RESERVOIR MODELING AND COMPOSITION SIMULATION OF PRIMARY DEPLETION, WATERFLOODING, AND CARBON DIOXIDE FLOODING OF A SMALL PENNSYLVANIAN CARBONATE MOUND COMPLEX, ANASAZI FIELD, PARADOX BASIN, UTAH

Volume I

by

Wilmer E. Culham
REGA Inc.
Houston, Texas 77057

and

Douglas M. Lorenz
Texaco E&P
Houston, Texas 77215

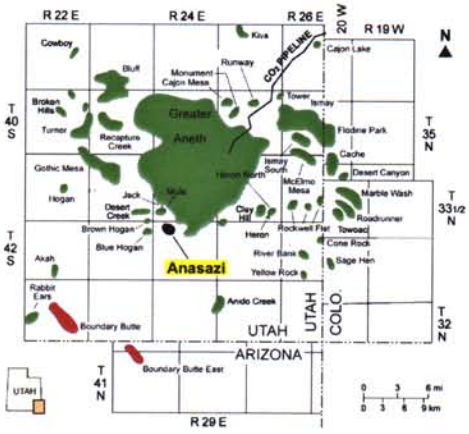

OPEN-FILE REPORT 420 **September 2003**
UTAH GEOLOGICAL SURVEY
a division of
UTAH DEPARTMENT OF NATURAL RESOURCES

This Open-File Report represents material that may not have undergone policy, technical, or editorial review required for other UGS publications. It provides information that, in part, may be interpretive or incomplete and readers are to exercise some degree of caution in the use of the data. Although this product represents the work of professional scientists, the Utah Department of Natural Resources, Utah Geological Survey, makes no warranty, stated or implied, regarding its suitability for a particular use. The Utah Department of Natural Resources, Utah Geological Survey, shall not be liable under any circumstances for any direct, indirect, special, incidental, or consequential damages with respect to claims by users of this product.

DISCLAIMER

This report was prepared as an account of work sponsored by an agency of the United States Government. Neither the United States Government nor any agency thereof, nor any of their employees, makes any warranty, express or implied, or assumes any legal liability or responsibility for the accuracy, completeness, or usefulness of any information, apparatus, product, or process disclosed, or represents that its use would not infringe privately owned rights. Reference herein to any specific commercial product, process, or service by trade name, trademark, manufacturer, or otherwise does not necessarily constitute or imply its endorsement, recommendation, or favoring by the United States Government or any agency thereof. The views and opinions of authors expressed herein do not necessarily state or reflect those of the United States Government or any agency thereof.

TABLE OF CONTENTS

LIST OF TABLES VII

LIST OF FIGURES XI

1. SUMMARY 1

2. INTRODUCTION 3

3. ANASAZI FIELD DEVELOPMENT AND GEOLOGICAL REVIEW 5

4. DATA REVIEW AND RESERVOIR DESCRIPTION 7

4.1. Well Data 7

4.1.1. Well Log Data 7

4.1.2. Core Data 9

4.1.3. Procedures for Estimating Permeability 9

4.1.4. Selection of Core Samples for SCAL Measurements . 10

4.1.5. Core Interpretation 12

4.1.6. Carbonate Lithotypes 12

4.1.7. Lithotype Layering 16

4.2. Outcrop Analogue Studies of Reservoir Architecture 16

4.3. Seismic Interpretation and Average Reservoir Porosity 16

5. RESERVOIR CHARACTERIZATION OVERVIEW 19

5.1. Gridding and Layering 19

5.2. Architectural Modeling 19

5.3. Porosity Modeling 20

5.4. Vertical Scaling 20

6. RESERVOIR MODELING 21

6.1. Lithotype Emplacement 21

6.1.1. Lithotype Geometry 21

6.1.2. Reservoir Volume 22

6.1.3. Boolean Modeling Procedure 22

6.2. Porosity Distribution Modeling 24

6.2.1. Simulated Annealing 24
6.2.2. Permeability Computation 27
6.2.3. Final Model Selection 28
7. VERTICAL UPSCALING: RESERVOIR CHARACTERIZATION TO SIMULATION MODEL 29
7.1. Lithotype Reassignment 29
7.2. Upscaling Reservoir Properties 29
8. REVIEW OF PRODUCTION HISTORY 31
9. WELL TEST DATA AND INTERPRETATION 32
9.1. Introduction 32
9.2. Anasazi Well 1 Tests 32
9.2.1. Anasazi Well No. 1 – Ana 1 – 0190 Test 33
9.2.2. Anasazi Well No. 1 – Ana 1 – 0290 Test 36
9.2.3. Anasazi Well No. 1 – Ana 1 – 0893 Test 37
9.3. Anasazi Well No. 5L–3 Tests 37
9.4. Anasazi Well No 6H–1 Tests 38
9.4.1. Introduction 38
9.4.2. Wireline Formation Testing 38
9.4.3. Dolomite Interval Flow and Build–up Test 39
9.4.4. Limestone Interval Pressure Monitoring 41
9.4.5. Summary of the Anasazi 6H–1 Tests 41
9.5. Sahgzie Well No. 1 Tests 42
9.5.1. Introduction 42
9.5.2. Sahgzie Well No. 1 Test 42
9.5.3. Other Sahgzie Well Tests 45
9.6. Other Paradox Basin Well Tests 45
10. RESERVOIR FLUID CHARACTERIZATION 46
10.1. Fluid Properties – Experimental Data 46
10.1.1. Original Reservoir Fluid Properties 46

10.1.2. CO_2 Process Fluid Property Characterization 46
10.1.2.1.Compositional Analysis 46
10.1.2.2.Constant Composition Expansion Test 48
10.1.2.3.CO_2 Swelling Test 48
10.1.2.4.Separator Tests 48
10.2. Equation of State Development 49
10.3. Equation of State Validation 51
11. RESERVOIR PETROPHYSICAL PROPERTY DETERMINATION . 54
11.1. General 54
11.2. Capillary Pressure and Relative Permeability Data – Dolomite Facies 54
11.2.1. Properties of Fluids Used for Special Core Tests 54
11.2.2. Experimental Procedures 55
11.2.3. Core Re–Saturation and Effective Permeability to Water (Kew) Measurements 55
11.2.4. Initial Oil/Brine Drainage Experiment and Aging 55
11.2.5. Brine/Oil Imbibition Capillary Pressure Test 56
11.2.6. Effective Water Permeability (Kew) Measurements and Oil/Brine Secondary Drainage Test 56
11.2.7. Brine/Oil Imbibition Relative Permeability Test 56
11.2.8. Oil/Brine Drainage Relative Permeability Test 56
11.2.9. Gas–Oil Capillary Pressure Experiment 56
11.2.10. Gas/Oil Relative Permeability Experiment 57
11.2.11. Final Saturation and Permeability Determinations . . 57
11.2.12. Primary Drainage Capillary Pressure Measurements 57
11.2.13. U.S.B.M. and Amott Wettability Indices 58
11.2.14. Bond Number versus Sor/Soi 58
11.2.15. Summary 58
11.3. Capillary Pressure and Relative Permeability – Limestone Facies 59

11.3.1. General 59
11.3.2. Core Re–Saturation and Effective Permeability to Water (Kew) Measurements 59
11.3.3. Primary Drainage Capillary Pressure Measurements and Aging 59
11.3.4. Brine/Oil Imbibition Capillary Pressure Test 59
11.3.5. Oil Brine Secondary Drainage Test 59
11.3.6. Brine/Oil Imbibition Relative Permeability Test 60
11.3.7. Oil/Brine Drainage Relative Permeability Test 60
11.3.8. Gas/Oil Capillary Pressure Experiment 60
11.3.9. Gas/Oil Relative Permeability Experiment 60
11.3.10. Final Saturation Determination via Dean–Stark 60
11.3.11. U.S.B.M. and Amott Wettability Indices 60
11.3.12. Bond Number vs. Sor/Soi 61
11.3.13. Oil/Gas Imbibition Capillary Pressure Experiment . . 61
11.3.14. Summary 61
11.4. Rock Compressibility Measurements 61
11.5. Gas Mercury Capillary Pressure Measurements 62
12. CARBON DIOXIDE PROCESS MECHANISM STUDIES 64
12.1. Introduction 64
12.2. Multiple Contact Phase Behavior of CO_2–Anasazi Fluid Systems 64
12.3. One Dimensional CO_2 Displacement Simulation Studies 67
12.4. Two Dimensional Mechanistic Simulation Studies 68
12.4.1. Introduction 68
12.4.2. Model Description 69
12.4.3. Fluid Properties and Production Data 69
12.4.4. Simulation Study Procedure 69
12.4.5. Study Results 70
12.4.6. Summary 71

13. RESERVOIR PERFORMANCE STUDY–SIMULATION MODEL SET UP 72
13.1. Simulator Selection 72
13.2. Fluid Properties 72
13.3. Rock Properties 73
13.4. Reservoir Characterization 73
13.5. Field/Reservoir Operational Data 74
13.6. Well Modelling 75
13.7. Separator Specifications 75
13.8. Reservoir Gridding and Region Definition 75
13.9. Simulation Initialization 76
14. RESERVOIR PERFORMANCE – HISTORY MATCH 77
14.1. Introduction 77
14.2. Review of History Match Studies 77
14.3. Final History match 83
15. RESERVOIR PERFORMANCE – PREDICTION CASES 88
15.1. Primary Production Performance 88
15.2. CO2 Flood Evaluation 89
15.2.1. Summary of CO_2 Flood Case Studies 89
15.2.2. Prediction Case Results and Reservoir Performance Interpretation 93
15.2.3. Optimized CO_2 Flood Performance Cases 98
15.3. Waterflood Evaluation 101
15.3.1. Summary of Waterflood Case Studies 101
15.3.2. Waterflood Prediction Case Results and Reservoir Performance Interpretation 103
16. ECONOMIC ASSESSMENT 108
16.1. Introduction 108
16.2. CO_2 Flood Implementation – Design and Costs 109
16.2.1. Production and Injection Wells 109

16.2.2. Surface Production and Injection Lines 110
16.2.3. Surface Production Facilities 111
16.2.4. CO_2 Supply Line 111
16.2.5. Main Injection Compressor 111
16.2.6. Gas Processing Plant 112
16.2.7. CO_2 Purchase Costs 112
16.2.8. Miscellaneous Fees 112
16.2.9. A New Seismic Survey and CO_2 Flood Re–Design . . . 113
16.3. Operating Cost Data 113
16.3.1. General Operating Costs 113
16.3.2. Gas Processing Plant Operating Expenses 114
16.3.3. CO_2 Supply Line Operating Expense 115
16.3.4. CO_2 Purchase 115
16.4. Economic Evaluations 115
16.4.1. Case Descriptions 115
16.4.2. Base Economic Parameters 118
16.4.3. Economic Evaluation Results 119
16.4.4. Economic Evaluation Summary 121
17. CONCLUSIONS 122
18. RECOMMENDATIONS 129
APPENDIX A A–1

LIST OF TABLES

Table 4–1 Desert Creek Stratigraphic Picks

Table 4–2 Average Porosity, Permeability and Water Saturation, Anasazi Field

Table 4–3 Average Reservoir Properties of Architectural Lithotypes, Anasazi Field

Table 4–4 Lithotype Layering, Anasazi #1

Table 4–5 Lithotype Layering, Anasazi #5L–3

Table 4–6 Lithotype Layering, Anasazi #6H–1

Table 4–7 Architectural Properties, Anasazi Lithotypes

Table 6–1 Boolean Emplacement Procedures

Table 6–2 Constraints on Simulated Annealing Procedures

Table 10–1 Paradox Basin Desert Creek Fields – Fluid Property Data

Table 10–2 Composition of Anasazi Well #5L–3 Separator Oil Sample at 73° F and 1014 psia

Table 10–3 Composition of Anasazi Well #5L–3 Separator Gas Cylinder #5EK088

Table 10–4 Dead Oil Liquid Composition of the Anasazi Flashed Separator Oils and Dead Oils

Table 10–5 Composition of Anasazi Well #5L–3 – Recombined Separator Oil at 70°F and 3014 psia

Table 10–6 PV–Isotherm Data for Anasazi Well #5L–3 Recombined Fluid at 130°F

Table 10–7 Composition of Recombined Anasazi Well #5L–3 Oil Flashed to 2050 psia at 130°F

Table 10–8 Composition of Recombined Anasazi Well #5L–3 Oil Flashed to 365.5 psia at 130°F

Table 10–9 Volumes of Liquid and Vapor Measured at Different Flash Conditions Anasazi Well #5L–3 Recombined Oil

Table 10–10 Relative Volumes of the Liquid and Vapor Phases as a Function of Pressure at 130°F

Table 10–11 Swelling Test Data for the Anasazi #5L–3 Oil at 130°F

Table 10–12 Composition of Anasazi Well #5L–3 Recombined Separator Oil at 70°F and 3014 psia – Pseudo Component Definition

Table 10–13 Composition of Anasazi Well #5L–3 Recombined Oil Flashed to 2050 psi at 130°F – Pseudo Component Definition

Table 10–14 Composition of Original Oil Anasazi Well #1 – Pseudo Component Definition

Table 10–15 Equation of State Parameters 11 Pseudo Component Version – Anasazi–Sahgzie Fluid System

Table 10–16 Pederson Viscosity Correlation Parameters

Table 10–17 Oil Viscosity of Recombined Anasazi #SL–3 Oil Flashed to 2050 psia and 130°F and Various Mole Fractions of CO_2

Table 11–1 Brine Composition for Capillary Pressure Measurements

Table 11–2 Fluid Properties for Capillary Pressure Measurements on the Dolomite Sample Test

Table 11–3 Permeability and Porosity Data Summary Anasazi #6H–1 Dolomite Sample

Table 11–4 Anasazi #6H–1 Dolomite and Anasazi #1 Limestone Samples Permeability and Porosity Data Summary

Table 11–5 Pre–Test Sample Conditions and Physical Properties for Selected Samples From Anasazi No. 1 and 6H–1 Wells

Table 11–6 Target Pressure for Simulated In–Situ Conditions

Table 11–7 Compressibilities Determined from Hydrostatic Compression for Samples from the Anasazi #1 and #6H–1 Wells

Table 11–8 Quasi–Static Mechanical Properties Determined from Triaxial Compression for Samples from the Anasazi #1 and #6H–1 Wells

Table 11–9 Parameters Determined During Uniaxial Strain/Pore Pressure Drawdown Segment

Table 14–1 Pressure Data Comparisons – Simulation versus Field Measurements

Table 15–1 Initial Fluids in Place – Harken Anasazi Full Field Compositional Model

Table 15–2 Oil and Gas Production – Primary Depletion Prediction Anasazi/Sahgzie Reservoir

Table 15–3 Region Summary of Fluid Volumes, Production, Injection and Fluid Influx at 1/1/2012

Table 15–4 Production/Injection Data CO_2 Flood Anasazi/Sahgzie Reservoir

Table 15–5 Region Summary of Fluid Volumes, Production, Injection and Fluid Influx at 1/1/1997

Table 15–6 Region Summary of Fluid Volumes, Production, Injection and Fluid Influx at 1/1/2012

Table 15–7 Production/Injection Data – Waterflood Anasazi/Sahgzie Reservoir

Table 16–1a Economic Evaluation Number 1
Table 16–1b Economic Evaluation Number 1
Table 16–2a Economic Evaluation Number 2
Table 16–2b Economic Evaluation Number 2
Table 16–3a Economic Evaluation Number 3
Table 16–3b Economic Evaluation Number 3
Table 16–4a Economic Evaluation Number 4
Table 16–4b Economic Evaluation Number 4
Table 16–5a Economic Evaluation Number 5
Table 16–5b Economic Evaluation Number 5
Table 16–6a Economic Evaluation Number 6
Table 16–6b Economic Evaluation Number 6
Table 16–7a Economic Evaluation Number 7
Table 16–7b Economic Evaluation Number 7
Table 16–8a Economic Evaluation Number 8
Table 16–8b Economic Evaluation Number 8
Table 16–9a Economic Evaluation Number 9
Table 16–9b Economic Evaluation Number 9
Table 16–10a Economic Evaluation Number 10
Table 16–10b Economic Evaluation Number 10
Table 16–11a Economic Evaluation Number 11
Table 16–11b Economic Evaluation Number 11
Table 16–12a Economic Evaluation Number 14
Table 16–12b Economic Evaluation Number 14
Table 16–13a Economic Evaluation Number 15
Table 16–13b Economic Evaluation Number 15
Table 16–14 CO_2 Project Investment Summary – Purchase Compressor
Table 16–15 CO_2 Project Investment Summary – Lease Compressor

LIST OF FIGURES

Figure 3–1 Regional Location Map, Anasazi Field

Figure 3–2 Isopach Map of the Anasazi Carbonate Mound Buildup

Figure 3–3 Anasazi #1 Log Suite (Unedited)

Figure 4–1 Computed Lithology Plot, Anasazi #1

Figure 4–2 Computed Lithology Plot, Anasazi #5L–3

Figure 4–3 Computed Lithology Plot, Sahgzie #1

Figure 4–4 Computed Lithology Plot, Anasazi #6H–1

Figure 4–5 Porosity/Permeability Crossplot, Mound Interval

Figure 4–6 Porosity/Permeability Crossplot, Supramound Interval

Figure 4–7 Horizontal/Vertical Permeability Crossplot, Mound Interval

Figure 4–8 Horizontal/Vertical Permeability Crossplot, Supramound Interval

Figure 4–9 Transverse CAT Scans for Relative Permeability and Rock Compressibility Sample Selection, Mound Interval Limestone, Anasazi #1

Figure 4–10 Transverse CAT scans for Reservoir Quality Comparison, Supramound Interval Dolomite, Anasazi #6H–1

Figure 4–11 Whole Core Photos of Interval (5691 ft MD) Sampled for Relative Permeability and Rock Compressibility, Supramound Interval Dolomite, Anasazi #6H–1

Figure 4–12 Core Plug Photos of Samples 1 and 2 (5691 ft MD), Supramound Interval Dolomite, Anasazi #6H–1

Figure 4–13 Core Plug Photos of Samples 3 and 4 (5691 ft MD), Supramound Interval Dolomite, Anasazi #6H–1

Figure 4–14 Longitudinal CAT Scans of Relative Permeability and Rock Compressibility Plug Samples, Supramound Interval Dolomite, Anasazi #6H–1

Figure 4–15 Anasazi Reservoir Stratigraphy From Core Interpretation.

Figure 4–16 (a,b) – Lithotype 1: Tight Carbonate Mudstone
(c,d) – Lithotype 2: Dolomitized Mudstone

Figure 4–17 (a,b) – Lithotype 3: Enhanced Porosity Mudstone
(c,d) – Lithotype 4: Tight Packstone/Wackestone

Figure 4–18 (a,b) – Lithotype 5: Porous Packstone/Wackestone
(c,d) – Lithotype 6: Porous Grainstone

Figure 4–19 (a,b) – Lithotype 7: Tight Grainstone
(c,d) – Lithotype 8: Tubular Tempestites

Figure 4–20 (a,b) – Lithotype 9: Phylloid Algal Limestone
(c,d) – Lithotype 10: Mound–Front Bioclastic Breccia

Figure 4–21 Location Map of Wild Horse Canyon Field Study Area, Lower Ismay Carbonate Mound Analogues

Figure 4–22 Lower Ismay Carbonate Mound Analogue, San Juan River, Utah

Figure 4–23 Block Diagram Interpretation of Facies Distributions, Anasazi and Other Analogous Carbonate Mound Buildups

Figure 4–24 Interpreted Seismic Lines Across Anasazi Field Showing Qualitative Basis for the Reservoir Quality Index (RQI)

Figure 4–25 Reservoir Quality Seismic Interpretation Across the Anasazi and Sahgzie Mound Buildups, Anasazi Field

Figure 4–26 Anasazi Reservoir Quality Index (RQI) Map, Based on Qualitative Seismic Interpretations

Figure 4–27 Anasazi Reservoir Quality Index (RQI)/Average Porosity Transfer Function Plot

Figure 4–28 Nearest–Neighbor Map of Reservoir Quality Index (RQI)/Average Porosity Transfer Function Slope

Figure 4–29 Anasazi Average Porosity Map

Figure 5–1 Anasazi Gridded Isolith Map

Figure 6–1 Bivariate Monte Carlo Distribution of Lithotype Volume Proportions: Tight Mudstone, Tight Packstone/Wackestone

Figure 6–2 Bivariate Monte Carlo Distribution of Lithotype Volume Proportions: Porous Grainstone, Tubular Tempestites

Figure 6–3 Bivariate Monte Carlo Distribution of Lithotype Volume Proportions: Tight Mudstone, Porous Grainstone

Figure 6–4 Lithotype Legend, 50–Layer Geostatistical Models

Figure 6–5 Anasazi Boolean Lithotype Emplacements: Layer 1

Figure 6–6 Anasazi Boolean Lithotype Emplacements: Layer 19

Figure 6–7 Anasazi Boolean Lithotype Emplacements: Layer 38

Figure 6–8 Anasazi Boolean Lithotype Emplacements: Layer 40

Figure 6–9 Anasazi Boolean Lithotype Cross–Section: Y = 10

Figure 6–10 Anasazi Boolean Lithotype Cross–Section: Y = 20
Figure 6–11 Anasazi RQI Average Porosity Grid
Figure 6–12 Anasazi Porosity Vertical Variogram Modeling
Figure 6–13 Anasazi Annealing Average Porosity Grid
Figure 6–14 Anasazi Simulated Annealing Constraints – Porosity Horizontal Variogram
Figure 6–15 Anasazi Simulated Annealing Constraints – Porosity Vertical Variogram
Figure 6–16 Anasazi Lithotype Distribution Grid: Layer 1
Figure 6–17 Anasazi Lithotype Distribution Grid: Layer 19
Figure 6–18 Anasazi Lithotype Distribution Grid: Layer 38
Figure 6–19 Anasazi Lithotype Distribution Grid: Layer 40
Figure 6–20 Anasazi Lithotype Cross–Section: Y = 10
Figure 6–21 Anasazi Lithotype Cross–Section: Y = 20
Figure 7–1 Lithotype Legend, 15–Layer Upscaled VIP Simulation Model
Figure 7–2 Lithotype Areal Grid, Layer 38 – 50 Layer Model
Figure 7–3 Lithotype Areal Grid, Layer 12 – 15 Layer Model
Figure 7–4 Lithotype Cross–Section (Y=20) – 50 Layer Model
Figure 7–5 Lithotype Cross–Section (Y=20) – 15 Layer Model
Figure 7–6 Porosity Areal Grid, Layer 38 – 50 Layer Model
Figure 7–7 Porosity Areal Grid, Layer 12 – 15 Layer Model
Figure 7–8 Porosity Cross–Section (Y=20) – 50 Layer Model
Figure 7–9 Porosity Cross–Section (Y=20) – 15 Layer Model
Figure 7–10 Horizontal Permeability Areal Grid, Layer 38 – 50 Layer Model
Figure 7–11 Horizontal Permeability Areal Grid, Layer 12 – 15 Layer Model
Figure 7–12 Lithotype Block – 15 Layer VIP Model
Figure 7–13 Porosity Block – 15 Layer VIP Model
Figure 7–14 Horizontal Permeability Block – 15 Layer VIP Model
Figure 8–1 Oil Production History Anasazi–Sahgzie Field
Figure 8–2 Gas Production History Anasazi–Sahgzie Field
Figure 8–3 Oil Production and GOR History Anasazi–Sahgzie Field

Figure 8–4 Oil Production History Anasazi Well #1
Figure 8–5 Oil Production History Anasazi Well #SL–3
Figure 8–6 Oil Production History Anasazi Well #6H–1
Figure 8–7 Oil Production History Sahgzie Well #1
Figure 8–8 Gas Production History Anasazi Well #1
Figure 8–9 Gas Production History Anasazi Well #5L–3
Figure 8–10 Gas Production History Anasazi Well #6H–1
Figure 8–11 Gas Production History Sahgzie Well #1
Figure 8–12 Oil Production and GOR History Anasazi Well #1
Figure 8–13 Oil Production and GOR History Anasazi Well #5L–3
Figure 8–14 Oil Production and GOR History Anasazi Well #6H–1
Figure 8–15 Oil Production and GOR History Anasazi Well #1
Figure 9–1 Anasazi Well #1 – 0190 Test Derivative Diagnostic
Figure 9–2 Anasazi Well #1 – 0190 Test Superposition Diagnostic
Figure 9–3 Anasazi Well #1 – 0190 Derivative Pressure Difference Match
Figure 9–4 Anasazi Well #1 – 0190 Test Superposition Pressure Match
Figure 9–5 Anasazi Well #1 – 0190 Test Pressure Data Match
Figure 9–6 Anasazi Well #1 – 0190 Test Derivative and Pressure Difference Match
Figure 9–7 Anasazi Well #1 – 0190 Test Superposition Pressure Match
Figure 9–8 Anasazi Well #1 – 0190 Test Pressure Data Match
Figure 9–9 Anasazi Well #1 – 0290 Test Derivative and Pressure Difference Match
Figure 9–10 Anasazi Well #1 – 0290 Test Superposition Pressure Match
Figure 9–11 Anasazi Well #1 – 0290 Test Pressure Data Match
Figure 9–12 Anasazi Well #6H–1 – Dolomite Test – Derivative and Pressure Difference Match
Figure 9–13 Anasazi Well #6H–1 – Dolomite Test – Superposition Pressure Match
Figure 9–14 Anasazi Well #6H–1 – Dolomite – Pressure Test Match – Last Swab Run
Figure 9–15 Sahgzie Well #1 – 1189 Test Derivative Diagnostics
Figure 9–16 Sahgzie Well #1 – 1189 Test Superposition Diagnostics

Figure 9–17 Sahgzie Well #1 – 1189 Test Derivative and Pressure Difference Match

Figure 9–18 Sahgzie Well #1 – 1189 Test Superposition Pressure Match

Figure 9–19 Sahgzie Well #1 – 1189 Test Pressure Data Match

Figure 9–20 Sahgzie Well #1 – 1189 Test Two Layer Model Derivative and Pressure Difference Match

Figure 9–21 Sahgzie Well #1 – 1189 Test Two Layer Model Superposition – Pressure Match

Figure 9–22 Sahgzie Well #1 – 1189 Test Two Layer Model Pressure Data Match

Figure 10–1 Comparison of Weight Percent Composition Measured for Anasazi Flashed Separator Oil and Dead Oil Samples

Figure 10–2 Anasazi Well #1 Constant Composition Expansion Experiment – Original Oil Relative Oil Volume

Figure 10–3 Anasazi Well #1 Differential Depletion Experiment – Original Oil Relative Oil Volume (Oil Formation Volume Factor)

Figure 10–4 Anasazi Well #1 Differential Depletion Experiment – Original Oil Solution Gas Oil Ratio

Figure 10–5 Anasazi Well #1 Differential Depletion Experiment – Original Oil Density

Figure 10–6 Anasazi Well #1 Differential Depletion Experiment – Original Oil Gas Gravity

Figure 10–7 Anasazi Well #1 Constant Composition Expansion Experiment – Recombined Oil Relative Oil Volume

Figure 10–8 Anasazi Field – Saturation Pressure Versus CO_2 Concentration

Figure 10–9 Anasazi Field CO_2 Swelling Test 20% CO_2 Case – Relative Volume

Figure 10–10 Anasazi Field CO_2 Swelling Test 20% CO_2 Case – Liquid Volume

Figure 10–11 Anasazi Field CO_2 Swelling Test 40% CO_2 Case – Relative Volume

Figure 10–12 Anasazi Field CO_2 Swelling Test 40% CO_2 Case – Liquid Volume

Figure 10–13 Anasazi Field CO_2 Swelling Test 60% CO_2 Case – Relative Volume

Figure 10–14 Anasazi Field CO_2 Swelling Test 60% CO_2 Case – Liquid Volume

Figure 10–15 Anasazi Field CO_2 Swelling Test 75% CO_2 Case – Relative Volume

Figure 10–16 Anasazi Field CO_2 Swelling Test 75% CO_2 Case – Liquid Volume

Figure 10–17 Anasazi Field CO_2 Swelling Factor Comparison

Figure 11–1 Brine – Oil Primary Imbibition Capillary Pressure Data Anasazi #6H–1 Dolomite Interval Elevated Temperature – Automated Centrifuge Data

Figure 11–2 Oil – Brine Secondary Drainage Capillary Pressure Data Anasazi #6H–1 Dolomite Interval Elevated Temperature – Automated Centrifuge Data

Figure 11–3 Relative Permeability Data – Comparison of Core Preparation Methods Anasazi #6H–1 Dolomite Interval Elevated Temperature – Automated Centrifuge Data

Figure 11–4 Oil – Brine Primary Drainage Capillary Pressure Data Anasazi #6H–1 Dolomite Interval Elevated Temperature – Automated Centrifuge Data

Figure 11–5 Gas – Oil Drainage Capillary Pressure Data Anasazi #6H–1 Dolomite Interval Elevated Temperature – Automated Centrifuge Data

Figure 11–6 Gas – Oil Relative Permeability – Comparison of Core Preparation Methods Anasazi #6H–1 Dolomite Interval Elevated Temperature –Automated Centrifuge Data

Figure 11–7 Bond Number versus Oil Saturation Ratio Anasazi #6H–1 Dolomite Interval Elevated Temperature – Automated Centrifuge Data

Figure 11–8 Oil – Brine Primary Drainage Capillary Pressure Data Anasazi #6H–1 – Limestone Interval Elevated Temperature – Automated Centrifuge Data

Figure 11–9 Brine – Oil Primary Imbibition Capillary Pressure Data Anasazi #1 – Limestone Interval Elevated Temperature – Automated Centrifuge Data

Figure 11–10 Oil – Brine Secondary Drainage Capillary Pressure Data Anasazi #1 – Limestone Interval Elevated Temperature – Automated Centrifuge Data

Figure 11–11 Oil – Brine Relative Permeability Anasazi #1 – Limestone Interval Elevated Temperature – Automated Centrifuge Data

Figure 11–12 Gas – Oil Drainage Capillary Pressure Data Anasazi #1 – Limestone Interval Elevated Temperature – Automated Centrifuge Data

Figure 11–13 Gas – Oil Drainage Relative Permeability Anasazi #1 – Limestone Interval Elevated Temperature – Automated Centrifuge Data

Figure 11–14 Bond Number versus Oil Saturation Ratio Anasazi #1 – Limestone Interval Elevated Temperature – Automated Centrifuge Data

Figure 11–15 Oil – Gas Imbibition Capillary Pressure Anasazi #1 – Limestone Interval Elevated Temperature – Automated Centrifuge Data

Figure 11–16 Mean Pore Size Distribution Anasazi #6H–1 Dolomite Interval – Mercury Capillary Pressure Data

Figure 11–17 Mercury Capillary Pressure Anasazi #6H–1 Dolomite Interval – Mercury Capillary Pressure Data

Figure 11–18 Mean Pore Size Distribution Anasazi #1 Limestone Interval – Mercury Capillary Pressure Data

Figure 11–19 Mercury Capillary Pressure Anasazi #1 Limestone Interval – Mercury Capillary Pressure Data

Figure 12–1 Pseudo Ternary Diagram – Original Oil at 2000 psia and 130°F Multiple Contact Immiscible Displacement

Figure 12–2 Pseudo Ternary Diagram – Original Oil at 2350 psia and 130°F Multiple Contact Immiscible Displacement

Figure 12–3 Pseudo Ternary Diagram – Original Oil at 2400 psia and 130°F Multiple Contact Miscible

Figure 12–4 Pseudo Ternary Diagram – Depleted Oil at 2500 psia and 130°F Multiple Contact Immiscible Displacement

Figure 12–5 Pseudo Ternary Diagram – Depleted Oil at 3000 psia and 130°F Multiple Contact Immiscible Displacement

Figure 12–6 Pseudo Ternary Diagram – Original Oil at 3100 psia and 130°F Multiple Contact Miscible

Figure 12–7 Oil Production Sensitivity to Grid Block Size

Figure 12–8 Oil Recovery Sensitivity to Grid Block Size

Figure 12–9 Oil Recovery Sensitivity to Displacement Pressure

Figure 12–10 Oil Recovery Sensitivity to Displacement Pressure

Figure 12–11 CO_2 Displacement at 2500 psia – Phase Saturation versus Time for Cell 217

Figure 12–12 CO_2 Displacement at 2500 psia – Composition versus Time for Cell 217 – Component CO_2

Figure 12–13 CO_2 Displacement at 2500 psia – Composition versus Time for Cell 217 – Component C1

Figure 12–14 CO_2 Displacement at 2500 psia – Composition versus Time for Cell 217 – Component C2

Figure 12–15 CO_2 Displacement at 2500 psia – Composition versus Time for Cell 217 – Component C3

Figure 12–16 CO_2 Displacement at 2500 psia – Composition versus Time for Cell 217 – Component C4–C5

Figure 12–17 CO_2 Displacement at 2500 psia – Composition versus Time for Cell 217 – Component C6–C8

Figure 12–18 CO_2 Displacement at 2500 psia – Composition versus Time for Cell 217 – Component C9–C11

Figure 12–19 CO_2 Displacement at 2500 psia – Composition versus Time for Cell 217 – Component C12–C15

Figure 12–20 CO_2 Displacement at 2500 psia – Composition versus Time for Cell 217 – Component C16–C19

Figure 12–21 CO_2 Displacement at 2500 psia – Composition versus Time for Cell 217 – Component C20–C29

Figure 12–22 CO_2 Displacement at 2500 psia – Composition versus Time for Cell 217 – Component C30P

Figure 12–23 CO_2 Displacement at 3000 psia – Composition versus Time for Cell 202 – Component CO2

Figure 12–24 CO_2 Displacement at 3000 psia – Composition versus Time for Cell 202 – Component C1

Figure 12–25 CO_2 Displacement at 3000 psia – Composition versus Time for Cell 202 – Component C2

Figure 12–26 CO_2 Displacement at 3000 psia – Composition versus Time for Cell 202 – Component C3

Figure 12–27 CO_2 Displacement at 3000 psia – Composition versus Time for Cell 202 – Component C4–C5

Figure 12–28 CO_2 Displacement at 3000 psia – Composition versus Time for Cell 202 – Component C6–C8

Figure 12–29 CO_2 Displacement at 3000 psia – Composition versus Time for Cell 202 – Component C9–C11

Figure 12–30 CO_2 Displacement at 3000 psia – Composition versus Time for Cell 202 – Component C12–C15

Figure 12–31 CO_2 Displacement at 3000 psia – Composition versus Time for Cell 202 – Component C16–C19

Figure 12–32 CO_2 Displacement at 3000 psia – Composition versus Time for Cell 202 – Component C20–C29

Figure 12–33 CO_2 Displacement at 3000 psia – Composition versus Time for Cell 202 – Component C30P

Figure 12–34 Oil Production Rate – Anasazi Field

Figure 12–35 Simulation versus Anasazi Field Data – Gas Production Rate

Figure 12–36 Simulation versus Anasazi Field Data – Gas Oil Ratio

Figure 12–37 Two Dimensional Simulation Predictions – Anasazi GOR and Pressure

Figure 12–38 Predicted Limestone and Dolomite Cumulative Oil Production

Figure 12–39 Predicted Interval Oil Production History

Figure 12–40 Gas Saturation Distribution – Two Dimensional Simulation
Figure 12–41 Gas–Oil Relative Permeability and Capillary Pressure for Dolomite Unit
Figure 12–42 Oil–Water Relative Permeability and Capillary Pressure for Dolomite Unit
Figure 12–43 Gas–Oil Relative Permeability and Capillary Pressure for Limestone Unit
Figure 12–44 Oil–Water Relative Permeability and Capillary Pressure for Limestone Unit
Figure 12–45 Areal Reservoir Geometry and Simulation Grid Definition
Figure 12–46 Vertical (Z–Direction) Grid Definition Y–Cross Section
Figure 12–47 Vertical (Z–Direction) Grid Definition X–Cross Section
Figure 12–48 Region Definition – Eight Regions Y–Cross Section
Figure 12–49 Region Definition – Map at Top of Core Mound Interval
Figure 12–50 Oil Production History Anasazi–Sahgzie Reservoirs
Figure 12–51 Gas Production History Match Anasazi–Sahgzie Reservoir
Figure 12–52 Oil Production History – Sahgzie Well #1
Figure 12–53 Gas Production History Match – Sahgzie Well #1
Figure 12–54 Oil Production History – Anasazi Well #1
Figure 12–55 Gas Production History Match – Anasazi Well #1
Figure 12–56 Oil Production History – Anasazi Well #5L–3
Figure 12–57 Gas Production History Match – Anasazi Well #5L–3
Figure 12–58 Oil and Gas Production Rate – Anasazi Well #1
Figure 12–59 Layer 11 Oil and Gas Production – Anasazi Well #1
Figure 12–60 Layer 12 Oil and Gas Production – Anasazi Well #1
Figure 12–61 Layer 13 Oil and Gas Production – Anasazi Well #1
Figure 12–62 Layer 14 Oil and Gas Production – Anasazi Well #1
Figure 12–63 Layer 12 Oil and Gas Production – Sahgzie Well #1
Figure 12–64 Layer 13 Oil and Gas Production – Sahgzie Well #1
Figure 12–65 Regional Influx and Efflux of Oil – Anasazi Mound
Figure 12–66 Regional Influx and Efflux of Oil – Anasazi Mound
Figure 12–67 Regional Influx and Efflux of Oil – Anasazi Mound
Figure 12–68 Regional Influx and Efflux of Oil – Sahgzie Mound

Figure 12–69 Regional Influx and Efflux of Oil – Sahgzie Mound

Figure 12–70 Regional Influx and Efflux of Oil – Sahgzie Mound

Figure 12–71 Limestone Production versus Supramound Oil Efflux – Anasazi Mound

Figure 12–72 Limestone Production versus Supramound Oil Efflux – Sahgzie Mound

Figure 12–73 Gas Saturation Distribution – Y–Direction Cross Section at Anasazi Well #1

Figure 12–74 Gas Saturation Distribution – Z–Direction Map at Top of Phylloid Algal Limestone

Figure 12–75 Gas Saturation Distribution – Z–Direction Map at Top of Supramound Interval

Figure 13–1 Gas–Oil Relative Permeability and Capillary Pressure for Dolomite Unit

Figure 13–2 Oil–Water Relative Permeability and Capillary Pressure for Dolomite Unit

Figure 13–3 Gas–Oil Relative Permeability and Capillary Pressure for Limestone Unit

Figure 13–4 Oil–Water Relative Permeability and Capillary Pressure for Limestone Unit

Figure 13–5 Areal Reservoir Geometry and Simulation Grid Definition

Figure 13–6 Vertical (Z–Direction) Grid Definition Y–Cross Section

Figure 13–7 Vertical (Z–Direction) Grid Definition X–Cross Section

Figure 13–8 Region Definition – Eight Regions Y–Cross Section

Figure 13–9 Region Definition – Map at Top of Core Mound Interval

Figure 14–1 Oil Production History Anasazi–Sahgzie Reservoir

Figure 14–2 Gas Production History Match Anasazi–Sahgzie Reservoir

Figure 14–3 Oil Production History – Sahgzie Well #1

Figure 14–4 Gas Production History Match – Sahgzie Well #1

Figure 14–5 Oil Production History – Anasazi Well #1

Figure 14–6 Gas Production History Match – Anasazi Well #1

Figure 14–7 Oil Production History – Anasazi Well #5L–3

Figure 14–8 Gas Production History Match – Anasazi Well #5L–3

Figure 14–9 Oil and Gas Production Rate – Anasazi Well #1

Figure 14–10 Layer 11 Oil and Gas Production – Anasazi Well #1

Figure 14–11 Layer 12 Oil and Gas Production – Anasazi Well #1

Figure 14–12 Layer 13 Oil and Gas Production – Anasazi Well #1

Figure 14–13 Layer 14 Oil and Gas Production – Anasazi Well #1
Figure 14–14 Layer 12 Oil and Gas Production – Sahgzie Well #1
Figure 14–15 Layer 13 Oil and Gas Production – Sahgzie Well #1
Figure 14–16 Regional Influx and Efflux of Oil – Anasazi Mound
Figure 14–17 Regional Influx and Efflux of Oil – Anasazi Mound
Figure 14–18 Regional Influx and Efflux of Oil – Anasazi Mound
Figure 14–19 Regional Influx and Efflux of Oil – Sahgzie Mound
Figure 14–20 Regional Influx and Efflux of Oil – Sahgzie Mound
Figure 14–21 Regional Influx and Efflux of Oil – Sahgzie Mound
Figure 14–22 Limestone Production versus Supramound Oil Efflux – Anasazi Mound
Figure 14–23 Limestone Production versus Supramound Oil Efflux – Sahgzie Mound
Figure 14–24 Gas Saturation Distribution – Y–Direction Cross Section at Anasazi Well #1
Figure 14–25 Gas Saturation Distribution – Z–Direction Map at Top of Phylloid Algal Limestone
Figure 15–1 Gas Saturation Distribution – Z–Direction Map at Top of Supramound Interval
Figure 15–2 Oil Production Primary Depletion Prediction Anasazi–Sahgzie Reservoir
Figure 15–3 Gas Production Primary Depletion Prediction Anasazi–Sahgzie Reservoir
Figure 15–4 Oil Production Primary Depletion Prediction –Sahgzie Well #1
Figure 15–5 Oil Production Primary Depletion Prediction –Anasazi Well #1
Figure 15–6 Oil Production Primary Depletion Prediction –Anasazi Well #5L–3
Figure 15–7 Oil Production Primary Depletion Prediction –Anasazi Well #6H–1
Figure 15–8 Cumulative Oil Recover as Function of Reservoir Operating Pressure
Figure 15–9 Oil Production Rate Variation with Number and Location of Injectors
Figure 15–10 Cumulative Oil Variation with Number and Location of Injectors
Figure 15–11 Sahgzie Well #1 Response to Single Anasazi CO_2 Injector
Figure 15–12 Oil Production Data – Horizontal versus Vertical Injectors
Figure 15–13 Oil Production Variation with Processing of Re–Injection Gas
Figure 15–14 Oil Production As Influenced by Operations during Fill–Up
Figure 15–15 Oil Production – Continuous CO_2 versus CO_2 Injection and Blowdown

Figure 15–16 Field Level Oil Production – CO_2 Flood versus Primary

Figure 15–17 Anasazi Well #1 Oil Production – CO_2 Flood versus Primary

Figure 15–18 Anasazi Well #5L–3 Oil Production – CO_2 Flood versus Primary

Figure 15–19 Anasazi Well #6H–1 Oil Production – CO_2 Flood versus Primary

Figure 15–20 Sahgzie Well #1 Oil Production – CO_2 Flood versus Primary

Figure 15–21 Gas Injection – Sahgzie Mound Well – Continuous CO_2 Injection

Figure 15–22 Gas Injection – Anasazi Mound Well – Continuous CO_2 Injection

Figure 15–23 Oil Production –Continuous CO_2 versus CO_2 Injection and Blowdown

Figure 15–24 Anasazi Well #1 Oil Production – Continuous CO_2 versus CO_2 Injection and Blowdown

Figure 15–25 Anasazi Well #5L–3 Oil Production – Continuous CO_2 versus CO_2 Injection and Blowdown

Figure 15–26 Sahgzie Well #1 Oil Production – Continuous CO_2 versus CO_2 Injection and Blowdown

Figure 15–27 Oil Saturation Distribution – Y–Direction Cross Section at Anasazi Well #1

Figure 15–28 C4–C5 Liquid Mole Fraction Minus C4–C5 Vapor Mole Fraction – Y–Direction Cross Section at Anasazi Well #1

Figure 15–29 Oil Saturation Distribution – Z–Direction Map – Layer 12 in Phylloid Algal Limestone

Figure 15–30 Oil Saturation Distribution – Z–Direction Map – Layer 5 in Supramound Interval

Figure 15–31 Oil Saturation Distribution – Z–Direction Map – Layer 12 in Phylloid Algal Limestone

Figure 15–32 Oil Saturation Distribution – Z–Direction Map – Layer 5 in Supramound Interval

Figure 15–33 C4–C5 Liquid Mole Fraction Minus C4–C5 Vapor Mole Fraction – Z–Direction Map – Layer 11 in Phylloid Algal Limestone

Figure 15–34 C4–C5 Liquid Mole Fraction Minus C4–C5 Vapor Mole Fraction – Z–Direction Map – Layer 5 in Supramound Interval

Figure 15–35 Oil Saturation Distribution – X–Direction Cross Section at Anasazi Mound Injector and Anasazi Well #6H–1

Figure 15–36 Oil Saturation Distribution – X–Direction Cross Section at Sahgzie Mound Injector

Figure 15–37 Oil Saturation Distribution
Figure 15–38 3–D Liquid Phase CO2 Mole Fraction Distribution
Figure 15–39 Field Level Oil Production – Water Flood versus Primary
Figure 15–40 Anasazi Well #1 Oil Production – Water Flood versus Primary
Figure 15–41 Anasazi Well #5L–3 Oil Production – Water Flood versus Primary
Figure 15–42 Sahgzie Well #1 Oil Production – Water Flood versus Primary
Figure 15–43 Anasazi Well #1 Oil Rate and Water Cut – Water Flood
Figure 15–44 Anasazi Well #5L–3 Oil Rate and Water Cut – Water Flood
Figure 15–45 Sahgzie Well #1 Oil Rate and Water Cut – Water Flood
Figure 15–46 Field Level Oil Production – Water Flood versus Primary
Figure 15–47 Anasazi Well #1 Oil Production – Water Flood versus Primary
Figure 15–48 Anasazi Well #5L–3 Oil Production – Water Flood versus Primary
Figure 15–49 Sahgzie Well #1 Oil Production – Water Flood versus Primary
Figure 15–50 Anasazi Well #1 Oil Rate and Water Cut – Water Flood
Figure 15–51 Anasazi Well #5L–3 Oil Rate and Water Cut – Water Flood
Figure 15–52 Sahgzie Well #1 Oil Rate and Water Cut – Water Flood
Figure 15–53 Water Injection Data – Anasazi Mound Injector
Figure 15–54 Water Injection Data – Sahgzie Mound Injector
Figure 15–55 Field Level Oil Production – Water Flood versus Primary
Figure 15–56 Anasazi Well #1 Oil Production – Water Flood versus Primary
Figure 15–57 Anasazi Well #5L–3 Oil Production – Water Flood versus Primary
Figure 15–58 Sahgzie Well #1 Oil Production – Water Flood versus Primary
Figure 15–59 Field Level Oil Production – Water Flood versus Primary
Figure 15–60 Field Level Oil Production – Water Flood versus Primary
Figure 15–61 Anasazi Well #1 Oil Production – Water Flood versus Primary
Figure 15–62 Anasazi Well #5L–3 Oil Production – Water Flood versus Primary
Figure 15–63 Anasazi Well #6H–1 Oil Production – Water Flood versus Primary
Figure 15–64 Sahgzie Well #1 Oil Production – Water Flood versus Primary
Figure 15–65 Anasazi Well #1 Oil Rate and Water Cut – Water Flood

Figure 15–66 Anasazi Well #5L–3 Oil Rate and Water Cut – Water Flood
Figure 15–67 Anasazi Well #6H–1 Oil Rate and Water Cut – Water Flood
Figure 15–68 Sahgzie Well #1 Oil Rate and Water Cut – Water Flood
Figure 15–69 Field Level Oil Production – Water Flood versus Primary
Figure 15–70 Anasazi Well #1 Oil Production – Water Flood versus Primary
Figure 15–71 Anasazi Well #5L–3 Oil Production – Water Flood versus Primary
Figure 15–72 Sahgzie Well #1 Oil Production – Water Flood versus Primary
Figure 15–73 Anasazi Well #1 Oil Rate and Water Cut – Water Flood
Figure 15–74 Anasazi Well #5L–3 Oil Rate and Water Cut – Water Flood
Figure 15–75 Sahgzie Well #1 Oil Rate and Water Cut – Water Flood
Figure 15–76 Residual Oil Saturation after CO_2 Flooding
Figure 15–77 Residual Oil Saturation after Water Flooding

1. SUMMARY

This report presents the results of a comprehensive reservoir description and reservoir engineering study completed on Harken Energy Corporation's Anasazi/Sahgzie reservoir in the Paradox Basin in Utah. The study is part of a larger assessment program designed to determine the geologic and reservoir production performance characteristics of small shallow–shelf carbonate reservoirs in the Paradox Basin of Utah, Colorado and Arizona. The overall program is sponsored under the Class II Oil Program of the U. S. Department of Energy.

The principal objectives of the study were to develop a detailed quantitative description of the subject reservoir and use this description coupled with composition simulation to predict the performance of the mound complex under three different reservoir recovery processes. The three processes included primary depletion, CO_2 flooding and water flooding.

The economic feasibility of implementing one or more recovery processes was also to be investigated. These objectives were successfully completed. The work required to accomplish the objectives and the final results are presented in this report. The scope of this work and a summary of results are reviewed below.

The geometry, lithology, internal architecture and reservoir properties of the Anasazi/Sahgzie mound complex were developed from a variety of data sources. Data sources included seismic, well logs, core, outcrop data and well test results. This data and its interpretation were used to construct geostatistically based architectural representations of a number of different reservoir models or realizations and the associated properties of the facies contained in the architectural elements. The procedures used to generate the models and changes necessary for implementation in the reservoir simulation studies are provided.

The reservoir production history is presented and the various stages of depletion are defined using production data, mechanistic and full field simulation studies.

To supplement the fluid and rock property data available prior to this study, a comprehensive data acquisition program was defined and completed. Fluid compositions, carbon dioxide swelling tests, capillary pressures, relative permeabilities and rock compressibility measurements were completed and results discussed in the report. Fluid property data was used to calibrate an equation of state which was subsequently used to conduct CO_2 process mechanistic studies and compositional simulation studies to define CO_2 miscibility conditions.

A complete review of existing well test data and new interpretations of this data were completed and reported. Interpretations provided new insight into fluid flow among the principal rock types and quantitative data to support reservoir characterization.

Utilizing new reservoir property data, the calibrated equation of state and a number of different geostatistically based reservoir models, a compositional simulator was used to history match past reservoir performance. The reservoir properties that required modification to obtain a history match are reviewed and the final predicted performance is compared with historic data.

Using the history matched simulator, continued primary depletion to the year 2012 was predicted. The ultimate recovery projected for primary depletion is 2.55 million STB of oil. This represents 54% of the original oil in place (OOIP) in the mound complex and 22% of the OOIP of the reservoir system that was modelled. The simulator was used to predict performances of both CO_2 floods and

waterfloods. The influence of the number of injectors, injector location, injector well configuration (vertical versus horizontal), and production well operating conditions were assessed for both CO_2 floods and waterflooding. In addition, the operating pressure required to maintain CO_2 – crude oil miscibility and the impact of re–injecting unprocessed (CO_2 and hydrocarbons not separated) produced gas on CO_2 flood performance was assessed. Simulation results indicate that CO_2 flooding is superior to waterflooding in terms of total oil recovered, time to complete the displacement and higher oil production rates. The best performing CO_2 flood had predicted total oil recovery in excess of 5.0 million STB and an incremental oil recovery over primary of approximately 2.5 million STB at the year 2012. Simulation results provide data to determine the CO_2 gas volume required and overall project injection requirements. Also, the performance of continued CO_2 injection versus CO_2 injection followed by reservoir blowdown is reported.

Based on the conclusion that CO_2 flooding is the only technically feasible recovery process suitable for the Anasazi/Sahgzie reservoir, CO_2 flood implementation costs were developed. Implementation costs in conjunction with reservoir performance production and injection predictions were used to complete a suite of economic assessment studies. Of the various CO_2 implementation options studied, a continuous CO_2 injection case utilizing re–injection of unprocessed produced gas, a leased main injection compressor and DOE cost sharing provided a before tax net present value discounted at 10% / year of over $12.5 million and a before tax rate of return of 62% on a total investment of $3.1 million. Harken's investment share would be $1.7 million. The profitability index of this particular implementation was determined to be 15.0 to 1.0.

Conclusions associated with the overall implementation of a CO_2 flood in the Anasazi–Sahgzie reservoir and the appropriate operational requirements to maximize the economic return are provided in the final chapter of the report.

The study results on predicted CO_2 flood response and the associated economics, support the extension of the overall shallow shelf carbonate evaluation program to Phase II. Phase II involves the implementation and completion of a CO_2 flood in the Anasazi/Sahgzie reservoir.

2. INTRODUCTION

As part of a comprehensive assessment program to determine the geologic and reservoir production performance characteristics of small shallow shelf carbonate reservoirs in the Paradox Basin a detailed reservoir description and reservoir engineering study was completed on Harken Energy Corporation's Anasazi/Sahgzie reservoir. The overall program and the subject study are sponsored under the Class II Oil Program of the U. S. Department of Energy. The Utah Geologic Survey heads a multi–disciplinary team responsible for the overall program administration and technical work program.

The subject study involved the acquisition of new geologic, fluid and reservoir property data and the integration of this information with existing data to develop geostatistically derived detailed geologic models of the reservoir for use in reservoir simulation studies. The simulation studies were designed to understand reservoir production mechanisms and history match the primary depletion stage of Anasazi/Sahgzie system and then predict the performance of the reservoir under CO_2 flooding and waterflooding. Using performance prediction history from the simulation studies, the economic feasibility of implementing a CO_2 flood was assessed.

The report provides a complete technical documentation of the work conducted to complete the study. It serves as documentation for Harken Energy Corporation as well as the DOE program requirements.

Chapters 3 to 7 cover the geology, description and quantitative characterization of the Anasazi reservoir. Chapter 3 summarizes the development history of the field and briefly describes the geometry, lithology, internal architecture and overall reservoir properties. Chapter 4 reviews the variety of seismic, well log/core and outcrop data utilized in constructing the reservoir model and provides detailed descriptions of reservoir properties at the four Anasazi wells. Reservoir modeling design is briefly outlined in Chapter 5, for which Chapter 6 provides details of the methods used to generate the architectural and properties–based geostatistical characterization. Chapter 7 concludes the reservoir modeling discussion with a description of the vertical upscaling procedures required to convert the quantitative characterization into a final flow simulation model.

Chapter 8 provides a brief review of the production history of the Anasazi–Sahgzie reservoir. It includes historic production data and a preliminary discussion of reservoir production mechanisms.

Chapter 9 presents data on transient well tests and wireline formation tests conducted on wells completed in the subject reservoir. Well test data interpretations are provided and discussed on selected tests where test data quality justified analysis. Quantitative data derived from the interpretations for use in developing the geologic model and conducting simulation history matches are presented.

To supplement existing fluid property measurements from a number of Paradox Basin small algal mound fields a series of new measurements designed to define interphase mass transfer between CO_2 and Anasazi crude were conducted. The results from these tests are presented and discussed. The development and validation of an equation of state is presented. Equation of state calibration procedures and a comparison of equation of state predictions versus experimental data are included. Fluid characterization related work is presented in Chapter 10.

To expand on existing rock property data a series of capillary pressure and relative permeability measurements using different core restoration procedures were completed. This set of data was

supplemented by wettability, mercury injection capillary pressure and rock compressibility measurements. The results from this work and interpretation of the data are given in Chapter 11.

Using the calibrated equation of state, multiple contact phase behavior calculations and one-dimensional compositional simulation studies, the CO_2–Anasazi crude interphase mass transfer process is analyzed and defined. Reservoir conditions required to develop miscibility between CO_2 and crude were determined and are presented in Chapter 12. In addition, two dimensional mechanistic studies are used to define and explain past and current Anasazi/Sahgzie reservoir processes.

Chapter 13 is used to document and explain the compositional reservoir simulator setup and initialization. This encompasses initial reservoir conditions and well/field operational constraints.

To develop a simulation model that could be used to predict reservoir performance under various operating conditions, a well and field level history match of production history from field discovery in late 1989 to December 31, 1996 was completed. The changes in reservoir description and fluid properties required to obtain a history match and a discussion of the need for these changes are presented in Chapter 14. A comparison of field production data with simulation results are provided.

Chapter 15 presents reservoir performance predictions for three different reservoir processes. These processes involve: continued primary depletion, CO_2 flooding and water flooding. The full field prediction for primary depletion further defines the three separate and distinct stages of depletion of the Anasazi/Sahgzie reservoir and identifies associated reserves. The influence of the number of injectors, injector location, injector well configuration, reservoir operating pressure and production gas processing on CO_2 flooding are examined. Both continuous CO_2 injection and CO_2 injection followed by reservoir blowdown are assessed. Ultimate recovery and gas injection requirements are defined. The potential of waterflooding and the influence of various operational constrains are presented and discussed. Production history and associated reservoir property maps are provided. The relative merits of CO_2 versus waterflooding are reviewed.

The costs of implementing a CO_2 flood and the economic performance of CO_2 flooding as applied to the Anasazi/Sahgzie reservoir are provided in Chapter 16 and Appendix A. The influence of leasing versus purchase of the main injector compressor and the economic impact of using a gas processing plant to separate CO_2 and hydrocarbons prior to re–injection of CO_2 are assessed. The benefits of DOE cost sharing are illustrated and the influence of different equipment/facilities installation options are assessed from an economic performance perspective.

Chapter 17 and 18 present conclusions and recommendations based on the work and results of the subject project.

3. ANASAZI FIELD DEVELOPMENT AND GEOLOGICAL REVIEW

The Desert Creek (Middle Pennsylvanian) carbonate mound build–up of the Anasazi field was originally identified as a seismic amplitude and interval–thickening anomaly on two–dimensional seismic surveys, situated 1 1/2 miles west–southwest of the White Mesa Unit, Aneth field in southeastern San Juan County, Utah (Figure 3–1). The first well drilled in what is now the Anasazi field was the Chuska (now Harken Energy) Sahgzie #1 (SE1/4,NE1/4,Sec.5,T42S,R24E,Salt Lake Base Line Survey), completed in November of 1989 in what was then thought to be a separate carbonate build–up immediately adjacent to the main Anasazi mound on the northeast (Figure 3–2). This well penetrated the entire Desert Creek mound and has been in production for the past eight years. Since that time, three additional wells have been drilled in the main mound build–up area of the Anasazi field. The Anasazi #1 was completed in the main mound build–up area in January, 1990 and since has proved to be the best producer in the field. The Anasazi #5L–3, located about 1060 feet (323 m) to the southeast of Anasazi #1 (Figure 3–2), was completed as an oil and gas producer a year later, in March, 1991. Finally, the Anasazi #6H–1 was drilled in June 1995 near the western end of the Anasazi build–up. This well proved to be a poor producer, and examination of the core revealed that the well missed the mound itself, penetrating instead an equivalent section of tight, largely cemented mound–front bioclastic debris.

As delineated by seismic and drilling, the Anasazi field is a lenticular, lobate carbonate mound trending west–northwest and measuring 0.9 miles (1.5 km) long and between about 2,000 and 3,000 feet (600–900 m) wide (Figure 3–2). It is situated on the eastern flank of the Desert Creek Anticline, with an east–northeasterly dip of about 0.7 degrees. The Anasazi #1 has a thick, well–developed Desert Creek carbonate section and illustrates the stratigraphy typical in the field (Figure 3–3). The Desert Creek in this well is 155 feet (47.2 m) thick, comprised of an upper 22–foot (6.7 m) thick bedded anhydrite, underlain by 133 feet (40.5 m) of predominantly carbonate, interspersed with scattered, thin, dark, laminated shales. These carbonates exhibit considerable heterogeneity, but are easily differentiated into three superimposed, lithically distinctive intervals representing the three major phases of Desert Creek mound–building at Anasazi.

At the top of the carbonate section, immediately beneath the capping anhydrite, is a 69–foot (21 m) sequence of mixed thin to medium–bedded dolomites and minor limestones. A variety of preserved carbonate textures are present (mudstones, packstones/wackestones, and grainstones) in heterogeneous bedding sequences, but nevertheless exhibiting abundant evidence of shallow restricted marine deposition and penecontemporaneous dolomitization, followed by selective early phreatic diagenesis, resulting in a closely associated mixture of enhanced porosity and both carbonate and anhydrite cementation. This sequence is termed the "Supramound Interval", and is easily recognized throughout the field. It represents the later stages of mound development, after the mounds were fully established but before they were entirely inundated and submerged during deposition of the overlying anhydrite. A variety of shallow, fluctuating, partially restricted marine microenvironments characterized Supramound deposition and alteration, which accounts for the heterogeneous nature of the lithology and reservoir properties in this interval. Although porosity averages about 15.5% in the Anasazi #1 Supramound Interval, in the cores and logs, porosity ranges from < 2% to over 24 %, and permeability between 0.1 md. and nearly 50 md. This interval exhibits the largest average porosity and originally contained most of the oil in the Anasazi field.

Immediately below the Supramound Interval in the Anasazi #1 well lies a 40–foot (12.2 m) thick phylloid algal limestone representing the major mound–building period of build–up development

and termed the "Mound Interval". Lithically, this limestone is more homogeneous than the overlying Supramound dolomites, varying from cement–rich to mud–rich bafflestone, with local porosities varying between 2% and 11% (average 7% in Anasazi #1) and permeabilities up to several darcies (averaging 150–250 md.). The pore system in these mound–building limestones is largely associated with the algal remains themselves, chiefly occurring as either pore space beneath the fronds sheltered from primary lime–mud sedimentation, or as secondary moldic porosity left by dissolved frond structures. Associated with the shelter porosity are local systems of collapse microfractures produced during compaction, which also contribute to the excellent permeability in this interval. Although both the Mound and Supramound Intervals are perforated in all three producing Anasazi wells, most of the Anasazi oil production has been attributed to the highly permeable Mound Interval limestones, a conclusion borne out by the simulation studies reported herein (see below, Chapter 15).

The lowest 24 feet (7.3 m) of Desert Creek carbonates in Anasazi #1 are comprised of regularly interbedded dolomitized carbonate mudstones and wackestones, carbonaceous crinoidal lime mudstones, and several feet of anhydrite–plugged phylloid algal limestone. This is the "Platform Interval", a generally flat substrate upon which the lowermost mound–building phylloid algal colonies were able to firmly established themselves. The isolated, cemented algal limestone developed in the Platform Interval of the Anasazi #1 well is an example of an early failed attempt to establish such a colony. The Platform limestones and dolomites are much tighter than the overlying intervals, with average porosities of 2–4% and permeabilities generally below 2 md. This is consistent with the properties of this interval reportedly encountered in the nearby Aneth field[3–2]. Although the Platform Interval was perforated in the Anasazi #5L–3 well, its contribution to overall Anasazi oil and gas production is inferred to be minimal.

The informal four–fold subdivision of the Desert Creek zone described above is present in all four Anasazi wells. The Desert Creek is underlain by the highly carbonaceous, dolomite–bearing Chimney Rock shale, which is considered the proximal source for Desert Creek hydrocarbons. Above the Desert Creek lies the 20–30 foot (6–9 m) anhydrite–bearing Gothic shale. Together, the upper Desert Creek anhydrite and Gothic shale form an effective seal over the Anasazi reservoir. Depositionally, both the Gothic and Chimney Rock shales represent sea–level highstand tracts, with the intervening Desert Creek carbonates laid down during periods of lower, more restricted marine incursion over the carbonate platform.

The Anasazi reservoir comprises the Mound and Supramound Intervals over the mound build–up area (Figure 3–2), ranging from 50 to 110 feet (15.25 to 33.5 m) thick and covering an area of 271 acres (109.7 ha). Surrounding the mound build–up area is the off–mound area, containing tight interbedded crinoidal lime mudstones, partially dolomitized mudstones, and wackestones, with isolated, locally restricted grainstones derived from the adjacent mound area. These grainstones may be porous or anhydrite–cemented, the latter being particularly prevalent on the northeast side of the mound area, between the Anasazi build–up and the nearby Aneth platform[3–2]. Desert Creek thickness in the off–mound area averages 110 feet (33.5 m), including 40–45 feet (12.2–13.7 m) in the section equivalent to the Mound and Supramound Intervals comprising the Anasazi reservoir.

Historical production figures for the Anasazi field and forecasts for future recovery under several different exploitation options are detailed below, in Chapters 8 and 15. An excellent supplementary synopsis of the Anasazi field can be found in reference (3–3).

4. DATA REVIEW AND RESERVOIR DESCRIPTION

The terms "reservoir description" and "reservoir characterization" commonly are used interchangeably in the literature. However, we find it useful to distinguish between them, depending on the spatial scales represented by the constituent measured data and confidence in the corresponding quantitative representation. Herein, "Reservoir Description" refers to the process of assembling a quantitative representation of the reservoir wherever "hard" (measured) data are available to document actual reservoir properties. Generally, such data are available only at the well locations. Reservoir Description thus requires no interpolation or other procedure (other than possible averaging) to generate estimates of reservoir properties away from the observed sampled data points.

Although other quantitative data usually are available (e.g. seismic, well test or production data), these commonly measured reservoir attributes at substantially larger spatial scales than that represented by a single grid cell in the reservoir model. Thus, although such data can be used to *constrain* the aggregate properties over larger reservoir volumes between the wells, they cannot be used to *assign* (or *condition*) the properties of individual grid blocks.

On the other hand, "Reservoir Characterization" comprises the procedures for generating estimates of reservoir properties throughout most of the reservoir volume, in all regions not directly sampled (i.e. away from the wells). Seismic, well test and other data, along with geological interpretations and information from analogous subsurface reservoirs and outcrops, if available, provide the *constraints* governing all characterized properties of the subject reservoir, however they are generated.

This Chapter describes the sources of data used as conditioning and constraining information in describing and characterizing the Anasazi reservoir, and the procedures used to develop the conditioning data at the well bores. Methods for determining the quantitative constraints used in characterization are discussed in Chapters 5 and 6.

4.1. Well Data

Conditioning data at the wells include well logs, core data and lithostratigraphic information from core descriptions. All four Anasazi wells were logged using standard open–hole combination tools: dual laterolog/micro–spherically focused logs, borehole–corrected sonic logs, and compensated neutron porosity/lithodensity logs. In addition, micrologs were run separately in the Anasazi #5L–3 and 6H–1 wells. The Anasazi #6H–1 was logged by Haliburton, the other three by Schlumberger. The log–based stratigraphic tops of the Desert Creek interval are given in Table 4–1.

4.1.1. Well Log Data

To facilitate comparison of the vertical profiles of lithology and porosity between the logs and cores in the three cored wells (Anasazi #1, Anasazi #5L–3, Anasazi 6H–1), lithologic logs were computed from the log data in the Desert Creek carbonate interval for each well (Figures 4–1, 4–2, 4–3, 4–4). Lithologies were computed as relative proportions of the three dominant minerals (calcite, dolomite, anhydrite) using the standard triangular field on the lithodensity rho_{maa} vs. U_{maa} crossplot. Log porosity was computed from the neutron–density crossplot and saturations from the porosity and deep resistivity using the standard Archie equation for clean formations, adjusted for invasion in the highly permeable Mound Interval limestones. These lithology log plots thus contain five

components: limestone, dolomite, anhydrite, oil and water. A number of notable features of Anasazi reservoir are apparent on these logplots.

1. The predominance of dolomite in the Supramound and Platform intervals, and limestone in the Mound Interval is consistent in all four wells.

2. At the top of the Mound Interval, the algal limestones in all three wells situated within the Mound Area (Anasazi #1, Anasazi #5L–3, Sahgzie #1) are plugged by anhydrite (Figures 4–1, 4–2, 4–3; Table 4–2). The Anasazi #6H–1 contains cemented limestone breccia and generally tight mound–fringe dolomites in the Mound Interval (Figure 4–4), with the exception of one six–foot (1.8 m.) porous but tight interval with high water saturation near the top of the dolomite (Table 4–2). The anhydrite–plugged limestone at the top of the Mound Interval is missing in the Anasazi #6H–1.

3. Water saturations in all four Anasazi wells are generally highest in the non– productive Platform Interval (Table 4–2). For the most part, this is associated with the tight, microcrystalline porosity in the fine–grained limestones and dolomitized limemuds comprising this interval. Water saturation in most of the Desert Creek carbonates is at irreducible, which is consistent with the reported oil–water contact at Aneth field of –960 feet (–293 m.) subsea, below the the lowest encountered Desert Creek at Anasazi field, at –925 feet (–282 m.) subsea (Table 4–1). Average water saturations computed from logs in the Mound and Supramound Intervals (13% and 9%, respectively) roughly agree with the values obtained from the oil–water capillary pressure endpoints computed from lab measurements (Chapter 11).

4. In two of the Mound Area wells, the average porosity in the Supramound Interval of the reservoir (14%) is 50% greater than in the Mound Interval (9%; Figures 4–1, 4–2; Table 4–2). In the Sahgzie #1, most of the lower half of the Supramound Interval is plugged with anhydrite (Figure 4–3), which could severely impact the drainage of hydrocarbons into the permeable, more productive limestones of the underlying Mound Interval. Although there is no direct geoscience evidence of the areal extent of this anhydrite plugging, the results of history matching the primary production in the Sahgzie build–up area demonstrate that the Supramound Interval is at least partially plugged throughout the northwestern flank of the Anasazi reservoir (see below, Chapter 14). This is consistent with prior studies which report extensive anhydrite plugging in stratigraphically equivalent washover fans on the southwestern flank of Aneth field[4–1,4–2], adjacent to the Sahgzie build–up portion of the Anasazi reservoir.

5. Although porosity in the Supramound Interval of Anasazi #6H–1 averages 10% and oil saturation is 84% (Figure 4–4; Table 4–2), reservoir properties in the underlying cemented mound–front breccias are poor (particularly permeability), which in the other productive mound wells can average 150–200 md (Table 4–1; Chapter 9). Thus, although the Supramound Interval in the vicinity of Anasazi #6H–1 contains significant hydrocarbon volume, production is poor because of the low permeability in the mound limestone.

6. Most of the stratigraphic tops reported in Table 4–1 are annotated on the lithologic logs. Generally, the dominant lithology changes from the dolomites of the Platform Interval

to Mound Interval limestone to Supramound Interval dolomites at these contacts in the three mound area wells (Figures 4–1, 4–2, 4–3). The base of the Mound Interval in the Anasazi #1 well, however, is picked near the middle of the 15–foot (4.6 m.) dolomite just below the main phylloid algal limestone (Figure 4–1). This pick is based on identification of a stratigraphically–equivalent flooding surface represented by a two–inch dark gray laminated shale (see below, Core Interpretation) which can be correlated among all four Anasazi wells and even up onto the Aneth platform[4–1]. Thus, during the earliest part of the mound–building period at Anasazi #5L–3 (Figure 4–2), platform deposition continued at Anasazi #1 and continued for some time thereafter, until the northward–spreading phylloid algal community reached that location. Indication of this thin shale break can be seen in the gamma ray curves in both wells (Figures 4–1, 4–2).

7. Finally, in the middle of the Platform Interval at the Anasazi #1 well occurs a 15–foot (4.6 m.) anhydrite–plugged limestone (Figure 4–1). This represents an early failed attempt by phylloid algae to establish a mound, which was subsequently drowned and cemented with anhydrite before being covered by typical platform dolomites.

Based on core description (see below), it was determined that the smallest effective thickness of carbonates with similar reservoir properties was 2–2.5 feet (0.6–0.75 m.). An equal–thickness layering design for the reservoir characterization grid model of 50 layers was established for the Anasazi reservoir, 20 in the Mound Interval and 30 in the Supramound Interval. Comparison of porosities between log and core data (Table 4–2) show sufficient consistency to warrant use of the log data as the basis for conditioning data in the model. The porosity assigned to each layer in the model in the four conditioning grid blocks, each containing one well, was the average of the effective porosity computed from the logs over the layer. These porosity data were held constant throughout the entire reservoir characterization and modeling procedure. Because water saturations were all irreducible, single saturation values derived from the relative permeability curve end points were utilized for the Supramound dolomites (8.4%) and mound limestone (11.55%) respectively.

4.1.2. Core Data

Whole cores were cut vertically through the Anasazi reservoir in three wells, Anasazi #1, Anasazi #5L–3 and Anasazi #6H–1. Conventional core analysis was carried out on the Anasazi #1 and Anasazi #5L–3 cores[4–3,4–4]; additional conventional analysis on selected plugs from these whole cores also was performed, plus plugs from the Anasazi #6H–1 core[4–5]. Sidewall cores were cut in the Sahgzie #1 well and analyzed for porosity and permeability[4–6].

Average values of core porosity and horizontal permeability are given in Table 4–2 for each interval in the mound area wells. These data show the higher porosity typical of the Supramound Interval and higher permeability exhibited by the Mound Interval limestones. In addition to providing a sample of average and variation (by well, and vertically in each well) for use in developing modeling constraints, these core data also provide a means for generating estimates of vertical and horizontal permeability.

4.1.3. Procedures for Estimating Permeability

Although there exist a number of standard algorithms for estimating permeability from wire–line log data[e.g.4–7,4–9,4–9], in the absence of new and not yet standard logs specifically intended to

measure permeability (e.g. the nuclear magnetic resonance log, or NML), only methods developed for those (largely clastic) reservoirs retaining the original depositional fabric are suitable for widespread application. Because of the high degree of pore–system heterogeneity in dolomitized, cemented, leached or otherwise altered carbonate reservoirs, studies of log responses to permeability in such reservoirs are generally applicable only to the specific reservoirs for which they were designed[4–10], despite some recent claims to the contrary[4–11]. In the absence of NML or similar log data, and with few well data, a simple approach was adopted for estimating lateral and vertical permeability from logs.

First, since not all conventional core analyses included two horizontal permeability measurements ($K_{h(max)}$, $K_{h(90)}$), in those data sets where both were reported, there was no systematic relationship and the effective range of the (log $K_{h(90)}$/log $K_{h(max)}$) ratio was relatively narrow (mean = 0.91; standard deviation = 0.43), an isotropic horizontal permeability was assumed throughout the Anasazi reservoir.

Second, scatterplots of log K_h vs. porosity from core data in the Mound and Supramound Intervals, respectively (Figures 4–5, 4–6) were used to define a transfer function from porosity to log K_h. Given a block porosity from the geostatistical modeling, horizontal permeability was computed as the predicted (expected) value from regression, plus a randomized term obtained as the product of the standard error of estimate for the expected value of log K_h and a number randomly selected from a Normal (Gassuian) distribution with mean = 0, standard deviation = 1. Geometric averages of these horizontal permeabilities in the Mound and Supramound Intervals over the Anasazi Mound Area (183 md and 2.6 md, respectively) are comparable to the results obtained from well tests (see below, Chapter 9).

Third, vertical permeability was measured only on the whole cores from the Anasazi #5L–3 well. Thus, only these data were available for estimating the K_v/K_h ratio from cores. Nevertheless, scatterplots of log K_v vs. log K_h for core from the Mound and Supramound Intervals, respectively (Figures 4–7, 4–8), demonstrate a clear relationship, with a K_v/K_h ratio averaging somewhat above or below 1.0, depending on the stratigraphic interval and the magnitude of K_h. A similar procedure to that described above for estimating log K_h from porosity was utilized, in turn, to obtain log K_v from log K_h. The resulting block log K_v/log K_h ratios have means and standard deviations of (0.96, 0.13) and (0.42, 0.21), for the Mound and Supramound Intervals, respectively. The Supramound ratio was later reduced to 0.2, based on flow simulation history match results (see below, Chapter 14), still not unreasonable, given the dispersion of the Supramound core measurements (Figure 4–8).

4.1.4. Selection of Core Samples for SCAL Measurements

Core and plug samples for obtaining laboratory measurements of relative permeability and rock compressibility were selected by an iterative process of high–grading the reservoir quality inferred from previous conventional core analysis and CAT scans. First, the previous conventional core data were consulted to determine which cored intervals in the Mound and Supramound Intervals represented typical reservoir quality. This survey yielded two short lengths of core, from measured depths of 5690–5693 feet (1734–1735 m) in the Supramound Interval of the Anasazi #6H–1 well, and 5646–5648.5 feet (1721–1722 m) in the Mound Interval of the Anasazi #1 well. Transverse CAT scan images of these 2.5–3–foot (.75–1 m) lengths of core were obtained at 3–inch (7.6 cm) intervals. These images for the Anasazi #1 core sample are shown in Figure 4–9. The color scale

represents bulk density, with yellow and red depicting high density (low porosity) and blues–greens indicating lower density (higher porosity). Since the plugs were cut perpendicular to the core axis, these scans are excellent indicators of horizontally–connected pore space, parallel to the plug axes. For the Mound Interval limestone relative permeability work, radial Section #5 (Figure 4–9) at 5647.4 feet (1721 m) measured depth was chosen as the plug sample location; for the rock compressibility work, a continuous one–foot (0.3 m) interval (5647.5–5648.5 feet; 1721 m) was selected. Computed log porosity for this interval is 12–14%, water saturation is 13.9–16% and horizontal permeability (whole core) is 522 md.

For the Supramound Interval, the following procedure was followed in selecting plug points for laboratory measurement of relative permeability:

1. Continuous core from the entire Supramound Interval was CAT scanned for lithologic consistency, to ensure that the oil/water and gas/oil relative permeability measurements were based on comparable pore systems. Selection of three cores was made from examination of six large–format multiple–image black and white films of whole core screening CAT scans of the entire length of the core from this interval.

2. Three transverse color CAT scans were obtained through each of the three selected core intervals, chosen as the three most homogeneous zones from the low–resolution screening CAT scan images. Using these images, one (core box #12) was chosen as the most homogeneous low–density (high porosity) interval.

3. A more detailed color CAT scan survey of the selected interval revealed that the upper half exhibited the most consistency in pore system geometry. These images (0 through 5, Figure 4–10) were taken at 1.5–inch (3.8 cm) intervals, top–to–bottom from 5691–5692 feet (1735 m) measured depth. Transverse plugs were taken from this section of core at positions represented by images 0, 2, 3 and 5.

4. Reflected light photographs of a) the whole 10–inch core section (Figure 4–11) and b) opposite sides of each of the four plugs (Figures 4–12, 4–13) show something of the pore– system heterogeneity in these Supramound dolomites. These photos illustrate the range of variations in reservoir fabric particularly well. Easily identifiable features include anhydrite–filled vugs, both micro–vuggy and intercrystalline porosity, patches of bitumen–filled pores and patches of nonporous carbonate mudstone.

5. A final set of color CAT scans (Figure 4–14) of two mutually perpendicular longitudinal (axial) sections of each of the four plugs to assess heterogeneity and select the most consistent for running porosity and standard (air) permeability as a final step before selecting the two half–plugs to be used in the restored and unrestored core relative permeability measurements (see below, Chapter 11).

6. The right half of plug 1 (5691.2 feet) and left half of plug 4 (5691.8 feet) were selected for preliminary lab screening. Also, porosity and permeability measurements were carried out on plug 2 (5691.5 feet), which was then transversely cut in half and the measurements repeated on each half, to assess whole plug heterogeneity. The plug 1 and plug 4 samples were finally selected for the SCAL relative permeability analysis. An additional half–plug (plug 1, left half) was chosen for conducting the "native state" relative permeability measurements as a benchmark comparison with the two

cleaned–plug (restored and unrestored) sets of lab data. Details of the lab procedures and results are covered below, in Chapter 11.

The sample for Supramound rock compressibility measurements was selected from the same core at 5691.2–5692.5 feet (1735 m) measured depth. Laboratory procedures and results of the rock compressibility analysis are detailed in Chapter 11. Porosity in the Supramound core used in the relative permeability and rock compressibility measurements averaged 11.9–14.6%, water saturation was 9.8–10.1% and horizontal permeability 3.8–30.0 millidarcies.

4.1.5. Core Interpretation

A total of 368 feet (112 m) of core was cut from three wells (Anasazi #1, Anasazi #5L–3, Anasazi #6H–1) in the Anasazi field. This core was photographed[4–12], described in detail and carbonate sedimentology and stratigraphy interpreted. These interpretations are summarized in the correlated core sections shown in Figure 4–15. As indicated in the figure, the three major intervals comprising the Desert Creek carbonate section are readily identifiable in the core. Lithologically, both the Platform and Supramound Intervals are mixed limestones and dolomites, while the Mound Interval is largely limestone in the two cored mound wells (Anasazi #1, Anasazi #5L–3). The reservoir is distinctly differentiated lithologically into the mud–rich phylloid algal limestones of the Mound Interval, overlain by the dominant dolomites and subordinate limestones of the Supramound Interval. Interspersed within this largely carbonate section are thin 0.5–3 inch (1–7.5 cm) dark gray laminated shales. Many of these isolated shales are associated with evidence of subaerial exposure in the underlying carbonates and occur at approximately the same stratigraphic position throughout the mound. They are interpreted to represent flooding surfaces, and thus can be correlated between the cored wells (Figure 4–15). Generally, these shales conform to the carbonate lithostratigraphy, with the major exception of the shale corresponding to flooding surface 1 (fs1, Figure 4–15) in the Anasazi #1 well, which occurs near the middle of a 16–foot (5 m) dolomite section immediately beneath the main algal limestone build–up. Although interpretation of this shale as representing fs1 does not accord with its occurrence just below the Mound Interval limestone in the Anasazi #5L–3, this placement maintains stratigraphic regularity of the Platform–Mound intervals across the mound (Figure 4–15) and is considered a chrono–stratigraphic marker. Although there is abundant evidence from well tests, production history and flow simulation results that these flooding surface shales do not represent continuously–developed fluid transmissibility barriers, most of the eight recognized markers in the Anasazi reservoir are found in all three wells, and they almost certainly had some impact on communication. Thus, for purposes of reservoir modeling, the base of the Mound Interval in Anasazi #1 is placed at fs1, ten feet below the base of the algal limestones.

4.1.6. Carbonate Lithotypes

Although porosity and permeability vary throughout the Mound Interval phylloid algal limestones, they are relatively homogeneous lithologically, with no sharp distinctive lithic boundaries which differentiate subintervals of contrasting reservoir properties. The reverse is true, however, for the interbedded dolomites and limestones of the Supramound Interval. These are heterolithic, with sharply differing sets of reservoir properties. They represent at least five successive stages of exposure and subsequent re–flooding of the remnant mound build–up areas, apparently continuing long after active mound–building by phylloid algae had ceased (Figure 4–15). A great variety of carbonate lithologies is present in these Supramound cores, including dolomitized and unaltered limestones, some tightly cemented or leached by phreatic circulation, or plugged with marine

(chiefly anhydrite) cements. Although many subtle variations in the original depositional texture and subsequent complex history of early diagenetic alteration have been interpreted, it is convenient to subdivide these carbonates into lithotype based on a) original texture, as closely as it can be determined, and b) the dominant mode of diagenetic alteration, if any. This classification yields a set of ten lithotypes (including the mound–building limestones) that are reasonably consistent with the original sedimentological interpretations. These lithotypes can be implemented as a basis for architecturally apportioning this complex reservoir volume into geologically significant subunits, as a practical means for representing the major differences in reservoir properties known to exist at Anasazi.

The ten lithotypes identified from core and thin section examination, together with average thickness, porosity, horizontal permeability and estimated reservoir volume proportion for each are listed in Table 4–3. These data were obtained from the Anasazi logs and cores. The volume proportion includes both on–mound and the adjacent off–mound areas which comprise the region included in the reservoir model (see below, Figure 5–1). These areas encompass 271 acres (1.1 million m^2) and 109 acres (0.44 million m^2), respectively. Approximate volume ratios for the uncored off–mound areas were obtained from well logs of three off–mound dry holes previously drilled nearby (Figure 3–2). This accounts for the large proportion of tight carbonate mudstone in Table 4–3. Photomicrographs illustrating typical pore geometries and whole core photographs of representative examples of the ten Anasazi lithotypes are depicted in Figures 4–16 through 4–20.

In addition to distinctly different lithologies, reservoir properties and pore geometries, these ten lithotypes are associated with specific depositional microenvironments. A considerable amount of geological information about these environments has been accumulated over the past 10 years, highlighting their differences in depositional processes and carbonate sediments, describing the normal placement of each facies in the mound and post–mound architecture, and detailing the effects of the various diagenetic processes which typically resulted in substantially altered lithic fabrics and reservoir properties[4–13,4–14]. Detailed descriptions and interpretations of the three Anasazi cores have been developed by carbonate sedimentologists and incorporated into the lithotype classification system, and similar interpretations from stratigraphically equivalent core at Aneth field are available in the literature[4–1]. The ten carbonate lithotypes present in the Anasazi reservoir are briefly summarized as follows:

1. **Tight Mudstone:** carbonate mudrocks (micrites), including limestones and partially to completely dolomitized mudstones (Figure 4–16a,b) with little or no preserved porosity; permeability less than 0.5 md and irreducible water saturation 80–100%. Tight mudstones comprise almost 25% of the total bulk volume of the reservoir model and more than 60% of the off–mound volume. Less than 5% of the Mound Interval and 20% of the Supramound Interval in the Mound Area, however, are tight mudstone. Environments represented include off–mound deep, quiet water to protected lagoonal areas in the Supramound Interval.

2. **Dolomitized Mudstone:** partially or pervasively dolomitized mudrocks in which intercrystalline porosity is associated largely with volume reduction during dolomitization (Figure 4–16c,d). Porosity can range up to 11% and permeability is generally less than 10 md. Oil saturation can be as high as 70%, but is normally 30–50%. This lithotype is most common in the Supramound Interval of the mound build–up area, although it also is common in off–mound aprons adjacent to the mound and mound–front areas. Dolomitized mudstones are much less common than tight mudstones, comprising

just under 6% of the total Desert Creek reservoir volume. In some instances, pervasively dolomitized packstones or wackestones, in which the original texture has been completely obliterated, may be mistaken for dolomitized mudstones.

3. **Porous Mudstone:** fine–grained limestone and/or dolomite which has been partially leached to produce vuggy or moldic porosity (Figure 4–17a,b). Average porosity and permeability are both enhanced somewhat from the precursor tight limestone or dolomite (Table 4–3). Porous mudstones are more common in the Supramound Interval of the mound area than in off–mound areas, contributing about 20% of the total Supramound volume. These porous mudrocks have been subjected to phreatic leaching and often contain secondary pore–lining calcite cements. In other cases, the leached pores may be completely filled with calcite or even anhydrite cement. Such cemented mudstones are classified with the tight or dolomitized mudstones, depending on the matrix.

4. **Tight Packstone/Wackestone:** these mixed skeletal–mudrocks are combined because there is no clear lithologic distinction between them in the Anasazi reservoir, and because they generally exhibit similar reservoir properties (Figure 4–17c,d). Differentiation between packstone and wackestone is strictly a function of the relative proportions of mud matrix and skeletal material, which at Anasazi appear to have been primarily a function of local current winnowing, resulting in a thorough admixture of the two. Because clear–cut differences in porosity and permeability are also lacking, they are combined in a single reservoir lithotype for purposes of reservoir description and characterization. Tight packstones/wackestones are generally limestone, although some may be partially dolomitized. Some also have been leached and subsequently re–cemented. Reservoir properties are generally similar to the tight mudstones, but the distribution of these lithotypes is strikingly different. Tight packstones/wackestones are primarily restricted to the Supramound Interval of the mound area, although they also constitute a much smaller proportion of the off–mound areas. Rocks of this lithotype contribute little to the hydrocarbon pore volume of the Anasazi reservoir, and may serve as partial barriers to communication in some areas.

5. **Porous Packstone/Wackestone:** this mixed lithotype bears a similar relation to the tight packstones/wackestones as do the porous mudstones to tight mudstones (Figure 4–18a,b). Vuggy and moldic porosity, primarily produced by phreatic leaching, predominate. Like the tight packstones/wackestones, this lithotype is most commonly found in the Supramound Interval of the mound area, although log responses in some off–mound wells indicate its scattered presence there also. Porosity and permeability are slightly greater than in the porous mudstones (Table 4–3).

6. **Porous Grainstone:** skeletal grainstones are a common lithic constituent of the Supramound Interval of the mound area, and also occur in washover fans extending out from the mound into adjacent off–mound areas (Figure 4–18c,d). These grainstones are primarily limestone, of which porous and permeable, poorly cemented textures comprise about half the total. Porosity averages 15%, ranging up to 25%, making this lithotype the most important single contributor to the total Anasazi hydrocarbon pore volume. In some areas, porous grainstones occur as tidal channel deposits, in others as washover fans, and elsewhere as thin biostromes on top of the mounds. Water saturations in these

porous grainstones are low, generally less than 15%. This lithotype contributes substantially to reservoir communication in the Supramound Interval, within and between individual mound build–up areas (Anasazi, Sahgzie) in the mound area, and also between the mound and off–mound areas.

7. **Tight Grainstone:** similar to Lithotype 6, except for the pervasive secondary cementation and consequently poor reservoir properties (Figure 4–19a,b). Secondary sparry calcite and anhydrite cementation occurs throughout the mound and off–mound areas, but seems to be most prevalent in the northern–northeastern parts of the reservoir, adjacent to similar coeval deposits on the southwestern fringes of nearby Aneth field[4–2], where anhydrite can entirely plug at least half the Supramound Interval (Figure 4–3). Reservoir properties of this lithotype are generally very poor, in some instances forming barriers to reservoir communication. Tight grainstones constitute about half of all Anasazi grainstones.

8. **Tubular Tempestite:** this exotic but distinctive Lithotype is found only in the Supramound Interval of the Anasazi #6H–1 core, but is inferred to be present in scattered patches over the mound area and adjacent off–mound areas as well. Tubular tempestites are characterized by a patchy mosaic of fine and coarse–grained carbonate matrix, each with a different set of reservoir properties, resulting in distinctly bimodal distributions of porosity and permeability (Figure 4–19c,d). These bimodal patches are a few square inches (cm) in cross–sectional area and are interpreted as calianassid shrimp burrows that have been injected with comminuted carbonate debris, whipped up by storm–driven turbulence[4–15]. Tubular tempestites exhibit a mixture of effective properties, averaging 9% porosity and an estimated 8 md effective permeability. They are distinguished as a separate lithotype because their genesis indicates a degree of continuity with a proximal source of the coarse–grained, permeable injecta, and also for the main lithotype units themselves. Thus, tubular tempestites are considered to be significant contributors to reservoir communication in the Supramound Interval and with the adjacent off–mound portions of the Anasazi reservoir.

9. **Phylloid Algal Limestone:** this lithotype is the primary constituent of the Mound Interval in the build–up areas of the reservoir (Figure 4–20a,b). Aside from some anhydrite cementation at the top of the Mound Interval and some scattered pore lining and plugging by anhydrite and sparry calcite elsewhere, the original pore system remains open. Average porosity is only fair (10%), but effective permeability is very high, up to several darcies locally and averaging 100–200 md. This lithotype represents the primary mound–building agent of the reservoir and has been altered very little since. Although the top of these limestones is cemented by anhydrite in the three Anasazi mound–area wells, there is abundant evidence from reservoir behavior that this cemented zone is discontinuously developed across the mound, allowing hydrocarbon drainage from the Supramound Interval above down into these limestones, which furnish most of the Anasazi production, and also to provide pressure communication (see below, Chapters 8, 14).

10. **Mound–Front Breccia:** finally, the bioclastic mound–front breccia (Figure 4–20c,d) consists of disoriented, brecciated fragments of mound–edge lithotypes (primarily algal limestone), broken off the upper part of the mound face by wave action and transported

down–slope to rest as part of the debris apron fronting the mound core. At Anasazi field, this lithotype is found only in the Anasazi #6H–1 core, but also is described from a well penetrating a similar proximal off–mound area at nearby Mule field[4–16]. It is inferred that this lithotype is present along the mound front, adjacent to Lithotype 9, at other locations in the Anasazi field. Mound–front breccia is characteristically cemented, but locally can exhibit porosity up to 10% and permeabilities of nearly 50 md.

4.1.7. Lithotype Layering

Based on these lithotype definitions and thicknesses, the reservoir at each of the three cored Anasazi wells was layered, using the minimum lithotype thickness observed in core of about 2 feet (0.6 m) as a rough guide. Requirements of the final flow simulation model, as well as field observations and detailed sequence–stratigraphic work in the Desert Creek at nearby Aneth field[4–1,4–2], indicated that layers of equal thickness in both the Mound and Supramound Intervals would satisfy both requirements, and an equal–thickness 50–layer model was defined for the Anasazi reservoir, comprised of 20 layers in the Mound Interval and 30 layers in the Supramound Interval. Layer lithotype designations are summarized in Tables 4–4, 4–5 and 4–6. These layering data provided the conditioning "hard" data for the stochastic simulation models (Chapters 5, 6), and were unaltered during the modeling process.

4.2. Outcrop Analogue Studies of Reservoir Architecture

Because direct detailed information about lateral variation of lithotype and reservoir properties distributions in the Anasazi reservoir is lacking, and to provide information about the three–dimensional architecture of the various lithotype bodies identified from core, a field study of a carbonate mound outcrop analogue from the Ismay zone of the Paradox Formation was undertaken at nearby Wild Horse Canyon[4–17]. A photographic cross section of a typical carbonate mound taken along the San Juan River a few miles from the study area illustrates the three–dimensional geometry of these reservoir analogue buildups (Figure 4–22).

The carbonate mound exposed at Wild Horse Canyon (Figure 4–23) is considered a close analogue to the Anasazi reservoir, comprised of direct analogues to the Platform, Mound and Supramound intervals, and to the carbonate lithotypes identified from Anasazi core. The geometry of stratigraphic boundaries, vertical facies successions and lateral facies relationships within the outcropping buildup provided much of the primary information on the geometry of the internal architecture of these carbonate mound reservoirs (Table 4–7). These data, described in the field and subsequently assembled in debriefing discussions, provided the quantitative basis for generating the architectural components of the Anasazi reservoir characterization modeling (Chapter 6).

Because systematic samples for determining patterns of lateral variation of reservoir properties were unobtainable from the Wild Horse Canyon outcrop, data from similar outcrop studies and subsurface information from the Aneth reservoir reported in the literature[4–18] were utilized in establishing the overall pattern of lateral variation in these Desert Creek/Ismay carbonate mound complexes, and applied to the Anasazi reservoir.

4.3. Seismic Interpretation and Average Reservoir Porosity

Six good–quality two–dimensional seismic lines were shot across the Anasazi field. Seismic response of the non–mound Desert Creek interval in the surrounding area is generally uniform,

providing a background against which the anomalous Desert Creek character can be calibrated. The typical high–amplitude non–mound Desert Creek seismic event is generated by the large velocity contrast between the dense, high–velocity upper Desert Creek anhydrite and tight carbonates and the overlying low–velocity 30–foot Gothic Shale. Amplitude dimming is caused by thinning of the Gothic Shale and underlying anhydrite over the buildup, and by increased porosity development in the upper Desert Creek. This combined mound buildup and increased porosity effect can be exploited both to map the Anasazi reservoir and to estimate average porosity development in the upper Desert Creek. Both the architectural information and the average porosity indicator were used in developing the reservoir model.

The Desert Creek isolith map of the Anasazi/Sahgzie algal mound complex was generated by calibrating the isopach values of the wells in the area (mound and off–mound wells) to an Ismay–to–Desert Creek isochron map (Figure 4–24). Thinning in the Ismay–to–Desert Creek interval is a good indicator of mound buildup and provides the basis for mapping the geometry of the mound. The contours of the isochron map were used as guides for contouring the isopach values calculated from well logs, and were further modified while mapping the seismic character of the Desert Creek event and overlying Ismay/Gothic shale trough.

Mapping of the seismic character within the mound was based on two general features: the character of the Desert Creek event and the character of the overlying trough. Dimming and doublet development within the Desert Creek event have proven to be good mound indicators. Changes in the trough character of the overlying Gothic Shale, although less significant than those of Desert Creek event, also seem to indicate the presence and higher porosity of the mound reservoir. The red and blue coded color lines on the seismic base map (Figure 4–24) and the seismic cross section across the main Anasazi mound buildup (Figure 4–25) illustrate these two indicators of reservoir quality.

To measure average reservoir quality, the color–coded seismic interpretations were assigned numerical index values, weighted, added and rescaled to yield a numerical index with a range of (0–10). The original indices were (0,1,2,3,4) for the Desert Creek doublet character and (0,1,2,3) for the Gothic Shale trough character, where reservoir quality increases with magnitude of both indices. Proportional weights of (2/3,1/3) were applied to these two variables, respectively, the results added and this sum rescaled to (0,10) by applying the multiplying factor 2.7273 (=30/11). Thus, the **R**eservoir **Q**uality **I**ndex (RQI) was computed as

$$\text{RQI} = (30/11) \times (\text{Desert Creek doublet index} + \text{Gothic Shale trough index})$$

for each data point on all six seismic lines and mapped (Figure 4–26). The topology of this map away from the seismic control points was drawn to be consistent with the Desert Creek isolith map (Figure 4–24).

The RQI index was then converted into an estimate of average reservoir porosity using a deterministic transfer function anchored to the four Anasazi wells. First, average porosity of the entire Desert Creek reservoir (Mound + Supramound intervals) was computed from the density–neutron crossplot porosity curve for each of the four Anasazi wells. Second, based on average porosities in the off–mound wells, the average porosity of the poorest quality reservoir was determined to be 4%. Thus, at the minimum RQI=0, porosity=4%. For each well, then, a linear transfer function from RQI to average porosity can be defined as

$$\text{Average Porosity} = 0.04 + (B \times \text{RQI}),$$

where the constant "B" is determined separately for each well. The scatterplot in Figure 4–27 shows these four (porosity,RQI) point–pairs (one for each well) and the transfer function associated with each. To obtain a smooth estimate of the coefficient "B" between the wells, it was mapped using simple inverse–distance weighting (Figure 4–28). Using this map grid and the RQI map grid (Figure 4–26), then, the map grid of average reservoir porosity can be computed as:

$$\text{Average Porosity Map Grid} = 0.04 + (\text{“B” map grid x RQI map grid}),$$

which map is shown in Figure 4–29. In the reservoir characterization modeling, this map grid was used as a global constraint on both the areal distribution of average reservoir porosity and the total reservoir pore volume (Chapters 5,6).

5. RESERVOIR CHARACTERIZATION OVERVIEW

The significant heterogeneity exhibited by both the lithotypes and the reservoir property distributions at Anasazi field required design and development of a multistage procedure for honoring the conditioning well data while at the same time incorporating into the reservoir model the variation known to exist from outcrop analogues and seismic interpretations. This chapter outlines the procedures followed in generating the final characterization used in the flow simulations.

5.1. Gridding and Layering

The size and shape of the mound build–up area, the inferred areal extent of lithotype architectural bodies known to be present in the reservoir, and the constraints imposed by numerical modeling provided the framework for defining the areal grid for the Anasazi reservoir characterization and simulation model. This model consists of 30 rows and 50 columns of grid cells, each measuring 105 feet (32m) square (Figure 5–1). The 50x30 grid just spans the reservoir build–up, encompassing an area of 380 acres (154 ha). Thus, the grid system used in characterizing the Anasazi reservoir consists of 50 equal–thickness layers and a 50x30 areal grid, for a total of 75,000 cells representing an overall bulk volume of 57.8 million cubic feet (2.04×10^6 m^3). Based on detailed examination of the cores and log data, and field observations from the Lower Ismay outcrop analogues, it was determined that a 50 layer model would adequately capture the lithologic variability in both the Mound Core and Supramound Intervals. They were designed as continuous, equal–thickness layers, ranging from approximately one foot thick in the off–mound areas to slightly more than two feet in the thickest parts of the Anasazi mound build–up. Observed lithologic, porosity and permeability data from the four Anasazi wells were incorporated into the layering at the well locations. These "conditioning" data were fixed throughout the subsequent modeling process.

5.2. Architectural Modeling

The internal architecture of the reservoir was modeled between the wells using a marked point (Boolean) process for emplacement of the ten constituent lithotypes. This process was constrained by both the relative volumetric percentages of the various lithotypes observed in the wells and outcrops, and the total reservoir pore volume estimated from volumetrics based on the well and seismic data. At the areal scale of 105 foot square grid blocks, simple rectangular geometries sufficed to adequately represent the individual lithotype bodies, dimensions for which were described by triangular probability distributions developed from outcrop observations and presented in Table 4–7. Emplacement sequences were established (e.g. cementation/dissolution following emplacement of the unaltered lithotype) and the relative lithotype proportions varied stochastically according to the field observations. In the Mound Interval, the phylloid algal limestones were emplaced deterministically, corresponding to the seismic build–up isolith data (Figure 5–1). The initial lithotype emplacement procedure resulted in a model with greater stratigraphic continuity than the wells and outcrops warrant. This regular stratigraphy was subsequently modified during fitting of the porosity model. A total of 50 preliminary geostatistical models were generated using this procedure, for later sensitivity studies of the impact of reservoir continuity on production performance.

5.3. Porosity Modeling

The initial architectural model was modified by pairwise exchange of grid blocks to fit porosity constraints of both local spatial variation and overall (global) average porosity distribution derived from the seismic interpretation using a stochastic relaxation simulated annealing procedure. These exchanges were moderated by rules governing block interface continuity at both locations of the proposed exchange to ensure that although local architectural geometry could be changed to accommodate the fitting of the porosity data, the total number of discrete bodies for each lithotype originally emplaced was conserved. Horizontal and vertical permeability were estimated by transformation from porosity–permeability crossplots based on whole core measurements (see Chapter 4; Figures 4–5 through 4–8).

5.4. Vertical Scaling

Finally, because of computer flow simulation run time limitations, the number of layers in the model was reduced from 50 to 15. Sensitivity studies indicated that most of the variation in effective properties could be retained with careful scaling of porosity and permeability. Lithotypes were assigned to each of the 15–layer grid blocks according to the dominant lithotype in the corresponding 3.5 layers of the parent 50–layer geostatistical model. If no single lithotype predominated, the block was assigned to one of two new lithotype categories termed "poor quality" and "good quality" mixed lithologies. Porosity was volume–averaged for the 15–layer model, and effective permeability was computed by solution of the pressure equation using the VIP preprocessing module GRIDGENR. Details of the architectural and porosity modeling are discussed in Chapter 6; vertical upscaling is treated in Chapter 7.

6. RESERVOIR MODELING

As outlined in Chapter 5, developing a quantitative characterization of the Anasazi reservoir which honors the well data, yet incorporates the complex lithology and associated heterogeneities in reservoir properties known to exist between the wells requires successive application of two geostatistical procedures. The first (boolean emplacement) generated the reservoir architecture, based on lithotype geometries and distributions observed in outcrop. The second (simulated annealing) fit the spatial distribution of reservoir properties within that architecture to vertical and horizontal patterns observed in the wells and in outcrop, respectively. Details of these procedures are covered in this chapter.

6.1. Lithotype Emplacement

It is apparent from the variable sequences of lithotypes in the Supramound Interval of the three Anasazi cores (Tables 4–4, 4–5, 4–6) and the lack of continuity of these lithotypes between the wells (Figure 4–15) that the Supramound carbonates form a complex facies association[6–1,6–2,6–3]. Because much of the reservoir–quality carbonate in off–mound areas have been transported from the mound area, similar facies variations are found there also. From the Anasazi core data, each of these lithotypes has a characteristic porosity distribution (Table 4–7). Since these distributions show distinct differences within the various lithotypes, porosity cannot be modeled as a single continuous variable. Thus, the internal reservoir architecture comprising the spatial distribution of lithotype bodies must be developed first, and the reservoir properties subsequently modeled for the individual lithotype compartments.

Five broad types of information are required for architectural modeling using a boolean emplacement procedure. These constraints are:

1. lithotype body geometry: size, shape, orientation
2. bulk reservoir volume properties of each lithotype (summing to one)
3. total reservoir pore volume obtained from volumetrics, based on the RQI porosity (Figure 4–29) and reservoir isolith data (Figure 5–1)
4. lithotype associations and preferred positions
5. sequences of lithotype emplacement.

Because the volumetric proportions of the various lithotypes in the Mound and Supramound Intervals are entirely different (e.g. Lithotypes 9 and 10, the algal limestones and mound–front breccias, are found only in the Mound Interval), they were modeled separately. However, emplacement procedures for the two intervals are almost identical, except that in the Mound Interval, the 16,500 limestone blocks are defined deterministically before boolean emplacement begins, and the 1,575 mound front blocks stochastically emplaced last, after all the other lithotypes. A detailed list of the geometric rules and constraints governing boolean emplacement is given in Table 6–1.

6.1.1. Lithotype Geometry

Estimates for the minimum, maximum and dominant (modal) lengths of carbonate bodies for Lithotypes 2–8 were based on outcrop observations (see above, Chapter 4, Table 4–7). These data

were discretized into block areal dimensions (105 feet; 32 m) for simulation purposes. Lithotype body width and thickness are determined as functions of body length using the width/length and thickness/length ratios, rounded to the nearest block dimension. Orientation was specifically modeled only for the transported grainstones on the periphery of the mound area. In these locations, the length of the grainstone "apron" was placed perpendicular to the mound front. To ensure the reservoir continuity of transported grainstones between on–mound and off–mound areas observed in outcrop[6–2], peripheral off–mound grainstone aprons were connected to the mound by narrow channels or "necks", 1–2 block wide and 2–10 blocks long, depending on the length of the apron (Table 6–1).

6.1.2. Reservoir Volume

Based on the observed and reconstructed lithotype properties in the Anasazi wells and in outcrop, estimates were made of the most probable (modal) values of proportional reservoir volume for each of the ten lithotypes in the Anasazi reservoir (Table 4–7). Because these estimates are necessarily imprecise, a range of uncertainty for each volume property also was developed in consultation with the field participants and carbonate sedimentologists who studied the Ismay outcrop analogy [6–4].

However, this collection of ten univariate distributions of reservoir bulk volume proportion for the ten carbonate lithotypes cannot be used directly as a modeling constraint. The volume proportions obtained by randomly sampling each of these distributions independently would not sum to 100%. Rather, the joint distribution of all ten lithologies must be determined, any single sample from which gives a set of the ten volume fractions that will, by definition, sum to 1.0.

Although it is theoretically possible to derive this joint probability density function (jpdf) analytically, it is much easier to generate a result that, for modeling purposes, is just as precise using Monte Carlo simulation[6–5]. A computer program was written to generate two five–million point distributions for modeling, a ten–variate jpdf for lithotype proportions in the Mound Interval and an eight–variate jpdf for the Supramound Interval (which, of course, contains no algal limestone or mound–front breccia lithotype bodies). Bivariate marginal distributions from these multivariate jpdf's are illustrated in Figures 6–1, 6–2 and 6–3. Generally, the lithotypes comprising most of the reservoir volume (tight mudstones, packstones and grainstones) are negatively correlated among themselves (Figure 6–1), whereas the high quality lithotypes are less strongly intercorrelated (Figure 6–2), and low quality/high quality lithotypes are mutually independent (Figure 6–3). As part of the boolean model initialization procedure, a random sample was selected from the appropriate (Mound or Supramound) distribution. This fixed the volume for each lithotype in that stochastic realization, a constant honored throughout the boolean emplacement modeling procedure.

6.1.3. Boolean Modeling Procedure

Using the block volume data (Table 4–7), the lithotype bodies were emplaced following the same general procedure for both the Mound and Supramound Intervals, which were modeled separately. First, the lithotype bodies present in the four Anasazi wells were generated by drawing a random sample from the appropriate size/shape distribution (Table 4–7). Since tight mudstones constitute the greatest single volume proportion of all the lithotypes and tend to comprise relatively unstratified intervals throughout the off–mound areas, individual bodies of this lithotype were not emplaced. Rather, tight mudstone was defined as the "matrix" lithotype that remained after all the other lithotypes had been generated. Likewise, the massive algal limestones in the Mound Interval were

initially generated deterministically, as two (Anasazi, Sahgzie) mound build–ups, with stratigraphic position defined by the wells and areal geometry determined by the 78–foot (23.8 m) reservoir isolith (Figure 5–1). Geometric bodies for the other eight lithotypes were emplaced for each layer encountered in each well, covering the position of the well. All grid cells comprising these bodies were then deducted from the reservoir volume available for stochastic lithotype emplacement established previously by the jpdf Monte Carlo sample (see above).

After generation of the conditioning lithotype bodies, filling in the remaining reservoir architecture proceeded as follows:

1. The two remaining primary lithotypes (grainstone, packstone/wackestone) were emplaced first, in that order. Geometric shapes were generated by random selection from the triangular pdf's defined in Table 4–7 and emplaced according to detailed rules (Table 6–1). Bodies of a single lithotype were sequentially generated and emplaced until the corresponding bulk volume proportion (Table 4–7) was reached, before proceeding to the next lithotype.

2. Next, in the Supramound Interval and off–mound areas, the tubular tempestites were carved out of the remaining mudstone volume and truncated where they intersected previously defined packstone/wackestone or grainstone bodies. These storm–generated mixed lithology bodies were emplaced adjacent to previously generated, spatially segregated facies, according to the dimensions and rules in Tables 4–7 and 6–1, respectively.

3. Third, the secondary lithotypes (dolomitized mudstone, enhanced porosity mudstone, enhanced porosity packstone/wackestone, enhanced porosity grainstone) were emplaced as subsets of the primary lithotype bodies. That is, areas of dolomitized and enhanced porosity mudstone were emplaced within the remaining mudstone volume in the off–mound areas of both intervals, and in the mound area of the Supramound Interval. Likewise, enhanced porosity packstones/wackestones and enhanced porosity grainstones were carved out of their previously emplaced primary lithotype bodies, respectively. Again, geometries and placement rules are given in Tables 4–7 and 6–1.

4. Because the process of fitting effective porosity to the spatial distribution constraints required grid cell exchange and, to preserve the integrity of overall mound geometry, only a limited amount of exchange was allowed on the mound periphery, emplacement of the mound–front breccias in the Mound Interval was delayed until after the reservoir properties had been generated (see below). Then, mound–front breccias were emplaced along the outside margin of the algal limestone build–ups, to a maximum width of two blocks (210 feet; 64 m.), replacing whatever off–mound lithotypes previously occupied those positions. Only about 15% of the mound periphery was fronted by these blocks, which were preferentially placed in clusters rather than randomly scattered over the mound front (Table 6–1).

A total of 50 equally–probable stochastic realizations of lithotype distribution using this boolean emplacement process were generated for the Mound and Supramound Intervals, respectively. Typical examples from the realization ultimately selected for the final flow simulations are shown as areal grids and cross sections in Figures 6–5 through 6–10. A legend for all the lithotype displays is given in Figure 6–4. In this realization, Layer 1 at the top Supramound Interval, just beneath the

Desert Creek anhydrite, is chiefly mudstone, about half of which is dolomitized or enhanced porosity (Figure 6–5). Less than 20% of Layer 1 is good quality reservoir (enhanced porosity grainstones and tubular tempestites over the Sahgzie mound area). Although the boolean bodies were generated as simple (x,y) rectangles, bodies of the same lithotype were allowed to overlap, producing the somewhat irregular shapes. The areal grid shown in Figure 6–6, near the middle of the Supramound Interval, shows a number of coalescing porous grainstones developed over and between the Anasazi and Sahgzie mound areas, contributing to the communication observed between these two parts of the reservoir (see above, Chapter 4). Connection between the two mound–core algal limestone build–ups themselves by good quality lithotypes is also seen in the middle of the Mound Interval (Figure 6–7). There, at least two coalescing porous grainstone aprons, originating from the southwest flank of the Sahgzie mound build–up, are continuous across to the main (Anasazi) mound area. In contrast, two layers below (Figure 6–8), there is virtually no communication between these two build–up areas. Northeast–southwest cross sections, along the y–direction and intersecting the Anasazi #6H–1 (Figure 6–9) and Anasazi #1 (Figure 6–10) wells, also illustrate this stratigraphic variation in the continuity of good quality lithotypes between the mound build–up areas. Although these models reflect the sizes and shapes of carbonate facies observed in the field (Chapter 4, Table 4–7), the heterogeneity of Supramound facies and lack of actual direct continuity between wells in the Anasazi reservoir suggests that the lithotype stratification should be less continuous. The block–exchange process by which reservoir properties were fit to the local and global pattern constraints during the second phase of modeling (see below) rectified this problem.

6.2. Porosity Distribution Modeling

Three types of information bearing on spatial patterns of porosity distribution in the Anasazi reservoir are available to constrain the characterization.

First, at the largest vertical scale, the areal distribution of average reservoir porosity is available from the seismic RQI/porosity maps (Figures 4–26, 4–29), for which the equivalent average porosity grid is shown in Figure 6–11. Second, the average porosities of the various lithotypes (Table 4–7) serve to characterize the main features of vertical and lateral spatial distribution on an intermediate scale, that of the average lithotype body geometry. Finally, information from detailed analyses of vertical porosity variation in the Anasazi wells and areal variation from published studies of analogous lithotypes from outcrop and the nearby Aneth reservoir[(6–6)] was used to develop spatial covariance models (variograms) for the patterns of vertical and lateral porosity variation (Figure 6–12). Prior work[(6–6)] and the Anasazi well data (Table 4–7) have suggested that although the actual porosity distributions within the various lithotypes may differ, their spatial patterns of variation within each lithotype, when properly normalized, are generally similar. Hence, these data are plotted using a normal transform by subtracting the mean and dividing by the standard deviation before plotting (Figure 6–12).

6.2.1. Simulated Annealing

These three types of constraints on porosity distribution can be integrated into the boolean model by the following procedure:

1. Generate random normal deviates with mean=0, standard deviation=1, and populate the 75,000 block Anasazi grid.

2. To condition the model, substitute the actual well layer average (normalized) porosities for their corresponding (randomly–generated) grid cell values. These conditioning porosities then remain fixed throughout the rest of the procedure.

3. Compute the lateral and vertical variograms* for the model of the normal (0,1) variates. Also compute the average porosity by transforming each normal (0,1) value back to equivalent porosity using

$$\phi_{eq} = N(0,1)\phi_{sd} + \phi_{\mu}$$

where ϕ_{μ} = lithotype porosity mean

ϕ_{sd} = lithotype porosity standard deviation

and averaging all the layers in each (x,y) areal cell (except for the four cells conditioned by well data).

4. A measure of the "fit" of these random data to all three spatial constraints can be defined as the "Objective Function" (O):

$$O = \omega_1 \sum_{x,y} (\Phi_{RQI} - \phi)^2$$

$$+ \omega_2 \sum_{h_H} (\Gamma_H - \gamma_H)^2$$

$$+ \omega_3 \sum_{h_V} (\Gamma_V - \gamma_V)^2$$

---

*The variogram is a functional measure of the spatial covariance of the sample porosity data points in a specified direction. It is defined as

$$\gamma(h) = \frac{1}{2n_h} \sum_{(i,j) \subset (h + -\Delta)} (\phi_i - \phi_j)^2$$

where
- h = nominal separation distance between sample data points i and j
- Δ = width of distance sampling bin defining the points included in (h), that is, all point–pairs separated by distances in the range ($h \pm \Delta$)
- n_h = number of point pairs included in ($h \pm \Delta$)
- $\phi_{i,j}$ = sampled porosities corresponding to the (i, j) point pair.

If the vertical and horizontal variograms alone were the only constraints, porosity modeling could proceed using one of the classical gaussian simulation procedures, which are guaranteed to fit the variogram models precisely[6–6]. However, inclusion of the added RQI average porosity constraint requires a more general simulation technique.

where

(Φ_{RQI},ϕ)	≡ average (RQI, computed) porosity
(H,V)	≡ (Horizontal, Vertical) variogram models
(Γ,γ)	≡ (fitted, computed) variogram values
$\omega_{1,2,3}$	≡ relative weights assigned to each component.

5. Initially, "O" will be a large value, reflecting a poor fit of the random porosity spatial distribution to the variogram and average porosity constraints imposed by Γ_H, Γ_V and Φ_{RQI}. To improve the fit, two grid cells are randomly selected as candidates for exchange. If exchanging these two blocks would improve the porosity distribution fit (i.e., reduce the value of "O"), and if both blocks meet specific requirements for lithotype contiguity designed to conserve the number of separate lithotype bodies (see below), they are exchanged, the value of "O" is updated to reflect the change, and another pair is selected. If contiguity requirements are met but degradation in "O" is small, the exchange may still be accepted, depending on the value of a stochastic moderating probability function, defined as

$$MPF = \exp[-(O_{new} - O_{old})/R]$$

where "R" is a relaxation factor which decreases according to a user–defined schedule as the block–exchange process progresses[6–7]. A uniform [0,1] random number (URN) is generated and compared with computed MPF. If URN > MPF, the exchange is rejected; otherwise the blocks are exchanged and the objective function "O" is updated.

6. The previous three steps are repeated until (a) a user–defined preset minimum threshold for MPF is reached, or (b) a user–defined preset maximum number of sequential iterations during which there are no acceptable block exchanges is exceeded, whichever comes first.

This iterative procedure for fitting the porosity spatial distribution to the variogram and average porosity constraints by regulated block exchange is one of a family of stochastic relaxation techniques commonly called "simulated annealing", for its origins in the thermodynamics of crystallization in cooling liquid melts[6–8]. In most ways, it is conceptually similar to standard linear programming procedures, except for the stochastic relaxation acceptance/rejection criterion. This departure from unconditional minimization is introduced to relax the requirement for inevitable descent of "O" into a local minimum on the complex objective function response surface, but rather allow escape from such non–optimal, local minima and promote a more global solution.

To ensure conservation of the number of lithotype bodies, either both grid cell exchange candidates must be the same lithotype, or both must interface with at least one block of the other lithotype. Additional block exchange restrictions apply to the algal limestones, to avoid unrealistic reconfiguration of overall mound geometry. Constraints on the entire simulated annealing block–exchange procedure are summarized in Table 6–2.

As an example, the fits of the geostatistical model ultimately selected for flow simulation to the average porosity and variogram constraints are shown in Figures 6–13, 6–14 and 6–15. Comparison of the average porosity grid generated by simulated annealing (Figure 6–13) with the RQI porosity grid (Figure 6–11) shows an excellent topological fit, although there are average differences of up to 2% in the mid–range porosities of the mound apron (proximal off–mound) areas. However,

because the model lithotype porosity distributions were based on observed porosity statistics from the four Anasazi wells (Table 4–7), the overall averages (5.15%) match exactly. Although some modifications in porosity were made in the Sahgzie mound area as a result of simulation history matching (see below, Chapter 14), the final average porosity (5.121%) and mound area original hydrocarbon pore volume (4.7 MMSTBO; 7.5×10^5 m^3) in Table 15–1 matches reasonably well the RQI average porosity (5.155%) and Harken's previous volumetric estimate of OOIP (5.3 MMSTBO; 8.4×10^5 m^3)[6–9], respectively. Fits of the final model to the normalized porosity variograms also are acceptable (Figures 6–14, 6–15). Although neither the vertical or horizontal variograms are fit precisely, they exhibit the same strong trends and are acceptable representations of the observed data (cf. Figure 6–12).

Comparisons of Figures 6–16 through 6–21 with Figures 6–5 through 6–10 show the changes in lithotype distribution produced by simulated annealing. All the areal grids (Figures 6–16 through 6–19) exhibit a marked increase in visual heterogeneity from the original boolean lithotype distributions (Figures 6–5 through 6–8), with apparently isolated blocks of only one or two contiguous lithotype bodies scattered everywhere. However, such apparent isolation is illusory. All these isolated blocks are connected vertically to the same lithotypes in the layers above and/or below, thus preserving both the lithic continuity and number of separate lithotype bodies originally generated. It is also apparent that the largest lithotype bodies have also been preserved after annealing. What has increased dramatically is the tortuosity of these lithotype bodies, one or two blocks (1–4 feet; 0.3–1.2 m) vertically and up to four or five blocks (420–525 feet; 128–160 m) laterally. This tortuosity effect is also evident in lithotype stratification, illustrated by comparison of Figures 6–20 and 6–21 with Figures 6–9 and 6–10. In both cross sections, the major stratigraphic features have been preserved, although the extreme regularity of the simple lithotype geometries produced by boolean emplacement is replaced by more realistic irregularities – thickening/thinning and lateral extension/displacement are common but not obtrusive. Rarely do the effects of the annealing block exchanges extend beyond two or three blocks from the original lithotype body. The patterns of lithotype connectivity between the mound build–up areas, however, have remained intact (e.g. Layer 19, cf. Figures 6–17 and 6–6; Layer 38, Figures 6–18 and 6–7). Similarly, internal communication in Layers 1 (cf. Figures 6–16, 6–5) and 40 (cf. Figures 6–19, 6–8) remains blocked.

Another obvious modification of the lithotype grids is the addition of mound–front breccia blocks (Figures 6–18 through 6–21). These were emplaced randomly, but with a preference (probability 0.75) for the outward–facing margins of the mound complex rather than reef–fronts facing the inner part of the complex, toward other build–ups. This is a tendency shared by mound–front facies in most ancient and modern carbonate build–ups[6–10].

6.2.2. Permeability Computation

Following completion of the boolean emplacement and simulated annealing modeling, horizontal and vertical permeability were estimated for each grid block by application of the results of whole core analysis (Chapter 4, Figures 4–5 through 4–8) to the final grid cell porosities. The similarity of the range of these data to the well test results (Chapter 9) indicated that elaborate upscaling of these predictive functions was unnecessary (Chapter 4). To ensure preservation of the entire range of permeability variation, a two–step procedure was used to obtain these estimates. First, the expected value of horizontal permeability, given grid cell porosity, was computed using the appropriate transfer function (Figures 4–5 and 4–7). Then, vertical permeability was computed from the horizontal permeability in the same manner, substituting vertical for horizontal

permeability and horizontal permeability for porosity, and using the transfer functions in Figures 4–6 and 4–8. So–called "cloud transforms" based on the data scatter in Figures 4–5 through 4–8 were not used because grid block averages do not preserve the entire range of variability exhibited by core data, only the expected values. For the grid cells at well locations, of course, the actual well layer–averaged data were honored, where available.

Thus, a total of four variables was generated, cell–by–cell, for the Anasazi characterization: lithotype, porosity, horizontal and vertical permeabilities. Although additional variables were required to complete the flow simulation model (e.g. initial water saturation, relative permeabilities, rock compressibilities, etc.), quantitative models of spatial variation between the wells were not constructed for these variables, but rather constant values were provided for the Supramound and Mound Intervals, respectively, from lab data determined from representative core samples selected from these intervals (Chapters 4, 11 and 13).

6.2.3. Final Model Selection

A total of fifty characterizations of the Anasazi reservoir were generated using the two–stage modeling process of boolean emplacement of lithotype bodies and simulated annealing of the porosity distribution described above. These were sorted according to the connectivity of good quality lithotypes between the mound build–up areas (e.g. Figures 6–17, 6–18). For each of the three connectivity classes (poor, average, good), one typical example was selected for conducting flow simulation sensitivity studies. The best example (Model 17) was selected for running the final flow simulations (Chapter 13). Vertical rescaling of this model into the final 15–layer model used in the numerical simulations is described in Chapter 7.

7. VERTICAL UPSCALING: RESERVOIR CHARACTERIZATION TO SIMULATION MODEL

The grid system used in developing the Anasazi reservoir characterization consists of 50 equal–thickness layers, 20 in the Mound Interval and 30 over the Supramound Interval (see above, Chapter 4). The entire model (50 columns x 30 rows x 50 layers) comprises 75,000 grid blocks. However, preliminary test runs demonstrated that if a model this large was used, the compositional simulator runs could not be completed in a reasonable amount of time. Consequently, the number of layers was reduced from 50 to 15, thereby reducing the number of cells to 22,500 and requiring reallocation of lithotype designations and re–computation of effective reservoir properties. Areal grid block definitions remained the same for both models. These readjustments constituted the vertical upscaling process.

Proportional allocation of the old layers to the new resulted in one new layer representing 3 1/3 old layers, with 6 layers in the Mound Interval and 9 layers in the Supramound Interval in the upscaled model. Each new layer averages approximately 6.7 feet (2 m) in thickness over the mound area, and 3.3 feet (1 m) in the off–mound areas. Under this reallocation scheme, every fourth layer of the 50–layer geostatistical model was subdivided, with 1/3 assigned to one new layer, 2/3 to the other.

7.1. Lithotype Reassignment

Because different lithotypes from the 50–layer model were allocated to the same new layer, rules were formulated for assigning lithotype names. Where one lithotype comprised more than 50% of the new layer thickness, that name was assigned to the new block. In cases where no single lithotype predominated, the new block was designated as a "mixed lithotype", which were subdivided into two new lithotype classes: a poor quality – mixed lithotype, and a good quality – mixed lithotype. The rule for assigning new blocks to one of the new classes was based on a subdivision of the original classes into "good" and "poor" quality lithotypes, on the basis of aggregate reservoir properties (Table 4–3). Lithotypes 3, 5, 6, 8 and 9 were defined as good–quality, the remainder (1, 2, 4, 7 and 10) as poor–quality. A "mixed" lithotype was assigned to one or the other of these two classes (11=poor, 12=good) according to whether poor or good lithotypes predominated in the 3 1/3–layer (geostatistical) interval comprising the new block (Figure 7–1). Comparisons of lithotype designations in typical 50–layer cross sections and maps with their equivalent 15–layer counterparts are shown in Figures 7–2 through 7–5. Approximately 15–20% of the grid cells in the 15–layer models were assigned to the mixed lithotype classes. Although upscaling resulted in blurring some of the finer detail of the 50–layer models, the main features of the original reservoir architecture remain intact. These designations were used in lithotype assignments in the flow simulator, but had no effect on the determination of effective properties; these are discussed below.

7.2. Upscaling Reservoir Properties

The effective porosity assigned to grid cells in the upscaled 15–layer model were computed by simple volume–weighted arithmetic averaging of porosities from the 3 1/3 constituent geostatistical model layers. Comparisons of porosity grids in the 50–layer and equivalent 15–layer models are shown in Figures 4–6 through 7–9. Porosity upscaling resulted in some reduction of small–scale vertical and lateral variation, but as with the upscaled lithotypes, the major differences between the

Mound and Supramound Intervals, and even among the major facies variations in the Supramound Interval, are preserved.

Upscaling of permeability is a controversial issue. Ideally, flow simulation would be carried out on the original grid system specifically designed to characterize the internal architecture and variation of reservoir properties. Unfortunately, current limitations on computational speed render this infeasible, and upscaling is, at the present time, a necessary expedient. However, although a variety of techniques exist for estimating effective permeabilities in upscaled grid cells that are purportedly equivalent to the ensemble of geostatistically generated permeabilities, no clear–cut consensus has been reached for either selection criteria or preference among the available methods.

The technique used for permeability upscaling in this study analytically recomputes the block–face transmissibilities from the original block permeabilities, harmonically weighted by the block interface areas. The pressure equation is then solved for the upscaled block. This procedure is implemented in Landmark Graphics' VIP simulator pre–processing program GRIDGENR[7–1]. Comparative examples of effective permeabilities for the original 50–layer and upscaled 15–layer models are shown in Figures 7–10 and 7–11. Although the effect of smoothing is apparent in the upscaled grid cells, differentiation between the Mound and Supramound Intervals is still readily apparent, and distinctions between the high and low–permeability zones in the Supramound Interval seem sharper than are the upscaled porosities (cf. Figures 7–6 through 7–9). Thus, the most significant patterns of variation have been preserved in upscaling the permeability. Despite the fact that some extremal (high and low) permeabilities have been lost, most of the sharpest small– scale contrasts remain intact.

The final upscaled 50x30x15 reservoir model was formatted for direct input to the VIP simulator. Defined variables were lithotype index (renamed "ISAT" in VIP), porosity, horizontal and vertical permeability, "IREGION" – a VIP index assigned to differentiate (off–mound, on–mound) areas, (Mound, Supramound) intervals, and (Anasazi, Sahgzie) build–ups; and rock compressibility (for which there were two values – one for the Mound Interval algal limestones, the other for all other, typically Supramound, lithotypes). Cutaway block diagrams of the final 15–layer VIP model (Figures 7–12, 7–13, 7–14) show the distributions of lithotype, porosity and horizontal permeability in the Anasazi reservoir.

8. REVIEW OF PRODUCTION HISTORY

The Anasazi and Sahgzie reservoirs have been producing for over 7.5 years. The Anasazi reservoir has three producing wells, Anasazi #1, Anasazi #5L–3 and the Anasazi #6H–1. The Sahgzie Field has one producer, the Sahgzie #1.

The Sahgzie #1, the first well completed in the subject field, was completed November 2, 1989 with an initial production rate (IP) of 1022 BOPD with 433 MSCF/D of gas. The Anasazi #1 Well was the second well completed. The Anasazi #1 was completed on January 29, 1990 with an IP of 1251 BOPD with 740 MMSCF/D of gas. The third well completed was the Anasazi #5L–3. It was completed March 21, 1991 with an IP of 260 BOPD with 169 MSCF/D of gas. The final well, the Anasazi #6H–1 was completed August 1, 1995. The initial production rate (swab test) was only 7 BOPD with 16 BWPD (load water).

All wells received acid treatments. In general the Supramound and Mound Intervals were perforated and acidized separately. Acid treatment volumes varied from 1600 gallons to 21,000 gallons and in some case acidization included the use of ball sealers to help in stimulating all sets of perforations. Details of each wells completion, initial well test data and pressure build–up test data are available in well files originally set up by Chuska Energy Company and subsequently acquired by Harken Energy Corporation.

Production history for each well and the field are provided in production data plots prepared as Figures 8–1 to 8–15. Field and well plots indicate that both the Anasazi and Sahgzie Fields (mounds) experienced a short period of primary production associated with liquid expansion. This period of production is characterized by a constant production gas–oil ratio (GOR). Both Anasazi Well 1 (Figure 8–12) and Sahgzie Well 1 (Figure 8–15) have a constant GOR rate from initial production in 1989 to a couple of months beyond January 1991. The Anasazi Wells 5L–3 and 6H–1 do not exhibit this initial production behavior because when both begin production, the liquid expansion phase of production is completed and free gas existed in the Anasazi mound.

Once liquid phase expansion is complete and reservoir pressure drops below the bubble point, GOR's and gas production increase and subsequently decrease. This type of production history is typical for dissolved gas depletion processes. The third stage of production exhibited by both well and field plots occur in the latter stages of production. The third stage of production is characterized by nearly constant or slowly declining oil and gas rates. The reservoir mechanism associated with this stage is continued dissolved gas depletion and secondary gas cap expansion coupled with gravity drainage of oil from the Supramound Interval into the Mound Interval. This last stage of production will be discussed and illustrated further in Chapters 12 and 14, entitled Carbon Dioxide Process Mechanism Studies and Reservoir Performance – History Match respectively.

9. WELL TEST DATA AND INTERPRETATION

9.1. Introduction

Well tests were conducted on the Anasazi Well 1, Anasazi Well 5L–3 and Sahgzie Well 1. In general, the quality of data obtained from these tests was poor. No original pressure–time data was available. The data available for analysis was derived from previous interpretations. The frequency at which pressure data was recorded was too low and the duration of the build–up was in general too short. Only a few data sets were considered of sufficient quality to be interpreted and those results are reported. The following sections identify all the tests that were conducted on each well and if the analysis provided no reasonable interpretation it is not documented. The reasons for not including the test data and its associated interpretation are discussed. Well test data, fluid production information and completion details on which the well test interpretations were based are not included in this report, but are available from general well files from the Anasazi/Sahgzie field. In subsequent discussions, specific references are not identified as to the source of information. When not cited it is implied that data and information was obtained from general well files. Test data and interpretation are reported below on a well basis.

9.2. Anasazi Well 1 Tests

The Anasazi Well 1 was perforated in the lower and upper Desert Creek units. The perforated intervals are reported as:

Upper Desert Creek (Dolomite) : 5,574′ – 5,630′
Lower Desert Creek (Limestone) : 5,646′ – 5,670′

The lower zone was acidized using ball sealers and produced for 8.0 hours and then for 6.0 hours a day later before completing the upper zone. The upper zone was acidized then re–perforated in the same interval and acidized for a second time. The upper zone was tested for 11.0 hours after the first acid job. Then the well was tested again for 5.0 hours on the following day. Subsequent to the second acid job on the upper interval, it was tested for 10.5 hours and then for 17.0 hours the following day. The testing of separate intervals was followed by a 110.5 hour flow test from both zones over a six day period from January 10, 1990 to January 21, 1990. This flow period was followed by a 44 hour pressure build–up during which pressure data was recorded. This test is referred to as the Ana 1–0190 test in discussions below.

Other tests were subsequently conducted on the Anasazi 1 Well. These tests, plus the first test, are summarized below with relevant comments.

Anasazi No. 1 Well Tests

Test Data	Test No.	Comments
Jan. 1990	Ana 1–0190	Analyzed (see below)
Feb. 1990	Ana 1–0290	Analyzed (see below)
Jan. 1992	Ana 1–0192	Not analyzed – Insufficient Pressure Data
Aug. 1993	Ana 1–0893	Analyzed (see below)

Results of analysis and/or comments on each test follows:

9.2.1. Anasazi Well No. 1 – Ana 1 – 0190 Test

Because no pressure build–up was recorded after each zone (lower and upper Desert Creek) was produced separately, reservoir properties for each interval could not be determined. Further, without resorting to simulation, the influence of individual interval tests on the combined interval test and build–up could not be accounted for in the analysis of the combined interval test. It was assumed that each interval had reverted to its original pressure prior to being produced jointly. The combined interval flow period lasted 110.5 hours over six days. Because the daily rates were approximately the same, a single average flow rate was determined and used for test analysis. This is summarized below:

Rate Schedule – Anasazi No. 1 (Ana 1–0190Test)

Period No.	Flow Type	Rate	Duration	Cumulative Hours	Comments
1	Flow	1362	110.5	110.5	Dual Zone Flow
2	Shut–in	0	48	1585	Final Shut–in

Well log data was used to calculate average porosity and water saturation for the producing intervals. This was used to set static properties for the interpretation of the test. Fluid property data was obtained from the Anasazi No. 1 Fluid property study [9–2]. Static data employed in the analysis is summarized below:

Static Properties – Anasazi 1 (Ana1–0190 Test)

Fluid Volume–Factor	:	1.2060	vol/vol	Datum depth	:	5622.00	Feet
Fluid Viscosity	:	0.900E+00	cp	Gauge depth	:	5622.00	Feet
Fluid Compressibility	:	0.962E–05	1/psi	Perf. depth	:	5622.00	Feet
Water Compressibility	:	0.300E–05	1/psi				
Porosity	:	14.1020	%				
Water Saturation	:	20.0000	%				
Net Thickness	:	98.000	Feet				
Rock Compressibility	:	0.200E–05	1/psi				
Wellbore Radius	:	0.208E+00	Feet	Total Compres	:	0.103E–04	1/psi

Production data and geologic information indicates that the Anasazi reservoir can be characterized as basically a two layer system comprised of the Upper Desert Creek (Supramound Interval) and the Lower Desert Creek (Mound Interval) intervals. These two basic intervals are the main flow units within a mound and thus a two layer model which allowed cross flow was used to analyze the test results. The Supramound Interval includes the perforations from 5574′ to 5641′ (67 feet) and the Mound Interval includes the perforations from 5642' to 5673' (31 feet) for a total thickness of 98 feet. Also, a homogeneous reservoir was used for preliminary interpretations. Fully penetrating

well models and reservoirs with no boundaries were employed for both the homogeneous and the two layer reservoir models.

All well test interpretations were conducted using P.I.E., an advanced interactive well test interpretation package developed by Simulation Modelling Consultancy, Ltd. The conventional interpretation of these two models is briefly discussed next and interpretation data provided. Plots presented for each model include:

Diagnostic Plots

1. Superposition Radial Flow Analysis
2. Derivative Analysis

Using data estimated from these diagnostic plots as initial estimates, a match of calculated and observed data was generated with results typically displayed in three types of plots. These plots compare calculated responses, using the parameters presented in the legend of each figure, and displayed as continuous curves with actual test data (discrete points). The three plots used include:

3. Pressure difference and pressure derivative data versus shut–in time.
4. Pressure versus superposition time.
5. Pressure versus time together with rate data for the test period.

Diagnostic plots are presented as Figures 9–1 and 9–2. Referring to Figure 9–1, the derivative plot, well bore storage data is not present. Thus, the unit slope line was simply chosen to the left of the first pressure data point. The stabilized flow was selected over the shut–in time interval of 1.0 to 10.0 hours which is believed to represent the total system response. This provided an estimated 78.9 md for the permeability. Figure 9–2, the superposition diagnostic plot, was used primarily to provide an estimate of reservoir pressure. Selecting the last 20 hours of build–up for extrapolation, the reservoir pressure was estimated at 1670 psi.

Using the reservoir parameters determined from the diagnostic plot analysis as initial estimates of reservoir parameters, a match of observed and computed data was attempted using two models. The first model was based on a homogeneous reservoir model with no boundaries (observable during test) coupled with a fully penetrating vertical well model. The second model employed a two–layer reservoir model with no boundaries and cross flow between layers coupled with a fully penetrating vertical well model.

Figures 9–3, 9–4 and 9–5 present the match of observed versus computed results for the homogeneous model. Because a homogeneous model is not representative of the total interval test the match between computed and observed is of poor quality. The results are presented merely to demonstrate that a homogeneous reservoir representation is not an appropriate model for the Anasazi Well No. 1.

Fully Penetrating Vertical Well – Two Layer Cross Flow Model

The two layer characterization of the Anasazi Well No. 1, based on well log data, used for well test interpretation is given below.

Anasazi Well No. 1 0190Test
Two Layer Properties

Layer 1			Layer 2			
Thickness	=	31.00	Thickness	=	67.0	Feet
Porosity	=	10.0000	Porosity	=	16.0000	%
Water Sat.	=	20.0000	Water Sat.	=	20.0000	%
Fluid Comp.	=	0.962E–05	Fluid Comp.	=	0.962E–05	1/psi
Rock Comp.	=	0.200E–04	Rock Comp.	=	0.200E–04	1/psi
Default Omega	=	0.224313	Default Omega	=	0.775687	
Boundary thickness between layers				=	.000	Feet
Global Static – data Water Compressibility				=	0.300E–05	1/psi
Global Static – data Total Thickness				=	98.0	Feet

Figures 9–6, 9–7 and 9–8 present data comparing observed and computed results using a two layer model which allows cross flow between layers.

As discussed previously, the Desert Creek Unit in the Anasazi/Sahgzie Field can be characterized as consisting of two principal intervals or flow units. One layer represents the dolomite (Supramound Interval) and the other the limestone (Mound Interval), each with their own characteristic reservoir properties. The observed well test response is governed or reflects the interaction of the dolomite facies with the limestone facies. This type of response is consistent with data available in the literature [9–3] which shows that the behavior of multi–layer systems or heterogeneous systems characterized by high contrasts in rock properties among layers or units of the heterogeneous system can be modelled by using two elements (i.e. two layers). That is, multi–layer systems or heterogeneous systems with two dominant set of properties behave like conventional two layer systems with cross flow between layers (or units). The above interpretation was applied to the Anasazi reservoir with consistent interpretation results.

The reservoir parameters associated with two layers models are defined below.

$$\omega = \frac{(\phi c_t h)_1}{(\phi c_t h)_1 + (\phi c_t h)_2}$$

$$\lambda = \frac{2r_w^2 \; k_v}{[(kh)_1 + (kh)_2][h_1 + h_2]}$$

$$\omega_1 + \omega_2 = 1.0$$

$$c_t = s_w c_w + s_o c_o + (1 - \phi) c_r$$

Variables used in the above equation are defined as:

c_t = total compressibility
c_o = oil compressibility

c_w	=	water compressibility
c_r	=	rock compressibility
r_w	=	well bore radius
k_v	=	vertical permeability
k_i	=	i = 1,2 layer permeability
h_i	=	i – 1,2 layer thickness
ω	=	storativity ratio parameter
λ	=	interporosity interlayer flow parameter
ϕ	=	porosity (fraction)

Figures 9–6, 9–7 and 9–8 illustrate the quality of the match possible with a two layer model which allows crossflow between layers. In general the match is reasonable given the quality of the data. Use of log data provides an initial estimate of the storage ratio "ω". From the above table the log based "ω" for the limestone interval was calculated to be 0.224. To fit the well test data, "ω" was decreased to 0.035. This implies that the actual high permeability interval contributing to the test has an effective ϕh much smaller than the log based value computed for the limestone interval (Mound Interval). Also the increase in derivative values for the last 20 hours of the test is not well matched in either Figure 9–6 or 9–7. This late time derivative increase may be attributable to additional layer interactions and/or boundaries. In summary the interpretation based on a two layer model provides the following reservoir parameter estimates:

Wellbore Storage	–	0.00128	Bbls/psi
Skin (both layers)	–	–0.9	
Permeability of Limestone Unit	–	185.0	md
Permeability of Dolomite Unit	–	1.28	md
Storage Ratio (ω)	–	0.035	
Interlayer Flow Parameter (λ)	–	0.64 E–05	
Static Reservoir Pressure	–	1664.0	psig

9.2.2. Anasazi Well No. 1 – Ana 1 – 0290 Test

The initial joint interval test on Anasazi Well No. 1 was followed by approximately one month of production and then shut–in for a 66 hour pressure build–up test. The flow rate schedule prior to shut–in is given below.

Rate Schedule Anasazi Well No. 1 – 0290 Test

Pt no.	Times Decimal Hours	Rates STB/D
1	.0	1272.0
2	79.0	893.0
3	247.0	687.0
4	511.0	461.0
5	679.0	328.0
6	823.5	280.0
7	824.1	0.0
29	890.0	0.0

Pressure data quality was again poor. The number of pressure points recorded was minimal and as a consequence, the pressure derivative data erratic and noisy. No clear indication of well bore storage or stabilized flow is evident in the pressure and pressure derivative plots. As in the 0190 test a late time increase in derivative value was recorded. Based on the 0190 test interpretation a two layer model was employed to analyze the 0290 test. These results are presented below:

Fully Penetrating Vertical Well – Two Layer Cross Flow Model

The initial properties of the two layers and the static data employed in analyzing the 0290 test is the same as the 0190. This data is available in the previous section.

Figures 9–9, 9–10 and 9–11 present results of the match between observed data and calculated response of a two layer model. The quality of the match is not as good as that obtained from the 0190 test interpretation. Specifically, the derivative match is particularly poor. The sparseness and quality of the observed pressure data results in a noisy derivative plot and hampers the matching effort. The storage ratio "ω" utilized in the match agrees with the log data. However, unlike the 0190 test, the predicted pressure response for the 0290 test was not particularly sensitive to changes in "ω" over the range of 0.09 to 0.25. In addition, λ variations did not significantly impact the match and a 100 fold increase did not significantly alter the fit and provided values closer to that obtained in the 0190 test interpretation. The reservoir parameters that gave the best match to observed data are presented in the above referenced Figures and summarized below:

Wellbore Storage	–	0.001	Bbls/psi
Skin (Limestone)	–	–2.40	
Skin (Dolomite)	–	–8.00	
Permeability of Limestone Unit	–	55	md
Permeability of Dolomite Unit	–	10	md
Storage Ratio (ω)	–	0.224	
Interlayer Flow Parameter λ	–	1.0×10^{-10}	
Static Reservoir Pressure	–	1328.0	psig

The static reservoir pressure shows a decline of approximately 336 psi after a month's production. The rapid pressure decline occurs during the liquid expansion portion of the primary production phase and reflects the relatively incompressible nature of the liquid saturated reservoir.

9.2.3. Anasazi Well No. 1 – Ana 1 – 0893 Test

The pressure build–up test was conducted after the Anasazi Well No. 1 had produced over 589,000 STB of oil and reservoir pressure had significantly decreased since discovery. The reservoir was in a two phase (oil and gas) state with a large portion of the pore space occupied by free gas.

The nature of the pressure build–up data again made interpretation difficult and late time recharging from low–quality higher–pressure intervals and possibly well interference effect prevented meaningful interpretation as the data and preliminary interpretations are not included.

The final pressure measured at the end of 47 hours of build–up was 228 psig. This illustrated the extent of local reservoir depletion.

9.3. Anasazi Well No. 5L–3 Tests

The Anasazi 5L–3 well was competed during March, 1991. The well did not flow upon completion of any of the five separate zones that were perforated. Zone 1 (5,726′ – 5,750′), the Akah unit,

was swabbed tested over 2 days (34 hours) and shut–in for a 48 hour pressure build–up. The pressure gauges however, were run during operation conducted in testing Zone 2 and the only meaningful data available for analysis was late time data on the static reservoir pressure. The final static pressure was computed to be approximately 126 psig.

Zone 2 (5,684′ – 9,711′), the Platform Interval, was swabbed over a three day period and shut–in for 48 hours to measure bottom hole pressures. No pressure data was available to analyze the test.

Zone 3 (5,652′ – 5,675′) the limestone interval, Zone 4 (5,611′ – 5,642′) and Zone 5 (5,587′ – 5,602′) the dolomite interval, were swabbed tested (isolated from Zone 1 and Zone 2) over a five day period and the well was shut–in for a 72 hour pressure build–up. Again, pressure data is of marginal quality and the only meaningful data extracted from the test was a shut–in reservoir pressure of approximately 870 psig.

9.4. Anasazi Well No 6H–1 Tests

9.4.1. Introduction

As part of the DOE sponsored project the Anasazi 6H–1 well was drilled and completed during June and July 1995. Subsequent to completing the well, it was logged and a series of wireline formation tests conducted at several points in the Desert Creek. Wireline formation testing provided a means of estimating formation (reservoir) pressure and calculating permeability from several short duration tests (flow and build–up) in a single wireline run. Five separate tests were completed over the Desert Creek Interval.

The completion was designed to separately complete and test (flow test followed by a pressure build–up) the limestone and dolomite intervals. During the flow tests of each zone, it was planned to collect fluid samples for compositional analysis and CO_2 swelling tests.

The limestone unit was initially perforated from 5,723′ to 5,730′ and acidized. Swab testing the well recovered only 19 barrels of total fluid (total load fluid to be recovered was 35 barrels) with minimum oil. The production test of the limestone unit was discontinued and the dolomite unit was perforated from 5,680′ to 5,694'. Prior to acidizing and testing the dolomite unit, pressure gauges were installed in the well to measure the limestone unit pressure during the test of the dolomite interval. The gauges were separated from the dolomite interval by a retrievable bridge plug. The limestone interval pressure was recorded during acidization and testing of the dolomite unit to establish the extent of pressure communication between the two intervals. Subsequent to the final two swab runs on the dolomite interval an additional set of pressure gauges were placed in the well to record the final bottom hole flowing pressure and pressure build–up of the dolomite interval.

The following sections summarize the results of the wireline formation tests, the analysis of the pressure build–up test of the dolomite interval and the pressure monitoring of the limestone interval during testing of the dolomite unit.

9.4.2. Wireline Formation Testing

Of the five tests conducted over the Desert Creek unit only the tests located at 5,692.5′ in the dolomite interval provided pressure data for the two flow and two completed pressure build–up periods. The other tests consisted of a single flow period followed by an incomplete pressure

build–up. The incomplete build–ups were attributable to low formation permeability. The following table summarizes the measurement of the subject fluid tests.

Anasazi Well No. 6H–1 Wireline Formation Tests

Test No.	Depth Feet	Interval Tested	Minimum FBHP psi	Duration of build–up in Minutes	Static Pressure psi	Comments
1	5737.0	Lower Dolomite Interval (Platform Interval)	88	27	> 990	Low permeability, build–up incomplete
2	5726.5	Limestone	204	20	> 314	Low permeability, build–up incomplete
3	5716.2	Limestone	120	6	> 137	Low permeability, build–up incomplete
4	5704.5	Dolomite	269	60	> 647	Low permeability, build–up incomplete
5	5692.5	Dolomite	62–136	3.7 – 6.5	475–477	build–up complete can be analyzed for permeability

Test 5 was analyzed with PIE and the permeability estimates obtained ranged from 0.565 to less than 15 md. PIE's capabilities do not include a rigorous option for analyzing wireline "point" flow/build–up tests. Specialized software that handles single point sources/sinks on the perimeter of a cylindrical wellbore is available for more rigorous analysis of the wireline tests.

Results of the subject wireline test were used primarily to obtain point values of pressure over the Desert Creek interval. Of the five completed tests, only Test 5 provides a final static pressure. This pressure is approximately 475 psi for one subunit of the dolomite interval. The other tests provide only bounds for the pressure levels of the tested depth. These estimates are:

Platform Interval	–	Pressure > 990 psi
Limestone Interval	–	Pressure > 314 psi
Dolomite Interval	–	Pressure = 475 psi
Separate Dolomite Subintervals	–	Pressure > 647 psi

The wireline tests data indicated that at the Anasazi 6H–1 location:

1. The Desert Creek, as expected, was depleted. However, the extent of depletion was not as great as that at the other two Anasazi wells at the time of testing.
2. The dolomite interval is less depleted than the limestone intervals (473 psi to 314 + psi)
3. Even within common lithologic units (i.e. limestone/dolomite) the pressure can vary. This is likely a result of limited communication within an interval which leads to differential depletion.
4. The platform interval is at a substantially higher pressure than the dolomite and limestone intervals of the Desert Creek.

9.4.3. Dolomite Interval Flow and Build–up Test

As stated above, the initial perforated interval of the dolomite interval was 5,680′ to 5,694′. It was acidized and swab tested. The production schedule, including the acidization treatment and the

subsequent swab test, is summarized below and was used in the analysis of the subsequent build–up using P.I.E.

Rate Schedule Anasazi Well No. 6H–1 Dolomite Interval Test

Pt no.	Times Decimal Hours	Rates STB/D
1	0.00	–267.24
2	2.00	1.50
3	4.50	0.00
4	20.50	12.12
10	32.50	0.00
16	44.50	2.250
22	56.50	0.00
28	68.50	2.401
33	78.50	0.00
94	91.78	2.85
159	102.19	0.00
358	302.63	0.00

Static reservoir properties used in the analysis of the test are given below:

Static Properties – Anasazi Well No. 6H–1 Dolomite Interval Test

Fluid Volume–Factor	:	1.1480	vol/vol	Datum depth	:	5684.00	Feet
Fluid Viscosity	:	0.105E+01	cp	Gauge depth	:	5500.00	Feet
Fluid Compressibility	:	0.232E–03	1/psi	Perf. depth	:	5684.00	Feet
Water Compressibility	:	0.300E–05	1/psi	Static grad.	:	.....	psi/Feet
Porosity	:	13.6000	%	Dynamic grad.	:	.....	psi/Feet
Water Saturation	:	15.0000	%	Field gradient	:	.....	psi/Feet
Net Thickness	:	10.000	Feet	Wellbore comp.	:	.....	1/PSI
Rock Compressibility	:	0.200E–05	1/psi	Wellbore vol.	:	.....	Bbls
Wellbore Radius	:	0.208E+00	Feet	Total Compres	:	0.200E–03	1/psi

Using a homogeneous reservoir model coupled with a fully penetrating well model the final swab bottomhole pressure value and build–up pressure were matched. The low production rate and nature of the flow period (swabbing causes an initial minimum bottomhole flowing pressure followed by an increasing bottomhole pressure as liquid flows into the wellbore, causing a temporary increase in pressure which results in a variable wellbore storage behavior) complicated interpretation of the test. A reasonable match of this final production (last swab) and build–up is presented in Figures 9–12, 9–13 and 9–14.

The reservoir properties estimated from this analysis are:

Wellbore Storage	–	0.00240	Bbls/psi
Skin	–	2.80	
Permeability	–	0.453	md
Initial Pressure	–	383	psig

The subject test was also analyzed employing the initial acid treatment (negative production) and four days of swabbing with overnight shut–in periods (see previous rate schedule) prior to the final build–up. To match the total pre shut–in rate, swab tests required some adjustment of the production rate schedule (deemed acceptable because fluid recovery was not measured accurately). A reasonable match of the final flowing bottom hole pressure at the end of each swab and the final build–up was obtained with the same reservoir properties as listed above.

9.4.4. Limestone Interval Pressure Monitoring

As discussed above the limestone interval pressure was monitored during the acidization and subsequent swab testing of the upper dolmite unit. Also, pressure measurements continued to be recorded when the upper dolomite was re–acidized and subsequently swabbed for a second test. During the sequence of acidizations the Anasazi 6H–1 well experienced well head pressure varying between 14.7 and 4,286 psi. The measured pressure versus time behavior of the limestone interval showed no response to the pressure fluctuation occurring in the upper dolomite interval immediately above. Thus, at least locally (Anasazi 6H–1 Location), no vertical communication exists between dolomite and limestone intervals. The final static pressure measured for the limestone interval was 291 psi. This final pressure was approached monotonically and showed no evidence of upper dolomite pressure influence.

9.4.5. Summary of the Anasazi 6H–1 Tests

The following observations can be made based on the pressure data obtained from the wireline formation tests, the swab test and subsequent pressure build–up of the dolomite interval and the pressure monitoring of the limestone interval.

1. No communication exists at the Anasazi 6H–1 well location between the dolomite and limestone intervals.

2. The limestone interval pressure at the 6H–1 location is approximately 290 psi.
   - The extended shut–in provided a value of 291 psi
   - The wireline tests provided a value of 314 psi

3. The dolomite interval pressure at the 6H–1 location is approximately 383 psi.
   - The extended build–up provided a value of 383 psi
   - The wireline tests provided a value between 425 and 647 psi.

4. Within each main geologic unit depletion appears to be non–uniform. Local sub intervals within the Supramound Interval (dolomite), for example, show pressures of 475 psig and 147 psig for two different sub–intervals.

5. Permeability estimates of the dolomite interval at the 6H–1 location provide value ranges from 0.5 to 15.0 md.

6. Initial estimates of the skin value for the dolomite were approximately 2.8. The influence of subsequent acid treatment could not be assessed since no pressure tests were conducted after the completion of the additional acid treatment. This contrasts with the negative skins exhibited by other Anasazi/Sahgzie wells.

9.5. Sahgzie Well No. 1 Tests

9.5.1. Introduction

The Sahgzie Well 1 was perforated in the lower and upper Desert Creek unit. The perforated intervals are reported as:

Upper Desert Creek (Dolomite Interval) – 5,590′ – 5,598′
Lower Desert Creek (Limestone Interval) – 5,644′ – 5,669′

The lower interval was perforated first and acidized using ball sealers. The lower interval was then production tested with the first flow period of 11.25 hours recovering 688 STB of oil. The well was subsequently killed with water and a retrievable bridge plug set to isolate the dolomite and limestone intervals.

9.5.2. Sahgzie Well No. 1 Test

In the November 1989 test both intervals were produced and the well shut–in for 48 hours following production of approximately 9,500 STB of oil. The rate schedule prior to shut–in is given below:

Rate Schedule Sahgzie Well No. 1 (1989 Test)

Pt no.	Times Decimal Hours	Rates STB/D
1	0.0	1046.0
2	14.0	1367.0
3	38.0	1312.0
4	62.0	1378.0
5	86.0	735.0
6	107.5	623.0
7	131.5	535.0
8	155.5	452.0
9	179.5	450.0
10	183.6	0.0
38	231.0	0.0

Well log data was used to calculate average porosity and water saturation for the producing intervals. Fluid properties employed were the same as used for the Anasazi test analysis. The following table summarizes the static data used to interpret the Sahgzie Well No. 1 tests.

Static Properties – Sahgzie Well No. 1 (189 Test)

Fluid Volume–Factor	:	1.2060	vol/vol	Datum depth	:	5578.00	Feet
Fluid Viscosity	:	0.200E+00	cp	Gauge depth	:	5578.00	Feet
Fluid Compressibility	:	0.962E–05	1/psi	Perf. depth	:	5590.00	Feet
Water Compressibility	:	0.300E–05	1/psi	Static grad.	:	.....	PSI/Feet
Porosity	:	10.8500	%	Dynamic grad.	:	.....	PSI/Feet
Water Saturation	:	25.0000	%	Field gradient	:	.....	PSI/Feet
Net Thickness	:	29.500	Feet	Wellbore comp.	:	.....	1/psi
Rock Compressibility	:	0.200E–05	1/psi	Wellbore vol.	:	.....	Bbls
Wellbore Radius	:	0.208E+00	Feet	Total Compres	:	0.996E–05	1/psi

As with most Paradox Basin well tests the pressure data quality is poor (i.e. frequency of data sampling and duration of the build–up insufficient), complicating interpretations. The pressure build–up data on the Sahgzie Well No. 1 exhibits at least two stabilized flow periods which could be attributable to multi–layers (or multiple intervals) contributing to production and/or lateral boundaries. Employing a homogeneous reservoir model and fully penetrating well model, diagnostic analysis using a linear lateral reservoir barrier was completed (Figures 9–15 and 9–16). Figure 9–15 indicates the test was dominated by well bore storage and that the derivative plot does not provide any straight forward interpretation trends. Figure 9–16 appears to illustrate the presence of a linear barrier since a line with double slope (relative to the first flow stabilization line) can be drawn through most of the data points for shut–in time greater than 21 hours. Reservoir properties obtained from this diagnostic analysis provide the following reservoir parameters:

Skin	–	–7.25	
Permeability	–	55.4	md
Linear Barrier Location	–	384 to 741	feet

Using this data as initial estimates for reservoir properties, several reservoir models were investigated in an attempt to match the observed pressure data. All models employed fully penetrating wells. Homogeneous and two layer models without lateral barriers did not provide a reservoir interpretation that would present a reasonable match of the data. A model employing two intersecting linear barriers provides a reasonable match, but the angle of intersection was between 150° and 180° suggesting that a single linear barrier was more appropriate. Thus, two models, a homogeneous reservoir and a two layer (with cross flow) reservoir model, containing a linear barrier were used to match the observed pressure data given the previous rate schedule and static data. Like the Anasazi reservoir the Sahgzie system can be characterized as consisting of two major flow units (dolomite and limestone intervals) with different properties. The log derived two layer characterization used in interpreting the test is given below.

Sahgzie Well No 1 (1102 Test)
Two Layer Properties

Layer 1			Layer 2			
Thickness	=	20.00	Thickness	=	9.50	Feet
Porosity	=	10.6000	Porosity	=	11.5000	%
Water Sat.	=	26.9000	Water Sat.	=	26.3000	%
Fluid Comp.	=	0.962E–05	Fluid Comp.	=	0.962E–05	1/psi
Rock Comp.	=	0.200E–05	Rock Comp.	=	0.200E–05	1/psi
Default Omega	=	0.659017	Default Omega	=	0.340983	

The relatively small thickness (9.5 feet) assigned the dolomite unit is based on a interpretation that a major portion of the dolomite interval is anhydrite filled and will not significantly contribute to the well response.

Fully Penetrating Vertical Well – Homogeneous Reservoir – Linear Barrier Model

Figures 9–17, 9–18 and 9–20 present the match between observed pressure data and model predictions employing the reservoir parameters presented in each figure. A reasonable match is obtained for all data except the late time period (30 to 48 hours) in the derivative plot. The increasing derivative during this time is not matched well and the increase maybe an indication of continuing layer cross flow for one or more layers. The reservoir parameters that provide this match are:

Wellbore Storage	–	0.256	Bbls/psi
Skin	–	–8.45	
Permeability	–	23.5	md
Linear Barrier Pressure	–	311	feet
Static Reservoir Pressure	–	1,618.0	psig

Fully Penetrating Vertical Well – Two Layer Model with Cross Flow – Linear Barrier Model

Figures 9–20, 9–21 and 9–22 present the match between observed pressure data and model predications employing the reservoir parameters presented in each plot.

An improved match for the late time pressure derivative curve is obtained but the derivative increase trend is not matched over the entire late time range (38 to 48 hours). Also, the possible flow stabilization at 10 hours (identified in diagnostic plots) does not match well. It is likely that the actual reservoir description is more complex than that represented in the simplified well test models. The reservoir parameters obtained from the match are:

Wellbore Storage	–	0.259	Bbls/psi
Skin (Limestone)	–	–8.81	
Skin (Dolomite)		–7.69	
Permeability (Limestone)	–	30.3	md
Permeability (Dolomite)	–	3.87	md
Storage Ration (ω)	–	0.659	
Interlayer Flow Parameters λ	–	0.206E07	
Distance to Linear Barrier	–	475	feet
Initial Pressure	–	1,686.0	psig

The storage ratio ω remained unchanged during the match process at the value calculated from the static data. The presence of a linear barrier within 300 to 476 feet of the well is consistent with the geologic model developed for the field. The Sahgzie Well No. 1 is located approximately 300 to 400 feet from the eastern edge of the main Sahgzie mound. Thus, it is likely that the presence of the eastern mound edge influenced the well test response. The radius of investigation after 13 hours of shut–in is estimated at between741 and 883 feet, thus encompassing the eastern mound edge and possibly even being influenced by the western mound edge (690 to 800 feet west of Sahgzie Well No. 1). The western boundary of the mound could be responsible for the additional increase in the derivative near the end of the build–up.

9.5.3. Other Sahgzie Well Tests

An additional Sahgzie Well No. 1 test was conducted during July, 1991. As with other tests, the poor quality of data complicated interpretation and parameters developed from the interpretation are questionable and not reported.

The Sahgzie Well No. 1 was the initial discovery well and the first test conducted in the Anasazi/Sahgzie reservoir was an open hole drillstem test on October 14, 1989. Extrapolation of the initial and final shut–in pressure data provided estimates of the initial reservoir pressure of 2,260 psi and 2,152 psi respectively. This data provides the best estimate of initial reservoir pressure of all tests conducted on the Anasazi/Sahgzie wells.

9.6. Other Paradox Basin Well Tests

Transient test data was available for well tests conducted on wells from the Brown Hogan, Blue Hogan, Mule and Runway. Test data available from all fields, except Runway, were of low quality (sparse sampling and insufficient build–up time) and either were not interpreted or the interpretations that were made were not considered reliable. Thus, since they could not be used to assist in the characterization of the Anasazi/Sahgzie reservoir, they are not included in this report.

Well test data from three Runway wells is of good quality and provided opportunities to determine reliable reservoir properties for individual intervals from each well. Results of these interpretations are provided in a separate Runway report assessing the viability of a CO_2 process.

10. RESERVOIR FLUID CHARACTERIZATION

10.1. Fluid Properties – Experimental Data

Two groups of fluid properties measurements were available for use in developing an equation of state for use in subsequent reservoir mechanistic and reservoir field performance predictions under various operating conditions. The two groups of fluid property data are classified as:

1. Original Reservoir Fluid Properties
2. CO_2 Process Fluid Property Characterization

10.1.1. Original Reservoir Fluid Properties

The first group of data consisted of nine conventional PVT studies[10–1 to 10–8] from eight different Paradox Basin fields. This group of data consisted of conventional reservoir fluid studies conducted on fluid samples normally acquired during initial production tests of the first well in the field. Data available on these studies usually consisted of constant composition expansion (CCE) and differential vaporization tests. These tests provided data on the bubblepoint, oil formation volume factors, solution gas oil ratios and oil compressibility. Reservoir fluid compositions were measured (usually only to the C_{7+} Fraction) and oil viscosity determined over the ranges of pressure used for the CCE tests. Table 10–1 summarizes selected data values from these studies to illustrate similarities or differences in fluid properties from these Paradox Basin Fields.

All the fields listed in Table 10–1 have similar fluid properties except for Runway. The fluid present in the Runway field is different because the methane, ethane, propane and butane content of the Runway Field is considerably higher than other Paradox Basin reservoir fluids. As a consequence the C_{7+} fraction is considerably lower. For example, both Runway fluid samples have methane and C_{7+} mole percents of 34% and 30% respectively. This contrasts to Anasazi, for example, which has methane and C_{7+} mole percents of 19% and 51% respectively. This difference in composition is responsible for the higher bubble point pressure, 2000 – 2100 psi for Runway versus 1023 psi for Anasazi and the higher initial GOR of 1000 SCF/STB versus 360 SCF/STB.

Primarily because of these fluid property differences, the Runway field is being studied separately. The Anasazi/Sahgzie field should serve as a reasonable analogue for the other Paradox Basin Fields because of fluid property similarities.

The Anasazi No. 1 fluid property data set was selected to represent the Anasazi/Sahgzie field and was used to supplement new fluid property measurements in developing an equation of state for the compositional simulation studies discussed later.

10.1.2. CO_2 Process Fluid Property Characterization

10.1.2.1.Compositional Analysis

New fluid property measurements were considered necessary to better characterize the potential of CO_2 flooding processes for the Paradox Basin fields. These new studies were designed to provide an extended compositional analysis of reservoir fluids at current reservoir conditions and to generate CO_2 swelling data. Compositional measurements provide concentration data for 43 components

extended to the C_{30+} fraction. This compares to the 12 component C_{7+} fraction fluid characterization of most of the above listed fluid property studies. The expanded heavy end characterization is required to model the complex CO_2 –crude oil mass transfer process at reservoir conditions.

The initial plan was to sample the newly completed Anasazi No. 6H–1 well during initial production tests. However, because of well productivity problems the Anasazi 6H–1 well could not be produced at a rate required to provide clean oil at a constant producing gas–oil ratio (GOR). Thus, fluid samples (oil and gas) were collected for the Anasazi 5L–3 well and these were recombined to provide the fluid employed in the CO_2 swelling tests. Dead oil samples were also collected from the Anasazi #6H–1 well and together with the Anasazi 5L–3 samples used for extended compositional analysis. The detailed results of these new fluid property measurements are provided in a report by D.B. Robinson [10–9]. Key results of the work are summarized next.

Samples obtained by D.B. Robinson for analysis included:

1. Three separator oil samples (1 gallon each) from the Anasazi 5L–3 separator.
2. Three separator gas samples (500 cc and 300 cc (two samples))
3. Dead oil samples (1 gallon) from the Anasazi 5L–3 location.
4. Dead oil samples (one from the dolomite interval test and one from the limestone interval test) from the Anasazi 6H–1 well.

The composition of these samples is analyzed and reported in Robinson's report[10–9]. One of the separator oil samples (cylinder #W8301) and a synthetic gas with a composition matched to the average composition of the separator gas samples, were recombined at a GOR of 1208 SCF/STB, and used for subsequent experiments. These are discussed below. The oil composition (cylinder W8301) and one of the gas composition data sets are included as Table 10–2 and 10–3 respectively.

Table 10–4 compares the composition of the dead oil samples to the composition of the flashed separator oils. Comparisons of dead oil composition were conducted to assess the uniformity of oil composition in the Anasazi field. The data for Table 10–4 is also presented graphically in Figure 10–1. The plot shows good agreement for all components for the flashed oil sample and the dead oil sample from Anasazi 5L–3. The composition of the two samples from the Anasazi 6H–1 well deviate considerably from the 5L–3 data for components lighter than C_{12}. The limestone unit sample exhibits the largest deviation. The explanation for this difference is not reservoir related. Both Anasazi 6H–1 samples were collected and stored in essentially non–sealed containers with the limestone sample stored outside and subject to large daily temperature changes. Because the containers were not sealed, it is likely that the lighter components of the oil were lost to the atmosphere and since the limestone was collected first and stored outside for several days, it would have experienced the greatest loss of components. The heavier components, C_{12} to C_{30+}, show comparable concentration for all oil samples.

Thus, because of the productivity problem of the Anasazi 6H–1 well and subsequent sample handling of the swabbed oil production, it was not possible to draw any conclusion regarding compositional changes resulting from reservoir related processes. If any composition changes had occurred that were reservoir flow related, it was expected that it would have been reflected in the lighter components. Consequently, the loss of the light ends because of sample storage conditions

has eliminated this opportunity to assess the influence of production and state of reservoir depletion on reservoir fluid composition. However, the similarity of concentrations of the heavier components at least confirms the presence of similar oil in different parts of the Anasazi reservoir.

10.1.2.2.Constant Composition Expansion Test

The reservoir fluid sample generated by recombining the separator oil and gas at a GOR of 1280 SCF/STB was analyzed for composition and used for a constant composition expansion (CCE) test to determine the bubblepoint pressure and the pressure volume isotherm at reservoir temperature. Table 10–5 presents the composition of the recombined sample. Table 10–6 presents relative volume data for the CCE test. The bubblepoint of this mixture was determined to be 2536 psig based on the intersection of the linear best fit line through the single and two phase PV data.

Preliminary reservoir simulation work indicated that if the Anasazi reservoir was repressured after undergoing primary depletion from the time of discovery to the current time, it would establish a single liquid phase (i.e., all free gas would re–dissolve in the liquid phase) at approximately 2050 psia.

Thus, the recombined oil/gas samples, with composition given in Table 10–6, was flashed to 2050 psia at reservoir temperature (130°F) and the liberated gas displaced. The remaining saturated liquid was used for a set of CO_2 swelling tests. Similarly the recombined oil/gas sample was also flashed to 365.5 psia at 130°F. The compositions for these two flash experiments are given in Tables 10–7 and 10–8 respectively. The associated volume of vapor and liquid for each flash condition are summarized in Table 10–9.

10.1.2.3.CO_2 Swelling Test

Starting with the saturated liquid obtained from the flash test to 2050 psia a series of CO_2 swelling tests were conducted to provide data for subsequent equation of state (EOS) calibration work. Swelling tests using 20, 40, 60 and 75 mole % of CO_2 were conducted. By adding known amounts of CO_2 to the hydrocarbon or hydrocarbon – CO_2 mixture, fluid with a known mole percent of CO_2 was created.

For each CO_2 concentration mixture, a constant composition expansion test was conducted to obtain the saturation pressure and a pressure volume isotherm at reservoir temperature. The viscosity of each CO_2 mixture was also measured. The results of the four CCE tests with 20,40, 60 and 75% CO_2 are presented in Table 10–10 and a summary of the saturation pressure, swelling factor and viscosity is presented in Table 10–11.

10.1.2.4.Separator Tests

A two stage separator test was conducted with first stage conditions set at 85°F and 35 psig. The second stage conditions (stock tank conditions) were 60°F and 0.0 psig. The original recombined oil was processed through these separator stages and the GOR data generated by this test is summarized below:

Separator Test Data

Stage	GOR SCF/STB	
	Per Stage	Cumulative
1st Stage Flash	1197.4	1197.4
2nd Stage Flash	20.4	1217.8
Total	1217.8	1217.8

10.2. Equation of State Development

The use of a compositional simulator requires equation of state data to calculate the behavior of the reservoir fluids under various operating conditions imposed on the reservoir. The objective of the subject study was to predict the performance of the Anasazi/Sahgzie reservoir for various CO_2 flood conditions and waterflooding. Prior to conducting reservoir performance predictions the simulator must be calibrated by history matching past reservoir performance. Thus, the simulator must be capable of modelling the initial primary solution gas drive depletion process, subsequent reservoir repressurization and miscible and near miscible CO_2 flooding followed by reservoir blowdown. In addition, reservoir repressurization via waterflooding after approximately eight years of primary production must be modelled. Thus, an equation of state must have the capability of calculating reservoir fluid behavior during each of the various production scenarios. To provide reliable fluid behavior predictions, it is necessary to calibrate the EOS using experimentally generated phase behavior data, employing reservoir fluid samples which are subjected to laboratory processes that emulate reservoir related processes. To calibrate the EOS for the Anasazi/Sahgzie reservoir fluid, both the original reservoir fluid study data plus the newly generated fluid data sets were employed. The original study data provides conditions appropriate for primary depletion process using original reservoir fluid. The new studies used current oil and employed CO_2 swelling tests to provide experimental data points that are expected to cover the CO_2–crude oil mixture likely to be encountered in a CO_2 flood.

The Computer Modelling Group's phase behavior package CMGPROP was used to develop an equation of state conditioned or tuned to the experimental data discussed above. A number of equations of state were set up to analyze and compare experimental data with predicted data. The final EOS selected employed 11 pseudo–components and provided a good match of experimental data, yet was still practical in terms of projected computer resources that would be required to conduct full field simulation studies. CMGPROP has the capability of regression fitting equation of state parameters to a variety of experimental data. The package also provides a number of options to investigate several common laboratory reservoir fluid analysis procedures. These options were employed to "tune" the various versions of the EOS for Anasazi/Sahgzie. EOS parameters adjusted included critical properties of the pseudo components, acentric factors, interaction coefficients and volume shift factors. The experimental data sets employed for EOS tuning included:

1. Saturation pressure measured on original Anasazi Well No. 1 fluid sample.[10–1]
2. Relative oil volume data at 21 pressure levels from the CCE study for the original Anasazi Well No. 1 fluid sample. [10–1]
3. Data for the differential liberation test at nine pressure levels for original Anasazi well #1 fluid sample.

4. Data at nine pressure levels from the differential liberation test for the original Anasazi Well No. 1 fluid. Specific data includes:

    a. Specific gravity of residual oil.

    b. Oil specific gravity at each pressure level.

    c. Relative oil value at each pressure level.

    d. Solution GOR at each pressure level.

    e. Deviation factor for the vapor at each pressure level.

    f. Gas specific gravity at each pressure level.

5. Separator test data for the original Anasazi Well No. 1 fluid.[10–1] This data includes API, oil formation volume factor and GOR.

6. Saturation pressure of the recombined fluid from the Anasazi Well No. 5L–3 study. [10–9]

7. Mass density of the recombined fluid from the Anasazi Well No. 5L–3 study. [10–9]

8. Relative oil volume data at eight pressure levels from the CCE test conducted on the recombined fluid from the Anasazi Well No. 5L–3.[10–9]

9. Data at 2050.0 and 365.3 psia generated by flashing the recombined fluid from the Anasazi Well No. 5L–3 as reported in the Robinson study.[10–9] The data includes mass density of the liquid and volume fractions of the liquid and vapor at each pressure level.

10. Data generated in the CO_2 swelling tests conducted on the saturated liquid sample obtained by flashing the recombined fluid sample from the Anasazi Well No. 5L–3 to 2050 psia and recombining with 0, 20, 40 60 and 75 mole % CO_2. This data included:

    a. Saturation pressure.

    b. Mass density of fluid at the saturated pressure.

    c. Volume fraction of vapor and liquid at several pressure levels of the CCE test conducted on each hydrocarbon– CO_2 mixture.

11. Separator test data generated in the fluid property study[10–9] using the recombined fluid from the Anasazi No. 5L–3 Well. The data included API gravity and GOR.

Using the above experimental data, a 13 pseudo–component equation of state was developed using the regression capabilities of CMGPROP. After a final match of experimental data was obtained, the 13 pseudo–component EOS was again modified to a 11 pseudo–component version and re–turned using the same experimental data set for regression. The number of pseudo–components was decreased to reduce the anticipated computer resource requirements needed for reservoir simulation studies. The composition of the three fluid systems used in conjunction with the experimental data were developed by either lumping or splitting components or pseudo–components from the compositions measured for each of these systems. Two fluid systems are associated with the most recent study,[10–9] and 43 components were measured for these two

systems (i.e. the recombined fluid at 3014 psia and the saturated liquid sample obtained by flashing the recombined fluid sample to 2050 psi). These 43 components were lumped into a 11 pseudo component system and are presented in Table 10–12 and 10–13. The original fluid from samples taken from the Anasazi Well No. 1[10–1] was characterized with 11 components, one of which was the C_{7+} pseudo– component. It was then necessary to recombine components lighter than the C_{7+} fraction and split the C_{7+} pseudo–component. The C_{7+} component was split into six pseudo–components. The distribution of these six components was based on the measured distribution obtained from the fluid obtained by flashing the recombined fluid from the Anasazi Well No. 5L–3 samples[10–9]. The redefined composition of the original fluid is given in Table 10–14. The parameters developed for the final 11 pseudo–component EOS version are provided as Table 10–15. The ability to match experimental data with this set of parameters using the 1978 version of the Peng Robinson EOS is demonstrated in the next Section.

Landmark Graphic Corporation's Desktop PVT software was used to develop a correlation for oil and gas viscosities. The Pederson correlation [10–10, 10–11] was used to predict viscosities. Desktop PVT provides regression capabilities to determine viscosity correlation parameters required by the Pederson model. CO_2 swelling fluid property measurement [10–9] provided viscosity data for various oil–CO_2 mixtures at the saturation pressure of the mixture and reservoir temperature (130°F). Regression provided estimates of the Pederson correlation constants (k_1 to k_7) for calculating the viscosity of the reference components and the binary interaction coefficients for calculating mixture critical temperatures. Table 10–16 provides the Pederson correlation parameters for the 11 pseudo–component fluid characterization.

10.3. Equation of State Validation

The data sets used for comparing predicted versus measured results were identified in the previous Section. The laboratory measured data includes results from the original black oil fluid property study[10–1] and the CO_2 swelling study[10–9]. The 11–pseudo component Peng–Robinson EOS with EOS parameters given in Table 10–15 was used to determine the predicted result in the comparisons.

In the following discussion the following definitions are used in terms of fluid compositions.

1. Composition 1 – Refers to the composition of the initial reservoir fluid as measured and reported in the original fluid study[10–11] (see Table 10–14).

2. Composition 2 – Refers to the composition of the recombined separator fluid from the Anasazi Well No. 5L–3 at a pressure of 3014 psia at a temperature of 70°F (see Table 10–12).

3. Composition 3 – Refers to the saturated liquid composition obtained by flashing Composition 2 to 2050 psia and 130°F (see Table 10–13).

The first set of comparisons used to validate the EOS involves Composition 1 and the associated properties measured on the initial reservoir fluid [10–9]. The bubblepoint calculated by the tuned EOS was 1033.3 psia. This agrees closely with the experimental value of 1037.4 psia. Figure 10–2 illustrates the excellent agreement between the relative oil volume for the constant composition expansion text.

Comparison between predicted and measured fluid property for the differential liberation test data sets are shown in Figures 10–3 to 10–6, inclusive. Agreement is excellent. For example, the relative

oil volume (Figure 10–3) predicted values are within approximately 2% of the measured values, the GOR is within less than 5% of the measured values and other comparisons exhibit a smaller percentage difference.

Using the separator data set for fluid Composition 1 shows API and GOR predicted values of 45.8° API and 362 SCF/STB compared to 42.1° API and 350.0 SCF/STB respectively.

The second set of comparisons illustrating the capabilities of the tuned EOS to predict measured fluid properties employs data associated with the fluid system with Composition 2. The following table compares predicted and measured data and Figure 10–7 compares relative oil volume values for a constant composition expansion test.

Predicted Versus Measured Fluid Properties
Composition 2 – 3014 psia at 70°F

Property	Predicted	Measured
Saturation Pressure – psia	2684.2	2550.6
Single Phase Fluid Mass Density (kg/m^3) at 3014 psia and 70°F	660.9	681.0
Flash to 2050 psia/130°F		
Mass Density (k_g/m^3)	654.4	664.0
Volume Fraction of Liquid Phase	0.848	0.863
Volume Fraction of Vapor Phase	0.152	0.137
Flash to 365.5– psia/130°F		
Mass Density (k_g/m^3)	743.9	741.0
Volume Fraction of Liquid Phase	0.141	0.144
Volume Fraction of Vapor Phase	0.859	0.856

Again, there is excellent agreement between predicted and measured data sets.

The third set of comparisons used to illustrate the calibration of the EOS involves the series of CO_2 swelling tests conducted on mixtures of hydrocarbon (with Composition 3) and CO_2. Figure 10–8 compares predicted and measured saturation pressures for various CO_2 concentrations. The EOS correctly predicted all phase states (all bubble points except the 75% CO_2 case which is a dewpoint), and with the exception of only the dewpoint pressure at 75% CO_2, accurately predicts the saturation pressure values. Because the 75% CO_2 concentration case generated is a near critical fluid and because the saturated pressure measurements exhibit a higher degree of uncertainty in accurately identifying a single dewpoint pressures the discrepancy between predicted and measured values is acceptable. In addition, the volume percent liquid present during the constant composition expansion is matched well (see Figure 10–16), further validating the EOS at high CO_2 concentrations. Figures 10–9 to 10–16 present a comparison of predicted and measured relative oil volumes (ratio of total volume to saturation volume) and percent liquid volumes at various pressure levels for the 20, 40, 60 and 75 percent CO_2 mixtures. All figures show excellent agreement between predicted and measured values. Finally, Figure 10–17 compares predicted and measured swelling factors for the hydrocarbon–CO_2 mixtures studied. This final plot also shows excellent agreement between the two data sets for swelling factors ranging from 1.0 to greater than 2.0.

An additional comparison used separator based data involving processing fluid with Composition 1 through two stages of separation. The comparison of predicted and measured data is given below:

Comparison of Separator Data for Composition 1 – Prediction versus Measured

Variable	Laboratory Value	Predicted Value
Residual Liquid API Gravity (API)	43.1	46.1
Total GOR (SCF/STB)	1217.8	1173.7

The final comparison provides data illustrating the fluid viscosity prediction capabilities of the tuned Pederson viscosity correlation. Table 10–17 compares oil viscosities measured at saturation conditions and 130°F for five mixtures of oil with Composition 3 and CO_2. The Pederson correlation provides a good viscosity prediction capability for the full range of CO_2 concentrations. This data also illustrates that CO_2 is capable of reducing oil viscosity by almost a factor of 2.0.

In summary, the overall match of predicted and measured data for both initial reservoir fluid properties and data generated by a series of CO_2 swelling tests is excellent. Thus, the EOS based on these parameters generated by matching a wide spectrum of laboratory data, will be capable of modelling the complex fluid behavior associated with the primary depletion process and subsequent CO_2 flooding processes. The calibrated equation of state was used to investigate the nature of CO_2 and crude oil interaction via a series of multiple contact experiments at constant pressure and temperature, investigate the phase behavior mechanisms of CO_2 displaying crude oil in a series of mechanistic studies (one and two dimensional simulation studies) and in finally assessing the performance of the Anasazi/Sahgzie Field under various CO_2 and water injection schemes. These various studies are discussed in subsequent chapters of this report.

11. RESERVOIR PETROPHYSICAL PROPERTY DETERMINATION

11.1. General

One of the key data sets required for reservoir recovery process evaluation via simulation is relative permeability data. Although an extensive core inventory exists for the Desert Creek reservoirs in the Paradox Basin area, all cores are in a de–preserved state. With the drilling of the Anasazi 6–H1 well in 1995, an opportunity existed to obtain a fresh core and preserve the core. Preserved cores could then be used to conduct wettability, capillary pressure and relative permeability measurements employing various core preparation procedures. Analysis of the resulting data from these measurements would thus provide guidelines for core preparation in future relative permeability work and furnish a valid data set for future reservoir simulation studies. To this end representative samples from the preserved Anasazi 6H–1 core were taken, based on cat–scan imaging of the core, and used for a suite of capillary pressure, wettability and relative permeability measurements.

Since a representative Desert Creek limestone interval was not present in the Anasazi 6–H well, the tests were performed on samples from the dolomite interval. After the proper core preparation procedures were identified, de–preserved core material from the Anasazi Well No. 1 was used for limestone relative permeability measurements. In addition to the above discussed tests, samples from the Anasazi 6H–1 (dolomite) and Anasazi #1 (limestone) were used for rock compressibility measurements. Because an important part of the production life of the Paradox Basin Desert Creek reservoirs involved liquid expansion and no compressibility data existed, it was important to obtain representative data to use in reservoir performance modeling.

In addition to the gas/oil and oil/brine capillary pressure data generated via ultra centrifuge technology, a suite of mercury injection capillary pressure data was completed. The core samples used for the gas–mercury capillary pressure measurements were end pieces from the plugs used for the gas–oil and oil–brine tests from the Anasazi 6H–1 well (dolomite interval) and the Anasazi No. 1 Well (limestone interval).

Results and a discussion of the results of laboratory programs to determine capillary pressure/relative permeability and rock compressibility are presented in the next two sections. Results and some discussions used extracted material from Westport Technology Center International [11–1, 11–2, 11–3] and TerraTek [11–4] reports.

11.2. Capillary Pressure and Relative Permeability Data – Dolomite Facies

11.2.1. Properties of Fluids Used for Special Core Tests

The brine used in these experiments was a synthetic formation brine using a composition provided by On Site Technologies, LTD. The water analysis was for a sample collected on July 28, 1995 from the Sahgzie #1 separator. The sample was filtered through a 0.45 micron filter (see Table 11–1) after mixing. The original brine was a saturated solution at ambient temperatures and was diluted to 3/4 strength to prevent salt precipitation during the temperature cycling the samples were subjected to in the course of the testing.

The crude oil was obtained from the surface separator for Anasazi 5L–3 well in August 1995 and used after filtering through a 0.45 micron filter at 73°F. Fluid properties were measured from 73°F

to 135°F since fluid saturations had to be measured at ambient conditions and the experiments conducted at 130°F. Data is provided for the oil properties in Table 11–2. The surface and interfacial tension measurements were made using a ring pull tensionmeter and thus are non equilibrium measurements.

11.2.2. Experimental Procedures

The ultra centrifuge experimental procedure followed is outlined below. Data collected was analyzed using techniques published in SPE 25290 [11–5]. The capillary pressure data was analyzed using a constrained Hassler–Brunner modeling technique. The relative permeability experiment is an unsteady state displacement in which only the displaced phase permeability is analyzed. The data is corrected for capillary hold up, invading phase mobility and speed ramp up effects, then fitted to a bimodal Corey model to account for mobility shock production.

The laboratory measurements and procedures were designed to not only provide capillary pressures and relative permeability data for gas–oil and brine–oil fluid systems, but also to investigate the influence of core preparation on the results.

Available cores included preserved cores from the Anasazi Well No. 6H–1 and de–preserved cores from all other Anasazi/Sahgzie Wells. By conducting the full suite of measurements on cores prepared by three different methods, it was possible to identify what method would be necessary for future tests that may use de–preserved cores. Six plugs were selected from the Anasazi Well No. 6H–1 preserved core using whole cores and plug size scale cat scan imaging. Plug size catscan images are presented in Westport's report [11–1] and discussed above in Chapter 4. Three similar plugs were selected from the set and used for the full set of tests with each plug prepared for testing using a different method. The three core preparation methods and sample numbers used to identify the plugs are summarized below. Core plug properties are summarized in Table 11–3.

Sample Identification and Core Preparation Method – Anasazi No. 6H–1

Core Number	Sample Depth – Feet	Core Preparation Method
1a	5,691.21	Solvent Cleaned But Not Aged
1b	5,691.21	Preserved
2b	5,691.21	Solvent Cleaned and Aged

11.2.3. Core Re–Saturation and Effective Permeability to Water (K_{ew}) Measurements

Because of the saturated condition of the reservoir brine, all samples were flushed with the lower salinity brine in an attempt to remove any precipitated salts from the materials. Samples 1a, 1b, 2 and 4a had "as received" flowing permeabilities measured using this brine. Core 2 was then cleaned using a sequential solvent flow cleaning procedure and cut into samples 2a and 2b. Core 1a was then flow cleaned using the same equivalent solvent cleaning technique. Cores 1a and 2b were then brine saturated under 500 psi back pressure and K_{ew} values measured at 100% brine saturation.

11.2.4. Initial Oil/Brine Drainage Experiment and Aging

An initial oil/brine drainage capillary pressure experiment was conducted on Cores 1b and 2b to establish a high initial oil saturation for the aging process. Aging was accomplished for 14 days at

130°F. Near the end of the aging process an oil/brine drainage capillary pressure experiment was conducted on Core 1a to establish a high initial oil saturation without the aging of the other cores.

11.2.5. Brine/Oil Imbibition Capillary Pressure Test

Initial flowing oil permeabilities were measured and then an imbibition capillary pressure experiment was conducted for use in wettability determination. A comparison of the data is given in Figure 11–1. The curve shapes indicate a wetting oil condition, since the oil saturation continues to decrease with increased capillary pressure until a value below 5% remaining oil is achieved near 100 psi. Comparisons of the core entry values indicate a slightly stronger oil wetting condition in the preserved and restored cores over the cleaned but unrestored core.

11.2.6. Effective Water Permeability (K_{ew}) Measurements and Oil/Brine Secondary Drainage Test

The samples were mounted in flow cells with an overburden of 1,000 psi and heated to 130°F. Brine was then introduced and a fluid pressure of 500 psi maintained while the K_{ew} at residual saturation (S_{or}) measurements were taken. The samples were cooled while maintaining the 500 psi fluid pressure. The samples were then placed in the centrifuge drainage cells. The cells were heated to 130°F and a multispeed experiment was conducted to determine the secondary drainage capillary pressure curves presented in Figure 11–2. The curves indicate stronger water wetting in Core 1a, with the preserved Core 1b having the least water wetting condition.

11.2.7. Brine/Oil Imbibition Relative Permeability Test

Initial flowing oil permeabilities were measured and then an imbibition capillary pressure experiment was conducted for use in wettability determination. A comparison of the data is given in Figure 11–3 (curves labeled Imbibition). The initial permeabilities were fixed to the measured initial flowing permeabilities and the data then history matched to produce the curves. The final oil saturation to which the curves are plotted is the final average saturation in the cores. This explains why the saturations are not as low as the capillary pressure final saturations, which are the saturations calculated at the inflow end of the core.

11.2.8. Oil/Brine Drainage Relative Permeability Test

Initial flowing brine permeabilities were measured and then a drainage capillary pressure experiment was conducted for use in wettability determination (Figure 11–4). A comparison of the data is given in Figure 11–3 (curves labeled drainage). The initial permeabilities were fixed to the measured flowing permeabilities and the data then history matched to produce the curves. The final oil saturations to which the curves are plotted is the final average saturation in the cores. This explains why the saturations are not as low as the capillary pressure final saturations, which are the saturations calculated at the inflow end of the core.

11.2.9. Gas–Oil Capillary Pressure Experiment

A gas/oil drainage capillary pressure experiment was conducted at S_{wir} determined by the preceding oil/brine relative permeability experiment. The data presented in Figures 11–5 indicate the expected oil wetting in the presence of gas. The residual oil value of between 0.8 and 2.5% is reflective of

the lack of trapping sites in the core material. The slightly higher capillary entry pressure when compared to the brine/oil system may be reflective of the non equilibrium tension measurements used.

11.2.10. Gas/Oil Relative Permeability Experiment

The samples were mounted in flow cells with an overburden of 1,000 psi and heated to 130°F. Oil was then introduced and a fluid pressure of 500 psi maintained during re–saturation and the effective permeability to oil (K_{eo}) at irreducible water saturation (S_{wr}) measurements taken. The samples were cooled while maintaining the 500 psi fluid pressure. The samples were then placed in the centrifuge drainage cells. The cells were heated to 130°F and a single speed experiment was conducted to determine the gas/oil drainage relative permeability curves to oil presented in Figure 11–6. The curves agree quite well with values of about 5×10^{-4}, at which point the cleaned core begins to deviate because of the inability of the bimodal model to provide a means of fitting the production data. At the conclusion of the experiment a gas permeability at residual oil and water saturation was measured and is presented in Table 11–3.

11.2.11. Final Saturation and Permeability Determinations

A Dean–Stark extraction was accomplished on the core material to determine the final oil and brine saturations to check the weight determined values used in the study. The material was then cleaned using a sequential solvent flow cleaning procedure involving first a 3% KCI brine to remove the precipitated salts from the extraction and then toluene and methanol flushes to properly clean the material.

Gas permeability and porosity measurements were made on the cleaned core material at 500 psi and 2000 psi net confining stress. Data is presented in Table 11–3

The dry cores were weighted and then evacuated, at which time degassed brine was introduced. The core holders were then pressurized to 2,000 psi and held for 16 hours at 73°F. The cores were removed from the cells and weighed. They were then placed in flow permeability cells with an overburden of 1,000 psi and a fluid pressure of 500 psi. Flow was established and when stabilized, the measurement was made (see Table 11–3).

11.2.12. Primary Drainage Capillary Pressure Measurements

After the flowing permeability measurements, the samples were mounted in the centrifuge drainage cells, surrounded with crude oil, and heated to 130°F. Thirteen speed steps were used to define the capillary pressure curves. Each speed was maintained for eight hours before moving on to the next speed. The final average saturations were then extrapolated to infinite time using the production data and a Corey exponent of 2.5 for the extrapolation. The resultant average saturation curve was then converted to the capillary pressure curve at the inflow end of the core using a constrained Hassler–Brunner fit. The samples were cooled to 73°F and weighed for saturation determinations. The resulting curves are seen in Figure 11–4 and indicate a stronger water wetting nature than the secondary drainage curves seen in Figure 11–2. This is evident from the higher entry pressure for the primary drainage curves. There appears to be a slight lowering in the entry pressure of the restored state core and an even lower value for the preserved core. This effect could be caused by a surface oil adsorption which is time dependent and which requires stronger solvent cleaning than was accomplished using toluene and methanol.

11.2.13. U.S.B.M. and Amott Wettability Indices

Both the U.S.B.M. and Amott wettability indices were determined from the primary waterflood and secondary oil flood capillary pressure experiments. The U.S.B.M. index is the ratio of the areas under the two capillary pressure curves. The areas were calculated to a common pressure of 90 psi. The results ranged in values from –0.33 to –0.49. These values are commonly classified as mixed wet values with a slightly stronger oil than water wetting. The Amott results are determined from the ratio of the production during the first speed step of the centrifuge divided by the total production during the experiment. This value is an upper limit for the "spontaneous" imbibition value since a slight amount of pressure was actually applied to the cores to produce the initial fluid. The values indicate no spontaneous water production and 6 to 25% spontaneous oil production. This spontaneous oil production was at an applied pressure of 0.6 psi while the water production values were taken at about 0.2 psi because of the difference in holder and sample configuration during the two experiments. If a spontaneous value for the oil production is calculated by extrapolating the curves to 0.2 psi, the values all become zero as in the water production case. This would be consistent with the U. S. B. M. results of mixed wettability. The higher entry pressure for the oil curves, when compared to the water entry pressures on the preserved and restored cores, support oil wetting. The AMOTT water and oil flood numbers were 0.249 and 0.0, respectively.

11.2.14. Bond Number versus S_{or}/S_{oi}

Figure 11–7 shows the relationship between the S_{or}/S_{oi} values versus the Bond Number for the waterflood capillary pressure experiments. The vertical lines are an artifact of the capillary entry pressure for the experiments. The remainder of the curves from about 10^{-7} to 10^{-5} show a film drainage mechanism common to thinning of oil films with increased pressure. The low residuals between 2 to 6% reflects the lack of trapping mentioned earlier.

11.2.15. Summary

Centrifuge tests were performed on three core plugs to provide oil–brine and gas–oil capillary pressure and oil–brine and gas–oil relative permeability curves. The samples were prepared in three ways: Core 1a was cleaned but not aged, Core 1b was preserved, and Core 2b was cleaned and aged to restore wettability. The tests were performed at 130°F and the confining pressure of approximately 200 psi was provided by shrinkable teflon jackets.

The data indicates a mixed wetting condition typical of carbonate systems with a slightly stronger oil wetting tendency in the preserved core and a nearly neutral wetting for the cleaned and unrestored core with the restored core falling between the others. The dominant feature of the cores is the lack of trapping sites yielding very low residuals in both the oil and brine phases. This feature overwhelms the slight differences in the measured data caused by the different wetting states resulting from the different core preparation techniques, and yields capillary pressure and relative permeability curves that compare quite well. The closest agreement among the various sets of data was between the preserved and restored state cores. Thus, even though capillary pressure and relative permeability data for all three core preparation methods are in relatively close agreement, the restored state option was used to prepare the limestone sample from the Anasazi Well No. 1 for a suite of capillary pressure and relative permeability measurements. The preserved core results for the dolomite facies was selected for generating capillary pressure and relative permeability data for simulation input.

11.3. Capillary Pressure and Relative Permeability – Limestone Facies

11.3.1. General

Centrifuge tests were performed on a core plug from depth 5647 feet 6 inches from Anasazi Well No. 1 to provide oil–brine and gas–oil capillary pressure, and gas–oil relative permeability curves. The sample was cleaned and aged for 18 days at 130°F to restore wettability. The tests were performed at 130°F and the confining pressure of approximately 200 psi provided by shrinkable teflon jackets.

The properties of the fluids used in the tests were the same as those used for the dolomite tests. They are presented in Tables 11–1 and 11–2. The experimental procedures employed are also the same as those used for the dolomite samples and were presented in Section 11–2–2. The only core preparation procedures used for the limestone sample was the restored state method.

11.3.2. Core Re–Saturation and Effective Permeability to Water (K_{ew}) Measurements

Because of the saturated condition of the reservoir brine, the sample was flushed with the lower salinity brine in an attempt to remove any precipitated salts from the material, then cleaned using a sequence of solvents flow cleaning. The core was dried and gas permeability and porosity measurements were made on the cleaned core material at 500 psi and 2000 psi net confining stress. Data is presented in Table 11–4, which also include the dolomite data for comparison. After drying, gas property measurements were taken and then the sample was brine saturated under 500 psi back pressure and K_{ew} values measured at 100% brine saturation

11.3.3. Primary Drainage Capillary Pressure Measurements and Aging

After the flowing permeability measurement, the samples were mounted in the centrifuge drainage cells, surrounded with crude oil, and heated to 130°F. Thirteen speed steps were used to define the capillary pressure curves. Each speed was maintained for eight hours before moving on to the next speed. The final average saturations were then extrapolated to infinite time using the production data and a Corey exponent of 2.5 for the extrapolation. The resultant average saturation curve was then converted to the capillary pressure curve at the inflow end of the core using a constrained Hassler–Brunner fit. The samples were cooled to 73°F and weighed for saturation determinations. The resulting curves are presented in Figure 11–8.

11.3.4. Brine/Oil Imbibition Capillary Pressure Test

An imbibition capillary pressure experiment was conducted for use in wettability determination. The data is given in Figure 11–9. The oil saturation continues to decrease with increased capillary pressure until a value of 13% remaining oil is achieved near 250 psi.

11.3.5. Oil Brine Secondary Drainage Test

The sample was cooled while in the centrifuge and removed for saturation determination. The sample was then placed in the centrifuge drainage cell. The cell was heated to 130°F and a multispeed experiment was conducted to determine the secondary drainage capillary pressure curve, presented in Figure 11–10. The curve indicates a less water wet condition than in the primary drainage case, as evidenced by the lower capillary entry pressure.

11.3.6. Brine/Oil Imbibition Relative Permeability Test

An initial flowing oil permeability was measured and then an imbibition relative permeability experiment was conducted for use in wettability determination., The results are given in Figure 11–11. The initial permeability was fixed to the measured initial flowing permeability and the data then history matched to produce the curves. The final oil saturations to which the curves are plotted is the final average saturation in the core. This explains why the saturations are not as low as the capillary pressure final saturations, which are the saturations calculated at the inflow end of the core.

11.3.7. Oil/Brine Drainage Relative Permeability Test

An initial flowing brine permeability was measured and then a drainage relative permeability experiment was conducted for use in wettability determination. The data is given in Figure 11–11. The initial permeability was fixed to the measured initial flowing permeability and the data then history matched to produce the curves. The final brine saturations to which the curves are plotted is the final average saturation in the core. This explains why the saturations are not as low as the capillary pressure final saturations, which are the saturations calculated at the inflow end of the core.

11.3.8. Gas/Oil Capillary Pressure Experiment

A gas/oil drainage capillary pressure experiment was conducted at irreducible water saturation (S_{wir}) determined by the preceding oil/brine relative permeability experiment. The data presented in Figure 11–12 indicates the expected oil wetting in the presence of gas. The residual oil value is near 16%.

11.3.9. Gas/Oil Relative Permeability Experiment

The sample was resaturated with oil and then placed in the centrifuge drainage cells. The cells were heated to 130°F and a single speed experiment was conducted to determine the gas/oil drainage relative permeability curves to oil presented in Figure 11–13. At the conclusion of the experiment a gas permeability at irreducible oil and water saturation (S_{or} and S_{wr}) was measured and is presented in Table 11–4. The sample was resaturated with oil and a drainage capillary pressure experiment was conducted. The centrifuge was stopped at three speed steps and the sample removed for flowing gas permeability measurements. The data were then fitted to a non wetting Corey Model and presented in Figure 11–13.

11.3.10. Final Saturation Determination via Dean–Stark

A Dean–Stark extraction was accomplished on the core material to determine the final oil and brine saturations, to check the weight determined values used in the study. The material was then cleaned using a sequence of solvents, involving first a 3# KCI brine to remove the precipitated salts from the extraction, and then toluene and methanol flushes to properly clean the material.

11.3.11. U.S.B.M. and Amott Wettability Indices

Both the U.S.B.M. and Amott wettability indices were determined from the primary waterflood and secondary oil flood capillary pressure experiments. The U.S.B.M. index is the ratio of the areas under the two capillary pressure curves. The areas were calculated to a common pressure of 120

psi. The value of +0.51 is commonly classified as a mixed wet value. The Amott results are calculated from the ratio of the production during the first speed step of the centrifuge, divided by the total production during the experiment. This value is an upper limit for the "spontaneous" imbibition value since a slight amount of pressure was actually applied to the cores to produce the initial fluid. The values indicate almost equal spontaneous water and oil production. Amott waterflood and oil flood numbers were 0.3378 and 0.335, respectively.

11.3.12. Bond Number vs. S_{or}/S_{oi}

Figure 11–14 shows the relationship between the S_{or}/S_{oi} values versus the Bond Number for the waterflood capillary pressure experiment. The vertical lines are an artifact of the capillary entry pressure for the experiment. The remainder of the curve from about 10^{-7} to 10^{-4} show a film drainage mechanism common to thinning of oil films with increased pressures. The low residual of 13% reflects the lack of trapping mentioned earlier.

11.3.13. Oil/Gas Imbibition Capillary Pressure Experiment

An oil/gas imbibition experiment was conducted on the core in an effort to determine a trapped gas saturation for the core. The data is presented in Figure 11–15. With an initial gas saturation of 70%, the core trapped 11.2% pore volume of gas. The experiment was conducted to a high capillary pressure to compress the trapped gas and establish a more accurate determination of the trapped gas saturation.

11.3.14. Summary

The presented oil–water and gas–oil capillary pressure and relative permeability data were used to develop data sets for the compositional simulation study. The simulation data sets are presented later (Chapter 13).

11.4. Rock Compressibility Measurements

Compressibility testing was conducted on two carbonate samples obtained from the Anasazi No. 1 and 6H–1 Wells. The core material was shipped to TerraTek by Westport Technology Center International and testing conditions were provided by Rega, Inc. The core material consisted of one sample of unpreserved limestone exhibiting irregular porosity from the No. 1 well, and one unpreserved microporous dolomite sample from the No. 6H–1 well.

Compressibility of a porous medium is defined as the relative volume change caused by a unit change in applied stress. Three types of compressibilities, consisting of the bulk compressibility, C_b, the solid (grain) compressibility, C_g, and the pore volume compressibility, C_p, were determined for both carbonate samples. The bulk compressibility represents the relative changes in bulk volume of the medium the grain compressibility represents the relative volumetric change of the solid portion of the medium, and the pore volume compressibility represents the relative change in pore volume. The sample depth, pre–test bulk density, effective grain density and effective porosity are presented in Table 11–5 below for both samples. In addition to the compressibility determinations, each specimen was loaded under triaxial conditions for determination of quasi–static elastic moduli and Poisson's ratio.

Table 11–5
Pre–test Sample Conditions and Physical Properties For Selected Samples From The Anasazi No. 1 and 6H–1 Wells

Sample Depth (Ft)	Rock Type	Length (in)	Diameter (in)	Pre–Test Density (gm/cm^3)			Porosity* (%)	Permeability to Gas (md)
				Saturated Bulk	Dry Bulk	Grain		
5648.5 – 5648.9	Limestone No. 1 Well	3.724	1.998	2.390	2.244	2.698	16.83	51.45
5692.0 – 5692.4	Dolomite No. 6H–1 Well	3.881	1.997	2.588	2.487	2.814	11.62	0.65

* Effective grain density and porosity determined – reflects only interconnected pore space

Simulated in–situ conditions were used for the compressibility and triaxial compression tests. The testing scenario was based on an approximate average horizontal stress gradient of 0.65 psi/ft, a reservoir (pore) pressure of 2000 psi and a vertical stress gradient of 1 psi/ft (overburden stress). The target in–situ pressures for this test program are shown in Table 11–6 below.

Table 11–6
Target Pressures for Simulated In–situ Conditions

Rock Type	Depth (in)	Target Confining Pressure (psi)	Target Pore Pressure (psi)	Target Stress Difference (psi)	Axial Stress (psi)
Limestone	5648.5–9	3670	2000	1980	5650
Dolomite	4592.0–.4	3700	2000	1990	5690

The TerraTek report [11–4] presents details on sample preparation and testing conditions.

Table 11–7 presents the compressibility and Biot's coefficient under hydrostatic stress conditions. Table 11–8 presents the quasi–static mechanical properties determined from the triaxial compression segment of the compressibility tests. Table 11–9 presents the compressibilities determined under uniaxial strain conditions. Both the bulk compressibility (defined under uniaxial strain boundary conditions as the axial compaction coefficient – C^u_{bp}) and pore volume compressibilities (C^u_{pp}) are provided in Table 11–9. The pore pressure range from which the compressibilities were calculated are also included in Table 11–9.

11.5. Gas Mercury Capillary Pressure Measurements

Gas–mercury capillary pressure curves were determined on two core plugs, Anasazi Well No. 1 from a depth of 5,647.5 feet and Anasazi Well No. 6H–1 from a depth of 5691.21 feet. The gas–mercury curves presented here were generated using an Autopore automated mercury capillary pressure device by Westport Laboratory [11–4].

The mean pore size distribution and capillary pressure data for the dolomite sample from the Anasazi Well No. 6H–1 are presented in Figures 11–16 and 11–17, respectively. Data for the limestone

sample from the Anasazi Well No. 1 are presented in Figures 11–18 and 11–19, respectively. The limestone sample clearly displays a bimodal pore size distribution, whereas the dolomite sample has a unimodal distribution.

The tests compare favorably with mercury injection tests performed by GeoCore for Chuska Energy Company [11–6] in 1990. In the GeoCore study two samples from the dolomite interval and two samples from the limestone interval, both from the Anasazi Well No. 1, were selected for mercury injection tests. The dolomite samples were from depths of 5,616′ – 5,616.3′ and 5,622′ – 5,623′. The limestone samples were from the intervals 5,650.3′ and 5,654′ – 5,655′. The GeoCore tests on the dolomite exhibited a unimodal pore size distribution with a pore entry diameter mode of 7.0 to 18.0 μ m. This agrees with the mode of distribution shown in Figure 11–16 for the sample from the Anasazi No. 6H–1 Well.

The GeoCore tests on the limestone sample exhibited a bimodal pore size distribution with a secondary mode of 0.07 to 0.1 μ m and a primary mode of approximately 100 μ m for pore entry diameters. This also agrees closely with Westport data [11–6] given in Figure 11–18, which exhibits a secondary mode of 0.11 μ m and a primary mode of approximately 90 μ m.

The agreement of the pore size distribution between the Anasazi Well No. 1 and Well No. 6H–1 provides support for the use of a dolomite sample from the Anasazi No. 6H–1 Well, even though it is a marginal producer, for petrophysical property measurements which were applied throughout the field.

12. CARBON DIOXIDE PROCESS MECHANISM STUDIES

12.1. Introduction

One of the preliminary steps in assessing the viability of a miscible process is to analyze the basic process mechanism associated with contacting a reservoir oil with a miscible injectant or solvent. The phase behavior interactions between solvent and oil can be analyzed by using an equation of state and simple process flow calculations. By conducting calculations at a series of pressures for a fixed temperature (say the reservoir temperature), it is possible to identify operating conditions that will support miscible displacement. These conditions can in turn be used to guide subsequent simulation studies. This approach was used with the Anasazi/Sahgzie field. Once a calibrated EOS had been developed, the influence of reservoir pressure on the development of miscibility was studied for two different oil compositions that were measured from Anasazi field samples. This preliminary mechanistic design work is presented and discussed below.

The dynamics of fluid flow can be introduced to the above outlined analysis by conducting one–dimensional compositional simulation studies. The use of one–dimensional simulation provides a means of analyzing in detail an actual displacement process and the associated process of miscibility development. The one dimensional process provides mechanistic insight into the miscible process and essentially represents what a small scale element of the reservoir would experience during a field scale displacement. The influence of fluid flow history, as governed by relative permeability data, and compositional changes on miscibility development were analyzed via a series of one dimensional displacement at different but relatively constant operating pressures. The results of these mechanistic simulation runs are presented and discussed in the following Section 12.3.

An additional mechanistic study was also conducted for the Anasazi/Sahgzie field. This involved two dimensional simulation studies to analyze the field scale reservoir process that could result during primary depletion of the reservoir. This study was used to identify important reservoir production mechanisms and qualitatively assess the impact of specific reservoir parameters on the primary depletion process. The results of this study are presented and discussed in Section 12.4.

12.2. Multiple Contact Phase Behavior of CO_2–Anasazi Fluid Systems

CMGPROP was used to conduct multiple contact experiments using 100% CO_2 as the solvent and the Anasazi crude compositions at two different depletion states to represent the oil. The original oil composition as measured from samples taken from the Anasazi Well No. 1 at discovery was used for one set of runs. The composition of this oil is given in Table 10–14 and is referred to as "original oil" in discussions in this Section. The oil composition used for the second set of tests was obtained from samples taken for the Anasazi 5L–3 well in 1995 and measured by D. B. Robinson [10–9]. This composition is presented in Table 10–13. This oil sample was generated by recombining separator oil and gas samples from the Anasazi Well No. 5L–3 at the well's producing GOR and subsequently flashing it to 2050 psia at 130°F. The remaining liquid was used for CO_2 swelling tests, as explained in Section 10, and is also used for the subject multiple contact experiments. In this Section this oil is designated as "depleted oil".

CMGPROP allows the study of multiple contact processes between a solvent and an oil at constant pressure and temperature. The results are expressed in the form of a ternary diagram. Starting with a solvent and an oil, the ternary diagram construction consists of three steps:

1. Solvent is added to the oil such that the solvent to oil molar ratio increases by a fixed amount at each point, until it becomes pure solvent. Flash calculations are performed at each point to determine the liquid/vapor split. If no two phase region is detected, it is judged first contact miscible and the calculation terminates; otherwise it proceeds to steps 2 and 3.

2. Using the first point in the two phase region detected above, remove all liquid. The remaining gas is combined with the original oil in a specified gas oil ratio. A flash calculation is performed and liquid removed. The procedure is repeated and simulates the vaporizing–gas drive process.

3. Again using the first point in the two phase region detected in Step 1, remove all vapor. The remaining liquid is combined with the original solvent in a specified solvent liquid ratio. A flash calculation is performed and vapor removed. The procedure is repeated until the oil can not be enriched further. This simulates the condensing gas drive process.

The improved oil recovery associated with gas injection processes are attributable to mass transfer effects between the injected fluid and the reservoir oil. Displacement processes can be classified, in a classical sense, by two types of processes:

1. Condensing gas drive: where the solvent, which is rich in intermediate components, through a multiple contact process enriches the in–place oil via condensation of its intermediate components. This usually occurs at the trailing edge of a mixing zone containing solvent and oil.

2. Vaporizing gas drive: where the injected solvent or gas via a multiple contact process is enriched in intermediate components vaporized from the in–place oil. This normally occurs from the front of the mixing zone.

The CO_2 process has been characterized as a vaporizing process [12–1], although some studies have identified it as a condensing process [12–2]. The subject multiple contact study and subsequent one–dimensional compositional studies were used to investigate the process and identify the potential for miscible displacement and the reservoir pressure required to achieve a miscible displacement.

Using the multiple contact option in CMGPROP, a set of numerical experiments were conducted using CO_2, the solvent, and the original oil (as defined above) at reservoir pressures of 2,000, 2,350 and 2,400 psia and a temperature of 130°F. The results are plotted as ternary diagrams in Figures 12–1, 12–2, and 12–3. An additional set of experiments using CO_2 and the depleted oil at reservoir pressures of 2,500, 3,000 and 3,100 psia at 130°F were conducted and the results are plotted in Figures 12–4, 12–5 and 12–6. In these ternary diagrams the following grouping of components is employed for the original and depleted oil cases.

Ternary Diagram Component Grouping – Original Oil

Component	Original Oil Mole %	Dry Gas	LPG	Solvent	Pseudo–Component 1	2	3
CO_2	1.1200	.00	100.00	100.0000			CO_2
C1	19.8409	100.00	.00	.0000		C1	
C2	7.5303	.00	.00	.0000		C2	
C3	6.5103	.00	.00	.0000		C3	
C4 to C5	9.6004	.00	.00	.0000			C4 to C5
C6 to C8	16.8284	.00	.00	.0000	C6 to C8		
C9 to C11	11.9115	.00	.00	.0000	C9 to C11		
C12 to C15	10.2250	.00	.00	.0000	C12 to C15		
C16 to C19	5.8775	.00	.00	.0000	C16 to C19		
C20 to C29	7.0277	.00	.00	.0000	C20 to C29		
FC30+	3.5280	.00	.00	.0000	FC30+		

Ternary Diagram Component Grouping – Depleted Oil

Component	Depleted Oil Mole %	Dry Gas	LPG	Solvent	Pseudo–Component 1	2	3
CO_2	.0000	.00	100.00	100.0000			CO_2
C1	34.2030	100.00	.00	.0000		C1	
C2	14.1570	.00	.00	.0000		C2	
C3	9.4470	.00	.00	.0000		C3	
C4 to C5	8.8880	.00	.00	.0000		C4 to C5	
C6 to C8	11.3440	.00	.00	.0000	C6 to C8		
C9 to C11	6.7730	.00	.00	.0000	C9 to C11		
C12 to C15	5.8140	.00	.00	.0000	C12 to C15		
C16 to C19	3.3420	.00	.00	.0000	C16 to C19		
C20 to C29	3.9960	.00	.00	.0000	C20 to C29		
FC30+	2.0060	.00	.00	.0000	FC30+		

Pseudo ternary diagrams can be used in a qualitative sense to identify multiple and first contact miscibility conditions. The requirements for multiple contact miscibility is that the oil composition be on the right side of the critical tie line (or critical tangent) in the pseudo–ternary diagram. The critical tie line is tangent to the critical point on the two phase envelope and parallel to the tie lines within the two phase envelope connecting the liquid and vapor composition points for each two phase mixture. Figures 12–1, 12–2 and 12–3 represent the original oil, at pressures of 2,000 and 2,350 and 2400 psia. For pressures of 2,000 and 2,350, the original oil composition lies on the left side of the two phase envelope which extends all the way across the ternary diagram. The CO_2 displacement under these conditions would be immiscible. However, above a pressure of 2,400 psia the two phase envelope shrinks, as shown in Figure 12–3 and the original oil composition now lies to the right of the critical tie line. Thus, CO_2 displacements at pressures above 2,400 psi and a

reservoir temperature of 130°F in a reservoir containing oil with a composition the same as the original oil would be multiple contact miscible.

Figures 12–4, 12–5 and 12–6 are a pseudo–ternary representations of a multiple contact process involving the depleted oil composition. At pressures of 2,500 and 3,000 psia, as explained above, CO_2 displacement of the depleted oil would be immiscible. However, at 3,100 psia and above the displacement would be multiple contact miscible.

This qualitative equation of state modelling indicated that the implementation of a CO_2 flood in the Anasazi/Sahgzie reservoirs would likely have to be conducted above a pressure of 3,100 psia to be miscible and significantly reduces residual oil values in areas contacted by CO_2. This guideline was used in both the one–dimensional and full field simulation work discussed below.

12.3. One Dimensional CO_2 Displacement Simulation Studies

The one dimensional simulation results were conducted using the compositional simulator VIP (discussed later – see Section 13.1). The calibrated equation of state parameters presented and discussed in Section 10.2 were used as input data to the simulator for mass transfer calculations. The one–dimensional simulation studies were conducted at essentially constant pressure. Relative permeability data based on laboratory measurement for the dolomite facies, as outlined in Section 11.2, were used in the one–dimensional CO_2 displacement runs. Relative permeabilities and capillary pressure were adjusted as a function of interfacial tension as discussed in Section 13. The one–dimensional model was dimensioned at field scale with the length set to 2,500 feet, width to 2,500 feet and thickness 100 feet. The porosity was constant at 10.0% and the absolute permeability was set to 2,500 md. The permeability was set to a high value to minimize the pressure drop during the displacement and allow the overall system pressure to remain relatively constant. The reservoir was initialized using the original oil composition (see Table 10–14). The initial oil in place was 8,395,500 STB. A single injector in the first block and a single producer in the last grid block were used to inject CO_2 and produce fluid.

Grid sensitivity studies were conducted prior to investigating the pressure required to develop miscibility. Figures 12–7 and 12–8 illustrate the influence of grid size on oil recovery rate and ultimate recovery, respectively. The two cases using 400 and 500 grid blocks exhibited similar recovery. The 500 grid block discretization was used in the simulation runs to investigate the effect of overall system pressure on miscibility. System or reservoir pressures from 1,000 to 3,000 psia were used in this study. Figures 12–9 and 12–10 illustrate the influence of pressure ranging from 2,000 psia to 3,000 psia on oil recovery rates and ultimate recovery, respectively. Figure 12–10 is an expanded view of the cumulative recovery during the last portion of the displacement. CO_2 injection approached miscible conditions at 3,000 psia and even at 2,000 psia the displacement efficiency is over 96% of the OOIP. The CO_2 process operating at 3,000 psi recovers 99.02% of the OOIP. The displacement at 2,000 psia exhibits the highest recovery during the initial part of the displacement. This is attributable to the more extensive transition zone (or mixing zone for CO_2 and hydrocarbon). However, it has the lowest ultimate recovery.

The detailed behavior of the compositional history of CO_2 displacing original oil is illustrated in the following series of plots for a displacements conducted at 2,500 psia and 3,000 psia. Figures 12–11 to 12–22 present the time history of hydrocarbon liquid and vapor saturations and the composition of each component used to characterize the fluid for cell 217 of the 500 cell one dimensional model for the 2,500 psia CO_2 displacement process. Figure 12–11 illustrates the vapor–liquid saturation

change at this grid block and Figures 12–12 to 12–22 present the concentration history of each hydrocarbon component in the liquid and vapor phase at block 217. Figures 12–23 to 12–33 present the concentration history of each component in the vapor and liquid phase at cell 202 for the 3,000 psia CO_2 displacement run.

Examining the 2,500 psia case first (Figures 12–11 to 12–22), the displacement process is characterized by a sharp transition from a 100% liquid system to a vapor dominated system at cell 217 after approximately 640 days of injection. Concurrently with this transition from liquid to vapor, the magnitude of the concentrations of each component in the liquid and vapor phases approach each other. The convergence of concentration to the same value is indicative of the development of a critical fluid and the initiation of a miscible displacement. However, convergence is not complete as clearly shown in the figures for pseudo–components C6–C8 to C30P (Figures 12–17 to 12–22). Thus, the displacement is nearly miscible and exhibits a high displacement efficiency (recovery greater than 98% of the OOIP).

The 3,000 psia displacement case does, however, exhibit apparent convergence of the concentration of each component in the liquid and vapor phases and a critical fluid is formed and propagates through the linear system, giving rise to a miscible displacement and over 99% recovery of the OOIP. Examination of the composition plots illustrates that the CO_2 process is vaporizing (extracting) hydrocarbon components from the liquid phase into vapor phase while CO_2 is condensing into the liquid phase (liquid phase composition of Figure 12–23 shows increasing CO_2 concentration). Prior to formation of the critical fluid, the CO_2 is extracting all hydrocarbon components (even the C30P component) into the vapor phase. Once the critical fluid is displaced from cell 202, it continues to extract or vaporize the lighter hydrocarbon components up to pseudo–component C9–C11. The concentration of CO_2 in the liquid phase reaches a maximum when the critical fluid forms and then stays relatively constant at approximately 75.0 mole %. With CO_2 concentration constant and components lighter than the C9–C11 component continuing to be vaporized, the concentration of the heavier components C12–C15 to C30P in the liquid phase show increasing concentrations. Because of the narrow transition zone (mixing zone) it is difficult to place the physical location of the critical fluid formation, but from examination of the data used to construct the plots it appears to be located at or near the leading edge. Thus, in terms of the Anasazi/Sahgzie Field, the CO_2 displacement is consistent with other interpretations of CO_2 floods.[12–1] That is, the process is a vaporizing process.

As exhibited in the pseudo ternary diagrams presented and discussed in Section 12.2, miscible displacement involving the original oil would require a pressure in excess of 2,400 psia. The one–dimensional simulation results indicate that under dynamic flow conditions, a displacement at 2,500 psia is not fully miscible. Under flow conditions, a pressure between 2,500 and 3,000 psia is needed to develop miscibility. These guidelines were used in setting displacement pressures for the full field model. Sensitivity runs were conducted at different operating pressures and the full field results are discussed and compared to Section 12 guidelines in Section 15.1.

12.4. Two Dimensional Mechanistic Simulation Studies

12.4.1. Introduction

To provide some initial insight into the basic production mechanism of the Anasazi/Sahgzie reservoir, some simple two dimensional compositional simulation studies were conducted prior to

developing final reservoir description models and conducting the final three dimensional simulation study. In addition to gaining insight into possible production mechanism, the simulation studies were used to estimate a fluid bubble point pressure that might be realized if the reservoir was repressured after producing the current volumes of oil and gas. This bubble point data was used for preparing fluid samples for CO_2 swelling tests discussed above.

12.4.2. Model Description

The bulk volume of the reservoir required to roughly match observed pressure–production conditions was established with a series of one dimensional simulation runs that adjusted reservoir bulk volume until a reasonable match of observed production data [gas–oil ratio(GOR)] was obtained. This volume was used to establish the overall volume of the two dimensional model. [2500′ x 2500′ x 100′ – Anasazi reservoir unit only.]

The geologic model was a simplistic two–layer model consisting of a dolomite unit and a limestone unit. The homogeneous layers were assigned an average Anasazi/Sahgzie thickness of 70′ and 30′ for the dolomite and limestone units, respectively. Several simulation runs were used to arrive at an overall vertical to horizontal absolute permeability ratio of 0.02. This gave the best GOR match for the permeability ratios investigated. The dolomite unit was assigned a uniform lateral permeability of 10.0 md and a vertical permeability of 0.2 md. The limestone unit, at the base of the Desert Creek, was assigned a uniform lateral permeability of 200 md and a vertical permeability of 4.0 md. The average uniform porosities assigned the dolomite and limestone units were 10.4% and 9.0%, respectively. An initial oil saturation of 85% and an initial irreducible water saturation of 15% was used. The initial pressure was set to 2260 psia. Studies incorporating both the Anasazi and Sahgzie units as well as just the Anasazi unit alone were investigated. The Anasazi reservoir system results are used here to illustrate the findings. The numerical grid was 200 x–direction blocks, one y–direction block and 20 z–direction blocks. Each geologic unit was assigned 10 layers.

12.4.3. Fluid Properties and Production Data

A preliminary equation of state was developed using black oil PVT data from the Anasazi Reservoir. The Jack Reservoir fluid properties study data was used to provide C_7+ characterization since the CO_2 swelling tests had not been completed prior to the mechanistic study.. A nine pseudo component representation of the fluid was developed which provided a good match of volumetric fluid property data available from the Anasazi reservoir fluid study. The calibrated equation of state was used in the compositional simulator to conduct the simple mechanistic reservoir studies.

As discussed earlier, the actual well by well, and thus field production data, was set up in data files formatted for comparison with simulation production results. The actual historic monthly production data was used as input to the two dimensional simulation during the history match phase.

12.4.4. Simulation Study Procedure

The simplistic two–dimensional reservoir models and compositional simulation were used to history match the production performance of the Anasazi unit through March 1995. The main parameter investigated was the overall vertical to lateral permeability ratio and the degree of communication between the dolomite and limestone units. A qualitative match rather than a detailed match was used for assessing the results.

12.4.5. Study Results

The first result of note was that to provide a reasonable match of reservoir response, particularly during the liquid expansion phase of production, an initial oil in place value of 8.2 MMSTB was needed (Anasazi unit only). This compares to an approximate volumetric value of 5.3 MMSTB. The oil in place needed to support the correct modelling of primary depletion thus exceeds volumetric data by over 3.0 MMSTB. The following full three dimensional studies are used to identify the basis for this difference.

Simulation results for the $k_v/k_h = 0.02$ case (for just the Anasazi reservoir) are presented in Figures 12–34 to 12–40. Figure 12–34 presents field oil production for the Anasazi reservoir versus time. This data was used as input to the model via single well monthly oil rate specifications. Figures 12–35 and 12–36 present the simulation production versus observed field gas production rate and the GOR (predicted value represented by solid line and historic data by + symbol). The match between predicted and observed data is considered reasonable, given the simplicity of the two dimensional geologic model, for understanding basic reservoir production mechanisms. The initial constant GOR period, representing the liquid expansion portions of the depletion, is well matched. The rate of GOR increase and ultimately levelling off is reflecting fluid migration between the dolomite/limestone units and gas segregation via gravity forces. The gas segregation after 1461 days of production clearly shows in Figure 12–40. This Figure shows higher gas saturation build–ups at the top of dolomite (Layer 1) unit and top of the limestone (Layer 11) unit.

Figure 12–37 illustrates the average reservoir pressure declines to the current expected value of 400 to 500 psi. Figures 12–38 and 12–39 represent oil production from and oil in place in the two geologic units, respectively. Figure 12–38 shows that over 90% of the production comes from the limestone interval. However, Figure 12–39 illustrates that despite the major portion of production being from the limestone interval, there is not a corresponding decrease in the oil–in–place in the limestone interval. This behavior clearly supports the gravity drainage of oil from the upper dolomite interval into the lower limestone unit from which the producing wells major share of production arises (Figure 12–39). Using this qualitative assessment prompted further analysis, and since the simulator provides data that summarizes the flow of oil between the dolomite and limestone unit, it was possible to determine the ratio of this flow to the limestone production. The schematic figure below identifies the various fluid rates used in the analysis and the accompanying table provides specific data on the relation of gravity drained oil into the limestone interval versus actual limestone production.

Schematic of Anasazi Reservoir

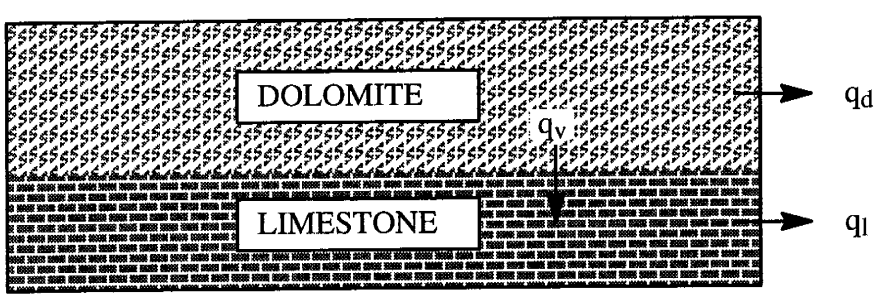

Analysis of Gravity Drainage Behavior

	Fluid Rates			
Month Ending	**q_d: BOPM**	**q_l: BOPM**	**q_v: BOPM**	**q_v / q_l**
1/31/90	1889.7	16,121.3	11,069.1	0.687
6/30/90	1787.0	15,222.9	10,553.6	0.693
1/31/91	2101.5	17,642.0	12,515.9	0.709
6/30/91	3826.0	33,645.9	24,458.2	0.727
1/31/92	2196.0	23,041.2	19,755.1	0.857
6/30/92	1910.3	21,461.6	17,970.1	0.837
1/31/93	1333.2	16,462.2	14,003.1	0.851
6/30/93	683.7	9,127.0	9,310.0	1.020
1/31/94	585.6	8,250.4	8,089.4	0.981
6/30/94	515.9	7,555.3	7,323.7	0.969
1/31/95	529.0	8,153.0	7,241.1	0.888

The above data, specifically q_v/q_l, shows that after June 1993, the production rate from the limestone interval approximately equals the volume of oil draining from the dolomite unit into the limestone unit. This type of production behavior is clearly evident in Figure 12–34. After the relatively rapid production rate decline, the production rate becomes constant at about 300 B/D. This corresponds to the time identified in the table above when q_v approximately equals q_l and is interpreted as representing the slower gravity drainage replenishment of oil in the limestone unit. The impact of dolomite production, q_d, is minimal since it represents a small fraction of the total production. Additional simulation runs projected a 22% recovery factor under primary depletion (through the year 2020).

12.4.6. Summary

The two dimensional mechanistic studies provided the following data and guidelines:

1. Repressurization of the depleted Anasazi reservoir from March 1995 indicated that all the free gas would be dissolved once the reservoir pressure reached 2,050 psia. This pressure was used to prepare fluid samples for the CO_2 swelling tests as discussed in Chapter 10.

2. Late stage production behavior is being controlled and supported by gravity drainage from the Supramound Interval (dolomite) into the limestone unit. The limestone unit contributes the major portion of actual production from the field, but is continually recharged from the Supramound.

3. The vertical to horizontal permeability ratio is a controlling reservoir parameter and is a key variable for history matching the reservoir.

4. The extent of dolomite/limestone communication also plays a key role in reservoir performance. These latter two observations were used in matching full field history as outlined in a later section.

13. RESERVOIR PERFORMANCE STUDY–SIMULATION MODEL SET UP

13.1. Simulator Selection

Because CO_2 flooding was to be investigated, a compositional simulation approach was necessary to account for the complex interphase mass transfer between hydrocarbon fluids and carbon dioxide. The ability to model immiscible – miscible flow transitions and incorporate the influence of interfacial tension on capillary pressures and relative permeability was required. The accurate prediction of hydrocarbon volume changes (swelling) and viscosity reduction when mixed with CO_2 is required to model convection flow. In addition to assessing the potential of CO_2 based processes, the primary production period (solution gas depletion) and waterflooding required simulation. History matching the primary production period was required to validate the reservoir models selected for reservoir performance simulation. Thus, the use of a compositional simulation approach was again deemed necessary for the primary depletion stage because of possible reservoir fluid composition changes that could impact future CO_2 processes. Although the primary depletion history could have been matched using a conventional black oil simulator, this would not have provided reservoir fluid composition data at the end of history. Reservoir fluid compositions are required for subsequent CO_2 process evaluation. Since both primary production and CO_2 process simulation required a compositional simulator approach it was convenient to employ the same simulation to assess waterflooding.

Landmark Graphics Corporation's (Formerly Western Atlas Software, Inc.) VIP–EXEC suite of software was selected for the reservoir simulation portion of the study. The VIP–COMP module of VIP–EXEC was employed. VIP–COMP is a n–component equation of state based reservoir simulator that can model fluid property changes associated with both pressure and fluid composition changes and incorporate multi–phase flow (three phases oil, gas, water) subject to viscous, gravity and capillary forces. Fluid properties and mass transfer between fluid phases are governed by a generalized cubic equation of state. The Peng–Robinson option was selected from several EOS options available in VIP–COMP for modeling the Anasazi/Sahgzie fluid system. This selection directly utilized EOS parameters determined and discussed in the Fluid Characterization work outlined in Chapter 10. VIP–COMP treats both oil and gas as mixtures containing an arbitrary number of hydrocarbon and non–hydrocarbon components. In addition, VIP–COMP provides a full spectrum of practical field operating condition options to model wells, various reservoir processes and complex geologic descriptions of the reservoir system.

13.2. Fluid Properties

A generalized n–component equation of state compositional simulator requires a full set of EOS parameters for the particular EOS employed. As indicated above, the Peng–Robinson EOS option in VIP–COMP was used. The EOS parameters employed in the simulation were developed by calibrating the EOS using a suite of experimental data. The EOS calibration and validity of the calibration were discussed and presented in Chapter 10. The EOS parameters developed for the above pseudo–component fluid system characterization were presented in Table 10–15 and were used as input data for VIP–COMP.

The hydrocarbon system viscosity as a function of pressure and composition was modelled using the Pederson [10–10,10–11] model. Parameters and validation of the model were also previously presented in Chapter 10. These parameters were also used directly as input data for the compositional simulator.

In a miscible displacement, parts of the reservoir will experience a transition from immiscible to miscible flow. Thus, some regions of the reservoir will experience fluid composition histories that lead to a critical point of the hydrocarbon mixture. For elements of the reservoir near the critical point, the composition of the vapor and liquid phase, when two phases exists, are nearly identical. Thus, interfacial tensions and capillary forces become small and approach zero. Also, the residual oil saturation decreases and the gas and oil relative permeability functions approach straight lines (linear functions of phase saturations). VIP–COMP provides an option that adjusts relative permeability and capillary pressure as functions of interfacial tension. Gas–oil interfacial tensions depend on composition and in VIP–COMP were calculated using the parachor approach[13–1]. A reference gas–oil interfacial tension of 12.74 dynes/cm and a threshold interfacial tension of 1.0 dynes/cm, below which the relative permeability adjustment is activated, was used in the simulation study.

In addition to the vapor and liquid phase properties of the hydrocarbon system defined by input EOS parameters, water properties were defined for the initial irreducible water phase present in the reservoir. Water density, water formation volume factor, viscosity and compressibility were defined as constants for the system studied.

13.3. Rock Properties

General purpose multi–phase reservoir simulation requires the use of relative permeability and capillary pressure data. Both gas–oil and water–oil capillary pressure and relative permeability data sets for the two principal production facies of the Anasazi/Sahgzie System were measured. This data was presented and discussed in Chapter 11. This data was adapted for use in VIP–COMP. The adjusted capillary pressure and relative permeability data actually employed in VIP–COMP for the principal dolomite and limestone facies are presented in Figures 13–1, 13–2, 13–3 and 13–4. Variations of these data sets were employed for the various facies identified in the Reservoir Characterization portion of the report (Charter 4) and employed in VIP–COMP (used 12 different rock types). The two phase sets of relative permeability (gas–oil and oil–water) were, as outlined above, selected from laboratory measurements for each main facies. For three phase flow VIP–COMP has several options for calculating the relative permeability to oil. The Stone II model[13–2, 13–3] was selected to predict three phase oil relative permeability. Since the subject field produces little water, the selection of three phase oil relative permeability models was not significant in simulating primary production or processes involving CO_2. It does impact waterflood predictions during fill–up. However, as will be discussed later, waterflooding is projected to be a marginal process for improving fluid recovery and thus again, the selection of a three phase oil relative permeability model is not of major concern.

Rock compressibility was treated as facies dependent within VIP–COMP and was based on laboratory measurements presented and discussed in Chapter 11. Laboratory values of 2.33×10^{-6} vol/vol/psi and 3.18×10^{-6} vol/vol/psi were used initially for the limestone and dolomite based facies, respectively. Rock compressibility values were subsequently adjusted during the history matching work. These adjustments are discussed further in Chapter 14.

Facies dependent reservoir parameters such as absolute permeability, porosity and thickness are discussed below in Section 13.4 on Reservoir Characterization Data.

13.4. Reservoir Characterization

Reservoir characterization includes the following data:

1. Reservoir geometry, including both areal and vertical (total thickness) definition.
2. Spatial variations of the various rock types or facies included in the model. Twelve rock types or facies were identified and used in the reservoir simulation work. The relations between the geologic lithotype and simulator rock type indicator (ISAT) are given below

Lithotype Definition

Simulator Rock Type Index	Lithotype
1	Tight Mudstone
2	Dolomitized Mudstone
3	Enhanced Porosity Mudstone
4	Tight Packstone/Wackestone
5	Enhanced Porosity Packstone/Wackestone
6	Enhanced Porosity Grainstone
7	Cemented Grainstone
8	Tubular Tempestites
9	Phylloid Algal Limestone
10	Mound–Front Breccia
11	Low quality mixed lithotypes
12	High quality mixed lithotypes

3. The structural depth variation of the reservoir.
4. The porosity and permeability defined as spatial variables for all reservoirs and non–reservoir rock.
5. The thickness of each rock type and its spatial variation.
6. Rock compressibility which is associated with each rock type and thus varies spatially within the reservoir.

Three dimensional data files were generated for each of these reservoir description parameters and used for VIP–COMP input data. The generation of data and the presentation of selected samples of the data were previously given in Chapters 4 through 7.

13.5. Field/Reservoir Operational Data

The actual drilling/completion schedules and the timing of each well's start of normal production operations were used as input to the simulator. The wells and total field production history was used to set monthly production schedules and this was in turn used as simulator input data. Oil production history was used to specific monthly production for each well and used as simulator input data from the initial production start up on November 1, 1989 through December 31, 1996. The gas production history and reservoir pressure measurement were employed as observation data to help in history matching the simulator to observed field performance. Individual well and total field production history was discussed and graphically presented in Chapter 8.

Simulation of reservoir performance past December 31, 1996 (prediction phase) did not invoke any production cut offs (i.e. gas–oil or water–oil ratios) or minimum economic rate specifications. Wells were modelled as being "pumped off" with a bottomhole pressure set at 15.0 psia.

13.6. Well Modelling

Actual well completion data was honored in the simulator. Only numerical layers that were perforated during the wells completion were active and could contribute to a well's production.

Well productivity indices were calculated for each well using initial production and well test data and used for initial input data to the simulator. Well productivity indices were subsequently adjusted during the history match to allow wells to meet specified oil production rates without bottomhole pressure constraint violations.

13.7. Separator Specifications

VIP–COMP provides different options for conducting separator calculations for prediction of surface recovery rates. Since the EOS was calibrated to both separator and reservoir condition data (see Chapter 10), a separate set of EOS parameters was not used for separator calculations. Separator conditions were specified to approximate field conditions with the first stage operating at 110°F and 50.0 psia and the second stage at 70°F and 14.65 psia.

13.8. Reservoir Gridding and Region Definition

A rectangular model that includes mound and off–mound Desert Creek carbonates was used in the simulation study. The areal description of the model contained 1,500 grid blocks, fifty grid blocks in the x–direction and 30 blocks in the y–direction. Each areal grid measured 105 feet by 105 feet. The interval of the Desert Creek used in the simulation study was sub divided into 15 layers. Layer thickness varied spatially. Figure 13–5 illustrates the areal grid system. Figures 13–6 and 13–7 illustrate the vertical gridding employed for a y–direction cross section and an x–direction cross section respectively. The vertical thickness is not scaled relative to the lateral dimensions for these illustrative plots.

To assist in understanding the fluid flow behavior within the Anasazi/Sahgzie reservoir system and to facilitate the history matching of the primary production phase, the region option of VIP–COMP was employed to partition the system into subregions. The region option provides fluid influx and efflux, pressure, fluid volume production and average fluid saturations histories of each region identified in the simulation model. The Anasazi/Sahgzie system was subdivided into the following eight regions.

Region Definition for Full Field Simulation

1.	Off–mound Area	Supramound Interval	Anasazi Mound
2.	Mound Area	Supramound Interval	Anasazi Mound
3.	Off–mound Area	Core Mound Interval	Anasazi Mound
4.	Mound Area	Core Mound Interval	Anasazi Mound
5.	Off–mound Area	Supramound Interval	Sahgzie Mound
6.	Mound Area	Supramodel Interval	Sahgzie Mound
7.	Off–mound Area	Core Mound Interval	Sahgzie Mound
8.	Mound Area	Core Mound Interval	Sahgzie Mound

Figure 13–8 illustrates the eight different regions for a y–direction cross section through both the Anasazi and Sahgzie mounds. Figure 13–9 illustrates the areal extent of the selected regions for the Core Mound Interval.

Using these region definition it was possible to understand and quantify the influx and efflux of oil and gas from the Supramound storage units to the Core Mound production units. The simulator provides both tabular and graphical output of data for each region as a function of time. Also, the historical variation of fluids in place, saturation and pressure of each region were used to understand the performance of the Anasazi/Sahgzie system. Reservoir performance interpretations using regional data are presented in Chapter 14. These regions are identified respectively as:

1	OMA–SMI	–	Anasazi
2.	MA–SMI	–	Anasazi
3.	OMA–CMI	–	Anasazi
4.	MA–CMI	–	Anasazi
5.	OMA–SMI	–	Sahgzie
6.	MA–SMI	–	Sahgzie
7.	OMA–CMI	–	Sahgzie
8.	MA–CMI	–	Sahgzie

in Figures 13–8 and 13–9.

13.9. Simulation Initialization

Initial reservoir data indicates that the Anasazi/Sahgzie reservoirs were under–saturated, with an initial reservoir pressure several hundred psi above the bubble point pressure of the reservoir fluid. Thus, no initial gas cap was present and no gas–oil contact existed in either reservoir. Further, since no significant free water production occurred and no active aquifer support exists, the model was initialized without an oil–water contact. Initial fluid saturations were not varied and the initial water saturation for dolomite associated rock was set at 8.41% and for limestone associated facies at 11.55%, based on previously presented capillary pressure / relative permeability measurements (Chapter 11)

The initial reservoir pressure identified in the first set of transient well tests conducted on the Anasazi Well No. 1 and the Sahgzie Well No. 1 provided values considerably lower than values obtained during the bottomhole fluid sampling of Anasazi No. 1 (prior to the first production test) and during the initial drillstem test of the Sahgzie Well No. 1. Referring to Chapter 9, initial transient tests conducted on the Anasazi Well No. 1 provided estimates of the initial reservoir pressure that varied from 1,653 to 1,664 psi, depending on the reservoir model selected. This compares to a pressure of 2,268 psi at 5,622′ recorded during bottomhole fluid sampling prior to production tests. Again, referring to Chapter 9, results on the initial Sahgzie Well No. 1 transient test provide initial reservoir pressure estimates that varied from 1,618 to 1,686 psi, depending on the reservoir model selected for the test interpretation. However, the initial drill stem for Sahgzie No. 1 provided an initial pressure of 2,260 psi at 5,558′. Since the higher value of pressure obtained for both Anasazi No. 1 and Sahgzie No. 1 were obtained prior to any major production testing, they are considered more representative of the true initial pressure condition. Thus, the reservoir simulator was initialized at 2,297.7 psia at a datum depth of 870 feet subsea. The use of this higher pressure was later verified during simulation of the liquid expansion portion of the primary depletion production period.

14. RESERVOIR PERFORMANCE - HISTORY MATCH

14.1. Introduction

The history match of the Anasazi/Sahgzie reservoir system during the primary production phase used historical monthly oil production data for each well as simulator input information. With the monthly oil data specified for each well, the simulator predicts the associated gas production, fluid composition, fluid saturations and reservoir pressure as functions of time. The production period used for history matching began on November 1, 1989 (field startup) and ended December 31, 1996. The principal variables used for history matching were the gas production history of each well and for the entire field, and local reservoir pressure at wells for which field data (either pressure build–up test data or fluid level data) were available. Because of the complexity of the lithology and the lack of detailed information on reservoir geometry, history matching of individual well performance and the field was difficult. To improve the agreement between prediction and observed reservoir data a number of reservoir related variables were modified. Listed below are the reservoir parameters which were investigated in terms of their influence on reservoir performance.

1. Complete reservoir description represented by the stochastic reservoir models described in Chapters 5,6 and 7.
2. Local areal (volume) adjustments of principal productive facies.
3. Local changes in porosity and lateral permeability of specific facies.
4. Facies specific changes in vertical permeability.
5. The addition of lateral and vertical fluid flow barriers between some well pairs, between a well and adjacent reservoir quality rock and between reservoir intervals (i.e. between the Supramound and Core Mound Intervals).
6. Rock compressibility.
7. Rock compaction.
8. Relative permeability functions.
9. Initial fluid compositions to accommodate changes in the initial producing GOR during the liquid expansion portion of reservoir production.
10. Adjustment of productivity indices of production wells.

14.2. Review of History Match Studies

Over 100 history match runs were conducted to arrive at the final history match. These history match runs involved various combination and or permutations of the reservoir parameters listed in the previous Section. Because of the large number of history match runs completed and because the influence of some changes were not assessed in conjunction with changes adopted later to improve the history match, it is not useful to review in detail each history match run. Rather, only the changes in reservoir parameters that were retained for the final history are discussed in terms of the need for adjusting these parameters relative to what was employed in the initial base model.

Early history match runs assessed the sensitivity of reservoir performance predictions to different stochastic realizations of the overall reservoir model. This included two geostatistical realizations (Model 1 and 17), an "upscaled" model using a 50 layer geostatistical realization for input and a homogeneous anisotropic model. The "upscaled" model employed a VIP based upscaling algorithm which provided values of porosity, lateral and vertical permeability and layer thickness for the reduced layer model (15 layers from 50 layers). The homogeneous model employed constant value for porosity and permeability for each main facies. The property used in the homogeneous model were:

	Limestone*	Dolomite**	All other Facies
Lateral Permeability (md)	200	10	2
Vertical Permeability (md)	10	2	0.2
Porosity	0.1	0.125	0.075

Although all models required modification to obtain a match between predicted and observed production data one of the geostatistical models was selected as the most representative. This Model 17, in conjunction with the specified fluid characterization, was used to generate production predictions that more closely matched observed data. It was selected as the model to conduct the final history match. The main reservoir description changes that were implemented in the model to obtain the final match were:

1. Vertical permeability.
2. Inclusion of transmissibility barriers.
3. Adjustment of reservoir pore volume via changes in porosity.
4. Expansion of the Core Mound Interval.
5. Local modifications to lateral permeability.
6. Adjustment of the initial (above bubblepoint) solution gas oil ratio of the fluid system via an initial fluid composition change.
7. Changes in rock compressibility values.
8. Miscellaneous reservoir parameters changes.

The necessity and justification for implementing each of these changes are discussed in a general context below. Each of these changes was adopted only after many history match runs were completed and the sensitivity of predicted reservoir response was quantified and supported the change. The change in reservoir descriptions also required generic justification from a geologic standpoint. Geologic justification is some cases involved direct data such as well log information, in other cases it was simply that a proposed change did not conflict with existing geologic data and/or geologic interpretation.

Vertical Permeability

The two dimensional mechanistic study conducted on a simplified representation of the Anasazi reservoir which was presented and discussed in Chapter 12 clearly illustrated one of the important

* Rock Type 9
** Rock type 3 or 5

production mechanisms associated with the Anasazi/Sahgzie field. This mechanism is the vertical segregation of liberated solution gas as reservoir pressure decreases. The segregated gas forms a secondary gas cap in the Supramound Interval and assists in moving oil from the principal reservoir storage unit into the lower limestone unit in the Core Mound Interval. Oil transfer is governed by gravitational forces and displacement by an expanding secondary gas cap. This production mechanism is also operational in the full field three dimensional simulation runs. It will be subsequently illustrated in a later Section which presents saturation maps for the final history match.

One of the key reservoir parameters controlling gas segregation and oil drainage is the vertical permeability of the rock facies overlying the Core Mound Interval. The geostatistically generated realization of the geologic models used in the simulation studies utilized vertical permeability that were based on whole core analysis from the Anasazi No. 1 and No. 5L–3 wells. To obtain the final match of predicted and observed gas production history it was necessary to adjust these initial values of vertical permeability. Initial vertical permeability values were too low and thus retarded gas segregation and caused the simulator to over predict gas production. One of the main focus areas in the history match was adjusting the magnitude and areal distribution of vertical permeability changes. The final adjustments involved increasing the original assigned vertical permeability of all rock types in the Supramound Interval by a factor of 7.5. The increase in vertical permeability was further restricted to the Supramound Interval of the Anasazi mound area east of the barrier (discussed later) inserted between the Anasazi Well No. 1 and the Anasazi Well No. 5L–3. Vertical permeability to the west of this barrier and in the Sahgzie mound were not changed, although changes in this area were systematically investigated in the various history match runs that were conducted. Final values used for vertical permeabilities are available in data files for VIP–COMP as well as in the original geostatistical models.

Transmissibility Barriers

History matching of reservoir performance supported the use of transmissibility barriers in both the Anasazi and Sahgzie mounds. In the Anasazi mound, to obtain a reasonable match of gas production for the Anasazi Well No. 1 and the Anasazi Well No. 5L–3, it was necessary to restrict the fluid flow between the two wells from that which was used in the unaltered geostatistical geologic model. Without a flow restriction between the two wells, production interference prevented a simultaneous match of the gas production of both production wells. The flow restriction are barriers placed approximately midway between the two wells and traversed from northeast to southwest through the mound area. This barrier was restricted to the bottom ten layers of the model. Thus, it included the entire Core Mound Interval and the bottom third of the Supramound Interval (simulation model layers 6 to 15 inclusive). Well production history and the overall Anasazi reservoir history support communication between the Anasazi No. 1 and No. 5L–3 wells. But, to obtain a match of gas production, the interwell transmissibility provided in the base geostatistically generated geologic model needed to be reduced. Again, several history match runs were used to position the barrier and the degree of transmissibility reduction applied. Communication strictly via the Core Mound Interval was not viable. In addition, complete isolation could not be supported, based on individual well production histories. Thus, a partial fluid flow restriction or barrier was adopted for the final match.

As currently interpreted (see Isolith map Figure 5–1), there is a re–entrant of lagoonal deposits (low permeability) which reduces phylloid algal limestone build–up immediately to the north of the main Anasazi mound. This feature could extend further south and possibly change the main mound

geometry from a "biscuit" shape to a "horseshoe" shape, thereby reducing Anasazi Well No. 1 and Well No. 5L–3 interwell communication. Lack of more detailed seismic data does not allow a more definitive geometric interpretation of the main Anasazi mound. Thus, incorporation of reduced fluid flow communication between the subject two wells could have geologic support, but there is no direct geologic evidence to support its inclusion in the model. The main support for its inclusion is associated with requirements of the history matching of the primary production period.

In matching gas production and reservoir pressure history of the Sahgzie Well No. 1, it was also necessary to introduce a flow restriction (or transmissibility reduction). To obtain the final match of the Sahgzie Well No. 1 gas production and reservoir pressure, it was necessary to restrict communication between the northern and southern segments of the Sahgzie mound.

Using the original geostatistically derived geologic model in initial simulation runs resulted in Sahgzie mound pressures that were several hundred pounds higher than observed field data. Support for this excess pressure was associated with the Sahgzie mound pore volume and the unrestricted north–south communication within the mound. To reduce computed Sahgzie mound pressure it was necessary to restrict north–south fluid flow and reduce the Supramound pore volume (discussed later). The reduction in mound pressure also enhanced gas production and improved the gas production match. To reduce north–south communication a transmissibility reduction (a barrier) was placed approximately in the middle of the main mound with a east–west trend. The actual north–south location was determined through a series of simulation runs assessing the impact of barrier placement on production. The final location is at the simulation y–direction grid block number eleven. Again, the vertical extent of the barrier included the entire Core Mound Interval and the bottom third of the Supramound Interval (simulation model Layers 6 to 15 inclusive). Simulation runs investigated several combinations of vertical flow restrictions (between the Supramound and Core Mound Intervals) and lateral barriers. The final selection was the lateral east–west barrier at y–direction grid block eleven.

Again, as in the Anasazi mound, there was no direct geologic evidence supporting the barrier placement and justification was based on primary production history match requirements. However, the interpreted seismic data supports a lower quality reservoir rock area trending east–west which separates the north and south portions of the Sahgzie mound. This east–west trend was used to guide the placement of the transmissibility barrier in the simulation studies.

Pore Volume Adjustment

As outlined above, the original geostatistically derived geologic model provided too much pressure support relative to field measurements. The pressure support was associated with the total pore volume in communication with the Sahgzie Well No. 1. To improve the match between observed and predicted Sahgzie mound pressures, the fluid flow between the north and south lobes of the Sahgzie mound was restricted (see transmissibility barrier discussion above) and the Supramound pore volume reduced.

The final pressure match employed a model with the Supramound Interval porosity for Lithotypes (3, 5, 6, 8 and 12) reduced by 50% within the Sahgzie mound area. Lithotypes are correlated with lithofacies in Chapter 13, Section 4. Thus, both porosity reduction of selected lithotypes as well as restricted north–south flow was implemented in the Sahgzie mound to improve the mound pressure match and overall gas production match.

The porosity reduction applied to the Supramound was justified to some extent by the partial plugging by anhydrite of the Supramound Interval in the Sahgzie Well No. 1 (Figure 4–6). This reduction in porosity was further extended to the entire Sahgzie mound in select facies to assist in obtaining a pressure history match. Extension of the partial plugging to the entire mound area was also supported geologically via a comparison of the depositional environment of the Sahgzie mound and the Aneth field (this was previously discussed in Chapter 4.)

Since there is no direct evidence for a Sahgzie mound wide porosity reduction in the Supramound Interval, it is also possible that a different transmissibility barrier–porosity reduction combination could have supported retention of the original Supramound porosity in the northern lobe of the Sahgzie mound. Even though several history match runs investigated different transmissibility barriers and porosity reduction combinations, these sensitivity runs were not exhaustive in their scope. Thus, it is still possible that an alternate interpretation exists, from a geologic model standpoint, that would provide a comparable history match for the Sahgzie well.

Expansion of Core Mound Interval

The implementation of a transmissibility barrier between the Anasazi Well No. 1 and Well No. 5L–3 was required to simultaneously match the historic gas production of both wells. Additional geologic description changes were required to improve the Anasazi Well No. 5L–3 match. Implementation of a barrier effectively reduced the pore volume contributing to the pressure and oil production support of the Anasazi 5L–3 well. Thus, it was necessary to extend the mound to the southwest of the Anasazi Well No. 5L–3. Approximately 3.5 acres of additional mound (both Core Mound and Supramound Intervals) were added to the geostatistically derived reservoir model. The additional mound volume in this area improved the overall gas production match and sustained late time primary oil production to be consistent with observed oil production rates.

The lack of seismic data southwest of the Anasazi Well No. 5L–3 was used to qualitatively support extension of the mound in this direction.

Local Modification to Permeability

The history match used, without modification, the original geostatistically derived lateral permeability of the base geologic model. Only in a restricted area adjacent to the Anasazi Well No. 5L–3 was it necessary to adjust the geostatistically assigned permeabilities. The original base geostatistical model restricted the communication between the Anasazi 5L–3 Well and the better quality permeability areas of the Supramound Interval outside of the immediate Anasazi 5L–3 Well vicinity. Oil production history of the Anasazi Well 1 and the Anasazi Well 5L–3 supported some changes in the lateral permeability in the vicinity of the Anasazi Well No. 5L–3. To improve the gas production match and sustain oil production at the observed level, the Supramound Interval lateral and vertical permeability in the vicinity of the well were increased from the base model values. This modification increased the lateral and vertical permeability by factors ranging from 2.0 to 10.0. The areal extent of the modifications around the Anasazi 5L–3 well varied from 6.0 to 15.0 acres and were applied to simulation layers three through nine (the major portion of the Supramound Interval). The enhancements applied to each layer were obtained via a qualitative assessment of the magnitude and spatial distribution of the permeability near the Anasazi Well 5L–3. The goal was to increase the permeability, but to restrict changes so that the enhanced permeability found near Anasazi 5L–3 was more consistent with permeability in the same layer further removed

form the well. These changes increased Supramound connectivity within the Anasazi Well No. 5L–3 drainage area and decreased the heterogeneity in the vicinity of the well. These changes, as pointed out above, assisted in improving the history match for the Anasazi Well 5L–3.

Solution Gas Oil Ratio Modification

The solution gas oil ratio measured in the differential vaporization test of the bottomhole fluid samples[10–1] taken from the Anasazi Well No. 1 was 387 SCF/STB at the measured bubblepoint pressure of 1023 psig. This and other data were used to tune the equation of state used in the compositional simulator as outlined in Chapter 10. As a result, the predicted initial gas–oil ratio (GOR) by the equation of state was close to this value. However, the field measured producing GOR during the liquid expansion phase of primary production was approximately 274 to 300 SCF/STB (See Chapter 8 data). The field production data provide an estimate of the initial GOR which is lower than the laboratory reported values.

During the history match phase most simulation runs produced too much gas, and the liquid expansion production phase exhibited GOR's 50 to 60 SCF/STB higher than the observed field values. To improve the GOR, and equivalently the gas production rate, match during the liquid expansion phase of production, the initial (GOR) predicted by the tuned equation of state was adjusted.

Because of the discrepancy between the reported production and laboratory based GORs, it was deemed necessary to adjust the equation of state predicted values which were "tuned" to the laboratory data. Because the laboratory data was based on a bottom hole sample and there was no surface production samples that could have been recombined at the correct field GOR rates, an adjustment of predicted GOR is appropriate. Further, no attempt was made to adjust the reported GOR of the bottomhole sample to be more consistent with field data.

The equation of state was used to generate liquid and vapor compositional data under field separation conditions. The vapor and liquid phases were then recombined at the field reported GOR (approximately 300 SCF/STB) during the liquid expansion portion of primary production. The overall composition computed from this recombination experiment was then used as the reservoir fluid composition for initialization of the simulator. With the revised initial reservoir fluid composition, the bubblepoint pressure required reduction from 1033.3 psia to 892.4 psia.

The adjustment of initial composition to improve the initial producing GOR match also assisted in matching individual well and total field gas production for both the liquid expansion phase of primary production as well as later production, once the reservoir pressure decreased below the bubblepoint pressure of the reservoir fluid. The revised initial fluid composition was retained for the final history match.

Rock Compressibility Modifications

Initial history match runs used previously reported laboratory measured[11–2] rock compressibilities. Several history match runs were completed to assess overall reservoir production sensitivity to changes in rock compressibility for the main production facies. Rock compressibilities changes were used to access their impact on the duration of the liquid expansion portion of the primary production period (largely controlled by rock and liquid compressibilities) and overall

reservoir pressure reduction during the dissolved gas production phase and the concurrent impact on gas production.

The values of rock compressibility accepted for the final history match were 2.33 x 10^{-6} vol/vol/psi for facies with simulation lithotype indices of nine and ten and 4.185 x 10^{-6} vol/vol/psi from all other facies types. Thus the limestone facies (phylloid algal limestone and front breccia) remained the same as was measured in the laboratory. The dolomite facies (simulation rock types 1–9, 12) were increased form the laboratory measured value of 3.185 x 10^{-6} vol/vol/psi to 4.185 x 10^{-6} vol/vol/psi.

Miscellaneous Reservoir Parameter Changes

In addition to the above reviewed changes in reservoir properties, several others were investigated as a means of improving the agreement between observed field history and simulation predictions. These included changes in the gas–oil relative permeabilities data, changes in absolute permeability of off–mound rock, reservoir compaction (employs pressure dependent and thus time dependent rock compressibilities) and various pore volume changes implemented by decreasing the overall rock volume and/or a particular rock facies (e.g. phylloid algal limestone). Changes in these parameters or reservoir mechanisms were used to influence reservoir pressure history and fluid flow and thus influence gas production history. Detailed analysis of the influence of these parameters on predicted field history was used to screen out these changes. None were adopted or used in the final history match.

14.3. Final History match

Input data for the simulation studies included the base reservoir description, which was adjusted as outlined above, fluid and rock properties and the monthly oil production on a well level basis. Historic gas production, on a field and well level, together with periodic reservoir pressure measurements taken from individual well surveys, were used as primary history match variables. Figure 14–1 presents the field level oil production rate which was specified on a monthly basis at the well level. Figure 14–2 presents the field level gas production rate and cumulative gas production predictions compared to historic data from November 1989 through December 31, 1996. The production forecast for both oil and gas from January 1, 1997 to January 1, 2012 is also included in both figures and was based on continuing primary production operations in effect on January 1, 1997 to January 1, 2012. The agreement between predicted and observed field level gas production history is excellent. There is some deviation between predicted and observed gas production for the last year of the comparison. This was caused primarily by the predicted response of the Anasazi Well No. 1 for gas production (discussed below).

Individual well comparisons are presented in Figures 14–3 to 14–8. Oil rates histories, which were used as simulator input for the history period, are given in Figures 14–3, 14–5 and 14–7. Comparison of predicted and observed gas production are given in Figures 14–4, 14–6 and 14–8. The initial well in the field, the Sahgzie Well No. 1, exhibits an excellent agreement between predicted and observed gas production history (Figures 14–4). The gas production history of the Anasazi Well No. 1 was the most difficult to match because of the complex fluid exchanges occurring between the Supramound and Core Mound Intervals and well level production interference with the Anasazi Well 5L–3. The observed peak gas production point at mid year 1992 was matched to within five to six months. The predicted peak gas production rate however, was higher (560 MSCF/D to 400 MSCF/D). Thus, the simulation model predicts too much gas

production for approximately six months and then under predicts gas production from 1993 to 1997. Then predicted gas production begins to agree more closely with observed produced gas rates at the start of 1997. Because the overall trend of gas production (peak followed by decreased rates) at both production times was matched and the initial history was well matched, the Anasazi Well No. 1 match was the accepted. It was judged that the additional effort to fine tune the Anasazi Well No. 1 match was not warranted since control of the production behavior (explained below) may have required further refining the Z–direction gridding which would have required re–generation of additional geostatistical models and further history matching work. Based on the subsequent CO_2 flood responses, precise matching of the gas–oil interface near the top of the phylloid algal limestone would not have influenced projected recovery significantly.

The gas production history for the Anasazi Well No. 5L–3 (Figure 14–8) is well matched, with the exception of approximately a one year period (1994). However, the impact of partial reservoir depletion and presence of free gas saturation that lead to the initial high gas production were well matched. Also, the late gas production rate trend from 1995 to 1997 is matched reasonably well.

As discussed above, the two principal history match parameters used to compare predicted and observed data were gas production and reservoir pressure. The gas production match was discussed above and the match of reservoir pressure will be outlined next.

One of the key criteria for assessing the validity of changes in reservoir description was the match of historical reservoir pressure data. The comparison used Harken Energy Corporation's reservoir pressure data obtained from several pressure build–up tests conducted on every well in the field during the primary production period. Reservoir simulation provides a means of simulating pressure build–up at a well at specified times. This simulation option conducts a pressure build–up of a specified time duration on selected wells at specified times. The simulator output provides the shut–in pressures (48 hours shut–in was specified) and also the bottom hole pressure at the well prior to shut–in. The simulation actually does a simulated build–up on each perforated layer and combines layer shut–in values in a production weighted procedure to obtain one value for the well.

Table 14–1 provides a comparison of full field measured shut–in pressure data and simulation derived pressure data. The simulation results presented in Table 14–1 contain three values for most tests. The first value reported is the simulated shut–in pressure. Since this shut–in value is a production weighted average of all perforation layers it tends to be a "high side" value since it incorporates contributions from the higher pressured Supramound Interval. The field value may be more representative of the main production intervals rather than a more uniform production weighted average. The second simulated related pressure value reported in Table 14–1 (described by BHP) is the average wellbore grid block pressure at the time of the shut–in. The final set of pressure values reported as simulation results is an approximate range of pressures for all grid blocks surrounding the well at the time of shut–in. This latter value is considered to be more representative and should compare move favorable with the reported field values.

Overall there is excellent agreement between field measured pressure and simulated pressure. Reported simulation values for the Sahgzie well in November 1989 are 230 to 300 psia higher than values reported from field measurements. This difference is caused by the pressure used to initialize the simulator. The initialization pressure was based on pressure recorded during the initial drill stem test of the Sahgzie grid Well No. 1 and during bottomhole fluid sampling of the Anasazi Well No. 1. The drill stem test value was 2260 psia (see Chapter 13). If this is used for comparison the simulation values are in good agreement with field data. The agreement between simulation and

field measured pressure values through the first four years of production is an indication that the pore volume, rock and fluid compressibilities and off–mound fluid influx into the mound complex are reasonable approximations of reservoir values and behavior.

Simulation data provides a means of interpreting the detailed performance mechanism of a reservoir. In Chapter 8, an analysis of the production data, both field and well, provided insight into possible production mechanism for the Anasazi/Sahgzie reservoir. Chapter 8 proposed three distinct production phases for the Anasazi/Sahgzie system. These are:

1. A liquid expansion phase characterized by a constant producing GOR until the reservoir pressure reaches the bubblepoint pressure of the reservoir fluid. This lasted approximately 1.5 years.
2. A dissolved gas depletion stage coupled with gas segregation. This period is characterized by increasing and subsequently decreasing gas production rates.
3. The third stage is referred as the gravity drainage period and is characterized by nearly constant or slowly declining oil and gas production rates. It is associated with continued dissolved gas depletion and secondary gas cap expansion coupled with gravity drainage of oil from the Supramound Interval into the Core Mound Interval.

During the history match and after the final history match was completed, the data available from the simulation study was used to confirm the reservoir production mechanism proposed above. Figures 14–9 to 14–26 provide data that is used to further explain and verify the proposed production mechanisms.

Figures 14–9 to 14–15 present the individual layer production histories for the Anasazi Well No. 1 and the Sahgzie Well No. 1. Since the phylloid algal limestone contributes over 95% of each well's production only the numerical layers that are completed in this unit are examined. Figures 14–9 to 14–13 present oil and gas production rate history for simulation layers 10 through 14 (these correspond to the actual perforated interval in Anasazi No. 1) respectively. Layers 10 and 11 exhibit a significant decrease in oil rate and increase in gas rate from just prior to 1992 to near the end of 1993. Examination of gas saturation maps shows a build–up of free gas saturation in these two layers in model. Thus, as free gas saturation builds up the gas rate increases rapidly. Increasing gas saturation results in a decrease in oil saturation and a corresponding decrease in oil relative permeability and thus the contribution of oil production from these two layers decreases. Eventually (just prior to 1993.8) the oil rates go to zero and Layers 10 and 11 contribute only gas production. These layers continue to produce any gas that accumulates near the top of the limestone unit. The lower permeability of the Supramound Interval retards the gas segregation and contributes to free gas saturation build–up at the Core Mound – Supramound interface. Layers 12, 13 and 14 (Figure 14–11, 14–12 and 14–13) show an increase in oil production rate at the same time Layers 10 and 11 are experiencing increasing gas production rates. The increase in oil production rates from Layers 12, 13 and 14 is required to meet the imposed overall oil production rate of the well. Layer 14 is producing at the solution gas oil ratio that prevails for the reservoir pressure level during this production period. The producing GOR's of Layers 12 and 13 are less than the GOR of Layer 14 since gas segregation is depleting these layers of evolving gas. Once the third stage (i.e. gravity drainage) of production starts oil, and gas production from the bottom three layers remains relatively constant and the bulk of the gas production occurs from the top two layers. Note that the oil rate from Layer 12 is beginning to decrease just prior to 1996. This is a prelude to increasing free gas production as the gas saturation of this layer begins to increase.

The Sahgzie Well No. 1 has only two numerical layers (corresponding to the physical field completions) completed in the limestone unit. The production behavior of these two layers are plotted in Figures 14–14 and 14–15. The same patterns of oil and gas production behavior occurs in the Sahgzie well as in the Anasazi No. 1 well. As free gas builds up in Layer 12 (based on corresponding gas saturation maps), oil and gas produce from the same layer, but because of relative permeability effects the oil rate must decrease, as shown in Figures 14–14. As the oil rate of Layer 12 decreases the oil rate of Layer 13 increases to meet the overall well level specified rate. Since liberated free gas segregates into both Layer 12 and the Supramound, no free gas build–up occurs in Layer 13 to decrease the oil saturation. Thus the oil rate remains relatively constant, despite an increasing GOR for the well.

This layer production analysis supports the proposed overall three stage reservoir production mechanism outlined above. Additional simulation data provides further supporting evidence. This is presented in Figures 14–16 to 14–23. These figures present the historical influx and efflux of oil from the simulation regions defined for the two mounds. These regions were defined in Chapter 13, Section 8. Figures 14–16 through 14–18 present oil flux data in terms of oil in place for the Anasazi mound. Figure 14–16 illustrates that despite the fact that the majority of oil production from the Anasazi mound is produced from the limestone unit perforations, the oil in place in the Core Mound limestone unit, after an initial decease, remains relatively constant. However, the overlying Supramound Interval exhibits a substantial and continuing decrease in the oil in place as gas segregates into the Supramound and oil is displaced into the underlying limestone unit. This process continually recharges the limestone unit and maintains the relatively constant oil production rate exhibited in Stage Three of the production history. Figures 14–17 shows that there is little recharge of the mound area – Core Mound Interval (i.e. limestone unit) from the laterally adjacent off–mound areas in the Core Mound Interval. However, Figure 14–18 indicates that the off–mound area of the Supramound Interval is recharging the mound area in the Supramound Interval as it in turn recharges the underlying limestone unit. Figure 14–22 compares the limestone unit production for the Anasazi mound to the continued efflux (or correspondingly, a decreasing oil–in place) of oil from the Supramound Interval. The combined decrease in oil–in–place of (or efflux from) the Supramound Interval roughly equals the total limestone unit production. Thus, since the oil–in place of the limestone unit remains relatively constant, the oil stored in the Supramound Interval is being produced via a fluid flow transfer process that involves gas segregation into the Supramound Interval and secondary gas cap expansion displacing Supramound oil into the underlaying limestone unit. Also, the gas displacement process is supplemented by gravity drainage of the oil. This overall process is identical to the process identified in the two–dimensional mechanistic studies presented earlier.

Figures 14–19 to 14–21 and Figure 14–23 present a similar set of data for the Sahgzie mound. An analogous explanation to that used for the Anasazi mound applies to the Sahgzie mound and supports the primary production mechanism of the Supramound recharging the primary limestone production interval.

Figures 14–24, 14–25 and 14–26 present gas saturation distribution maps that clearly illustrate the gas segregation and gas accumulation in the overlying Supramound and supports the free gas saturation distribution history developed in the above discussion. Figures 14–24 present a y–direction cross section plot of gas saturation at the Anasazi Well No. 1. Since, in a y–direction, this cross section is between the Sahgzie Well No. 1 and the Anasazi Well No. 5L–3, it also approximates the saturation distribution at these two wells. This figure clearly illustrates the

presence of free gas in Layers 10 and 11 at the Anasazi Well No. 1 (grid coordinates 26,20) as explained in the above discussion on layer production history. This cross–sectional plot also clearly illustrates the presence of gas segregation and free gas accumulation in the upper portion of the Supramound Interval. The limestone interval in both the Anasazi and Sahgzie mounds (Layers 8, 12, 13, 14 and 15) remain oil saturated with no free gas present. Solution gas liberated in these layers immediately segregates to the top of the limestone interval (Layers 10 and 11) and develops a region of high gas saturation at the Supramound – Core Mound interface. Gas continues to segregate and reaches higher saturation values in the upper portions of the Supramound Interval. Figures 14–25 and 14–26 illustrate the expanding areal extent of free gas as it moves from the top of the Core Mound Interval (Layer 10) to the top of the Supramound Interval.

Some direct field evidence of the gas segregation and accumulation exists. An upper interval re–completion of the North Heron 35C well showed production evidence of gas segregation. Prior to recompletion the producing GOR was relatively constant. Once the upper section of the Desert Creek was re–completed, the producing GOR rose quickly and continued to increase as the reservoir was depleted.

In addition to the production behavior of the North Heron 35C well, the well log data obtained from the Anasazi well No. 5L–3 indicates the presence of free gas in the upper half of the Core Mound Interval. The Anasazi Well No. 5L–33 was drilled, logged and completed in February, 1991. This was approximately 17 months after the Sahgzie Well No. 1 started production and 15 months after the Anasazi Well No. 1 was placed on production. Thus, in the vicinity of the Anasazi Well No. 1 (based on simulation results), the reservoir pressure had already dropped below the bubblepoint pressure and free gas had segregated to the top of the Core Mound Interval. In the vicinity of the Anasazi Well No. 5L–3 the simulated reservoir pressure is at the bubblepoint pressure and is starting to liberate gas. Thus, log data for the Anasazi Well No. 5L–3 supports gas segregation (it was present in the upper half of the Core Mound Interval) and the reservoir pressure at the time of its completion also correlates with simulator pressure levels that would allow solution gas to evolve.

In summary, the Anasazi/Sahgzie reservoir performance has been history matched. Both gas production and reservoir pressure were matched and the simulator results used to demonstrate and confirm a complex reservoir production mechanism. With the primary production history matched, it was then possible to utilize the simulator to predict reservoir performance under three different production schemes. The three processes include continued primary production, CO_2 flooding and waterflooding. The next chapter will present and compare these reservoir performance projections.

15. RESERVOIR PERFORMANCE – PREDICTION CASES

15.1. Primary Production Performance

Once the reservoir performance history match was completed, the simulation model was used for projecting the performance of the Anasazi/Sahgzie reservoir under various oil recovery options. To be able to quantify the projected incremental benefit of any recovery scheme, it was necessary to predict the performance of continuing to produce the reservoir under the current primary depletion mode.

Starting on January 1, 1997 the wells currently active were used for production until January 1, 2012. The individual production rates in effect on January 1, 1997 were imposed and maintained on each well until the reservoir pressure declined to the point that the specified rate could not be maintained. At this time the well was placed on a bottomhole pressure constraint (pumped off condition) and production continued at the specified pressure level.

Figures 15–1 and 15–2 present the projected primary depletion performance for the Anasazi/Sahgzie field. Figure 15–1 presents the historical and predicted oil production rate and cumulative oil production through January 1, 2012. Figure 15–2 present the historical and predicted gas production rate and cumulative gas production for the same time period. Figures 15–3, 15–4, 15–5 and 15–6 present the individual well oil production histories for the same time period. Table 15–1 presents data on the initial fluids in place, on a region specified basis, before the start of production. Table 15–2 presents individual well and total field oil and gas production data from January 1, 1997 through January 1, 2012 on an annual basis. Table 15–3 presents data on the final fluid in place on a region and total field basis, as well as average pressure, cumulative production and regional influx data.

The total original oil in place for the model is 11,433,000 STB. The original oil in place for the mound system is given in the table below.

Original Oil in Place – Anasazi/Sahgzie Mounds (MSTB)

Interval	Anasazi Mound	Sahgzie Mound	Total
Supramound	1932	1366	3298
Core Mound	803	605	1408
Total	2735	1971	4706

Thus, roughly 41% of the original oil in place (OOIP) is in the mound complex proper and 59% (6,727,000 STB) is in the associated off–mound structure.

The projected primary recovery at 1/1/2012 is 2,554,427 STB. This represents 54% of the OOIP in the mound complex and 23.3% of the OOIP in the total system. Approximately 2,408,000 STB, or 94%, was produced from the Core Mound Interval (phylloid algal limestone). However, at 1/1/2012 the oil in place is the Core Mound Interval in the mound area is 1,156,000 STB compared to the original volume of 1,408,000 STB. Thus, despite producing over 2,400,000 STB from the Core Mound Interval in the mound area the oil volume decreased by only 252,000 STB. This clearly illustrates the importance of the Supramound and off–mound system in recharging the Core Mound

Interval. This recharge was explained in the history match discussions of Chapter 14 and the two–dimensional mechanistic simulation studies section of Chapter 12.

The projected oil production rate from the field (see Figure 15–1) remains essentially constant at the January, 1997 rate up to the year 2000. From the year 2000 to 2012 the oil production declines in almost a linear fashion. Oil production decline, as illustrated in Chapter 14, is associated with free gas saturation build–up at the top of the Core Mound Interval in the core mound area and general pressure decline.

15.2. CO_2 Flood Evaluation

15.2.1. Summary of CO_2 Flood Case Studies

To assess the potential of CO_2 flooding as a process to increase oil recovery from the Anasazi/Sahgzie reservoir, 35 simulation prediction cases were completed. They are identified with the prediction simulation case codes of ASP1 to ASP35 inclusive. The prediction cases were designed to systematically investigate various operational aspects of CO_2 flooding implementations and identify the requirements for maximizing oil recovery from the reservoir of interest. The main areas assessed in terms of CO_2 flood performance were:

1. Reservoir operating pressure.
2. Injection well location, numbers and configuration.
3. Produced gas conditioning for re–injection.
4. Production operations during reservoir fill–up.
5. Continued injection versus blowdown.

In addition to reservoir performance prediction cases needed to investigate the above operational/implementation issues, the potential of waterflooding was also assessed. Waterflood response is addressed in a separate section of this report.

The above listed areas of investigation are discussed separately below and the specific simulation runs used in the assessment are identified. Relevant operational data that was varied and/or used in each specific area of investigation is also provided. Presentation and discussion of the results of the prediction cases are provided in Section 15.2.2

Carbon dioxide injection for the prediction cases was either initiated April 1, 1996 or January 1, 1997. Start of injection can be identified by examining the oil production history plots presented for the various cases.

<u>Reservoir Operating Pressure</u>

Reservoir operating pressure requirements for developing and maintaining miscibility for the CO_2 Anasazi/Sahgzie hydrocarbon fluid system were investigated and guidelines developed in the one–dimensional mechanistic studies presented and discussed in Chapter 12. The sensitivity of oil recovery to the CO_2 flood operating pressure was investigated further using the history matched full field model.

Basic operational/model parameters employed for a set of three prediction cases are summarized below:

1. Gas conditioning plant active to process produced gas and re–inject recovered CO_2.
2. One injection well active and located in simulation grid blocks (18,10,1–5). This is the Anasazi Well No. 6H–1 location, but with the 6H–1 well re–completed in the upper half of the Supramound (simulation Layers 1–5) Interval.
3. Anasazi production wells (#1 and #5L–3) shut–in at start of injection and remained shut–in until the bottomhole pressure equalled or exceeded either 2000, 2500 or 3000 psi (cases ASP6, ASP7, ASP8 respectively). To obtain improved oil recovery from the Sahgzie Well No. 1 with only one injector, the well was shut–in only until its bottomhole pressure exceeded 500 psi, (discussed later under injection well placement). In general, all production wells were re–completed so that only the Core Mound Interval layers were active or perforated. This completion configuration was applied to all prediction cases except as noted in the waterflood cases.
4. The maximum injection pressure was restricted to 3000, 3500 and 4000 psi for prediction cases ASP6, ASP7 and ASP8 respectively.

The key parameter varied for this set of runs were the producing pressure of the Anasazi production wells and the injection pressure. Specification of the pressure controlled the reservoir operating pressure during the CO_2 flood. Results and discussion follow in Section 15.2.2.

Injection Well Location/Number of Injectors and Configuration

The complete series of runs used to identify both the optimum location, based on total oil recovery and number of injectors to employ used the gas conditioning option. In addition, production wells were shut–in until each well's bottomhole pressure equalled or exceeded the imposed pressure constraints. The key parameter that was varied was well location. The Anasazi Well No. 6H–1 was identified as a re–completion candidate (producer to injector) because of its location and initial and current low productivity. A summary of the prediction cases and relevant data are given in the table below. Injection well location refers to the simulation grid numbers (see Figure 13–5). The first grid number refers to the x–direction coordinate, the second number refers to the y–direction coordinate and the third set of numbers refers to the simulation layers completed (i.e. perforated) in the simulator. As a point of reference, the simulation grid coordinates for current producers are given below:

Simulation Grid Locations of Producer

Well	X and Y Simulation Grid Coordinates	Layers Completed
Anasazi Well No. 1	(25, 20)	(1–5, 6–19)
Anasazi Well No. 5L–3	(17, 24)	(1–2, 4–8, 11–14)
Anasazi Well No. 6H–1	(18, 10)	(1, 3–4, 6–7, 10–11, 14)
Sahgzie Well No. 1	(41, 19)	(3, 12–13)

In general, all the above layers were active for primary production predictions and history matching. For the CO_2 prediction cases, only Core Mound Interval perforations (simulation Layers 10 to 15) were active. The waterflood cases had a different perforation set active and are discussed separately. The bottomhole pressure constraint data refers to the minimum bottomhole pressure requirement before the production well is allowed to produce or flow.

CO_2 Flood Prediction Cases – Injection Well Location

Case No.	Injector No. 1 Location	Injection No. 2 Location	Production Well Bottomhole Pressure Constraint (psia)			
			A#1	A#5L–3	A#6H–1	S#1
ASP4A	Not Active	(20, 14, 1–5)	2000	2000	2000	2000
ASP5/5A	Not Active	(20, 14, 1–5)	2000	2000	2000	500
ASP9	Not Active	(31, 12, 1–5)	2500	2500	2500	2500
ASP10	(37, 8, 1–5)	(18, 10, 1–5)	2500	2500	2500	2500
ASP11	(35, 12, 1–5)	(18, 10, 1–5)	2500	2500	2500	2500
ASP12/12A	(35, 6, 1–5)	(18, 10, 1–5)	2500	2500	2500	2500
ASP13	← Horizontal Injectors * →		2500	2500	2500	2500

* Horizontal Injectors were completed in the Supramound Interval (simulation layer 3). The areal coordinates are given in Section 15.2.2

For cases ASP4A and ASP5/5A the maximum injection pressure was set at 3000 psia. For cases ASP9 through ASP12 the maximum injection pressure was set at 3500 psia.

Produced Gas Conditioning for Re–Injection

One of the key operational decisions in connection with CO_2 flood implementation in the Paradox Basin for small algal reef mounds is whether the produced gas from a CO_2 injection project should be processed through a gas conditioning plant. The gas conditioning plant is designed to separate CO_2 from hydrocarbon components and provide two outlet streams. One outlet stream will be essentially pure CO_2 which can be re–injected and thus used to reduce the cost of purchasing CO_2. The other outlet stream will be a hydrocarbon gas, with a small mole fraction of CO_2 (less than the concentration required for pipeline sales). The hydrocarbon outlet stream could be either sold or used as lease fuel. There are two basic operating questions that must be addressed concerning the use of a gas conditioning plant. These are:

1. If the produced gas is re–injected without conditioning to remove hydrocarbon components, will the presence of the hydrocarbons adversely impact the development of miscibly and lower oil recovery?

2. Because of the significant operating costs associated with commissioning a gas conditioning plant, will the value of sales and fuel gas provide economic justification for its use?

Two basic sets of runs were used to generate data that could be used to answer the above two questions. Prediction cases ASP29 and ASP30 were conducted to furnish this specific data. In both

cases, two injectors were used (located at (35, 6, 1–5) and (18, 10, 1–9)) and production wells were allowed to produce during reservoir fill–up. Injectors used a maximum injection pressure of 3500 psia. The only difference between the two runs was that ASP30 used a gas conditioning plant to separate the CO_2 and hydrocarbon and recycled pure CO_2. ASP29, however, did not treat the produced gas and re–injected all produced gas once CO_2 concentration was sufficiently high to prevent sales or its use as fuel.

Results and the discussion of the results are presented in Section 15.2.2.

Production During Reservoir Fill–up

In most CO_2 prediction cases, production wells were shut–in until the reservoir pressure was increased to the point that a miscible displacement process would develop. From a practical operational stand point, continued production during reservoir fill–up is preferred. Under these conditions the project will still be generating revenue while the reservoir is being re–pressured. Prediction case ASP29 was also used to determine if continuous production during reservoir fill–up would adversely impact the CO_2 flood. ASP29 is a companion run to ASP15 in that it uses the same injection well location and pressure constraints. Also, ASP15 and ASP29 did not use a gas plant for gas conditioning, but rather re–cycled (i.e. re–injected) untreated produced gas. ASP15 shut–in the producer until a 2500 psi bottomhole pressure constraint was exceeded. ASP29 allowed production to continue at the production rate in effect on December 31, 1996 and continued at this rate until its bottomhole pressure exceeded 2500 psi. At this time the well was allowed to flow at any rate sustainable by the bottomhole pressure, provided it did not exceed a specified limit of 500 STB/D. The other difference between the two runs was that an updated history match ran was used for primary production predictions with ASP29. This difference did not prevent the two runs from being used to address the impact of continued oil production during reservoir fill–up.

Again, the results and associated discussion are presented in Section 15.2.2. Since data from prediction cases ASP29 and ASP30 were subsequently used to conduct economic assessment studies, a more comprehensive set of production plots and reservoir parameter maps are presented to provide insight into the CO_2 flood process. These are presented in Section 15.2.3.

Continued Injection versus Blowdown

Another principal operating and economic question that requires reservoir performance information to resolve, concerns how long CO_2 injection should continue before reservoir blowdown (or natural depletion) is initiated. Reservoir performance data is required to decide if it is economically more attractive to stop CO_2 injection, eliminating compressor costs and CO_2 make–up gas purchases but possibly reducing overall recovery, than it is to continue a CO_2 injection and recover more oil. Prediction case ASP35 was conducted to obtain reservoir performance data under blow down conditions and compare to a continuous injection case (ASP29). ASP35 is a continuation (or restart) of ASP29. ASP29 results are used up to January 1, 2003. At this time, injection is terminated and reservoir blow down started. The blow down phase allows the production wells (A#1, A#5L–3, and S#1) to produce against a specified tubing head pressure of 100 psia. Wellbore hydraulics data provided input data to allow the simulator to compute bottomhole flowing pressures. Each well was initially specified as a gas well because of the high gas production (essentially CO_2). Once gas production decreased to a lower rate and the bottomhole pressure had declined well below the CO_2 flood operating pressure, the production wells were specified as oil wells and allowed to produce

against a fixed bottomhole pressure of 50 psia (close to a pumped off condition). This production condition then prevailed until the end of the prediction case.

Results of this case are also presented in Section 15.2.2.

15.2.2. Prediction Case Results and Reservoir Performance Interpretation

Similar to the review of the different prediction cases completed for evaluating CO_2 flooding, the results of these cases are grouped and presented under the same topic heading as used in Section 15.2.1. That is results will be summarized under the following topics:

1. Reservoir operating pressure.
2. Injection well location, number and configuration.
3. Produced gas conditioning for re–injection.
4. Production operations during reservoir fill–up.
5. Continuous CO_2 injection versus blowdown.

In reviewing the results from the prediction cases under these topic headings, only essential results sufficient to illustrate the influence the parameter being investigated has on reservoir performance will be given. Only in the case of ASP29, ASP30 and ASP35 will detailed production data and reservoir parameter maps be given. Results from each of these three cases are used to assess the economic viability of CO_2 flooding and this merits more extensive documentation. More comprehensive results and complete data files from all runs are available, if needed.

Reservoir Operating Pressures

One dimensional simulation studies identified a CO_2 flood operating pressure of 2500 psia to develop and maintain miscibility and obtain a high displacement efficiency. Prediction cases ASP6, ASP7 and ASP8 were conducted to further quantify the pressure level needed for a field implementation of CO_2 flooding. Prediction case ASP6 operated the CO_2 flooding between the maximum injection pressure of 3000 psi and minimum bottomhole production well pressure of 2000 psi. The range of pressure for ASP7 was 2500 to 3500 psi, and for ASP8 it was 3000 to 4000 psi.

Figure 15–7 presents cumulative oil recovery versus time for the three pressure levels. Prediction cases ASP7 ($P > 2500$ psia) and ASP8 ($P > 3000$ psia) exhibit higher oil recovery than the lower operating pressure ASP6 ($P > 2000$ psia) case. ASP7 recovers approximately 268,000 STB more oil than the ASP6 case at 1/1/2005 and ASP8 recovers 359,000 STB more than the ASP6 case.

Comparison of gas and oil saturation maps for various layers of the model for ASP7 and ASP6 show that ASP7 displacement efficiency is greater than that of the lower pressure run (ASP6) in the CO_2 swept regions. Residual oil saturation values in the ASP7 case are approximately 5%, whereas in ASP6 they are approximately 10%. In addition, to improved displacement efficiency, a production increase for the Sahgzie Well No. 1 was noticed for the higher operating pressure case (ASP7). This is likely caused by a larger pressure differential between the mound area and the off–mound area in the Core Mound Interval in the Sahgzie mound. This is a result of a higher Anasazi Core Mound Interval pressure. Thus, increased recovery of the ASP7 prediction case relative to ASP6 is

attributable to both improved CO_2 displacement efficiency because of a higher operating pressure and a pressure differential induced improvement in the Sahgzie Well No. 1 production.

The additional recovery exhibited by the ASP8 run versus ASP7 is only 91,000 STB. This again is attributable to a slight improvement in CO_2 displacement efficiency as determined via saturation map analysis. Since the ASP7 case exhibited a slightly better CO_2 utilization ratio (14.2 MSCF CO_2/ STB) versus the ASP8 Case (14.7 MSCF/STB) and recovers only slightly less oil, its operating pressure was considered to be the best for conducting the remaining CO_2 flood predictions. This operating pressure level (2500 – 3500 psia) is consistent with the pressure level identified via the mechanistic studies presented in Chapter 12.

Injection Well Location, Number and Configuration

Because of the cost of drilling new wells and the limited size of the resource target, the number of injection wells must be minimized. Also, both the location of existing producing wells and overall geometric configuration of the mounds and distribution of mound and off–mound rock make the placement of injection wells critical. Several prediction cases, ASP4A, ASP5/5A, ASP9, ASP10, ASP11 and ASP 12/12A, and ASP13 as outlined in the previous section, were used to investigate the number of wells required and their location to maximize recovery from the Anasazi/Sahgzie reservoir.

For these cases, the following table presents the cumulative oil and gas production for the field, total gas injection and CO_2 purchase requirements for the field up to 1/1/2005.

Oil and Gas Production and Injection Requirements at 1/1/2005
Sensitivity to Number of Injectors and Location

Case No.	Cumulative Oil MSTB	Cumulative Gas BSCF	Cumulative CO_2 Injected BSCF	Cumulative CO_2 Purchased BSCF
ASP4A	2762	42.4	48.3	–
ASP5/5A	3535	39.6	46.5	9.4
ASP9	2574	16.7	23.2	8.1
ASP10	3865	34.3	43.9	11.9
ASP11	3672	35.0	44.0	11.2
ASP12/12A	4028	32.8	42.7	12.4
ASP13	3397	37.0	44.7	9.6

Injection was started April 1, 1996. Figures 15–8 and 15–9 present the oil production rate history and cumulative oil production history for the field for cases ASP9, ASP10, ASP11 and ASP12/12A respectively.

Prediction cases ASP4A and ASP5/5A compare CO_2 flood performance using one injector placed in the Anasazi mound located in the upper apex (closest to Anasazi 6H–1) of the triangle formed by connecting straight lines to the simulation grid location of the three Anasazi producers (Anasazi No. 1, No. 5L–3 and No. 6H–1). As modelled, the main limestone unit (phylloid algal limestone

facies) is not continuous between the Anasazi No. 6H–1 well and the other two Anasazi wells. Thus, there is no direct vertical communication paths from the Supramound Interval in the injector into the highly conductive phylloid algal facies. The injector was placed at this location because of the indirect path needed to move CO_2 from the injector's top five layers into the limestone unit. The difference between the two cases is the bottomhole pressure constraint placed on the Sahgzie Well No. 1. In the ASP4A case, the Sahgzie well was restricted from producing until the bottomhole pressure reached 2000 psia, the same as the Anasazi wells. In ASP5/5A the pressure constraint was 500 psia for the Sahgzie well. The principal difference in field oil recovery is attributable to the difference in Sahgzie well production. Field production to 1/1/2005 was roughly 800,000 STB higher for ASP5/5A, and the Sahgzie Well contributed the same amount of additional oil. Because CO_2 injected at (20, 14) must move through the off–mound rock to reach the Sahgzie mound and subsequently the Sahgzie Well No. 1 (the predicted fluid flow path for the CO_2 was via the Supramound Interval connecting the two mounds) the time required to pressurize the Sahgzie well location is much longer than for the Anasazi wells. In the ASP4A run the Sahgzie well location did not reach 2000 psi until about four years after the start of injection. In the case of ASP5/5A the delay was almost two years, even though the Sahgzie well could have started producing once the bottomhole pressure reaches 500 psi. This is shown in Figure 15–10. In contrast, Anasazi Well No. 1 started production approximately two months after injection started and the Anasazi Well No. 5L–3, 12 months after commencement of injection. The larger pressure differential under producing conditions for the Sahgzie well for the ASP5/5A case, 1500 psia, versus only a few hundred psi for the ASP4 case is the reason for the additional 800,000 STB of production for ASP5/5A.

The results of ASP5/5A and ASP4A indicated that if only one injector is used and it is located in the central portion of the Anasazi mound, the Sahgzie mound will not be effectively flooded. If the Sahgzie wells production is curtailed until sufficient pressure builds up to achieve miscibility the time delay between injection and production is excessive (> 4 years) and recovery is low because a CO_2 rich gas phase is not propagated into the Sahgzie mound. If the minimum bottomhole pressure is reduced to, say, 500 psia, fluid propagation between the Anasazi and Sahgzie mound is enhanced, but displacement efficiency is reduced because of a lack of miscibility caused by the lower Sahgzie mound pressures. Also, the production delay for the Sahgzie well was still in excess of two years. Thus, the results of these two cases suggested that either the single injection be placed midway between the two mounds or an additional injector be added to flood the Sahgzie complex. These options were investigated in the other prediction cases identified above.

Prediction case ASP9 examined the benefit of moving the single injector from the Anasazi Mound area to an off–mound location between the Anasazi and Sahgzie mounds (see previous table). Placing the injector between mounds resulted in two major changes in the predicted CO_2 displacement. Lower reservoir quality between the mounds reduced the rate at which CO_2 could be injected and still honor the injection well pressure constraint of 3500 psi. The reduced injection rate essentially reduces the total volume of CO_2 injected to 1/1/2005 by almost 50%. Also, the transmissibility barrier added between the Anasazi Well No. 1 and the Anasazi Well No. 5L–3 to obtain the history match and the direct production interference of the Anasazi Well No. 1 adversely affected the CO_2 fluid movement from the injector into the drainage area of the Anasazi 5L–3 well. This reduced the CO_2 flood enhanced recovery from the Anasazi Well No. 5L–3 by over 500,000 STB relative to the response prediction in Case 5/5A. The response of Sahgzie Well No. 1 to the close proximity of the injector allowed the Sahgzie well to produce 500,000 STB more oil, relative

to its response for Case 4A, and also to meet the imposed pressure constraint of 2500 psi set in Case ASP9.

The overall results of the single CO_2 injector cases (Case IA, Case 5/5A and ASP9) indicated that if both mounds are to be flooded effectively and the three main producers are to benefit from miscible CO_2 injection, at least two injectors are required. An injector for each mound is needed. To minimize injection well costs, the Anasazi mound injector could use a re–completion of the Anasazi Well No. 6H–1. Thus, the next series of prediction cases, Case ASP10, ASP11 and ASP12, were used to investigate alternative locations for the Sahgzie mound injector.

Data presented in the above production table and Figures 15–8 and 15–9 indicate that the most northerly location of the three locations examined for the Sahgzie mound injection recovered the most oil and effectively swept (along with injection into the Anasazi Well No. 6H–1 location) both mounds. The incremental oil production, over primary production, through 1/1/2005 was close to 2.0 MMSTB.

To assess the benefits of using a horizontal injector in place of vertical wells an additional prediction case, ASP13, was completed. Horizontal injectors were anticipated to possibly provide improved vertical CO_2 sweep by injecting the CO_2 at the top of the Supramound internal and also possibly enhance lateral sweep of the CO_2 by distributing the CO_2 over the entire length of the injector. Both the Anasazi and Sahgzie mound horizontal wells were completed in the third layer of the Supramound internal. The lateral location of the wells in terms of the simulation (x,y) grid is given below:

Sahgzie Horizontal well:

– (33,8), (34,9), (39,9), (35,10), (33,11), (38,12) (39,2), (40,13) (41,14) and (42,15)

Anasazi Horizontal Well:

– (18,10–11), (19,12–14), (20,15–16), (21,17–19) and (22,20–22)

In comparing the horizontal injector well case ASP13, to the best vertical well case involving two injectors, ASP12/12A, the horizontal injector case recovered approximately 902,000 STB less oil at 1/1/2005. A comparison of the oil production rate and cumulative oil production for these two cases is presented in Figures 15–11. The horizontal well case results in earlier CO_2 breakthrough and more gas production than the companion vertical well case (ASP12/12A). The horizontal injectors extend from the northern portion of both mounds to the southern portion of the mound where the producers are located. Since the horizontal injectors directly overlie the limestone unit in the Core Mound Interval in the proximity of the producers, CO_2 quickly moves from the Supramound Interval into the limestone unit below the well. The limestone unit in the Core Mound Interval provides a high permeability path for the CO_2 to move towards the producer. The early breakthrough of CO_2 reduces oil production and also inhibits the CO_2 from increasing its volumetric sweep in the northern region of both mounds.

In summary, the prediction cases completed to access oil recovery sensitivity to injection well number, location and configuration indicated that:

1. The best sweep and thus the maximum oil recovery requires two injectors, one in the Anasazi mound the other in the Sahgzie mound.

2. The most northern Sahgzie injector provided the best Sahgzie mound recovery when the Anasazi Well No. 6H–1 location was used for the Anasazi mound injector location.

3. Vertical wells located in the northern region of the mound provide better sweep and more oil recovery than the use of two horizontal injectors trending north to south in each mound.

Produced Gas Conditioning for Re–injection

As outlined above, prediction cases ASP29 and ASP30 were completed to answer two basic questions:

1. If the produced gas is re–injected without conditioning to remove hydrocarbon components, will the presence of the hydrocarbons adversely impact the CO_2 displacement process and lower recovery?

2. Will the use of a gas conditioning plant provide sufficient revenue from sales gas and/or lease fuel to justify its capital resource requirements?

Operating conditions employed in these two cases were discussed above.

Figure 15–12 compares oil production rates and cumulative oil production for prediction cases ASP29 and ASP30. Prediction case ASP30 used a gas conditioning plant which separated hydrocarbon components and CO_2 from the produced gas. The CO_2 stream was re–injected and the hydrocarbon rich stream was used for sales and/or fuel. Prediction case ASP29 did not use a gas conditioning plant, all of the produced gas was re–injected and make–up CO_2 was purchased to meet gas injection requirements. As shown in Figure 15–12, there is little difference in predicted performance between the two cases.

The cumulative oil recovery was approximately 58,000 STB higher for the case using unprocessed produced gas for re–injection. The additional recovery, because it is small (only 2% of incremental over primary recovery) could not be explained quantitatively without considerably more detailed analysis. The principal result is that use of unprocessed produced gas for re–injection does not adversely influence oil recovery. However, gas processing provided 4.2 BSCF of sales gas through 1/1/2012. In addition, if the produced gas was processed and CO_2 injection continued to 1/1/2012 an additional 4.2 BSCF of CO_2 make–up gas would be required. The economic benefits of produced gas conditioning will be addressed in Chapter 16. However, from a reservoir process standpoint, oil recovery is essentially insensitive to re–injection gas processing as used in the subject study.

Production During Reservoir Fill–up

To maintain a revenue stream from the Anasazi–Sahgzie reservoir, continued oil production during reservoir fill–up is the preferred option. To assess the impact of continued production during fill–up, prediction cases ASP15 and ASP29 were used to investigate the influence on overall process efficiency and oil recovery. As explained above, ASP15 shut–in producers at the start of injection and production remained shut–in until the reservoir pressure in the vicinity of the producer reached 2500 psi. ASP29 allowed oil production from all wells at the rate in effect on 12/31/96 during reservoir fill–up. Because injection exceeded production on a reservoir volume basis, reservoir pressure increased and the wells were allowed to produce unconstrained once local pressure exceeded 2500 psia. Figure 15–13 compares oil production history for these two prediction cases. As the production plots in Figure 15–13 illustrate, continued production during fill–up did not significantly impact the CO_2 flood process. Cumulative production through 1/1/2012 differed by

only 10,000 STB (ASP29 recovered more oil). Thus, as long as injectivity of the injection wells allows CO_2 injection at rates substantially in excess of pre CO_2 flood oil rates, no adverse impacts are expected. However, once reservoir pressure begins to build–up production rates should be constrained until the reservoir pressure in the vicinity of the producers exceeds 2500 psi. Once the reservoir is repressured, higher oil rates are possible, while still maintaining CO_2 – crude oil miscibility.

Continued CO_2 Injection versus Blowdown

The continuous CO_2 injection case used prediction run ASP29. Prediction case ASP35 (ASP35 and various restarts up to ASP35D) provides data to analyze the performance of CO_2 injection followed by blowdown. Use of a blowdown period eliminates the cost of injecting CO_2 from the start of blowdown to the end of production. However, the reduced operating costs is usually accompanied by loss of oil production. Economic analysis will provide a means of optimizing the time at which to commence blowdown.

Figure 15–14 compares predicted oil production rates and cumulative oil recovery for prediction cases ASP29 and ASP35. Blowdown in ASP35 commences on 01/01/2003. Initially the wells produced against a fixed tubing head pressure (100 psi in this case). Once reservoir pressure declines and the wells could no longer support vertical flow at sufficiency higher rates, the wells were converted to pump and produced against a fixed bottom hole pressure. This is the point at which oil rates after decreasing from 1/1/2003 to approximately midyear 2004, started to increase (01/05/2004). Cumulative oil recovery for the continuous injection case at 1/1/2012 was predicted to be 5,039,000 STB approximately 2.48 MMSTB over projected primary recovery to the same time. Cumulative recovery for CO_2 injection followed by blowdown was predicted to be approximately 4,269,000 STB, or 1.72 MMSTB incremental above primary. The total CO_2 purchase requirements for the blowdown case were 2.7 BSCF less than for continued CO_2 injection to the end of production.

Chapter 16 presents data to compare these two methods of operation from an economic performance standpoint. This accounts for the value of produced oil and the associated operating costs to produce the oil under the two different production scenarios.

15.2.3. Optimized CO_2 Flood Performance Cases

Over 35 prediction cases evaluating CO_2 flooding and waterflooding were completed. Nineteen of these cases involved CO_2 flooding. These runs were used to assess CO_2 flood performance as influenced by CO_2 flood operating pressure, the number of injection wells, the location and configuration (horizontal versus vertical) of injectors, the use of unprocessed versus processed production gas for use in re–injection and finally continuous CO_2 injection versus CO_2 injection followed by blowdown. Based on the results of these various prediction runs, three cases were selected to predict the optimum performance of the Anasazi/Sahgzie reservoir CO_2 flooding. The data from these three runs was also used to conduct the economic assessment discussed in Chapter 16. The three prediction cases were:

1. ASP29 – continuous CO_2 injection using re–injection of produced gas without gas conditioning to remove hydrocarbon components.
2. ASP30 – continuous CO_2 injection using gas re–injection of reclaimed CO_2 from the produced gas.

3. ASP35 – continuous CO_2 injection using gas re–injection of produced gas without gas conditioning to remove hydrocarbon components, followed by reservoir blowdown.

Table 15–4 summarizes relevant production/injection data for the three cases. As discussed above, the results from cases ASP29 and ASP30 simulation studies are similar. Thus, except for Table 15–4, only results from Case ASP29 will be presented. Case ASP30 results, except for the composition of the re–injected gas, are essentially identical to ASP29 and thus do not need to be presented.

From Table 15–4, oil recovery for the continuous CO_2 injection Case ASP29 exceeds predicted primary depletion oil recovery by 1.91 MMSTB and 2.48 MMSTB at 1/1/2006 and 1/1/2012, respectively. The incremental recovery of 2.48 MMSTB required the injection of 74.0 BSCF of gas and the purchase of 12.9 BSCF of CO_2 to provide the initial volume of injection gas and subsequent make–up gas. Field and well level oil production history comparisons between continued primary depletion and the continuous CO_2 injection (ASP29) are presented in Figures 15–15 to Figures 15–19, inclusive.

Figures 15–20 and 15–21 show the gas injection history for the two injectors. The reduction in injection rates is a result of the Supramound Interval being unable to accept the specified injection rate of 7.0 MMScF/D for each well while constraining the injection pressure to less than 3500 psia.

Figures 15–18, which presents oil production data for the Anasazi well No. 6H–1, show no production for the well for Case ASP29. As discussed previously, the Anasazi 6H–1 was converted to an injector for this series of runs. All three production wells show significant incremental oil recovery above primary. Incremental oil recovery above primary was 1009, 821 and 717 MSTB for Anasazi Wells No. 1 and No. 5L–3 and Sahgzie Well No. 1, respectively. The injection of CO_2 miscibly displaces oil from the Supramound Interval and off–mound areas into the Core Mound Interval of the mound area in both the Anasazi and Sahgzie mounds. Referring to Tables 15–5 and 15–6, which are Region summaries generated for Case ASP29 at 1/1/997 (the start of injection) and 1/1/2012 (the end of production), the oil in place in both the off–mound and Core Mound areas of the Supramound Interval of the Anasazi mound were reduced by roughly 1.1 MSTB and 629 MSTB respectively. The average oil saturation decreased from 77.4 and 60.5 to 52.8 and 38.5% respectively. Correspondingly, the average gas saturation (mostly CO_2) increased form 12.2 and 29.0 to 36.9 and 51.4% respectively. This indicates the replacement of oil by CO_2. In addition, the oil in place in the Core Mound Interval of the mound area was reduced from 766 MSTB to 289 MSTB. The net influx of oil into this same region from 1/1/1997 to 1/1/2012 was over 1.8 MMSTB of oil. Similar saturation changes and oil influx occur in the Sahgzie mound, as shown in Tables 15–5 and 15–6.

Figures 15–26 to Figure 15–36 present oil saturation and liquid phase composition differences data for various cross sections and areal maps at two different time intervals for prediction case ASP29 (ASP30 will be the same). Figure 15–26 presents the oil saturation at the beginning of CO_2 injection for a cross section through the Anasazi Well No. 1 (y=20 plane). This x–z plane is midway (y–direction) between the Anasazi Well No. 5L–3 and Sahgzie Well No. 1. The plot shows the lower portion of the mound interval to be oil saturated (zero gas saturation (dark blue in color – Layers 13 to 15) for both the Anasazi and Sahgzie mounds. The top two layers of the Core Mound Interval (Layers 10 and 11) and the Supramound Interval above the limestone show decreased oil saturation ($\cong$45 to 50%) caused by the evolution and segregation of the free gas. At the end of the CO_2 flood, both the Core Mound and Supramound Intervals have oil saturations below 0.10. This is clearly shown in Figure 15–27. Note that under miscible conditions the mole fraction of each hydrocarbon

component in the liquid and vapor phase are equal or nearly equal and that their difference should approach zero (or their ratio should approach 1.0). Thus, Figure 15–28 shows that the area in both mounds, for the x–z plane at y = 20, exhibit miscible or near miscible conditions. The map of the difference of the liquid and vapor mole fractions of the C4–C5 component identifies the miscible region (red color area). Difference plots of other components show the same behavior. Thus, since miscible to near miscible conditions exist in the two areas contacted by CO_2 the remaining oil saturation should be low, as shown in Figure 15–27.

Figures 15–29 to 15–34 present the same suite of plots (i.e. oil saturation at 1/1/2006 and 1/1/2012 and mole fraction difference data for the C4–C5 component) for two different x–y planes. The first plane is for simulation Layer 12 which is near the top of the Mound (i.e. phylloid algal limestone) Interval. The second plane is for Layer 5 which is at the bottom of the CO_2 injection interval in the Supramound Interval. This set of plots clearly illustrates the extent of the CO_2 movement, the lower residual oil saturation and the areal extent of the miscibly displaced region.

Figures 15–35 and 15–36 present oil saturations at 1/1/2012 for two x–direction cross sections. The cross section for x = 18 (Figure 15–35) runs through the Anasazi mound injector [(18,10) simulation grid location] and the cross section for x = 35 (Figure 15–36) intersects the location of the Sahgzie mound injector [simulation grid location (35,6)]. Both sections show effective oil displacement occurred from the injector locations to the southern extent of the two mounds. Examination of a time series of these plots clearly shows the propagation of CO_2 through the Supramound Interval and eventually invading the Mound Interval limestone once this lithotype appears below the Supramound Interval.

Figures 15–32 and 15–38 present the three dimensional (i.e. 3–D) distribution of oil saturation and the liquid phase mole fraction of CO_2 at 1/1/2008. The three dimensional representation of the simulation model uses a cut out section bounded to the north by the Anasazi injector (grid location 18,10) and the Anasazi Well No. 5L–3 producer to the west. The surface displayed internally represents the bottom of the top layer of the Core Mound Interval (Layer 10) and thus illustrates saturations and CO_2 concentrations in the limestone unit. The three large green arrows (along with the vertical white lines) mark the location of the three producers. The two red arrows mark the injector locations. The Anasazi mound injector (northwest corner) is located at the site of the Anasazi Well No. 6H–1 producer. As mentioned above the producer was re–completed as an injector. The five red disks at the Anasazi 6H–1 location mark the completed layers in the injector (Layers 1 to 5 in the Supramound Interval). Both plots illustrate the extent of the CO_2 movement and the displacement efficiency. In these plots, dark blue corresponds to an oil saturation of zero to 0.1 (previous plots used a red color). The CO_2 concentration data shown in Figure 15–38 shows the remaining hydrocarbon liquid has a CO_2 concentration in excess of 70%. The CO_2 has extracted the light hydrocarbon component in the liquid.

Prediction case ASP35 models CO_2 injection, followed by reservoir blowdown. Figures 15–22 presents field level oil production data for this case. The blowdown case is compared to the continuous CO_2 injection case, which employed re–injection of un–processed production gas (i.e. ASP29). Individual well level comparisons for these two cases are presented in Figures 15–23 to 15–25. Blowdown was initiated at 1/1/2003 and was modelled by imposing a tubing head pressure of 100 psi on the producers. The wells were then allowed to produce at a rate constrained only by the tubing head pressure. This explains the brief oil rate peak above the continuous CO_2 curve at 1/1/2003. The second oil production peak (just prior to 1/1/2006) occurs when switching the wells

from flowing conditions constrained by the tubing head to pumping conditions. Under pumping conditions the rate of oil production rate decline is reduced.

Relative to continuous CO_2 injection, employing blowdown reduces oil recovery through 1/1/2006 by 278,000 STB and by 770,000 STB through 1/1/2012. However, operating costs will be reduced substantially since gas injection and associated compression is not needed and no additional CO_2 purchases are required after 1/1/2003. The economic merits of early termination of CO_2 injection followed by blowdown are examined in Chapter 16.

15.3. Waterflood Evaluation

15.3.1. Summary of Waterflood Case Studies

To assess the potential of waterflooding to increase oil recovery form the Anasazi/Sahgzie reservoir six simulation prediction cases were completed. The production cases investigated three operational aspects of waterflooding. These are:

1. Injection well location.
2. Production well back pressure which influences overall reservoir pressure.
3. Completion interval of injectors and producers.

These areas of investigation are discussed separately below, where the specific runs used in the assessment are identified and key operational data incorporated in each run are identified. Presentation and discussions of the results of these six prediction cases are provided in Section 15.3.2.

Injection Well Location

Based on the CO_2 flood prediction results, at least two water injectors were considered necessary to effectively waterflood both mounds. One injector was not effective in implementing the CO_2 flood and because of the lower mobility of water, it is unlikely that one injection well would be effective for waterflooding. Thus, in all six cases two injectors, one in each mound, were used. The location of the injectors is given in the table below. This table also contains data on the completion intervals and production well back pressures used in each case. The latter two operational parameters will be discussed below.

Waterflood Prediction Cases – Injection / Production Well Data

			Production Well Bottomhole Pressure Constraints (psia)			
Case No.	Injector 1 Location	Injector 2 Location	A–1	A#5L–3	A#6H–1	S#1
ASP18	(35, 12, 1–15)	(18, 10, 1–15)	2000	2000	Shut–In	2000
ASP19	(35, 6, 1–15)	(18, 10, 1–15)	108	31	Shut–In	369
ASP20	(35, 12, 1–15)	(18, 10, 1–15)	108	31	Shut–In	369
ASP25*	(35, 12, 12–14)	(22, 14, 12–14)	2000	2000	Shut–In	2000
ASP26*	(35, 12, 12–14)	(22, 14, 12–14)	107	31	598	364
ASP28*	(35, 6, 12–14)	(18, 10, 11–14)	107	31	Shut–In	364

* For these cases the production wells were restricted to produce from the Supramound Interval using only the top five simulation layers.

Two injector well locations in each mound were investigated. In the Sahgzie mound the injection was located at either (35,12) or (35,6). Location (35,12) moved the injector south in the mound and closer to the Sahgzie Well No. 1. In the Anasazi mound the injector was either located at (18,10), which was the location of the Anasazi Well No. 6H–1 producer, or at (22,14). Using a straight line to connect the Anasazi Well No. 1 and Well No. 6H–1 locations, the (22,14) location placed the injector approximately midway between these two wells just north of the northern limit of the limestone unit (i. e. it was placed outside the mound area (phylloid algal limestone) of the main southern lobe of the Anasazi mound).

Production Well Back Pressure

The presence of free gas in a reservoir during waterflood operations results in three phase flow and reduced oil relative permeability. Reduced oil permeability reduces oil production rates and inhibits the "banking" of oil as injected water displaces reservoir fluid. Normal waterflood practices usually require reservoir re–pressurization to dissolve free gas to improve the displacement process. Because the Anasazi/Sahgzie mounds both will contain free gas saturation at the start of a waterflood, the back pressure imposed on the production wells was initially set to 2000 psia to stop or restrict production until reservoir fill–up had occurred. The cases which employed a 2000 psia back pressure are identified in the table above.

Because of low injectivity and slow propagation of water in the subject reservoir, it was found necessary to increase the pressure drops between injectors and producers to accelerate water movement. This was accomplished by lowering the back pressure on producers. In general, the back pressure on each producer was set to the bottomhole pressure calculated by the simulator at the end of primary depletion and the start of water injection. This data is provided in the table above. Thus, waterflood cases ASP19, ASP20, ASP26 and ASP28 used reduced back pressure values at the producers.

Completion Intervals of Injectors and Producers

In the first set of runs the injector wells were completed in all layers of the model (Layers 1 to 15). Thus, injection into both the Supramound and Core Mound Intervals, at the location of the injectors, was used. In these cases the associated producer wells were completed only in Core Mound Interval. At the producer locations the completions were thus in only the limestone unit.

Recognizing that water will segregate in the reservoir because of gravity forces an alternate injector/producer strategy was tried. This involved injection in the Core Mound Interval and production from the upper portion of the Supramound Interval. The completion intervals used for the injectors are identified in the table above for each case. Producers were completed only in the limestone unit (Core Mound Interval) for cases ASP18, ASP19 and ASP20. Producers for prediction cases ASP29, ASP26 and ASP28 were completed in the top five layers in the model, or essentially the top half at the Supramound Interval.

In addition to the specific operating variables used above, each waterflood also used the following controls.

1. The maximum water injection rate for a single injector was set to 750 BWPD.
2. Water injection started at 1/1/1997.

3. The maximum water injection pressure (bottomhole pressure restriction) was set to 3500 psia.

4. No economic limit or maximum water cut was invoked to control producers.

5. It was necessary to continue the waterflood past 1/1/2012 to identify positive waterflood behavior. In most cases simulation continued to 1/1/2022. Note that primary production predictions ended at 1/1/2012. Thus, no incremental recovery values for floods conducted past 1/1/2012 are presented.

15.3.2. Waterflood Prediction Case Results and Reservoir Performance Interpretation

Oil recovery and water injection/production on a field level basis is presented in Table 15–7 for all six waterflood cases. Figures 15–39 to 15–75, inclusive, present field and well level production/injection data for each of the five cases. Each waterflood case is compared to an extended primary depletion case using the history matched model employed in case ASC101. History match case ASC101 is nearly identical to case ASC102, which was used for some of the later CO_2 injection case prediction runs. Waterflood results will be reviewed on a case by case basis with a general overall summary at the end of this Section.

Waterflood Prediction Case ASP18

Prediction case ASP18 uses the Anasazi Well No. 6H–1 location for the Anasazi mound injector and the (35,12) location for the Sahgzie mound. In an attempt to pressure up the reservoir during reservoir fill–up, the three producers used a 2000 psia bottom hole pressure constraint. Thus, the reservoir pressure at the producer had to exceed 2,000 psia before the well was allowed to produce. The producers were completed only in the Core Mound Interval using original well completion intervals.

Figure 15–39 presents field level oil production data and contrasts the waterflood performance to the extended primary depletion case. As shown in Figure 15–39, no significant waterflood response occurs until the year 2007, 10 years after the start of injection. Well level production plots in Figures 15–40 to 15–45 show similar delays in production for both Anasazi wells. The Sahgzie Well No. 1 responded with oil production approximately 3.3 years after injection started on 1/1/1997. Note, water production in the Anasazi wells did not occur for several years after the start of oil production and their oil production rates are relatively low because of a low transmissibility between mounds and injector locations. However, for the Sahgzie Well No. 1 water production started at the same time oil production started and the watercut rapidly increased to over 95%. Analysis of water saturation and pressure maps for various time intervals indicated that because producers were not allowed to produce until local reservoir pressure exceeded 2000 psia, water injection had already displaced oil beyond the Sahgzie Well No. 1 and the reservoir was largely water saturated when local reservoir pressure build–up was sufficient to allow production.

Oil recovery for the field for this case was below primary and only after producing until 1/1/2022 did oil recovery approach primary recovery at 1/1/2012 (see Table 15–7). Oil recovery from both Anasazi wells exceeded 1/1/2012 primary recovery, but the waterflood had to be in operation for 20 years before this occurred. Low water injectivity prevented rapid pressure build–up and the requirement to re–pressure the reservoir to over 2000 psia to dissolve free gas is not practical with

the given reservoir description. The 2000 psia back pressure delayed water encroachment into mound and in the case of Sahgzie Well No. 1, allows mobilized oil to bypass the well and become water saturated before production starts.

To promote more rapid influx of water from the injectors into the producing well's drainage areas, the production wells need to be allowed to produce during fill–up. Also, to prevent possible oil bypass at Sahgzie Well No 1 the Sahgzie injector should be moved farther to the north in the mound. These options were evaluated in the next waterflood case.

Waterflood Prediction Case ASP19

Case ASP19 is a repeat of ASP18, but employs two important operating changes. First, the three producers are allowed to produce during reservoir fill–up. The bottomhole pressure constraint for each well was set to the calculated bottomhole pressure at the well at the time water injection is started (at 1/1/1997). Thus, since injection exceeds production, reservoir pressure build–up will occur and each well will remain on production during reservoir fill–up. In this case waterflooding improves oil recovery over primary. Once the initial declines in oil rate are reversed, Figure 15–46, and Table 15–8 data indicate that waterflood performance increases oil recovery over primary by approximately 618,000 STB at 1/1/2012. The initial decline in oil production is primarily attributable to the Anasazi Well No. 1 response, (see well level production data in Figures 15–47, 15–48 and 15–49). Injection of water temporarily retards oil influx into the core mound area of the Core Mound Interval. Only after water injection mobilizes and "banks" oil does oil influx into the Anasazi mound increase and the well respond with an increasing oil rate. The brief oil spike in the Sahgzie Well No. 1 history, which lasts for approximately 1.5 years is caused by water preferentially flooding the limestone unit in the Core Mound Interval. This preferential water movement occurs despite the injector being located farther north than in Case ASP18. Also, the Sahgzie mound injector is able to sustain injection rates in excess of 500 STB/D without violating the 3500 psi pressure constraint (See Figures 15–53 and 15–52). Once the limestone interval is flushed, the oil rate declines below primary (water drive less efficient in recharging the limestone unit than pressure depletion and gravity segregation) and only gradually increases above the primary rate. Once, the oil flushing of the limestone interval is complete, the oil rate declines and the water cut increases rapidly. This is shown in Figure 15–52, which plots oil rate and water cut for the Sahgzie Well No. 1. The delayed water production, relative to the Sahgzie well, shown in Figures 15–50 and 15–51 is indicative of a different water displacement mechanism in the Anasazi mound. Although water invades the limestone in the Anasazi mound it occurs less rapidly than in the Sahgzie mound and the displacement of oil from the Supramound is more complete. Oil rates are improved over those for the ASP18 case but still reach only a peak value of approximately 200 STB/D per well. The substantial increase in the pressure gradient between injectors and producers (caused by the low pressure constraint imposed on the producers) is responsible for the increased oil rate. Low reservoir pressure in the vicinity of the producing wells enhances oil influx into their respective drainage areas and supports higher production rates. The lower reservoir pressure also is responsible for the presence of free gas in the reservoir. As indicated above, the presence of gas can result in three phase flow and the reduction of oil relative permeability, which causes decreases of oil flow into the wells.

The overall waterflood response for Case ASP19 is the best of all cases studied. However, in terms of oil rates, total recovery and time required to recover the oil it finished a poor second to the best CO_2 flood case.

Waterflood Prediction Case ASP20

Waterflood case ASP20 is a repeat of Case ASP19, except the Sahgzie injector was moved farther south (35,6), closer to the Sahgzie producers. Production plots are presented in Figures 15–55 to 15–58. Moving the Sahgzie injector closer to the Sahgzie Well No. 1 producer resulted in a more rapid flushing of the limestone interval by water, followed by lower oil rates than exhibited in ASP19. The proximity of the injector to the producer results in higher water saturations in the well vicinity and causes the waterflood rate for the Sahgzie well to be lower than the primary rate predicted for almost the entire duration of the waterflood (see Figure 15–58).

Also, the Sahgzie injection is closer to the Anasazi Well No. 1 well than in prediction case ASP19. This has a detrimental impact on the Anasazi Well No. 1 waterflood response relative to that predicted in the ASP19 case. Increased water invasion, or less oil displacement, lowers the Anasazi Well No. 1 waterflood recovery (relative to ASP19 – compare Figure 15–47 and 15–56). Thus, with both the Sahgzie well and the Anasazi Well No. 1 negatively impacted by the different location of the Sahgzie injector, the overall field incremental oil recovery is lowered by over 37% (387,000 STB for ASP20 versus 618,000 STB for ASP19). This occurs despite improved performance of the Anasazi Well No. 5L–3 response (compare Figures 15–48 and 15–57).

Waterflood Prediction Case ASP25

In an attempt to delay water breakthrough and improve volumetric sweep, the completion intervals of both injectors and producers were altered relative to previous cases and the Anasazi mound injector location also was altered. In prediction cases ASP25, ASP26 and ASP 28, water injection was restricted to the Core Mound Interval and production was restricted to the upper half of the Supramound Interval (Layers 1 to 5). This approach was designed to have viscous and gravity forces oppose each other in regard to water movement from the Core Mound Interval to the Supramound Interval. In addition, the pressure gradient imposed on the Mound Interval limestone would be reduced (if injectors and producers were connected in different intervals). Prediction case ASP25 tested this approach with the production wells shut–in until local reservoir pressure exceeded 2000 psi (similar pressure control to ASP18). Total predicted oil recovery for ASP25 showed improvement over that for ASP18 (see Table 15–7 and Figure 15–59), but the requirement of re–pressurizing the reservoir to 2000 psi was too restrictive. Thus, recovery to 1/1/2012 was much worse than predicted primary recovery.

Waterflood Prediction Case ASP26

Prediction case ASP26 is a repeat of ASP25, the only change being alteration of the bottom hole pressure constraints set for the producers. As in ASP19, the bottomhole pressures were set to those calculated for each well at the start of injection (see the Table on page 101). Field and well level oil production data is provided in Figures 15–60 to 15–68. Overall field performance is worse than for Case ASP19 and only slightly better (78,000 STB more) than primary depletion through 1/1/2012. The relocation of the Anasazi mound injector adversely impacted the performance of the Anasazi Well No. 1. Water breakthrough occurred roughly four years earlier in ASP25 than ASP19. Also, the lower transmissibility of the Supramound Interval relative to the Core Mound Interval at the Anasazi Well No. 1 location adversely impacts the oil rate. In contrast, the total oil recovery prediction for the Anasazi Well No. 5L–3 remained about the same. However, the oil production history changed substantially and the peak oil production time was delayed relative to that predicted

in Case ASP19 (compare Figures 15–62 and 15–48). The rapid response of the Sahgzie well noted in ASP19 was damped as the water invasion pattern changed from a rapid flushing of the limestone interval to a more gradual invasion from the limestone interval into the Supramound Interval (now the production interval). However, the overall Sahgzie Well No. 1 response was still adversely impacted relative to that predicted in ASP19.

In general, the waterflood sweep is good with water invasion occurring from the lower limestone unit upwards into the Supramound Interval. This change in water movement was even accompanied by some local water coning. In a final attempt to improve the waterflood using this revised completion strategy, ASP25 was repeated but the Anasazi mound injector was relocated to the Anasazi Well No. 6H–1 location. Thus, a more direct comparison (not influenced by injector location) can be made with ASP19 and the change in reservoir performance caused by revised injector/producer completion more clearly identified.

Waterflood Prediction Case ASP28

Prediction Case ASP28 is a repeat of ASP25, but with the Anasazi injector returned to the Anasazi Well No. 6H–1 producer location. Production plots are presented in Figure 15–69 to 15–75. In contrasting the performance of ASP28 with ASP19, the relocation of injector/producer completions, as discussed above, caused the following changes in waterflood performance.

1. Water breakthrough was substantially delayed (> 6 years for the Anasazi wells and approximately 2 years for the Sahgzie; compare Figures 15–73 to 15–75 with Figures 15–50 to 15–52).

2. The change in water movement caused by the change in completions resulted in a significant delay in waterflood response. The time to the peak oil rate response occurs much later in ASP28 and than in ASP19. As discussed above, the water movement for the ASP25 case is upward from Core Mound Interval to Supramound Interval. In ASP19, water movement is generally from Supramound into the Core Mound and laterally in the Core Mound Interval. The earlier recovery of oil in ASP19 is attributable to the direct limestone interval displacement of oil toward limestone interval producers. In ASP28, the oil in the limestone unit must now be displaced upward into the Supramound Interval and then laterally in the Supramound Interval to the producers. This causes the delay in production response exhibited by ASP28.

3. Overall recovery from both the Anasazi Well No. 1 and Sahgzie Well No 1 are less for Case ASP28 than for Case ASP19. However, the response in terms of total oil recovery for Anasazi 5L–3 is improved for ASP28. Nevertheless, the delayed production response predicted for Case ASP28 adversely impacts the net present value of the oil production.

4. Total field recovery favors the completion strategy used in ASP19. This approach recovers more oil and exhibits a more favorable rate history.

General Waterflood Summary

In general, the lower mobility of water relative to CO_2 and the corresponding poor injectivity of the water injectors significantly delays waterflood response relative to CO_2 flooding response. The

need to operate producers at low bottomhole pressure to enhance water influx and improve waterflood response time results in three phase flow conditions in the reservoir and reduces oil mobility. This contrasts to the two phase flow present in a CO_2 flood. The increase in oil volume caused by CO_2 swelling and the reduced oil viscosity caused by CO_2 oil mixing, all favor higher oil mobility. The relatively lower displacement efficiency of water relative to CO_2 decreases total recovery. Figures 15–76 and 15–77 clearly illustrate the impact displacement efficiency has on mobilizing oil. Figures 15–76 and 15–77 present residual oil saturation predictions for a cross section through the Anasazi injection location (18,10) for both CO_2 flooding and waterflooding. Figure 15–76 shows the effectiveness of the CO_2 in displacing oil. In Figure 15–76, the red color represents essentially zero oil saturation. CO_2 has mobilized essentially all the oil in the CO_2 swept zone at the end of the flood (1/1/2012). In contrast, residual oil saturation present in the water swept zone in Figures 15–77 vary from 25% to in excess of 40%. Thus, immiscible waterflood displacement is relatively ineffective in contrast to the CO_2 process, which reduces oil saturations below waterflood residuals via a mass transfer mechanism.

Contrasting the best waterflood recovery to the best CO_2 recovery at 1/1/2012 shows that the CO_2 incremental recovery, relative to primary depletion, is 2,484,000 STB versus an incremental recovery from waterflooding of 618,000 STB. This represents roughly a 1,800,000 STB difference. Waterflood performance can be improved but would require an additional 10 years of operation to gain an additional 500,000 STB of oil.

Comparison of the CO_2 and waterflood predictions favor CO_2 because of:

1. Higher oil recovery.
2. Substantially higher oil rates which provide improved cash flow.
3. Shorter project life.
4. Return to primary depletion is possible with a shortened or aborted CO_2 project. A return to primary depletion, after attempting a waterflood, will be ineffective because the mound area will be largely water saturated, resulting in three phase flow and a gravity response unfavorable to returning oil to the Core Mound Interval.

Other factors which may adversely impact waterflooding include obtaining or developing a water source and the potential cost of water. These two factors have not been investigated, but could likely further reduce the potential.

For these reasons, CO_2 flooding was accepted as the best alternative to improving oil recovery from the Anasazi–Sahgzie reservoir and similar algal mound fields. Thus, the economic assessment is focused on CO_2 alone.

16. ECONOMIC ASSESSMENT

16.1. Introduction

Completion of the history match using the simulator and associated geologic model provided the basis for predicting performance of the Anasazi–Sahgzie reservoir for various production processes. Chapter 15 provided details and data for the projected performance of the subject reservoir for three processes. These processes included:

1. Primary depletion based on continuation of current production operations.
2. Carbon dioxide flooding under these different operating conditions. These three conditions are:
   a. Continuous CO_2 injection with the produced gas re–injected without processing.
   b. Continuous CO_2 injection with re–injection of produced CO_2 removed from the produced gas stream via a gas conditioning plant.
   c. Continuous CO_2 injection with produced gas re–injected for a period of six years, followed by reservoir blow down.
3. Waterflooding under various operating conditions and well placement configurations.

Because the waterflood case predictions indicated that the projected performance of waterflooding was marginal from an incremental recovery standpoint (compared to continued primary depletion), economic assessment of this option was not undertaken.

The remaining optional reservoir management approaches, continued primary depletion and CO_2 flooding, were subjected to a complete economic assessment.

Primary depletion required no additional capital investment and the production profile provided via the simulation studies was used together with current operating costs to determine the economic viability of continuing the current operation through the year 1/1/2012.

In economically evaluating the CO_2 flooding option, several implementation strategies required assessment. Because of the corrosive nature of the injectant and produced fluids, and high operating pressure required for developing miscibility in the reservoir, a major upgrading of well and production equipment was required. In addition, a CO_2 flood will require the addition of new wells for CO_2 injection, construction of a CO_2 supply line, installation of new lease flow lines and injection lines and installation of a main injection compressor. In addition, to assess the economic viability of using a gas conditioning plant to process produced gas to separate the CO_2 (used for re–injection) from hydrocarbon components of the gas (used for fuel or sales), the capital and/or leasing costs of this facility need to be developed and used in the economic assessment. Thus, costs associated with the CO_2 implementation need to be determined. Prior to presenting results of the economic assessment, the new well completions and facilities requirements for CO_2 implementation are reviewed and appropriate costs presented for capital and/or leasing, as well as the associated operating costs. This is presented in the next Section of the report, followed by an economic assessment section.

16.2. CO_2 Flood Implementation – Design and Costs

The changes to existing production facilities and addition of new systems are discussed under the following main topics:

1. Production and injection wells.
2. Surface production and injection lines.
3. Surface production facilities.
4. CO_2 supply line.
5. Main injection compressor.
6. Gas processing plant.
7. CO_2 purchase costs.
8. Miscellaneous fees.
9. Seismic survey and CO_2 flood re–design.

16.2.1. Production and Injection Wells

Previously discussed simulation prediction cases defined the operating conditions and well location requirements for the maximizing oil recovery from the Anasazi–Sahgzie reservoirs using CO_2 flooding. These prediction cases defined the required reservoir operating pressure and associated injection and production well fluid flow (injection or production) rate history. The prediction cases selected for economic assessment employed the following conditions.

1. Injection wells:
   - Maximum injection rate per well set at 7.0 MMSCF/D.
   - Maximum bottomhole injection pressure set at 3500 psia.
   - Bottomhole temperature 130°F and surface temperature 70°F.
2. Production wells
   - Flowing condition during CO_2 flood restricted to maintain a minimum bottomhole flowing pressure of 2000 psia.
   - Maximum flow restriction imposed during blowdown against a flowing tubing head pressure of 100 psia was set to 5.0 MMSCF/D based on production equipment (separator) design for each well.
   - Maximum surface pressure expected was less than 1000 psia.
   - Bottomhole temperature 130°F and surface temperature 70°F.

Based on two phase flow calculations for the above identified injection well operating conditions and possible injection well shut–in, a maximum surface pressure of 2000 psia was used for design

of well head and tubulars for the injector. Using simulation based injection/production fluid rates, 2 7/8″ O.D. tubing for injectors and 2 3/8″ O.D. tubing for producers were selected. All well equipment was designed for CO_2 service. CO_2 service impose special metallurgy requirements on both wellhead and down hole equipment. In addition, tubing requires internal coating, and casing exposed to produced fluids was specified to be a chrome–molybdenum alloy. Design specification and associated costs are provided in Appendix A. Costs for equipment are based on local suppliers quotes during 1997. For special equipment (i.e.: compressors and gas conditioning plants), quotes were obtained from qualified field equipment suppliers.

Appendix A provides the design specifications employed and cost breakdown for:

1. Re–completing three producers for CO_2 service (Anasazi Wells 1 and 5L–3 and the Sahgzie Well 1).
2. Drilling and completing a new injection well located (see Chapter 15) on the northern portion of the Sahgzie mound.
3. Re–completing the Anasazi Well No. 6H–1 producer as a CO_2 injector.

16.2.2. Surface Production and Injection Lines

Because of the corrosive nature of CO_2 and high injection pressures all new lease surface lines are proposed. Required surface lines would include:

1. Injection lines.
2. Co–mingled oil and gas production lines.
3. Separated gas (CO_2 and hydrocarbons) lines.

These line requirements are based on the current Anasazi/Sahgzie production system and utilize existing well sites for placement of surface production facilities (either new or replacement systems). Currently, the Anasazi Well No. 1 produces into separation facilities at the Sahgzie well site, the Anasazi Wells 5L–3 and the 6H–1 produce into separator facilities at the Anasazi Well 1 site and the Sahgzie Well No. 1 produces into facilities located on the Sahgzie well site. The main injection compressor was located at the Anasazi Well No. 1 Well site. If all produced gas is re–injected, fuel gas will be required from other locations. Thus, the existing sales gas line from Anasazi/Sahgzie to the Elkhorn transfer point is being proposed as either a fuel gas supply line or a fuel gas sales line, depending on the production history of the field. Retaining the current production system layout, the surface line requirements are:

1. Injection lines from the proposed compressor site to the Anasazi 6H–1 location and the new Sahgzie mound injector will require 7200 feet of line. This line is proposed to be located along existing right of way, with a new connection between the Anasazi 6H–1 site and the new Sahgzie injection site. This will require 5000 feet of line for the Sahgzie injector and 2200 feet for the Anasazi 6H–1 injector (total of 7200 feet).
2. Retaining the existing production facility setup, 6300 feet of new co–mingled oil and gas production lines are required. This consists of 1800 feet from the Anasazi 5L–3 well to the Anasazi Well No. 1 site, 4000 feet from the Anasazi Well No. 1 to the Sahgzie Well

No. 1 site and 500 feet of line from the Sahgzie Well No. 1 to the Sahgzie separation facility at the Sahgzie Well No. 1 site.

3. Separated gas (CO_2 plus hydrocarbons) needs to be transported from the various separation facilities at the well sites to the main compressor and/or gas plant at the Anasazi Well No. 1 site. This requires 4500 feet of new surface line, 4000 feet from the Sahgzie site to the Anasazi site and 500 feet at the Anasazi site (connects Anasazi Well No. 5L–3 to the compressor/gas plant).

The subject surface injector lines are designed to carry up to 15 MMSCF/D of CO_2 and will require internal coating to prevent or reduce CO_2 induced corrosion. Similarly oil and gas production lines and separated gas lines will require coating because of the presence of CO_2.

Details on the specifications, installation and costs are provided in Appendix A.

16.2.3. Surface Production Facilities

Surface equipment includes vertical separators and horizontal heater treaters for each well. Separators are specified with a corrosion tolerance and treaters are internally coated. A central glycol dehydrator for removing water from the separated gas is included and is designed to process a maximum of 15.0 MMSCF/D. Current equipment needs to be replaced to handle the higher volumes of produced gas expected (5.0 MMSCF/D) with the CO_2 flood, and also require redesign for CO_2 corrosion operation. In addition to the produced fluid treatment facility, new lined storage tanks are also included in the overall facility design.

16.2.4. CO_2 Supply Line

It is proposed to transport the CO_2 required for the project from the closest anticipated source point via pipeline. Two source points are possible. One is the Mobil Oil Ratherford Unit located approximately 13 miles from the Anasazi Well 1 site and the other is at the San Juan river crossing, approximately 17 miles from the Anasazi. The 13 mile option was selected for estimating the cost of installing a CO_2 supply line. The CO_2 supply line was designed to transport 15 MMSCF/D at a pressure of 2200 psi.

As discussed in Appendix A for the flow/injection line installation, quotes from the same two construction companies were obtained for the CO_2 supply line. Also, as outlined in the flow/injection line discussions, six different installation options were available. These involved various combinations of mechanical coupling options (ZAPLOCK versus Heatpro's CCB connectors), surface versus buried installations and different construction costs from two different construction companies. As outlined in Appendix A a minimum and maximum installation set of cost data were selected and used for economic assessment. The final design will likely use a combination of ZAPLOCK and Heatpro connectors and the cost will likely be bracketed by the proposed minimum/maximum limits. Details on the line specification and costs are provided in Appendix A.

16.2.5. Main Injection Compressor

The main injection compressor is designed to compress and deliver a maximum of 15.0 MMSCF/D of CO_2 at 2000 psi. The main compressor could be purchased or leased. Appendix A provides

general compressor specifications, purchase costs and supplier information. Installation costs, including an enclosed building, are also provided in Appendix A. The lease option costs are discussed in Section 16.4

16.2.6. Gas Processing Plant

One of the operating options that required evaluation was the use of a gas conditioning plant designed to separate CO_2 from hydrocarbon components of the produced gas. The separated CO_2 stream was to be re–injected to reduce the cost of purchasing CO_2 , while the hydrocarbon rich stream would be used as lease fuel and/or sold at prevailing gas prices. Continued injection of essentially pure CO_2 could impact reservoir performance and thus influence oil rate production history. The use of the hydrocarbon stream would reduce lease operating costs and/or generate revenue from the sale of gas. These benefits are offset by the cost of purchasing, installing and operating a natural gas purification system. The design and estimated cost of a membrane separation system was provided by the Cynara Company. The membrane system used hollow fiber technology and was designed to reduce the CO_2 content of the produced gas to below 4.0 mole percent. The plant was designed to treat a maximum of 15.0 MMSCF/D and required an inlet gas pressure of 450 psig. Separator gas thus required compression from the separator pressure (less than 100 psi) to 450 psig. This would be provided by a separate gas compression system. The gas compressor design is also included in the overall gas plant specification. Details of the system and associated costs are provided in Appendix A.

16.2.7. CO_2 Purchase Costs

Preliminary cost estimates for purchasing CO_2 from Mobil Oil, based on communication with Harken Energy, provided an estimate of $0.85/MSCF. Simulation prediction cases provided CO_2 injection rate requirements over the duration of each project. Re–injection of either unprocessed production gas or pure CO_2 separated for the produced gas substantially reduces CO_2 purchase costs. The schedule of these costs were developed from each prediction case and input as a lease operating cost into the economic evaluation program. Two additional CO_2 supply options are possible. The first is the development of a Harken owned CO_2 reservoir, in the Paradox Basin area. The cost of developing this CO_2 source and transporting the produced CO_2 to the Anasazi/Sahgzie reservoir however, has not been assessed. The second option is the direct purchase of CO_2 form the well head at McKelmo Dome. The approximate cost for CO_2 at the wellhead is $0.50/MSCF. However, a supply pipeline would have to be constructed from McKelmo Dome to Anasazi and the difference in CO_2 costs ($0.85 versus $0.50 MSCF) would have to economically justify this option. Based on CO_2 requirements for the Anasazi/Sahgzie system alone this is not an economically viable option. However, if two or more small algal mound systems were CO_2 flooded at the same time a direct source option could possibly be supported.

16.2.8. Miscellaneous Fees

Harken Energy staff provided an estimate for archeology permits, surveys and cattle grazing charges that would be payable to the Navajo Nation for installing new flow lines for the project. Total fees for the CO_2 supply line and lease lines for injection of CO_2 and transporting separated gas to the main compressor were estimated at $201,000. Details are provided in Appendix A.

16.2.9. A New Seismic Survey and CO_2 Flood Re–Design

As discussed in the history matching section of the report (Chapter 14), both the Anasazi and Sahgzie mound required modifications from a internal fluid communication standpoint. One of the possible reasons it was the necessary to introduce internal fluid flow communication barriers, was that the external geometry of the main mounds is not completely defined using the current seismic interpretation.

To improve the overall geometric interpretation of both mounds and provide direct information to help locate injector wells, a three–dimensional (3–D) seismic survey should be run prior to a CO_2 flood implementation. If a 3–D survey is conducted and it leads to an alternate reservoir description that is sufficiently different than the current interpretation, it would be necessary to re–design the CO_2 flood from the standpoint of injector well locations. Thus, in addition to the cost of a 3–D seismic survey and its associated interpretation, the current reservoir geologic model would require revision. Also, additional simulation runs would be required to optimize the CO_2 flood implementation from a well location standpoint. This would also entail an update of the history match. Details of the costs of these activities are provided in Appendix A.

Tables 16–14 and 16–15 provide a summary of total investments for the cases that included purchase of the main injection compressor and the case where the compressor is leased. Projected DOE cost sharing estimates based on the Phase I participation percentage are also included.

16.3. Operating Cost Data

16.3.1. General Operating Costs

Basic current operating costs for the Anasazi–Sahgzie field were provided by Harken Energy Corporation based on past operations. This was estimated as $2,000/well/month. This basic operating cost was used as needed in the various economic assessments carried out for continued primary depletion and the various CO_2 projects. For the economic cases evaluated, this cost was treated as constant for the life of a project. No inflation escalation was used.

Basic field operating expenses were increased by 50% to $3,000/well/month for all CO_2 projects. Again, no operating expense escalation was used during the project. The operating expenses were increased to reflect increased costs associated with CO_2 operations and higher operating pressures. Also, the proposed operating expense for CO_2 operations is in general agreement with other data[16–1]. In addition to basic operating costs, fuel requirements for treaters and the glycol dehydrator were calculated and treated as a separate cost stream in the economic evaluations. Fuel could be treated as being supplied from available produced gas or, in the case of CO_2 projects which re–injected produced gas without processing to separate the CO_2, as a monthly expense. Fuel requirements for basic production equipment was determined to be approximately 73 MSCF/D. Using $1.80/MSCF as the purchase price for fuel, a monthly operating cost of approximately $4,000 was included as an ongoing expense while the field produces.

Operating costs associated with the main CO_2 injection compressor include supplies such as lubricants, antifreeze, etc., regular maintenance and service and fuel requirements. Tide Aire and Gas Company's service organization, Tidewater Compression Services, Inc. (TCS) estimates months consumable (lubricants, antifreeze, etc.) at $2,000/month for the proposed compressor system (See Appendix A). In addition, TCS estimates for providing a full time technician to run

and service the gas compressor system are $9,000/month. In conducting the economic assessment for the subject project, this operating expense was modified based on Harken providing a technician. Because the gas compression system is fully instrumented and designed for continuous unattended operation, the Harken provided service technician for the system was charged at $4,000/month, assuming some of the technician's time could be billed to other activities. Thus, the monthly operating expense for the gas compressor system was set at a constant monthly charge of $6,000.

For CO_2 injection projects, the fuel requirement for the injection compressor is an ongoing expense while the compressor is operating. Fuel requirements, based on the designed brake horse power of the compressor, were calculated as 450 MSCF/D. In those cases were fuel could not be provided from the produced gas, a monthly operating expense of $25,000 (based on $1.80/MSCF gas) was charged to the project. This charge was initiated, for example, once the CO_2 concentration of the produced gas prevented it from being used as fuel if no gas processing was provided.

Thus, the operating expenses charged to the project for use of the compressor was $6,000/month for supplies, maintenance and service and $25,000/month for fuel when operations required fuel purchase. Also, for those cases where produced gas did not meet fuel requirements, the current sales gas line from Anasazi to the Elkhorn transfer point would be used as a fuel line and a monthly fee of $2,500 charged to the project for fuel gas compression at Elkhorn to cover rental of a compressor system.

One further operating expense that could be incurred for a CO_2 project would be a monthly charge for leasing the gas compressor system instead of purchasing the system at the start of the project. Lease quotes were provided by Tidewater Compressor Services, Inc. of Houston, Texas. Lease option of three and five years were provided. Also, lease terms could be with or without maintenance. In evaluating the lease option, a five year contract without maintenance was selected. The quoted charge for this type of lease for the gas compressor system outlined in Appendix A was $28,000/month. Supplies, maintenance and service were charged the project as outlined above for a purchased system. Thus, the full cost of a leased compressor system was $34,000/month (lease $28,000/month, supplies $2,000/month and maintenance/service $4,000/month).

16.3.2. Gas Processing Plant Operating Expenses

Operating expenses for the gas processing plant are associated with the gas compressor system and the main filter system. Gas compressor operating expenses for the small compressor required to compress gas to 450 psig and the filter system were set at :

Consumable Supplies (lubricant, antifreeze, etc..)	$1,000/month
Maintenance Services (shared w/main injection compressor)	$2,000/month
Membrane filter system (assume no filter replacement)	$2,000/month
Total	$5,000/month

In addition to the above monthly operating expenses, which were assumed constant for the project, a fuel gas cost will be incurred. Fuel consumption was calculated at 350 MSCF/D. If fuel had to be purchased, a monthly charge of approximately $19,000 would be assessed the project. In prediction cases involving gas processing, fuel requirements were first met from processed

produced gas. Only if fuel gas requirements exceeded the volume of produced hydrocarbon gases would fuel purchase be required.

16.3.3. CO_2 Supply Line Operating Expense

Operating expenses for the CO_2 supply line were obtained form a report prepared by Science Applications, Incorporated on behalf of the U.S. Department of Energy[16-2]. These reports estimate annual operating expenses at 1.0% of total capital expenditure for the pipeline. The subject economic assessment evaluation identified a range of capital cost for the CO_2 supply line (a minimum and a maximum were selected for economic runs). The maximum capital option was used for all cases when providing the operating costs, which were again assumed constant for the life of the project. Based on the $2,031,000 pipeline cost (See Appendix A), the operating expense for the pipeline was calculated as roughly $20,000/year or $1,600/month.

16.3.4. CO_2 Purchase

The price employed for purchasing, CO_2, as well as other supply sources for CO_2, were discussed previously in Section 16.2.7. In providing monthly CO_2 purchase cost data for economic assessment work, simulation data for each prediction was post processed and CO_2 make–up volumes were calculated. Using $0.85/MSCF, a monthly CO_2 cost was then calculated using the makeup volume and provided as input to the economic evaluation software.

The simulation results provide the CO_2 make up volume requirements by using the injection volume calculated for each well, subject to the well constraints imposed in the simulation, and the volume of gas available for re–injection. When the CO_2 project starts, all injected CO_2 must be purchased. However, for prediction cases evaluating gas processing, the reclaimed CO_2 from the produced gas is re–injected, thus reducing the volume of CO_2 that must be purchased. For the cases where the produced gas is re–injected without processing, the entire volume of produced gas could be used to reduce CO_2 purchases. In this case the produced gas was used as fuel and/or sold until the CO_2 concentration exceeded sales and fuel gas constraints on CO_2 concentrations. At this point it was re–injected and subsequently reduced the CO_2 purchase cost. Thus, the CO_2 purchase history was determined directly from simulation results and the cost of CO_2 treated as a monthly operating expense.

16.4. Economic Evaluations

Prior to presenting results of the economic evaluation cases completed and reported in the report each case is defined and basic input data and economic evaluations are reviewed. Following this, the results of each case are summarized and tables containing detailed economic results are presented. Finally, the economic evaluation work is summarized.

16.4.1. Case Descriptions

A number of economic sensitivity evaluations were completed. These evaluations provided economic performance data to compare and assess various CO_2 process implementation options. The following options were evaluated:

1. Basic reservoir recovery processes (i.e. primary versus various CO_2 flood implementations)

2. Gas processing.

3. Installation options for the CO_2 supply line.

4. Purchase versus lease of the main compressor.

5. DOE cost sharing.

The descriptions for each evaluation follows. A list of these evaluations is followed by a brief description.

In the following table, the column heading "CO_2 Supply Line" refers to the costs associated with various options for installing both flow and injection lines on the lease and the CO_2 supply line. The minimum cost options indicates that flow/injection lines and the CO_2 supply line were installed on the surface using ZAPLOCK mechanical connectors. The maximum cost option indicates that flow/injector lines and the CO_2 supply lines were taped and buried and the HeatPro CCB connectors were used to join pipe segments. The DOE cost sharing column provides a means of identifying whether the economics were run with the DOE sharing approximately 45.0% of the capital investment required to implement the specific case.

List of Economic Evaluation Cases

Evaluation Number	Reservoir Process	Compressor		CO_2 Supply Line		Gas Processing	DOE Cost Sharing
		Leased	Purchase	Minimum	Maximum		
1	CO_2 Inj	–	Yes	Yes	–	Yes	No
2	Primary	–	–	–	–	–	No
3	CO_2 Inj	–	Yes	Yes	–	No	No
4	CO_2 Inj	Yes	–	Yes	–	No	No
5	CO_2 Inj	–	Yes	Yes	–	No	Yes
6	CO_2 Inj	Yes	–	Yes	–	No	Yes
7	CO_2 Inj	–	Yes	–	Yes	Yes	No
8	CO_2 Inj	–	Yes	–	Yes	No	No
9	CO_2 Inj	Yes	–	–	Yes	No	No
10	CO_2 Inj	–	Yes	–	Yes	No	Yes
11	CO_2 Inj	Yes	–	–	Yes	No	Yes
12	CO_2 Inj	N/A	N/A	N/A	N/A	N/A	N/A
13	CO_2 Inj	N/A	N/A	N/A	N/A	N/A	N/A
14	CO_2 + Blowdown	–	Yes	Yes	–	No	No
15	CO_2 + Blowdown	–	Yes	–	Yes	No	No

A brief description of each of these economic evaluations follows:

Evaluation1

This evaluation uses continuous CO_2 injection employing gas re–injection. It assumes purchase of a new injector compressor and minimum pipe line installation costs. Use of a gas processing plant to separate the CO_2 and hydrocarbons is included. No DOE cost sharing is provided.

Evaluation 2

This evaluation uses the predicted performance of continued primary depletion reservoir performance, coupled with current operating costs and no new capital investments.

Evaluation 3

This evaluation is based on the simulated prediction performance of continuous CO_2 injection utilizing total gas re–injection, with no gas processing to remove hydrocarbons coupled with purchase of the main injection compressor, minimum pipeline installation costs and no DOE cost sharing.

Evaluation 4

This evaluation is a repeat of Evaluation 3, but with the main injection compressor leased instead of purchased at the start of the project.

Evaluation 5

This evaluation is a repeat of Evaluation 3, but with DOE cost sharing. The DOE projected 45% cost sharing of capital costs would reduce Harken's capital outlay by approximately $2,200,000.

Evaluation 6

Evaluation 6 is a repeat of Evaluation 4, but with cost sharing. Evaluation 6 can also be described as a repeat of Evaluation 3, but with the main compressor leased and DOE sharing tangible capital costs.

Evaluation 7

Evaluation 7 is a repeat of Evaluation 1, but with pipeline/flow line cost assessed at a maximum cost instead of the minimum capital expenditure.

Evaluation 8

Evaluation 8 is a repeat of Evaluation 3, but with pipeline/flow line costs assessed at the maximum cost.

Evaluation 9

Evaluation 9 is a repeat of Evaluation 4, except that the pipeline/flow line costs are assessed at the maximum cost.

Evaluation 10

Evaluation 10 is a repeat of Evaluation 5, except that pipeline/flow costs are assessed at the maximum case.

Evaluation 11

Evaluation 11 is a repeat of Evaluation 6, except that pipeline/flow line costs are assessed at the maximum case.

Evaluation 12

Evaluation 12 uses continuous CO_2 injection predicted performance data employing unprocessed gas re–injection until the year 2003. At 1/1/2003, reservoir blowdown is started and production performance follows a natural depletion course. The evaluation includes a purchased compressor, minimum pipeline/flow line costs and no DOE cost sharing.

Evaluation 13

Evaluation 13 is a repeat of Evaluation 12, except that pipeline/flow line costs are assessed at the maximum cost.

16.4.2. Base Economic Parameters

Base economic parameters that were used for all economic evaluations included:

1. Oil Price – $20.00/Bbl (Flat)
2. Gas Price – $1.80/MSCF (Flat)
3. Projects start in June 1996 with continuous production via natural depletion until 1/1/1997. At 1/1/997 CO_2 projects were started with the initiation of CO_2 injection.
4. Project life was set at 187 months (1/1/2012), the expiration date of current leases.
5. Royalty was set at 20% for oil for prices below $22/Bbl and 23% for oil prices above $22/Bbl. Gas royalty was set at a fixed 20%. Harken's oil and gas revenue interest was thus 80% for the project life, since a flat oil price schedule was used.
6. The federal tax rate was set at 34%.
7. Leasehold, geological and geophysical and intangibles were expensed at 100% in the year they were incurred.
8. Depreciation of tangible investments used the declining balance method at 200% of the straight line rate, with a switch to straight line at the optimum time.
9. Discounted revenue streams were calculated using a 10% discount rate.
10. A before tax profitability index (PI) is calculated by dividing the sum of total undiscounted net cash flow before tax plus the total net investment by the total net

investments. The after tax PI is calculated in the same way, except that the total undiscounted net before tax cash flow is replaced by the total undiscounted net after tax cash flow.

16.4.3. Economic Evaluation Results

The detailed results for each evaluation are presented in Tables 16–1 to 16–13. These tables have a letter "a" or "b" attached to table number, depending on the nature of the output. Both the "a" and "b" tables present yearly data on gross oil and gas production and net sales revenue. The "a" tables also present lease operating expenses, investments and undiscounted and discounted cash flow streams. The "b" tables report additional data on net total revenues and net lease revenues, net taxes and net taxable income plus after tax cash flow streams. Net present values at different discount rates, payouts, profitability indices and rates of return are summarized for each case. Reserves are reported for each case. The cumulative reserves refer to the field's production at June 1, 1996. The remaining reserves reflect the predicted cumulative recovery from June 1, 1996 to the end of the project (1/1/2012). The ultimate reserves are given as the total of the cumulative and remaining reserves. In addition, a brief description of the particular evaluation is provided which identifies key parameters used in the evaluation.

The following table summarizes the economic evaluation for 13 different conditions. These conditions reflect various CO_2 implementation options and the availability or absence of DOE cost sharing.

Summary of Economic Evaluations

Evaluation Number	Table Number	Gross Oil Production MSTB	Before Tax NPV @10% M $	Before Tax R of R%	Payout Months	P I
1	16–1a,b	3286	9,111	30	47	3.8
2	16–2a,b	880	–	–	–	–
3	16–3a,b	3344	12,145	42	41	6.4
4	16–4a,b	3344	11,230	48	39	8.2
5	16–5a,b	3344	14,179	57	37	11.7
6	16–6a,b	3344	12,500	62	37	14.9
7	16–7a,b	3286	7,967	26	49	3.3
8	16–8a,b	3344	11,255	37	42	5.4
9	16–9a,b	3344	10,399	41	41	6.3
10	16–10a,b	3344	13,686	52	38	9.8
11	16–11a,b	3344	12,068	56	37	17.2
14	16–12a,b	2571	9,759	40	41	5.0
15	16–13a,b	2571	8,869	35	42	4.2

Investment criteria for the primary depletion evaluation are not entered in the above table (see Table 16–2a and 16–2b for data) since the initial investment for the field was not included in this evaluation

and thus net present values, rates of return, etc. are misleading. The current evaluation just assesses the profitability of continuing operation, without the influence of prior (before June 1996) investments.

The best overall CO_2 implementation option is identified in Evaluations 6 and 11. Evaluations 6 and 11 use continuous CO_2 injection with unprocessed, produced gas re–injection, coupled with a leased injection compressor and DOE cost sharing. Evaluation 6 uses the minimum capital cost option for pipeline/flowline installation and Evaluation 11 uses the maximum cost option for the line installations. Evaluation 6 provides a rate of return of 62%, a payout of 37 months, a profitability index of 15 to 1 and discounted net present value in excess of $12,500,000. Utilizing the more costly pipeline/flowline installation option (a capital investment difference of almost $1,000,000) reduces the rate of return to 56% and the profitability index to 12 to 1. Both project implementations are economically robust.

If these two implementation options were conducted without DOE cost sharing,* the resulting economics are provided in Evaluations 4 and 9. Evaluation 4 exhibits a rate of return of 48%, a 39 month payout and a profitability index of 8 to 1, with the NPV reduced by approximately $2.0 million. The corresponding economic parameters for Evaluation 9 are a rate of return of 41%, a 41 month payout and a profitability index of 5 to 1. Thus, even without DOE, the CO_2 project still exhibits economic robustness.

Comparison of Evaluations 5 and 6 or Evaluations 3 and 4 illustrate the impact of purchase versus lease for the main injection compressor. Evaluations 3 and 4 (no DOE cost sharing) show that leasing the compressor improves the rate of return by 6.0 percentage points (42% to 48%), but reduces the NPV by approximately $1.0 million. For the cases with DOE cost sharing, compressor leasing versus purchase improves the rate of return from 57% to 62% and improves the profitability index from 11.7 to 14.7, although the NPV is reduced as before by approximately $1.0 million. Similar comparisons can be made between Evaluations 8 and 9 and Evaluations 10 and 11. Thus, compressor leasing is the preferred alternative. It also involves the least financial risk if the CO_2 project required early termination.

The economic evaluation of the CO_2 injection followed by blow down case is summarized in the above table and Evaluations 14 and 15. Detailed economic data are presented in Tables 16–12a, 16–12b, 16–13a and 16–13b. The economic evaluation of the blowdown option can be compared to Evaluations 3 and 8. Comparison of Evaluations 3 and 14 show that for the blowdown cases rates of return, payouts and profitability indices are comparable. However, the NPV for the blowdown was roughly $2.4 million less than the continuous CO_2 injection case. The lower NPV results from the lower oil recovery (approximately 800,000 STB less) from the blowdown option. Similar economic parameters difference exist between Evaluations 8 and 15 (comparison for maximum line installation costs).

The financial impact of using a gas conditioning plant to separate CO_2 and hydrocarbons from the produced gas prior to re–injecting the separated CO_2 can be assessed by comparing Evaluations 1 and 3 with Evaluations 7 and 8. This comparison shows that the large capital investment (over $3.0 million) reduces the NPV of the project by close to $3.0 million, reduces the rate of return by approximately 12 percentage points (42% to 30%) and reduces the profitability index by over 40%. However, the economic parameters still are reasonable even if the project is subjected to this large

DOE's projected capital expenditure outlay for the project is approximately $1.4 million and $1.8 million for the minimum and maximum pipeline/flow line option, respectively.

investment. The use of a gas conditioning plant is not required based on reservoir performance (see previous discussions), and now in terms of economic viability, it is substantially below CO_2 implementation options that do not use gas conditioning. The added financial benefits from providing lease fuel and sales gas does not offset the capital and operating costs required for the gas plant. Results in Table 16–1a illustrate the impact of gas conditioning on fuel and sales gas history. This table indicates that during the first six years of the project, fuel gas purchases will be necessary even with a gas plant to process the produced gas. Only after the sixth year is gas available for sale. However, the revenue stream is small and the costs of operating the gas plant and its initial capital requirements weaken the economic robustness of CO_2 injection. Thus, unless the fuel gas supply cannot be purchased, the use of a gas conditioning plant is not recommended.

16.4.4. Economic Evaluation Summary

The above discussed evaluations indicate that the best CO_2 flood implementation option involves no gas processing and the lease of the main injection compressor. Without DOE cost sharing, continuous CO_2 injection with all of the produced gas recycled provides a rate of return of 48%, a payout of 39 months, a profitability index of 8 to 1 and a NPV of over $11.0 million. This data indicates the project is economically robust. DOE cost sharing substantially improves the economics while reducing the economic risk by sharing front end capital costs.

Gas processing does not improve the economics and substantially increases the initial capital outlay, thus increasing the financial risk. With fuel gas purchase it is not needed and not recommended, since re–injection of unprocessed produced gas does not negatively impact the predicted reservoir process and associated recovery.

Use of the higher cost pipeline/flow line installation option will not prevent implementation from an economic viability standpoint. The actual choice between minimum and maximum cost installation options, or some combination of the two options, should be made from an engineering and safety perspective. If CO_2 injection operations needed to be shut down, the blowdown prediction cases also exhibit strong economic parameters and would be a reasonable option to continuing CO_2 injection to the end of the project.

In summary, if the CO_2 flood performs as predicted, it is a financially attractive process for increasing the reserves of the Anasazi–Sahgzie reservoir.

17. CONCLUSIONS

The integrated reservoir study completed on Harken Energy Corporation's Anasazi and Sahgzie reservoir in the Paradox Basin provided predictions on the performance of the reservoir under three different depletion/recovery scenarios. Performance predictions for continued primary depletion performance and the projected performance of waterflooding and CO_2 flooding are provided. These reservoir performance predictions and the companion economic assessment of implementing a CO_2 flood are based on several study components. Study components included:

1. Reservoir description and characterization.
2. A well testing and well test interpretation program.
3. Acquisition of fluid property data and its interpretation and characterization via an equation of state.
4. Acquisition and interpretation of reservoir petrophysical properties.
5. Reservoir mechanistic studies of CO_2 flooding and primary depletion performance.
6. History matching of the past reservoir performance to understand reservoir performance and serve as a basis for reservoir performance.
7. Reservoir performance predictions via CO_2 and waterflooding simulation.
8. Economic assessment of implementing a CO_2 flood.

Conclusions developed based on work conducted for the study are grouped into the above identified broad categories of work and summarized below.

Reservoir Description and Characterization

Most of the main features of the Anasazi reservoir were successfully modeled using a hybrid conditional geostatistical procedure. Patterned heterogeneities of both lithotype distribution and reservoir properties in the model conform closely to the constraints imposed by both the well and seismic data, and information from outcrop and reservoir analogues. With the exception of average porosity in the Supramound Interval of the Sahgzie build–up (see below), these reservoir properties required only minor local adjustments during the history match. This robust geostatistical model design should be directly applicable to other similar carbonate mound reservoirs.

However, attempts to match production history indicated the need to include major architectural features not present in the initial model. Communication barriers in both the Anasazi and Sahgzie mound build–ups, a minor southern extension of the main Anasazi mound near the Anasazi #5L–3 well, and substantial porosity reduction (inferred to be anhydrite plugging) in the Sahgzie build–up were required to achieve a satisfactory history match, yet were not detected in the existing 2–D seismic data. To satisfactorily verify the presence and determine the configurations of these features will require a 3–D seismic survey over the Anasazi field. In addition, because similar features are likely to be present in other carbonate mound reservoirs, we recommend that 3–D surveys be included in any future data acquisition programs.

Well Test Program and Well Test Interpretation

Prior to initiation of the subject study several well tests on the three Anasazi/Sahgzie wells were conducted. In addition, the most recently completed Anasazi well, the Anasazi 6H–1 well, was

tested extensively using conventional transient well tests and repeat wireline formation tests prior to completion. In general the quality of data available from the initial well tests was of poor quality. The frequency at which pressure data was recorded was too low and the duration of the build–up was in general too short for quantification of reservoir properties.

Specific conclusions that were made based on the interpretation of the tests that were interpreted are:

1. All tests provided estimates of the reservoir pressure. These pressure estimates, available at various stages of depletion, were used as data in the history matching portion of the study. The specific values that were utilized are given in Chapter 14. The initial reservoir pressure was determined to be approximately 2298 psia.

2. Two tests from the Anasazi Well 1 were used to estimate reservoir properties. The reservoir model which provided the best interpretation of the data was based on a two layer representation of the reservoir with cross flow between layers. These layers were interpreted to represent the two main productive facies of the reservoir, the dolomite and the limestone units. This interpretation is consistent with other reservoir data and performance interpretations that support a multiple layer system. Permeability estimates for the limestone interval varied from 55 to 180 md. The range of permeability for the dolomite unit was 1.2 to 10.0 md. Both tests exhibited a negative skin factor consistent with acidization treatments the wells received upon initial completion.

3. Wireline formation tests and pressure build–up tests in the Anasazi Well 6H–1 supported the following conclusions.

    a. The dolomite and limestone units at the well location are not in direct pressure communication (essentially isolated).

    b. The limestone unit is more pressure depleted than the dolomite unit.

    c. Within each main production unit (i.e. dolomite versus limestone) depletion is non uniform, with pressure differences approaching 200 psi.

    d. Most likely permeability values for the dolomite interval at the 6H–1 location is less than 0.5 md.

4. Interpretation of the Sahgzie Well No. 1 November 1989 test provided the following conclusions.

    a. A two layer model can be supported for the Sahgzie mound.

    b. The permeability ranges for the limestone unit was estimated at 23 to 30 md. The dolomite unit exhibited a permeability of approximately 4.0 md.

    c. A linear barrier, interpreted as the western edge of the Sahgzie mound, is located approximately 300 to 475 feet from the Sahgzie well.

    d. Acidization was effective in providing local well stimulation as support by calculated negative skins.

Reservoir Fluid Characterization

An experimental program to characterize carbon dioxide and Anasazi crude interaction was successfully completed. These CO_2 swelling tests and associated fluid property measurements for

density and viscosity were combined with conventional black oil property measurements on original reservoir fluid samples to provide an extensive data set for equation of state calibration.

A 11 pseudo–component calibrated equation of state was successfully developed. The calibrated equation of state provided an excellent match of all fluid property data associated with the Anasazi reservoirs. Thus, it is capable of modelling the complex fluid behavior associated with both the current primary depletion process and the proposed CO_2 flooding processes.

Petrophysical Properties Acquisition Program

A comprehensive petrophysical property acquisition program was completed using core samples from the Anasazi Well No. 6H–1 and Anasazi Well No. 1. The following sets of data were developed using ultra centrifuge technology.

1. Complete sets of drainage and imbibition capillary pressure data for gas–oil and oil–water fluid system for representative dolomite and limestone samples.

2. Complete sets of gas–oil and oil–water relative permeability data for both dolomite and limestone samples.

Additional tests were used to draw the following conclusion:

1. The samples tested demonstrated a mixed wetting condition tending towards an oil wet condition.

2. Both facies exhibited a lack of fluid trapping sites, yielding low residuals in both oil and brine phases.

3. Based on tests conducted using three different core preparation conditions, cores can be restored and used to determine valid capillary pressure and relative permeability data.

Mercury injection tests conducted on end pieces from core plugs used for ultra centrifuge measurements confirm the biomodal pore size distribution of the main productive limestone unit and the unimodal pore size distribution of the overlying dolmite unit.

Rock compressibility measurements provided the following uniaxial stress/pore pressure drawdown pore volume compressibility values for the two principal productive rock types.

Limestone	– 2.33×10^{-6} 1/psi
Dolomite	– 3.18×10^{-6} 1/psi

Reservoir Mechanistic Studies

Using the developed calibrated equation of state, multiple contact phase behavior calculations and one–dimensional compositional studies, it was concluded that:

1. The Anasazi–Sahgzie crude can be miscibility displaced by CO_2.

2. The CO_2 – crude mass transfer process can be characterized as a vaporizing gas drive process where the injected CO_2 ,via a multiple contact process, is enriched in intermediate components vaporized or extracted from the in–place oil.

3. Using oil compositions representative of the original oil and depleted oil, miscible displacement occurs over the pressure range of 2400 to 3100 psia. A pressure of 3100 psia was used as a guideline for field full simulation studies assessing CO_2 injection.

Two dimensional mechanistic reservoir performance studies modelling the primary depletion stages of the Anasazi–Sahgzie reservoir provided the following insights into basic reservoir prediction mechanisms.

1. The initial Anasazi–Sahgzie reservoir production behavior can be characterized as liquid expansion processes followed by a solution gas drive. The solution gas drive is accompanied by free gas segregation into the Supramound Interval and the development of a secondary gas cap. The latter stage of production is characterized by secondary gas cap expansion and gravity drainage of oil from the Supramound Interval into the underlying Core Mound Interval (i.e. limestone unit).

2. The limestone unit (Core Mound Interval) contributes the major portion of production (> 99%), but is continually recharged from the overlying Supramound Interval.

3. Vertical permeability is a key parameter that controls reservoir processes. The extent and nature of the Supramound/Core Mound (i.e. dolomite/limestone) communication plays a controlling role in reservoir performance.

History Match of Reservoir Performance

The performance of the Anasazi–Sahgzie reservoir from discovery to January 1, 1997, was successfully history matched. The producing GOR history of each well and the entire field were matched. The measured reservoir pressure history was also matched to verify the simulator and associated geologic model. The history match required the following reservoir description modifications and fluid property changes.

1. Vertical permeability influencing gas segregation.

2. Inclusion of transmissibility barriers within both the Anasazi and Sahgzie mounds. This suggests that the three dimensional architecture of the mound complex needs further definition.

3. Adjustment of the reservoir pore volume of the Sahgzie mound.

4. Limited but local changes to lateral permeability.

5. Limited changes to rock compressibility initially set from laboratory measurements.

6. An increase in the Core Mound Interval volume in the Anasazi mound.

7. Adjustment of the initial solution gas oil ratio of the fluid system via original fluid composition changes.

The history matching process confirmed the production mechanism of the subject reservoir identified from analysis of the production history and mechanistic simulation studies. The Anasazi–Sahgzie reservoir performance is characterized by three distinct phases. These phases are:

1. A liquid expansion phase characterized by a constant producing GOR until reservoir pressure reaches the bubble point pressure of the original oil.

2. A dissolved gas depletion stage coupled with free gas segregation. This phase is characterized by an increasing and then a decreasing gas production rate.
3. A gravity drainage period characterized by nearly constant or slowly declining oil and gas rates. This period is associated with continued dissolved gas depletion and secondary gas expansion coupled with influx of oil, via gravity forces, from the Supramound Interval into the Core Mound Interval.
4. Over 99% of the total production is produced from the Core Mound Interval, but the limestone is continually recharged from the Supramound.

These production mechanisms are supported by the ability of the simulator to match gas production and reservoir pressure history as well as field data directly supporting the accumulation of free gas in the Supramound Interval.

The final total pore volume of the model used to obtain the history match was 15.2 million barrels. The total original oil in place (OOIP) was estimated to be 11.4 million STB. Roughly 41%, or 4.7 million STB, of the OOIP is contained in the mound complex. Over 6.7 million STB, or 59% of the total is contained in the associated off–mound structure. With primary production matched, the simulator provides a validated means of predicting the performance of the reservoir under various depletion processes.

Reservoir Performance Predictions

The history matched simulator was used to predict the performance of the Anasazi–Sahgzie reservoir under continued primary depletion, assess the potential of CO_2 flooding and identify operating conditions needed to maximize CO_2 enhanced recovery. In addition, the potential of waterflooding was assessed. Major conclusions from the predicted performances of the subject reservoir are:

1. The projected primary production through 1/1/2012 is 2.55 million STB. This represents 54% of the OOIP in the mound complex proper and 22.3 % of the OOIP in the total system.
2. An optimized CO_2 flood is predicted to recover a total 5.04 million STB. This represents an increase of 1.91 million STB and 2.48 million STB over predicted primary depletion recovery at 1/1/2006 and 1/1/2012, respectively. The projected 5.04 million STB of oil production represents in excess of 100% of the OOIP in the mound complex and 44% of the oil in place of the total system modelled. The incremental recovery of 2.48 million STB requires the injection of 74.0 BSCF of gas and the purchase of 12.9 BSCF of CO_2.
3. Projected maximum CO_2 enhanced oil recovery will require pressurization of the reservoir to over 2700 psia (Core Mound pressure in excess of 2500 psia). This is the projected average operating pressure needed to provide miscibility, given past production and compositional changes.
4. Optimum recovery from CO_2 flooding will require one injector for each mound. These injectors need to be located in the mound complex north of the current wells (Anasazi #1, #5L–3 and Sahgzie #1).
5. Vertical injection wells with injection restricted to the Supramound Interval provide the best recovery. Horizontal CO_2 injection wells have associated poor recovery and early CO_2 break through.

6. Conditioning of produced gas to remove hydrocarbons prior to re–injection is not required to maintain miscible conditions in the reservoir and obtain high oil recovery.

7. The subject reservoir can maintain current production levels during reservoir fill–up without adversely impacting the CO_2 enhanced recovery process.

8. Continuous CO_2 injection versus CO_2 injection followed by blowdown favors using continuous injection, since it is projected to recover 800,000 STB more oil than the case using blowdown.

9. Predicted waterflooding recovery was substantially below the projected CO_2 flood performance. The best waterflood exhibited an incremental recovery over primary of 618,000 STB of oil versus 2.48 million STB for the best CO_2 flood.

10. The low mobility of water (relative to CO_2) and the corresponding poor injectivity of water injectors would require producers to operate at low bottomhole pressure to enhance water influx and improve waterflood response time. Low reservoir pressure would result in three phase flow contributing to lower oil production rates and recovery.

11. CO_2 is favored over waterflooding because of:

    a. Higher oil recovery.

    b. Substantially higher oil mobility which improves oil flow (CO_2 exhibited a maximum constrained rate of 1500 STB/D versus a maximum waterflood rate of less than 400 STB/D).

    c. Project life is shorter.

    d. A return to primary depletion is possible after injecting CO_2; it is not likely after injection of water.

12. The results of the Anasazi–Sahgzie study can be used to qualitatively assess the CO_2 recovery potential of other Paradox Basin small algal mound reservoirs containing fluids with similar properties. However, the experience gained in history matching and predicting the performance of the Anasazi–Sahgzie reservoir indicates that the overall mound geometry and internal facies architecture is critical to matching and predicting performance. Thus, each mound will likely require an individual reservoir study to quantify its CO_2 potential and identify the appropriate implementation strategy to maximum oil recovery.

Economic Assessment of CO_2 Flood

Using reservoir simulation based performance predictions and current CO_2 flood implementation costs, detailed economic assessments were conducted for a number of different CO_2 flood options. These set of studies indicated that:

1. A CO_2 flood of the Anasazi–Sahgzie reservoir has robust economics. With DOE participation the project would have a rate of return of 62%, a payout of 35 months, a profitability index of 15 to 1 and a discounted (10%) net present value in excess of $12,500,000. Harken's capital outlay would be $1,728,000. Even without DOE

participation the economics remain robust with a rate of return of 48%, a payout of 39 months, a profitability index of 8 to 1 and a discounted net present value of over $11,000,000. The capital requirements would be $3,146,000.

2. Leasing the compressor on a five year contract basis is better economically than purchasing the compressor. Leasing improves the rate of return by approximately 6.0 percentage points (42% versus 48%) but reduces the NPV by approximately $1.0 million.

3. The benefit from processing produced gas to separate CO_2 from the hydrocarbons and using the hydrocarbons for fuel and sales are offset by the large capital investment required for a membrane separation facility. Thus, re–injection of all produced gas without conditioning is economically more attractive than implementing a CO_2 flood with gas processing.

4. The difference between a minimum and maximum cost option for installation of flow/injection lines and the CO_2 supply is approximately $1,000,000. However, the economics are still robust. With DOE cost sharing, the rate of return is 56% with a profitability index of 11.5 to 1.

5. Comparison of the economics of a process using blowdown after six years of CO_2 injection versus the continuous CO_2 injection case indicates that the rate of return and the profitability index are not significantly different, but the NPV is substantially decreased (approximately $1.4 million). The lower NPV is a result of lower oil recovery for the blowdown case (800,000 STB less than the continuous injection case).

In summary, if the CO_2 flood performs as predicted, it is a financially robust process for increasing the reserves of the Anasazi–Sahgzie reservoir.

18. RECOMMENDATIONS

Based on the results of the completed geologic and reservoir engineering study and the associated economic assessment of implementing a CO_2 flood in the Anasazi–Sahgzie reservoir, the following principal recommendations are proposed.

1. Reservoir performance predictions and economic evaluations support implementation of a CO_2 injection project in the Anasazi–Sahgzie reservoir.

2. Study results support the initiation and completion of Phase II of the Anasazi project sponsored under the Class II Oil Program of the U.S. Department of Energy.

3. Additional simulation work on oil recovery sensitivity to CO_2 injection rate should be conducted. In addition, a field injectivity test using CO_2 should be conducted on the Anasazi Well 6H–1 to establish long term injection rate data before committing to further Phase II work.

4. Prior to implementing a CO_2 flood, a three dimensional seismic survey of the Anasazi/Sahgzie reservoir should be conducted and the results interpreted to update the current reservoir description. If the reservoir description requires changes, based on the 3–D survey, that could significantly alter current projected reservoir performance, update the CO_2 flood design. If revised performance predictions retain robust economics, implementation of a CO_2 pilot flood should proceed.

5. The main injection compressor should be leased rather than purchased to provide the most operating flexibility and least financial risk.

6. Produced gas processing is not required for a single field CO_2 implementation case. It is not required from a reservoir processing standpoint nor it is justified economically.

7. The potential of CO_2 flooding other Paradox Basin small algal mound reservoirs should be evaluated and the financial impact of simultaneous or sequential flooding of a series of reservoirs assessed. This will identify the upside potential of CO_2 flooding for the entire Basin from both a reserves and an economic standpoint.

8. The feasibility and benefits of using cross well seismic surveys to supplement 3–D seismic study should be assessed.

REFERENCES

Chapter 3

3–1 Chidsey, T.C., Jr., D.E. Eby, and D.M. Lorenz, 1994, "Geological and Reservoir Characterization of Small Shallow–Shelf Carbonate Fields, Southern Paradox Basin, Utah", in Huffman, A.C., W.R. Lund, and L.H. Goodwin, eds., Geology and Resources of the Paradox Basin, Utah Geological Association Guidebook 25, p. 39–56.

3–2 Weber, L.J., J.F. Sarg, F.M. Wright, and A.C. Huffman, 1994, "High–Resolution Sequence Stratigraphy: Reservoir Description and Geologic Setting of the Giant Aneth Oil Field, SE Utah", AAPG/RMAG Field Guide, Field Trip #2, 1994 AAPG Annual Convention, Denver, Colorado.

3–3 Chidsey, T.C., Jr., D.E. Eby, W.G. Groen, Kris Hartmann, and M.C. Watson, 1996, "Anasazi Field", in Hill, B.G., and Bereskin, S.R., eds., Oil and gas fields of Utah, Utah Geological Association Publication 22 (Second Edition).

Chapter 4

4–1 Weber, L.J., J.F. Sarg, F.M. Wright, and A.C. Huffman, 1994, "High–Resolution Sequence Stratigraphy: Reservoir Description and Geologic Setting of the Giant Aneth Oil Field, SE Utah", AAPG/RMAG Field Guide, Field Trip #2, 1994 AAPG Annual Convention, Denver, Colorado.

4–2 Weber, L.J., F.M. Wright, J.F. Sarg, Ed Shaw, L.P. Harman, J.B. Vanderhill and D.A. Best, 1995, "Reservoir Delineation and Performance: Application of Sequence Stratigraphy and Integration of Petrophysics and Engineering Data, Aneth Field, Southeast Utah, U.S.A.", in Stoudt, E.L., and P.M. Harris (eds.), Hydrocarbon Reservoir Characterization – Geologic Framework and Flow Unit Modeling, Notes – SEPM Short Course 34, Houston, March 4–5, 1995, p. 1–29.

4–3 Improved Recoveries, Inc., February 15, 1991, Anasazi No. 1, Desert Creek Reservoir, Core Analysis Report, Covington, La., 13 p.

4–4 Core Laboratories, March 18, 1991, Core Analysis Results, Anasazi 5L–3 Well, San Juan County, Utah, File No. 57121–91CHU024, 14p.

4–5 Precision Core Analysis, Inc., December 27, 1995, Core Plug Analysis, Anasazi 6H #1, San Juan County, Utah, 8 p.

4–6 Improved Recoveries, Inc., February 21, 1991, Sahgzie No. 1, Desert Creek Reservoir, Core Analysis Report, Covington, La., 13 p.

4–7 Bateman, R.M., 1985, "Open–hole log analysis and formation evaluation", Internat. Human Resources Development Corp., Boston, p. 118–120.

4–8 Schlumberger, Inc., 1991, "Log interpretation: principles/applications", Schlumberger Educational Serv., p. 101–105.

4–9 Hearst, J.R., and P.H. Nelson, 1985, "Well logging for physical properties", McGraw–Hill, New York, p. 421–433.

4–10 Amaefule, J.O.M., M.Altunbay, D. Tiab, D.G. Kersey, and D.K. Keelan, 1991, "Enhanced reservoir description using core and log to identify hydraulic (flow) units and predict permeability in uncored intervals/wells", SPE paper

4–11 Martin, A.J., S.T. Solomon, and D.J. Hartmann, 1997, "Characterization of petrophysical flow units in carbonate reservoirs", American Assoc. Petroleum Geologists Bull., v. 81, no. 5, p. 734–759.

4–12 Triple–O Slabbing, 1990–1995, Core photographs for the Anasazi 31, Anasazi #5L–3 and Anasazi 6H–1 wells, Harken Energy Corp. files.

4–13 Brinton, Lisë, 1986, "Deposition and diagenesis of middle Pennsylvanian (Desmoinesian) phylloid algal banks, Paradox Formation, Ismay zone, Ismay field and San Juan Canyon, Paradox Basin, Utah and Colorado", inpub. MS thesis, Colorado School of Mines, Golden, Colorado, 315 p.

4–14 White, J.V., and B.L. Kirkland, 1996, "Diagenesis and porosity distribution of Pennsylvanian Paradox Formation carbonates (Upper Ismay), southeastern Utah", in Huffman, A.C., Jr., W.R. Lund and L.H. Goodwin, eds., Geology and Resources of the Paradox Basin, Utah Geol. Assoc. and Four Corners Geol. Soc. Guidebook 25, p. 151–160.

4–15 Eby, D.E., personal communication, December, 1995.

4–16 Chidsey, T.C., Jr., D.E. Eby and D.M. Lorenz, 1996, "Geological and reservoir characterization of small shallow–shelf carbonate fields, southern Paradox Basin, Utah", in Huffman, A.C., Jr., W.R. Lund and L.H. Goodwin, eds., Geology and Resources of the Paradox Basin, Utah Geol. Assoc. and Four Corners Geol. Soc. Guidebook 25, p. 39–56.

4–17 Chidsey, T.C., Jr., L. Brinton, D.E. Eby and K. Hartmann, 1996, "Carbonate–mound reservoirs in the Paradox Formation: an outcrop analogue along the San Juan River, southeastern Utah", in Huffman, A.C., Jr., W.R. Lund and L.H. Goodwin, eds., Geology and Resources of the Paradox Basin, Utah Geol. Assoc. and Four Corners Geol. Soc. Guidebook 25, p. 139–150.

4–18 Best, D.A., F.M. Wright, Jr., R. Sagar and L.J. Weber, 1995, "Contribution of outcrop data to improve understanding of field performance: rock exposures at Eight Foot Rapids tied to Aneth field", in Stoudt, E.L., and P.M. Harris, eds., Hydrocarbon Reservoir Characterization – Geologic Framework and Flow Unit Modeling, Notes– Soc Econ. Petrologists and Mineralogists Short Course 34, Houston, March 4–5, 1995, p. 31–50.

Chapter 6

6–1 Chidsey, T.C., Jr., D.E. Eby, and D.M. Lorenz, 1994, "Geological and Reservoir Characterization of Small Shallow–Shelf Carbonate Fields, Southern Paradox Basin, Utah", in Huffman, A.C., W.R. Lund, and L.H. Goodwin, eds., Geology and Resources of the Paradox Basin, Utah Geological Association Guidebook 25, p. 39–56.

6–2 Chidsey, T.C., Jr., L. Brinton, D.E. Eby and K. Hartmann, 1996, "Carbonate–mound reservoirs in the Paradox Formation: an outcrop analogue along the San Juan River, southeastern Utah", in Huffman, A.C., Jr., W.R. Lund and L.H. Goodwin, eds., Geology and Resources of the Paradox Basin, Utah Geol. Assoc. and Four Corners Geol. Soc. Guidebook 25, p. 139–150.

6–3 Weber, L.J., J.F. Sarg, F.M. Wright, and A.C. Huffman, 1994, "High–Resolution Sequence Stratigraphy: Reservoir Description and Geologic Setting of the Giant Aneth Oil Field, SE Utah", AAPG/RMAG Field Guide, Field Trip #2, 1994 AAPG Annual Convention, Denver, Colorado.

6–4 Eby, D.E., L. Brinton, T. Chidsey, and K. Hartmann – personal communication, January, 1996.

6–5 Bratley, Paul, B.L. Fox and L.E. Schrage, 1983, "A guide to simulation", Springer–Verlag, New York, 383 p.

6–6 Journel, A.G., and Ch.J. Huijbregts, 1978, "Mining geostatistics", Academic Press, New York, p. 491–498.

6–7 Ohen, R.F.J.M., and L.P.P.P. vanGinnekeu, 1989, "The annealing algorithm", Kluwer Press, Boston, Mass.

6–8 Metropolis, N., A. Rosenbluth, M. Rosenbluth. A. Teller, and E. Teller, 1953,"Equation of state calculations by fast computing machines", J. Chem. Physics, v. 21, p. 1087–1092.

6–9 Watson, M.C., 1994, "A Study of Waterflooding Aneth Area Algal Mound Oil Fields: Sahgzie/Mule/Anasazi", Harken Energy Corp., internal report.

6–10 Eby, D.E., personal communication, January, 1996.

Chapter 7

7–1 Landmark Graphics Corp., 1996, "GRIDGENR User's Guide", Version 3.3.1, p.H1–H16.

Chapter 9

9–1 McCarthy, Tom: Bottomhole Pressure Buildup and Material Balance Analysis, Anasazi No.1., Chusku Energy Company Internal Memorandum, March 15, 1990.

9–2 Core Laboratories: Reservoir Fluid Study, Anasazi No. 1 Well, Wildcat, San Juan County, Utah, File no. ARFL–900012, Feb. 20, 1990.

9–3 Bourdet, D. "Pressure Behavior of Layered Reservoirs with Cross Flow" SPE 13628 presented at the SPE 1985 California Regional Meeting, Bakersfield, CA, March, 1985.

Chapter 10

10–1 Core Laboratories: Reservoir Fluid Study For Chuska Energy Company, Anasazi No. 1 Well, Wildcat, San Juan County, Utah, File No. ARFL–900012, Feb. 20, 1990.

10–2 Core Laboratories: Reservoir Fluid Study For Chuska Energy Company, Sahgzie No. 1 Well, Wildcat, San Juan County, Utah, File No. ARFL 89012, Nov. 20, 1989.

10–3 Core Laboratories: Reservoir Fluid Study For Chuska Energy Company, Mule No. 31–M, Aneth Field Wildcat, San Juan County, Utah, File No. RFL 920107 April 16, 1992.

10–4 Core Laboratories: Reservoir Fluid Study For Chuska Energy Company, Blue Hogan No. 1J–1 Well, Wildcat, San Juan County, Utah, File No. ARFL–910014, March 19, 1991.

10–5 Core Laboratories: Reservoir Fluid Study For Chuska Energy Company, Brown Hogan No. 1A Well, Wildcat, San Juan County, Utah, File No. ARFL–910035, May 13, 1991.

10–6 Core Laboratories: Reservoir Fluid Study For Chuska Energy Company, North Heron No. 35–C Well, Undesignated Field, San Juan County, Utah, File No. ARFL–910078, Nov. 11, 1991.

10–7 Core Laboratories: Reservoir Fluid Study For Chuska Energy Company, Runway No. 10E–2 Well (Middle Zone), Wildcat, San Juan County, Utah, File No. RFLM 90092, Jan. 24, 1991.

10–8 Core Laboratories: Reservoir Fluid Study For Chuska Energy Company, Navajo Tribal Jock – 31–G, San Juan County, Utah, File No. RFL 920169, July 21, 1992.

10–9 D. B. Robinson Research Ltd.: Laboratory PVT Program for Harken Energy Reservoir Fluid – Phase I, File No. DBRR 205136, Nov. 17, 19

10–10 Pedersen, K. S. and Fredenslund, A. "An Improved Corresponding States Model for the Prediction of Oil and Gas Viscosities and Thermal Conductivities," *Chem. Eng. Sci.*, 42, pp. 182–187 (1987).

10–11 Pedersen, K. S. and Fredenslund, A. and Christensen, P.L.: "Viscosity of Crud Oils," *Chem. Eng. Sci.*, 39, pp. 1011–1016 (1984).

Chapter 11

11–1 Westport Technology Center International, "Harken Energy Special Core Analysis – Anasazi 6H." Report No. WTC195–201, December 1995.

11–2 TerraTek; "Compressibility of Carbonate from the Anasazi No. 1 and No 6H–1 Wells." Report No. TR96–23, December 1995.

11–3 Westport Technology Center International, "Harken Energy Special Core Analysis – Limestone, " Report No. WTE1–96–094, April 1996.

11–4 Westport Technology Center International; "Mercury and Oil–Brine Capillary Pressure Comparison on Anasazi Core Material for Harken Energy Corporation," Report No. WTCI–96–173, August 1996.

11–5 Hirasaki, G. J., Rohan, J.A. and Dubey, S.T.; "Wettability Evaluation During Restored–State Core Analysis," SPE 20506, September 1990.

Chapter 12

12–1 Rathmell, J. J., Stalkup, F. I., and Hassinger, H. C., "A Laboratory Investigation of Miscible Displacement by Carbon Dioxide," SPE paper 3483 presented at the SPE Annual Meeting, New Orleans, October 3–6, 1971.

12–2 Leach, M. P. and Yellig, W. F., "Compositional Model Studies – CO_2 Oil Displacement Mechanism," *Soc. Pet. Eng. J.*, February 1981.

Chapter 13

13–1 Reid, R. C., Prausnitz, J. M., and Sherwood, T. K., "*The Properties of Gases and Liquids,*" 3rd Editon, McGraw–Hill, New York, 1977.

13–2 Stone, H. L. "Probability model for estimating three–phase relative permeability, Trans. SPE of AIME, 249, pp. 214–18 (JPT) (1970).

13–3 Stone, H. L. "Estimate of three–phase relative permeability and residual oil data," *J. Can. Petrol. Technol.*, 12, No. 4, pp. 53–61 (1973)

Chapter 16

16–1 National Petroleum Council, "Enhanced Oil Recovery," 1984 publication.

16–2 Science Applications, Inc. "Feasibility and Economics of By Product CO_2 Supply for Enhanced Oil Recovery," Volume I, Technical Report, prepared by Science Applications, Inc. for U. S. D. O. E., Contract DE–AT21–78MC 0 8333, Task 36, Jan., 1982.

APPENDIX A

CO_2 IMPLEMENTATION – EQUIPMENT DESIGN AND COST

Production and Injection Well Design and Costs

Production Wells

The following equipment is specified for re–completing producers:

Tubing

Specification: – 6000 feet per well of 2 3/8″ O.D., 4.7 lbs. R–11, J–55 Bellville tubing with EUE 8–round thread pin and coupling connectors.

– Tubing fully lined with fiberglass–epoxy lining.

Price: – $28,300 per well including 8.5% tax, F.O.B. Aneth, Utah

Suppliers: – Pipe and Shipping: Cave Enterprises, Farmington, New Mexico

– Lining: ICO Permian, Odessa, Texas

Wellhead Equipment

Specification: – All wellhead and associated equipment uses T23 stainless steel and includes tubing head and tubing hangers, tubing head adaptors and double master valves, and 216 stainless steel wing valves.

Price: – $23,300/well including 8.5% tax, FOB Farmington, New Mexico

Suppliers: – WSI–Cameron, Farmington, New Mexico

Downhole Equipment

Note that three distinct options exist for downhole equipment based on design and metallurgy. All are quoted below, but the most expensive and corrosion resistant option is used for subsequent economic assessments. Other options are included to provide lower cost completion alternatives, if needed, to improve economic return at greater risk.

Specifications:– Option 1
- Baker Model L–316 Stainless on/off tool
- Baker Model B Two–way downhole shut off valve (chrome–molybdenum alloy)
- Baker inverted Lock–set packer assembly with Inconel mandrel

– Option 2
- Baker Model L–316 Stainless on/off tool
- Baker Model B Two–way downhole shut off valve

(chrome–molybdenum alloy)
- Baker Model J–Lock retrievable single string packer assembly using nickel plating

- Option 3 – Baker Model L–316 Stainless on/off tool
  - Baker Model J–Lock retrievable single string packer assembly using nickel plating

Price:
- Option 1 – $24,800/well with 8.5% tax
- Option 2 – $12,200/well with 8.5% tax
- Option 3 – $ 6,800/well with 8.5% tax

Supplier – Baker Oil Tools, Farmington, New Mexico

Casing Liner

Specification – 900 feet of 4 1/2″ chrome–molybdenum casing/liner and hanger

Price:
- Casing – $6,000
- Hanger – $2,500

Suppliers: – Secondary market estimation

Summary of Producing Well Recompletion Costs

Item	Cost	Classification
Tubing	$ 28,200	Tangible
Liner/Hanger	$ 8,500	Tangible
Wellhead	$ 23,300	Tangible
Downhole Equipment	$ 24,800	Tangible
Rig Daytime Recompletion	$ 3,000	Intangible
Day Time for Running Liner	$ 4,500	Intangible
Casing Crew and Tongs	$ 8,000	Intangible
	$100,330	
Total Costs for Three Wells		
	Tangible	$254,000
	Intangible	47,000
	Total	$301,000

Injection Wells

Two injection wells are proposed for the CO_2 flood project. The Sahgzie mound will utilize a new well completed as an injector. The Anasazi mound will re–complete the Anasazi 6H–1 well from a producer to an injector. The costs differ and are specified separately for each well.

Recompleting Producer to Injector

Tubing

Specification: – 6,000 feet per well of 2 7/8″ O.D., 6.50 lbs., R–11, J–55, Bellville tubing with EUE 8–round thread pin and coupling connector and fully lined with fiber glass–epoxy lining.

Price: – $36,200 per well including 8.5% tax.

Suppliers: – Pipe and shipping: Cave Enterprises, Farmington, New Mexico

– Lining: ICO Permian, Odessa, Texas

Wellhead Equipment

Same as producers, except price is $32,500 per well, including tax

Downhole Equipment

Same as producers, again only Option 1 is used in the economic assessment

Casing Liner

Same as production wells, except for the new injector.

Drilling and Completing New Injector

Drilling and completion cost estimates are based on the costs to drill and complete the Anasazi 6H–1 Well.

Drilling and Completion Costs

Drilling Costs		
Item	**Cost**	**Classification**
Drilling – Day Rate	$ 87,000	Intangible
Rig Supervisor	$ 11,000	Intangible
Location Preparation	$ 30,000	Intangible
Cementing	$ 45,000	Intangible
Water/Mud/Fuel	$ 26,000	Intangible
Bits/Equipment	$ 14,000	Intangible
Trucking	$ 6,000	Intangible
Coring	$ 12,000	Intangible
Mud Logging	$ 5,000	Intangible
Clean up	$ 5,000	Intangible
Total	$241,000	

Completion Costs		
Item	**Cost**	**Classification**
Surface Casing	$ 16,000	Tangible
Production Casing (all chrome molybdenum)	$ 40,000	Tangible
Casing Crew and Tong Rental	$ 8,000	Intangible
Logging	$ 25,000	Intangible
Perforating	$ 4,000	Intangible
Acidization	$ 11,000	Intangible
Pressure Testing	$ 10,000	Intangible
Trucking/Supplies	$ 5,000	Intangible
Total	$119,000	
Total Drilling & Completion Costs	$360,000	

Summary Recompleting Anasazi 6H–1 Well		
Item	**Cost**	**Classification**
Tubing	$ 36,200	Tangible
Liner/Hanger	$ 8,500	Tangible
Wellhead	$ 32,500	Tangible
Downhole Equipment	$ 24,800	Tangible
Rig Day Time – Recompletion	$ 3,000	Intangible
Day Time for Running Liner	$ 4,500	Tangible
Casing Crew on Tongs	$ 8,000	Tangible
Total	$117,500	

Summary Drilling/Initial Completing/Injector Completion – New Injector		
Item	**Cost**	**Classification**
Drilling	$241,000	Intangible
Initial Completion*		
Tangible	$ 56,000	Intangible
Intangible	$ 63.000	Intangible
Tubing	$ 36,200	Tangible
Wellhead	$ 32,500	Tangible
Downhole Equipment	$ 24.800	Tangible
Day time	$ 3,000	Intangible
Rig Up Facility	$ 8,000	Intangible
Total	$464,500	Intangible
* See previous details		

Injection Well Cost Summary			
Item	**Tangible**	**Intangible**	**Total**
Total Injection Well Costs			
Recompletion of Anasazi 6H–1	$102,000	$ 15,500	$117,500
Drilling Completion New Injection	$ 56,000	$304,000	$360,000
Completing New Injector for CO_2	$ 93,500	$ 11,000	$104,500
Total (Rounded)	$252,000	$331,000	$583,000
Total Well Costs			
	Tangible	**Intangible**	**Total**
	$506,000	$378,000	$884,000

Surface Production/Injection Line Design and Costs

The following material provides specifications and costs for the various surface lines required for implementation of a CO_2 injection process.

Injection Lines

Specifications:– 7,200 feet of 1 1/2″ O.D., 10.79/lb, x .337″ wall, DRL, BFW, X42 new line pipe with ICO Permian IPC – 505 epoxy internal coating.

Price: – $6.02/foot. Total cost of $47,000 with 8.5% sales tax. FOB Aneth, Utah

Supplier: – Pipe and shipping – Cave Enterprises, Farmington, New Mexico

– Internal Coating – ICO Permian, Odessa, Texas

CO_2 Mingled Oil and Gas Production Lines

Specifications:– 6300 feet of 4 1/2″ O.D., 8.66/lbs, x .188″ wall, DRL, BFW X42 new line pipe with ICO Permian IPC–505 epoxy internal coating.

Price – $5.32/foot. Total cost of $36,000 with 8.5% sales tax, FOB Aneth, Utah

Supplier: – Line pipe and shipping – Cave Enterprises, Farmington, New Mexico

– Internal Coating – ICO Permian, Odessa, Texas

Separator Gas Lines

Specifications:– 4500 feet of 4.5″ O.D., x .188″ wall, DRL, BFW, X42 with ICO Permian IPC–505 epoxy internal coating.

Price: – $5.32/foot. Total cost of $26,000 with 8.5% sales tax, FOB Aneth, Utah

Suppliers: – Pipe and shipping – Cave Enterprises, Farmington, New Mexico

– Internal Coating – ICO Permian, Odessa, Texas

Surface Production/Injection Line Installation

To minimize the potential of internal flow line CO_2 corrosion, new lines must be mechanically connected. Two current options exist for mechanical connection. These are Zaplock and the cylindrical corrosion barrier (CCB) welded connector from Heat–Pro Systems, Inc. Zaplock is a mechanical pipe connection which requires the "belling" of one end of each pipe joint and the joining of two sections of pipe, in the field with special Zaplock equipment.

The CCB welded connection utilizes a special designed coupling which prevents the welding process used to connect the pipe from damaging the internal coating. In addition to mechanical connector costs, the flow/injector lines could be laid on the surface or taped and buried with each option incurring different costs. Two sets of quotes were obtained for flow/injection line installation. These quotes were obtained from Foutz and Bursum Construction Company, Inc. of Farmington, New Mexico and BWR Incorporated of Cortez, New Mexico. Cost options were developed for six different combinations of connectors and the type of installation. Total costs for flow line, connectors and installation varied from a low of $220,000 to a high of $380,000. Economic evaluations were run for two cases, a minimum cost case and a high end cost case. The design and cost breakdown of these two cases are given below. The Foutz and Bursum quote uses a 30% escalation to account for terrain variations and special fees and labor requirements for Navajo land operation. The BWR quote includes a 25% estimate for rock ditching in addition to normal installment costs as well as a surcharge of 3% for use of a Navajo crew. The following costs are based on 18,000 feet of new flow and injection lines (see above note for breakdown)

Minimum Cost Installation – Surface Lines and Zaplock Connection

Specifications:– Surface installation of taped line using existing right of way and non welded Zaplock connectors.

– Zaplock pipe and preparation and Zaplock installation equipment rental and associated transportation costs.

Price:

– Line Installation – $5.50/foot – Total cost for 1800′ is $99,000

– Zaplock Pipe preparation and installation – $10,600

Supplier: – Line installation – BWR Incorporated, Cortez, New Mexico

– Connectors – Zaplock Pipe Line Systems, Inc. Houston, Texas

Maximum Cost Installation – Buried Lines and Heat Pro Connectors

Specifications:– Welded, taped and buried line using existing right of way and Heat Pro CCB connectors

– 600 Heat Pro connectors plus epoxy/lubricant for installation.

Price:

– Line Installation – $10/foot – Total cost for 18,000 feet is $180,000 plus $43,000 for rock ditching (approximately 25% of line length) for a total of $223,000.

– Coupling – 600 couplings at $78.00/coupling plus epoxy/lubricant for cost of $47,448.

Supplier: – Line installation – BWR Incorporated, Cortez, New Mexico

– Couplings – Heat Pro Systems, Inc. Houston, Texas

Total Flow/Injection Line Cost Summary

Minimum Cost			
Item	**Tangible**	**Intangible**	**Total**
Line Pipe	$110,000		$110,000
Coupling (Zap Lock)		$ 11,000	$ 11,000
Installation		$ 99,000	$ 99,000
Total	$110,000	$110,000	$220,000

Maximum Cost			
Item	**Intangible**	**Intangible**	**Total**
Line Pipe	$110,000		$110,000
Coupling (Heat Pro)	$ 47,000		$ 47,000
Installation		$223,000	$223,000
Total	$157,000	$223,000	$380,000

Surface Production Facilities – Design and Costs

The following summary provides specifications and costs for surface facility equipment.

Specification: – Vertical Separators: 32″O.D. by 7′6″with 100 psi MAWP, 2 phase vertical and 1/4" corrosion allowance.

– Horizontal Treaters: 48″ O.D. by 20′ with 75 psi MAWP internally coated with a 0.75MMBtu/Hr. firebox.

- Glycol Dehydration System consisting of:
  1. Inlet separator 36" OD by 7'6" with 285 psi MAWP, 2 phase vertical with 1/8" corrosion allowance
  2. Glycol Absorber: 60" O.D. with 15 tray equivalency, 285 psi MAWP with 1/8" corrosion allowance with bottom five trays specified as stainless steel.
  3. Glycol Regenerator: 0.8 MMBTU/hr
  4. Still column: stainless steel
  5. Glycol/Glycol Heat Exchanger
  6. Glycol/Gas Heat Exchanger
- Tanks 1500 barrel coated steel welded tanks

Price			
	– Vertical Separators	$ 13,000	Includes 8.5% Sales Tax
	– Treaters	$ 26,000	
	– Glycol Dehydrator	$130,000	
	– Tanks	$ 20,000	

Suppliers: – Process Equipment & Service Company, Inc. Farmington, New Mexico

Summary of Surface Production Facilities

	Cost		
Item	**Tangible**	**Intangible**	**Total**
Separators (total 3)	$ 39,000	–	$ 39,000
Treaters (total 3)	78,000	–	78,000
Glycol Dehydrator	130,000	–	130,000
Tanks (3 at 1500 Bbls)	60,000	–	60,000
Installation of Tanks	–	$ 6,000	6,000
Installation of Facilities	–	$ 25,000	25,000
Total	$307,000	$ 31,000	$ 338,000

CO_2 Supply Line Design and Costs

The following summarizes the design and costs of providing a 13 mile, 8 5/8 " CO_2 supply line from Mobil Oil's Ratherford Unit to the Anasazi Field. The same choices of installation, couplings and contractors were used to develop six different cost scenarios as explained in the flow/injection line section above. The minimum and maximum cost options were selected to provide further details, costs and specifications.

Specification: – 68,640 feet of 8 5/8" Maxicon API rated line pipe rated at 2,530 psi with beveled pipe ends for welding.

- ICO Permian internal IPC505 epoxy coating.

Price:
- $6.82/foot. total cost of $468,129 including transportation to and from ICO Permian's Odessa plant.
- $5.41/foot for applying IPC505 epoxy coating for total of $371,342

Supplier:
- Pipe and shipping – Cave Enterprises, Farmington, New Mexico
- Internal coating – ICO Permian, Odessa, TX

Pipe Line Installation

Minimum Costs Option – Surface Installation and Zaplock Connectors

Specification:
- Surface installation of taped line using new right–a–way and non–welded ZapLock mechanical connectors.
- ZapLock pipe end preparation completed at the coating plant plus ZapLock installation equipment rental and associated transportation costs.

Price:
- Line Installation : $5.20/foot – Total cost for 68,640 feet is $356,928
- Coupling: ZapLock Pipe preparation and installation is $0.77/foot total cost for 68,640 feet is $52,852 plus $2,500 for transportation of installation equipment.
- Total Cost (rounded) $413,000

Supplier:
- Line Installation: BWR Incorporated, Cortez, New Mexico
- Connectors: ZapLock Pipeline Systems, Inc. Houston, Texas

Maximum Cost Option – Buried Line and Heat Pro Connectors

Specification:
- Welded, taped and buried line using new right–of–way and HeatPro CCB connectors
- 2288 8 5/8″ HeatPro connectors plus epoxy/lubricant for installation

Price:
- Line Installation: $10.70/foot – total cost for 68,640 feet is $734,448 plus $155,000 for excavating rock ditches (approximately 25% of line at $9.00/foot) for total of $889,448 (use $890,000)
- Couplings: 2288 at $128.75 each for $294,580 plus $6400 for epoxy/ lubricant. Total coupling costs is $300,980 (use $301,000)

Supplier: – Installation: BWR Incorporated, Farmington, N.M.

– Couplings: HeatPro Systems, Inc. Houston, Texas

Total CO_2 Supply Line Cost Summary

Minimum Cost			
Item	**Tangible**	**Intangible**	**Total**
Line Pipe	$840,000		$ 840,000
Coupling (ZapLock)		$ 56,000	$ 56,000
Installation		$356,000	$ 356,000
	$840,000	$413,000	$1,253,000

Maximum Cost			
Item	**Tangible**	**Intangible**	**Total**
Line Pipe	$ 840,000		$ 840,000
Coupling (HeatPro)	$ 301,000		$ 301,000
Installation		$890,000	
	$1,141,000	$890,000	$2,031,000

Main Injection Compressor Design and Costs

A summary of the compressor design and associated cost is presented below. Detailed design specification and associated system options can be provided as required.

Specification: – Gas Compression System: Complete packaged, skid mounted Ariel Model JGD/4 compressor direct connected to a Caterpillar G3612LE130 natural gas fueled engine with gas starter and associated control system.

– Pad and building for gas compression system.

Price: – Gas Compressor system priced at $1,508,000 including 8.5% sales tax.

– Cost for installation and construction of pad and building is $120,000.

Supplier: –TideAir and Gas, Houston, Texas

Main Compressor Cost Summary

Item	Tangible	Intangible	Total
Compressor	$1,508,000		$1,508,000
Installation	$ 72,000	$ 48,000	$ 120,000
Freight		$ 35,000	$ 35,000
	$1,580.000	$ 83,000	$1,663,000

Gas Processing Plant – Design and Costs

A summary of the gas processing plant employing hollow fiber membrane separation systems and associated process equipment is presented below. Additional details on design can be provided.

Specification:
- Gas Purification System: Multi stage, multi case membrane filter system incorporates a pre–treatment system and membrane separation system.
- Gas Compressor System: Complete packaged Ariel Model JGC/2 single stage compressor direct connected to a Caterpillar G3608 natural gas fueled engine with gas starter and associated control system.

Price:
- Membrane Filter Processing Plant priced at $2,000,000.
- Gas Compressor System priced at $750,000 including 8.5% sales tax.
- Installation Costs quoted as $250,000 for the gas plant and $65,000 for the compressor.
- Freight estimated at a total of $90,000.

Supplier:
- Gas Plant: The Cynara Company, Houston, Texas
- Compressor: Tide Air and Gas, Houston, Texas

Gas Plant Cost Summary

Item	Tangible	Intangible	Total
Gas Plant	$2,000,000	–	$2,000,000
Compressor	$ 700,000	–	$ 700,000
Compressor Building	$ 30,000	–	$ 30,000
Installation	–	–	
Gas Plant	–	$250,000	$ 250,000
Compressor	–	$ 35,000	$ 35,000
Freight	–	$ 90,000	$ 90,000
Total	$2,730,000	$375,000	$3,105,000

CO_2 Purchase Costs

Project economics are based on a CO_2 purchase price of $0.85/MSCF and a collection point for the local CO_2 supply line approximately 13 miles from the Anasazi/Sahgzie reservoir.

Miscellaneous Fees

Archeology, permits, survey, and cattle grazing and damage fees payable to the Navajo Nation are estimated at $2.50/foot. These are charged to any new pipeline or flow line. Thus, the CO_2 supply line, the CO_2 injection line from the main compressor to the injectors and the produced gas line (separators to compressor) would be assessed a fee. Replacement of the existing flow line with new coated lines would not be assessed a fee.

Cost Breakdown of Fees

Item	Cost
CO_2 Injection Line (78,200 feet)	$ 18,000
Separator Gas Lines (4,500 feet)	$ 11,250
CO_2 Supply Lines (68,640 feet)	$171,000
Total	$200,850 (rounded to $201,000)

New Seismic Survey and CO_2 Flood Re–design

Projected costs associated with a 3–D seismic survey, revised reservoir description work, updated history matching and CO_2 flood re–design are provided below:

3–D Seismic Survey

Acquisition Costs	$ 70,000
Processing/Interpretation	$ 30,000
Contingency or Possible Cross Well Survey	$ 50,000
	$150,000

CO_2 Flood Redesign

Revised Reservoir Description	$ 35,000
Updated History Match	$ 35,000
CO_2 Flood Re–design	$ 30,000
Total	$100,000

RESERVOIR MODELING AND COMPOSITION SIMULATION OF PRIMARY DEPLETION, WATERFLOODING, AND CARBON DIOXIDE FLOODING OF A SMALL PENNSYLVANIAN CARBONATE MOUND COMPLEX, ANASAZI FIELD, PARADOX BASIN, UTAH

Supplement

CO_2 Flood Recovery Sensitivity to CO_2 Injection Rate

INTRODUCTION

Two additional simulation prediction cases were conducted to assess the sensitivity of CO_2 flood performance of the Anasazi–Sahgzie fields to reductions in the CO_2 injection rate. This report documents the results of these two new prediction cases and provides economic analysis of the projected performance of one of the floods.

BACKGROUND

The technical report* prepared by REGA, Inc. provides CO_2 flood performance data for two optimized flood cases using CO_2 injection rates governed by a flowing bottom hole pressure constraint of 3,500 psia and a single well maximum CO_2 injection rate of 7.0 MMSCF/D. Pressure constraints restricted the injection rate just after initiation of injection and just before CO_2 breakthrough at the producers. Based on data from Mobil Oil's Aneth field CO_2 projects, Harken believes these rates may be too high. Thus, additional CO_2 flood prediction cases were completed to assess changes in CO_2 injection rates on flood performance. Two cases using CO_2 injection rates of 2.0 MMSCF/Day/well and 4.0 MMSCF/Day/well were completed. The 2.0 MMSCF/D/well rate is based on an average rate reported by Mobil for vertical injectors and the 4.0 MMSCF/D/well rate is representative of well injection rates for some of Mobil's horizontal injectors. The operating conditions and reservoir rock quality in the wells upon which these reported rates are based is unknown. It is believed that water injection was attempted prior to CO_2 injection and if this is the case then this would reduce CO_2 injectivity in the Mobil wells through fluid mobility changes in the reservoir. More information is required to determine if this data would be representative of conditions at Anasazi–Sahgzie. However, the data does provide some guidance and was used, as indicated above, to assess what impact lower CO_2 injection rates would have on predicted Anasazi–Sahgzie CO_2 flood performance.

CO_2 FLOOD SIMULATION PREDICTION CONDITIONS

The operating conditions used for the subject two CO_2 flood cases are the same as those defined in the final technical report for prediction case ASP29. The principal operating parameters and simulation related data in effect for these runs were:

1. Uses history match simulation run ASC102 as a base for restarting the simulation.
2. CO_2 injection starts on 1/1/2000 instead of 1/1/1997.
3. Simulation run ASP36 uses an injection rate of 2.0 MMSCF/D/well and ASP37 uses an injection rate of 4.0 MMSCF/D/well. Each mound (Anasazi and Sahgzie) uses one injection well in the same location as defined in the final report for run ASP29.
4. Production wells Anasazi #1, #5L–3 and Sahgzie #1 were allowed to produce at the rate in effective on 1/1/2000 during reservoir fill–up. This, however was modified as discussed below.
5. Produced gas was recycled to reduce CO_2 make–up gas purchases. Thus, no gas conditioning was employed.
6. CO_2 injection was continuous from the start of injection on 1/1/2000 to the end of the project at 1/1/2012. Although production past 1/1/2012 was possible in terms of reservoir performance it was curtailed to be consistent with Harken's current leasing arrangements.

* "Paradox Basin–Improved Oil Recovery Assessment – Anasazi–Sahgzie Fields" submitted to Harken Energy Corporation, October 1997.

CO_2 FLOOD PERFORMANCE RESULTS

Table 1 (extension of Table 15–4 from final report) summarizes relevant production/injection data for the two new CO_2 flood cases (ASP36 and ASP37) and compares the results to cases presented and discussed in the previously referenced final report. Figures 1 to 9 present production data for the subject two cases and compares CO_2 flood performance under reduced injection conditions to previous high injection rate cases. Results of the two new cases are presented and discussed separately below.

ASP36 Case – CO_2 Flood Using an Injection Rate of 2.0 MMSCF/D/Well

As discussed above, continued production during reservoir fill–up was attempted for both new cases using the lower CO_2 injection rate. In setting up the simulation runs it is necessary to estimate the point at which constrained production can stop and unconstrained production in terms of rates can begin. Unconstrained production is permitted once the reservoir pressure at the producers reaches 2,500 psia. This well related pressure ensures that the average reservoir pressure exceeds the pressure needed for miscibility development. Unconstrained production, subject to a minimum flowing bottom hole pressure of 2,500 psia is allowed from this point to the end of the project. In Case ASP36, the conversion from constrained to unconstrained production was set at 10/1/2001, ten months after the start of CO_2 injection. However, using an injection rate of 2.0 MMSCF/D/well, reservoir pressure had not increased to 2,500 psia at the producers at 10/1/2001 and thus, they were shut–in. The wells remained shut–in until 10/1/2004, three years later. At this time CO_2 injection had raised the reservoir pressure to the required 2,500 psia and production was allowed. An iterative process would have been required to determine when fill–up would have been completed, without a shut–in of producers, if the production wells were allowed to produce at the rates in effect at 1/1/2000. This obviously would have exceeded three years. This was considered excessive in terms of Harken's production needs and the rate of 2.0 MMSCF/D/well was considered impractical. However, the run was allowed to complete (to 1/1/2012) to generate production data for comparison to other cases. Table 1 data shows that incremental oil recovery above primary was 951,000 barrels at 1/1/2012. This required injection of 17.5 BSCF of CO_2 and produced gas and purchase of 10.1 BSCF of CO_2. Relative to case ASP29 (total Injection of 14.0 MMSCF/D versus 4.0 MMSCF/D for ASP36), CO_2 flooding recovered 1.53 MMSTB less oil. Production performance for the field relative to continued primary production is illustrated in Figure 8. Figure 9 compares the predicted performance of Case ASP29 versus Case ASP36 .

In case ASP29. using 14.0 MMSCF/D of CO_2 injection, reservoir fill–up was accomplished (as determined by a minimum bottom hole producing pressure of 2,500 psia) in about 1.5 years with continued production rates in effect at the start of CO_2 injection. In case ASP36, using 4.0 MMSCF/D of CO_2 injection, fill–up was not complete until after 4.75 years of injection (even with production shut–in for 3.0 years)., If the project was allowed to continue past the 1/1/2012 termination date, additional oil would have been recovered and possibly could approach the projected ultimate recovery (less primary production between 1/1/1997 and 1/1/2000) predicted for ASP29 flood .

ASP37 – CO_2 Flood Using an Injection Rate of 4.0 MMSCF/D/Well

Under conditions imposed for this prediction case, reservoir fill–up occurred approximately 22 months after CO_2 injection commenced on 1/1/2000. This period included an eight month shut–in of production. Again, an iterative process to identify reservoir fill–up time with continued production throughout the entire fill–up period without a production shut–in period could have been determined, but ASP37 results were considered acceptable in terms of quantifying CO_2 performance for 8.0 MSCF/D CO_2 injection rate.

Table 1 data indicates that incremental oil recovery over primary was 1,654,000 STB at 1/1/2012. This required injection of 35.0 BSCF of CO_2 and produced gas and purchase of 11.5 BSCF of CO_2. Relative to ASP 29 (14.0 MMSCF/D CO_2 injection), injecting CO_2 at a total rate of 8.0 MSCF/D would recover 830,000 STB less oil. Figure 1 compares CO_2 flood performance to continued primary production for the field and Figures 2, 3 and 4 present the same comparison for the individual wells. Figures 5 and 6 present the injection rate and cumulative injection volume for the two injectors. Figures 7 compares the CO_2 flood for the 14.0 MMSCF/D case (ASP29) and the current case using 8.0 MMSCF/D (ASP37).

Again, continued operation beyond 1/1/2012 would have provided additional recovery of the remaining oil and would have likely approached projected ASP29 recovery. At 1/1/2012 the ASP37 case exhibits 910,000 STB more oil in place and is producing at a lower GOR than is case ASP29. Thus, another four or five years of production under ASP37 conditions would have provided a significant percent of the difference in ultimate oil production between ASP29 and ASP37.

ECONOMIC ASSESSMENT

Production data and injection gas requirements, including CO_2 make–up purchases, from ASP37 case information were used to assess, from an economic standpoint, the financial merits of a CO_2 flood using a 8.0 MMSCF/D injection rate commencing 1/1/2000. The economic assessment was conducted assuming the following conditions:

1. Leased compressor.
2. CO_2 supply line construction using the minimum costs option.
3. No gas processing.
4. DOE cost sharing.

In conducting the economic assessment, the CO_2 supply line was down sized to handle smaller CO_2 throughput (8.0 MMSCF/D vs 15.0 MMSCF/D). This reduced CO_2 supply pipeline installation costs for the minimum cost option to $825,000 from $1,253,000. It reduced the maximum cost option to $1,488,000 from $2,031,000. No down sizing was utilized for lease lines, injection well tubing or production facilities. However, the scaled down CO_2 injection rate could have been used to reduce the capital requirements for these facilities.

A revised estimate for the main injection compressor costs for these lower injection rate cases based on a five year lease option, without vendor supplied maintenance, reduces compressor lease costs from $28,000/month to $19,500/month for compressor Option 1 and to $23,500/month for compressor Option 2. Compressor Option 1 is based on an Ariel JGC–4 compressor connected to a Caterpillar G3606 natural gas engine. Compressor Option 2 is based on the same compressor, but uses a Caterpillar G3608 engine. Compressor and lease fuel requirements were scaled down from 15,899 MSCF/month to 10,300 MSCF/month for compressor Option 1 and to 13,000 MSCF/month for Option 2 when using produced gas to supply fuel. Once the CO_2 concentration prevented the use of lease gas for fuel then gas needs to be purchased. Using the down–sized compressor and prime mover the fuel costs were reduced from $29,000/month to $18,500 for Option 1 and to $23,400/month for Option 2. Also with lower capital requirements, the DOE cost sharing element was reduced proportionately. Details on DOE cost sharing are presented in Table 2. All other costs/expenditures were kept the same as those used in the final report. Also, all economic parameters remained unchanged.

Under these conditions, the 8.0 MMSCF/D CO_2 injection rate flood commencing in 1/1/2000 provided the following economic performance data:

Economic Performance Parameters for Low Injection Rate Cases

Evaluation	Compressor Option	Before Tax NPV @ 10% M$	Before Tax R of R	Payout Months	PI
18	1	5,930	32	36	10.4
17	2	5,300	30	48	9.7

Details on the economic evaluations are provided in Tables 3a, 3b, 4a and 4b.

Comparing the compressor Option 1 case with it's counterpart case in the original report (Evaluation 6) shows that the reduced CO_2 injection rate case decreased the rate of return from 62% to 32%, the net present value from $12,500,000 to $5,900,000 and the profitability index from 15 to 1 to 10.4 to 1. The lower economic performance criteria result from:

1. A longer time to fill–up and thus reach the peak oil production period (22 months for ASP37 versus 15 months for ASP29). Also the lower injection rate cases included an eight month production shut–in period.

2. Longer project life and premature termination of the flood because of the January 1, 2012 lease termination date.

3. Lower peak oil production rates caused by the lower CO_2 injection rates reduces cash flow.

Economics could be improved by using reduced capital requirements associated with scale down of un–modified surface facilities and well completions retained from the high CO_2 injection cases. In addition, allowing oil production during the entire fill–up period would improve initial cash flow.

SUMMARY AND CONCLUSIONS

Two reduced CO_2 injection rate simulation prediction cases were completed and compared to optimum cases presented in the final technical report. Injection rates of 2.0 and 4.0 MMSCF/D/well were used to assess the impact of CO_2 injection rate on flood performance and associated economics. Simulation prediction results indicate that a CO_2 injection rate of 2.0 MMSCF/D/well would not be sufficient to meet ongoing production needs of Harken and generate acceptable economic returns. If would however, increase recovery by close to 1.0 MMSTB over predicted primary recovery at 1/1/2012.

CO_2 flooding at 4.0 MMSCF/D/well did provide adequate flood response and an acceptable economic return. Specifically, using a 4.0 MMSCF/D/well injection rate from two injectors could provide:

1. The CO_2 flood will recovery 4.21 MMSTB. This represents an increase of 1.65 MMSTB over predicted primary recovery at 1/1/2012. The projected 4.21 MMSTB represents more than 89% of the oil in the mound complex and 36.8% of the original oil in place in the total system modelled. The incremental recovery of 1.65 MMSTB requires injection of 35.0 BSCF of gas with purchase of 11.5 BSCF of CO_2.

2. An economic rate of return of 32%, a payout of 36 months and a discounted (10%) net percent value of $5.9 million could be realized by implementing a CO_2 flood under the proposed conditions. Harken's capital outlay with DOE participation would be $1,493,000.

RECOMMENDATIONS

As the results of these two lower CO_2 injection rate cases illustrate, injection rate and CO_2 flood implementation timing are important factors influencing flood performance and economics. Thus it is recommended that:

1. CO_2 flooding should be implemented as early as possible because of the lease expiration date of 1/1/2012.

2. As recommended in the final report, a full injectivity test using CO_2 should be conducted on the Anasazi 6H–1 well to establish injection data before committing to further work.

3. Horizontal well injectivity should be predicted from the appropriate well test model after calibration with vertical well test data.

4. Further work is needed before accepting reported Mobil Oil injection rate information as guide lines for Anasazi–Sahgzie or any other Harken operated Paradox Basin reservoirs. Specifically, reservoir operating history prior to CO_2 injection (ie. water injection) needs to be determined. Also, reservoir geology and rock quality together with reservoir fluid mobility conditions need to be compared among specific Mobil and Harken wells.

Table 1
Production/Injection Data CO_2 Flood
Anasazi/Sahgzie Reservoir

Case No.	Cum Oil MSTB	Cum Gas /BSCF	Incremental over Primary MSTB	Total Gas Inj. BSCF	Total CO_2 Purchase BSCF	Total Gas Recycled BSCF
Production / Injection at 1/1/2003						
ASC102	2194	1.9	NA	NA	NA	N/A
ASP29	3665	19.1	1471	28.0	10.2	17.8
ASP30	3659	19.2	1460	28.0	11.5	16.5
ASP35	3665	19.1	1471	28.0	10.2	17.8
ASP36	2116	1.7	–78	4.4	4.2	0.2
ASP37	2293	2.6	99	8.8	7.8	1.0
Production / Injection at 1/1/2006						
ASC102	2392	2.2	NA	NA	NA	NA
ASP29	4261	33.3	1909	43.3	11.4	31.9
ASP30	4232	33.4	1881	43.4	13.6	29.8
ASP35	3983	30.0	1631	28.0	10.2	17.8
ASP36	2385	2.4	–7	8.8	8.0	0.8
ASP37	3302	9.4	910	17.5	9.8	7.7
Production / Injection at 1/1/2012						
ASC102	2554	2.5	NA	NA	NA	NA
ASP29	5039	62.5	2484	74.0	12.9	61.1
ASP30	4980	62.5	2426	74.1	17.2	56.9
ASP35	4269	30.8	1775	28.0	10.2	17.8
ASP36	3505	9.1	951	17.5	10.1	7.4
ASP37	4208	25.2	1654	35.0	11.5	23.5

Table 2
DOE Cost Sharing (Reduced Injection Rate Cases)

	Minimum Cost Case (Surface–Zaplock)		
Item	**Tangible**	**Intangible**	**Total**
Drilling/Completion	$ 506,000	$ 378,000	$ 884,000
Surface Production Facilities	$ 307,000	$ 31,000	$ 338,000
Lease Lines	$ 110,000	$ 110,000	$ 220,000
CO_2 Supply Line	$ 413,000	$ 412,000	$ 825,000
Miscellaneous Fees	–	$ 201,000	$ 201,000
G&G	–	$ 250,000	$ 250,000
	$ 1,336,000	$ 1,382,000	$ 2,718,000
DOE Share (45.08%)	$ 602,000	$ 623,000	

Table 3a

EVALUATION ANAC1.17

ECONOMIC EVALUATION
HARKEN PARADOX BASIN
REGA INCORPORATED

RUN DATE:12-18-1997
RUN TIME: 11:05:27

AS OF DATE: JUN99

		NPV	5.0%	8359.157	BFIT
		NPV	10.0%	5299.527	BFIT
NAME:	ANASAZI CO2 FLOOD LEASE DOE	CONTINUOUS CO2 GAS RECYCLE	NPV	15.0%	3202.053	BFIT
FIELD:	ANASAZI-SAHGZIE	NO GAS PROCESSING BUY FUEL	NPV	20.0%	1733.149	BFIT
LOCATION:	UTAH	LEASE INJECTION COMPRESSOR	NPV	25.0%	686.288	BFIT
FORMATION:	DESERT CREEK	SURFACE LINES - ZAPLOCK	IRR		30%	BFIT
OPERATOR:	HARKEN ENERGY	LOW INJECTION RATE - 8.0MMSCF/D	PAYOUT		JAN04	BFIT
			PI		9.67:1	BFIT

====== INTERESTS AND EFFECTIVE DATE ======

COST	OIL	GAS	COND	PRODT	DATE
1.00000	0.80000	0.80000	0.80000	0.80000	JUN99

	======== PRICES ========			========== GROSS RESERVES ==========				
	BEGINING	ENDING	AVERAGE	CUMULATIVE	REMAINING	ULTIMATE	%REMAINING	
OIL	20.00	20.00	20.00	1952.420	2252.763	4205.183	53.57	OIL
GAS	1.80	0.00	1.80	1578.320	80.214	1658.534	4.84	GAS
COND	0.00	0.00	0.00	0.000	0.000	0.000	0.00	COND
PRDT	0.00	0.00	0.00	0.000	0.000	0.000	0.00	PRDT

YEAR ========	GROSS OIL PRODUCTION ==MBBLS==	NET OIL PRODUCTION ==MBBLS==	GROSS GAS PRODUCTION ==MMSCF==	GROSS GAS AS FUEL ==MMSCF==	NET GAS PRODUCTION ==MMSCF==	AVERAGE OIL PRICE ===$/B===	AVERAGE GAS PRICE ==$/MSCF==	NET OIL SALES ===M$===	NET GAS SALES ===M$===	NET TOTAL REVENUE ===M$===
1999(7 Mo)	47.473	37.978	42.968	15.323	34.374	20.000	1.800	759.568	39.809	799.377
2000	70.314	56.251	37.246	78.000	29.797	20.000	1.800	1125.024	-58.686	1066.338
2001	20.250	16.200	0.000	0.000	0.000	20.000	0.000	324.000	0.000	324.000
2002	201.653	161.322	0.000	0.000	0.000	20.000	0.000	3226.448	0.000	3226.448
2003	450.294	360.235	0.000	0.000	0.000	20.000	0.000	7204.704	0.000	7204.704
2004	306.985	245.588	0.000	0.000	0.000	20.000	0.000	4911.760	0.000	4911.760
2005	250.266	200.213	0.000	0.000	0.000	20.000	0.000	4004.256	0.000	4004.256
2006	206.479	165.183	0.000	0.000	0.000	20.000	0.000	3303.664	0.000	3303.664
2007	173.842	139.074	0.000	0.000	0.000	20.000	0.000	2781.472	0.000	2781.472
2008	151.757	121.406	0.000	0.000	0.000	20.000	0.000	2428.112	0.000	2428.112
2009	135.547	108.438	0.000	0.000	0.000	20.000	0.000	2168.752	0.000	2168.752
2010	123.466	98.773	0.000	0.000	0.000	20.000	0.000	1975.456	0.000	1975.456
2011(12Mo)	114.437	91.550	0.000	0.000	0.000	20.000	0.000	1830.992	0.000	1830.992
2012	0.000	0.000	0.000	0.000	0.000	0.000	0.000	0.000	0.000	0.000
2013	0.000	0.000	0.000	0.000	0.000	0.000	0.000	0.000	0.000	0.000
SUBTOTAL	2252.763	1802.210	80.214	93.323	64.171	20.000	1.800	36044.207	-18.877	36025.332
REMAINING	0.000	0.000	0.000	0.000	0.000	0.000	0.000	0.000	0.000	0.000
TOT 12.6Yr	2252.763	1802.210	80.214	93.323	64.171	20.000	1.800	36044.207	-18.877	36025.332

YEAR ========	NET TOTAL LOE ===M$===	NET TANGIBLES ===M$===	NET INTANGIBLES ===M$===	NET G&G ===M$===	NET TOTAL INVESTMENTS ===M$===	NET LEASE REVENUE ===M$B===	NET BFIT CASHFLOW ===M$===	CUM BFIT CASHFLOW ===M$===	BFIT CF DISC 10.0% ===M$===	CUMBFIT CF DISC 10.0% ===M$===
1999(7 Mo)	56.000	1336.000	1133.000	250.000	2719.000	743.377	-1975.623	-1975.623	-1918.012	-1918.012
2000	3259.195	-602.000	-511.000	-112.000	-1225.000	-2192.857	-967.857	-2943.480	-818.398	-2736.410
2001	3419.433	0.000	0.000	0.000	0.000	-3095.433	-3095.433	-6038.914	-2533.435	-5269.846
2002	2798.734	0.000	0.000	0.000	0.000	427.714	427.714	-5611.199	273.434	-4996.411
2003	1746.636	0.000	0.000	0.000	0.000	5458.068	5458.068	-153.131	3690.932	-1305.479
2004	1484.661	0.000	0.000	0.000	0.000	3427.099	3427.099	3273.968	2108.066	802.587
2005	1393.112	0.000	0.000	0.000	0.000	2611.144	2611.144	5885.112	1459.166	2261.753
2006	1322.835	0.000	0.000	0.000	0.000	1980.829	1980.829	7865.941	1006.509	3268.262
2007	1275.553	0.000	0.000	0.000	0.000	1505.919	1505.919	9371.860	695.439	3963.701
2008	1241.708	0.000	0.000	0.000	0.000	1186.404	1186.404	10558.265	497.914	4461.615
2009	1215.756	0.000	0.000	0.000	0.000	952.996	952.996	11511.261	363.569	4825.184
2010	1196.643	0.000	0.000	0.000	0.000	778.813	778.813	12290.074	270.006	5095.189
2011(12Mo)	1182.529	0.000	0.000	0.000	0.000	648.463	648.463	12938.537	204.338	5299.528
2012	0.000	0.000	0.000	0.000	0.000	0.000	0.000	0.000	0.000	0.000
2013	0.000	0.000	0.000	0.000	0.000	0.000	0.000	0.000	0.000	0.000
SUBTOTAL	21592.795	734.000	622.000	138.000	1494.000	14432.537	12938.537	12938.537	5299.528	5299.528
REMAINING	0.000	0.000	0.000	0.000	0.000	0.000	0.000	0.000	0.000	0.000
TOT 12.6Yr	21592.795	734.000	622.000	138.000	1494.000	14432.537	12938.537	12938.537	5299.528	5299.528

Table 3b

EVALUATION ANAC1.17

ECONOMIC EVALUATION
HARKEN PARADOX BASIN
REGA INCORPORATED

RUN DATE: 12-18-1997
RUN TIME: 11:06:44

AS OF DATE: JUN99

NAME: ANASAZI CO2 FLOOD LEASE DOE
FIELD: ANASAZI-SAHGZIE
LOCATION: UTAH
FORMATION: DESERT CREEK
OPERATOR: HARKEN ENERGY

CONTINUOUS CO2 GAS RECYCLE
NO GAS PROCESSING BUY FUEL
LEASE INJECTION COMPRESSOR
SURFACE LINES - ZAPLOCK
LOW INJECTION RATE - 8.0MMSCF/D

NPV	5.0%	8359.157	BFIT	5344.880	AFIT
NPV	10.0%	5299.527	BFIT	3177.490	AFIT
NPV	15.0%	3202.053	BFIT	1672.521	AFIT
NPV	20.0%	1733.149	BFIT	607.699	AFIT
NPV	25.0%	686.288	BFIT	-157.017	AFIT
IRR		30%	BFIT	24%	AFIT
PAYOUT		JAN04	BFIT	JAN04	AFIT
PI		9.67:1	BFIT	6.72:1	AFIT

====== INTERESTS AND EFFECTIVE DATE ======

COST	OIL	GAS	COND	PRODT	DATE
1.00000	0.80000	0.80000	0.80000	0.80000	JUN99

	======== PRICES ========			========== GROSS RESERVES ==========				
	BEGINING	ENDING	AVERAGE	CUMULATIVE	REMAINING	ULTIMATE	%REMAINING	
OIL	20.00	20.00	20.00	1952.420	2252.763	4205.183	53.57	OIL
GAS	1.80	0.00	1.80	1578.320	80.214	1658.534	4.84	GAS
COND	0.00	0.00	0.00	0.000	0.000	0.000	0.00	COND
PRDT	0.00	0.00	0.00	0.000	0.000	0.000	0.00	PRDT

YEAR	GROSS OIL PRODUCTION	NET OIL PRODUCTION	GROSS GAS PRODUCTION	GROSS GAS AS FUEL	NET GAS PRODUCTION	AVERAGE OIL PRICE	AVERAGE GAS PRICE	NET OIL SALES	NET GAS SALES	NET TOTAL REVENUE
========	==MBBLS==	==MBBLS==	==MMSCF==	==MMSCF==	==MMSCF==	===$/B===	==$/MSCF==	===M$===	===M$===	===M$===
1999(7 Mo)	47.473	37.978	42.968	15.323	34.374	20.000	1.800	759.568	39.809	799.377
2000	70.314	56.251	37.246	78.000	29.797	20.000	1.800	1125.024	-58.686	1066.338
2001	20.250	16.200	0.000	0.000	0.000	20.000	0.000	324.000	0.000	324.000
2002	201.653	161.322	0.000	0.000	0.000	20.000	0.000	3226.448	0.000	3226.448
2003	450.294	360.235	0.000	0.000	0.000	20.000	0.000	7204.704	0.000	7204.704
2004	306.985	245.588	0.000	0.000	0.000	20.000	0.000	4911.760	0.000	4911.760
2005	250.266	200.213	0.000	0.000	0.000	20.000	0.000	4004.256	0.000	4004.256
2006	206.479	165.183	0.000	0.000	0.000	20.000	0.000	3303.664	0.000	3303.664
2007	173.842	139.074	0.000	0.000	0.000	20.000	0.000	2781.472	0.000	2781.472
2008	151.757	121.406	0.000	0.000	0.000	20.000	0.000	2428.112	0.000	2428.112
2009	135.547	108.438	0.000	0.000	0.000	20.000	0.000	2168.752	0.000	2168.752
2010	123.466	98.773	0.000	0.000	0.000	20.000	0.000	1975.456	0.000	1975.456
2011(12Mo)	114.437	91.550	0.000	0.000	0.000	20.000	0.000	1830.992	0.000	1830.992
2012	0.000	0.000	0.000	0.000	0.000	0.000	0.000	0.000	0.000	0.000
2013	0.000	0.000	0.000	0.000	0.000	0.000	0.000	0.000	0.000	0.000
SUBTOTAL	2252.763	1802.210	80.214	93.323	64.171	20.000	1.800	36044.207	-18.877	36025.332
REMAINING	0.000	0.000	0.000	0.000	0.000	0.000	0.000	0.000	0.000	0.000
TOT 12.6Yr	2252.763	1802.210	80.214	93.323	64.171	20.000	1.800	36044.207	-18.877	36025.332

YEAR	NET TOTAL INVESTMENTS	NET TOTAL REVENUE	NET LEASE REVENUE	NET BFIT CASHFLOW	NET TAX DEPREC	NET TAXABLE INCOME	NET INCOME TAXES PAID	NET AFIT CASHFLOW	CUM AFIT CASHFLOW	AFIT CF DISC 10.0%
========	===M$===	===M$===	===M$===	===M$===	===M$===	===M$B===	===M$===	===M$===	===M$===	===M$===
1999(7 Mo)	2719.000	799.377	743.377	-1975.623	190.857	-830.480	0.000	-1975.623	-1975.623	-1918.012
2000	-1225.000	1066.338	-2192.857	-967.857	-274.816	-1295.041	0.000	-967.857	-2943.480	-818.398
2001	0.000	324.000	-3095.433	-3095.433	233.703	-3329.136	0.000	-3095.433	-6038.914	-2533.435
2002	0.000	3226.448	427.714	427.714	166.930	260.784	0.000	427.714	-5611.199	273.434
2003	0.000	7204.704	5458.068	5458.068	119.236	5338.833	49.286	5408.782	-202.417	3659.090
2004	0.000	4911.760	3427.099	3427.099	119.236	3307.863	1124.673	2302.426	2100.009	1447.498
2005	0.000	4004.256	2611.144	2611.144	119.236	2491.908	847.249	1763.896	3863.904	1006.780
2006	0.000	3303.664	1980.829	1980.829	59.618	1921.211	653.212	1327.617	5191.521	689.436
2007	0.000	2781.472	1505.919	1505.919	0.000	1505.919	512.013	993.907	6185.428	469.499
2008	0.000	2428.112	1186.404	1186.404	0.000	1186.404	403.377	783.027	6968.455	336.094
2009	0.000	2168.752	952.996	952.996	0.000	952.996	324.019	628.977	7597.433	245.401
2010	0.000	1975.456	778.813	778.813	0.000	778.813	264.796	514.017	8111.449	182.216
2011(12Mo)	0.000	1830.992	648.463	648.463	0.000	648.463	220.477	427.986	8539.435	137.887
2012	0.000	0.000	0.000	0.000	0.000	0.000	0.000	0.000	8539.435	0.000
2013	0.000	0.000	0.000	0.000	0.000	0.000	0.000	0.000	0.000	0.000
SUBTOTAL	1494.000	36025.332	14432.537	12938.537	734.000	12938.537	4399.103	8539.435	8539.435	3177.489
REMAINING	0.000	0.000	0.000	0.000	0.000	0.000	0.000	0.000	0.000	0.000
TOT 12.6Yr	1494.000	36025.332	14432.537	12938.537	734.000	12938.537	4399.103	8539.435	8539.435	3177.489

Table 4a

EVALUATION ANAC1.18

ECONOMIC EVALUATION
HARKEN PARADOX BASIN
REGA INCORPORATED

RUN DATE: 12-18-1997
RUN TIME: 11:29:42

AS OF DATE: JUN99

NPV	5.0%	9184.550	BFIT
NPV	10.0%	5929.458	BFIT
NPV	15.0%	3699.717	BFIT
NPV	20.0%	2138.012	BFIT
NPV	25.0%	1023.880	BFIT
IRR		32%	BFIT
PAYOUT		DEC03	BFIT
PI		10.42:1	BFIT

NAME: ANASAZI CO2 FLOOD LEASE DOE
FIELD: ANASAZI-SAHGZIE
LOCATION: UTAH
FORMATION: DESERT CREEK
OPERATOR: HARKEN ENERGY

CONTINUOUS CO2 GAS RECYCLE
NO GAS PROCESSING BUY FUEL
LEASE INJECTION COMPRESSOR
SURFACE LINES - ZAPLOCK
LOW INJECTION RATE - 8.0 MMSCF/D

====== INTERESTS AND EFFECTIVE DATE ======

COST	OIL	GAS	COND	PRODT	DATE
1.00000	0.80000	0.80000	0.80000	0.80000	JUN99

	======== PRICES ========			========== GROSS RESERVES ==========				
	BEGINING	ENDING	AVERAGE	CUMULATIVE	REMAINING	ULTIMATE	%REMAINING	
OIL	20.00	20.00	20.00	1952.420	2252.763	4205.183	53.57	OIL
GAS	1.80	0.00	1.80	1578.320	80.214	1658.534	4.84	GAS
COND	0.00	0.00	0.00	0.000	0.000	0.000	0.00	COND
PRDT	0.00	0.00	0.00	0.000	0.000	0.000	0.00	PRDT

YEAR	GROSS OIL PRODUCTION	NET OIL PRODUCTION	GROSS GAS PRODUCTION	GROSS GAS AS FUEL	NET GAS PRODUCTION	AVERAGE OIL PRICE	AVERAGE GAS PRICE	NET OIL SALES	NET GAS SALES	NET TOTAL REVENUE
========	==MBBLS==	==MBBLS==	==MMSCF==	==MMSCF==	==MMSCF==	===$/B===	==$/MSCF==	===M$===	===M$===	===M$===
1999(7 Mo)	47.473	37.978	42.968	15.323	34.374	20.000	1.800	759.568	39.809	799.377
2000	70.314	56.251	37.246	61.800	29.797	20.000	1.800	1125.024	-35.358	1089.666
2001	20.250	16.200	0.000	0.000	0.000	20.000	0.000	324.000	0.000	324.000
2002	201.653	161.322	0.000	0.000	0.000	20.000	0.000	3226.448	0.000	3226.448
2003	450.294	360.235	0.000	0.000	0.000	20.000	0.000	7204.704	0.000	7204.704
2004	306.985	245.588	0.000	0.000	0.000	20.000	0.000	4911.760	0.000	4911.760
2005	250.266	200.213	0.000	0.000	0.000	20.000	0.000	4004.256	0.000	4004.256
2006	206.479	165.183	0.000	0.000	0.000	20.000	0.000	3303.664	0.000	3303.664
2007	173.842	139.074	0.000	0.000	0.000	20.000	0.000	2781.472	0.000	2781.472
2008	151.757	121.406	0.000	0.000	0.000	20.000	0.000	2428.112	0.000	2428.112
2009	135.547	108.438	0.000	0.000	0.000	20.000	0.000	2168.752	0.000	2168.752
2010	123.466	98.773	0.000	0.000	0.000	20.000	0.000	1975.456	0.000	1975.456
2011(12Mo)	114.437	91.550	0.000	0.000	0.000	20.000	0.000	1830.992	0.000	1830.992
2012	0.000	0.000	0.000	0.000	0.000	0.000	0.000	0.000	0.000	0.000
2013	0.000	0.000	0.000	0.000	0.000	0.000	0.000	0.000	0.000	0.000
SUBTOTAL	2252.763	1802.210	80.214	77.123	64.171	20.000	1.800	36044.207	4.451	36048.660
REMAINING	0.000	0.000	0.000	0.000	0.000	0.000	0.000	0.000	0.000	0.000
TOT 12.6Yr	2252.763	1802.210	80.214	77.123	64.171	20.000	1.800	36044.207	4.451	36048.660

YEAR	NET TOTAL LOE	NET TANGIBLES	NET INTANGIBLES	NET G&G	NET TOTAL INVESTMENTS	NET LEASE REVENUE	NET BFIT CASHFLOW	CUM BFIT CASHFLOW	BFIT CF DISC 10.0%	CUMBFIT CF DISC 10.0%
========	==MBBLS==	==MBBLS==	==MMSCF==	==MMSCF==	==MMSCF==	===$/B===	==$/MSCF==	===M$===	===M$===	===M$===
1999(7 Mo)	56.000	1336.000	1133.000	250.000	2719.000	743.377	-1975.623	-1975.623	-1918.012	-1918.012
2000	3194.035	-602.000	-511.000	-112.000	-1225.000	-2104.369	-879.369	-2854.992	-739.002	-2657.014
2001	3325.113	0.000	0.000	0.000	0.000	-3001.113	-3001.113	-5856.105	-2456.379	-5113.394
2002	2704.414	0.000	0.000	0.000	0.000	522.034	522.034	-5334.071	343.486	-4769.908
2003	1652.316	0.000	0.000	0.000	0.000	5552.388	5552.388	218.317	3754.615	-1015.293
2004	1390.341	0.000	0.000	0.000	0.000	3521.419	3521.419	3739.736	2165.960	1150.667
2005	1298.792	0.000	0.000	0.000	0.000	2705.464	2705.464	6445.200	1511.796	2662.463
2006	1228.515	0.000	0.000	0.000	0.000	2075.149	2075.149	8520.350	1054.355	3716.818
2007	1181.233	0.000	0.000	0.000	0.000	1600.239	1600.239	10120.589	738.935	4455.753
2008	1147.388	0.000	0.000	0.000	0.000	1280.724	1280.724	11401.313	537.456	4993.208
2009	1121.436	0.000	0.000	0.000	0.000	1047.316	1047.316	12448.629	399.516	5392.724
2010	1102.323	0.000	0.000	0.000	0.000	873.133	873.133	13321.762	302.685	5695.409
2011(12Mo)	1088.209	0.000	0.000	0.000	0.000	742.783	742.783	14064.545	234.047	5929.456
2012	0.000	0.000	0.000	0.000	0.000	0.000	0.000	0.000	0.000	0.000
2013	0.000	0.000	0.000	0.000	0.000	0.000	0.000	0.000	0.000	0.000
SUBTOTAL	20490.115	734.000	622.000	138.000	1494.000	15558.545	14064.545	14064.545	5929.456	5929.456
REMAINING	0.000	0.000	0.000	0.000	0.000	0.000	0.000	0.000	0.000	0.000
TOT 12.6Yr	20490.115	734.000	622.000	138.000	1494.000	15558.545	14064.545	14064.545	5929.456	5929.456

Table 4b

EVALUATION ANAC1.18

ECONOMIC EVALUATION
HARKEN PARADOX BASIN
REGA INCORPORATED

RUN DATE: 12-18-1997
RUN TIME: 11:30:32

AS OF DATE: JUN99

NAME: ANASAZI CO2 FLOOD LEASE DOE
FIELD: ANASAZI-SAHGZIE
LOCATION: UTAH
FORMATION: DESERT CREEK
OPERATOR: HARKEN ENERGY

CONTINUOUS CO2 GAS RECYCLE-LO2
NO GAS PROCESSING BUY FUEL
LEASE INJECTION COMPRESSOR
SURFACE LINES - ZAPLOCK
LOW INJECTION RATE - 8.0 MMSCF/D

NPV	5.0%	9184.550	BFIT	5903.555	AFIT
NPV	10.0%	5929.458	BFIT	3615.290	AFIT
NPV	15.0%	3699.717	BFIT	2027.794	AFIT
NPV	20.0%	2138.012	BFIT	904.446	AFIT
NPV	25.0%	1023.880	BFIT	96.770	AFIT
IRR		32%	BFIT	26%	AFIT
PAYOUT		DEC03	BFIT	DEC03	AFIT
PI		10.42:1	BFIT	7.22:1	AFIT

====== INTERESTS AND EFFECTIVE DATE ======

COST	OIL	GAS	COND	PRODT	DATE
1.00000	0.80000	0.80000	0.80000	0.80000	JUN99

	======== PRICES ========			========== GROSS RESERVES ==========				
	BEGINING	ENDING	AVERAGE	CUMULATIVE	REMAINING	ULTIMATE	%REMAINING	
OIL	20.00	20.00	20.00	1952.420	2252.763	4205.183	53.57	OIL
GAS	1.80	0.00	1.80	1578.320	80.214	1658.534	4.84	GAS
COND	0.00	0.00	0.00	0.000	0.000	0.000	0.00	COND
PRDT	0.00	0.00	0.00	0.000	0.000	0.000	0.00	PRDT

YEAR	GROSS OIL PRODUCTION	NET OIL PRODUCTION	GROSS GAS PRODUCTION	GROSS GAS AS FUEL	NET GAS PRODUCTION	AVERAGE OIL PRICE	AVERAGE GAS PRICE	NET OIL SALES	NET GAS SALES	NET TOTAL REVENUE
========	==MBBLS==	==MBBLS==	==MMSCF==	==MMSCF==	==MMSCF==	===$/B===	==$/MSCF==	===M$===	===M$===	===M$===
1999(7 Mo)	47.473	37.978	42.968	15.323	34.374	20.000	1.800	759.568	39.809	799.377
2000	70.314	56.251	37.246	61.800	29.797	20.000	1.800	1125.024	-35.358	1089.666
2001	20.250	16.200	0.000	0.000	0.000	20.000	0.000	324.000	0.000	324.000
2002	201.653	161.322	0.000	0.000	0.000	20.000	0.000	3226.448	0.000	3226.448
2003	450.294	360.235	0.000	0.000	0.000	20.000	0.000	7204.704	0.000	7204.704
2004	306.985	245.588	0.000	0.000	0.000	20.000	0.000	4911.760	0.000	4911.760
2005	250.266	200.213	0.000	0.000	0.000	20.000	0.000	4004.256	0.000	4004.256
2006	206.479	165.183	0.000	0.000	0.000	20.000	0.000	3303.664	0.000	3303.664
2007	173.842	139.074	0.000	0.000	0.000	20.000	0.000	2781.472	0.000	2781.472
2008	151.757	121.406	0.000	0.000	0.000	20.000	0.000	2428.112	0.000	2428.112
2009	135.547	108.438	0.000	0.000	0.000	20.000	0.000	2168.752	0.000	2168.752
2010	123.466	98.773	0.000	0.000	0.000	20.000	0.000	1975.456	0.000	1975.456
2011(12Mo)	114.437	91.550	0.000	0.000	0.000	20.000	0.000	1830.992	0.000	1830.992
2012	0.000	0.000	0.000	0.000	0.000	0.000	0.000	0.000	0.000	0.000
2013	0.000	0.000	0.000	0.000	0.000	0.000	0.000	0.000	0.000	0.000
SUBTOTAL	2252.763	1802.210	80.214	77.123	64.171	20.000	1.800	36044.207	4.451	36048.660
REMAINING	0.000	0.000	0.000	0.000	0.000	0.000	0.000	0.000	0.000	0.000
TOT 12.6Yr	2252.763	1802.210	80.214	77.123	64.171	20.000	1.800	36044.207	4.451	36048.660

YEAR	NET TOTAL INVESTMENTS	NET TOTAL REVENUE	NET LEASE REVENUE	NET BFIT CASHFLOW	NET TAX DEPREC	NET TAXABLE INCOME	NET INCOME TAXES PAID	NET AFIT CASHFLOW	CUM AFIT CASHFLOW	AFIT CF DISC 10.0%
========	===M$===	===M$===	===M$===	===M$===	===M$===	===M$B===	===M$===	===M$===	===M$===	===M$===
1999(7 Mo)	2719.000	799.377	743.377	-1975.623	190.857	-830.480	0.000	-1975.623	-1975.623	-1918.012
2000	-1225.000	1089.666	-2104.369	-879.369	-274.816	-1206.553	0.000	-879.369	-2854.992	-739.002
2001	0.000	324.000	-3001.113	-3001.113	233.703	-3234.815	0.000	-3001.113	-5856.105	-2456.379
2002	0.000	3226.448	522.034	522.034	166.930	355.103	0.000	522.034	-5334.071	343.486
2003	0.000	7204.704	5552.388	5552.388	119.236	5433.152	175.578	5376.810	42.738	3641.178
2004	0.000	4911.760	3521.419	3521.419	119.236	3402.183	1156.742	2364.677	2407.415	1486.557
2005	0.000	4004.256	2705.464	2705.464	119.236	2586.228	879.318	1826.147	4233.562	1042.287
2006	0.000	3303.664	2075.149	2075.149	59.618	2015.531	685.281	1389.869	5623.430	721.716
2007	0.000	2781.472	1600.239	1600.239	0.000	1600.239	544.081	1056.158	6679.588	498.844
2008	0.000	2428.112	1280.724	1280.724	0.000	1280.724	435.446	845.278	7524.866	362.771
2009	0.000	2168.752	1047.316	1047.316	0.000	1047.316	356.087	691.229	8216.094	269.653
2010	0.000	1975.456	873.133	873.133	0.000	873.133	296.865	576.268	8792.361	204.263
2011(12Mo)	0.000	1830.992	742.783	742.783	0.000	742.783	252.546	490.237	9282.598	157.930
2012	0.000	0.000	0.000	0.000	0.000	0.000	0.000	0.000	9282.598	0.000
2013	0.000	0.000	0.000	0.000	0.000	0.000	0.000	0.000	0.000	0.000
SUBTOTAL	1494.000	36048.660	15558.545	14064.545	734.000	14064.545	4781.946	9282.598	9282.598	3615.290
REMAINING	0.000	0.000	0.000	0.000	0.000	0.000	0.000	0.000	0.000	0.000
TOT 12.6Yr	1494.000	36048.660	15558.545	14064.545	734.000	14064.545	4781.946	9282.598	9282.598	3615.290

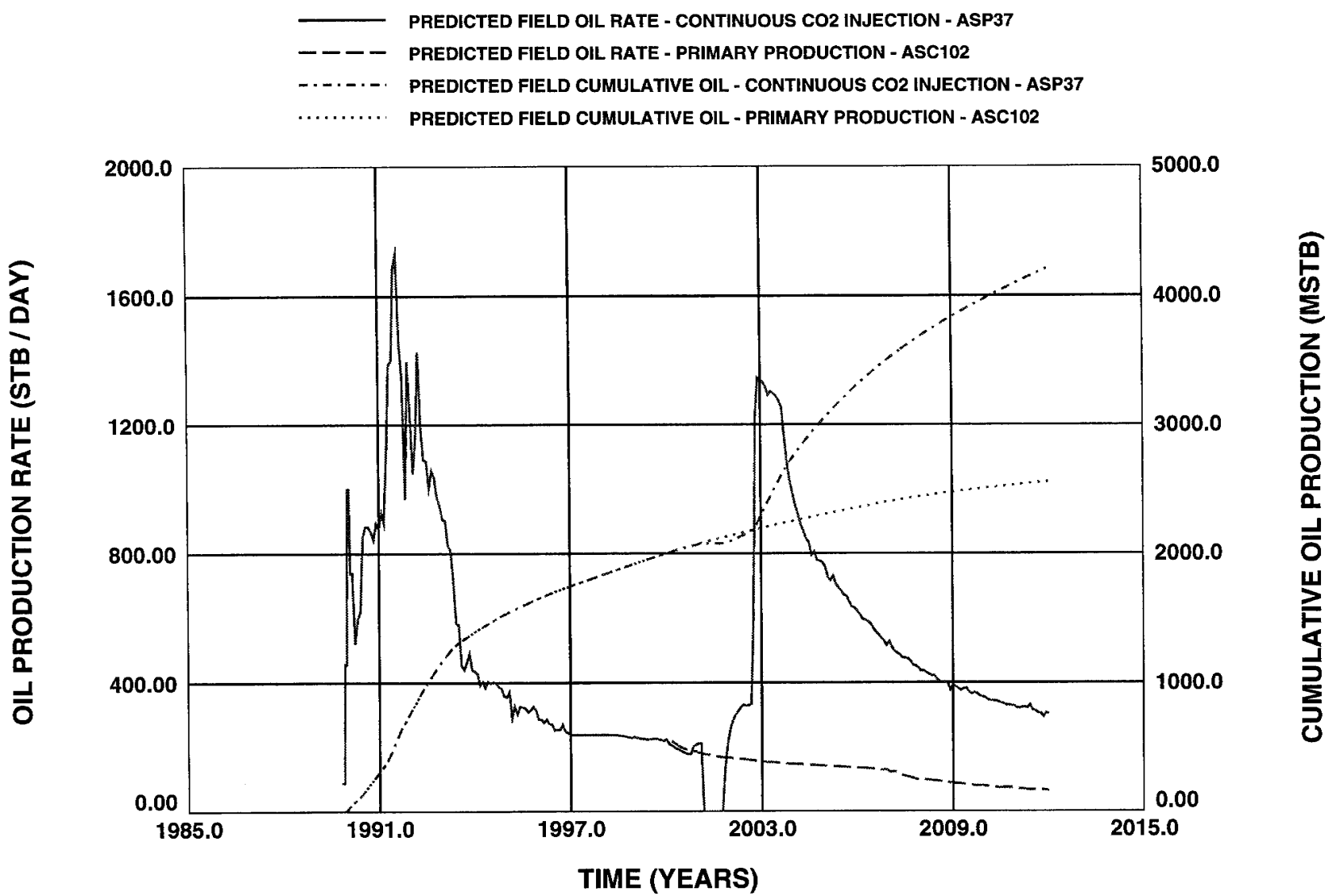

Figure 1 Field Level Oil Production - CO2 Flood versus Primary

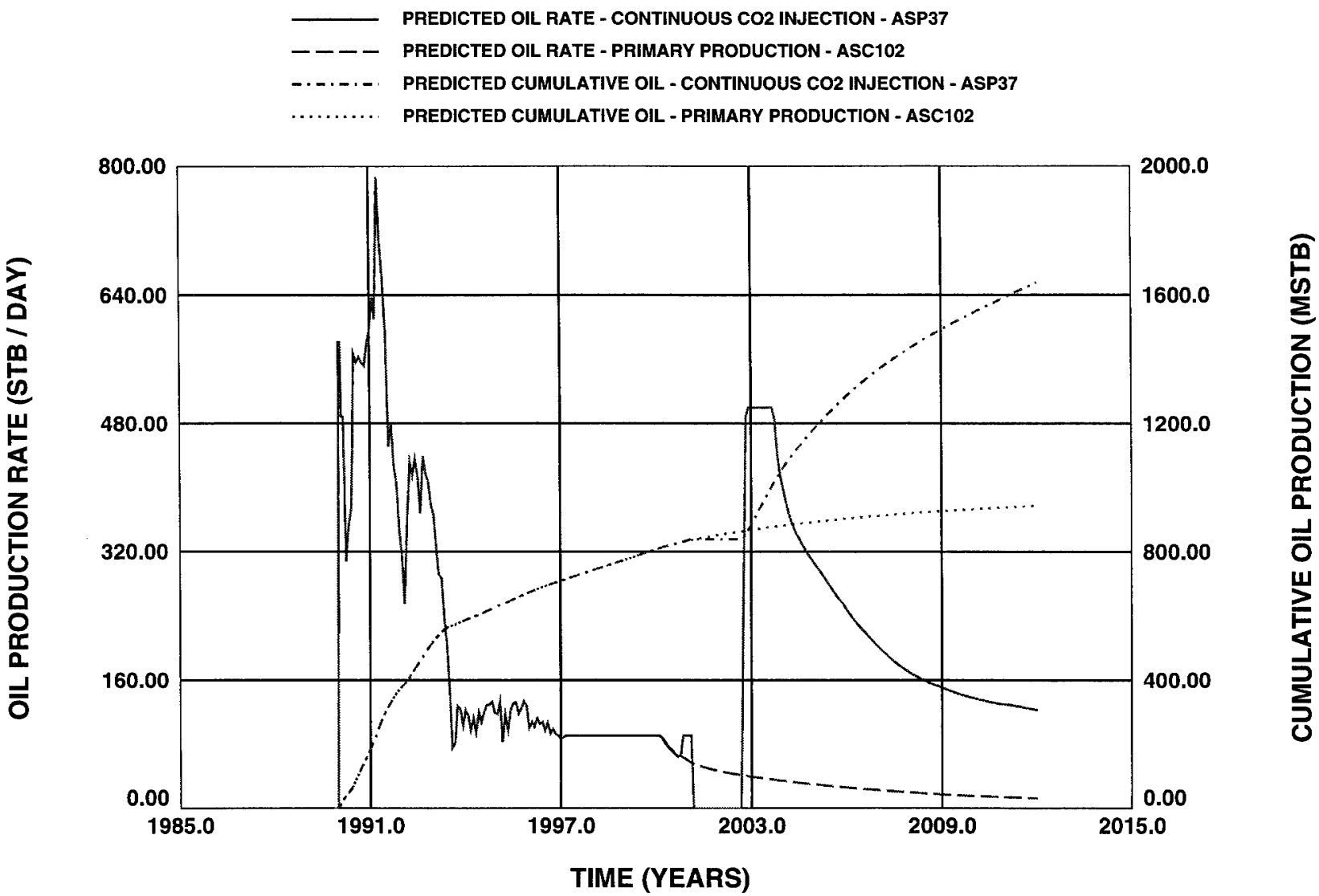

Figure 2 Anasazi Well No 1 Oil Production - CO2 Flood versus Primary

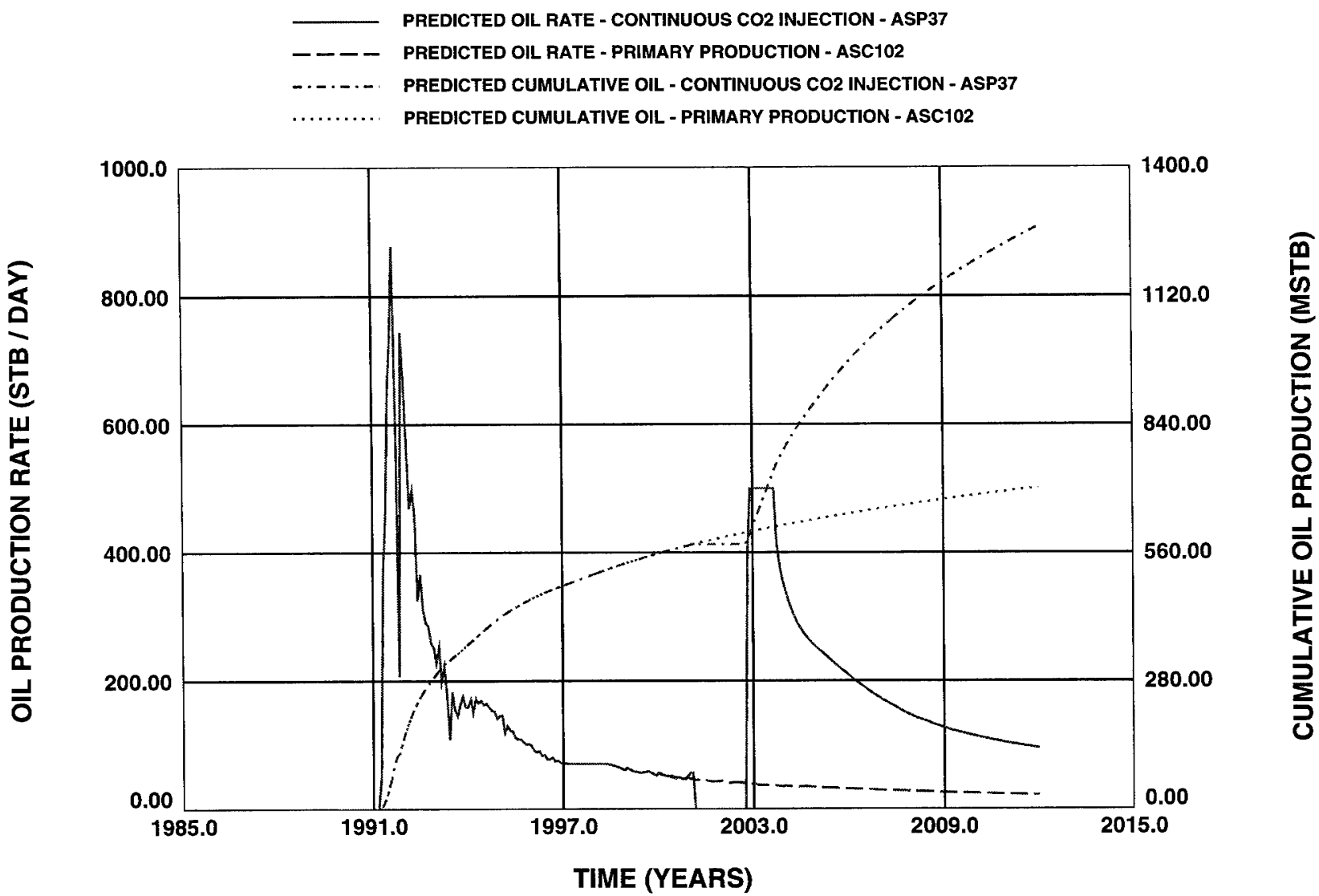

Figure 3 Anasazi Well No 5L-3 Oil Production - CO2 Flood versus Primary

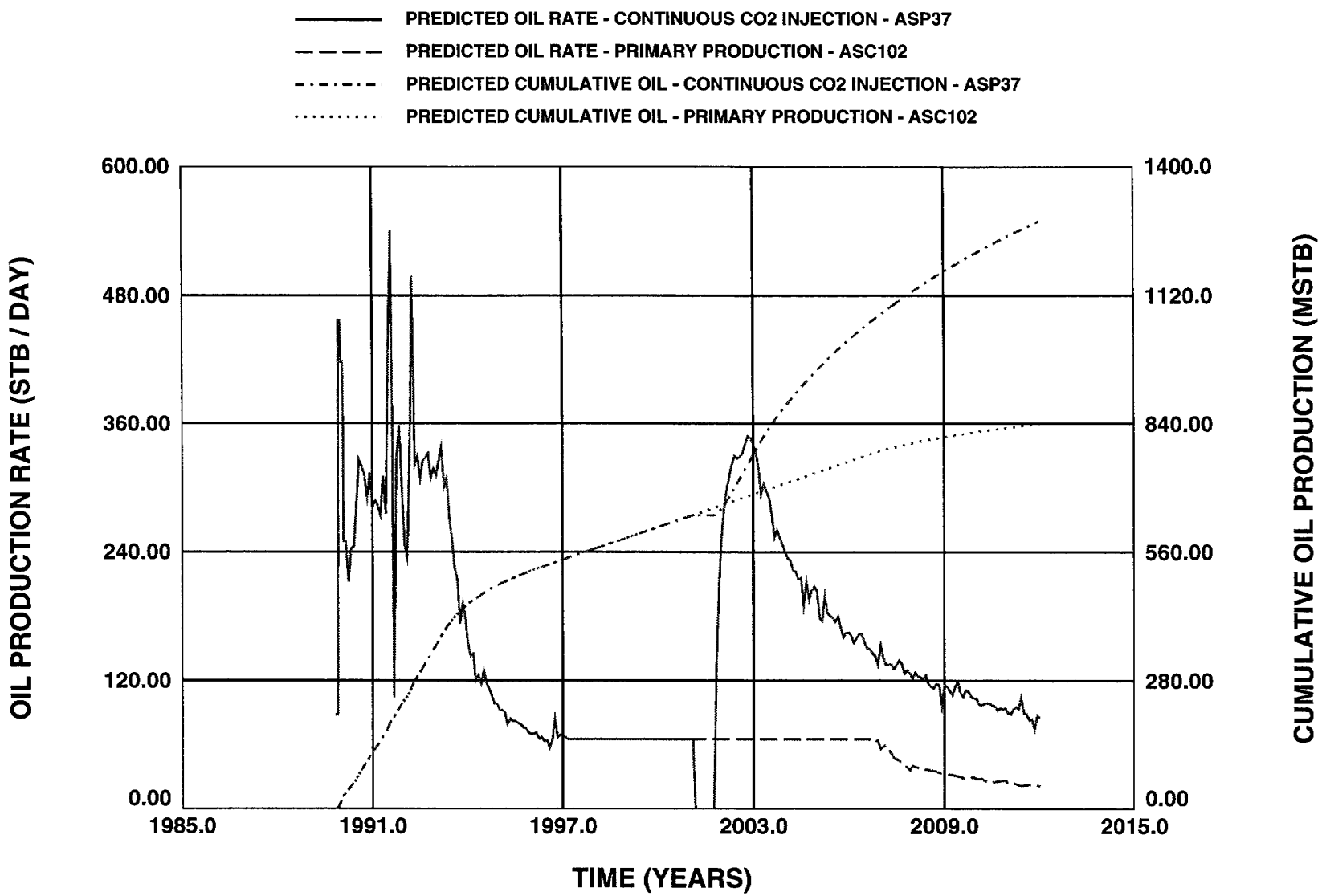

Figure 4 Sahgzie Well No 1 Oil Production - CO2 Flood versus Primary

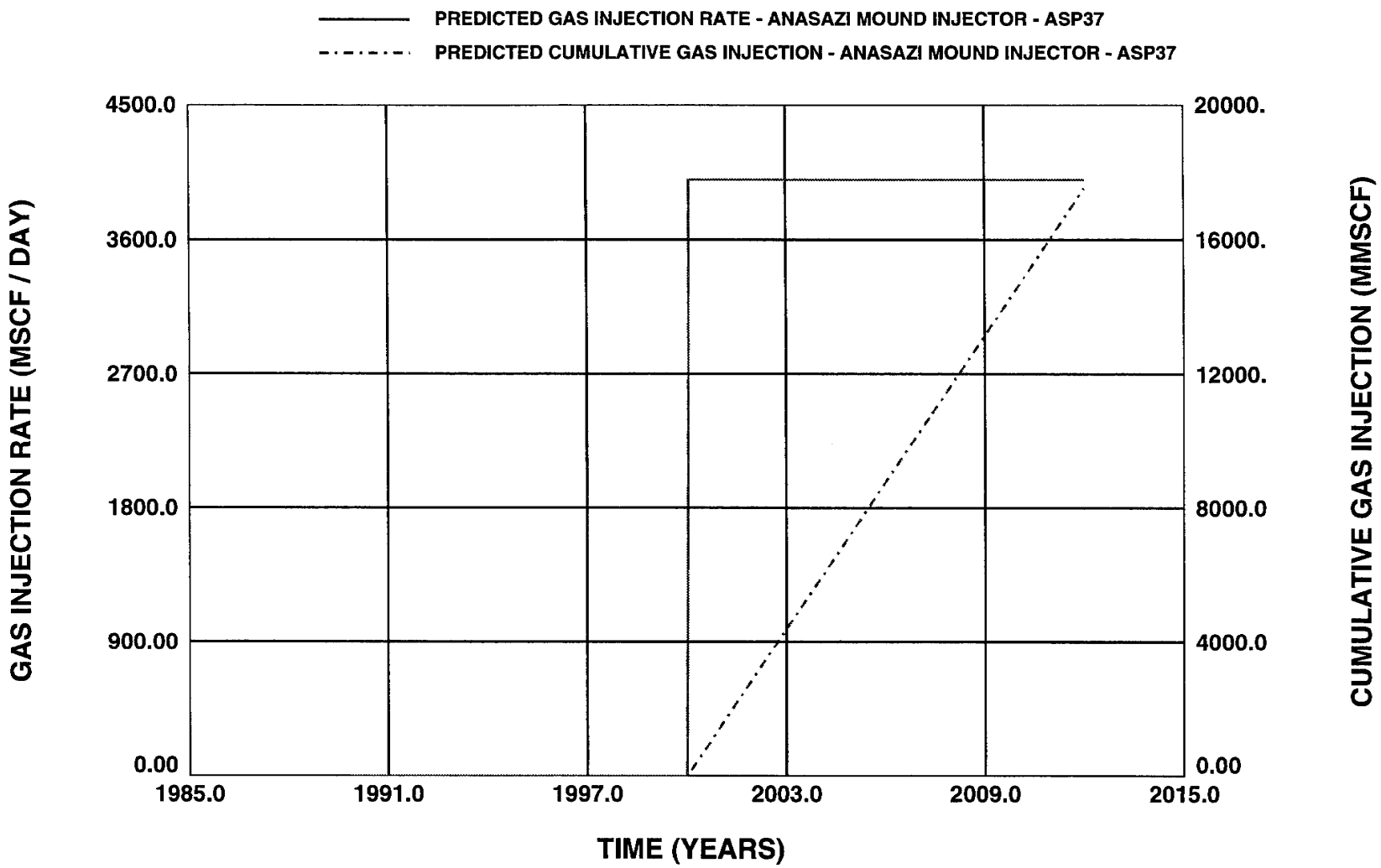

Figure 5 Gas Injection- Anasazi Mound Well - Continuous CO2 Injection

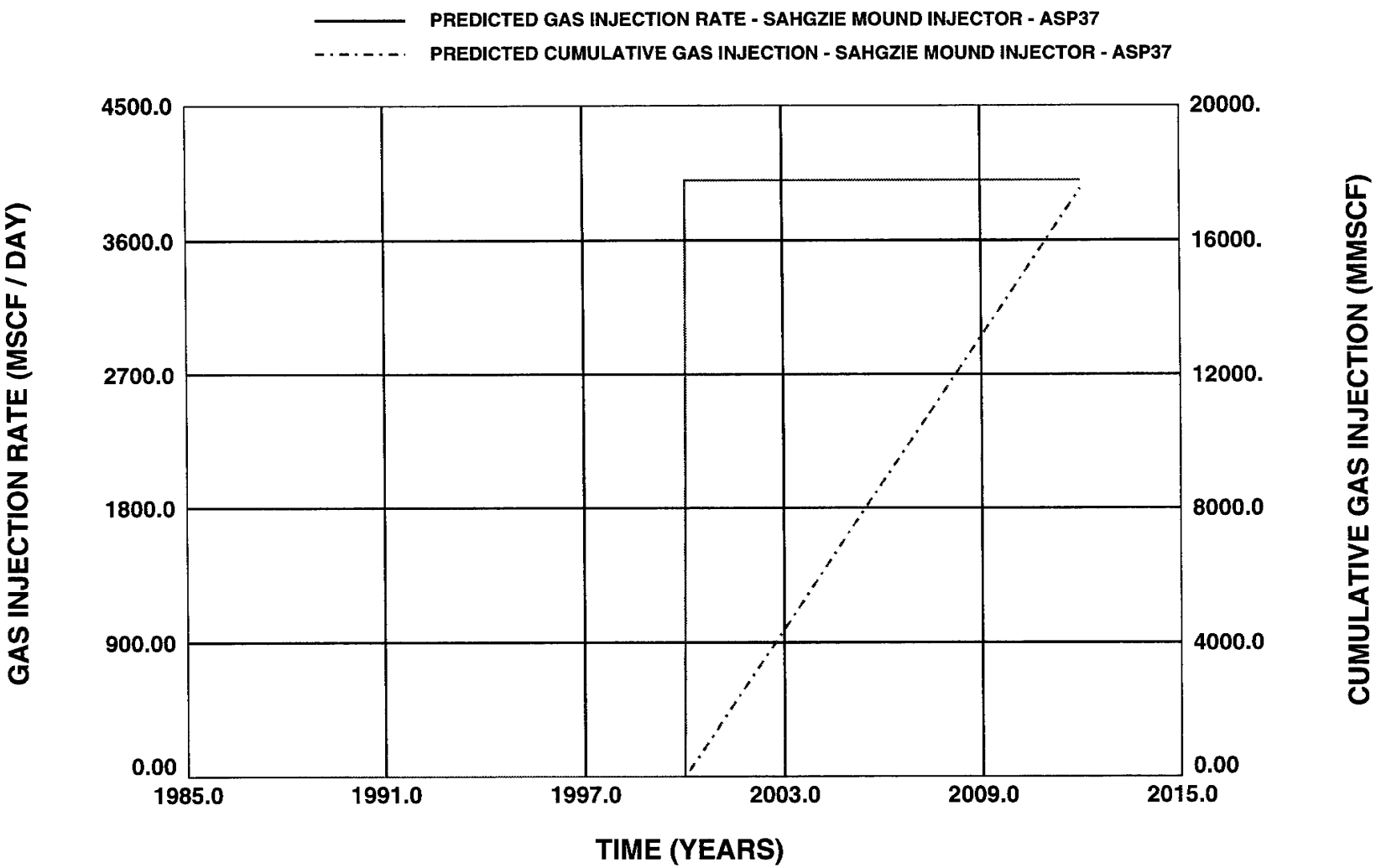

Figure 6 Gas Injection- Sahgzie Mound Well - Continuous CO2 Injection

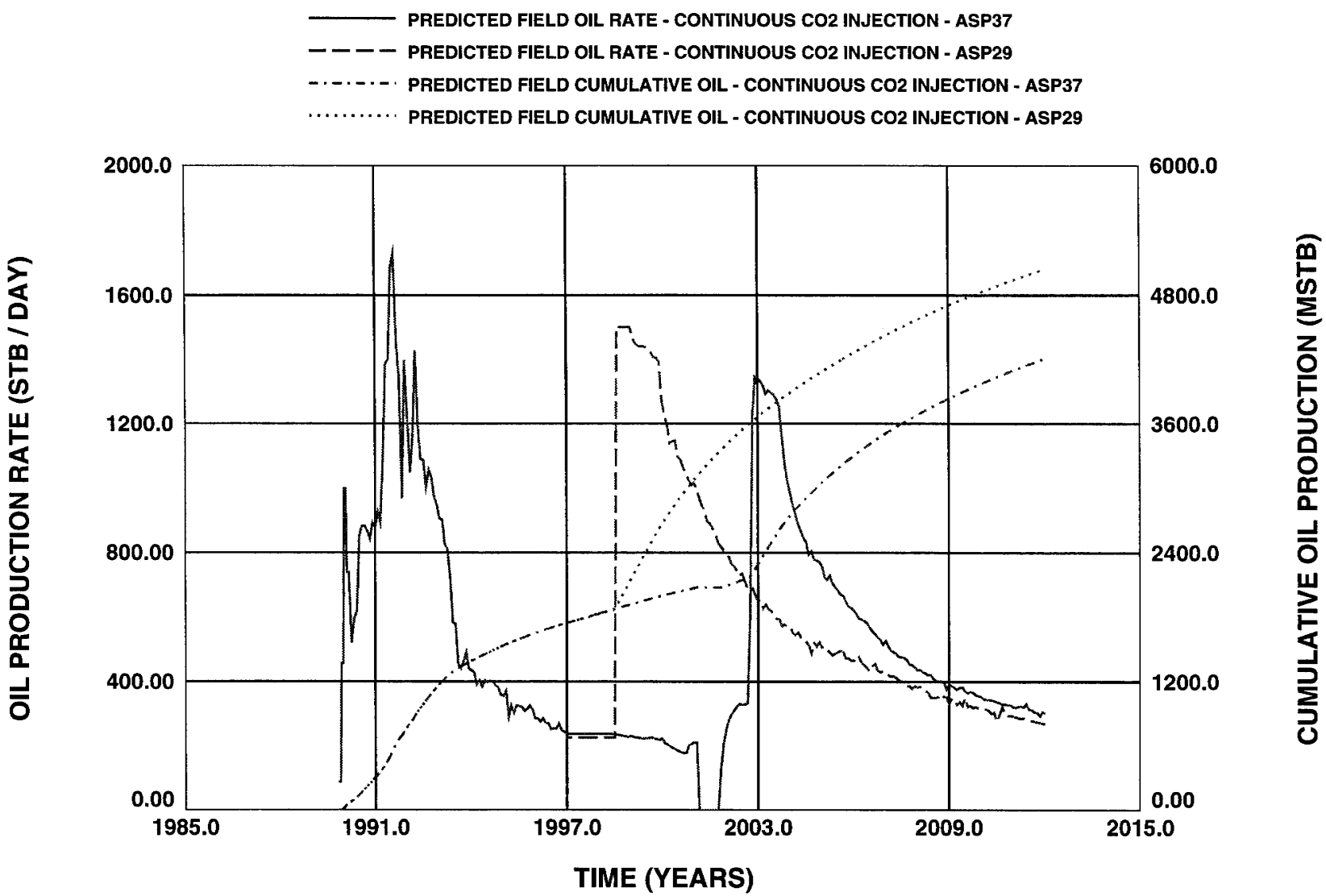

Figure 7 Comparison of CO2 Flood Predictions for 14.0 and 8.0 MMSCF/D Injection

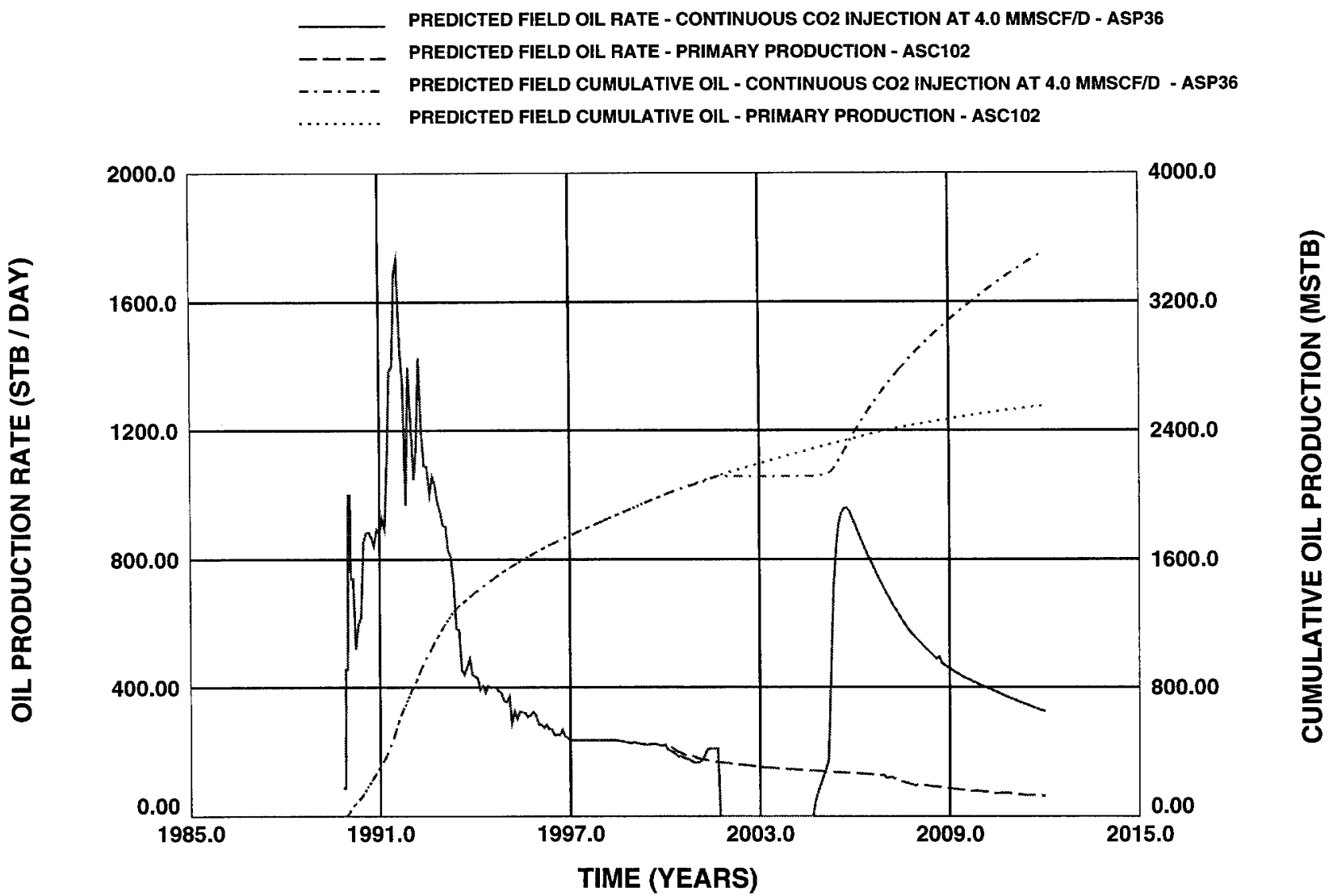

Figure 8 Field Level Oil Production - CO2 Flood versus Primary

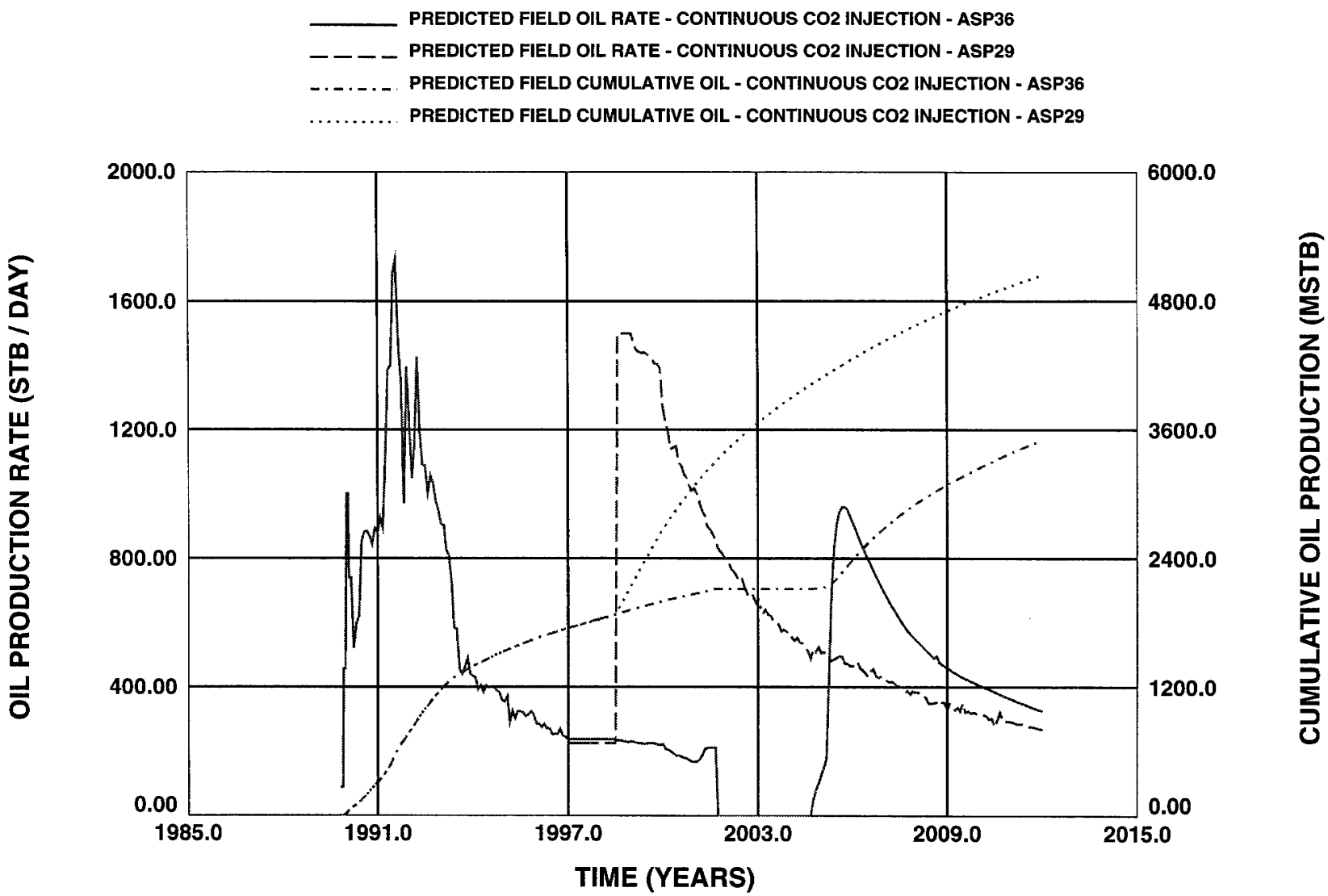

Figure 9 Comparison of CO2 Flood Predictions for 14.0 and 4.0 MMSCF/D Injection Rates

RESERVOIR MODELING AND COMPOSITION SIMULATION OF PRIMARY DEPLETION, WATERFLOODING, AND CARBON DIOXIDE FLOODING OF A SMALL PENNSYLVANIAN CARBONATE MOUND COMPLEX, ANASAZI FIELD, PARADOX BASIN, UTAH

Volume II

by

William E. Culham
REGA Inc.
Houston, Texas 77057

and

Douglas M. Lorenz
Texaco E&P
Houston, Texas 77215

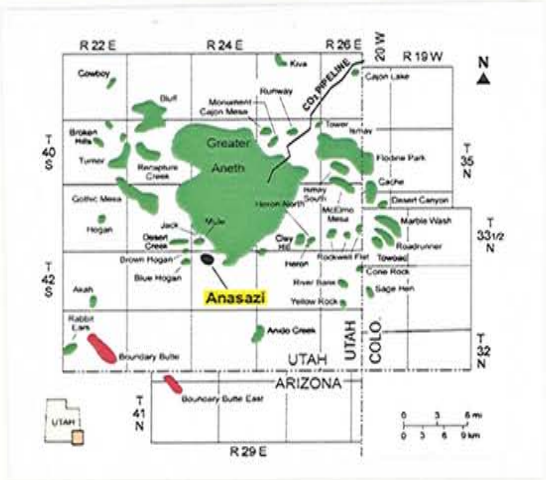

OPEN-FILE REPORT 420 **September 2003**
UTAH GEOLOGICAL SURVEY
a division of
UTAH DEPARTMENT OF NATURAL RESOURCES

This Open-File Report represents material that may not have undergone policy, technical, or editorial review required for other UGS publications. It provides information that, in part, may be interpretive or incomplete and readers are to exercise some degree of caution in the use of the data. Although this product represents the work of professional scientists, the Utah Department of Natural Resources, Utah Geological Survey, makes no warranty, stated or implied, regarding its suitability for a particular use. The Utah Department of Natural Resources, Utah Geological Survey, shall not be liable under any circumstances for any direct, indirect, special, incidental, or consequential damages with respect to claims by users of this product.

DISCLAIMER

This report was prepared as an account of work sponsored by an agency of the United States Government. Neither the United States Government nor any agency thereof, nor any of their employees, makes any warranty, express or implied, or assumes any legal liability or responsibility for the accuracy, completeness, or usefulness of any information, apparatus, product, or process disclosed, or represents that its use would not infringe privately owned rights. Reference herein to any specific commercial product, process, or service by trade name, trademark, manufacturer, or otherwise does not necessarily constitute or imply its endorsement, recommendation, or favoring by the United States Government or any agency thereof. The views and opinions of authors expressed herein do not necessarily state or reflect those of the United States Government or any agency thereof.

TABLES AND FIGURES

TABLES

Table 4–1
Desert Creek Stratigraphic Picks
(Anasazi Reservoir = Mound + Supramound Intervals)

Desert Creek Stratigraphy	Anasazi #1 KB = 4792′ (1461m)		Anasazi #5L3 KB = 4809′ (1466m)		Sahgzie #1 KB = 4785′ (1458m)		Anasazi #6H KB = 4885′ (1489m)	
	MD	SSD	MD	SSD	MD	SSD	MD	SSD
Top Desert Creek	5552′ (1692m)	–760′ (–232m)	5551′ (1692m)	–742′ (–226m)	5541′ (1689m)	–756′ (–230m)	5634′ (1717m)	–749′ (–228m)
Top Supramound Interval	5574′ (1699m)	–781′ (–238m)	5589′ (1704m)	–780′ (–238m)	5578′ (1700m)	–793′ (–242m)	5666′ (1727m)	–776′ (–237m)
Top Mound Interval	5642′ (1720m)	–850′ (–259m)	5644′ (1720m)	–835′ (–255m)	5634′ (1717m)	–849′ (–259m)	5720′ (1743m)	–835′ (–255m)
Top Platform Interval	5682′ (1732m)	–890′ (–271m)	5681′ (1732m)	–872′ (–266m)	5680′ (1731m)	–895′ (–273m)	5751′ (1753m)	–866′ (–264m)
Base Desert Creek	5707′ (1740m)	–915′ (–279m)	5704′ (1739m)	–895′ (–273m)	5710′ (1740m)	–925′ (–282m)	>5760′ >(1756m)	> –875′ >(–267m)

Table 4–2
Average Porosity, Permeability and Water Saturation
Anasazi Field

	Log Properties		Core Properties	
Well by Interval	**Ave. Porosity (%)**	**Ave. S_w (%)**	**Ave. Porosity (%)**	**Ave. K_h ** (md)**
Anasazi #1				
Supramound	16.3	12.0	14.4	31.7
Mound	10.1	8.4	8.8	235.1
Platform	5.9	36.1	6.0	1.1
Anasazi #5L–3				
Supramound	11.4	13.3	10.9	11.3
Mound	8.5	11.7	9.0	183.7
Platform	8.6	39.2	5.0	0.2
Sahgzie #1				
Supramound	12.1*	17.5*	12.4***	1.32***
Mound	10.0*	12.5*	11.0***	8.18***
Platform	5.8	41.7		
Anasazi #6H–1				
Supramound	10.3	15.8	13.7	18.2
Mound	6.4	19.1	6.2	9.3
Platform	9.6	41.4	10.2	0.9
* pay intervals only ** geometric averages *** sidewall plugs				

Table 4–3
Average Reservoir Properties of Architectural Lithotypes, Anasazi Field

Lithotype	Average Bed Thickness (ft)	Average Porosity (%)	Average Horizontal Permeability (md)	Volume Proportion
1. Tight Carbonate Mudstone	3.7	2	0.25	0.24
2. Dolomitized Mudstone	5.5	9	1.51	0.06
3. Enhanced Porosity Mudstone	2.9	11	2.00	0.05
4. Tight Packstone/Wackestone	2.4	2	0.02	0.14
5. Enhanced Porosity Packstone/Wackestone	3.8	10	1.80	0.05
6. Porous Grainstone	3.2	15	15.00	0.08
7. Cemented Grainstone	2.2	2	0.15	0.07
8. Tubular Tempestites in Mudstone/Wackestone/Packstone	6.7	9	8.00 (est)	0.07
9. Phylloid Algal Limestone (Bafflestone)	42.0	10	150.00	0.22
10. Mound–Front Bioclastic Breccia	13.0	8	30.00 (est)	0.02

Table 4–4
Lithotype Layering, Anasazi #1

MD (ft)	Layers	Lithotype Code	Description
Top Supramound Interval			
5574–88*	1–2	2	Mixed dolomitized mudstone/wackestone; anhydrite–plugged at top
	3–4	4	
	5–6	1	
5588–92	7–8	1	Tight dolomitized mudstone w/shale partings
5592–98	9–11	1	Tight dolomitized mudstone
5598–5600	12	6	Fine–grained lime grainstone w/moldic porosity
5600–02	13	3	Enhanced porosity mudstone
5602–13	14–18	1	Tight dolomitized mudstone
5613–22	19–21	6	Mixed lithology: 60% porous grainstone
	22–23	2	40% dolomitized mudstone
5622–26	24–25	3	Porous lime mudstone
5626–31	26–27	1	Tight dolomitized mudstone; anhydrite modules at base
5631–33*	28	5	Porous dolomitized wackestone
5633–38*	29–30	5	Porous packstone/wackestone
Top Mound Interval			
5638–42*	31	9	Phylloid algal limestone; anhydrite–plugged
5642–45	32	6	Porous grainstone
5645–70	33–44	9	Permeable phylloid algal limestone
5670–73	45	9	Phylloid algal limestone; anhydrite–plugged
5673–83	46–50	2	Dolomitized mudstone/wackestone
Base Mound Interval			

*Uncored intervals, or no core recovery; lithology inferred from logs.

Table 4–5
Lithotype Layering, Anasazi #5L–3

MD (ft)	Layers	Lithotype Code	Description
Top Supramound Interval			
5589–94*	1–3	1	Dolonitic lime–mudstone; tight
5594–5600*	4–6	6	Dolomitized grainstone; porous, permeable
5600–03	7	2	Dolomitized mudstone; slight porosity
5603–06	8	4	Argillaceous dolomitized wackestone; very tight
5606–08	9	1	Tight lime mudstone
5608–13	10–11	5	Dolomitized wackestone; porous
5613–15	12	1	Argillaceous dolomitized mudstone
5615–16	13	6	Dolomitized packstone/grainstone; porous, permeable
5616–20	14–15	5	Variably porous lime–packstone/wackestone
5620–22	16	5	Porous dolomitized packstone/grainstone
5622–25	17–18	4	Partially dolomitized packstone; cemented, tight
5625–26	19	7	Cemented lime–grainstone; very tight
5626–30	20–21	4	Lime–packstone/wackestone; tight
5630–35	22–24	5	Porous, dolomitized bioturbated wackestone
5635–37	25	5	Muddy, porous dolomitized wackestone; scoured base
5637–39	26	5	Dolomitized, brecciated porous packstone
5639–40	27	4	Cemented lime–wackestone; tight
5640–46	28–30	5	Dolomitized, porous burrowed packstone/ wackestone
Top Mound Interval			
5646–48	31	9	Anhydrite–plugged phylloid algal limestone
5648–58	32–36	9	Permeable phylloid algal limestone
5658–76*	37–47	9	Permeable phylloid algal limestone
5676–80*	48–49	9	Anhydrite–plugged phylloid algal limestone
5680–82	50	1	Tight lime–mudstone
Base Mound Interval			
* uncored intervals, or no core recovery; lithology inferred from logs			

Table 4–6
Lithotype Layering, Anasazi #6H–1

MD (ft)	Layers	Lithotype Code	Description
Top Supramound Interval			
5665–69	1–2	1	Dark, tight micro–crystalline dolomite
5669–76	3–6	6	Fine–grained dolomitized porous grainstone
5676–78	7	4	Tight, dolomitized burrowed wackestone
5678–93	8–15	2/5	Heterogeneous dolomitized mudstones and packstones; porous
5693–5701	16–19	1	Tight dolomitized mudstone
5701–08	20–23	8	Dolomitized tubular tempestites; porous
5708–13	24–27	8	Undolomitized tubular tempestites; tight
5713–19	28–30	6	Dolomitized porous grainstone (tidal channel)
Top Mound Interval			
5719–33	31–38	10	Brecciated, cemented mound–front limestone; tight
5733–39	39–42	5	Dolomitized porous wackestone
5739–41	43–44	6	Dolomitized porous grainstone
5741–51	45–50	1	Tight dolomitic lime–mudstone
Base Mound Interval			

Table 4–7
Architectural Properties, Anasazi Lithotypes

Lithotype	Length (Blocks) Feet			Width/Length Ratio			Percent Reservoir Volume			Percent Porosity	
	min	max	mode	min	max	mode	min	max	mode	mean	st dev
1. Tight Mudstone	no individual lithotype bodies defined						25	65	35	1.9	1.7
2. Dolomitized Mudstone	10	18	14	0.8	1.0	0.9				9.2	3.1
3. Enhanced Porosity Mudstone	2	8	5	0.6	1.0	0.8				10.8	2.9
4. Tight Packstone/Wackestone	3	9	6	0.8	1.0	0.9	10	40	19	2.4	1.9
5. Porous Packstone/Wackestone	2	8	5	0.5	1.0	0.75				10.2	3.2
6. Enhanced Porosity Grainstone	6	18	12	0.4	1.0	0.8	5	40	19	14.9	2.8
7. Cemented Grainstone	2	10	6	0.2	1.0	0.6				2.3	1.8
8. Tubular Tempestites	3	9	6	0.8	1.0	0.9	0	15	6.5	9.3	2.7
9. Phylloid Algal Limestone	no individual lithotype bodies defined						22	22	22	10.0	3.3
10. Mound Front Breccia	1	1	1	1	1	1	2.5	2.5	2.5	7.6	2.3

Table 6–1
Boolean Emplacement Procedures

*** Emplacement of Grainstones:**

a) Apron Length:
mode = 12 blocks;
range = {6 blocks – 18 blocks}

b) Apron Width:
mode = (Length/2) blocks;
range = {(Length/4) blocks – (3*Length/4) blocks}

c) Apron Thickness:
i) all peripheral blocks = 1 layer
ii) if (30 blocks <= Length*Width <= 60 blocks), then
P(all interior blocks = 2 layers) = 0.5,
P(all interior blocks = 1 layer) = 0.5.
iii) if (Length*Width > 60 blocks), then
P(all interior blocks = 1 layer) = 0.25,
P(all interior blocks = 2 layers) = 0.5,
P(1–layer outer rind + 2–layer inner rind + 3 layer interior blocks) = 0.25.

d) Neck Length:
mode = (3*Apron Length/5) blocks
range = {(2*Apron Length/5) blocks – (4*Apron Length/5) blocks}

e) Neck Width:
i) if Neck Length <= 4 blocks, then Neck Width = 1 block
ii) if (4 blocks < Neck Length <= 10 blocks), then
P(Neck Width = 2 blocks) = [(Neck Length/2) – 2]/3,
P(Neck Width = 1 block) = 1 – P(Neck Width = 2 blocks)
iii) if Neck Length > 10 blocks, then Neck Width = 2.

f) Neck Thickness = Maximum Apron Thickness

g) position of proximal block on Neck chosen from Mound Margin Probability Map

h) orientation of Apron/Neck complex perpendicular to Mound Margin; if this is diagonal, both x and y orientations are equally probable.

i) continue until the Primary Grainstone volume proportion is reached (Table 4–7).

*** Emplacement of Primary Packstones/Wackestones:**

follow same procedure as for Tubular Tempestites above, except that
a) length, width mode = 19 blocks; range = (3 blocks – 6 blocks), and
b) reject only if > 70% of the P/W body is truncated

*** Emplacement of Tubular Tempestites:**

a) emplace bodies (1 layer thick) with mode = 6 blocks; range = (3 blocks – 9 blocks) for both length and width, chosen independently

b) x,y position of TT body selected randomly within remaining Mudstone volume

c) truncate where blocks overlap mound blocks, grainstone blocks, or the model edge

d) as above, reject if >30% of TT body is truncated

e) continue until selected volume proportion for Tubular Tempestites is reached (Table 4–7).

Table 6–1 (continued)

*** Emplacement of Dolomitized Mudstones, Enhanced Porosity Mudstones, and Enhanced Porosity Packstones/Wackestones:**

for each of these secondary lithotypes, randomly place individual blocks within the respective primary lithotype field (i.e. mudstone or packstone/wackestone) until the corresponding volume proportion is reached (Table 4–3).

*** Emplacement of Enhanced Grainstones:**

a) on Aprons, use the same Length/Width generating pdf's as for the Primary Grainstones themselves; all Enhanced Grainstone bodies are 1 layer thick.

b) position is determined by randomly selecting a Primary (unaltered) Apron; then randomly selecting a block each from the original grainstone body and the corresponding Enhanced Porosity Grainstone body, which are then superimposed with identical orientations and Enhanced Porosity Grainstone gridblocks substituted wherever they overlap with the Primary Grainstone blocks

c) if less than 70% of the Enhanced Grainstone body can be substituted for Primary Grainstone blocks, the alteration is rejected and another candidate Grainstone body chosen.

d) continue until the Enhanced Grainstone volume proportion is reached (Table 4–3).

*** Emplacement of Mound Front Lithotype Blocks:**

(subsequent to completion of the Simulated Annealing Procedure)

a) replace a total of 1575 blocks laterally adjacent to mound blocks with Mound Front blocks

b) randomly select blocks to be replaced using the following formula:

- randomly select 50% of the mound–edge block x–y positions for replacement
- select the number of blocks to replace at each (x,y) location by drawing from a uniform pdf over the number of stacked mound blocks adjacent to the selected location.
- determine the base of the mound front by random selection from a uniform pdf over the {number of adjacent stacked mound blocks – number of stacked mound–front replacement blocks} to determine the position of the vertical mound–front stack relative to the base of the adjacent mound stack.

Table 6–2
Constraints on Simulated Annealing Procedures

*** Block Exchange Constraints:**

- the only Phylloid Algal Mound blocks eligible for exchange are those contiguous with at least one non–mound block, and they must be exchanged with non–mound blocks with at least one face contiguous with a mound block. In addition, such an exchange cannot create a vertical mound/non–mound/mound "sandwich" sequence at either location. If the potential exchange violates any of these restrictions, it is rejected.
- the same rules apply to the Grainstone/Enhanced Porosity Grainstone lithotypes. The two may be interchanged freely, but are subject to comparable restrictions to those above for exchanges with non–grainstone lithotypes.
- prior to block exchange, at least one adjacent block must be the same lithotype as the other block exchange candidate. This rule applies to both candidates.

*** Objective Function Weighting:**

- start with weighting the average porosity map by 2/3, the horizontal and vertical variogram by 1/3 each;
- adjust if required

*** R–Parameter Scheduling:**

- start with R = 10x(average magnitude of the objective function change per exchange) established by experiment over 10,000 random changes to determine average
- schedule initially set to reduce by .01 of its magnitude every exchange frequency, corresponding to an average of one exchange per block, or 1500*20 = 30,000 successful block exchanges.

*** Process Termination Criteria:**

- Square Root {Objective Function} <= .01, or uninterrupted sequence of 10,000 block exchange rejections by Objective Function.

Table 10–1
Paradox Basin Desert Creek Fields – Fluid Property Data

Field/Well	Res Temp. °F	API @60°F	BPP psia	Bo*** RB/STB	Rs*** SCF/STB	Oil Density		MW	
						Overall*	C_{7+}**	Overall*	C_{7+}
Anasazi #1	130	39.2	1023	1.213	364	0.7344	0.8243	124.4	206.0
Sahgzie #1	130	38.7	1120	1.215	365	0.7365	0.8306	123.0	211.0
Mule #31M	132	37.4	1478	1.245	450	0.7378	0.8460	116.9	220.2
Blue Hogan #1J–1	128	37.6	1590	1.260	450	0.7308	0.8360	117.3	225.0
Brown Hogan #1A	128	37.1	1524	1.260	458	0.7311	0.8386	115.1	215.0
North Heron #35–C	132	36.2	1922	1.303	581	0.7204	0.8429	106.6	225.9
Runway #10E–2	136	43.4	2003	1.516	941	0.6594	0.8300	81.6	198.0
Runway #10G–1	138	38.5	2141	1.512	967	0.6578	0.8313	81.7	200.0
Navajo Tribal	130	42.2	1086	1.190	305	0.7341	0.7889	127.0	224.0
Jack #31G									

* At reservoir temperature and bubblepoint pressure (BPP)

** Gravity of Residual Oil at 60°F

*** Adjusted to Separator Conditioning

Table 10–2
Composition of Anasazi Well 5L–3 Separator Oil Sample at 73°F and 1014 psia

Component	MW	Gas Mole %	Liquid Wt %	Overall Wt %	Mole %
CO2	44.010	0.000	0.000	0.000	0.000
H2S	34.080	0.000	0.000	0.000	0.000
N2	28.013	0.000	0.000	0.000	0.000
C1	16.043	12.818	0.000	0.061	0.673
C2	30.070	24.311	0.050	0.266	1.568
C3	44.097	30.424	0.382	0.775	3.112
I–C4	58.124	5.552	0.236	0.329	1.001
N–C4	58.124	14.474	0.966	1.203	3.665
I–C5	72.151	3.652	0.791	0.859	2.108
N–C5	72.151	4.214	1.253	1.327	3.257
C6	86.200	2.301	2.760	2.782	5.718
MCYC–C5	84.160	0.431	0.767	0.768	1.616
Benzene	78.110	0.109	0.177	0.177	0.402
CYCL–C6	84.160	0.282	0.715	0.712	1.536
C7	100.200	0.692	3.268	3.246	5.738
MCYCL–C6	98.190	0.231	1.460	1.447	2.611
Toluene	92.140	0.062	0.453	0.449	0.863
C8	114.230	0.275	4.270	4.223	6.549
C2–Benzene	106.170	0.012	0.176	0.174	0.290
M&P–XYLENE	106.170	0.019	0.497	0.491	0.819
O–XYLENE	106.170	0.007	0.343	0.339	0.565
C9	128.300	0.083	4.137	4.086	5.641
C10	134.000	0.033	4.996	4.932	6.519
C11	147.000	0.009	4.406	4.348	5.240
C12	161.000	0.003	3.751	3.702	4.073
C13	175.000	0.002	4.336	4.279	4.331
C14	190.000	0.001	3.868	3.817	3.559
C15	206.000	0.001	3.615	3.567	3.068
C16	222.000	0.001	3.052	3.012	2.403
C17	237.000	0.000	3.039	2.999	2.242
C18	251.000	0.000	3.086	3.045	2.149
C19	263.000	0.000	2.891	2.853	1.922
C20	275.000	0.000	2.643	2.608	1.680
C21	291.000	0.000	2.346	2.315	1.409
C22	305.000	0.000	2.295	2.265	1.315
C23	318.000	0.000	2.134	2.106	1.173
C24	331.000	0.000	1.947	1.921	1.028
C25	345.000	0.000	1.888	1.863	0.957
C26	359.000	0.000	1.755	1.732	0.855
C27	374.000	0.000	1.725	1.702	0.806
C28	388.000	0.000	1.639	1.617	0.738
C29	402.000	0.000	1.519	1.499	0.661
C30+	580.000	0.000	20.371	20.104	6.140
MW (g/mol) =		44.274	184.503		177.137
Density (g/cc) = 0.809					
GOR (SCF/BBL) = 34.3					

Table 10–3
Composition of Anasazi Well 5L–3 Separator Gas Cylinder #5EK088

Component	MW	Recombine Gas Analyses	Convert Recombined Gas Composition to Mole % Basis	
			w/MW	Mole %
CO2	44.010	0.103	0.002	0.062
H2S	34.080	0.000	0.000	0.000
N2	28.013	10.57	0.038	1.002
C1	16.043	35.181	2.193	58.211
C2	30.070	23.285	0.774	20.555
C3	44.097	19.624	0.445	11.813
I–C4	58.124	3.485	0.060	1.592
N–C4	48.314	8.472	0.146	3.869
I–C5	72.151	2.158	0.030	0.794
N–C5	72.151	2.524	0.035	0.928
C6	86.200	1.797	0.021	0.553
MCYC–C5	84.160	0.337	0.004	0.106
Benzene	78.110	0.083	0.001	0.028
CYCL–C6	84.160	0.225	0.003	0.071
C7	100.200	0.717	0.007	0.190
MCYCL–C6	98.190	0.232	0.002	0.063
Toluene	92.140	0.063	0.001	0.018
C8	114.230	0.359	0.003	0.083
C2–Benzene	106.170	0.015	0.000	0.004
M&P–XYLENE	106.170	0.025	0.000	0.006
O–XYLENE	106.170	0.012	0.000	0.003
C9	128.300	0.133	0.001	0.028
C10	134.000	0.066	0.000	0.013
C11	147.000	0.024	0.000	0.004
C12	161.000	0.009	0.000	0.001
C13	175.000	0.004	0.000	0.001
C14	190.000	0.001	0.000	0.000
C15	206.000	0.001	0.000	0.000
C16	222.000	0.001	0.000	0.000
C17	237.000	0.002	0.000	0.000
C18	251.000	0.002	0.000	0.000
C19	263.000	0.005	0.000	0.000
C20	275.000	0.000	0.000	0.000
C21	291.000	0.000	0.000	0.000
C22	305.000	0.000	0.000	0.000
C23	318.000	0.000	0.000	0.000
C24	331.000	0.000	0.000	0.000
C25	345.000	0.000	0.000	0.000
C26	359.000	0.000	0.000	0.000
C27	374.000	0.000	0.000	0.000
C28	388.000	0.000	0.000	0.000
C29	402.000	0.000	0.000	0.000
C30+	580.000	0.000	0.000	0.000
MW (g/mol) =	26.54			

Table 10–4
Dead Oil Liquid Composition of the Anasazi Flashed Separator Oils And Dead Oils

		Flashed Oil 5L–3		Dead Oil		
Component	**MW**	**Cyl #W4635**	**Cyl #W8301**	**6H–1 Limestone**	**6H–1 Dolomite**	**5L–3**
CO2	44.010	0.000	0.000	0.000	0.000	0.000
H2S	34.080	0.000	0.000	0.000	0.000	0.000
N2	28.013	0.000	0.000	0.000	0.000	0.000
C1	16.043	0.000	0.000	0.000	0.000	0.000
C2	30.070	0.053	0.050	0.001	0.022	0.049
C3	44.097	0.392	0.382	0.009	0.145	0.343
I–C4	58.124	0.239	0.236	0.009	0.093	0.212
N–C4	48.314	0.975	0.966	0.035	0.383	0.870
I–C5	72.151	0.793	0.791	0.049	0.383	0.745
N–C5	72.151	1.256	1.253	0.082	0.694	1.196
C6	86.200	2.767	2.760	0.265	1.473	1.979
MCYC–C5	84.160	0.768	0.767	0.206	1.127	1.504
Benzene	78.110	0.178	0.177	0.024	0.134	0.175
CYCL–C6	84.160	0.717	0.715	0.137	0.614	0.714
C7	100.200	3.284	3.268	0.701	3.060	3.293
MCYCL–C6	98.190	1.466	1.460	0.366	1.406	1.472
Toluene	92.140	0.456	0.453	0.108	0.413	0.454
C8	114.230	4.306	4.270	1.286	4.206	4.335
C2–Benzene	106.170	0.176	0.176	0.105	0.176	0.177
M&P–XYLENE	106.170	0.500	0.497	0.413	0.472	0.500
O–XYLENE	106.170	0.360	0.343	0.323	0.331	0.362
C9	128.300	4.160	4.137	1.538	4.066	4.154
C10	134.000	5.006	4.996	2.529	4.881	4.913
C11	147.000	4.447	4.406	3.128	4.376	4.286
C12	161.000	3.732	3.751	3.284	4.737	3.635
C13	175.000	4.373	4.336	4.301	4.347	4.138
C14	190.000	3.919	3.868	3.994	3.924	3.652
C15	206.000	3.610	3.615	3.943	3.701	3.208
C16	222.000	3.104	3.052	3.427	3.124	2.830
C17	237.000	3.089	3.039	3.336	3.082	2.763
C18	251.000	3.111	3.086	3.494	3.152	2.823
C19	263.000	2.907	2.891	3.160	2.987	2.596
C20	275.000	2.647	2.643	2.825	2.401	2.375
C21	291.000	2.362	2.346	2.660	2.360	2.101
C22	305.000	2.319	2.295	2.635	2.295	2.058
C23	318.000	2.152	2.134	2.468	2.155	1.922
C24	331.000	1.950	1.947	2.304	1.917	1.729
C25	345.000	1.929	1.888	2.277	2.229	1.692
C26	359.000	1.783	1.755	1.954	1.378	1.437
C27	374.000	1.844	1.725	2.275	1.782	1.549
C28	388.000	1.693	1.639	1.944	1.473	1.573
C29	402.00	1.446	1.519	1.740	1.521	1.300
C30+	580.000	19.732	20.371	36.664	23.980	24.885
MW (g/mol)		186.634	184.503	272.062	200.546	189.014

Table10–5
Composition of Anasazi Well 5L–3 Recombined Separator Oil at 70°F and 3014 psia

Component	MW	Gas Mole %	Liquid Wt %	Overall Wt %	Mole %
CO2	44.010	0.078	0.000	0.031	0.055
H2S	34.080	0.000	0.000	0.000	0.000
N2	28.013	1.003	0.000	0.255	0.702
C1	16.043	55.141	0.011	8.052	38.647
C2	30.070	19.748	0.076	5.456	13.971
C3	44.097	12.165	0.274	5.080	8.872
I–C4	58.124	1.902	0.143	1.111	1.472
N–C4	58.124	4.792	0.565	2.951	3.909
I–C5	72.151	1.241	0.481	1.170	1.249
N–C5	72.151	1.561	0.829	1.637	1.748
C6	86.200	1.123	2.404	2.659	2.375
MCYC–C5	84.160	0.194	0.601	0.594	0.543
Benzene	78.110	0.051	0.142	0.142	0.140
CYCL–C6	84.160	0.135	0.605	0.551	0.504
C7	100.200	0.397	3.247	2.765	2.125
MCYCL–C6	98.190	0.128	1.390	1.143	0.896
Toluene	92.140	0.037	0.442	0.358	0.299
C8	14.230	0.170	4.465	3.480	2.346
C2–Benzene	106.170	0.008	0.165	0.130	0.094
M&P–XYLENE	106.170	0.013	0.521	0.398	0.289
O–XYLENE	106.170	0.005	0.383	0.288	0.209
C9	128.300	0.056	4.412	3.330	1.999
C10	134.000	0.027	5.293	3.950	2.270
C11	147.000	0.011	4.617	3.432	1.798
C12	161.000	0.005	3.851	2.857	1.367
C13	175.000	0.003	4.500	3.335	1.467
C14	190.000	0.002	3.965	2.937	1.191
C15	206.000	0.002	3.644	2.700	1.009
C16	222.000	0.001	3.175	2.352	0.816
C17	237.000	0.001	3.139	2.324	0.755
C18	251.000	0.000	3.218	2.382	0.731
C19	263.000	0.000	2.991	2.214	0.648
C20	275.000	0.000	2.651	1.962	0.549
C21	291.000	0.000	2.413	1.786	0.473
C22	305.000	0.000	2.351	1.740	0.439
C23	318.000	0.000	2.205	1.632	0.395
C24	331.000	0.000	1.971	1.459	0.339
C25	345.000	0.000	1.938	1.434	0.320
C26	359.000	0.000	1.687	1.248	0.268
C27	374.000	0.000	1.842	1.363	0.281
C28	388.000	0.000	1.552	1.149	0.228
C29	402.000	0.000	1.533	1.134	0.217
C30+	580.000	0.000	20.309	15.029	1.995
MW (g/mol)		28.591	190.065		77.005
Density (g/cc) = 0.681 @ 70°F and 3014 psia					

Table 10–6
PV–Isotherm Data for Anasazi Well No. 5L–3
Recombined Fluid at 130°F

Pressure (psig)	Total Volume (cm^3)	Relative* Volume (cm^3/cm^3)	Phase Volume (cm^3)		Observations
			Liquid	Vapor	
5000	51.91	0.969	51.91	0.00	single phase
4000	52.52	0.980	52.52	0.00	single phase
3500	52.88	0.987	52.88	0.00	single phase
3000	53.25	0.994	53.25	0.00	single phase
2500	53.86	1.005	53.86	0.00	single phase
2400	54.63	1.019	52.29	2.34	two phase
2290	55.52	1.036	51.92	3.60	two phase
2036	58.27	1.087	50.26	8.00	two phase

* Defined as the ratio of the total volume to the saturation volume (53.59 cm^3)

Table 10–7
Composition of Recombined Anasazi Well 5L–3 Oil Flashed to 2050 psia at 130°F

Component	MW	Gas Mole %	Liquid Wt %	Overall Wt %	Mole %
CO2	44.010	0.000	0.000	0.000	0.000
H2S	34.080	0.000	0.000	0.000	0.000
N2	28.013	0.928	0.000	0.191	0.586
C1	16.043	53.274	0.000	6.291	33.617
C2	30.070	22.122	0.087	4.965	14.157
C3	44.097	14.215	0.328	4.875	9.477
I–C4	58.124	2.023	0.232	1.050	1.549
N–C4	58.124	4.668	1.005	2.796	4.125
I–C5	72.151	0.872	0.832	1.125	1.336
N–C5	72.151	0.960	1.346	1.580	1.878
C6	86.200	0.488	3.043	2.730	2.715
MCYC–C5	84.160	0.079	0.709	0.613	0.624
Benzene	78.110	0.021	0.165	0.143	0.157
CYCL–C6	84.160	0.052	0.677	0.571	0.582
C7	100.200	0.141	3.451	2.849	2.437
MCYCL–C6	98.190	0.001	1.435	1.142	0.997
Toluene	92.140	0.012	0.449	0.365	0.340
C8	14.230	0.092	4.416	3.589	2.694
C2–Benzene	106.170	0.003	0.177	0.143	0.115
M&P–XYLENE	106.170	0.005	0.502	0.403	0.325
O–XYLENE	106.170	0.002	0.555	0.443	0.358
C9	128.300	0.020	4.015	3.212	2.146
C10	134.000	0.013	5.055	4.033	2.581
C11	147.000	0.005	4.405	3.509	2.046
C12	161.000	0.001	3.759	2.991	1.593
C13	175.000	0.000	4.351	3.461	1.696
C14	190.000	0.000	3.789	3.014	1.360
C15	206.000	0.000	3.520	2.800	1.165
C16	222.000	0.000	3.003	2.389	0.923
C17	237.000	0.000	2.963	2.357	0.853
C18	251.000	0.000	3.029	2.409	0.823
C19	263.000	0.000	2.867	2.280	0.743
C20	275.000	0.000	2.307	1.835	0.572
C21	291.000	0.000	2.290	1.821	0.537
C22	305.000	0.000	2.240	1.781	0.501
C23	318.000	0.000	2.094	1.665	0.449
C24	331.000	0.000	1.879	1.494	0.387
C25	345.000	0.000	1.964	1.562	0.388
C26	359.000	0.000	1.616	1.285	0.307
C27	374.000	0.000	1.805	1.436	0.329
C28	388.000	0.000	1.626	1.293	0.286
C29	402.000	0.000	1.419	1.129	0.241
C30+	580.000	0.000	20.596	16.380	2.006
MW (g/mol)		27.811	184.796		85.734
GOR (SCF/BBL) = 1037					
Density (g/cc) = 0.664 @ 130°F and 2050 psia					

Table 10–8
Composition of Recombined Anasazi Well 5L–3 Oil Flashed to 365.5 psia at 130°F

Component	MW	Gas Mole %	Liquid Wt %	Overall Wt %	Mole %
CO2	44.010	0.000	0.000	0.000	0.000
H2S	34.080	0.000	0.000	0.000	0.000
N2	28.013	0.000	0.000	0.000	0.000
C1	16.043	22.558	0.000	0.693	6.234
C2	30.070	26.125	0.075	1.573	7.552
C3	44.097	26.693	0.444	2.664	8.720
I–C4	58.124	4.649	0.266	0.763	1.896
N–C4	58.124	11.544	1.043	2.249	5.585
I–C5	72.151	2.554	0.787	1.081	2.162
N–C5	72.151	2.935	1.268	1.578	3.157
C6	86.200	1.564	2.937	2.974	4.980
MCYC–C5	84.160	0.251	0.691	0.679	1.165
Benzene	78.110	0.065	0.161	0.159	0.293
CYCL–C6	84.160	0.169	0.665	0.642	1.127
C7	100.200	0.448	3.418	3.247	4.677
MCYCL–C6	98.190	0.141	1.428	1.347	1.980
Toluene	92.140	0.038	0.447	0.420	0.658
C8	14.230	0.167	4.417	4.121	5.207
C2–Benzene	106.170	0.007	0.178	0.166	0.226
M&P–XYLENE	106.170	0.011	0.506	0.470	0.639
O–XYLENE	106.170	0.004	0.559	0.518	0.704
C9	128.300	0.048	4.042	3.749	4.218
C10	134.000	0.018	5.114	4.734	5.099
C11	147.000	0.005	4.460	4.126	4.051
C12	161.000	0.002	3.744	3.463	3.104
C13	175.000	0.001	4.337	4.011	3.308
C14	190.000	0.001	3.855	3.565	2.708
C15	206.000	0.001	3.598	3.327	2.331
C16	222.000	0.000	3.013	2.786	1.812
C17	237.000	0.000	2.957	2.735	1.665
C18	251.000	0.001	3.018	2.791	1.605
C19	263.000	0.001	2.924	2.704	1.484
C20	275.000	0.000	2.365	2.187	1.148
C21	291.000	0.000	2.252	2.082	1.033
C22	305.000	0.000	2.069	1.913	0.905
C23	318.000	0.000	2.063	1.908	0.866
C24	331.000	0.000	1.855	1.715	0.748
C25	345.000	0.000	1.924	1.779	0.744
C26	359.000	0.000	1.597	1.477	0.594
C27	374.000	0.000	1.822	1.685	0.650
C28	388.000	0.000	1.466	1.356	0.504
C29	402.000	0.000	1.532	1.417	0.509
C30+	700.000	0.000	20.705	19.147	3.948
MW (g/mol)		39.309	184.453		144.343
GOR (SCF/BBL) = 234					
Density (g/cc) = 0.741 @ 130°F and 365.5 psia					

Table 10–9
Volumes of Liquid and Vapor Measured at Different Flash Conditions
Anasazi Well 5L–3 Recombined Oil

2050 psia & 130°F		365.5 psia & 130°F	
Liquid vol. %	Vapor vol. %	Liquid vol. %	Vapor vol. %
86.26	13.74	14.37	85.63

Table 10–10
Relative Volumes of the Liquid and Vapor Phases as a Function of Pressure at 130°F
(CO_2 Concentration = 20, 40, 60 and 75 Mole %)

Pressure (psig)	Total Volume (cm^3)	Relative Volume* (cm^3/cm^3)	Phase Volume (cm^3)		Observations
			Liquid	Vapor	
20% CO_2 Case					
3986	64.09	0.974	64.09	0.00	Single Phase
3486	64.61	0.981	64.61	0.00	Single Phase
2987	65.07	0.988	65.07	0.00	Single Phase
2487	65.64	0.997	65.64	0.00	Single Phase
2227	66.55	1.011	66.55	0.00	Single Phase
2177	67.11	1.019	64.31	2.80	Two Phase
2127	67.83	1.030	63.89	3.94	Two Phase
1986	70.70	1.064	62.32	7.75	Two Phase
40% CO_2 Case					
4486	70.04	0.967	70.04	0.00	Single Phase
3987	70.61	0.975	70.61	0.00	Single Phase
3486	71.21	0.983	71.21	0.00	Single Phase
2986	71.97	0.993	71.97	0.00	Single Phase
2525	72.93	1.007	not measurable	not measurable	Two Phase
2430	73.73	1.018	60.46	4.69	Two Phase
2351	74.58	1.029	67.32	7.26	Two Phase
1986	80.99	1.118	61.84	19.15	Two Phase
60% CO_2 Case					
4986	70.42	0.957	70.42	0.00	Single Phase
4487	71.18	0.968	71.18	0.00	Single Phase
3987	72.05	0.980	72.05	0.00	Single Phase
3487	73.03	0.993	73.03	0.00	Single Phase
3076	74.01	1.006	74.01	0.00	Single Phase
2914	74.67	1.015	44.55	30.12	Two Phase
2776	75.46	1.026	43.60	31.86	Two Phase
1987	85.48	1.162	46.83	36.65	Two Phase
75% CO_2 Case					
7986	75.43	0.965	0.00		Single Phase
7486	75.69	0.968	0.00		Single Phase
6986	76.49	0.978	0.00		Single Phase
6487	77.07	0.986	0.00		Single Phase
5986	77.87	0.996	0.00		Single Phase
5487	78.76	1.007	not measurable		Two Phase
4987	79.72	1.019	1.25		Two Phase
4486	80.90	1.035	4.94		Two Phase
3986	82.36	1.053	10.32		Two Phase
3486	84.05	1.075	16.42		Two Phase
2986	86.43	1.105	21.75		Two Phase
2486	90.46	1.157	26.86		Two Phase
2036	98.23	1.256	29.83		Two Phase

Table 10–11
Swelling Test Data for the Anasazi 5L–3 Oil at 130°F

CO_2 Concentration Mole %	Saturation Pressure psia-Measured	V_{sat}	Adjusted V_{sat}* cm^3	Bulk Density g/cm^3	Molar Volume cm^3/mol	Swelling Factor** cm^3/cm^3	μ cP
00.0	2050†	59.61	59.61	0.664	129.12	1.000	0.464
20.0	2294†	65.83	65.83	0.678	114.14	1.104	0.349
40.0	2585†	72.45	76.24	0.697	99.63	1.279	0.270
60.0	3176†	73.55	96.60	0.725	83.72	1.621	0.215
75.0	5800‡	78.20	125.21	0.805	67.63	2.101	0.210

† Graphically
‡ Visually
*Based on originally charged virgin oil (i.e., accounts for the sample volumes displaced after each CO_2 concentration swelling test to measure the respective viscosity and/or density).
**Swelling Factor = adjusted Vsat (of CO_2 + oil mixture)/V_{sat} (virgin oil).
where V_{sat} (virgin oil) = 59.61cm^3

Table 10–12
Composition of Anasazi Well 5L–3 Recombined Separator Oil at 70°F and 3014 psia
Pseudo Component Definition

Pseudo	Component	MW	Gas Mole%	Liquid WT%	Overall Wt%	Mole %	Pseudo Mole%
	CO2	44.010	0.078	0.000	0.031	0.055	
CO2							0.055
	N2	28.013	1.03	0.000	0.255	0.702	
	C1	16.043	55.141	0.011	8.082	38.647	
C1							39.349
	C2	30.070	19.748	0.076	5.456	13.971	
C2							13.971
	C3	44.097	12.165	0.274	5.080	8.872	
C3							8.872
	I–C4	58.124	1.902	0.143	1.111	1.472	
	N–C4	58.124	4.792	0.565	2.951	3.909	
	I–C5	72.151	1.241	0.481	1.170	1.249	
	N–C5	72.151	1.561	0.829	1.637	1.748	
C4 to C–5							8.378
	C6	86.200	1.123	2.404	2.659	2.375	
	MCYC–C5	84.160	0.194	0.601	0.594	0.543	
	Benzene	78.110	0.051	0.142	0.142	0.140	
	CYCL–C6	84.160	0.135	0.605	0.551	0.504	
	C7	100.200	0.397	3.247	2.765	2.125	
	MCYCL–C6	98.190	0.128	1.390	1.143	0.896	
	Toluene	92.140	0.037	0.442	0.358	0.299	
	C8	114.230	0.170	4.465	3.480	2.346	
	C2–Benzene	106.170	0.008	0.165	0.130	0.094	
	M&P–XYLENE	106.170	0.013	0.521	0.398	0.289	
	O–XYLENE	106.170	0.005	0.383	0.288	0.209	
C6 to C8							9.820
	C9	128.300	0.056	4.412	3.330	1.999	
	C10	134.000	0.027	5.293	3.950	2.270	
	C11	147.000	0.011	4.617	3.432	1.798	
C9 to C11							6.067
	C12	161.000	0.005	3.851	2.857	1.367	
	C13	175.000	0.003	4.500	3.335	1.467	
	C14	190.000	0.002	3.965	2.937	1.191	
	C15	206.000	0.002	3.644	2.700	1.009	
C12 to C15							5.034
	C16	222.000	0.001	3.175	2.352	0.816	
	C17	237.000	0.001	3.139	2.324	0.755	
	C18	251.000	0.000	3.218	2.382	0.731	
	C19	263.000	0.000	2.991	2.214	0.648	
C16 to C19							2.950

Table 10–12 – continued
Composition of Anasazi Well 5L–3 Recombined Separator Oil at 70°F and 3014 psia
Pseudo Component Definition

	C20	275.000	0.000	2.651	1.962	0.549	
	C21	291.00	0.000	2.413	1.786	0.473	
	C22	305.000	0.000	2.351	1.740	0.439	
	C23	318.000	0.000	2.205	1.632	0.395	
	C24	331.000	0.000	1.971	1.459	0.339	
	C25	345.000	0.000	1.938	1.434	0.320	
	C26	359.000	0.000	1.687	1.248	0.268	
	C27	374.000	0.000	1.842	1.363	0.281	
	C28	388.000	0.000	1.552	1.149	0.228	
	FC29	402.00	0.000	1.533	1.134	0.217	
C20 to C29							3.509
FC30+	FC30+	580.000	0.000	20.309	15.029	1.995	1.995
MW (g/mol)			28.591	190.065	77.005		
Density (g/cc) = 0.681 @ 70°F & 3014 psia							

Table 10–13
Composition of Anasazi Well 5L–3 Recombined Oil Flashed to 2050 psia at 130°F
Pseudo Component Definition

Pseudo	Component	MW	Gas Mole%	Liquid WT%	Overall Wt%	Mole %	Pseudo Mole%
CO2	CO2	44.010	0.000	0.000	0.000	0.000	0.000
	N2	28.013	0.928	0.000	0.191	0.586	
	C1	16.043	53.274	0.000	6.291	33.617	
C1							34.208
	C2	30.070	22.122	0.087	4.965	14.157	
C2							14.157
	C3	44.097	14.215	0.328	4.875	9.477	
C3							9.477
	I–C4	58.124	2.023	0.232	1.050	1.549	
	N–C4	58.124	4.668	1.005	2.796	4.125	
	I–C5	72.151	0.872	0.832	1.125	1.336	
	N–C5	72.151	0.960	1.346	1.580	1.878	
C4 to C–5							8.888
	C6	86.200	0.488	3.043	2.730	2.715	
	MCYC–C5	84.160	0.079	0.709	0.613	0.624	
	Benzene	78.110	0.021	0.165	0.143	0.157	
	CYCL–C6	84.160	0.052	0.677	0.571	0.582	
	C7	100.200	0.141	3.451	2.849	2.437	
	MCYCL–C6	98.190	0.001	1.435	1.142	0.997	
	Toluene	92.140	0.012	0.449	0.365	0.340	
	C8	114.230	0.092	4.416	3.589	2.694	
	C2–Benzene	106.170	0.003	0.177	0.143	0.15	
	M&P–XYLENE	106.170	0.005	0.502	0.403	0.325	
	O–XYLENE	106.170	0.002	0.555	0.443	0.358	
C6 to C8							11.344
	C9	128.300	0.020	4.015	3.212	2.146	
	C10	134.000	0.013	2.055	4.033	2.581	
	C9 to C11	147.000	0.005	4.405	3.509	2.046	
C9 to C11							6.773
	C12	161.000	0.001	3.759	2.991	1.593	
	C13	175.000	0.000	4.351	3.461	1.696	
	C14	190.000	0.000	3.789	3.014	1.360	
	C12 to C15	206.000	0.000	3.520	2.800	1.165	
C12 to C15							5.814
	C16	222.000	0.000	3.003	2.389	0.923	
	C17	237.000	0.000	2.963	2.357	0.853	
	C18	251.000	0.000	3.029	2.409	0.823	
	C19	263.000	0.000	2.867	2.280	0.743	
C 16 to C19							3.342

Table 10–13 continued
Composition of Anasazi Well 5L–3 Recombined Oil Flashed to 2050 psia at 130°F
Pseudo Component Definition

	C20	275.000	0.000	2.307	1.835	0.572	
	C21	291.000	0.000	2.290	1.821	0.537	
	C22	305.000	0.000	2.240	1.781	0.501	
	C23	318.000	0.000	2.094	1.665	0.449	
	C24	331.000	0.000	1.879	1.494	0.387	
	C25	345.000	0.000	1.964	1.3562	0.388	
	C26	359.000	0.000	1.616	1.285	0.307	
	C27	374.000	0.000	1.805	1.436	0.329	
	C28	388.000	0.000	1.626	1.293	0.286	
	C±20 to C29	402.000	0.000	1.419	1.129	0.241	
C20 to C29							3.996
	FC30+	700.000		20.596	16.380	2.006	
FC30+							2.006
MW (gmol)			27.811	184.796	85.734		
GOR (SCF/BBL) = 1037							
Density (g/cc) = 0.664 @ 130°F & 2050 psia							

Table 10–14
Composition of Original Oil Anasazi Well No. 1
Pseudo – Component Definition

Pseudo	Component	MW	Mole %	Pseudo Mole %
CO_2	CO_2	44.010	1.12	1.1200
	N_2	28.013	0.40	
C_1	C_1	16.043	19.44	19.8408
C_2	C_2	30.070	7.53	7.5303
C_3	C_3	44.097	6.51	6.5103
	iC_4	58.124	1.34	
	nC_4	58.124	3.94	
	iC_5	72.151	1.55	
	nC_5	72.151	2.77	
C_4 to C_5	–	–	–	9.6004
C_6 to C_8	–	–	–	16.8284
C_9 to C_{11}	–	–	–	11.9115
C_{12} to C_{15}	–	–	–	10.2250
C_{16} to C_{19}	–	–	–	5.8775
C_{20} to C_{29}	–	–	–	7.0277
FC_{30+}	–	–	–	3.5280

Table 10−15
Equation of State Parameters
11−Pseudo−Component Version
Anasazi−Sahgzie Fluid System

	CO2	C1	C2	C3	C4toC5	C6toC8	C9toC11	C12toC15	C16toC19	C20toC29	FC30+
Sg	.48748	.26542	.44301	.52191	.59700	.67411	.69884	.84209	.88247	1.04925	.99206
Tb, deg K	168.793	112.517	183.312	229.564	281.579	361.428	404.889	499.477	564.979	795.685	909.712
pc, atm	72.8280	45.4001	48.2002	41.9012	35.6920	26.5606	22.2081	21.0636	17.6592	11.9538	7.5885
vc, m3/kmol	.09299	.09901	.14803	.20300	.27429	.42633	.53810	.69511	.91508	1.29636	2.91351
Tc, deg K	301.106	190.600	305.400	369.800	437.680	529.579	573.561	693.994	758.867	998.278	1047.578
Zc	.274100	.287400	.284700	.280300	.272580	.260569	.253900	.257100	.259500	.191158	.260994
Acentric Factor	.22611	.00800	.09800	.15200	.20793	.34360	.46410	.59460	.76300	1.12896	1.12323
Molecular Weight	44.010	16.040	30.070	44.100	63.193	99.483	139.270	180.880	242.090	283.760	700.000
Omega A	.4572355	.4572355	.4572355	.4572355	.4572355	.4572355	.4572355	.4572355	.4572355	.4572355	.4572355
Omega B	.0777961	.0777961	.0777961	.0777961	.0777961	.0777961	.0777961	.0777961	.0777961	.0777961	.0777961
vc for viscosity	.09299	.09901	.14803	.20300	.27429	.42633	.53810	.69511	.91508	1.29636	2.91351
Parachor	125.7429	45.8286	85.9143	126.0000	180.5526	284.2386	397.9143	516.8000	691.6857	810.7429	2000.0000
Rackett Const, Zra	.388942	.287400	.242194	.271591	.273080	.262453	.272572	.255779	.255629	.184437	.235933
Vol Shift, m3/kmol	.0004701	−.0061806	−.0105228	−.0041298	−.0006110	.0234714	.0051946	.0286750	.0376525	.0817225	.1440720
EOS bc, m3/kmol	.02639	.02680	.04045	.05634	.07828	.12729	.16488	.21034	.27434	.53313	.88129
EOS Cappa Term	.70957	.38696	.52319	.60283	.68365	.87269	1.03227	1.20801	1.42440	1.87060	1.86385
H−ideal parameter A	.000E+00	.000E+00	.000E+00	.000E+00	.000E+00	.000E+00	.000E+00	.000E+00	.000E+00	.000E+00	.000E+00
H−ideal parameter B	−5.352E−01	−3.957E+01	−3.265E+00	−9.109E−01	−2.062E−01	−4.815E−02	−4.717E−02	−2.553E−02	−2.697E−02	−3.875E−02	−8.401E−03
H−ideal parameter C	1.145E−03	5.143E−02	4.713E−03	1.645E−03	7.043E−04	4.796E−04	4.793E−04	3.830E−04	3.815E−04	3.620E−04	3.824E−04
H−ideal parameter D	−2.395E−07	−1.262E−05	−1.135E−06	−3.682E−07	−1.306E−07	−7.392E−08	−7.404E−08	−5.362E−08	−5.363E−08	−5.235E−08	−5.138E−08
H−ideal parameter E	.000E+00	.000E+00	.000E+00	.000E+00	.000E+00	.000E+00	.000E+00	.000E+00	.000E+00	.000E+00	.000E+00
H−ideal parameter F	.000E+00	.000E+00	.000E+00	.000E+00	.000E+00	.000E+00	.000E+00	.000E+00	.000E+00	.000E+00	.000E+00

Ideal Enthalpy, H−ideal = A + B*T + C*T**2 + D*T**3 + E*T**4 + F*T**5 with T in deg R and H−ideal in BTU/lb

Viscosity correlation parameters: COEMU(1:5), EMIXVC

1.02300E−01 2.33640E−02 5.85330E−02 −4.07580E−02 9.33240E−03 1.00000E+00

Interaction Coefficient Table

dij = 1 − (2*sqrt(vc3i*vc3j)/(vc3i+vc3j)) ** 1.00000

vc3i= vci**(1/3)

CO2	.00000										
C1	.00000	.00000									
C2	.00258	.00269	.00000								
C3	.00811	.00954	.00166	.00000							
C4toC5	.01776	.01783	.00685	.00184	.00000						
C6toC8	.15132	.03633	.01511	.00800	.00219	.00000					
C9toC11	.04772	.06015	.02335	.01617	.00614	.00157	.00000				
C12toC15	.11808	.07233	.02984	.02221	.00955	.0036	.00056	.00000			
C16toC19	.05308	.07230	.04034	.03519	.01576	00831	.00331	.00116	.00000		
C20toC29	.05423	.05105	.06462	.04798	.02327	.0147	.00824	.00454	.00112	.00000	
FC30+	.02173	.05602	.09772	.07483	.03978	.03021	.02212	.01579	.00848	.00347	.00000

VSHIFT − Final Values

1.7810000E−02 −2.3061000E−01 −2.6015000E−01 −7.3300000E−02 −7.8052521E−03
1.8439868E−01 3.1505940E−02 1.3633000E−01 1.3725000E−01 1.5328843E−01 1.6347938E−01

Table 10–16
Pederson Viscosity Correlation Parameters

Reference Component Viscosity Coefficients

k_1	=	0.8862322597E+01
k_2	=	0.1842077768E+02
k_3	=	0.4912304900E+04
k_4	=	0.4253428222E+02
k_5	=	0.7822237626E+00
k_6	=	0.5837289021E+02
k_7	=	0.1846321666E+05

Binary Interaction Coefficients

VISKJ		
1	8	0.1317577930E+00
1	9	0.1317577930E+00
1	10	0.2117241466E+00
1	11	0.2117241466E+00
2	8	0.9168434822E+01
2	9	0.9168434822E+01
2	10	0.1471782926E+00
2	11	0.1471782926E+00

All other pairs have a zero coefficient

Table 10–17
Oil Viscosity of Recombined Anasazi 5L–3 Oil Flashed to 2050 psia and 130°F and Various Mole Fractions of CO_2

Mole % CO_2	Viscosity – cp	
	Experimental	Calculated
0	0.4640	0.4152
20.0	0.3490	0.3500
40.0	0.2700	0.2724
60.0	0.2150	0.2035
75.0	0.2100	0.2153

Table 11–1 Brine Composition for Capillary Pressure Measurements on the Dolomite Sample

	Wt %
Sodium Chloride (NaC1)	9.1
Calcium Chloride ($CaC1_2 . 2H_2O$)	6.0
Magnesium Chloride ($MgC1_2.6H_2O$)	2.0
Potassium Chloride (KC1)	0.23

Table 11–2 Fluid Properties for Capillary Pressure Measurements on the Dolomite Sample Test

Fluid	Temp °F	Density grams/cc	Viscosity cp	Interfacial Tension Dyne/cm	Surface Tension Dyne/cm
Brine	75	1.1930	1.975	17.2	
Brine	130	1.1791	1.005	15.6	
Crude	75	0.8229	4.73		26.8
Crude	130	0.8014	2.58		25.5

Table 11–3
Permeability and Porosity Data Summary
Anasazi 6H #1 Dolomite Sample

	Test #	Core 1a*	Core 1b*	Core 2	Core 2a	Core 2b*	Core 4a
Initial Core Properties at 500 psi NCS							
Depth	ft.	5691.21	5691.21	5691.46	5691.46	5691.46	5691.8
Length, L	cm	4.097	4.252	9.073	4.470	4.257	4.262
Average Area	sqcm	11.158	11.159	11.187	11.194	11.194	11.153
Bulk Volume	cc	45.716	47.447	101.502	50.044	47.652	47.534
Gas Pore Volume	cc	8.211	8.273	17.715	8.070	9.054	7.454
Grain Volume	cc	37.495	39.174	83.787	41.974	38.598	40.080
Gas Porosity	%PV	17.982	17.436	17.453	16.125	19.000	15.681
Grain Density	gm/cc	2.849	2.840	2.826	2.821	2.825	2.771
Gas Permeability	md	30.0	26.4	15.1	13.6	26.7	3.8
Oil Permeability #1	md	12.95	20.71			18.42	
Core Properties at 2000 psi NCS							
Length, L	cm	4.097	4.252	9.073	4.470	4.257	4.262
Average Area	sqcm	11.125	11.106	11.148	11.15	11.16	11.111
Bulk Volume	cc	45.578	47.224	101.149	49.487	47.509	47.355
Gas Pore Volume	cc	8.083	8.050	17.362	7.873	8.911	7.275
Gas Porosity	%PV	17.735	17.046	17.165	15.794	18.756	15.362
Gas Permeability	md	26.5	23.1	13.2	12.3	24.4	2.9
Brine Permeability as Received	md	10.4	8.3	4.3	–	–	1.0
Brine Permeability @ Cleaning	md	20.2	–	–	–	13.8	
Centrifuge Values							
Initial Residual Water Saturation (S_{wri})	S_w% PV	8.99	10.24			7.95	
K_{eo} @ S_{wri}	md	12.95	20.71			18.42	
Residual Oil Saturation (S_{or})	S_o% PV	6.01	5.48			6.86	
Water Saturation at S_{or} (S_w @ S_{or})	S_w% PV	93.99	94.52			93.14	
K_{ew} @ S_{or}	md	16.4	16.8			10.9	
Residual Water Saturation (Swrf)	S_w% PV	10.79	7.91			9.30	
K_{eo} @ S_{wrf}	md	9.4	18.9			14.5	
Residual Oil Saturation (S_{or})	S_o% PV	10.1	10.40			11.70	
Water Saturation at S_{or} (S_w @ S_{or})	S_w% PV	89.99	89.60			90.72	
K_{ew} @ S_{or}	md	12.7	15.1			9.86	
Final Residual Water Saturation (S_{wrf})	S_w% PV	9.49	7.18			5.92	
K_{eo} @ S_{wrf}	md	15.22	19.18			19.37	
Residual Oil Saturation (S_{or})	S_o% PV	2.41	8.22			3.22	
K_{eg} @ S_{or}	md	25.7	25.9			22.3	
Final Brine 100% saturated	md	23.7	13.4			14.2	

*Centrifuge Cores
1a – Cleaned
1b – Preserved
2b – Restored

Table 11–4
Anasazi No. 6H–1 Dolomite and Anasazi Limestone Samples
Permeability and Porosity Data Summary

		Test #	Core 1a	Core 1b	Core 2	Core 2a	Core 2b	Core 4a	Limestone
Initial Core Properties at 500 psi NCS									
Depth	ft.		5691.21	5691.21	5691.46	5691.46	5691.46	5691.8	697.6
Length, L		cm	4.097	4.252	9.073	4.470	4.257	4.262	4.978
Average Area		sqcm	11.158	11.159	11.187	11.194	11.194	11.153	10.818
Bulk Volume		cc	45.716	47.447	101.502	50.044	47.652	47.534	53.857
Gas Pore Volume		cc	8.211	8.273	17.715	8.070	9.054	7.454	7.269
Grain Volume		cc	37.495	39.174	83.787	41.974	38.598	40.080	46.588
Gas Porosity		%BV	17.982	17.436	17.453	16.125	19.000	15.681	13.498
Grain Density		gm/cc	2.849	2.840	2.826	2.821	2.825	2.771	2.66
Gas Permeability		md	30.0	26.4	15.1	13.6	26.7	3.8	56.0
Oil Permeability #1		md	12.95	20.71			18.42		
Core Properties at 2000 psi NCS									
Length, L		cm	4.097	4.252	9.073	4.470	4.257	4.262	4.978
Average Area		sqcm	11.125	11.106	11.148	11.15	11.16	11.111	10.780
Bulk Volume		cc	45.578	47.224	101.149	49.487	47.509	47.355	53.667
Gas Pore Volume		cc	8.083	8.050	17.362	7.873	8.911	7.275	7.079
Gas Porosity		%BV	17.735	17.046	17.165	15.794	18.756	15.362	13.191
Gas Permeability		md	26.5	23.1	13.2	12.3	24.4	2.9	54.0
Brine Permeability as Received		md	10.4	8.3	4.3	–	–	1.0	
Brine Permeability @ Cleaning		md	20.2	–	–	–	13.8		42.3
Centrifuge Values		Test #	1a	1b			2b		
Initial Residual Water Saturation (S_{wri})		S_w% PV	8.99	10.24			7.95		11.55
K_{eo} @ S_{wri}		md	12.95	20.71			18.42		
Residual Oil Saturation (S_{or})		S_o% PV	6.01	5.48			6.86		13.0
Water Saturation at S_{or} (S_w @ S_{or})		S_w% PV	93.99	94.52			93.14		87.0
K_{ew} @ S_{or}		md	16.4	16.8			10.9		
Residual Water Saturation (Swrf)		S_w% PV	10.79	7.91			9.30		11.07
K_{eo} @ S_{wrf}		md	9.4	18.9			14.5		54.06
Residual Oil Saturation (S_{or})		S_o% PV	10.1	10.40			11.70		18.23
Water Saturation at S_{or} (S_w @ S_{or})		S_w% PV	89.99	89.60			90.72		81.77
K_{ew} @ S_{or}		md	12.7	15.1			9.86		35.36
Final Residual Water Saturation (S_{wrf})		S_w% PV	9.49	7.18			5.92		12.34
K_{eo} @ S_{wrf}		md	15.22	19.18			19.37		
Residual Oil Saturation (S_{or})		S_o% PV	2.41	8.22			3.22		
K_{eg} @ S_{or}		md	25.7	25.9			22.3		21.0
Final Brine 100% saturated		md	23.7	13.4			14.2		

*Centrifuge Cores
1a – Cleaned
1b – Preserved
2b – Restored

Table 11–7 Compressibilities Determined From Hydrostatic Compression For Samples From The Anasazi No. 1 and 6H–1 Wells

Sample Depth (ft)	Rock Type	Stress Range (psi)	Grain Compressibility ($10^{-8}psi^{-1}$)	Bulk Compressibility ($10^{-6}psi^{-1}$)	Pore Volume Compressibility ($10^{-5}psi^{-1}$)	Biot's Constant α
5648.5 – 5648.9	Limestone No. 1 Well	60 to 320	–	21.593	12.830	0.998
		525 to 1956	5.1203			
		2243 to 2807	–	4.0396	2.4002	0.987
		3083 t 3636	–	1.7226	1.0235	0.970
5692.0 – 5692.4	Dolomite No. 6H–1 Well	75 to 315	–	1.6797	1.4468	0.994
		547 to 1805	1.0400			
		2368 to 2910	–	1.7074	1.4706	0.994
		3050 to 3690	–	1.2950	1.1154	0.992

Table 11–8 Quasi–Static Mechanical Properties Determined From Triaxial Compression For Samples From The Anasazi No. 1 and 6H–1 Wells

Sample Depth (ft)	Rock Type	Axial Stress Difference Range for Properties Calculations (psi)		Triaxial Compression – Moduli (10^6 psi)		
				Young's	Bulk	Shear
5648.5 –.9	Limestone	610 to 1390	0.20	2.37	1.30	0.99
5692.0 –.4	Dolomite	605 to 1390	0.15	3.21	1.51	1.40

Table 11–9 Parameters Determined During Uniaxial Strain/ Pore Pressure Drawdown Segment

Sample Depth (ft)	Rock Type	Pore Pressure Stress Range (psi)	Compaction Coefficient ($C_b{}^u$ 10^{-7}/psi)	Pore Volume Compressibility ($C_p{}^u$ 10^{-6}/psi)
5648.5 –.9	Limestone	1935 to 300	3.9263	2.3329
5692.0 –.4	Dolomite	1915 to 275	3.6977	3.1849

Table 14–1
Pressure Data Comparisons – Simulation versus Field Measurements

Date	Anasazi Well No. 1				Sahgzie Well No. 1				Anasazi Well No. 5L–3			
	Field Shut–in	Simulation			Field Shut–in	Simulation			Field Shut–in	Simulation		
		Shut–in	BHP	Grid Value		Shut–in	BHP	Grid Value		Shut–in	BHP	Grid Values
11/05/89					1930(2260)*	2231	2189	2181–2215				
1/20/90	1708	1819	1747									
2/28/90	1386			1590–1620								
3/25/91									870–952	908	900	900–924
7/08/91					750	864	606	680–710				
1/17/92	580	638	589	590–620								
8/10/93	240	247	229	230–270								
8/14/93					175	504	241	240–330				
9/14/93									154	227	137	140–180

* The 2260 psi was reported as the initial reservoir pressure based on the initial drill stem test of the Sahgzie No. 1

Table 15–1

INITIAL FLUIDS IN PLACE

HARKEN ANASAZI FULL FIELD COMPOSITIONAL MODEL

RESERVOIR PROCESS – PRIMARY DEPLETION

VIP–CORE

		REGION	REGION	REGION	REGION	REGION	REGION	REGION	REGION	TOTAL
REGION NUMBER		1	2	3	4	5	6	7	8	
REGION NAME		A–OMAS	A–MASM	A–OMAC	A–MACM	S–OMAS	S–MASM	S–OMAC	S–MACM	
AVERAGE PRESSURE, PSIA										
WEIGHTED BY HC PV AT DATUM		2297.8	2297.8	2297.8	2297.7	2297.8	2297.8	2297.7	2297.7	2297.8
WEIGHTED BY TOTAL PV AT DATUM		2297.8	2297.8	2297.8	2297.7	2297.8	2297.8	2297.	72297.7	2297.8
WEIGHTED BY HC PV		2280.3	2280.6	2291.0	2294.9	2291.1	2283.8	2300.9	2299.0	2286.3
WEIGHTED BY TOTAL PV		2280.3	2280.7	2291.1	2294.9	2291.1	2283.9	2300.9	2299.0	2286.5
FLUIDS IN PLACE										
TOTAL PORE VOLUME	(MRB)	4562.	2540.	1832.	1120.	1740.	1800.	755	846.	15196.
HC PORE VOLUME	(MRB)	4093.	2279.	1629.	947.	1550.	1612.	664.	714.	13489.
TOTAL OIL	(MSTB)	3469.	1932.	1381.	803.	1314.	1366.	563	605.	11433.
CONDENSATE IN F.G.	(MSTB)	0.	0.	0.	0.	0.	0.	0	0.	0.
TOTAL GAS	(MMSCF)	1010.6	562.7	402.2	233.9	382.6	398.1	164.0	176.2	3330.4
FREE GAS	(MMSCF)	0.	0.	0.	0.	0.	0.	0.	0.	0.
WATER	(MSTB)	464.9	258.9	201.8	171.5	188.5	186.4	90.2	131.3	1693.4
RESERVOIR OIL	(MRB)	4093.	2279.	1629.	947.	1550.	1612.	664.	714.	13489.
RESERVOIR GAS	(MMRCF)	0.	0.	0.	0.	0.	0.	0.	0.	0
RESERVOIR WATER	(MRB)	468.6	260.9	203.4	172.9	190.0	187.9	90.9	132.3	1707.0
MOBILE RES OIL	(MRB)	3619.	2015.	1436.	802.	1369.	1425.	584.	604.	11853.
MOBILE RES GAS	(MMRCF)	0.	0.	0.	0.	0.	0.	0.	0.	0.
MOBILE RES WATER	(MRB)	84.98	47.32	46.83	43.49	43.71	36.53	25.03	34.62	362.50
AVG OIL SATURATION	(FPV)	.897274	.897273	.889005	.845681	.890777	.895610	.879595	.843576	.887664
AVG GAS SATURATION	(FPV)	.000000	.000000	.000000	.000000	.000000	.000000	.000000	0.	0.
AVG WTR SATURATION	(FPV)	.102726	.102727	.110995	.154319	.109223	.104390	.120405	.156424	.112336
AVERAGE COMPOSITIONS										
CO2		.0100	.0100	.0100	.0100	.0100	.0100	.0100	.0100	.0100
C1		.1755	.1755	.1755	.1755	.1755	.1755	.175	5.1755	.1755
C2		.0671	.0671	.0671	.0671	.0671	.0671	.0671	.0671	.0671
C3		.0594	.0594	.0594	.0594	.0594	.0594	.0594	.0594	.0594
C4–C5		.0943	.0943	.0943	.0943	.0943	.0943	.0943	.0943	.0943
C6–C8		.1795	.1795	.1795	.1795	.1795	.1795	.1795	.1795	.1795
C9–C11		.1278	.1278	.1278	.1278	.1278	.1278	.1278	.1278	.1278
C12–C15		.1098	.1098	.1098	.1098	.1098	.1098	.1098	.1098	.1098
C16–C19		.0631	.0631	.0631	.0631	.0631	.0631	.0631	.0631	.0631
C20–C29		.0755	.0755	.0755	.0755	.0755	.0755	.0755	.0755	.0755
C30P		.0379	.0379	.0379	.0379	.0379	.0379	.0379	.0379	.0379
TOTAL MOLES		8031921.	4472194.	3196436.	1859253.	3040947.	3163621.	1303421	.1400612.	26468403.

Table 15–2
Oil and Gas Production – Primary Depletion Prediction
Anasazi/Sahgzie Reservoir
Oil – MSTB – Gas – MMSCF

Date	Cumulative Well Production								Cumulative Field Production	
	Sahgzie #1		Anasazi #1		Anasazi #5L–3		Anasazi #6H–1			
	Oil	Gas	Oil	Gas	Oil	Gas	Oil	Gas	Oil	Gas
1/1/1997	543	338	709	502	487	518	7	3	1746	1362
1/1/1998	567	354	741	538	512	550	12	6	1833	1449
1/1/1999	591	374	775	577	537	579	16	10	1918	1540
1/1/2000	615	396	807	620	558	603	20	14	2000	1634
1/1/2001	638	421	834	658	576	624	25	20	2073	1724
1/1/2002	662	451	853	688	592	644	29	26	2136	1809
1/1/2003	686	487	868	715	607	661	33	34	2194	1897
1/1/2004	710	527	882	739	621	678	38	42	2249	1986
1/1/2005	733	570	893	760	633	693	42	52	2302	2075
1/1/2006	757	614	903	778	645	707	47	62	2352	2162
1/1/2007	780	657	912	796	655	720	51	73	2399	2246
1/1/2008	797	690	920	811	666	732	55	84	2438	2317
1/1/2009	810	716	927	824	676	744	60	95	2473	2378
1/1/2010	822	738	933	835	685	754	63	105	2503	2433
1/1/2011	831	757	938	845	694	765	67	114	2530	2481
1/1/2012	839	773	943	855	702	774	70	123	2556	2524

Table 15–3 Region Summary of Fluid Volumes, Production, Injection and Fluid Influx at 1/1/2012

VIP–EXEC REGION SUMMARY

DAY/MO/YR: 01/01/2012 TIME: 8096.0 DAYS

		REGION	REGION	REGION	REGION	REGION	REGION	REGION	REGION	TOTAL
REGION NUMBER		1	2	3	4	5	6	7	8	
REGION NAME		A–OMAS	A–MASM	A–OMAC	A–MACM	S–OMAS	S–MASM	S–OMAC	S–MACM	
AVERAGE PRESSURE, PSIA										
WEIGHTED BY HC PV AT DATUM		261.2	60.4	292.9	42.2	175.0	121.3	161.0	89.5	175.1
WEIGHTED BY TOTAL PV AT DATUM		260.8	60.3	291.6	42.2	175.0	121.2	160.7	89.5	174.0
WEIGHTED BY HC PV		247.6	49.9	286.9	40.4	170.3	112.0	163.9	91.1	166.9
WEIGHTED BY TOTAL PV		247.2	49.9	285.7	40.4	170.3	112.0	163.7	91.1	165.9
FLUIDS IN PLACE										
TOTAL PORE VOLUME	(MRB)	4523.27	2516.46	1817.22	1114.44	1724.24	1783.84	748.64	841.69	15069.80
HC PORE VOLUME	(MRB)	4052.65	2255.37	1612.57	938.12	1533.39	1595.12	657.06	707.85	13352.12
TOTAL OIL	(MSTB)	2743.395	1271.087	1257.751	654.059	1000.742	965.327	503.568	501.798	8897.728
CONDENSATE IN F.G.	(MSTB)	.000000	.024104	.000000	.024596	.000000	.000000	.000000	.000002	.048702
TOTAL GAS	(MMSCF)	342.6013	27.5243	159.7132	8.4592	97.1573	63.8977	41.6458	22.9579	763.9565
FREE GAS	(MMSCF)	81.0163	14.5087	22.3119	3.1038	25.8807	21.8543	6.0707	5.0529	179.7994
WATER	(MSTB)	464.006	257.275	201.791	173.741	188.129	185.999	90.270	131.900	1693.112
RESERVOIR OIL	(MRB)	3007.352	1330.819	1388.731	684.152	1084.789	1030.900	545.786	533.488	9606.018
RESERVOIR GAS	(MMRCF)	5.8689	5.1910	1.2568	1.4259	2.5187	3.1678	.6247	.9790	21.0328
RESERVOIR WATER	(MRB)	470.618	261.094	204.647	176.325	190.853	188.724	91.579	133.841	1717.682
AVG OIL SATURATION	(FPV)	.664862	.528845	.764206	.613897	.629141	.577910	.729040	.633831	.637435
AVG GAS SATURATION	(FPV)	.231094	.367400	.123179	.227884	.260171	.316293	.148633	.207154	.248583
AVG WTR SATURATION	(FPV)	.104044	.103755	.112615	.158219	.110688	.105797	.122327	159015	.113982
CUMULATIVE PRODUCTION										
TOTAL OIL	(MSTB)	45.916	69.287	23.940	1576.131	.000	7.458	.000	831.695	2554.427
TOTAL GAS	(MMSCF)	107.737	204.586	14.541	1424.131	.000	13.377	.000	759.810	2524.182
WATER	(MSTB)	.075286	.153262	.019769	.056841	.000000	.007609	.000000	.022036	.334803
CUMULATIVE INJECTION										
TOTAL GAS	(MMSCF)	0.	0.	0.	0.	0.	0.	0	0.	0. .
WATER	(MSTB)	0.	0.	0.	0.	0.	0.	0.	0.	0.
NET INFLUX										
TOTAL OIL	(MSTB)	−680.009	−591.353	−98.982	1427.101	−312.770	−393.714	−59.433	728.5108	.0000
TOTAL GAS	(MMSCF)	−560.294	−330.612	−227.943	1198.647	−285.476	−320.794	−122.360	606.5328	.0000
WATER	(MSTB)	−.8222	−1.4318	.0556	2.2832	−.3724	−.4171	.0748	.629789	.000000
WATER – AQUIFER	(MSTB)	0.	0.	0.	0.	0.	0.	0.	0	0.

Table 15–4
Production/Injection Data CO_2 Flood
Anasazi/Sahgzie Reservoir

Case No.	Cum Oil MSTB	Cum Gas /BSCF	Incremental over Primary MSTB	Total Gas Inj. BSCF	Total CO_2 Purchase BSCF	Total Gas Recycled BSCF
Production / Injection at 1/1/2003						
ASC102	2194	1.9	NA	NA	NA	N/A
ASP29	3665	19.1	1471	28.0	10.2	17.8
ASP30	3659	19.2	1460	28.0	11.5	16.5
ASP35	3665	19.1	1471	28.0	10.2	17.8
Production / Injection at 1/1/2006						
ASC102	2392	2.2	NA	NA	NA	NA
ASP29	4261	33.3	1909	43.3	11.4	31.9
ASP30	4232	33.4	1881	43.4	13.6	29.8
ASP35	3983	30.0	1631	28.0	10.2	17.8
Production / Injection at 1/1/2012						
ASC102	2554	2.5	NA	NA	NA	NA
ASP29	5039	62.5	2484	74.0	12.9	61.1
ASP30	4980	62.5	2426	74.1	17.2	56.9
ASP35	4269	30.8	1775	28.0	10.2	17.8

Table 15–5 Region Summary of Fluid Volumes, Production, Injection and Fluid Influx at 1/1/1997

VIP–EXEC REGION SUMMARY

DAY/MO/YR: 01/01/1997 TIME: 2618.0 DAYS

		REGION	REGION	REGION	REGION	REGION	REGION	REGION	REGION	TOTAL
REGION NUMBER		1	2	3	4	5	6	7	8	
REGION NAME		A–OMAS	A–MASM	A–OMAC	A–MACM	S–OMAS	S–MASM	S–OMAC	S–MACM	
AVERAGE PRESSURE, PSIA										
WEIGHTED BY HC PV AT DATUM		590.6	186.8	625.6	141.4	580.2	504.6	558.3	455.6	474.9
WEIGHTED BY TOTAL PV AT DATUM		589.9	186.7	623.8	141.2	580.1	504.4	557.8	455.5	473.2
WEIGHTED BY HC PV		574.8	174.7	619.2	139.4	574.5	493.3	561.2	465.4	
WEIGHTED BY TOTAL PV		574.1	174.6	617.4	139.2	574.4	493.1	560.8	457.1	463.8
FLUIDS IN PLACE										
TOTAL PORE VOLUME	(MRB)	4529.51	2517.79	1819.74	1114.70	1727.18	1786.71	749.84	842.41	15087.87
HC PORE VOLUME	(MRB)	4058.82	2255.83	1615.36	939.70	1536.34	1597.97	658.44	709.03	13371.48
TOTAL OIL	(MSTB)	3038.165	1410.374	1262.617	706.560	1118.507	1095.770	504.887	565.595	9702.47
CONDENSATE IN F.G.	(MSTB)	.044465	.000000	.000000	.000000	.000000	.055217	.000000	.000000	.099681
TOTAL GAS	(MMSCF)	714.675	132.475	299.563	44.693	278.371	263.272	115.658	103.374	1952.082
FREE GAS	(MMSCF)	91.6011	36.9810	27.8923	6.8652	48.4668	60.9304	15.1434	11.0823	298.9624
WATER	(MSTB)	464.537	258.219	201.722	172.488	188.352	186.230	90.197	131.596	1693.341
RESERVOIR OIL	(MRB)	3504.09	1524.14	1462.68	758.11	1291.55	1253.59	581.18	640.53	11015.87
RESERVOIR GAS	(MMRCF)	3.1145	4.1081	.8572	1.0195	1.3744	1.9335	.4338	3846	13.2258
RESERVOIR WATER	(MRB)	470.695	261.954	204.375	175.002	190.846	188.742	91.396	133.385	1716.395
AVG OIL SATURATION	(FPV)	.773614	.605350	.803787	.680102	.747779	.701619	.775073	.760351	.730114
AVG GAS SATURATION	(FPV)	.122469	.290609	.083903	.162903	.141726	.192744	.103040	.081312	.156126
AVG WTR SATURATION	(FPV)	.103917	.104041	.112310	.156995	.110496	.105636	.121887	.158337	.113760
CUMULATIVE PRODUCTION										
TOTAL OIL	(MSTB)	5.500	62.053	1.695	1134.162	.000	6.225	.000	536.838	1746.474
TOTAL GAS	(MMSCF)	2.718	113.053	.764	906.529	.000	5.257	.000	333.397	1361.717
WATER	(MSTB)	.002644	.067538	.000732	.022955	.000000	.003449	000000	.008460	.105779
CUMULATIVE INJECTION										
TOTAL GAS	(MMSCF)	7.0000	.0000	.0000	.0000	.0000	7.0000	0000	.0000	14.0000
WATER	(MSTB)	0.	0.	0.	0.	0.	0	0	.0	0.
CO2		.9859	.0000	.0000	.0000	.0000	.9859	.0000	.0000	.9859
NET INFLUX										
TOTAL OIL	(MSTB)	−425.656	−459.299	−116.361	1037.634	−195.005	−264.505	−58.115	497.4510	.0000
TOTAL GAS	(MMSCF)	−300.2388	−317.1946	−101.8709	717.2778	−104.2617	−136.5396	−48.3478	260.5358	.0000
WATER	(MSTB)	−.364025	−.573984	−.032445	.996336	−.149463	−.190473	.002078	.311976	.000000
WATER – AQUIFER	(MSTB)	0.	0.	0.	0.	0.	0.	0.	0.	0.

Table 15−6 Region Summary of Fluid Volumes, Production, Injection and Fluid Influx at 1/1/2012

VIP−EXEC REGION SUMMARY

DAY/MO/YR: 01/01/2012 TIME: 8096.0 DAYS

		REGION	REGION	REGION	REGION	REGION	REGION	REGION	REGION	TOTAL
REGION NUMBER		1	2	3	4	5	6	7	8	
REGION NAME		A−OMAS	A−MASM	A−OMAC	A−MACM	S−OMAS	S−MASM	S−OMAC	S−MACM	
AVERAGE PRESSURE, PSIA										
WEIGHTED BY HC PV AT DATUM		2716.8	2560.7	2733.3	2542.7	2704.8	2694.4	2666.2	2645.8	2669.9
WEIGHTED BY TOTAL PV AT DATUM		2716.4	2560.6	2732.6	2542.6	2704.5	2694.2	2666.1	2645.7	2669.1
WEIGHTED BY HC PV		2699.5	2544.1	2726.6	2540.1	2698.3	2680.9	2669.5	2647.1	2658.8
WEIGHTED BY TOTAL PV		2699.2	2544.0	2725.9	2540.0	2698.1	2680.7	2669.4	2647.0	2658.1
FLUIDS IN PLACE										
TOTAL PORE VOLUME	(MRB)	4570.09	2542.98	1835.57	1120.97	1742.64	1803.19	756.19	846.73	15218.37
HC PORE VOLUME	(MRB)	4102.64	2282.87	1632.50	946.91	1553.07	1615.90	665.41	714.03	13513.32
TOTAL OIL	(MSTB)	1942.700	781.886	1106.801	285.523	723.569	409.665	404.072	115.582	5769.798
CONDENSATE IN F.G.	(MSTB)	43.9328	39.7724	12.9614	18.8731	20.0847	18.6411	5.3283	11.6153	171.2090
TOTAL GAS	(MMSCF)	4331.89	3019.62	1015.65	1344.64	1671.37	2468.19	516.69	1230.66	15598.70
FREE GAS	(MMSCF)	3389.89	2557.39	587.97	1137.81	1289.05	2208.15	329.85	1100.00	12600.10
WATER	(MSTB)	464.298	258.237	201.707	172.807	188.291	186.021	90.161	131.790	1693.312
RESERVOIR OIL	(MRB)	2414.693	976.352	1337.147	363.963	910.064	527.123	501.080	163.791	7194.214
RESERVOIR GAS	(MMRCF)	9.4771	7.3355	1.6583	3.2730	3.6102	6.1130	.9226	3.0894	35.4792
RESERVOIR WATER	(MRB)	467.454	260.111	203.063	174.064	189.571	187.295	90.781	132.705	1705.044
AVG OIL SATURATION	(FPV)	.528369	.383940	.728466	.324685	.522232	.292328	.662637	.193438	.472732
AVG GAS SATURATION	(FPV)	.369346	.513774	.160908	.520036	.368984	.603804	.217312	649836	.415229
AVG WTR SATURATION	(FPV)	.102285	.102286	.110627	.155279	.108784	.103869	.120051	.156726	.112039
CUMULATIVE PRODUCTION										
TOTAL OIL	(MSTB)	5.500	62.053	1.695	3413.388	.000	6.225	.000	1549.919	5038.780
TOTAL GAS	(MMSCF)	2.72	113.05	.76	34524.18	.00	5.26	00	27820.07	62466.04
WATER	(MSTB)	.002644	.067538	.000732	.040796	.000000	.003449	.000000	.019188	.134348
CUMULATIVE INJECTION										
TOTAL GAS	(MMSCF)	37600.07	.00	.00	.00	.00	36385.58	.00	.00	73985.65
WATER	(MSTB)	0.	0.	0.	0.	0.	0.	0.	0.	0.
NET INFLUX										
TOTAL OIL	(MSTB)	−1521.120	−1087.788	−272.178	2895.823	−589.942	−950.610	−158.930	1060.518	.000
TOTAL GAS	(MMSCF)	−34276.10	2569.95	614.22	35634.87	1288.74	−34310.20	352.68	28874.49	.00
WATER	(MSTB)	−.6028	−.5559	−.0483	1.3333	−.2106	−.3987	−.0337	.516743	.000000
WATER − AQUIFER	(MSTB)	0.	0.	0.	0.	0.	0.	0.	0.	0.

Table 15–7
Production/Injection Data – Waterflood
Anasazi/Sahgzie Reservoir

Case No.	Cum Oil MSTB	Cum Gas BSCF	Incremental over Primary MSTB	Total Water Injected MSTB	Water ProductionTotal MSTB
Production / Injection at 1/1/2006					
ASC101	2354	2.2	N/A	N/A	N/A
ASP18	1753	1.4	–601	2927	124
ASP19	2728	1.7	374	3014	593
ASP20	2496	1.6	142	3652	1488
ASP25	1782	1.4	–572	2338	5
ASP26	2674	1.5	–280	2517	54
ASP28	2030	1.5	–324	2267	8
Production / Injection at 1/1/2012					
ASC102	2558	2.5	N/A	N/A	N/A
ASP18	1995	1.4	–563	4251	1495
ASP19	3176	1.8	618	4831	1574
ASP20	2945	1.7	387	5976	3072
ASP25	2080	1.4	–478	2902	59
ASP26	2636	1.6	78	3619	294
ASP28	2538	1.6	–20	3182	52
Production / Injection at 1/1/2022					
ASC101	NA	N/A	N/A	N/A	N/A
ASP18	2446	1.4	–	6510	3264
ASP19	3672	1.8	–	8197	4177
ASP20	–	–	–	–	–
ASP25	–	–	–	–	–
ASP26	3029	1.6	–	5156	1252
ASP28	3407	1.7	–	4447	220

* Primary Depletion Case Based on History Match Run ASC101

Table 16–1a

EVALUATION ANAC1.1

ECONOMIC EVALUATION
HARKEN PARADOX BASIN
REGA INCORPORATED

RUN DATE: 07–02–1997
RUN TIME: 09:56:37

AS OF DATE: JUN96

NAME: ANASAZI CO2 FLOOD–GAS PLANT
FIELD: ANASAZI–SAHGZIE
LOCATION: UTAH
FORMATION: DESERT CREEK
OPERATOR: HARKEN ENERGY

CONTINUOUS CO2 GAS RECYCLE
GAS PROCESSING FOR CO2 REMOVAL
SURFACE LINES – ZAPLOCK

NPV	5.0%	14327.741	BFIT
NPV	10.0%	9111.382	BFIT
NPV	15.0%	5567.312	BFIT
NPV	20.0%	3076.025	BFIT
NPV	25.0%	1275.586	BFIT
IRR		30%	BFIT
PAYOUT		MAY00	BFIT
PI		3.83:1	BFIT

====== INTERESTS AND EFFECTIVE DATE ======

COST	OIL	GAS	COND	PRODT	DATE
1.00000	0.80000	0.80000	0.80000	0.80000	JUN96

	====== PRICES ========			========== GROSS RESERVES ==========				
	BEGINING	ENDING	AVERAGE	CUMULATIVE	REMAINING	ULTIMATE	%REMAINING	
OIL	20.00	20.00	20.00	1692.690	3285.841	4978.531	66.00	OIL
GAS	1.80	1.80	1.80	1308.810	4306.441	5615.251	76.69	GAS
COND	0.00	0.00	0.00	0.000	0.000	0.000	0.00	COND
PRDT	0.00	0.00	0.00	0.000	0.000	0.000	0.00	PRDT

YEAR	GROSS OIL PRODUCTION	NET OIL PRODUCTION	GROSS GAS PRODUCTION	GROSS GAS AS FUEL	NET GAS PRODUCTION	AVERAGE OIL PRICE	AVERAGE GAS PRICE	NET OIL SALES	NET GAS SALES	NET TOTAL REVENUE
========	==MBBLS==	==MBBLS==	==MMSCF==	==MMSCF==	==MMSCF==	===$/B===	==$/MSCF==	===M$===	===M$===	===M$===
1996(7 Mo)	54.774	43.819	52.810	15.323	42.248	20.000	1.800	876.384	53.981	930.365
1997	82.120	65.696	40.118	254.628	32.094	20.000	1.800	1313.920	−308.894	1005.026
1998	316.729	253.383	90.895	318.468	72.716	20.000	1.800	5067.664	−327.705	4739.959
1999	520.906	416.725	232.213	318.468	185.770	20.000	1.800	8334.496	−124.207	8210.289
2000	404.129	323.303	275.282	318.468	220.226	20.000	1.800	6466.064	−62.188	6403.876
2001	323.119	258.495	304.552	318.468	243.642	20.000	1.800	5169.904	−20.039	5149.865
2002	258.865	207.092	317.958	318.468	254.366	20.000	1.800	4141.840	−0.734	4141.105
2003	217.046	173.637	325.510	318.468	260.408	20.000	1.800	3472.736	10.140	3482.877
2004	188.999	151.199	330.359	318.468	264.287	20.000	1.800	3023.984	17.123	3041.107
2005	171.519	137.215	333.830	318.468	267.064	20.000	1.800	2744.304	22.121	2766.425
2006	157.493	125.994	335.640	318.468	268.512	20.000	1.800	2519.888	24.728	2544.616
2007	142.196	113.757	337.926	318.468	270.341	20.000	1.800	2275.136	28.020	2303.156
2008	127.824	102.259	334.630	318.468	267.704	20.000	1.800	2045.184	23.273	2068.457
2009	115.919	92.735	333.677	318.468	266.942	20.000	1.800	1854.704	21.901	1876.605
2010	106.654	85.323	331.217	318.468	264.974	20.000	1.800	1706.464	18.359	1724.823
SUBTOTAL	3188.292	2550.634	3976.617	4410.035	3181.294	20.000	1.800	51012.672	−624.122	50388.555
REMAINING	97.549	78.039	329.824	318.468	263.859	20.000	1.800	1560.784	16.353	1577.137
TOT 15.6Yr	3285.841	2628.673	4306.441	4728.503	3445.153	20.000	1.800	52573.457	−607.769	51965.691

YEAR	NET TOTAL LOE	NET TANGIBLES	NET INTANGIBLES	NET G&G	NET TOTAL INVESTMENTS	NET LEASE REVENUE	NET BFIT CASHFLOW	CUM BFIT CASHFLOW	BFIT CF DISC 10.0%	CUMBFIT CF DISC 10.0%
========	===M$===	===M$===	===M$===	===M$===	===M$===	===M$===	===M$===	===M$===	===M$===	===M$===
1996(7 Mo)	56.000	3343.000	1216.000	250.000	4809.000	874.365	−3934.635	−3934.635	−3805.880	−3805.880
1997	4609.612	2730.000	375.000	0.000	3105.000	−3604.587	−6709.587	−10644.222	−5953.668	−9759.549
1998	2643.576	0.000	0.000	0.000	0.000	2096.383	2096.383	−8547.839	1620.992	−8138.557
1999	1459.535	0.000	0.000	0.000	0.000	6750.754	6750.754	−1797.085	5012.956	−3125.601
2000	1391.053	0.000	0.000	0.000	0.000	5012.823	5012.823	3215.738	3390.181	264.580
2001	1278.564	0.000	0.000	0.000	0.000	3871.301	3871.301	7087.040	2380.495	2645.075
2002	1183.695	0.000	0.000	0.000	0.000	2957.411	2957.411	10044.450	1652.453	4297.528
2003	1122.793	0.000	0.000	0.000	0.000	2360.084	2360.084	12404.534	1198.617	5496.145
2004	1079.716	0.000	0.000	0.000	0.000	1961.391	1961.391	14365.926	905.188	6401.332
2005	1052.281	0.000	0.000	0.000	0.000	1714.144	1714.144	16080.070	718.840	7120.172
2006	1029.693	0.000	0.000	0.000	0.000	1514.923	1514.923	17594.994	577.698	7697.870
2007	1004.162	0.000	0.000	0.000	0.000	1298.994	1298.994	18893.988	450.389	8148.260
2008	979.660	0.000	0.000	0.000	0.000	1088.797	1088.797	19982.785	343.189	8491.449
2009	960.336	0.000	0.000	0.000	0.000	916.269	916.269	20899.055	262.528	8753.978
2010	943.448	0.000	0.000	0.000	0.000	781.375	781.375	21680.430	203.475	8957.453
SUBTOTAL	20794.125	6073.000	1591.000	250.000	7914.000	29594.428	21680.430	21680.430	8957.453	8957.453
REMAINING	926.966	0.000	0.000	0.000	0.000	650.171	650.171	22330.600	153.933	9111.386
TOT 15.6Yr	21721.092	6073.000	1591.000	250.000	7914.000	30244.598	22330.600	22330.600	9111.386	9111.386

Table 16-1b

EVALUATION ANAC1.1

ECONOMIC EVALUATION
HARKEN PARADOX BASIN
REGA INCORPORATED

RUN DATE: 07-02-1997
RUN TIME: 10:01:40

AS OF DATE: JUN96

NAME: ANASAZI CO2 FLOOD-GAS PLANT
FIELD: ANASAZI-SAHGZIE
LOCATION: UTAH
FORMATION: DESERT CREEK
OPERATOR: HARKEN ENERGY

CONTINUOUS CO2 GAS RECYCLE
GAS PROCESSING FOR CO2 REMOVAL
SURFACE LINES - ZAPLOCK

NPV	5.0%	14327.741	BFIT	9163.573	AFIT
NPV	10.0%	9111.382	BFIT	5458.879	AFIT
NPV	15.0%	5567.312	BFIT	2899.006	AFIT
NPV	20.0%	3076.025	BFIT	1073.546	AFIT
NPV	25.0%	1275.586	BFIT	-261.466	AFIT
IRR		30%	BFIT	24%	AFIT
PAYOUT		MAY00	BFIT	JUL00	AFIT
PI		3.83:1	BFIT	2.87:1	AFIT

====== INTERESTS AND EFFECTIVE DATE ======

COST	OIL	GAS	COND	PRODT	DATE
1.00000	0.80000	0.80000	0.80000	0.80000	JUN96

	======== PRICES ========			========== GROSS RESERVES ==========				
	BEGINING	ENDING	AVERAGE	CUMULATIVE	REMAINING	ULTIMATE	% REMAINING	
OIL	20.00	20.00	20.00	1692.690	3285.841	4978.531	66.00	OIL
GAS	1.80	1.80	1.80	1308.810	4306.441	5615.251	76.69	GAS
COND	0.00	0.00	0.00	0.000	0.000	0.000	0.00	COND
PRDT	0.00	0.00	0.00	0.000	0.000	0.000	0.00	PRDT

YEAR	GROSS OIL PRODUCTION	NET OIL PRODUCTION	GROSS GAS PRODUCTION	GROSS GAS AS FUEL	NET GAS PRODUCTION	AVERAGE OIL PRICE	AVERAGE GAS PRICE	NET OIL SALES	NET GAS SALES	NET TOTAL REVENUE
========	==MBBLS==	==MBBLS==	==MMSCF==	==MMSCF==	==MMSCF==	===$/B===	==$/MSCF==	===M$===	===M$===	===M$===
1996(7 Mo)	54.774	43.819	52.810	15.323	42.248	20.000	1.800	876.384	53.981	930.365
1997	82.120	65.696	40.118	254.628	32.094	20.000	1.800	1313.920	-308.894	1005.026
1998	316.729	253.383	90.895	318.468	72.716	20.000	1.800	5067.664	-327.705	4739.959
1999	520.906	416.725	232.213	318.468	185.770	20.000	1.800	8334.496	-124.207	8210.289
2000	404.129	323.303	275.282	318.468	220.226	20.000	1.800	6466.064	-62.188	6403.876
2001	323.119	258.495	304.552	318.468	243.642	20.000	1.800	5169.904	-20.039	5149.865
2002	258.865	207.092	317.958	318.468	254.366	20.000	1.800	4141.840	-0.734	4141.105
2003	217.046	173.637	325.510	318.468	260.408	20.000	1.800	3472.736	10.140	3482.877
2004	188.999	151.199	330.359	318.468	264.287	20.000	1.800	3023.984	17.123	3041.107
2005	171.519	137.215	333.830	318.468	267.064	20.000	1.800	2744.304	22.121	2766.425
2006	157.493	125.994	335.640	318.468	268.512	20.000	1.800	2519.888	24.728	2544.616
2007	142.196	113.757	337.926	318.468	270.341	20.000	1.800	2275.136	28.020	2303.156
2008	127.824	102.259	334.630	318.468	267.704	20.000	1.800	2045.184	23.273	2068.457
2009	115.919	92.735	333.677	318.468	266.942	20.000	1.800	1854.704	21.901	1876.605
2010	106.654	85.323	331.217	318.468	264.974	20.000	1.800	1706.464	18.359	1724.823
SUBTOTAL	3188.292	2550.634	3976.617	4410.035	3181.294	20.000	1.800	51012.672	-624.122	50388.555
REMAINING	97.549	78.039	329.824	318.468	263.859	20.000	1.800	1560.784	16.353	1577.137
TOT 15.6Yr	3285.841	2628.673	4306.441	4728.503	3445.153	20.000	1.800	52573.457	-607.769	51965.691

YEAR	NET TOTAL INVESTMENTS	NET TOTAL REVENUE	NET LEASE REVENUE	NET BFIT CASHFLOW	NET TAX DEPREC	NET TAXABLE INCOME	NET INCOME TAXES PAID	NET AFIT CASHFLOW	CUM AFIT CASHFLOW	AFIT CF DISC 10.0%
========	===M$===	===M$===	===M$===	===M$===	===M$===	===M$B===	===M$===	===M$===	===M$===	===M$===
1996(7 Mo)	4809.000	930.365	874.365	-3934.635	477.571	-1069.206	0.000	-3934.635	-3934.635	-3805.880
1997	3105.000	1005.026	-3604.587	-6709.587	1208.694	-5188.281	0.000	-6709.587	-10644.222	-5953.668
1998	0.000	4739.959	2096.383	2096.383	1253.353	843.030	0.000	2096.383	-8547.839	1620.992
1999	0.000	8210.289	6750.754	6750.754	895.252	5855.502	149.955	6600.799	-1947.040	4906.385
2000	0.000	6403.876	5012.823	5012.823	639.466	4373.357	1486.942	3525.882	1578.842	2429.504
2001	0.000	5149.865	3871.301	3871.301	542.006	3329.295	1131.960	2739.341	4318.183	1715.648
2002	0.000	4141.105	2957.411	2957.411	542.006	2415.404	821.237	2136.173	6454.355	1213.956
2003	0.000	3482.877	2360.084	2360.084	392.827	1967.256	668.867	1691.217	8145.572	873.944
2004	0.000	3041.107	1961.391	1961.391	121.824	1839.567	625.453	1335.938	9481.511	629.189
2005	0.000	2766.425	1714.144	1714.144	0.000	1714.144	582.809	1131.335	10612.846	485.039
2006	0.000	2544.616	1514.923	1514.923	0.000	1514.923	515.074	999.849	11612.695	389.854
2007	0.000	2303.156	1298.994	1298.994	0.000	1298.994	441.658	857.336	12470.031	303.963
2008	0.000	2068.457	1088.797	1088.797	0.000	1088.797	370.191	718.606	13188.638	231.614
2009	0.000	1876.605	916.269	916.269	0.000	916.269	311.531	604.737	13793.375	177.169
2010	0.000	1724.823	781.375	781.375	0.000	781.375	265.667	515.707	14309.082	137.300
SUBTOTAL	7914.000	50388.555	29594.428	21680.430	6073.000	21680.428	7371.345	14309.082	14309.082	5355.007
REMAINING	0.000	1577.137	650.171	650.171	0.000	650.171	221.058	429.113	14738.194	103.875
TOT 15.6Yr	7914.000	51965.691	30244.598	22330.600	6073.000	22330.598	7592.403	14738.194	14738.194	5458.882

Table 16–2a

EVALUATION ANAC1.2

ECONOMIC EVALUATION

RUN DATE: 09–04–1997

HARKEN PARADOX BASIN

RUN TIME: 15:18:18

REGA INCORPORATED

AS OF DATE: JUN96

NAME: ANASAZI PRIMARY DEPLETION

FIELD: ANASAZI–SAHGZIE

LOCATION: UTAH

FORMATION: DESERT CREEK

OPERATOR: HARKEN ENERGY

CONTINUED PRIMARY DEPLETION

NPV	5.0%	10440.517	BFIT
NPV	10.0%	8299.962	BFIT
NPV	15.0%	6852.402	BFIT
NPV	20.0%	5828.308	BFIT
NPV	25.0%	5075.080	BFIT
IRR		>100%	BFIT
PAYOUT		JUN96	BFIT
PI		N/A	BFIT

====== INTERESTS AND EFFECTIVE DATE ======							======== PRICES ========			========== GROSS RESERVES ==========				
COST	OIL	GAS	COND	PRODT	DATE		BEGINING	ENDING	AVERAGE	CUMULATIVE	REMAINING	ULTIMATE	% REMAINING	
1.00000	0.80000	0.80000	0.80000	0.80000	JUN96	OIL	20.00	20.00	20.00	1692.690	879.533	2572.223	34.19	OIL
						GAS	1.80	1.80	1.80	1308.810	1240.814	2549.624	48.67	GAS
						COND	0.00	0.00	0.00	0.000	0.000	0.000	0.00	COND
						PRDT	0.00	0.00	0.00	0.000	0.000	0.000	0.00	PRDT

GROSS OIL YEAR ========	NET OIL PRODUCTION ==MBBLS==	GROSS GAS PRODUCTION ==MBBLS==	GROSS PRODUCTION ==MMSCF==	NET GAS GAS AS FUEL ==MMSCF==	AVERAGE PRODUCTION ==MMSCF==	AVERAGE OIL PRICE ===$/B===	NET GAS PRICE ==$/MSCF==	NET OIL SALES ===M$===	NET TOTAL GAS SALES ===M$===	REVENUE ===M$===
1996(7 Mo)	54.714	43.771	54.273	15.323	43.418	20.000	1.800	875.424	56.088	931.512
1997	86.601	69.281	86.366	26.268	69.093	20.000	1.800	1385.616	86.541	1472.157
1998	85.635	68.508	90.733	26.268	72.586	20.000	1.800	1370.160	92.830	1462.990
1999	81.935	65.548	93.873	26.268	75.098	20.000	1.800	1310.960	97.351	1408.311
2000	74.122	59.298	90.366	26.268	72.293	20.000	1.800	1185.952	92.301	1278.253
2001	63.532	50.826	85.752	26.268	68.602	20.000	1.800	1016.512	85.657	1102.169
2002	58.584	46.867	87.194	26.268	69.755	20.000	1.800	937.344	87.733	1025.077
2003	55.225	44.180	89.142	26.268	71.314	20.000	1.800	883.600	90.539	974.139
2004	52.380	41.904	88.762	26.268	71.010	20.000	1.800	838.080	89.991	928.071
2005	50.157	40.126	86.942	26.268	69.554	20.000	1.800	802.512	87.371	889.883
2006	48.254	38.603	85.269	26.268	68.215	20.000	1.800	772.064	84.961	857.025
2007	44.378	35.502	79.289	26.268	63.431	20.000	1.800	710.048	76.350	786.398
2008	37.047	29.638	66.941	26.268	53.553	20.000	1.800	592.752	58.569	651.321
2009	32.376	25.901	58.430	26.268	46.744	20.000	1.800	518.016	46.313	564.329
2010	28.653	22.922	51.467	26.268	41.174	20.000	1.800	458.448	36.287	494.735
SUBTOTAL	853.593	682.874	1194.799	383.075	955.839	20.000	1.800	13657.486	1168.883	14826.370
REMAINING	25.940	20.752	46.015	26.268	36.812	20.000	1.800	415.040	28.436	443.476
TOT 15.6Yr	879.533	703.626	1240.814	409.343	992.651	20.000	1.800	14072.526	1197.318	15269.846

YEAR ========	NET TOTAL LOE ===M$===	NET TANGIBLES ===M$===	NET INTANGIBLES ===M$===	NET G&G ===M$===	NET TOTAL INVESTMENTS ===M$===	NET LEASE REVENUE ===M$B===	NET BFIT CASHFLOW ===M$===	CUM BFIT CASHFLOW ===M$===	BFIT CF DISC 10.0% ===M$===	CUMBFIT CF DISC 10.0% ===M$===
1996(7 Mo)	56.000	0.000	0.000	0.000	0.000	875.512	875.512	875.512	848.504	848.504
1997	96.000	0.000	0.000	0.000	0.000	1376.157	1376.157	2251.669	1236.439	2084.942
1998	96.000	0.000	0.000	0.000	0.000	1366.990	1366.990	3618.659	1116.793	3201.735
1999	96.000	0.000	0.000	0.000	0.000	1312.311	1312.311	4930.970	974.677	4176.412
2000	96.000	0.000	0.000	0.000	0.000	1182.253	1182.253	6113.223	799.366	4975.778
2001	96.000	0.000	0.000	0.000	0.000	1006.169	1006.169	7119.392	617.953	5593.731
2002	96.000	0.000	0.000	0.000	0.000	929.077	929.077	8048.469	518.550	6112.281
2003	96.000	0.000	0.000	0.000	0.000	878.139	878.139	8926.607	445.522	6557.803
2004	96.000	0.000	0.000	0.000	0.000	832.071	832.071	9758.679	383.773	6941.576
2005	96.000	0.000	0.000	0.000	0.000	793.883	793.883	10552.562	332.839	7274.415
2006	96.000	0.000	0.000	0.000	0.000	761.025	761.025	11313.587	290.047	7564.462
2007	96.000	0.000	0.000	0.000	0.000	690.398	690.398	12003.985	239.730	7804.192
2008	96.000	0.000	0.000	0.000	0.000	555.321	555.321	12559.307	175.186	7979.378
2009	96.000	0.000	0.000	0.000	0.000	468.329	468.329	13027.636	134.302	8113.681
2010	96.000	0.000	0.000	0.000	0.000	398.735	398.735	13426.370	103.955	8217.636
SUBTOTAL	1400.000	0.000	0.000	0.000	0.000	13426.370	13426.370	13426.370	8217.636	8217.636
REMAINING	96.000	0.000	0.000	0.000	0.000	347.476	347.476	13773.846	82.327	8299.963
TOT 15.6Yr	1496.000	0.000	0.000	0.000	0.000	13773.846	13773.846	13773.846	8299.963	8299.963

Table 16–2b

EVALUATION ANAC1.2

ECONOMIC EVALUATION

RUN DATE: 09–04–1997

HARKEN PARADOX BASIN

RUN TIME: 15:24:12

REGA INCORPORATED

AS OF DATE: JUN96

NAME: ANASAZI PRIMARY DEPLETION

FIELD: ANASAZI–SAHGZIE

LOCATION: UTAH

FORMATION: DESERT CREEK

OPERATOR: HARKEN ENERGY

CONTINUED PRIMARY DEPLETION

NPV	5.0%	10440.517	BFIT	6967.401	AFIT
NPV	10.0%	8299.962	BFIT	5595.011	AFIT
NPV	15.0%	6852.402	BFIT	4661.930	AFIT
NPV	20.0%	5828.308	BFIT	3998.829	AFIT
NPV	25.0%	5075.080	BFIT	3509.220	AFIT
IRR		>100%	BFIT	>100%	AFIT
PAYOUT		JUN96	BFIT	JUN96	AFIT
PI		N/A	BFIT	N/A	AFIT

====== INTERESTS AND EFFECTIVE DATE ======						======== PRICES ========				========== GROSS RESERVES ==========				
COST	OIL	GAS	COND	PRODT	DATE		BEGINING	ENDING	AVERAGE	CUMULATIVE	REMAINING	ULTIMATE	% REMAINING	
1.00000	0.80000	0.80000	0.80000	0.80000	JUN96	OIL	20.00	20.00	20.00	1692.690	879.533	2572.223	34.19	OIL
						GAS	1.80	1.80	1.80	1308.810	1240.814	2549.624	48.67	GAS
						COND	0.00	0.00	0.00	0.000	0.000	0.000	0.00	COND
						PRDT	0.00	0.00	0.00	0.000	0.000	0.000	0.00	PRDT

GROSS OIL YEAR	NET OIL PRODUCTION	GROSS GAS PRODUCTION	GROSS PRODUCTION	NET GAS GAS AS FUEL	AVERAGE PRODUCTION	AVERAGE OIL PRICE	NET GAS PRICE	NET OIL SALES	NET TOTAL GAS SALES	REVENUE
========	==MBBLS==	==MBBLS==	==MMSCF==	==MMSCF==	==MMSCF==	===$/B===	==$/MSCF==	===M$===	===M$===	===M$===
1996(7 Mo)	54.714	43.771	54.273	15.323	43.418	20.000	1.800	875.424	56.088	931.512
1997	86.601	69.281	86.366	26.268	69.093	20.000	1.800	1385.616	86.541	1472.157
1998	85.635	68.508	90.733	26.268	72.586	20.000	1.800	1370.160	92.830	1462.990
1999	81.935	65.548	93.873	26.268	75.098	20.000	1.800	1310.960	97.351	1408.311
2000	74.122	59.298	90.366	26.268	72.293	20.000	1.800	1185.952	92.301	1278.253
2001	63.532	50.826	85.752	26.268	68.602	20.000	1.800	1016.512	85.657	1102.169
2002	58.584	46.867	87.194	26.268	69.755	20.000	1.800	937.344	87.733	1025.077
2003	55.225	44.180	89.142	26.268	71.314	20.000	1.800	883.600	90.539	974.139
2004	52.380	41.904	88.762	26.268	71.010	20.000	1.800	838.080	89.991	928.071
2005	50.157	40.126	86.942	26.268	69.554	20.000	1.800	802.512	87.371	889.883
2006	48.254	38.603	85.269	26.268	68.215	20.000	1.800	772.064	84.961	857.025
2007	44.378	35.502	79.289	26.268	63.431	20.000	1.800	710.048	76.350	786.398
2008	37.047	29.638	66.941	26.268	53.553	20.000	1.800	592.752	58.569	651.321
2009	32.376	25.901	58.430	26.268	46.744	20.000	1.800	518.016	46.313	564.329
2010	28.653	22.922	51.467	26.268	41.174	20.000	1.800	458.448	36.287	494.735
SUBTOTAL	853.593	682.874	1194.799	383.075	955.839	20.000	1.800	13657.486	1168.883	14826.370
REMAINING	25.940	20.752	46.015	26.268	36.812	20.000	1.800	415.040	28.436	443.476
TOT 15.6Yr	879.533	703.626	1240.814	409.343	992.651	20.000	1.800	14072.526	1197.318	15269.846

YEAR	NET TOTAL INVESTMENTS	NET TOTAL REVENUE	NET LEASE REVENUE	NET BFIT CASHFLOW	NET TAX DEPREC	NET TAXABLE INCOME	NET INCOME TAXES PAID	NET AFIT CASHFLOW	CUM AFIT CASHFLOW	AFIT CF DISC 10.0%
========	===M$===	===M$===	===M$===	===M$===	===M$===	===M$B===	===M$===	===M$===	===M$===	===M$===
1996(7 Mo)	0.000	931.512	875.512	875.512	0.000	875.512	297.674	577.838	577.838	566.928
1997	0.000	1472.157	1376.157	1376.157	0.000	1376.157	467.893	908.264	1486.102	834.084
1998	0.000	1462.990	1366.990	1366.990	0.000	1366.990	464.776	902.213	2388.315	753.453
1999	0.000	1408.311	1312.311	1312.311	0.000	1312.311	446.186	866.125	3254.440	657.580
2000	0.000	1278.253	1182.253	1182.253	0.000	1182.253	401.966	780.287	4034.727	539.666
2001	0.000	1102.169	1006.169	1006.169	0.000	1006.169	342.097	664.072	4698.799	417.024
2002	0.000	1025.077	929.077	929.077	0.000	929.077	315.886	613.191	5311.990	349.884
2003	0.000	974.139	878.139	878.139	0.000	878.139	298.567	579.571	5891.561	300.596
2004	0.000	928.071	832.071	832.071	0.000	832.071	282.904	549.167	6440.728	258.934
2005	0.000	889.883	793.883	793.883	0.000	793.883	269.920	523.963	6964.690	224.557
2006	0.000	857.025	761.025	761.025	0.000	761.025	258.749	502.277	7466.967	195.683
2007	0.000	786.398	690.398	690.398	0.000	690.398	234.735	455.663	7922.630	161.906
2008	0.000	651.321	555.321	555.321	0.000	555.321	188.809	366.512	8289.142	118.279
2009	0.000	564.329	468.329	468.329	0.000	468.329	159.232	309.097	8598.239	90.673
2010	0.000	494.735	398.735	398.735	0.000	398.735	135.570	263.165	8861.404	70.186
SUBTOTAL	0.000	14826.370	13426.370	13426.370	0.000	13426.370	4564.966	8861.404	8861.404	5539.433
REMAINING	0.000	443.476	347.476	347.476	0.000	347.476	118.142	229.334	9090.738	55.575
TOT 15.6Yr	0.000	15269.846	13773.846	13773.846	0.000	13773.846	4683.107	9090.738	9090.738	5595.008

Table 16--3b

EVALUATION ANAC1.3

ECONOMIC EVALUATION
HARKEN PARADOX BASIN
REGA INCORPORATED

RUN DATE: 07-10-1997
RUN TIME: 17:12:59

AS OF DATE: JUN96

NPV	5.0%	17630.217	BFIT	11490.055	AFIT
NPV	10.0%	12144.982	BFIT	7707.753	AFIT
NPV	15.0%	8379.468	BFIT	5069.691	AFIT
NPV	20.0%	5700.107	BFIT	3165.975	AFIT
NPV	25.0%	3736.405	BFIT	1753.528	AFIT
IRR		42%	BFIT	34%	AFIT
PAYOUT		OCT 99	BFIT	NOV 99	AFIT
PI		6.41:1	BFIT	4.57:1	AFIT

NAME: ANASAZI CO2 FLOOD RECYCLE ALL
FIELD: ANASAZI-SAHGZIE
LOCATION: UTAH
FORMATION: DESERT CREEK
OPERATOR: HARKEN ENERGY

CONTINUOUS CO2 GAS RECYCLE
NO GAS PROCESSING BUY FUEL
SURFACE LINES - ZAPLOCK

====== INTERESTS AND EFFECTIVE DATE ======						======== PRICES ========				========== GROSS RESERVES ==========			
COST	OIL	GAS	COND	PRODT	DATE		BEGINING	ENDING	AVERAGE	CUMULATIVE	REMAINING	ULTIMATE	%REMAINING	
1.00000	0.80000	0.80000	0.80000	0.80000	JUN96	OIL	20.00	20.00	20.00	1692.690	3344.399	5037.089	66.40	OIL
						GAS	1.80	0.00	1.80	1308.810	88.141	1396.951	6.31	GAS
						COND	0.00	0.00	0.00	0.000	0.000	0.000	0.00	COND
						PRDT	0.00	0.00	0.00	0.000	0.000	0.000	0.00	PRDT

GROSS OIL YEAR	NET OIL PRODUCTION	GROSS GAS PRODUCTION	GROSS PRODUCTION	NET GAS GAS AS FUEL	AVERAGE PRODUCTION	AVERAGE OIL PRICE	NET GAS PRICE	NET OIL SALES	NET TOTAL GAS SALES	REVENUE
========	==MBBLS==	==MBBLS==	==MMSCF==	==MMSCF==	==MMSCF==	===$/B===	==$/MSCF==	===M$===	===M$===	===M$===
1996(7 Mo)	54.774	43.819	52.810	15.323	42.248	20.000	1.800	876.384	53.981	930.365
1997	82.120	65.696	35.331	95.394	28.265	20.000	1.800	1313.920	-86.491	1227.429
1998	316.729	253.383	0.000	0.000	0.000	20.000	0.000	5067.664	0.000	5067.664
1999	521.095	416.876	0.000	0.000	0.000	20.000	0.000	8337.521	0.000	8337.521
2000	406.741	325.393	0.000	0.000	0.000	20.000	0.000	6507.856	0.000	6507.856
2001	326.351	261.081	0.000	0.000	0.000	20.000	0.000	5221.615	0.000	5221.615
2002	263.997	211.198	0.000	0.000	0.000	20.000	0.000	4223.952	0.000	4223.952
2003	222.703	178.162	0.000	0.000	0.000	20.000	0.000	3563.248	0.000	3563.248
2004	194.597	155.678	0.000	0.000	0.000	20.000	0.000	3113.552	0.000	3113.552
2005	177.929	142.343	0.000	0.000	0.000	20.000	0.000	2846.864	0.000	2846.864
2006	163.003	130.402	0.000	0.000	0.000	20.000	0.000	2608.048	0.000	2608.048
2007	147.588	118.070	0.000	0.000	0.000	20.000	0.000	2361.408	0.000	2361.408
2008	133.133	106.506	0.000	0.000	0.000	20.000	0.000	2130.128	0.000	2130.128
2009	120.594	96.475	0.000	0.000	0.000	20.000	0.000	1929.504	0.000	1929.504
2010	110.609	88.487	0.000	0.000	0.000	20.000	0.000	1769.744	0.000	1769.744
SUBTOTAL	3241.962	2593.570	88.141	110.717	70.513	20.000	1.800	51871.406	-32.509	51838.898
REMAINING	102.437	81.950	0.000	0.000	0.000	20.000	0.000	1638.992	0.000	1638.992
TOT 15.6Yr	3344.399	2675.520	88.141	110.717	70.513	20.000	1.800	53510.398	-32.509	53477.891

YEAR	NET TOTAL INVESTMENTS	NET TOTAL REVENUE	NET LEASE REVENUE	NET BFIT CASHFLOW	NET TAX DEPREC	NET TAXABLE INCOME	NET INCOME TAXES PAID	NET AFIT CASHFLOW	CUM AFIT CASHFLOW	AFIT CF DISC 10.0%
========	===M$===	===M$===	===M$===	===M$===	===M$===	===M$B===	===M$===	===M$===	===M$===	===M$===
1996(7 Mo)	4809.000	930.365	874.365	-3934.635	477.571	-1069.206	0.000	-3934.635	-3934.635	-3805.880
1997	0.000	1227.429	-3502.995	-3502.995	818.694	-4321.689	0.000	-3502.995	-7437.630	-3150.424
1998	0.000	5067.664	2194.898	2194.898	584.781	1610.117	0.000	2194.898	-5242.732	1702.295
1999	0.000	8337.521	6761.355	6761.355	417.701	6343.654	871.378	5889.978	647.246	4401.961
2000	0.000	6507.856	5034.356	5034.356	298.358	4735.998	1610.239	3424.117	4071.362	2364.593
2001	0.000	5221.615	3884.380	3884.380	298.358	3586.022	1219.248	2665.133	6736.495	1672.314
2002	0.000	4223.952	2992.865	2992.865	298.358	2694.507	916.133	2076.733	8813.228	1183.075
2003	0.000	3563.248	2398.423	2398.423	149.179	2249.244	764.743	1633.680	10446.908	846.807
2004	0.000	3113.552	1996.198	1996.198	0.000	1996.198	678.707	1317.491	11764.398	621.735
2005	0.000	2846.864	1759.164	1759.164	0.000	1759.164	598.116	1161.048	12925.446	497.875
2006	0.000	2608.048	1545.431	1545.431	0.000	1545.431	525.447	1019.985	13945.431	397.707
2007	0.000	2361.408	1324.956	1324.956	0.000	1324.956	450.485	874.471	14819.901	310.029
2008	0.000	2130.128	1117.419	1117.419	0.000	1117.419	379.922	737.496	15557.397	237.686
2009	0.000	1929.504	936.016	936.016	0.000	936.016	318.245	617.771	16175.168	181.008
2010	0.000	1769.744	791.603	791.603	0.000	791.603	269.145	522.458	16697.627	139.154
SUBTOTAL	4809.000	51838.898	30108.436	25299.436	3343.000	25299.436	8601.809	16697.627	16697.627	7599.935
REMAINING	0.000	1638.992	674.789	674.789	0.000	674.789	229.428	445.361	17142.988	107.819
TOT 15.6Yr	4809.000	53477.891	30783.225	25974.225	3343.000	25974.225	8831.236	17142.988	17142.988	7707.754

Table 16–4a

EVALUATION ANAC1.4

ECONOMIC EVALUATION

RUN DATE: 07–10–1997

HARKEN PARADOX BASIN

RUN TIME: 17:40:47

REGA INCORPORATED

AS OF DATE: JUN96

NAME: ANASAZI CO2 FLOOD LEASE COMP
FIELD: ANASAZI–SAHGZIE
LOCATION: UTAH
FORMATION: DESERT CREEK
OPERATOR: HARKEN ENERGY

CONTINUOUS CO2 GAS RECYCLE
NO GAS PROCESSING BUY FUEL
LEASE INJECTION COMPRESSOR
SURFACE LINES – ZAPLOCK

NPV	5.0%	15799.687	BFIT
NPV	10.0%	11229.655	BFIT
NPV	15.0%	8034.524	BFIT
NPV	20.0%	5727.375	BFIT
NPV	25.0%	4016.556	BFIT
IRR		48%	BFIT
PAYOUT		AUG99	BFIT
PI		8.19:1	BFIT

====== INTERESTS AND EFFECTIVE DATE ======						======== PRICES ========			========== GROSS RESERVES ==========				
COST	OIL	GAS	COND	PRODT	DATE		BEGINING	ENDING	AVERAGE	CUMULATIVE	REMAINING	ULTIMATE	% REMAINING	
1.00000	0.80000	0.80000	0.80000	0.80000	JUN96	OIL	20.00	20.00	20.00	1692.690	3344.399	5037.089	66.40	OIL
						GAS	1.80	0.00	1.80	1308.810	88.141	1396.951	6.31	GAS
						COND	0.00	0.00	0.00	0.000	0.000	0.000	0.00	COND
						PRDT	0.00	0.00	0.00	0.000	0.000	0.000	0.00	PRDT

YEAR	GROSS OIL PRODUCTION	NET OIL PRODUCTION	GROSS GAS PRODUCTION	GROSS GAS AS FUEL	NET GAS PRODUCTION	AVERAGE OIL PRICE	AVERAGE GAS PRICE	NET OIL SALES	NET GAS SALES	NET TOTAL REVENUE
========	==MBBLS==	==MBBLS==	==MMSCF==	==MMSCF==	==MMSCF==	===$/B===	==$/MSCF==	===M$===	===M$===	===M$===
1996(7 Mo)	54.774	43.819	52.810	15.323	42.248	20.000	1.800	876.384	53.981	930.365
1997	82.120	65.696	35.331	95.394	28.265	20.000	1.800	1313.920	−86.491	1227.429
1998	316.729	253.383	0.000	0.000	0.000	20.000	0.000	5067.664	0.000	5067.664
1999	521.095	416.876	0.000	0.000	0.000	20.000	0.000	8337.521	0.000	8337.521
2000	406.741	325.393	0.000	0.000	0.000	20.000	0.000	6507.856	0.000	6507.856
2001	326.351	261.081	0.000	0.000	0.000	20.000	0.000	5221.615	0.000	5221.615
2002	263.997	211.198	0.000	0.000	0.000	20.000	0.000	4223.952	0.000	4223.952
2003	222.703	178.162	0.000	0.000	0.000	20.000	0.000	3563.248	0.000	3563.248
2004	194.597	155.678	0.000	0.000	0.000	20.000	0.000	3113.552	0.000	3113.552
2005	177.929	142.343	0.000	0.000	0.000	20.000	0.000	2846.864	0.000	2846.864
2006	163.003	130.402	0.000	0.000	0.000	20.000	0.000	2608.048	0.000	2608.048
2007	147.588	118.070	0.000	0.000	0.000	20.000	0.000	2361.408	0.000	2361.408
2008	133.133	106.506	0.000	0.000	0.000	20.000	0.000	2130.128	0.000	2130.128
2009	120.594	96.475	0.000	0.000	0.000	20.000	0.000	1929.504	0.000	1929.504
2010	110.609	88.487	0.000	0.000	0.000	20.000	0.000	1769.744	0.000	1769.744
SUBTOTAL	3241.962	2593.570	88.141	110.717	70.513	20.000	1.800	51871.406	−32.509	51838.898
REMAINING	102.437	81.950	0.000	0.000	0.000	20.000	0.000	1638.992	0.000	1638.992
TOT 15.6Yr	3344.399	2675.520	88.141	110.717	70.513	20.000	1.800	53510.398	−32.509	53477.891

YEAR	NET TOTAL LOE	NET TANGIBLES	NET INTANGIBLES	NET G&G	NET TOTAL INVESTMENTS	NET LEASE REVENUE	NET BFIT CASH FLOW	CUM BFIT CASH FLOW	BFIT CF DISC 10.0%	CUM BFITCF DISC 10.0%
========	==MBBLS==	==MBBLS==	==MMSCF==	==MMSCF==	==MMSCF==	===$/B===	==$/MSCF==	===M$===	===M$===	===M$===
1996(7 Mo)	56.000	1763.000	1133.000	250.000	3146.000	874.365	−2271.635	−2271.635	−2194.884	−2194.884
1997	5066.424	0.000	0.000	0.000	0.000	−3838.995	−3838.995	−6110.629	−3452.374	−5647.258
1998	3208.766	0.000	0.000	0.000	0.000	1858.898	1858.898	−4251.731	1427.794	−4219.463
1999	1912.165	0.000	0.000	0.000	0.000	6425.355	6425.355	2173.624	4771.689	552.226
2000	1809.500	0.000	0.000	0.000	0.000	4698.356	4698.356	6871.980	3178.069	3730.295
2001	1673.235	0.000	0.000	0.000	0.000	3548.380	3548.380	10420.360	2182.193	5912.488
2002	1567.087	0.000	0.000	0.000	0.000	2656.865	2656.865	13077.226	1484.754	7397.242
2003	1500.825	0.000	0.000	0.000	0.000	2062.423	2062.423	15139.648	1047.575	8444.816
2004	1453.354	0.000	0.000	0.000	0.000	1660.198	1660.198	16799.846	766.286	9211.102
2005	1423.700	0.000	0.000	0.000	0.000	1423.164	1423.164	18223.010	596.955	9808.057
2006	1398.617	0.000	0.000	0.000	0.000	1209.432	1209.432	19432.441	461.277	10269.333
2007	1372.452	0.000	0.000	0.000	0.000	988.956	988.956	20421.396	342.967	10612.301
2008	1348.708	0.000	0.000	0.000	0.000	781.420	781.420	21202.816	246.363	10858.664
2009	1329.487	0.000	0.000	0.000	0.000	600.017	600.017	21802.834	171.996	11030.660
2010	1314.141	0.000	0.000	0.000	0.000	455.603	455.603	22258.438	118.732	11149.392
SUBTOTAL	26434.459	1763.000	1133.000	250.000	3146.000	25404.438	22258.438	22258.438	11149.392	11149.392
REMAINING	1300.203	0.000	0.000	0.000	0.000	338.789	338.789	22597.227	80.259	11229.650
TOT 15.6Yr	27734.662	1763.000	1133.000	250.000	3146.000	25743.227	22597.227	22597.227	11229.650	11229.650

Table 16–4b

EVALUATION ANAC1.4

ECONOMIC EVALUATION

RUN DATE: 07–10–1997

HARKEN PARADOX BASIN

RUN TIME: 17:41:35

REGA INCORPORATED

AS OF DATE: JUN96

NAME: ANASAZI CO2 FLOOD LEASE COMP

FIELD: ANASAZI–SAHGZIE

LOCATION: UTAH

FORMATION: DESERT CREEK

OPERATOR: HARKEN ENERGY

CONTINUOUS CO2 GAS RECYCLE
NO GAS PROCESSING BUY FUEL
LEASE INJECTION COMPRESSOR
SURFACE LINES – ZAPLOCK

NPV	5.0%	15799.687	BFIT	10337.381	AFIT
NPV	10.0%	11229.655	BFIT	7210.232	AFIT
NPV	15.0%	8034.524	BFIT	4992.118	AFIT
NPV	20.0%	5727.375	BFIT	3369.987	AFIT
NPV	25.0%	4016.556	BFIT	2153.813	AFIT
IRR		48%	BFIT	39%	AFIT
PAYOUT		AUG99	BFIT	OCT99	AFIT
PI		8.19:1	BFIT	5.75:1	AFIT

====== INTERESTS AND EFFECTIVE DATE ======					
COST	OIL	GAS	COND	PRODT	DATE
1.00000	0.80000	0.80000	0.80000	0.80000	JUN96

	======== PRICES ========			========== GROSS RESERVES ==========				
	BEGINING	ENDING	AVERAGE	CUMULATIVE	REMAINING	ULTIMATE	% REMAINING	
OIL	20.00	20.00	20.00	1692.690	3344.399	5037.089	66.40	OIL
GAS	1.80	0.00	1.80	1308.810	88.141	1396.951	6.31	GAS
COND	0.00	0.00	0.00	0.000	0.000	0.000	0.00	COND
PRDT	0.00	0.00	0.00	0.000	0.000	0.000	0.00	PRDT

GROSS OIL YEAR ========	NET OIL PRODUCTION ==MBBLS==	GROSS GAS PRODUCTION ==MBBLS==	GROSS PRODUCTION ==MMSCF==	NET GAS GAS AS FUEL ==MMSCF==	AVERAGE PRODUCTION ==MMSCF==	AVERAGE OIL PRICE ===$/B===	NET GAS PRICE ==$/MSCF==	NET OIL SALES ===M$===	NET TOTAL GAS SALES ===M$===	REVENUE ===M$===
1996(7 Mo)	54.774	43.819	52.810	15.323	42.248	20.000	1.800	876.384	53.981	930.365
1997	82.120	65.696	35.331	95.394	28.265	20.000	1.800	1313.920	−86.491	1227.429
1998	316.729	253.383	0.000	0.000	0.000	20.000	0.000	5067.664	0.000	5067.664
1999	521.095	416.876	0.000	0.000	0.000	20.000	0.000	8337.521	0.000	8337.521
2000	406.741	325.393	0.000	0.000	0.000	20.000	0.000	6507.856	0.000	6507.856
2001	326.351	261.081	0.000	0.000	0.000	20.000	0.000	5221.615	0.000	5221.615
2002	263.997	211.198	0.000	0.000	0.000	20.000	0.000	4223.952	0.000	4223.952
2003	222.703	178.162	0.000	0.000	0.000	20.000	0.000	3563.248	0.000	3563.248
2004	194.597	155.678	0.000	0.000	0.000	20.000	0.000	3113.552	0.000	3113.552
2005	177.929	142.343	0.000	0.000	0.000	20.000	0.000	2846.864	0.000	2846.864
2006	163.003	130.402	0.000	0.000	0.000	20.000	0.000	2608.048	0.000	2608.048
2007	147.588	118.070	0.000	0.000	0.000	20.000	0.000	2361.408	0.000	2361.408
2008	133.133	106.506	0.000	0.000	0.000	20.000	0.000	2130.128	0.000	2130.128
2009	120.594	96.475	0.000	0.000	0.000	20.000	0.000	1929.504	0.000	1929.504
2010	110.609	88.487	0.000	0.000	0.000	20.000	0.000	1769.744	0.000	1769.744
SUBTOTAL	3241.962	2593.570	88.141	110.717	70.513	20.000	1.800	51871.406	−32.509	51838.898
REMAINING	102.437	81.950	0.000	0.000	0.000	20.000	0.000	1638.992	0.000	1638.992
TOT 15.6Yr	3344.399	2675.520	88.141	110.717	70.513	20.000	1.800	53510.398	−32.509	53477.891

YEAR ========	NET TOTAL INVESTMENTS ===M$===	NET TOTAL REVENUE ===M$===	NET LEASE REVENUE ===M$===	NET BFIT CASHFLOW ===M$===	NET TAX DEPREC ===M$===	NET TAXABLE INCOME ===M$B===	NET INCOME TAXES PAID ===M$===	NET AFIT CASH FLOW ===M$===	CUM AFIT CASH FLOW ===M$===	AFIT CF DISC 10.0% ===M$===
1996(7 Mo)	3146.000	930.365	874.365	−2271.635	251.857	−760.492	0.000	−2271.635	−2271.635	−2194.884
1997	0.000	1227.429	−3838.995	−3838.995	431.755	−4270.750	0.000	−3838.995	−6110.629	−3452.374
1998	0.000	5067.664	1858.898	1858.898	308.396	1550.501	0.000	1858.898	−4251.731	1427.794
1999	0.000	8337.521	6425.355	6425.355	220.283	6205.072	926.273	5499.083	1247.351	4113.403
2000	0.000	6507.856	4698.356	4698.356	157.345	4541.011	1543.944	3154.412	4401.763	2180.565
2001	0.000	5221.615	3548.380	3548.380	157.345	3391.035	1152.952	2395.428	6797.191	1505.016
2002	0.000	4223.952	2656.865	2656.865	157.345	2499.520	849.837	1807.028	8604.220	1030.986
2003	0.000	3563.248	2062.423	2062.423	78.673	1983.751	674.475	1387.948	9992.168	720.180
2004	0.000	3113.552	1660.198	1660.198	0.000	1660.198	564.467	1095.731	11087.898	517.198
2005	0.000	2846.864	1423.164	1423.164	0.000	1423.164	483.876	939.288	12027.187	402.842
2006	0.000	2608.048	1209.432	1209.432	0.000	1209.432	411.207	798.225	12825.411	311.313
2007	0.000	2361.408	988.956	988.956	0.000	988.956	336.245	652.711	13478.122	231.489
2008	0.000	2130.128	781.420	781.420	0.000	781.420	265.683	515.737	13993.859	166.287
2009	0.000	1929.504	600.017	600.017	0.000	600.017	204.006	396.011	14389.870	116.099
2010	0.000	1769.744	455.603	455.603	0.000	455.603	154.905	300.698	14690.568	80.146
SUBTOTAL	3146.000	51838.898	25404.438	22258.438	1763.000	22258.438	7567.869	14690.568	14690.568	7156.061
REMAINING	0.000	1638.992	338.789	338.789	0.000	338.789	115.188	223.601	14914.169	54.175
TOT 15.6Yr	3146.000	53477.891	25743.227	22597.227	1763.000	22597.227	7683.057	14914.169	14914.169	7210.236

Table 16–5a

EVALUATION ANAC1.5

ECONOMIC EVALUATION
HARKEN PARADOX BASIN
REGA INCORPORATED

RUN DATE: 07–10–1997
RUN TIME: 18:15:10

AS OF DATE: JUN96

NAME: ANASAZI CO2 FLOOD DOE SHARE
FIELD: ANASAZI–SAHGZIE
LOCATION: UTAH
FORMATION: DESERT CREEK
OPERATOR: HARKEN ENERGY

CONTINUOUS CO2 GAS RECYCLE
NO GAS PROCESSING BUY FUEL
DOE COST SHARING
SURFACE LINES – ZAPLOCK

NPV	5.0%	19727.865	BFIT
NPV	10.0%	14178.574	BFIT
NPV	15.0%	10353.683	BFIT
NPV	20.0%	7619.092	BFIT
NPV	25.0%	5603.872	BFIT
IRR		57%	BFIT
PAYOUT		JUN99	BFIT
PI		11.66:1	BFIT

====== INTERESTS AND EFFECTIVE DATE ======							======== PRICES ========			========== GROSS RESERVES ==========				
COST	OIL	GAS	COND	PRODT	DATE		BEGINING	ENDING	AVERAGE	CUMULATIVE	REMAINING	ULTIMATE	% REMAINING	
1.00000	0.80000	0.80000	0.80000	0.80000	JUN96	OIL	20.00	20.00	20.00	1692.690	3344.399	5037.089	66.40	OIL
						GAS	1.80	0.00	1.80	1308.810	88.141	1396.951	6.31	GAS
						COND	0.00	0.00	0.00	0.000	0.000	0.000	0.00	COND
						PRDT	0.00	0.00	0.00	0.000	0.000	0.000	0.00	PRDT

YEAR	GROSS OIL PRODUCTION	NET OIL PRODUCTION	GROSS GAS PRODUCTION	GROSS GAS AS FUEL	NET GAS PRODUCTION	AVERAGE OIL PRICE	AVERAGE GAS PRICE	NET OIL SALES	NET GAS SALES	NET TOTAL REVENUE
========	==MBBLS==	==MBBLS==	==MMSCF==	==MMSCF==	==MMSCF==	===$/B===	==$/MSCF==	===M$===	===M$===	===M$===
1996(7 Mo)	54.774	43.819	52.810	15.323	42.248	20.000	1.800	876.384	53.981	930.365
1997	82.120	65.696	35.331	95.394	28.265	20.000	1.800	1313.920	−86.491	1227.429
1998	316.729	253.383	0.000	0.000	0.000	20.000	0.000	5067.664	0.000	5067.664
1999	521.095	416.876	0.000	0.000	0.000	20.000	0.000	8337.521	0.000	8337.521
2000	406.741	325.393	0.000	0.000	0.000	20.000	0.000	6507.856	0.000	6507.856
2001	326.351	261.081	0.000	0.000	0.000	20.000	0.000	5221.615	0.000	5221.615
2002	263.997	211.198	0.000	0.000	0.000	20.000	0.000	4223.952	0.000	4223.952
2003	222.703	178.162	0.000	0.000	0.000	20.000	0.000	3563.248	0.000	3563.248
2004	194.597	155.678	0.000	0.000	0.000	20.000	0.000	3113.552	0.000	3113.552
2005	177.929	142.343	0.000	0.000	0.000	20.000	0.000	2846.864	0.000	2846.864
2006	163.003	130.402	0.000	0.000	0.000	20.000	0.000	2608.048	0.000	2608.048
2007	147.588	118.070	0.000	0.000	0.000	20.000	0.000	2361.408	0.000	2361.408
2008	133.133	106.506	0.000	0.000	0.000	20.000	0.000	2130.128	0.000	2130.128
2009	120.594	96.475	0.000	0.000	0.000	20.000	0.000	1929.504	0.000	1929.504
2010	110.609	88.487	0.000	0.000	0.000	20.000	0.000	1769.744	0.000	1769.744
SUBTOTAL	3241.962	2593.570	88.141	110.717	70.513	20.000	1.800	51871.406	−32.509	51838.898
REMAINING	102.437	81.950	0.000	0.000	0.000	20.000	0.000	1638.992	0.000	1638.992
TOT 15.6Yr	3344.399	2675.520	88.141	110.717	70.513	20.000	1.800	53510.398	−32.509	53477.891

YEAR	NET TOTAL LOE	NET TANGIBLES	NET INTANGIBLES	NET &G	NET TOTAL INVESTMENTS	NET LEASE REVENUE	NET BFIT CASHLOW	CUM BFIT CASHLOW	BFIT CF DISC 10.0%	CUMBFIT CF DISC 10.0%
========	===M$===	===M$===	===M$===	===M$===	===M$===	===M$B===	===M$===	===M$===	===M$===	===M$===
1996(7 Mo)	56.000	3343.000	1216.000	250.000	4809.000	874.365	−3934.635	−3934.635	−3805.880	−3805.880
1997	4730.424	−1507.000	−548.000	−112.000	−2167.000	−3502.995	−1335.995	−5270.630	−1116.832	−4922.712
1998	2872.766	0.000	0.000	0.000	0.000	2194.898	2194.898	−3075.732	1702.295	−3220.417
1999	1576.165	0.000	0.000	0.000	0.000	6761.355	6761.355	3685.624	5021.235	1800.818
2000	1473.500	0.000	0.000	0.000	0.000	5034.356	5034.356	8719.979	3404.929	5205.747
2001	1337.235	0.000	0.000	0.000	0.000	3884.380	3884.380	12604.359	2388.429	7594.176
2002	1231.087	0.000	0.000	0.000	0.000	2992.865	2992.865	15597.225	1672.241	9266.417
2003	1164.825	0.000	0.000	0.000	0.000	2398.423	2398.423	17995.648	1218.018	10484.435
2004	1117.354	0.000	0.000	0.000	0.000	1996.198	1996.198	19991.846	921.234	11405.669
2005	1087.700	0.000	0.000	0.000	0.000	1759.164	1759.164	21751.010	737.817	12143.486
2006	1062.617	0.000	0.000	0.000	0.000	1545.431	1545.431	23296.441	589.333	12732.819
2007	1036.452	0.000	0.000	0.000	0.000	1324.956	1324.956	24621.396	459.382	13192.201
2008	1012.709	0.000	0.000	0.000	0.000	1117.419	1117.419	25738.816	352.195	13544.396
2009	993.487	0.000	0.000	0.000	0.000	936.017	936.017	26674.834	268.207	13812.603
2010	978.141	0.000	0.000	0.000	0.000	791.603	791.603	27466.438	206.196	14018.799
SUBTOTAL	21730.461	1836.000	668.000	138.000	2642.000	30108.438	27466.438	27466.438	14018.799	14018.799
REMAINING	964.203	0.000	0.000	0.000	0.000	674.789	674.789	28141.227	159.772	14178.570
TOT 15.6Yr	22694.664	1836.000	668.000	138.000	2642.000	30783.227	28141.227	28141.227	14178.570	14178.570

Table 16–5b

EVALUATION ANAC1.5

ECONOMIC EVALUATION
HARKEN PARADOX BASIN
REGA INCORPORATED

RUN DATE: 07–10–1997
RUN TIME: 18:15:54

AS OF DATE: JUN96

NAME: ANASAZI CO2 FLOOD DOE SHARE
FIELD: ANASAZI–SAHGZIE
LOCATION: UTAH
FORMATION: DESERT CREEK
OPERATOR: HARKEN ENERGY

CONTINUOUS CO2 GAS RECYCLE
NO GAS PROCESSING BUY FUEL
DOE COST SHARING
SURFACE LINES – ZAPLOCK

NPV	5.0%	19727.865	BFIT	12969.105	AFIT
NPV	10.0%	14178.574	BFIT	9217.732	AFIT
NPV	15.0%	10353.683	BFIT	6597.384	AFIT
NPV	20.0%	7619.092	BFIT	4701.600	AFIT
NPV	25.0%	5603.872	BFIT	3289.802	AFIT
IRR		57%	BFIT	47%	AFIT
PAYOUT		JUN99	BFIT	AUG99	AFIT
PI		11.66:1	BFIT	8.03:1	AFIT

====== INTERESTS AND EFFECTIVE DATE ======

COST	OIL	GAS	COND	PRODT	DATE
1.00000	0.80000	0.80000	0.80000	0.80000	JUN96

	======== PRICES ========			========== GROSS RESERVES ==========				
	BEGINING	ENDING	AVERAGE	CUMULATIVE	REMAINING	ULTIMATE	% REMAINING	
OIL	20.00	20.00	20.00	1692.690	3344.399	5037.089	66.40	OIL
GAS	1.80	0.00	1.80	1308.810	88.141	1396.951	6.31	GAS
COND	0.00	0.00	0.00	0.000	0.000	0.000	0.00	COND
PRDT	0.00	0.00	0.00	0.000	0.000	0.000	0.00	PRDT

YEAR	GROSS OIL PRODUCTION	NET OIL PRODUCTION	GROSS GAS PRODUCTION	GROSS GAS AS FUEL	NET GAS PRODUCTION	AVERAGE OIL PRICE	AVERAGE GAS PRICE	NET OIL SALES	NET GAS SALES	NET TOTAL REVENUE
========	==MBBLS==	==MBBLS==	==MMSCF==	==MMSCF==	==MMSCF==	===$/B===	==$/MSCF==	===M$===	===M$===	===M$===
1996(7 Mo)	54.774	43.819	52.810	15.323	42.248	20.000	1.800	876.384	53.981	930.365
1997	82.120	65.696	35.331	95.394	28.265	20.000	1.800	1313.920	−86.491	1227.429
1998	316.729	253.383	0.000	0.000	0.000	20.000	0.000	5067.664	0.000	5067.664
1999	521.095	416.876	0.000	0.000	0.000	20.000	0.000	8337.521	0.000	8337.521
2000	406.741	325.393	0.000	0.000	0.000	20.000	0.000	6507.856	0.000	6507.856
2001	326.351	261.081	0.000	0.000	0.000	20.000	0.000	5221.615	0.000	5221.615
2002	263.997	211.198	0.000	0.000	0.000	20.000	0.000	4223.952	0.000	4223.952
2003	222.703	178.162	0.000	0.000	0.000	20.000	0.000	3563.248	0.000	3563.248
2004	194.597	155.678	0.000	0.000	0.000	20.000	0.000	3113.552	0.000	3113.552
2005	177.929	142.343	0.000	0.000	0.000	20.000	0.000	2846.864	0.000	2846.864
2006	163.003	130.402	0.000	0.000	0.000	20.000	0.000	2608.048	0.000	2608.048
2007	147.588	118.070	0.000	0.000	0.000	20.000	0.000	2361.408	0.000	2361.408
2008	133.133	106.506	0.000	0.000	0.000	20.000	0.000	2130.128	0.000	2130.128
2009	120.594	96.475	0.000	0.000	0.000	20.000	0.000	1929.504	0.000	1929.504
2010	110.609	88.487	0.000	0.000	0.000	20.000	0.000	1769.744	0.000	1769.744
SUBTOTAL	3241.962	2593.570	88.141	110.717	70.513	20.000	1.800	51871.406	−32.509	51838.898
REMAINING	102.437	81.950	0.000	0.000	0.000	20.000	0.000	1638.992	0.000	1638.992
TOT 15.6Yr	3344.399	2675.520	88.141	110.717	70.513	20.000	1.800	53510.398	−32.509	53477.891

YEAR	NET TOTAL INVESTMENTS	NET TOTAL REVENUE	NET LEASE REVENUE	NET BFIT CASH FLOW	NET TAX DEPREC	NET TAXABLE INCOME	NET INCOME TAXES PAID	NET AFIT CASH FLOW	CUM AFIT CASHFLOW	AFIT CF DISC 10.0%
========	===M$===	===M$===	===M$===	===M$===	===M$===	===M$B===	===M$===	===M$===	===M$===	===M$===
1996(7 Mo)	4809.000	930.365	874.365	−3934.635	477.571	−1069.206	0.000	−3934.635	−3934.635	−3805.880
1997	−2167.000	1227.429	−3502.995	−1335.995	−688.306	−2154.689	0.000	−1335.995	−5270.630	−1116.832
1998	0.000	5067.664	2194.898	2194.898	584.781	1610.117	0.000	2194.898	−3075.732	1702.295
1999	0.000	8337.521	6761.355	6761.355	417.701	6343.654	1608.158	5153.198	2077.466	3878.344
2000	0.000	6507.856	5034.356	5034.356	298.358	4735.998	1610.239	3424.117	5501.583	2364.593
2001	0.000	5221.615	3884.380	3884.380	298.358	3586.022	1219.248	2665.133	8166.715	1672.314
2002	0.000	4223.952	2992.865	2992.865	298.358	2694.507	916.133	2076.733	10243.448	1183.075
2003	0.000	3563.248	2398.423	2398.423	149.179	2249.244	764.743	1633.680	11877.129	846.807
2004	0.000	3113.552	1996.198	1996.198	0.000	1996.198	678.707	1317.491	13194.619	621.735
2005	0.000	2846.864	1759.164	1759.164	0.000	1759.164	598.116	1161.048	14355.667	497.875
2006	0.000	2608.048	1545.431	1545.431	0.000	1545.431	525.447	1019.985	15375.651	397.707
2007	0.000	2361.408	1324.956	1324.956	0.000	1324.956	450.485	874.471	16250.122	310.029
2008	0.000	2130.128	1117.419	1117.419	0.000	1117.419	379.922	737.496	16987.619	237.686
2009	0.000	1929.504	936.017	936.017	0.000	936.017	318.246	617.771	17605.391	181.008
2010	0.000	1769.744	791.603	791.603	0.000	791.603	269.145	522.458	18127.850	139.154
SUBTOTAL	2642.000	51838.898	30108.438	27466.438	1836.000	27466.438	9338.590	18127.850	18127.850	9109.910
REMAINING	0.000	1638.992	674.789	674.789	0.000	674.789	229.428	445.361	18573.211	107.819
TOT 15.6Yr	2642.000	53477.891	30783.227	28141.227	1836.000	28141.227	9568.018	18573.211	18573.211	9217.729

Table 16–6a

EVALUATION ANAC1.6

ECONOMIC EVALUATION
HARKEN PARADOX BASIN
REGA INCORPORATED

RUN DATE: 09–08–1997
RUN TIME: 17:51:55

AS OF DATE: JUN96

NAME: ANASAZI CO2 FLOOD LEASE DOE
FIELD: ANASAZI–SAHGZIE
LOCATION: UTAH
FORMATION: DESERT CREEK
OPERATOR: HARKEN ENERGY

CONTINUOUS CO2 GAS RECYCLE
NO GAS PROCESSING BUY FUEL
LEASE INJECTION COMPRESSOR
DOE COST SHARING
SURFACE LINES – ZAPLOCK

NPV	5.0%	17172.307	BFIT
NPV	10.0%	12560.359	BFIT
NPV	15.0%	9326.369	BFIT
NPV	20.0%	6983.083	BFIT
NPV	25.0%	5238.548	BFIT
IRR		62%	BFIT
PAYOUT		JUN99	BFIT
PI		14.90:1	BFIT

====== INTERESTS AND EFFECTIVE DATE ======

COST	OIL	GAS	COND	PRODT	DATE
1.00000	0.80000	0.80000	0.80000	0.80000	JUN96

	======== PRICES ========			========== GROSS RESERVES ==========				
	BEGINING	ENDING	AVERAGE	CUMULATIVE	REMAINING	ULTIMATE	% REMAINING	
OIL	20.00	20.00	20.00	1692.690	3344.399	5037.089	66.40	OIL
GAS	1.80	0.00	1.80	1308.810	88.141	1396.951	6.31	GAS
COND	0.00	0.00	0.00	0.000	0.000	0.000	0.00	COND
PRDT	0.00	0.00	0.00	0.000	0.000	0.000	0.00	PRDT

YEAR	GROSS OIL PRODUCTION	NET OIL PRODUCTION	GROSS GAS PRODUCTION	GROSS GAS AS FUEL	NET GAS PRODUCTION	AVERAGE OIL PRICE	AVERAGE GAS PRICE	NET OIL SALES	NET GAS SALES	NET TOTAL REVENUE
========	==MBBLS==	==MBBLS==	==MMSCF==	==MMSCF==	==MMSCF==	===$/B===	==$/MSCF==	===M$===	===M$===	===M$===
1996(7 Mo)	54.774	43.819	52.810	15.323	42.248	20.000	1.800	876.384	53.981	930.365
1997	82.120	65.696	35.331	95.394	28.265	20.000	1.800	1313.920	−86.491	1227.429
1998	316.729	253.383	0.000	0.000	0.000	20.000	0.000	5067.664	0.000	5067.664
1999	521.095	416.876	0.000	0.000	0.000	20.000	0.000	8337.521	0.000	8337.521
2000	406.741	325.393	0.000	0.000	0.000	20.000	0.000	6507.856	0.000	6507.856
2001	326.351	261.081	0.000	0.000	0.000	20.000	0.000	5221.615	0.000	5221.615
2002	263.997	211.198	0.000	0.000	0.000	20.000	0.000	4223.952	0.000	4223.952
2003	222.703	178.162	0.000	0.000	0.000	20.000	0.000	3563.248	0.000	3563.248
2004	194.597	155.678	0.000	0.000	0.000	20.000	0.000	3113.552	0.000	3113.552
2005	177.929	142.343	0.000	0.000	0.000	20.000	0.000	2846.864	0.000	2846.864
2006	163.003	130.402	0.000	0.000	0.000	20.000	0.000	2608.048	0.000	2608.048
2007	147.588	118.070	0.000	0.000	0.000	20.000	0.000	2361.408	0.000	2361.408
2008	133.133	106.506	0.000	0.000	0.000	20.000	0.000	2130.128	0.000	2130.128
2009	120.594	96.475	0.000	0.000	0.000	20.000	0.000	1929.504	0.000	1929.504
2010	110.609	88.487	0.000	0.000	0.000	20.000	0.000	1769.744	0.000	1769.744
SUBTOTAL	3241.962	2593.570	88.141	110.717	70.513	20.000	1.800	51871.406	−32.509	51838.898
REMAINING	102.437	81.950	0.000	0.000	0.000	20.000	0.000	1638.992	0.000	1638.992
TOT 15.6Yr	3344.399	2675.520	88.141	110.717	70.513	20.000	1.800	53510.398	−32.509	53477.891

YEAR	NET TOTAL LOE	NET TANGIBLES	NET INTANGIBLES	NET G&G	NET TOTAL INVESTMENTS	NET LEASE REVENUE	NET BFIT CASH FLOW	CUM BFIT CASH FLOW	BFIT CF DISC 10.0%	CUMBFIT CF DISC 10.0%
========	===M$===	===M$===	===M$===	===M$===	===M$===	===M$B===	===M$===	===M$===	===M$===	===M$===
1996(7 Mo)	56.000	1763.000	1133.000	250.000	3146.000	874.365	−2271.635	−2271.635	−2194.884	−2194.884
1997	5066.424	−795.000	−511.000	−112.000	−1418.000	−3838.995	−2420.995	−4692.629	−2121.671	−4316.555
1998	3208.766	0.000	0.000	0.000	0.000	1858.898	1858.898	−2833.731	1427.794	−2888.761
1999	1912.165	0.000	0.000	0.000	0.000	6425.355	6425.355	3591.624	4771.689	1882.929
2000	1809.500	0.000	0.000	0.000	0.000	4698.356	4698.356	8289.980	3178.069	5060.998
2001	1673.235	0.000	0.000	0.000	0.000	3548.380	3548.380	11838.360	2182.193	7243.191
2002	1567.087	0.000	0.000	0.000	0.000	2656.865	2656.865	14495.226	1484.754	8727.944
2003	1500.825	0.000	0.000	0.000	0.000	2062.423	2062.423	16557.648	1047.575	9775.520
2004	1453.354	0.000	0.000	0.000	0.000	1660.198	1660.198	18217.846	766.286	10541.805
2005	1423.700	0.000	0.000	0.000	0.000	1423.164	1423.164	19641.010	596.955	11138.760
2006	1398.617	0.000	0.000	0.000	0.000	1209.432	1209.432	20850.441	461.277	11600.036
2007	1372.452	0.000	0.000	0.000	0.000	988.956	988.956	21839.396	342.967	11943.004
2008	1348.709	0.000	0.000	0.000	0.000	781.419	781.419	22620.816	246.363	12189.367
2009	1329.487	0.000	0.000	0.000	0.000	600.017	600.017	23220.834	171.996	12361.363
2010	1314.141	0.000	0.000	0.000	0.000	455.603	455.603	23676.438	118.732	12480.095
SUBTOTAL	26434.459	968.000	622.000	138.000	1728.000	25404.438	23676.438	23676.438	12480.095	12480.095
REMAINING	1300.203	0.000	0.000	0.000	0.000	338.789	338.789	24015.227	80.259	12560.354
TOT 15.6Yr	27734.662	968.000	622.000	138.000	1728.000	25743.227	24015.227	24015.227	12560.354	12560.354

Table 16–6b

EVALUATION ANAC1.6

ECONOMIC EVALUATION
HARKEN PARADOX BASIN
REGA INCORPORATED

RUN DATE: 09–08–1997
RUN TIME: 17:52:55

AS OF DATE: JUN96

NAME: ANASAZI CO2 FLOOD LEASE DOE
FIELD: ANASAZI–SAHGZIE
LOCATION: UTAH
FORMATION: DESERT CREEK
OPERATOR: HARKEN ENERGY

CONTINUOUS CO2 GAS RECYCLE
NO GAS PROCESSING BUY FUEL
LEASE INJECTION COMPRESSOR
DOE COST SHARING
SURFACE LINES – ZAPLOCK

NPV	5.0%	17172.307	BFIT	11305.211	AFIT
NPV	10.0%	12560.359	BFIT	8198.299	AFIT
NPV	15.0%	9326.369	BFIT	5991.782	AFIT
NPV	20.0%	6983.083	BFIT	4374.841	AFIT
NPV	25.0%	5238.548	BFIT	3159.090	AFIT
IRR		62%	BFIT	51%	AFIT
PAYOUT		JUN99	BFIT	JUL99	AFIT
PI		14.90:1	BFIT	10.18:1	AFIT

====== INTERESTS AND EFFECTIVE DATE ======

COST	OIL	GAS	COND	PRODT	DATE
1.00000	0.80000	0.80000	0.80000	0.80000	JUN96

	======= PRICES =======			========== GROSS RESERVES ==========				
	BEGINING	ENDING	AVERAGE	CUMULATIVE	REMAINING	ULTIMATE	%REMAINING	
OIL	20.00	20.00	20.00	1692.690	3344.399	5037.089	66.40	OIL
GAS	1.80	0.00	1.80	1308.810	88.141	1396.951	6.31	GAS
COND	0.00	0.00	0.00	0.000	0.000	0.000	0.00	COND
PRDT	0.00	0.00	0.00	0.000	0.000	0.000	0.00	PRDT

YEAR	GROSS OIL PRODUCTION	NET OIL PRODUCTION	GROSS GAS PRODUCTION	GROSS GAS AS FUEL	NET GAS PRODUCTION	AVERAGE OIL PRICE	AVERAGE GAS PRICE	NET OIL SALES	NET GAS SALES	NET TOTAL REVENUE
========	==MBBLS==	==MBBLS==	==MMSCF==	==MMSCF==	==MMSCF==	===$/B===	==$/MSCF==	===M$===	===M$===	===M$===
1996(7 Mo)	54.774	43.819	52.810	15.323	42.248	20.000	1.800	876.384	53.981	930.365
1997	82.120	65.696	35.331	95.394	28.265	20.000	1.800	1313.920	−86.491	1227.429
1998	316.729	253.383	0.000	0.000	0.000	20.000	0.000	5067.664	0.000	5067.664
1999	521.095	416.876	0.000	0.000	0.000	20.000	0.000	8337.521	0.000	8337.521
2000	406.741	325.393	0.000	0.000	0.000	20.000	0.000	6507.856	0.000	6507.856
2001	326.351	261.081	0.000	0.000	0.000	20.000	0.000	5221.615	0.000	5221.615
2002	263.997	211.198	0.000	0.000	0.000	20.000	0.000	4223.952	0.000	4223.952
2003	222.703	178.162	0.000	0.000	0.000	20.000	0.000	3563.248	0.000	3563.248
2004	194.597	155.678	0.000	0.000	0.000	20.000	0.000	3113.552	0.000	3113.552
2005	177.929	142.343	0.000	0.000	0.000	20.000	0.000	2846.864	0.000	2846.864
2006	163.003	130.402	0.000	0.000	0.000	20.000	0.000	2608.048	0.000	2608.048
2007	147.588	118.070	0.000	0.000	0.000	20.000	0.000	2361.408	0.000	2361.408
2008	133.133	106.506	0.000	0.000	0.000	20.000	0.000	2130.128	0.000	2130.128
2009	120.594	96.475	0.000	0.000	0.000	20.000	0.000	1929.504	0.000	1929.504
2010	110.609	88.487	0.000	0.000	0.000	20.000	0.000	1769.744	0.000	1769.744
SUBTOTAL	3241.962	2593.570	88.141	110.717	70.513	20.000	1.800	51871.406	−32.509	51838.898
REMAINING	102.437	81.950	0.000	0.000	0.000	20.000	0.000	1638.992	0.000	1638.992
TOT 15.6Yr	3344.399	2675.520	88.141	110.717	70.513	20.000	1.800	53510.398	−32.509	53477.891

YEAR	NET TOTAL INVESTMENTS	NET TOTAL REVENUE	NET LEASE REVENUE	NET BFIT CASHFLOW	NET TAX DEPREC	NET TAXABLE INCOME	NET INCOME TAXES PAID	NET AFIT CASHFLOW	CUM AFIT CASHFLOW	AFIT CF DISC 10.0%
========	===M$===	===M$===	===M$===	===M$===	===M$===	===M$B===	===M$===	===M$===	===M$===	===M$===
1996(7 Mo)	3146.000	930.365	874.365	−2271.635	251.857	−760.492	0.000	−2271.635	−2271.635	−2194.884
1997	−1418.000	1227.429	−3838.995	−2420.995	−363.245	−2852.750	0.000	−2420.995	−4692.629	−2121.671
1998	0.000	5067.664	1858.898	1858.898	308.396	1550.501	0.000	1858.898	−2833.731	1427.794
1999	0.000	8337.521	6425.355	6425.355	220.283	6205.072	1408.393	5016.962	2183.231	3770.768
2000	0.000	6507.856	4698.356	4698.356	157.345	4541.011	1543.944	3154.412	5337.643	2180.565
2001	0.000	5221.615	3548.380	3548.380	157.345	3391.035	1152.952	2395.428	7733.071	1505.016
2002	0.000	4223.952	2656.865	2656.865	157.345	2499.520	849.837	1807.028	9540.100	1030.986
2003	0.000	3563.248	2062.423	2062.423	78.673	1983.751	674.475	1387.948	10928.048	720.180
2004	0.000	3113.552	1660.198	1660.198	0.000	1660.198	564.467	1095.731	12023.778	517.198
2005	0.000	2846.864	1423.164	1423.164	0.000	1423.164	483.876	939.288	12963.066	402.842
2006	0.000	2608.048	1209.432	1209.432	0.000	1209.432	411.207	798.225	13761.291	311.313
2007	0.000	2361.408	988.956	988.956	0.000	988.956	336.245	652.711	14414.002	231.489
2008	0.000	2130.128	781.419	781.419	0.000	781.419	265.682	515.737	14929.738	166.286
2009	0.000	1929.504	600.017	600.017	0.000	600.017	204.006	396.011	15325.749	116.099
2010	0.000	1769.744	455.603	455.603	0.000	455.603	154.905	300.698	15626.447	80.146
SUBTOTAL	1728.000	51838.898	25404.438	23676.438	968.000	23676.438	8049.989	15626.447	15626.447	8144.129
REMAINING	0.000	1638.992	338.789	338.789	0.000	338.789	115.188	223.601	15850.048	54.175
TOT 15.6Yr	1728.000	53477.891	25743.227	24015.227	968.000	24015.227	8165.177	15850.048	15850.048	8198.304

Table 16–7a

EVALUATION ANAC1.7

ECONOMIC EVALUATION
HARKEN PARADOX BASIN
REGA INCORPORATED

RUN DATE: 07–02–1997
RUN TIME: 10:24:54

AS OF DATE: JUN96

NAME: ANASAZI CO2 FLOOD–GAS PLANT
FIELD: ANASAZI–SAHGZIE
LOCATION: UTAH
FORMATION: DESERT CREEK
OPERATOR: HARKEN ENERGY

CONTINUOUS CO2 GAS RECYCLE
GAS PROCESSING FOR CO2 REMOVAL
BURIED LINES – HEATPRO

NPV	5.0%	13153.339	BFIT
NPV	10.0%	7967.233	BFIT
NPV	15.0%	4451.335	BFIT
NPV	20.0%	1986.364	BFIT
NPV	25.0%	210.581	BFIT
IRR		26%	BFIT
PAYOUT		JUL00	BFIT
PI		3.32:1	BFIT

====== INTERESTS AND EFFECTIVE DATE ======

COST	OIL	GAS	COND	PRODT	DATE
1.00000	0.80000	0.80000	0.80000	0.80000	JUN96

	======== PRICES ========			========== GROSS RESERVES ==========				
	BEGINING	ENDING	AVERAGE	CUMULATIVE	REMAINING	ULTIMATE	% REMAINING	
OIL	20.00	20.00	20.00	1692.690	3285.841	4978.531	66.00	OIL
GAS	1.80	1.80	1.80	1308.810	4306.441	5615.251	76.69	GAS
COND	0.00	0.00	0.00	0.000	0.000	0.000	0.00	COND
PRDT	0.00	0.00	0.00	0.000	0.000	0.000	0.00	PRDT

YEAR	GROSS OIL PRODUCTION	NET OIL PRODUCTION	GROSS GAS PRODUCTION	GROSS GAS AS FUEL	NET GAS PRODUCTION	AVERAGE OIL PRICE	AVERAGE GAS PRICE	NET OIL SALES	NET GAS SALES	NET TOTAL REVENUE
========	==MBBLS==	==MBBLS==	==MMSCF==	==MMSCF==	==MMSCF==	===$/B===	==$/MSCF==	===M$===	===M$===	===M$===
1996(7 Mo)	54.774	43.819	52.810	15.323	42.248	20.000	1.800	876.384	53.981	930.365
1997	82.120	65.696	40.118	254.628	32.094	20.000	1.800	1313.920	–308.894	1005.026
1998	316.729	253.383	90.895	318.468	72.716	20.000	1.800	5067.664	–327.705	4739.959
1999	520.906	416.725	232.213	318.468	185.770	20.000	1.800	8334.496	–124.207	8210.289
2000	404.129	323.303	275.282	318.468	220.226	20.000	1.800	6466.064	–62.188	6403.876
2001	323.119	258.495	304.552	318.468	243.642	20.000	1.800	5169.904	–20.039	5149.865
2002	258.865	207.092	317.958	318.468	254.366	20.000	1.800	4141.840	–0.734	4141.105
2003	217.046	173.637	325.510	318.468	260.408	20.000	1.800	3472.736	10.140	3482.877
2004	188.999	151.199	330.359	318.468	264.287	20.000	1.800	3023.984	17.123	3041.107
2005	171.519	137.215	333.830	318.468	267.064	20.000	1.800	2744.304	22.121	2766.425
2006	157.493	125.994	335.640	318.468	268.512	20.000	1.800	2519.888	24.728	2544.616
2007	142.196	113.757	337.926	318.468	270.341	20.000	1.800	2275.136	28.020	2303.156
2008	127.824	102.259	334.630	318.468	267.704	20.000	1.800	2045.184	23.273	2068.457
2009	115.919	92.735	333.677	318.468	266.942	20.000	1.800	1854.704	21.901	1876.605
2010	106.654	85.323	331.217	318.468	264.974	20.000	1.800	1706.464	18.359	1724.823
SUBTOTAL	3188.292	2550.634	3976.617	4410.035	3181.294	20.000	1.800	51012.672	–624.122	50388.555
REMAINING	97.549	78.039	329.824	318.468	263.859	20.000	1.800	1560.784	16.353	1577.137
TOT 15.6Yr	3285.841	2628.673	4306.441	4728.503	3445.153	20.000	1.800	52573.457	–607.769	51965.691

YEAR	NET TOTAL LOE	NET TANGIBLES	NET INTANGIBLES	NET G&G	NET TOTAL INVESTMENTS	NET LEASE REVENUE	NET BFIT CASH FLOW	CUM BFIT CASH FLOW	BFIT CF DISC 10.0%	CUMBFIT CF DISC 10.0%
========	===M$===	===M$===	===M$===	===M$===	===M$===	===M$B===	===M$===	===M$===	===M$===	===M$===
1996(7 Mo)	56.000	3960.000	1806.000	250.000	6016.000	874.365	–5141.635	–5141.635	–4950.029	–4950.029
1997	4609.612	2730.000	375.000	0.000	3105.000	–3604.587	–6709.587	–11851.222	–5953.668	–10903.697
1998	2643.576	0.000	0.000	0.000	0.000	2096.383	2096.383	–9754.839	1620.992	–9282.705
1999	1459.535	0.000	0.000	0.000	0.000	6750.754	6750.754	–3004.085	5012.956	–4269.750
2000	1391.053	0.000	0.000	0.000	0.000	5012.823	5012.823	2008.738	3390.181	–879.569
2001	1278.564	0.000	0.000	0.000	0.000	3871.301	3871.301	5880.040	2380.495	1500.927
2002	1183.695	0.000	0.000	0.000	0.000	2957.411	2957.411	8837.450	1652.453	3153.379
2003	1122.793	0.000	0.000	0.000	0.000	2360.084	2360.084	11197.534	1198.617	4351.996
2004	1079.716	0.000	0.000	0.000	0.000	1961.391	1961.391	13158.926	905.188	5257.184
2005	1052.281	0.000	0.000	0.000	0.000	1714.144	1714.144	14873.070	718.840	5976.023
2006	1029.693	0.000	0.000	0.000	0.000	1514.923	1514.923	16387.994	577.698	6553.722
2007	1004.162	0.000	0.000	0.000	0.000	1298.994	1298.994	17686.988	450.389	7004.111
2008	979.660	0.000	0.000	0.000	0.000	1088.797	1088.797	18775.785	343.189	7347.301
2009	960.336	0.000	0.000	0.000	0.000	916.269	916.269	19692.055	262.528	7609.829
2010	943.448	0.000	0.000	0.000	0.000	781.375	781.375	20473.430	203.475	7813.304
SUBTOTAL	20794.125	6690.000	2181.000	250.000	9121.000	29594.428	20473.430	20473.430	7813.304	7813.304
REMAINING	926.966	0.000	0.000	0.000	0.000	650.171	650.171	21123.600	153.933	7967.237
TOT 15.6Yr	21721.092	6690.000	2181.000	250.000	9121.000	30244.598	21123.600	21123.600	7967.237	7967.237

Table 16–7b

EVALUATION ANAC1.7

ECONOMIC EVALUATION
HARKEN PARADOX BASIN
REGA INCORPORATED

RUN DATE: 07–02–1997
RUN TIME: 10:27:23

AS OF DATE: JUN96

NAME: ANASAZI CO2 FLOOD–GAS PLANT
FIELD: ANASAZI–SAHGZIE
LOCATION: UTAH
FORMATION: DESERT CREEK
OPERATOR: HARKEN ENERGY

CONTINUOUS CO2 GAS RECYCLE
GAS PROCESSING FOR CO2 REMOVAL
BURIED LINES – HEATPRO

NPV	5.0%	13153.339	BFIT	8320.194	AFIT
NPV	10.0%	7967.233	BFIT	4584.852	AFIT
NPV	15.0%	4451.335	BFIT	2005.763	AFIT
NPV	20.0%	1986.364	BFIT	169.285	AFIT
NPV	25.0%	210.581	BFIT	–1170.828	AFIT
IRR		26%	BFIT	21%	AFIT
PAYOUT		JUL00	BFIT	OCT00	AFIT
PI		3.32:1	BFIT	2.53:1	AFIT

====== INTERESTS AND EFFECTIVE DATE ======

COST	OIL	GAS	COND	PRODT	DATE
1.00000	0.80000	0.80000	0.80000	0.80000	JUN96

	======== PRICES ========			========== GROSS RESERVES ==========				
	BEGINING	ENDING	AVERAGE	CUMULATIVE	REMAINING	ULTIMATE	% REMAINING	
OIL	20.00	20.00	20.00	1692.690	3285.841	4978.531	66.00	OIL
GAS	1.80	1.80	1.80	1308.810	4306.441	5615.251	76.69	GAS
COND	0.00	0.00	0.00	0.000	0.000	0.000	0.00	COND
PRDT	0.00	0.00	0.00	0.000	0.000	0.000	0.00	PRDT

YEAR	GROSS OIL PRODUCTION	NET OIL PRODUCTION	GROSS GAS PRODUCTION	GROSS GAS AS FUEL	NET GAS PRODUCTION	AVERAGE OIL PRICE	AVERAGE GAS PRICE	NET OIL SALES	NET GAS SALES	NET TOTAL REVENUE
========	==MBBLS==	==MBBLS==	==MMSCF==	==MMSCF==	==MMSCF==	===$/B===	==$/MSCF==	===M$===	===M$===	===M$===
1996(7 Mo)	54.774	43.819	52.810	15.323	42.248	20.000	1.800	876.384	53.981	930.365
1997	82.120	65.696	40.118	254.628	32.094	20.000	1.800	1313.920	–308.894	1005.026
1998	316.729	253.383	90.895	318.468	72.716	20.000	1.800	5067.664	–327.705	4739.959
1999	520.906	416.725	232.213	318.468	185.770	20.000	1.800	8334.496	–124.207	8210.289
2000	404.129	323.303	275.282	318.468	220.226	20.000	1.800	6466.064	–62.188	6403.876
2001	323.119	258.495	304.552	318.468	243.642	20.000	1.800	5169.904	–20.039	5149.865
2002	258.865	207.092	317.958	318.468	254.366	20.000	1.800	4141.840	–0.734	4141.105
2003	217.046	173.637	325.510	318.468	260.408	20.000	1.800	3472.736	10.140	3482.877
2004	188.999	151.199	330.359	318.468	264.287	20.000	1.800	3023.984	17.123	3041.107
2005	171.519	137.215	333.830	318.468	267.064	20.000	1.800	2744.304	22.121	2766.425
2006	157.493	125.994	335.640	318.468	268.512	20.000	1.800	2519.888	24.728	2544.616
2007	142.196	113.757	337.926	318.468	270.341	20.000	1.800	2275.136	28.020	2303.156
2008	127.824	102.259	334.630	318.468	267.704	20.000	1.800	2045.184	23.273	2068.457
2009	115.919	92.735	333.677	318.468	266.942	20.000	1.800	1854.704	21.901	1876.605
2010	106.654	85.323	331.217	318.468	264.974	20.000	1.800	1706.464	18.359	1724.823
SUBTOTAL	3188.292	2550.634	3976.617	4410.035	3181.294	20.000	1.800	51012.672	–624.122	50388.555
REMAINING	97.549	78.039	329.824	318.468	263.859	20.000	1.800	1560.784	16.353	1577.137
TOT 15.6Yr	3285.841	2628.673	4306.441	4728.503	3445.153	20.000	1.800	52573.457	–607.769	51965.691

YEAR	NET TOTAL INVESTMENTS	NET TOTAL REVENUE	NET LEASE REVENUE	NET BFIT CASH FLOW	NET TAX DEPREC	NET TAXABLE INCOME	NET INCOME TAXES PAID	NET AFIT CASH FLOW	CUM AFIT CASHFLOW	AFIT CF DISC 10.0%
========	===M$===	===M$===	===M$===	===M$===	===M$===	===M$B===	===M$===	===M$===	===M$===	===M$===
1996(7 Mo)	6016.000	930.365	874.365	–5141.635	565.714	–1747.349	0.000	–5141.635	–5141.635	–4950.029
1997	3105.000	1005.026	–3604.587	–6709.587	1359.796	–5339.383	0.000	–6709.587	–11851.222	–5953.668
1998	0.000	4739.959	2096.383	2096.383	1361.283	735.100	0.000	2096.383	–9754.839	1620.992
1999	0.000	8210.289	6750.754	6750.754	972.345	5778.409	0.000	6750.754	–3004.085	5012.956
2000	0.000	6403.876	5012.823	5012.823	694.532	4318.291	1273.323	3739.500	735.415	2567.517
2001	0.000	5149.865	3871.301	3871.301	597.073	3274.229	1113.238	2758.063	3493.478	1726.645
2002	0.000	4141.105	2957.411	2957.411	597.073	2360.338	802.515	2154.896	5648.374	1223.953
2003	0.000	3482.877	2360.084	2360.084	420.361	1939.723	659.506	1700.578	7348.952	878.488
2004	0.000	3041.107	1961.391	1961.391	121.824	1839.567	625.453	1335.938	8684.891	629.189
2005	0.000	2766.425	1714.144	1714.144	0.000	1714.144	582.809	1131.335	9816.226	485.039
2006	0.000	2544.616	1514.923	1514.923	0.000	1514.923	515.074	999.849	10816.075	389.854
2007	0.000	2303.156	1298.994	1298.994	0.000	1298.994	441.658	857.336	11673.411	303.963
2008	0.000	2068.457	1088.797	1088.797	0.000	1088.797	370.191	718.606	12392.018	231.614
2009	0.000	1876.605	916.269	916.269	0.000	916.269	311.531	604.737	12996.755	177.169
2010	0.000	1724.823	781.375	781.375	0.000	781.375	265.667	515.707	13512.462	137.300
SUBTOTAL	9121.000	50388.555	29594.428	20473.430	6690.000	20473.428	6960.965	13512.462	13512.462	4480.980
REMAINING	0.000	1577.137	650.171	650.171	0.000	650.171	221.058	429.113	13941.574	103.875
TOT 15.6Yr	9121.000	51965.691	30244.598	21123.600	6690.000	21123.598	7182.023	13941.574	13941.574	4584.855

Table 16–8a

EVALUATION ANAC1.8

ECONOMIC EVALUATION

RUN DATE: 07–10–1997

HARKEN PARADOX BASIN

REGA INCORPORATED

RUN TIME: 17:28:04

AS OF DATE: JUN96

NAME: ANASAZI CO2 FLOOD RECYCLE ALL
FIELD: ANASAZI–SAHGZIE
LOCATION: UTAH
FORMATION: DESERT CREEK
OPERATOR: HARKEN ENERGY

CONTINUOUS CO2 GAS RECYCLE
NO GAS PROCESSING BUY FUEL
BURIED LINES – HEATPRO

NPV	5.0%	16717.268	BFIT
NPV	10.0%	11255.285	BFIT
NPV	15.0%	7511.433	BFIT
NPV	20.0%	4852.308	BFIT
NPV	25.0%	2907.567	BFIT
IRR		37%	BFIT
PAYOUT		NOV99	BFIT
PI		5.36:1	BFIT

====== INTERESTS AND EFFECTIVE DATE ======

COST	OIL	GAS	COND	PRODT	DATE
1.00000	0.80000	0.80000	0.80000	0.80000	JUN96

	======== PRICES ========			========== GROSS RESERVES ==========				
	BEGINING	ENDING	AVERAGE	CUMULATIVE	REMAINING	ULTIMATE	%REMAINING	
OIL	20.00	20.00	20.00	1692.690	3344.399	5037.089	66.40	OIL
GAS	1.80	0.00	1.80	1308.810	88.141	1396.951	6.31	GAS
COND	0.00	0.00	0.00	0.000	0.000	0.000	0.00	COND
PRDT	0.00	0.00	0.00	0.000	0.000	0.000	0.00	PRDT

YEAR	GROSS OIL PRODUCTION	NET OIL PRODUCTION	GROSS GAS PRODUCTION	GROSS GAS AS FUEL	NET GAS PRODUCTION	AVERAGE OIL PRICE	AVERAGE GAS PRICE	NET OIL SALES	NET GAS SALES	NET TOTAL REVENUE
========	==MBBLS==	==MBBLS==	==MMSCF==	==MMSCF==	==MMSCF==	===$/B===	==$/MSCF==	===M$===	===M$===	===M$===
1996(7 Mo)	54.774	43.819	52.810	15.323	42.248	20.000	1.800	876.384	53.981	930.365
1997	82.120	65.696	35.331	95.394	28.265	20.000	1.800	1313.920	−86.491	1227.429
1998	316.729	253.383	0.000	0.000	0.000	20.000	0.000	5067.664	0.000	5067.664
1999	521.095	416.876	0.000	0.000	0.000	20.000	0.000	8337.521	0.000	8337.521
2000	406.741	325.393	0.000	0.000	0.000	20.000	0.000	6507.856	0.000	6507.856
2001	326.351	261.081	0.000	0.000	0.000	20.000	0.000	5221.615	0.000	5221.615
2002	263.997	211.198	0.000	0.000	0.000	20.000	0.000	4223.952	0.000	4223.952
2003	222.703	178.162	0.000	0.000	0.000	20.000	0.000	3563.248	0.000	3563.248
2004	194.597	155.678	0.000	0.000	0.000	20.000	0.000	3113.552	0.000	3113.552
2005	177.929	142.343	0.000	0.000	0.000	20.000	0.000	2846.864	0.000	2846.864
2006	163.003	130.402	0.000	0.000	0.000	20.000	0.000	2608.048	0.000	2608.048
2007	147.588	118.070	0.000	0.000	0.000	20.000	0.000	2361.408	0.000	2361.408
2008	133.133	106.506	0.000	0.000	0.000	20.000	0.000	2130.128	0.000	2130.128
2009	120.594	96.475	0.000	0.000	0.000	20.000	0.000	1929.504	0.000	1929.504
2010	110.609	88.487	0.000	0.000	0.000	20.000	0.000	1769.744	0.000	1769.744
SUBTOTAL	3241.962	2593.570	88.141	110.717	70.513	20.000	1.800	51871.406	−32.509	51838.898
REMAINING	102.437	81.950	0.000	0.000	0.000	20.000	0.000	1638.992	0.000	1638.992
TOT 15.6Yr	3344.399	2675.520	88.141	110.717	70.513	20.000	1.800	53510.398	−32.509	53477.891

YEAR	NET TOTAL LOE	NET TANGIBLES	NET INTANGIBLES	NET G&G	NET TOTAL INVESTMENTS	NET LEASE REVENUE	NET BFIT CASHFLOW	CUM BFIT CASHFLOW	BFIT CF DISC 10.0%	CUMBFIT CF DISC 10.0%
========	===M$===	===M$===	===M$===	===M$===	===M$===	===M$B===	===M$===	===M$===	===M$===	===M$===
1996(7 Mo)	56.000	3691.000	1806.000	250.000	5747.000	874.365	−4872.635	−4872.635	−4695.577	−4695.577
1997	4730.424	0.000	0.000	0.000	0.000	−3502.995	−3502.995	−8375.630	−3150.424	−7846.000
1998	2872.766	0.000	0.000	0.000	0.000	2194.898	2194.898	−6180.732	1702.295	−6143.706
1999	1576.165	0.000	0.000	0.000	0.000	6761.355	6761.355	580.624	5021.235	−1122.470
2000	1473.500	0.000	0.000	0.000	0.000	5034.356	5034.356	5614.979	3404.929	2282.459
2001	1337.235	0.000	0.000	0.000	0.000	3884.380	3884.380	9499.359	2388.429	4670.888
2002	1231.087	0.000	0.000	0.000	0.000	2992.865	2992.865	12492.225	1672.241	6343.129
2003	1164.825	0.000	0.000	0.000	0.000	2398.423	2398.423	14890.648	1218.018	7561.146
2004	1117.354	0.000	0.000	0.000	0.000	1996.198	1996.198	16886.846	921.234	8482.381
2005	1087.700	0.000	0.000	0.000	0.000	1759.164	1759.164	18646.010	737.817	9220.197
2006	1062.617	0.000	0.000	0.000	0.000	1545.431	1545.431	20191.441	589.333	9809.530
2007	1036.452	0.000	0.000	0.000	0.000	1324.956	1324.956	21516.396	459.382	10268.912
2008	1012.709	0.000	0.000	0.000	0.000	1117.419	1117.419	22633.816	352.195	10621.106
2009	993.487	0.000	0.000	0.000	0.000	936.017	936.017	23569.834	268.207	10889.313
2010	978.141	0.000	0.000	0.000	0.000	791.603	791.603	24361.438	206.196	11095.510
SUBTOTAL	21730.461	3691.000	1806.000	250.000	5747.000	30108.438	24361.438	24361.438	11095.510	11095.510
REMAINING	964.203	0.000	0.000	0.000	0.000	674.789	674.789	25036.227	159.772	11255.281
TOT 15.6Yr	22694.664	3691.000	1806.000	250.000	5747.000	30783.227	25036.227	25036.227	11255.281	11255.281

Table 16-8b

EVALUATION ANAC1.8

ECONOMIC EVALUATION
HARKEN PARADOX BASIN
REGA INCORPORATED

RUN DATE: 07-10-1997
RUN TIME: 17:28:53

AS OF DATE: JUN96

NAME: ANASAZI CO2 FLOOD RECYCLE ALL
FIELD: ANASAZI-SAHGZIE
LOCATION: UTAH
FORMATION: DESERT CREEK
OPERATOR: HARKEN ENERGY

CONTINUOUS CO2 GAS RECYCLE
NO GAS PROCESSING BUY FUEL
BURIED LINES - HEATPRO

NPV	5.0%	16717.268	BFIT	10841.632	AFIT
NPV	10.0%	11255.285	BFIT	7039.667	AFIT
NPV	15.0%	7511.433	BFIT	4388.974	AFIT
NPV	20.0%	4852.308	BFIT	2477.783	AFIT
NPV	25.0%	2907.567	BFIT	1061.672	AFIT
IRR		37%	BFIT	30%	AFIT
PAYOUT		NOV99	BFIT	JAN00	AFIT
PI		5.36:1	BFIT	3.88:1	AFIT

====== INTERESTS AND EFFECTIVE DATE ======

COST	OIL	GAS	COND	PRODT	DATE
1.00000	0.80000	0.80000	0.80000	0.80000	JUN96

	======== PRICES ========			========== GROSS RESERVES ==========				
	BEGINING	ENDING	AVERAGE	CUMULATIVE	REMAINING	ULTIMATE	%REMAINING	
OIL	20.00	20.00	20.00	1692.690	3344.399	5037.089	66.40	OIL
GAS	1.80	0.00	1.80	1308.810	88.141	1396.951	6.31	GAS
COND	0.00	0.00	0.00	0.000	0.000	0.000	0.00	COND
PRDT	0.00	0.00	0.00	0.000	0.000	0.000	0.00	PRDT

YEAR	GROSS OIL PRODUCTION	NET OIL PRODUCTION	GROSS GAS PRODUCTION	GROSS GAS AS FUEL	NET GAS PRODUCTION	AVERAGE OIL PRICE	AVERAGE GAS PRICE	NET OIL SALES	NET GAS SALES	NET TOTAL REVENUE
========	==MBBLS==	==MBBLS==	==MMSCF==	==MMSCF==	==MMSCF==	===$/B===	==$/MSCF==	===M$===	===M$===	===M$===
1996(7 Mo)	54.774	43.819	52.810	15.323	42.248	20.000	1.800	876.384	53.981	930.365
1997	82.120	65.696	35.331	95.394	28.265	20.000	1.800	1313.920	-86.491	1227.429
1998	316.729	253.383	0.000	0.000	0.000	20.000	0.000	5067.664	0.000	5067.664
1999	521.095	416.876	0.000	0.000	0.000	20.000	0.000	8337.521	0.000	8337.521
2000	406.741	325.393	0.000	0.000	0.000	20.000	0.000	6507.856	0.000	6507.856
2001	326.351	261.081	0.000	0.000	0.000	20.000	0.000	5221.615	0.000	5221.615
2002	263.997	211.198	0.000	0.000	0.000	20.000	0.000	4223.952	0.000	4223.952
2003	222.703	178.162	0.000	0.000	0.000	20.000	0.000	3563.248	0.000	3563.248
2004	194.597	155.678	0.000	0.000	0.000	20.000	0.000	3113.552	0.000	3113.552
2005	177.929	142.343	0.000	0.000	0.000	20.000	0.000	2846.864	0.000	2846.864
2006	163.003	130.402	0.000	0.000	0.000	20.000	0.000	2608.048	0.000	2608.048
2007	147.588	118.070	0.000	0.000	0.000	20.000	0.000	2361.408	0.000	2361.408
2008	133.133	106.506	0.000	0.000	0.000	20.000	0.000	2130.128	0.000	2130.128
2009	120.594	96.475	0.000	0.000	0.000	20.000	0.000	1929.504	0.000	1929.504
2010	110.609	88.487	0.000	0.000	0.000	20.000	0.000	1769.744	0.000	1769.744
SUBTOTAL	3241.962	2593.570	88.141	110.717	70.513	20.000	1.800	51871.406	-32.509	51838.898
REMAINING	102.437	81.950	0.000	0.000	0.000	20.000	0.000	1638.992	0.000	1638.992
TOT 15.6Yr	3344.399	2675.520	88.141	110.717	70.513	20.000	1.800	53510.398	-32.509	53477.891

YEAR	NET TOTAL INVESTMENTS	NET TOTAL REVENUE	NET LEASE REVENUE	NET BFIT CASHFLOW	NET TAX DEPREC	NET TAXABLE INCOME	NET INCOME TAXES PAID	NET AFIT CASHFLOW	CUM AFIT CASHFLOW	AFIT CF DISC 10.0%
========	===M$===	===M$===	===M$===	===M$===	===M$===	===M$B===	===M$===	===M$===	===M$===	===M$===
1996(7 Mo)	5747.000	930.365	874.365	-4872.635	527.286	-1708.921	0.000	-4872.635	-4872.635	-4695.577
1997	0.000	1227.429	-3502.995	-3502.995	903.918	-4406.914	0.000	-3502.995	-8375.630	-3150.424
1998	0.000	5067.664	2194.898	2194.898	645.656	1549.242	0.000	2194.898	-6180.732	1702.295
1999	0.000	8337.521	6761.355	6761.355	461.183	6300.173	589.417	6171.938	-8.794	4602.346
2000	0.000	6507.856	5034.356	5034.356	329.416	4704.939	1599.679	3434.677	3425.883	2371.415
2001	0.000	5221.615	3884.380	3884.380	329.416	3554.964	1208.688	2675.692	6101.575	1678.516
2002	0.000	4223.952	2992.865	2992.865	329.416	2663.449	905.573	2087.292	8188.868	1188.714
2003	0.000	3563.248	2398.423	2398.423	164.708	2233.715	759.463	1638.960	9827.828	849.370
2004	0.000	3113.552	1996.198	1996.198	0.000	1996.198	678.707	1317.491	11145.318	621.735
2005	0.000	2846.864	1759.164	1759.164	0.000	1759.164	598.116	1161.048	12306.366	497.875
2006	0.000	2608.048	1545.431	1545.431	0.000	1545.431	525.447	1019.985	13326.351	397.707
2007	0.000	2361.408	1324.956	1324.956	0.000	1324.956	450.485	874.471	14200.821	310.029
2008	0.000	2130.128	1117.419	1117.419	0.000	1117.419	379.922	737.496	14938.317	237.686
2009	0.000	1929.504	936.017	936.017	0.000	936.017	318.246	617.771	15556.089	181.008
2010	0.000	1769.744	791.603	791.603	0.000	791.603	269.145	522.458	16078.547	139.154
SUBTOTAL	5747.000	51838.898	30108.438	24361.438	3691.000	24361.438	8282.889	16078.547	16078.547	6931.850
REMAINING	0.000	1638.992	674.789	674.789	0.000	674.789	229.428	445.361	16523.908	107.819
TOT 15.6Yr	5747.000	53477.891	30783.227	25036.227	3691.000	25036.227	8512.316	16523.908	16523.908	7039.669

Table 16–9a

EVALUATION ANAC1.9

ECONOMIC EVALUATION
HARKEN PARADOX BASIN
REGA INCORPORATED

RUN DATE: 07–10–1997
RUN TIME: 18:02:41

AS OF DATE: JUN96

NAME: ANASAZI CO2 FLOOD LEASE COMP
FIELD: ANASAZI–SAHGZIE
LOCATION: UTAH
FORMATION: DESERT CREEK
OPERATOR: HARKEN ENERGY

CONTINUOUS CO2 GAS RECYCLE
NO GAS PROCESSING BUY FUEL
LEASE INJECTION COMPRESSOR
BURIED LINES – HEATPRO

NPV	5.0%	14886.736	BFIT
NPV	10.0%	10339.958	BFIT
NPV	15.0%	7166.487	BFIT
NPV	20.0%	4879.573	BFIT
NPV	25.0%	3187.718	BFIT
IRR		41%	BFIT
PAYOUT		OCT99	BFIT
PI		6.31:1	BFIT

====== INTERESTS AND EFFECTIVE DATE ======							======== PRICES ========			========== GROSS RESERVES ==========				
COST	OIL	GAS	COND	PRODT	DATE		BEGINING	ENDING	AVERAGE	CUMULATIVE	REMAINING	ULTIMATE	%REMAINING	
1.00000	0.80000	0.80000	0.80000	0.80000	JUN96	OIL	20.00	20.00	20.00	1692.690	3344.399	5037.089	66.40	OIL
						GAS	1.80	0.00	1.80	1308.810	88.141	1396.951	6.31	GAS
						COND	0.00	0.00	0.00	0.000	0.000	0.000	0.00	COND
						PRDT	0.00	0.00	0.00	0.000	0.000	0.000	0.00	PRDT

YEAR	GROSS OIL PRODUCTION	NET OIL PRODUCTION	GROSS GAS PRODUCTION	GROSS GAS AS FUEL	NET GAS RODUCTION	AVERAGE OIL PRICE	AVERAGE GAS PRICE	NET OIL SALES	NET GAS SALES	NET TOTAL REVENUE
========	==MBBLS==	==MBBLS==	==MMSCF==	==MMSCF==	==MMSCF==	===$/B===	==$/MSCF==	===M$===	===M$===	===M$===
1996(7 Mo)	54.774	43.819	52.810	15.323	42.248	20.000	1.800	876.384	53.981	930.365
1997	82.120	65.696	35.331	95.394	28.265	20.000	1.800	1313.920	–86.491	1227.429
1998	316.729	253.383	0.000	0.000	0.000	20.000	0.000	5067.664	0.000	5067.664
1999	521.095	416.876	0.000	0.000	0.000	20.000	0.000	8337.521	0.000	8337.521
2000	406.741	325.393	0.000	0.000	0.000	20.000	0.000	6507.856	0.000	6507.856
2001	326.351	261.081	0.000	0.000	0.000	20.000	0.000	5221.615	0.000	5221.615
2002	263.997	211.198	0.000	0.000	0.000	20.000	0.000	4223.952	0.000	4223.952
2003	222.703	178.162	0.000	0.000	0.000	20.000	0.000	3563.248	0.000	3563.248
2004	194.597	155.678	0.000	0.000	0.000	20.000	0.000	3113.552	0.000	3113.552
2005	177.929	142.343	0.000	0.000	0.000	20.000	0.000	2846.864	0.000	2846.864
2006	163.003	130.402	0.000	0.000	0.000	20.000	0.000	2608.048	0.000	2608.048
2007	147.588	118.070	0.000	0.000	0.000	20.000	0.000	2361.408	0.000	2361.408
2008	133.133	106.506	0.000	0.000	0.000	20.000	0.000	2130.128	0.000	2130.128
2009	120.594	96.475	0.000	0.000	0.000	20.000	0.000	1929.504	0.000	1929.504
2010	110.609	88.487	0.000	0.000	0.000	20.000	0.000	1769.744	0.000	1769.744
SUBTOTAL	3241.962	2593.570	88.141	110.717	70.513	20.000	1.800	51871.406	–32.509	51838.898
REMAINING	102.437	81.950	0.000	0.000	0.000	20.000	0.000	1638.992	0.000	1638.992
TOT 15.6Yr	3344.399	2675.520	88.141	110.717	70.513	20.000	1.800	53510.398	–32.509	53477.891

YEAR	NET TOTAL LOE	NET TANGIBLES	NET INTANGIBLES	NET G&G	NET TOTAL INVESTMENTS	NET LEASE REVENUE	NET BFIT CASHFLOW	CUM BFIT CASHFLOW	BFIT CF DISC 10.0%	CUMBFIT CF DISC 10.0%
========	===M$===	===M$===	===M$===	===M$===	===M$===	===M$B===	===M$===	===M$===	===M$===	===M$===
1996(7 Mo)	56.000	2111.000	1723.000	250.000	4084.000	874.365	–3209.635	–3209.635	–3084.580	–3084.580
1997	5066.424	0.000	0.000	0.000	0.000	–3838.995	–3838.995	–7048.629	–3452.374	–6536.953
1998	3208.766	0.000	0.000	0.000	0.000	1858.898	1858.898	–5189.731	1427.794	–5109.159
1999	1912.165	0.000	0.000	0.000	0.000	6425.355	6425.355	1235.624	4771.689	–337.469
2000	1809.500	0.000	0.000	0.000	0.000	4698.356	4698.356	5933.980	3178.069	2840.600
2001	1673.235	0.000	0.000	0.000	0.000	3548.380	3548.380	9482.360	2182.193	5022.793
2002	1567.087	0.000	0.000	0.000	0.000	2656.865	2656.865	12139.226	1484.754	6507.546
2003	1500.825	0.000	0.000	0.000	0.000	2062.423	2062.423	14201.648	1047.575	7555.121
2004	1453.354	0.000	0.000	0.000	0.000	1660.198	1660.198	15861.847	766.286	8321.406
2005	1423.700	0.000	0.000	0.000	0.000	1423.164	1423.164	17285.012	596.955	8918.361
2006	1398.617	0.000	0.000	0.000	0.000	1209.432	1209.432	18494.443	461.277	9379.638
2007	1372.452	0.000	0.000	0.000	0.000	988.956	988.956	19483.398	342.967	9722.605
2008	1348.709	0.000	0.000	0.000	0.000	781.419	781.419	20264.816	246.363	9968.969
2009	1329.487	0.000	0.000	0.000	0.000	600.017	600.017	20864.834	171.996	10140.965
2010	1314.141	0.000	0.000	0.000	0.000	455.603	455.603	21320.438	118.732	10259.696
SUBTOTAL	26434.459	2111.000	1723.000	250.000	4084.000	25404.438	21320.438	21320.438	10259.696	10259.696
REMAINING	1300.203	0.000	0.000	0.000	0.000	338.789	338.789	21659.227	80.259	10339.955
TOT 15.6Yr	27734.662	2111.000	1723.000	250.000	4084.000	25743.227	21659.227	21659.227	10339.955	10339.955

Table 16–9b

EVALUATION ANAC1.9

ECONOMIC EVALUATION
HARKEN PARADOX BASIN
REGA INCORPORATED

RUN DATE: 07–10–1997
RUN TIME: 18:03:48

AS OF DATE: JUN96

NAME: ANASAZI CO2 FLOOD LEASE COMP
FIELD: ANASAZI–SAHGZIE
LOCATION: UTAH
FORMATION: DESERT CREEK
OPERATOR: HARKEN ENERGY

CONTINUOUS CO2 GAS RECYCLE
NO GAS PROCESSING BUY FUEL
LEASE INJECTION COMPRESSOR
BURIED LINES – HEATPRO

NPV	5.0%	14886.736	BFIT	9688.957	AFIT
NPV	10.0%	10339.958	BFIT	6542.146	AFIT
NPV	15.0%	7166.487	BFIT	4311.401	AFIT
NPV	20.0%	4879.573	BFIT	2681.793	AFIT
NPV	25.0%	3187.718	BFIT	1461.956	AFIT
IRR		41%	BFIT	34%	AFIT
PAYOUT		OCT99	BFIT	NOV99	AFIT
PI		6.31:1	BFIT	4.51:1	AFIT

====== INTERESTS AND EFFECTIVE DATE ======

COST	OIL	GAS	COND	PRODT	DATE
1.00000	0.80000	0.80000	0.80000	0.80000	JUN96

	======== PRICES ========			========== GROSS RESERVES ==========				
	BEGINING	ENDING	AVERAGE	CUMULATIVE	REMAINING	ULTIMATE	%REMAINING	
OIL	20.00	20.00	20.00	1692.690	3344.399	5037.089	66.40	OIL
GAS	1.80	0.00	1.80	1308.810	88.141	1396.951	6.31	GAS
COND	0.00	0.00	0.00	0.000	0.000	0.000	0.00	COND
PRDT	0.00	0.00	0.00	0.000	0.000	0.000	0.00	PRDT

YEAR	GROSS OIL PRODUCTION	NET OIL PRODUCTION	GROSS GAS PRODUCTION	GROSS GAS AS FUEL	NET GAS PRODUCTION	AVERAGE OIL PRICE	AVERAGE GAS PRICE	NET OIL SALES	NET GAS SALES	NET TOTAL REVENUE
========	==MBBLS==	==MBBLS==	==MMSCF==	==MMSCF==	==MMSCF==	===$/B===	==$/MSCF==	===M$===	===M$===	===M$===
1996(7 Mo)	54.774	43.819	52.810	15.323	42.248	20.000	1.800	876.384	53.981	930.365
1997	82.120	65.696	35.331	95.394	28.265	20.000	1.800	1313.920	−86.491	1227.429
1998	316.729	253.383	0.000	0.000	0.000	20.000	0.000	5067.664	0.000	5067.664
1999	521.095	416.876	0.000	0.000	0.000	20.000	0.000	8337.521	0.000	8337.521
2000	406.741	325.393	0.000	0.000	0.000	20.000	0.000	6507.856	0.000	6507.856
2001	326.351	261.081	0.000	0.000	0.000	20.000	0.000	5221.615	0.000	5221.615
2002	263.997	211.198	0.000	0.000	0.000	20.000	0.000	4223.952	0.000	4223.952
2003	222.703	178.162	0.000	0.000	0.000	20.000	0.000	3563.248	0.000	3563.248
2004	194.597	155.678	0.000	0.000	0.000	20.000	0.000	3113.552	0.000	3113.552
2005	177.929	142.343	0.000	0.000	0.000	20.000	0.000	2846.864	0.000	2846.864
2006	163.003	130.402	0.000	0.000	0.000	20.000	0.000	2608.048	0.000	2608.048
2007	147.588	118.070	0.000	0.000	0.000	20.000	0.000	2361.408	0.000	2361.408
2008	133.133	106.506	0.000	0.000	0.000	20.000	0.000	2130.128	0.000	2130.128
2009	120.594	96.475	0.000	0.000	0.000	20.000	0.000	1929.504	0.000	1929.504
2010	110.609	88.487	0.000	0.000	0.000	20.000	0.000	1769.744	0.000	1769.744
SUBTOTAL	3241.962	2593.570	88.141	110.717	70.513	20.000	1.800	51871.406	−32.509	51838.898
REMAINING	102.437	81.950	0.000	0.000	0.000	20.000	0.000	1638.992	0.000	1638.992
TOT 15.6Yr	3344.399	2675.520	88.141	110.717	70.513	20.000	1.800	53510.398	−32.509	53477.891

YEAR	NET TOTAL INVESTMENTS	NET TOTAL REVENUE	NET LEASE REVENUE	NET BFIT CASHFLOW	NET TAX DEPREC	NET TAXABLE INCOME	NET INCOME TAXES PAID	NET AFIT CASHFLOW	CUM AFIT CASHFLOW	AFIT CF DISC 10.0%
========	===M$===	===M$===	===M$===	===M$===	===M$===	===M$B===	===M$===	===M$===	===M$===	===M$===
1996(7 Mo)	4084.000	930.365	874.365	−3209.635	301.571	−1400.206	0.000	−3209.635	−3209.635	−3084.580
1997	0.000	1227.429	−3838.995	−3838.995	516.980	−4355.974	0.000	−3838.995	−7048.629	−3452.374
1998	0.000	5067.664	1858.898	1858.898	369.271	1489.627	0.000	1858.898	−5189.731	1427.794
1999	0.000	8337.521	6425.355	6425.355	263.765	6161.590	644.313	5781.043	591.312	4313.787
2000	0.000	6507.856	4698.356	4698.356	188.404	4509.952	1533.384	3164.972	3756.284	2187.387
2001	0.000	5221.615	3548.380	3548.380	188.404	3359.977	1142.392	2405.988	6162.271	1511.219
2002	0.000	4223.952	2656.865	2656.865	188.404	2468.461	839.277	1817.588	7979.859	1036.624
2003	0.000	3563.248	2062.423	2062.423	94.202	1968.222	669.195	1393.228	9373.088	722.743
2004	0.000	3113.552	1660.198	1660.198	0.000	1660.198	564.467	1095.731	10468.818	517.198
2005	0.000	2846.864	1423.164	1423.164	0.000	1423.164	483.876	939.288	11408.106	402.842
2006	0.000	2608.048	1209.432	1209.432	0.000	1209.432	411.207	798.225	12206.331	311.313
2007	0.000	2361.408	988.956	988.956	0.000	988.956	336.245	652.711	12859.042	231.489
2008	0.000	2130.128	781.419	781.419	0.000	781.419	265.682	515.737	13374.778	166.286
2009	0.000	1929.504	600.017	600.017	0.000	600.017	204.006	396.011	13770.789	116.099
2010	0.000	1769.744	455.603	455.603	0.000	455.603	154.905	300.698	14071.487	80.146
SUBTOTAL	4084.000	51838.898	25404.438	21320.438	2111.000	21320.438	7248.949	14071.487	14071.487	6487.976
REMAINING	0.000	1638.992	338.789	338.789	0.000	338.789	115.188	223.601	14295.088	54.175
TOT 15.6Yr	4084.000	53477.891	25743.227	21659.227	2111.000	21659.227	7364.137	14295.088	14295.088	6542.151

Table 16-10a

EVALUATION ANAC1.10

ECONOMIC EVALUATION

RUN DATE: 07-10-1997

HARKEN PARADOX BASIN

REGA INCORPORATED

RUN TIME: 18:27:10

AS OF DATE: JUN96

NAME: ANASAZI CO2 FLOOD DOE SHARE
FIELD: ANASAZI-SAHGZIE
LOCATION: UTAH
FORMATION: DESERT CREEK
OPERATOR: HARKEN ENERGY

CONTINUOUS CO2 GAS RECYCLE
NO GAS PROCESSING BUY FUEL
DOE COST SHARING
BURIED LINES - HEATPRO

NPV	5.0%	19224.379	BFIT
NPV	10.0%	13685.836	BFIT
NPV	15.0%	9871.013	BFIT
NPV	20.0%	7145.878	BFIT
NPV	25.0%	5139.563	BFIT
IRR		52%	BFIT
PAYOUT		JUL99	BFIT
PI		9.76:1	BFIT

====== INTERESTS AND EFFECTIVE DATE ======

COST	OIL	GAS	COND	PRODT	DATE
1.00000	0.80000	0.80000	0.80000	0.80000	JUN96

	======== PRICES ========			========== GROSS RESERVES ==========				
	BEGINING	ENDING	AVERAGE	CUMULATIVE	REMAINING	ULTIMATE	%REMAINING	
OIL	20.00	20.00	20.00	1692.690	3344.399	5037.089	66.40	OIL
GAS	1.80	0.00	1.80	1308.810	88.141	1396.951	6.31	GAS
COND	0.00	0.00	0.00	0.000	0.000	0.000	0.00	COND
PRDT	0.00	0.00	0.00	0.000	0.000	0.000	0.00	PRDT

YEAR	GROSS OIL PRODUCTION	NET OIL PRODUCTION	GROSS GAS PRODUCTION	GROSS GAS AS FUEL	NET GAS PRODUCTION	AVERAGE OIL PRICE	AVERAGE GAS PRICE	NET OIL SALES	NET GAS SALES	NET TOTAL REVENUE
========	==MBBLS==	==MBBLS==	==MMSCF==	==MMSCF==	==MMSCF==	===$/B===	==$/MSCF==	===M$===	===M$===	===M$===
1996(7 Mo)	54.774	43.819	52.810	15.323	42.248	20.000	1.800	876.384	53.981	930.365
1997	82.120	65.696	35.331	95.394	28.265	20.000	1.800	1313.920	-86.491	1227.429
1998	316.729	253.383	0.000	0.000	0.000	20.000	0.000	5067.664	0.000	5067.664
1999	521.095	416.876	0.000	0.000	0.000	20.000	0.000	8337.521	0.000	8337.521
2000	406.741	325.393	0.000	0.000	0.000	20.000	0.000	6507.856	0.000	6507.856
2001	326.351	261.081	0.000	0.000	0.000	20.000	0.000	5221.615	0.000	5221.615
2002	263.997	211.198	0.000	0.000	0.000	20.000	0.000	4223.952	0.000	4223.952
2003	222.703	178.162	0.000	0.000	0.000	20.000	0.000	3563.248	0.000	3563.248
2004	194.597	155.678	0.000	0.000	0.000	20.000	0.000	3113.552	0.000	3113.552
2005	177.929	142.343	0.000	0.000	0.000	20.000	0.000	2846.864	0.000	2846.864
2006	163.003	130.402	0.000	0.000	0.000	20.000	0.000	2608.048	0.000	2608.048
2007	147.588	118.070	0.000	0.000	0.000	20.000	0.000	2361.408	0.000	2361.408
2008	133.133	106.506	0.000	0.000	0.000	20.000	0.000	2130.128	0.000	2130.128
2009	120.594	96.475	0.000	0.000	0.000	20.000	0.000	1929.504	0.000	1929.504
2010	110.609	88.487	0.000	0.000	0.000	20.000	0.000	1769.744	0.000	1769.744
SUBTOTAL	3241.962	2593.570	88.141	110.717	70.513	20.000	1.800	51871.406	-32.509	51838.898
REMAINING	102.437	81.950	0.000	0.000	0.000	20.000	0.000	1638.992	0.000	1638.992
TOT 15.6Yr	3344.399	2675.520	88.141	110.717	70.513	20.000	1.800	53510.398	-32.509	53477.891

YEAR	NET TOTAL LOE	NET TANGIBLES	NET INTANGIBLES	NET G&G	NET TOTAL INVESTMENTS	NET LEASE REVENUE	NET BFIT CASHFLOW	CUM BFIT CASHFLOW	BFIT CF DISC 10.0%	CUMBFIT CF DISC 10.0%
========	===M$===	===M$===	===M$===	===M$===	===M$===	===M$B===	===M$===	===M$===	===M$===	===M$===
1996(7 Mo)	56.000	3691.000	1806.000	250.000	5747.000	874.365	-4872.635	-4872.635	-4695.577	-4695.577
1997	4730.424	-1664.000	-814.000	-112.000	-2590.000	-3502.995	-912.995	-5785.630	-719.873	-5415.450
1998	2872.766	0.000	0.000	0.000	0.000	2194.898	2194.898	-3590.732	1702.295	-3713.155
1999	1576.165	0.000	0.000	0.000	0.000	6761.355	6761.355	3170.624	5021.235	1308.080
2000	1473.500	0.000	0.000	0.000	0.000	5034.356	5034.356	8204.979	3404.929	4713.009
2001	1337.235	0.000	0.000	0.000	0.000	3884.380	3884.380	12089.359	2388.429	7101.438
2002	1231.087	0.000	0.000	0.000	0.000	2992.865	2992.865	15082.225	1672.241	8773.680
2003	1164.825	0.000	0.000	0.000	0.000	2398.423	2398.423	17480.648	1218.018	9991.697
2004	1117.354	0.000	0.000	0.000	0.000	1996.198	1996.198	19476.846	921.234	10912.932
2005	1087.700	0.000	0.000	0.000	0.000	1759.164	1759.164	21236.010	737.817	11650.748
2006	1062.617	0.000	0.000	0.000	0.000	1545.431	1545.431	22781.441	589.333	12240.081
2007	1036.452	0.000	0.000	0.000	0.000	1324.956	1324.956	24106.396	459.382	12699.463
2008	1012.709	0.000	0.000	0.000	0.000	1117.419	1117.419	25223.816	352.195	13051.657
2009	993.487	0.000	0.000	0.000	0.000	936.017	936.017	26159.834	268.207	13319.864
2010	978.141	0.000	0.000	0.000	0.000	791.603	791.603	26951.438	206.196	13526.061
SUBTOTAL	21730.461	2027.000	992.000	138.000	3157.000	30108.438	26951.438	26951.438	13526.061	13526.061
REMAINING	964.203	0.000	0.000	0.000	0.000	674.789	674.789	27626.227	159.772	13685.832
TOT 15.6Yr	22694.664	2027.000	992.000	138.000	3157.000	30783.227	27626.227	27626.227	13685.832	13685.832

Table 16–10b

EVALUATION ANAC1.10

ECONOMIC EVALUATION
HARKEN PARADOX BASIN
REGA INCORPORATED

RUN DATE: 07–10–1997
RUN TIME: 18:27:56

AS OF DATE: JUN96

NAME: ANASAZI CO2 FLOOD DOE SHARE
FIELD: ANASAZI–SAHGZIE
LOCATION: UTAH
FORMATION: DESERT CREEK
OPERATOR: HARKEN ENERGY

CONTINUOUS CO2 GAS RECYCLE
NO GAS PROCESSING BUY FUEL
DOE COST SHARING
BURIED LINES – HEATPRO

NPV	5.0%	19224.379	BFIT	12609.391	AFIT
NPV	10.0%	13685.836	BFIT	8844.394	AFIT
NPV	15.0%	9871.013	BFIT	6214.876	AFIT
NPV	20.0%	7145.878	BFIT	4313.163	AFIT
NPV	25.0%	5139.563	BFIT	2897.827	AFIT
IRR		52%	BFIT	43%	AFIT
PAYOUT		JUL99	BFIT	SEP99	AFIT
PI		9.76:1	BFIT	6.78:1	AFIT

====== INTERESTS AND EFFECTIVE DATE ======

COST	OIL	GAS	COND	PRODT	DATE
1.00000	0.80000	0.80000	0.80000	0.80000	JUN96

	======== PRICES ========			========== GROSS RESERVES ==========				
	BEGINING	ENDING	AVERAGE	CUMULATIVE	REMAINING	ULTIMATE	%REMAINING	
OIL	20.00	20.00	20.00	1692.690	3344.399	5037.089	66.40	OIL
GAS	1.80	0.00	1.80	1308.810	88.141	1396.951	6.31	GAS
COND	0.00	0.00	0.00	0.000	0.000	0.000	0.00	COND
PRDT	0.00	0.00	0.00	0.000	0.000	0.000	0.00	PRDT

YEAR	GROSS OIL PRODUCTION	NET OIL PRODUCTION	GROSS GAS PRODUCTION	GROSS GAS AS FUEL	NET GAS PRODUCTION	AVERAGE OIL PRICE	AVERAGE GAS PRICE	NET OIL SALES	NET GAS SALES	NET TOTAL REVENUE
========	==MBBLS==	==MBBLS==	==MMSCF==	==MMSCF==	==MMSCF==	===$/B===	==$/MSCF==	===M$===	===M$===	===M$===
1996(7 Mo)	54.774	43.819	52.810	15.323	42.248	20.000	1.800	876.384	53.981	930.365
1997	82.120	65.696	35.331	95.394	28.265	20.000	1.800	1313.920	−86.491	1227.429
1998	316.729	253.383	0.000	0.000	0.000	20.000	0.000	5067.664	0.000	5067.664
1999	521.095	416.876	0.000	0.000	0.000	20.000	0.000	8337.521	0.000	8337.521
2000	406.741	325.393	0.000	0.000	0.000	20.000	0.000	6507.856	0.000	6507.856
2001	326.351	261.081	0.000	0.000	0.000	20.000	0.000	5221.615	0.000	5221.615
2002	263.997	211.198	0.000	0.000	0.000	20.000	0.000	4223.952	0.000	4223.952
2003	222.703	178.162	0.000	0.000	0.000	20.000	0.000	3563.248	0.000	3563.248
2004	194.597	155.678	0.000	0.000	0.000	20.000	0.000	3113.552	0.000	3113.552
2005	177.929	142.343	0.000	0.000	0.000	20.000	0.000	2846.864	0.000	2846.864
2006	163.003	130.402	0.000	0.000	0.000	20.000	0.000	2608.048	0.000	2608.048
2007	147.588	118.070	0.000	0.000	0.000	20.000	0.000	2361.408	0.000	2361.408
2008	133.133	106.506	0.000	0.000	0.000	20.000	0.000	2130.128	0.000	2130.128
2009	120.594	96.475	0.000	0.000	0.000	20.000	0.000	1929.504	0.000	1929.504
2010	110.609	88.487	0.000	0.000	0.000	20.000	0.000	1769.744	0.000	1769.744
SUBTOTAL	3241.962	2593.570	88.141	110.717	70.513	20.000	1.800	51871.406	−32.509	51838.898
REMAINING	102.437	81.950	0.000	0.000	0.000	20.000	0.000	1638.992	0.000	1638.992
TOT 15.6Yr	3344.399	2675.520	88.141	110.717	70.513	20.000	1.800	53510.398	−32.509	53477.891

YEAR	NET TOTAL INVESTMENTS	NET TOTAL REVENUE	NET LEASE REVENUE	NET BFIT CASHFLOW	NET TAX DEPREC	NET TAXABLE INCOME	NET INCOME TAXES PAID	NET AFIT CASHFLOW	CUM AFIT CASHFLOW	AFIT CF DISC 10.0%
========	===M$===	===M$===	===M$===	===M$===	===M$===	===M$B===	===M$===	===M$===	===M$===	===M$===
1996(7 Mo)	5747.000	930.365	874.365	−4872.635	527.286	−1708.921	0.000	−4872.635	−4872.635	−4695.577
1997	−2590.000	1227.429	−3502.995	−912.995	−760.082	−1816.914	0.000	−912.995	−5785.630	−719.873
1998	0.000	5067.664	2194.898	2194.898	645.656	1549.242	0.000	2194.898	−3590.732	1702.295
1999	0.000	8337.521	6761.355	6761.355	461.183	6300.173	1470.018	5291.338	1700.606	3976.518
2000	0.000	6507.856	5034.356	5034.356	329.416	4704.939	1599.679	3434.677	5135.282	2371.415
2001	0.000	5221.615	3884.380	3884.380	329.416	3554.964	1208.688	2675.692	7810.975	1678.516
2002	0.000	4223.952	2992.865	2992.865	329.416	2663.449	905.573	2087.292	9898.268	1188.714
2003	0.000	3563.248	2398.423	2398.423	164.708	2233.715	759.463	1638.960	11537.228	849.370
2004	0.000	3113.552	1996.198	1996.198	0.000	1996.198	678.707	1317.491	12854.719	621.735
2005	0.000	2846.864	1759.164	1759.164	0.000	1759.164	598.116	1161.048	14015.767	497.875
2006	0.000	2608.048	1545.431	1545.431	0.000	1545.431	525.447	1019.985	15035.751	397.707
2007	0.000	2361.408	1324.956	1324.956	0.000	1324.956	450.485	874.471	15910.222	310.029
2008	0.000	2130.128	1117.419	1117.419	0.000	1117.419	379.922	737.496	16647.719	237.686
2009	0.000	1929.504	936.017	936.017	0.000	936.017	318.246	617.771	17265.490	181.008
2010	0.000	1769.744	791.603	791.603	0.000	791.603	269.145	522.458	17787.949	139.154
SUBTOTAL	3157.000	51838.898	30108.438	26951.438	2027.000	26951.438	9163.490	17787.949	17787.949	8736.571
REMAINING	0.000	1638.992	674.789	674.789	0.000	674.789	229.428	445.361	18233.311	107.819
TOT 15.6Yr	3157.000	53477.891	30783.227	27626.227	2027.000	27626.227	9392.918	18233.311	18233.311	8844.390

Table 16–11a

EVALUATION ANAC1.11

ECONOMIC EVALUATION
HARKEN PARADOX BASIN
REGA INCORPORATED

RUN DATE: 09–08–1997
RUN TIME: 18:11:26

AS OF DATE: JUN96

NAME: ANASAZI CO2 FLOOD LEASE DOE
FIELD: ANASAZI–SAHGZIE
LOCATION: UTAH
FORMATION: DESERT CREEK
OPERATOR: HARKEN ENERGY

CONTINUOUS CO2 GAS RECYCLE
NO GAS PROCESSING BUY FUEL
LEASE INJECTION COMPRESSOR
DOE COST SHARING
BURIED LINES – HEATPRO

NPV	5.0%	16668.814	BFIT
NPV	10.0%	12067.621	BFIT
NPV	15.0%	8843.700	BFIT
NPV	20.0%	6509.871	BFIT
NPV	25.0%	4774.241	BFIT
IRR		56%	BFIT
PAYOUT		JUL99	BFIT
PI		11.48:1	BFIT

====== INTERESTS AND EFFECTIVE DATE ======

COST	OIL	GAS	COND	PRODT	DATE
1.00000	0.80000	0.80000	0.80000	0.80000	JUN96

	======== PRICES ========			========== GROSS RESERVES ==========				
	BEGINING	ENDING	AVERAGE	CUMULATIVE	REMAINING	ULTIMATE	%REMAINING	
OIL	20.00	20.00	20.00	1692.690	3344.399	5037.089	66.40	OIL
GAS	1.80	0.00	1.80	1308.810	88.141	1396.951	6.31	GAS
COND	0.00	0.00	0.00	0.000	0.000	0.000	0.00	COND
PRDT	0.00	0.00	0.00	0.000	0.000	0.000	0.00	PRDT

YEAR	GROSS OIL PRODUCTION	NET OIL PRODUCTION	GROSS GAS PRODUCTION	GROSS GAS AS FUEL	NET GAS PRODUCTION	AVERAGE OIL PRICE	AVERAGE GAS PRICE	NET OIL SALES	NET GAS SALES	NET TOTAL REVENUE
========	==MBBLS==	==MBBLS==	==MMSCF==	==MMSCF==	==MMSCF==	===$/B===	==$/MSCF==	===M$===	===M$===	===M$===
1996(7 Mo)	54.774	43.819	52.810	15.323	42.248	20.000	1.800	876.384	53.981	930.365
1997	82.120	65.696	35.331	95.394	28.265	20.000	1.800	1313.920	−86.491	1227.429
1998	316.729	253.383	0.000	0.000	0.000	20.000	0.000	5067.664	0.000	5067.664
1999	521.095	416.876	0.000	0.000	0.000	20.000	0.000	8337.521	0.000	8337.521
2000	406.741	325.393	0.000	0.000	0.000	20.000	0.000	6507.856	0.000	6507.856
2001	326.351	261.081	0.000	0.000	0.000	20.000	0.000	5221.615	0.000	5221.615
2002	263.997	211.198	0.000	0.000	0.000	20.000	0.000	4223.952	0.000	4223.952
2003	222.703	178.162	0.000	0.000	0.000	20.000	0.000	3563.248	0.000	3563.248
2004	194.597	155.678	0.000	0.000	0.000	20.000	0.000	3113.552	0.000	3113.552
2005	177.929	142.343	0.000	0.000	0.000	20.000	0.000	2846.864	0.000	2846.864
2006	163.003	130.402	0.000	0.000	0.000	20.000	0.000	2608.048	0.000	2608.048
2007	147.588	118.070	0.000	0.000	0.000	20.000	0.000	2361.408	0.000	2361.408
2008	133.133	106.506	0.000	0.000	0.000	20.000	0.000	2130.128	0.000	2130.128
2009	120.594	96.475	0.000	0.000	0.000	20.000	0.000	1929.504	0.000	1929.504
2010	110.609	88.487	0.000	0.000	0.000	20.000	0.000	1769.744	0.000	1769.744
SUBTOTAL	3241.962	2593.570	88.141	110.717	70.513	20.000	1.800	51871.406	−32.509	51838.898
REMAINING	102.437	81.950	0.000	0.000	0.000	20.000	0.000	1638.992	0.000	1638.992
TOT 15.6Yr	3344.399	2675.520	88.141	110.717	70.513	20.000	1.800	53510.398	−32.509	53477.891

YEAR	NET TOTAL LOE	NET TANGIBLES	NET INTANGIBLES	NET G&G	NET TOTAL INVESTMENTS	NET LEASE REVENUE	NET BFIT CASHFLOW	CUM BFIT CASHFLOW	BFIT CF DISC 10.0%	CUMBFIT CF DISC 10.0%
========	===M$===	===M$===	===M$===	===M$===	===M$===	===M$B===	===M$===	===M$===	===M$===	===M$===
1996(7 Mo)	56.000	2111.000	1723.000	250.000	4084.000	874.365	−3209.635	−3209.635	−3084.580	−3084.580
1997	5066.424	−952.000	−777.000	−112.000	−1841.000	−3838.995	−1997.995	−5207.629	−1724.713	−4809.292
1998	3208.766	0.000	0.000	0.000	0.000	1858.898	1858.898	−3348.731	1427.794	−3381.498
1999	1912.165	0.000	0.000	0.000	0.000	6425.355	6425.355	3076.624	4771.689	1390.191
2000	1809.500	0.000	0.000	0.000	0.000	4698.356	4698.356	7774.980	3178.069	4568.261
2001	1673.235	0.000	0.000	0.000	0.000	3548.380	3548.380	11323.360	2182.193	6750.454
2002	1567.087	0.000	0.000	0.000	0.000	2656.865	2656.865	13980.226	1484.754	8235.207
2003	1500.825	0.000	0.000	0.000	0.000	2062.423	2062.423	16042.648	1047.575	9282.782
2004	1453.354	0.000	0.000	0.000	0.000	1660.198	1660.198	17702.846	766.286	10049.068
2005	1423.700	0.000	0.000	0.000	0.000	1423.164	1423.164	19126.010	596.955	10646.023
2006	1398.617	0.000	0.000	0.000	0.000	1209.432	1209.432	20335.441	461.277	11107.300
2007	1372.452	0.000	0.000	0.000	0.000	988.956	988.956	21324.396	342.967	11450.268
2008	1348.709	0.000	0.000	0.000	0.000	781.419	781.419	22105.816	246.363	11696.631
2009	1329.487	0.000	0.000	0.000	0.000	600.017	600.017	22705.834	171.996	11868.627
2010	1314.141	0.000	0.000	0.000	0.000	455.603	455.603	23161.438	118.732	11987.358
SUBTOTAL	26434.459	1159.000	946.000	138.000	2243.000	25404.438	23161.438	23161.438	11987.358	11987.358
REMAINING	1300.203	0.000	0.000	0.000	0.000	338.789	338.789	23500.227	80.259	12067.617
TOT 15.6Yr	27734.662	1159.000	946.000	138.000	2243.000	25743.227	23500.227	23500.227	12067.617	12067.617

Table 16–11b

EVALUATION ANAC1.11

ECONOMIC EVALUATION
HARKEN PARADOX BASIN
REGA INCORPORATED

RUN DATE: 09–08–1997
RUN TIME: 18:12:15

AS OF DATE: JUN96

NAME: ANASAZI CO2 FLOOD LEASE DOE
FIELD: ANASAZI–SAHGZIE
LOCATION: UTAH
FORMATION: DESERT CREEK
OPERATOR: HARKEN ENERGY

CONTINUOUS CO2 GAS RECYCLE
NO GAS PROCESSING BUY FUEL
LEASE INJECTION COMPRESSOR
DOE COST SHARING
BURIED LINES – HEATPRO

NPV	5.0%	16668.814	BFIT	10945.498	AFIT
NPV	10.0%	12067.621	BFIT	7824.961	AFIT
NPV	15.0%	8843.700	BFIT	5609.272	AFIT
NPV	20.0%	6509.871	BFIT	3986.404	AFIT
NPV	25.0%	4774.241	BFIT	2767.116	AFIT
IRR		56%	BFIT	46%	AFIT
PAYOUT		JUL99	BFIT	AUG99	AFIT
PI		11.48:1	BFIT	7.92:1	AFIT

====== INTERESTS AND EFFECTIVE DATE ======							======== PRICES ========			========== GROSS RESERVES ==========				
COST	OIL	GAS	COND	PRODT	DATE		BEGINING	ENDING	AVERAGE	CUMULATIVE	REMAINING	ULTIMATE	%REMAINING	
1.00000	0.80000	0.80000	0.80000	0.80000	JUN96	OIL	20.00	20.00	20.00	1692.690	3344.399	5037.089	66.40	OIL
						GAS	1.80	0.00	1.80	1308.810	88.141	1396.951	6.31	GAS
						COND	0.00	0.00	0.00	0.000	0.000	0.000	0.00	COND
						PRDT	0.00	0.00	0.00	0.000	0.000	0.000	0.00	PRDT

YEAR	GROSS OIL PRODUCTION	NET OIL PRODUCTION	GROSS GAS PRODUCTION	GROSS GAS AS FUEL	NET GAS PRODUCTION	AVERAGE OIL PRICE	AVERAGE GAS PRICE	NET OIL SALES	NET GAS SALES	NET TOTAL REVENUE
========	==MBBLS==	==MBBLS==	==MMSCF==	==MMSCF==	==MMSCF==	===$/B===	==$/MSCF==	===M$===	===M$===	===M$===
1996(7 Mo)	54.774	43.819	52.810	15.323	42.248	20.000	1.800	876.384	53.981	930.365
1997	82.120	65.696	35.331	95.394	28.265	20.000	1.800	1313.920	−86.491	1227.429
1998	316.729	253.383	0.000	0.000	0.000	20.000	0.000	5067.664	0.000	5067.664
1999	521.095	416.876	0.000	0.000	0.000	20.000	0.000	8337.521	0.000	8337.521
2000	406.741	325.393	0.000	0.000	0.000	20.000	0.000	6507.856	0.000	6507.856
2001	326.351	261.081	0.000	0.000	0.000	20.000	0.000	5221.615	0.000	5221.615
2002	263.997	211.198	0.000	0.000	0.000	20.000	0.000	4223.952	0.000	4223.952
2003	222.703	178.162	0.000	0.000	0.000	20.000	0.000	3563.248	0.000	3563.248
2004	194.597	155.678	0.000	0.000	0.000	20.000	0.000	3113.552	0.000	3113.552
2005	177.929	142.343	0.000	0.000	0.000	20.000	0.000	2846.864	0.000	2846.864
2006	163.003	130.402	0.000	0.000	0.000	20.000	0.000	2608.048	0.000	2608.048
2007	147.588	118.070	0.000	0.000	0.000	20.000	0.000	2361.408	0.000	2361.408
2008	133.133	106.506	0.000	0.000	0.000	20.000	0.000	2130.128	0.000	2130.128
2009	120.594	96.475	0.000	0.000	0.000	20.000	0.000	1929.504	0.000	1929.504
2010	110.609	88.487	0.000	0.000	0.000	20.000	0.000	1769.744	0.000	1769.744
SUBTOTAL	3241.962	2593.570	88.141	110.717	70.513	20.000	1.800	51871.406	−32.509	51838.898
REMAINING	102.437	81.950	0.000	0.000	0.000	20.000	0.000	1638.992	0.000	1638.992
TOT 15.6Yr	3344.399	2675.520	88.141	110.717	70.513	20.000	1.800	53510.398	−32.509	53477.891

YEAR	NET TOTAL INVESTMENTS	NET TOTAL REVENUE	NET LEASE REVENUE	NET BFIT CASHFLOW	NET TAX DEPREC	NET TAXABLE INCOME	NET INCOME TAXES PAID	NET AFIT CASHFLOW	CUM AFIT CASHFLOW	AFIT CF DISC 10.0%
========	===M$===	===M$===	===M$===	===M$===	===M$===	===M$B===	===M$===	===M$===	===M$===	===M$===
1996(7 Mo)	4084.000	930.365	874.365	−3209.635	301.571	−1400.206	0.000	−3209.635	−3209.635	−3084.580
1997	−1841.000	1227.429	−3838.995	−1997.995	−435.020	−2514.974	0.000	−1997.995	−5207.629	−1724.713
1998	0.000	5067.664	1858.898	1858.898	369.271	1489.627	0.000	1858.898	−3348.731	1427.794
1999	0.000	8337.521	6425.355	6425.355	263.765	6161.590	1270.253	5155.103	1806.372	3868.942
2000	0.000	6507.856	4698.356	4698.356	188.404	4509.952	1533.384	3164.972	4971.344	2187.387
2001	0.000	5221.615	3548.380	3548.380	188.404	3359.977	1142.392	2405.988	7377.332	1511.219
2002	0.000	4223.952	2656.865	2656.865	188.404	2468.461	839.277	1817.588	9194.920	1036.624
2003	0.000	3563.248	2062.423	2062.423	94.202	1968.222	669.195	1393.228	10588.148	722.743
2004	0.000	3113.552	1660.198	1660.198	0.000	1660.198	564.467	1095.731	11683.879	517.198
2005	0.000	2846.864	1423.164	1423.164	0.000	1423.164	483.876	939.288	12623.167	402.842
2006	0.000	2608.048	1209.432	1209.432	0.000	1209.432	411.207	798.225	13421.392	311.313
2007	0.000	2361.408	988.956	988.956	0.000	988.956	336.245	652.711	14074.103	231.489
2008	0.000	2130.128	781.419	781.419	0.000	781.419	265.682	515.737	14589.839	166.286
2009	0.000	1929.504	600.017	600.017	0.000	600.017	204.006	396.011	14985.850	116.099
2010	0.000	1769.744	455.603	455.603	0.000	455.603	154.905	300.698	15286.548	80.146
SUBTOTAL	2243.000	51838.898	25404.438	23161.438	1159.000	23161.438	7874.889	15286.548	15286.548	7770.792
REMAINING	0.000	1638.992	338.789	338.789	0.000	338.789	115.188	223.601	15510.148	54.175
TOT 15.6Yr	2243.000	53477.891	25743.227	23500.227	1159.000	23500.227	7990.077	15510.148	15510.148	7824.966

Table 16–12a

EVALUATION ANAC1.14

ECONOMIC EVALUATION
HARKEN PARADOX BASIN
REGA INCORPORATED

RUN DATE: 09–05–1997
RUN TIME: 08:47:09

AS OF DATE: JUN96

NAME: ANASAZI CO2 FLOOD RECYCLE ALL
FIELD: ANASAZI–SAHGZIE
LOCATION: UTAH
FORMATION: DESERT CREEK
OPERATOR: HARKEN ENERGY

CO2 INJ/RECYCLE & BLOWDOWN–2
NO GAS PROCESSING BUY FUEL
SURFACE LINES – ZAPLOCK

NPV	5.0%	13745.337	BFIT
NPV	10.0%	9759.158	BFIT
NPV	15.0%	6862.502	BFIT
NPV	20.0%	4705.629	BFIT
NPV	25.0%	3066.648	BFIT
IRR		40%	BFIT
PAYOUT		OCT99	BFIT
PI		5.04:1	BFIT

====== INTERESTS AND EFFECTIVE DATE ======						======== PRICES ========				========== GROSS RESERVES ==========				
COST	OIL	GAS	COND	PRODT	DATE		BEGINING	ENDING	AVERAGE	CUMULATIVE	REMAINING	ULTIMATE	%REMAINING	
1.00000	0.80000	0.80000	0.80000	0.80000	JUN96	OIL	20.00	20.00	20.00	1692.690	2570.691	4263.381	60.30	OIL
						GAS	1.80	0.00	1.80	1308.810	88.141	1396.951	6.31	GAS
						COND	0.00	0.00	0.00	0.000	0.000	0.000	0.00	COND
						PRDT	0.00	0.00	0.00	0.000	0.000	0.000	0.00	PRDT

YEAR	GROSS OIL PRODUCTION	NET OIL PRODUCTION	GROSS GAS PRODUCTION	GROSS GAS AS FUEL	NET GAS PRODUCTION	AVERAGE OIL PRICE	AVERAGE GAS PRICE	NET OIL SALES	NET GAS SALES	NET TOTAL REVENUE
========	==MBBLS==	==MBBLS==	==MMSCF==	==MMSCF==	==MMSCF==	===$/B===	==$/MSCF==	===M$===	===M$===	===M$===
1996(7 Mo)	54.774	43.819	52.810	15.323	42.248	20.000	1.800	876.384	53.981	930.365
1997	82.120	65.696	35.331	95.394	28.265	20.000	1.800	1313.920	–86.491	1227.429
1998	316.729	253.383	0.000	0.000	0.000	20.000	0.000	5067.664	0.000	5067.664
1999	521.095	416.876	0.000	0.000	0.000	20.000	0.000	8337.521	0.000	8337.521
2000	406.741	325.393	0.000	0.000	0.000	20.000	0.000	6507.856	0.000	6507.856
2001	326.351	261.081	0.000	0.000	0.000	20.000	0.000	5221.615	0.000	5221.615
2002	263.997	211.198	0.000	0.000	0.000	20.000	0.000	4223.952	0.000	4223.952
2003	125.336	100.269	0.000	0.000	0.000	20.000	0.000	2005.376	0.000	2005.376
2004	56.885	45.508	0.000	0.000	0.000	20.000	0.000	910.160	0.000	910.160
2005	135.149	108.119	0.000	0.000	0.000	20.000	0.000	2162.384	0.000	2162.384
2006	86.287	69.030	0.000	0.000	0.000	20.000	0.000	1380.592	0.000	1380.592
2007	56.760	45.408	0.000	0.000	0.000	20.000	0.000	908.160	0.000	908.160
2008	43.917	35.134	0.000	0.000	0.000	20.000	0.000	702.672	0.000	702.672
2009	34.184	27.347	0.000	0.000	0.000	20.000	0.000	546.944	0.000	546.944
2010	30.366	24.293	0.000	0.000	0.000	20.000	0.000	485.856	0.000	485.856
SUBTOTAL	2540.691	2032.553	88.141	110.717	70.513	20.000	1.800	40651.055	–32.509	40618.547
REMAINING	30.000	24.000	0.000	0.000	0.000	20.000	0.000	480.000	0.000	480.000
TOT 15.6Yr	2570.691	2056.553	88.141	110.717	70.513	20.000	1.800	41131.055	–32.509	41098.547

YEAR	NET TOTAL LOE	NET TANGIBLES	NET INTANGIBLES	NET G&G	NET TOTAL INVESTMENTS	NET LEASE REVENUE	NET BFIT CASHFLOW	CUM BFIT CASHFLOW	BFIT CF DISC 10.0%	CUMBFIT CF DISC 10.0%
========	===M$===	===M$===	===M$===	===M$===	===M$===	===M$B===	===M$===	===M$===	===M$===	===M$===
1996(7 Mo)	56.000	3343.000	1216.000	250.000	4809.000	874.365	–3934.635	–3934.635	–3805.880	–3805.880
1997	4730.424	0.000	0.000	0.000	0.000	–3502.995	–3502.995	–7437.630	–3150.424	–6956.304
1998	2872.766	0.000	0.000	0.000	0.000	2194.898	2194.898	–5242.732	1702.295	–5254.009
1999	1576.165	0.000	0.000	0.000	0.000	6761.355	6761.355	1518.624	5021.235	–232.774
2000	1473.500	0.000	0.000	0.000	0.000	5034.356	5034.356	6552.979	3404.929	3172.155
2001	1337.235	0.000	0.000	0.000	0.000	3884.380	3884.380	10437.359	2388.429	5560.584
2002	1231.087	0.000	0.000	0.000	0.000	2992.865	2992.865	13430.225	1672.241	7232.825
2003	402.000	0.000	0.000	0.000	0.000	1603.376	1603.376	15033.601	830.560	8063.386
2004	402.000	0.000	0.000	0.000	0.000	508.160	508.160	15541.761	228.972	8292.357
2005	402.000	0.000	0.000	0.000	0.000	1760.384	1760.384	17302.145	738.692	9031.049
2006	402.000	0.000	0.000	0.000	0.000	978.592	978.592	18280.736	374.959	9406.008
2007	402.000	0.000	0.000	0.000	0.000	506.160	506.160	18786.896	175.989	9581.997
2008	402.000	0.000	0.000	0.000	0.000	300.672	300.672	19087.568	95.121	9677.118
2009	402.000	0.000	0.000	0.000	0.000	144.944	144.944	19232.512	41.698	9718.816
2010	402.000	0.000	0.000	0.000	0.000	83.856	83.856	19316.367	21.885	9740.701
SUBTOTAL	16493.178	3343.000	1216.000	250.000	4809.000	24125.367	19316.367	19316.367	9740.701	9740.701
REMAINING	402.000	0.000	0.000	0.000	0.000	78.000	78.000	19394.367	18.458	9759.159
TOT 15.6Yr	16895.178	3343.000	1216.000	250.000	4809.000	24203.367	19394.367	19394.367	9759.159	9759.159

Table 16–12b

EVALUATION ANAC1.14

ECONOMIC EVALUATION
HARKEN PARADOX BASIN
REGA INCORPORATED

RUN DATE: 09–05–1997
RUN TIME: 08:52:04

AS OF DATE: JUN96

NAME: ANASAZI CO2 FLOOD RECYCLE ALL
FIELD: ANASAZI–SAHGZIE
LOCATION: UTAH
FORMATION: DESERT CREEK
OPERATOR: HARKEN ENERGY

CO2 INJ/RECYCLE & BLOWDOWN–2
NO GAS PROCESSING BUY FUEL
SURFACE LINES – ZAPLOCK

NPV	5.0%	13745.337	BFIT	8899.573	AFIT
NPV	10.0%	9759.158	BFIT	6102.101	AFIT
NPV	15.0%	6862.502	BFIT	4040.250	AFIT
NPV	20.0%	4705.629	BFIT	2486.015	AFIT
NPV	25.0%	3066.648	BFIT	1292.473	AFIT
IRR		40%	BFIT	32%	AFIT
PAYOUT		OCT99	BFIT	NOV99	AFIT
PI		5.04:1	BFIT	3.67:1	AFIT

====== INTERESTS AND EFFECTIVE DATE ======

COST	OIL	GAS	COND	PRODT	DATE
1.00000	0.80000	0.80000	0.80000	0.80000	JUN96

	======== PRICES ========			========== GROSS RESERVES ==========				
	BEGINING	ENDING	AVERAGE	CUMULATIVE	REMAINING	ULTIMATE	%REMAINING	
OIL	20.00	20.00	20.00	1692.690	2570.691	4263.381	60.30	OIL
GAS	1.80	0.00	1.80	1308.810	88.141	1396.951	6.31	GAS
COND	0.00	0.00	0.00	0.000	0.000	0.000	0.00	COND
PRDT	0.00	0.00	0.00	0.000	0.000	0.000	0.00	PRDT

YEAR	GROSS OIL PRODUCTION	NET OIL PRODUCTION	GROSS GAS PRODUCTION	GROSS GAS AS FUEL	NET GAS PRODUCTION	AVERAGE OIL PRICE	AVERAGE GAS PRICE	NET OIL SALES	NET GAS SALES	NET TOTAL REVENUE
========	==MBBLS==	==MBBLS==	==MMSCF==	==MMSCF==	==MMSCF==	===$/B===	==$/MSCF==	===M$===	===M$===	===M$===
1996(7 Mo)	54.774	43.819	52.810	15.323	42.248	20.000	1.800	876.384	53.981	930.365
1997	82.120	65.696	35.331	95.394	28.265	20.000	1.800	1313.920	−86.491	1227.429
1998	316.729	253.383	0.000	0.000	0.000	20.000	0.000	5067.664	0.000	5067.664
1999	521.095	416.876	0.000	0.000	0.000	20.000	0.000	8337.521	0.000	8337.521
2000	406.741	325.393	0.000	0.000	0.000	20.000	0.000	6507.856	0.000	6507.856
2001	326.351	261.081	0.000	0.000	0.000	20.000	0.000	5221.615	0.000	5221.615
2002	263.997	211.198	0.000	0.000	0.000	20.000	0.000	4223.952	0.000	4223.952
2003	125.336	100.269	0.000	0.000	0.000	20.000	0.000	2005.376	0.000	2005.376
2004	56.885	45.508	0.000	0.000	0.000	20.000	0.000	910.160	0.000	910.160
2005	135.149	108.119	0.000	0.000	0.000	20.000	0.000	2162.384	0.000	2162.384
2006	86.287	69.030	0.000	0.000	0.000	20.000	0.000	1380.592	0.000	1380.592
2007	56.760	45.408	0.000	0.000	0.000	20.000	0.000	908.160	0.000	908.160
2008	43.917	35.134	0.000	0.000	0.000	20.000	0.000	702.672	0.000	702.672
2009	34.184	27.347	0.000	0.000	0.000	20.000	0.000	546.944	0.000	546.944
2010	30.366	24.293	0.000	0.000	0.000	20.000	0.000	485.856	0.000	485.856
SUBTOTAL	2540.691	2032.553	88.141	110.717	70.513	20.000	1.800	40651.055	−32.509	40618.547
REMAINING	30.000	24.000	0.000	0.000	0.000	20.000	0.000	480.000	0.000	480.000
TOT 15.6Yr	2570.691	2056.553	88.141	110.717	70.513	20.000	1.800	41131.055	−32.509	41098.547

YEAR	NET TOTAL INVESTMENTS	NET TOTAL REVENUE	NET LEASE REVENUE	NET BFIT CASHFLOW	NET TAX DEPREC	NET TAXABLE INCOME	NET INCOME TAXES PAID	NET AFIT CASHFLOW	CUM AFIT CASHFLOW	AFIT CF DISC 10.0%
========	===M$===	===M$===	===M$===	===M$===	===M$===	===M$B===	===M$===	===M$===	===M$===	===M$===
1996(7 Mo)	4809.000	930.365	874.365	−3934.635	477.571	−1069.206	0.000	−3934.635	−3934.635	−3805.880
1997	0.000	1227.429	−3502.995	−3502.995	818.694	−4321.689	0.000	−3502.995	−7437.630	−3150.424
1998	0.000	5067.664	2194.898	2194.898	584.781	1610.117	0.000	2194.898	−5242.732	1702.295
1999	0.000	8337.521	6761.355	6761.355	417.701	6343.654	871.378	5889.978	647.246	4401.961
2000	0.000	6507.856	5034.356	5034.356	298.358	4735.998	1610.239	3424.117	4071.362	2364.593
2001	0.000	5221.615	3884.380	3884.380	298.358	3586.022	1219.248	2665.133	6736.495	1672.314
2002	0.000	4223.952	2992.865	2992.865	298.358	2694.507	916.133	2076.733	8813.228	1183.075
2003	0.000	2005.376	1603.376	1603.376	149.179	1454.197	494.427	1108.949	9922.177	590.563
2004	0.000	910.160	508.160	508.160	0.000	508.160	172.774	335.386	10257.563	152.730
2005	0.000	2162.384	1760.384	1760.384	0.000	1760.384	598.531	1161.854	11419.416	498.584
2006	0.000	1380.592	978.592	978.592	0.000	978.592	332.721	645.871	12065.287	253.618
2007	0.000	908.160	506.160	506.160	0.000	506.160	172.094	334.066	12399.353	118.933
2008	0.000	702.672	300.672	300.672	0.000	300.672	102.228	198.443	12597.796	64.310
2009	0.000	546.944	144.944	144.944	0.000	144.944	49.281	95.663	12693.459	28.195
2010	0.000	485.856	83.856	83.856	0.000	83.856	28.511	55.345	12748.804	14.783
SUBTOTAL	4809.000	40618.547	24125.367	19316.367	3343.000	19316.369	6567.565	12748.804	12748.804	6089.648
REMAINING	0.000	480.000	78.000	78.000	0.000	78.000	26.520	51.480	12800.284	12.453
TOT 15.6Yr	4809.000	41098.547	24203.367	19394.367	3343.000	19394.369	6594.085	12800.284	12800.284	6102.102

Table 16–13a

EVALUATION ANAC1.15

ECONOMIC EVALUATION
HARKEN PARADOX BASIN
REGA INCORPORATED

RUN DATE: 09–05–1997
RUN TIME: 09:11:27

AS OF DATE: JUN96

NAME: ANASAZI CO2 FLOOD RECYCLE ALL
FIELD: ANASAZI–SAHGZIE
LOCATION: UTAH
FORMATION: DESERT CREEK
OPERATOR: HARKEN ENERGY

CO2 INJ/RECYCLE & BLOWDOWN–2
NO GAS PROCESSING BUY FUEL
BURIED LINES – HEATPRO

NPV	5.0%	12832.387	BFIT
NPV	10.0%	8869.462	BFIT
NPV	15.0%	5994.467	BFIT
NPV	20.0%	3857.830	BFIT
NPV	25.0%	2237.810	BFIT
IRR		35%	BFIT
PAYOUT		NOV99	BFIT
PI		4.22:1	BFIT

====== INTERESTS AND EFFECTIVE DATE ======

COST	OIL	GAS	COND	PRODT	DATE
1.00000	0.80000	0.80000	0.80000	0.80000	JUN96

	======== PRICES ========			========== GROSS RESERVES ==========				
	BEGINING	ENDING	AVERAGE	CUMULATIVE	REMAINING	ULTIMATE	%REMAINING	
OIL	20.00	20.00	20.00	1692.690	2570.691	4263.381	60.30	OIL
GAS	1.80	0.00	1.80	1308.810	88.141	1396.951	6.31	GAS
COND	0.00	0.00	0.00	0.000	0.000	0.000	0.00	COND
PRDT	0.00	0.00	0.00	0.000	0.000	0.000	0.00	PRDT

YEAR	GROSS OIL PRODUCTION	NET OIL PRODUCTION	GROSS GAS PRODUCTION	GROSS GAS AS FUEL	NET GAS PRODUCTION	AVERAGE OIL PRICE	AVERAGE GAS PRICE	NET OIL SALES	NET GAS SALES	NET TOTAL REVENUE
========	==MBBLS==	==MBBLS==	==MMSCF==	==MMSCF==	==MMSCF==	===$/B===	==$/MSCF==	===M$===	===M$===	===M$===
1996(7 Mo)	54.774	43.819	52.810	15.323	42.248	20.000	1.800	876.384	53.981	930.365
1997	82.120	65.696	35.331	95.394	28.265	20.000	1.800	1313.920	−86.491	1227.429
1998	316.729	253.383	0.000	0.000	0.000	20.000	0.000	5067.664	0.000	5067.664
1999	521.095	416.876	0.000	0.000	0.000	20.000	0.000	8337.521	0.000	8337.521
2000	406.741	325.393	0.000	0.000	0.000	20.000	0.000	6507.856	0.000	6507.856
2001	326.351	261.081	0.000	0.000	0.000	20.000	0.000	5221.615	0.000	5221.615
2002	263.997	211.198	0.000	0.000	0.000	20.000	0.000	4223.952	0.000	4223.952
2003	125.336	100.269	0.000	0.000	0.000	20.000	0.000	2005.376	0.000	2005.376
2004	56.885	45.508	0.000	0.000	0.000	20.000	0.000	910.160	0.000	910.160
2005	135.149	108.119	0.000	0.000	0.000	20.000	0.000	2162.384	0.000	2162.384
2006	86.287	69.030	0.000	0.000	0.000	20.000	0.000	1380.592	0.000	1380.592
2007	56.760	45.408	0.000	0.000	0.000	20.000	0.000	908.160	0.000	908.160
2008	43.917	35.134	0.000	0.000	0.000	20.000	0.000	702.672	0.000	702.672
2009	34.184	27.347	0.000	0.000	0.000	20.000	0.000	546.944	0.000	546.944
2010	30.366	24.293	0.000	0.000	0.000	20.000	0.000	485.856	0.000	485.856
SUBTOTAL	2540.691	2032.553	88.141	110.717	70.513	20.000	1.800	40651.055	−32.509	40618.547
REMAINING	30.000	24.000	0.000	0.000	0.000	20.000	0.000	480.000	0.000	480.000
TOT 15.6Yr	2570.691	2056.553	88.141	110.717	70.513	20.000	1.800	41131.055	−32.509	41098.547

YEAR	NET TOTAL LOE	NET TANGIBLES	NET INTANGIBLES	NET G&G	NET TOTAL INVESTMENTS	NET LEASE REVENUE	NET BFIT CASHFLOW	CUM BFIT CASHFLOW	BFIT CF DISC 10.0%	CUMBFIT CF DISC 10.0%
========	===M$===	===M$===	===M$===	===M$===	===M$===	===M$B===	===M$===	===M$===	===M$===	===M$===
1996(7 Mo)	56.000	3691.000	1806.000	250.000	5747.000	874.365	−4872.635	−4872.635	−4695.577	−4695.577
1997	4730.424	0.000	0.000	0.000	0.000	−3502.995	−3502.995	−8375.630	−3150.424	−7846.000
1998	2872.766	0.000	0.000	0.000	0.000	2194.898	2194.898	−6180.732	1702.295	−6143.706
1999	1576.165	0.000	0.000	0.000	0.000	6761.355	6761.355	580.624	5021.235	−1122.470
2000	1473.500	0.000	0.000	0.000	0.000	5034.356	5034.356	5614.979	3404.929	2282.459
2001	1337.235	0.000	0.000	0.000	0.000	3884.380	3884.380	9499.359	2388.429	4670.888
2002	1231.087	0.000	0.000	0.000	0.000	2992.865	2992.865	12492.225	1672.241	6343.129
2003	402.000	0.000	0.000	0.000	0.000	1603.376	1603.376	14095.601	830.560	7173.689
2004	402.000	0.000	0.000	0.000	0.000	508.160	508.160	14603.761	228.972	7402.661
2005	402.000	0.000	0.000	0.000	0.000	1760.384	1760.384	16364.145	738.692	8141.353
2006	402.000	0.000	0.000	0.000	0.000	978.592	978.592	17342.736	374.959	8516.312
2007	402.000	0.000	0.000	0.000	0.000	506.160	506.160	17848.896	175.989	8692.301
2008	402.000	0.000	0.000	0.000	0.000	300.672	300.672	18149.568	95.121	8787.422
2009	402.000	0.000	0.000	0.000	0.000	144.944	144.944	18294.512	41.698	8829.120
2010	402.000	0.000	0.000	0.000	0.000	83.856	83.856	18378.367	21.885	8851.005
SUBTOTAL	16493.178	3691.000	1806.000	250.000	5747.000	24125.367	18378.367	18378.367	8851.005	8851.005
REMAINING	402.000	0.000	0.000	0.000	0.000	78.000	78.000	18456.367	18.458	8869.463
TOT 15.6Yr	16895.178	3691.000	1806.000	250.000	5747.000	24203.367	18456.367	18456.367	8869.463	8869.463

Table 16–13b

EVALUATION ANAC1.15

ECONOMIC EVALUATION
HARKEN PARADOX BASIN
REGA INCORPORATED

RUN DATE: 09–05–1997
RUN TIME: 09:16:11

AS OF DATE: JUN96

NAME: ANASAZI CO2 FLOOD RECYCLE ALL
FIELD: ANASAZI–SAHGZIE
LOCATION: UTAH
FORMATION: DESERT CREEK
OPERATOR: HARKEN ENERGY

CO2 INJ/RECYCLE & BLOWDOWN–2
NO GAS PROCESSING BUY FUEL
BURIED LINES – HEATPRO

NPV	5.0%	12832.387	BFIT	8251.146	AFIT
NPV	10.0%	8869.462	BFIT	5434.015	AFIT
NPV	15.0%	5994.467	BFIT	3359.533	AFIT
NPV	20.0%	3857.830	BFIT	1797.824	AFIT
NPV	25.0%	2237.810	BFIT	600.617	AFIT
IRR		35%	BFIT	28%	AFIT
PAYOUT		NOV99	BFIT	JAN00	AFIT
PI		4.22:1	BFIT	3.12:1	AFIT

====== INTERESTS AND EFFECTIVE DATE ======						======== PRICES ========				========== GROSS RESERVES ==========				
COST	OIL	GAS	COND	PRODT	DATE		BEGINING	ENDING	AVERAGE	CUMULATIVE	REMAINING	ULTIMATE	%REMAINING	
1.00000	0.80000	0.80000	0.80000	0.80000	JUN96	OIL	20.00	20.00	20.00	1692.690	2570.691	4263.381	60.30	OIL
						GAS	1.80	0.00	1.80	1308.810	88.141	1396.951	6.31	GAS
						COND	0.00	0.00	0.00	0.000	0.000	0.000	0.00	COND
						PRDT	0.00	0.00	0.00	0.000	0.000	0.000	0.00	PRDT

YEAR	GROSS OIL PRODUCTION	NET OIL PRODUCTION	GROSS GAS PRODUCTION	GROSS GAS AS FUEL	NET GAS PRODUCTION	AVERAGE OIL PRICE	AVERAGE GAS PRICE	NET OIL SALES	NET GAS SALES	NET TOTAL REVENUE
========	==MBBLS==	==MBBLS==	==MMSCF==	==MMSCF==	==MMSCF==	===$/B===	==$/MSCF==	===M$===	===M$===	===M$===
1996(7 Mo)	54.774	43.819	52.810	15.323	42.248	20.000	1.800	876.384	53.981	930.365
1997	82.120	65.696	35.331	95.394	28.265	20.000	1.800	1313.920	−86.491	1227.429
1998	316.729	253.383	0.000	0.000	0.000	20.000	0.000	5067.664	0.000	5067.664
1999	521.095	416.876	0.000	0.000	0.000	20.000	0.000	8337.521	0.000	8337.521
2000	406.741	325.393	0.000	0.000	0.000	20.000	0.000	6507.856	0.000	6507.856
2001	326.351	261.081	0.000	0.000	0.000	20.000	0.000	5221.615	0.000	5221.615
2002	263.997	211.198	0.000	0.000	0.000	20.000	0.000	4223.952	0.000	4223.952
2003	125.336	100.269	0.000	0.000	0.000	20.000	0.000	2005.376	0.000	2005.376
2004	56.885	45.508	0.000	0.000	0.000	20.000	0.000	910.160	0.000	910.160
2005	135.149	108.119	0.000	0.000	0.000	20.000	0.000	2162.384	0.000	2162.384
2006	86.287	69.030	0.000	0.000	0.000	20.000	0.000	1380.592	0.000	1380.592
2007	56.760	45.408	0.000	0.000	0.000	20.000	0.000	908.160	0.000	908.160
2008	43.917	35.134	0.000	0.000	0.000	20.000	0.000	702.672	0.000	702.672
2009	34.184	27.347	0.000	0.000	0.000	20.000	0.000	546.944	0.000	546.944
2010	30.366	24.293	0.000	0.000	0.000	20.000	0.000	485.856	0.000	485.856
SUBTOTAL	2540.691	2032.553	88.141	110.717	70.513	20.000	1.800	40651.055	−32.509	40618.547
REMAINING	30.000	24.000	0.000	0.000	0.000	20.000	0.000	480.000	0.000	480.000
TOT 15.6Yr	2570.691	2056.553	88.141	110.717	70.513	20.000	1.800	41131.055	−32.509	41098.547

YEAR	NET TOTAL INVESTMENTS	NET TOTAL REVENUE	NET LEASE REVENUE	NET BFIT CASHFLOW	NET TAX DEPREC	NET TAXABLE INCOME	NET INCOME TAXES PAID	NET AFIT CASHFLOW	CUM AFIT CASHFLOW	AFIT CF DISC 10.0%
========	===M$===	===M$===	===M$===	===M$===	===M$===	===M$B===	===M$===	===M$===	===M$===	===M$===
1996(7 Mo)	5747.000	930.365	874.365	−4872.635	527.286	−1708.921	0.000	−4872.635	−4872.635	−4695.577
1997	0.000	1227.429	−3502.995	−3502.995	903.918	−4406.914	0.000	−3502.995	−8375.630	−3150.424
1998	0.000	5067.664	2194.898	2194.898	645.656	1549.242	0.000	2194.898	−6180.732	1702.295
1999	0.000	8337.521	6761.355	6761.355	461.183	6300.173	589.417	6171.938	−8.794	4602.346
2000	0.000	6507.856	5034.356	5034.356	329.416	4704.939	1599.679	3434.677	3425.883	2371.415
2001	0.000	5221.615	3884.380	3884.380	329.416	3554.964	1208.688	2675.692	6101.575	1678.516
2002	0.000	4223.952	2992.865	2992.865	329.416	2663.449	905.573	2087.292	8188.868	1188.714
2003	0.000	2005.376	1603.376	1603.376	164.708	1438.668	489.147	1114.229	9303.097	593.125
2004	0.000	910.160	508.160	508.160	0.000	508.160	172.774	335.386	9638.482	152.730
2005	0.000	2162.384	1760.384	1760.384	0.000	1760.384	598.531	1161.854	10800.336	498.584
2006	0.000	1380.592	978.592	978.592	0.000	978.592	332.721	645.871	11446.207	253.618
2007	0.000	908.160	506.160	506.160	0.000	506.160	172.094	334.066	11780.272	118.933
2008	0.000	702.672	300.672	300.672	0.000	300.672	102.228	198.443	11978.716	64.310
2009	0.000	546.944	144.944	144.944	0.000	144.944	49.281	95.663	12074.379	28.195
2010	0.000	485.856	83.856	83.856	0.000	83.856	28.511	55.345	12129.724	14.783
SUBTOTAL	5747.000	40618.547	24125.367	18378.367	3691.000	18378.369	6248.646	12129.724	12129.724	5421.563
REMAINING	0.000	480.000	78.000	78.000	0.000	78.000	26.520	51.480	12181.204	12.453
TOT 15.6Yr	5747.000	41098.547	24203.367	18456.367	3691.000	18456.369	6275.166	12181.204	12181.204	5434.017

Table 16–14
CO_2 Project Investment Summary
Purchase Compressor

Item	Minimum Cost*	Maximum Cost*
Drilling Completions	$ 884,000	$ 884,000
Surface Production Facilities	338,000	338,000
Lease Injection/Production Line	220,000	380,000
CO_2 Supply Line	1,253,000	2,031,000
Injection Compressor	1,663,000	1,663,000
Miscellaneous Fees	201,000	201,000
GSG Expenses	250,000	250,000
Gross Total	4,809,000	5,747,000
Less DOE Cost Sharing	(2,167,000)	(2,590,000)
Net Total	$ 2,642,000	$ 3,197,000

* Refers to installation option for flow/injection lines and CO_2 supply line

Table 16–15
CO_2 Project Investment Summary
Lease Compressor

Item	Minimum Cost*	Maximum Cost*
Drilling/Completion	$ 884,000	$ 884,000
Surface Production Facilities	338,000	338,000
Lease Injection/Production Line	220,000	380,000
CO_2 Supply Line	1,253,000	2,031,000
Miscellaneous Fees	201,000	201,000
G&G Expenses	259,000	250,000
Gross Total	3,146,000	4,084,000
Less DOE Cost Sharing	(1,418,000)	(1,841,000)
Net Total	$ 1,728,000	$ 2,243,000

* Refers to installation option for flow/injection lines and CO_2 supply line

FIGURES

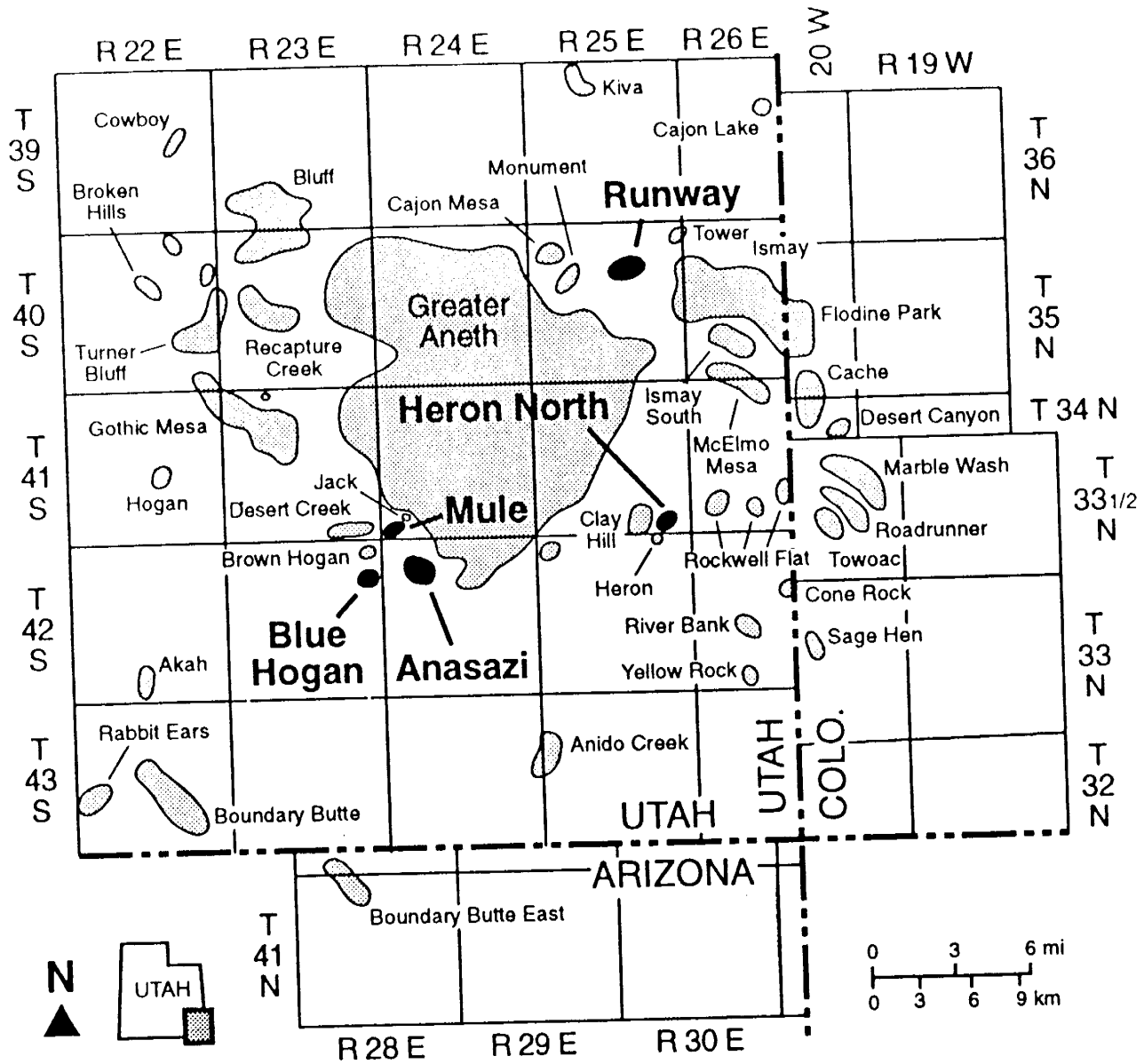

Figure 3–1. Regional Location Map, Anasazi Field.
(courtesy of the Utah Geological Survey)

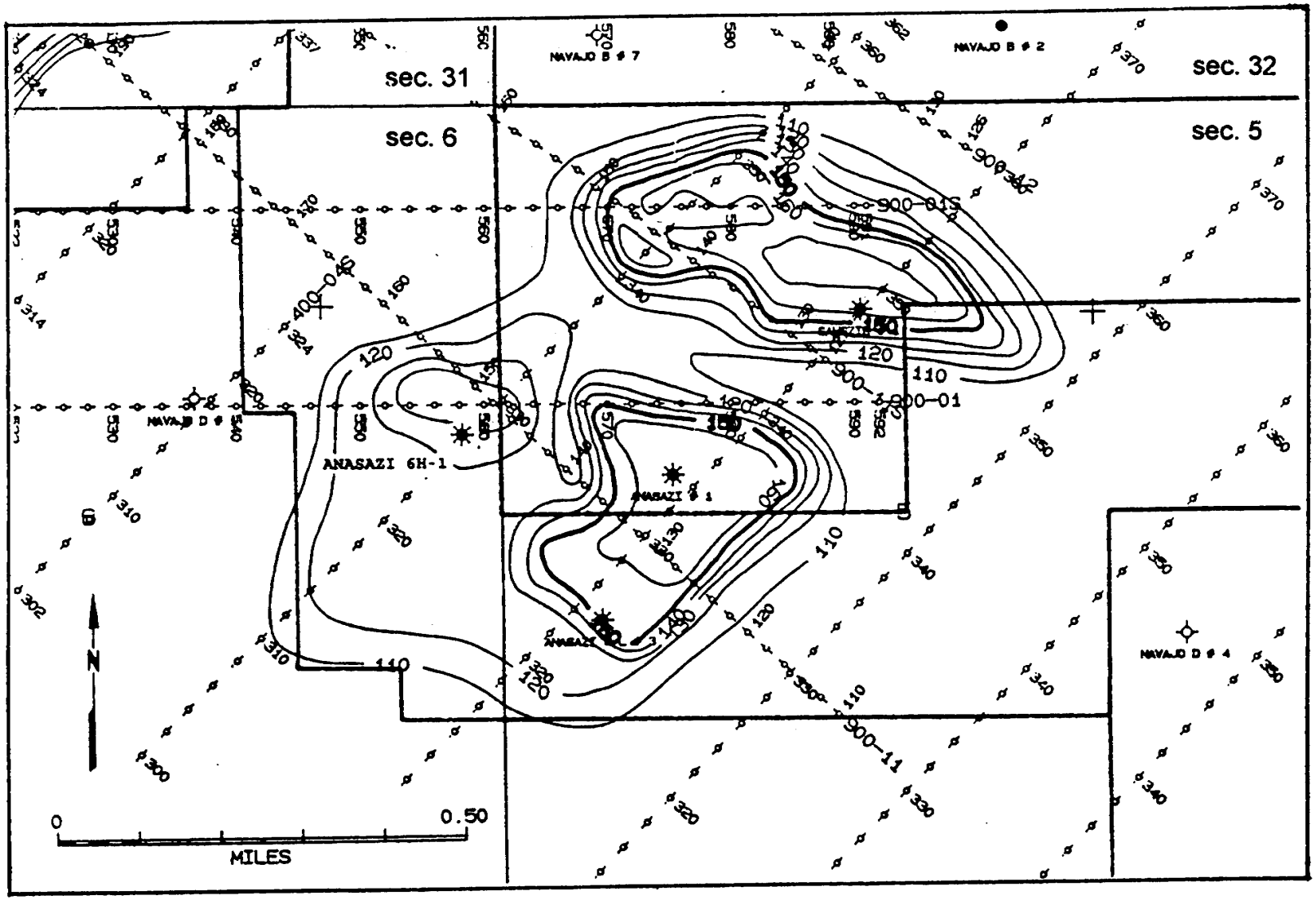

Figure 3–2. Isopach Map of the Anasazi Carbonate Mound Buildup. (courtesy of Harken Southwest Corp. and the Utah Geological Survey)

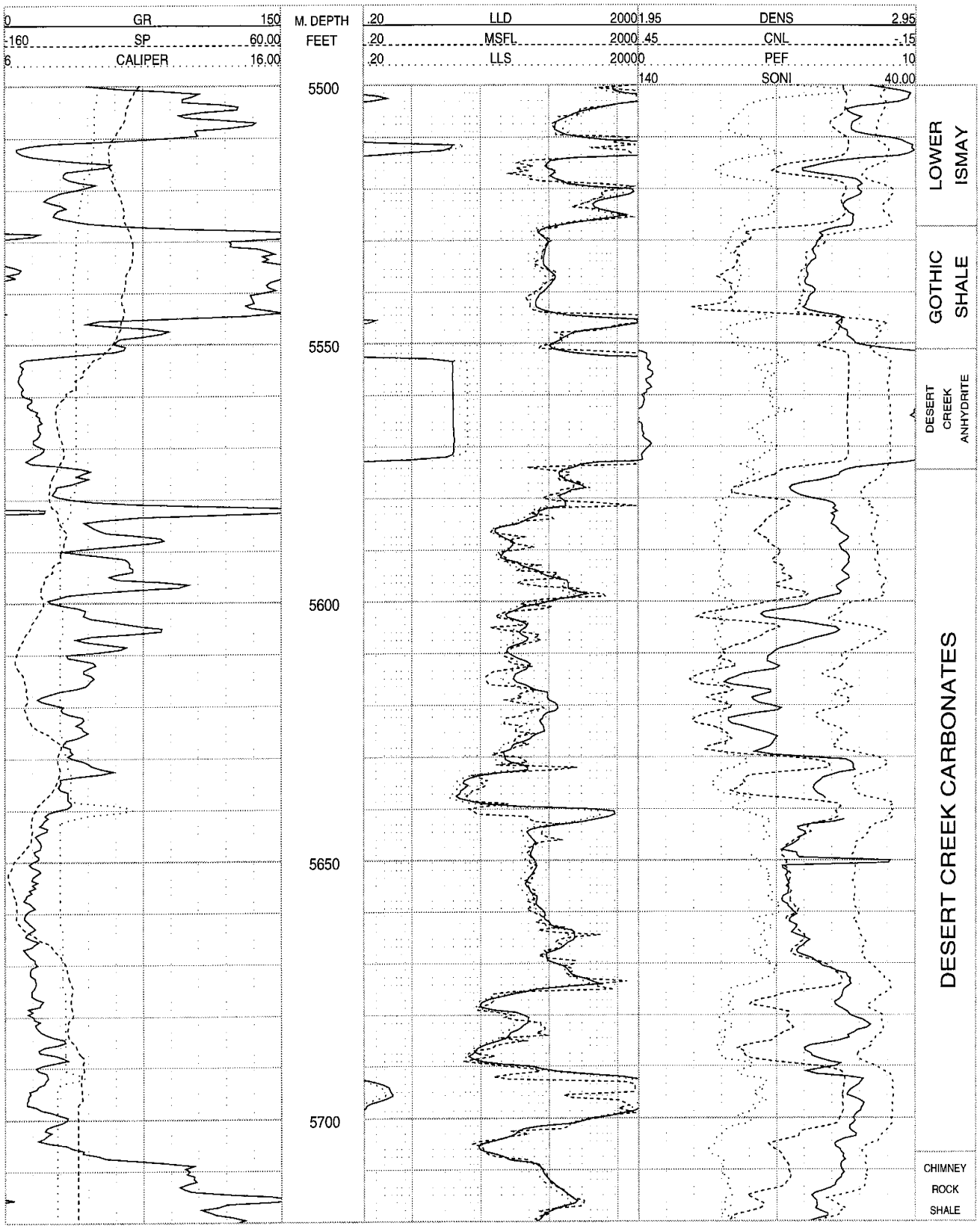

Figure 3.3 Anasazi #1 Log Suite - Unedited

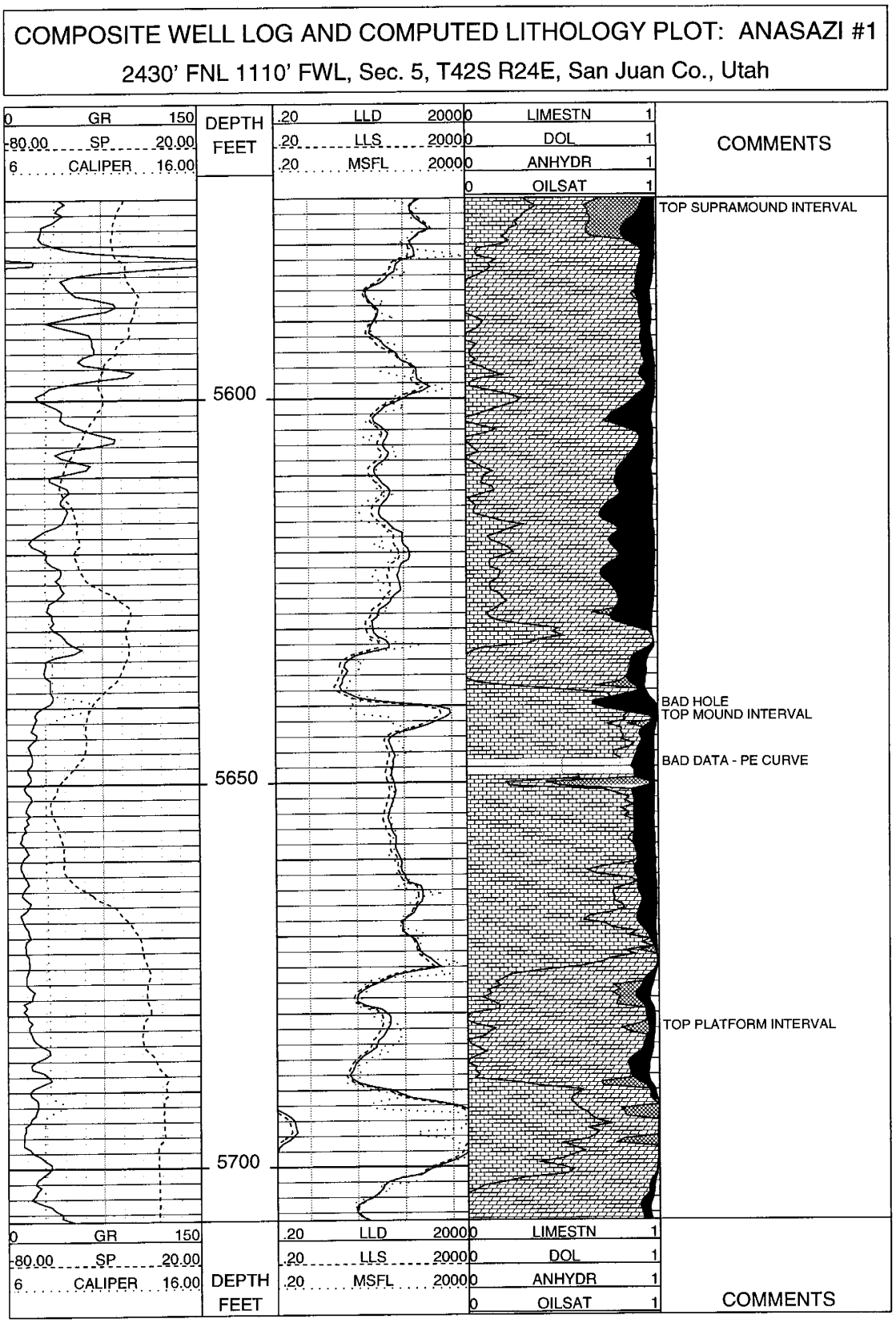

Figure 4-1. Computed Lithology Plot, Anasazi #1

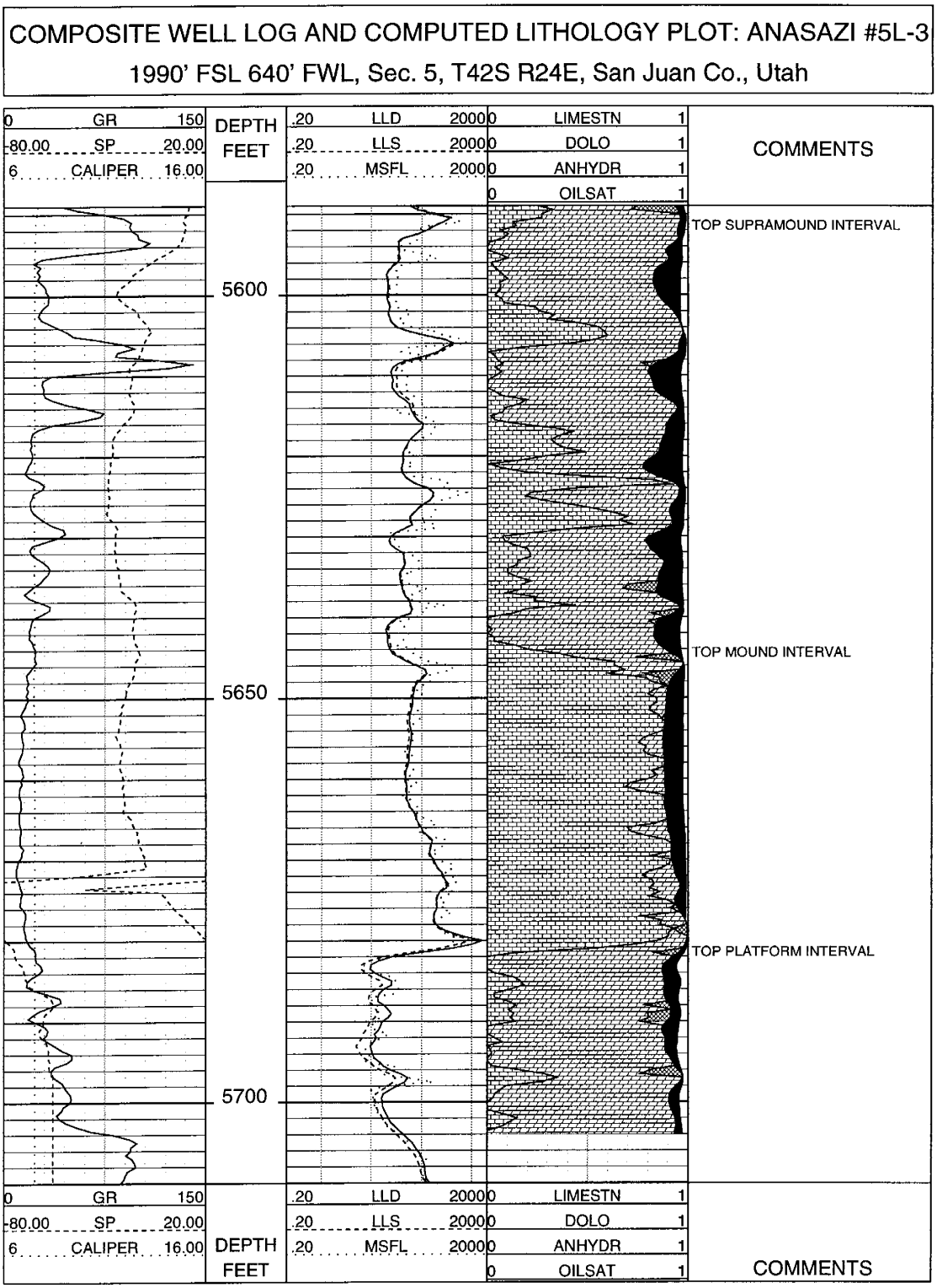

Figure 4-2. Computed Lithology Plot, Anasazi #5L-3

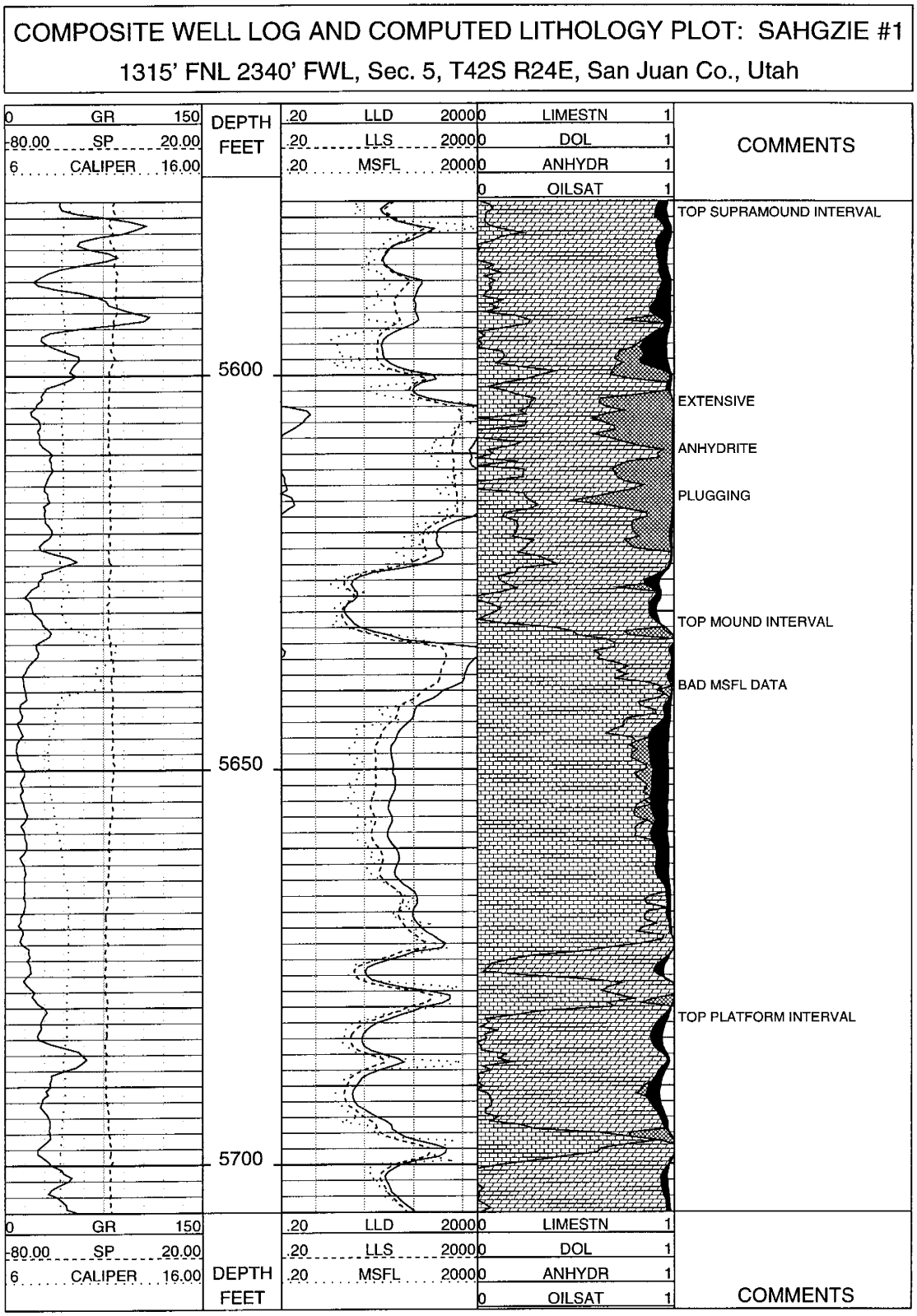

Figure 4-3. Computed Lithology Plot, Sahgzie #1

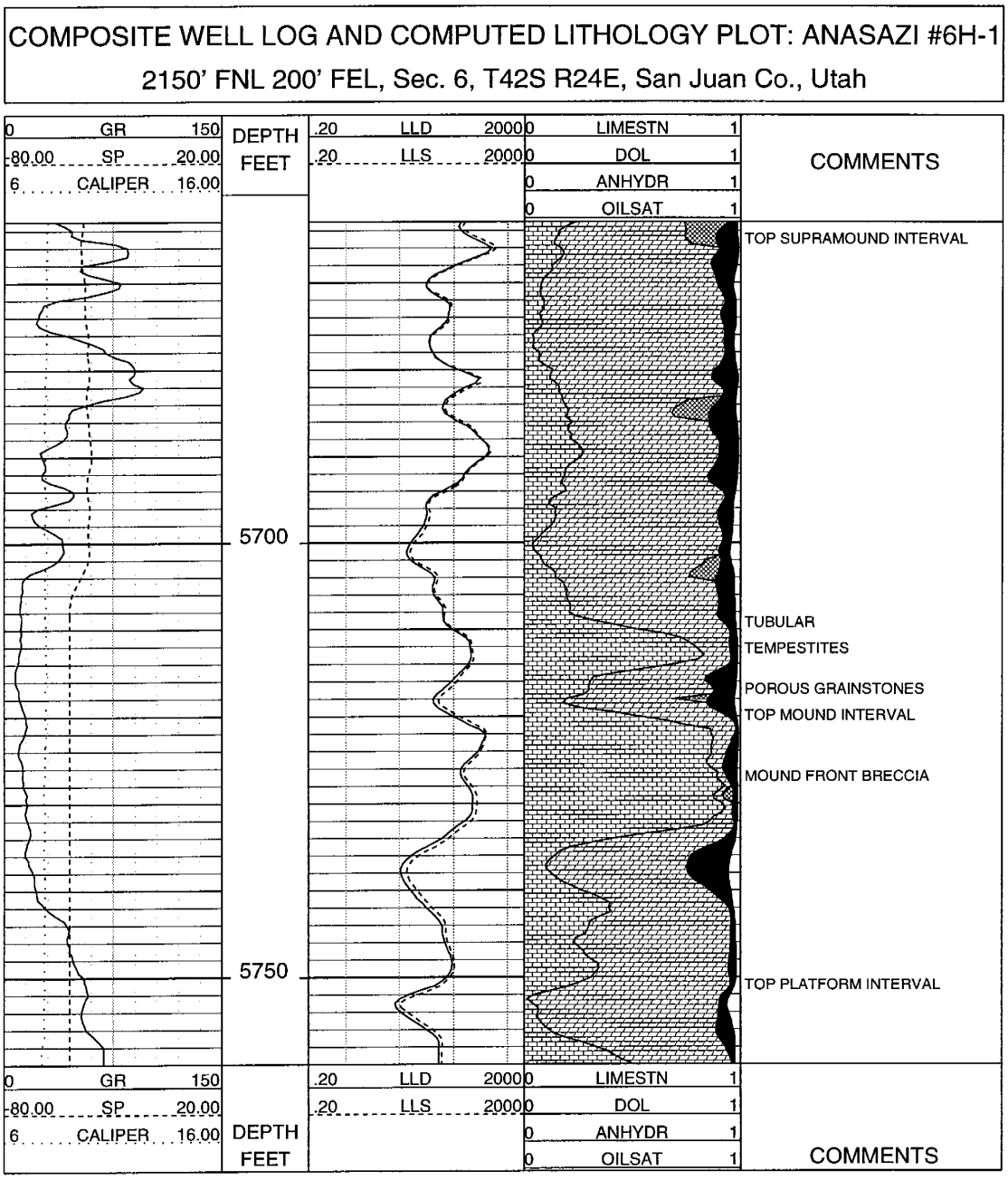

Figure 4-4. Computed Lithology Plot, Anasazi #6H-1

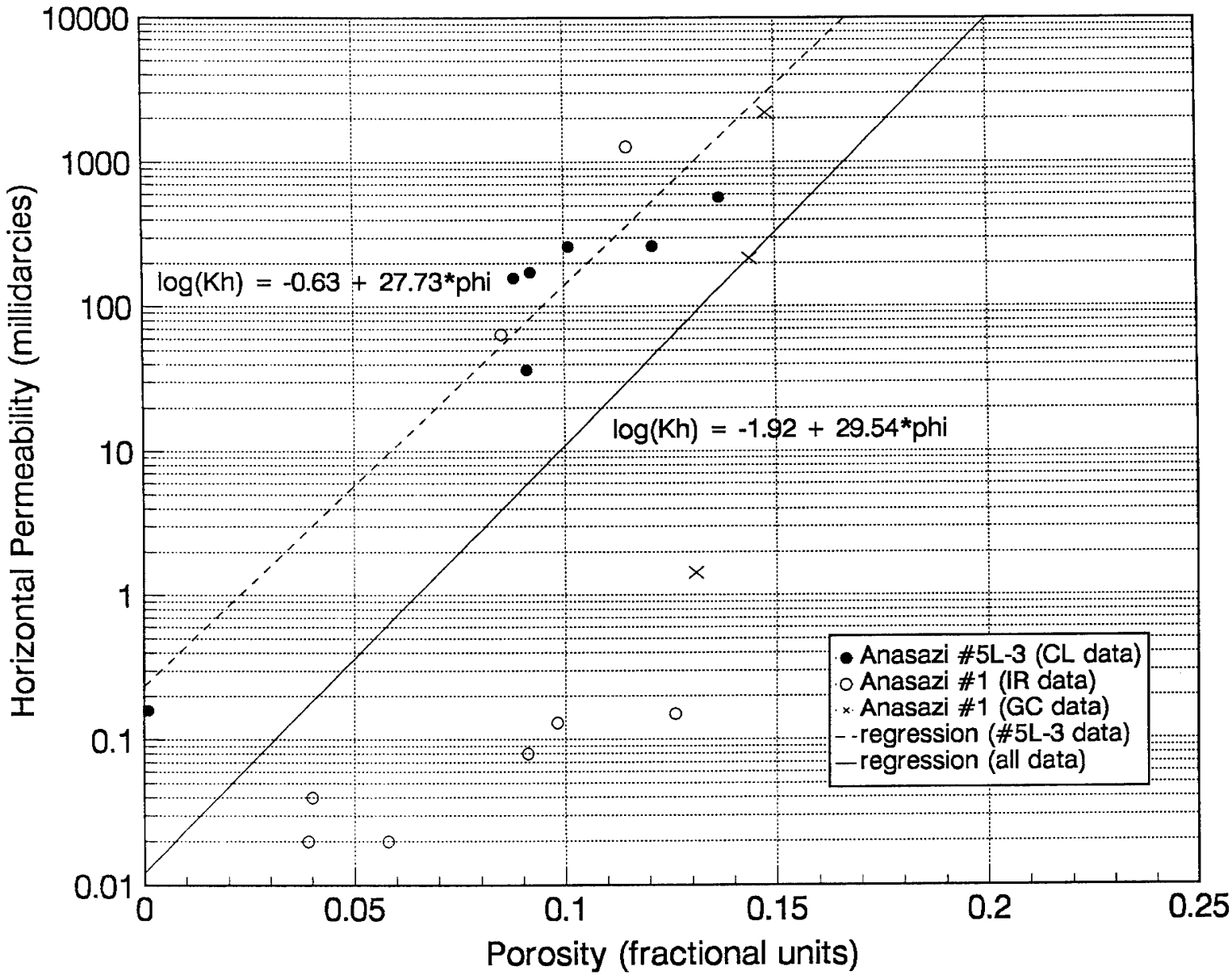

FIGURE 4-5. POROSITY/PERMEABILITY CROSSPLOT
MOUND INTERVAL, ANASAZI #1, #5L-3 (Combined Data)

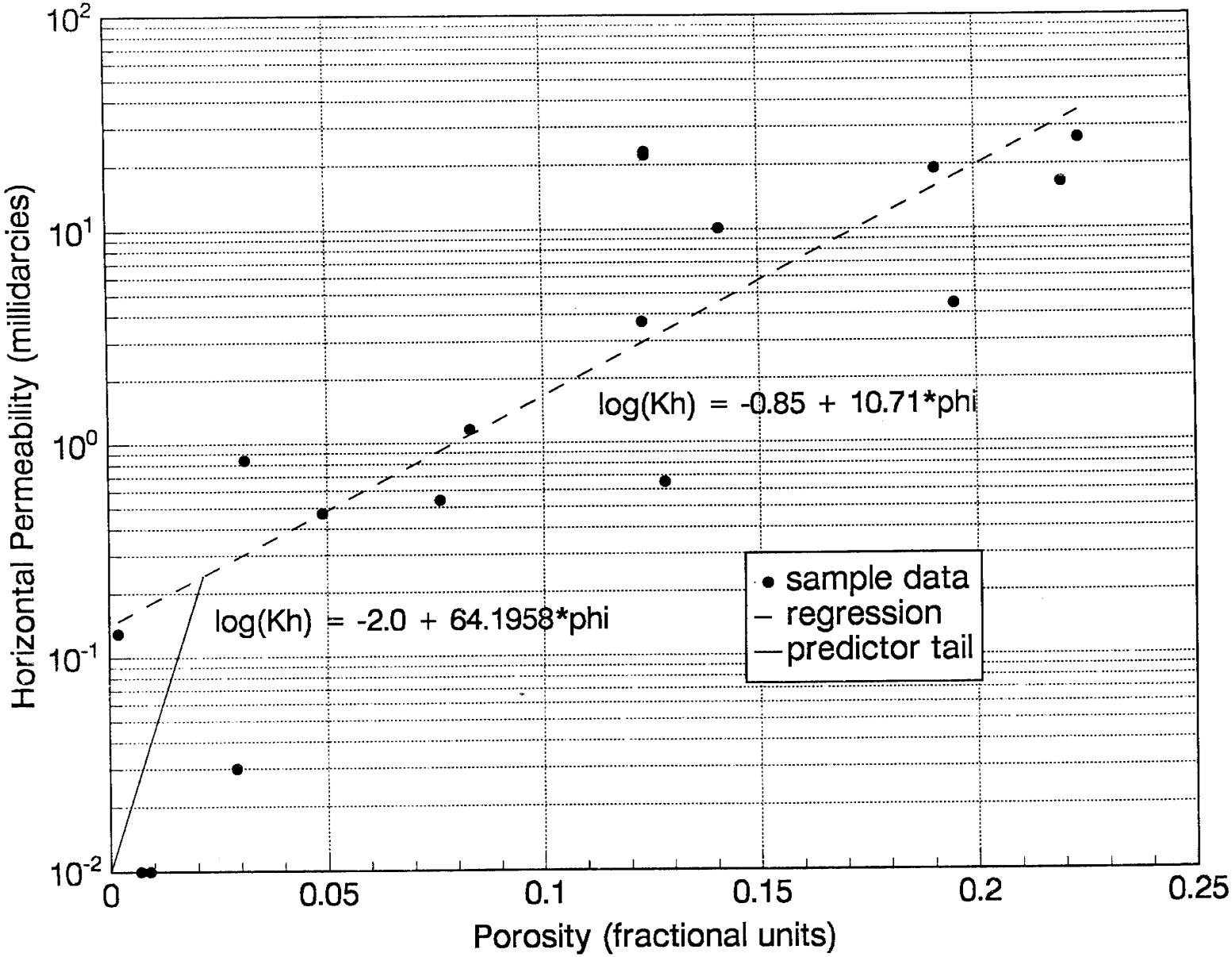

FIGURE 4-6. POROSITY/PERMEABILITY CROSSPLOT
SUPRAMOUND INTERVAL, ANASAZI #5L-3 (Corelabs Data)

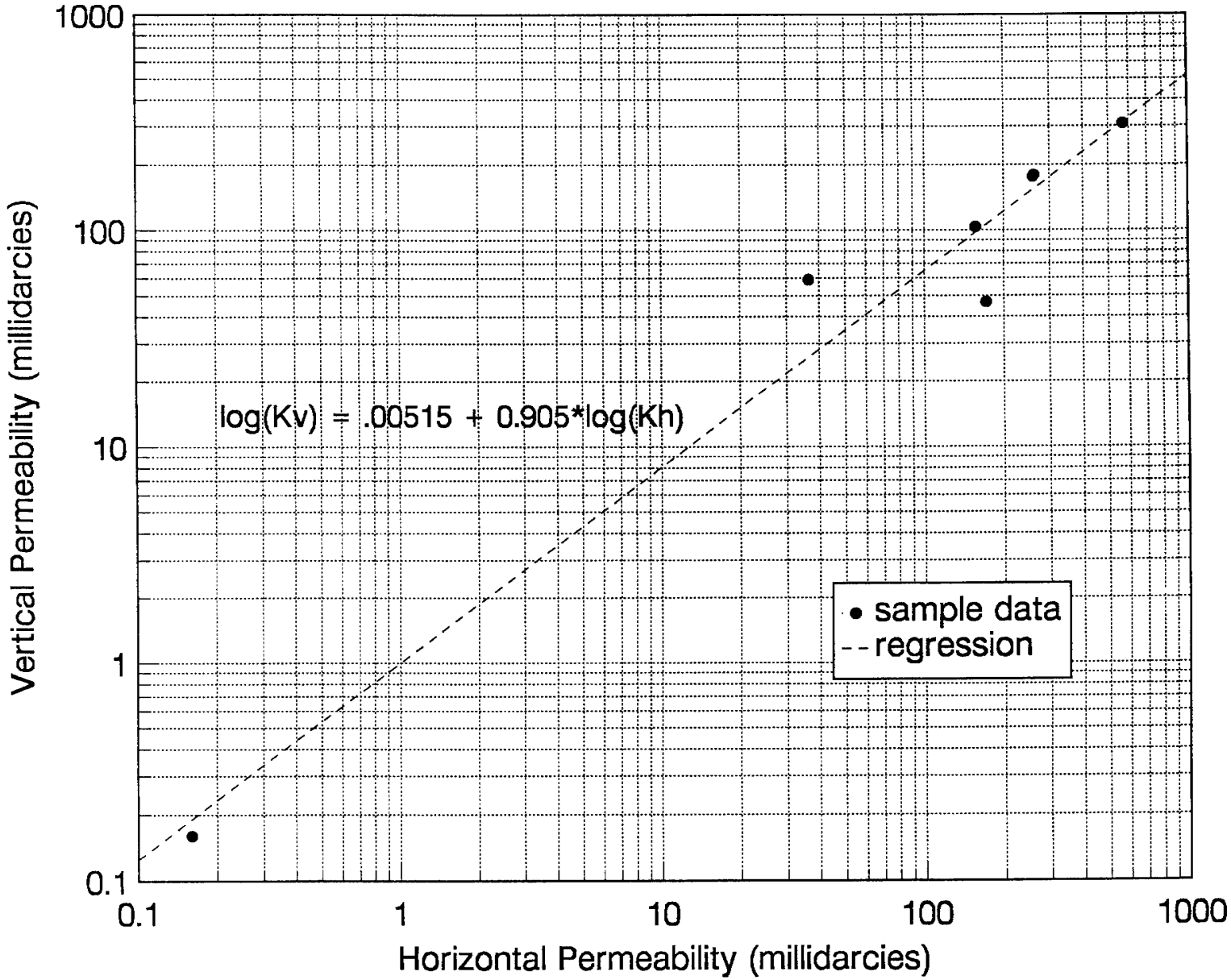

FIGURE 4-7. HORIZONTAL/VERTICAL PERMEABILITY CROSSPLOT
MOUND INTERVAL, ANASAZI #5L-3 (Corelabs Data)

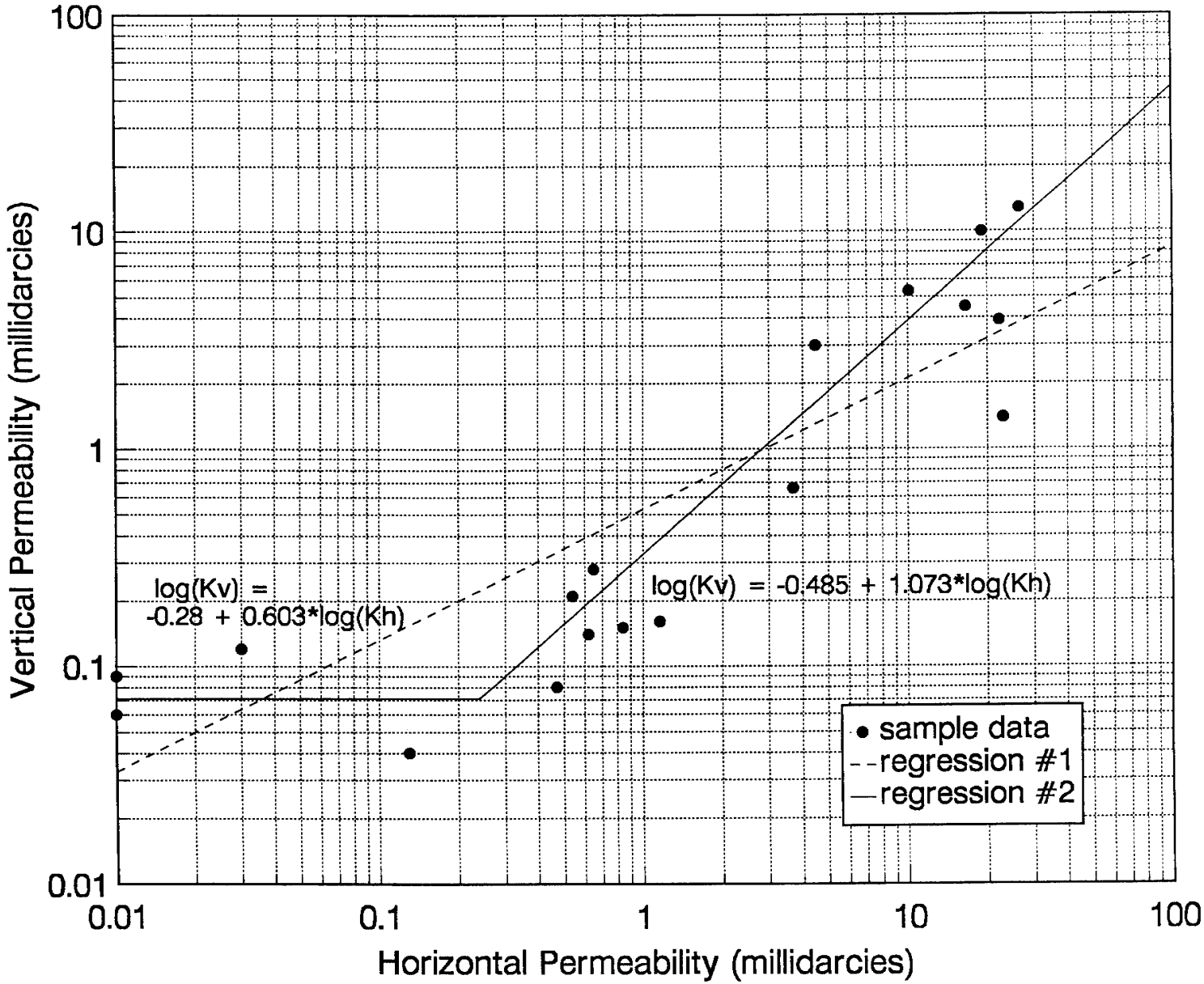

FIGURE 4-8. HORIZONTAL/VERTICAL PERMEABILITY CROSSPLOT
SUPRAMOUND INTERVAL, ANASAZI #5L-3 (Corelabs Data)

IIT RESEARCH INSTITUTE

Westport Technology Center International

Computed Tomography Section

Harken Energy

Field: Aneth

San Juan Co., Utah

ASN	Distance (inches) from edge of core box	Interval
115893	1.5	5646.0 - 5648.5 Anasazi No. 1
115894	4.5	
115895	7.5	
115896	10.5	
115897	13.5	
115898	16.5	
115899	19.5	
115900	22.5	
115901	25.5	
115902	28.5	
115903	31.5	
115904	34.5	

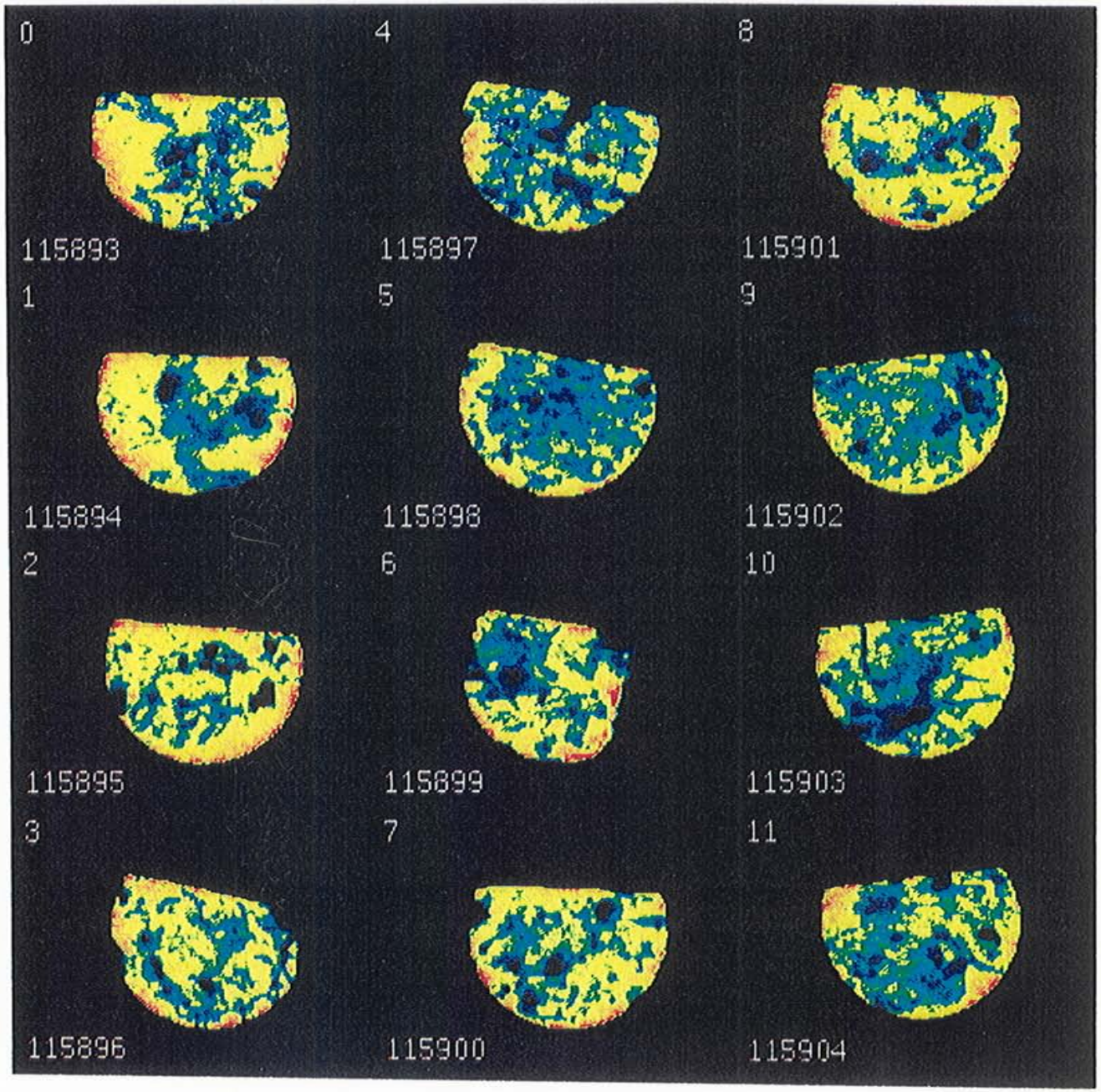

Figure 4–9. Transverse CAT Scans For Relative Permeability and Rock Compressibility Sample Selection. Mound Interval Limestone (5646–5648.5 ft MD), Anasazi #1

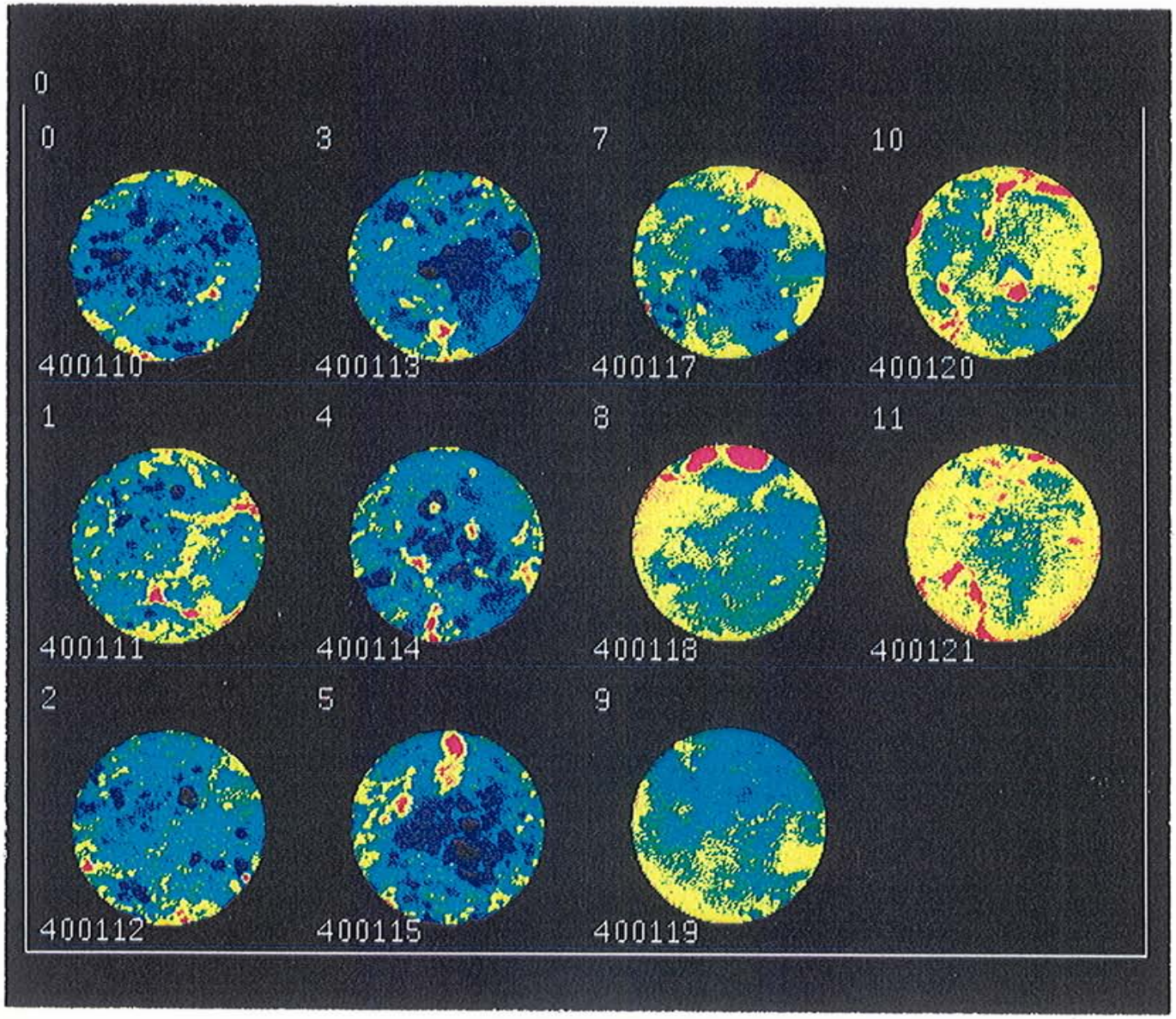

Figure 4–10. Transverse CAT Scans for Reservoir Quality Comparison. Supramound Interval Dolomite (5691–5692 ft MD), Anasazi #6H–1

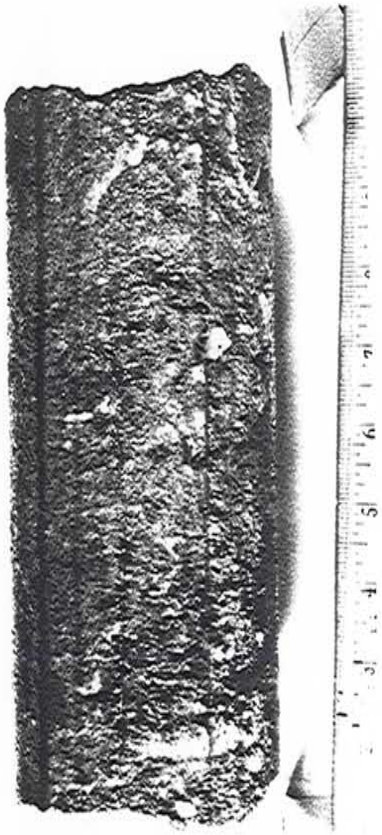

(a) Entire 10–inch Core Segment

(b) Close–up of Cat–Scanned Interval

Figure 4–11. Whole Core Photos of Interval (5491 ft MD) for Relative Permeability and Rock Compressibility, Supramound Interval Dolomite, Anasazi #6H–1

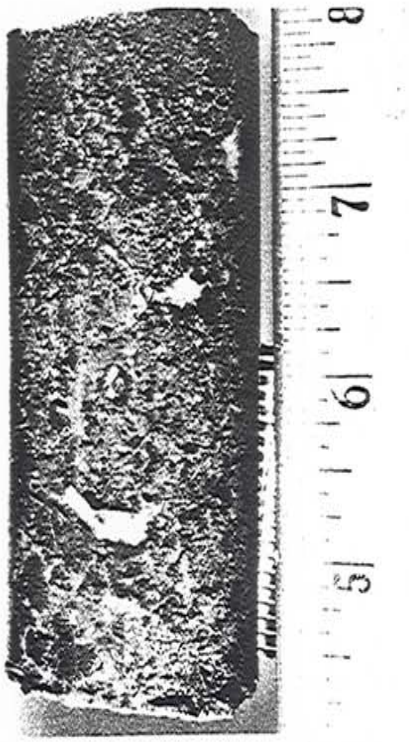

(a) Plug Sample #1 – front

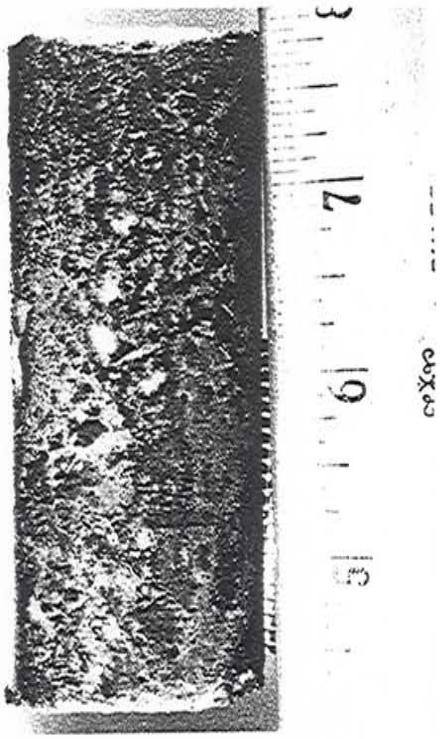

(b) Plug Sample #1 – back

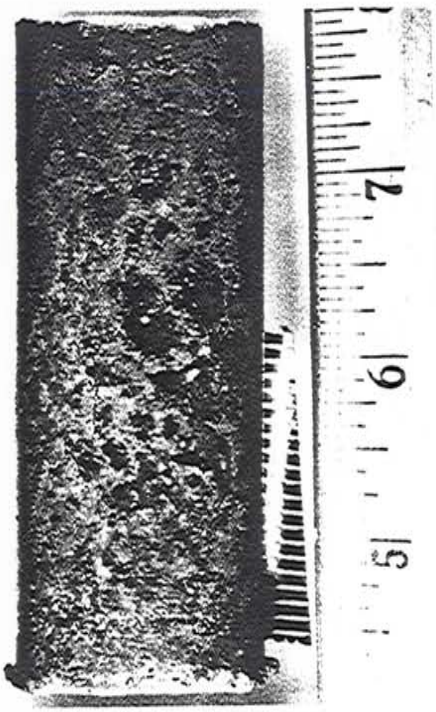

(c) Plug Sample #2 – front

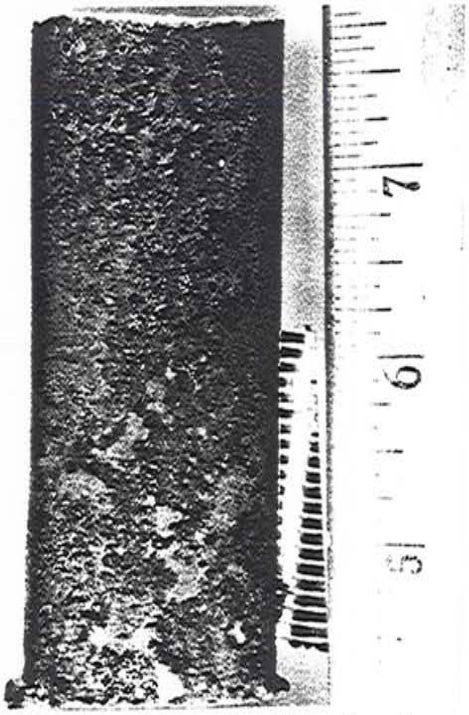

(d) Plug Sample #2 – back

Figure 4–12. Core Plug Photos of Samples 1 and 2 (5691 ft MD), Supramound Interval Dolomite, Anasazi #6H–1

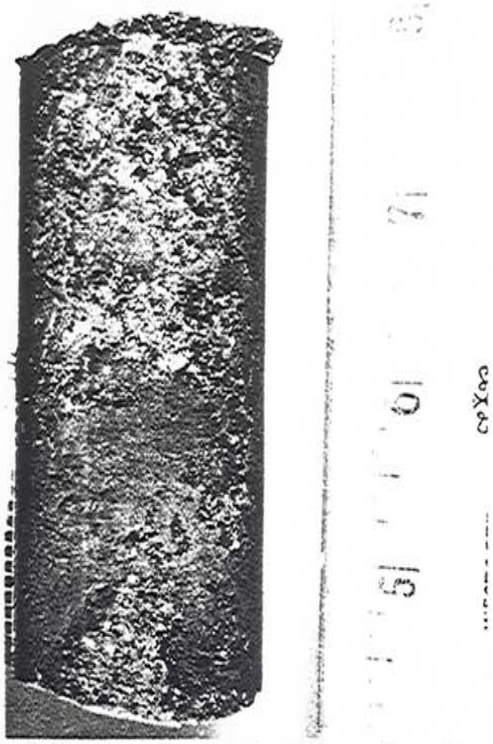

(a) Plug Sample #3 – front

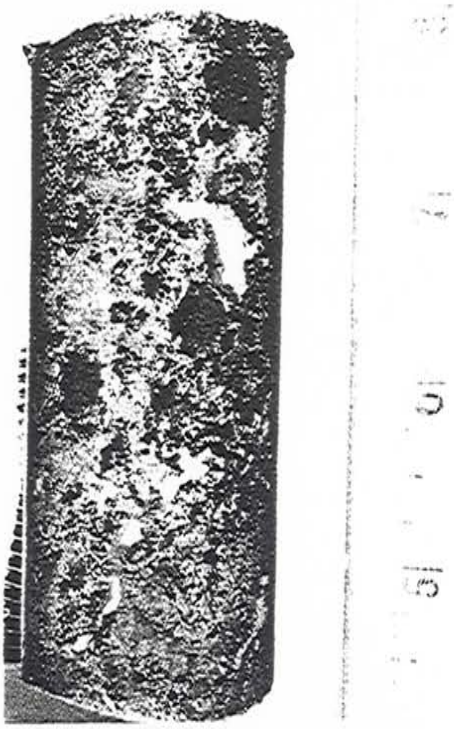

(b) Plug Sample #3 – back

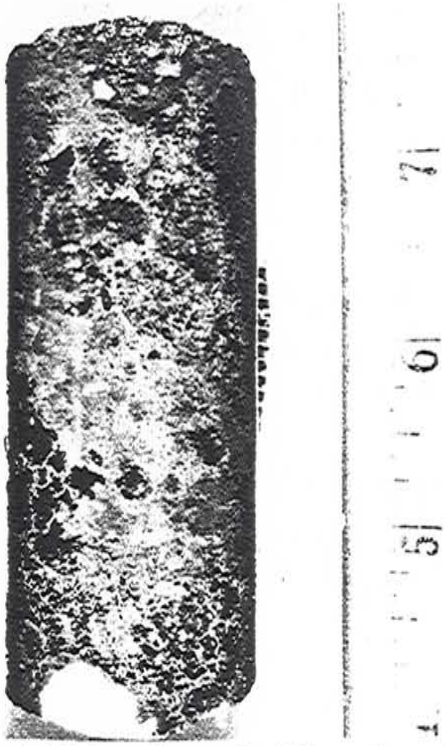

(c) Plug Sample #4 – front

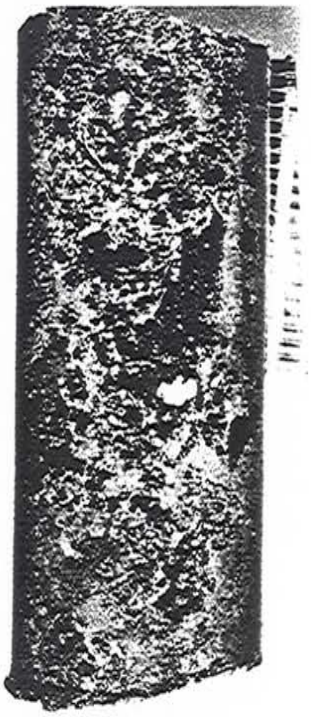

(d) Plug Sample #4 – back

Figure 4–13. Core Plug Photos of Samples 3 and 4 (5691 ft MD), Supramound Interval Dolomite, Anasazi #6H–1

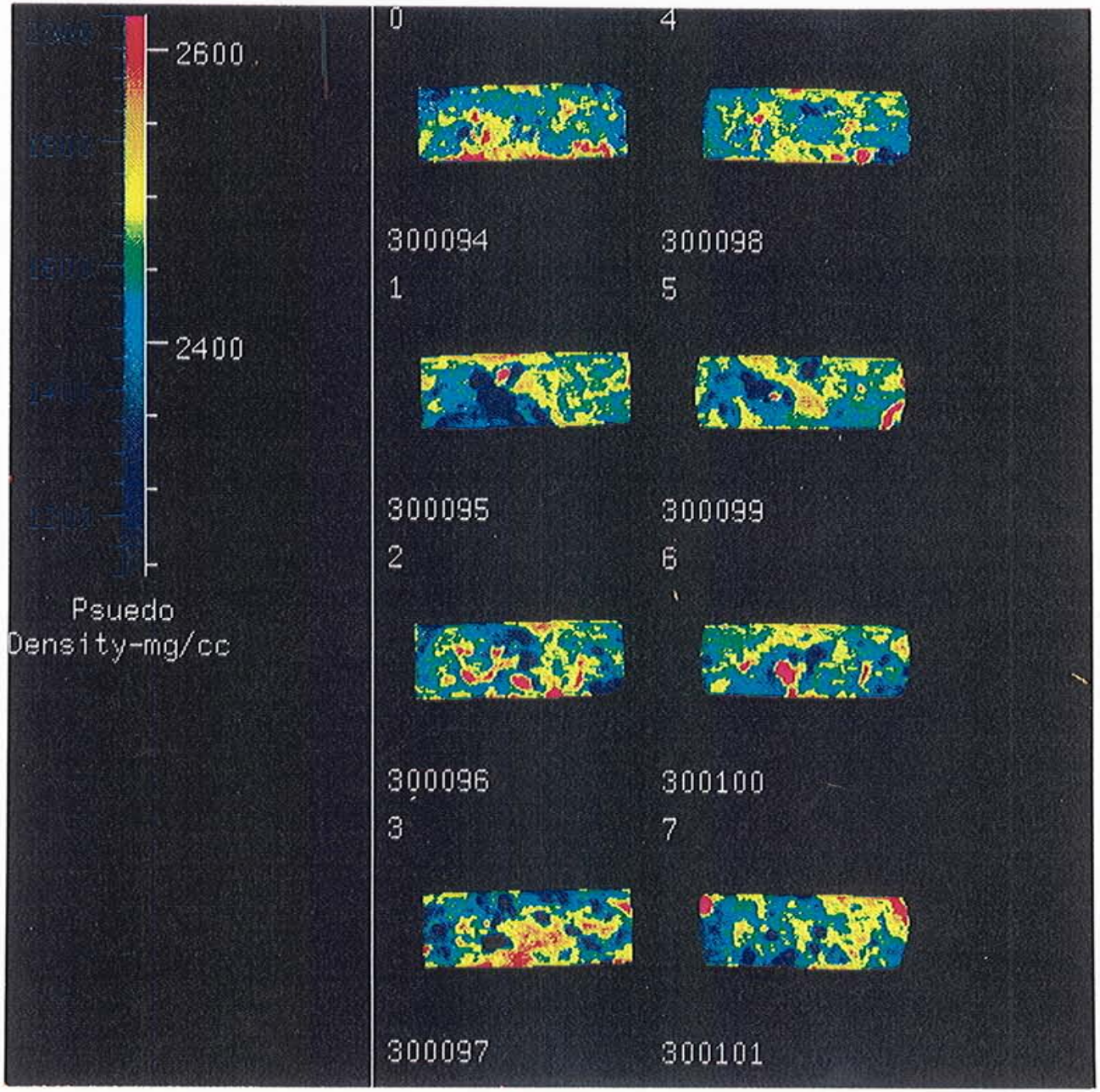

Figure 4–14. Longitudinal CAT Scans of Relative Permeability and Rock Compressibility Plug Samples. Supramound Interval Dolomite, Anasazi #6H–1.

(plug#1 = images (0,1); plug#2 = images (2,3); plug#3 = images (4,5); plug#4 = images (6,7))

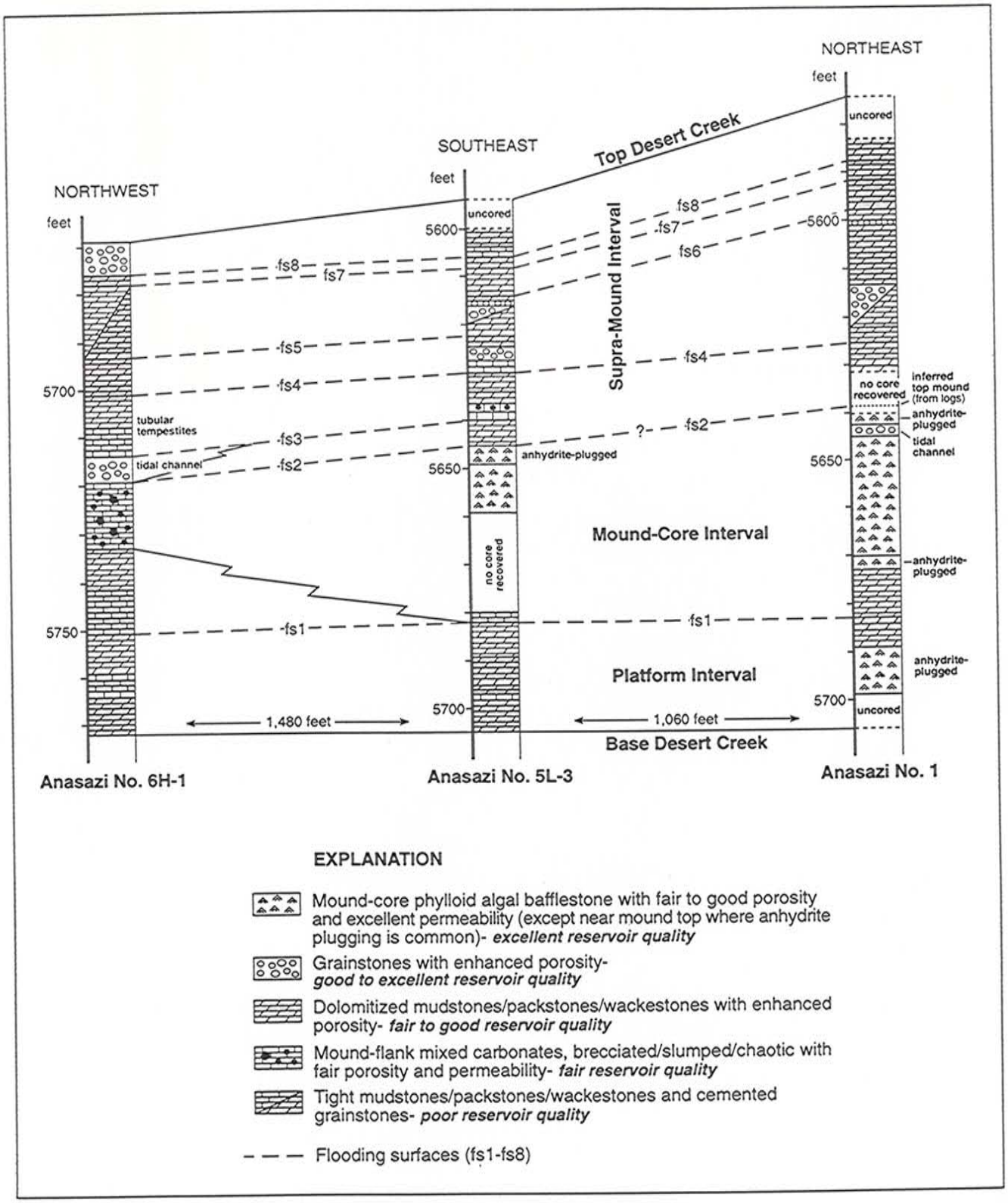

Figure 4–15. Anasazi Reservoir Stratigraphy from Core Interpretation. (drafting courtesy of the Utah Geological Survey)

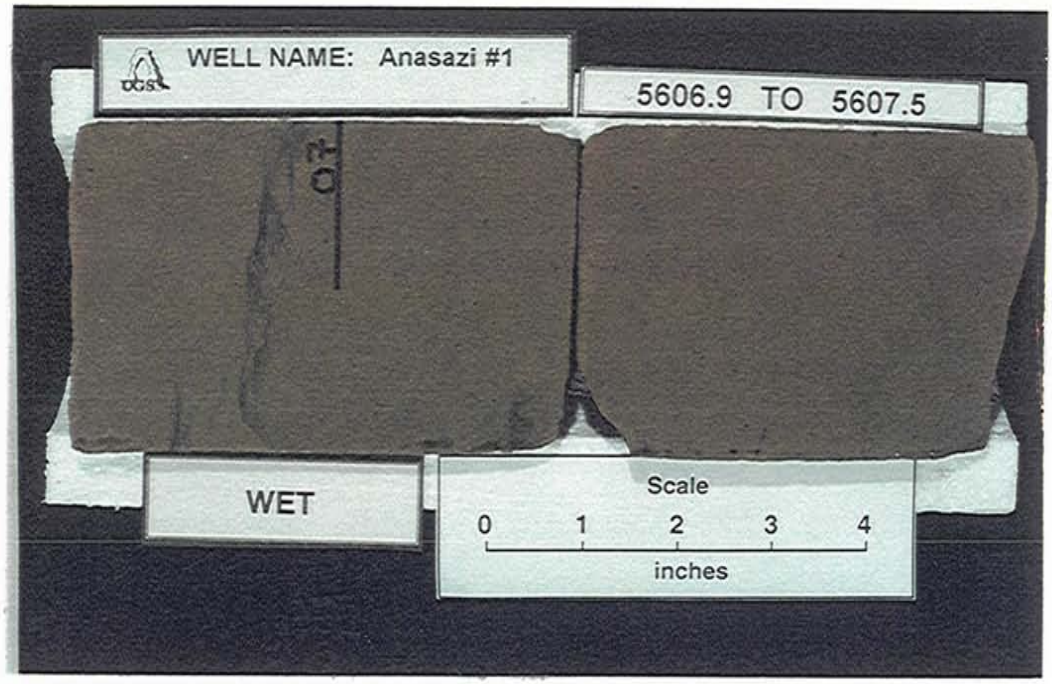

(a) Core Photograph (courtesy Utah Geological Survey)

(b) Photomicrograph (plane polarized light; 47.5x)

Figure 4–16 (a,b). Lithotype 1: Tight Carbonate Mudstone.

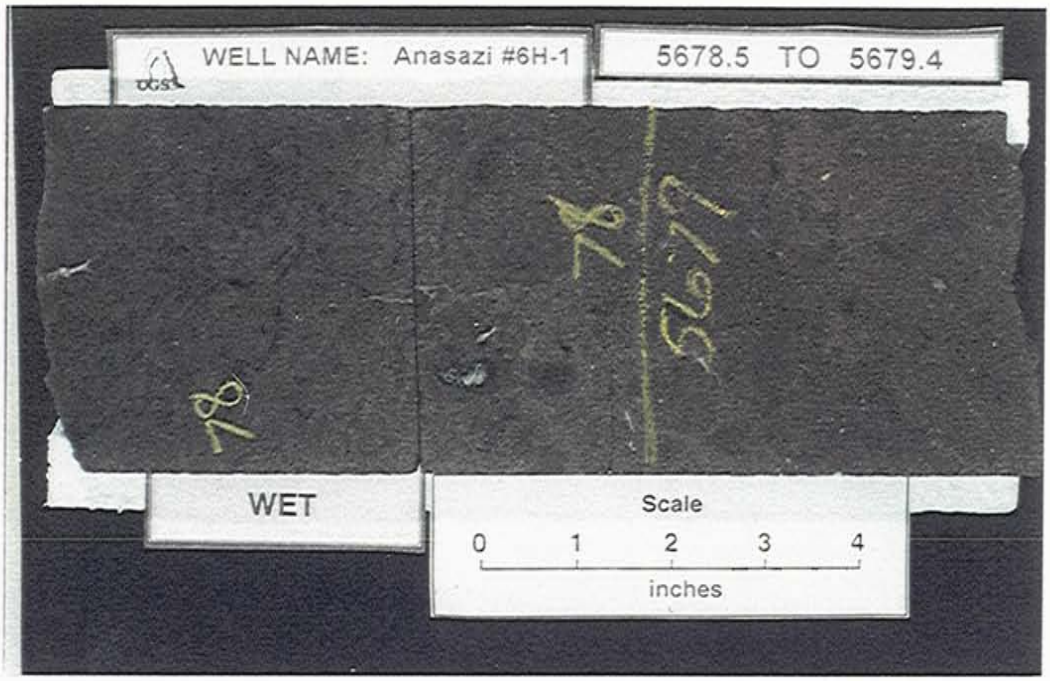

(c) **Core Photograph (courtesy Utah Geological Survey)**

(d) **Photomicrograph (plane polarized light; 47.5x)**

Figure 4–16 (c,d). Lithotype 2: Dolomitized Mudstone.

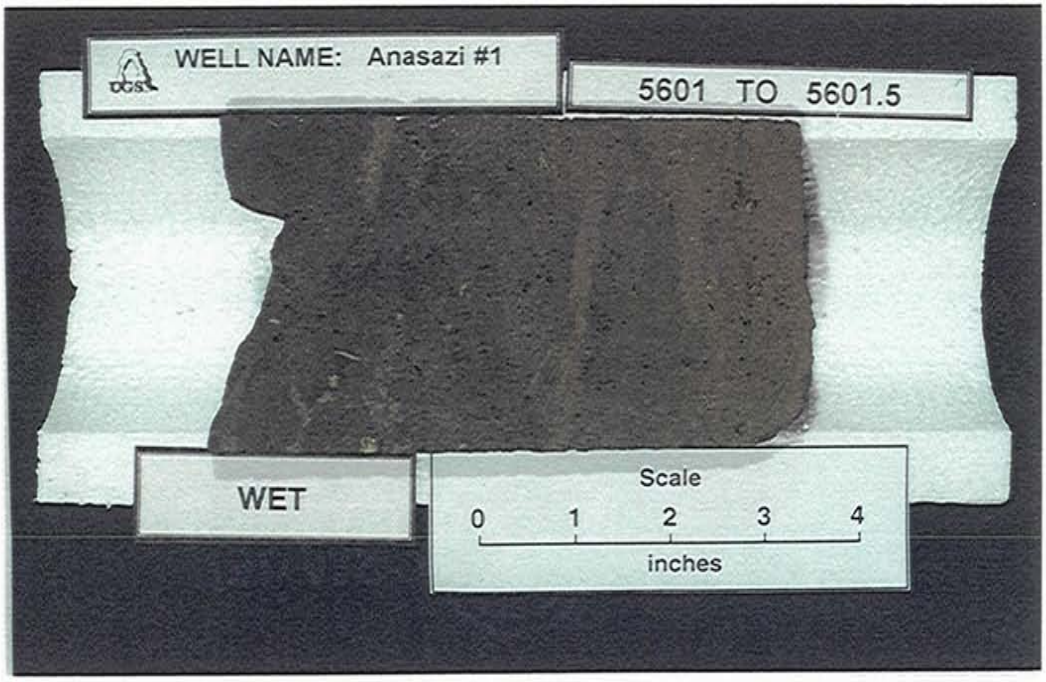

(a) Core Photograph (courtesy Utah Geological Survey)

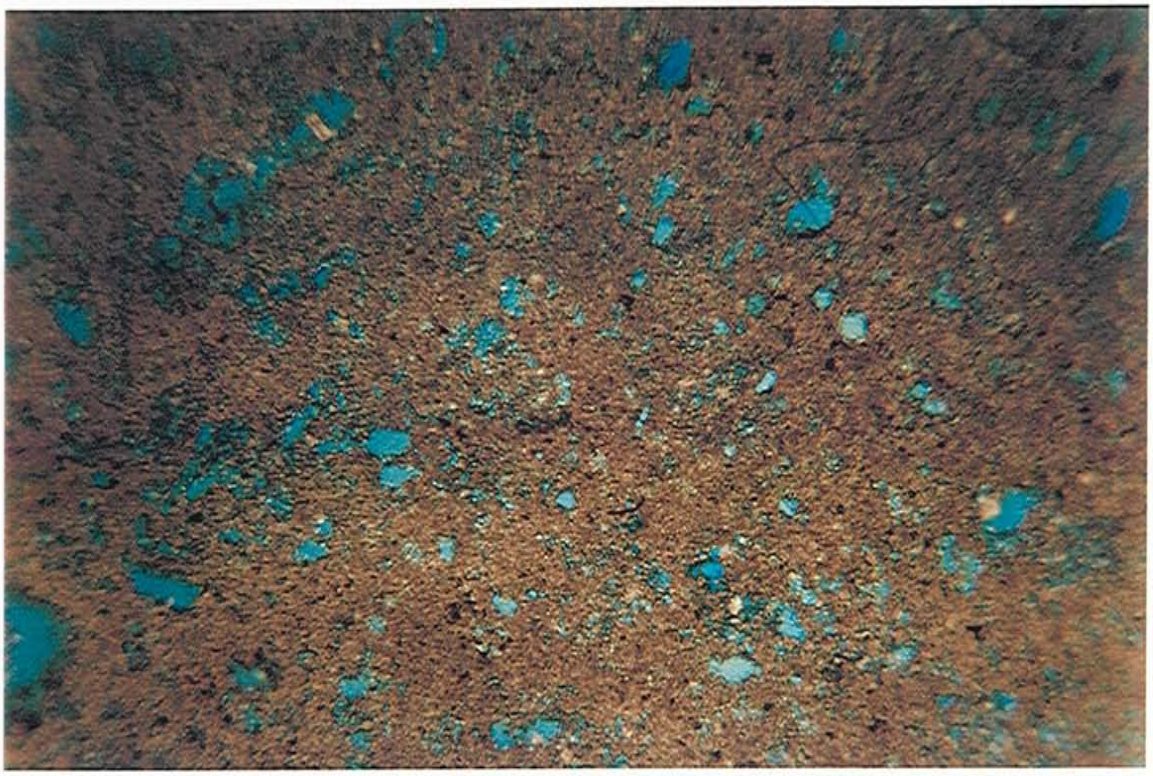

(b) Photomicrograph (plane polarized light; 47.5x)

Figure 4–17 (a,b). Lithotype 3: Enhanced Porosity Mudstone.

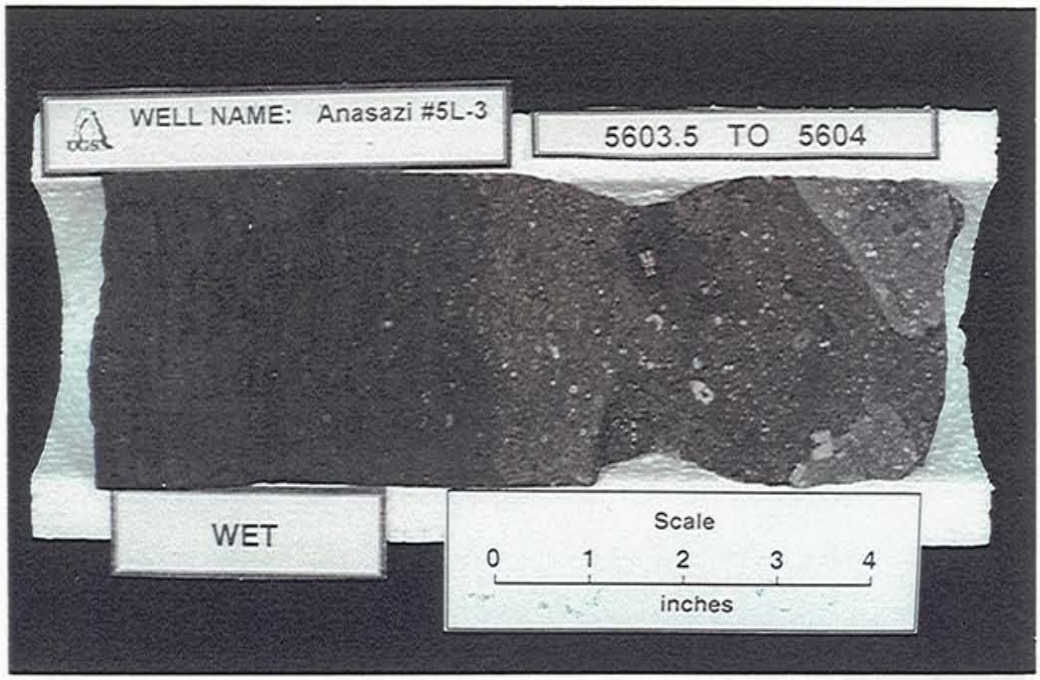

(c) Core Photograph (courtesy Utah Geological Survey)

(d) Photomicrograph (plane polarized light; 47.5x)

Figure 4–17 (c,d). Lithotype 4: Tight Packstone/Wackestone.

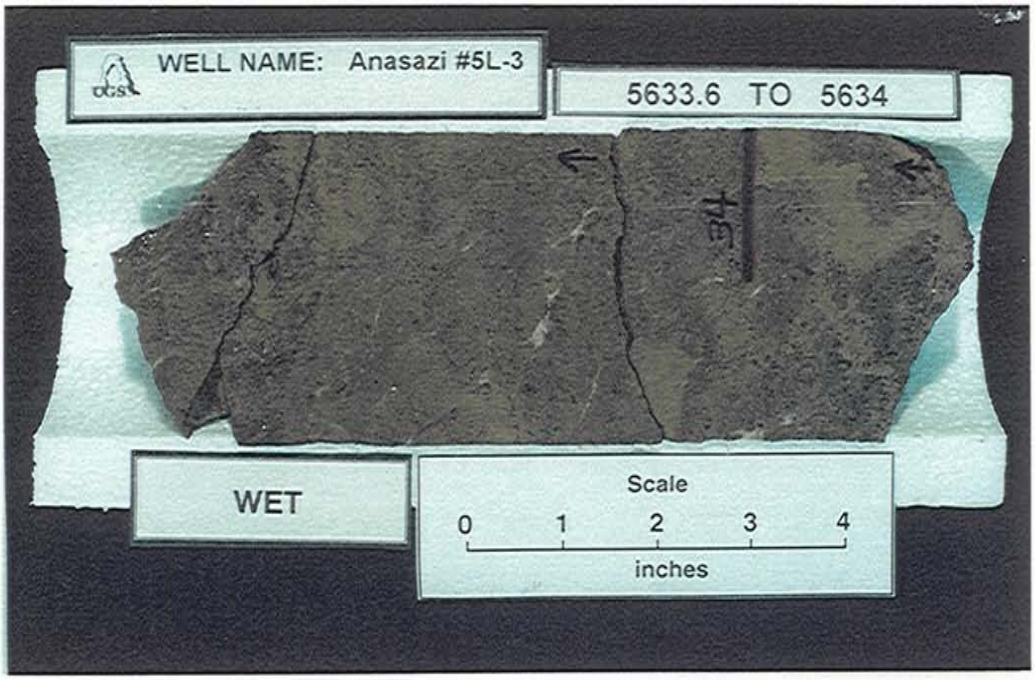

(a) Core Photograph (courtesy Utah Geological Survey)

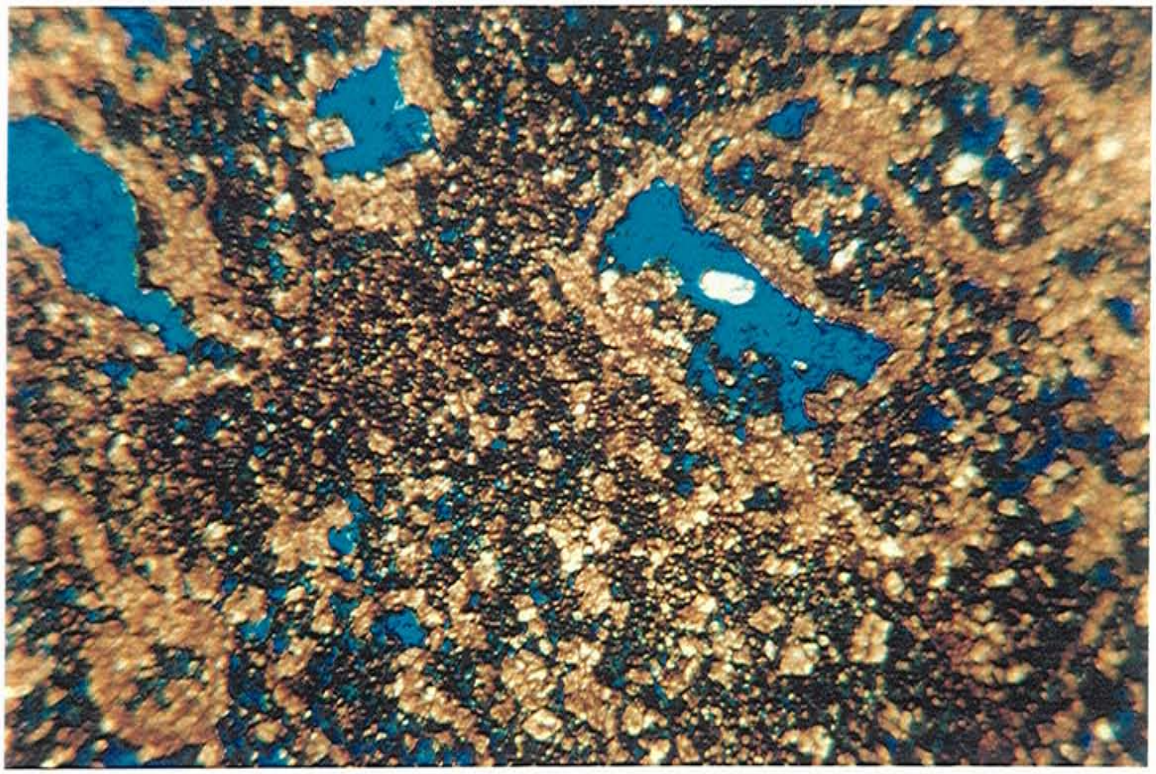

(b) Photomicrograph (plane polarized light; 47.5x)

Figure 4–18 (a,b). Lithotype 5: Porous Packstone/Wackestone.

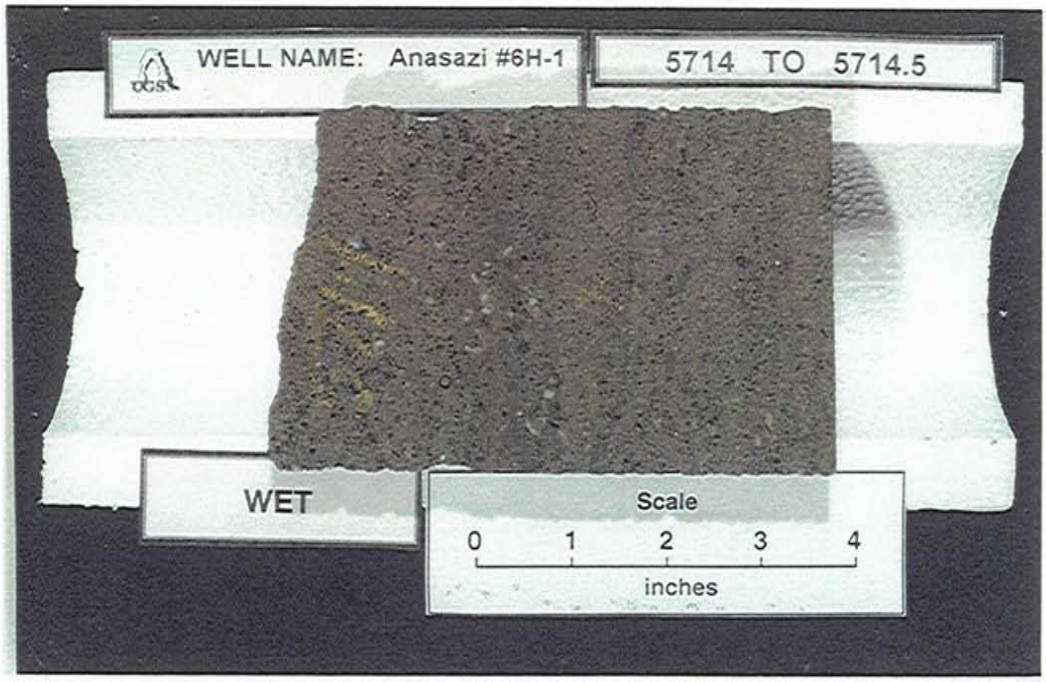

(c) Core Photograph (courtesy Utah Geological Survey)

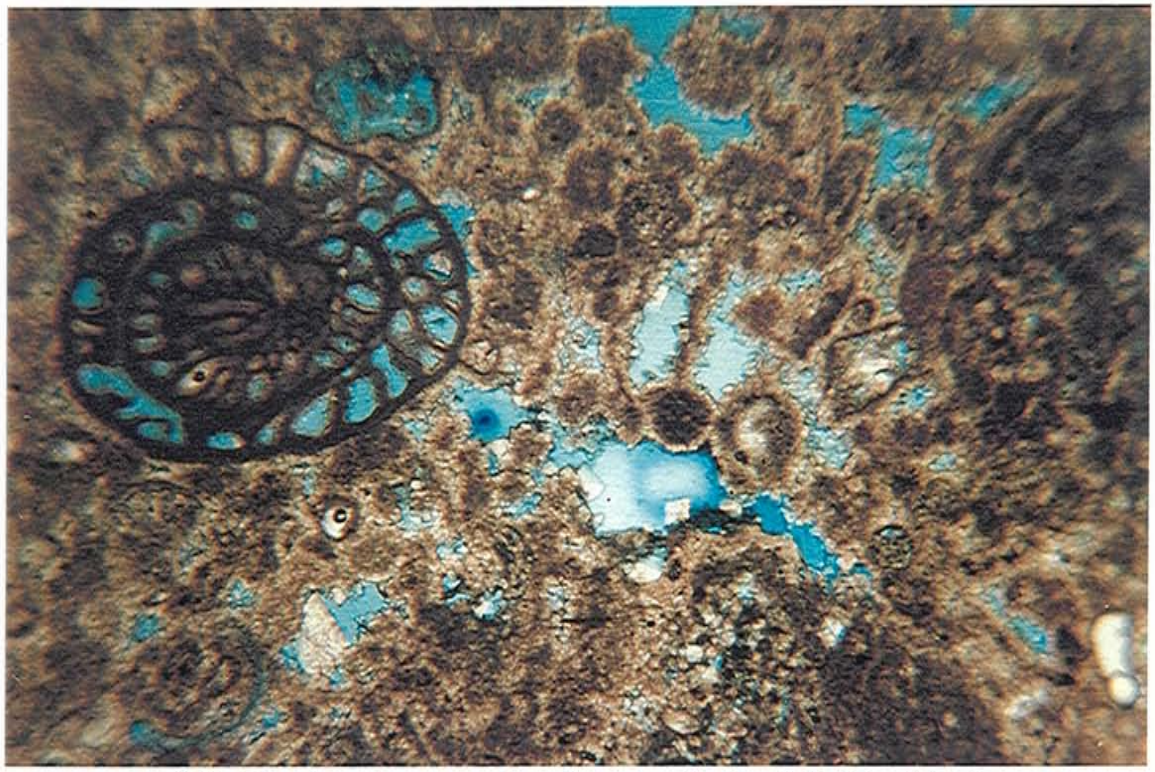

(d) Photomicrograph (plane polarized light; 47.5x)

Figure 4–18 (c,d). Lithotype 6: Porous Grainstone.

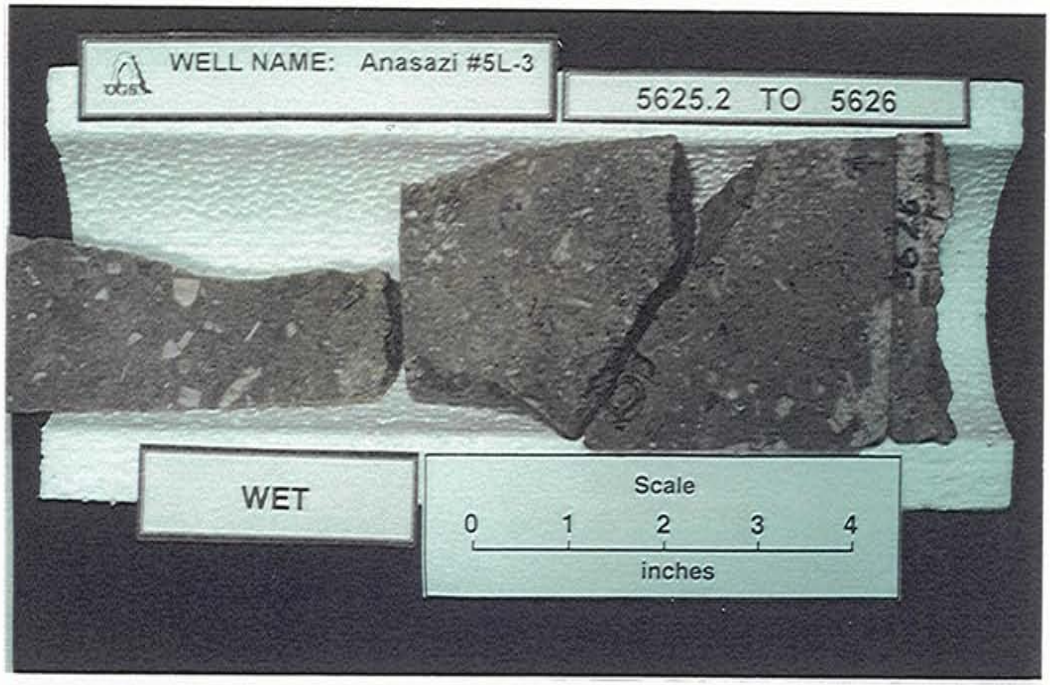

(a) Core Photograph (courtesy Utah Geological Survey)

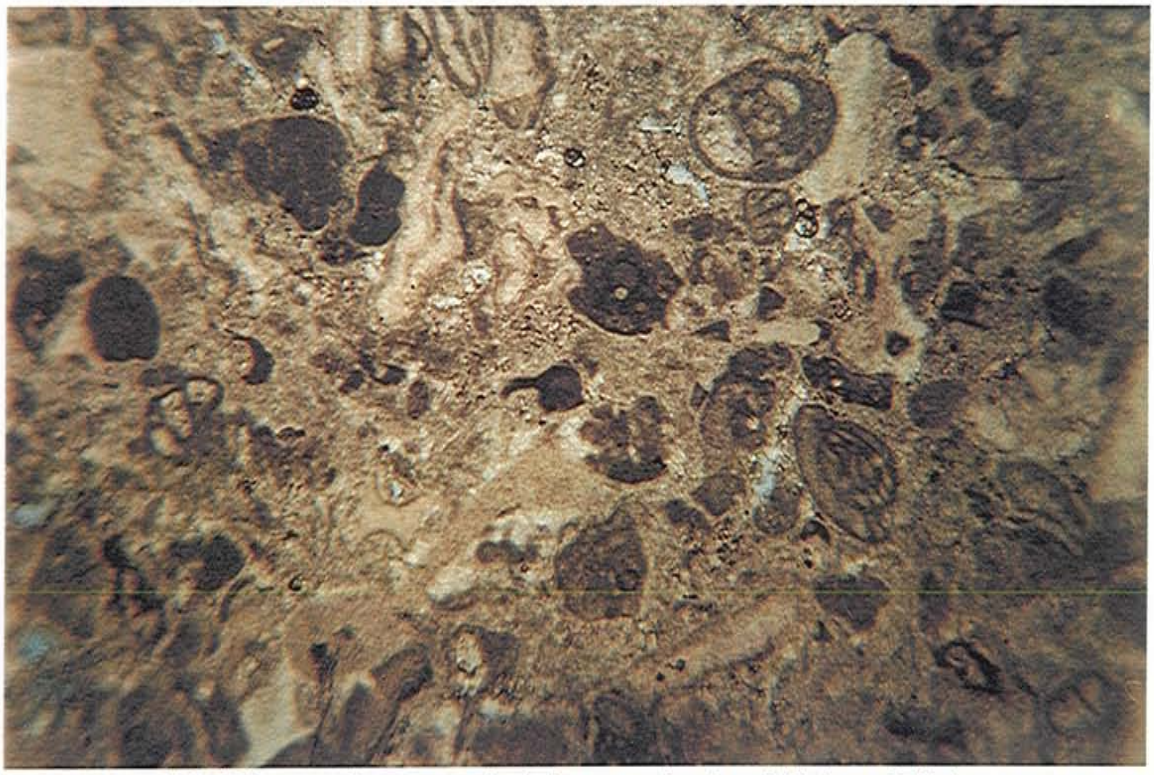

(b) Photomicrograph (plane polarized light; 47.5x)

Figure 4–19 (a,b). Lithotype 7: Tight Grainstone.

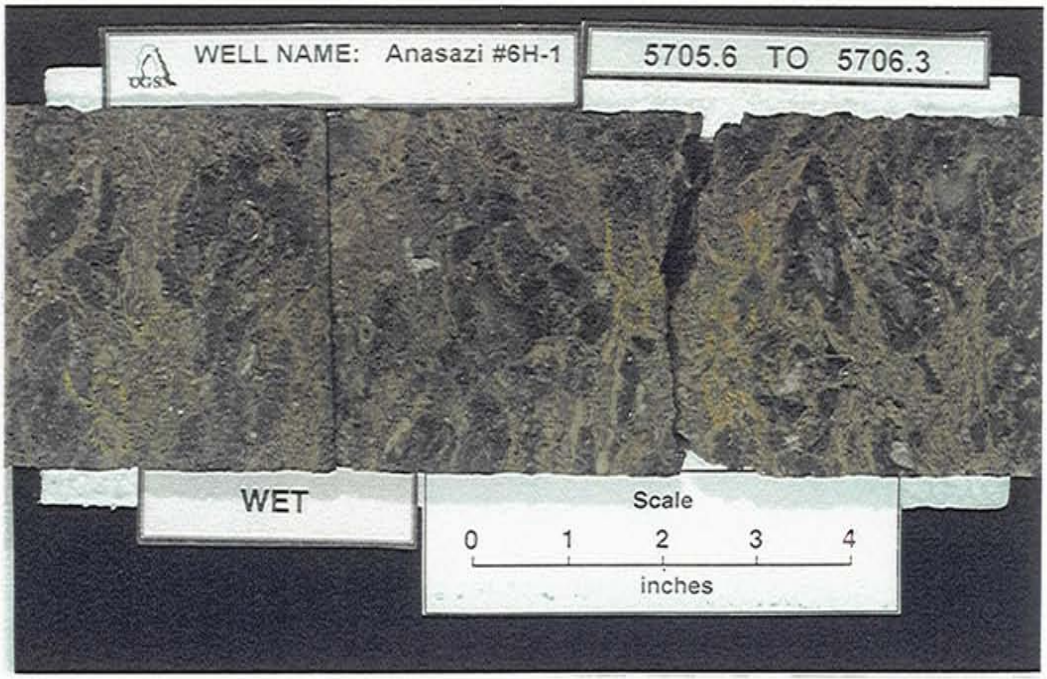

(c) Core Photograph (courtesy Utah Geological Survey)

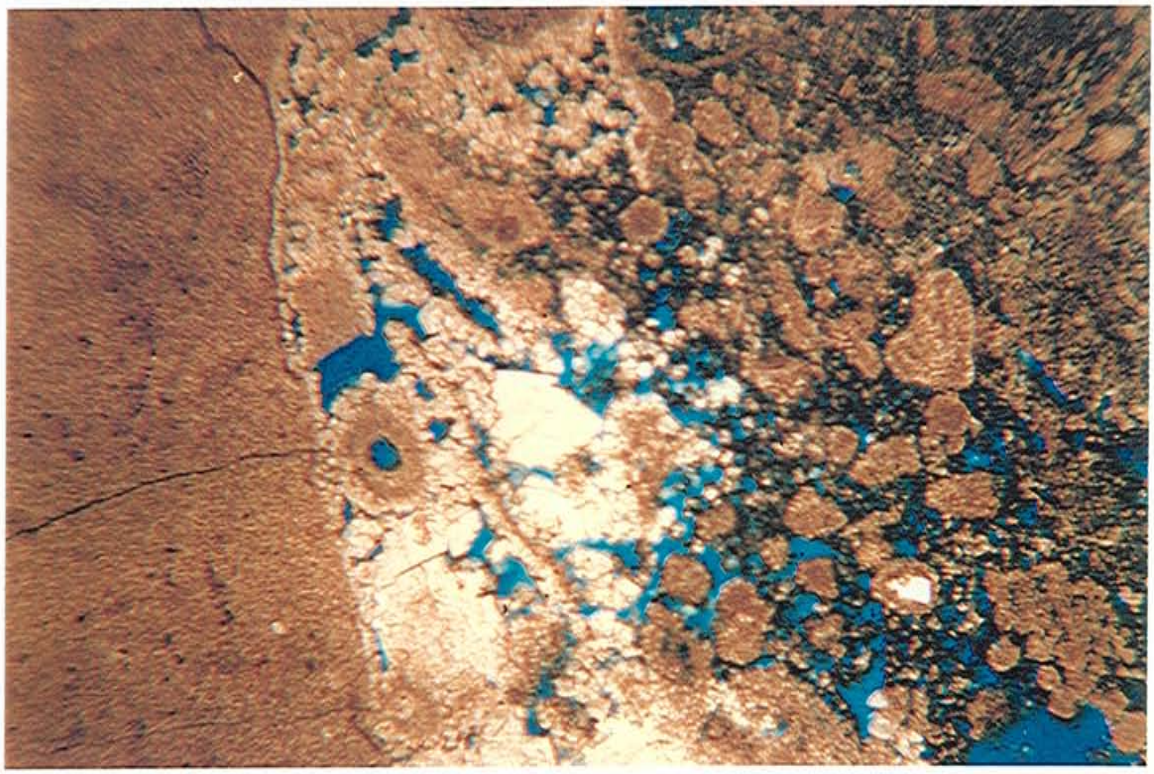

(d) Photomicrograph (plane polarized light; 47.5x)

Figure 4–19 (c,d). Lithotype 8: Tubular Tempestites.

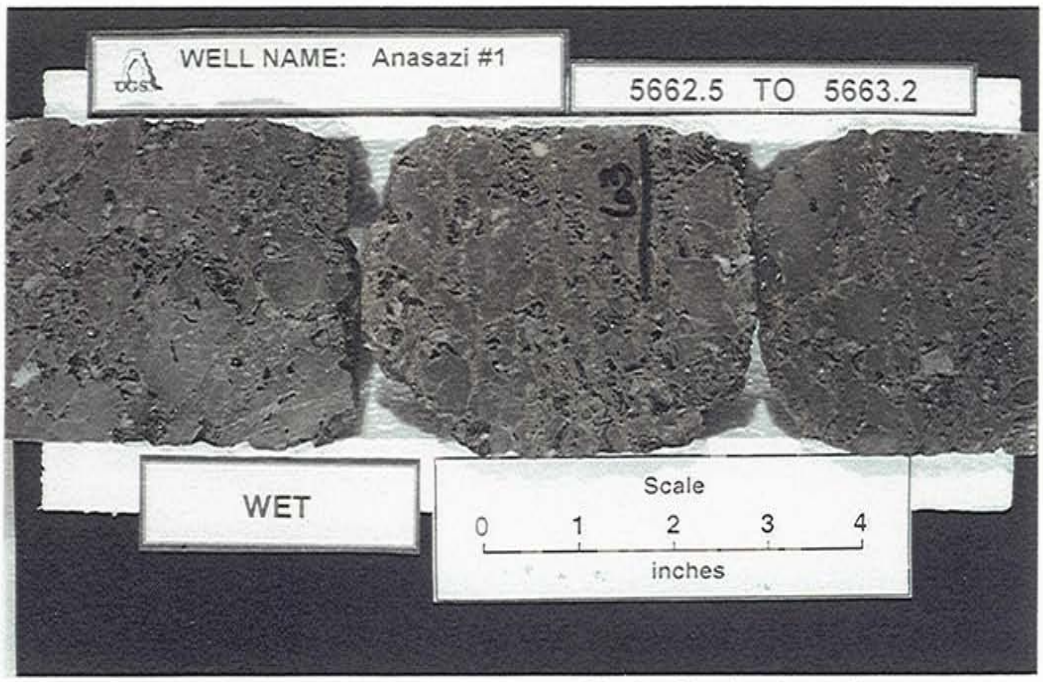

(a) Core Photograph (courtesy Utah Geological Survey)

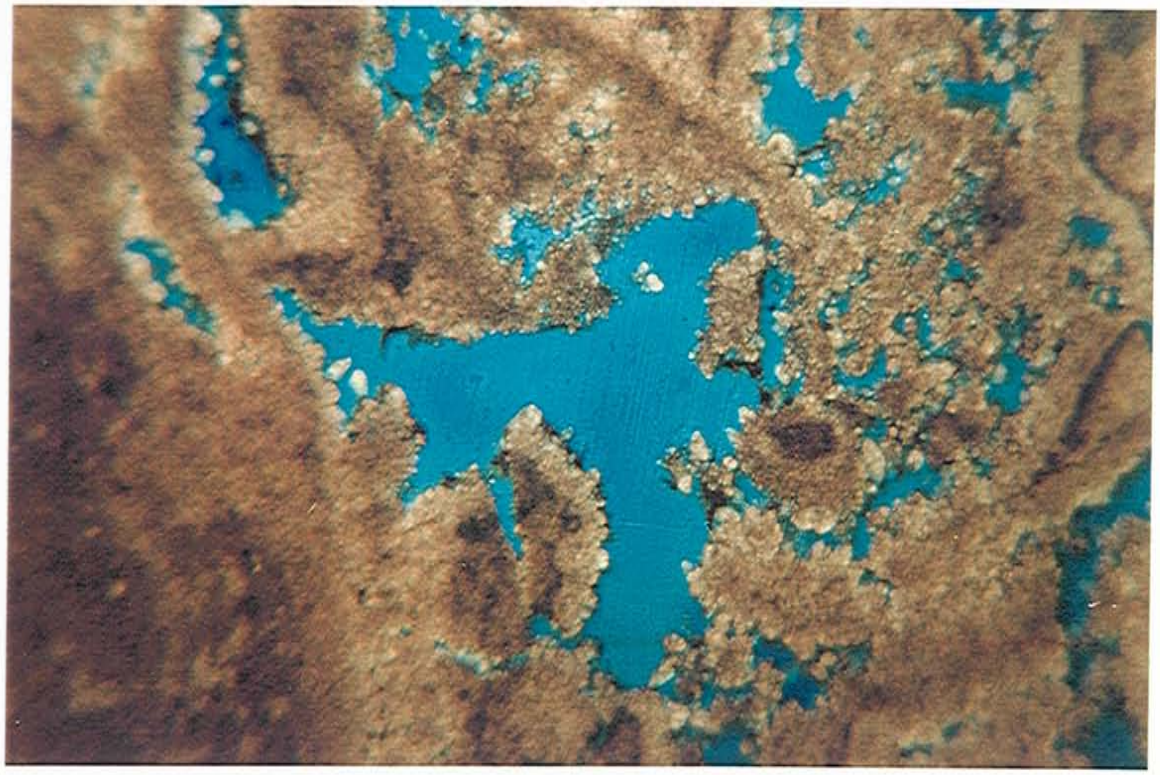

(b) Photomicrograph (plane polarized light; 47.5x)

Figure 4–20 (a,b). Lithotype 9: Phylloid Algal Limestone.

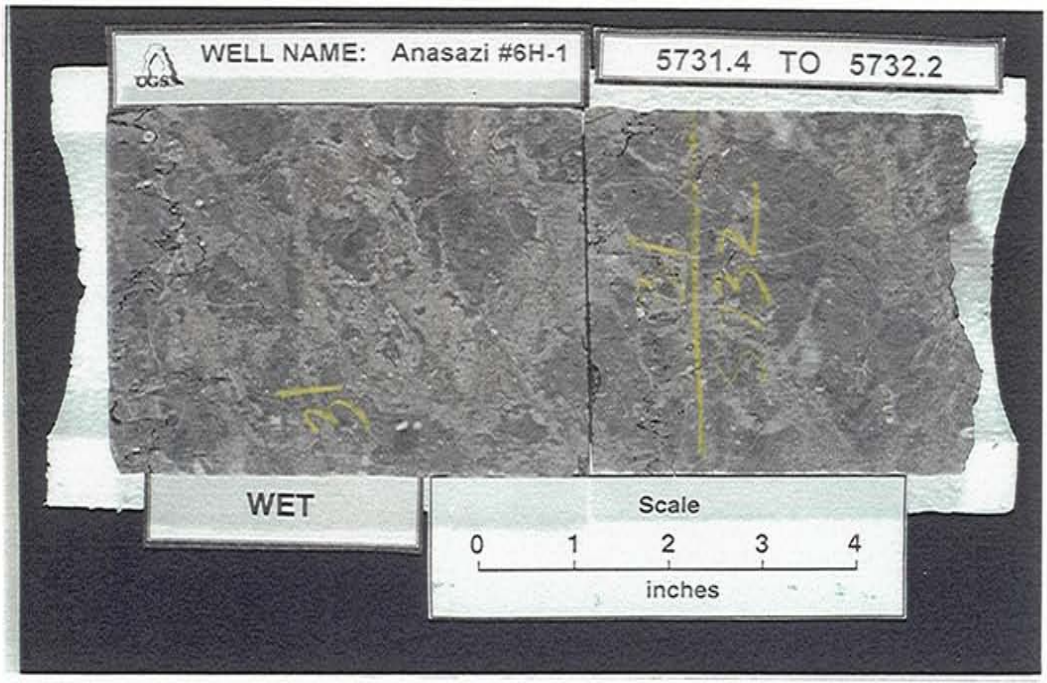

(c) Core Photograph (courtesy Utah Geological Survey)

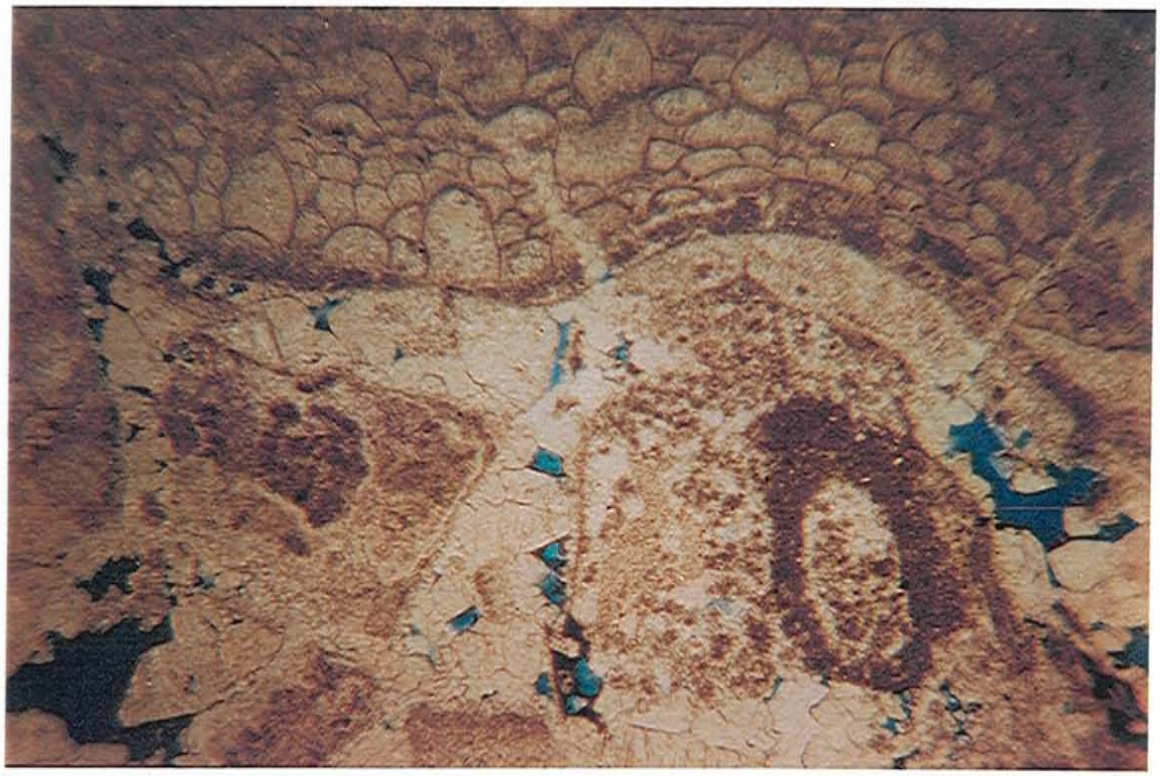

(d) Photomicrograph (plane polarized light; 47.5x)

Figure 4–20 (c,d). Lithotype 10: Mound–Front Bioclastic Breccia.

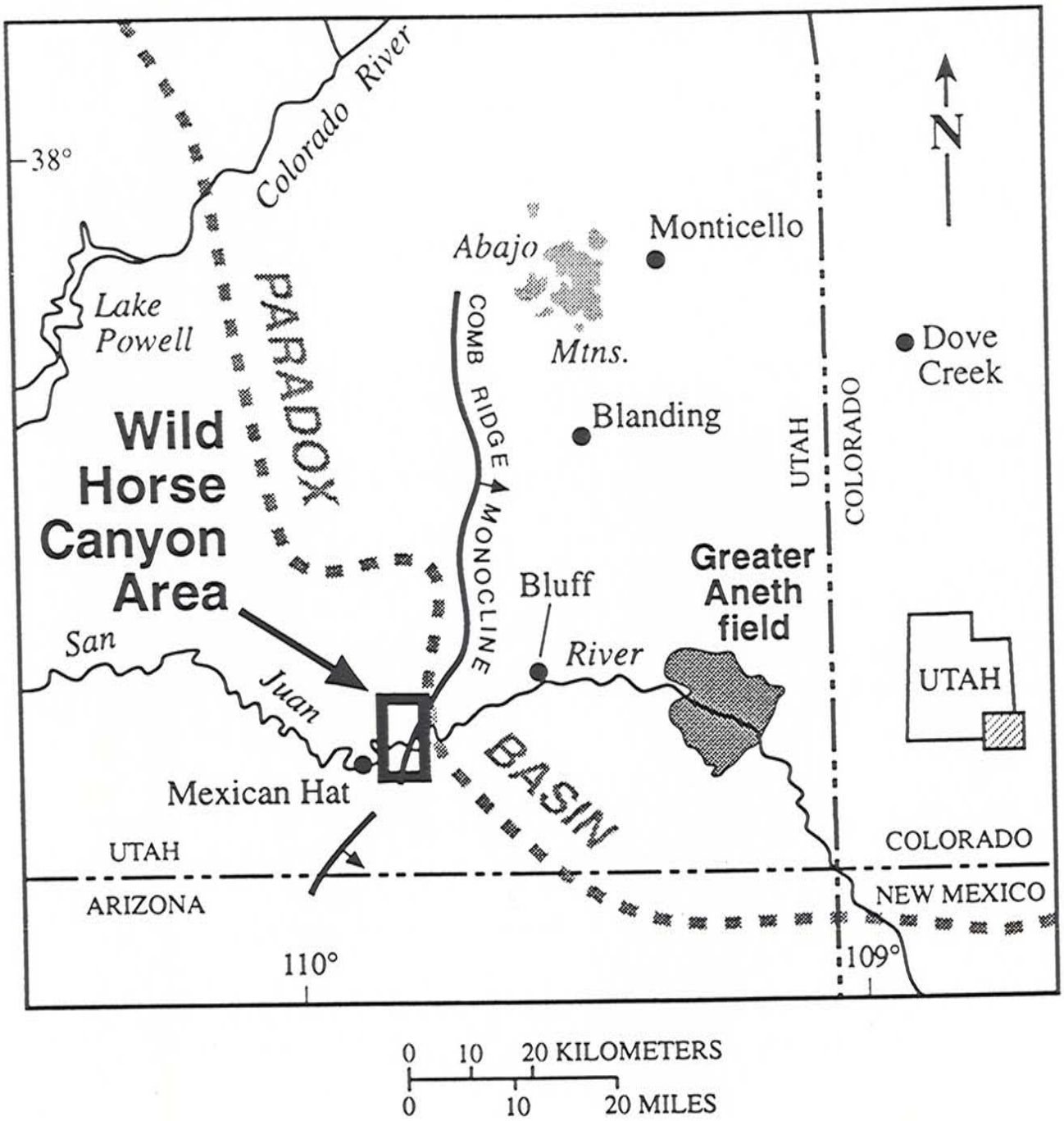

Figure 4–21. Location Map of Wild Horse Canyon Field Study Area, Lower Ismay Carbonate Mound Analogues. (courtesy of the Utah Geological Survey)

Figure 4–22. Lower Ismay Carbonate Mound Analogue, San Juan River, Utah (photo courtesy of T.C. Chidsey, Jr., Utah Geological Survey)

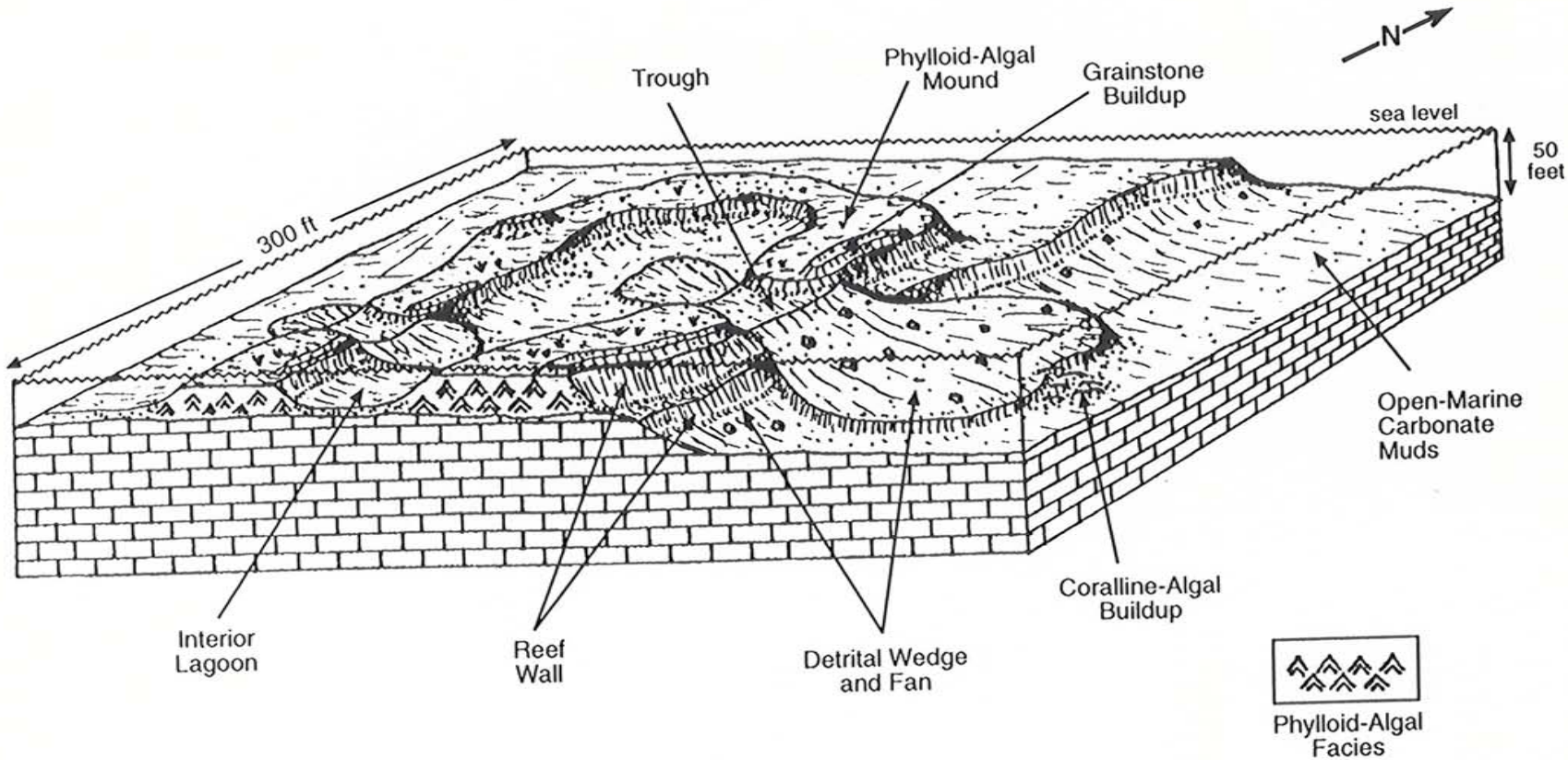

Figure 4–23. Block Diagram Interpretation of Facies Distributions, Anasazi and Other Analogous Carbonate Mound Buildups. (courtesy of T.C. Chidsey, Jr., the Utah Geological Survey)

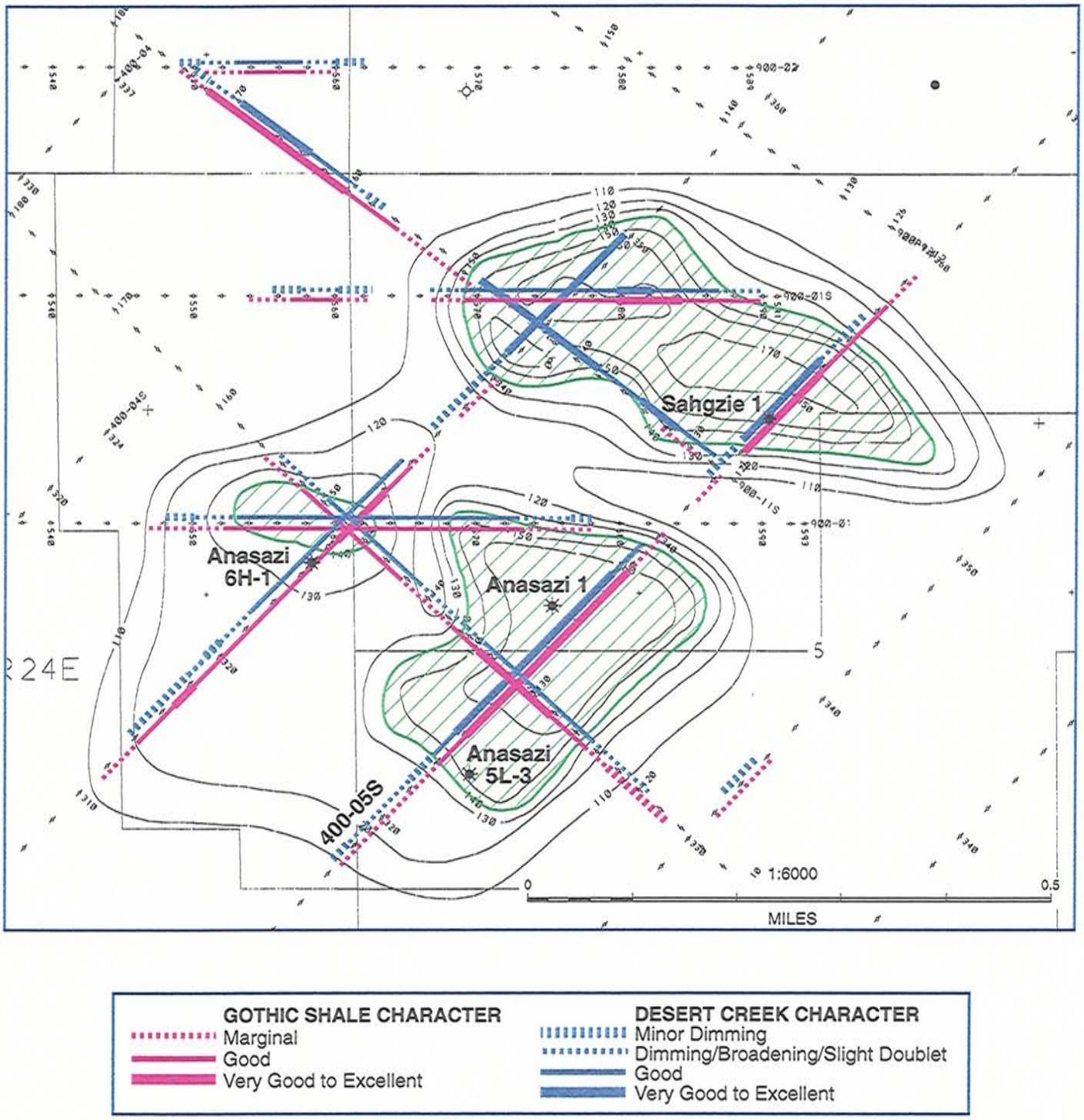

Figure 4–24. Interpreted Seismic Lines Across Anasazi Field Showing Qualitative Basis for the Reservoir Quality Index (RQI) (courtesy Harken Southwest Corp. and the Utah Geological Survey)

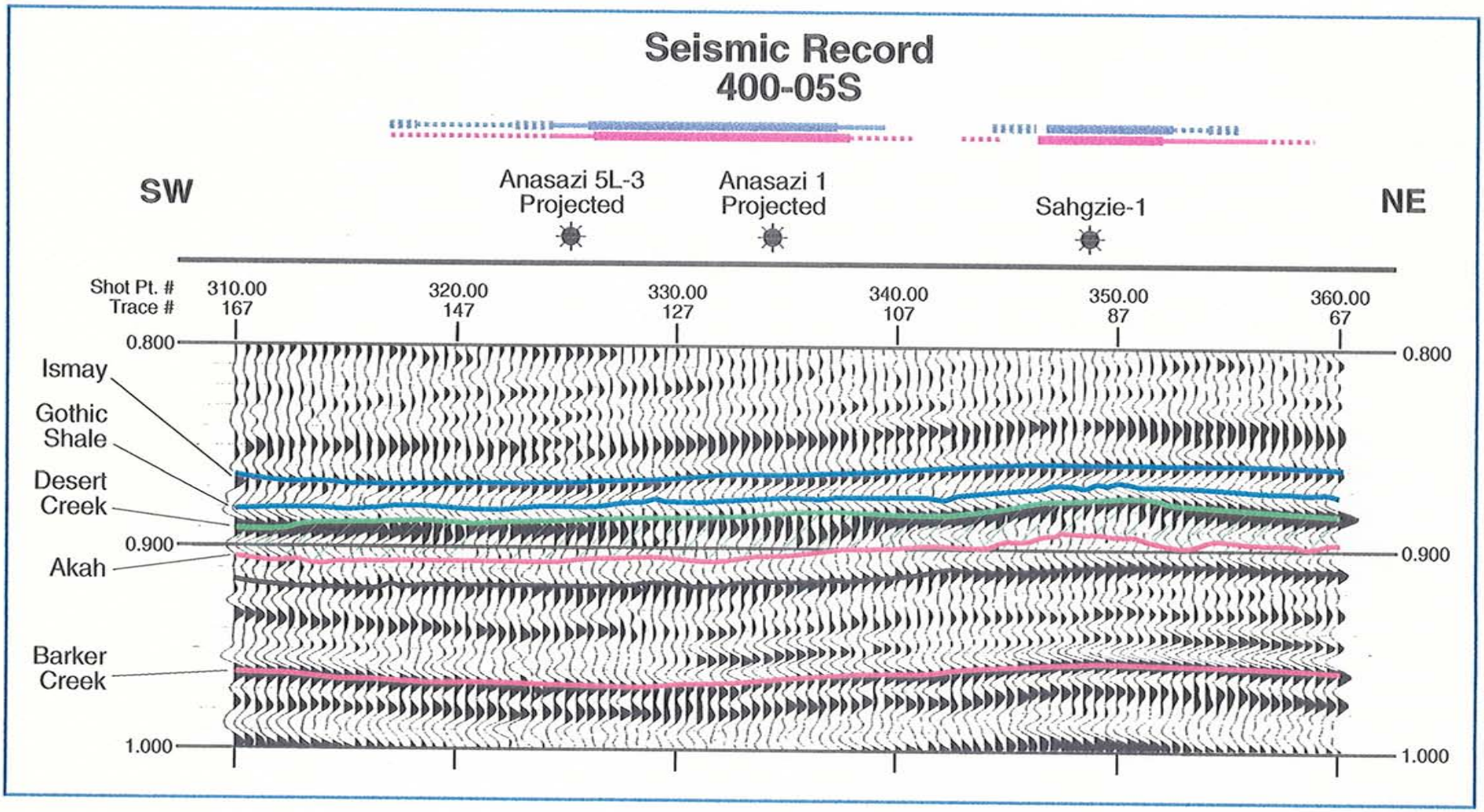

Figure 4–25. Reservoir Quality Seismic Interpretation Across the Anasazi and Sahgzie Carbonate Mound Buildups, Anasazi Field.
(courtesy of Harken Southwest Corp. and the Utah Geological Survey)

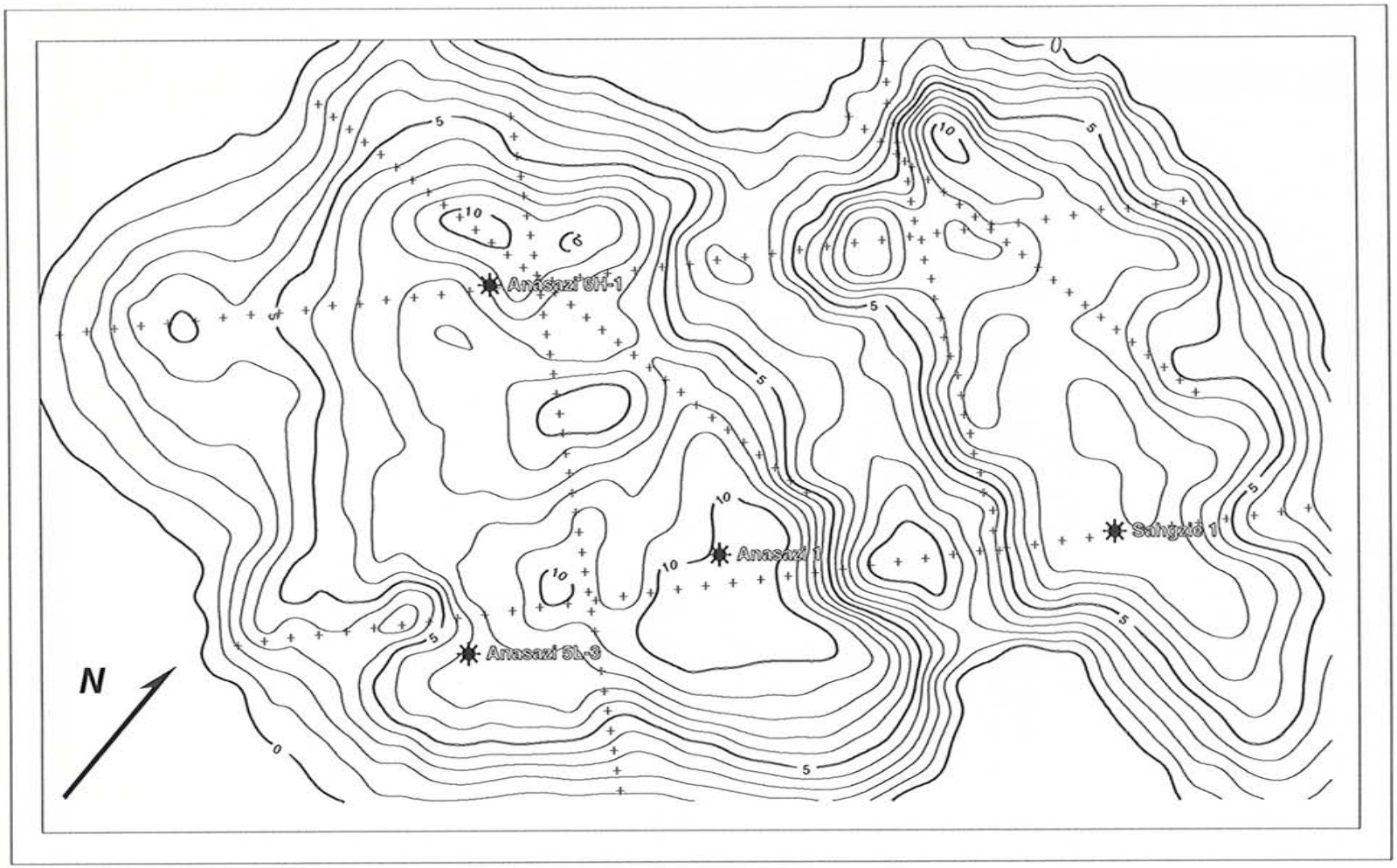

500 0 500 1000 1500 2000 2500 Feet

Scale

Figure 4-26. Anasazi Reservoir Quality Index Map
Based On Qualitative Seismic Interpretations

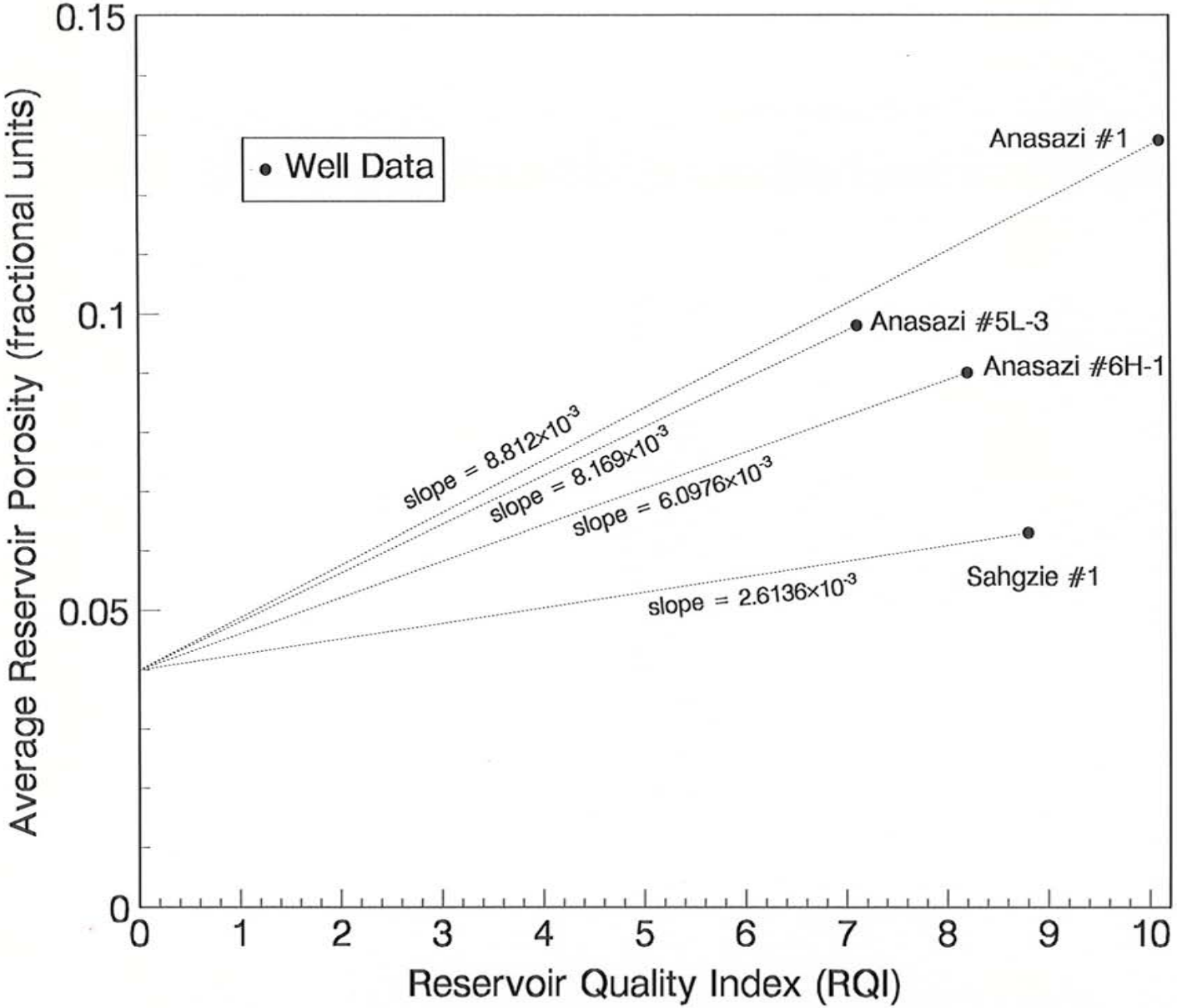

Figure 4-27. Anasazi Reservoir Quality Index (RQI)/ Average Porosity Transfer Function Plot.

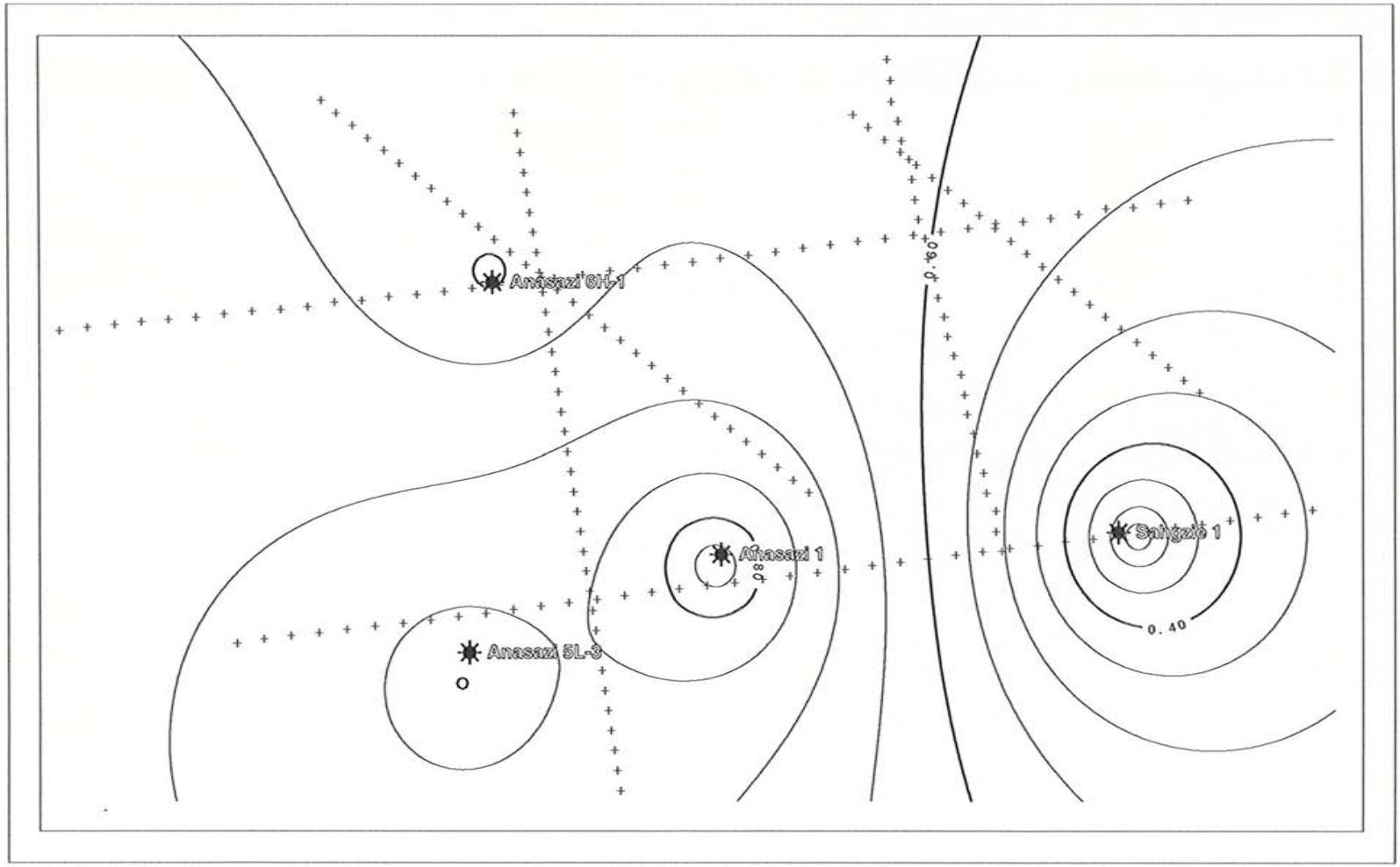

Figure 4-28. Nearest-Neighbor Map of Reservoir Quality vs. Average Porosity Transfer Function Slope

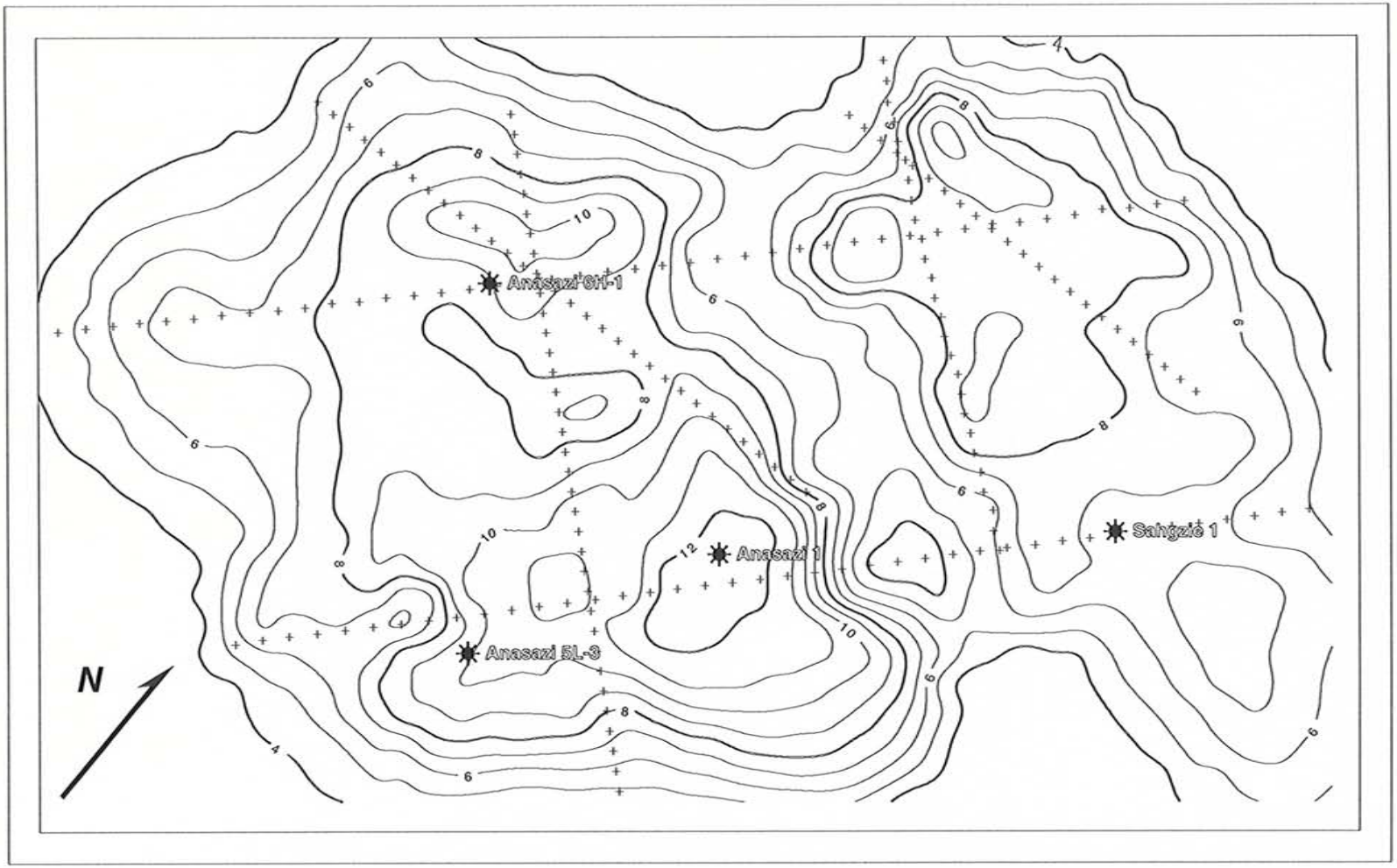

500 0 500 1000 1500 2000 2500 Feet

Scale

Figure 4-29. Anasazi Average Porosity Map

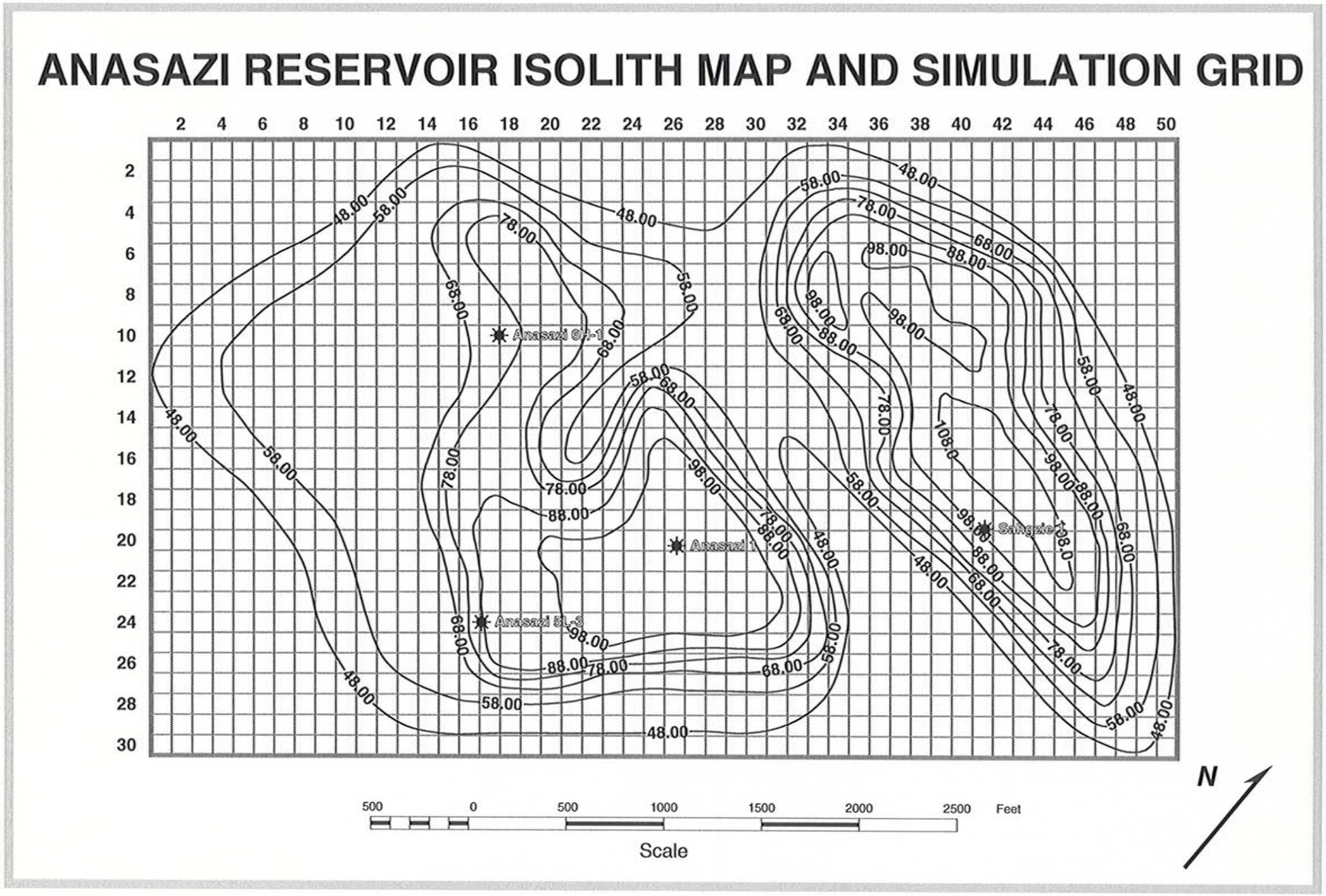

Figure 5-1. Anasazi Gridded Isolith Map

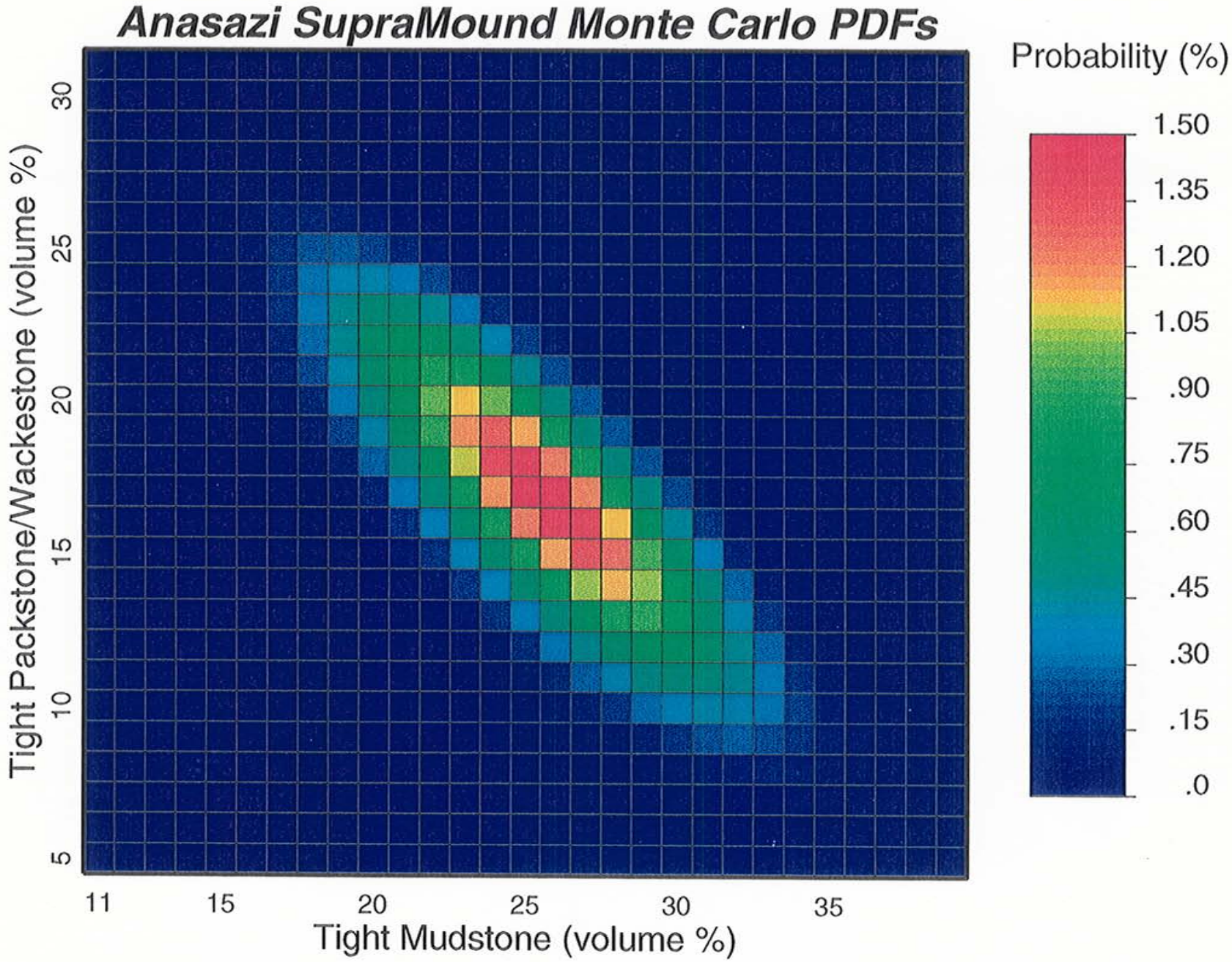

Figure 6–1. Bivariate Monte Carlo Distribution of Lithotype Volume Proportions: Tight Mudstone, Tight Packstone/Wackestone

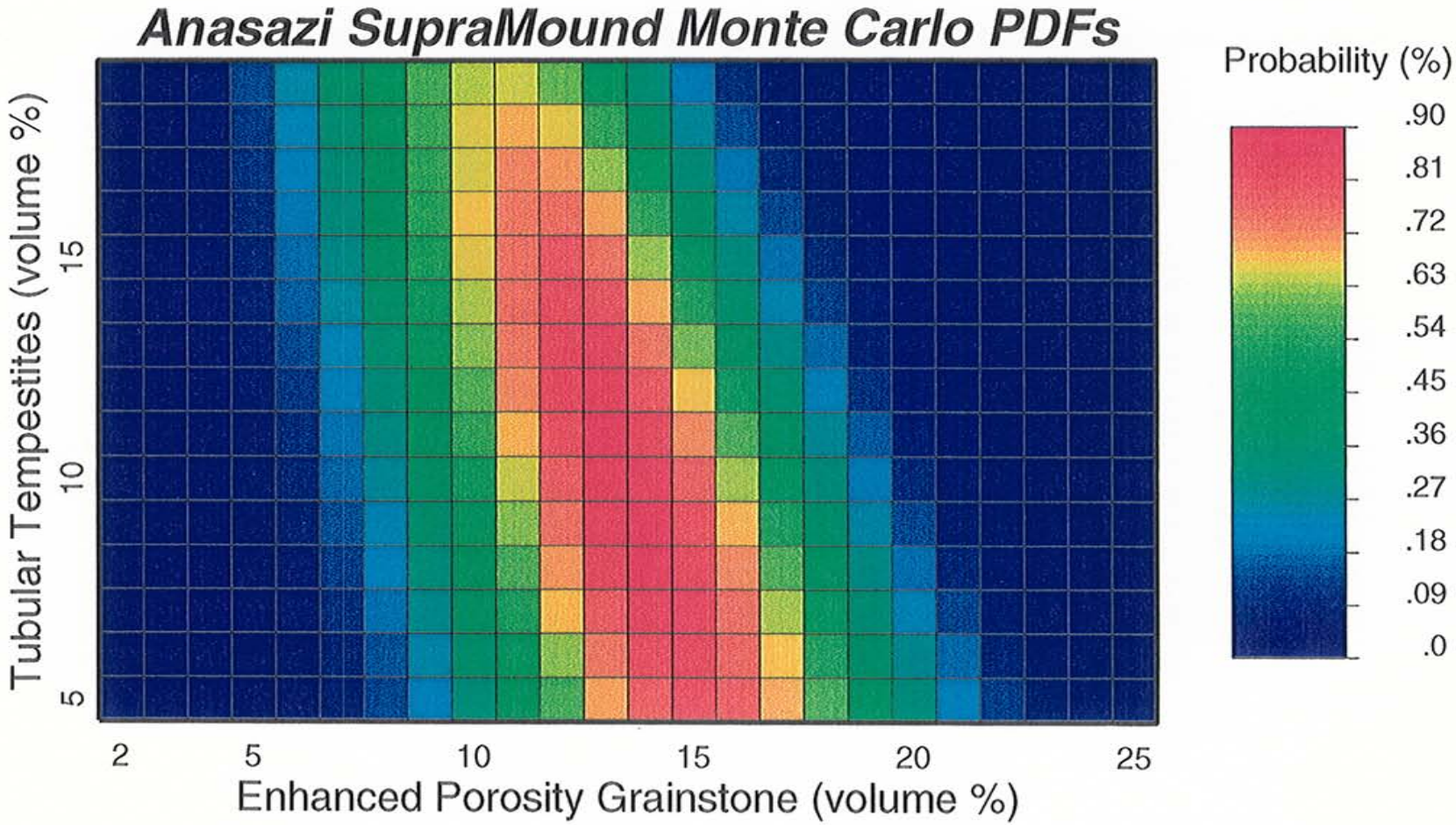

Figure 6–2. Bivariate Monte Carlo Distribution of Lithotype Volume Proportions: Porous Grainstone, Tubular Tempestites

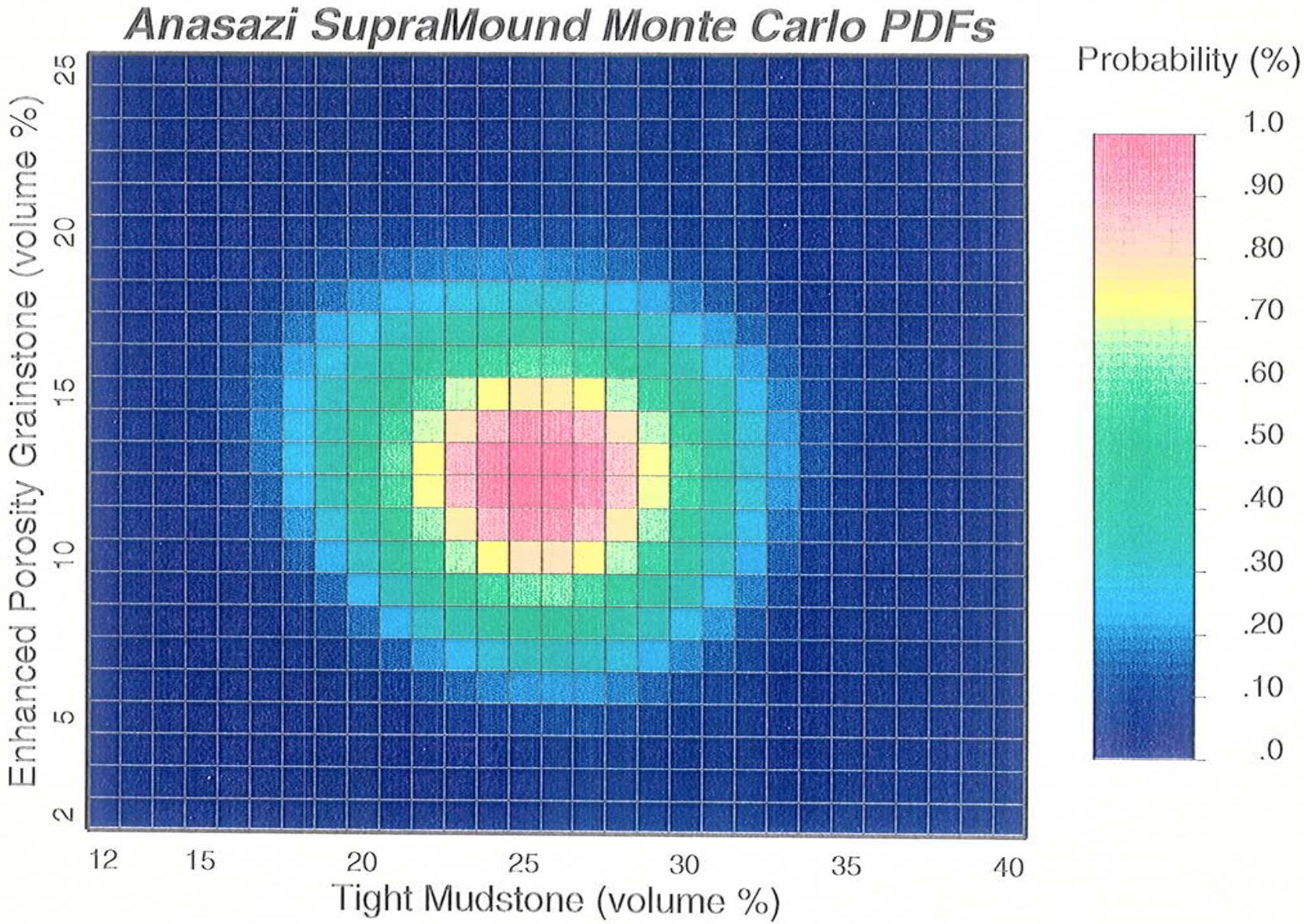

Figure 6–3. Bivariate Monte Carlo Distribution of Lithotype Volume Proportions: Tight Mudstone, Porous Grainstone

Enhanced Porosity Mudstone

Dolomitized Mudstone

Tight Carbonate Mudstone

Enhanced Porosity Packstone/Wackestone

Tight Packstone/Wackestone

Porous Grainstone

Cemented Grainstone

Tubular Tempestites

Phylloid Algal Limestone

Mound-Front Bioclastic Breccia

Figure 6-4. Lithotype Legend
50-Layer Geostatistical Model

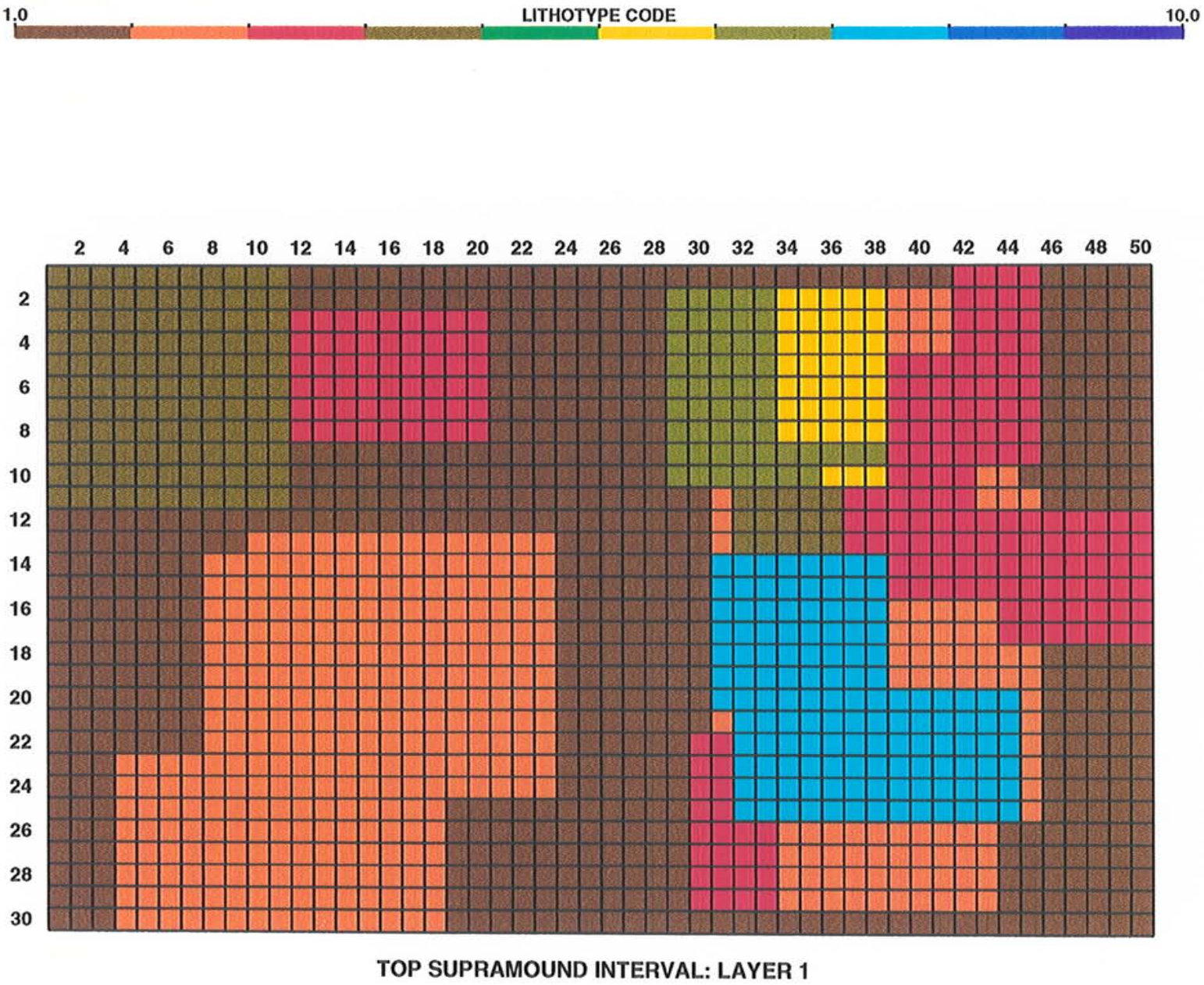

Figure 6-5. Anasazi Boolean Lithotype Emplacements: Layer 1

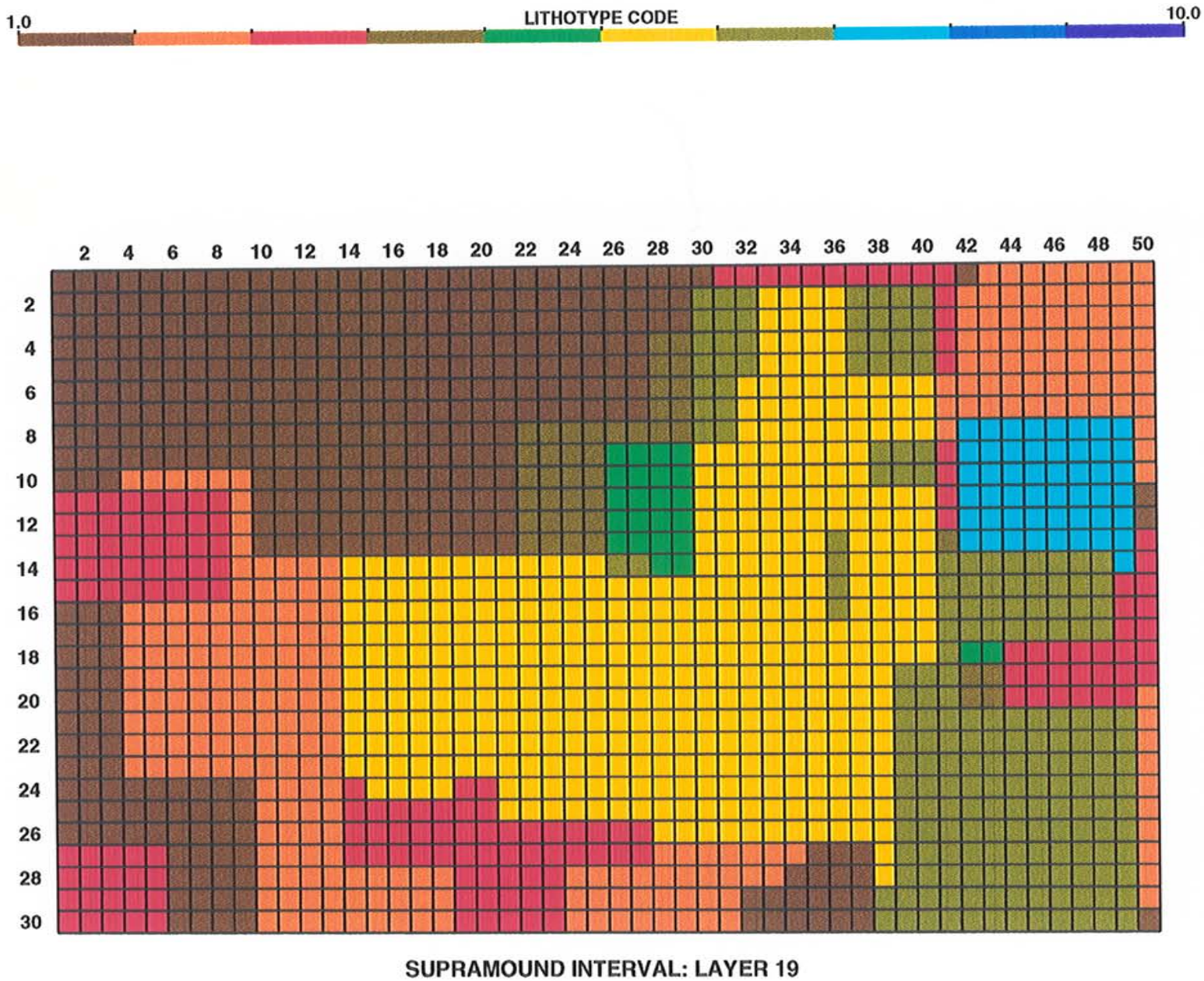

Figure 6-6. Anasazi Boolean Lithotype Emplacements: Layer 19

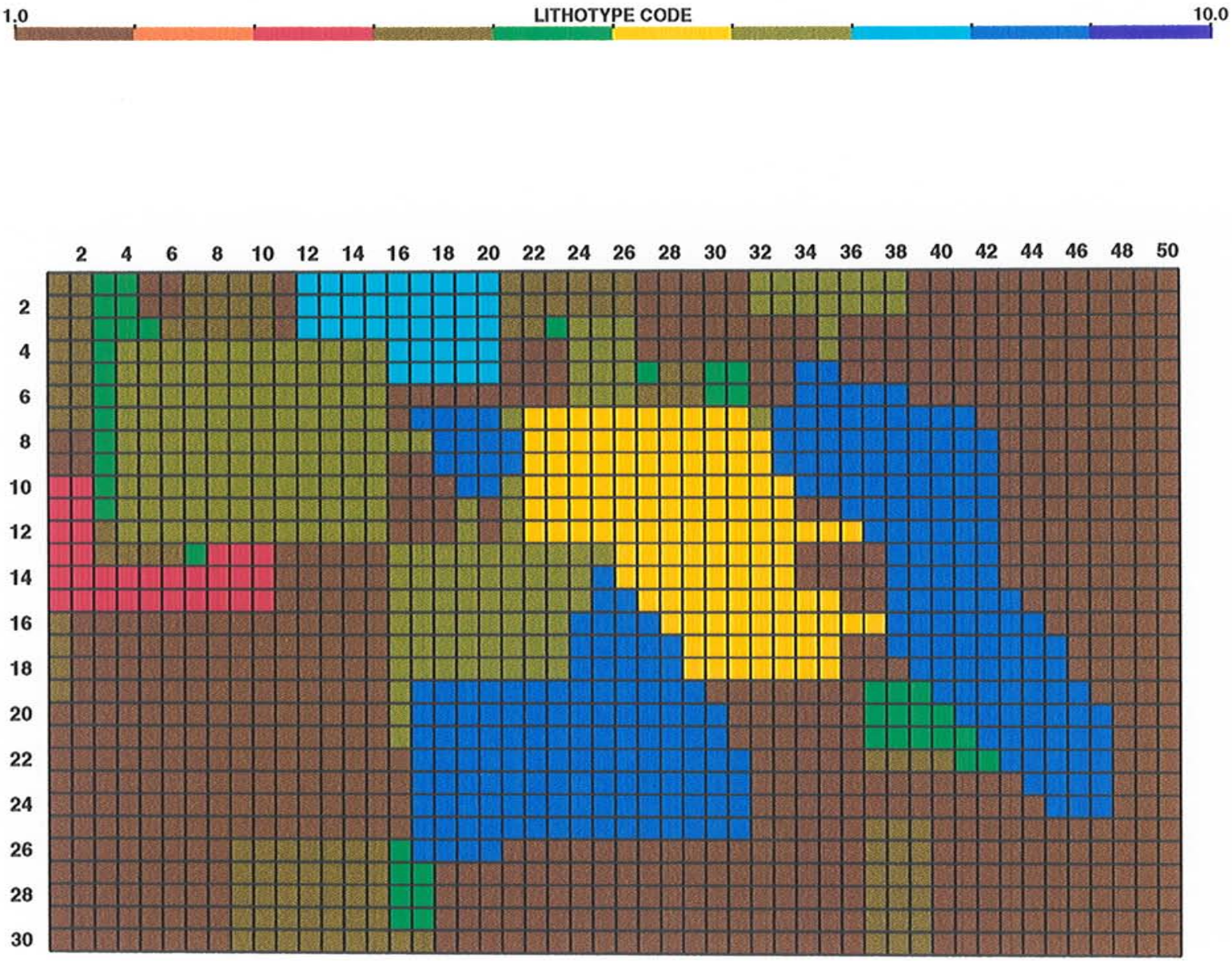

Figure 6-7. Anasazi Boolean Lithotype Emplacements: Layer 38

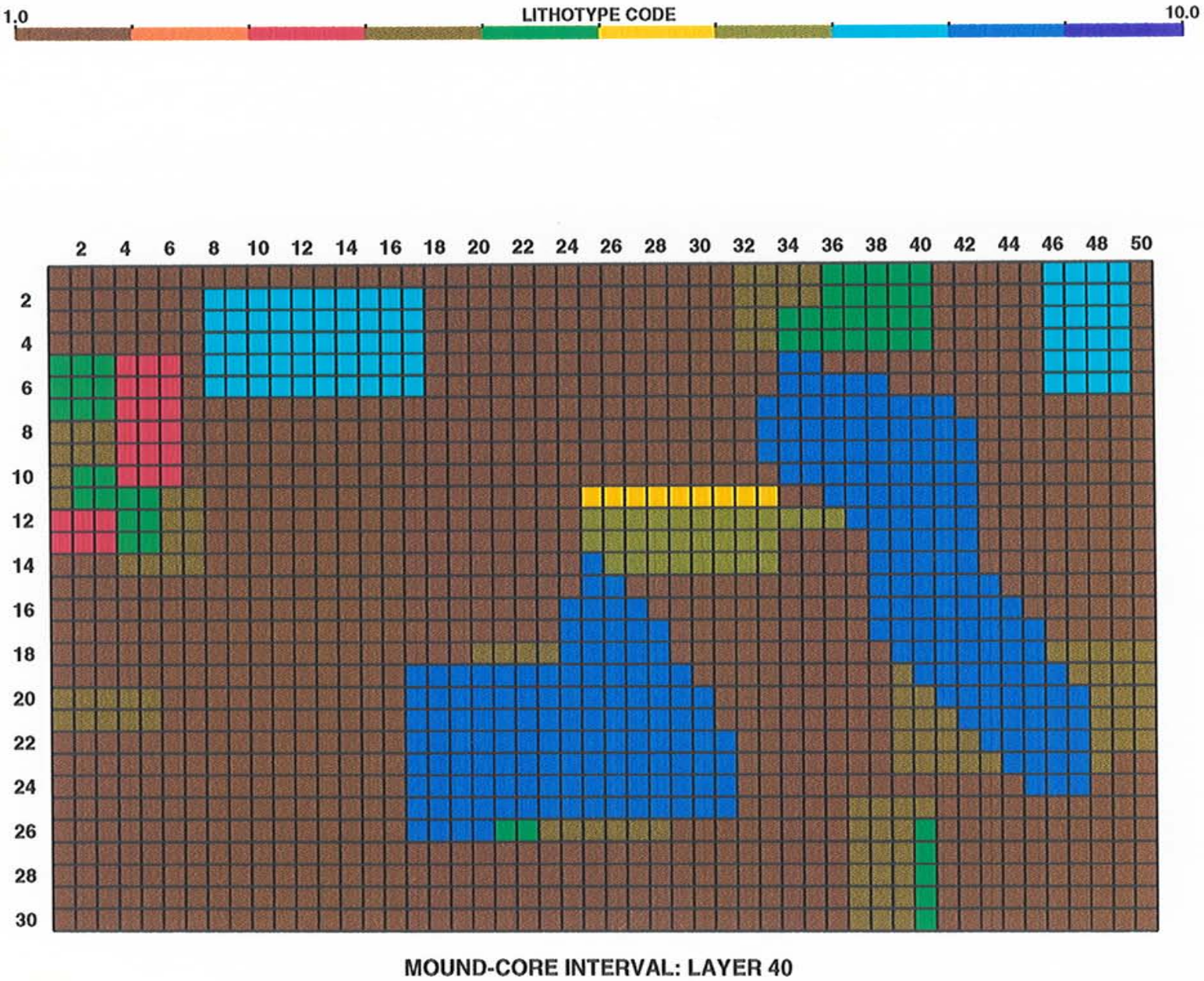

Figure 6-8. Anasazi Boolean Lithotype Emplacements: Layer 40

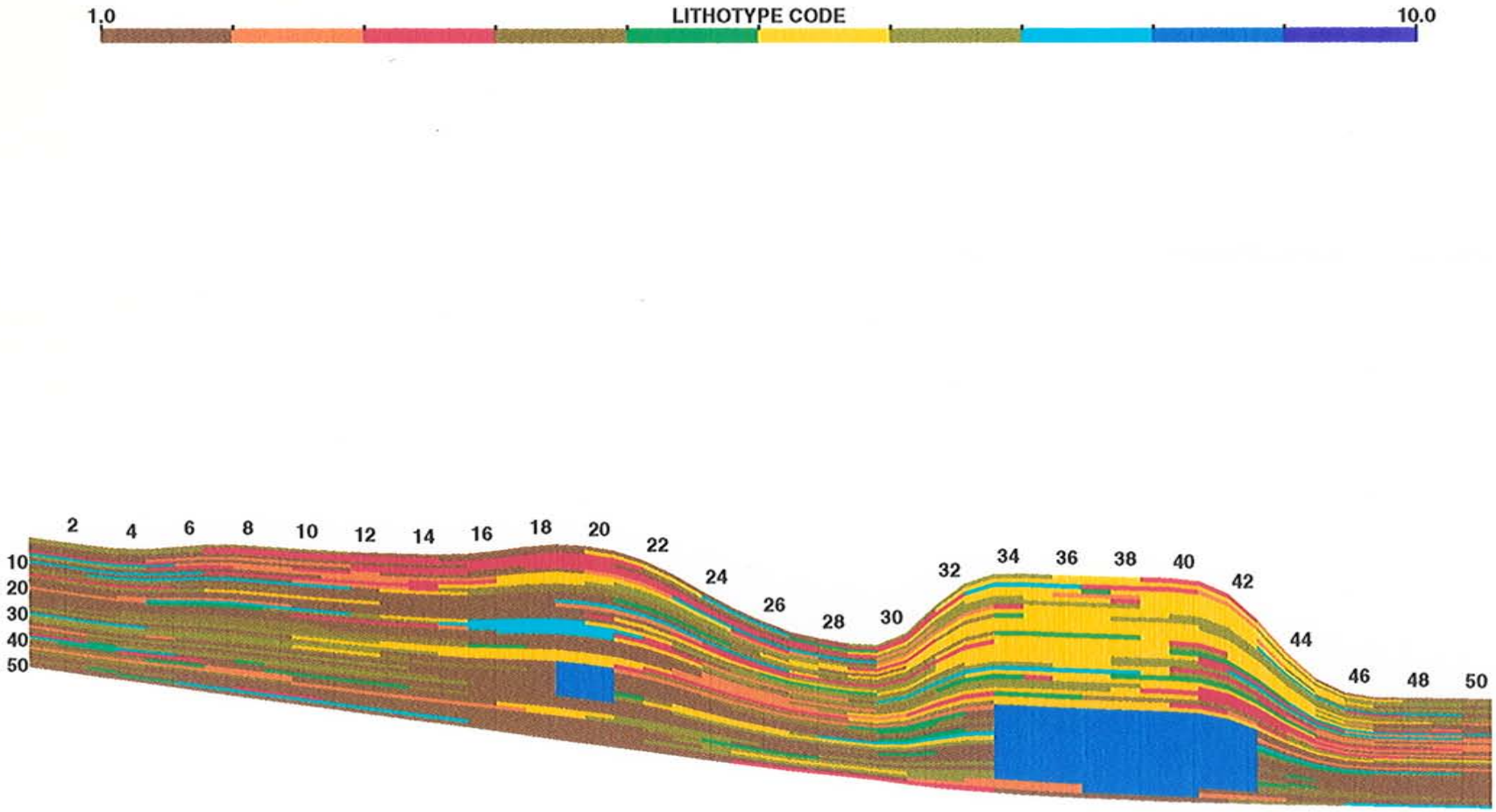

Vertical Exaggeration: 7.5X

Figure 6-9. Anasazi Boolean Lithotype Cross-Section: Y=10

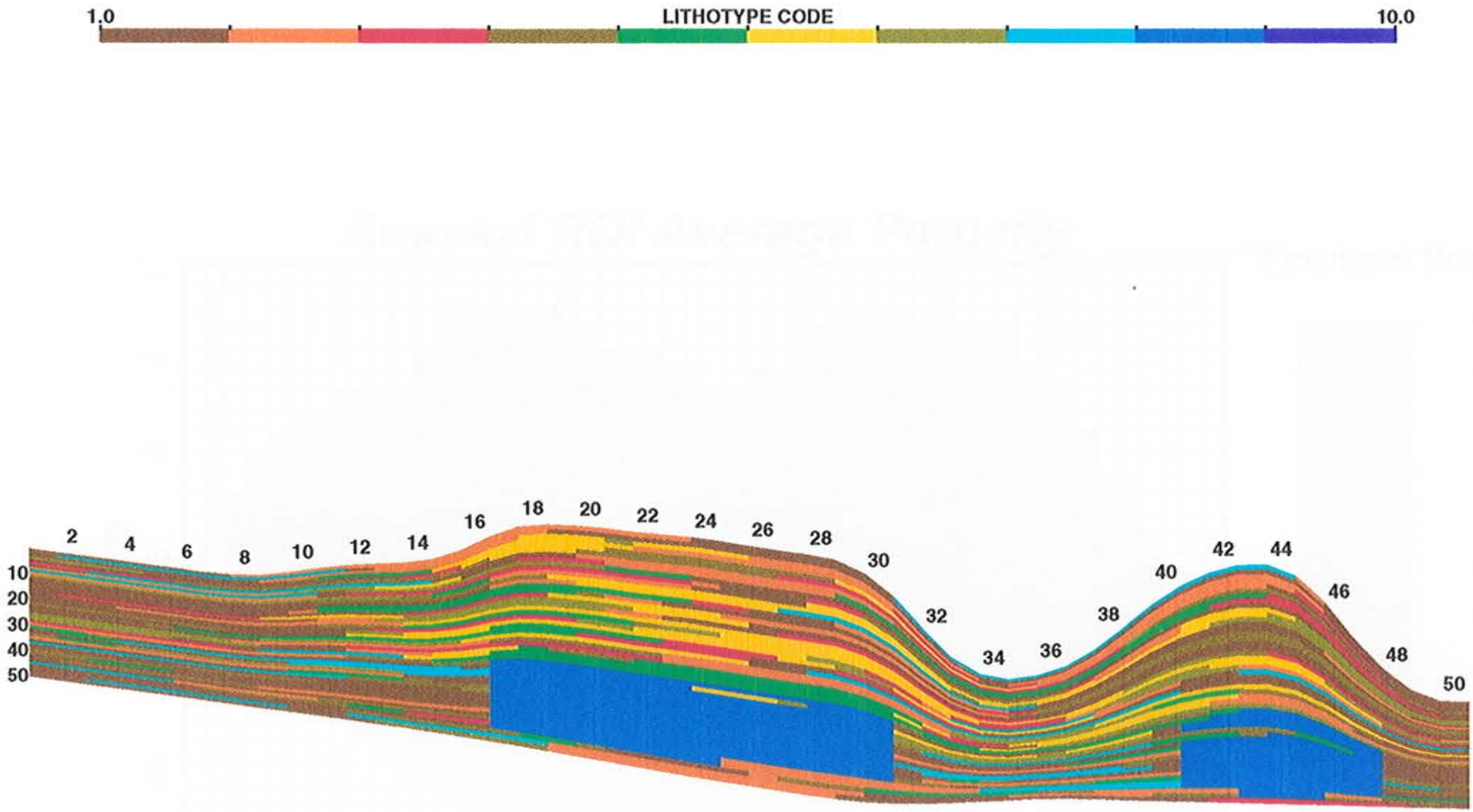

Vertical Exaggeration: 7.5X

Figure 6-10. Anasazi Boolean Lithotype Cross-Section: Y=20

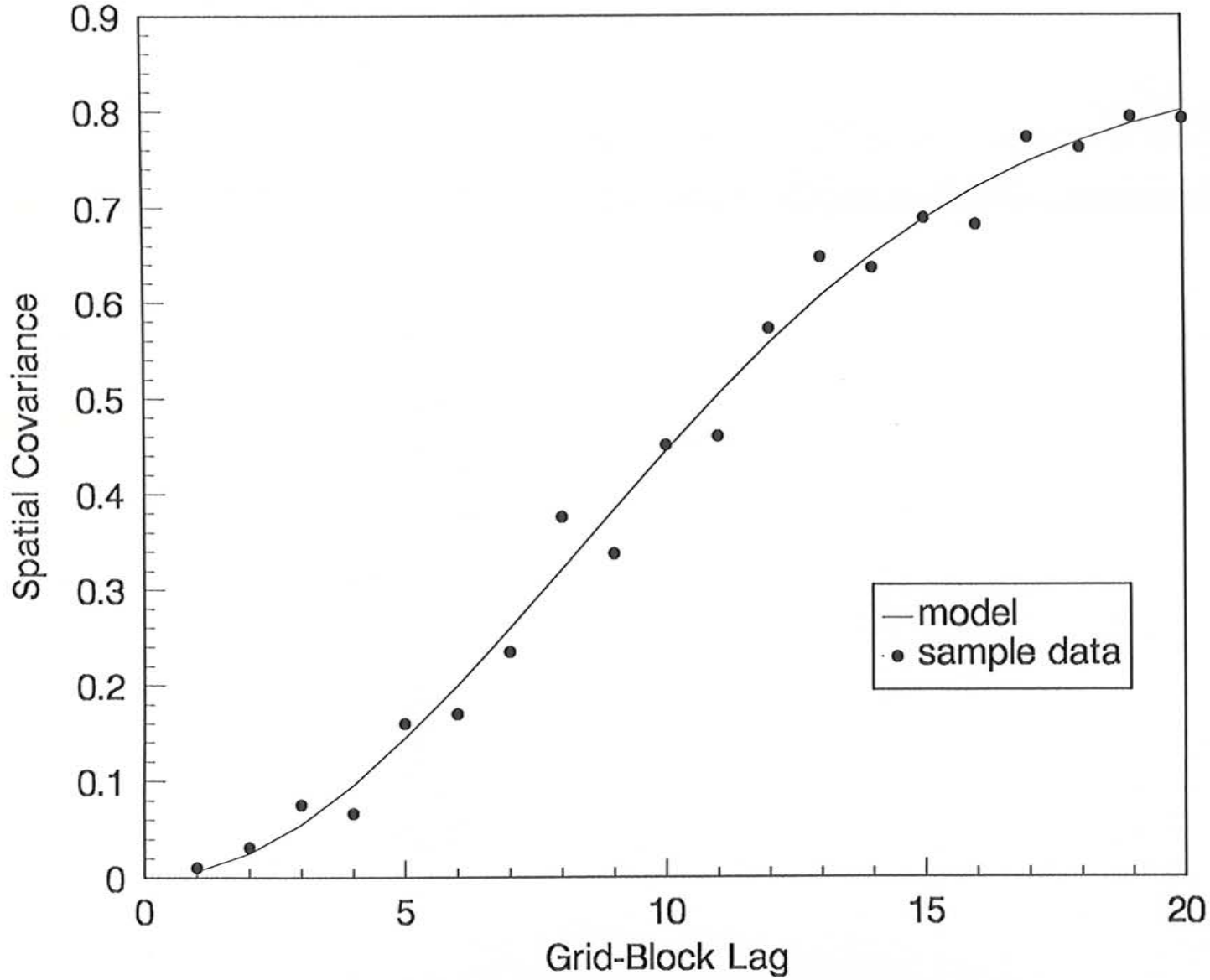

FIGURE 6-12. ANASAZI POROSITY VERTICAL VARIOGRAM MODELING

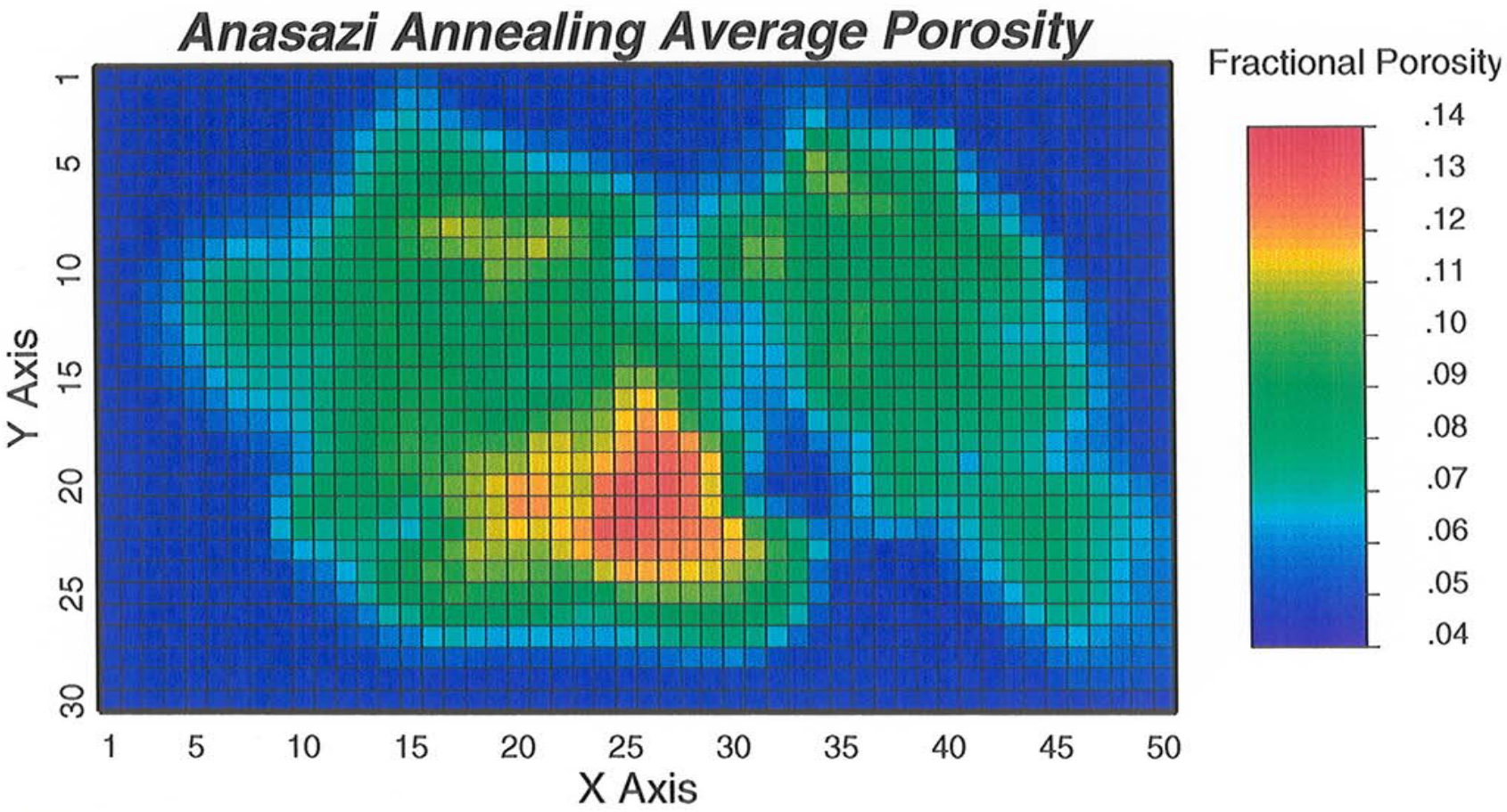

Figure 6-13. Anasazi Annealing Average Porosity Grid

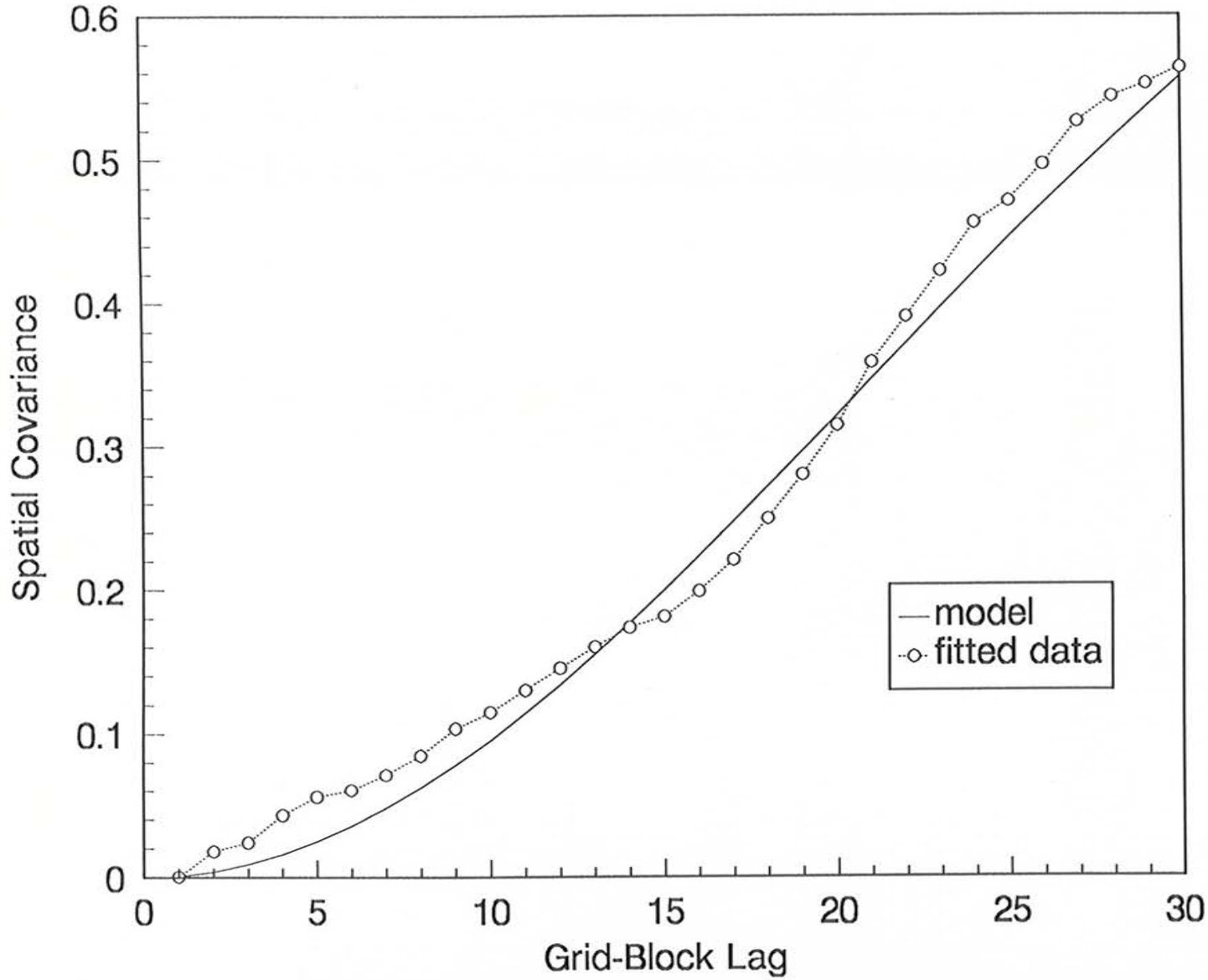

FIGURE 6-14. ANASAZI SIMULATED ANNEALING CONSTRAINTS POROSITY HORIZONTAL VARIOGRAM

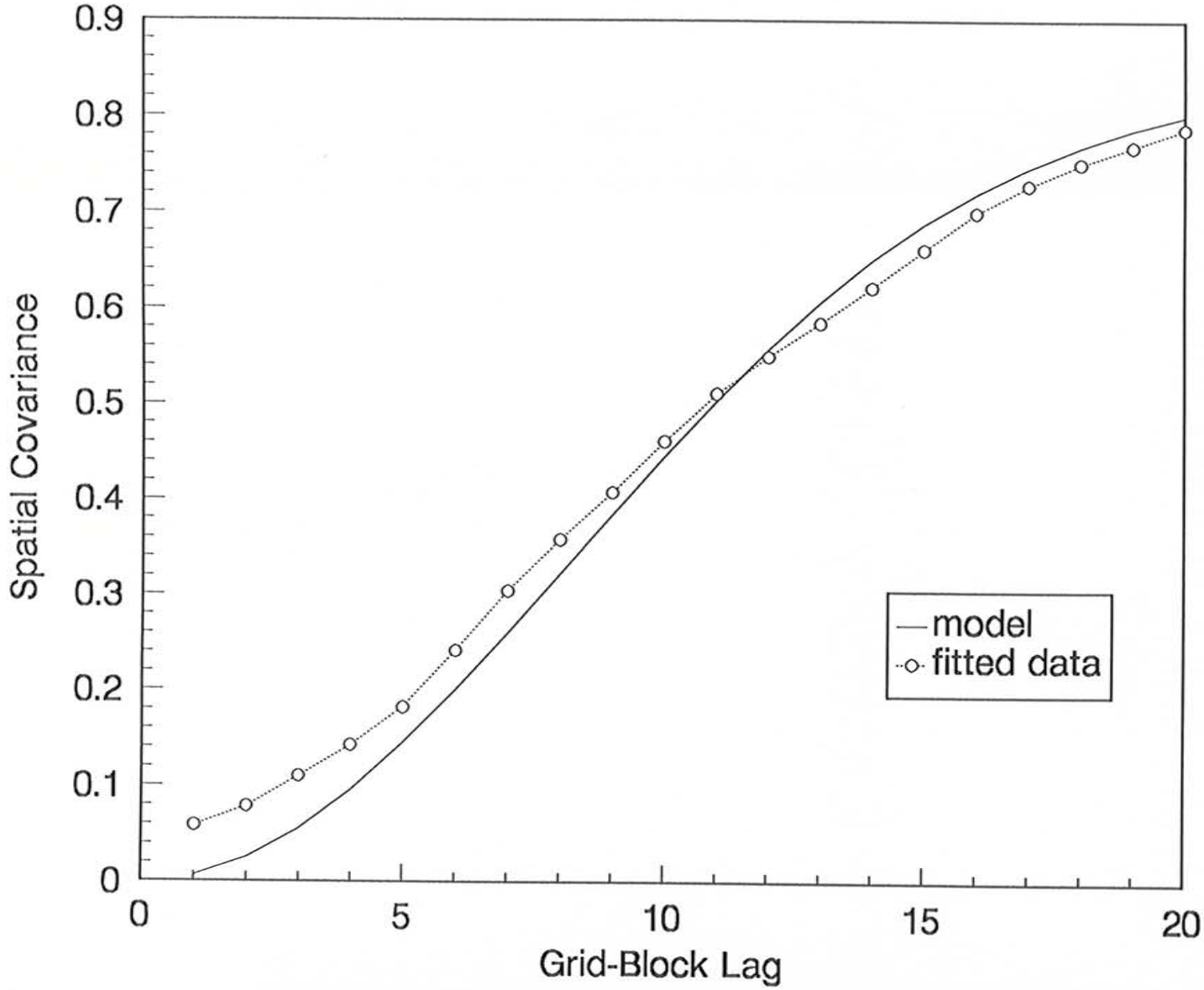

FIGURE 6-15. ANASAZI SIMULATED ANNEALING CONSTRAINTS POROSITY VERTICAL VARIOGRAM

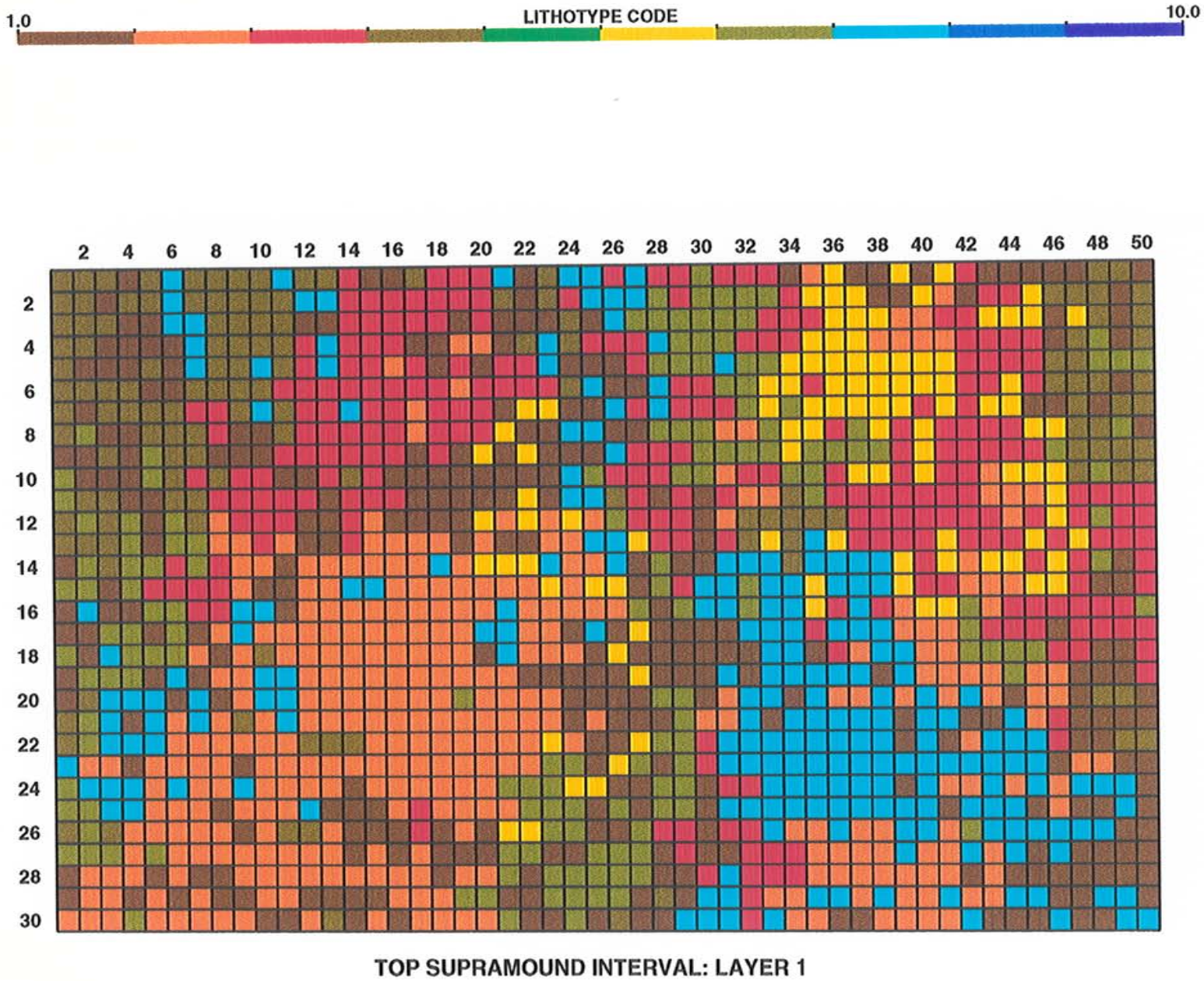

Figure 6-16. Anasazi Lithotype Distribution Grid: Layer 1

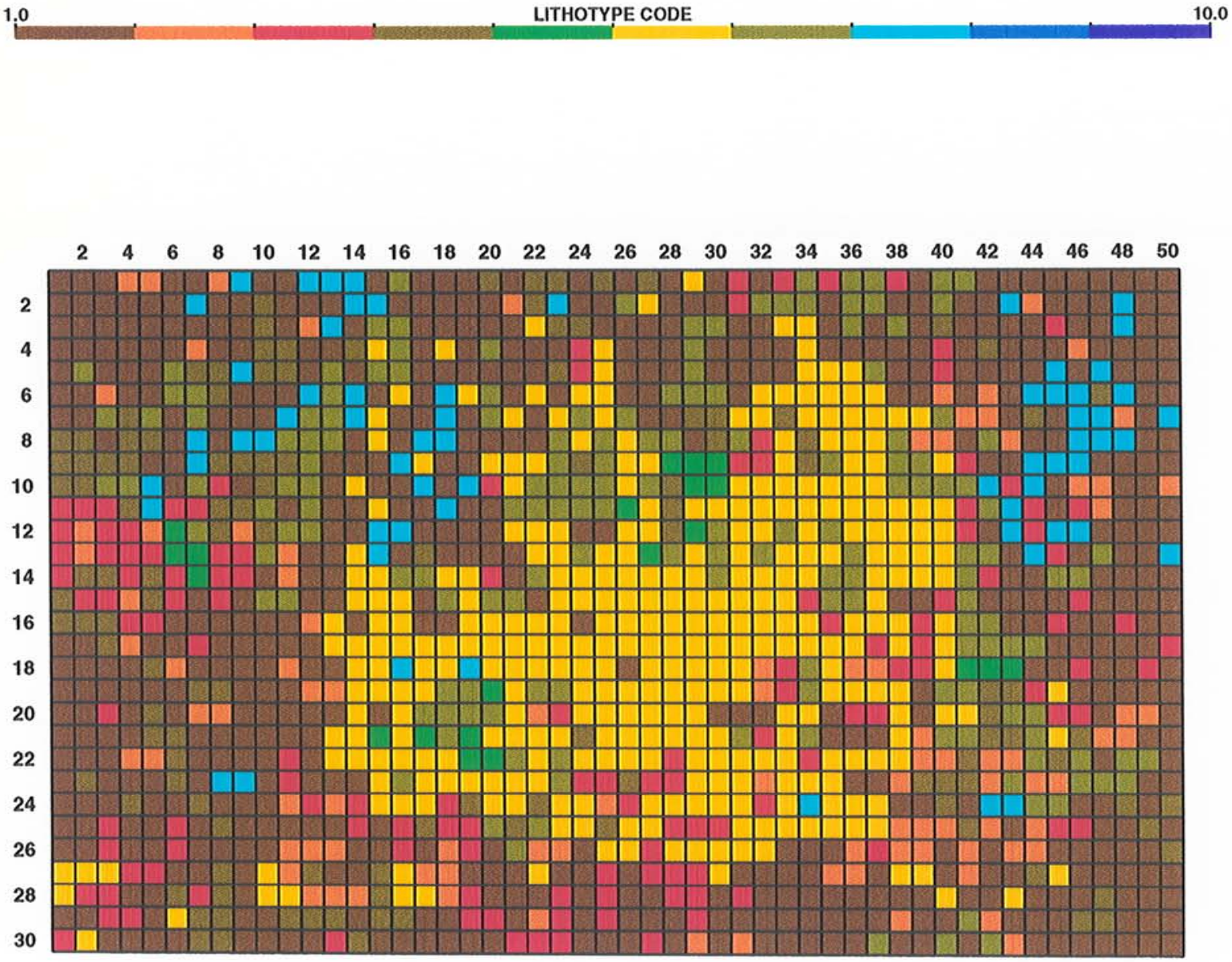

Figure 6-17. Anasazi Lithotype Distribution Grid: Layer 19

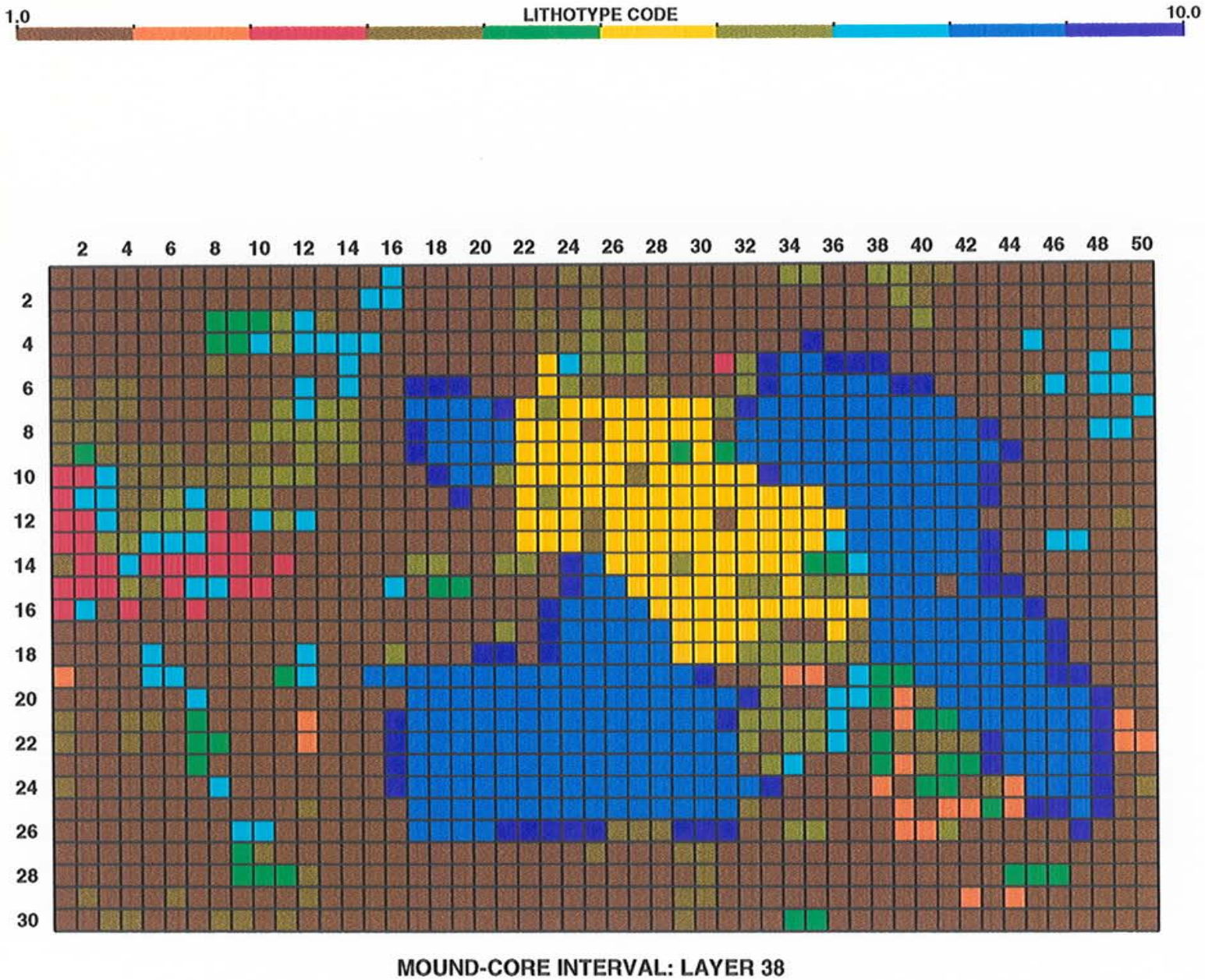

Figure 6-18. Anasazi Lithotype Distribution Grid: Layer 38

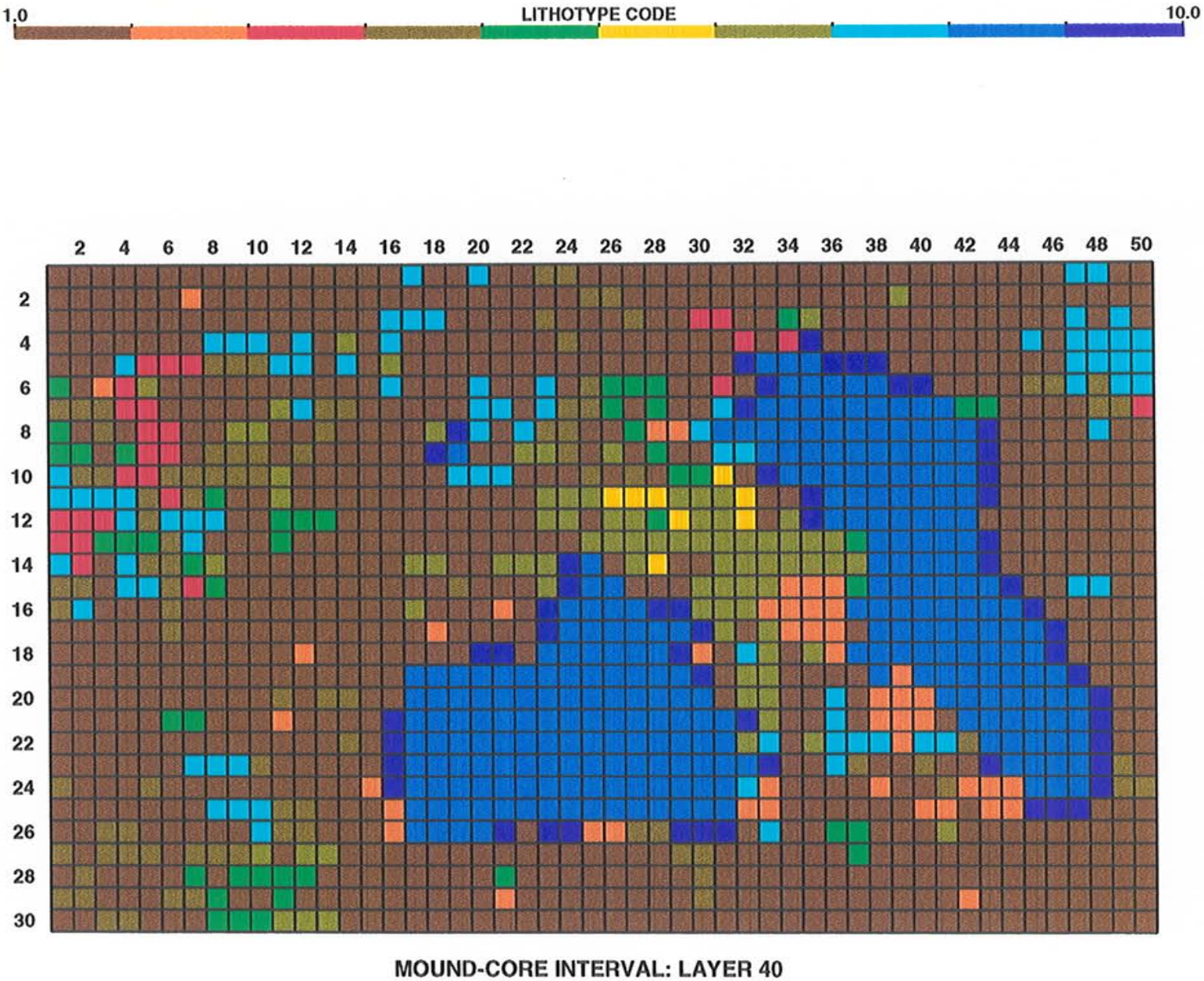

Figure 6-19. Anasazi Lithotype Distribution Grid: Layer 40

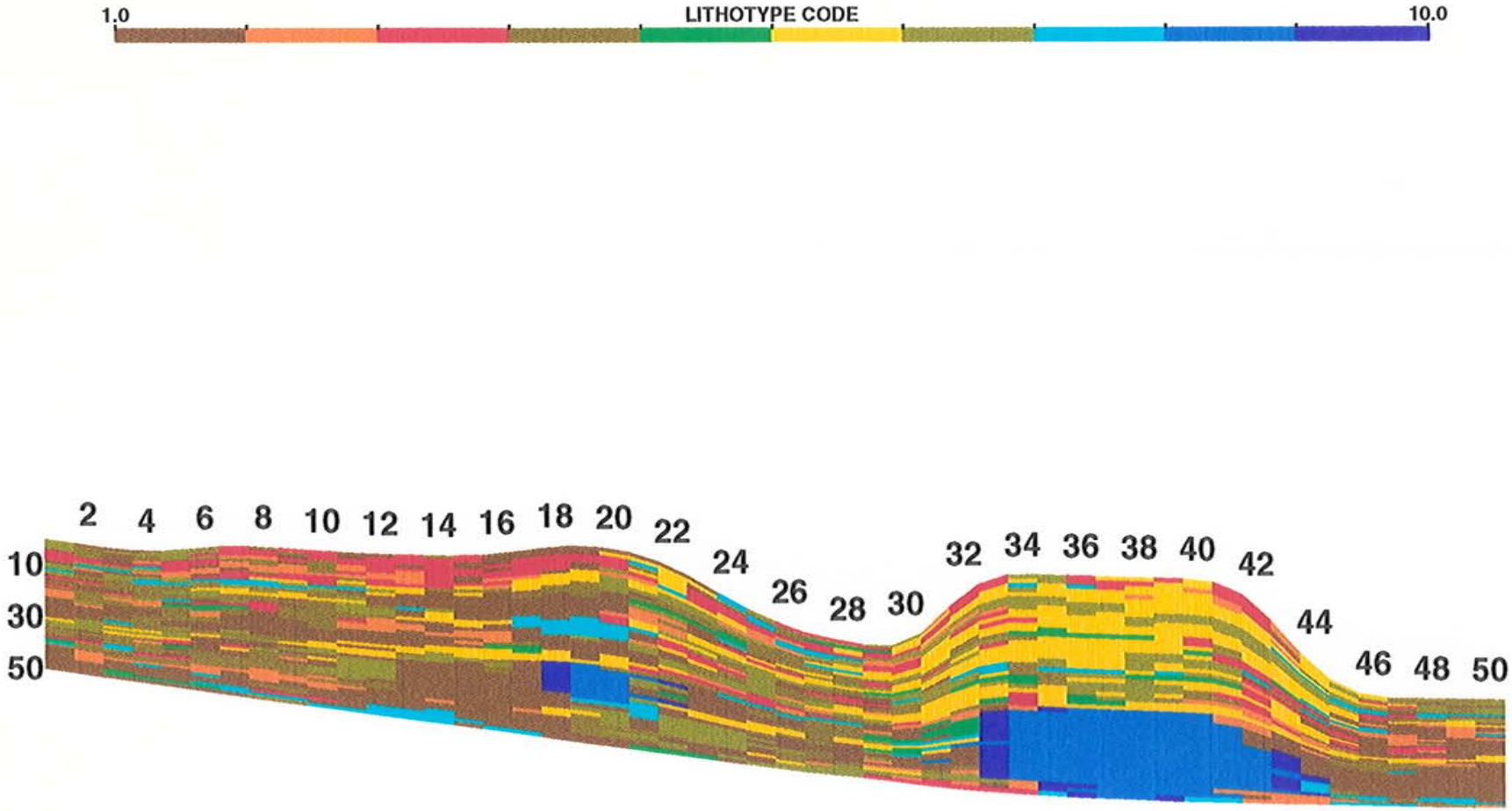

Vertical Exaggeration: 7.5X

Figure 6-20. Anasazi Lithotype Cross-Section: Y=10

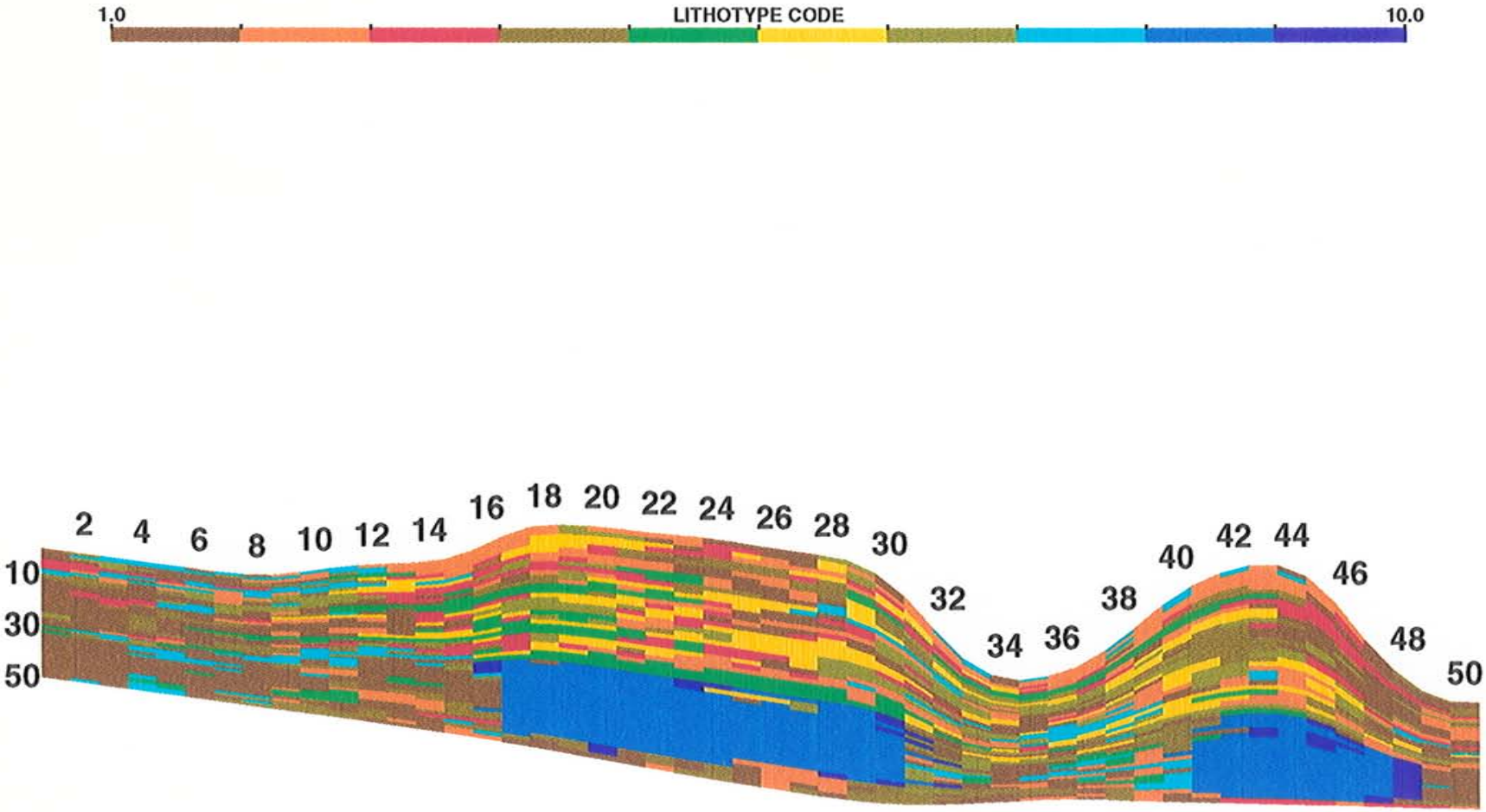

Vertical Exaggeration: 7.5X

Figure 6-21. Anasazi Lithotype Cross-Section: Y=20

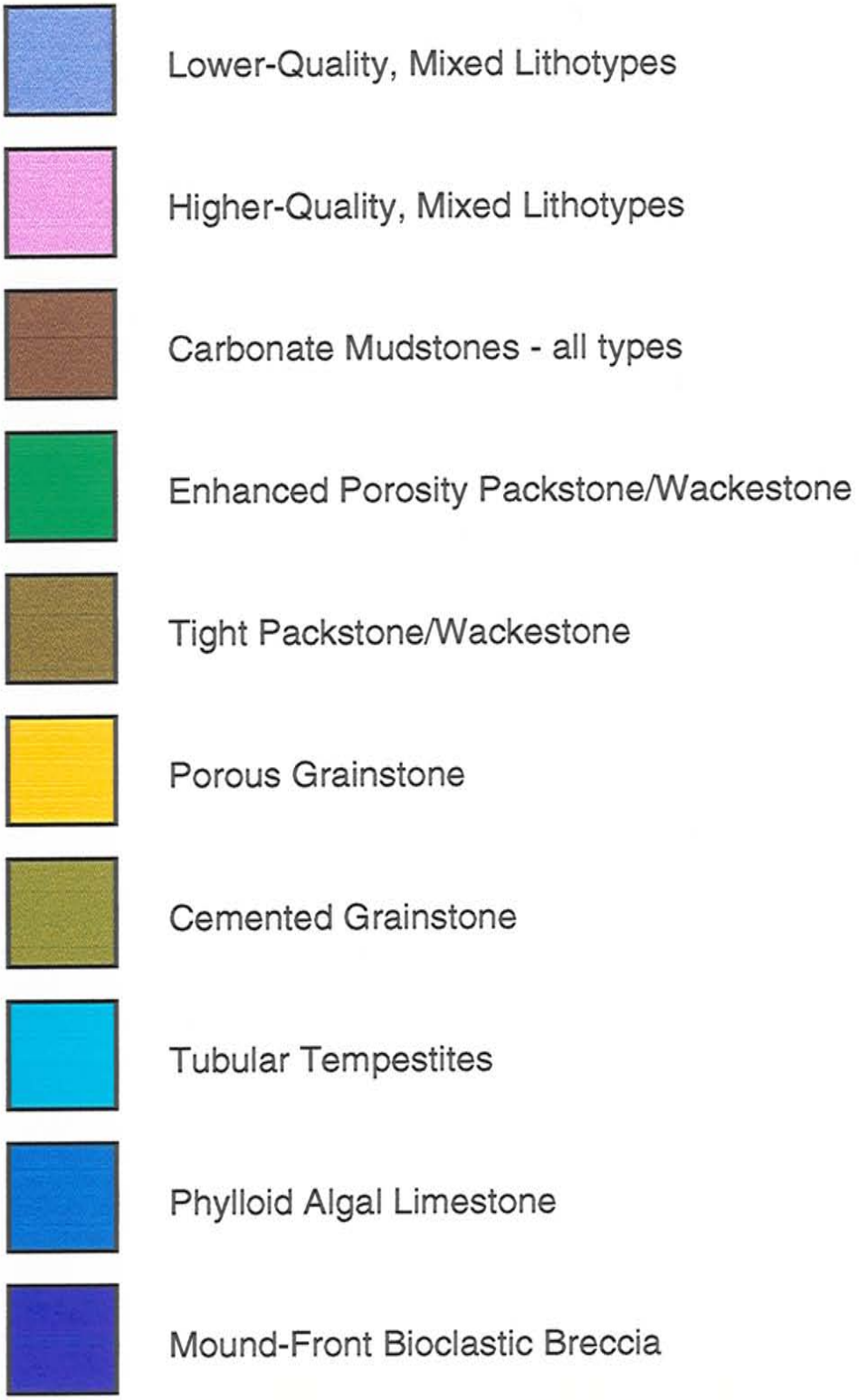

Figure 7-1. Lithotype Legend
15-Layer Upscaled VIP Simulation Model

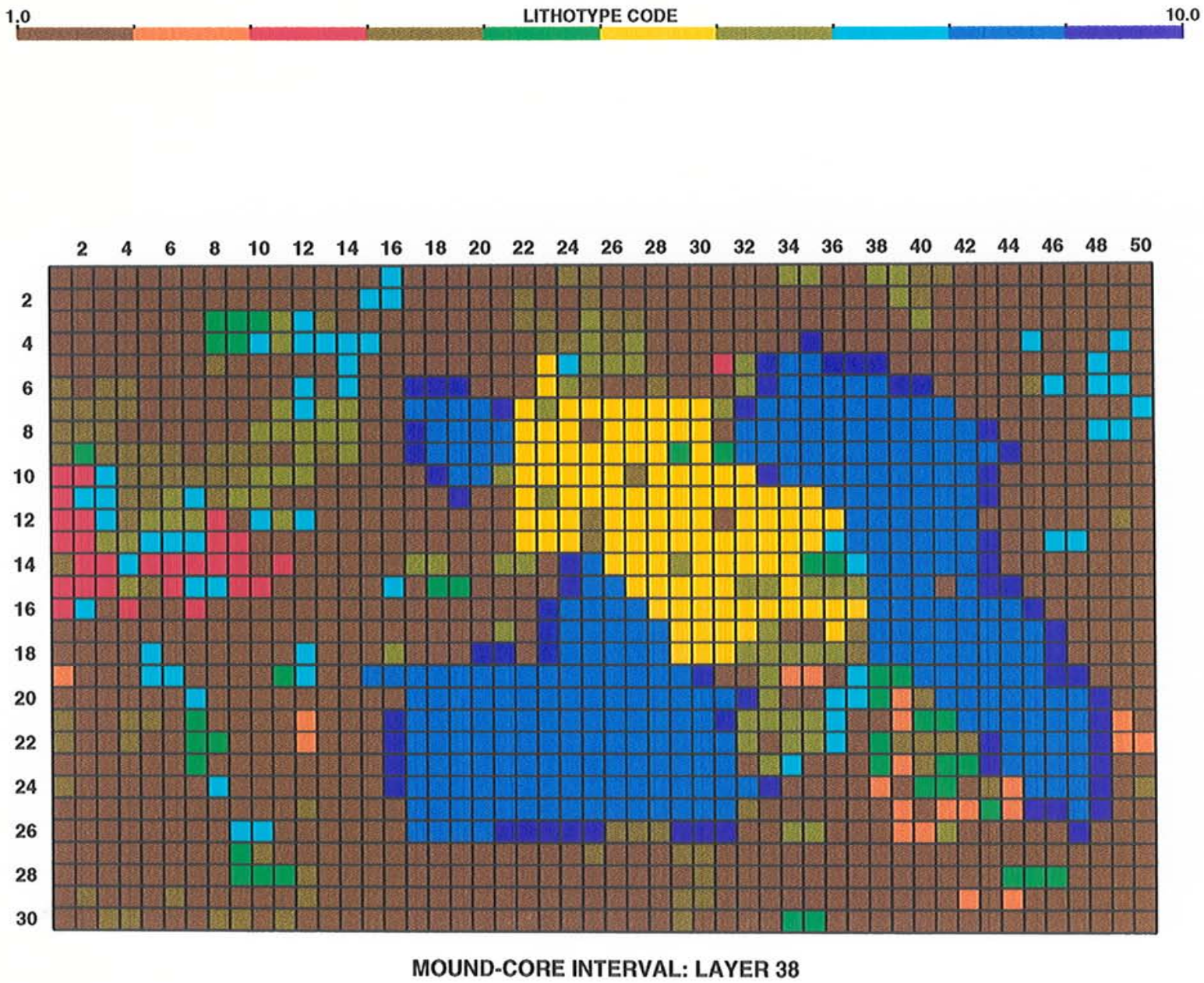

Figure 7-2. Lithotype Areal Grid, Layer 38
50 Layer Geostatistical Model

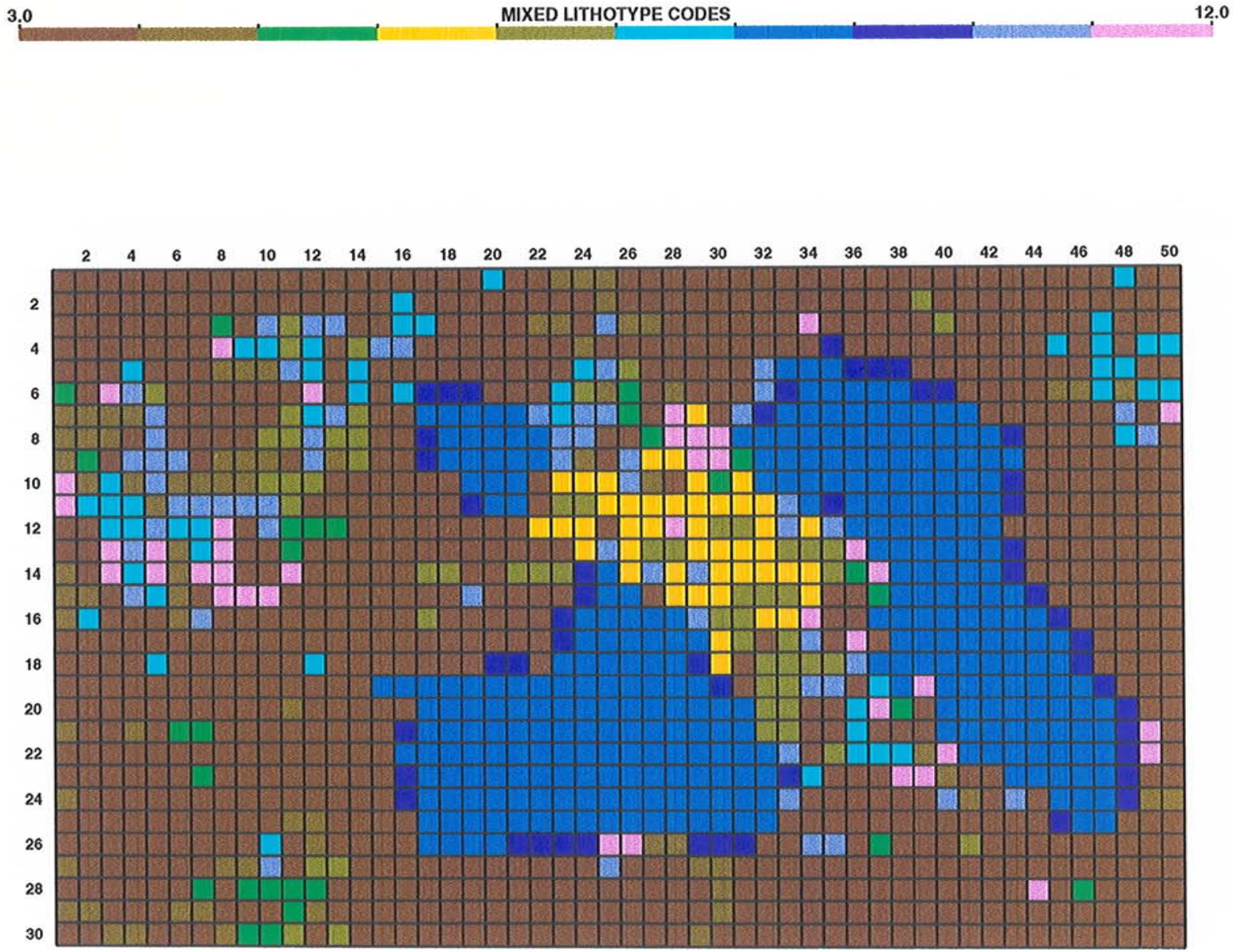

Figure 7-3. Lithotype Areal Grid, Layer 12
Upscaled Simulation 15-Layer Model

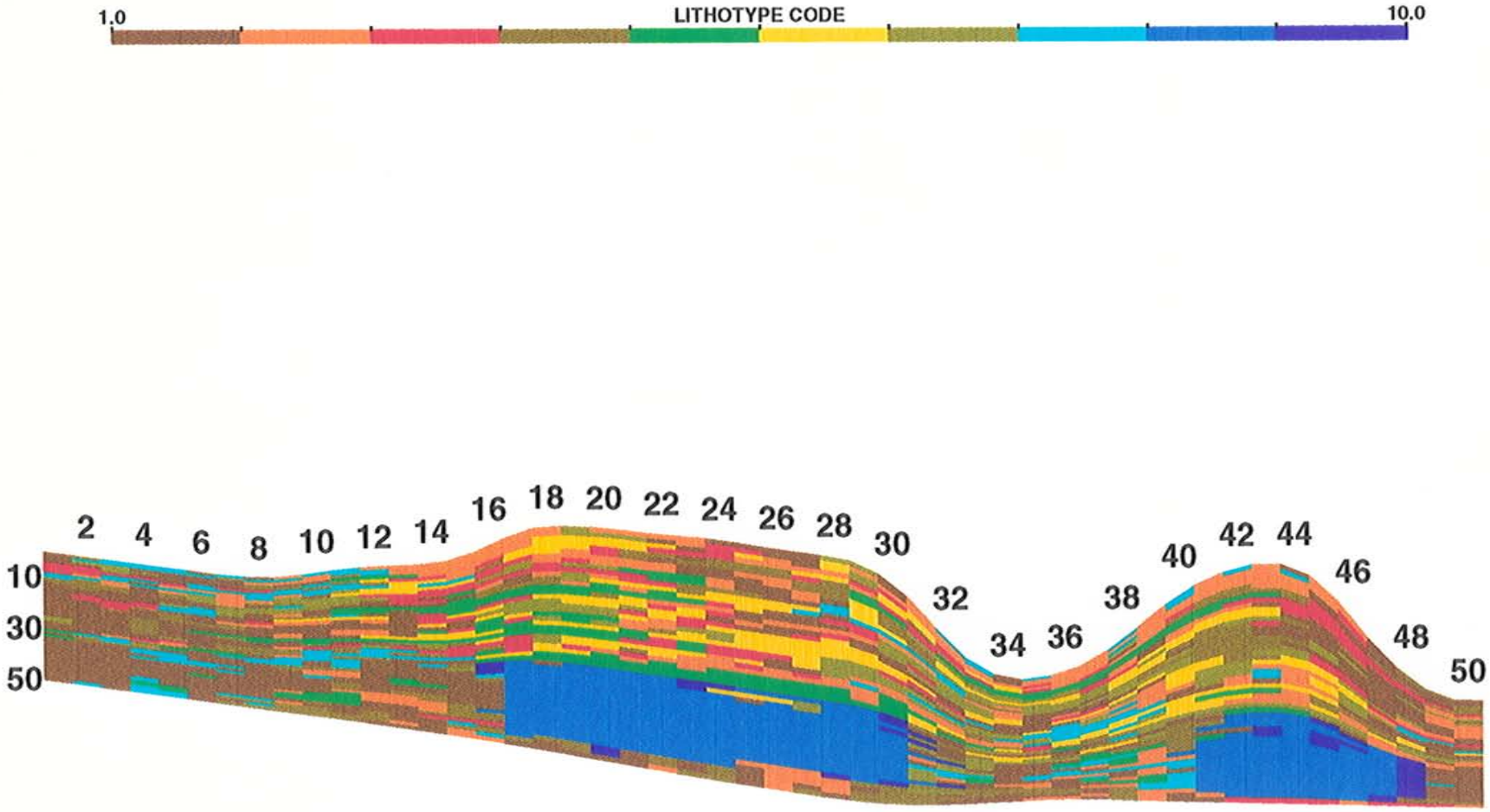

Vertical Exaggeration: 7.5X

Figure 7-4. Lithotype Cross-Section (Y=20)
50 Layer Geostatistical Model

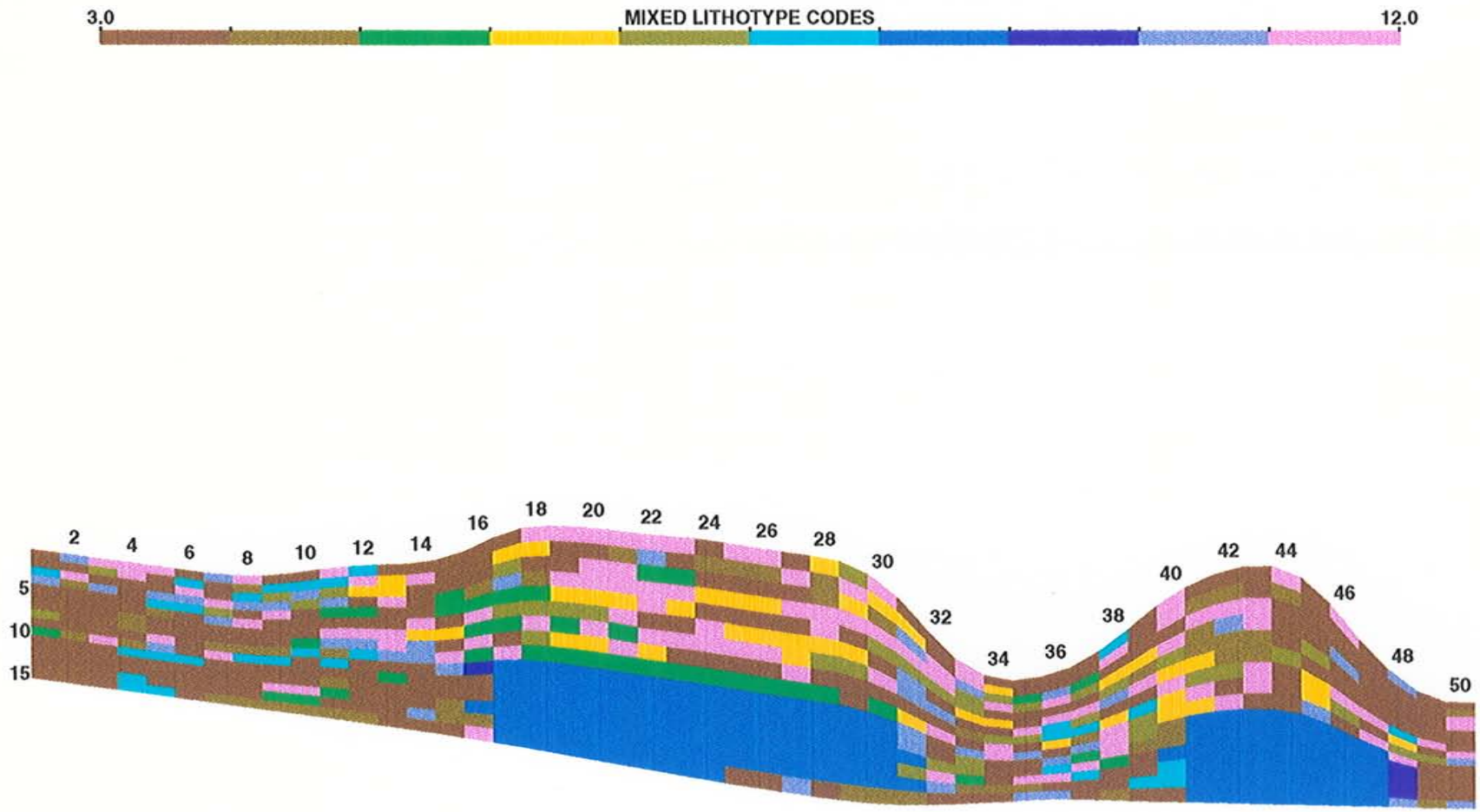

Vertical Exaggeration: 7.5X

Figure 7-5. Lithotype Cross-Section (Y=20)
Upscaled Simulation 15-Layer Model

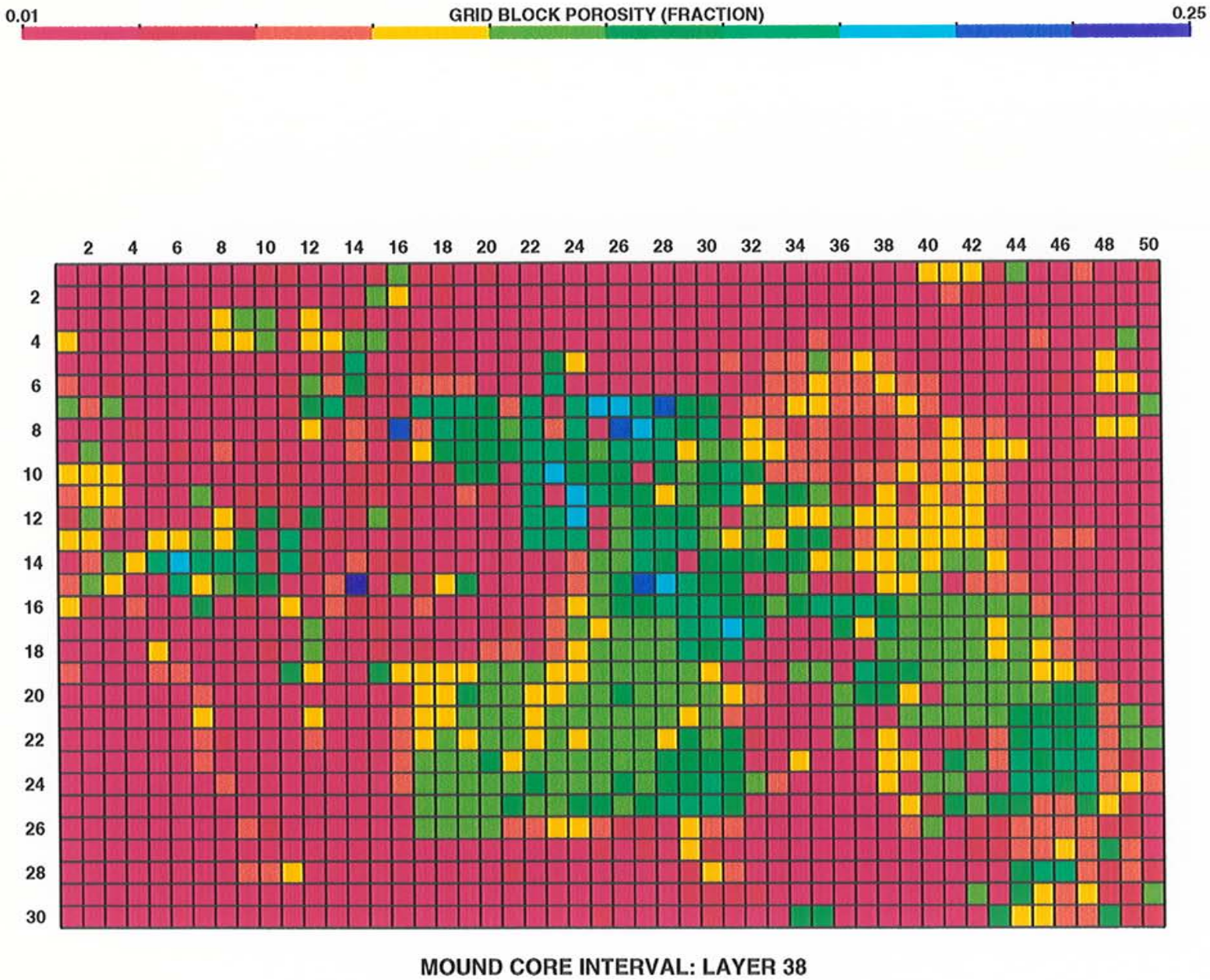

Figure 7-6. Porosity Areal Grid, Layer 38
50 Layer Geostatistical Model

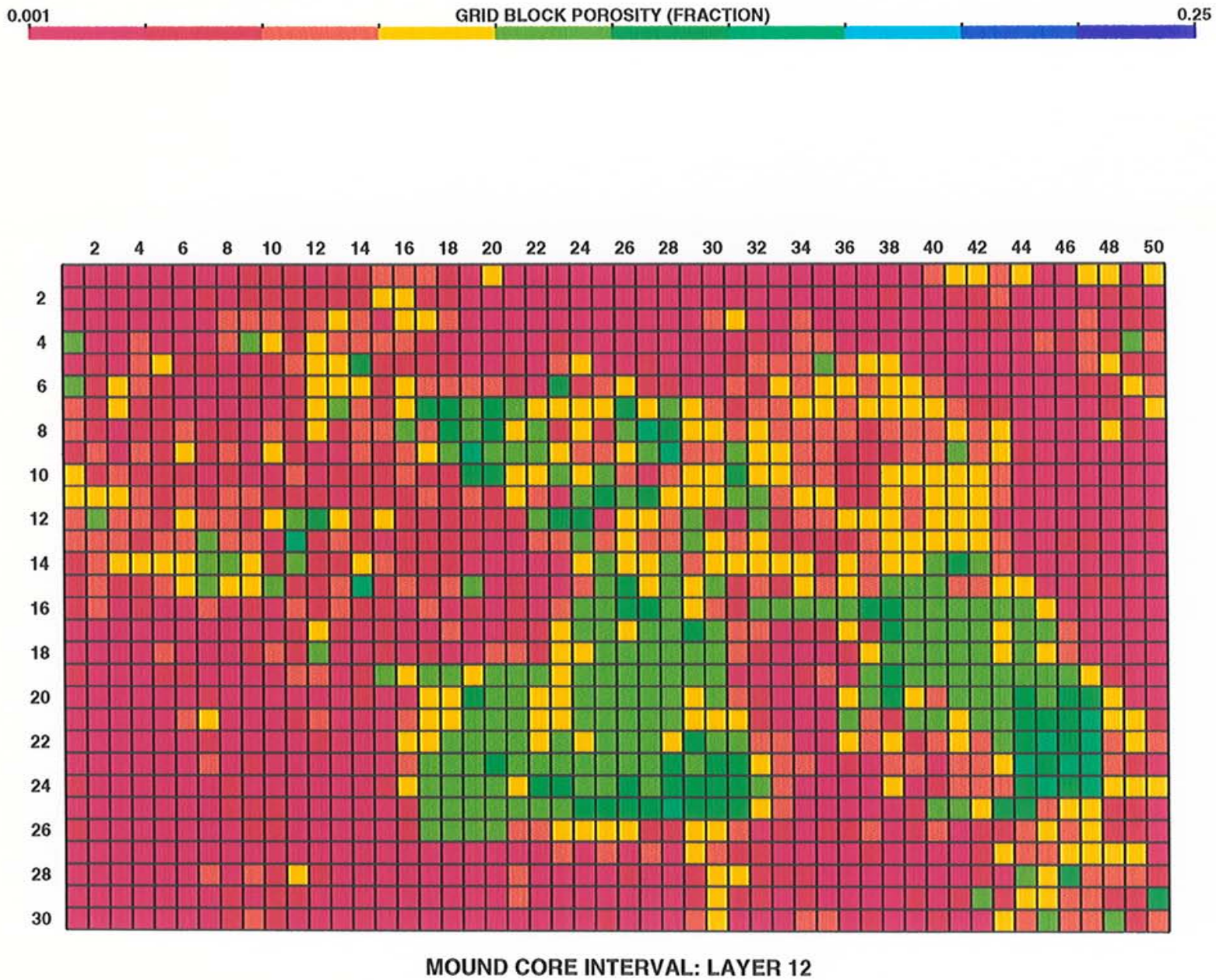

Figure 7-7. Porosity Areal Grid, Layer 12
Upscaled Simulation 15-Layer Model

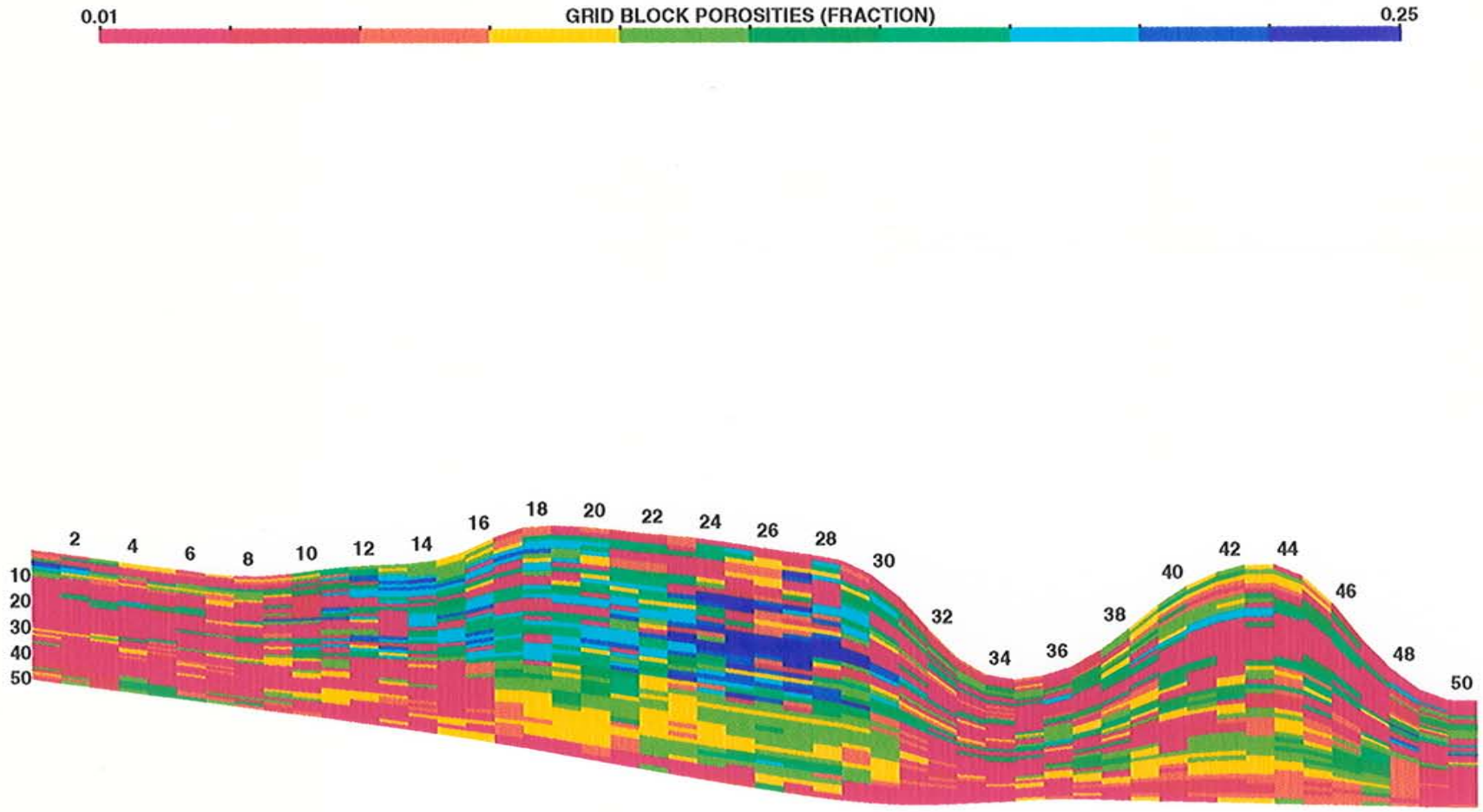

Figure 7-8. Porosity Cross-Section (Y=20)
50 Layer Geostatistical Model

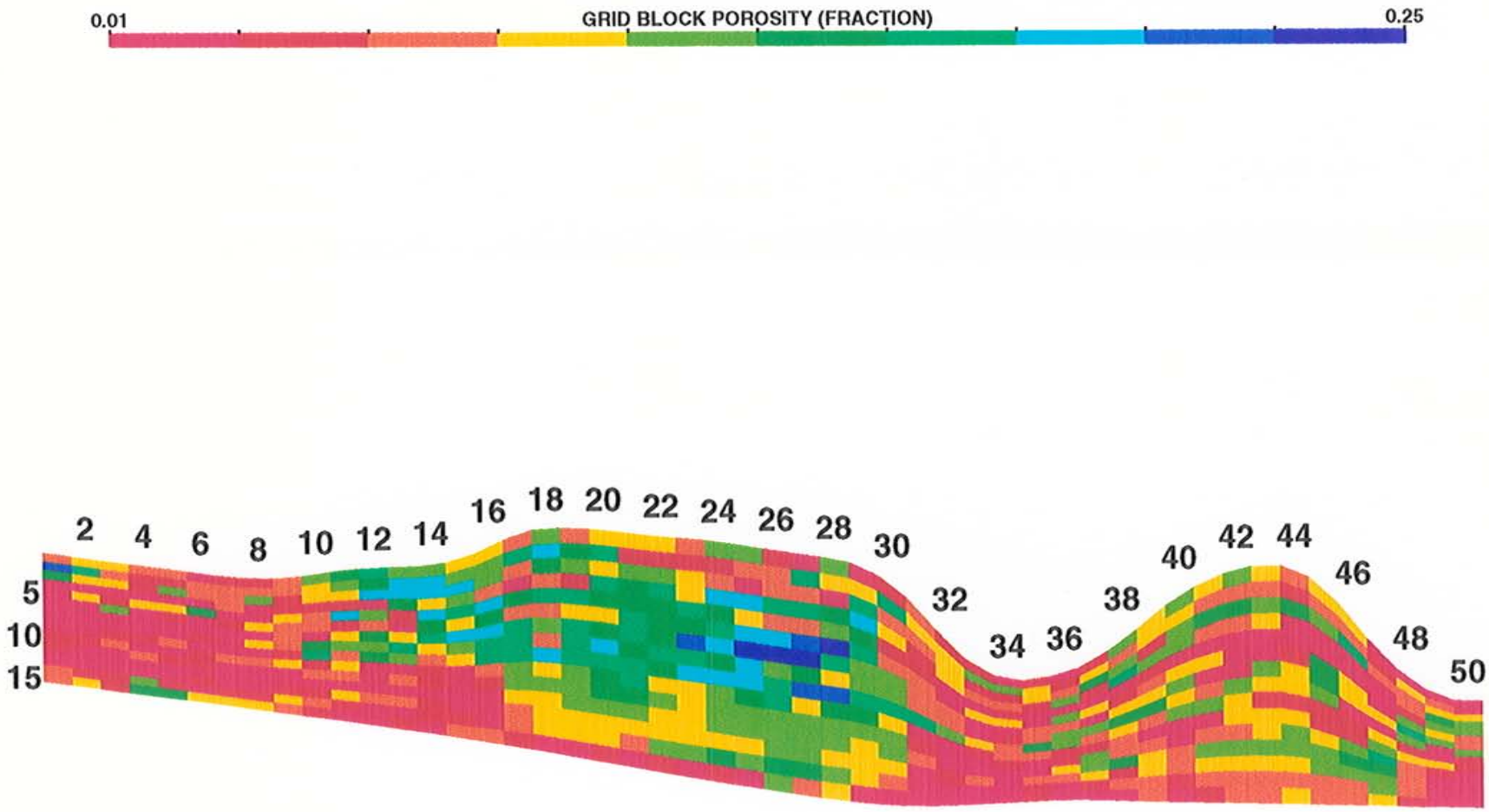

Vertical Exaggeration: 7.5X

Figure 7-9. Porosity Cross-Section (Y=20)
Upscaled Simulation 15-Layer Model

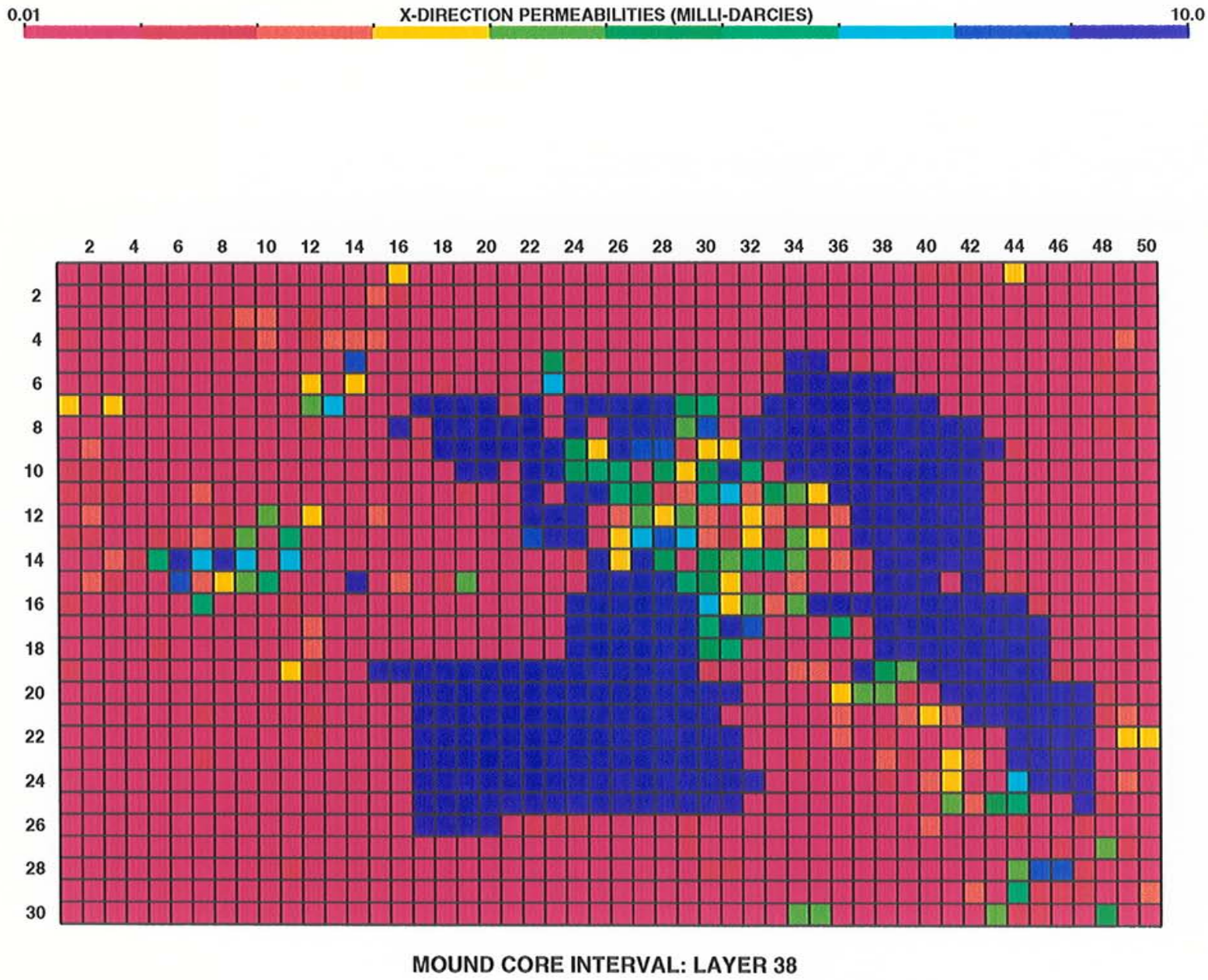

Figure 7-10. Horizontal Permeability Areal Grid, Layer 38
50 Layer Geostatistical Model

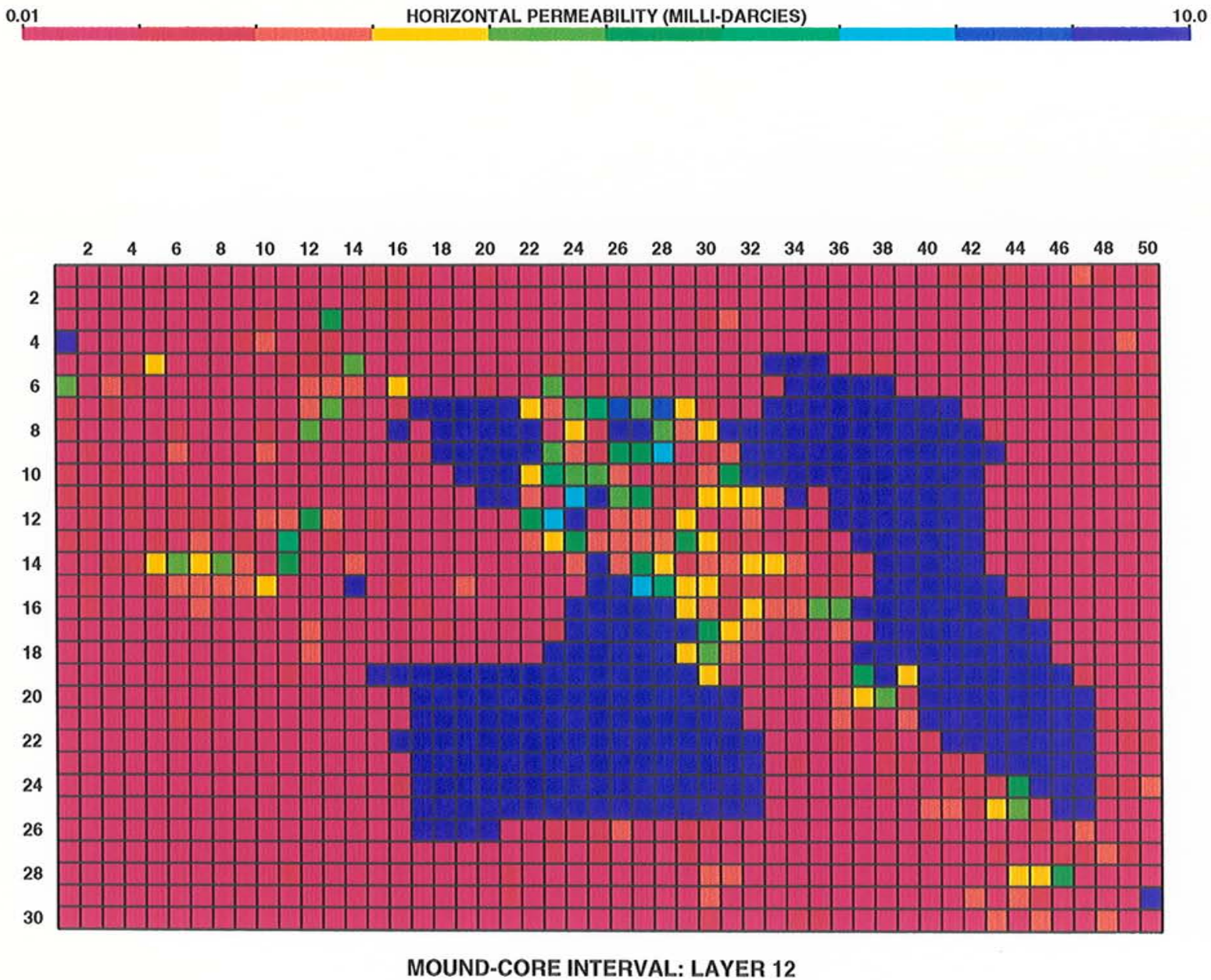

Figure 7-11. Horizontal Permeability Areal Grid, Layer 12
Upscaled Simulation 15-Layer Model

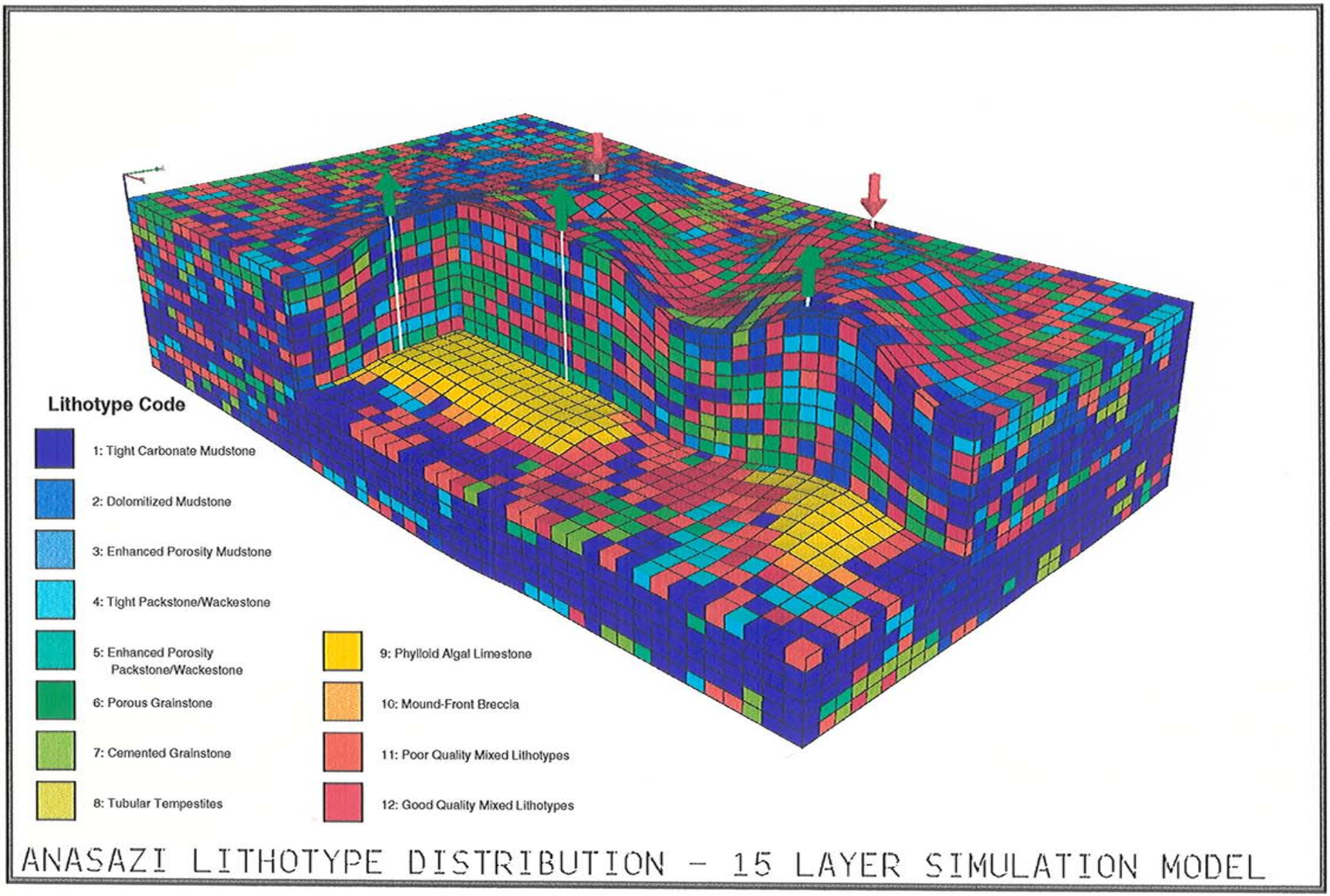

Figure 7-12. 3-D Lithotypes - 15 Layer VIP Model

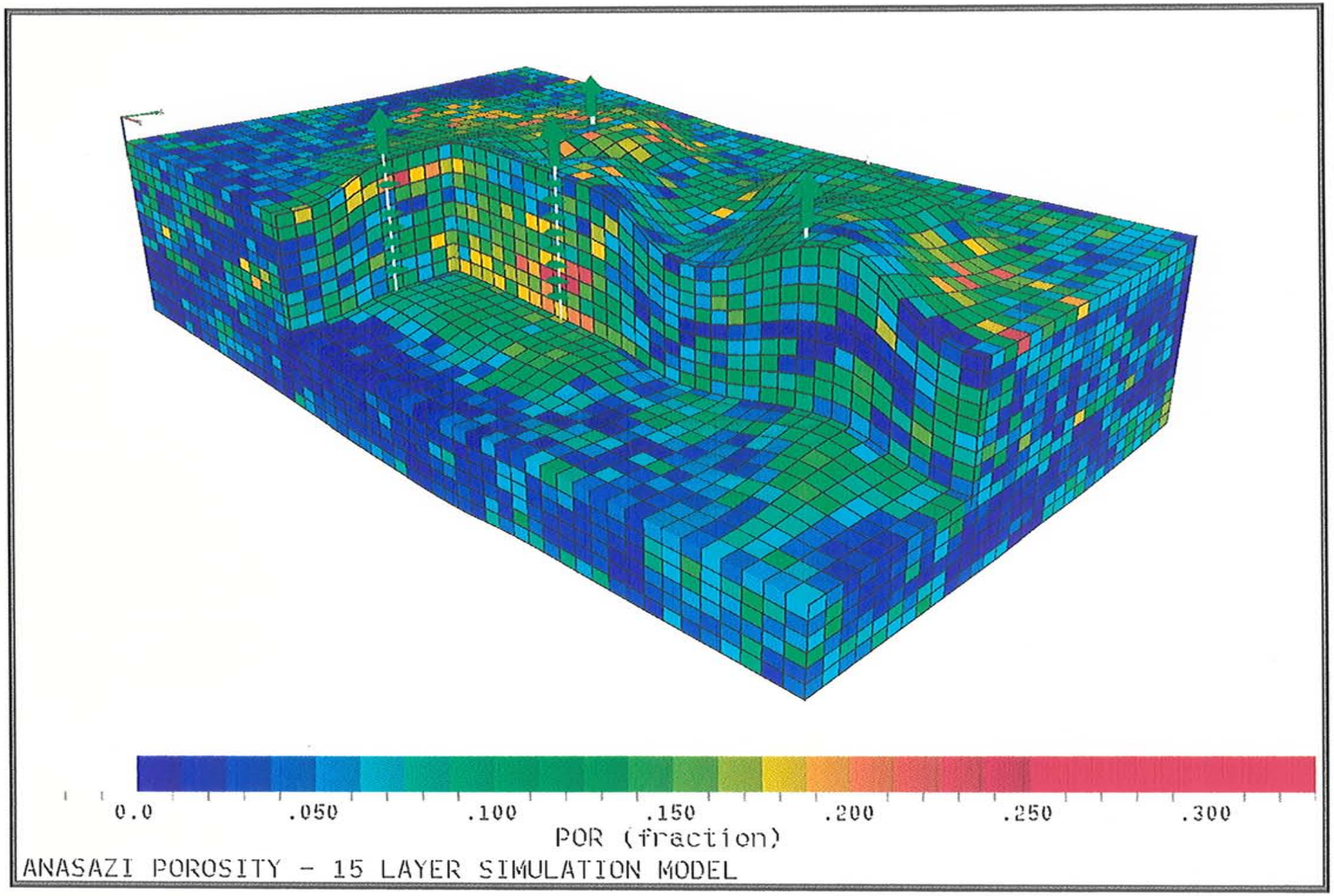

Figure 7-13. 3-D Porosity - 15 Layer VIP Model

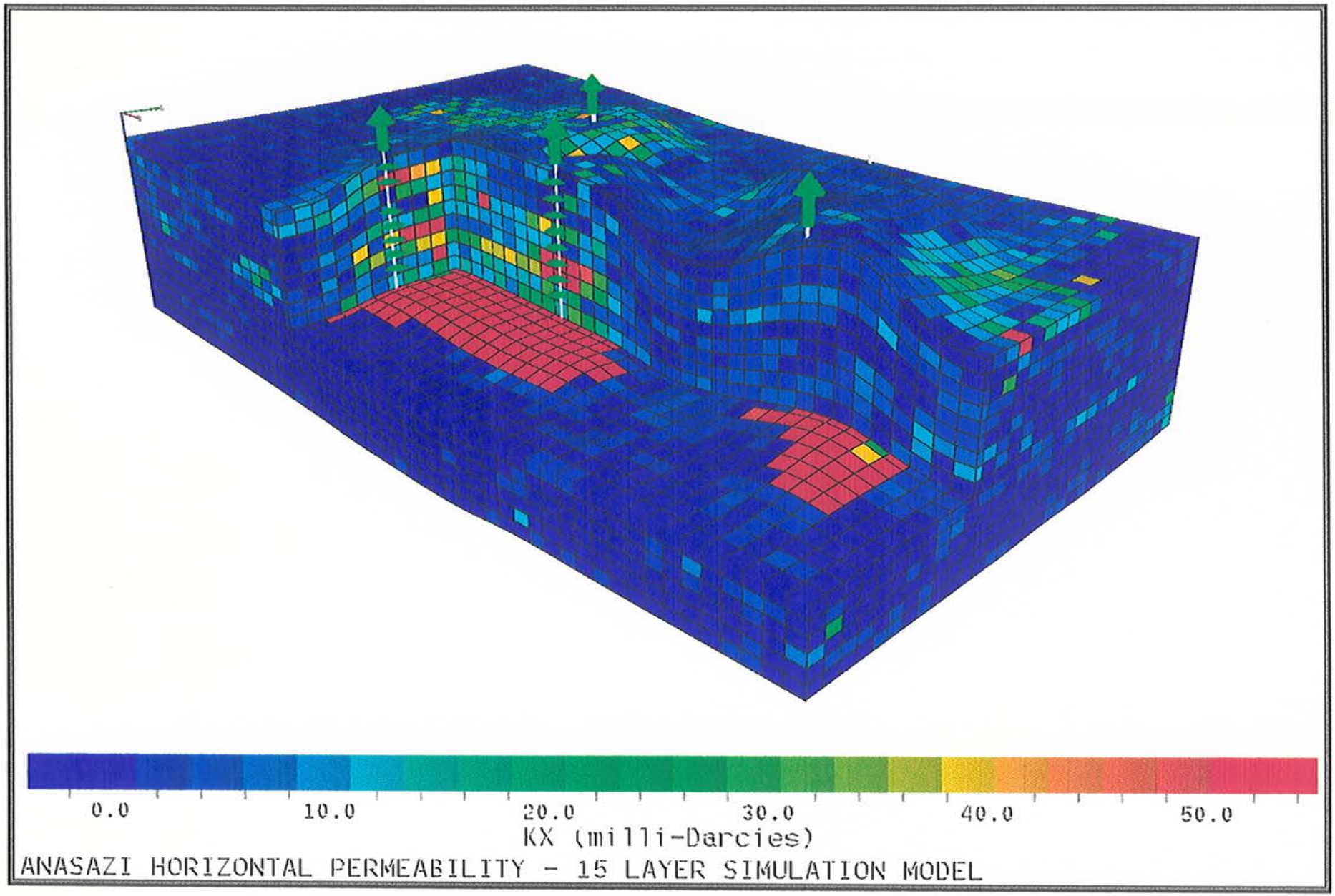

Figure 7-14. 3-D Horizontal Permeability - 15 Layer VIP Model

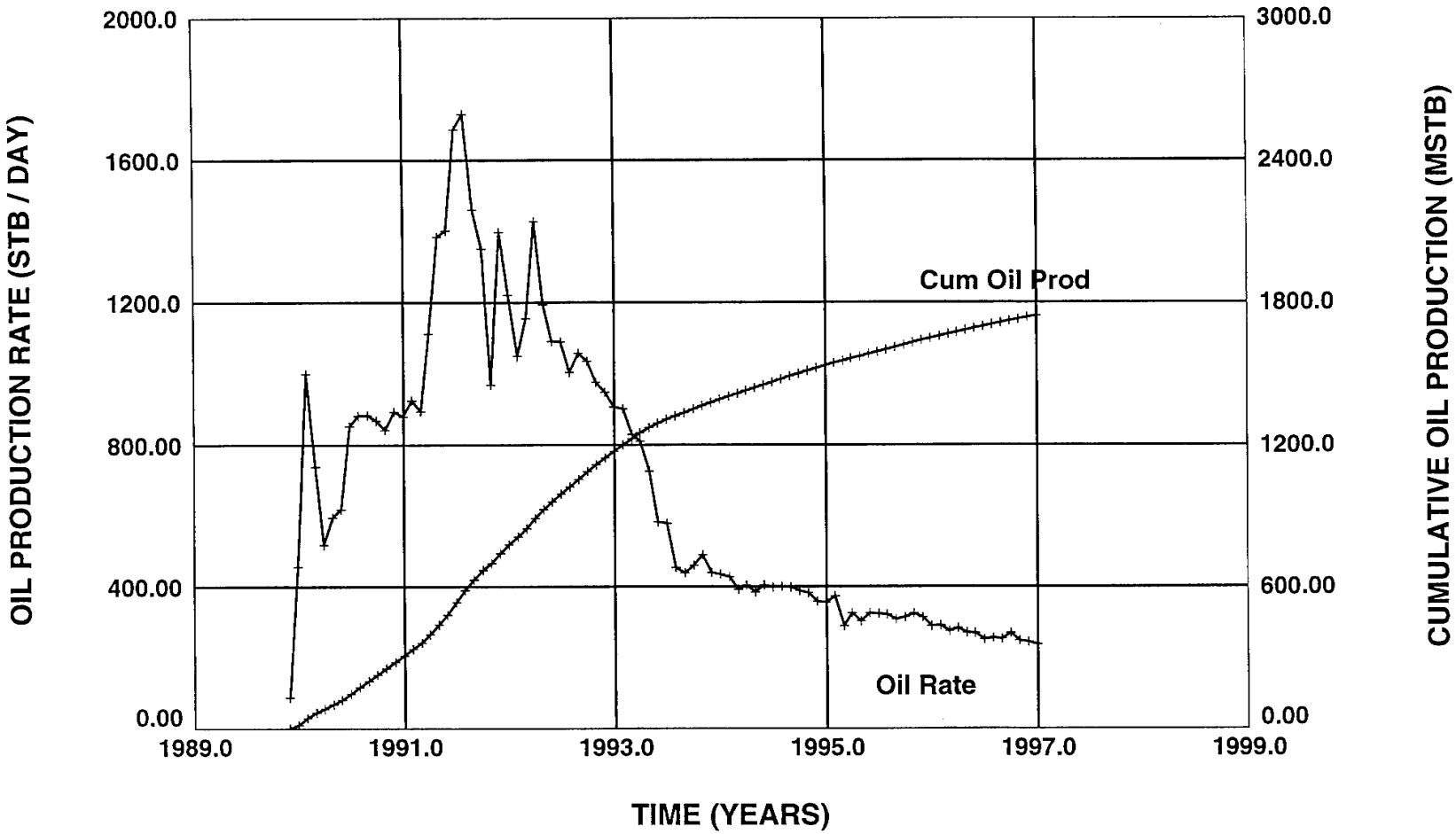

Figure 8-1 Oil Production History Anasazi-Sahgzie Field

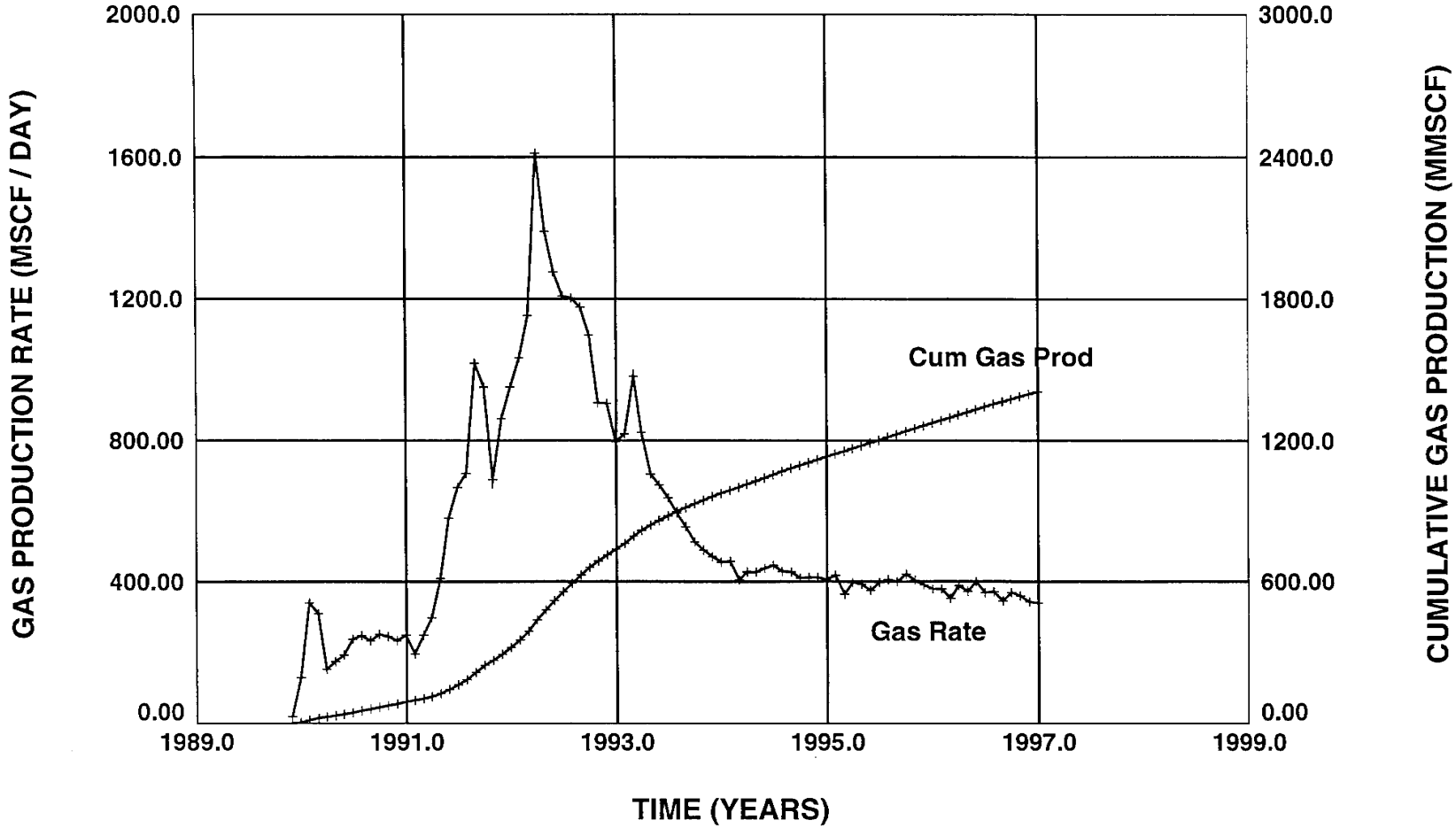

Figure 8-2 Gas Production History Anasazi-Sahgzie Field

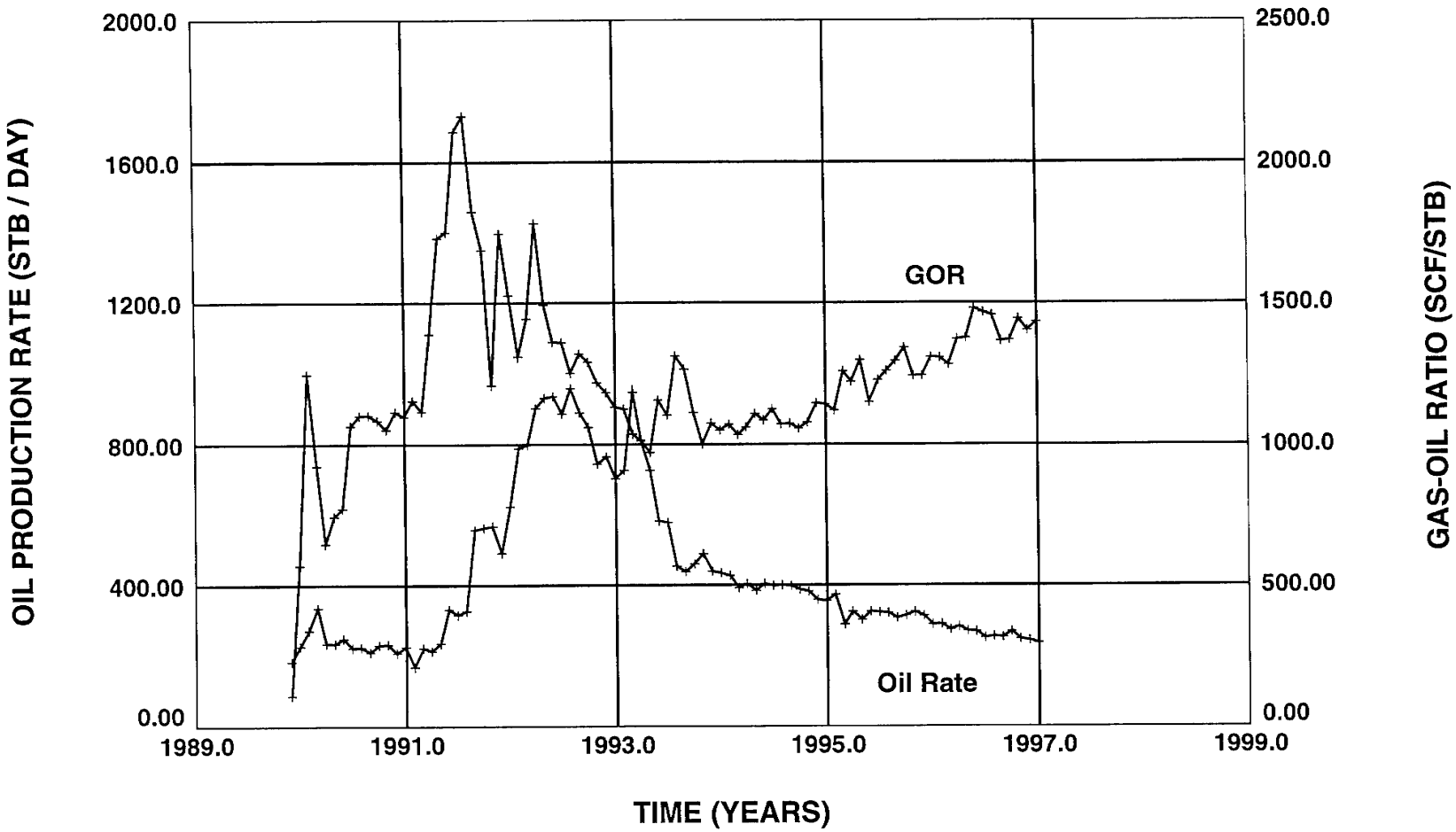

Figure 8-3 Oil Production and GOR History Anasazi-Sahgzie Field

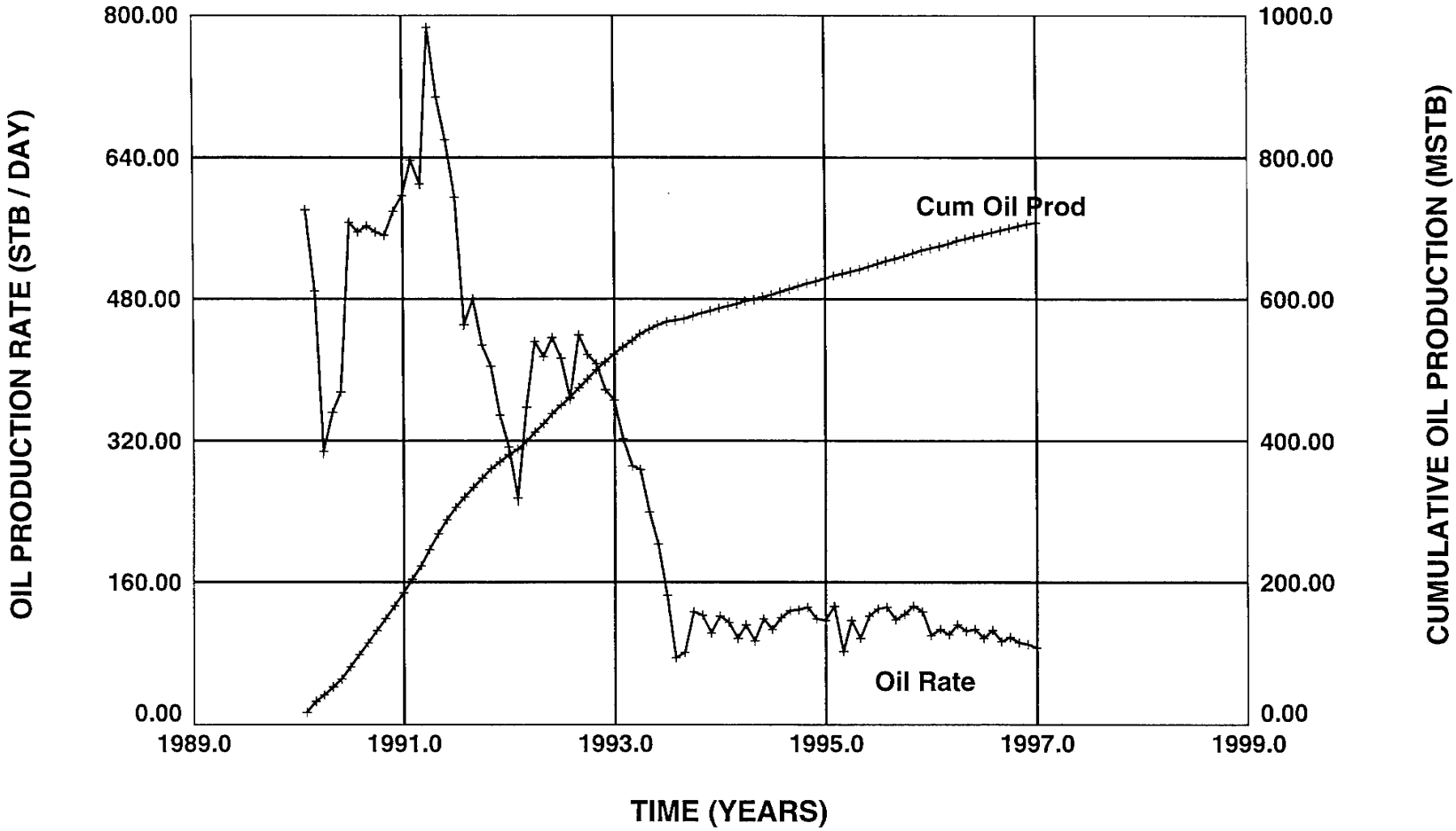

Figure 8-4 Oil Production History Anasazi Well 1

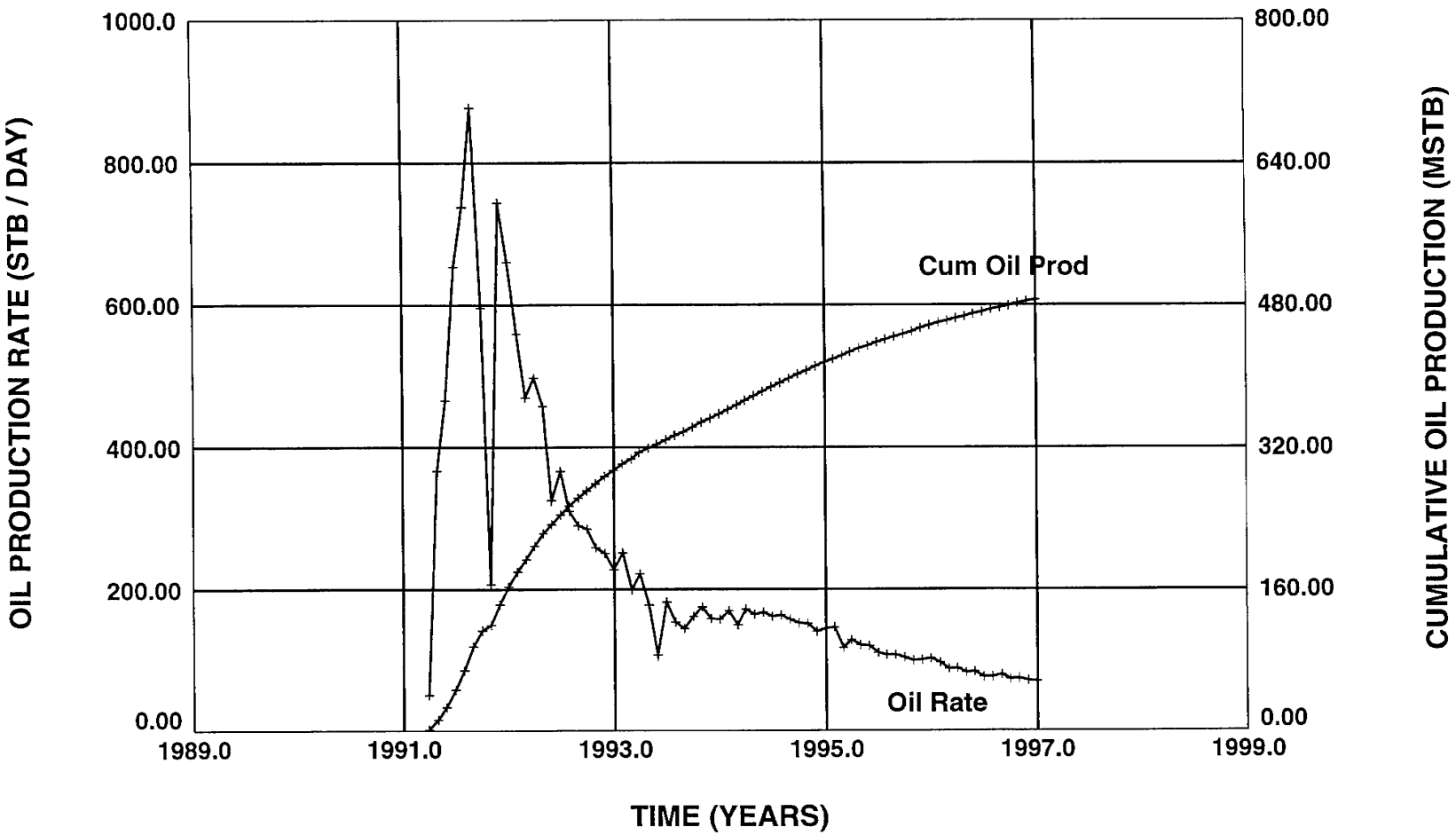

Figure 8-5 Oil Production History Anasazi Well 5L-3

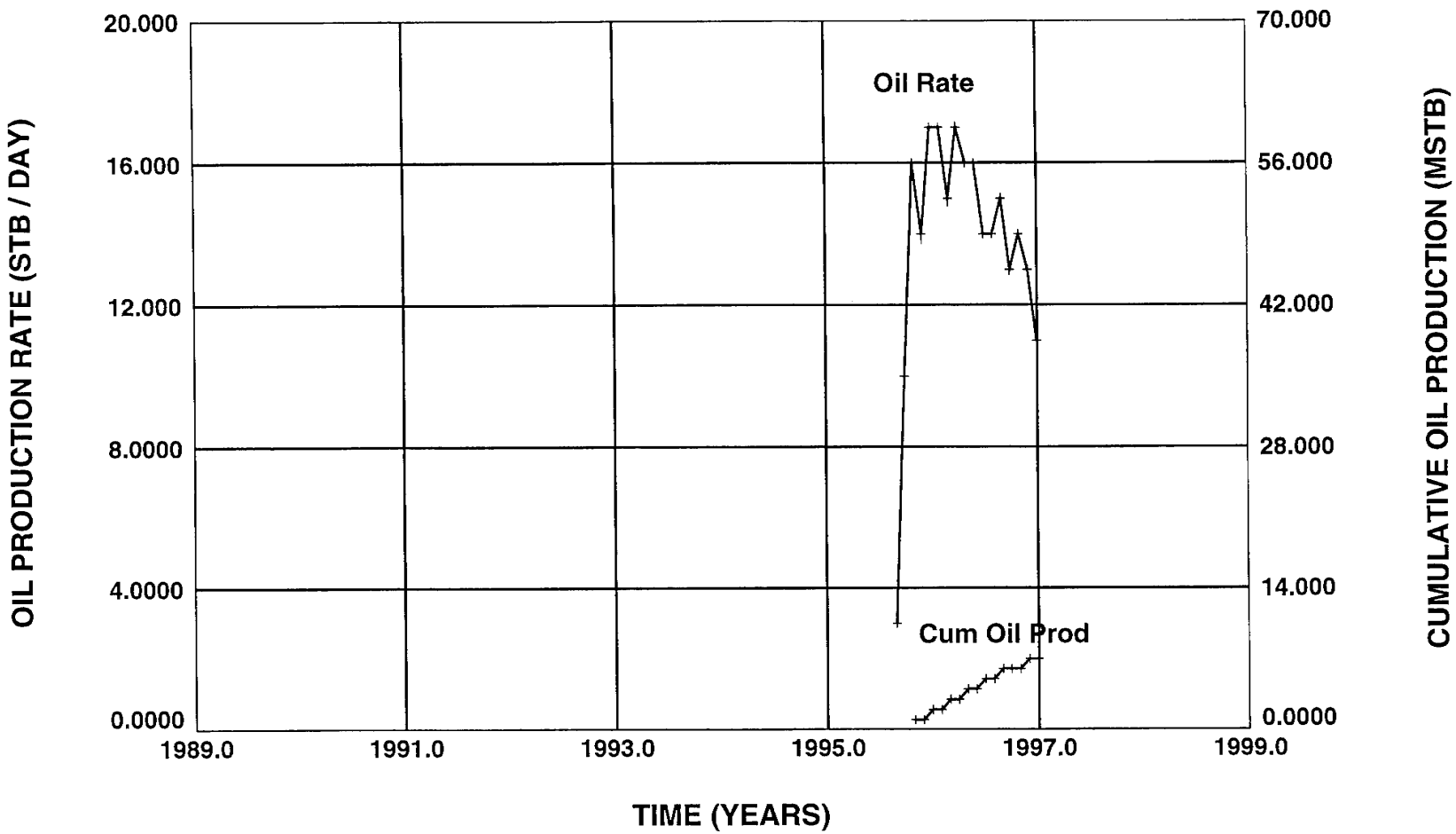

Figure 8-6 Oil Production History Anasazi Well 6H-1

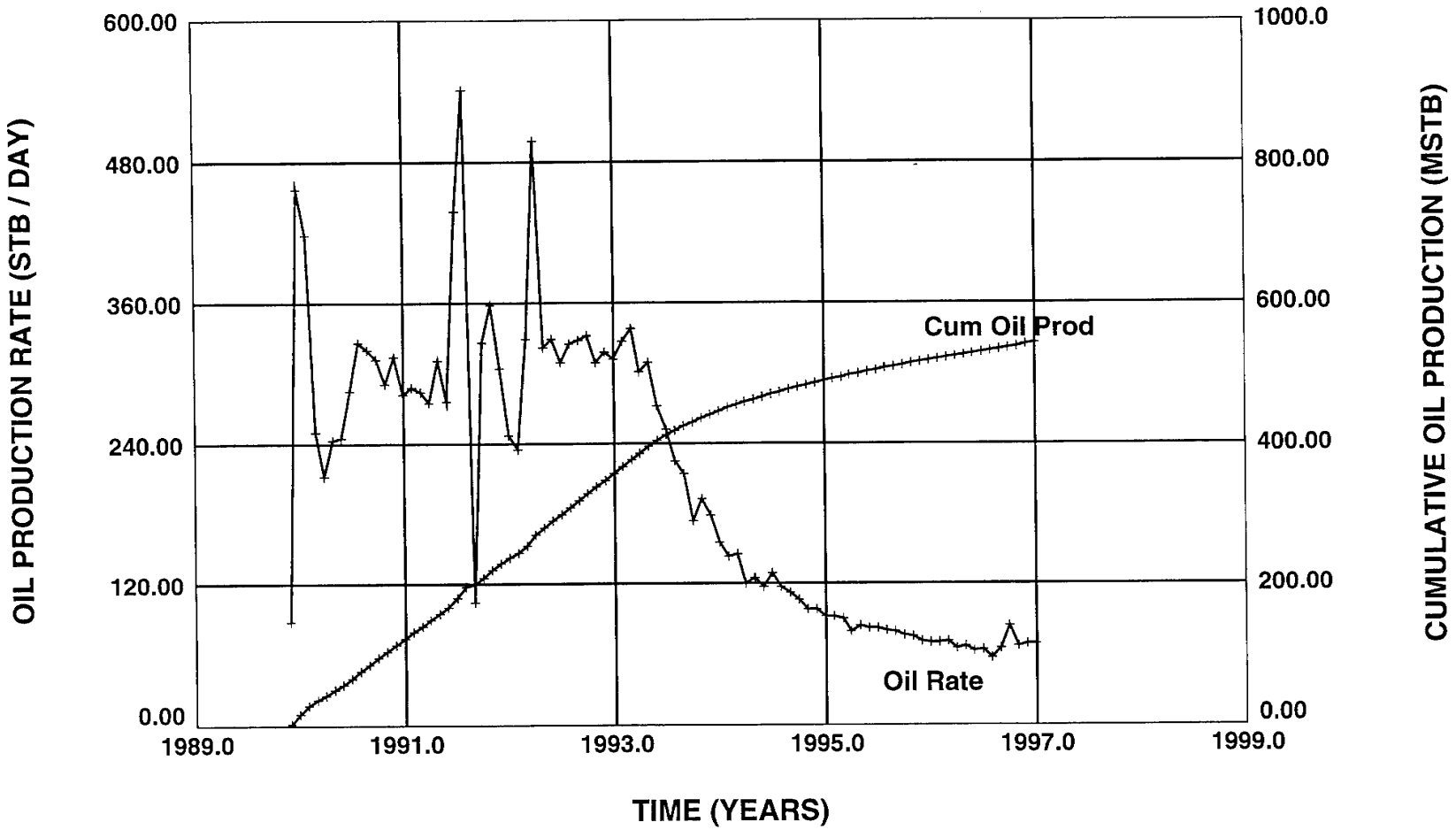

Figure 8-7 Oil Production History Sahgzie Well 1

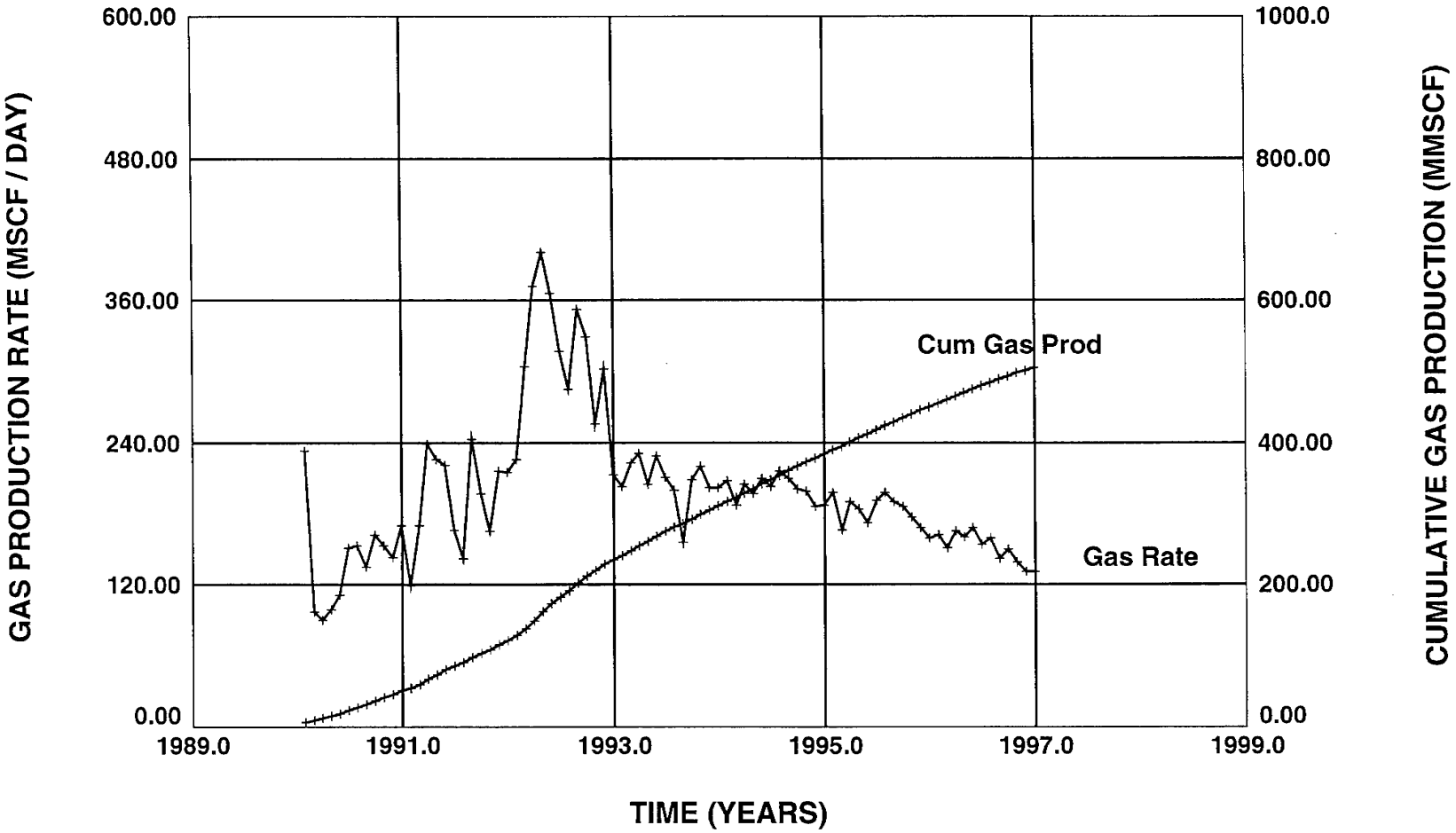

Figure 8-8 Gas Production History Anasazi Well 1

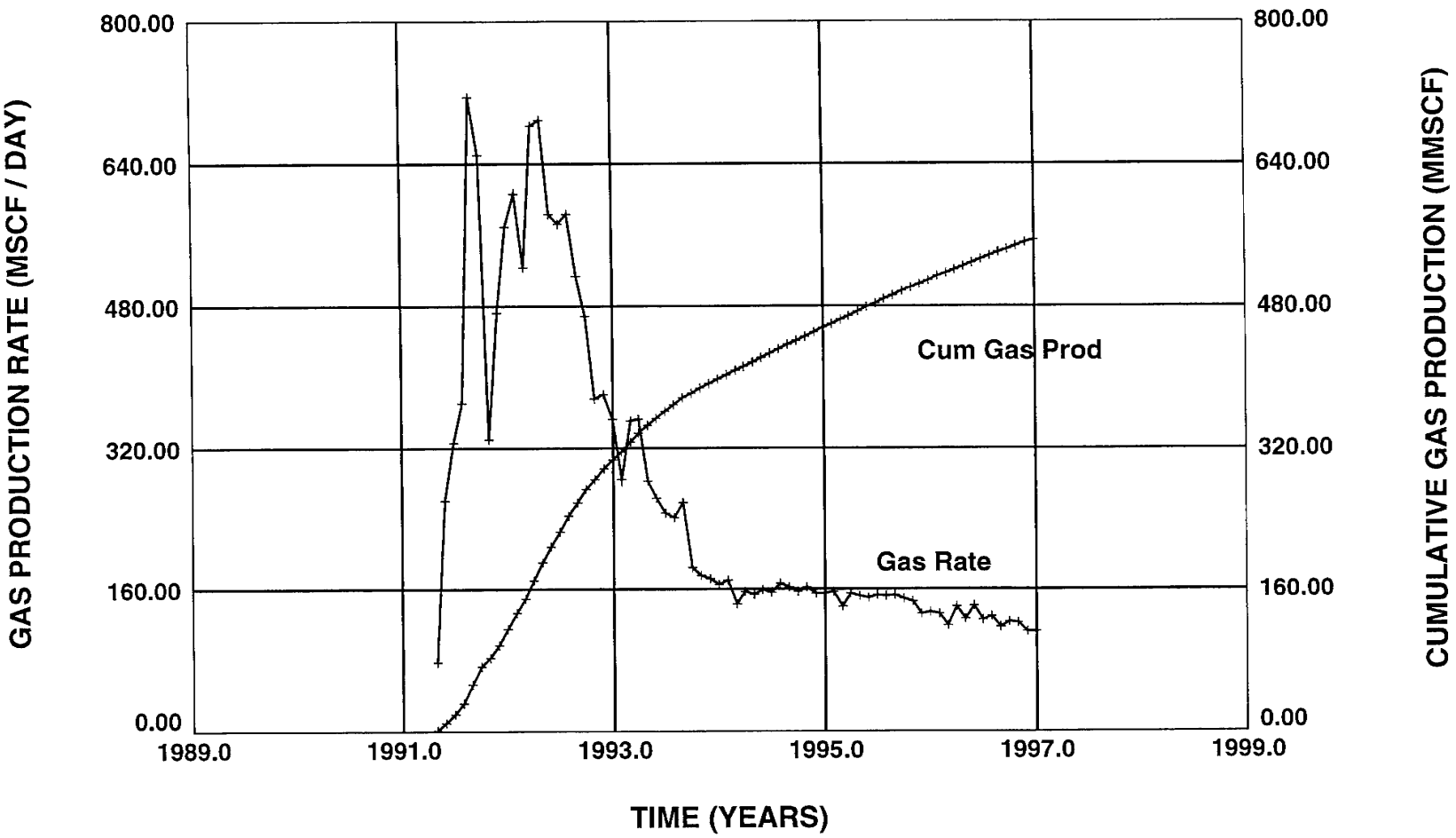

Figure 8-9 Gas production History Anasazi Well 5L-3

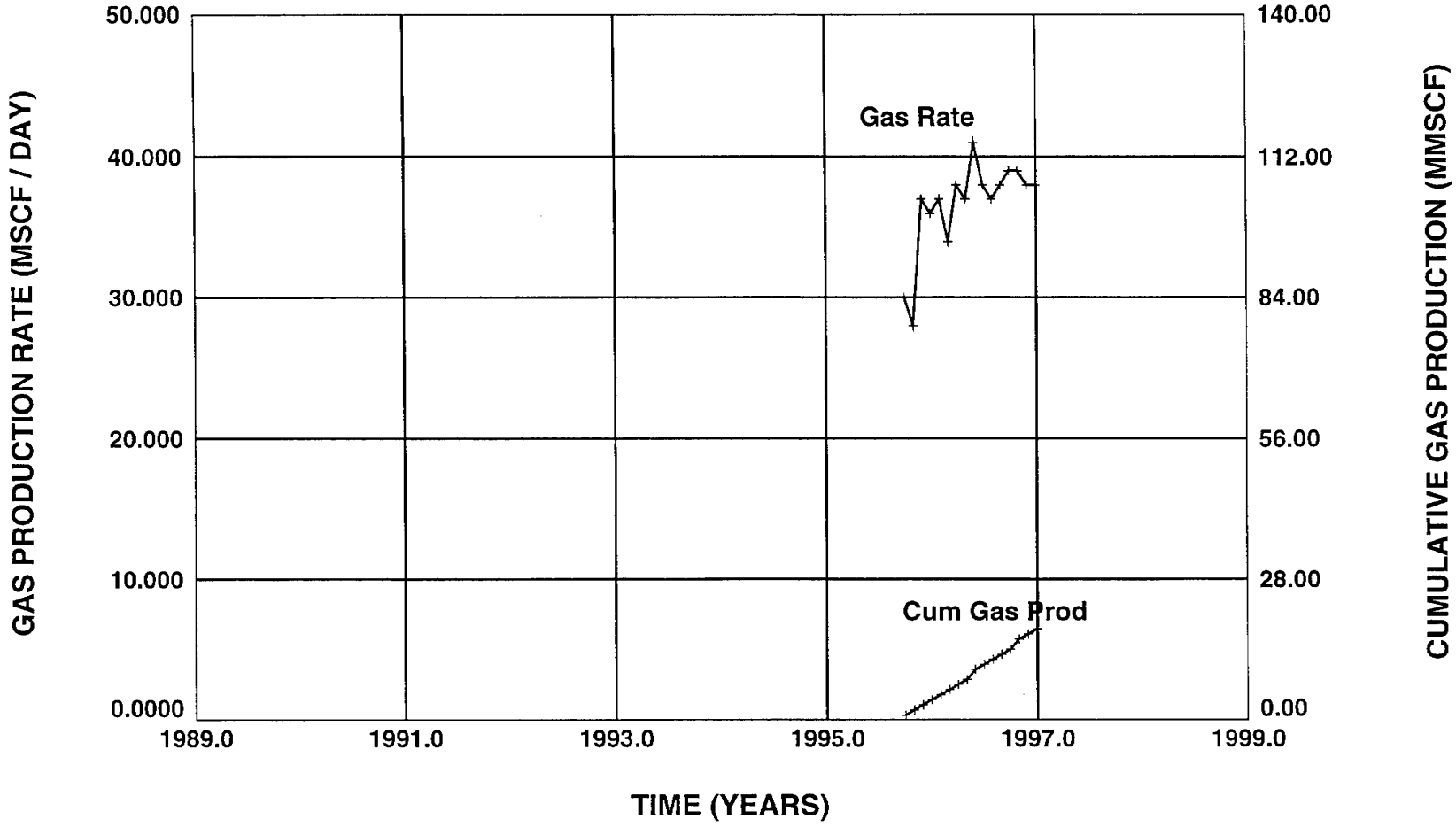

Figure 8-10 Gas Production History Anasazi Well 6H-1

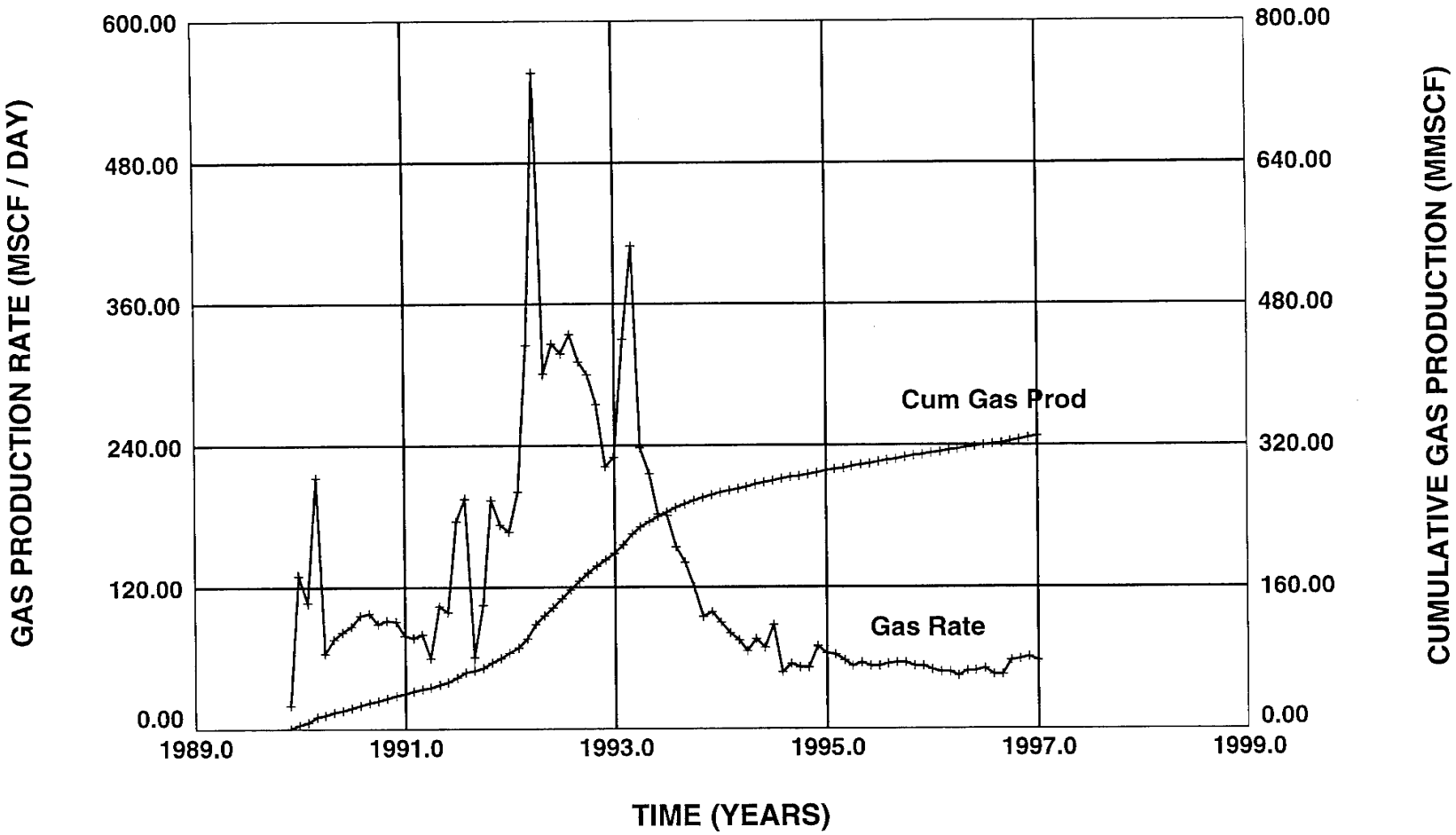

Figure 8-11 Gas Production History Sahgzie Well 1

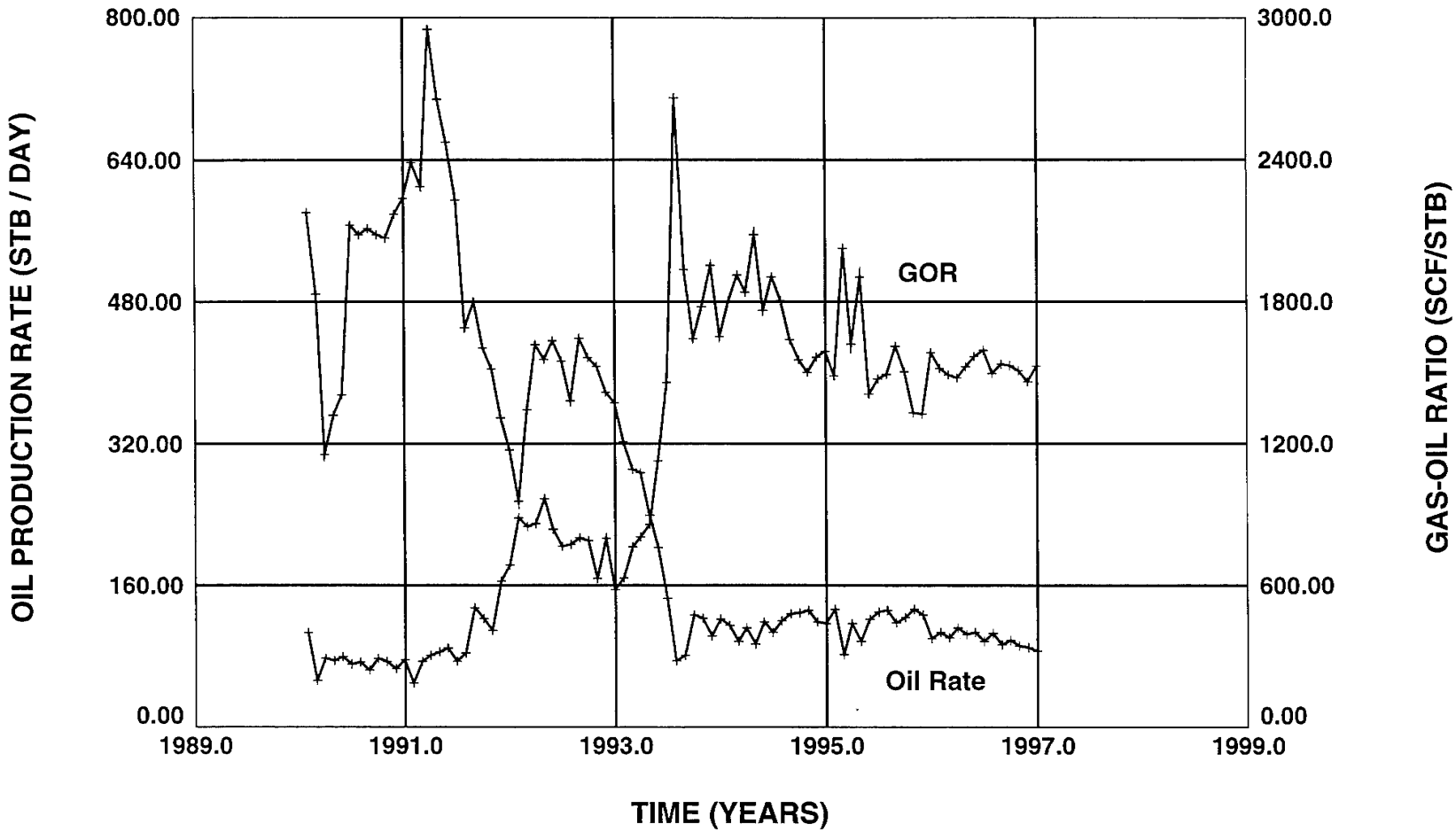

Figure 8-12 Oil Production and GOR History Anasazi Well 1

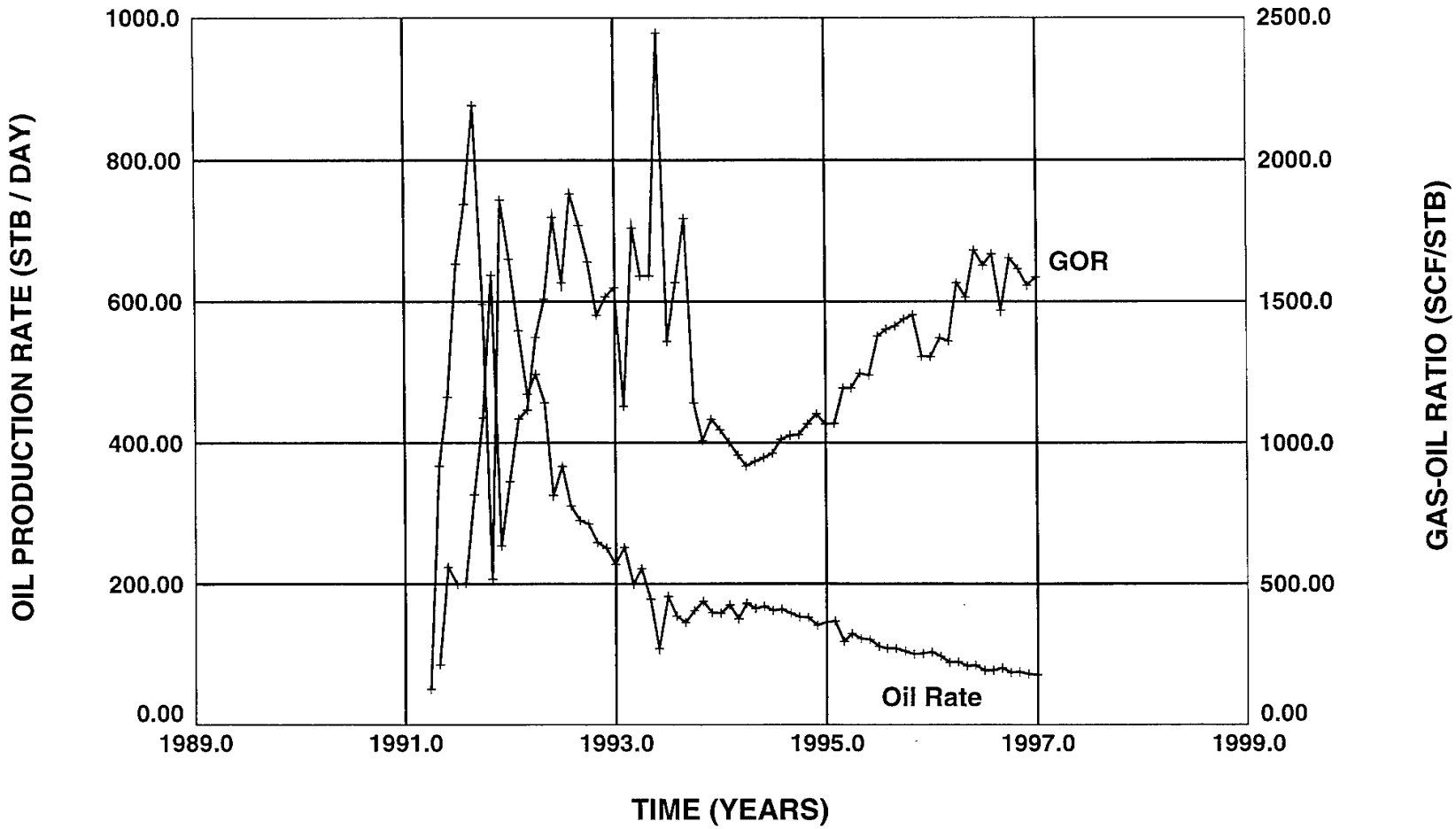

Figure 8-13 Oil Production and GOR History Anasazi Well 5L-3

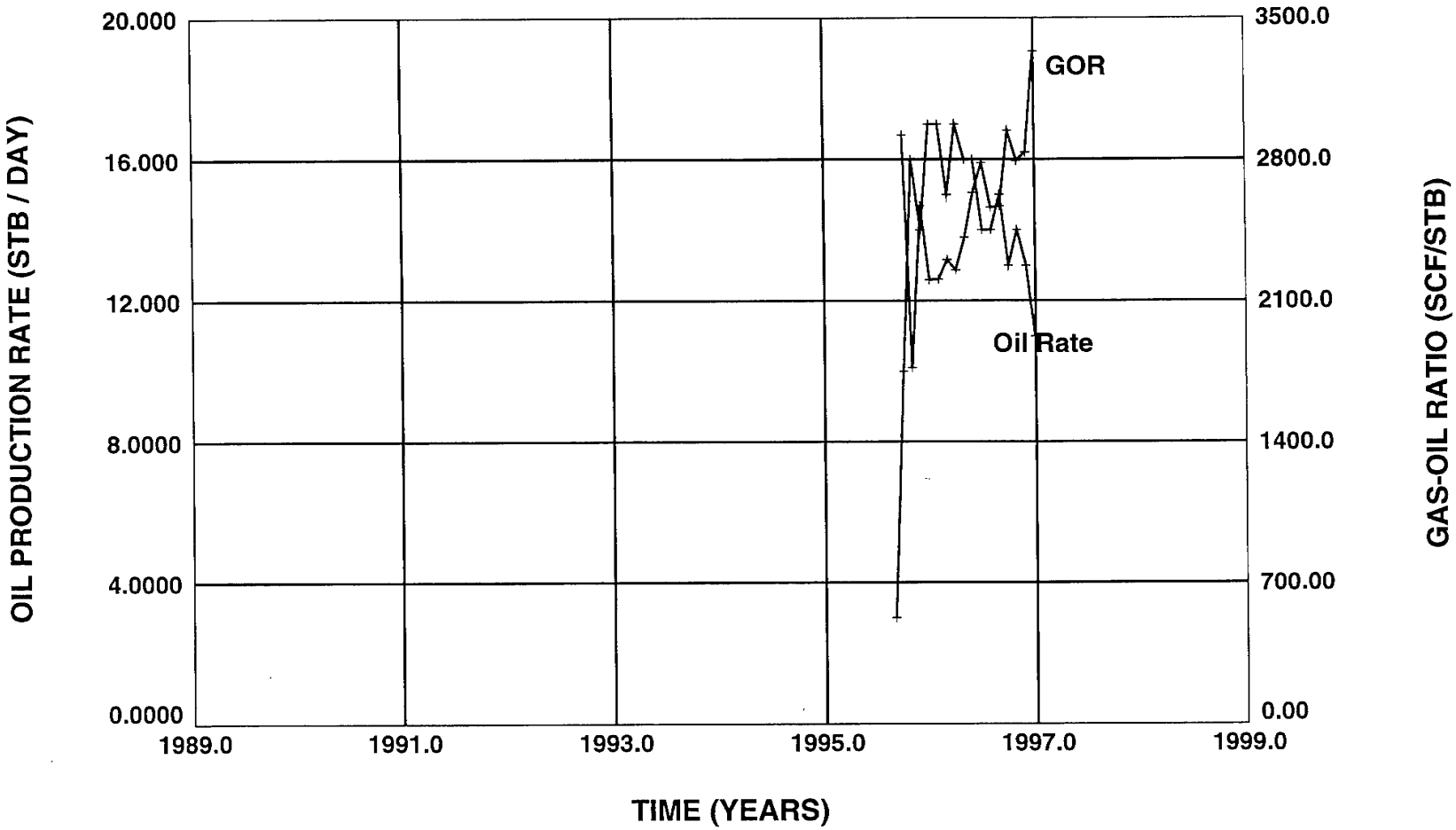

Figure 8-14 Oil Production and GOR History Anasazi Well 6H-1

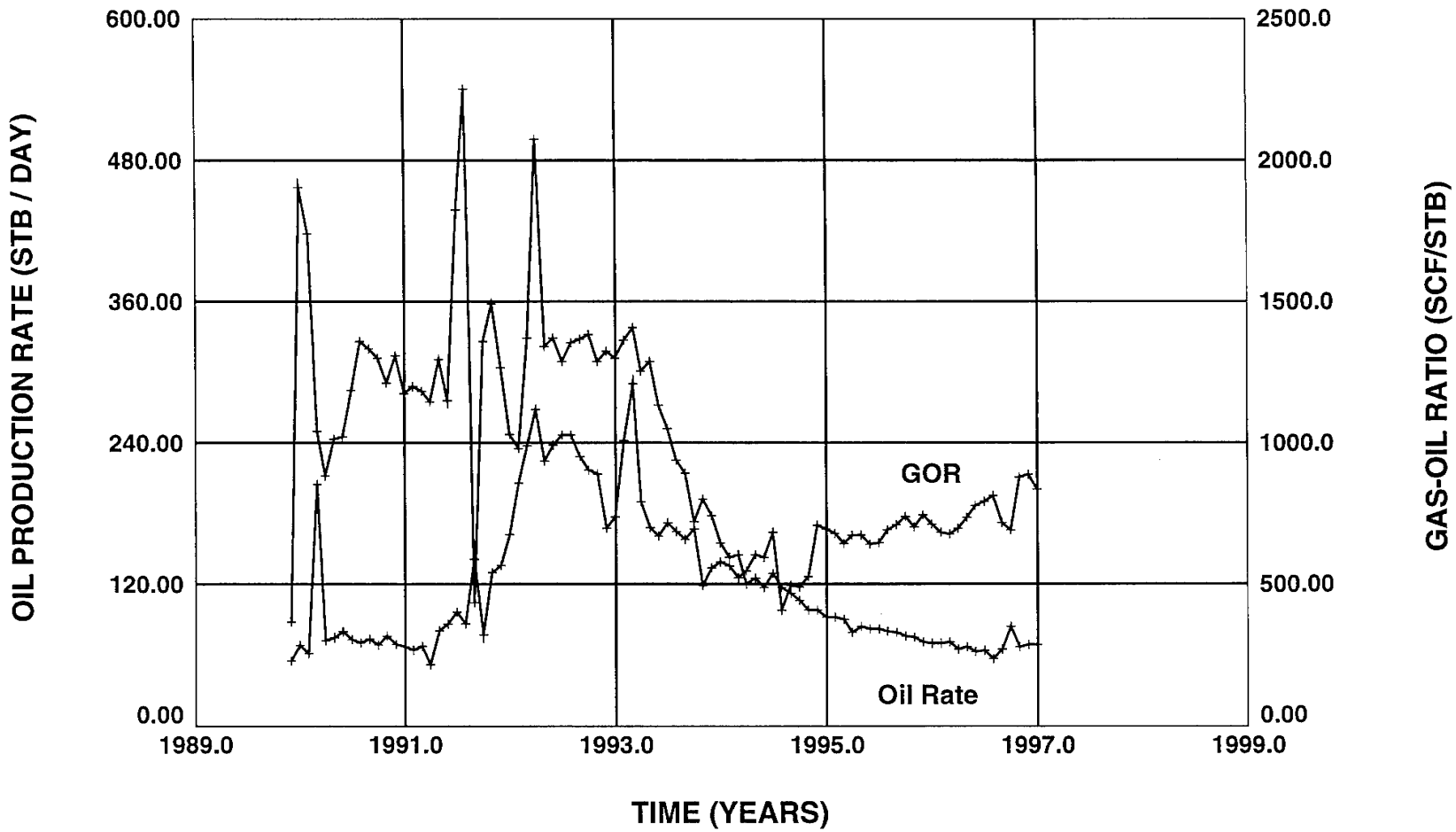

Figure 8-15 Oil Production and GOR History Sahgzie Well 1

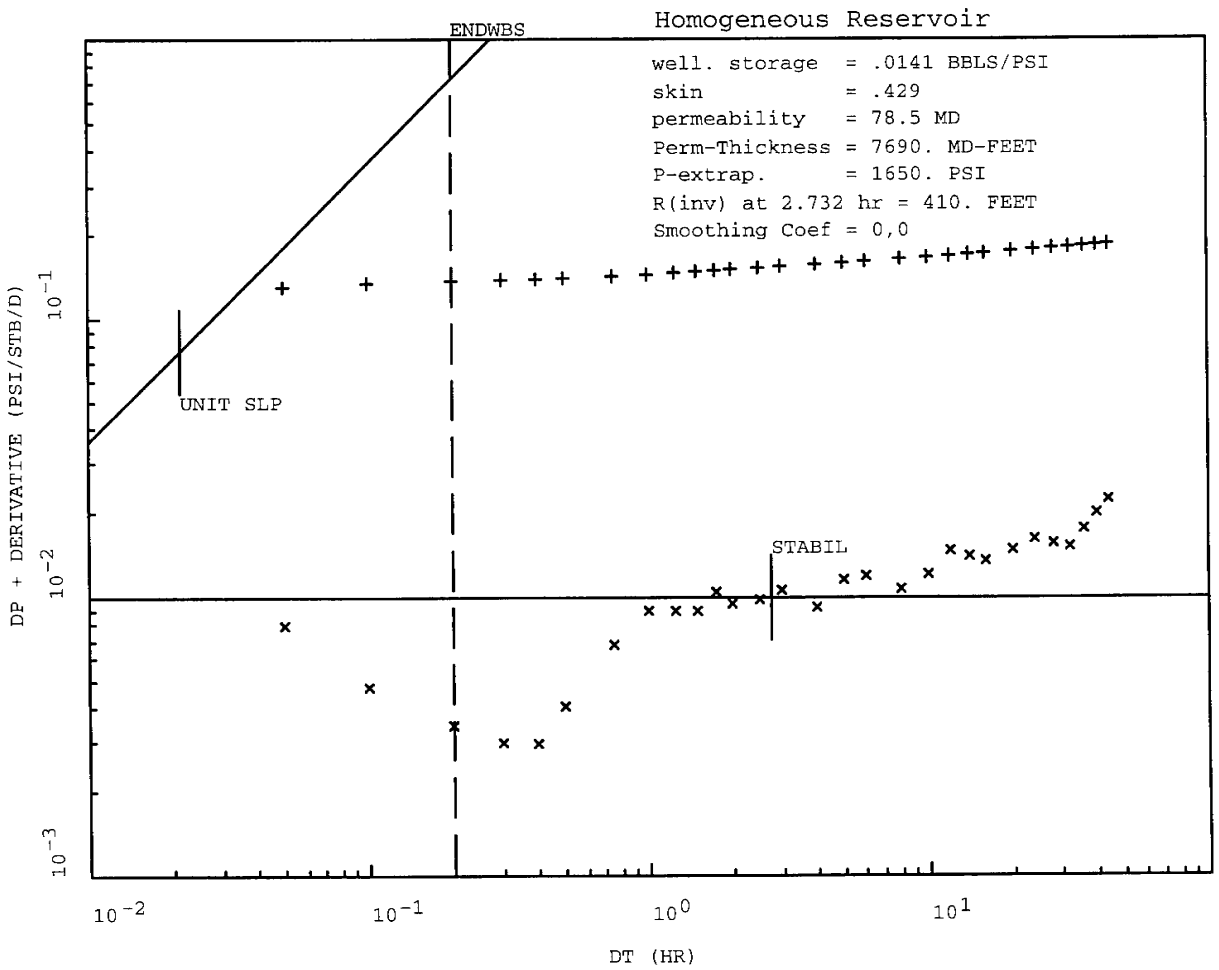

Figure 9–1 Anasazi Well No. 1 0190 Test – Derivative Diagnostics

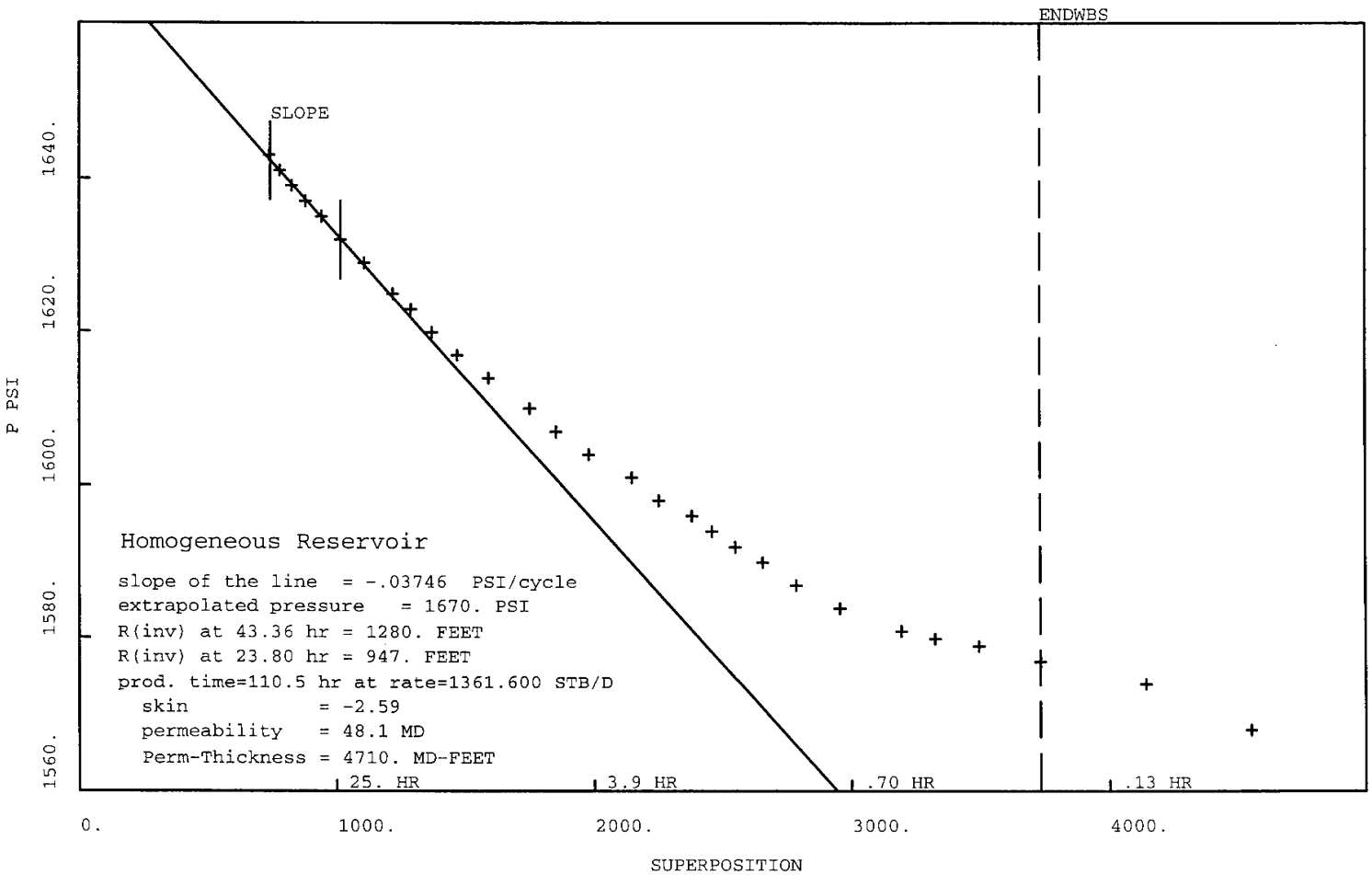

Figure 9–2 Anasazi Well No. 1 0190 Test – Superposition Diagnostics

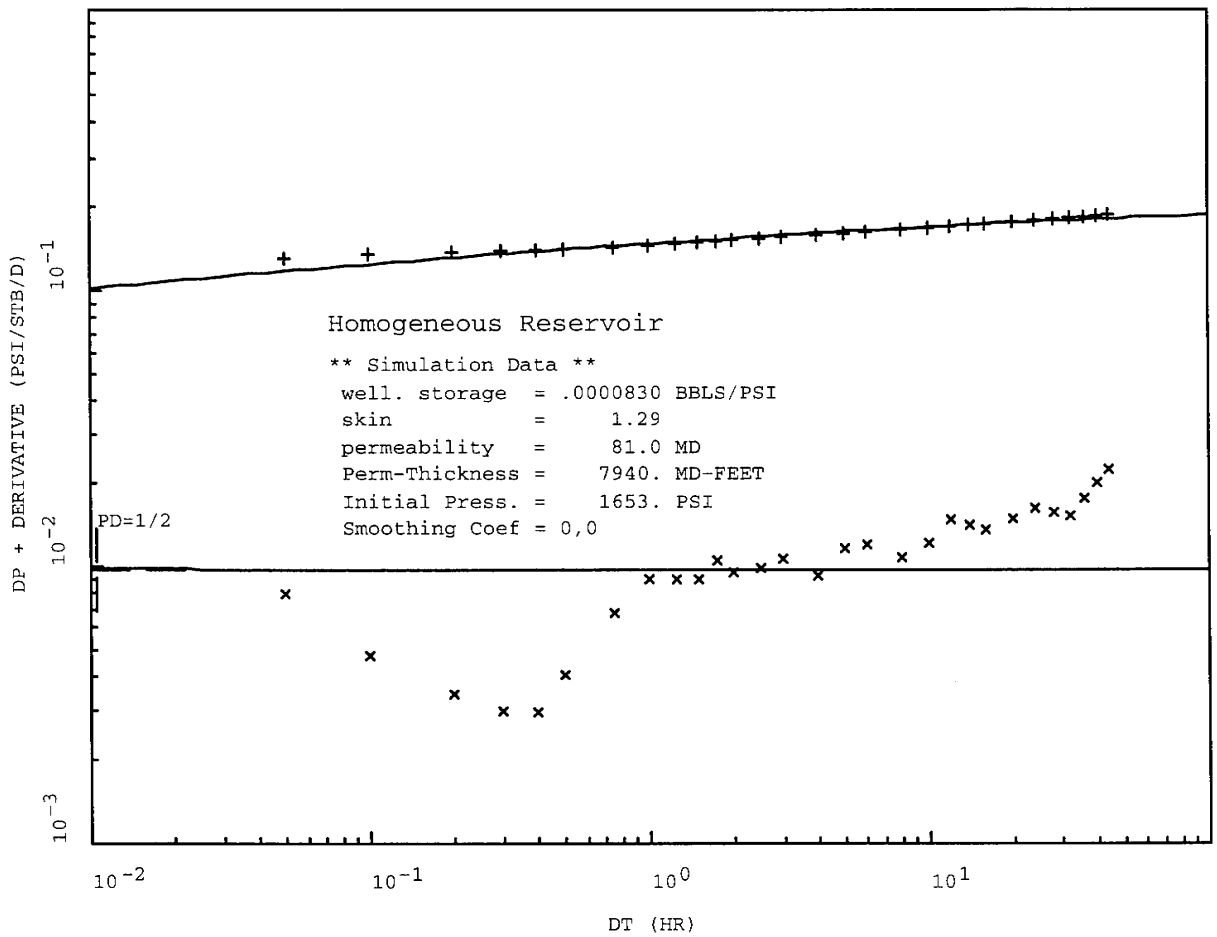

Figure 9–3 Anasazi Well No. 1 0190 Test – Derivative and Pressure Difference Match

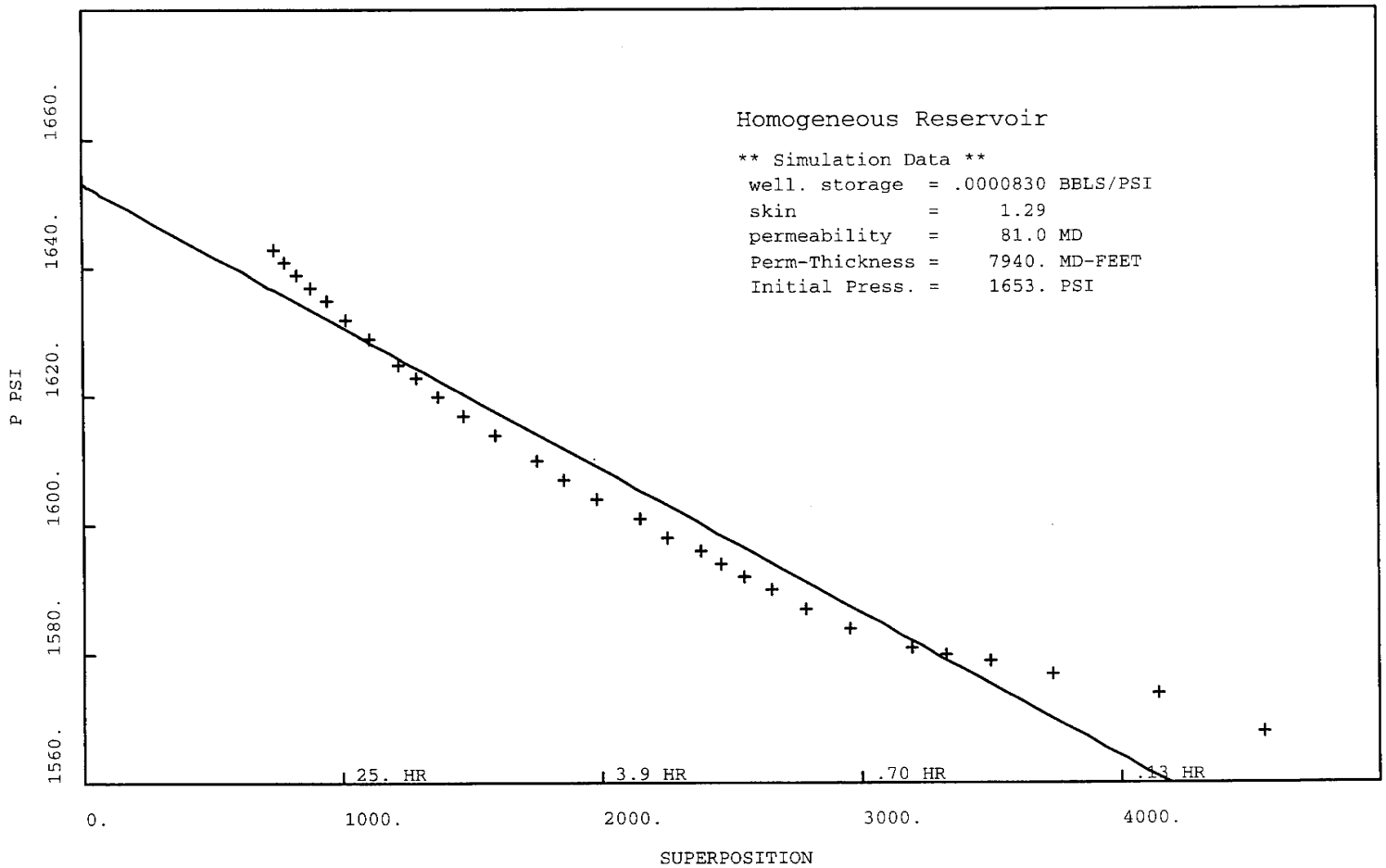

Figure 9–4 Anasazi Well No. 1 0190 Test – Superposition Match – Pressure

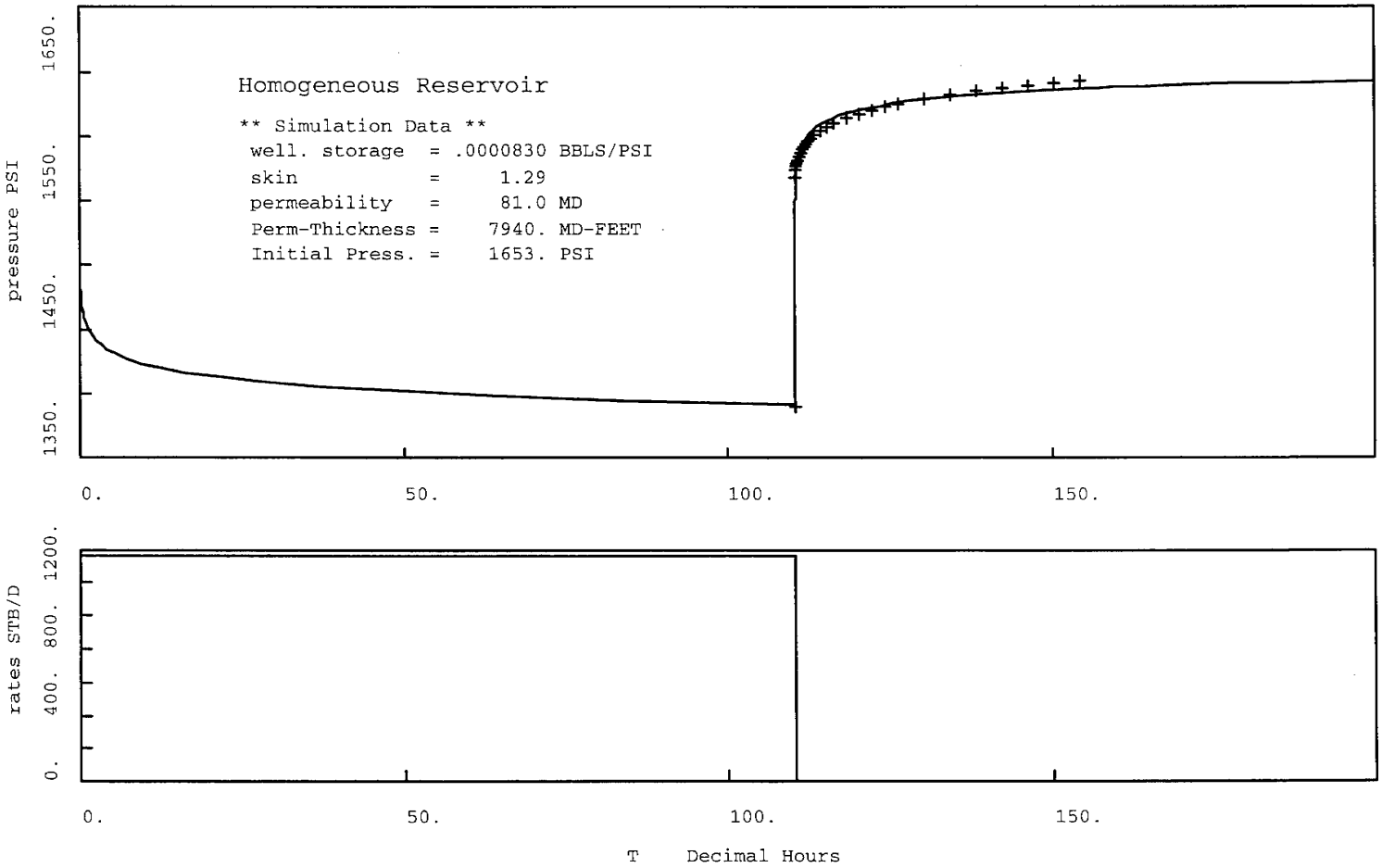

Figure 9–5 Anasazi Well No. 1 0190 Test – Pressure Data Match

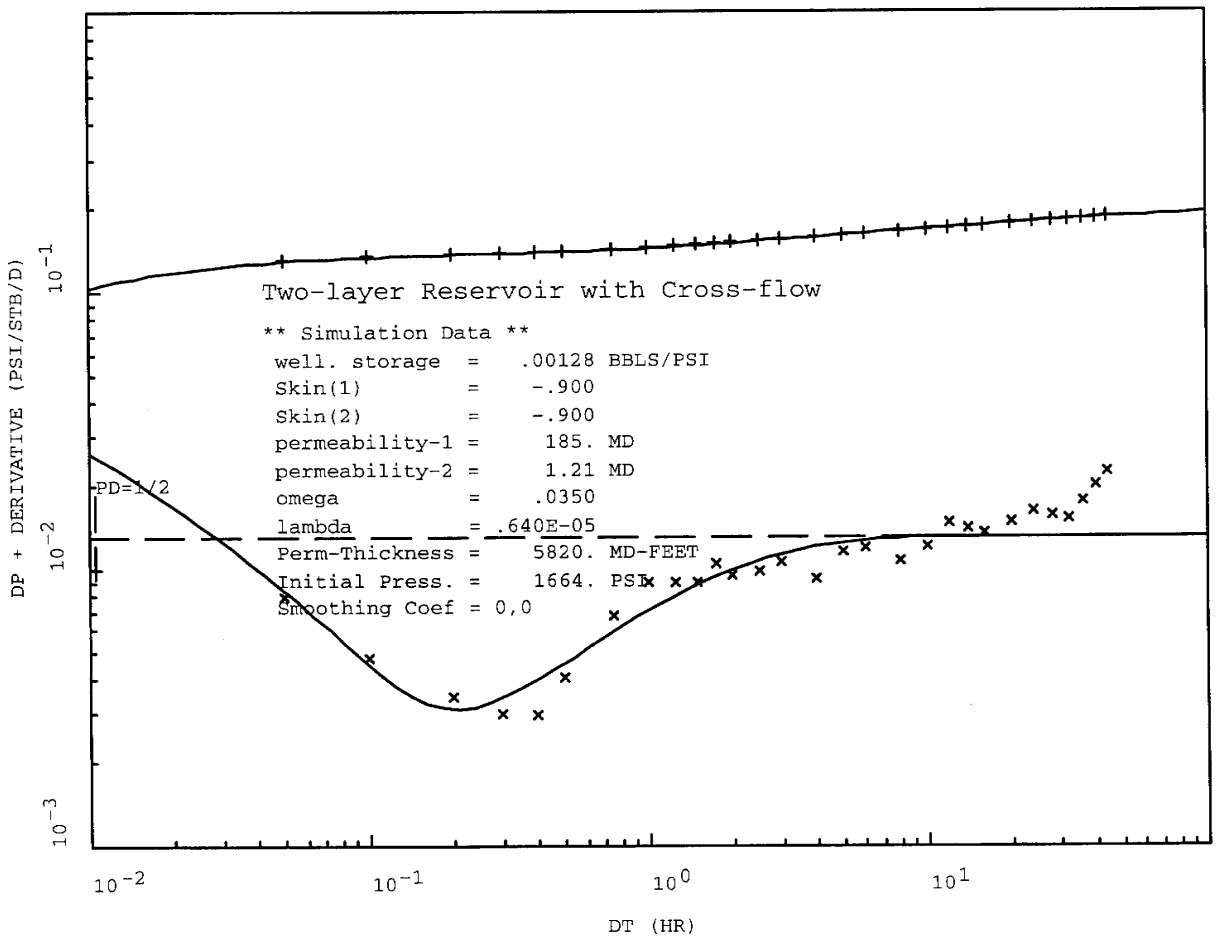

Figure 9–6 Anasazi Well No. 1 0190 Test – Derivative and Pressure Diffeence Match

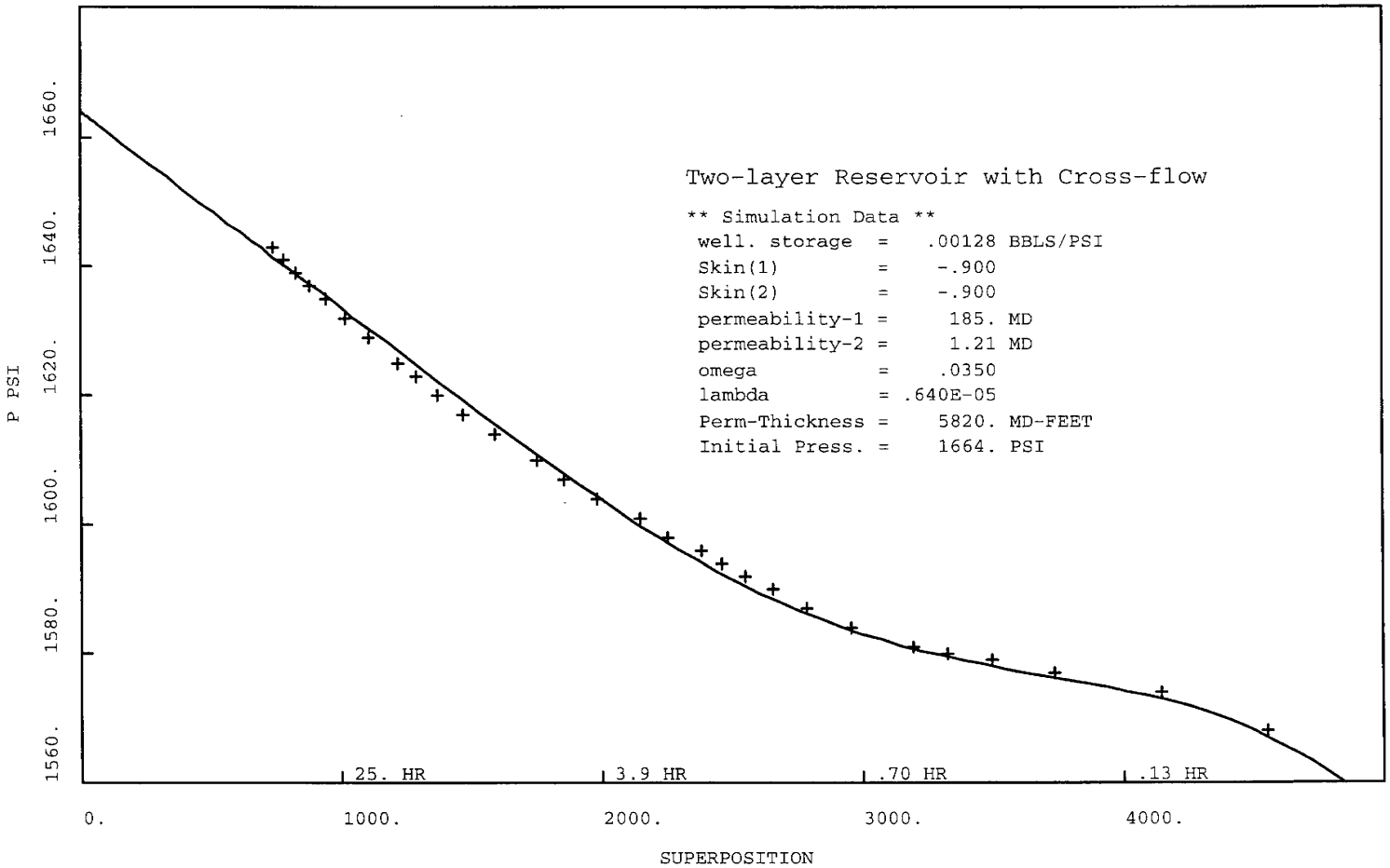

Figure 9–7 Anasazi Well No. 1 0190 Test – Superposition Pressure Match

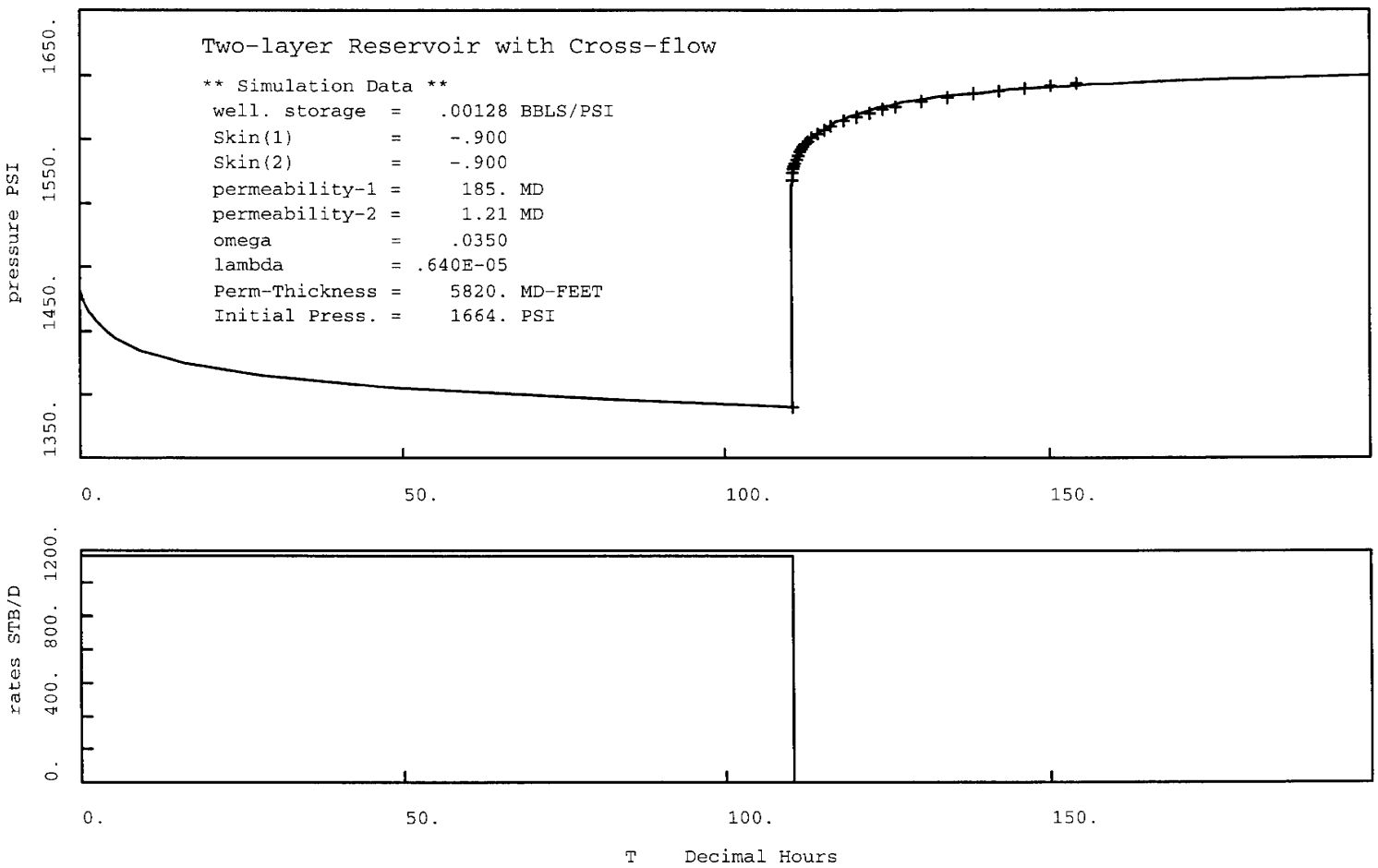

Figure 9–8 Anasazi Well No. 1 0190 Test – Pressure Data Match

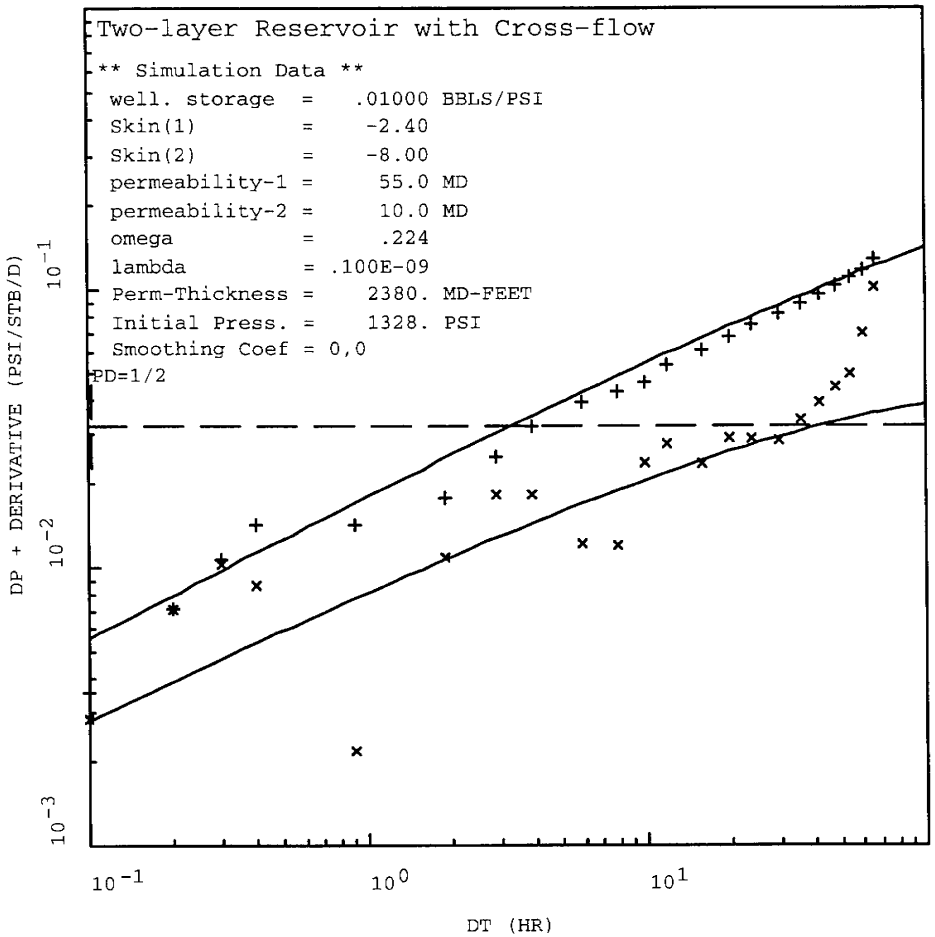

Figure 9–9 Anasazi Well No. 1 – 0290 Test Derivative and Pressure Difference Match

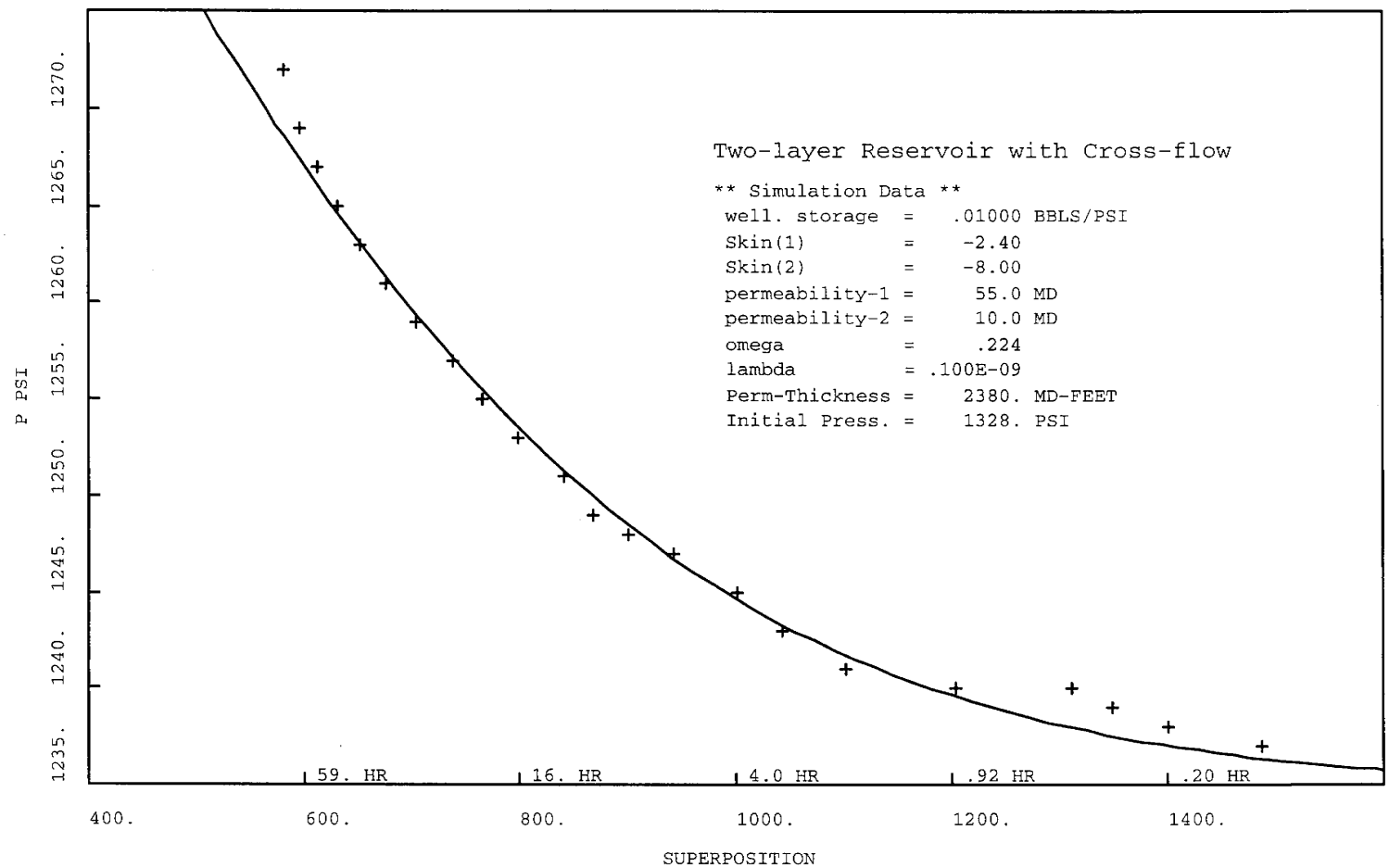

Figure 9–10 Anasazi Well No. 1 – 0290 Test Diagnostic Pressure Match

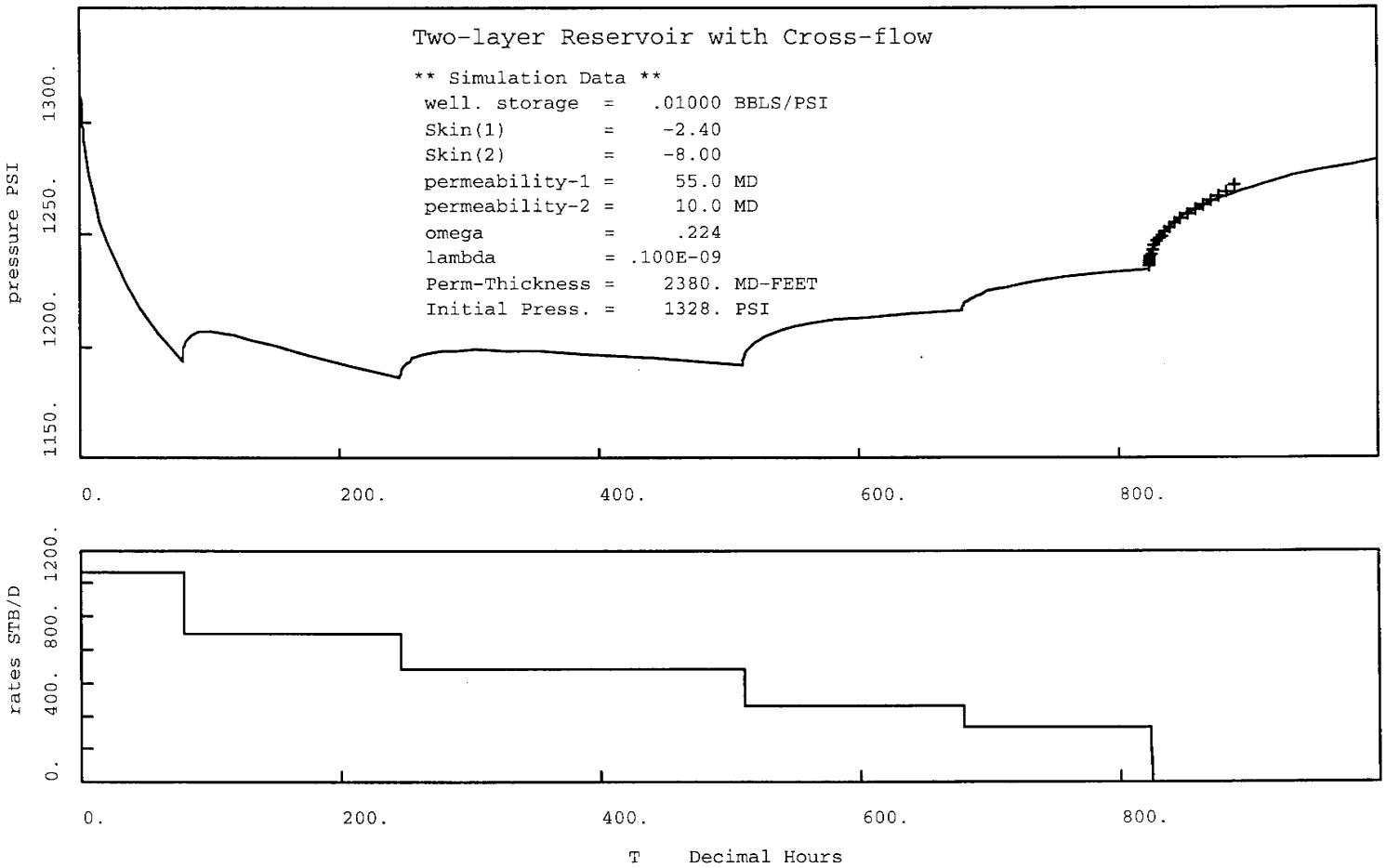

Figure 9–11 Anasazi Well No. 1 – 0290 Test Pressure Data Match

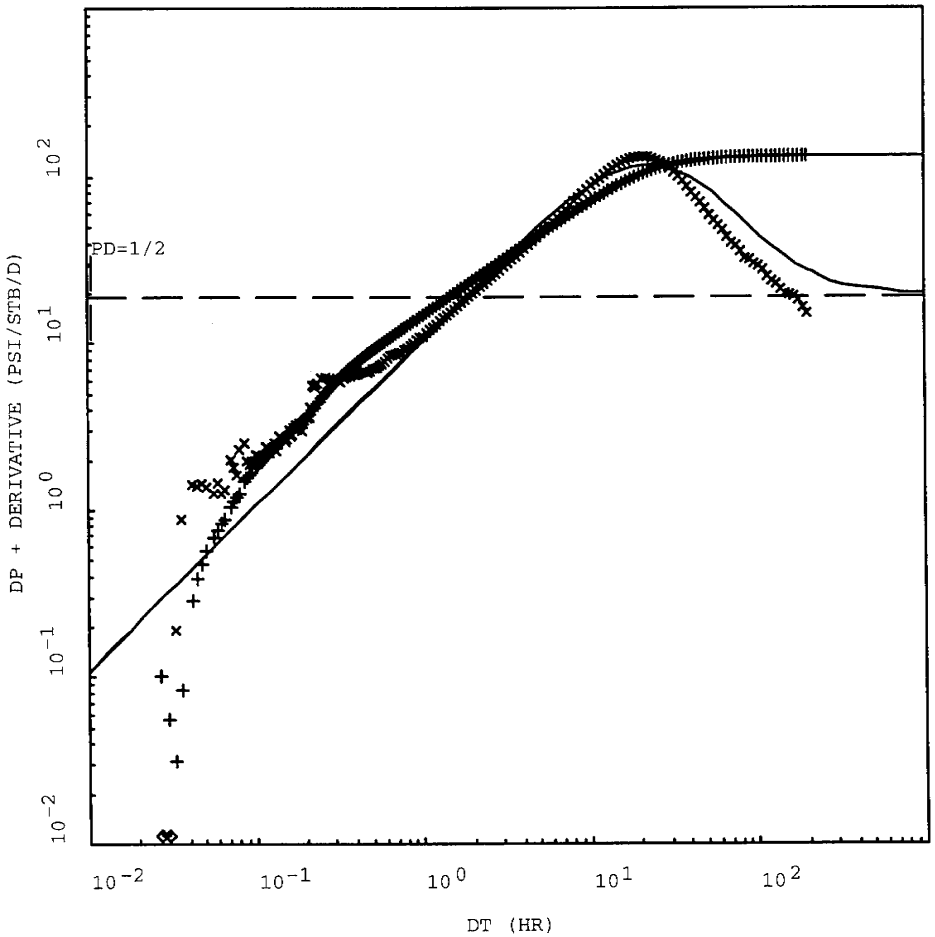

Homogeneous Reservoir

** Simulation Data **

well. storage	=	.00249 BBLS/PSI
skin	=	2.80
permeability	=	.453 MD
Perm-Thickness	=	4.53 MD-FEET
Initial Press.	=	383.0 PSI
Smoothing Coef	=	0,0

Figure 9–12 Anasazi Well No. 6H–1 – Dolomite Test Derivative and Pressure Difference Match

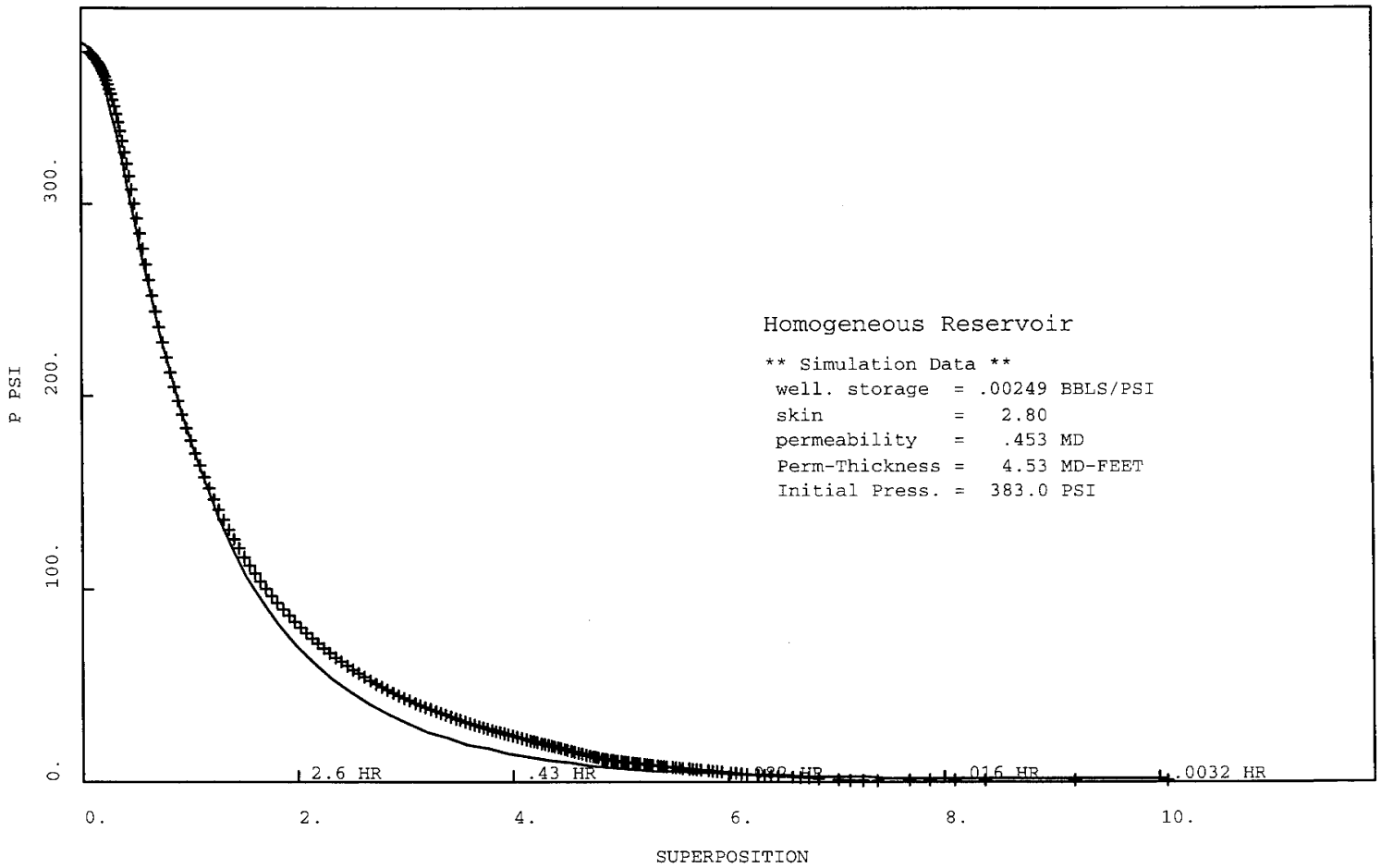

Figure 9–13 Anasazi Well No. 6H–1 – Dolomite Test Superposition Pressure Match

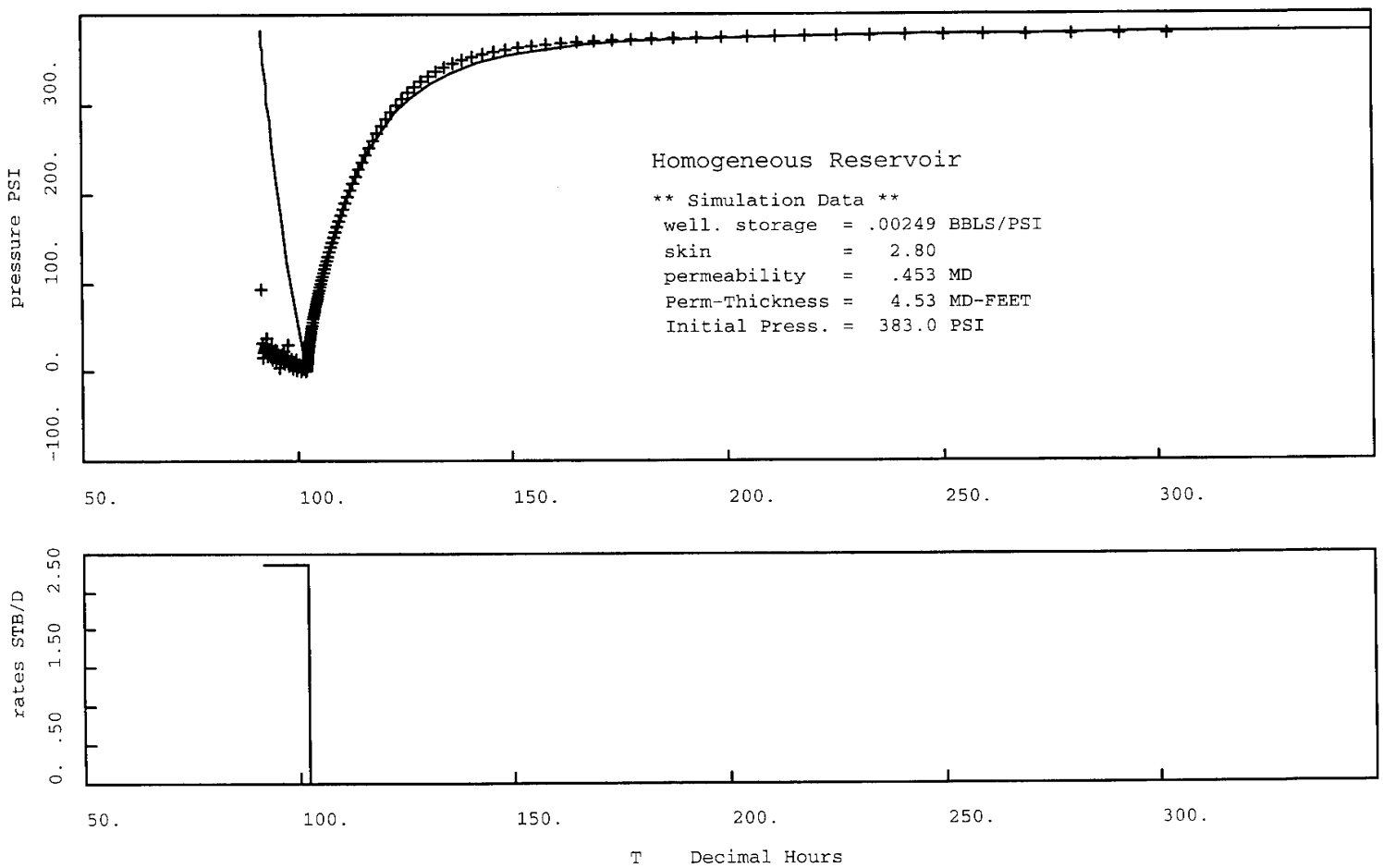

Figure 9–14 Anasazi Well No. 6H–1 – Dolomite Test Pressure Match – Last Swab Run

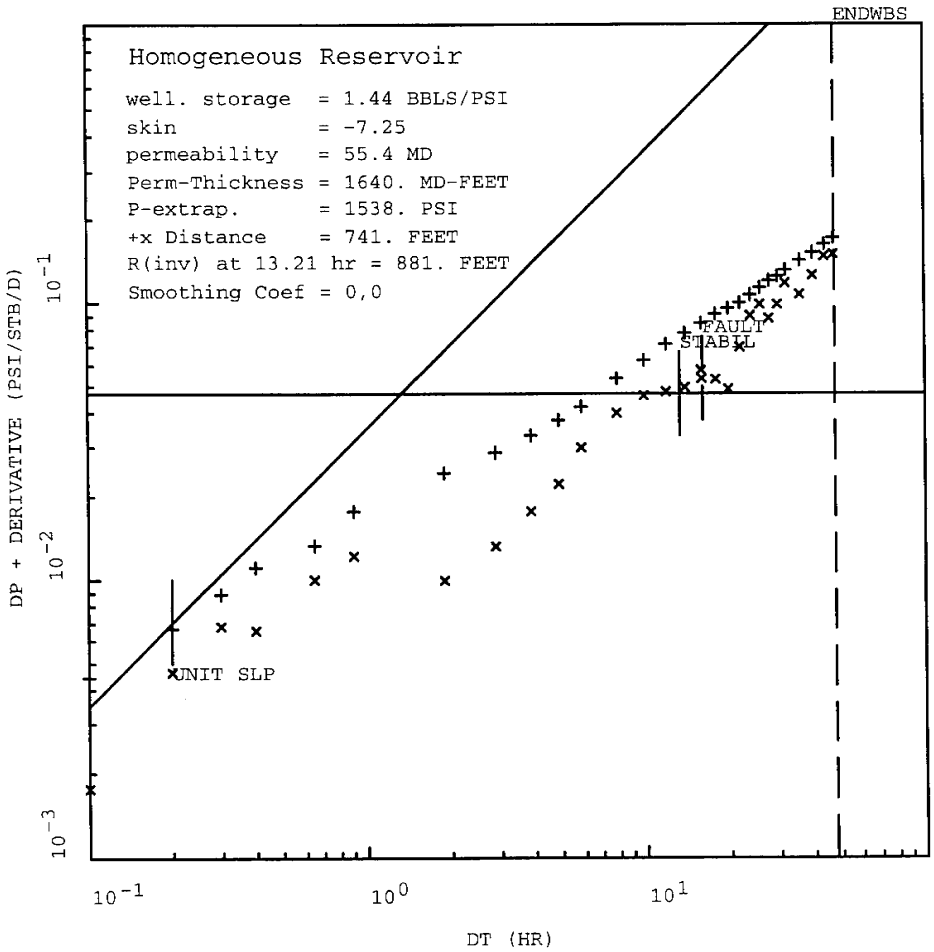

Figure 9–15 Sahgzie Well No. 1 – 1189 Derivative Diagnostics

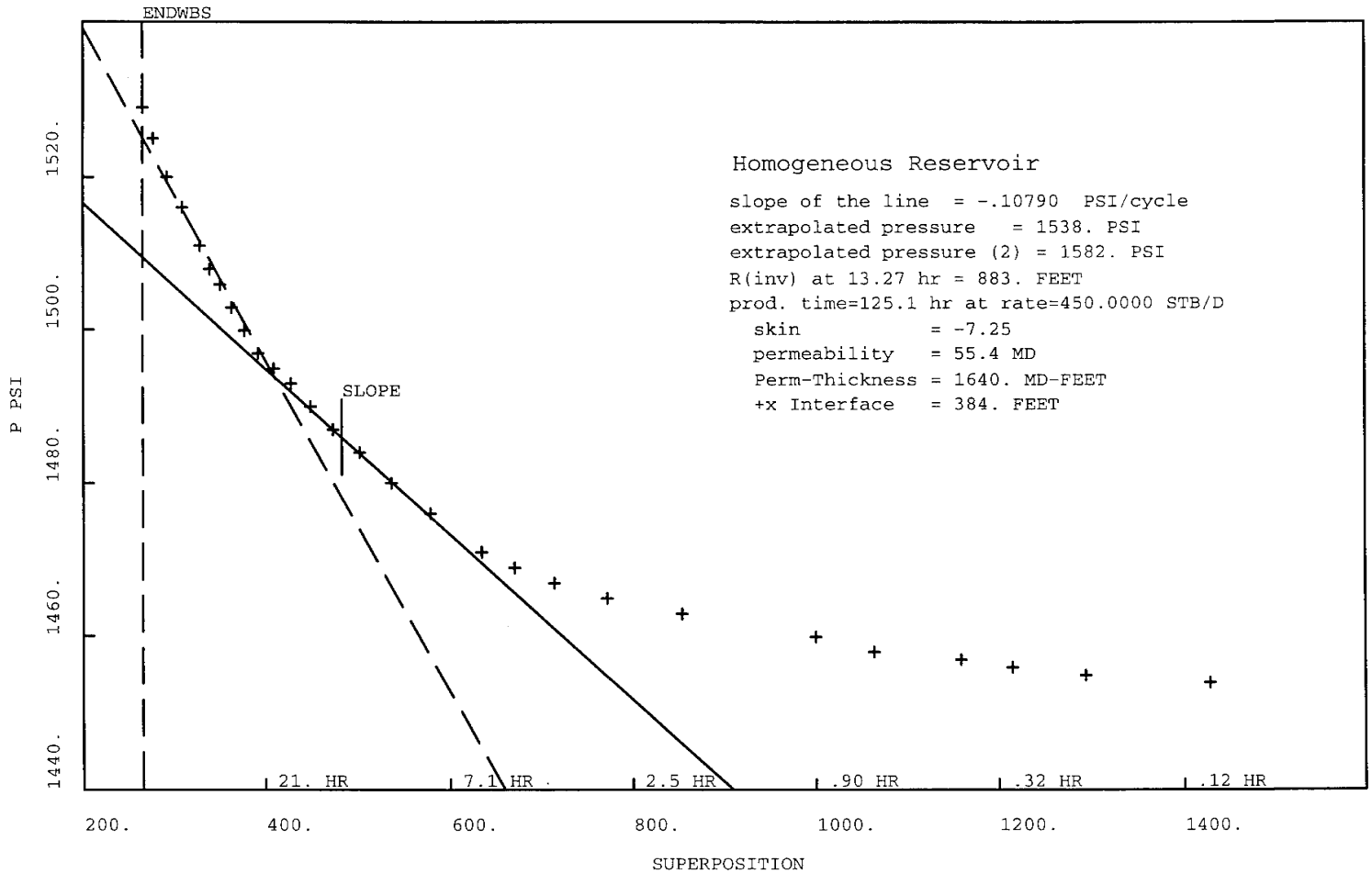

Figure 9–16 Sahgzie Well No. 1 – 1189 Superposition Diagnostics

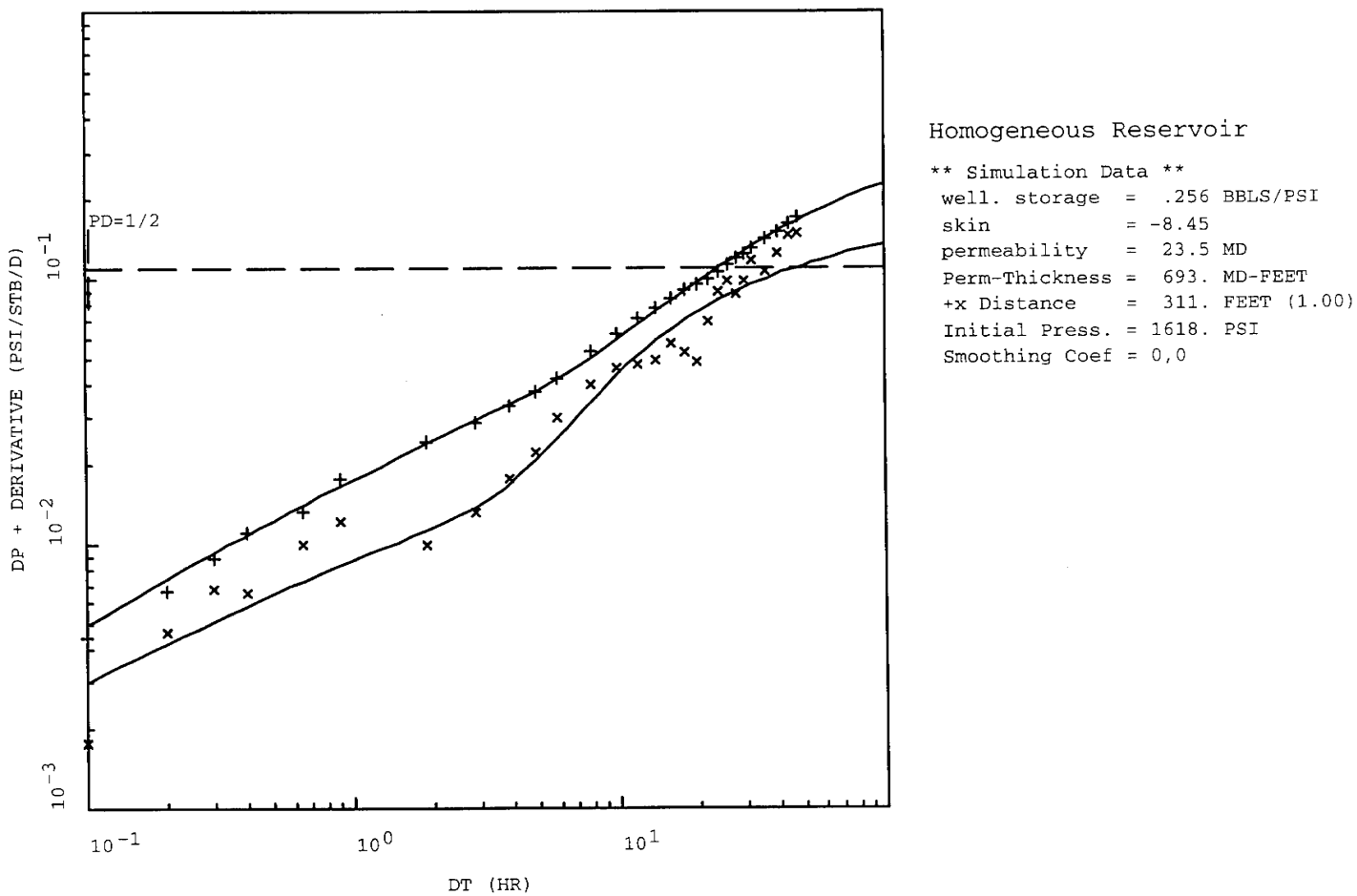

Figure 9–17 Sahgzie Well No. 6H–1 – 1189 Test Derivative Diagnostics

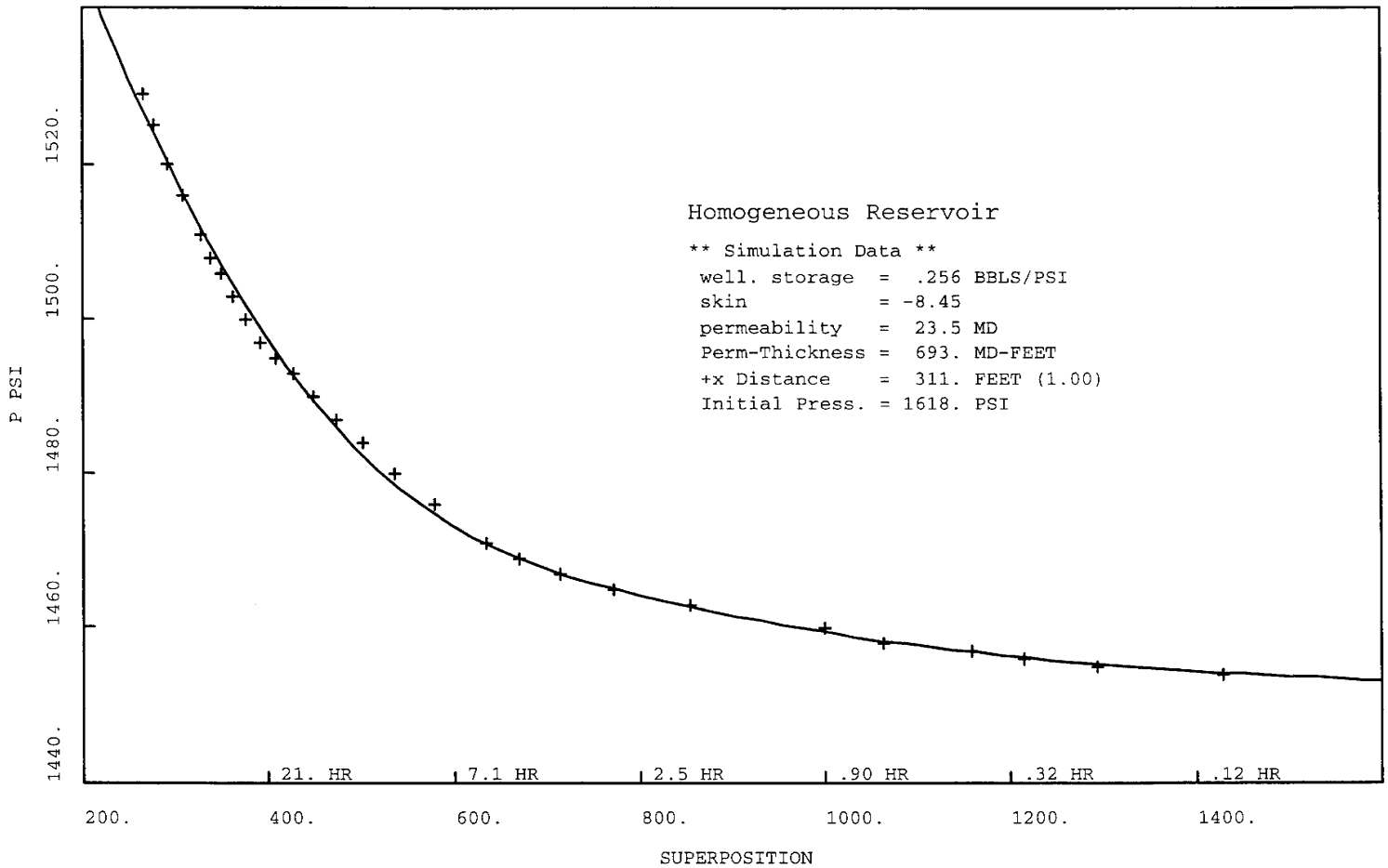

Figure 9–18 Sahgzie Well No. 1 – 1189 Superposition Pressure Match

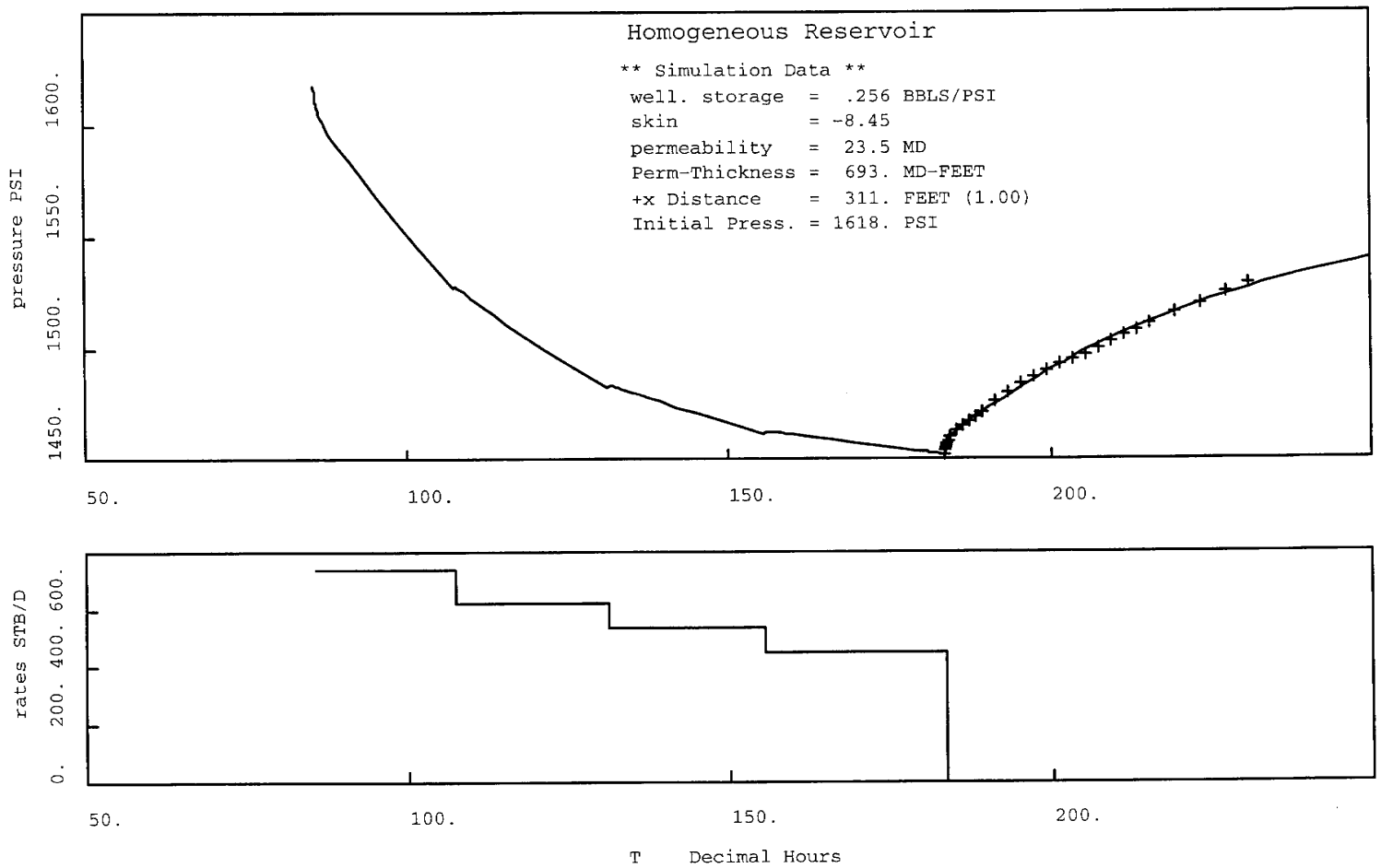

Figure 9–19 Sahgzie Well No. 1 – 1189 Pressure Data Match

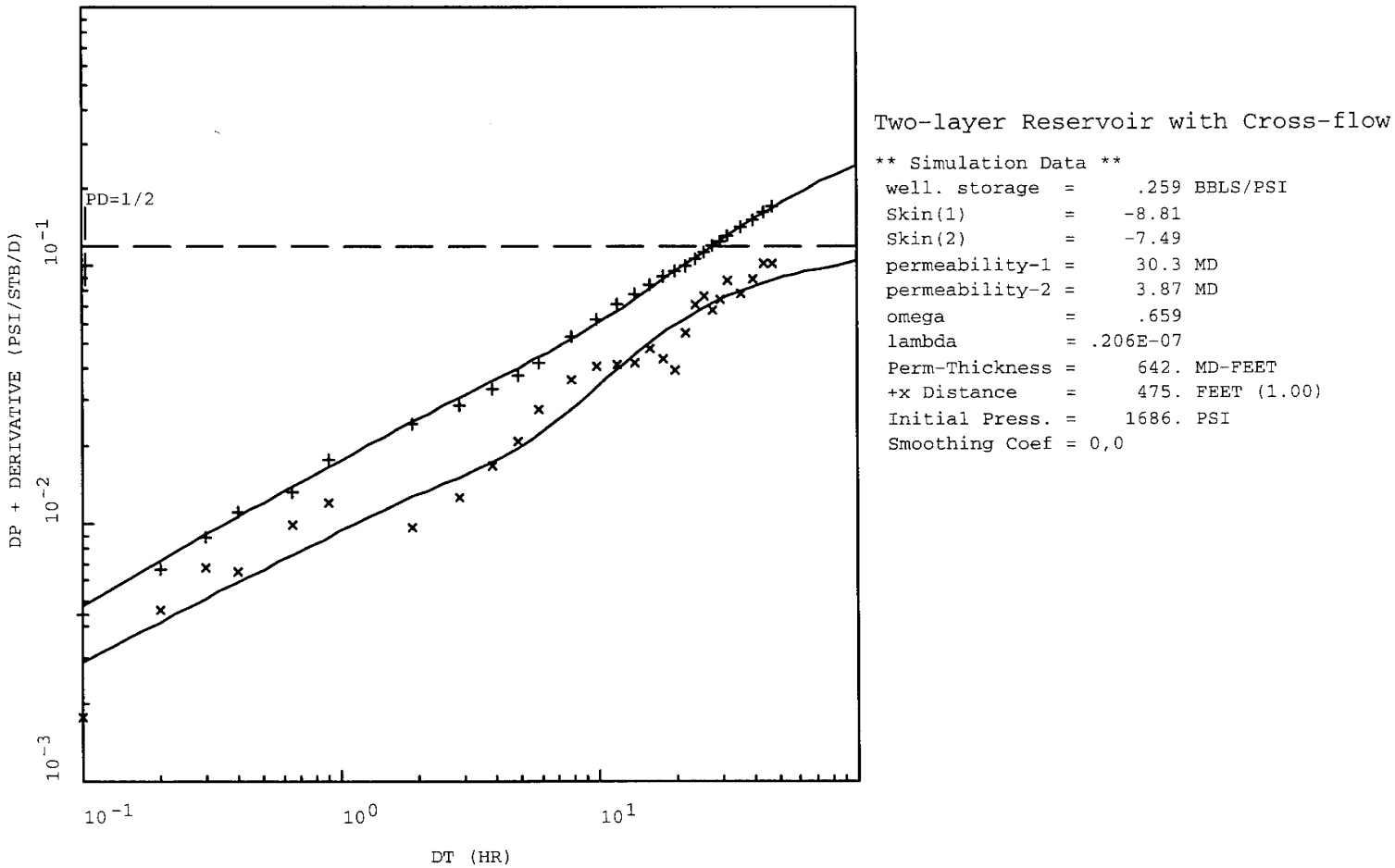

Figure 9–20 Sahgzie Well No. 1 – 1189 Two Layer Model Derivative Pressure Difference Match

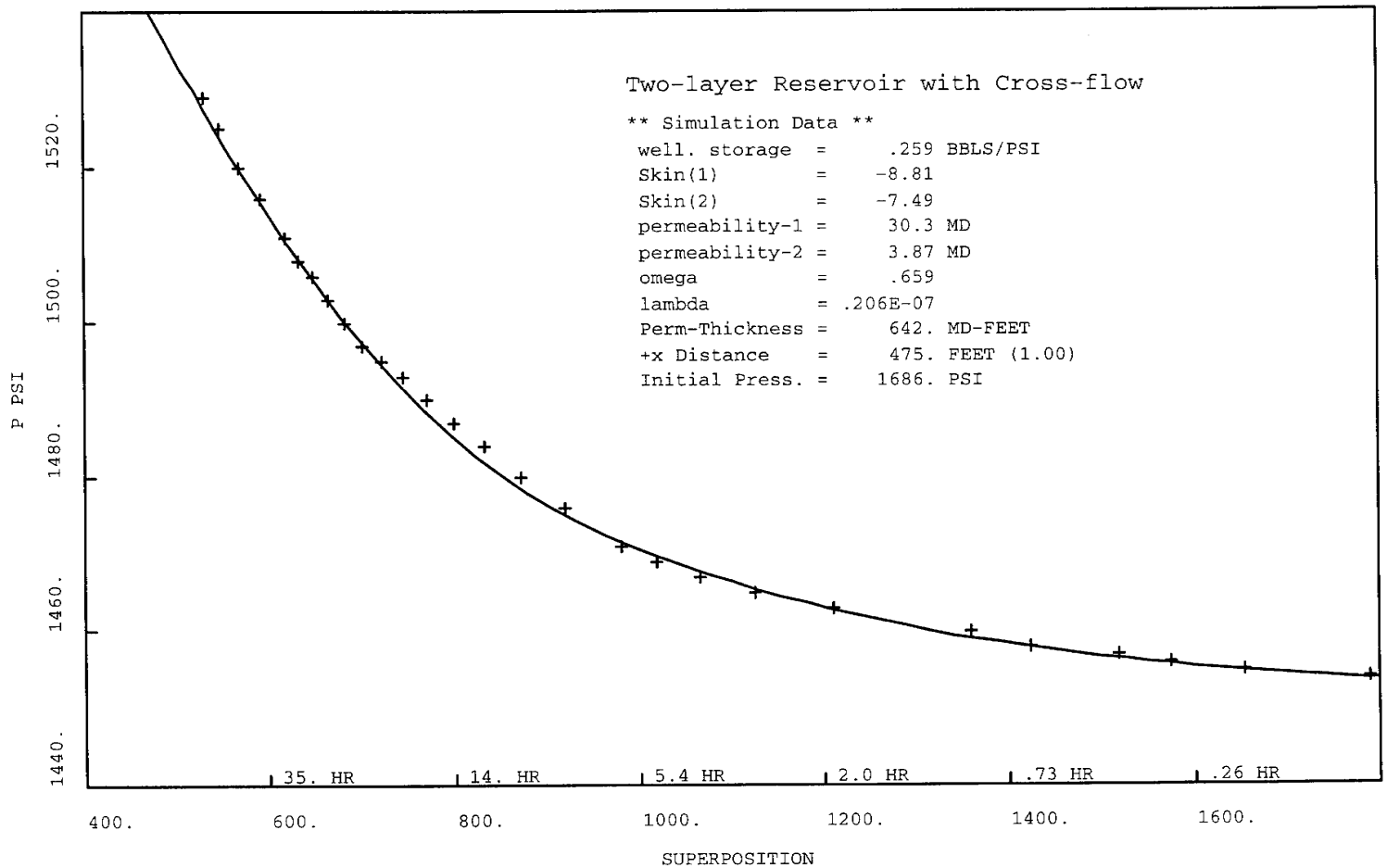

Figure 9–21 Sahgzie Well No. 1 – 1189 Two Layer Model Superposition Pressure Match

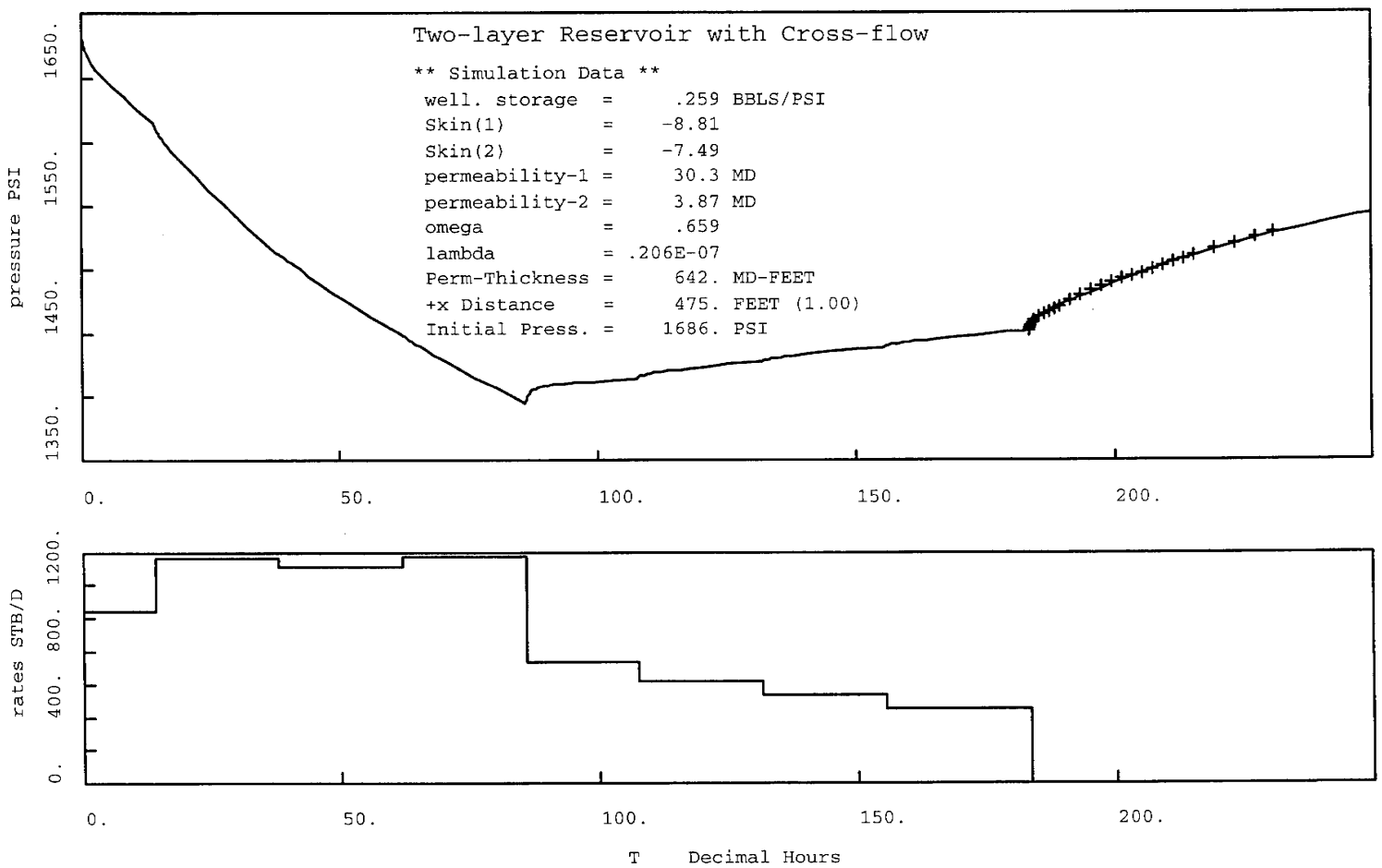

Figure 9–22 Sahgzie Well No. 1 – 1189 Two Layer Model Pressure Data Match

RESERVOIR MODELING AND COMPOSITION SIMULATION OF PRIMARY DEPLETION, WATERFLOODING, AND CARBON DIOXIDE FLOODING OF A SMALL PENNSYLVANIAN CARBONATE MOUND COMPLEX, ANASAZI FIELD, PARADOX BASIN, UTAH

Volume III

by

William E. Culham
REGA Inc.
Houston, Texas 77057

and

Douglas M. Lorenz
Texaco E&P
Houston, Texas 77215

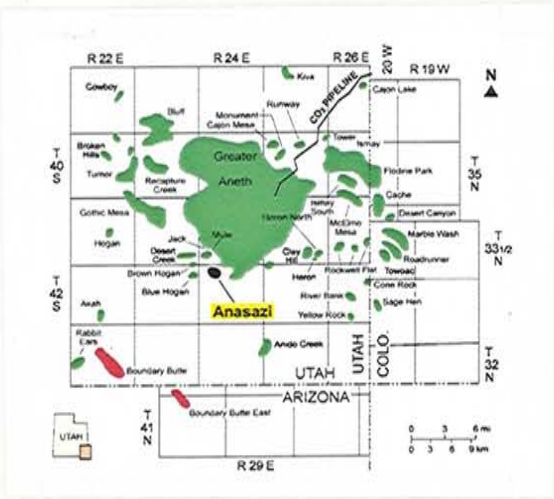

OPEN-FILE REPORT 420 **September 2003**
UTAH GEOLOGICAL SURVEY
a division of
UTAH DEPARTMENT OF NATURAL RESOURCES

This Open-File Report represents material that may not have undergone policy, technical, or editorial review required for other UGS publications. It provides information that, in part, may be interpretive or incomplete and readers are to exercise some degree of caution in the use of the data. Although this product represents the work of professional scientists, the Utah Department of Natural Resources, Utah Geological Survey, makes no warranty, stated or implied, regarding its suitability for a particular use. The Utah Department of Natural Resources, Utah Geological Survey, shall not be liable under any circumstances for any direct, indirect, special, incidental, or consequential damages with respect to claims by users of this product.

DISCLAIMER

This report was prepared as an account of work sponsored by an agency of the United States Government. Neither the United States Government nor any agency thereof, nor any of their employees, makes any warranty, express or implied, or assumes any legal liability or responsibility for the accuracy, completeness, or usefulness of any information, apparatus, product, or process disclosed, or represents that its use would not infringe privately owned rights. Reference herein to any specific commercial product, process, or service by trade name, trademark, manufacturer, or otherwise does not necessarily constitute or imply its endorsement, recommendation, or favoring by the United States Government or any agency thereof. The views and opinions of authors expressed herein do not necessarily state or reflect those of the United States Government or any agency thereof.

FIGURES

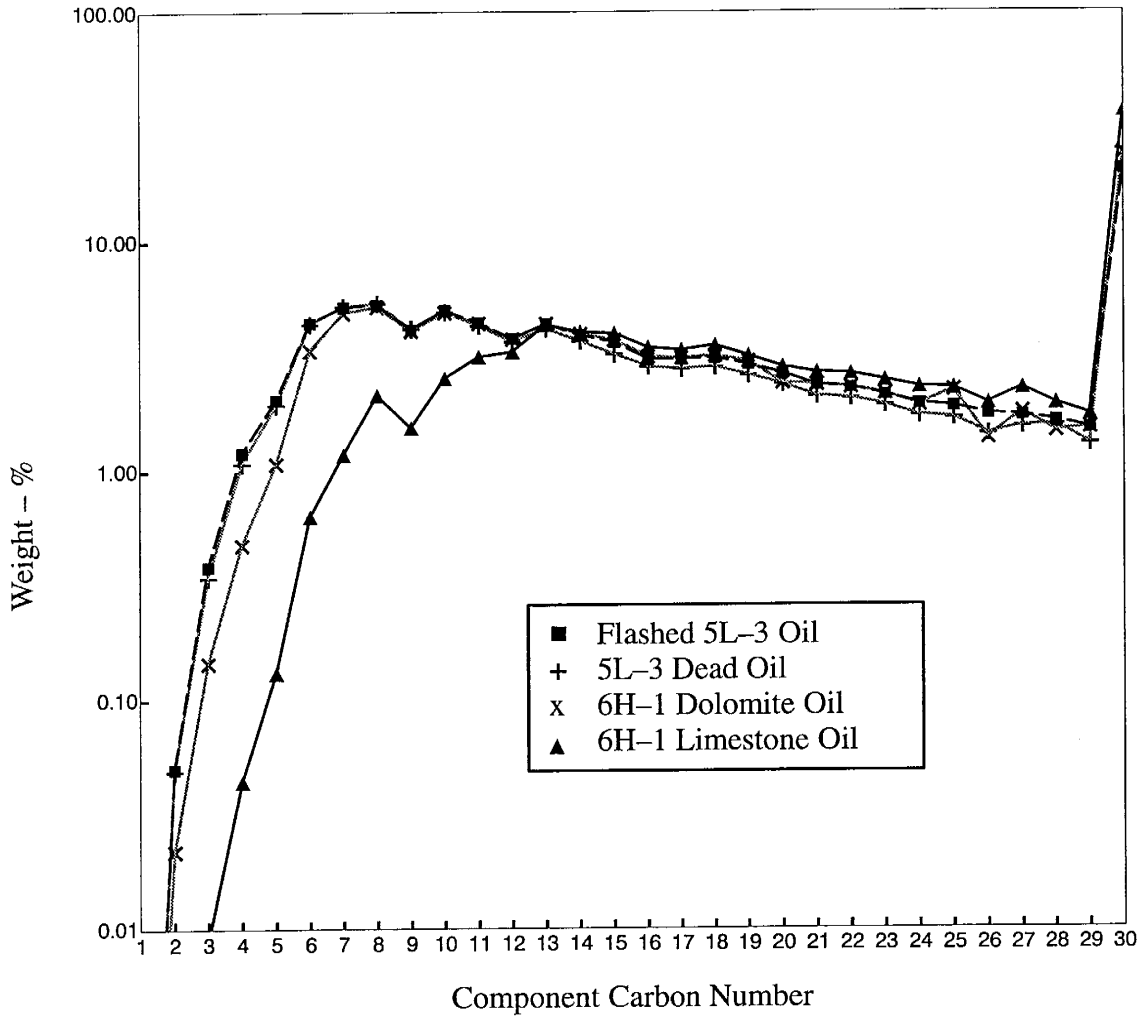

Figure 10–1 – Comparison of Weight Percent Composition Measured for Anasazi Flashed Separator Oil and Dead Oil Samples

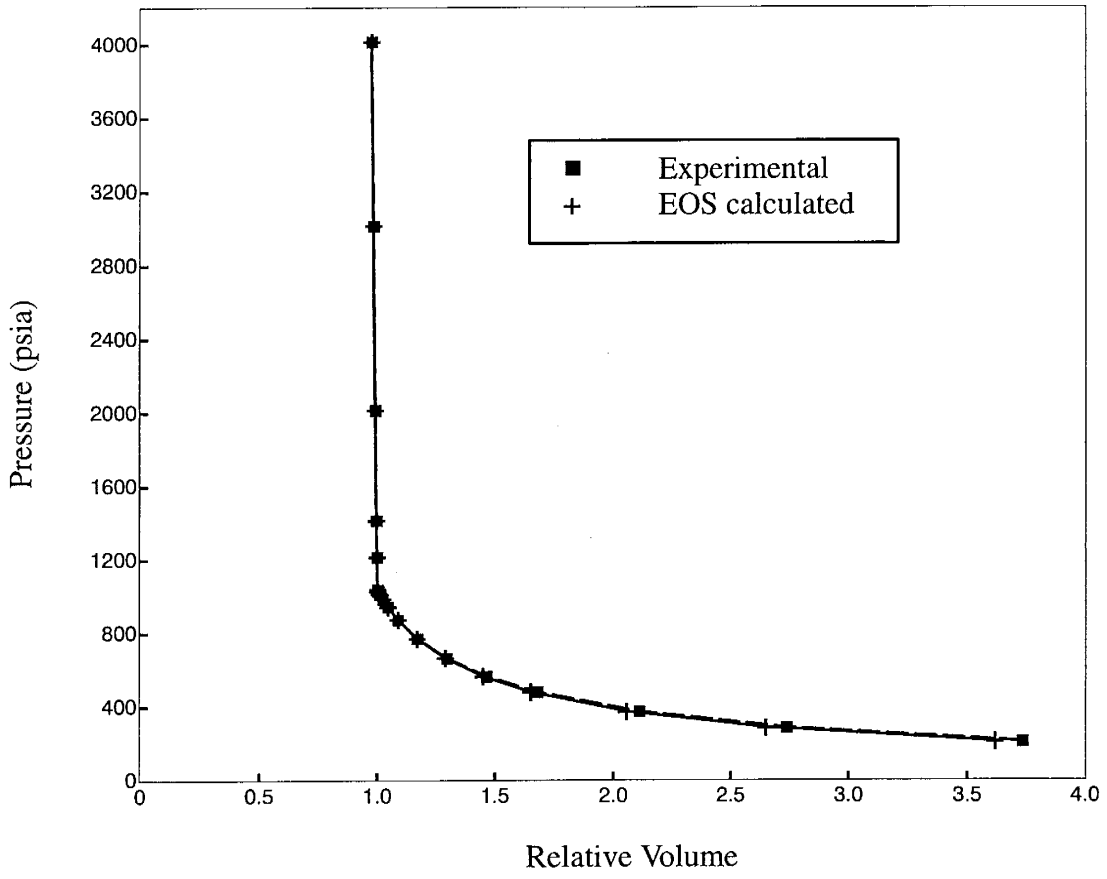

Figure 10–2 – Anasazi Well 1 Constant Composition Expansion Experiment–Original Oil Relative Oil Volume

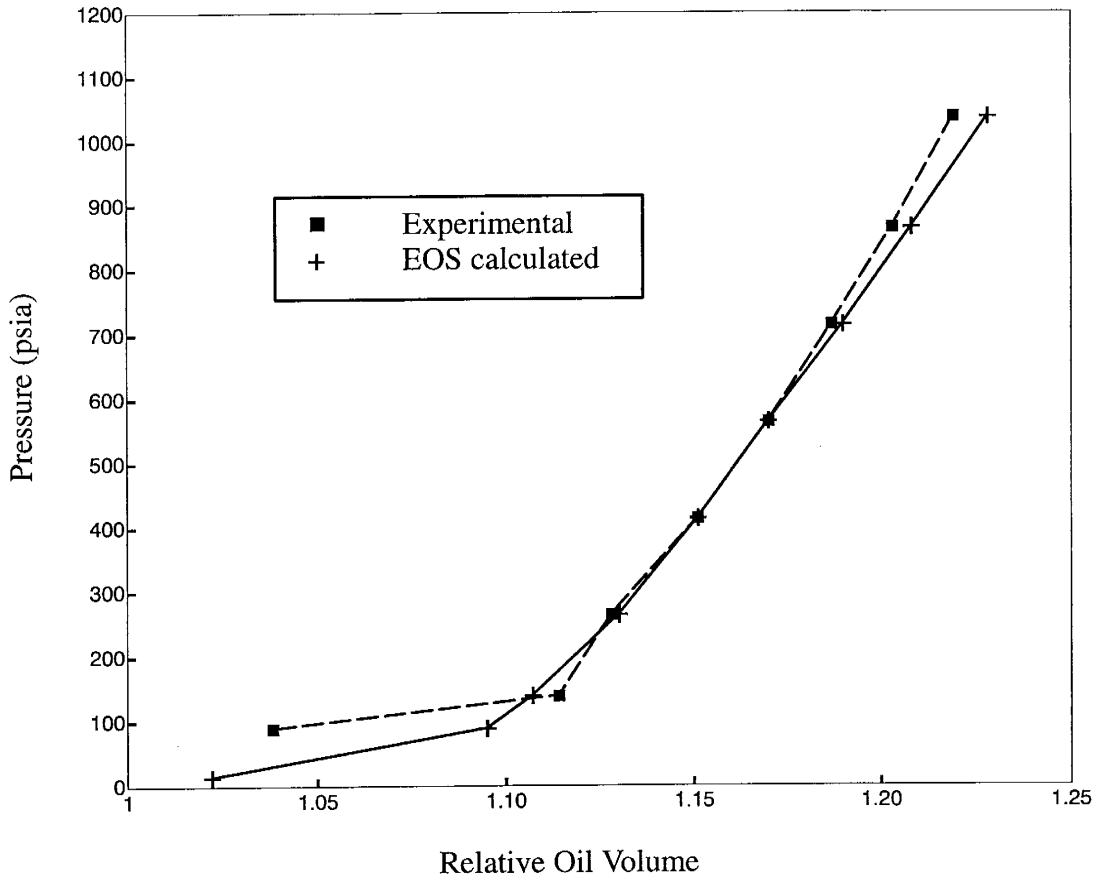

Figure 10–3 – Anasazi Well 1 Differential Depletion Experiment–Original Oil Relative Oil Volume (Oil Formation Volume Factor)

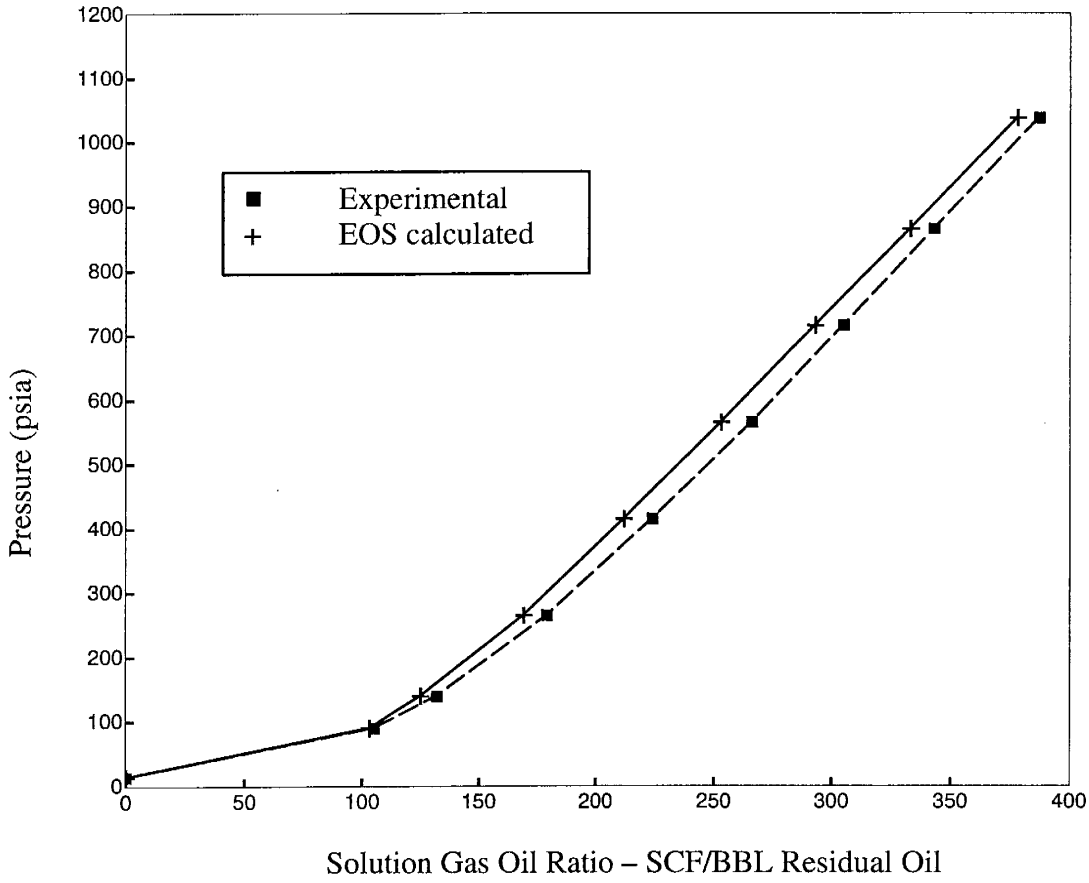

Figure 10–4 – Anasazi Well 1 Differential Depletion Experiment–Original Oil Solution Gas Oil Ratio

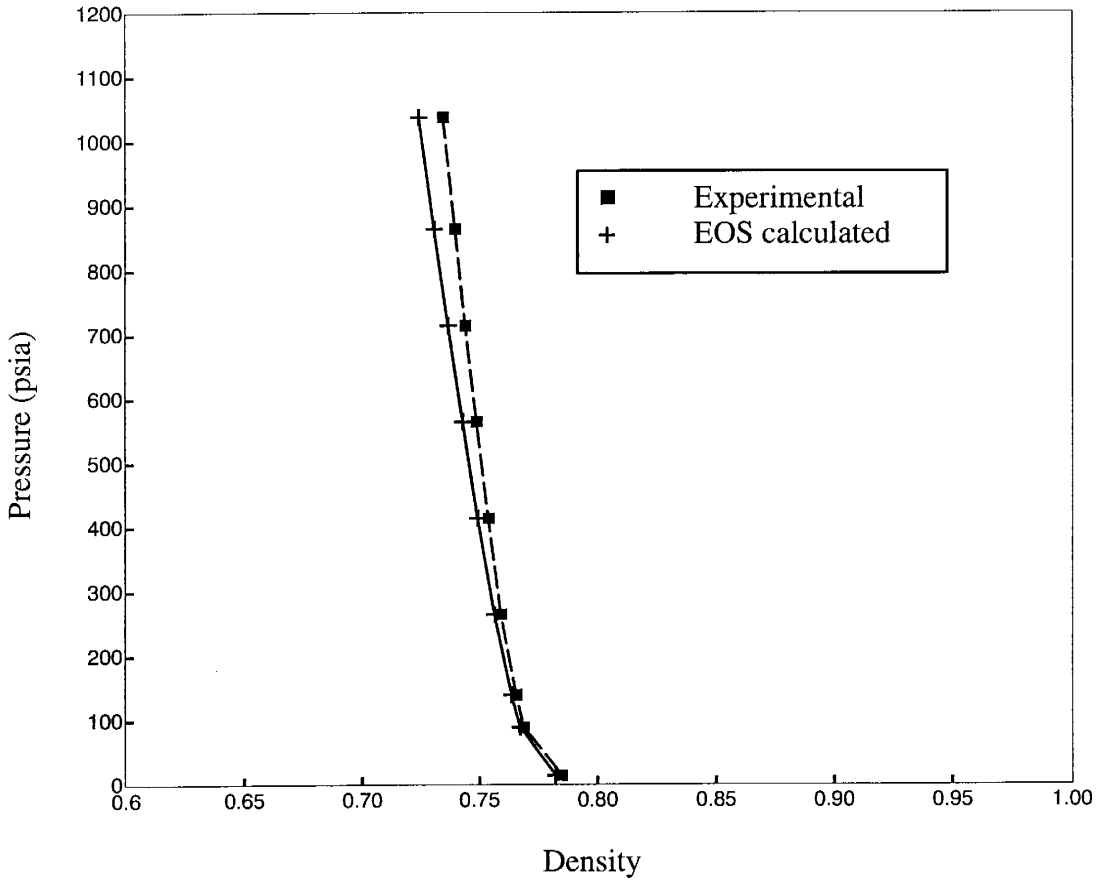

Figure 10–5 – Anasazi Well 1 Differential Depletion Experiment–Original Oil Oil Density

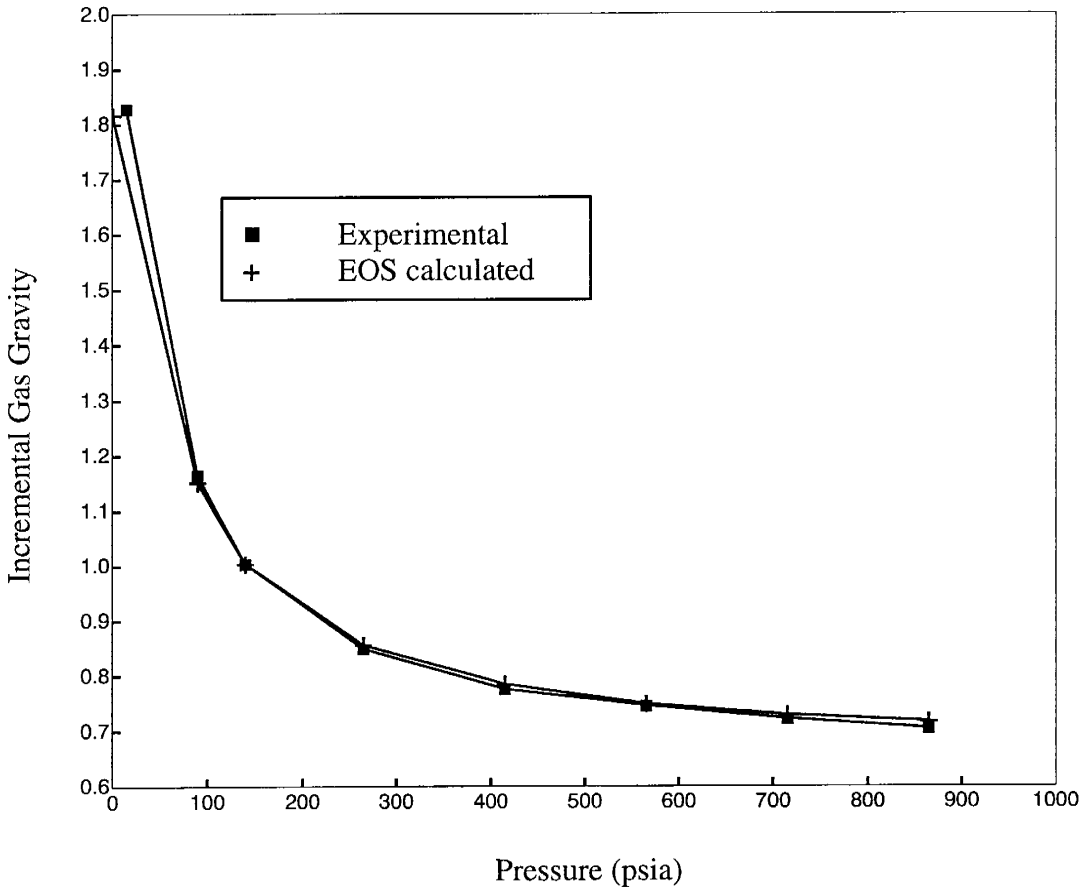

Figure 10–6 – Anasazi Well 1 Differential Depletion Experiment–Oiginal Oil Gas Gravity

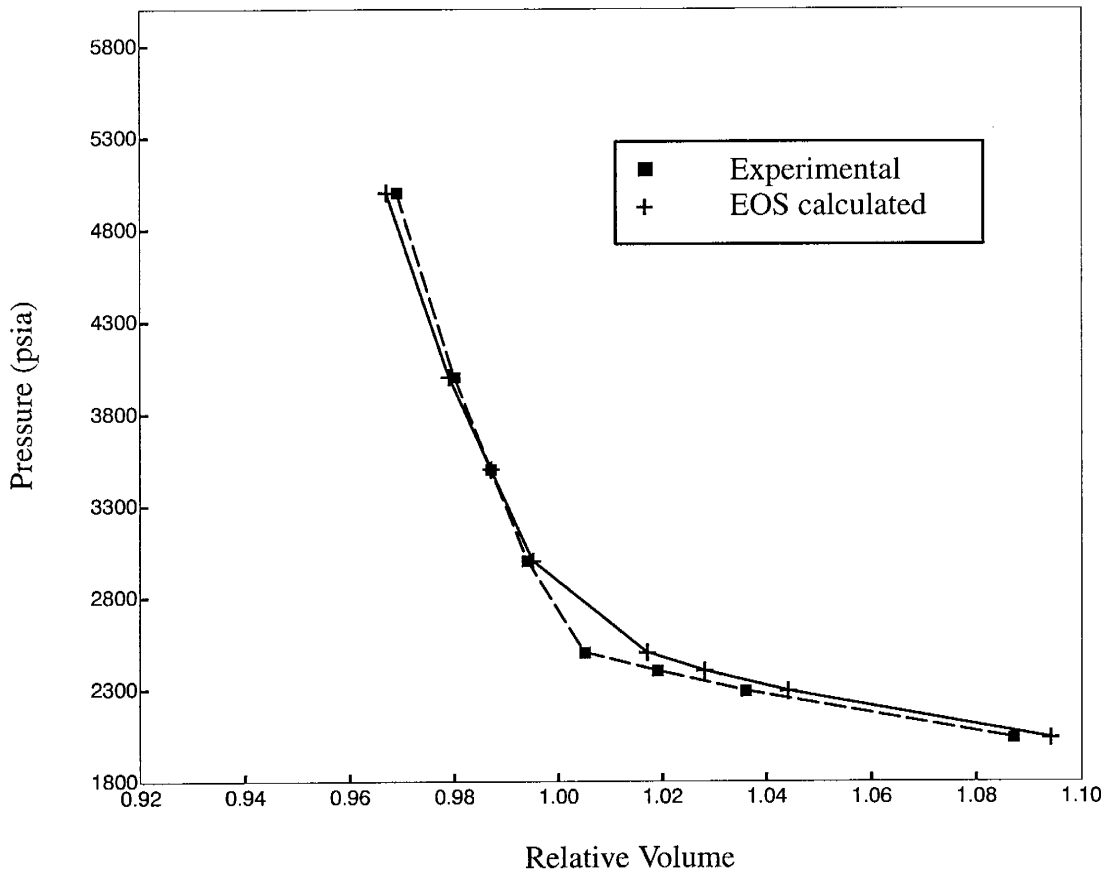

Figure 10–7 – Anasazi Well 1 Constant Composition Expansion Experiment–Recombined Oil
Relative Oil Volume

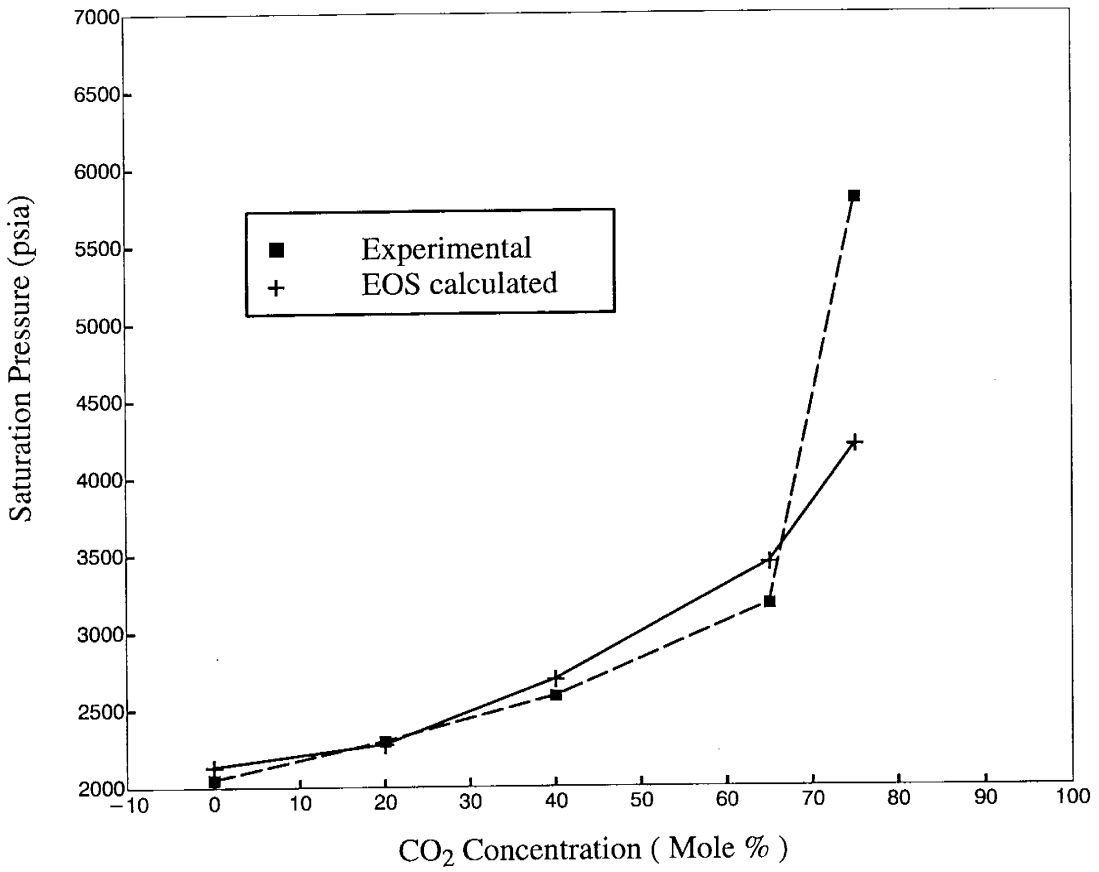

Figure 10–8 – Anasazi Field – Saturation Pressure Versus CO_2 Concentration

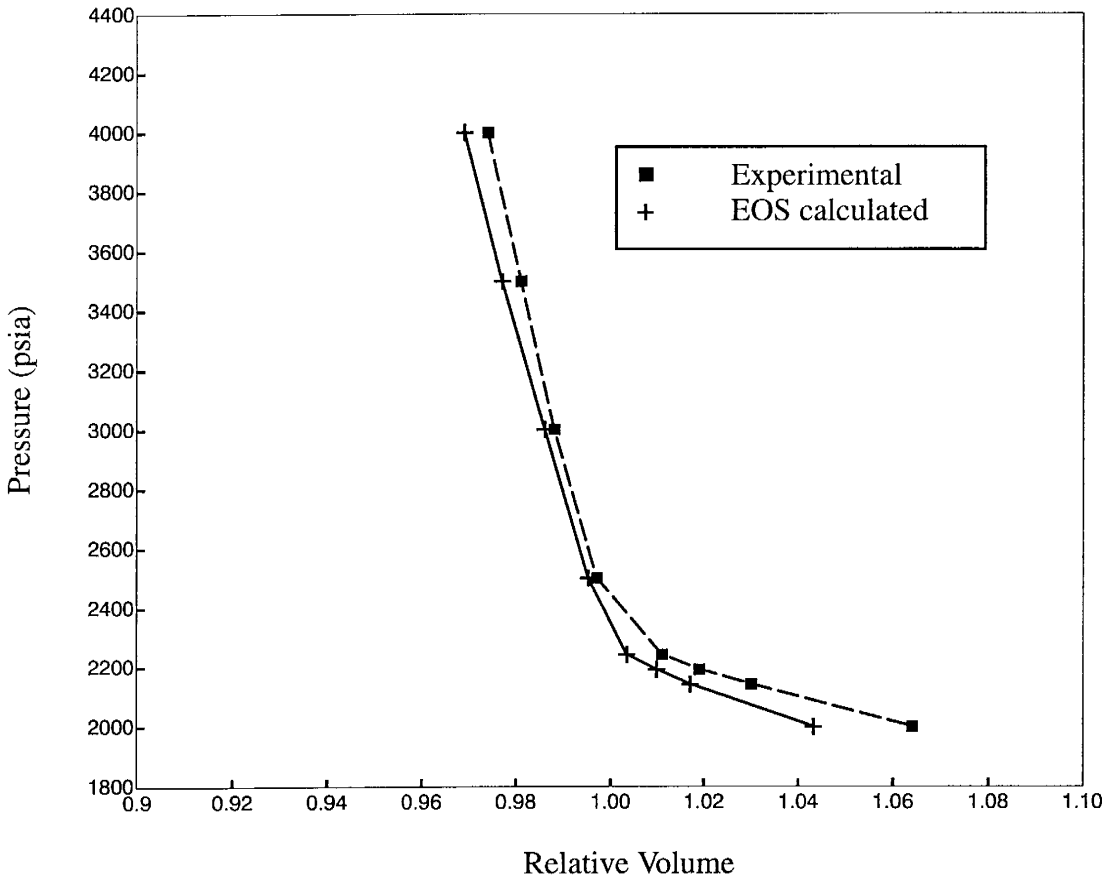

Figure 10–9 – Anasazi Field CO_2 Swelling Test 20% CO_2 Case – Relative Volume

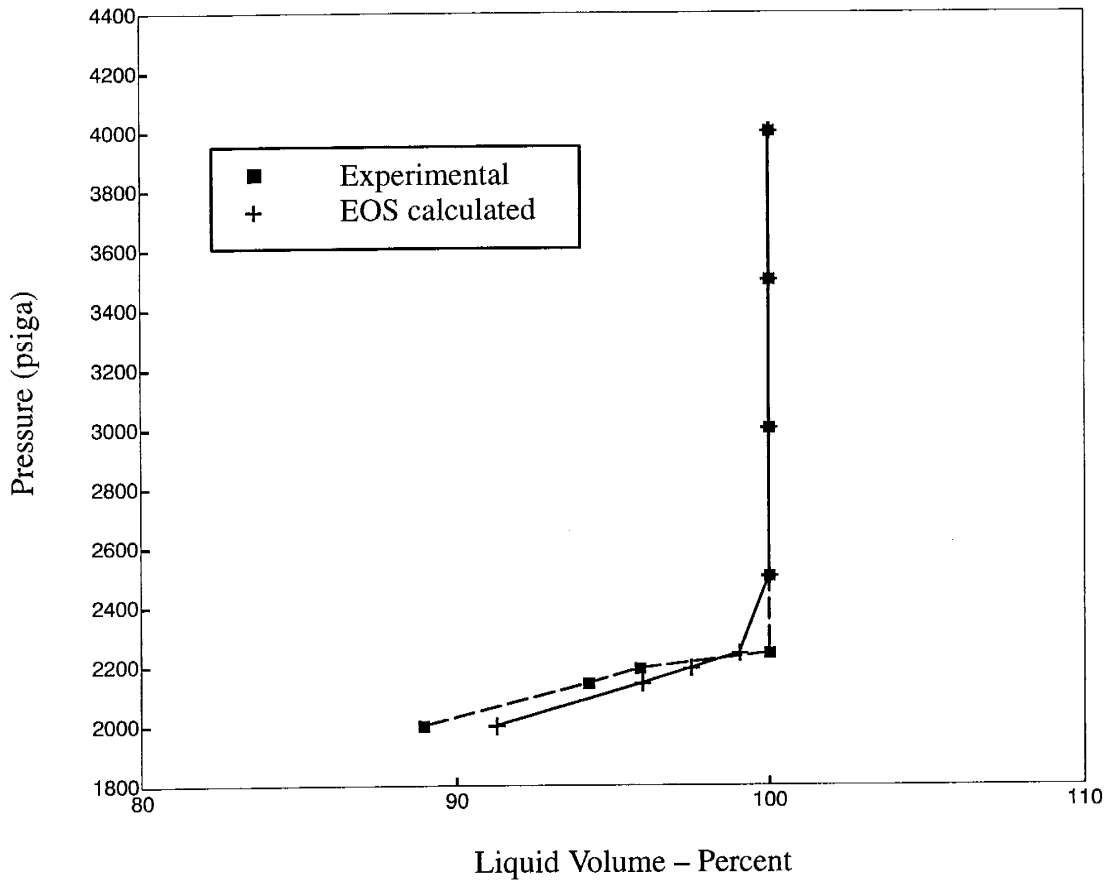

Figure 10–10 – Anasazi Field CO_2 Swelling Test 20% CO_2 Case – Liquid Volume

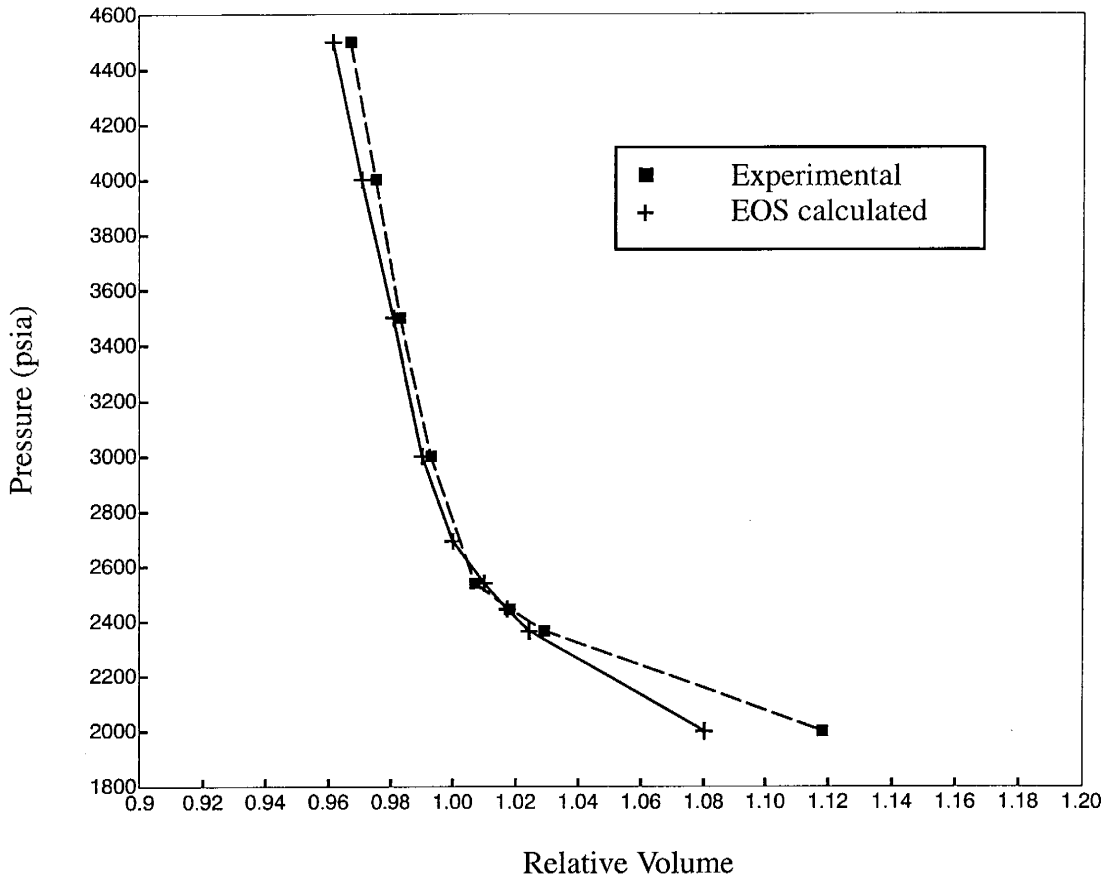

Figure 10–11 – Anasazi Field CO_2 Swelling Test 40% CO_2 Case – Relative Volume

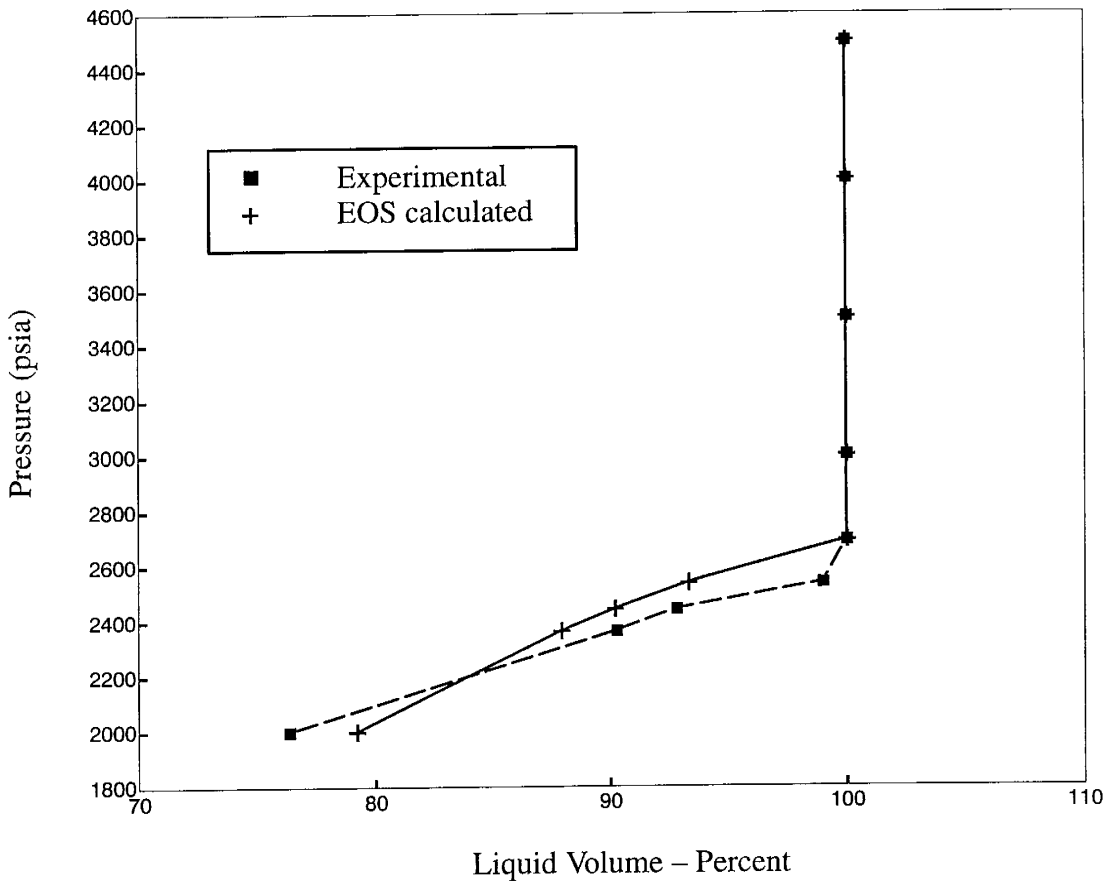

Figure 10–12 – Anasazi Field CO_2 Swelling Test 40% CO_2 Case – Liquid Volume

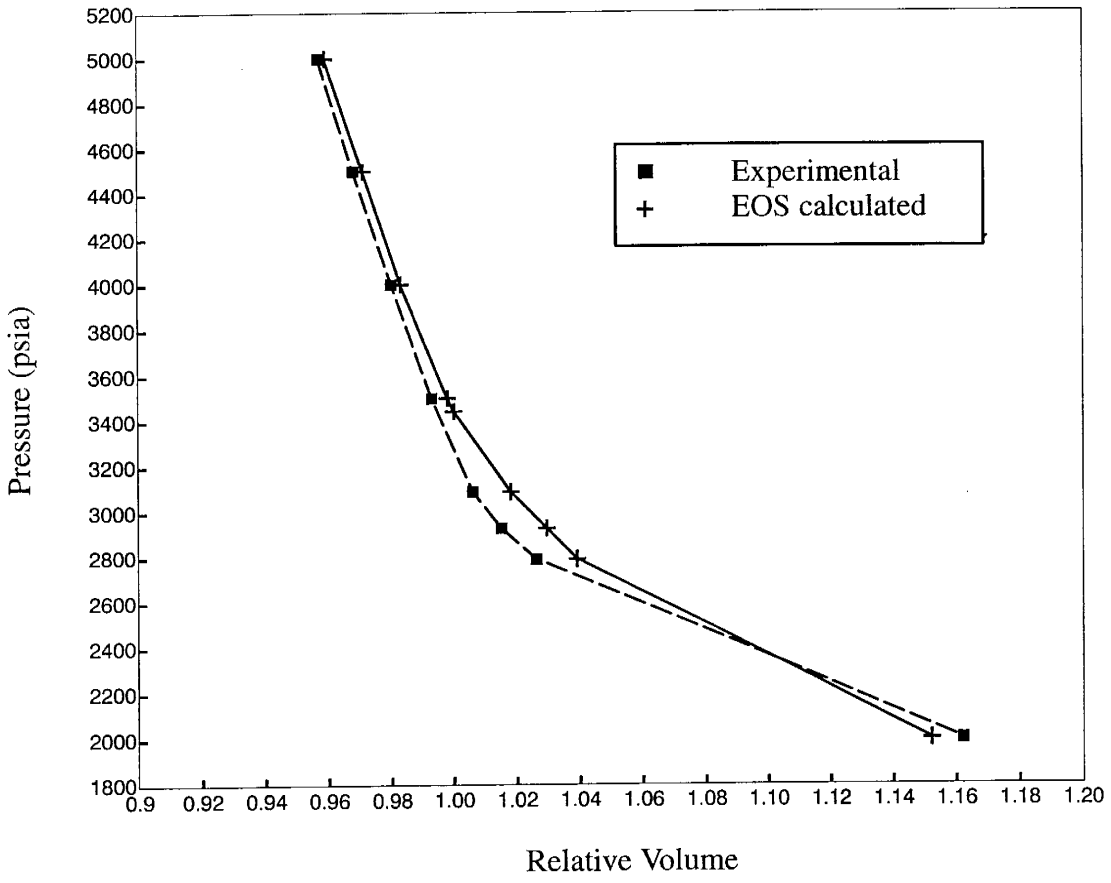

Figure 10–13 – Anasazi Field CO_2 Swelling Test 60% CO_2 Case – Relative Volume

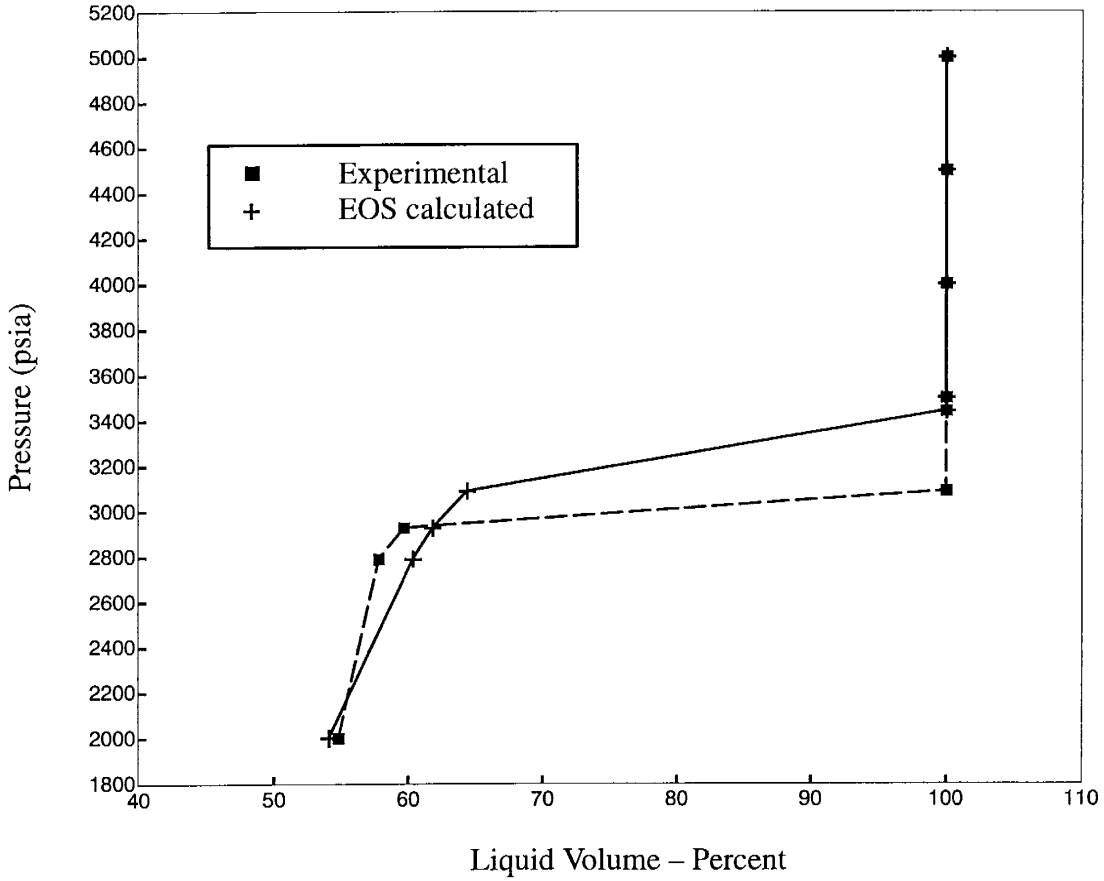

Figure 10–14 – Anasazi Field CO_2 Swelling Test 60% CO_2 Case –Liquid Volume

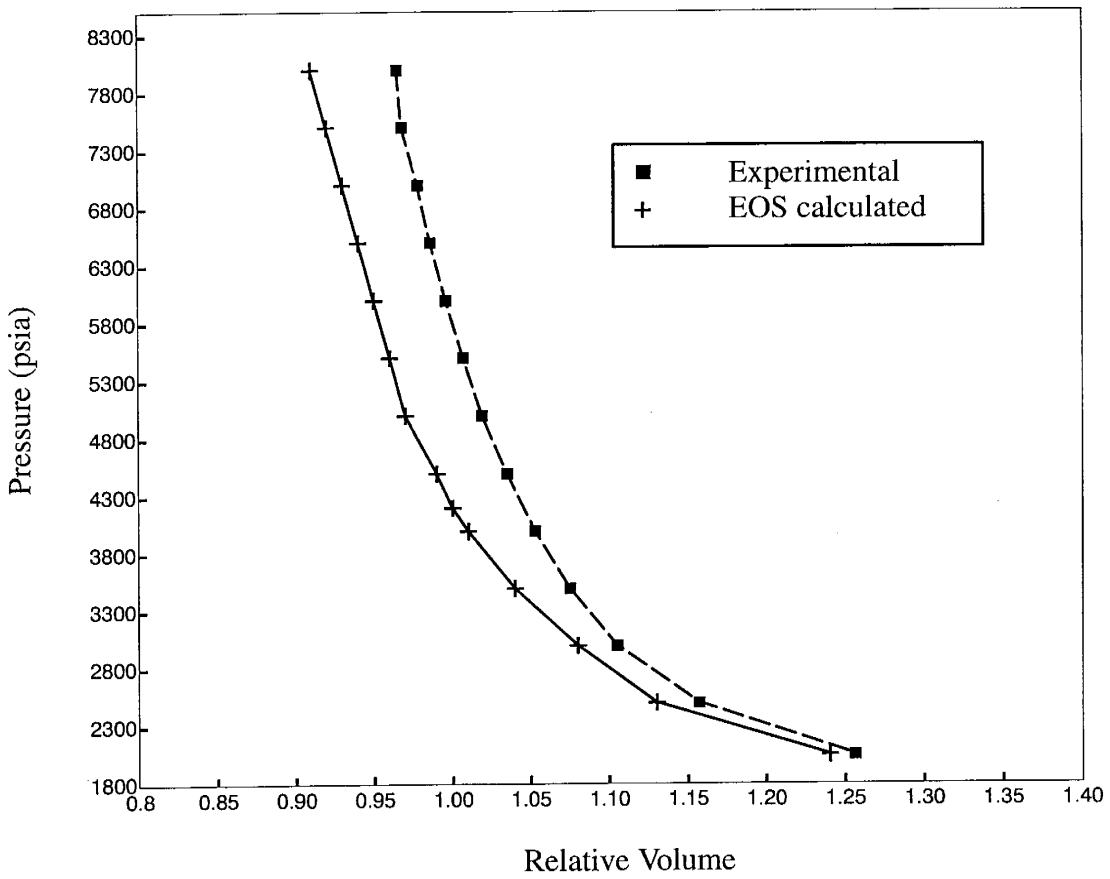

Figure 10–15 – Anasazi Field CO_2 Swelling Test 75% CO_2 Case – Relative Volume

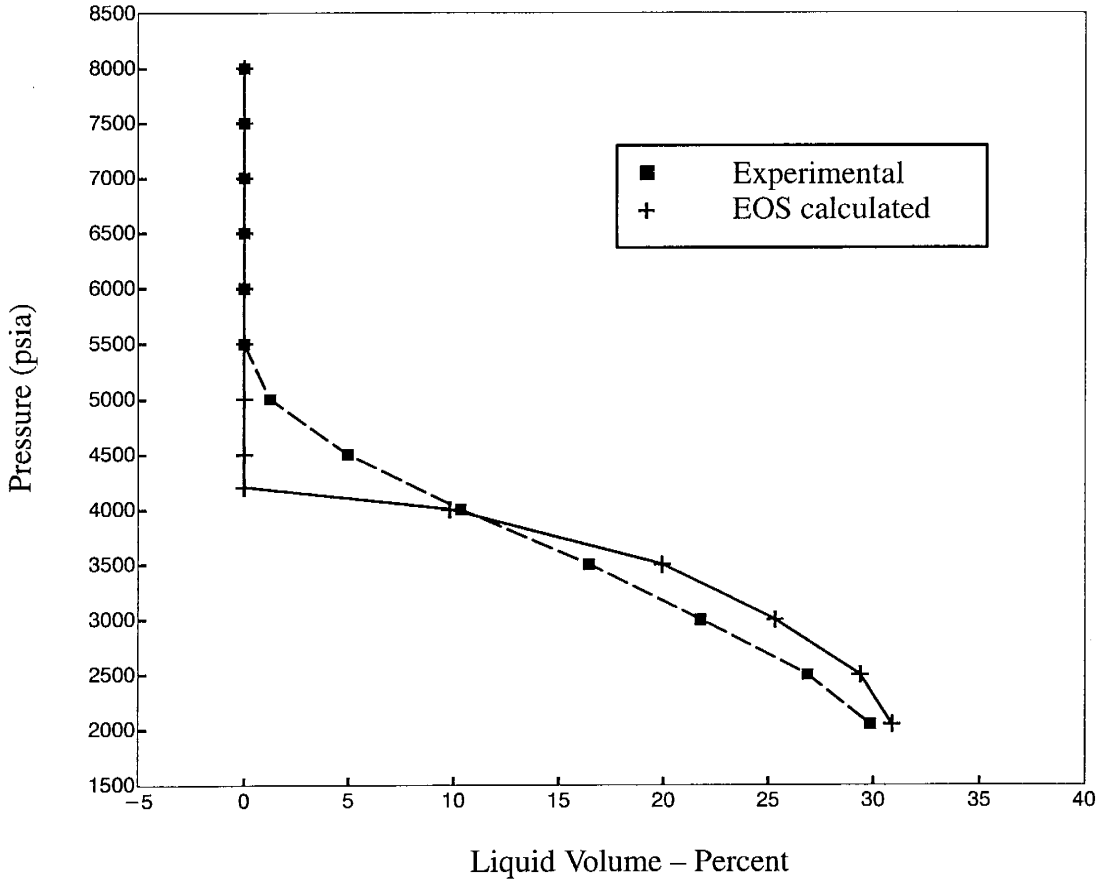

Figure 10–16 – Anasazi Field CO_2 Swelling Test 75% CO_2 Case – Liquid Volume

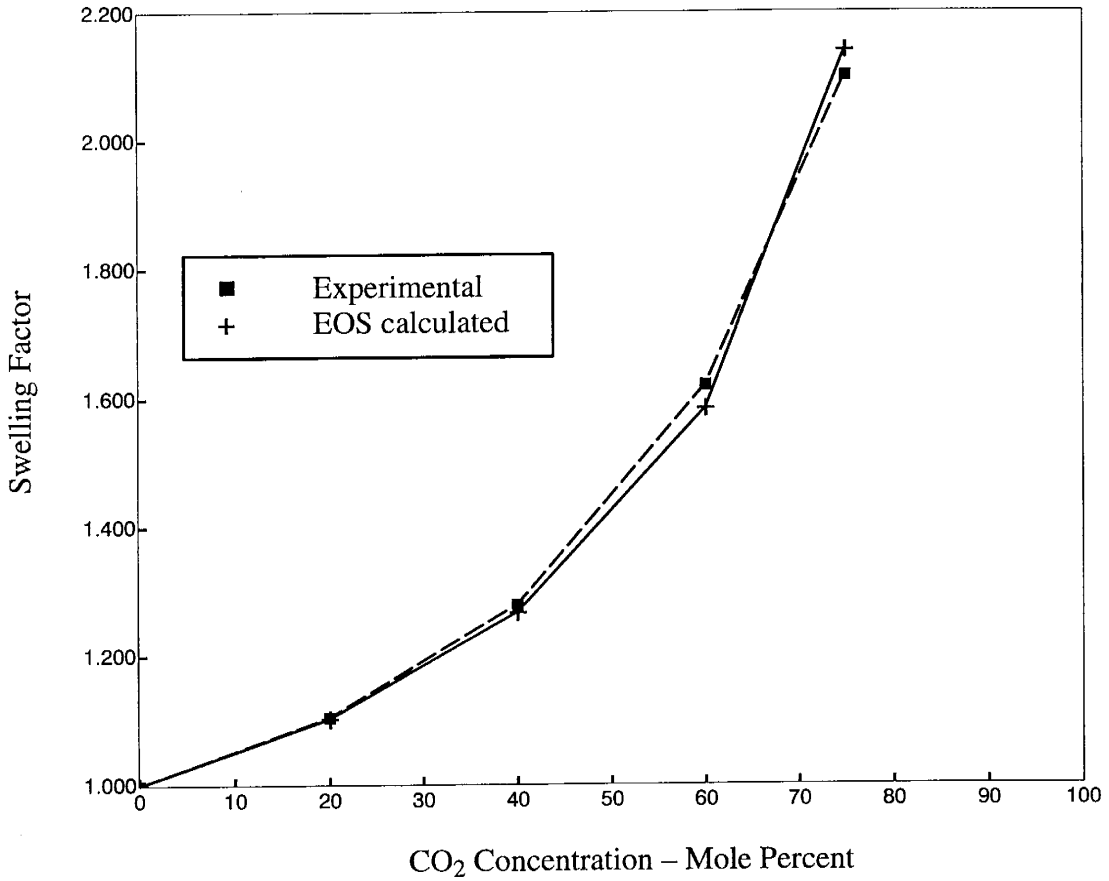

Figure 10–17 – Anasazi Field CO_2 Swelling Factor Comparison

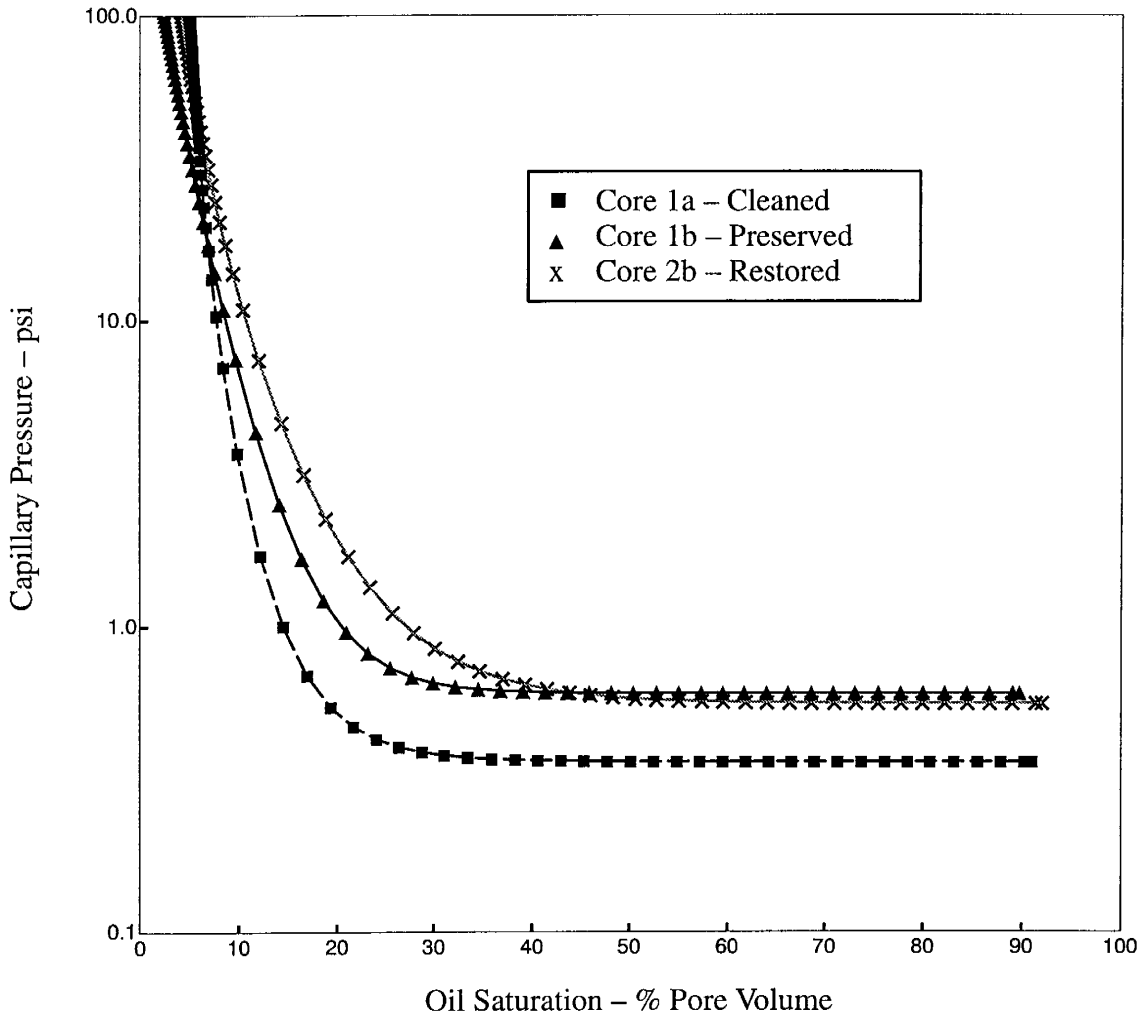

Figure 11–1 Brine – Oil Primary Imbibition Capillary Pressure Data
Anasazi # 6H–1 Dolomite Interval
Elevated Temperature – Automated Centrifuge Data

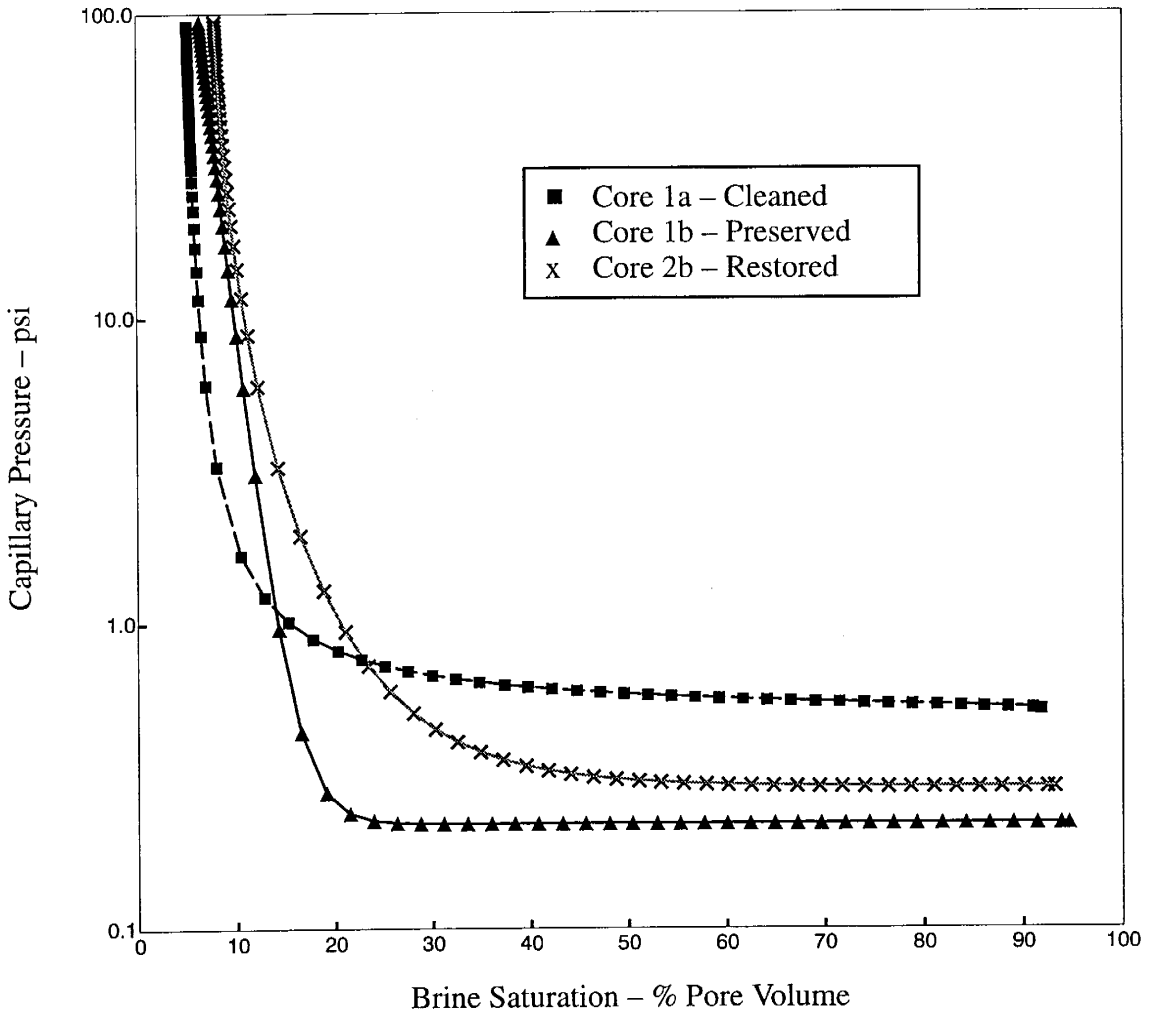

Figure 11–2 Oil – Brine Secondary Drainage Capillary Pressure Data
Anasaz1 # 6H–1 Dolomite Interval
Elevated Temperature – Automated Centrifuge Data

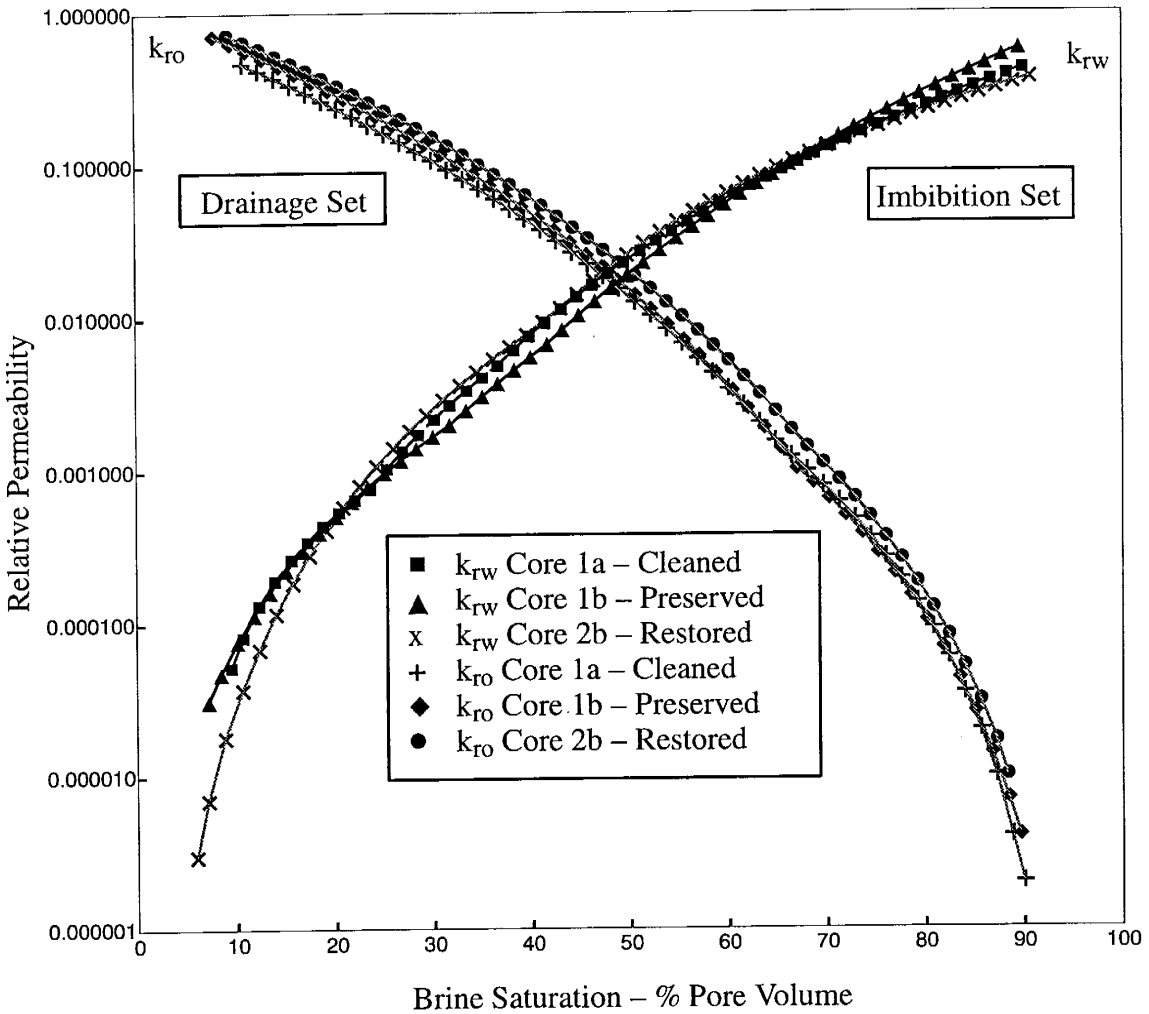

Figure 11–3 Relative Permeability Data – Comparison of Core Preparation Methods
Anasazi # 6H–1 Dolomite Interval
Elevated Temperature – Automated Centrifuge Data

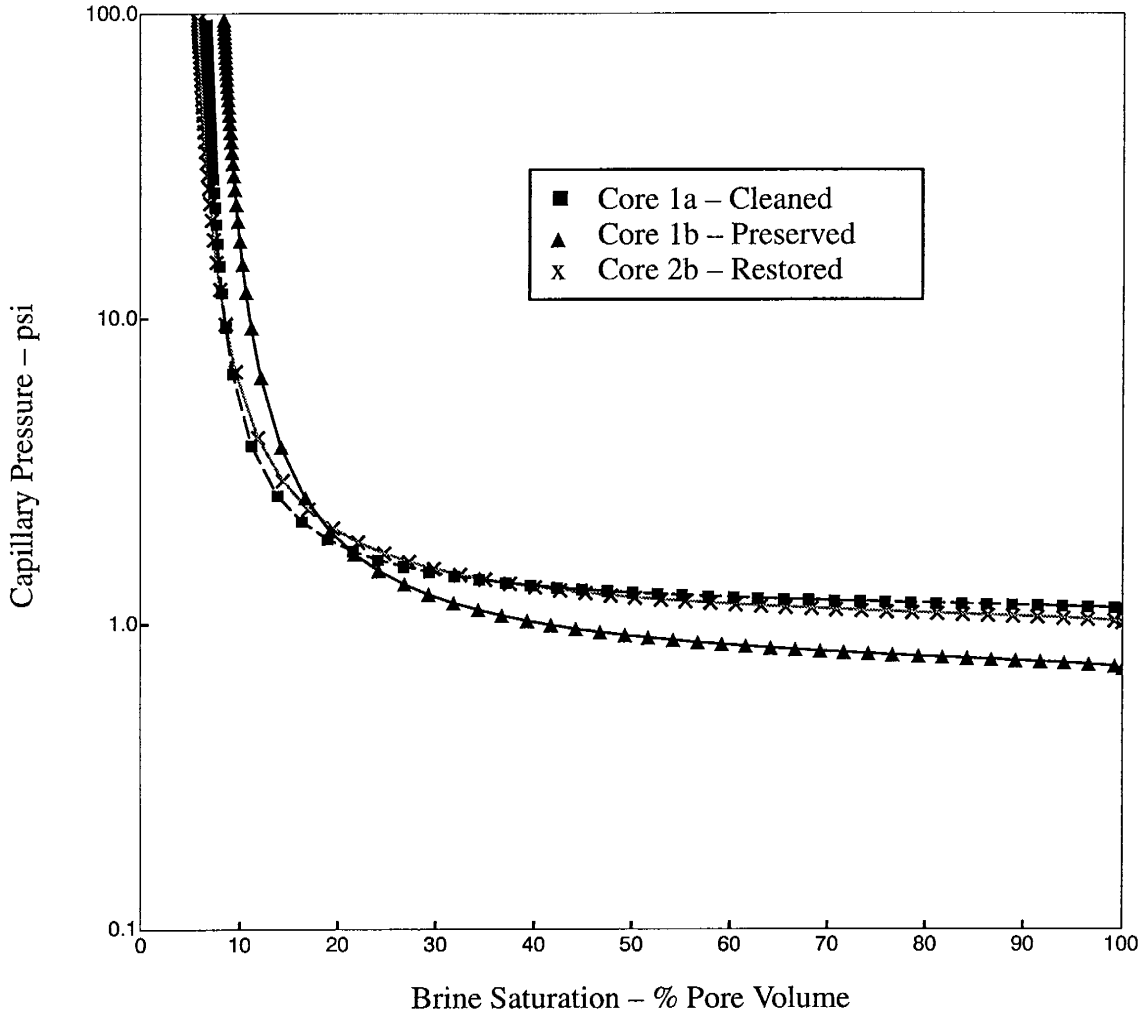

Figure 11–4 Oil – Brine Primary Drainage Capillary Pressure Data
Anasazi # 6H–1 Dolomite Interval
Elevated Temperature – Automated Centrifuge Data

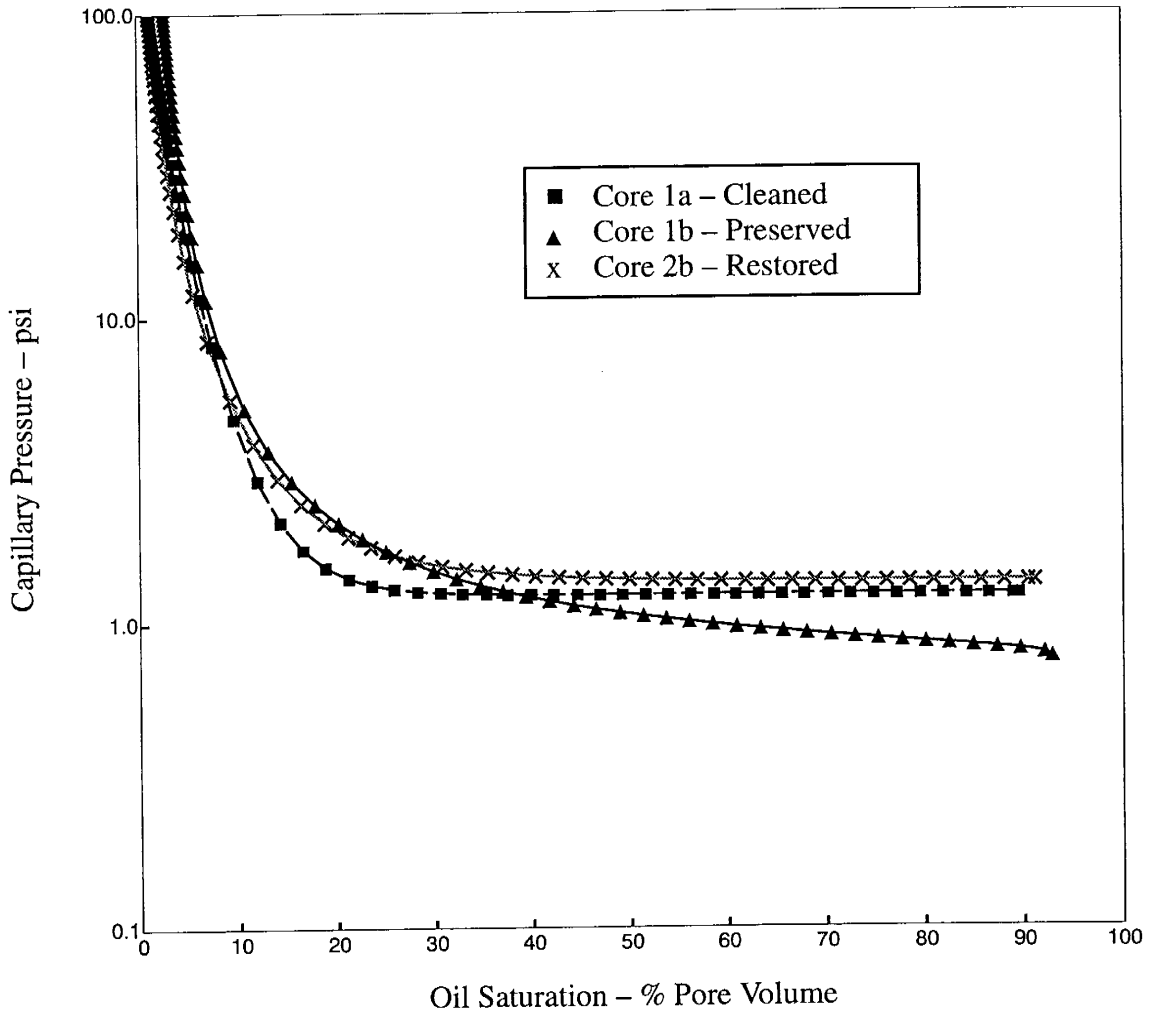

Figure 11–5 Gas – Oil Drainage Capillary Pressure Data
Anasazi # 6H–1 Dolomite Interval
Elevated Temperature – Automated Centrifuge Data

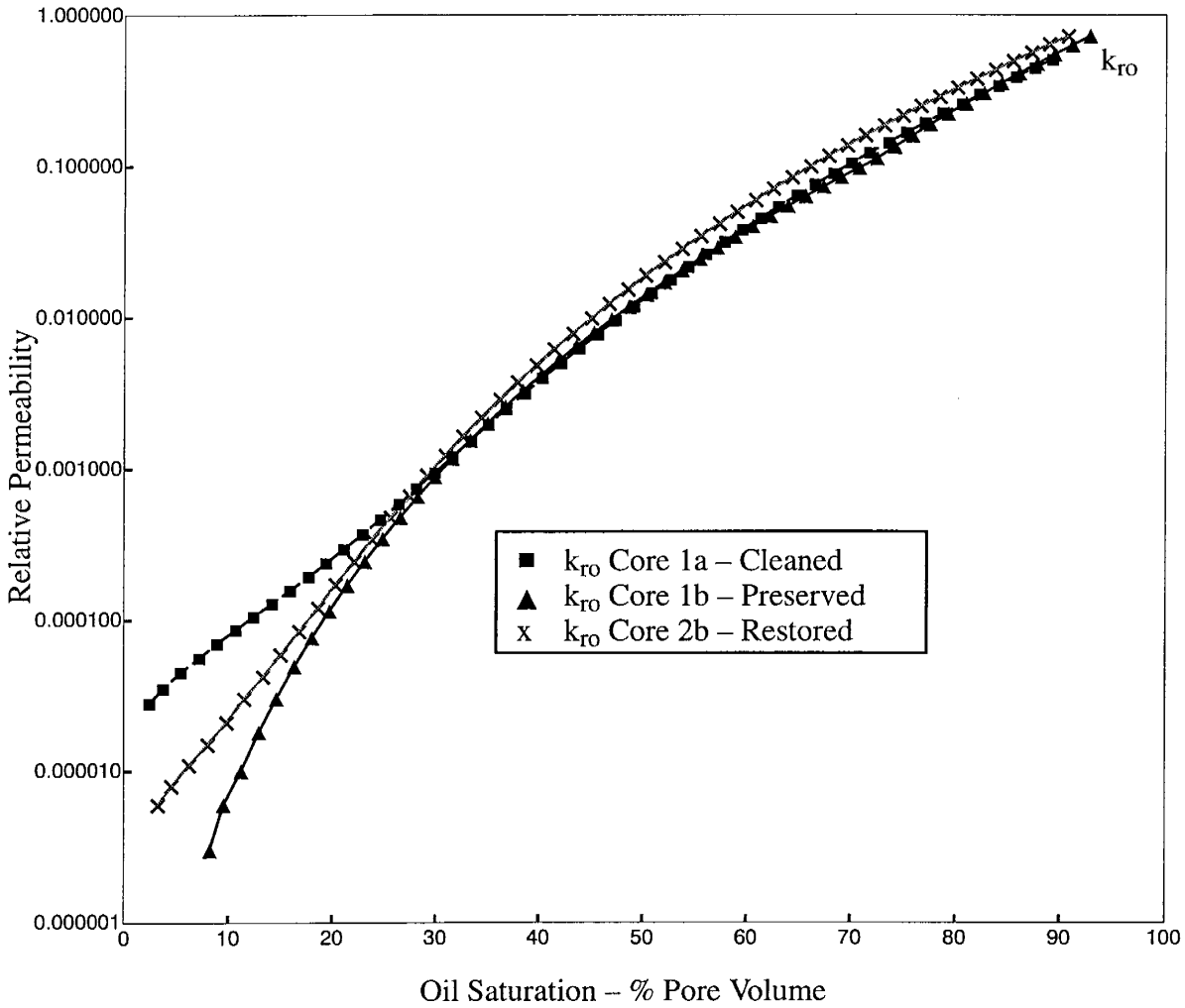

Figure 11–6 Gas – Oil Relative Permeability – Comparison of Core Preparation Methods
Anasazi # 6H–1 Dolomite Interval
Elevated Temperature – Automated Centrifuge Data

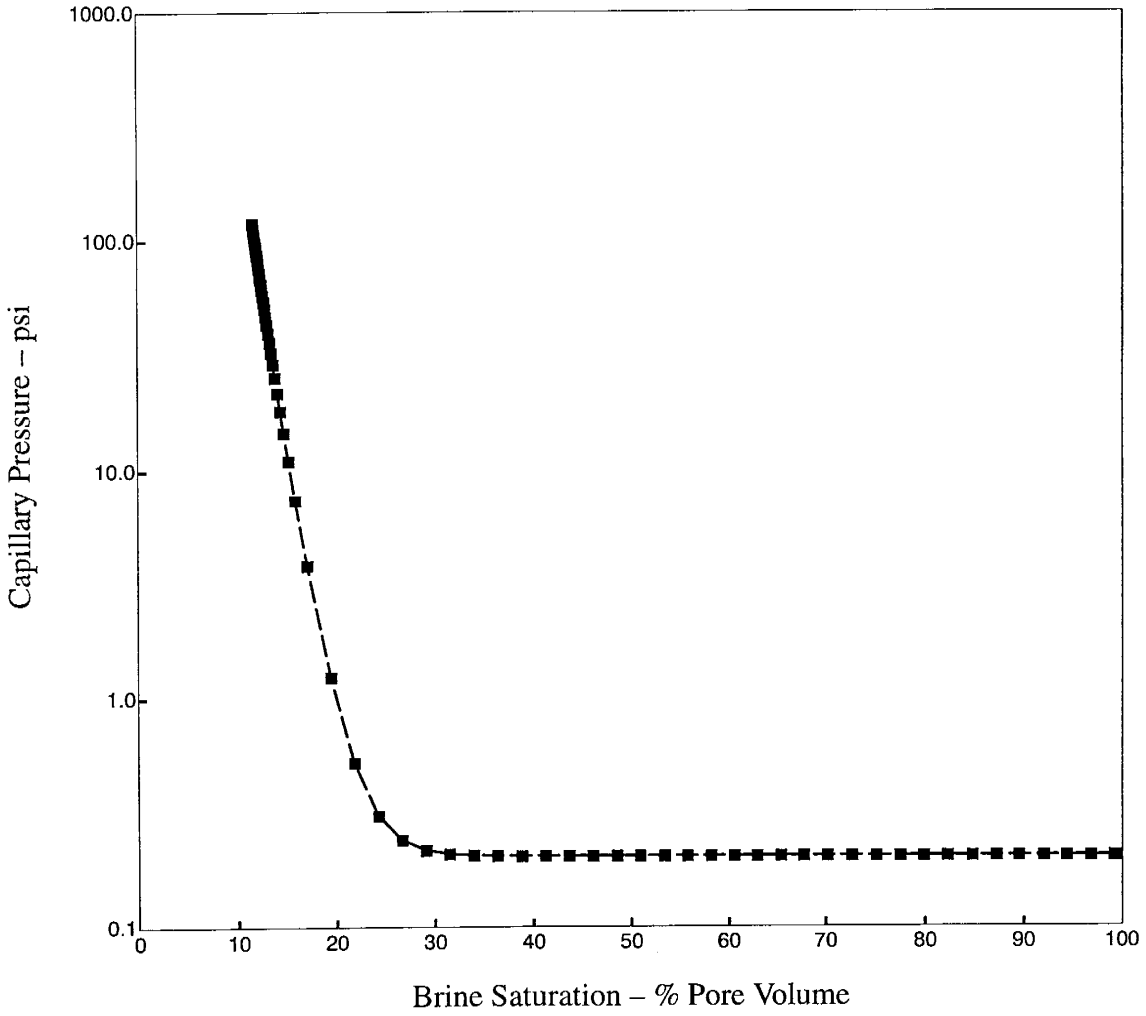

Figure 11–8 Oil – Brine Primary Drainage Capillary Pressure Data
Anasazi #1 – Limestone Interval
Elevated Temperature – Automated Centrifuge Data

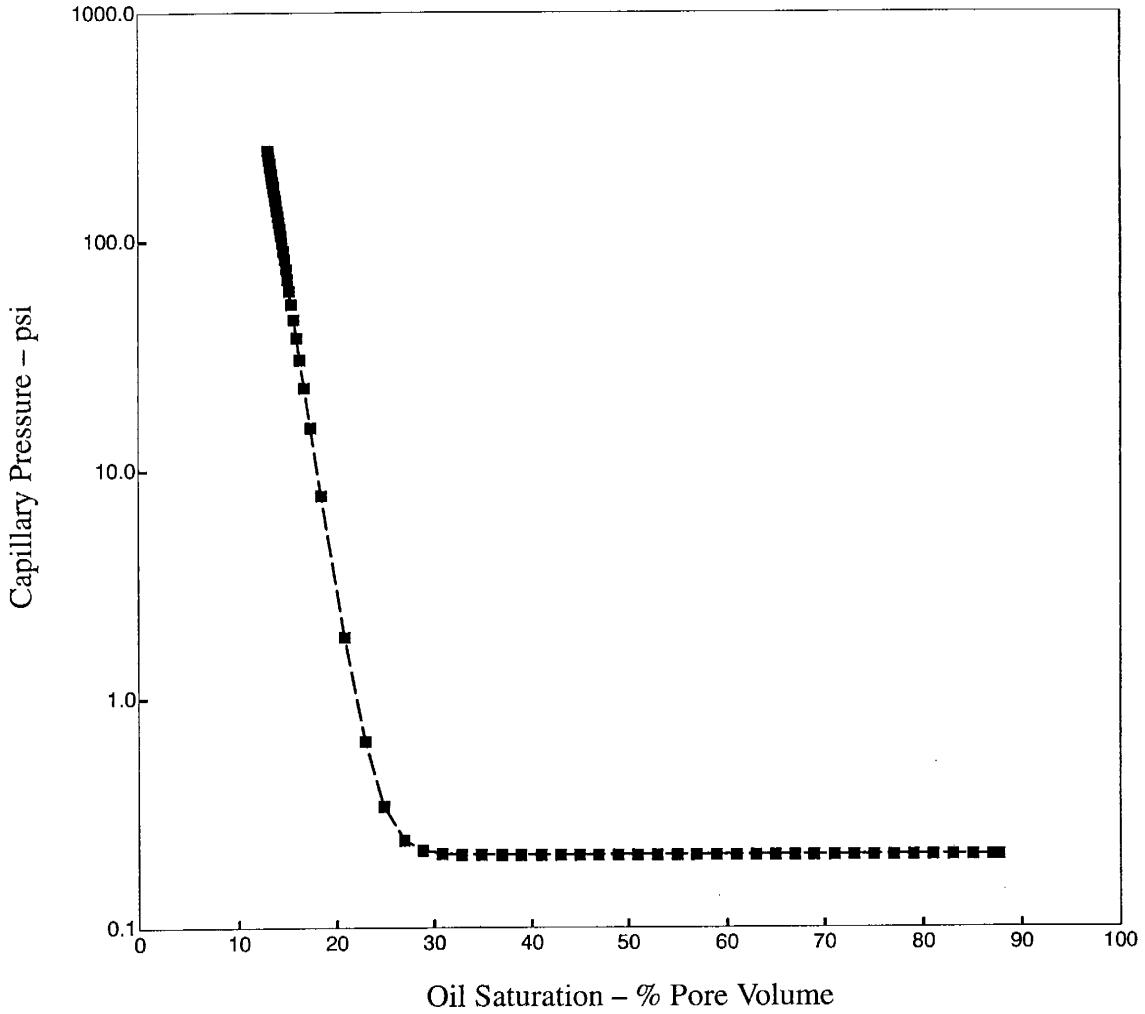

Figure 11–9 Brine – Oil Primary Imbibition Capillary Pressure Data
Anasazi #1 – Limestone Interval
Elevated Temperature – Automated Centrifuge Data

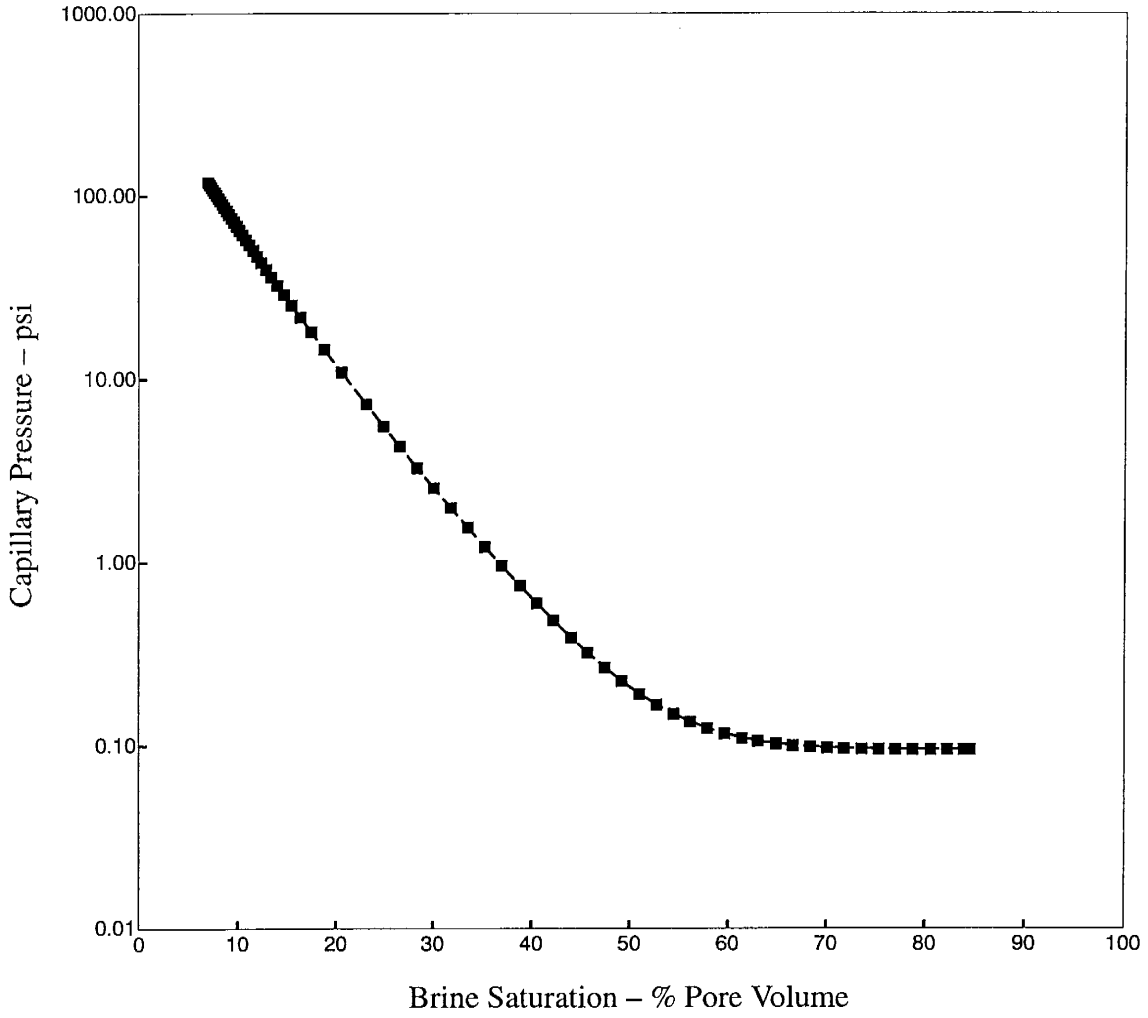

Figure 11–10 Oil – Brine Secondary Drainage Capillary Pressure Data
Anasazi #1 – Limestone Interval
Elevated Temperature – Automated Centrifuge Data

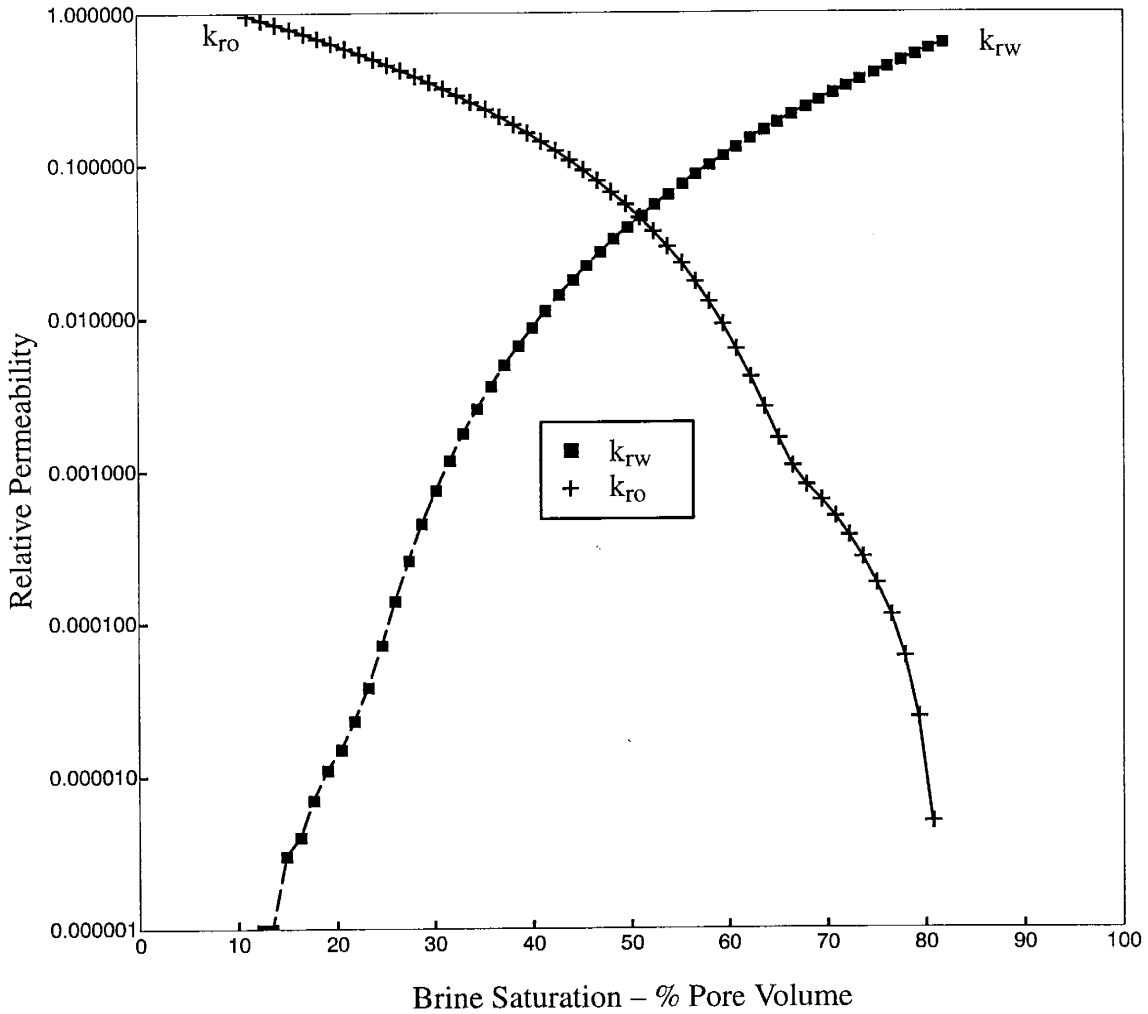

Figure 11–11 Oil – Brine Relative Permeability – Anasazi # 1 Limestone Interval
Elevated Temperature – Automated Centrifuge Data

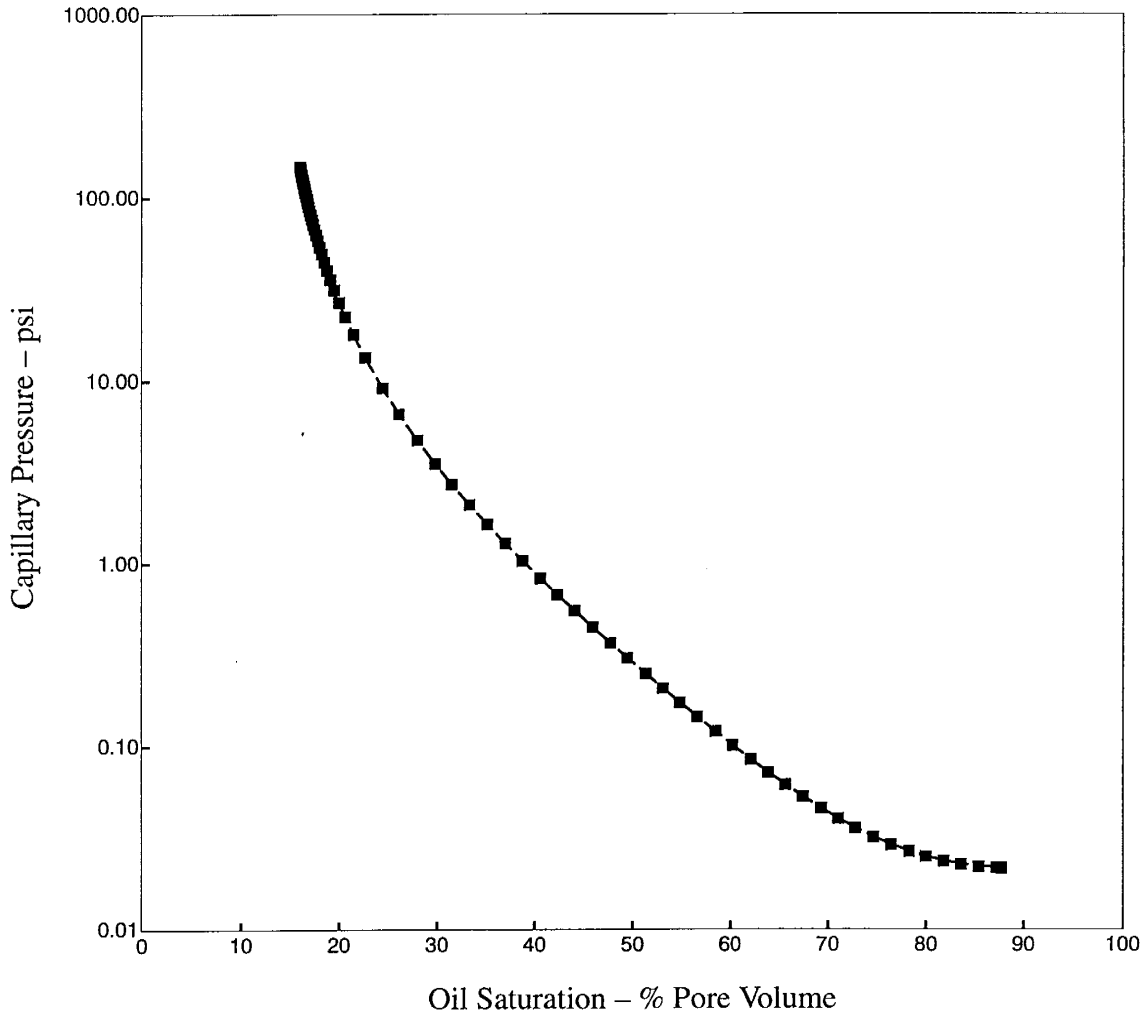

Figure 11–12 Gas – Oil Drainage Capillary Pressure Data
Anasazi #1 – Limestone Interval
Elevated Temperature – Automated Centrifuge Data

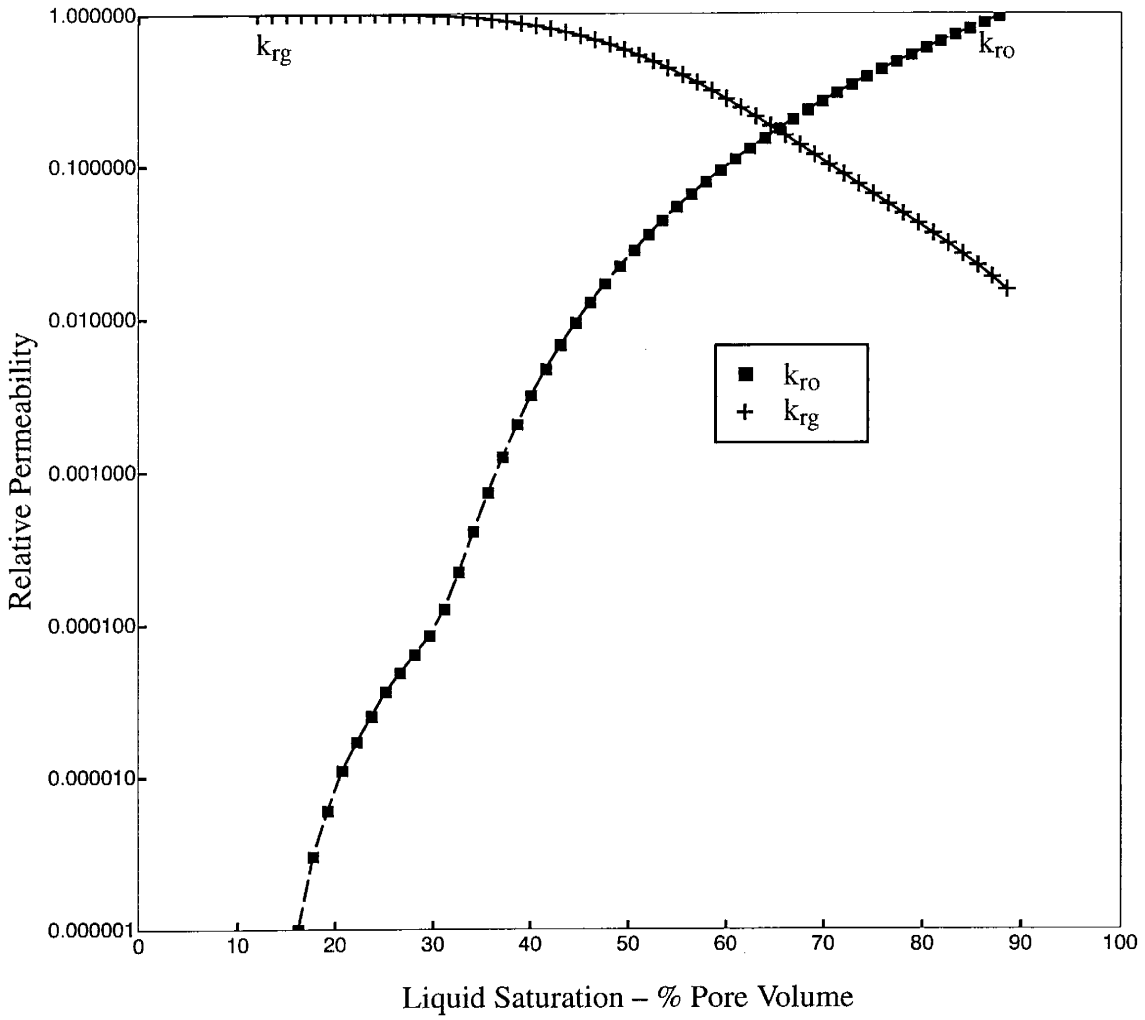

Figure 11–13 Gas – Oil Drainage Relative Permeability – Anasazi # 1 Limestone Interval
Elevated Temperature – Automated Centrifuge Data

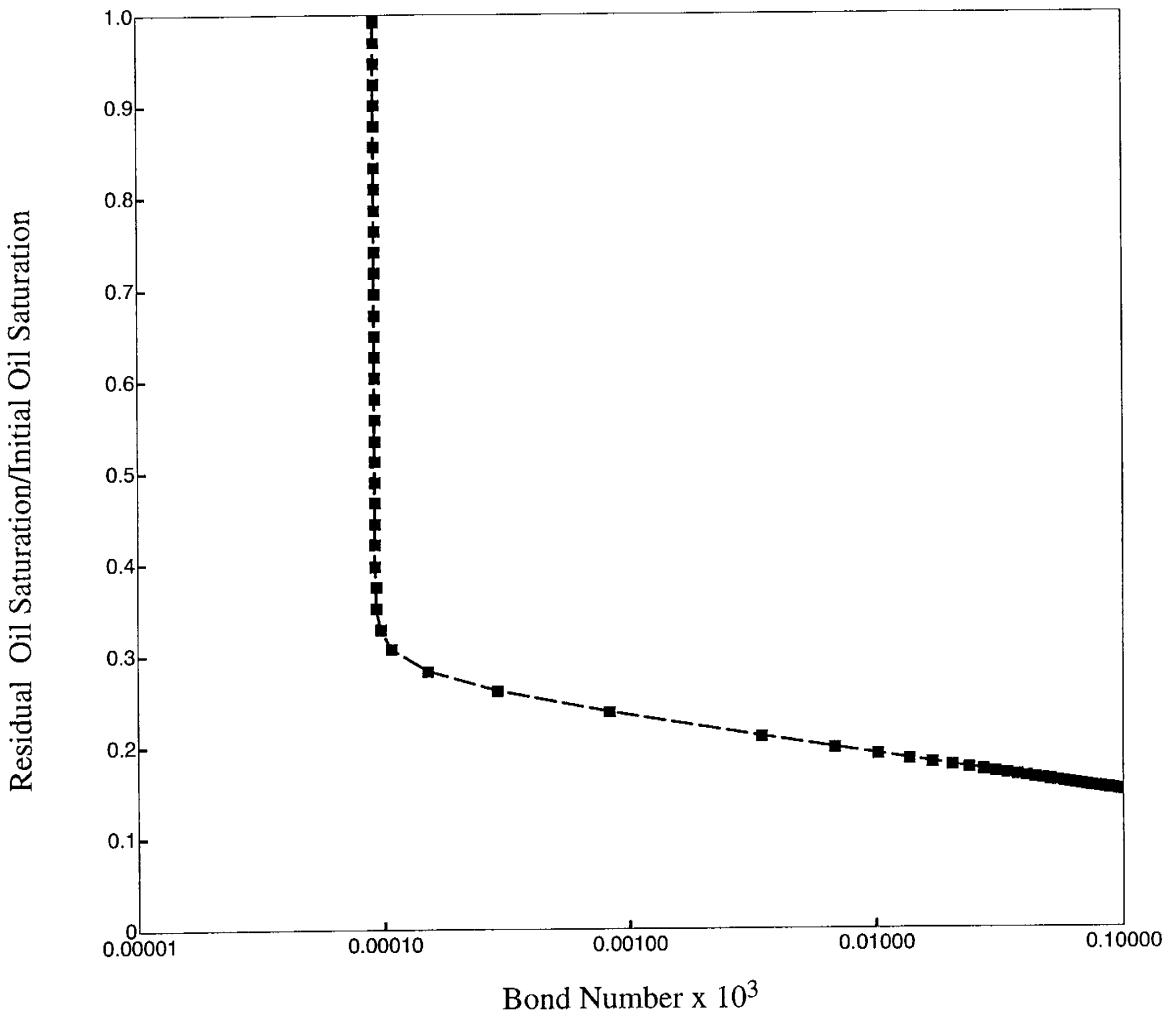

Figure 11–14 Bond Number versus Oil Saturation Ratio
Anasazi # 1 Limestone Interval
Elevated Temperature – Automated Centrifuge Data

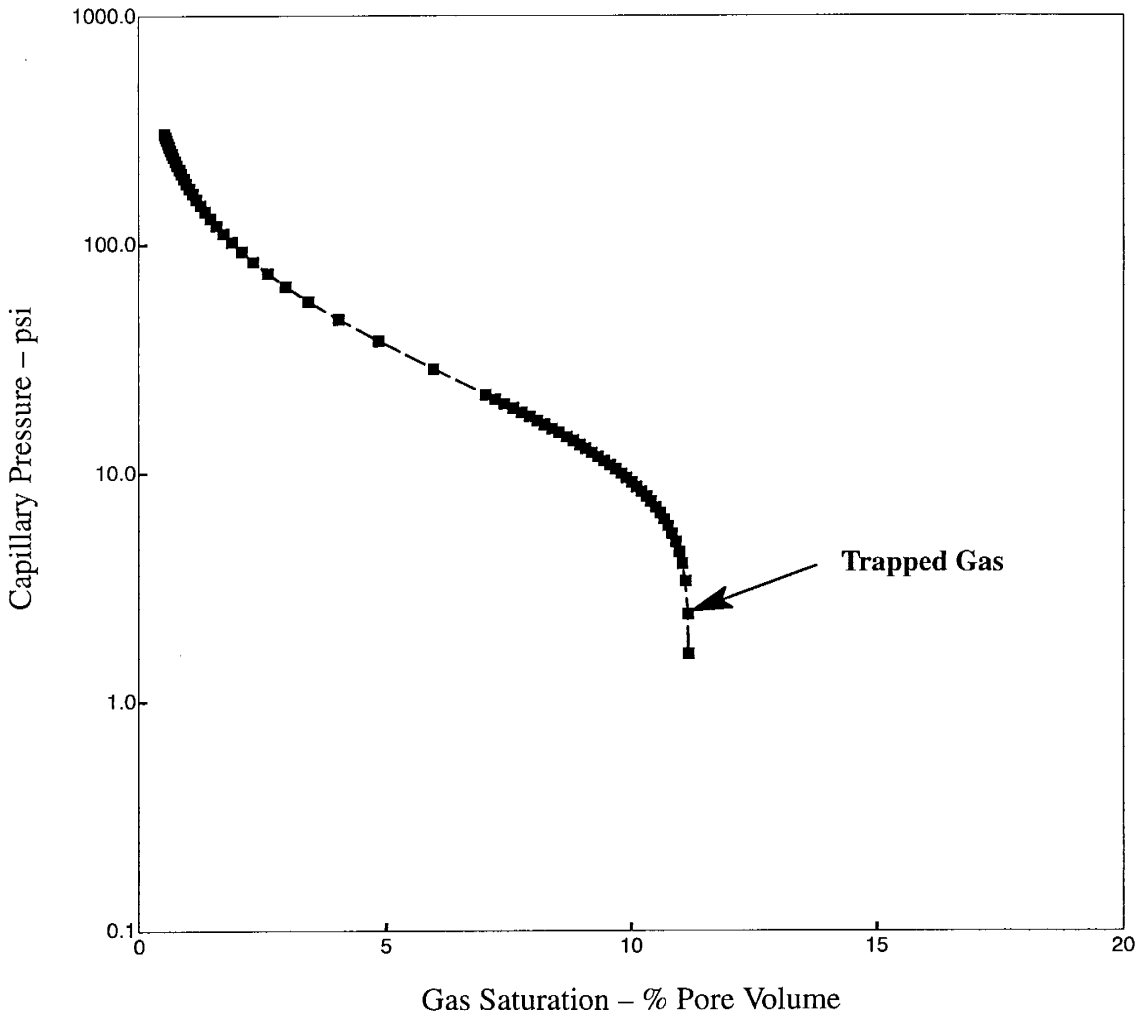

Figure 11–15 Oil – Gas Imbibition Capillary Pressure
Anasazi # 1 Limestone Interval
Elevated Temperature – Automated Centrifuge Data

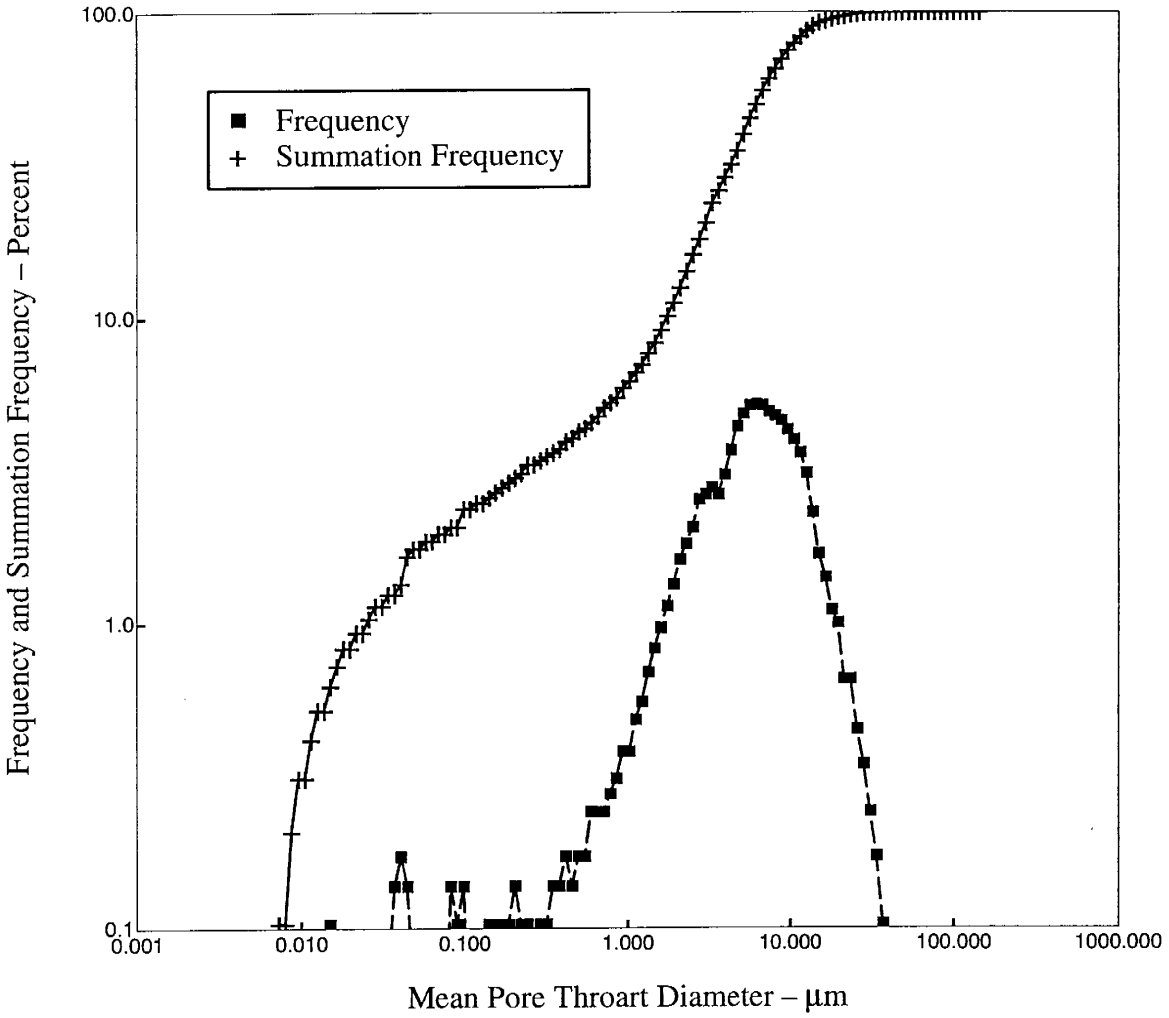

Figure 11–16 Mean Pore Size Distribution
Anasazi # 6H–1 Dolomite Interval
Mercury Capillary Pressure Data

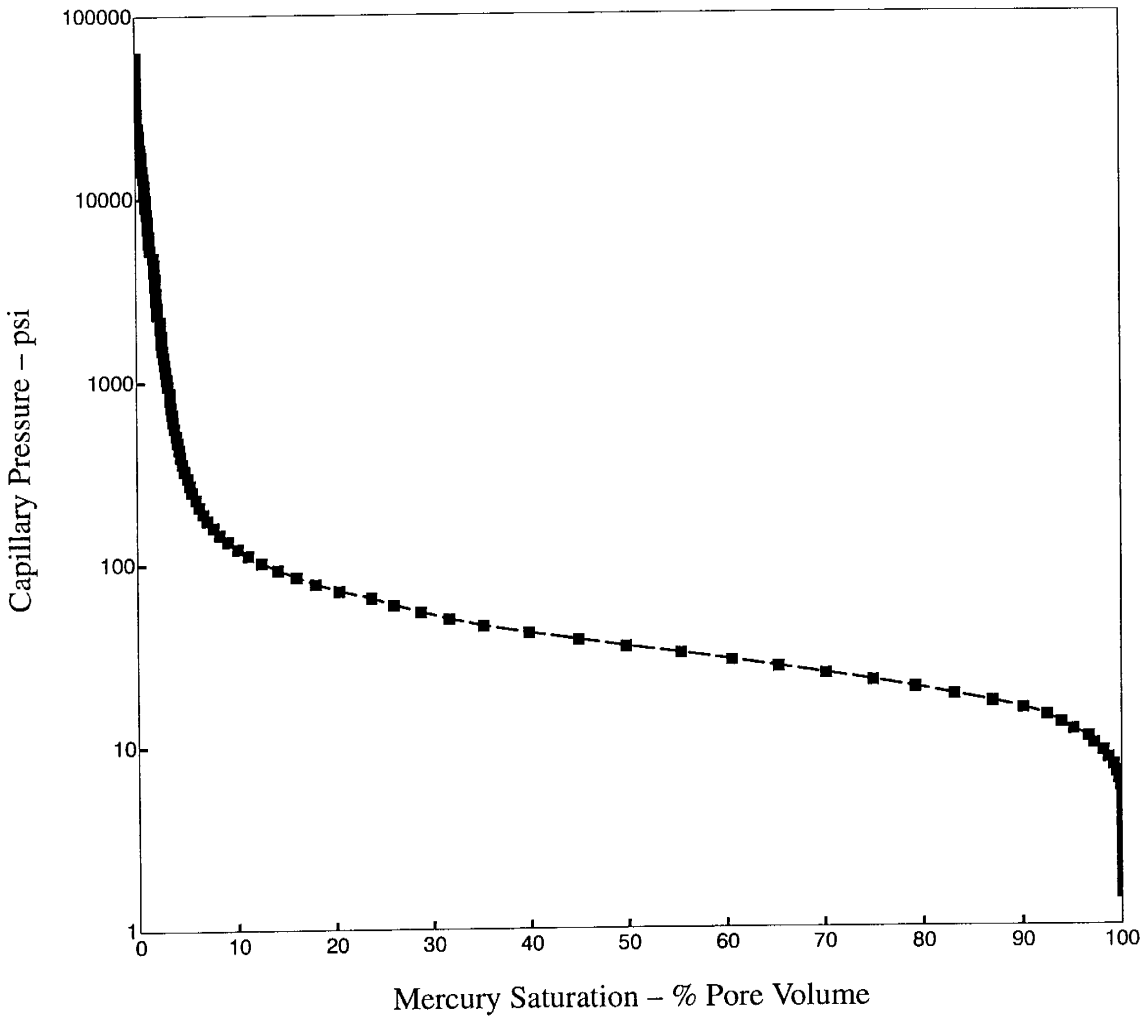

Figure 11–17 Mercury Capillary Pressure
Anasazi # 6H–1 Dolomite Interval
Mercury Capillary Pressure Data

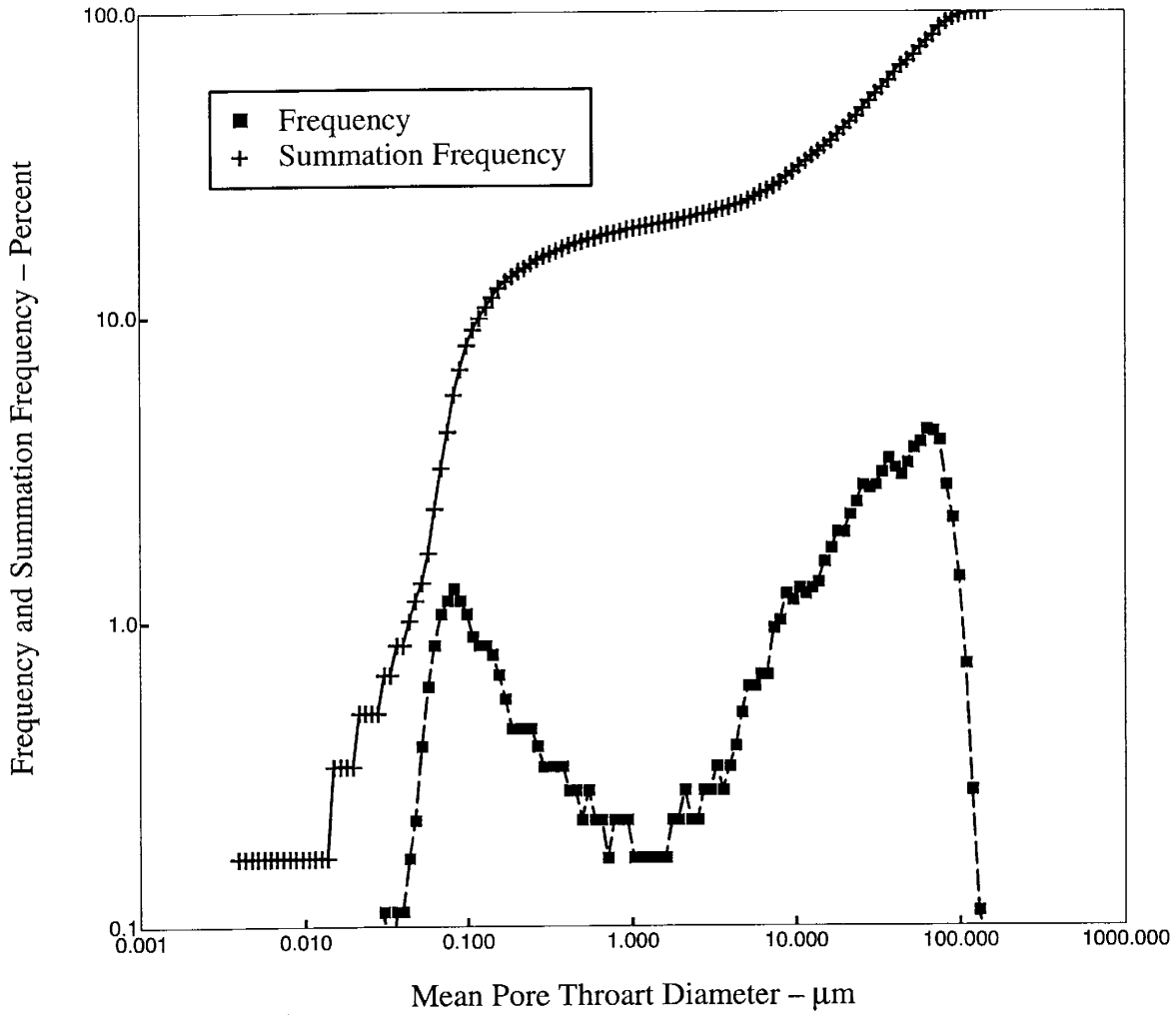

Figure 11–18 Mean Pore Size Distribution
Anasazi # 1 Limestone Interval
Mercury Capillary Pressure Data

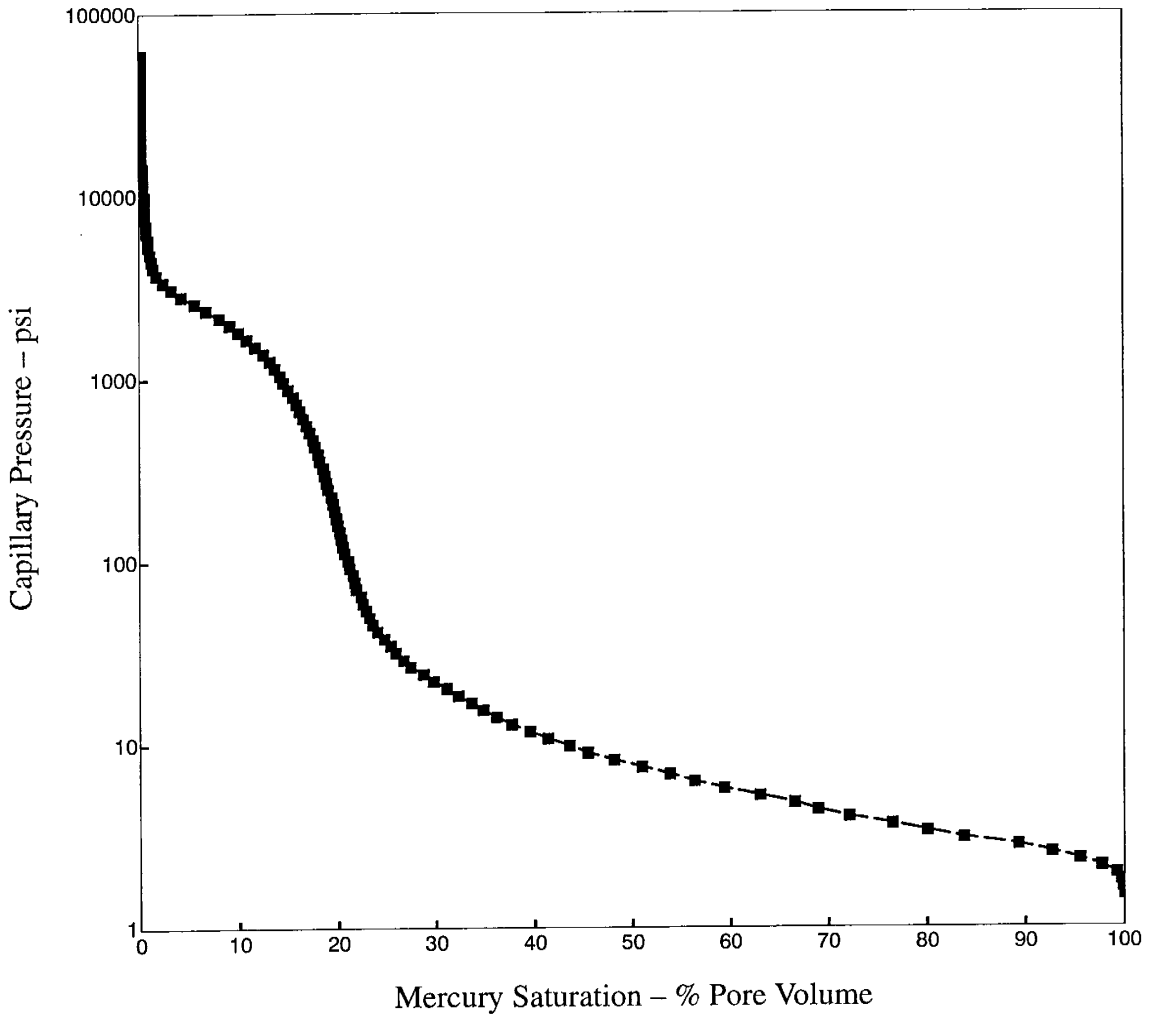

Figure 11–19 Mercury Capillary Pressure
Anasazi # 1 Limestone Interval
Mercury Capillary Pressure Data

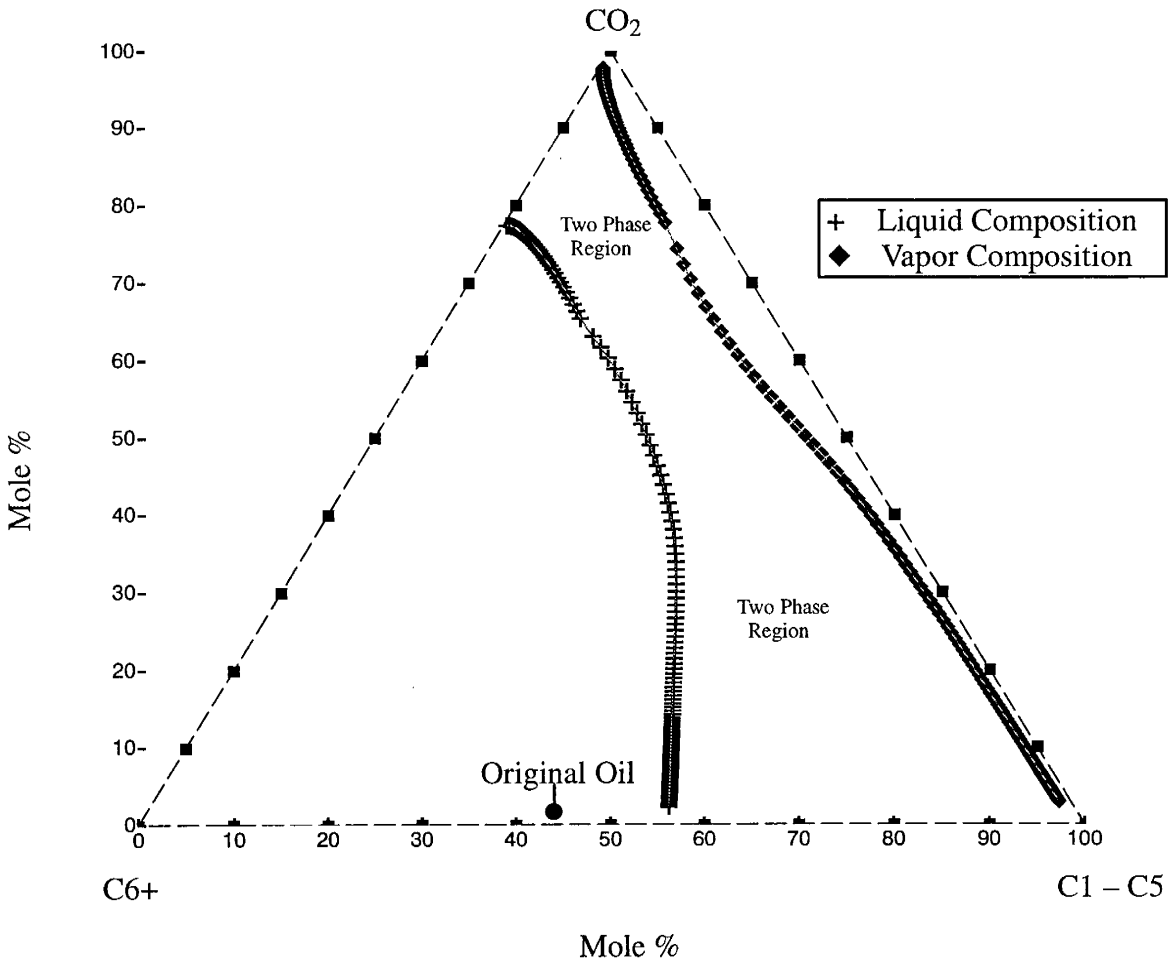

Figure 12–1 – Pseudo Ternary Diagram – Original Oil at 2000 psia and 130°F
Multiple Contact Immiscible Displacement

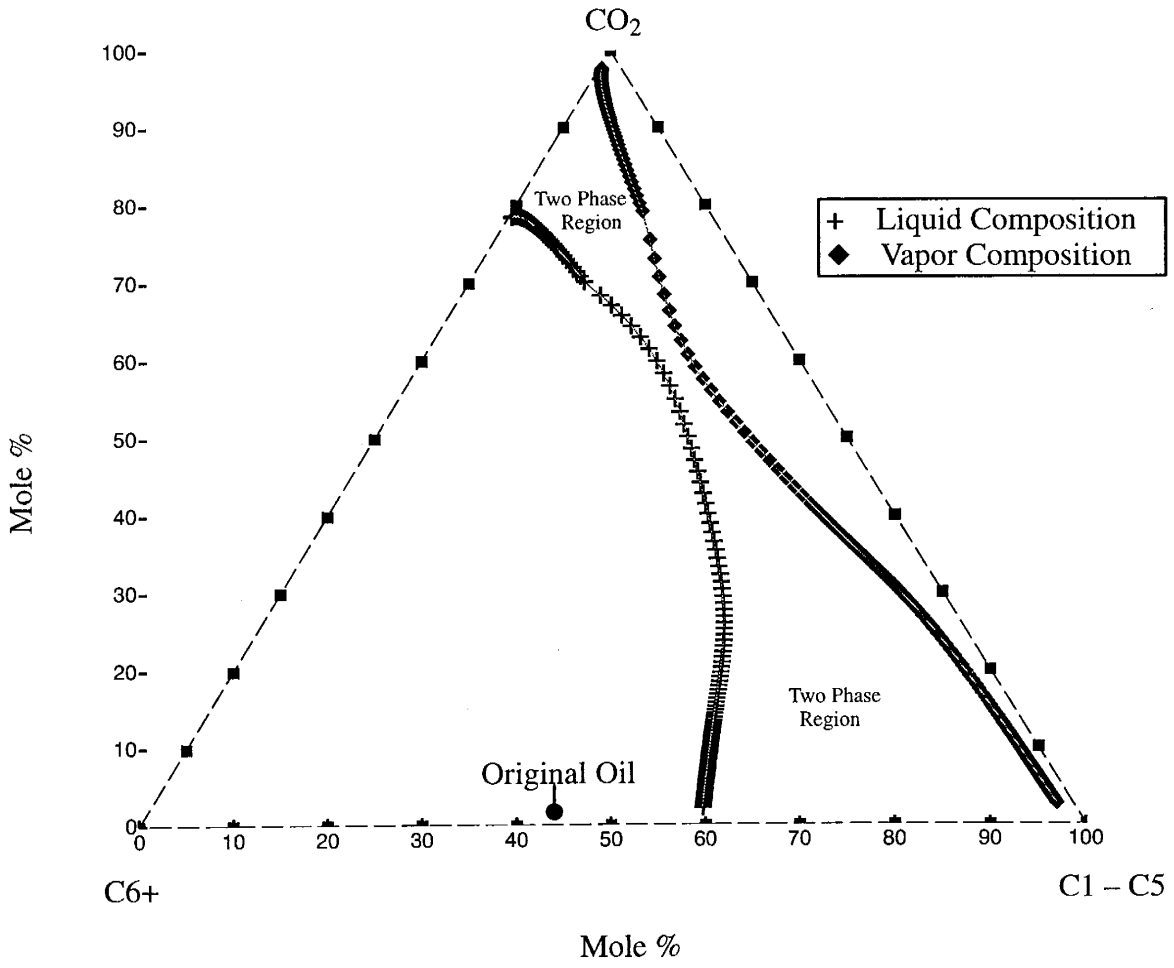

Figure 12–2 – Pseudo Ternary Diagram – Original Oil at 2350 psia and 130°F
Multiple Contact Immiscible Displacement

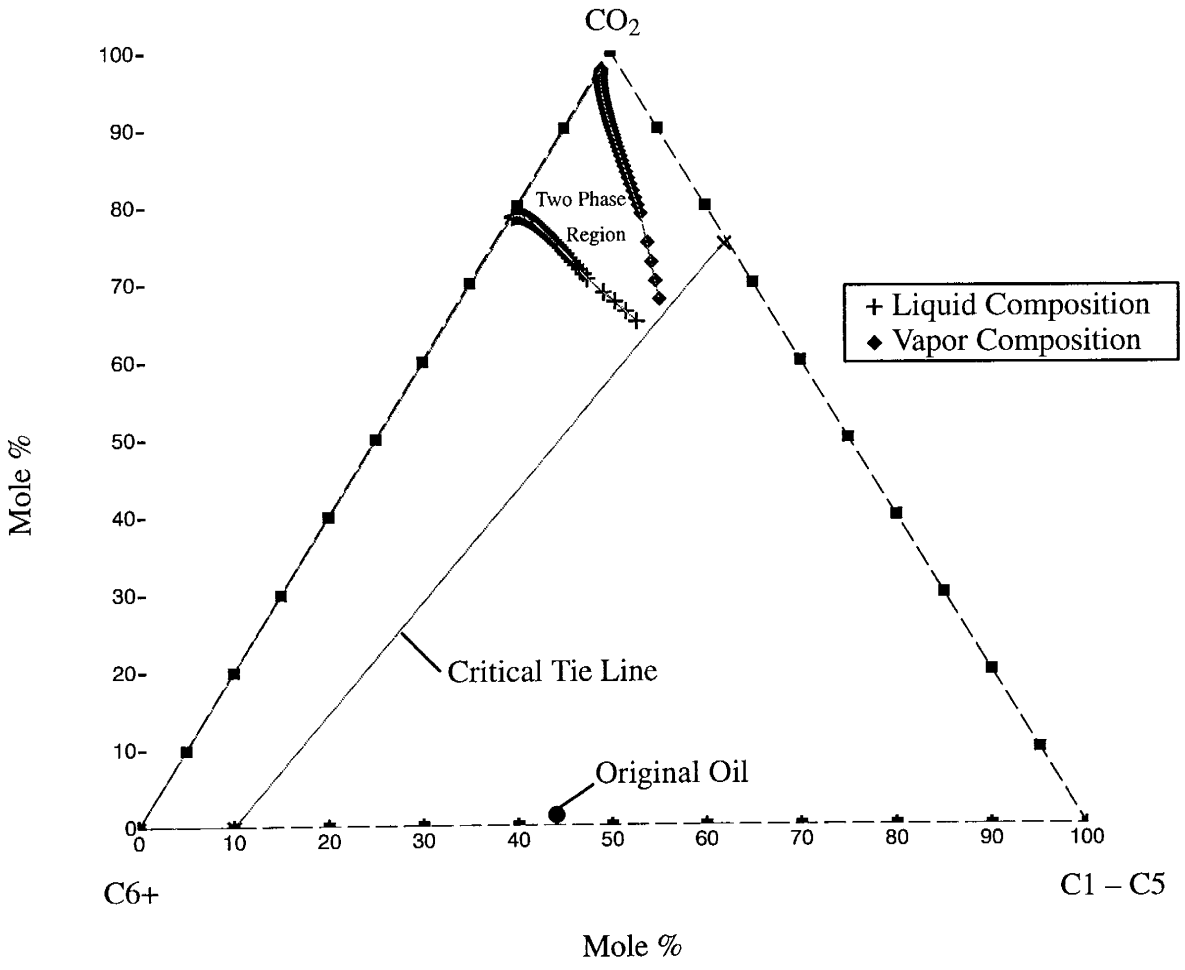

Figure 12–3 – Pseudo Ternary Diagram – Original Oil at 2400 psia and 130°F
Multiple Contact Miscible

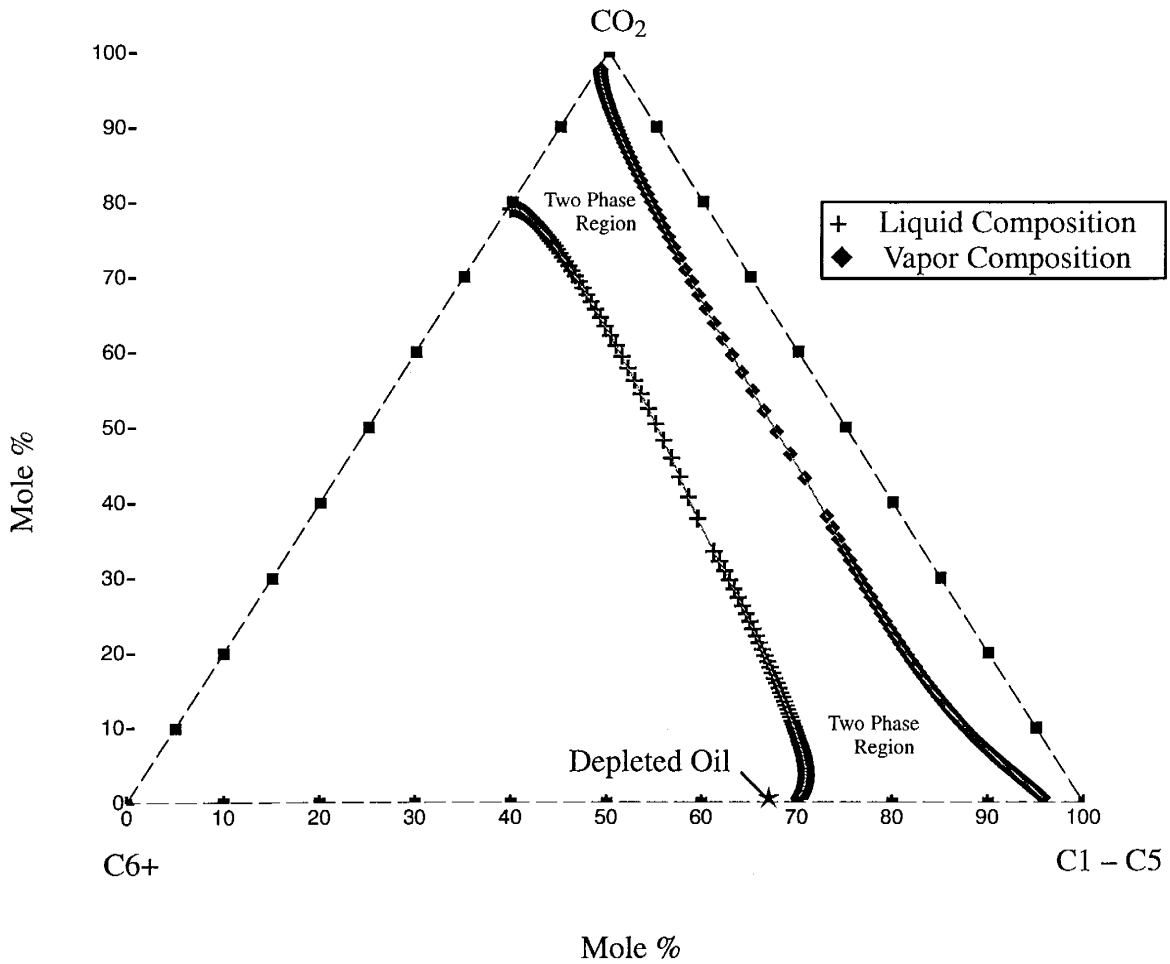

Figure 12–4 – Pseudo Ternary Diagram – Depleted Oil at 2500 psia and 130°F
Multiple Contact Immiscible Displacement

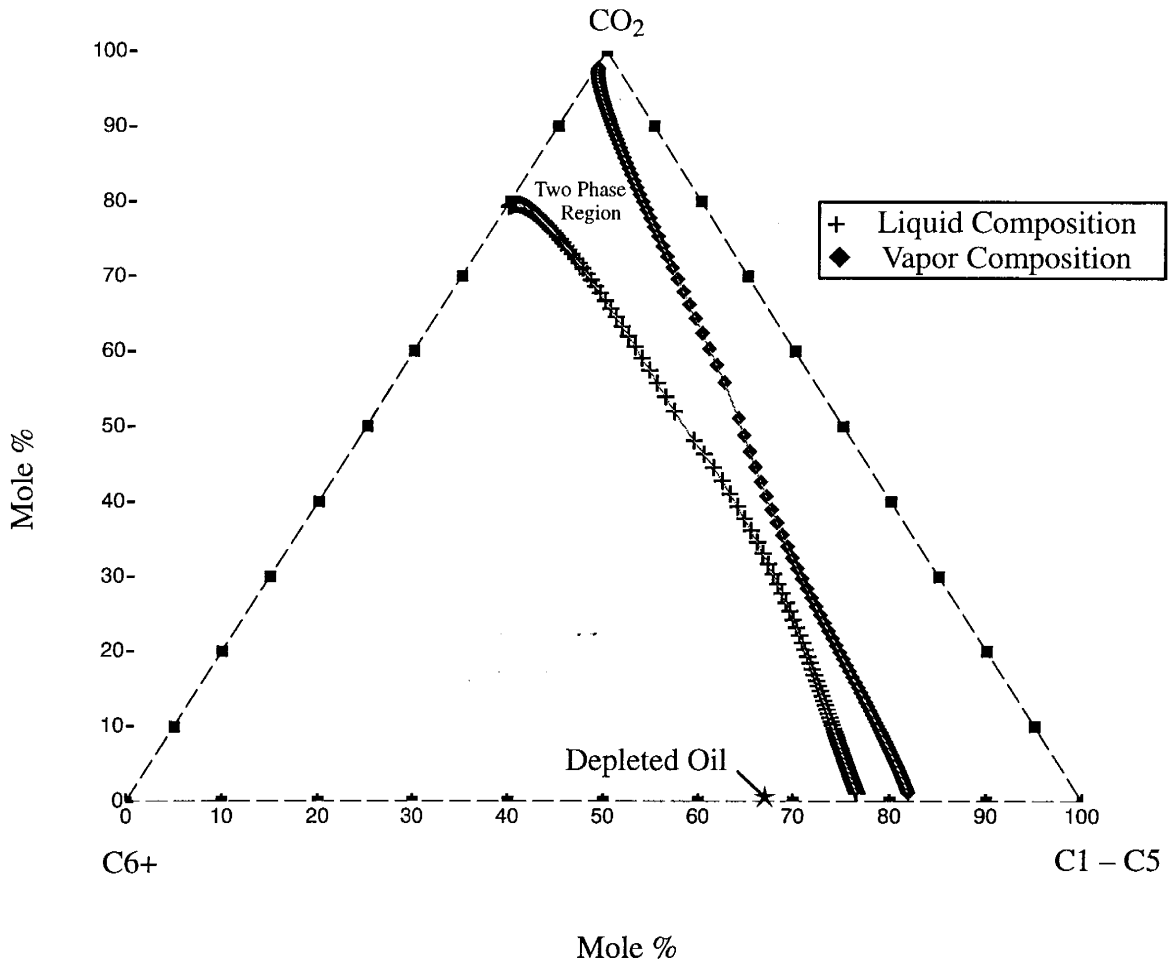

Figure 12–5 – Pseudo Psuedo Ternary Diagram – Depleted Oil at 3000 psia and 130°F
Multiple Contact Immiscible Displacement

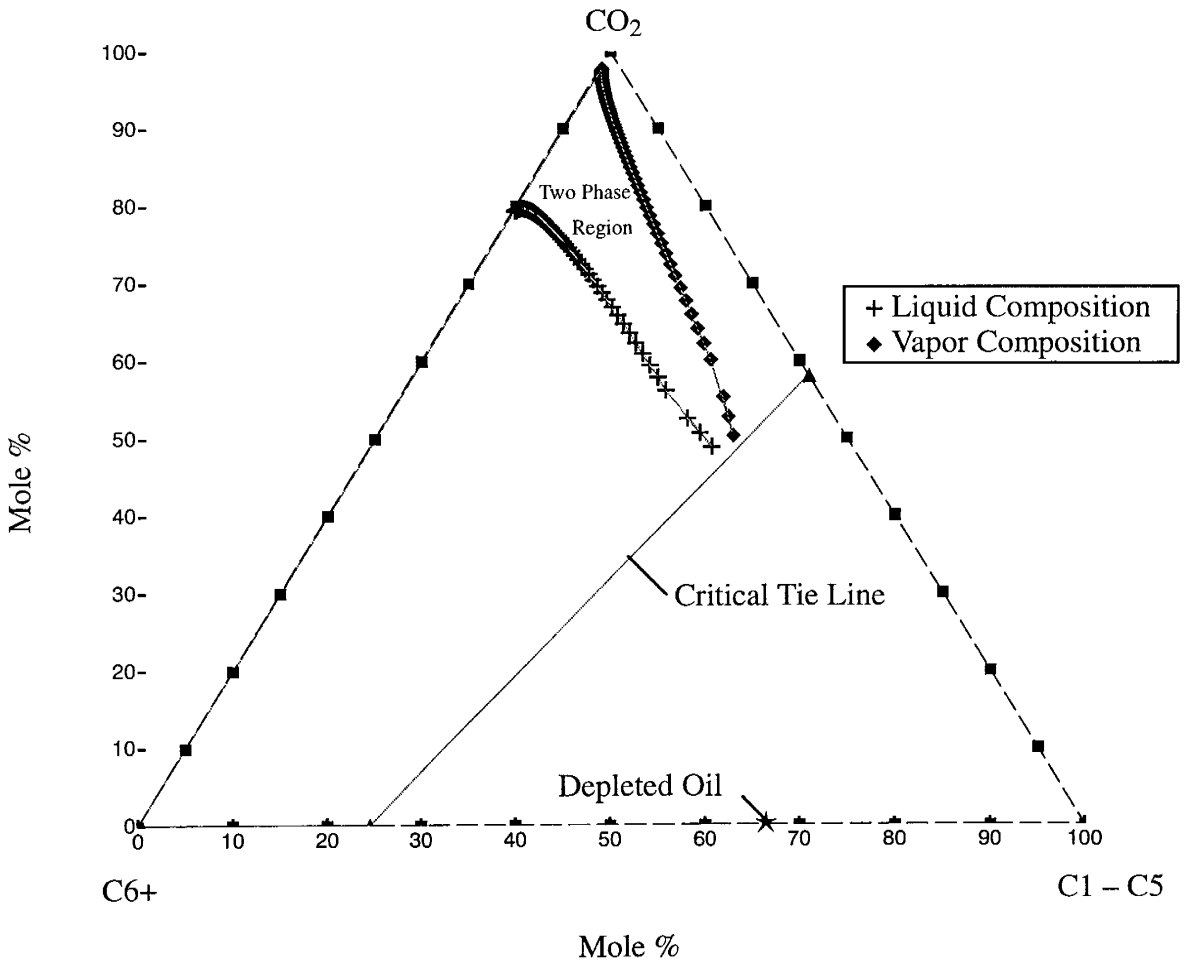

Figure 12–6 Pseudo Ternary Diagram – Original Oil at 3100 psia and 130°F
Multiple Contact Miscible

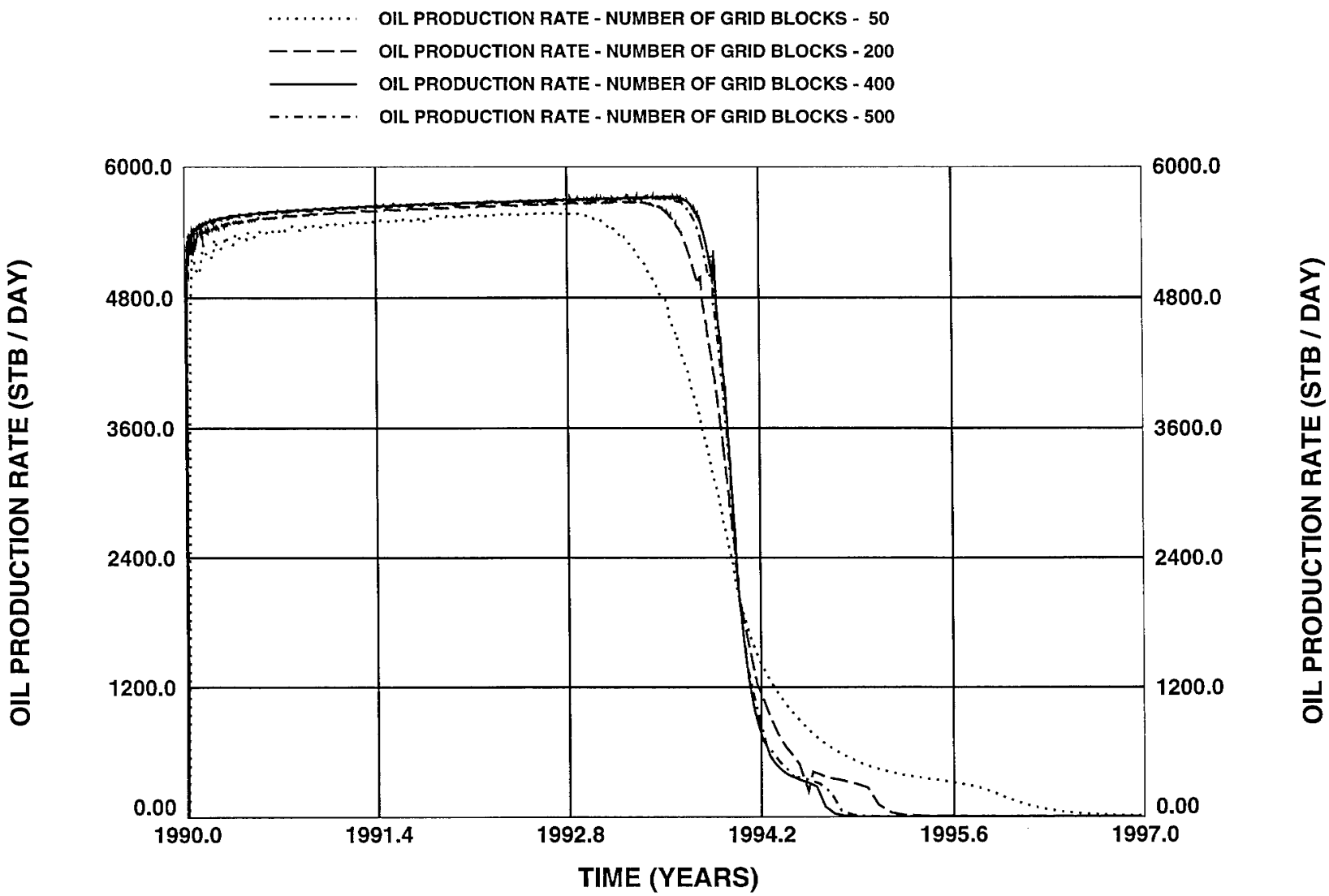

Figure 12-7 Oil Production Sensitivity to Grid Block Size

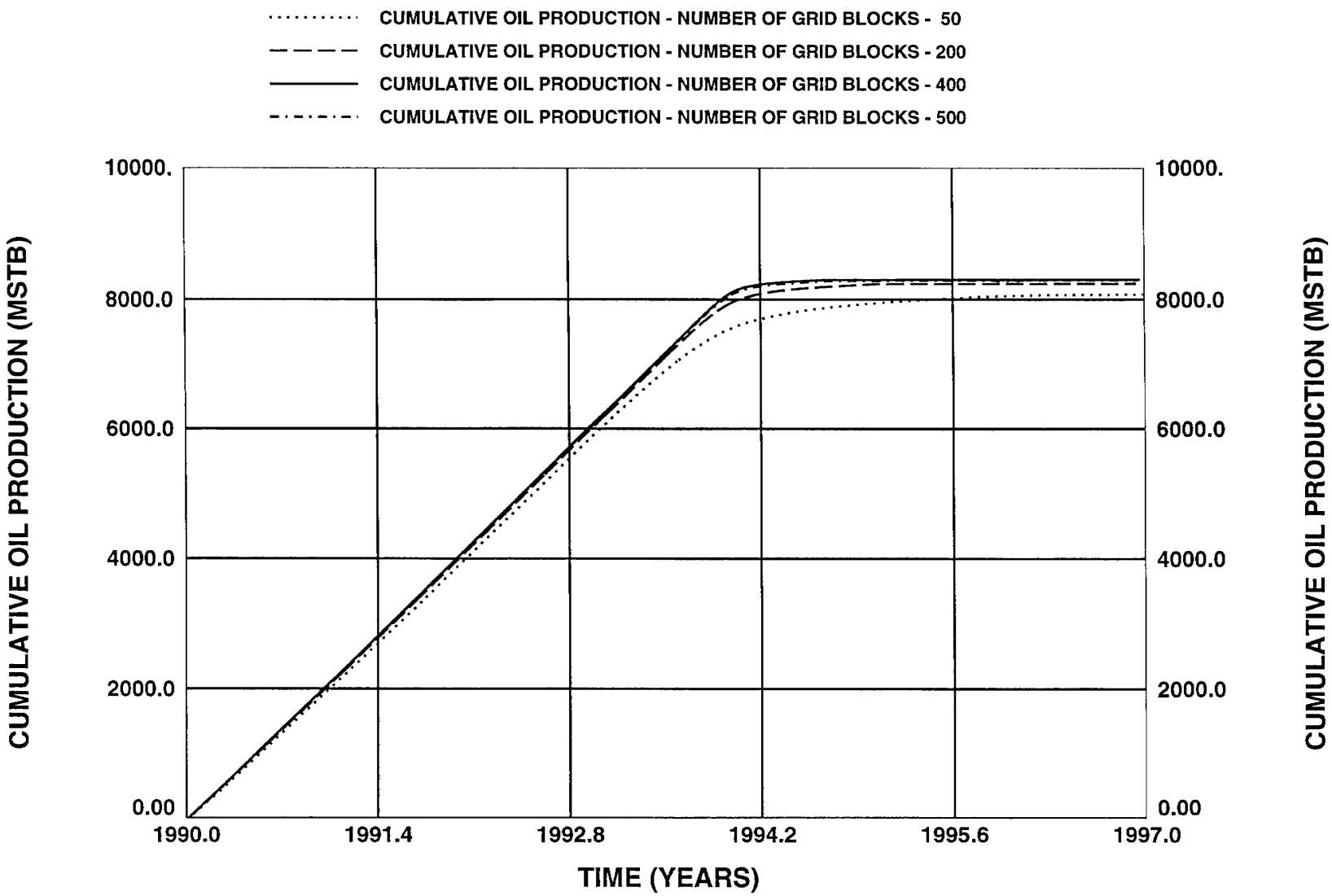

Figure 12-8 Oil Recovery Sensitivity to Grid Block Size

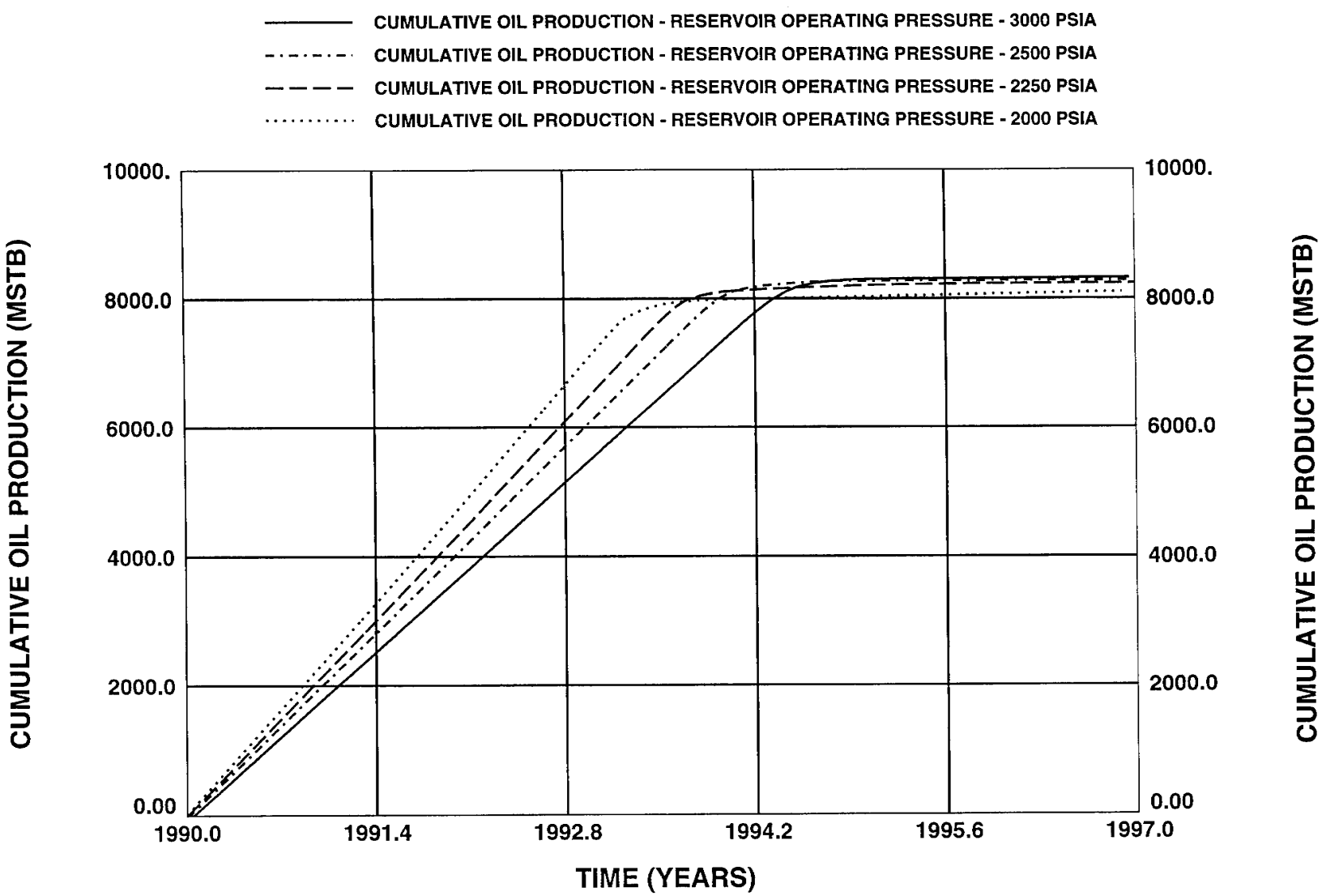

Figure 12-9 Oil Recovery Sensitivity to Displacement Pressure

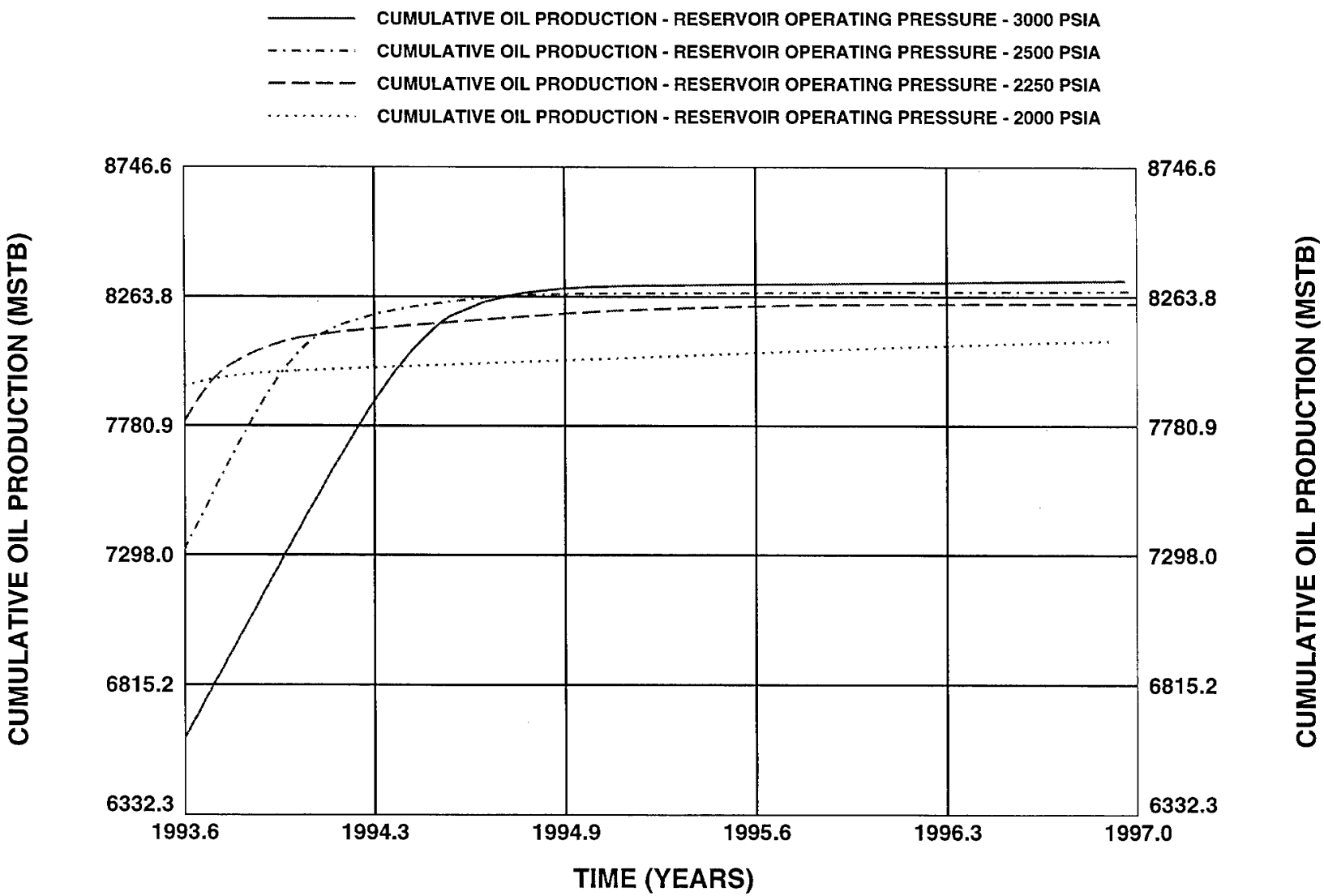

Figure 12-10 Oil Recovery Sensitivity to Displacement Pressure - Expanded View

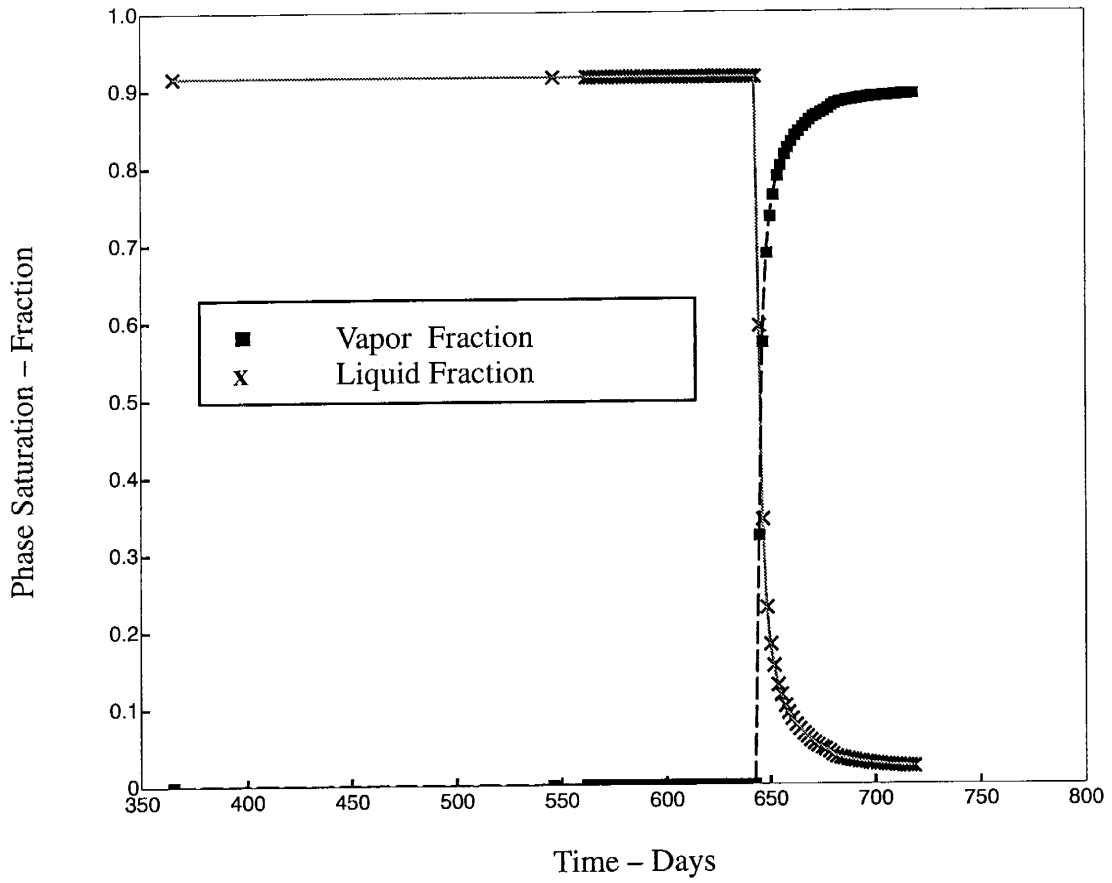

Figure 12–11 CO_2 Displacement at 2500 PSIA – Phase Saturation Versus Time for Cell 217

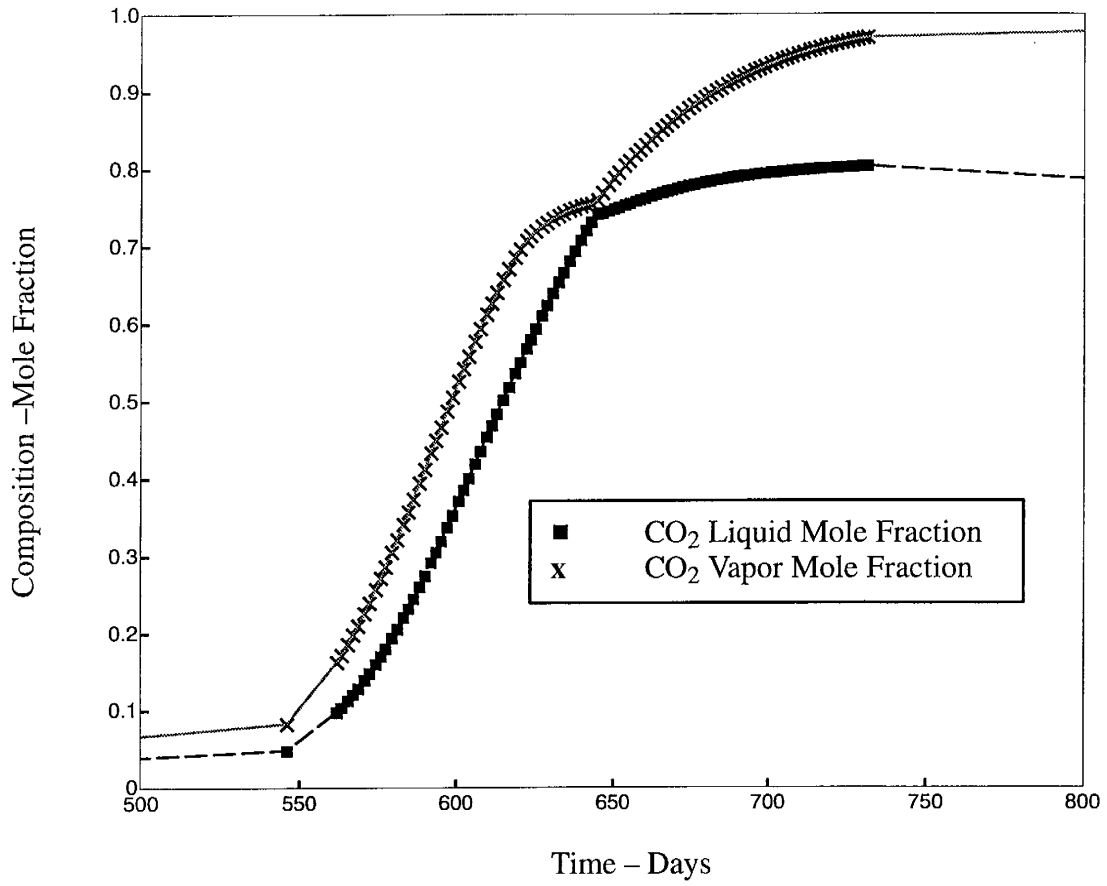

Figure 12–12 CO_2 Displacement at 2500 PSIA – Composition Versus Time for Cell 217 Component CO_2

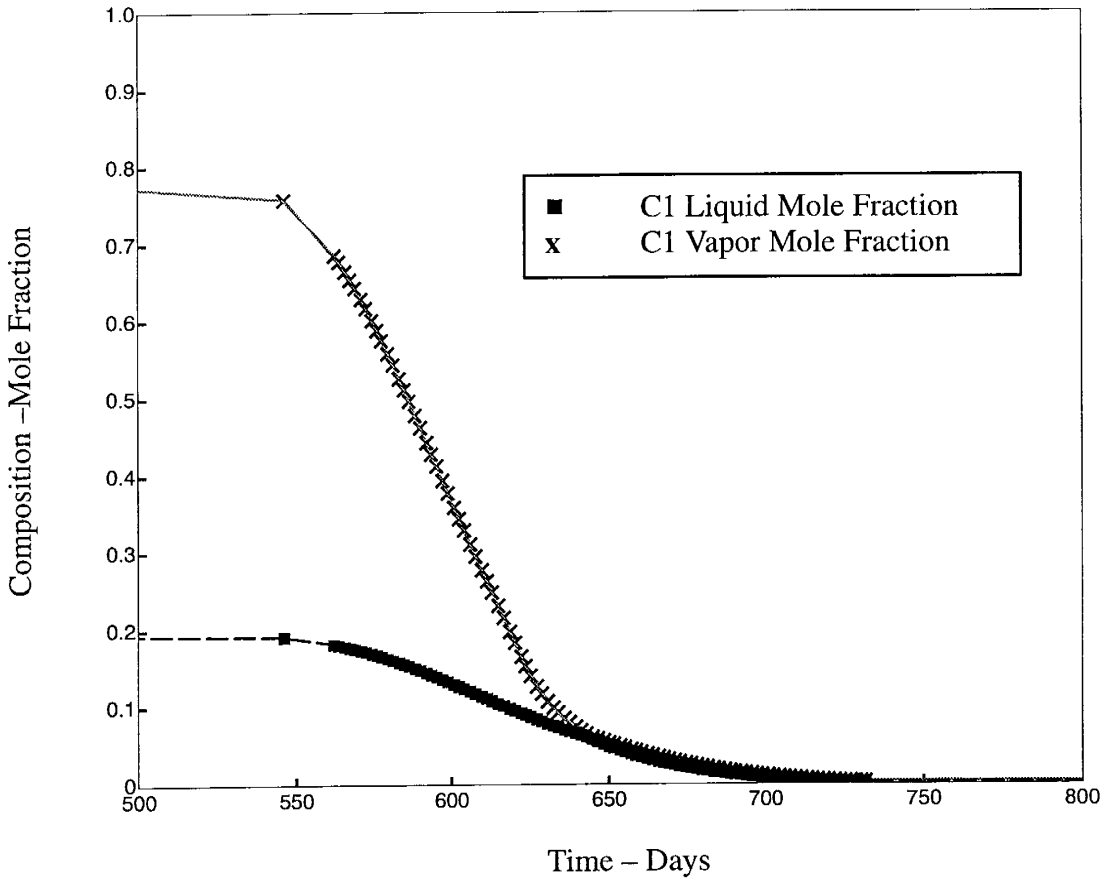

Figure 12–13 CO_2 Displacement at 2500 PSIA – Composition Versus Time for Cell 217 Component C1

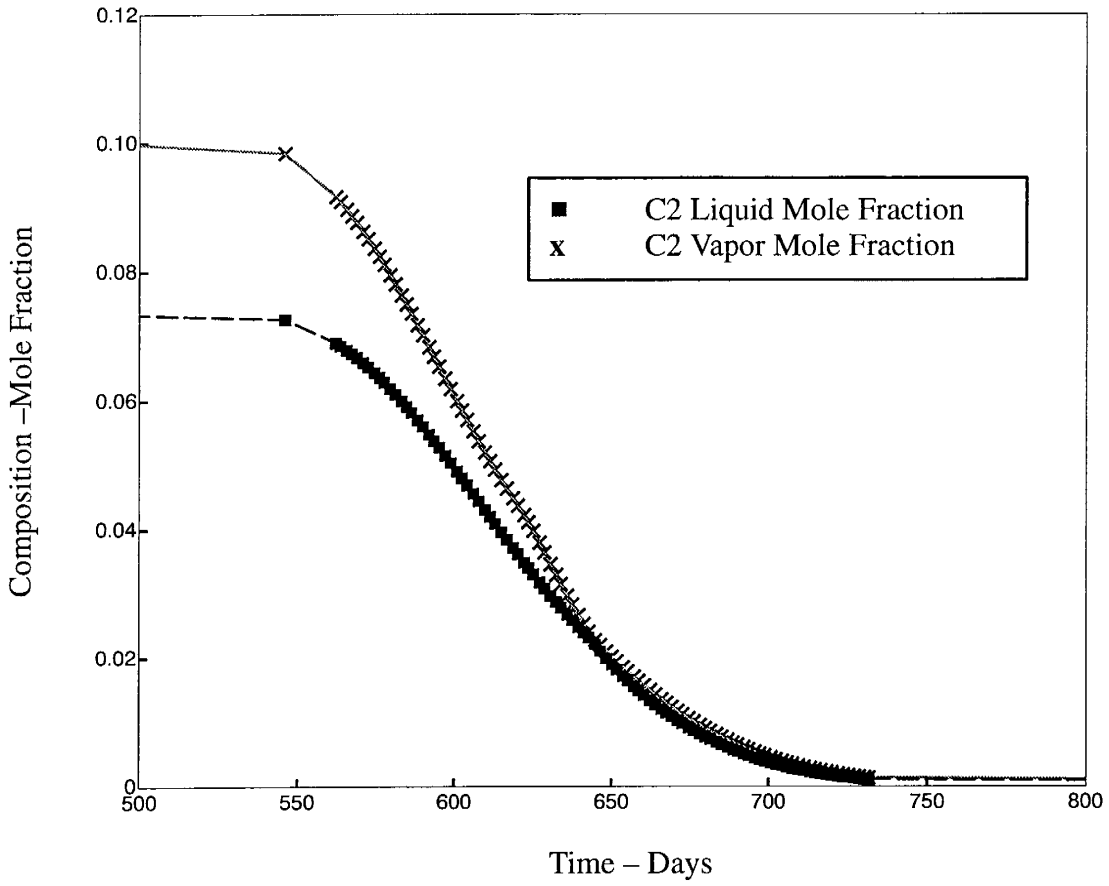

Figure 12–14 CO_2 Displacement at 2500 PSIA – Composition Versus Time for Cell 217 Component C2

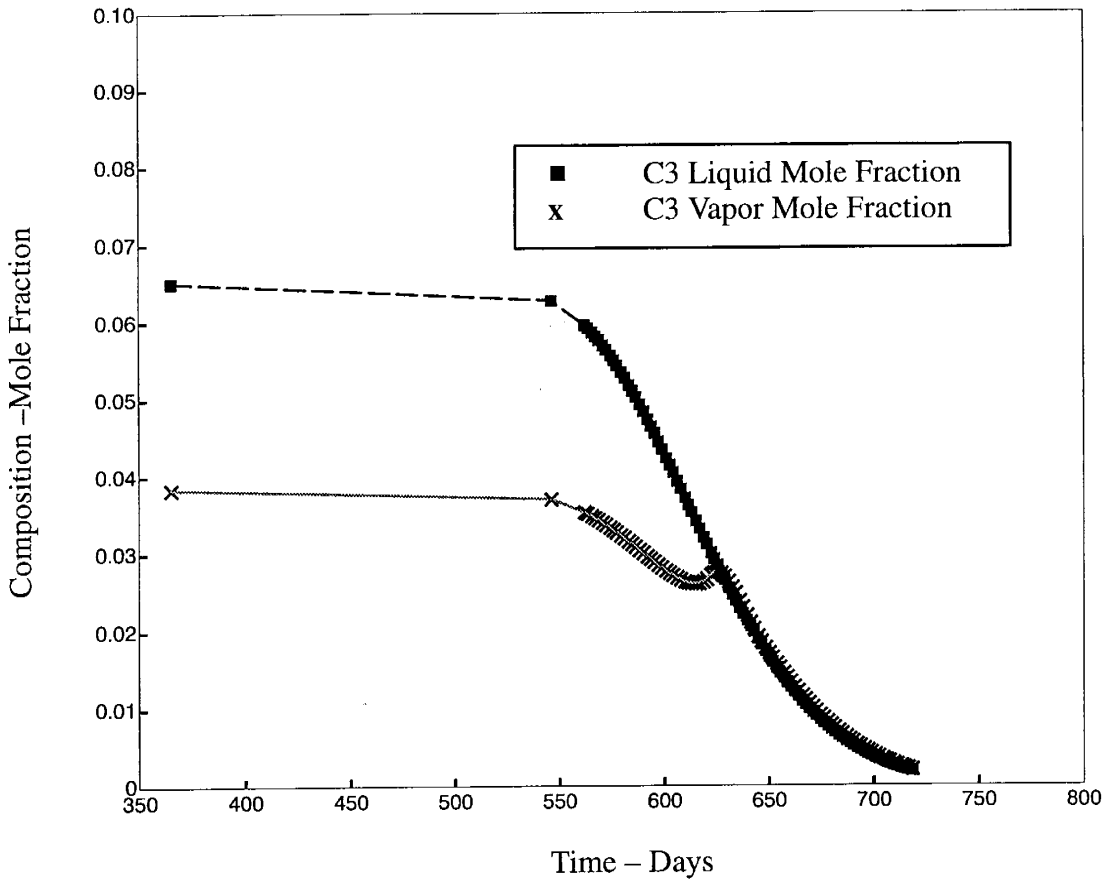

Figure 12–15 CO_2 Displacement at 2500 PSIA – Composition Versus Time for Cell 217 Component C3

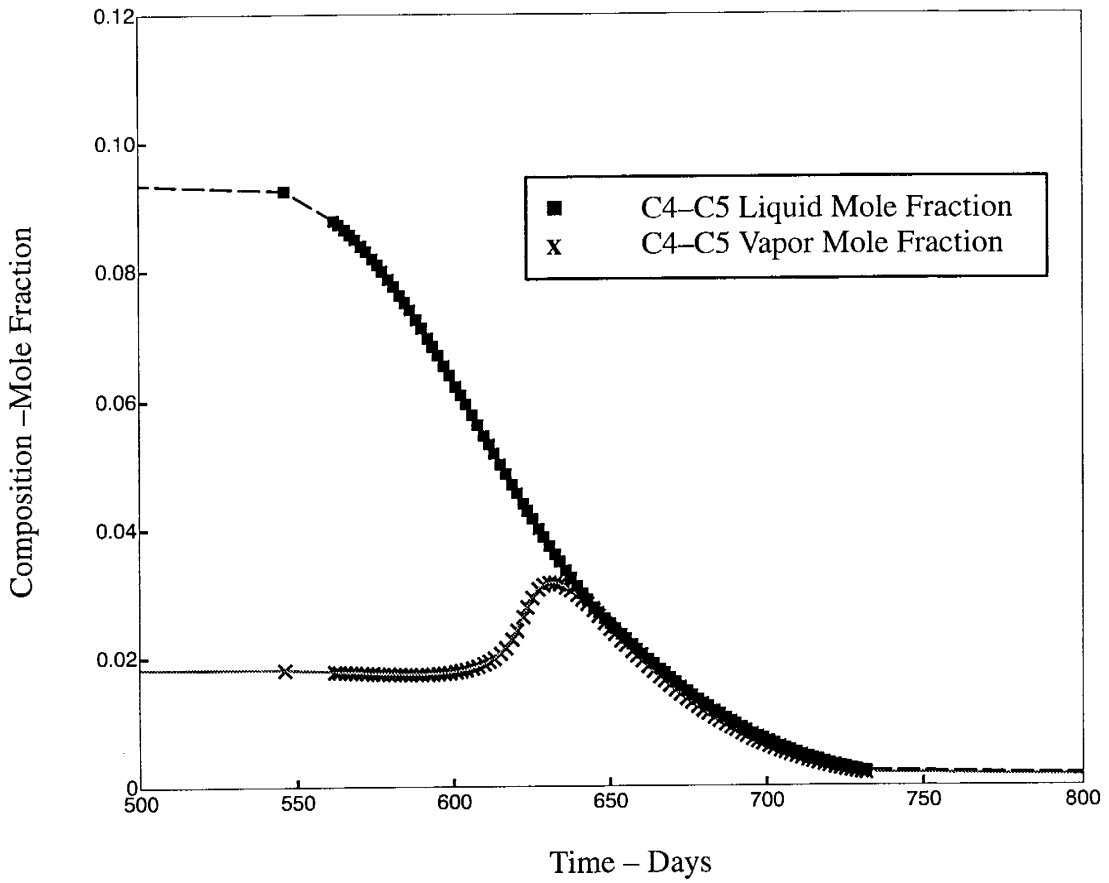

Figure 12–16 CO_2 Displacement at 2500 PSIA – Composition Versus Time for Cell 217 Component C4–C5

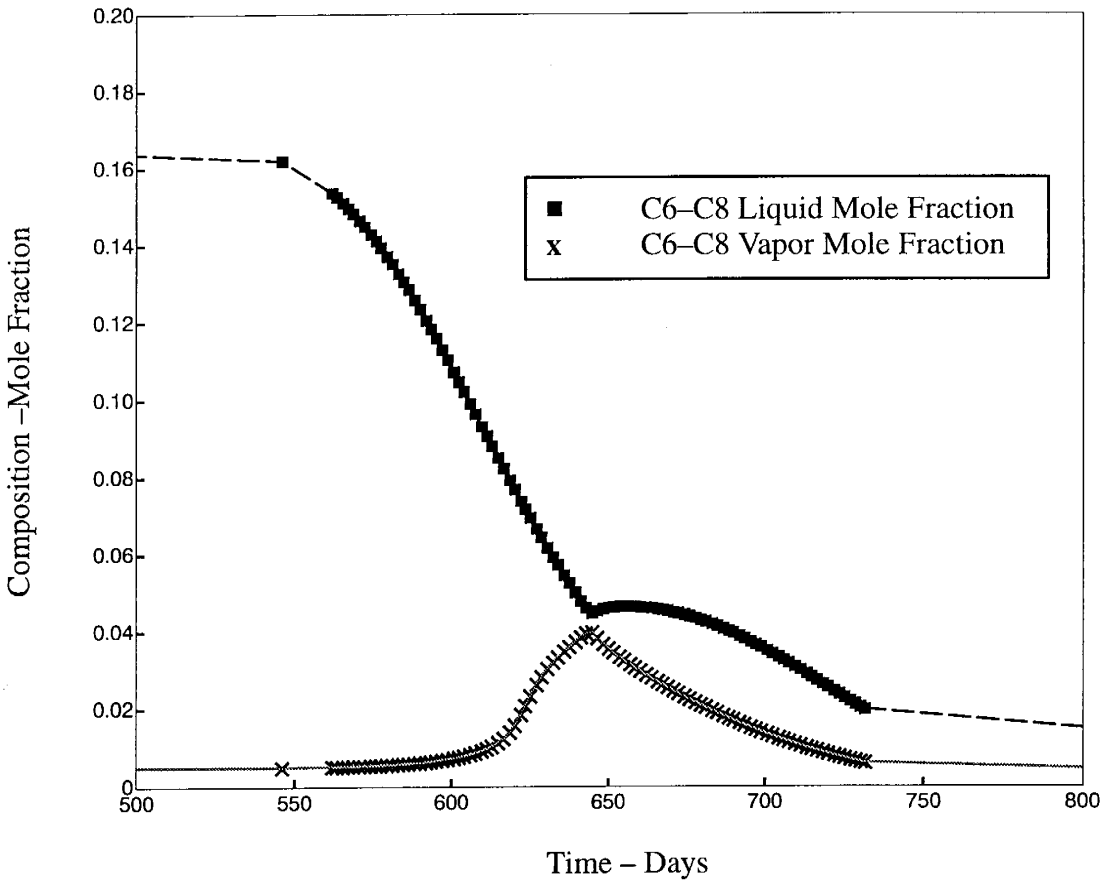

Figure 12–17 CO_2 Displacement at 2500 PSIA – Composition Versus Time for Cell 217 Component C6–C8

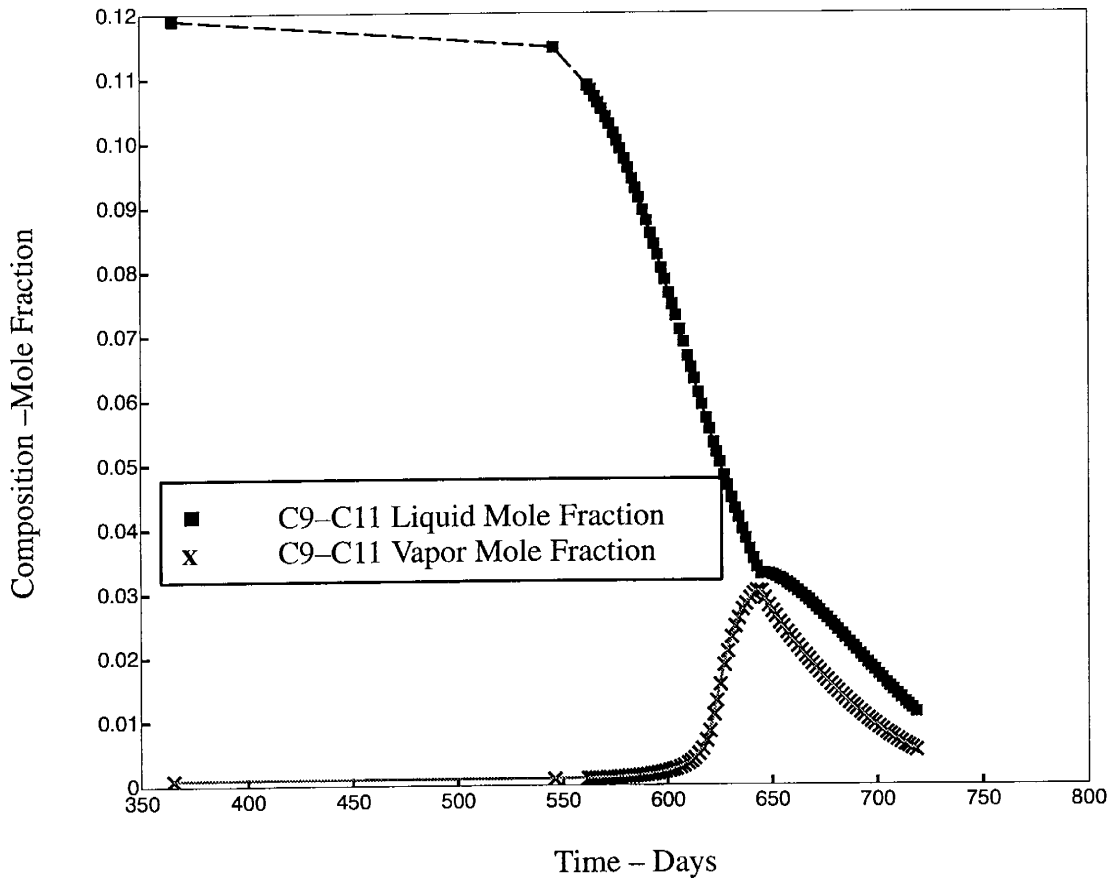

Figure 12–18 CO_2 Displacement at 2500 PSIA – Composition Versus Time for Cell 217 Component C9–C11

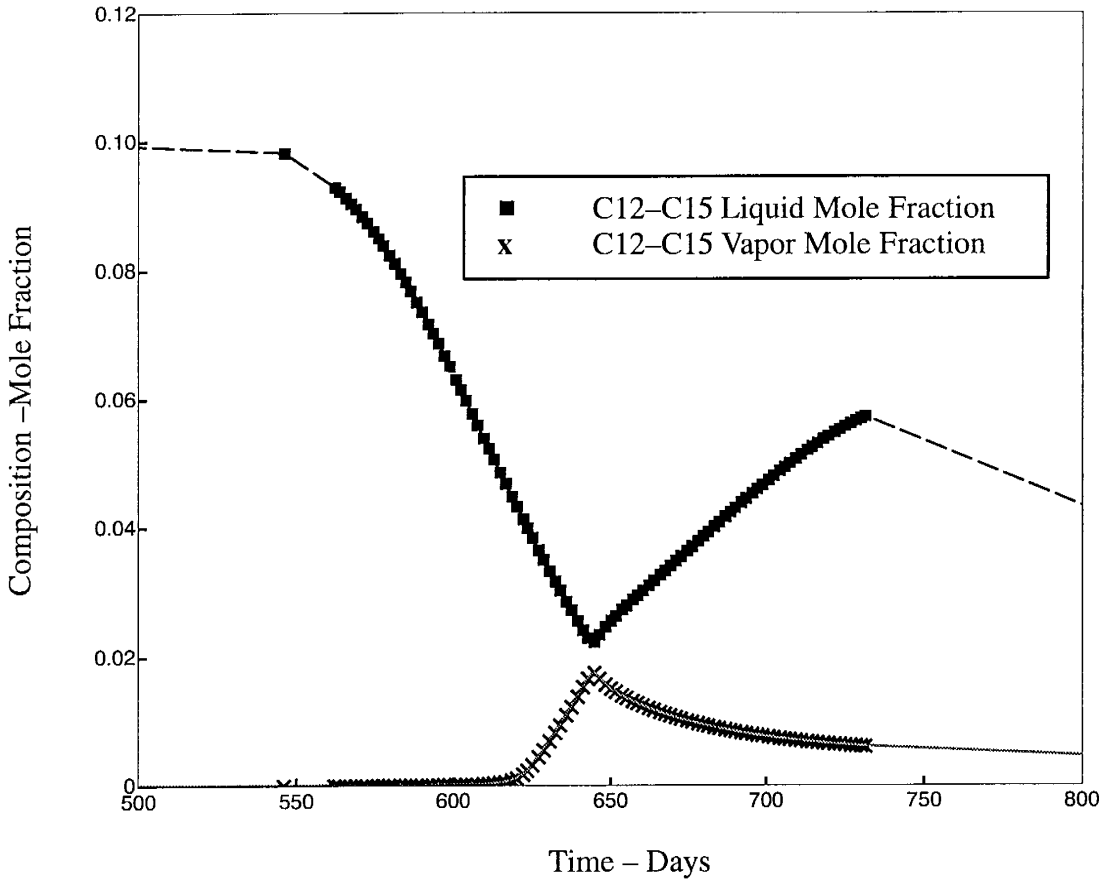

Figure 12–19 CO_2 Displacement at 2500 PSIA – Composition Versus Time for Cell 217 Component C12–C15

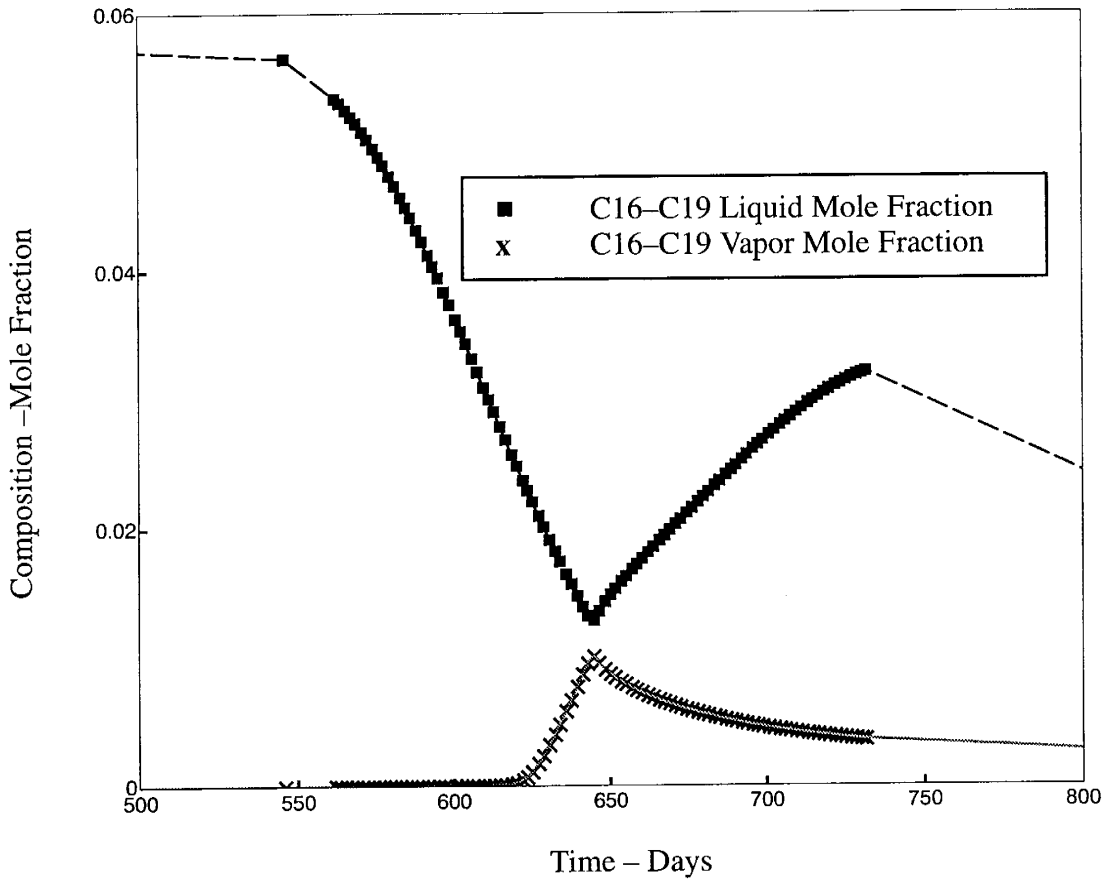

Figure 12–20 CO_2 Displacement at 2500 PSIA – Composition Versus Time for Cell 217 Component C16–C19

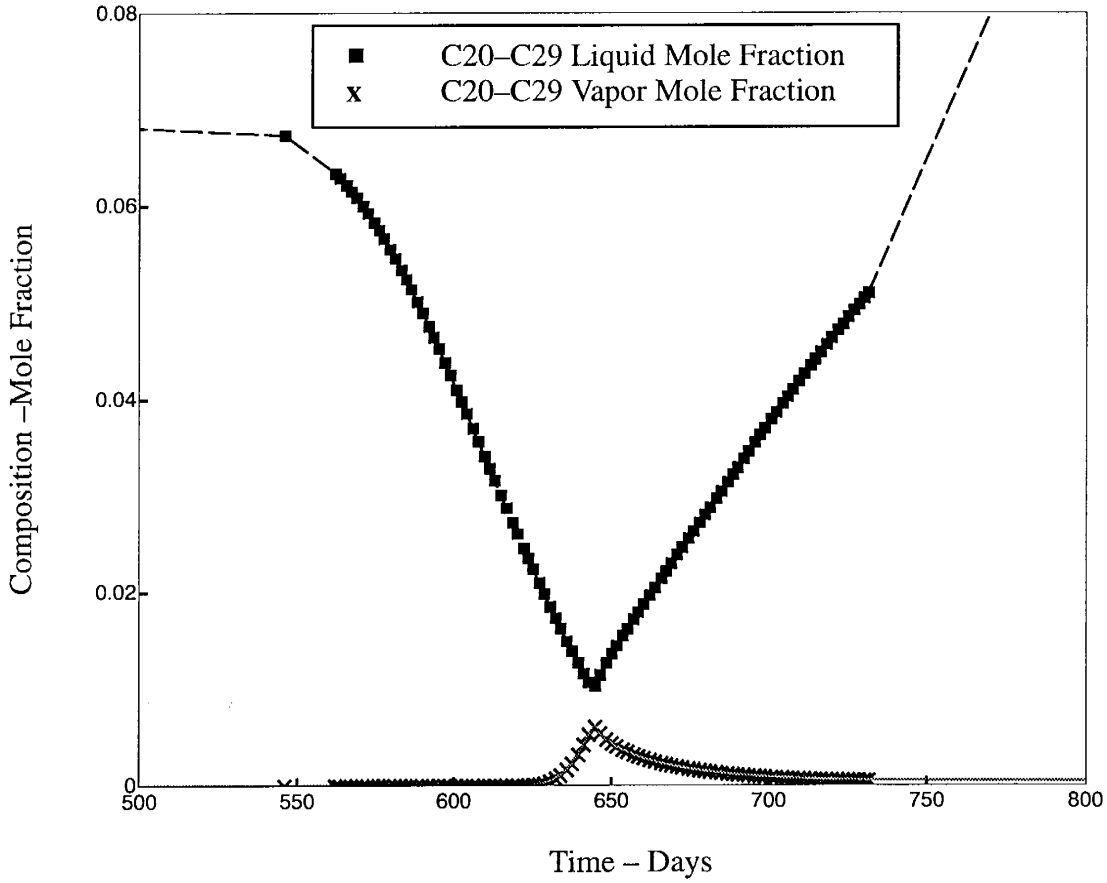

Figure 12–21 CO_2 Displacement at 2500 PSIA – Composition Versus Time for Cell 217 Component C20–C29

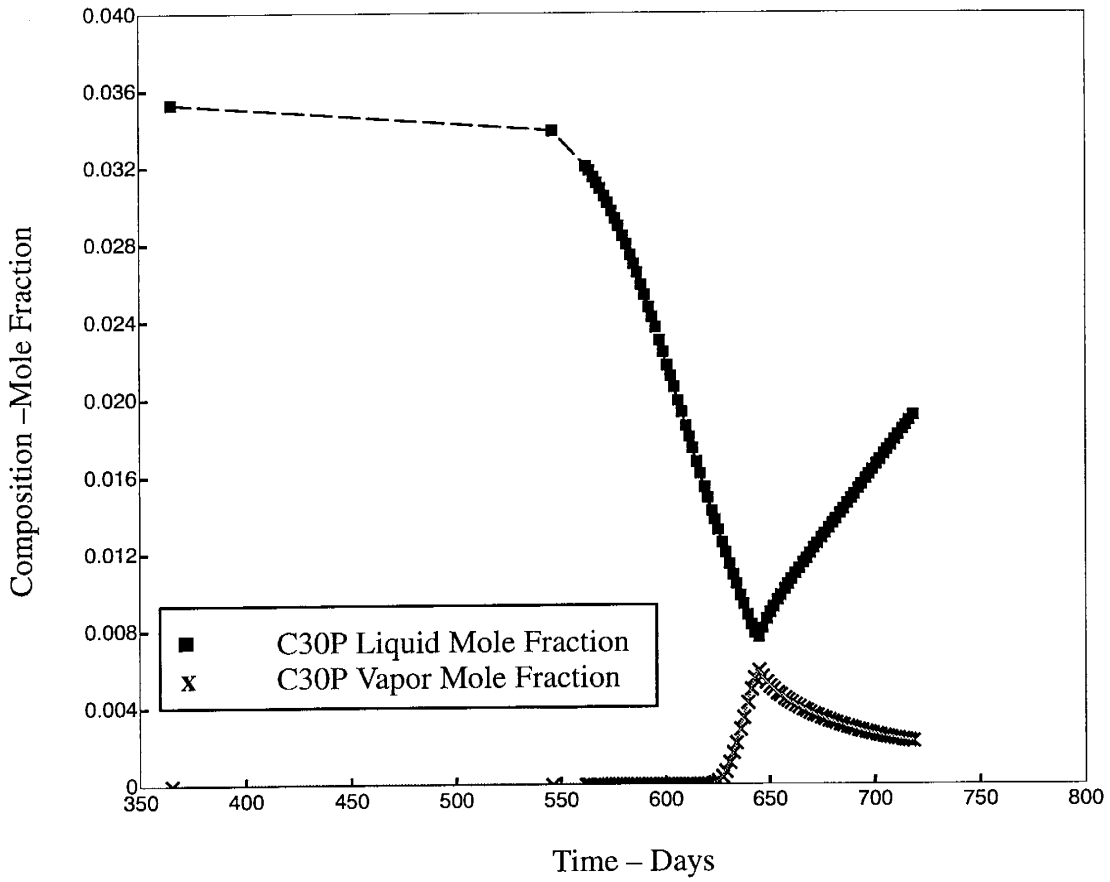

Figure 12–22 CO_2 Displacement at 2500 PSIA – Composition Versus Time for Cell 217 Component C30P

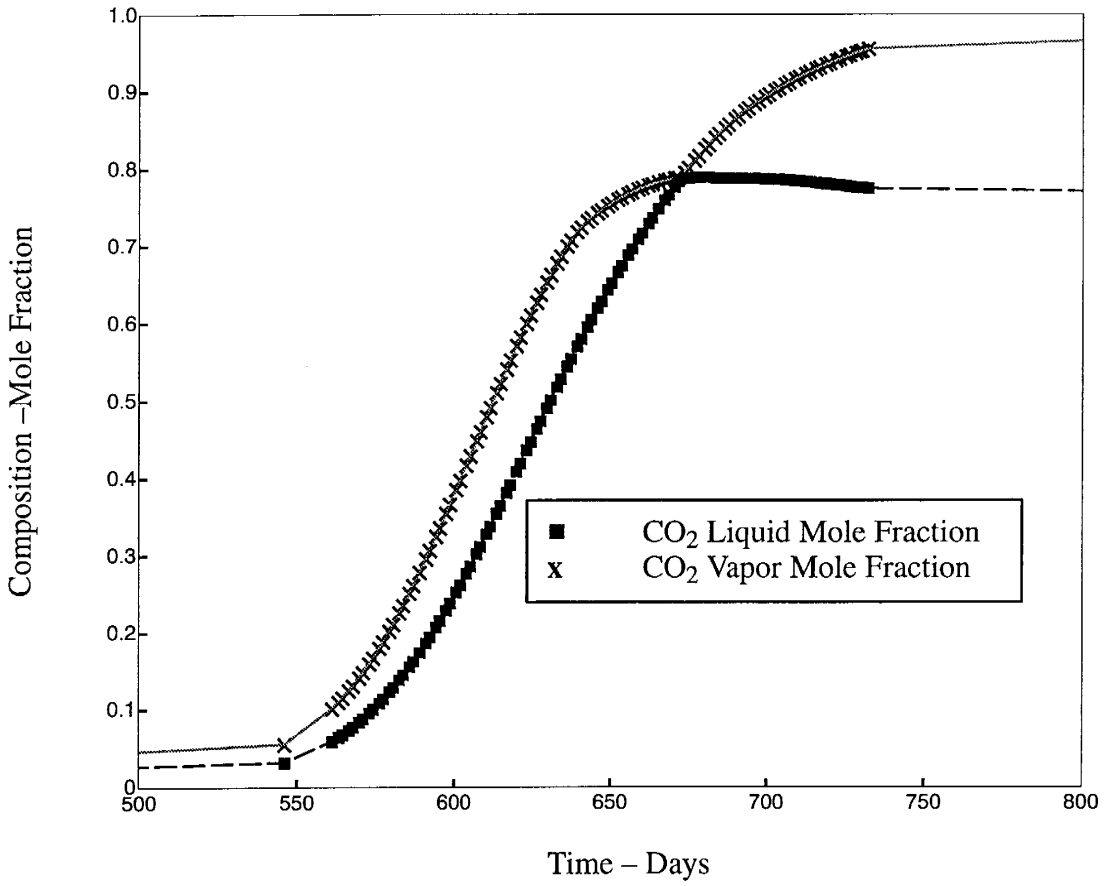

Figure 12–23 CO_2 Displacement at 3000 PSIA – Composition Versus Time for Cell 202 Component CO_2

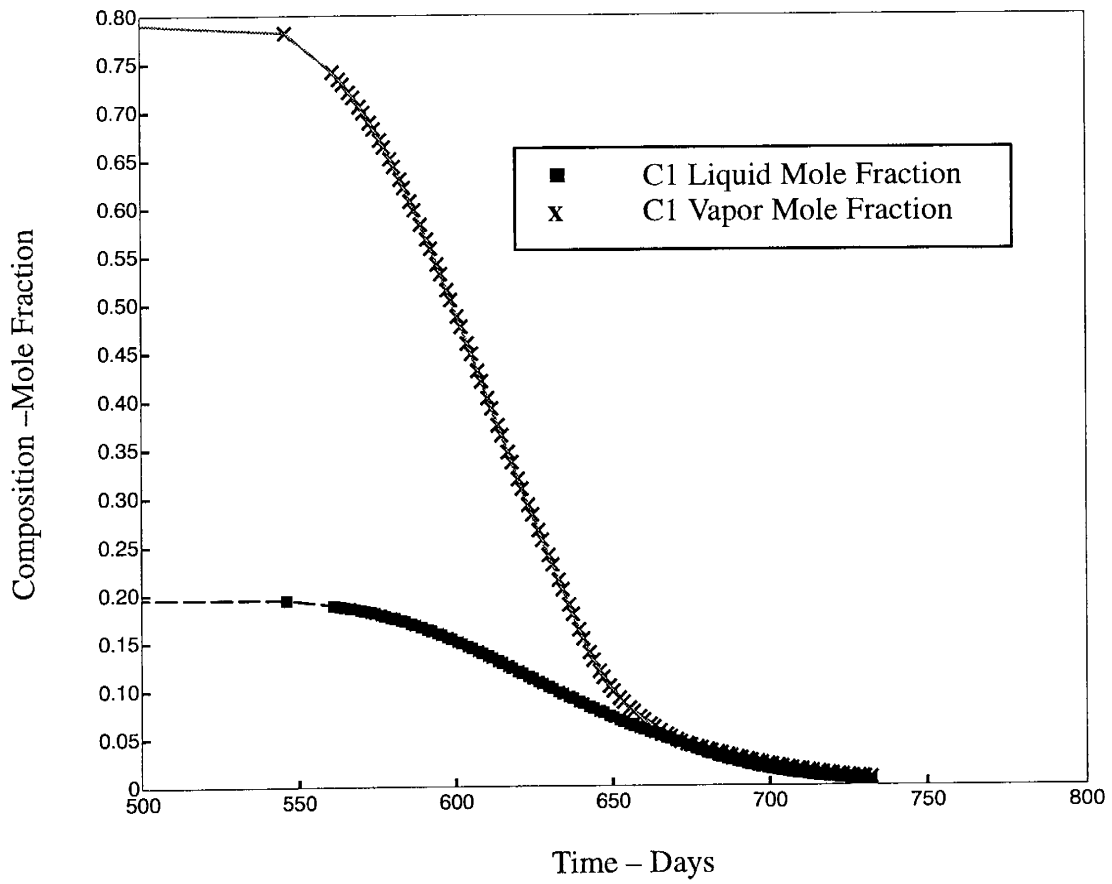

Figure 12–24 CO_2 Displacement at 3000 PSIA – Composition Versus Time for Cell 202 Component C1

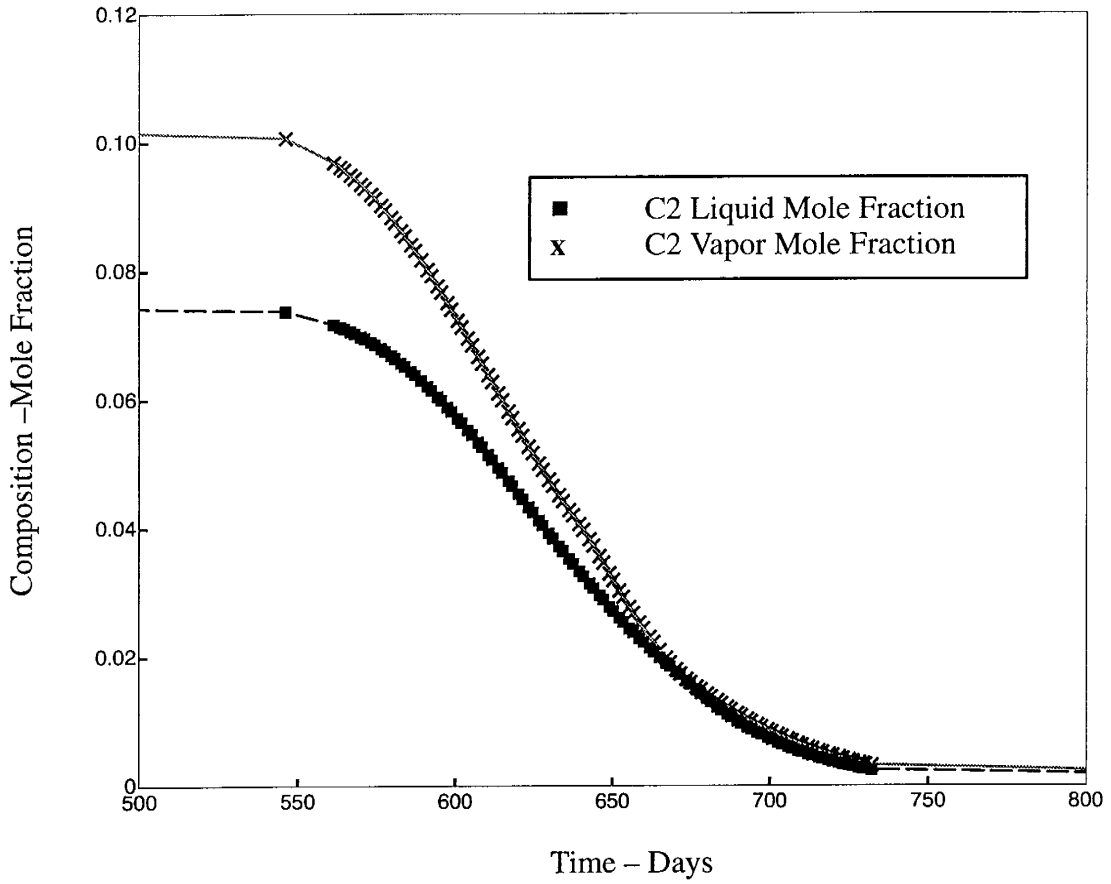

Figure 12–25 CO_2 Displacement at 3000 PSIA – Composition Versus Time for Cell 202 Component C2

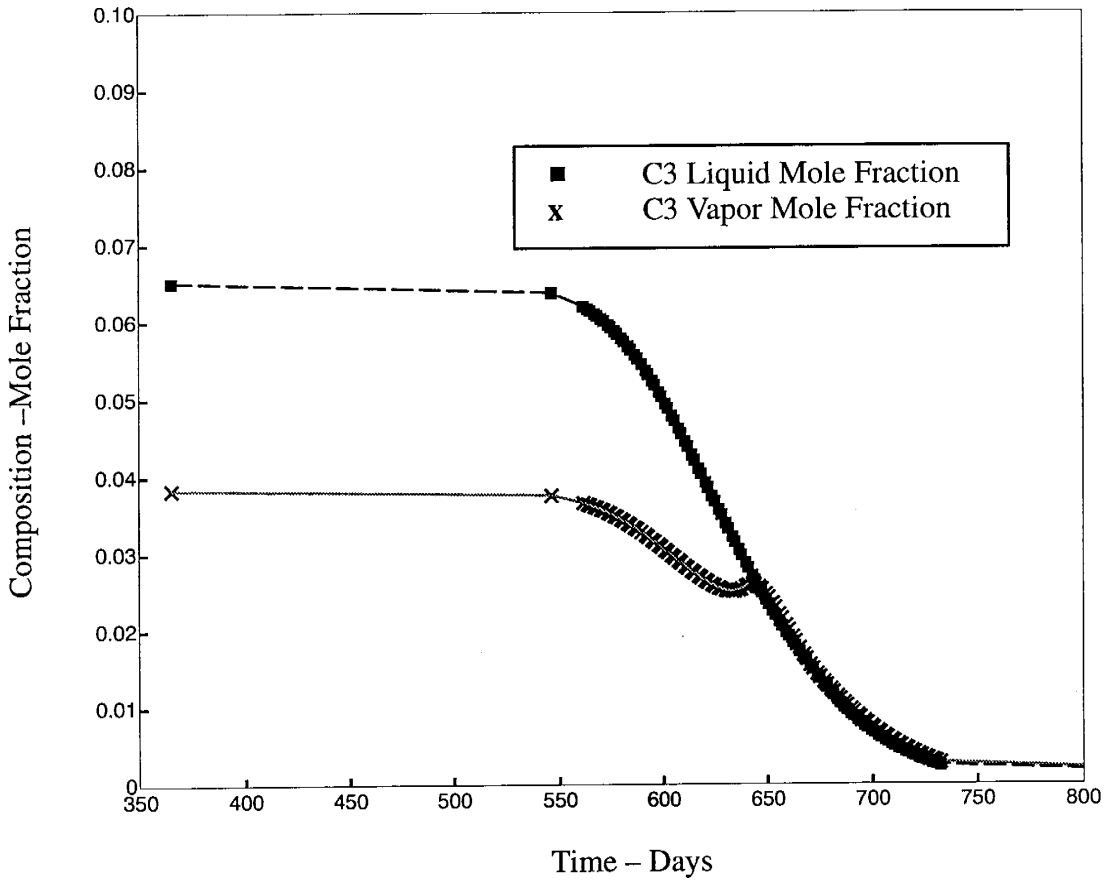

Figure 12–26 CO_2 Displacement at 3000 PSIA – Composition Versus Time for Cell 202 Component C3

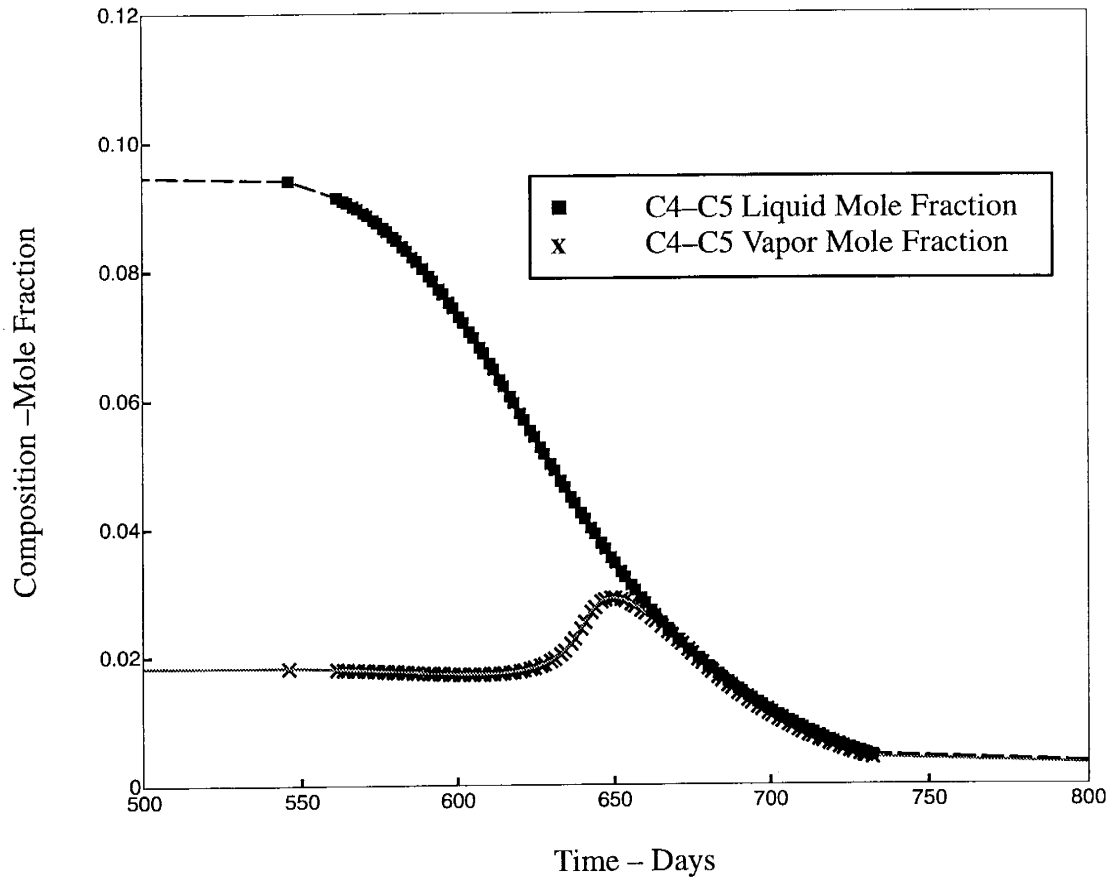

Figure 12–27 CO_2 Displacement at 3000 PSIA – Composition Versus Time for Cell 202 Component C4–C5

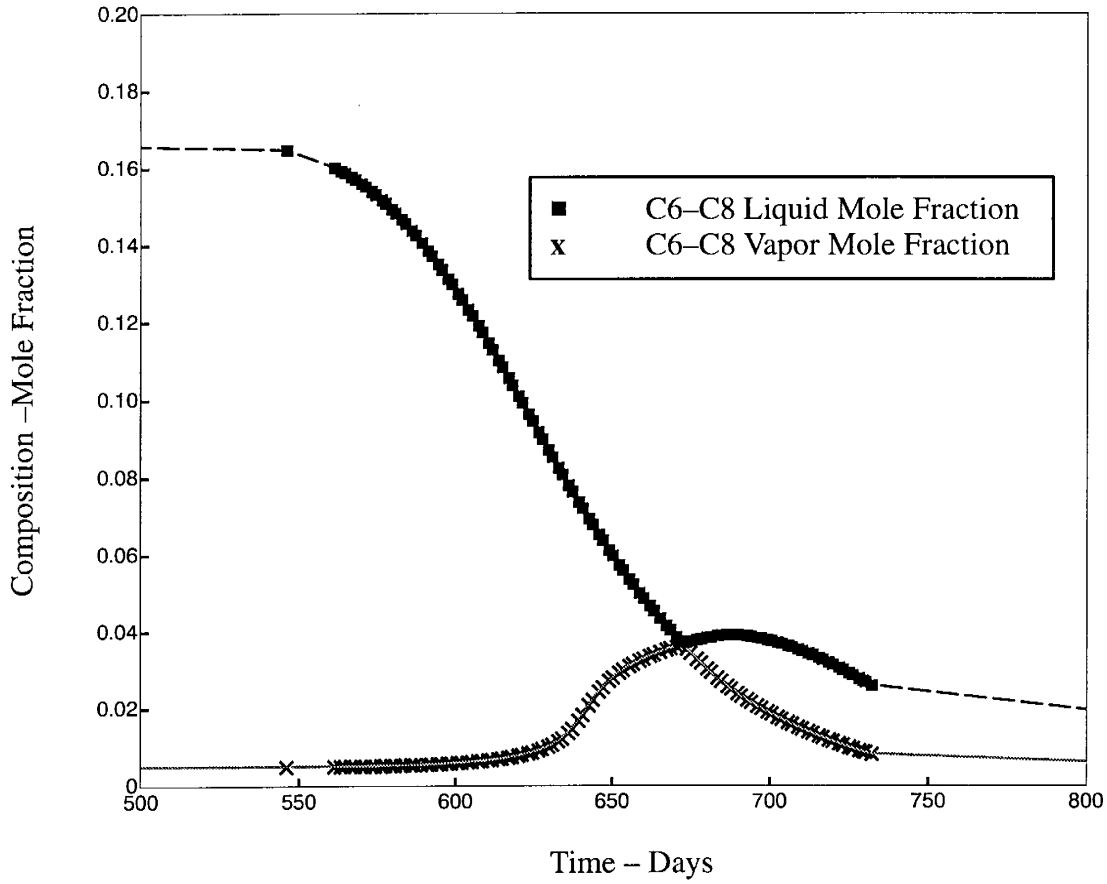

Figure 12–28 CO_2 Displacement at 3000 PSIA – Composition Versus Time for Cell 202 Component C6–C8

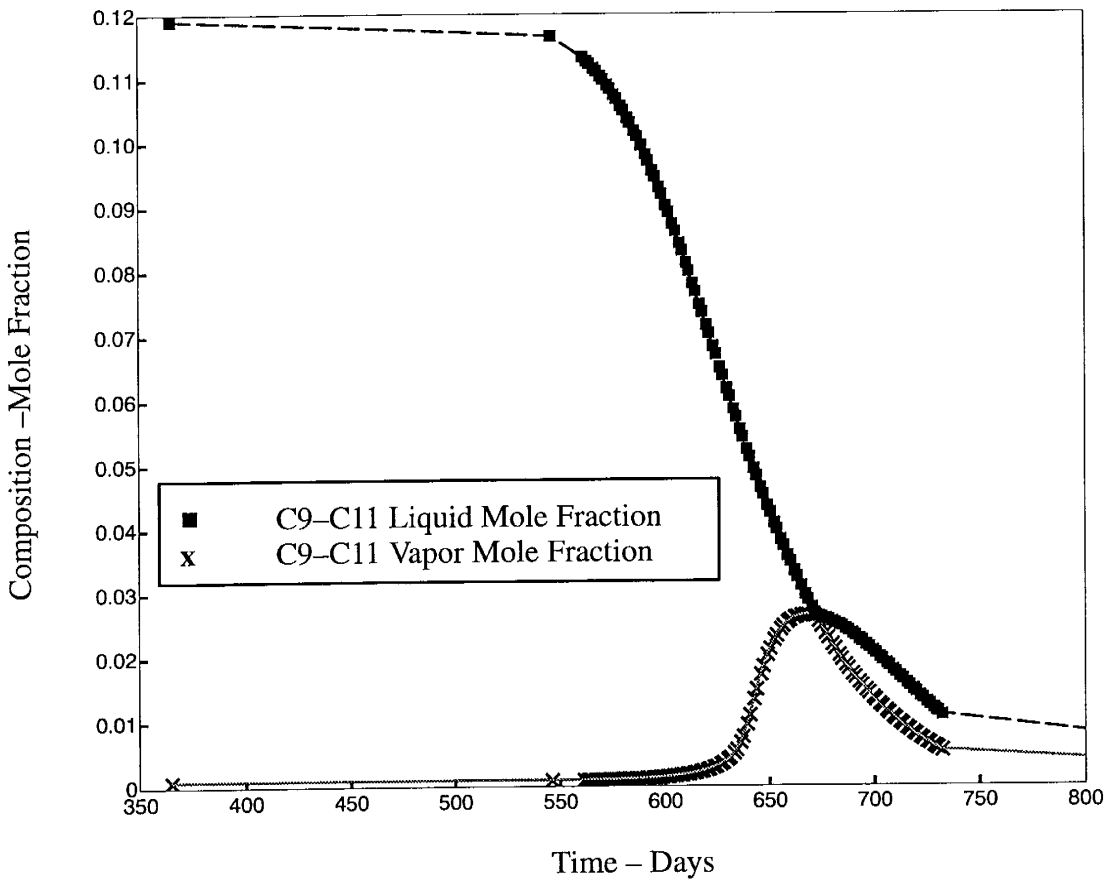

Figure 12–29 CO_2 Displacement at 3000 PSIA – Composition Versus Time for Cell 202 Component C9–C11

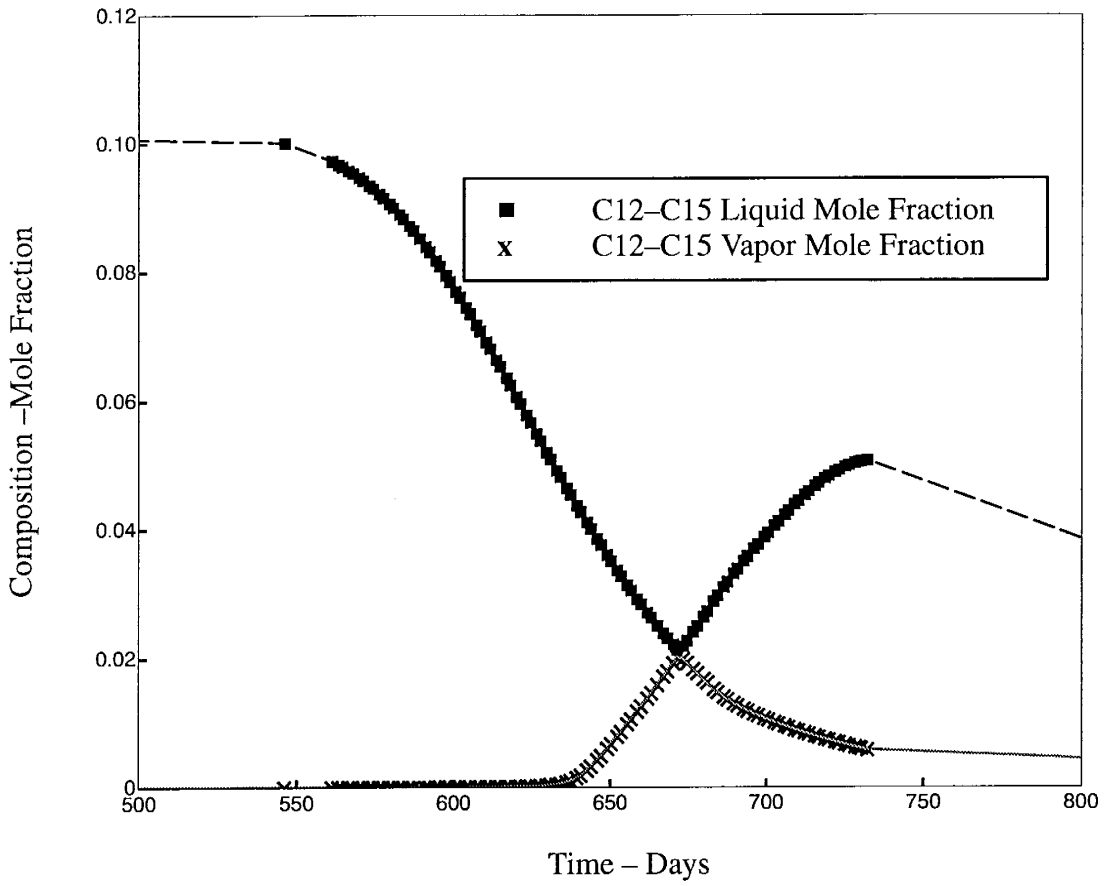

Figure 12–30 CO_2 Displacement at 3000 PSIA – Composition Versus Time for Cell 202 Component C12–C15

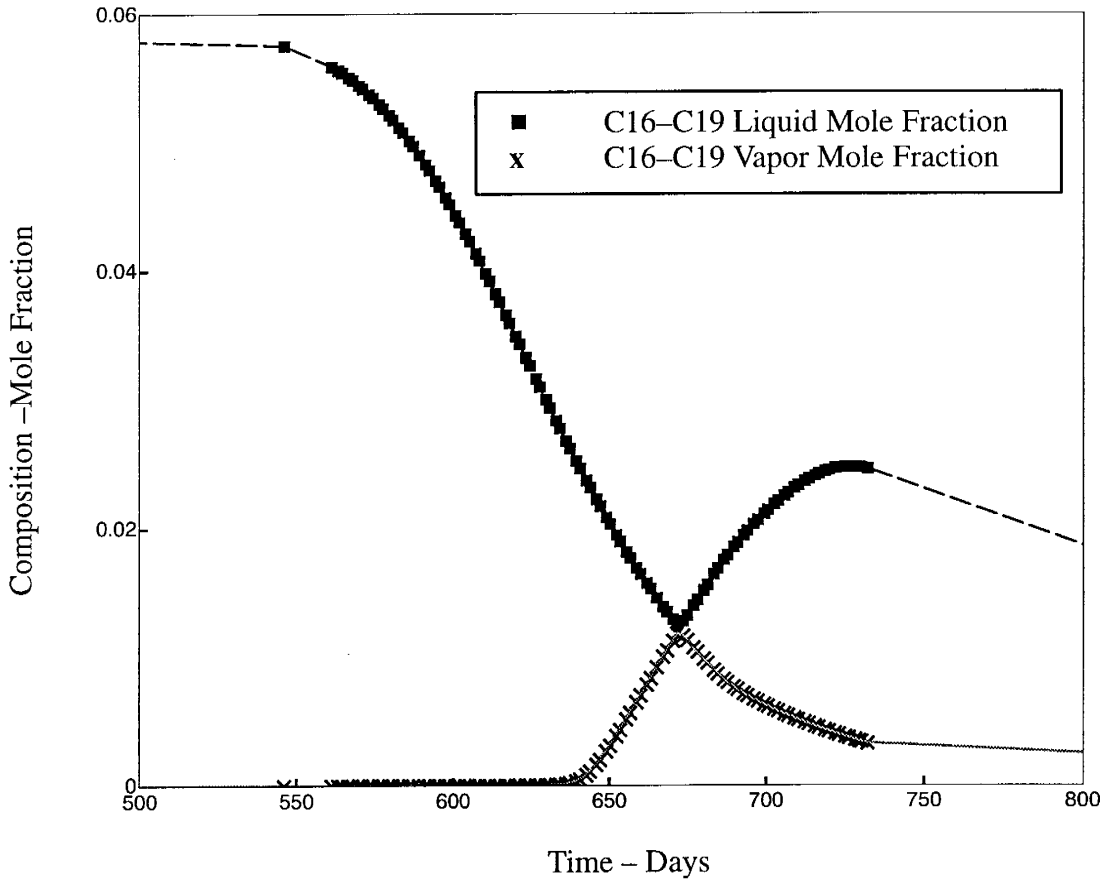

Figure 12–31 CO_2 Displacement at 3000 PSIA – Composition Versus Time for Cell 202 Component C16–C19

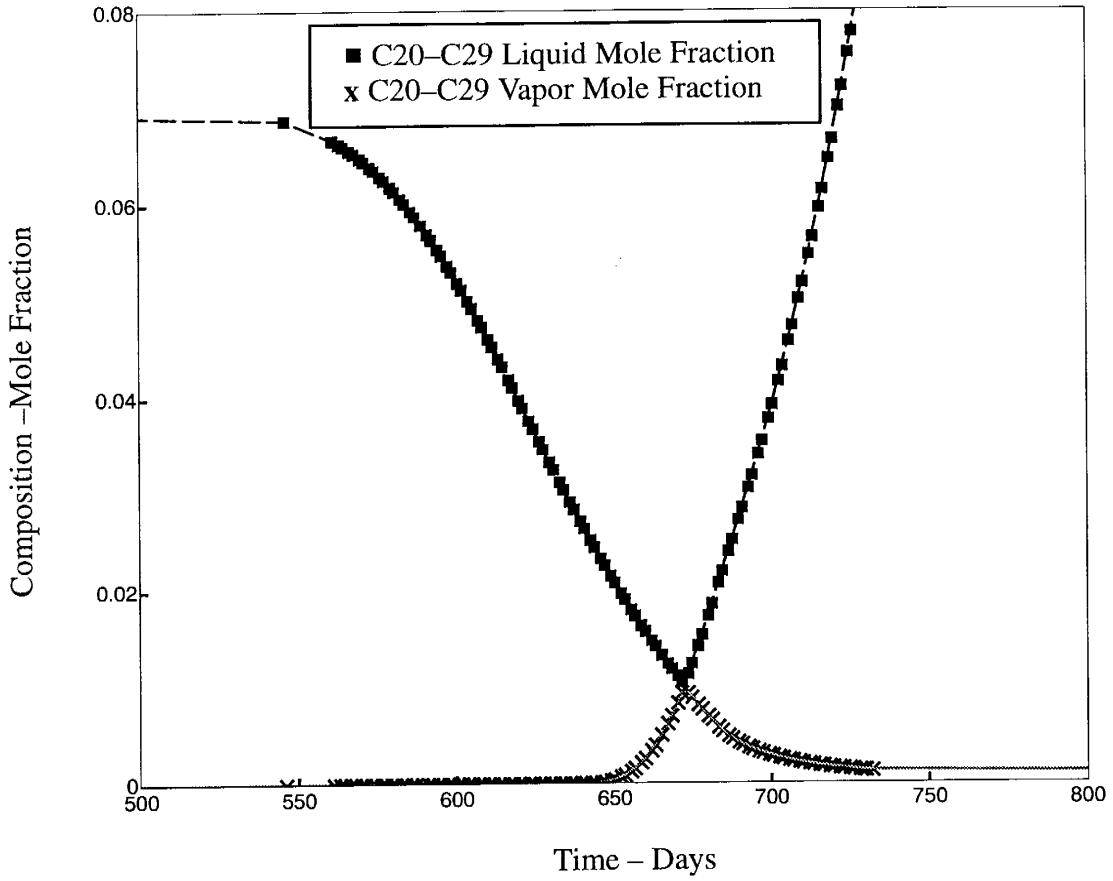

Figure 12–32 CO_2 Displacement at 3000 PSIA – Composition Versus Time for Cell 202 Component C20–C29

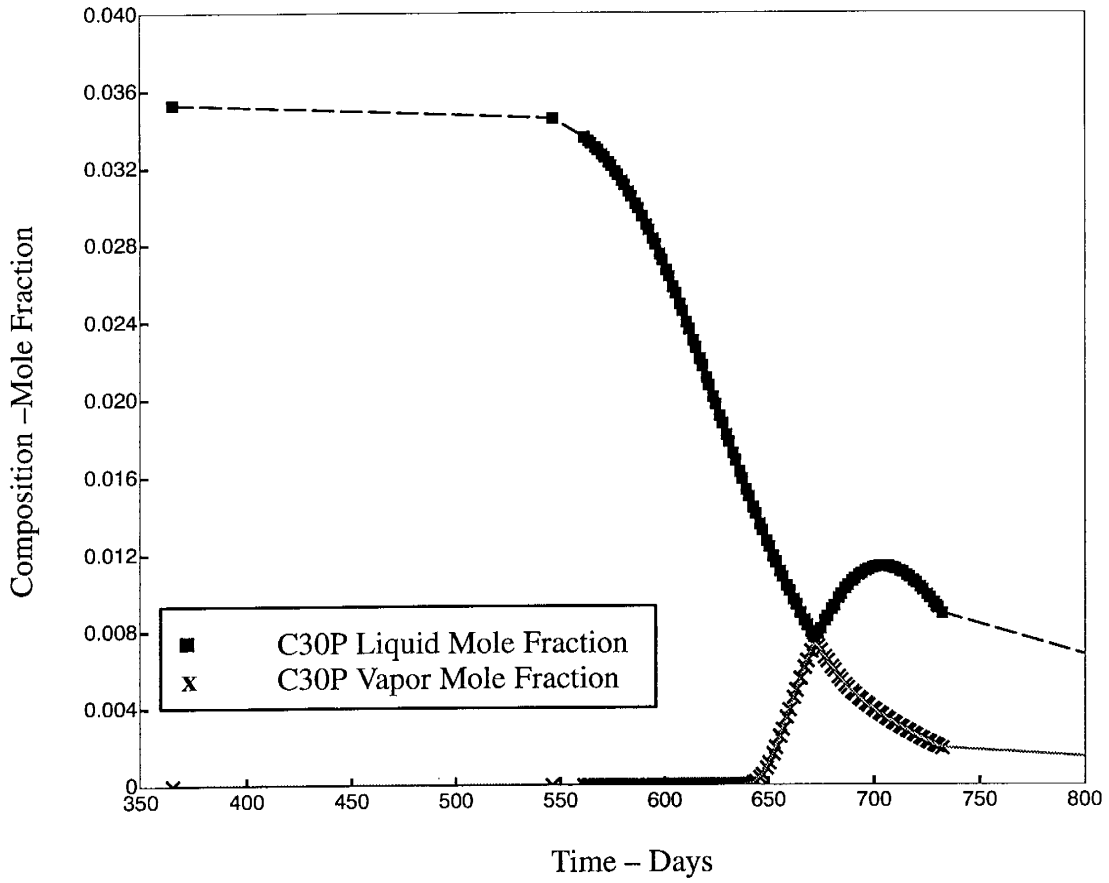

Figure 12–33 CO_2 Displacement at 3000 PSIA – Composition Versus Time for Cell 202 Component C30P

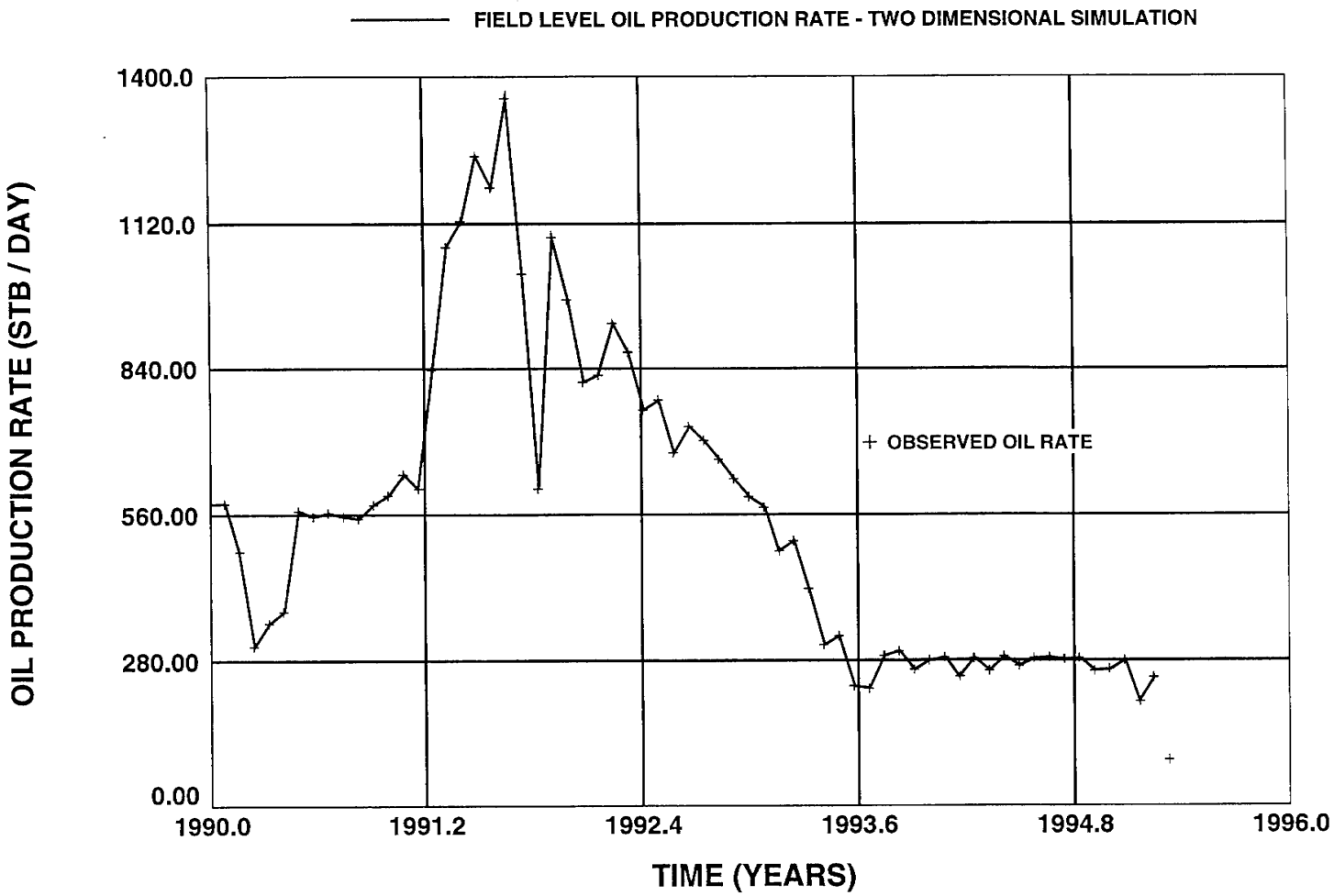

Figure 12-34 Oil Production Rate - Anasazi Field

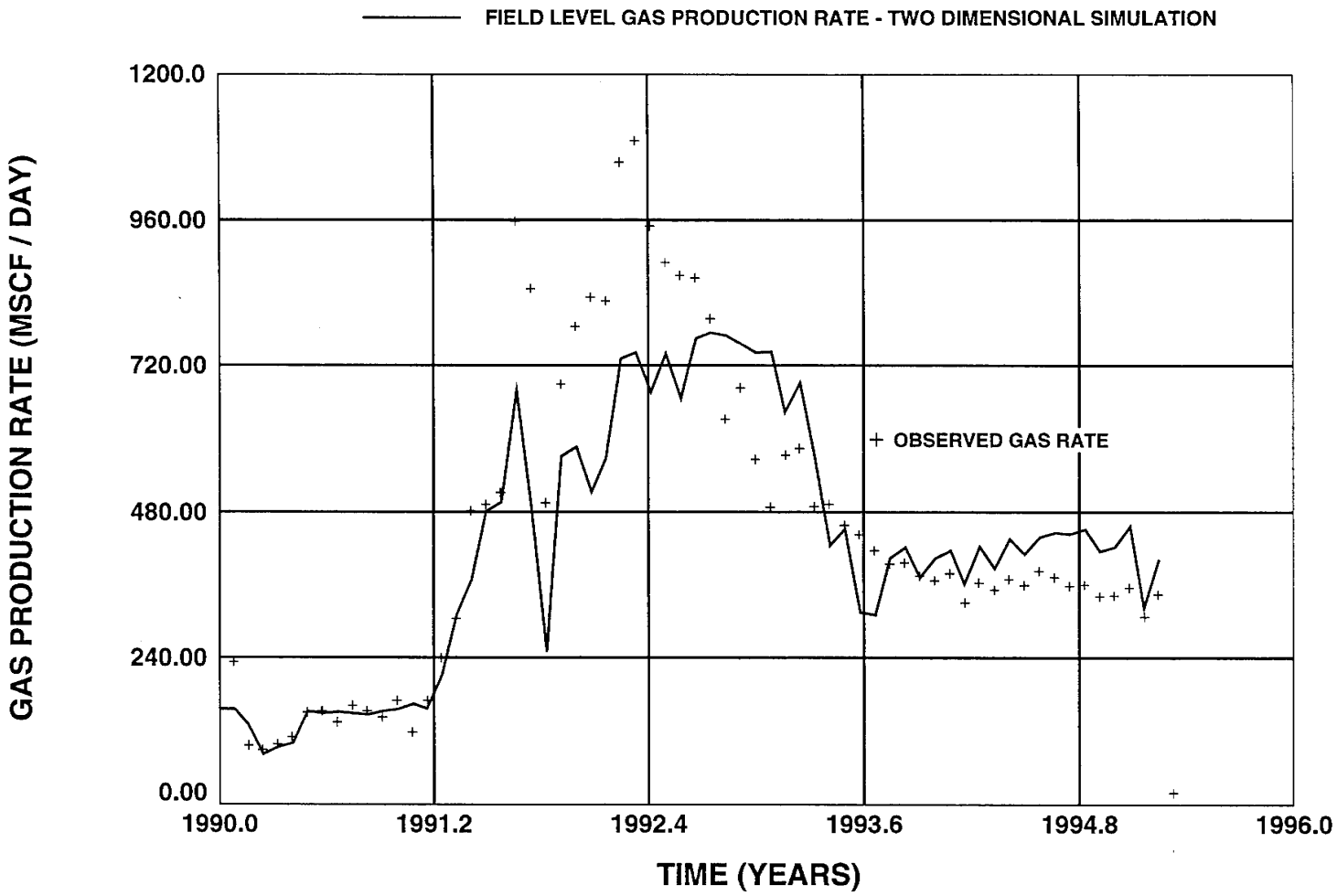

Figure 12-35 Simulation vs Anasazi Field Data - Gas Production Rate

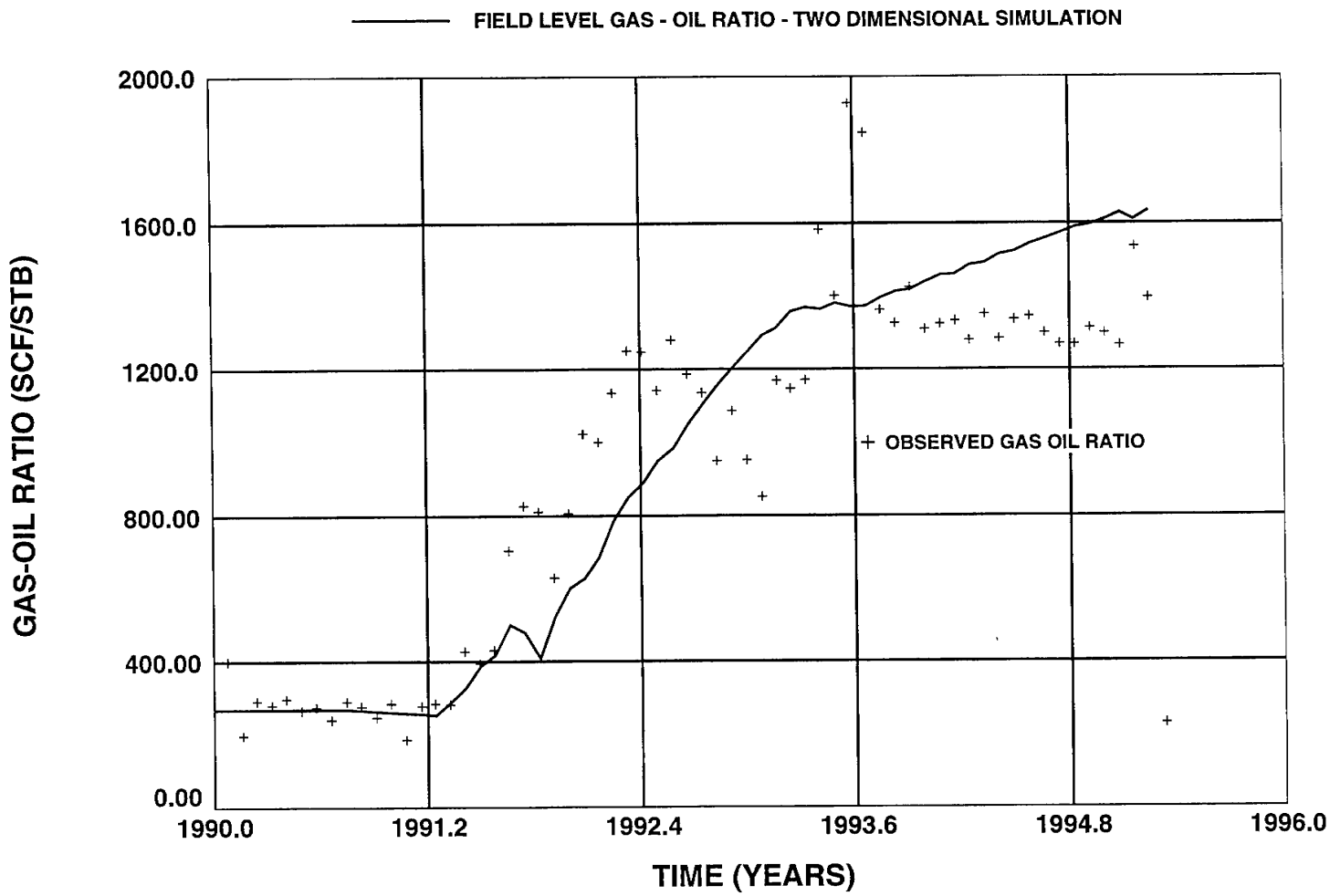

Figure 12-36 Simulation vs Anasazi Field Data - Gas Oil Ratio

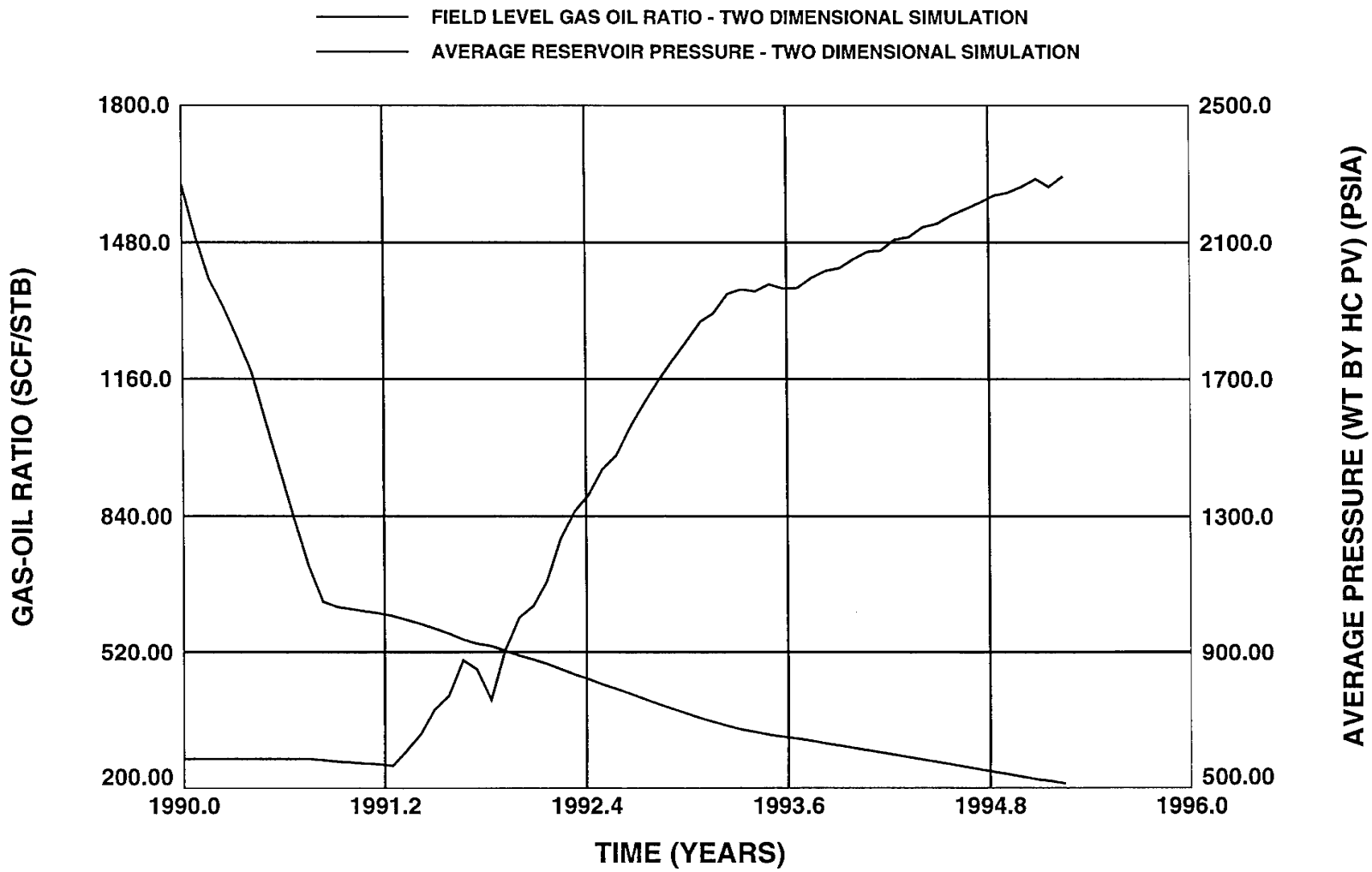

Figure 12-37 Two Dimensional Simulation Predictions - Anasazi GOR and Pressure

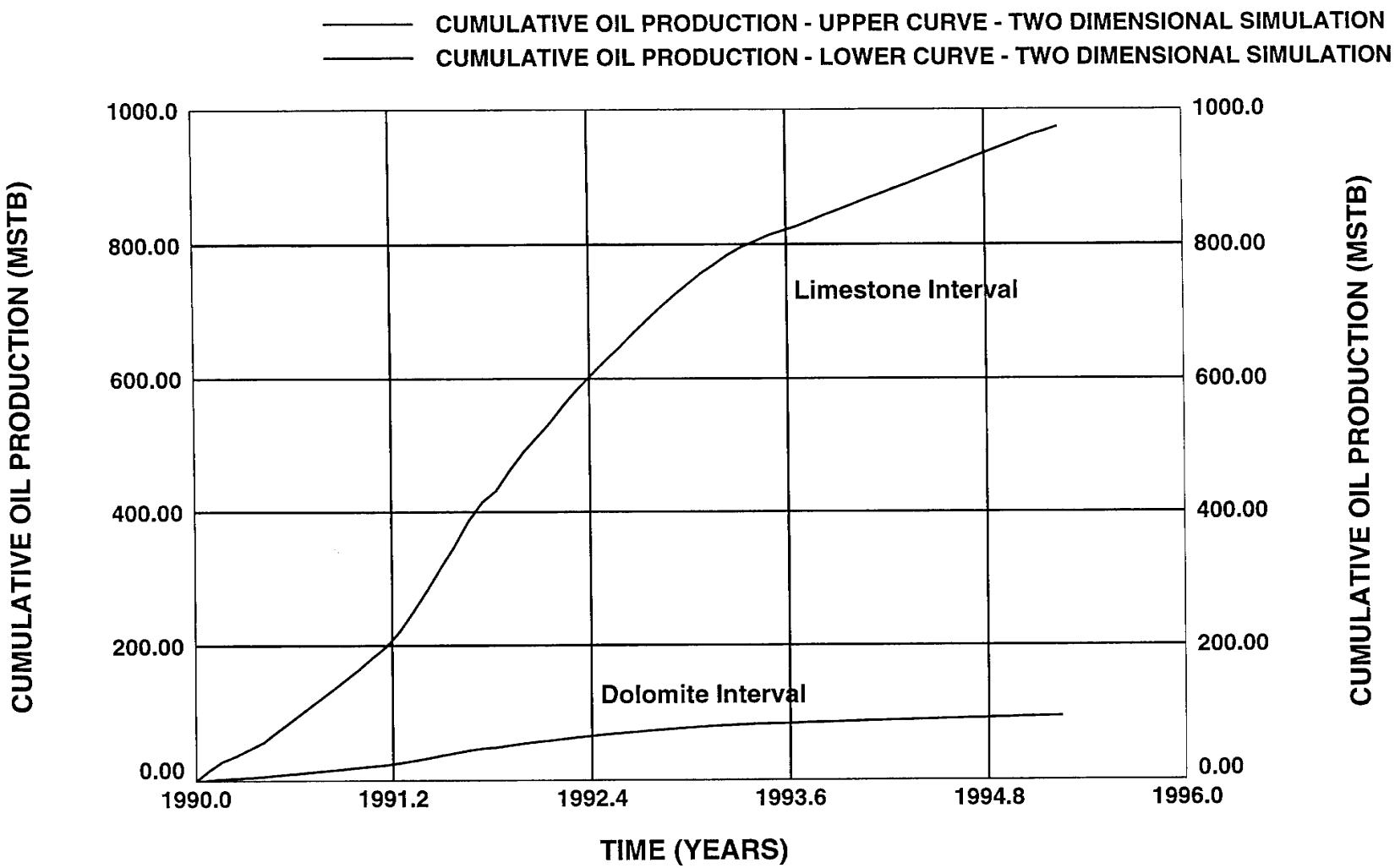

Figure 12-38 Predicted Limestone and Dolomite Cumulative Oil Production

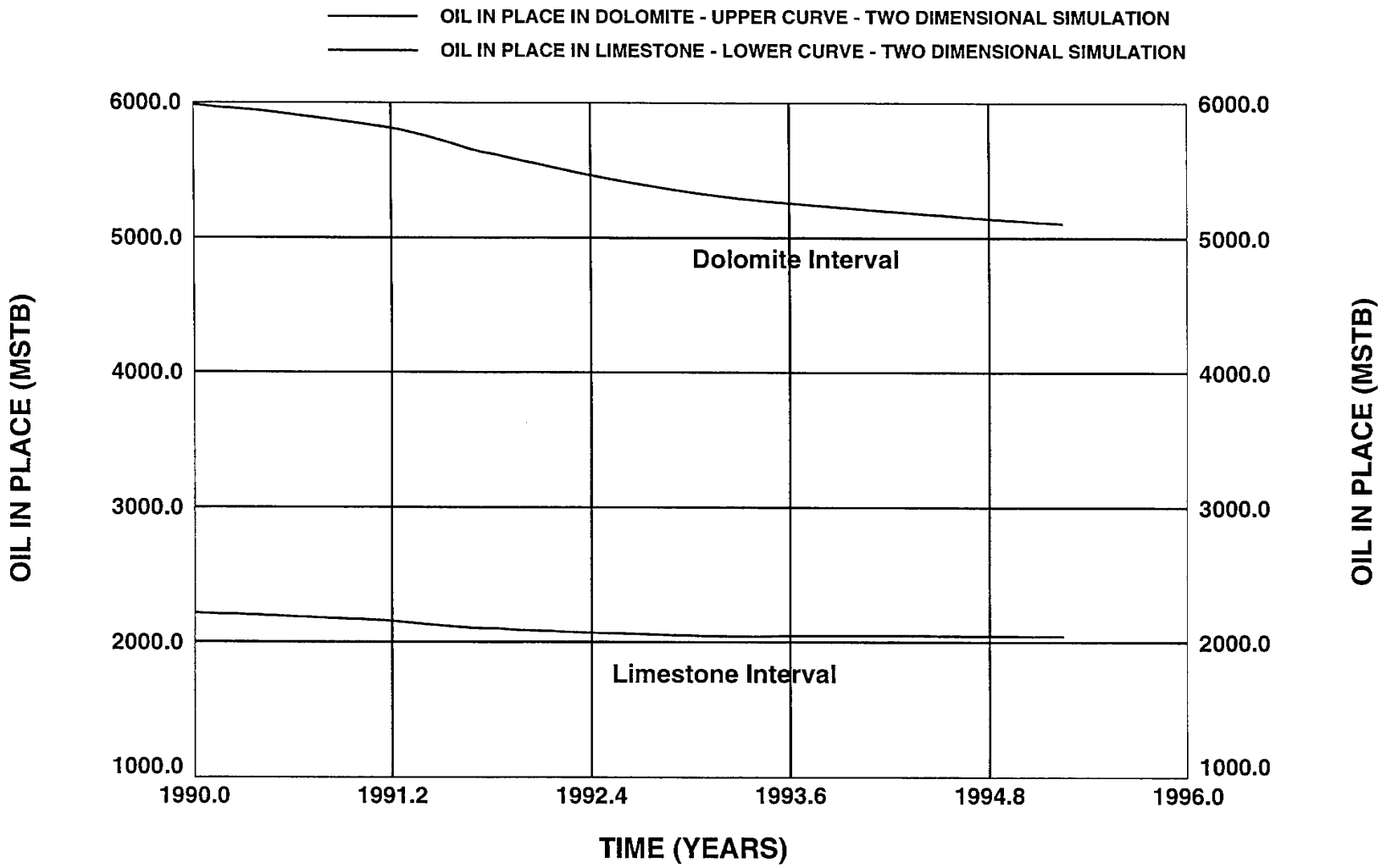

Figure 12-39 Predicted Interval Oil Production History

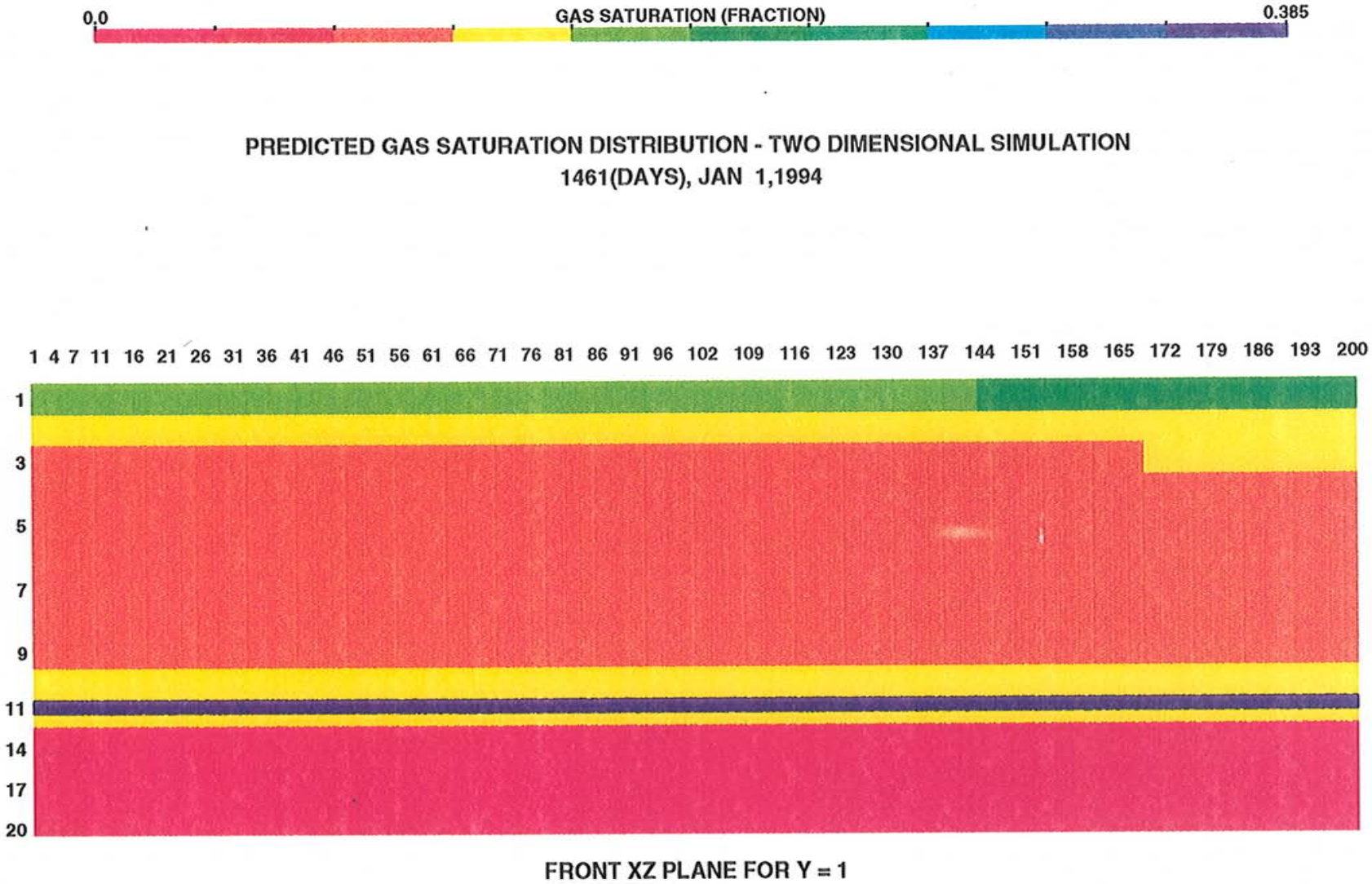

Figure 12-40 Gas Saturation Distribution - Two Dimensional Simulation

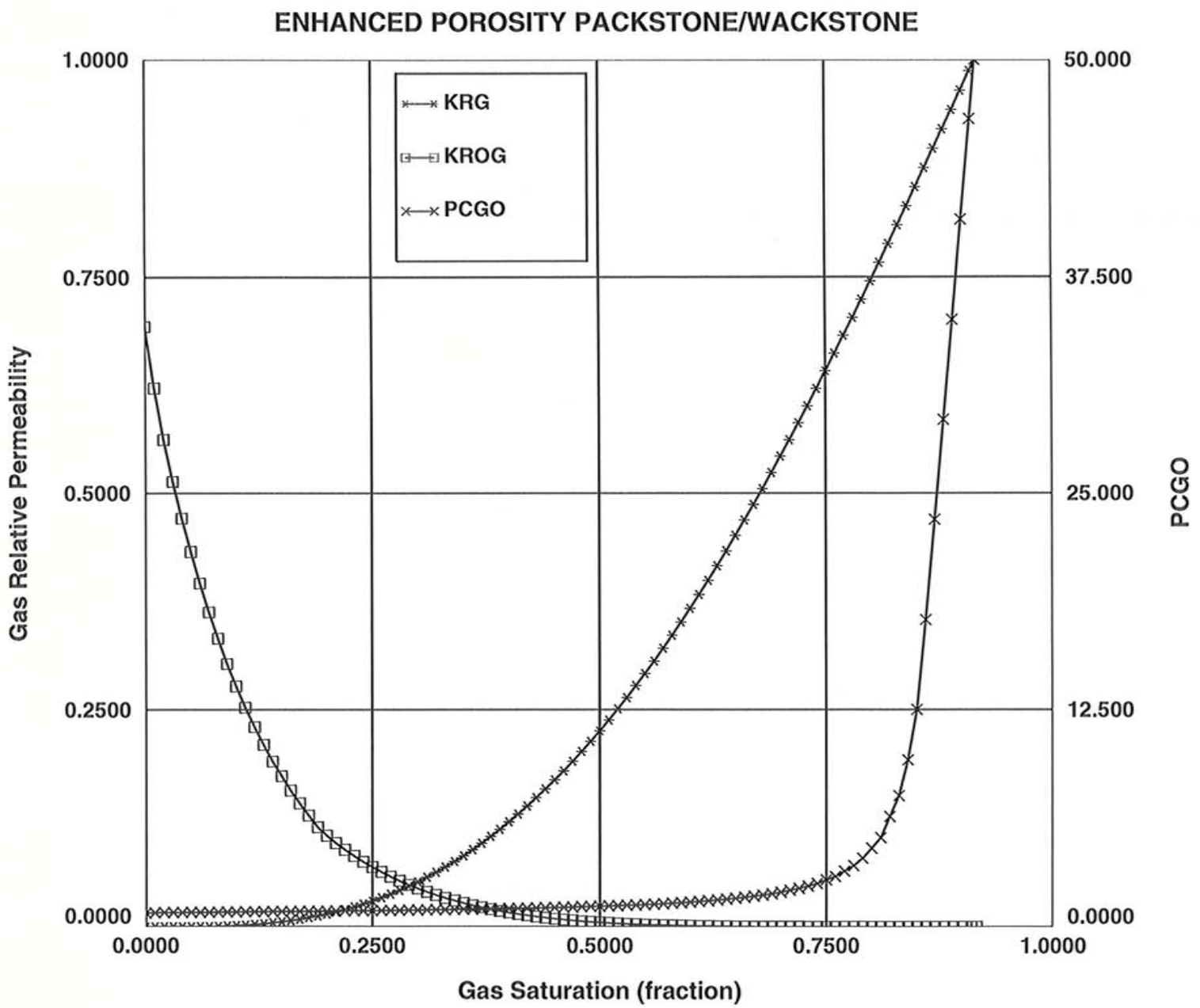

Figure 13-1 Gas-Oil Relative Permeability and Capillary Pressure for Dolomite Unit

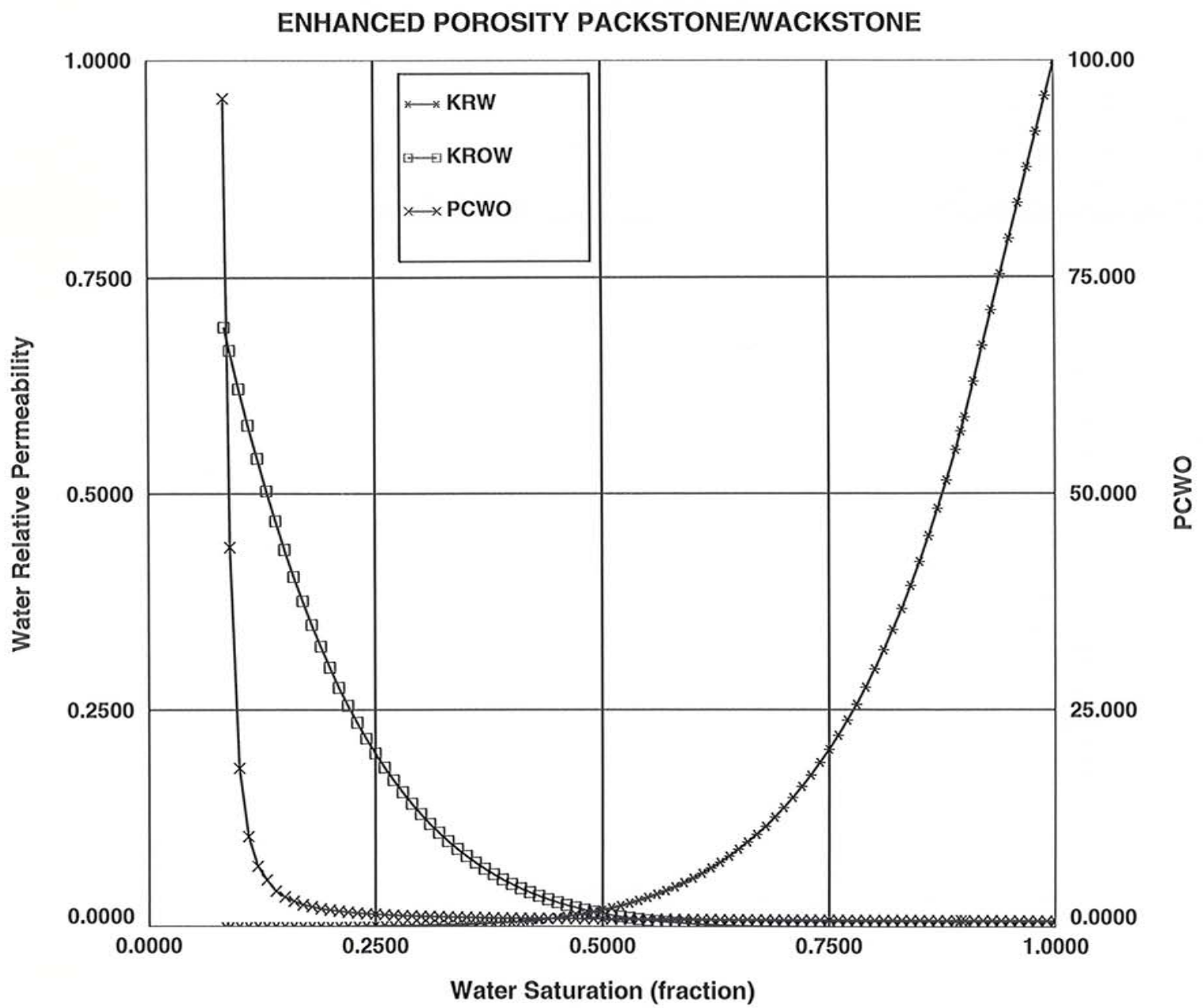

Figure 13-2 Oil-Water Relative Permeability and Capillary Pressure for Dolomite Unit

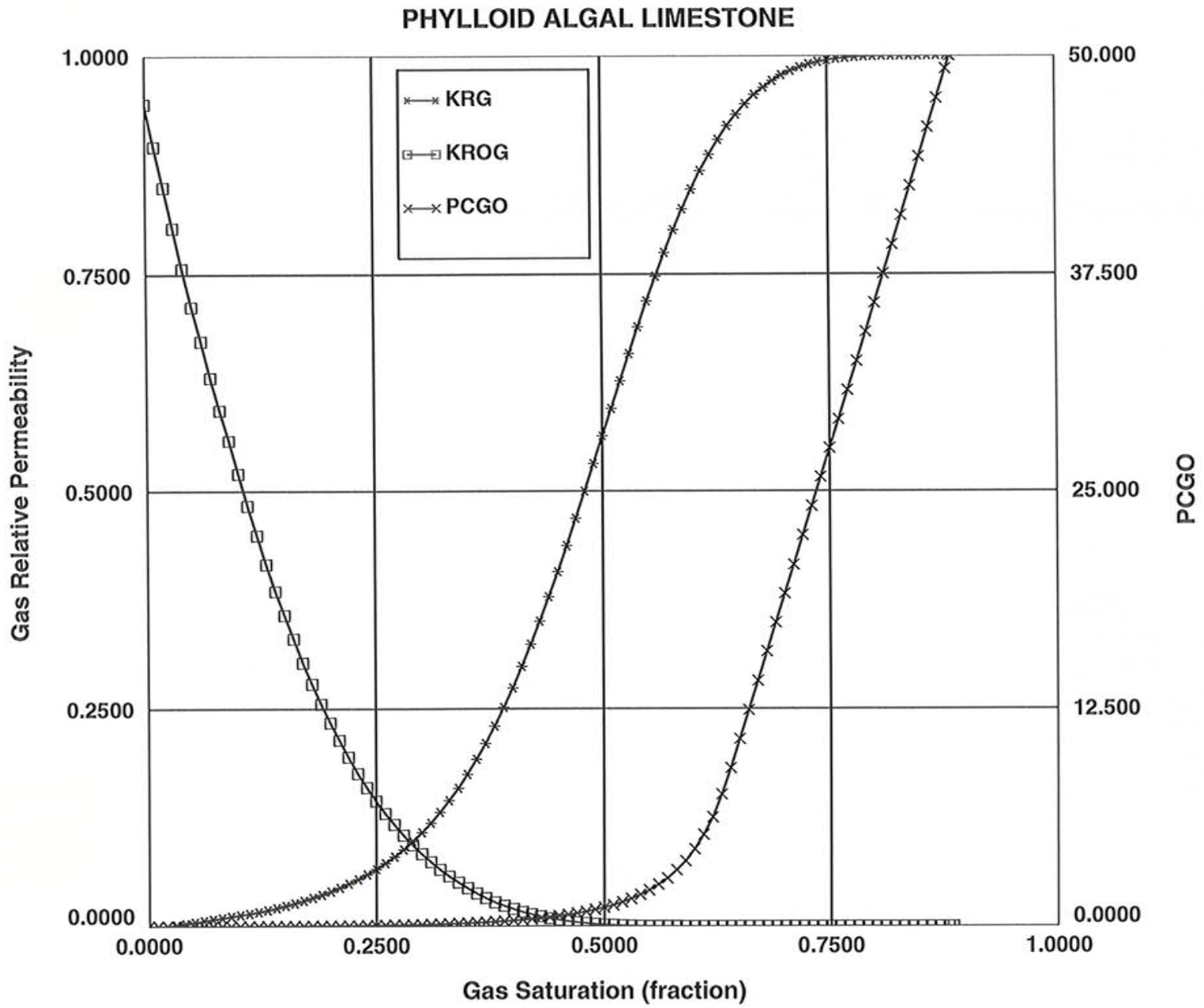

Figure 13-3 Gas-Oil Relative Permeability and Capillary Pressure for Limestone Unit

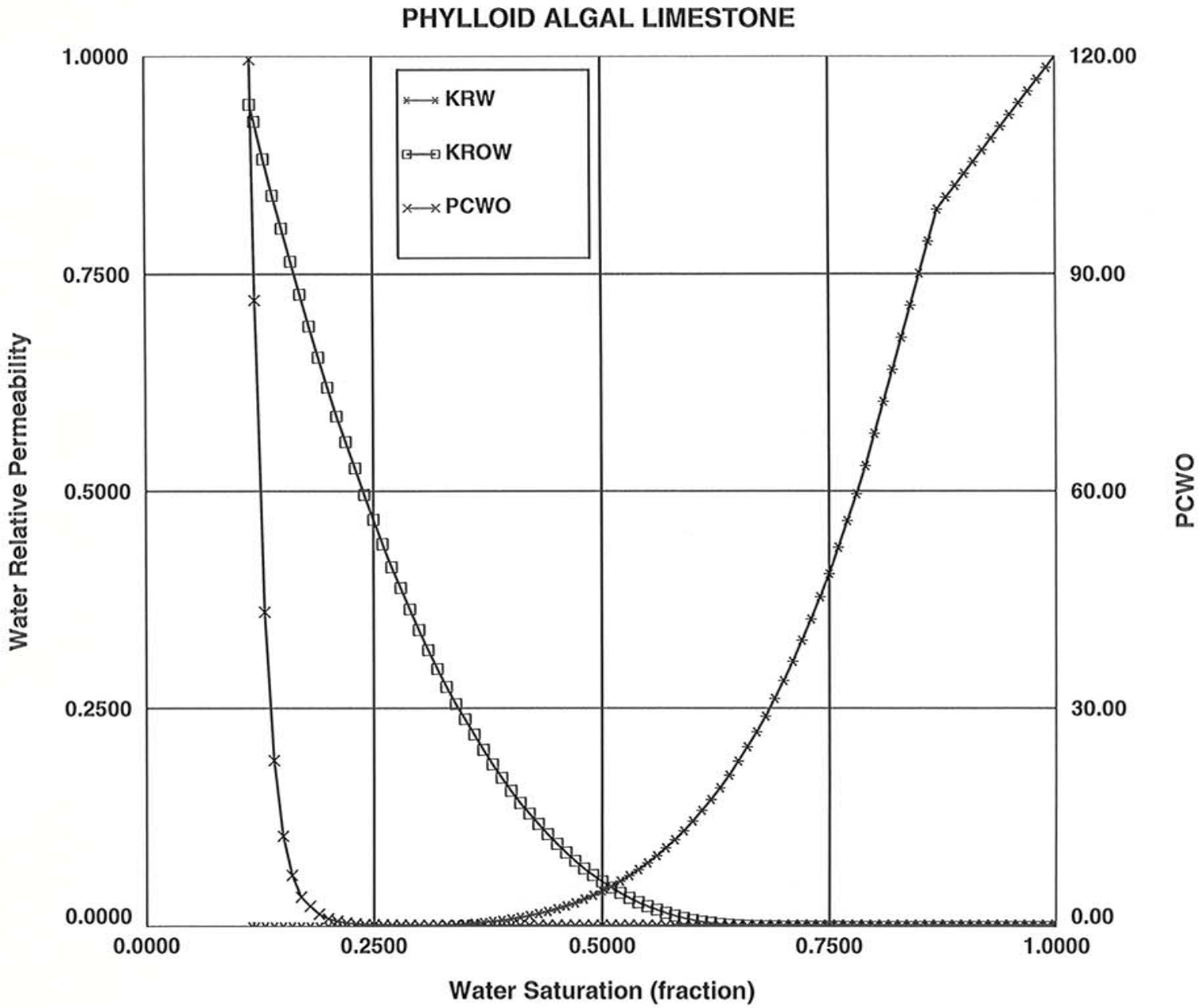

Figure 13-4 Oil-Water Relative Permeability and Capillary Pressure for Limestone Unit

X-Direction and Y-Direction Grid Sizes - 105 Feet

Number of X-Direction Cells = 50

Number of Y-Direction Cells = 30

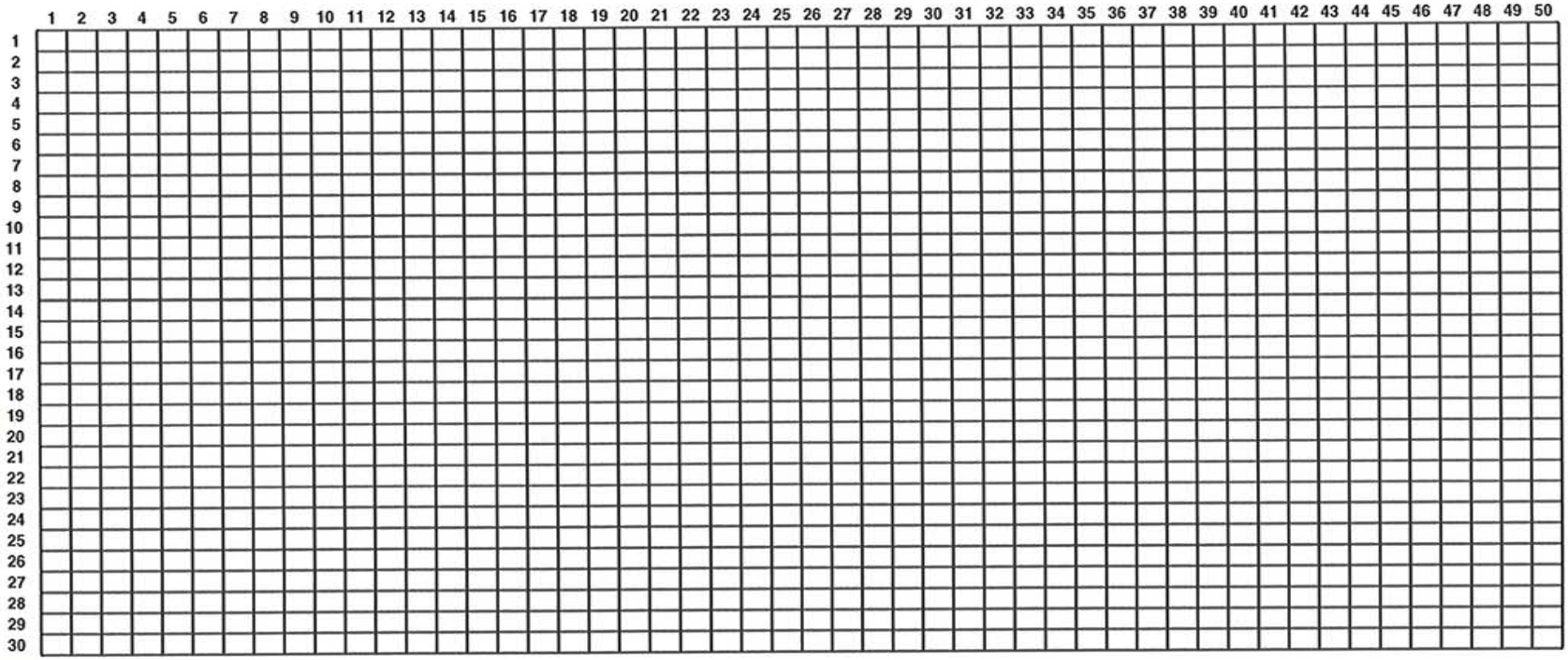

Figure 13-5 Areal Reservoir Geometry and Simulation Grid Definition

Z - Direction Grid Size - Variable

Number of Z - Direction Cells = 15

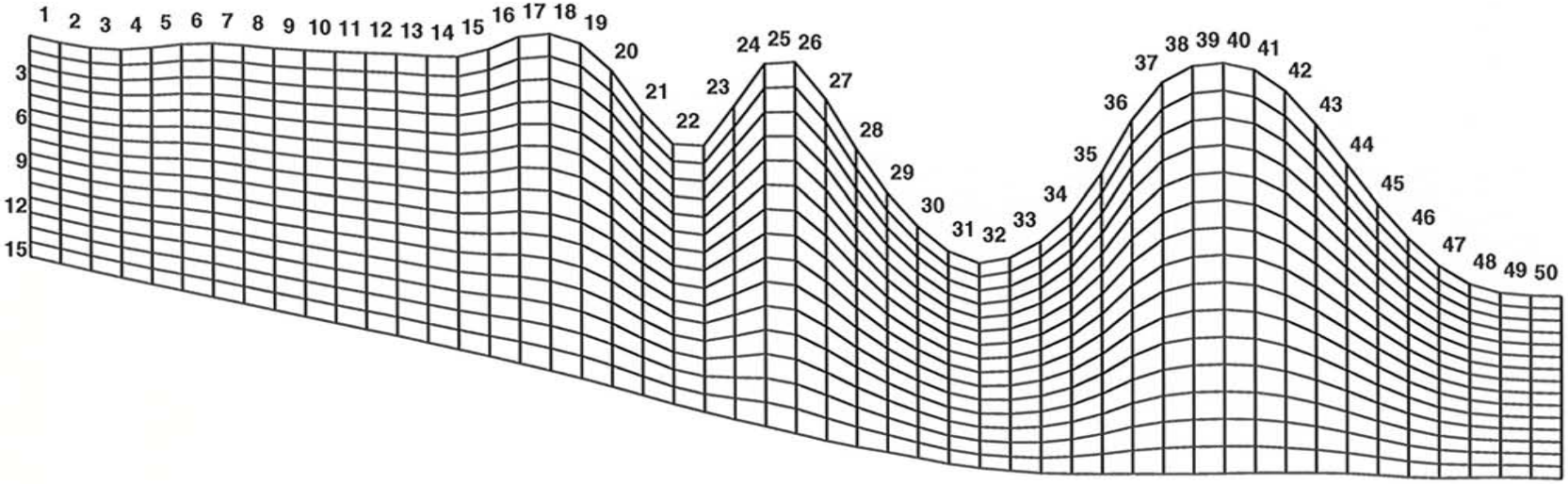

FRONT XZ PLANE FOR Y =15

Figure 13-6 Vertical(Z-Direction) Grid Definition Y - Cross Section

Z - Direction Grid Size - Variable

Number of Z - Direction Cells = 15

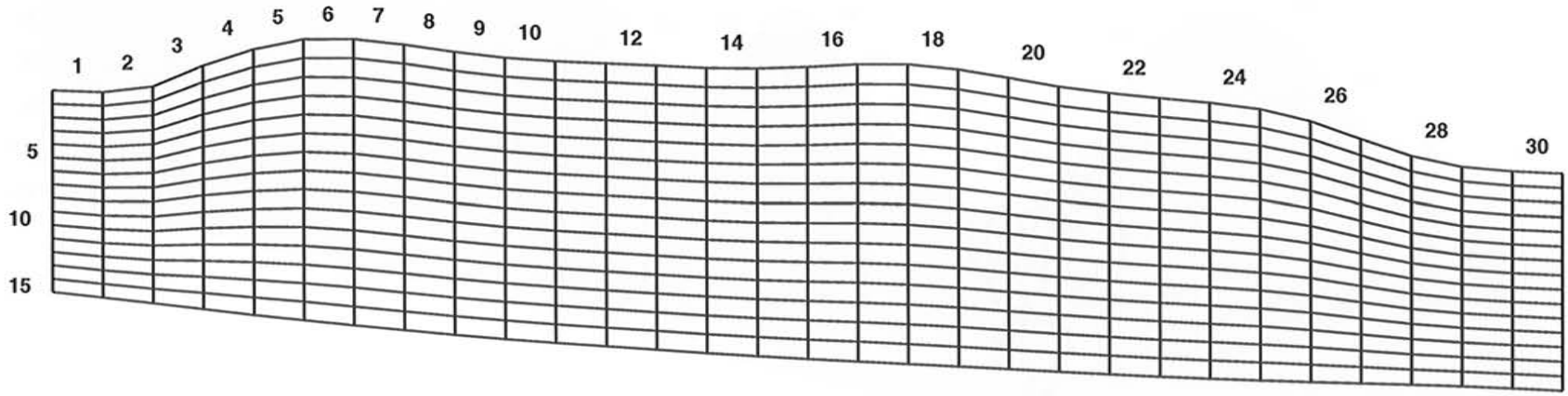

FRONT YZ PLANE FOR X =15

Figure 13-7 Vertical(Z-Direction) Grid Definition X - Cross Section

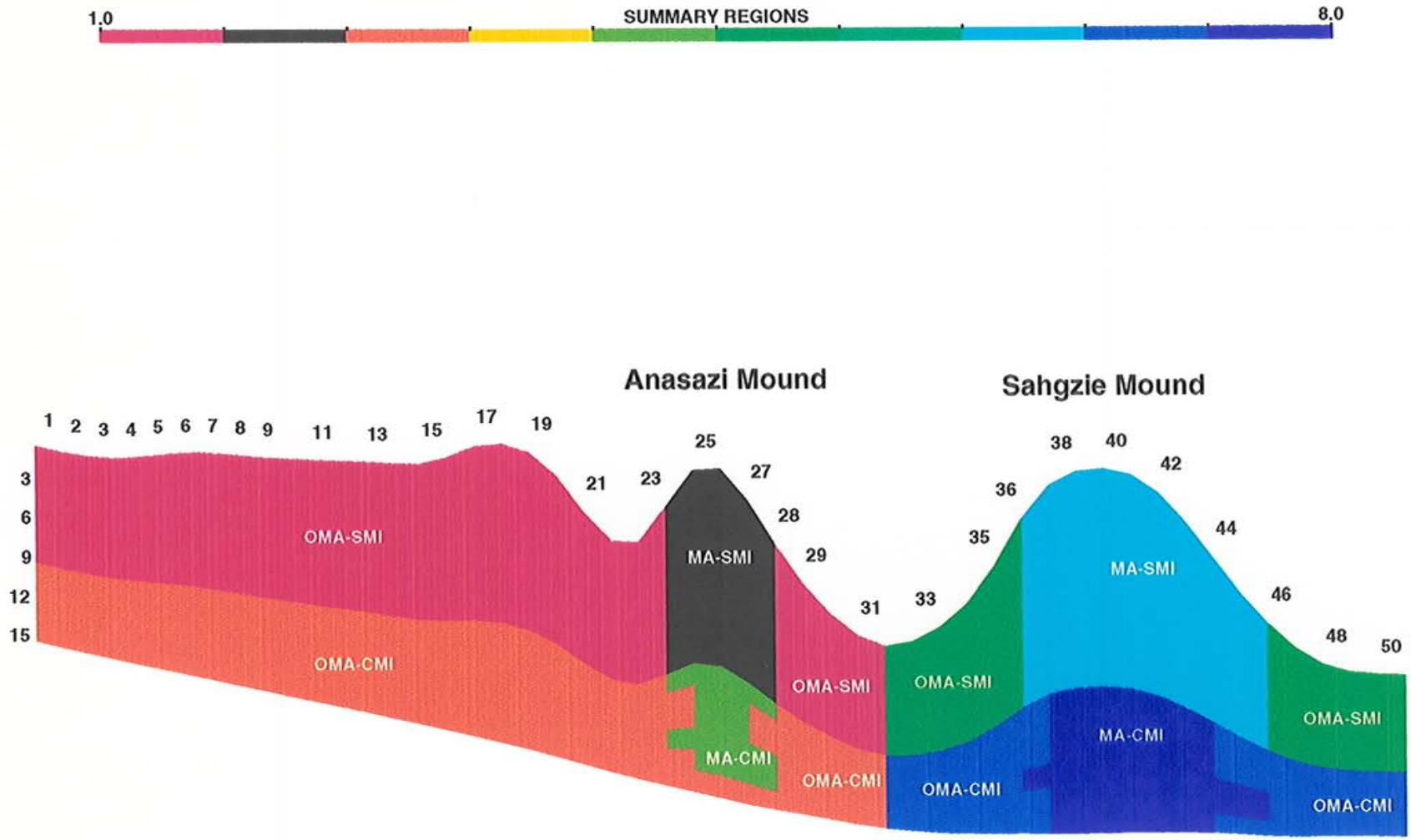

FRONT XZ PLANE FOR Y =15

Figure 13-8 Region Definition - Eight Regions Y Cross Section

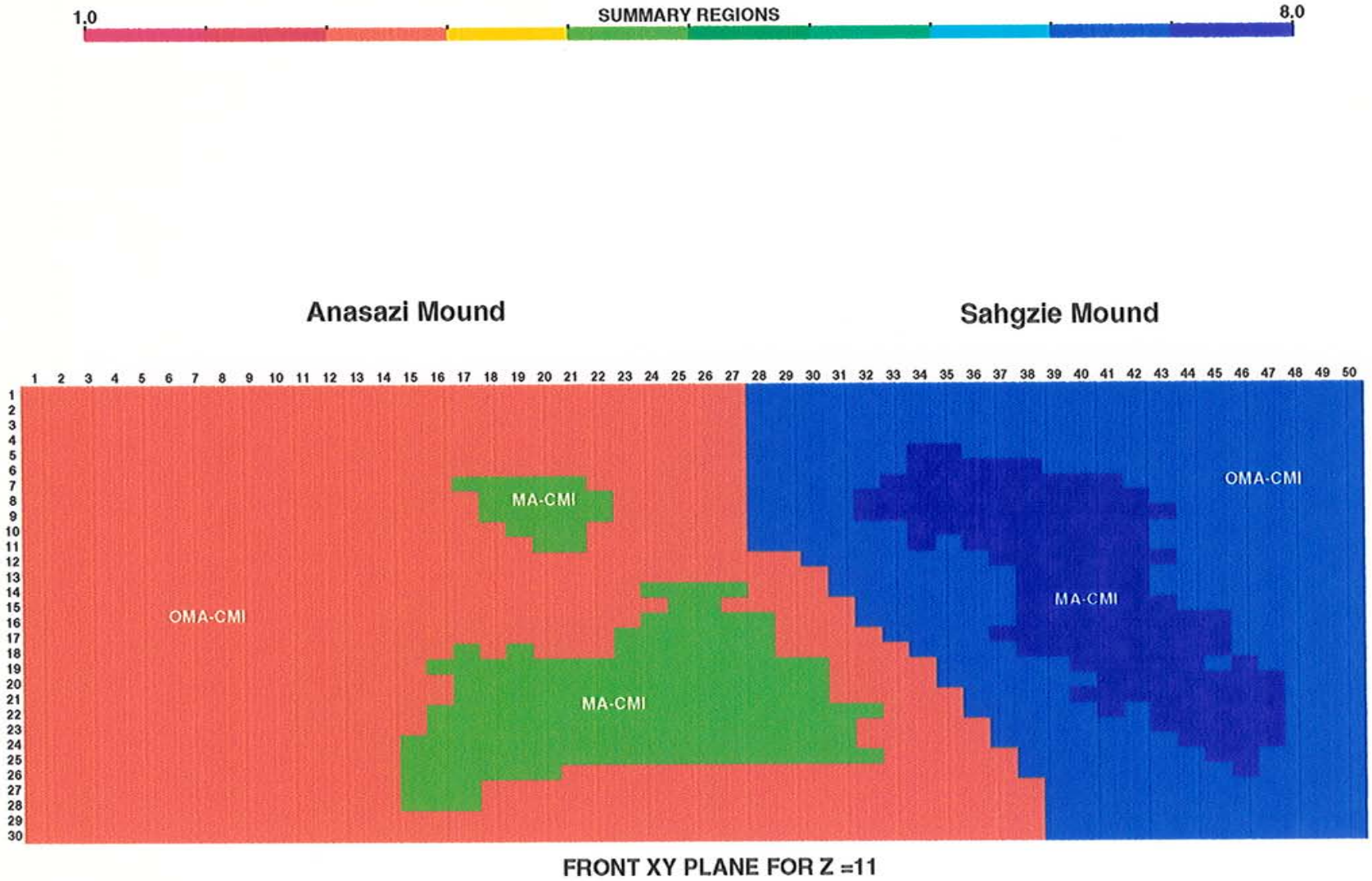

Figure 13-9 Region Definition - Map at Top of Core Mound Interval

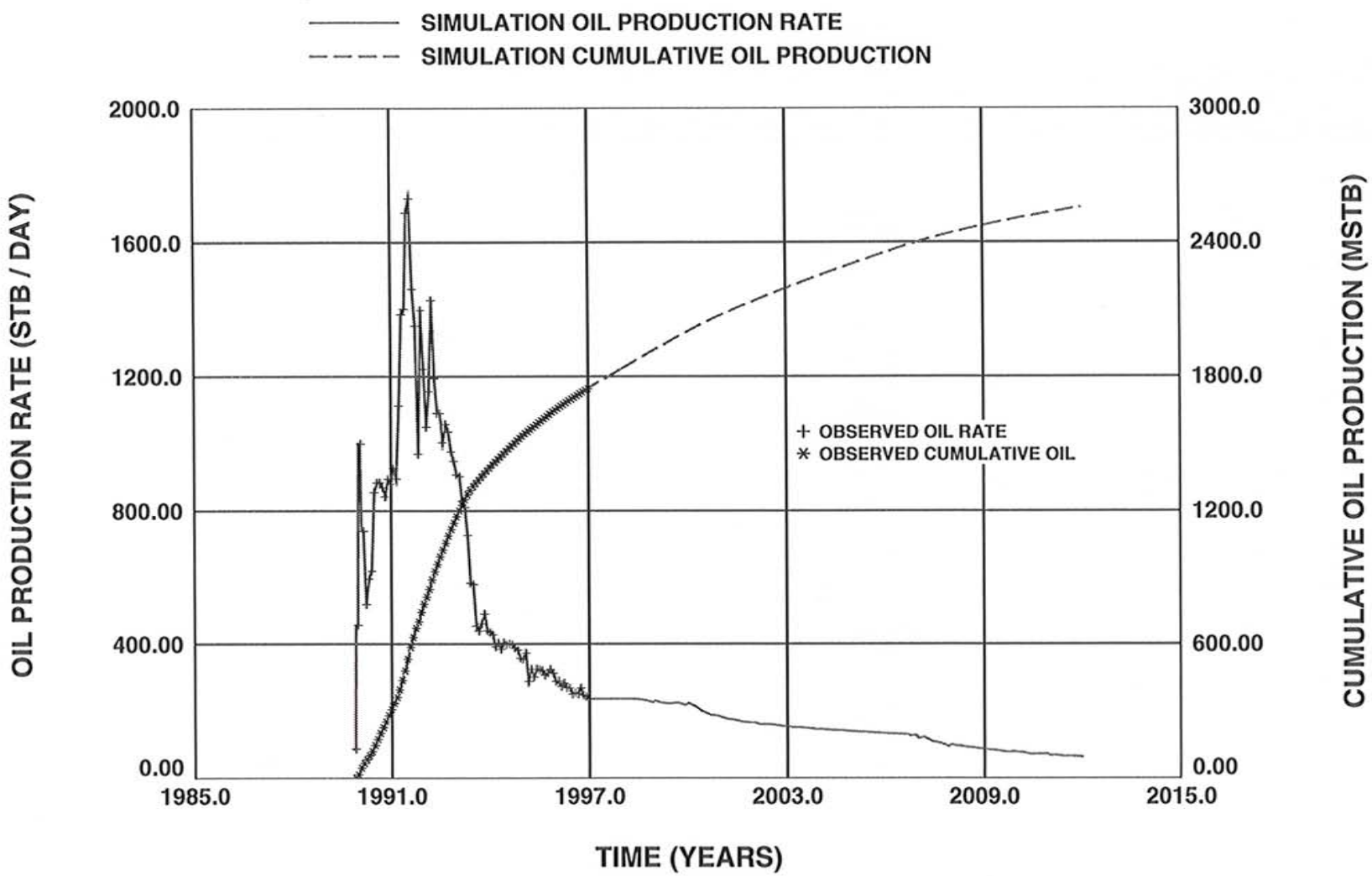

Figure 14-1 Oil Production History Anasazi-Sahgzie Reservoir

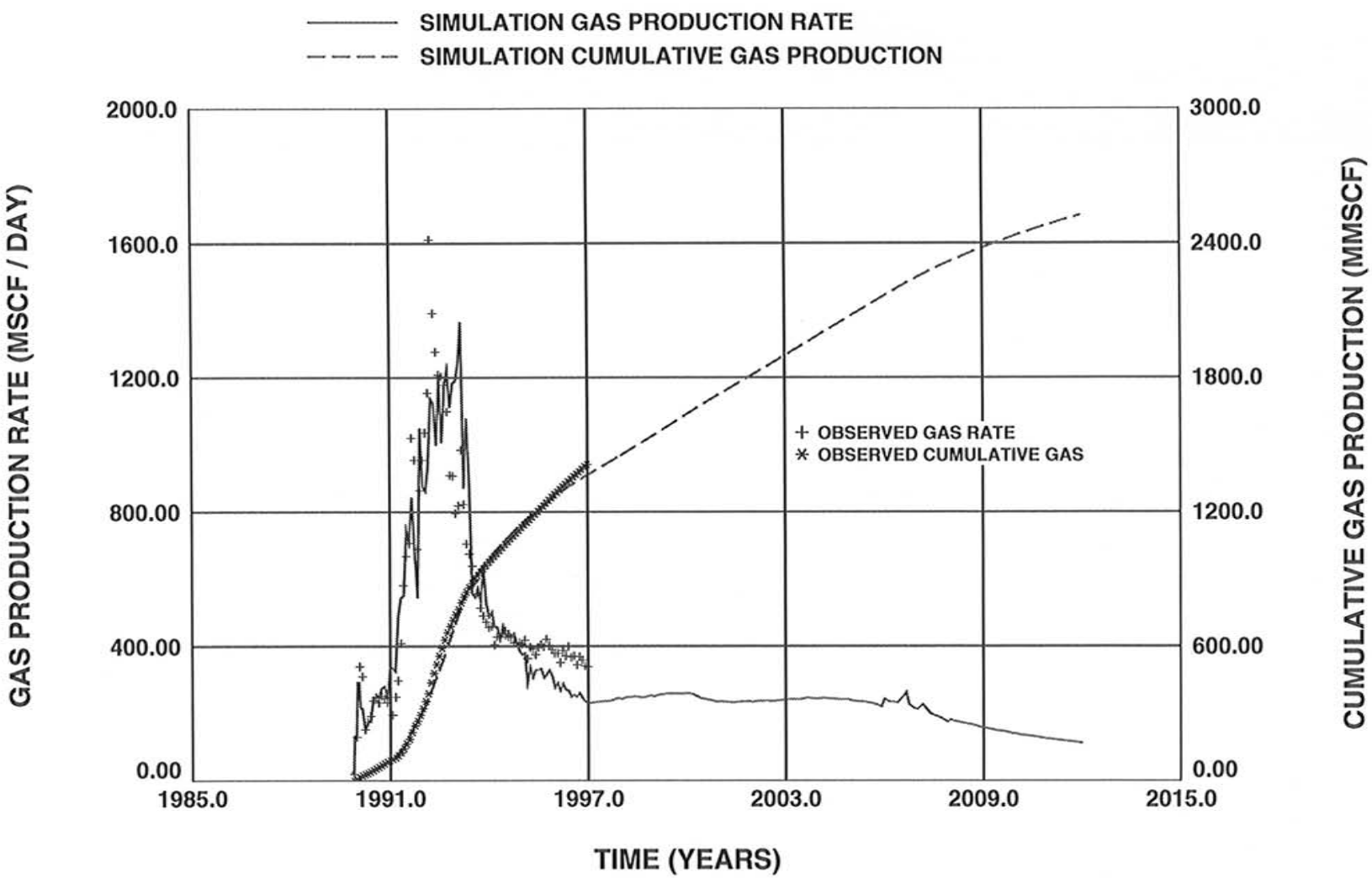

Figure 14-2 Gas Production History Match Anasazi-Sahgzie Reservoir

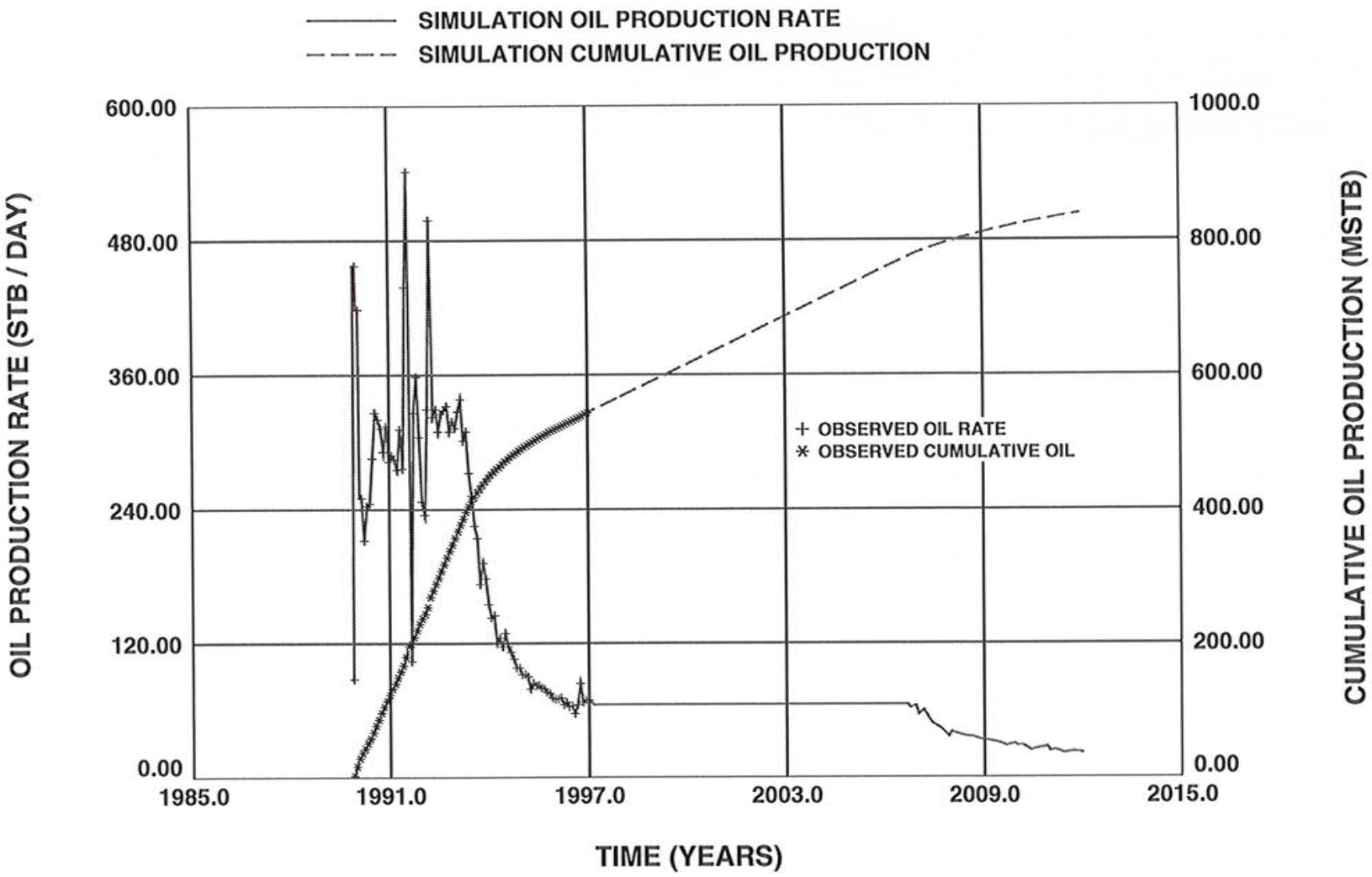

Figure 14-3 Oil Production History - Sahgzie Well No 1

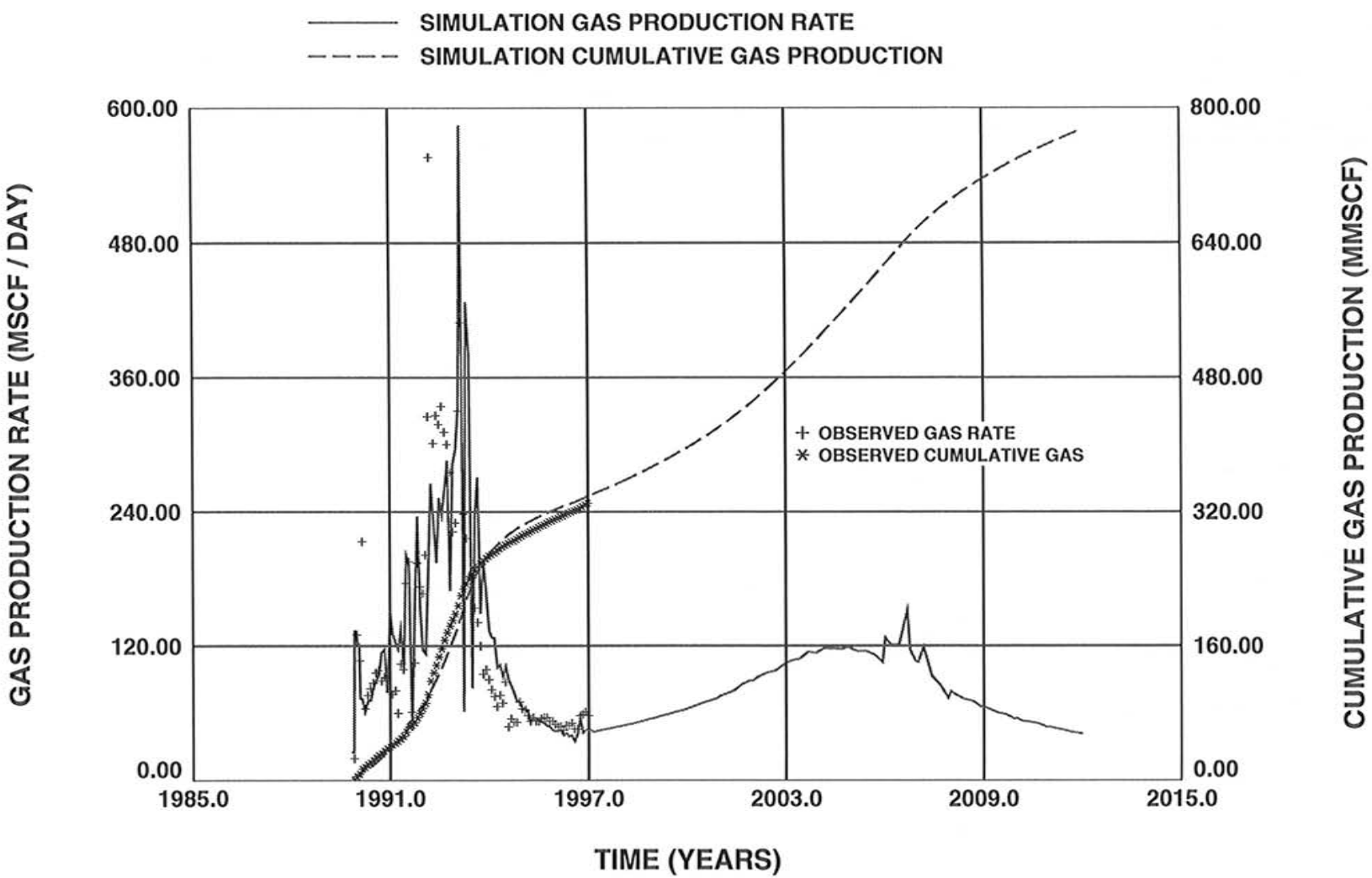

Figure 14-4 Gas Production History Match - Sahgzie Well No 1

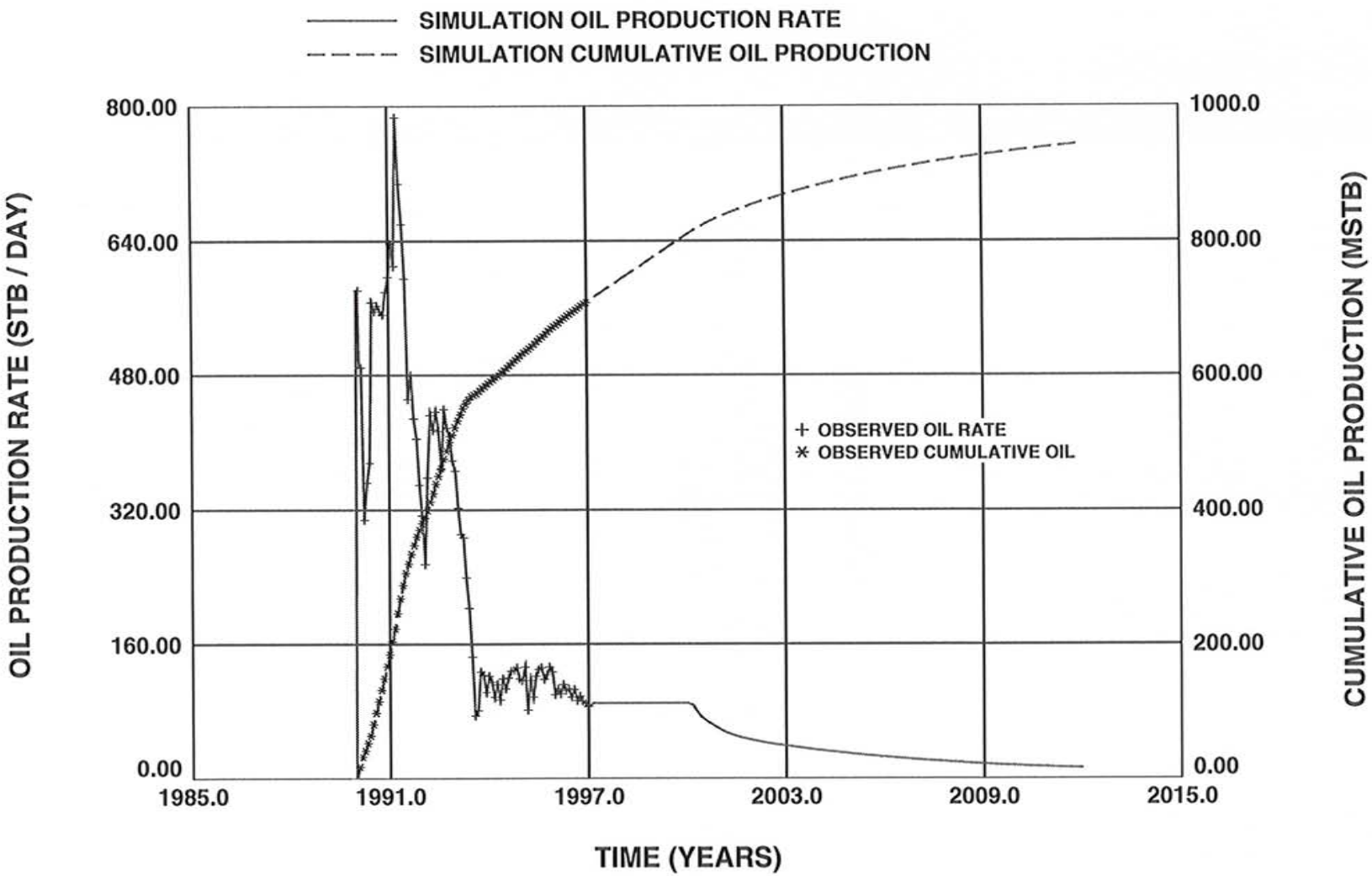

Figure 14-5 Oil Production History - Anasazi Well No 1

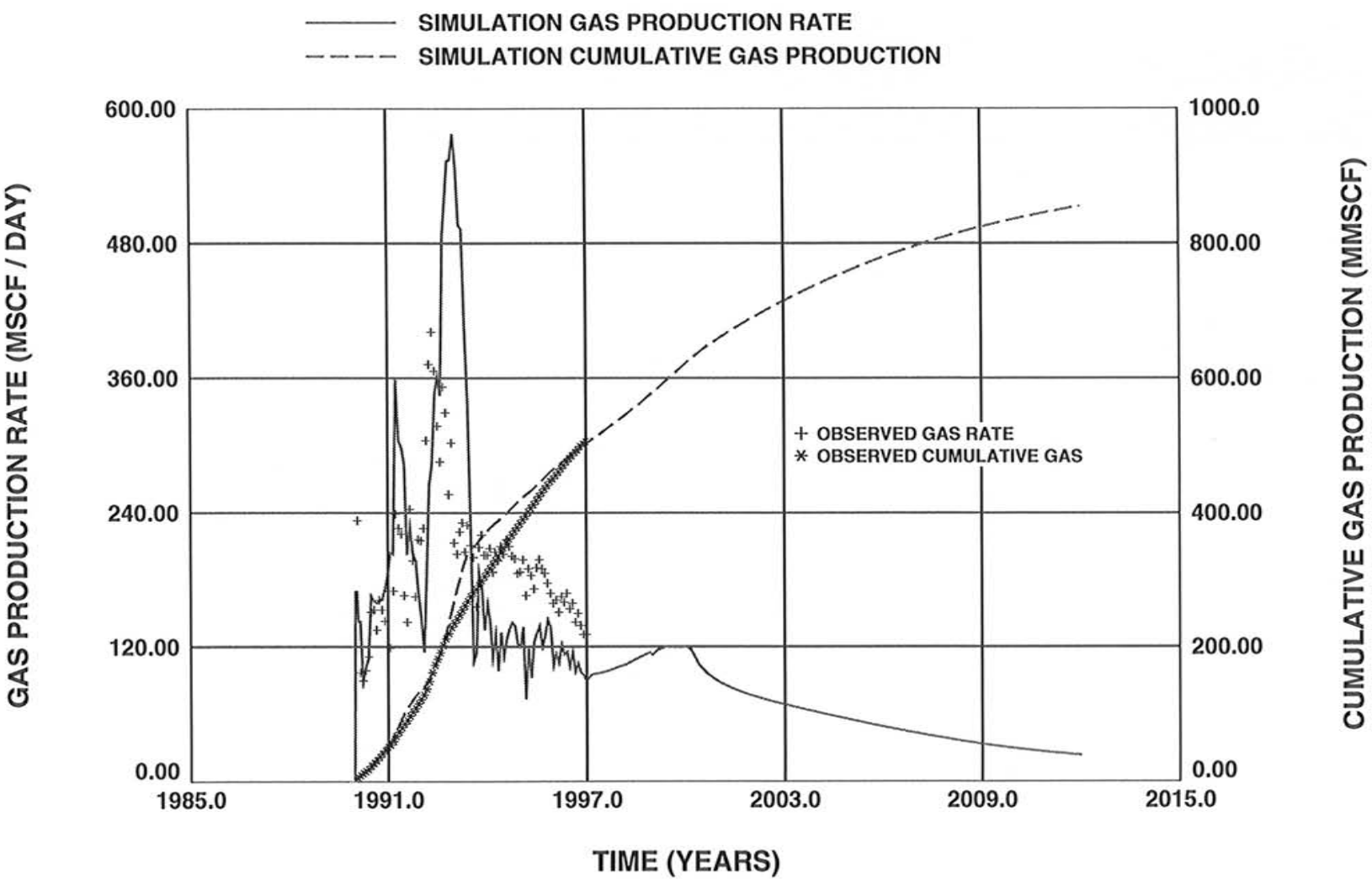

Figure 14-6 Gas Production History Match - Anasazi Well No 1

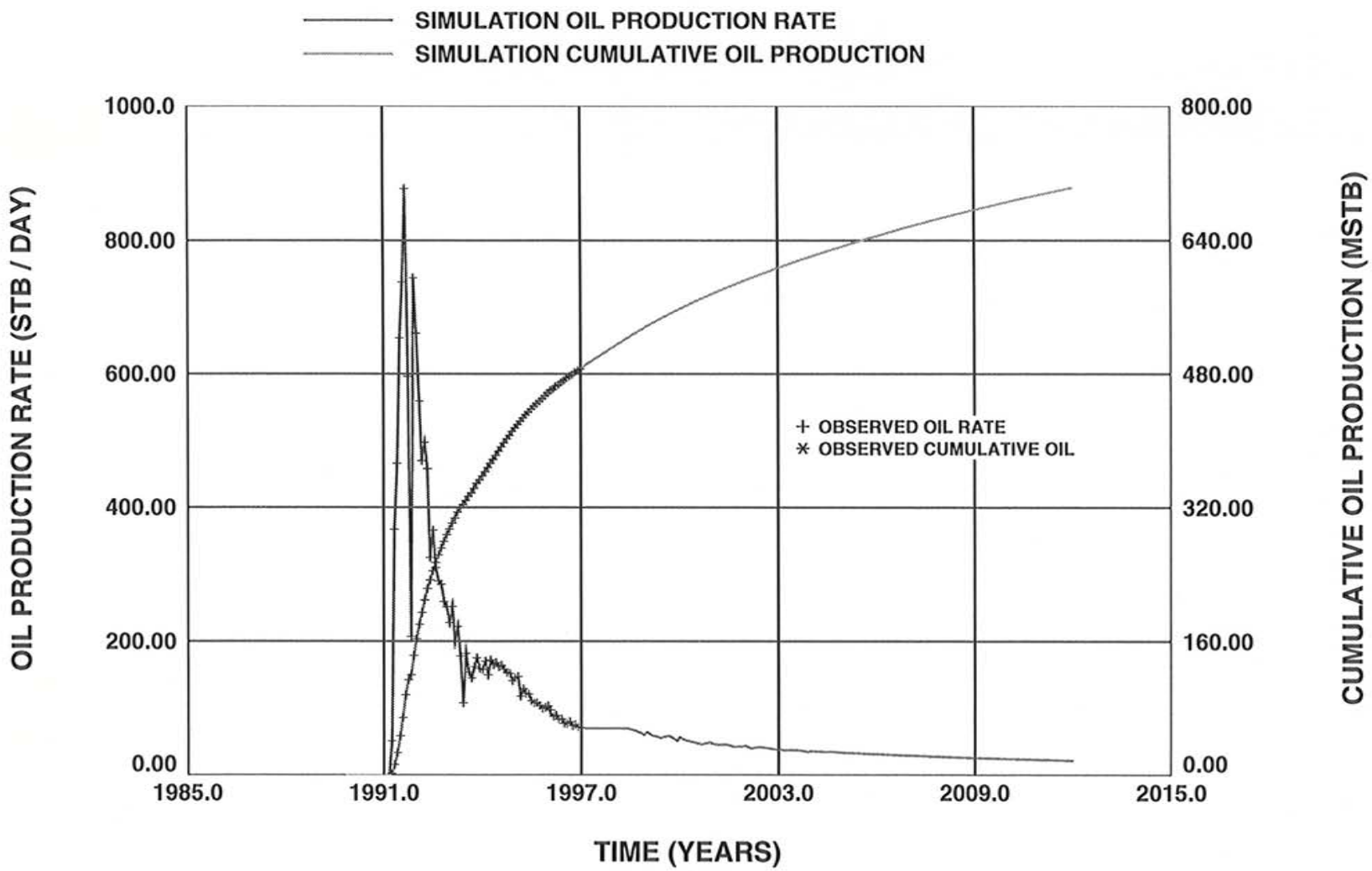

Figure 14-7 Oil Production History - Anasazi Well No 5L-3

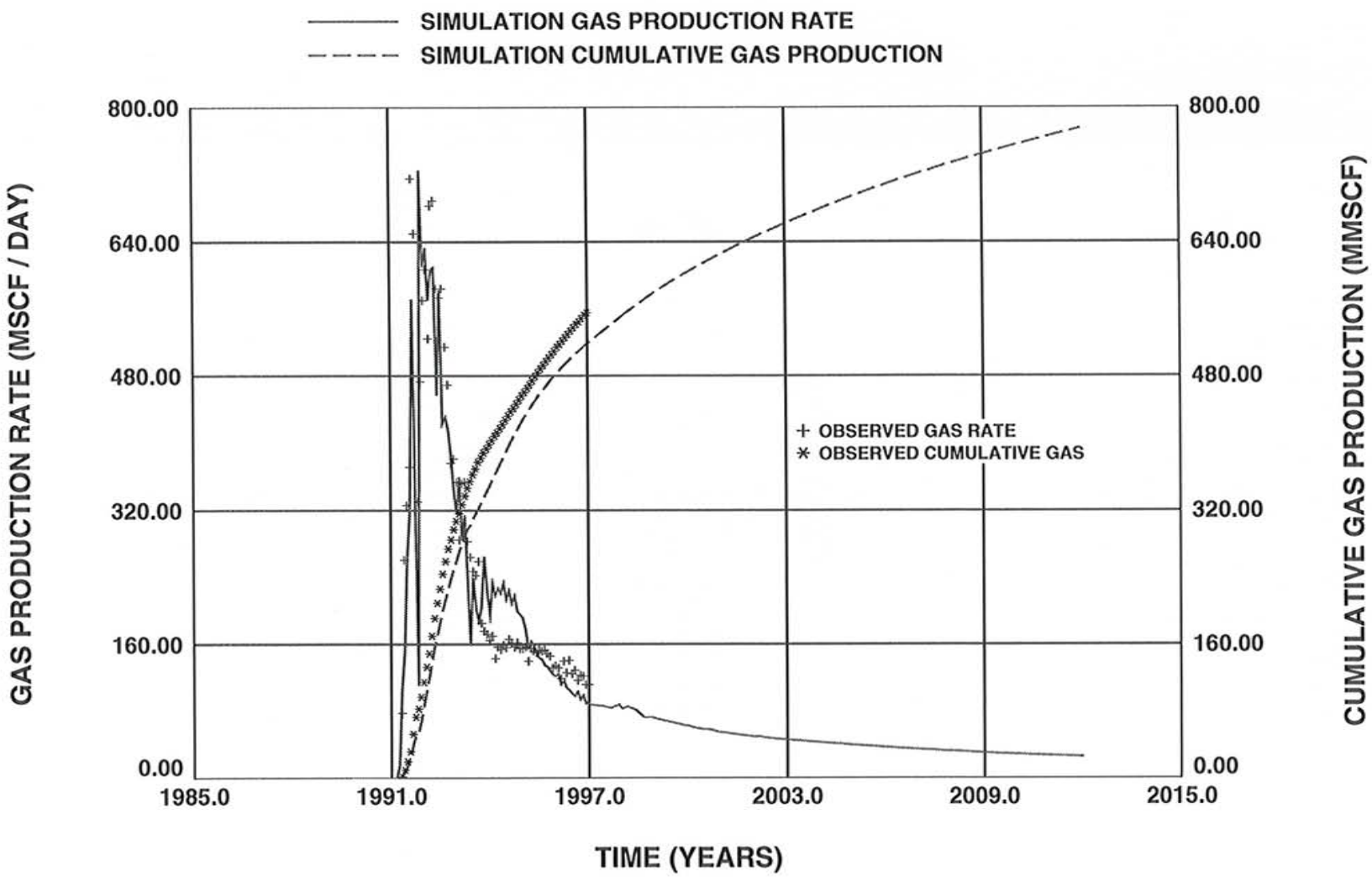

Figure 14-8 Gas Production History Match - Anasazi Well No 5L-3

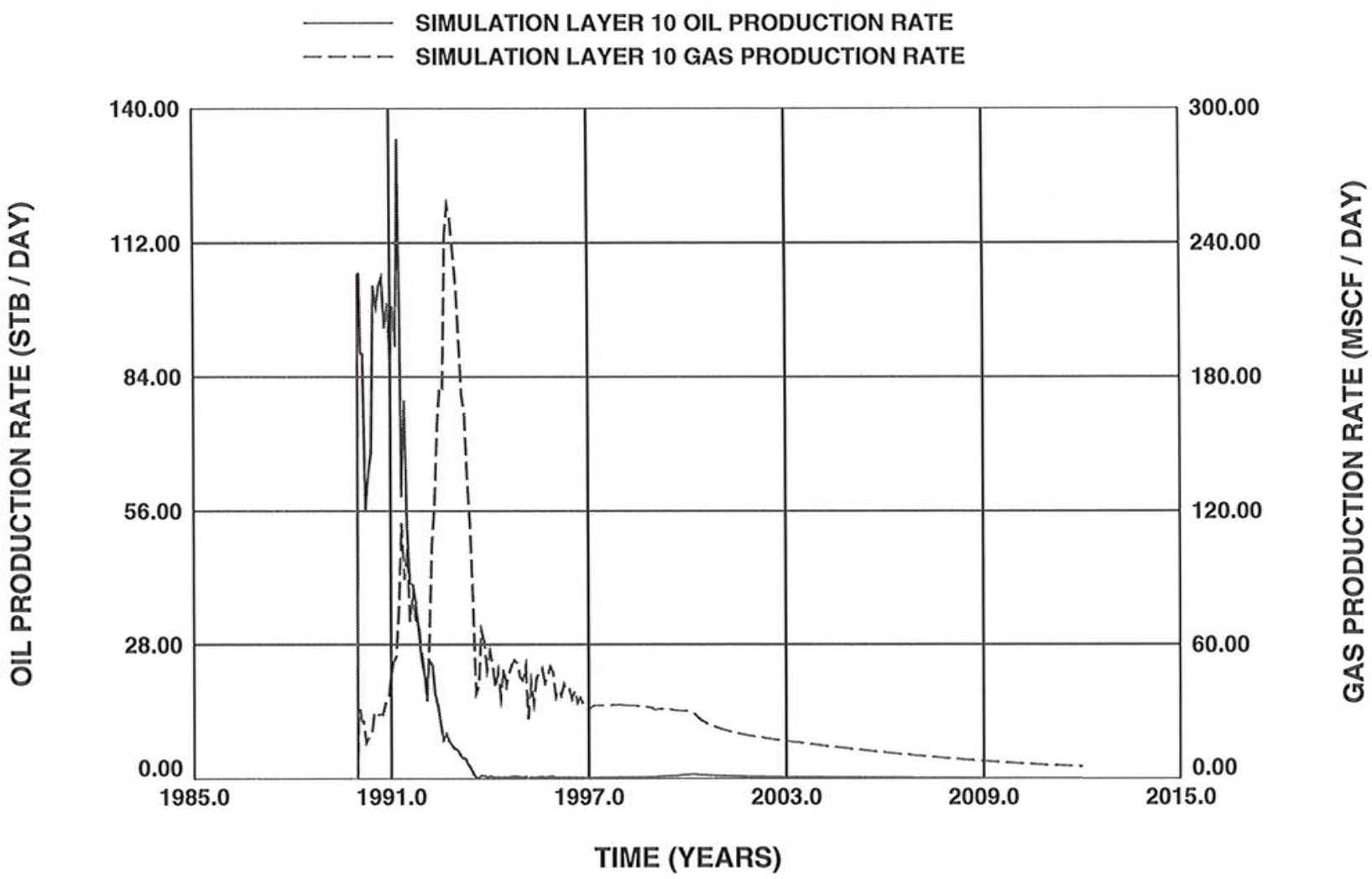

Figure 14-9 Layer 10 Oil and Gas Production Rate - Anasazi Well No 1

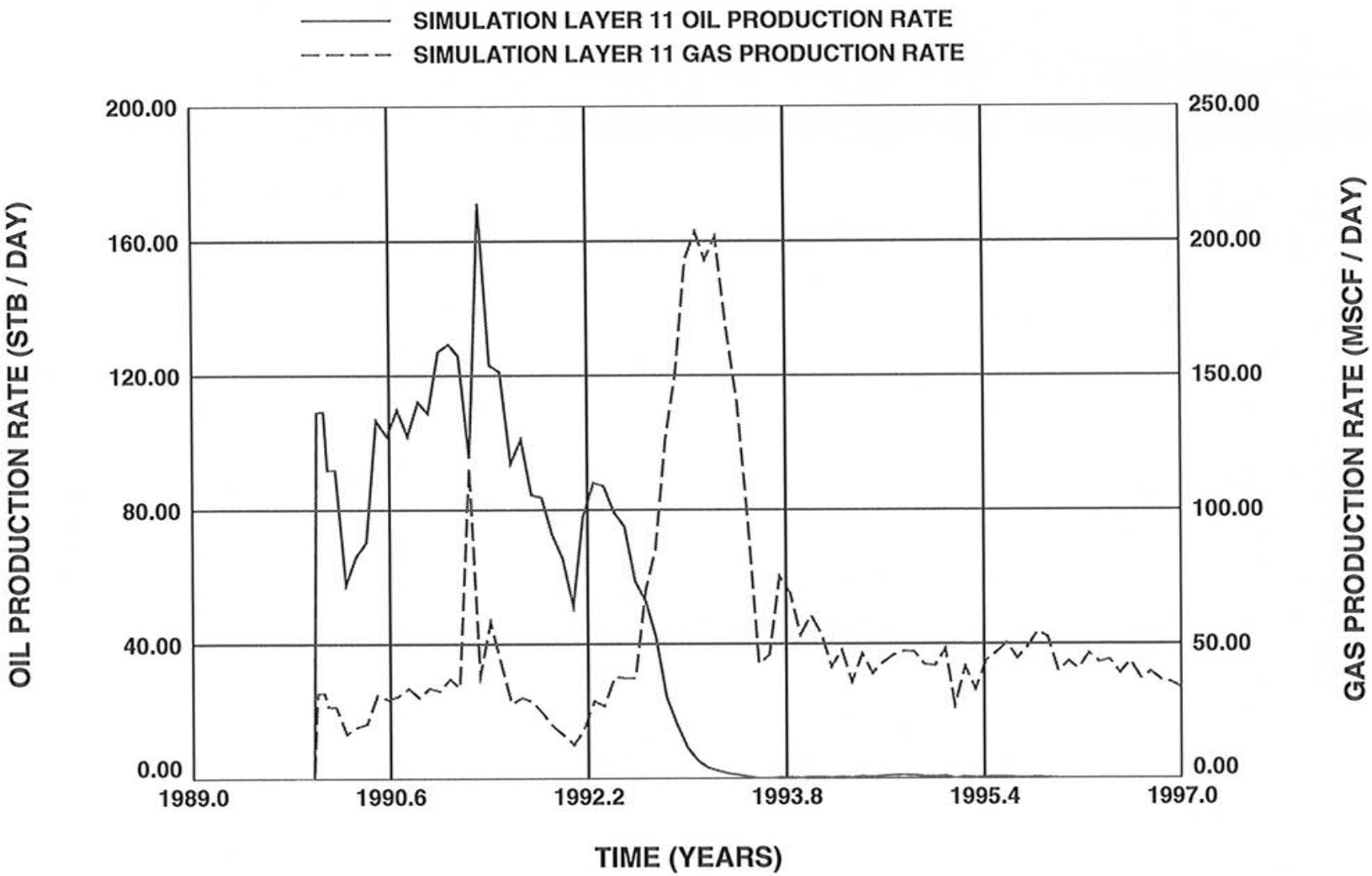

Figure 14-10 Layer 11 Oil and Gas Production - Anasazi Well No 1

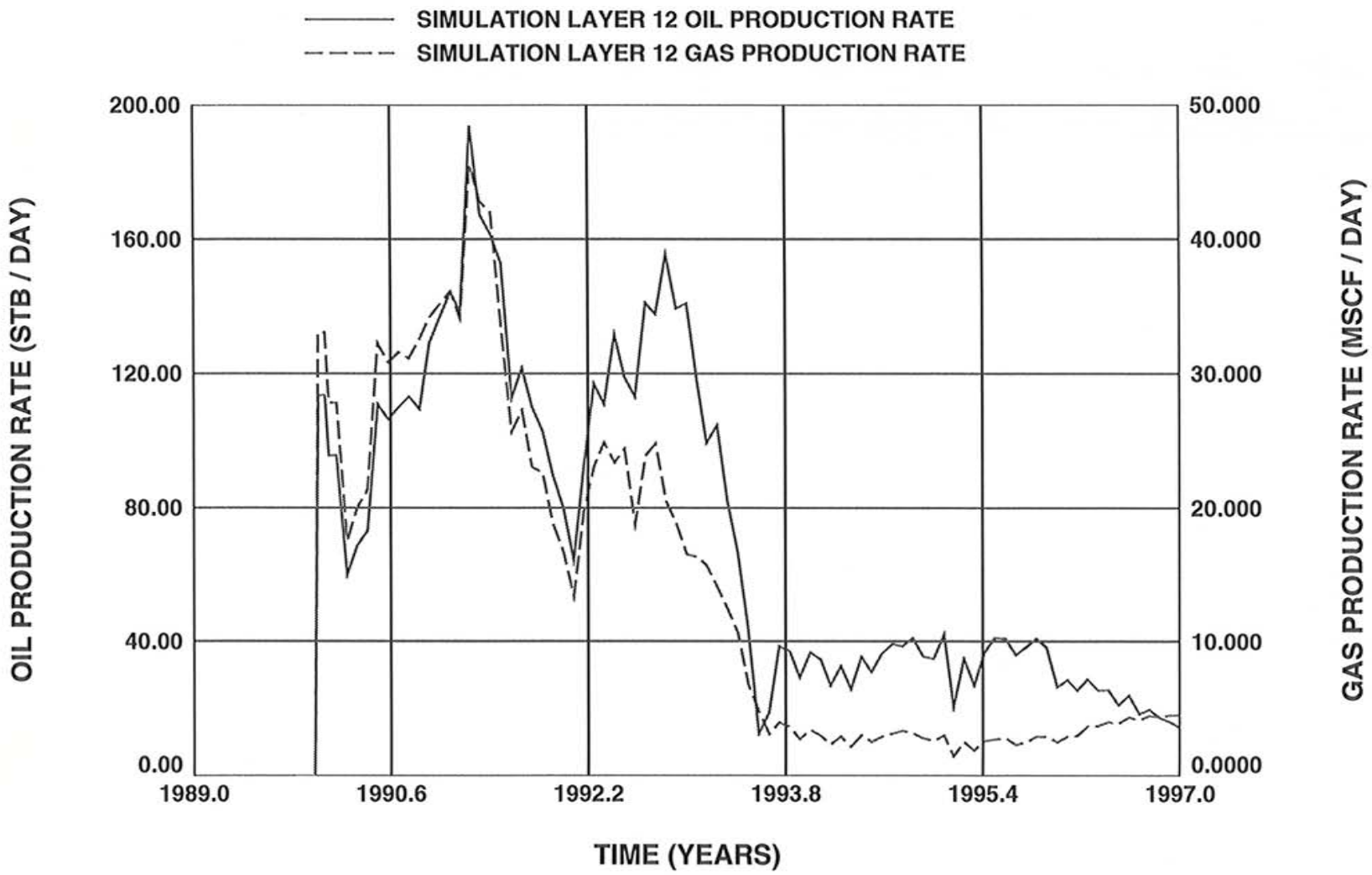

Figure 14-11 Layer 12 Oil and Gas Production - Anasazi Well No 1

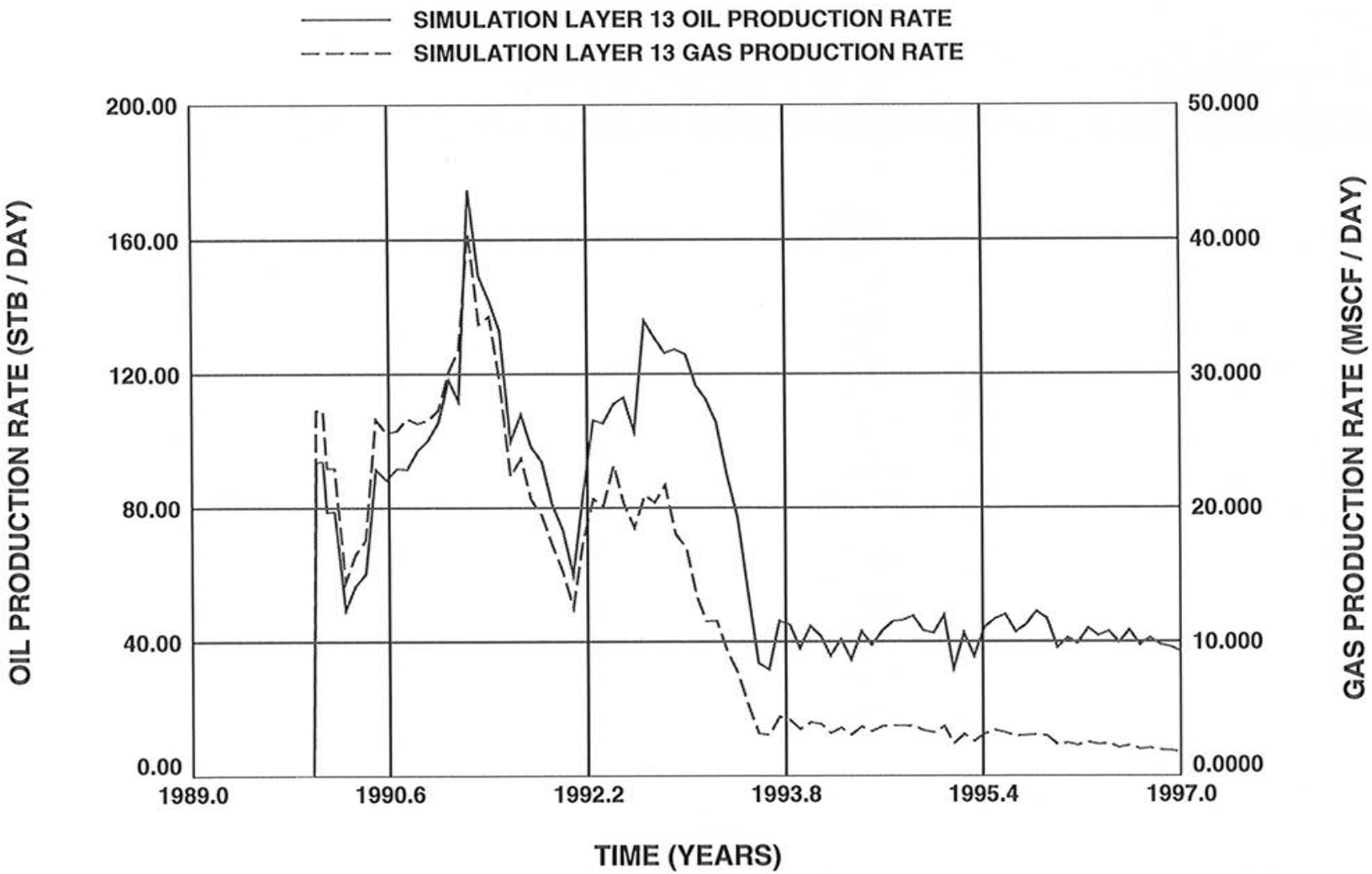

Figure 14-12 Layer 13 Oil and Gas Production - Anasazi Well No 1

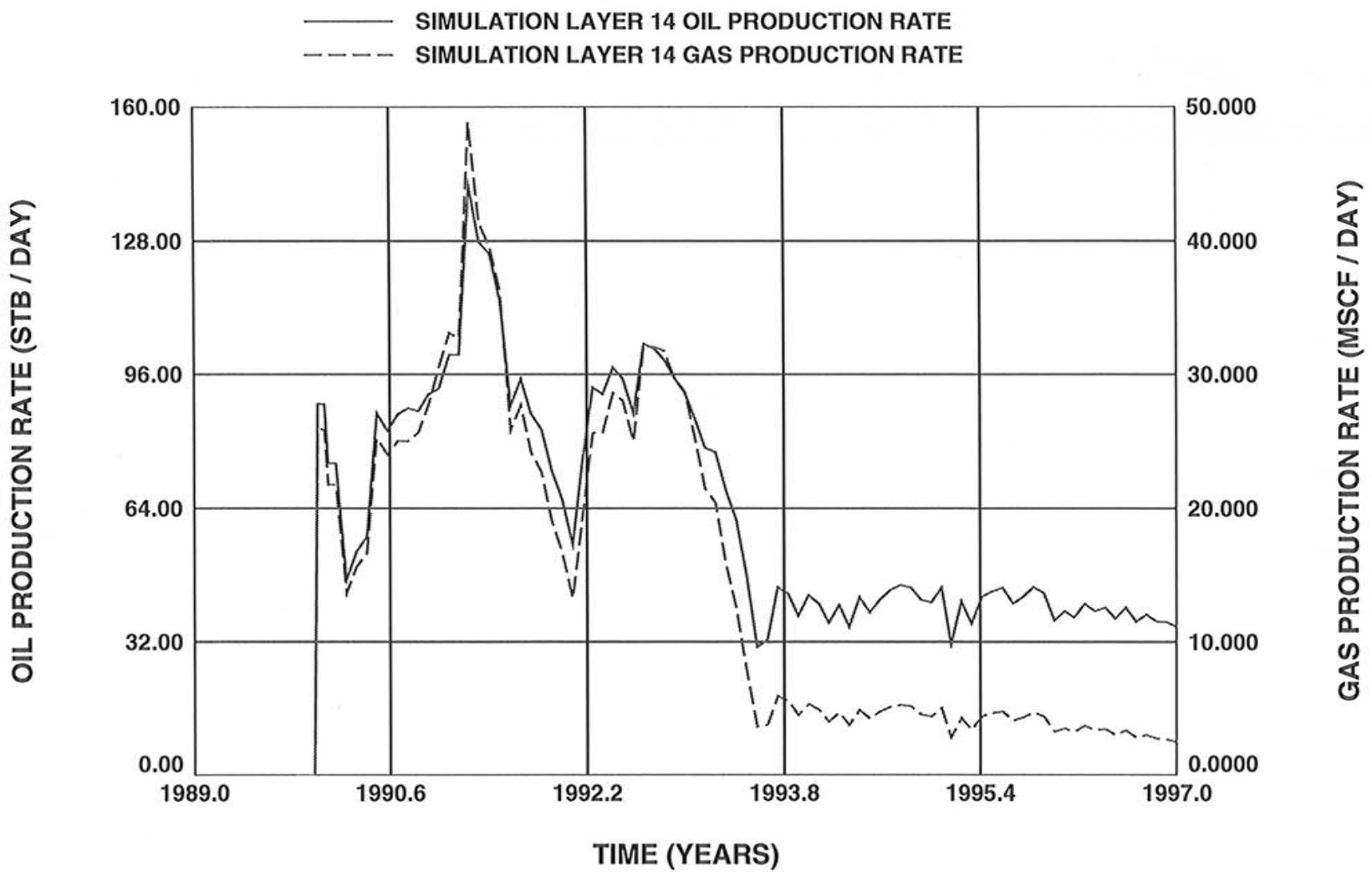

Figure 14-13 Layer 14 Oil and Gas Production - Anasazi Well No 1

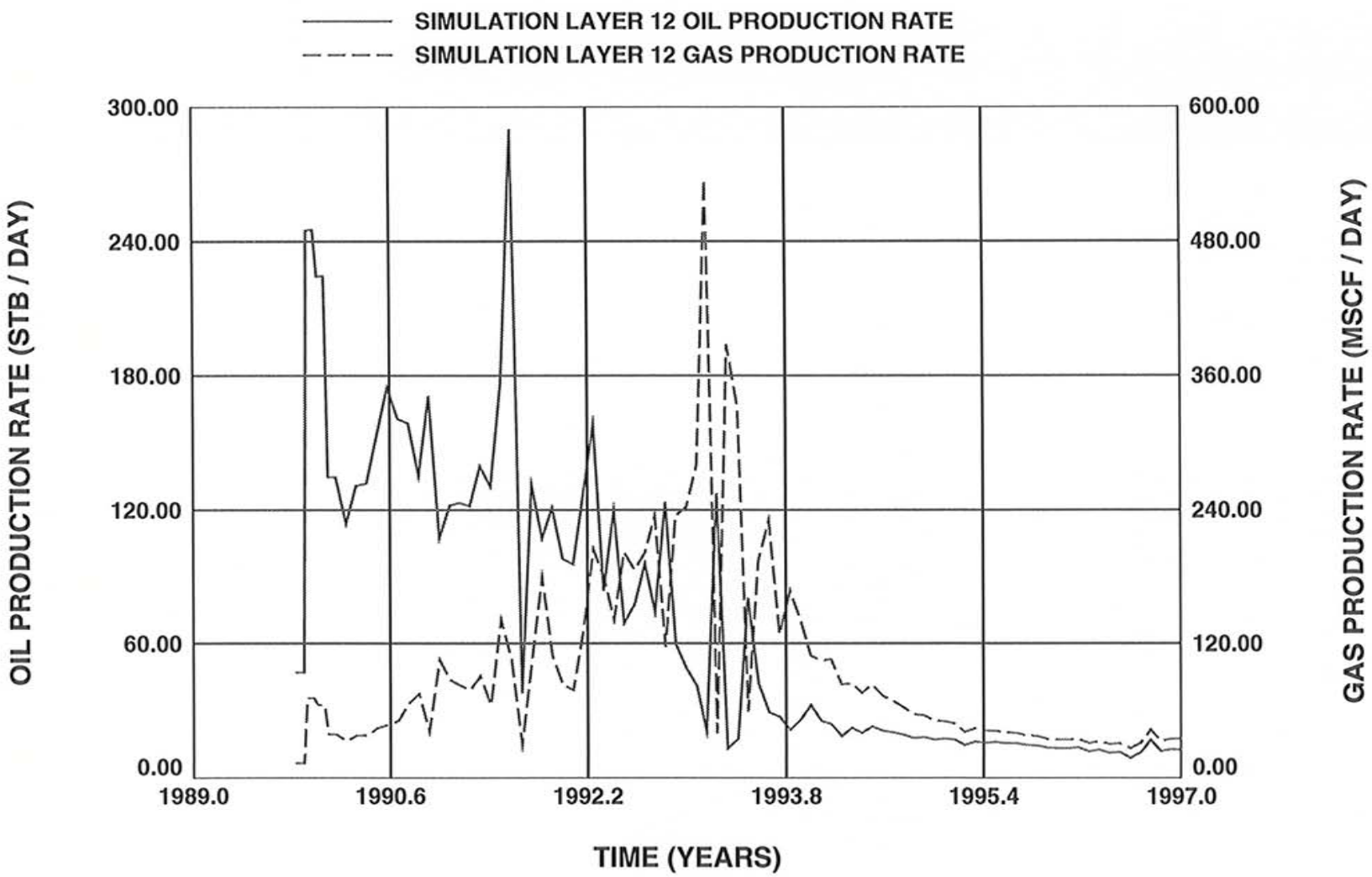

Figure 14-14 Layer 12 Oil and Gas Production - Sahgzie Well No 1

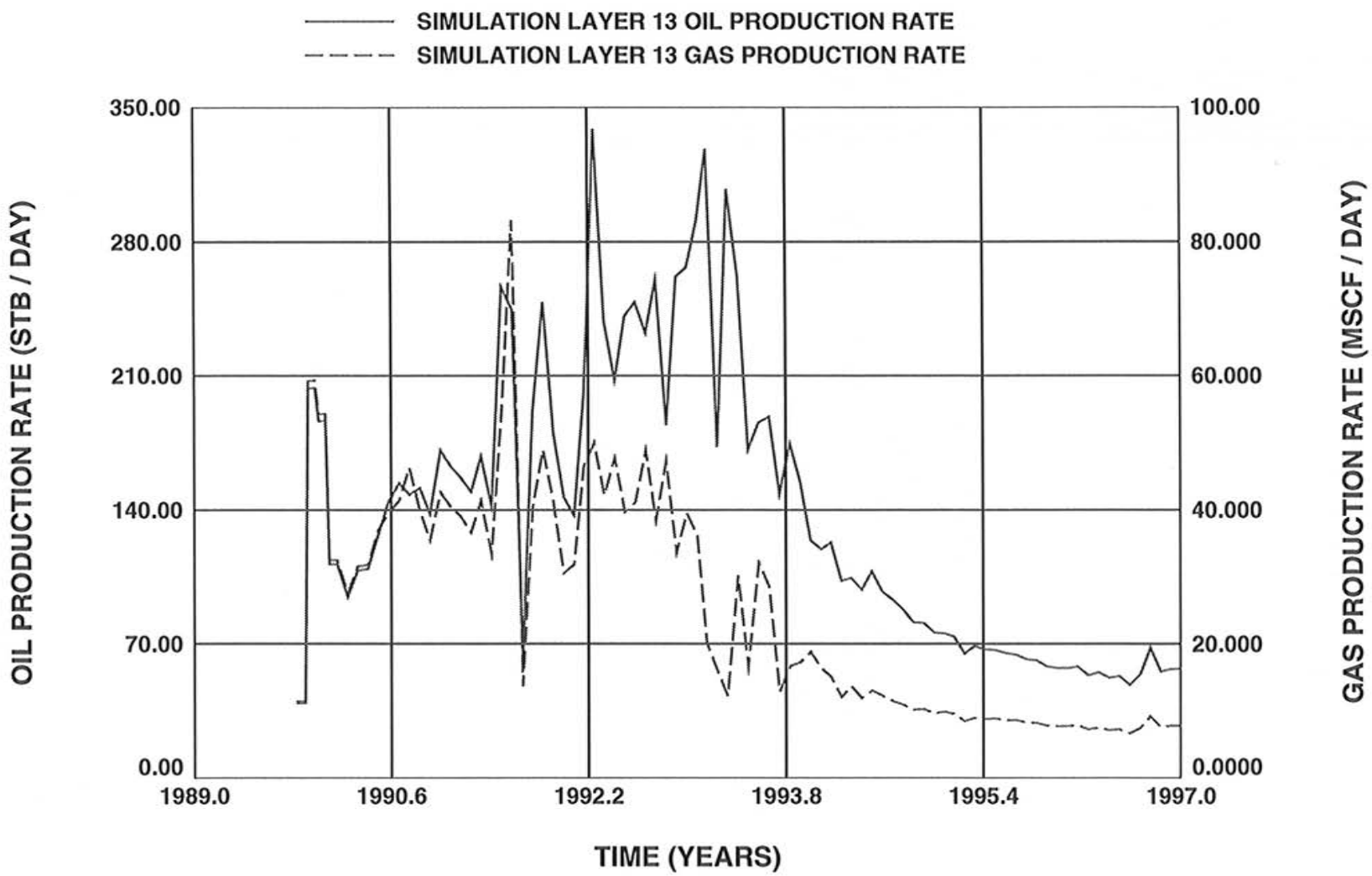

Figure 14-15 Layer 13 Oil and Gas Production - Sahgzie Well No 1

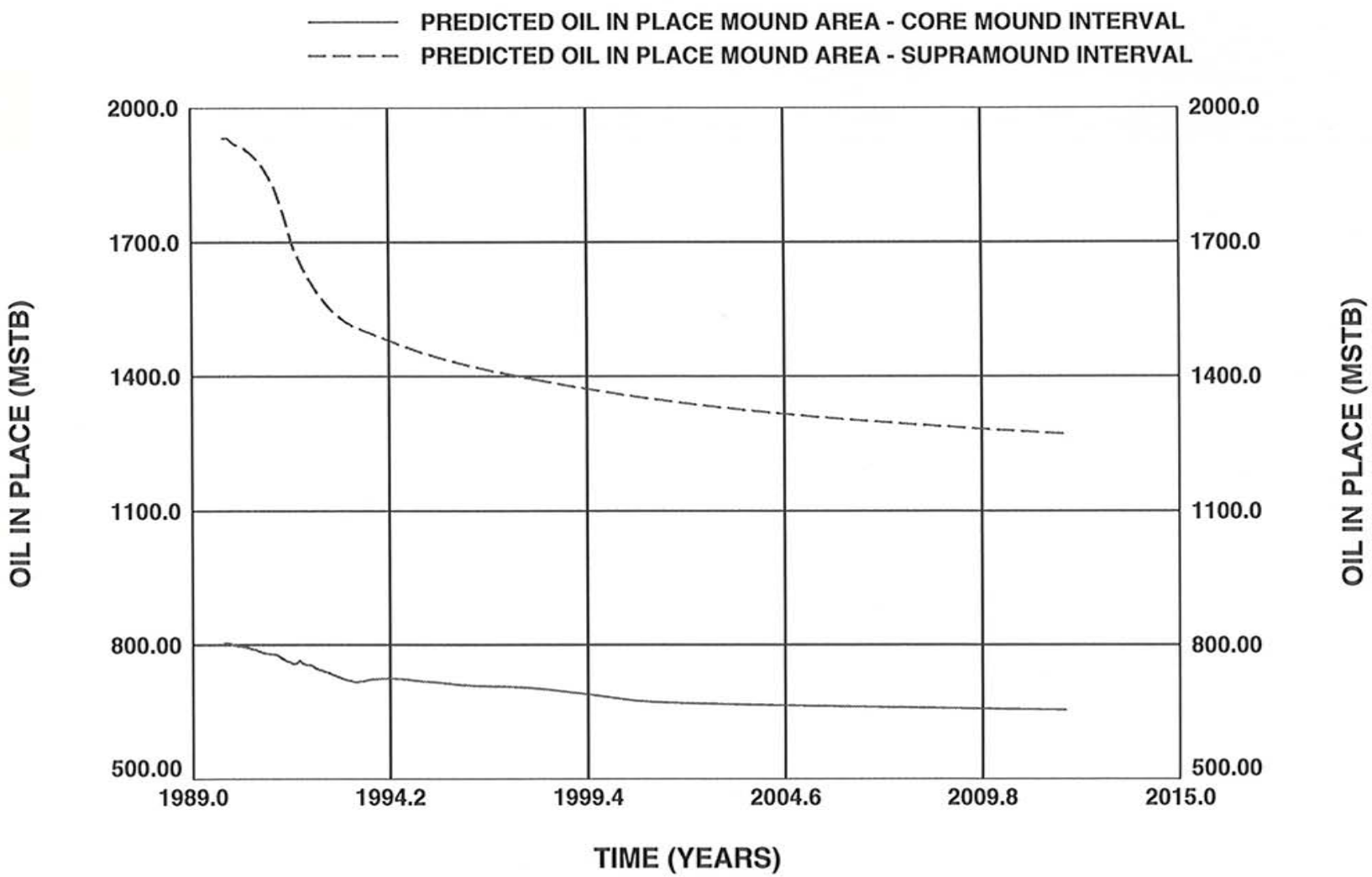

Figure 14-16 Regional Influx and Efflux of Oil - Anasazi Mound

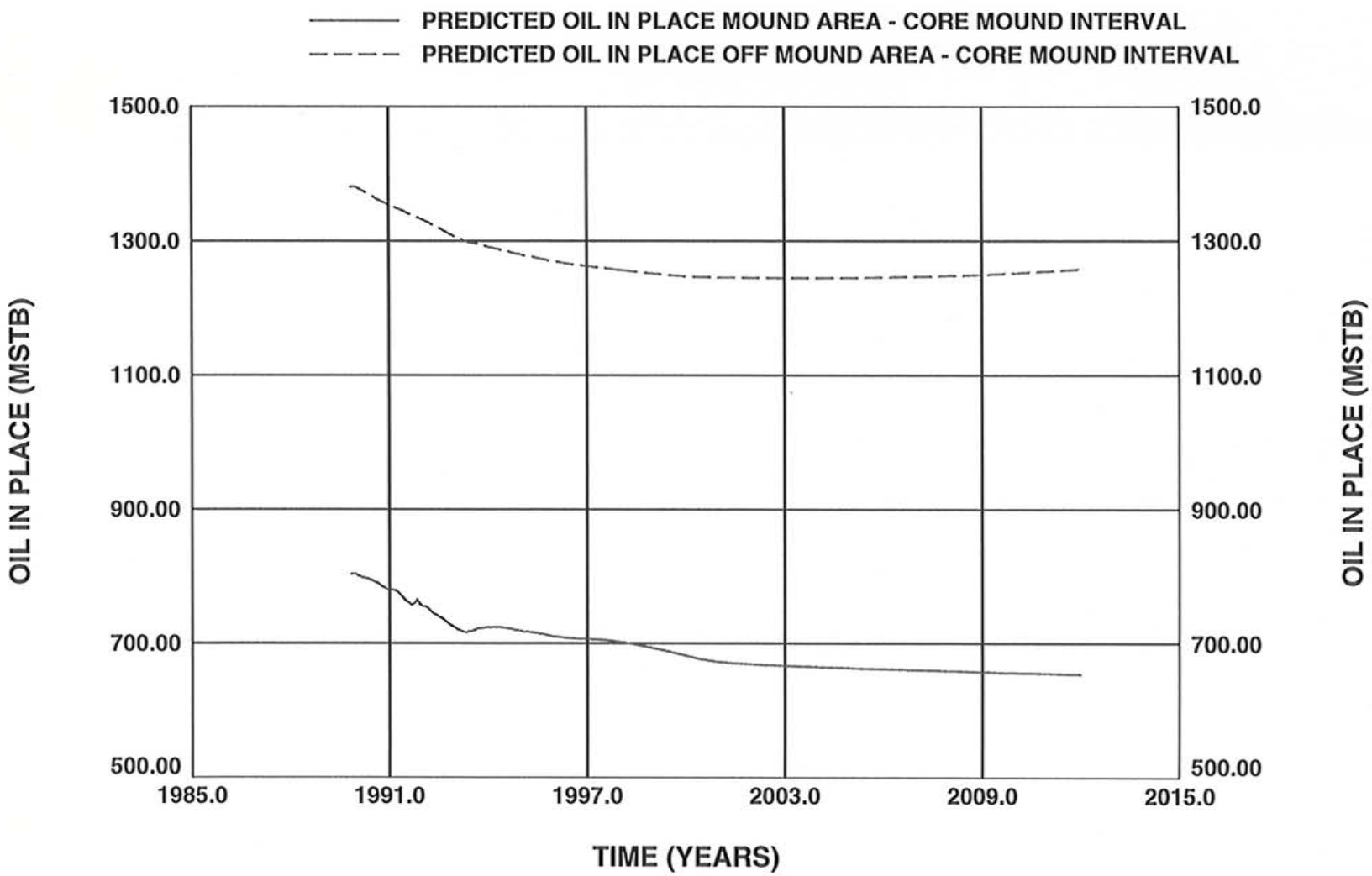

Figure 14-17 Regional Influx and Efflux of Oil - Anasazi Mound

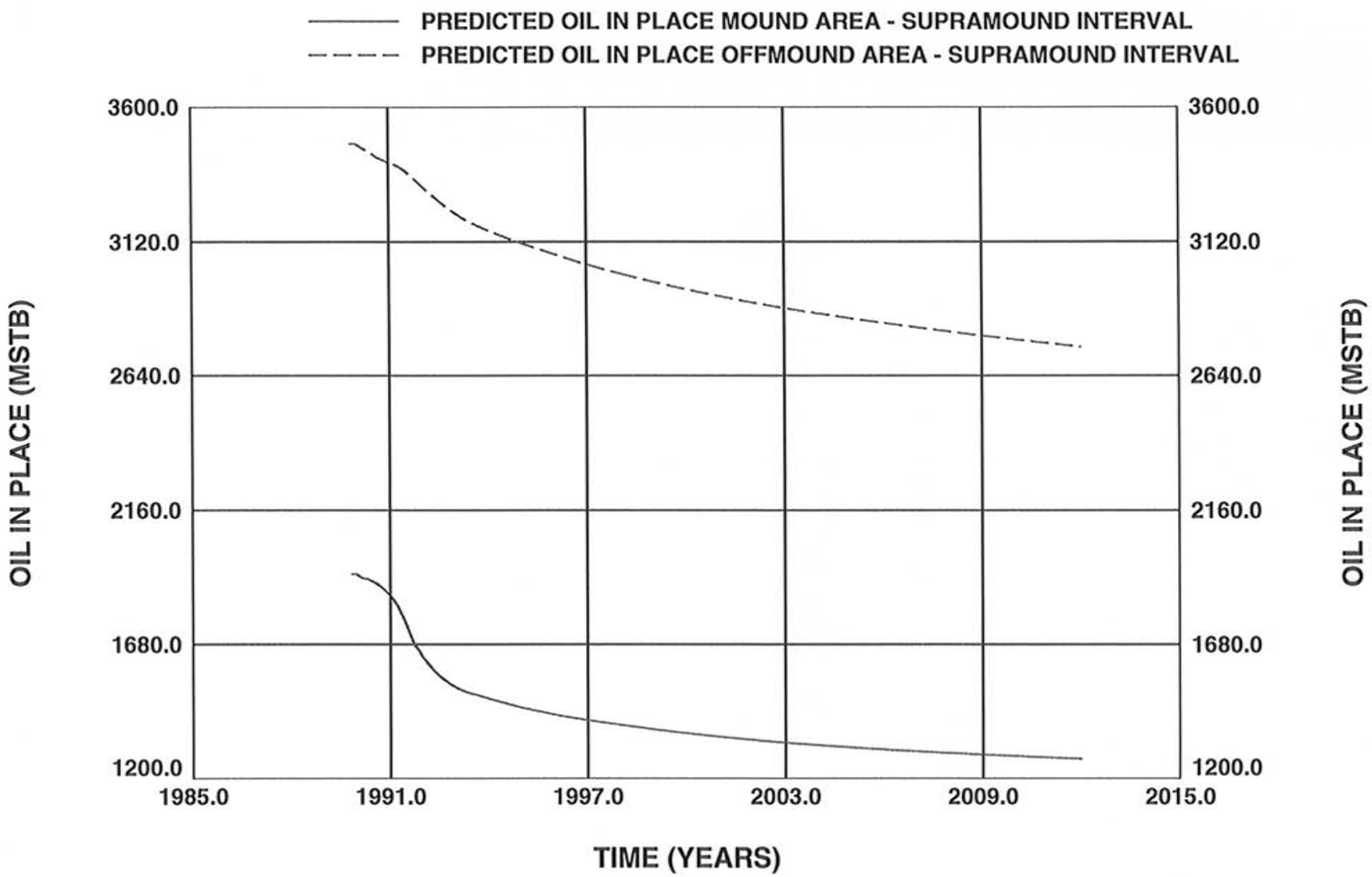

Figure 14-18 Regional Influx and Efflux of Oil - Anasazi Mound

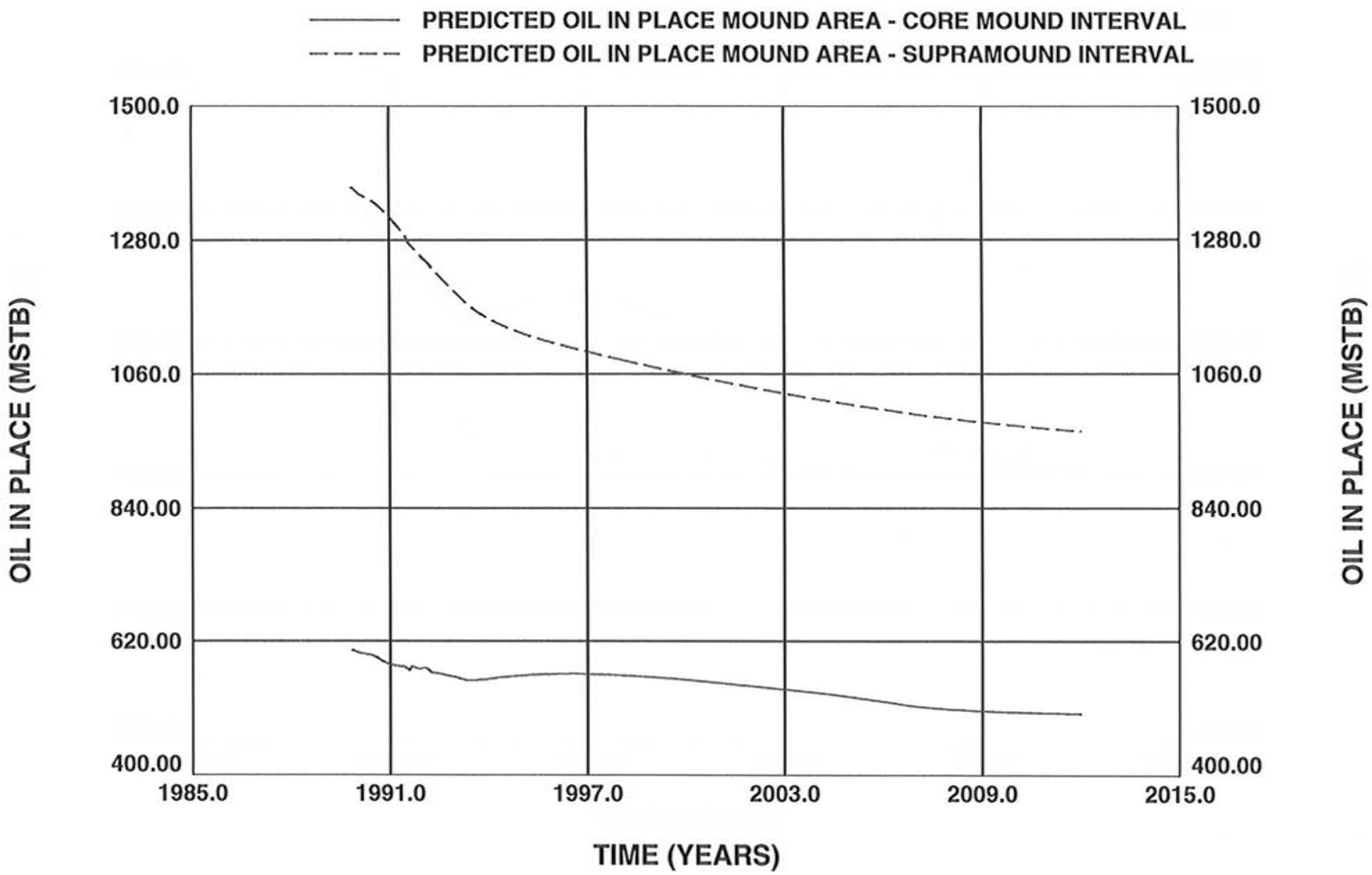

Figure 14-19 Regional Influx and Efflux of Oil - Sahgzie Mound

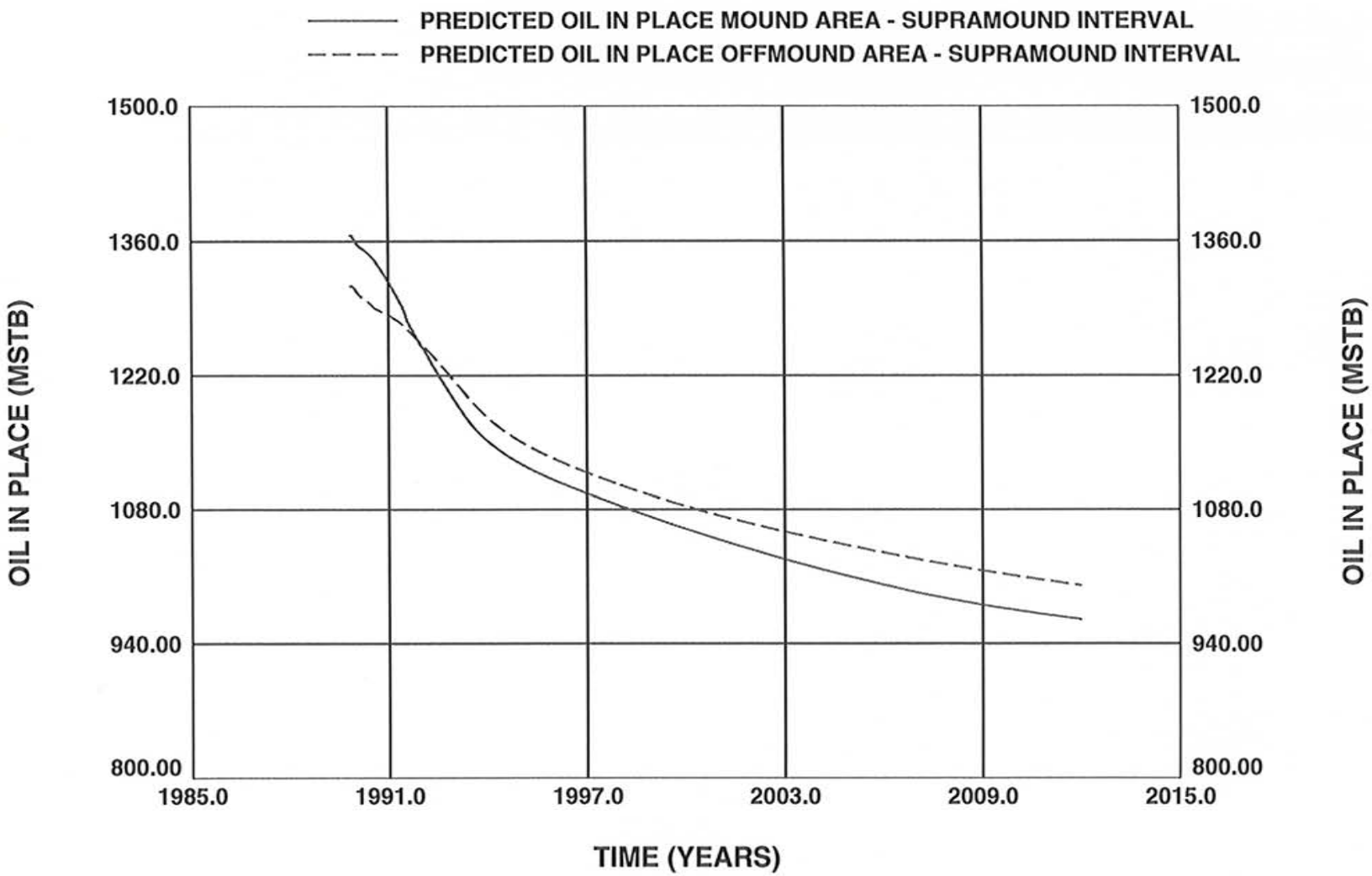

Figure 14-21 Regional Influx and Efflux of Oil - Sahgzie Mound

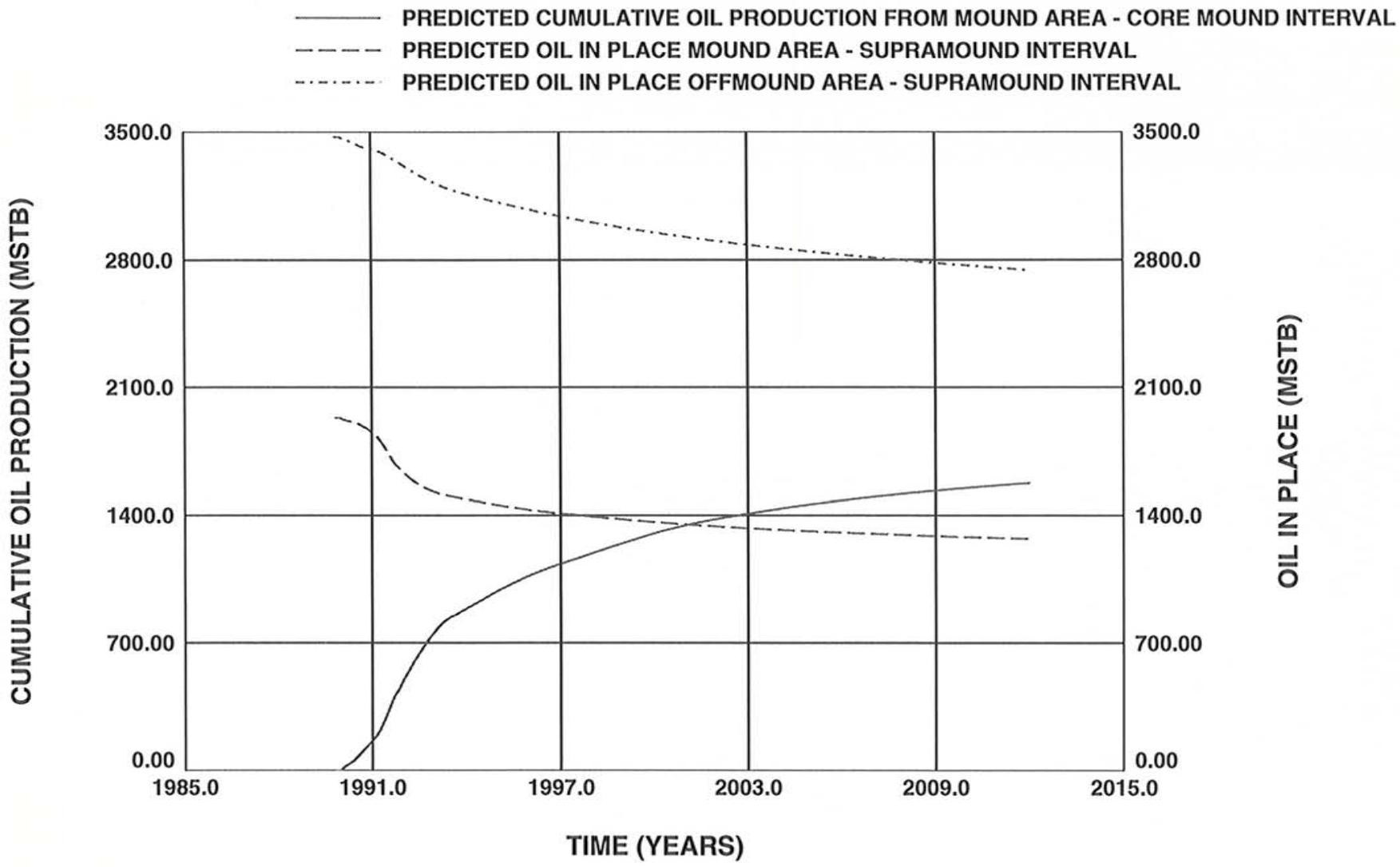

Figure 14-22 Limestone Production versus Supramound Oil Efflux - Anasazi Mound

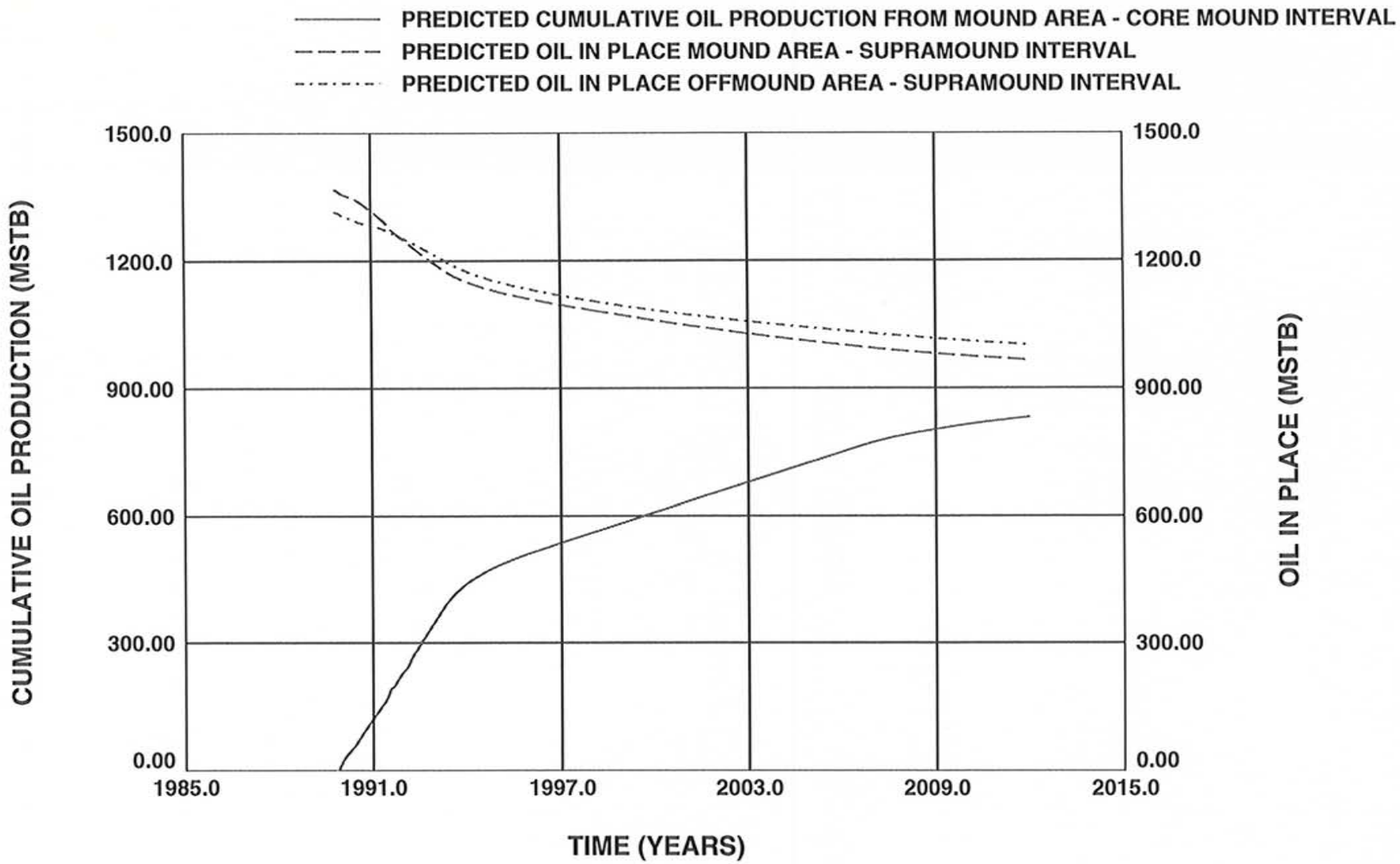

Figure 14-23 Limestone Production versus Supramound Oil Efflux - Sahgzie Mound

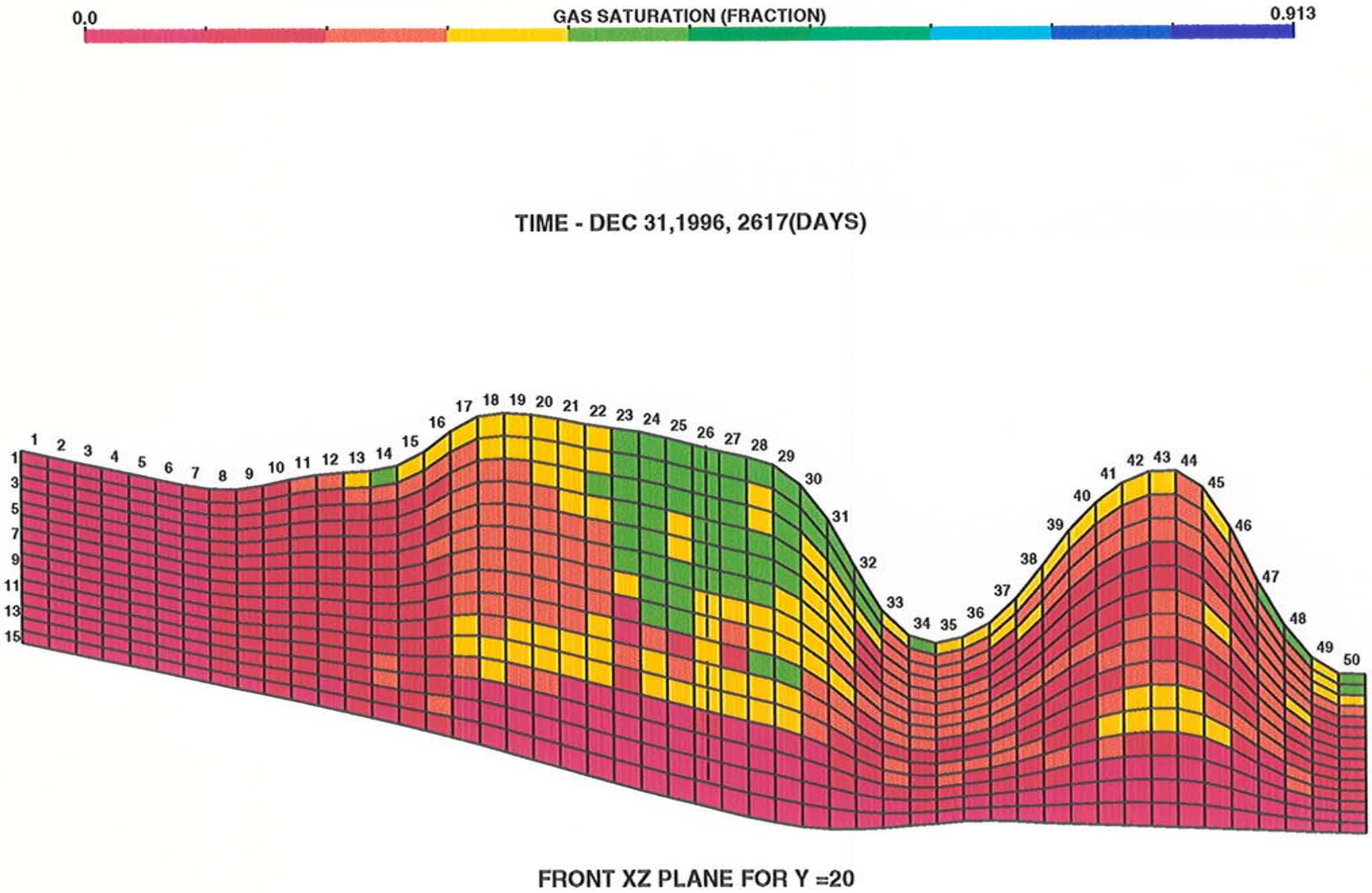

Figure 14-24 Gas Saturation Distribution

Y-Direction Cross Section at Anasazi Well No 1

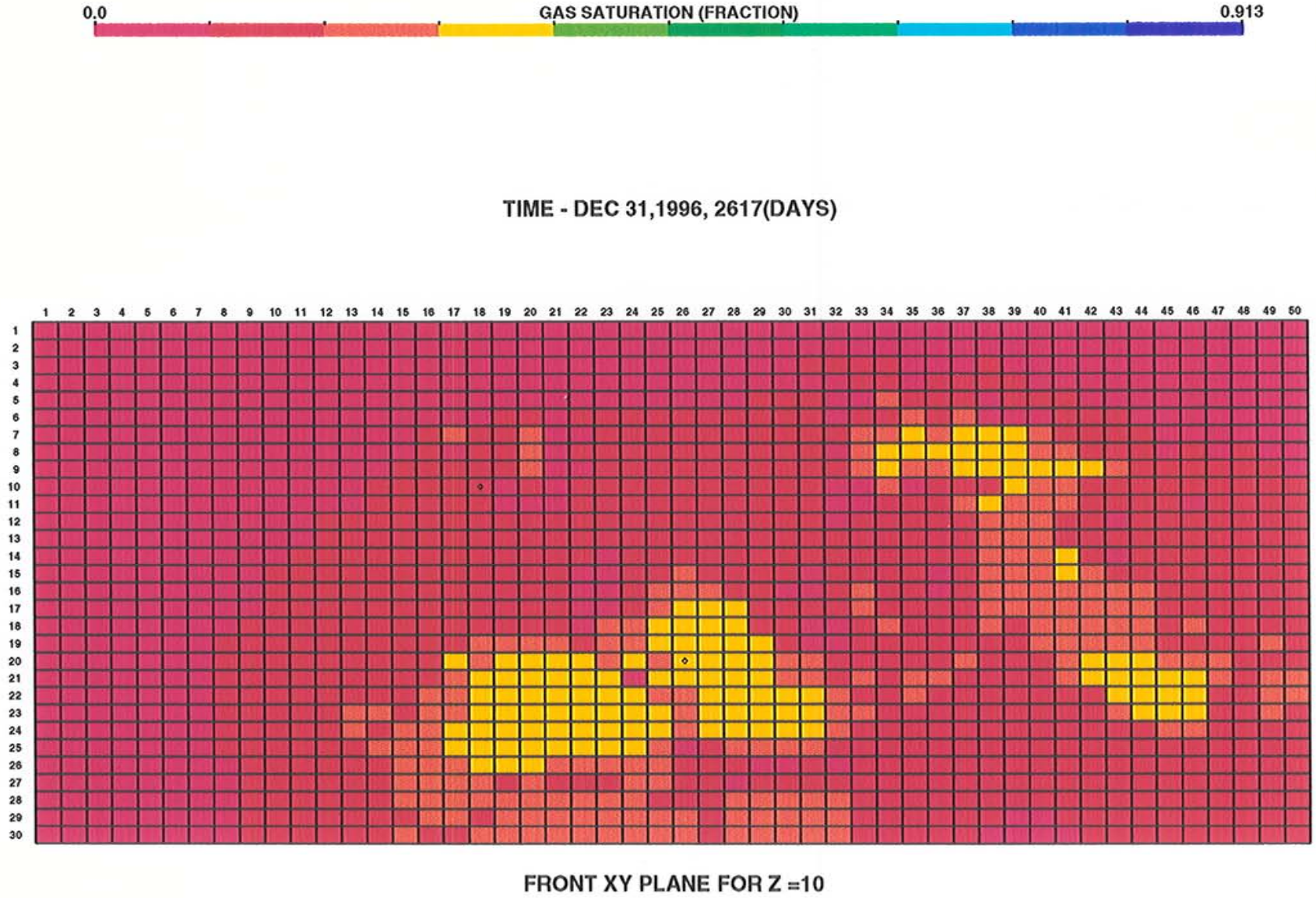

Figure 14-25 Gas Saturation Distribution Z-Direction Map at Top of Phylloid Algal Limestone

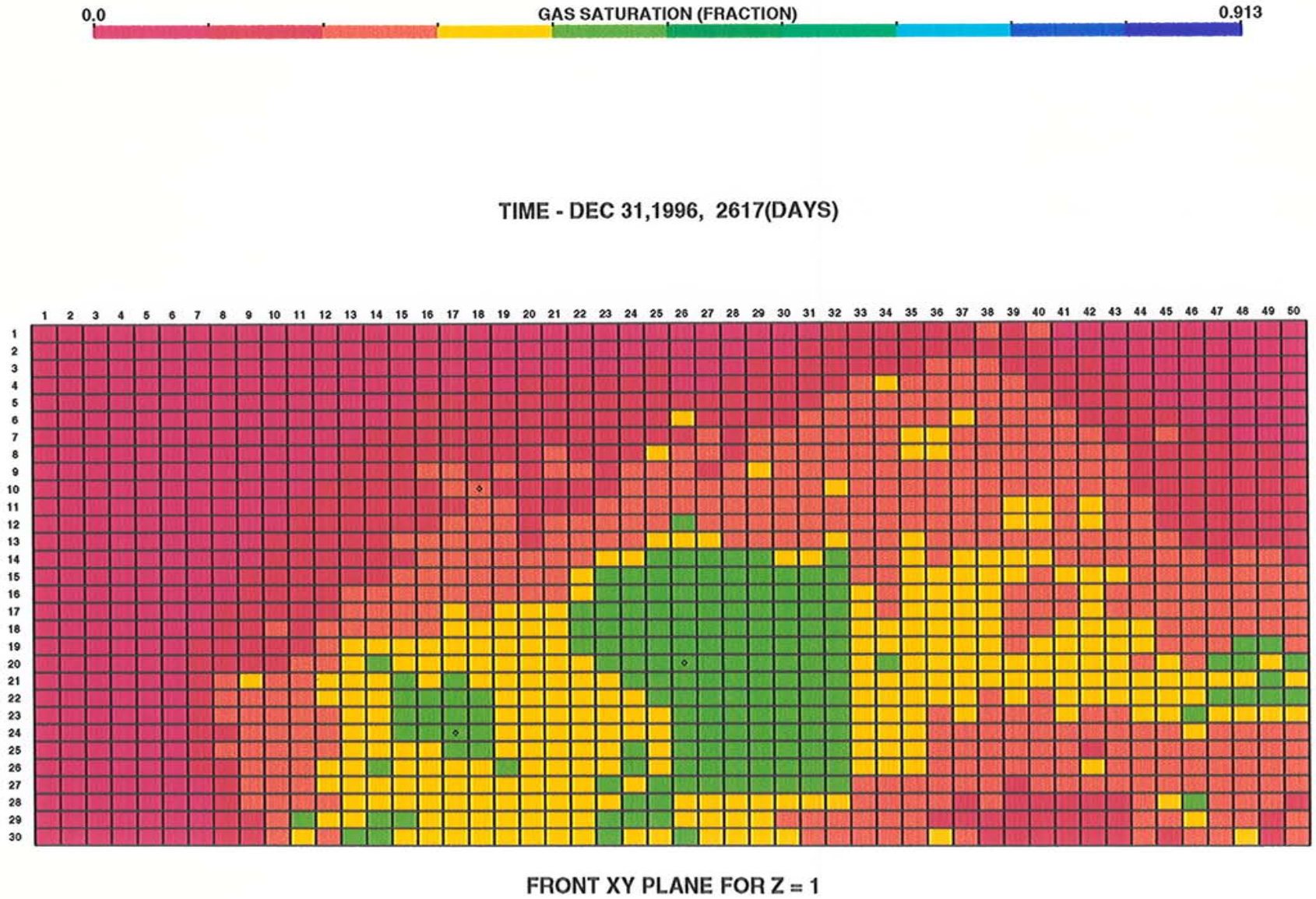

Figure 14-26 Gas Saturation Distribution Z-Direction Map at Top of Supramound Interval

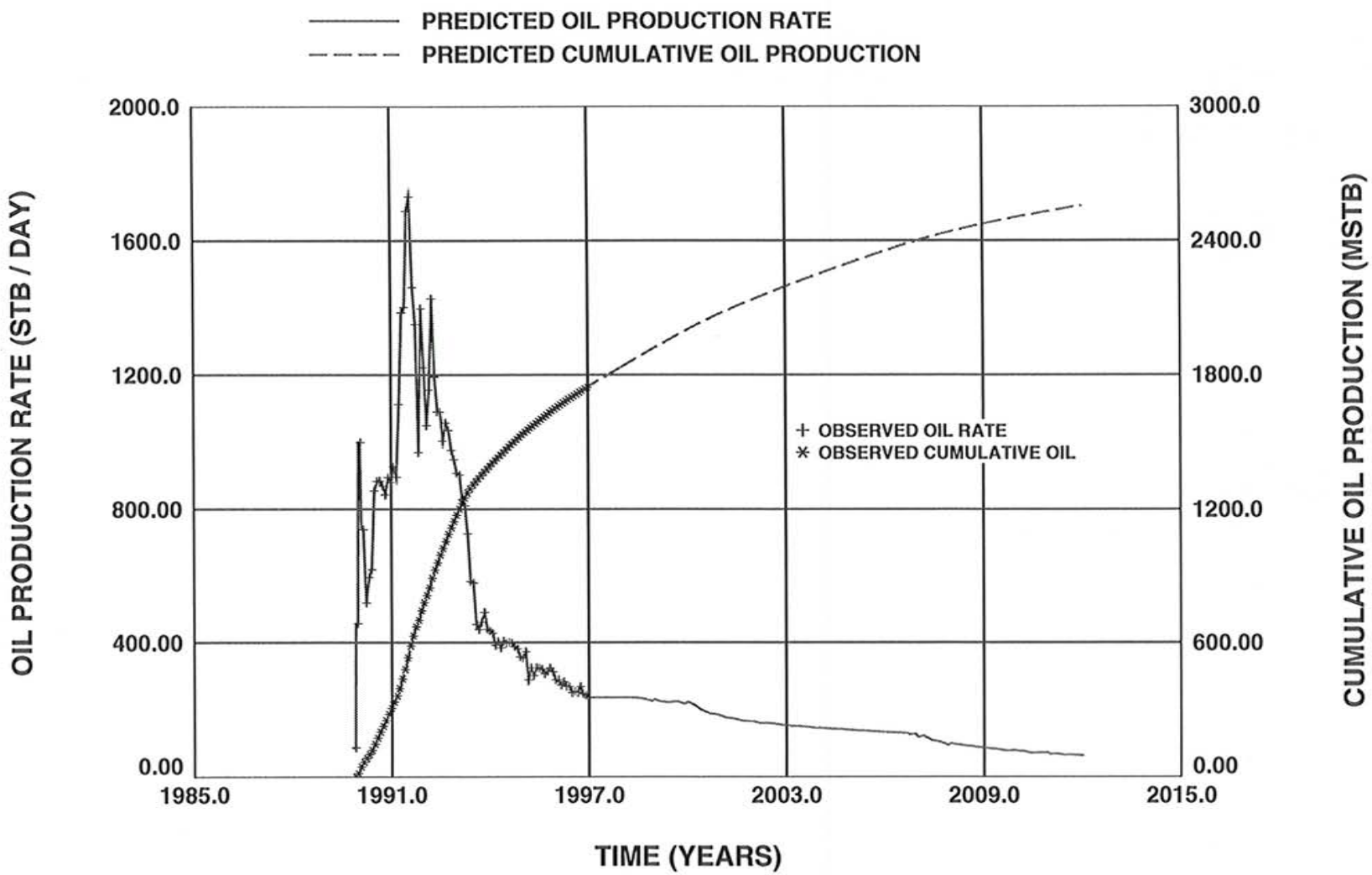

Figure 15-1 Oil Production Primary Depletion Prediction Anasazi-Sahgzie Reservoir

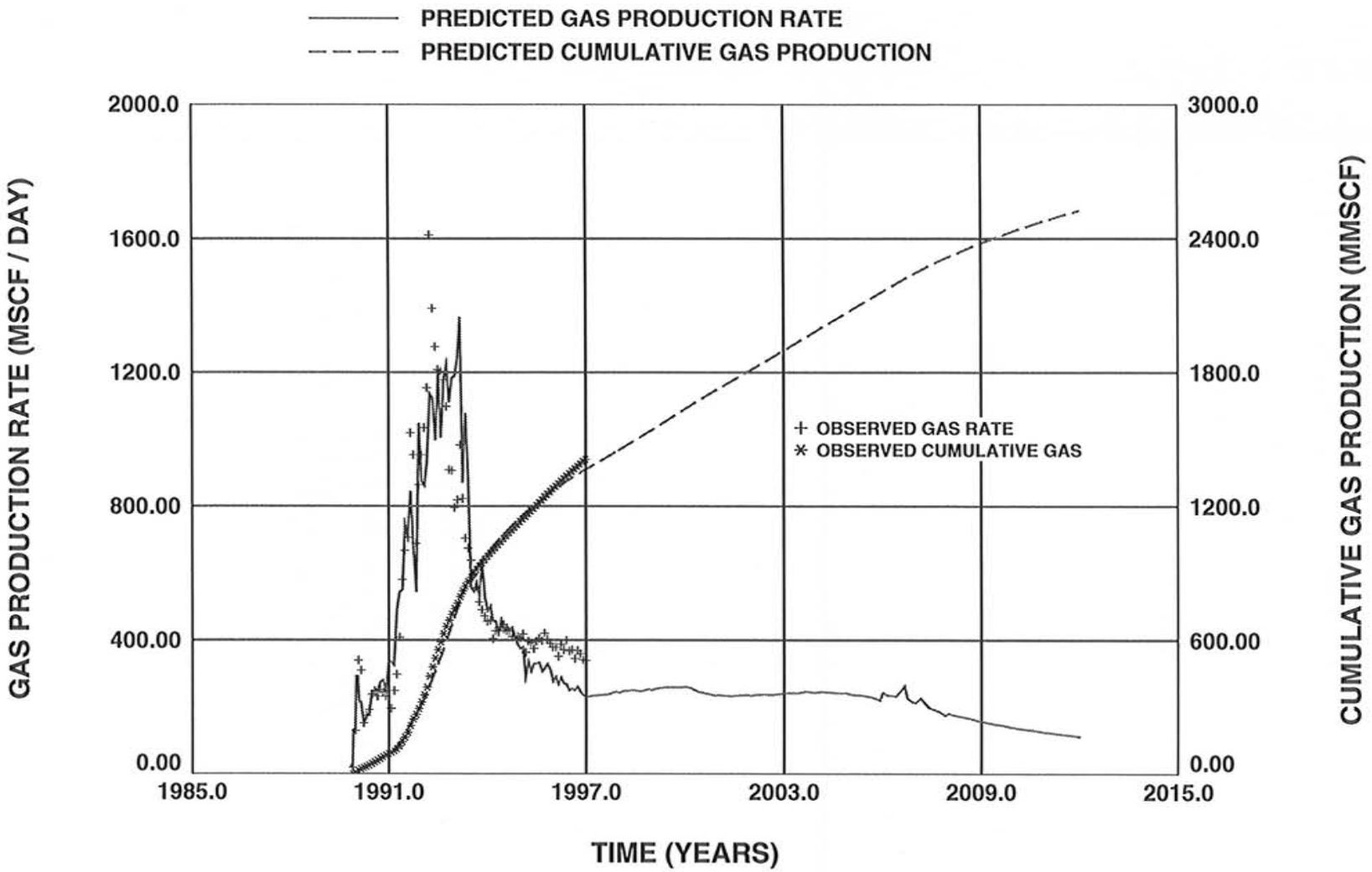

Figure 15-2 Gas Production Primary Depletion Prediction Anasazi-Sahgzie Reservoir

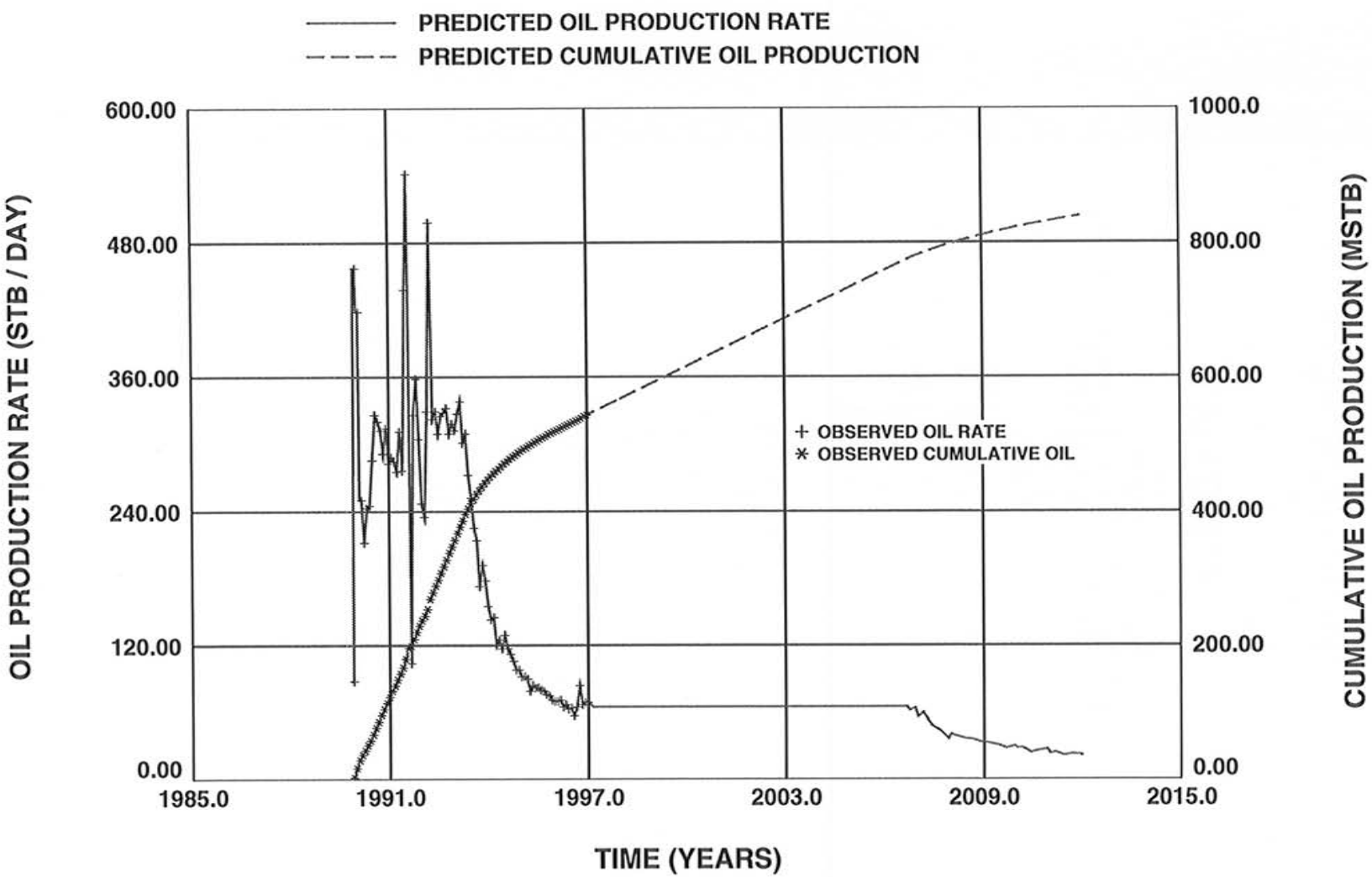

Figure 15-3 Oil Production Primary Depletion Prediction - Sahgzie Well No 1

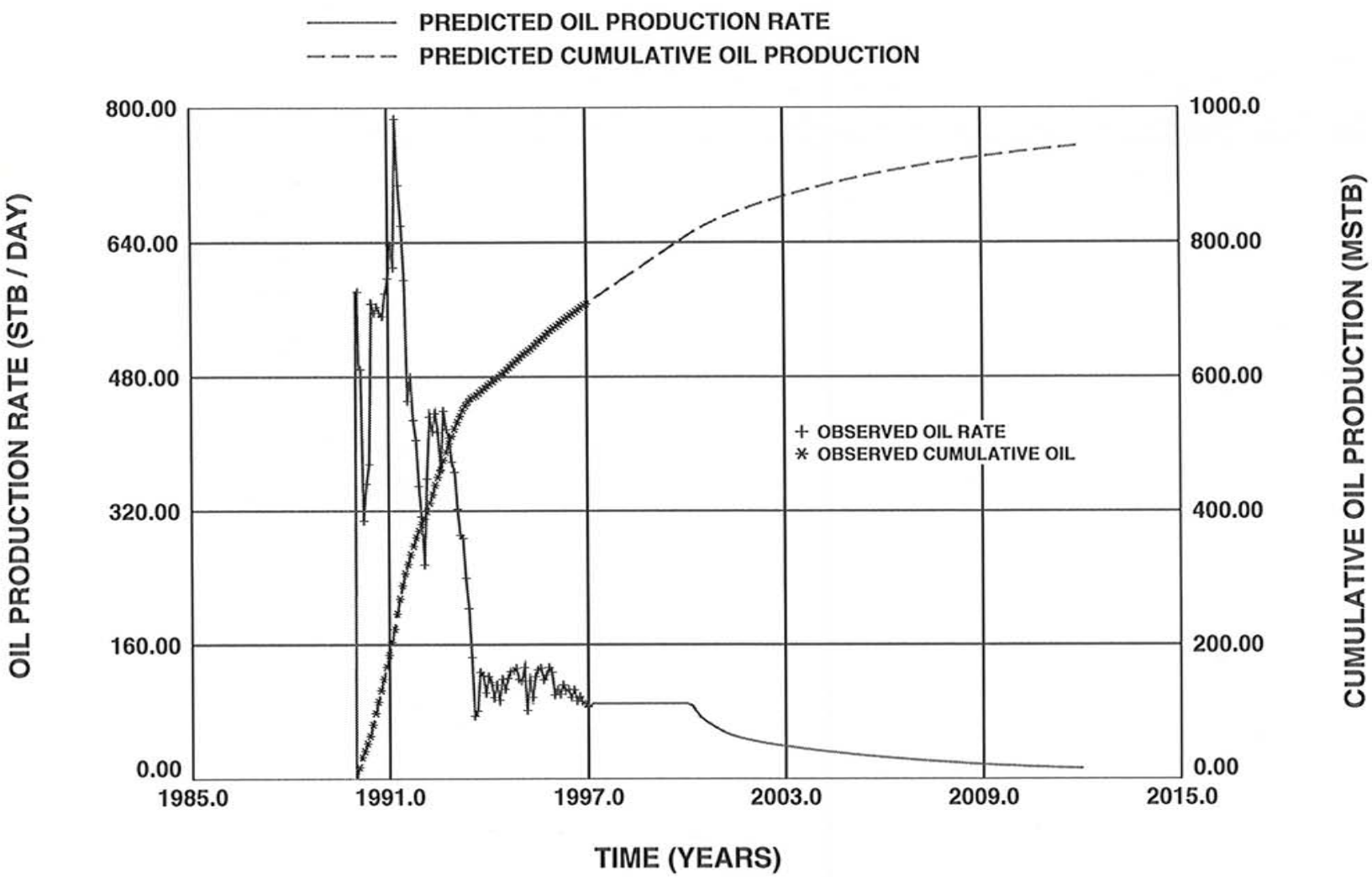

Figure 15-4 Oil Production Primary Depletion Prediction - Anasazi Well No 1

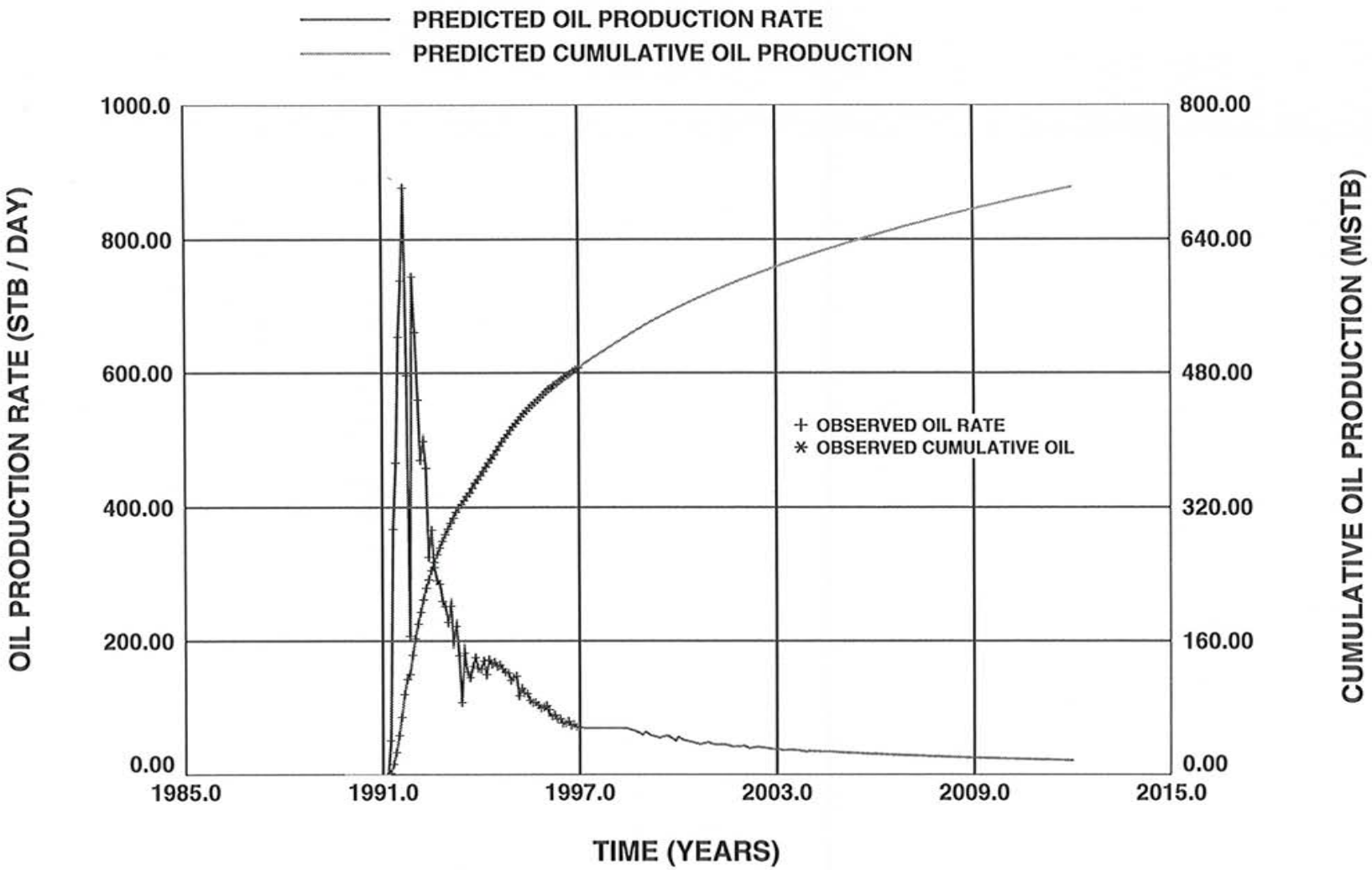

Figure 15-5 Oil Production Primary Depletion Prediction - Anasazi Well No 5L-3

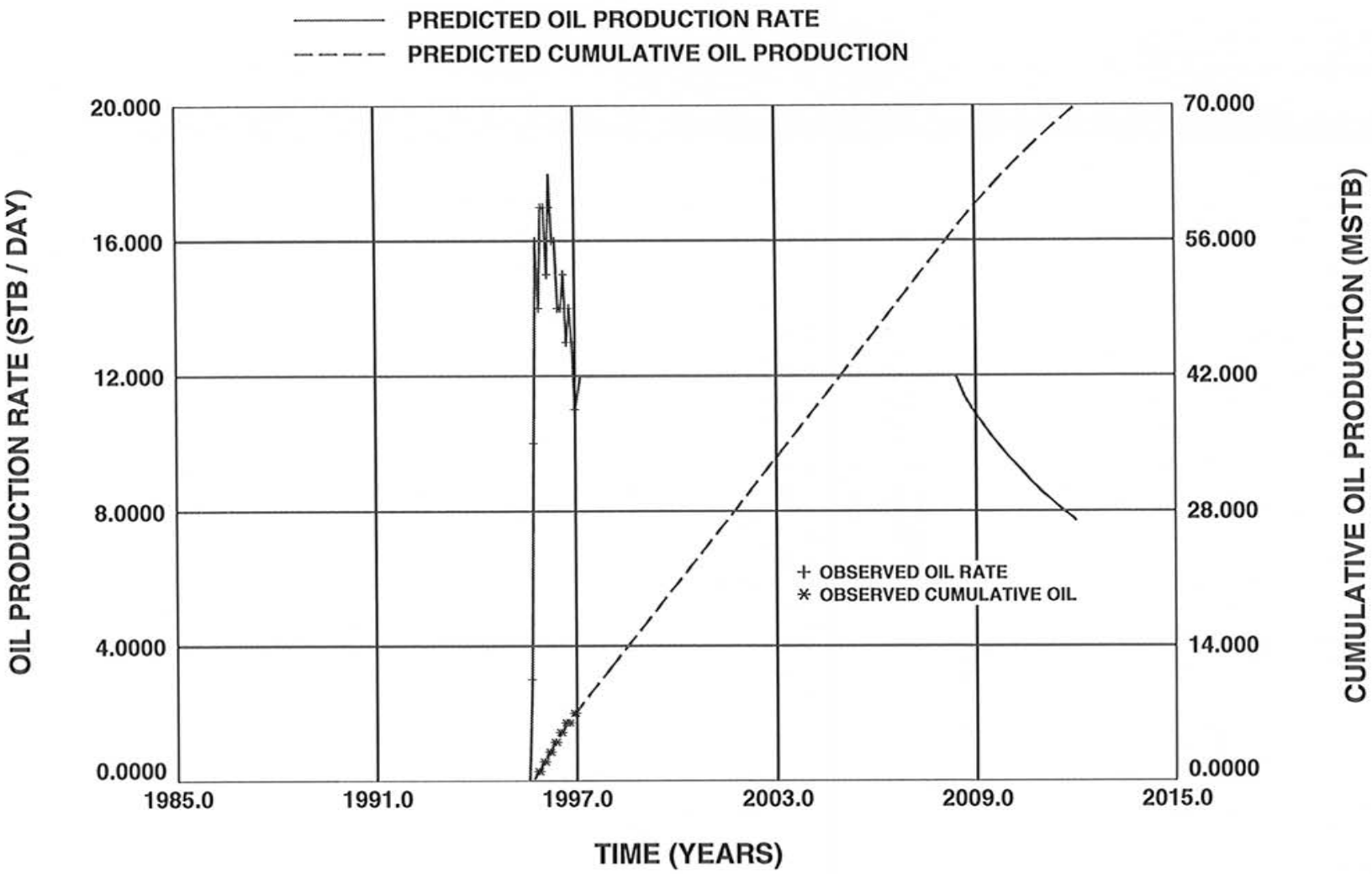

Figure 15-6 Oil Production Primary Depletion Prediction - Anasazi Well No 6H-1

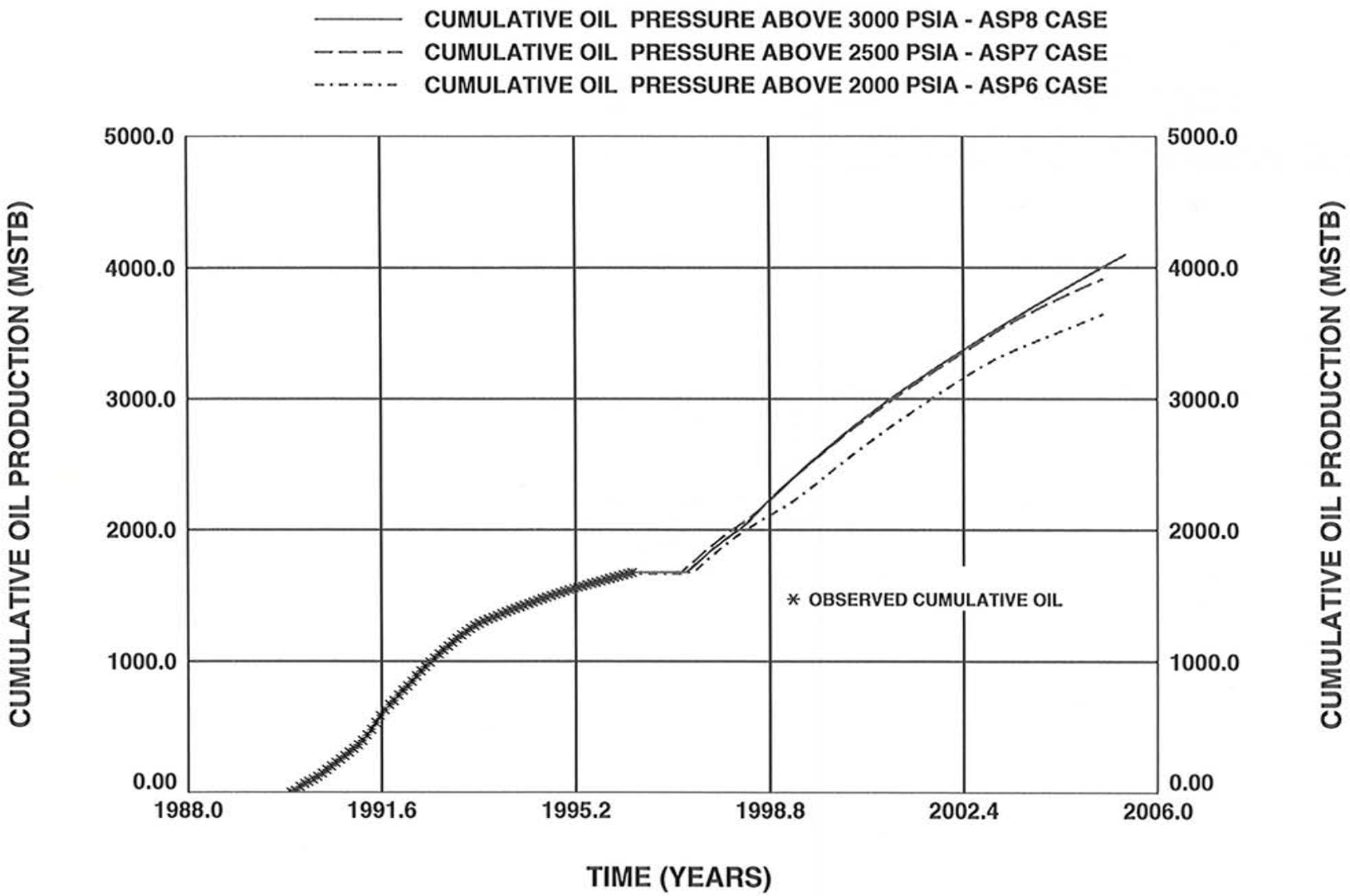

Figure 15-7 Cumulative Oil Recovery as Function of Reservoir Operating Pressure

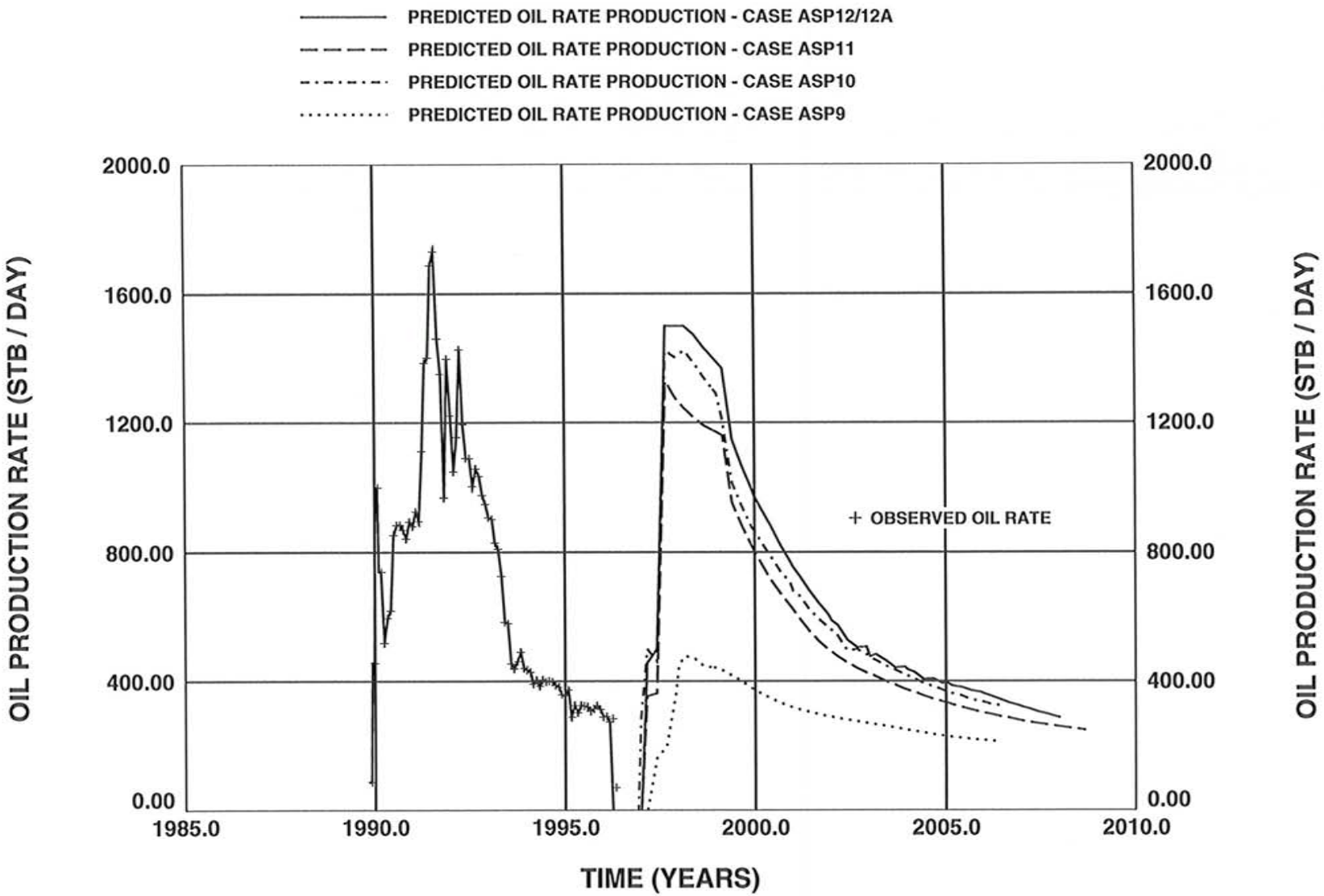

Figure 15-8 Oil Production Rate Variation with Number and Location of Injectors

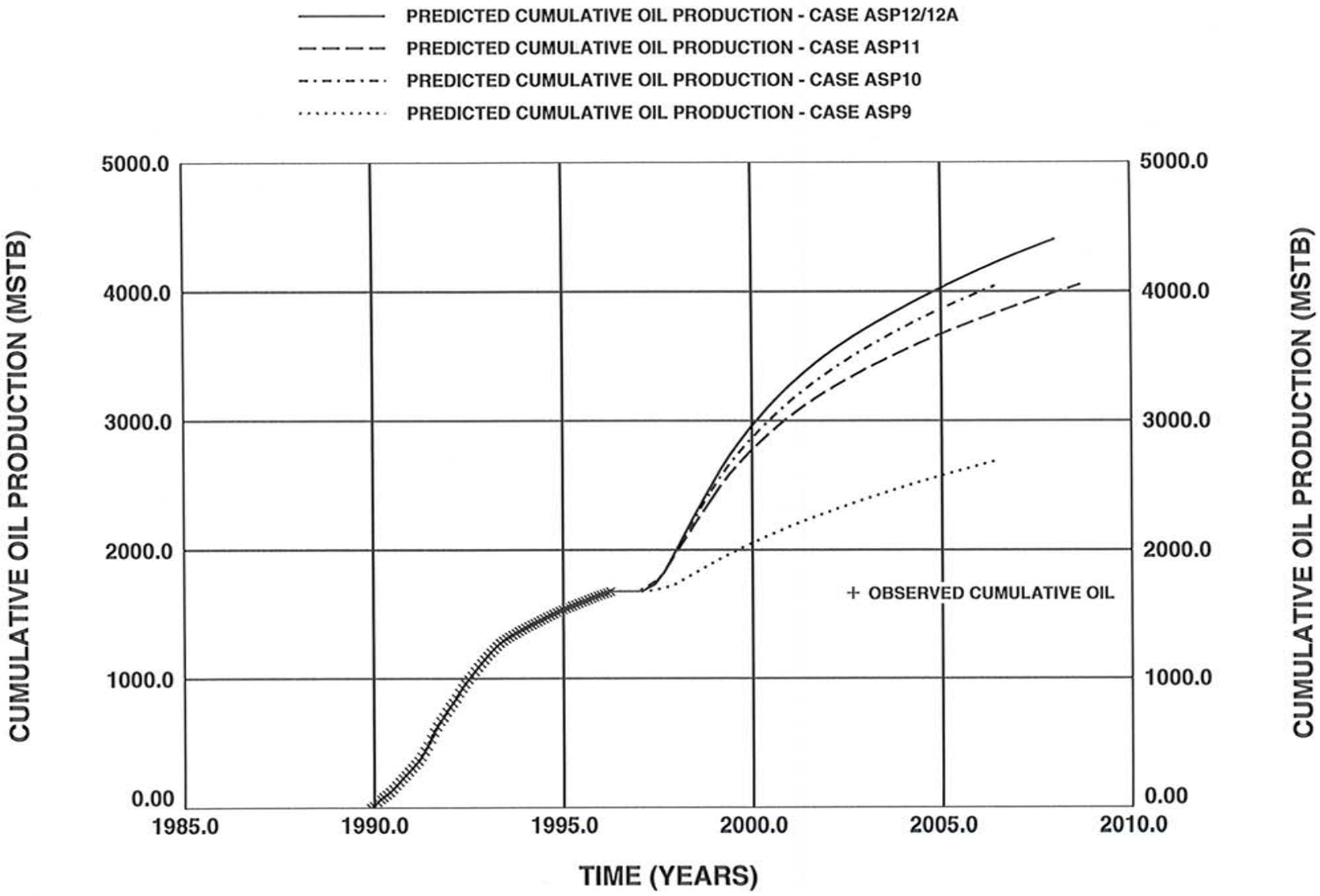

Figure 15-9 Cumulative Oil Variation with Number and Location of Injectors

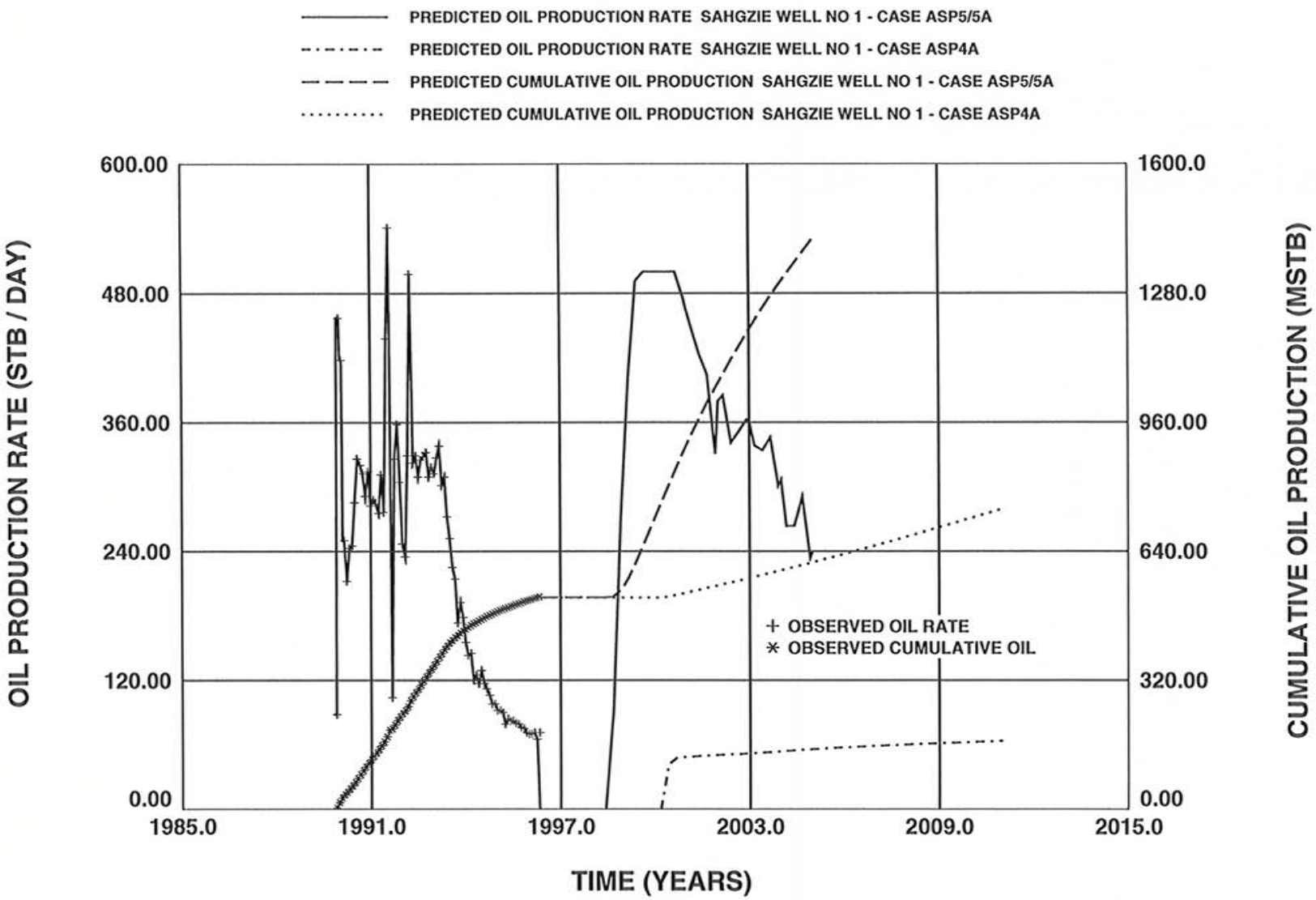

Figure 15-10 Sahgzie Well No 1 Response to Single Anasazie CO2 Injector

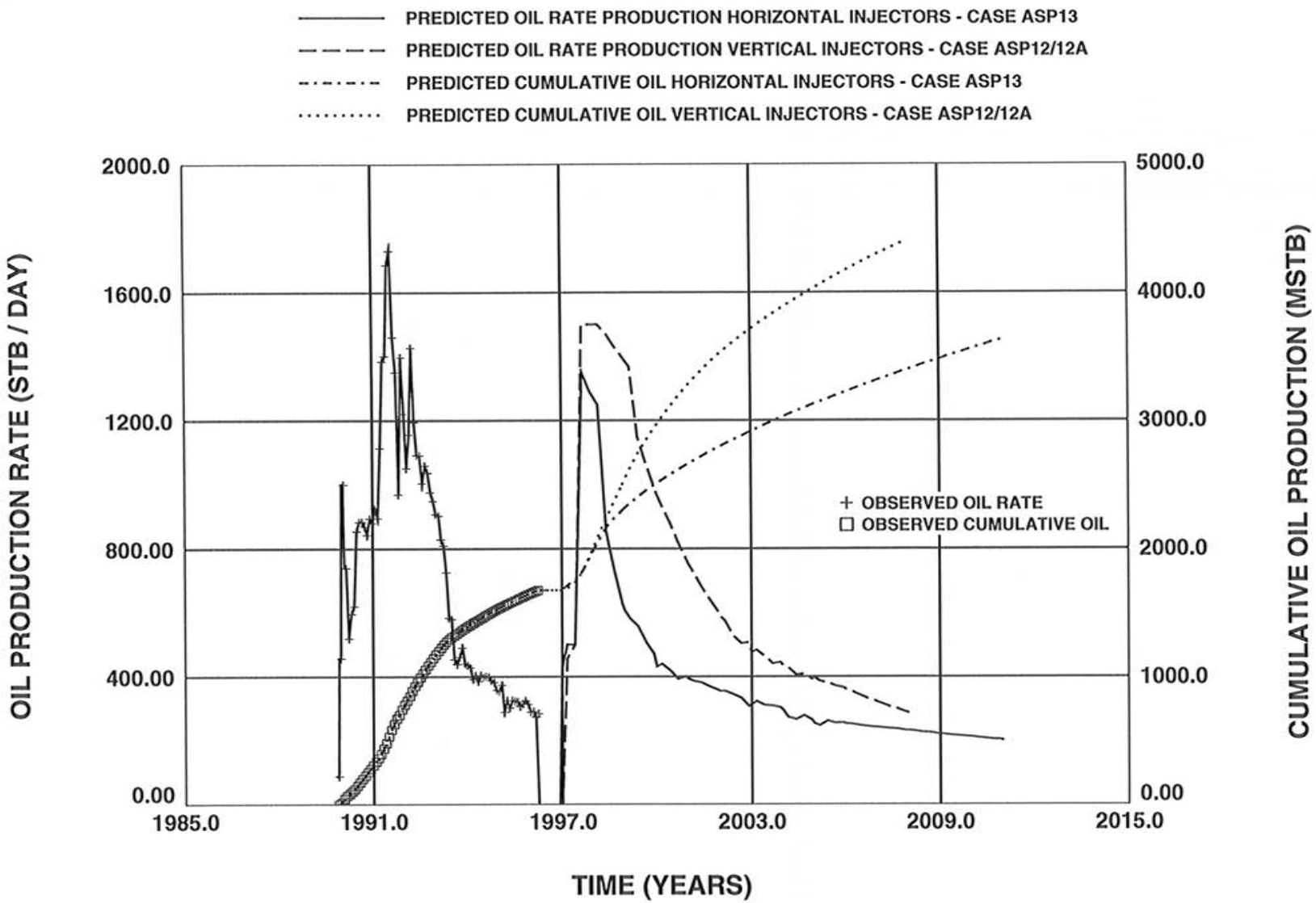

Figure 15-11 Oil Production Data - Horizontal versus Vertical Injectors

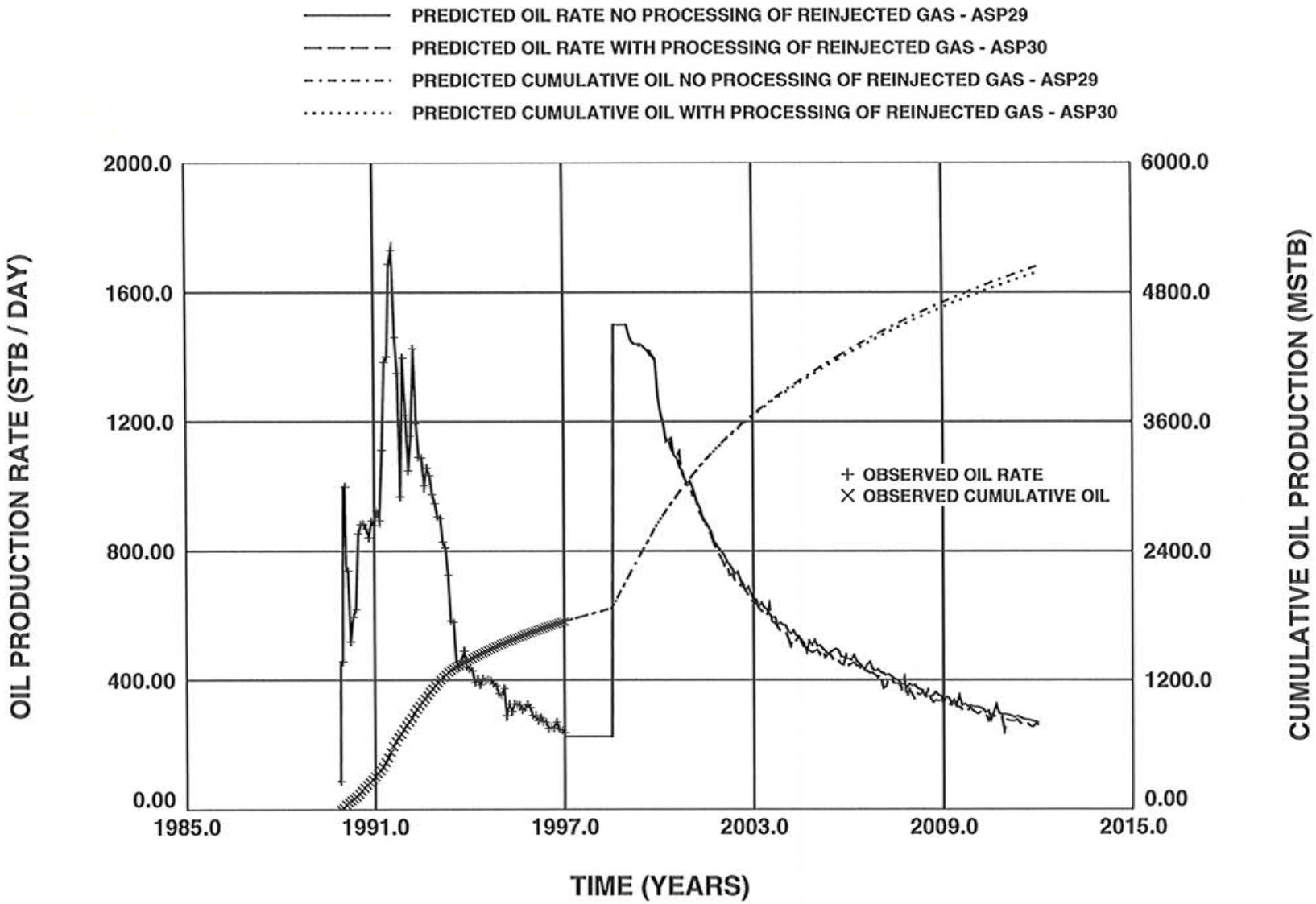

Figure 15-12 Oil Production Variation with Processing of Re-Injection Gas

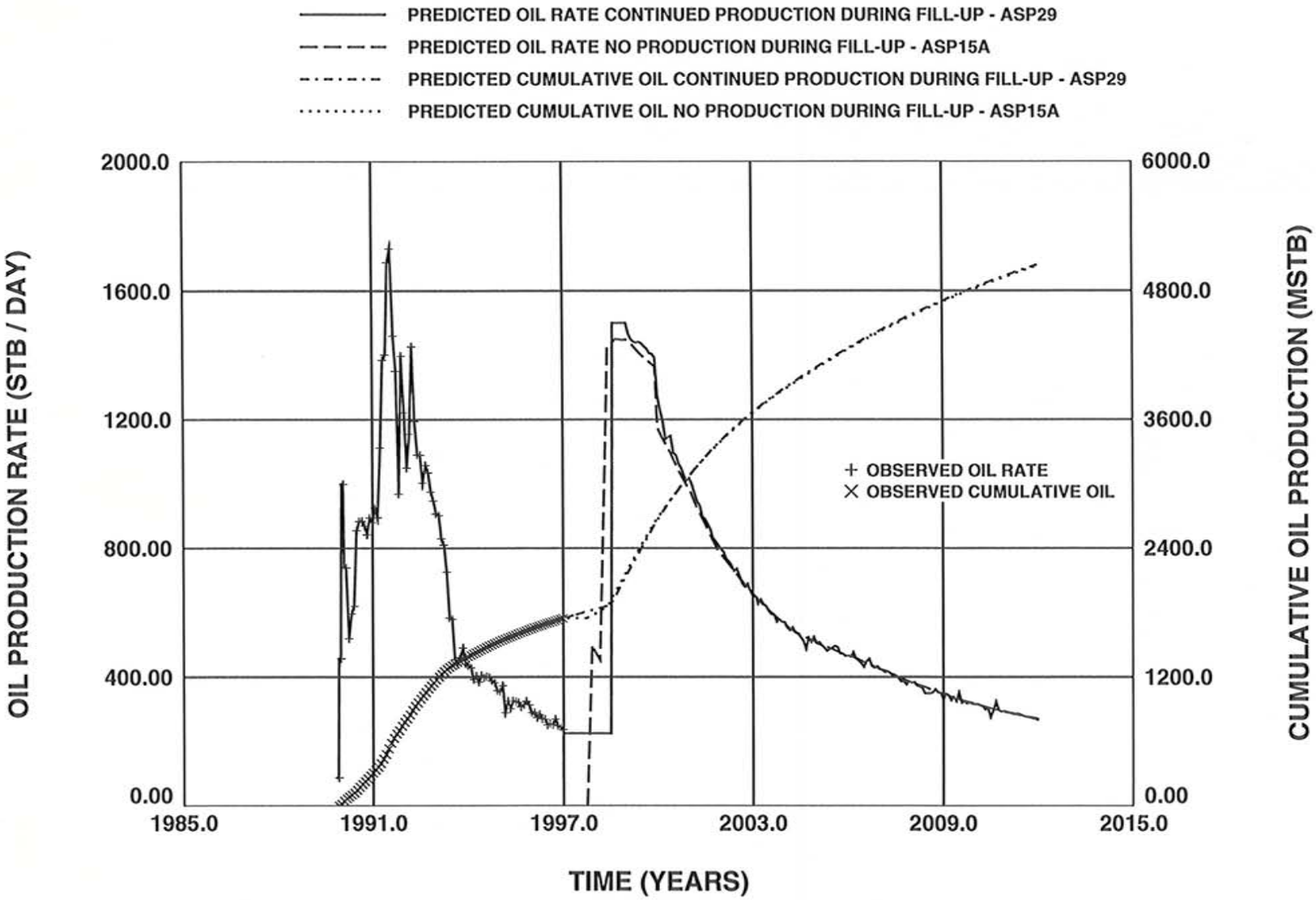

Figure 15-13 Oil Production as Influenced by Operations during Fill-Up

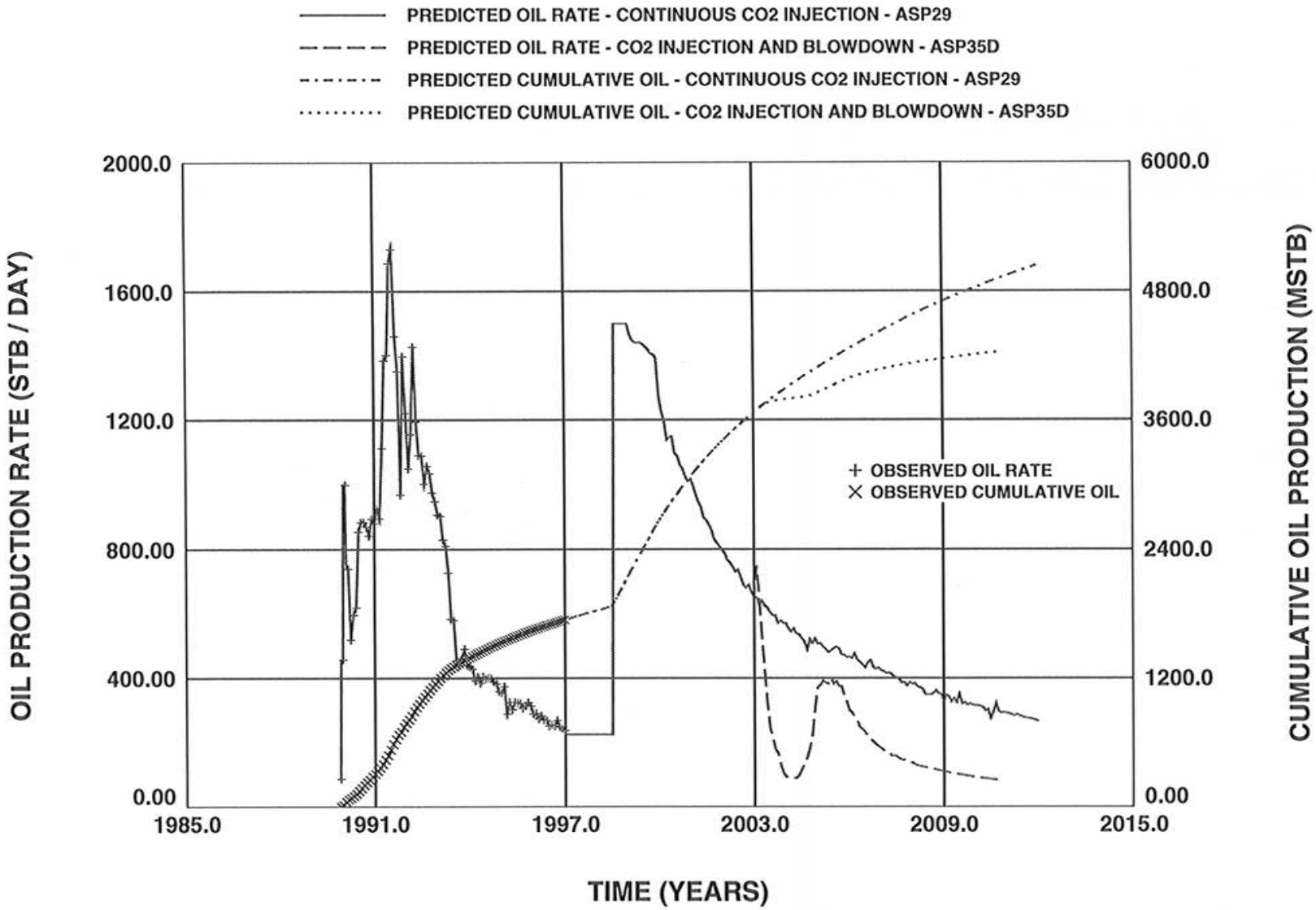

Figure 15-14 Oil Production - Continuous CO2 versus CO2 Injection and Blowdown

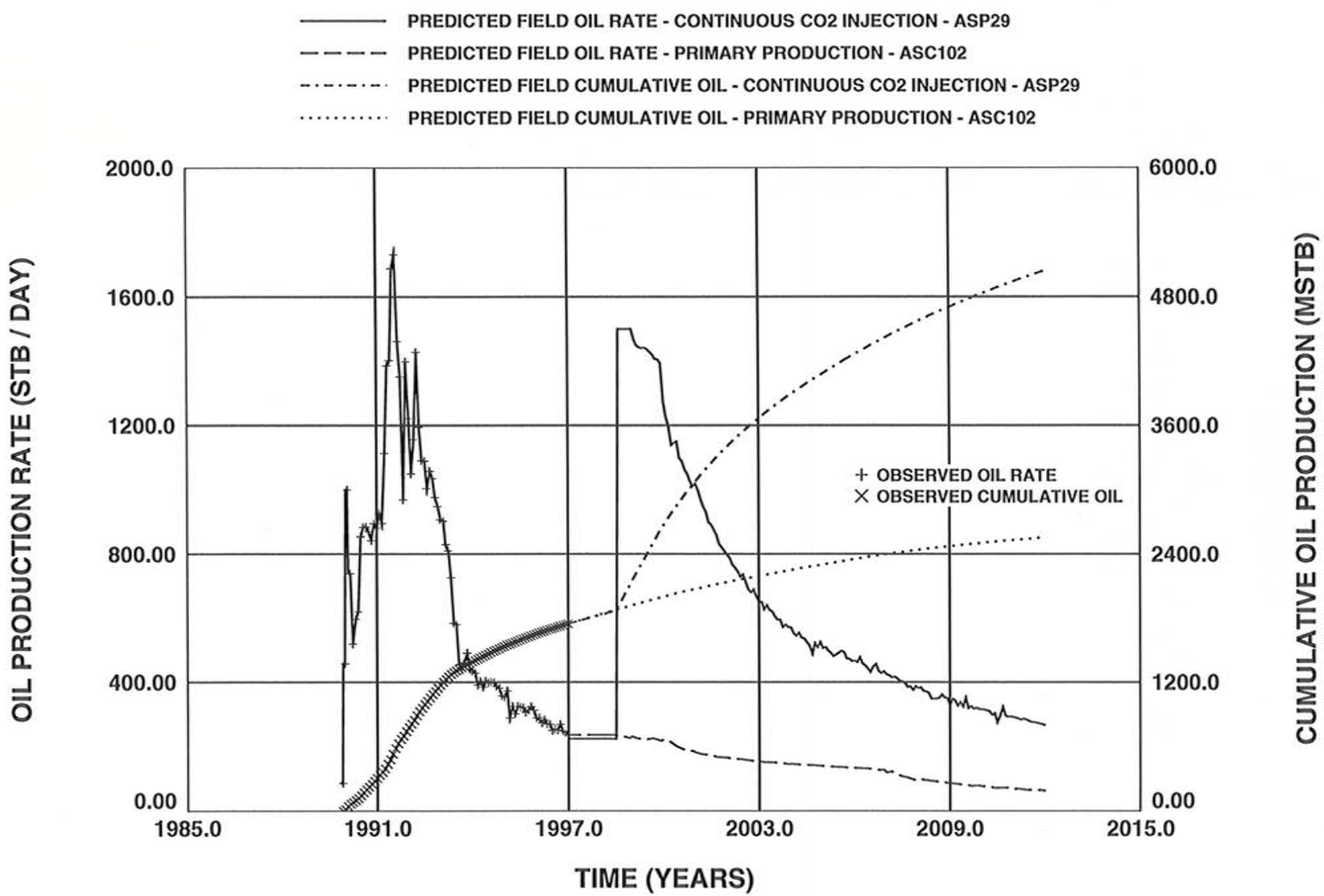

Figure 15-15 Field Level Oil Production - CO2 Flood versus Primary

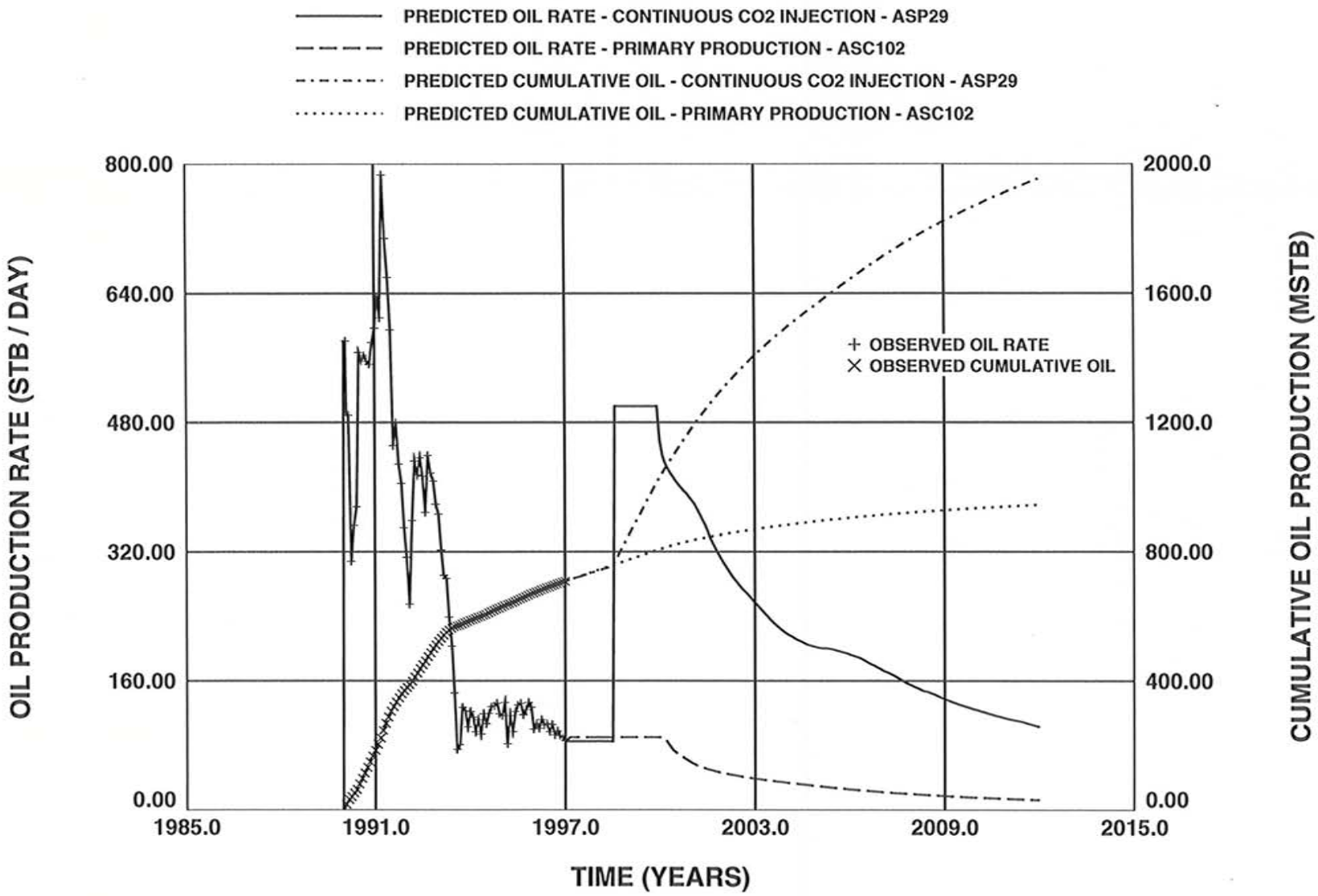

Figure 15-16 Anasazi Well No 1 Oil Production - CO2 Flood versus Primary

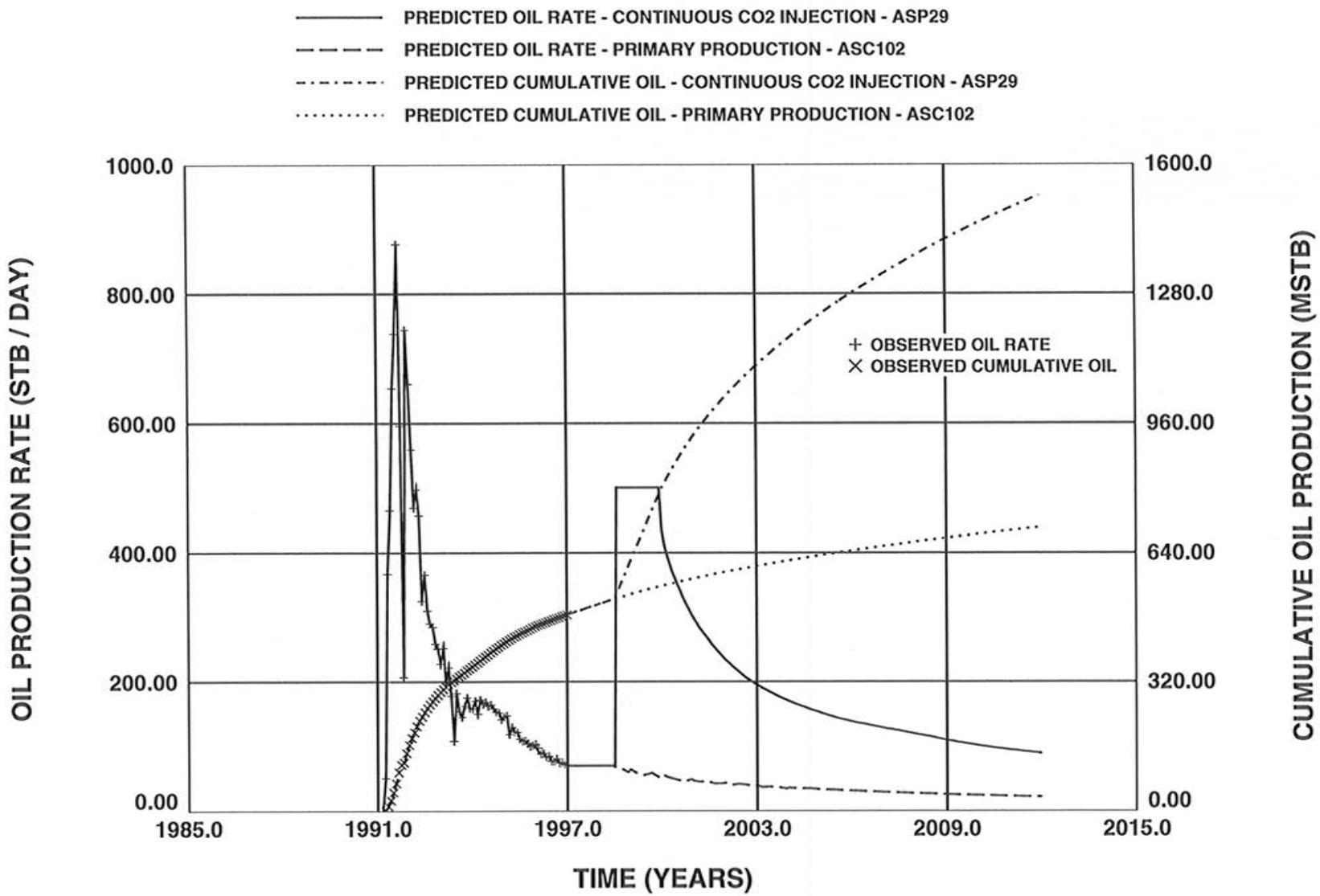

Figure 15-17 Anasazi Well No 5L-3 Oil Production - CO2 Flood versus Primary

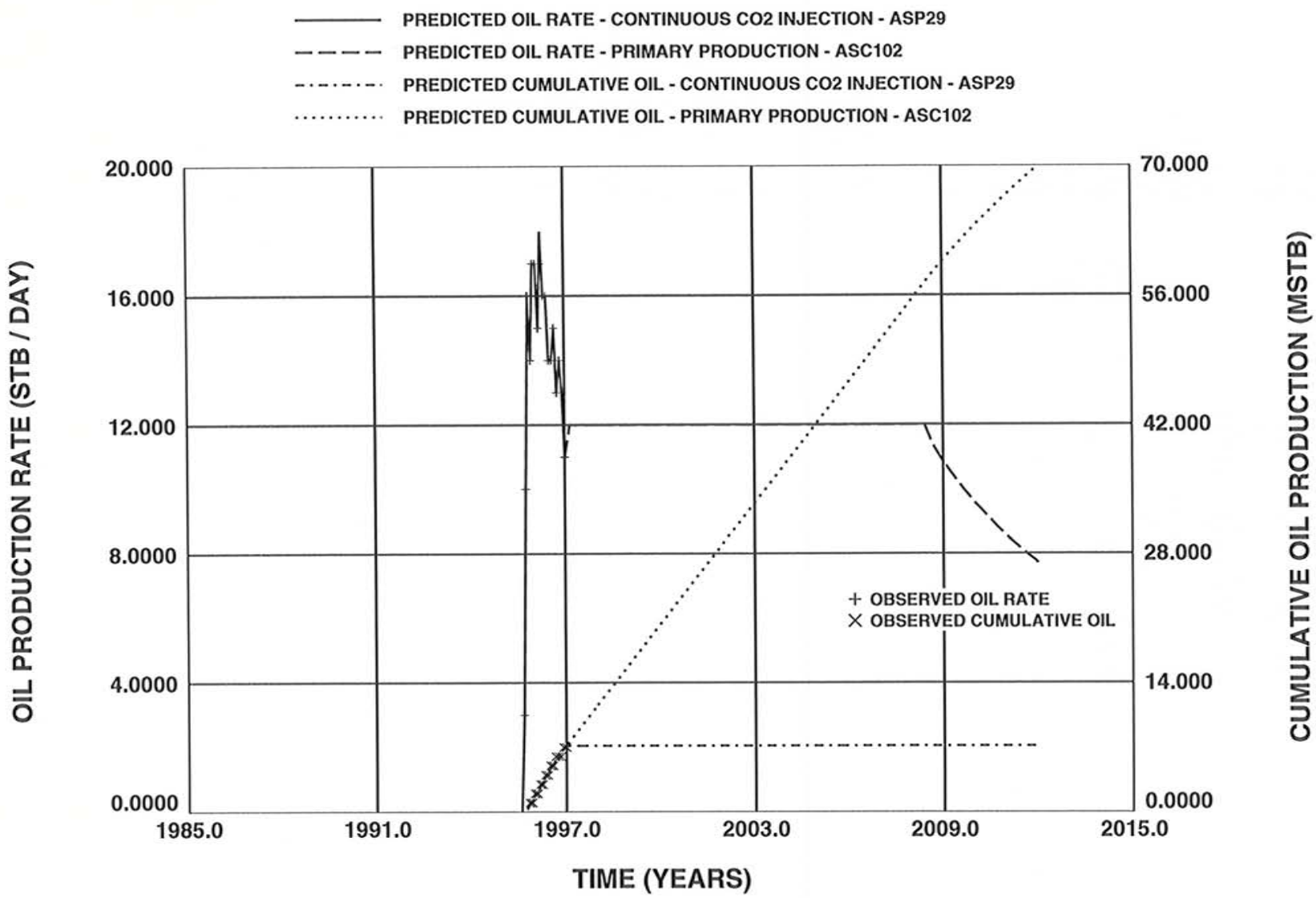

Figure 15-18 Anasazi Well No 6H-1 Oil Production - CO2 Flood versus Primary

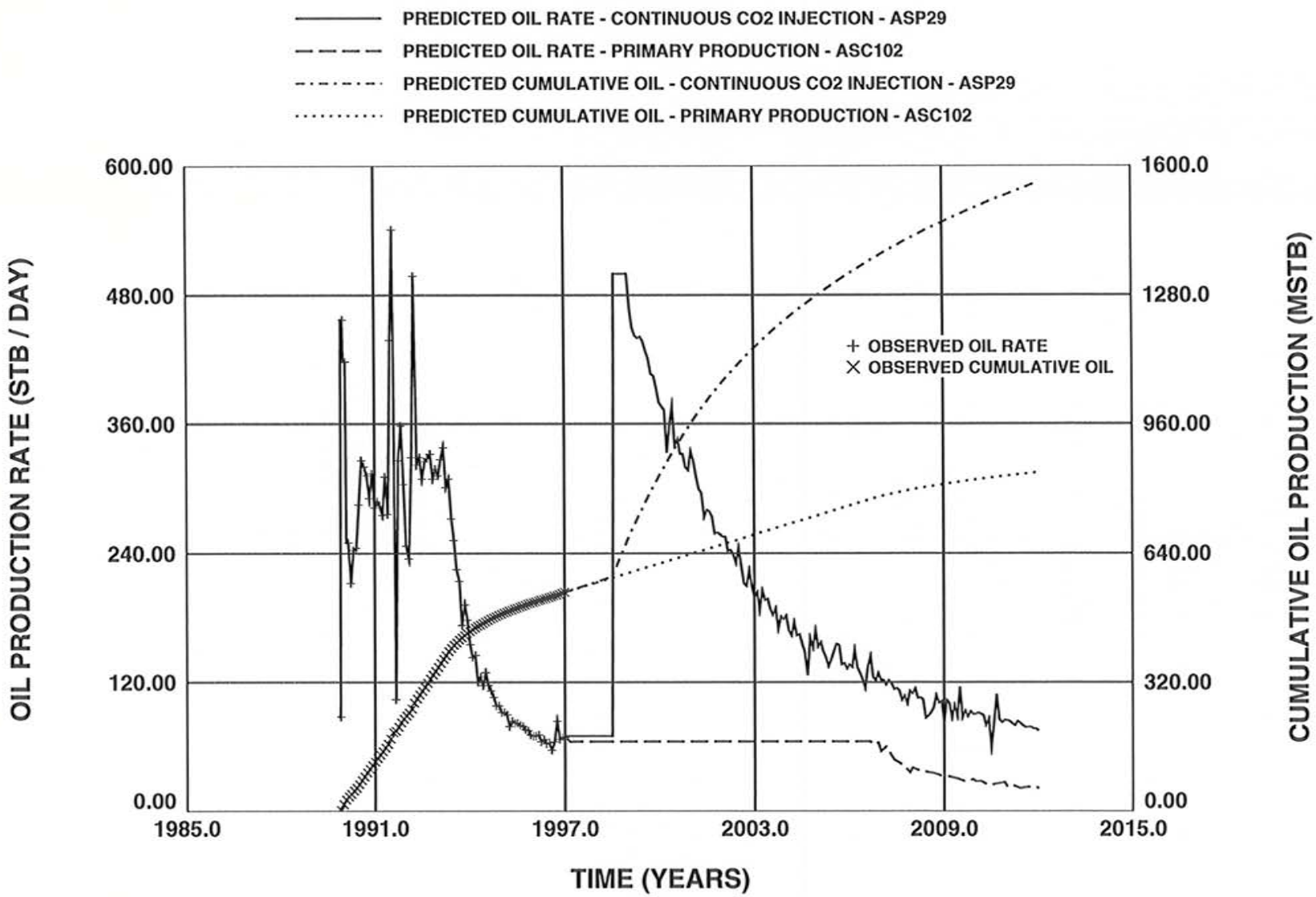

Figure 15-19 Sahgzie Well No 1 Oil Production - CO2 Flood versus Primary

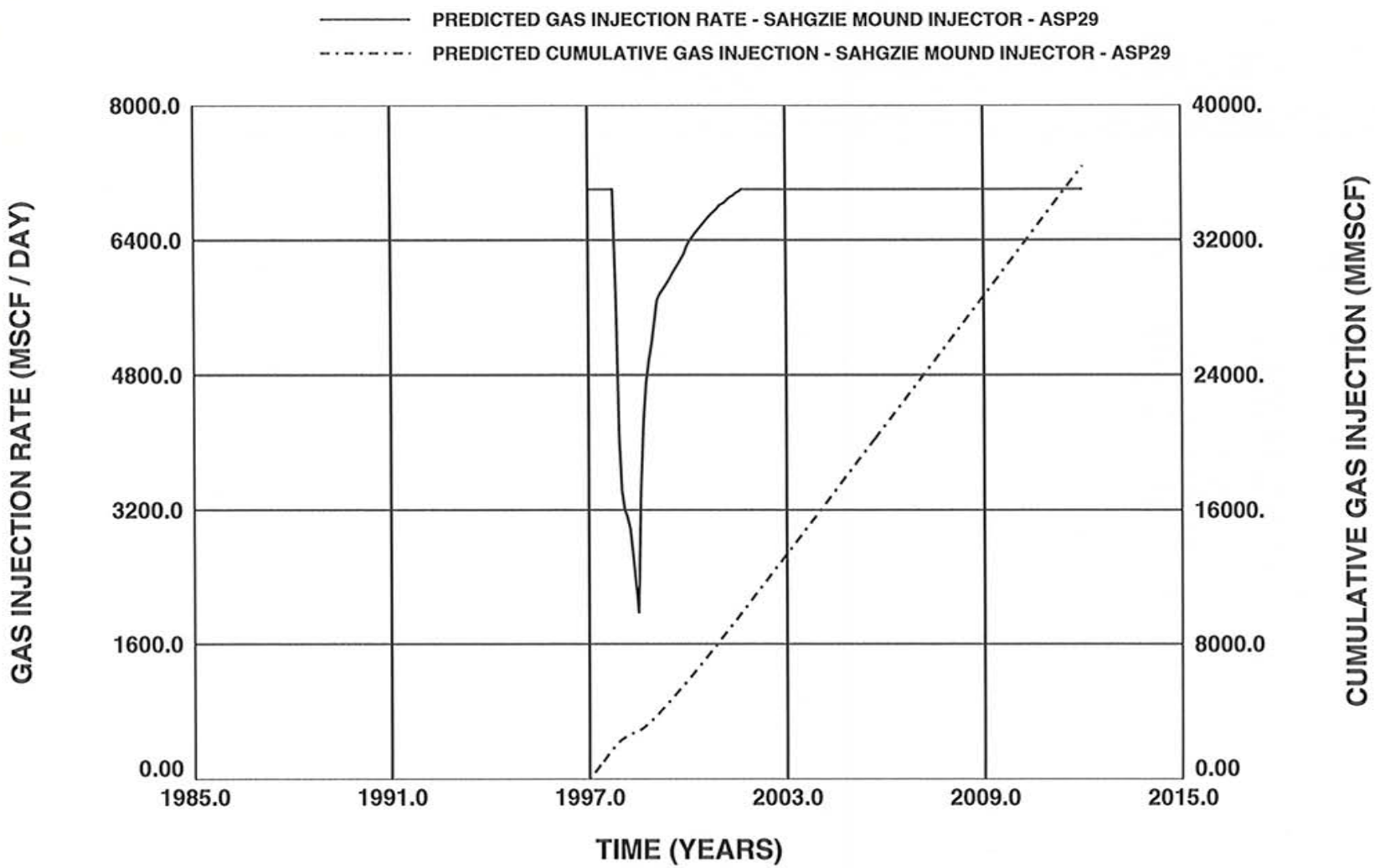

Figure 15-20 Gas Injection - Sahgzie Mound Well - Continuous CO2 Injection

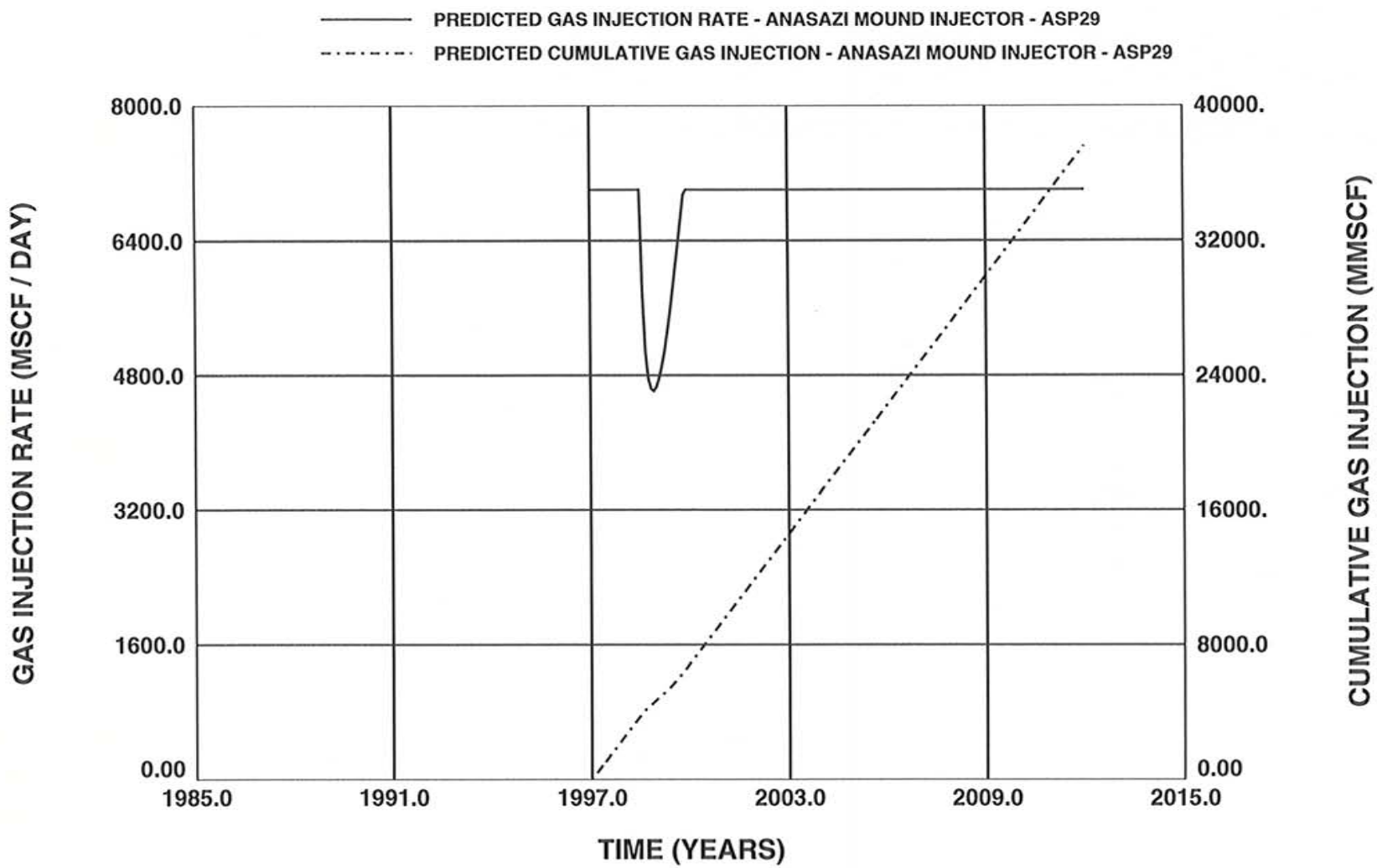

Figure 15-21 Gas Injection - Anasazi Mound Well - Continuous CO2 Injection

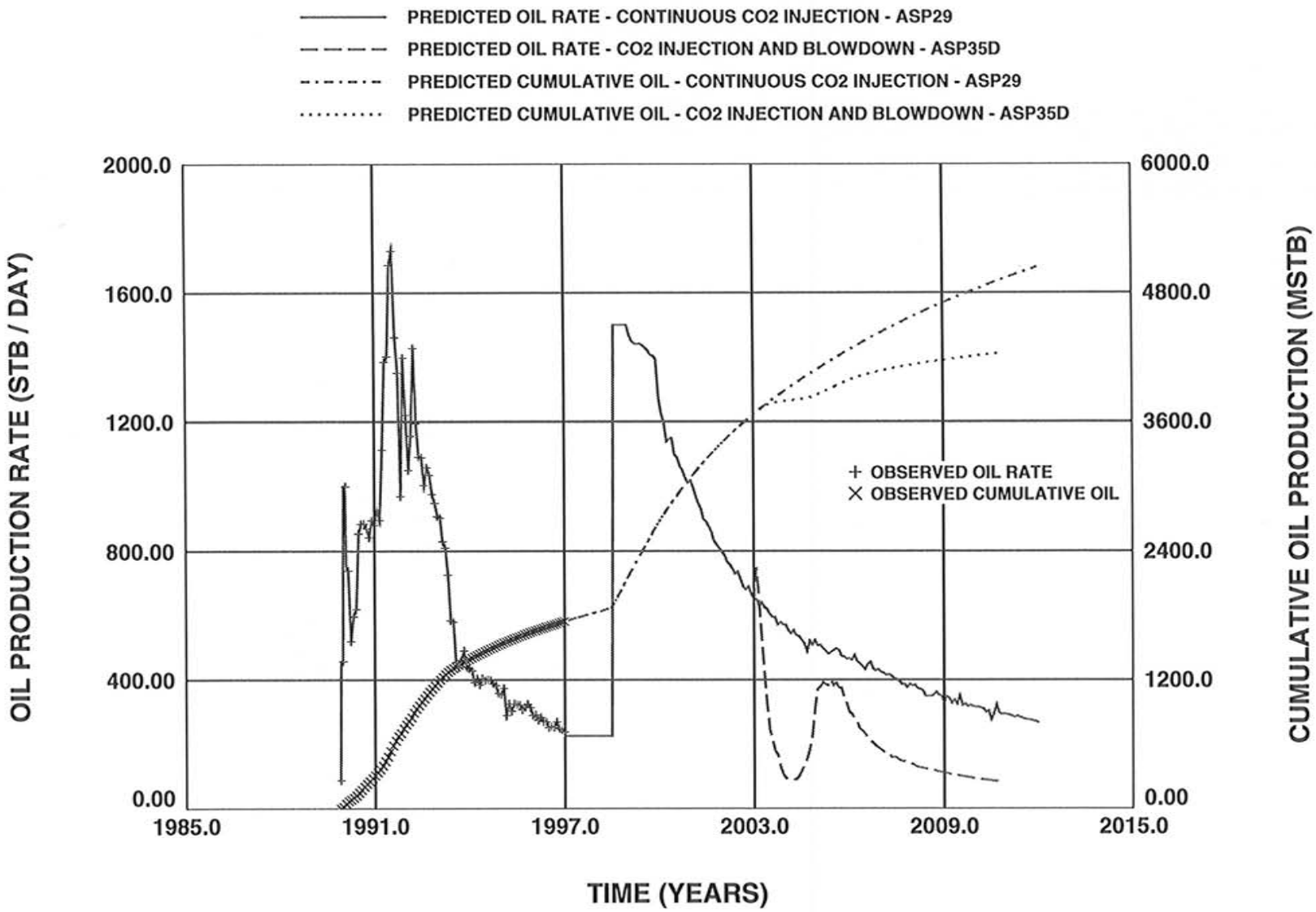

Figure 15-22 Oil Production - Continuous CO2 versus CO2 Injection and Blowdown

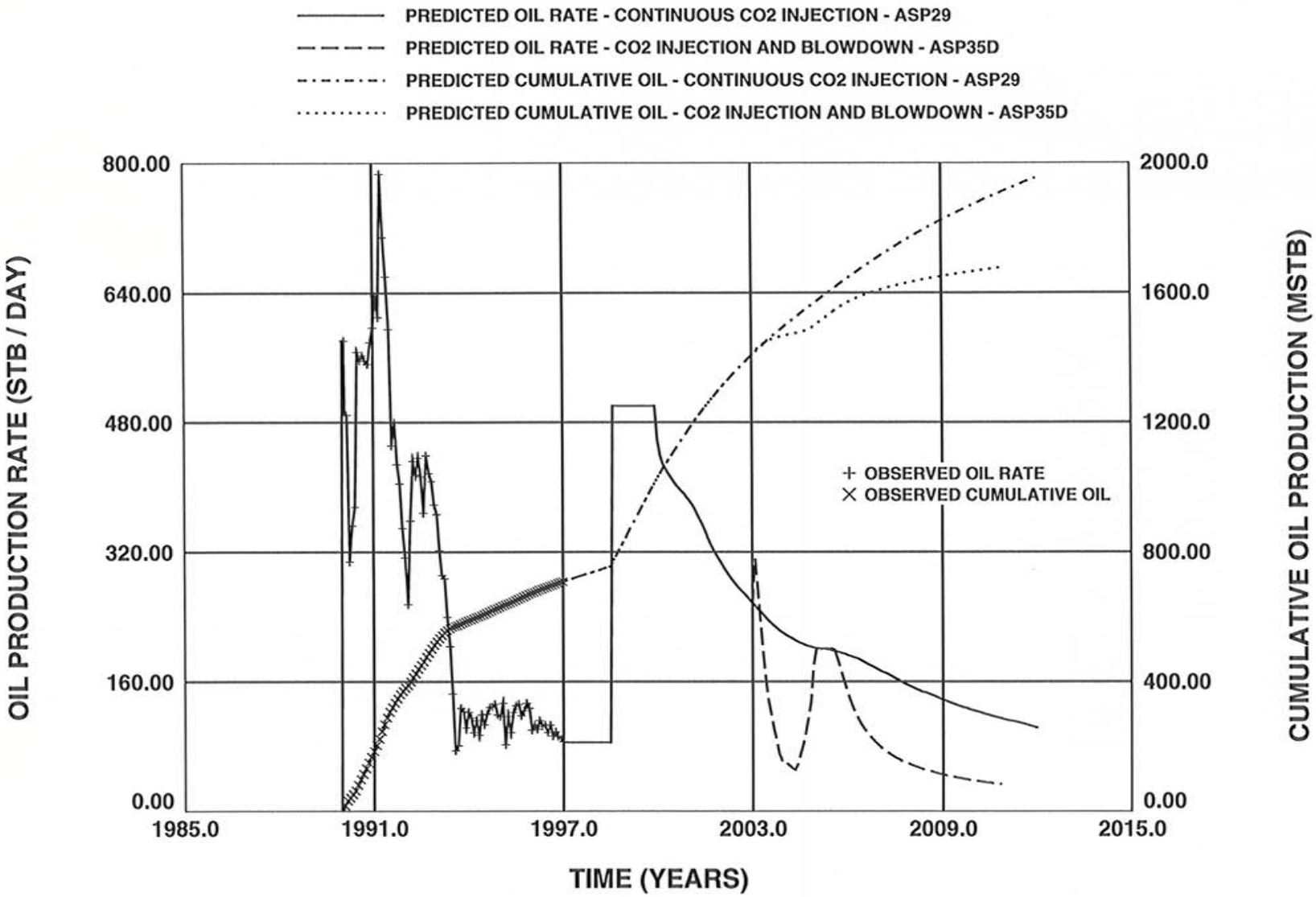

Figure 15-23 Anasazi Well No 1 Oil Production
Continuous CO2 versus CO2 Injection and Blowdown

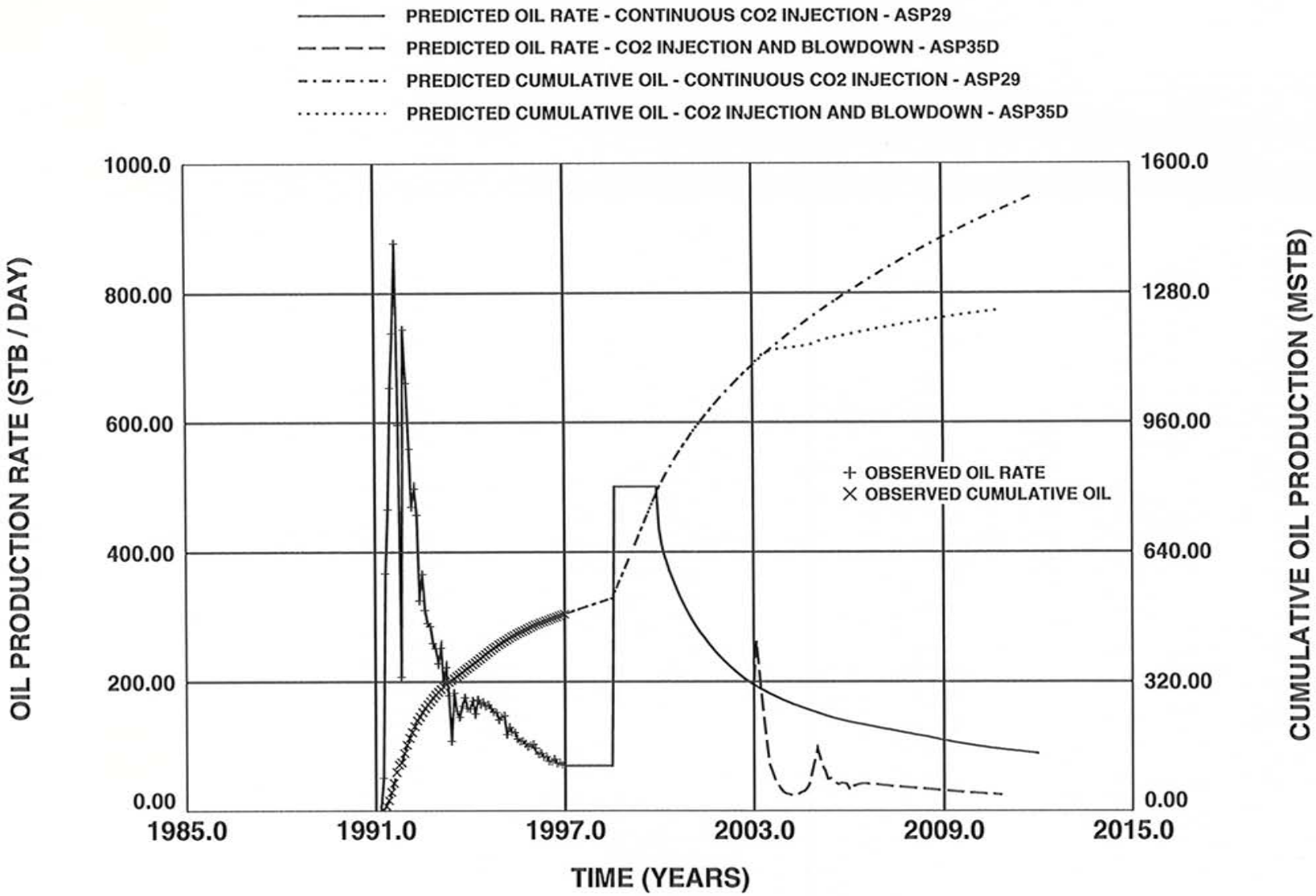

Figure 15-24 Anasazi Well No 5L-3 Oil Production Continuous CO2 versus CO2 Injection and Blowdown

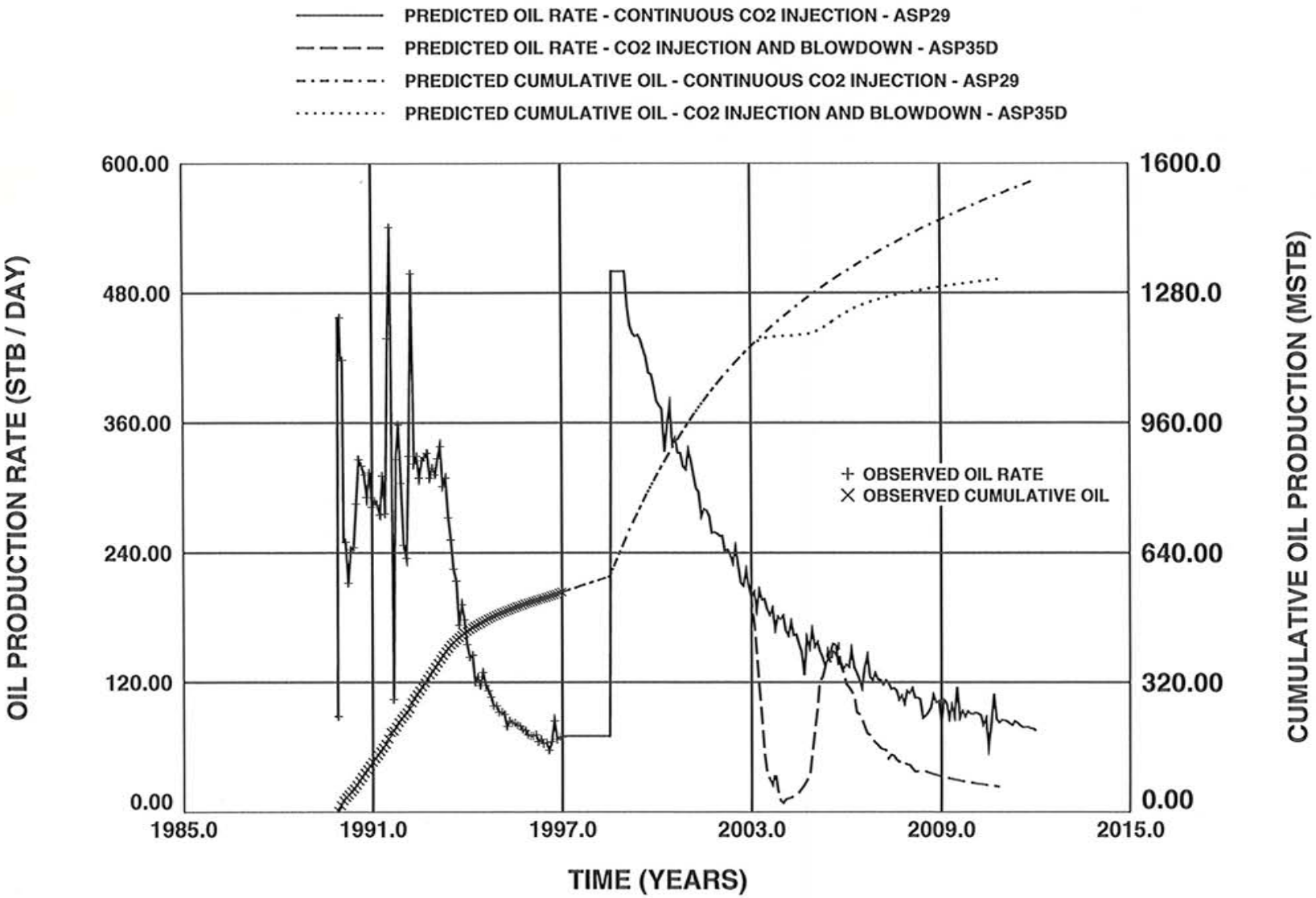

Figure 15-25 Sahgzie Well No 1 Oil Production
Continuous CO2 versus CO2 Injection and Blowdown

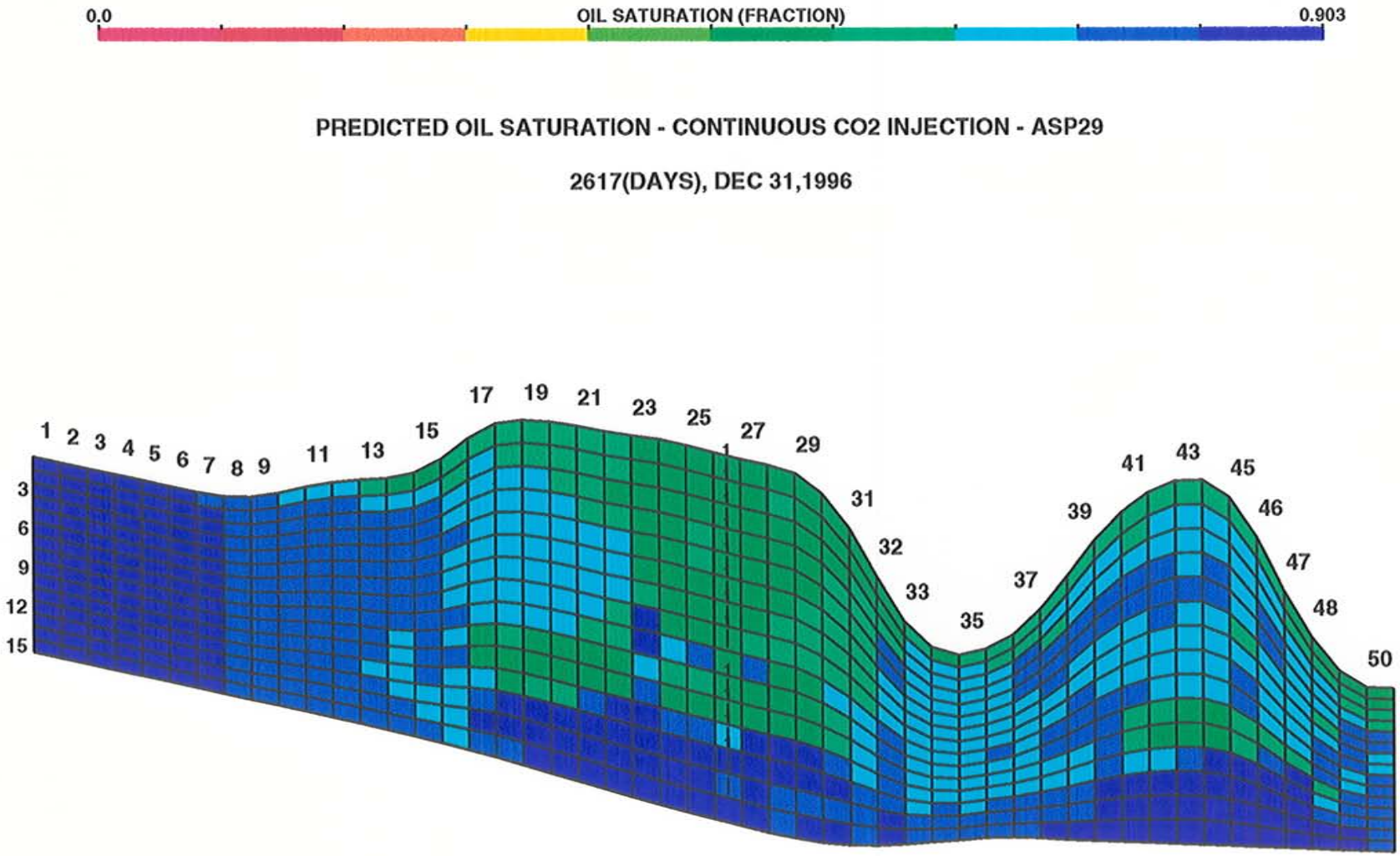

Figure 15-26 Oil Saturation Distribution

Y-Direction Cross Section at Anasazi Well No 1

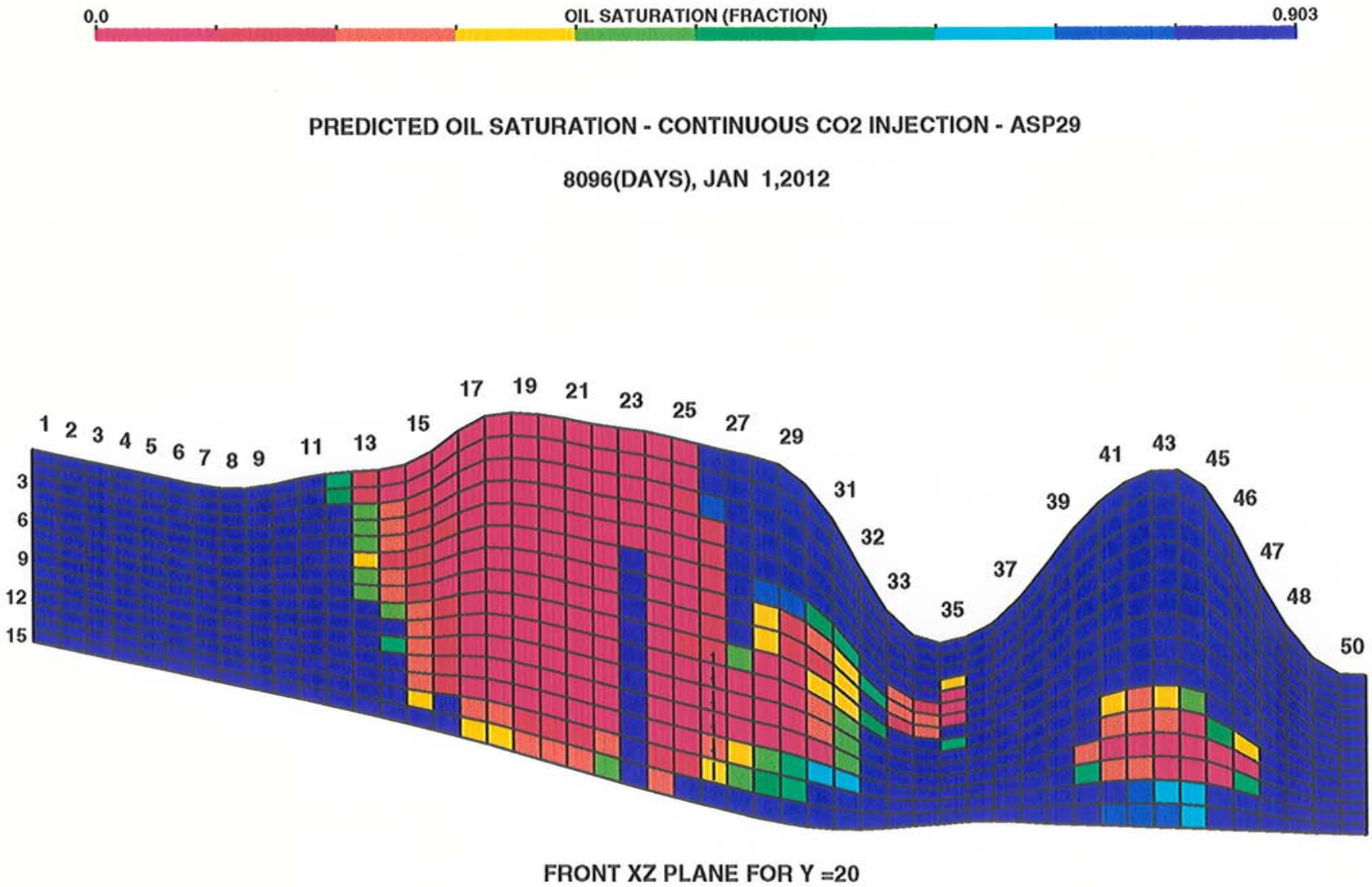

Figure 15-27 Oil Saturation Distribution

Y-Direction Cross Section at Anasazi Well No 1

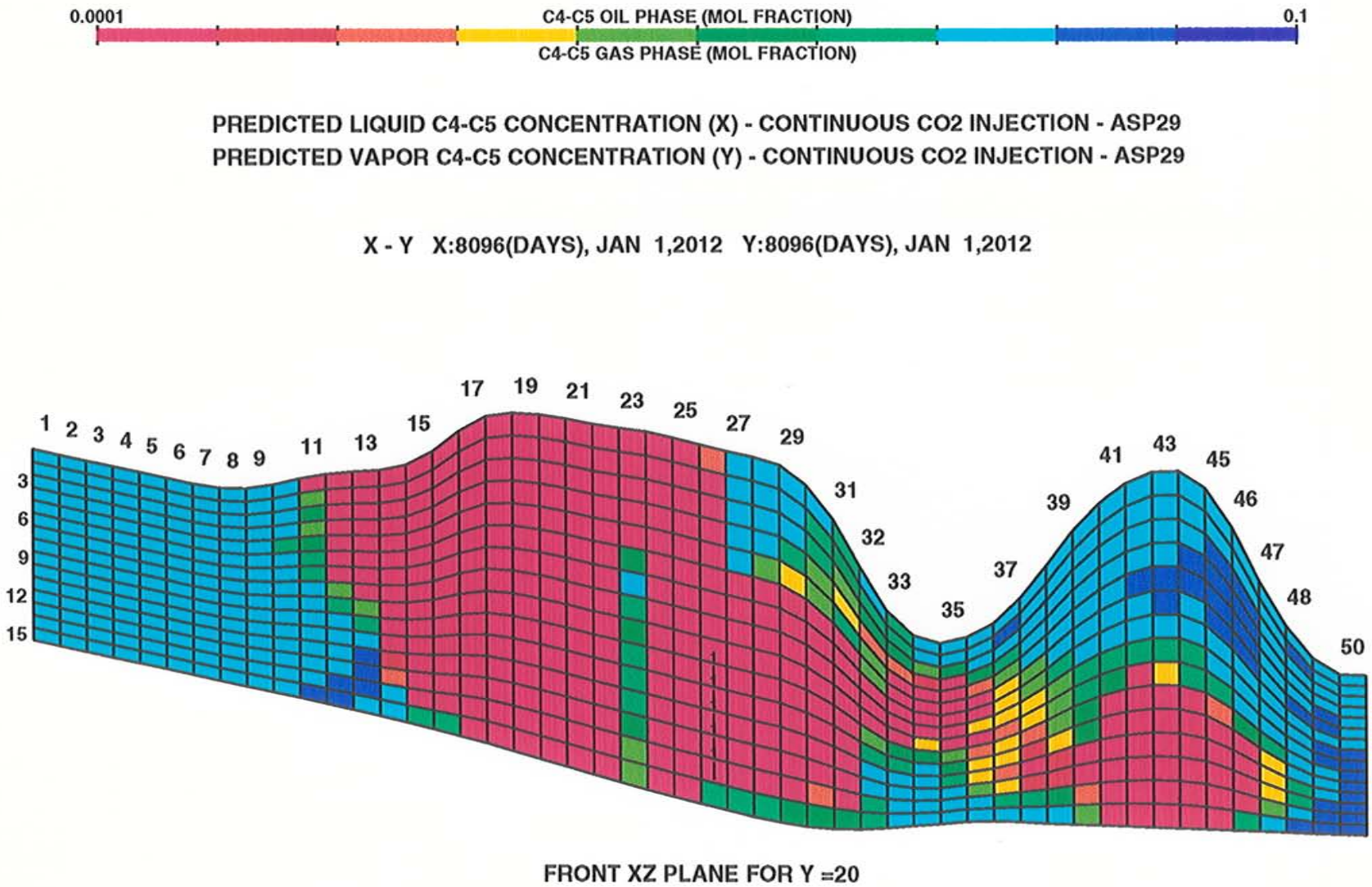

Figure 15-28 C4-C5 Liquid Mole Fraction Minus C4-C5 Vapor Mole Fraction Y-Direction Cross Section at Anasazi Well No 1

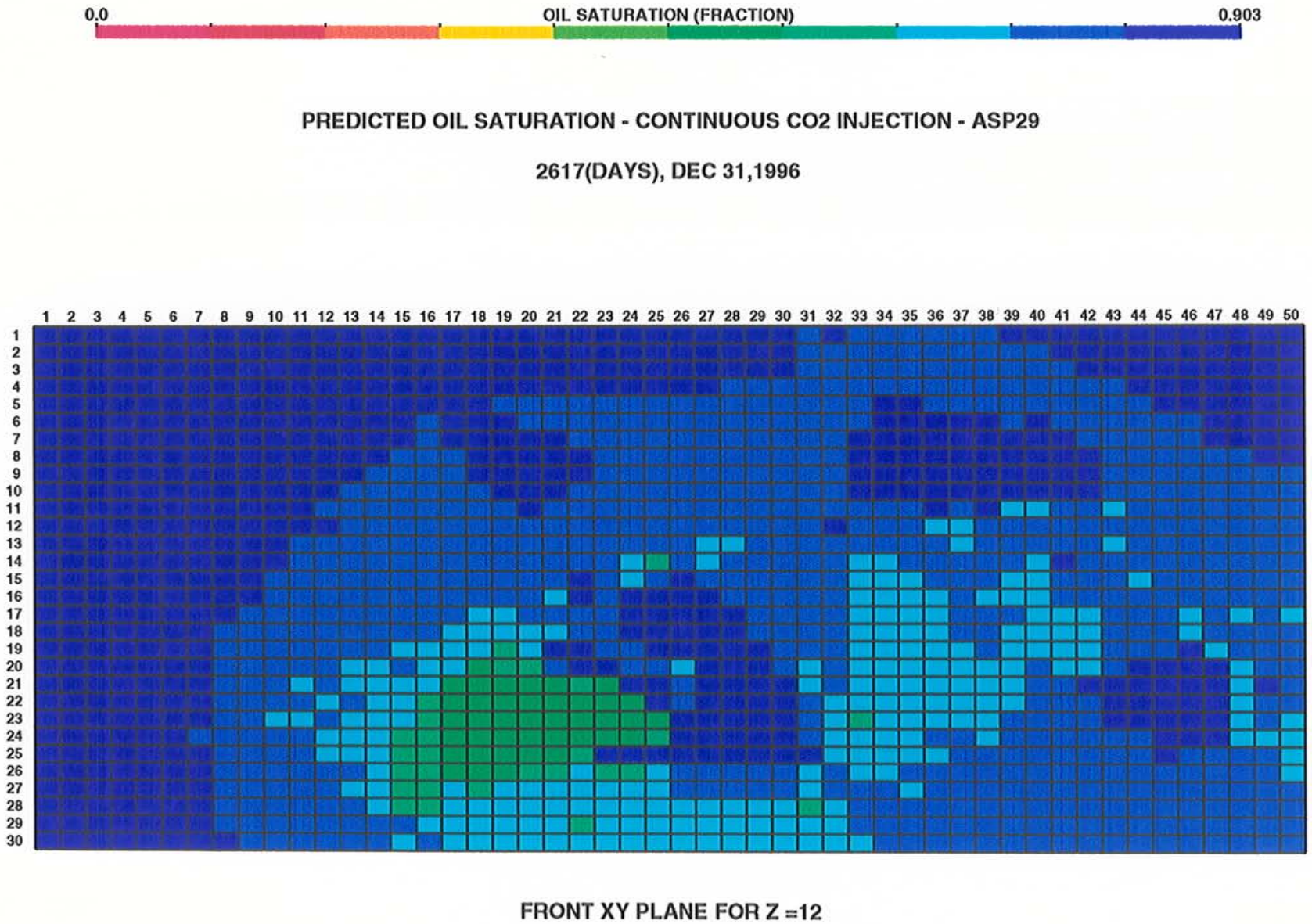

Figure 15-29 Oil Saturation Distribution
Z-Direction Map - Layer 12 in Phylloid Algal Limestone

PREDICTED OIL SATURATION - CONTINUOUS CO2 INJECTION - ASP29

2617(DAYS), DEC 31,1996

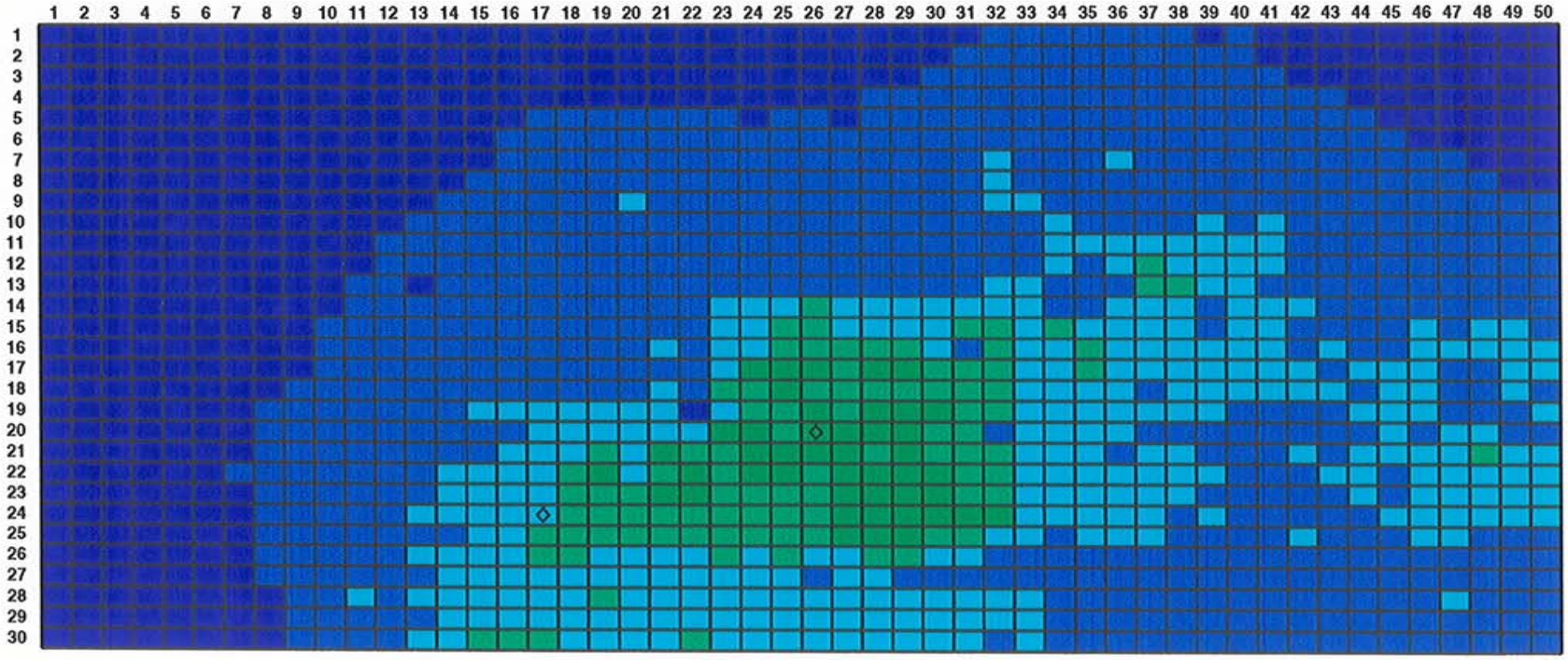

FRONT XY PLANE FOR Z = 5

Figure 15-30 Oil Saturation Distribution
Z-Direction Map - Layer 5 in Supramound Interval

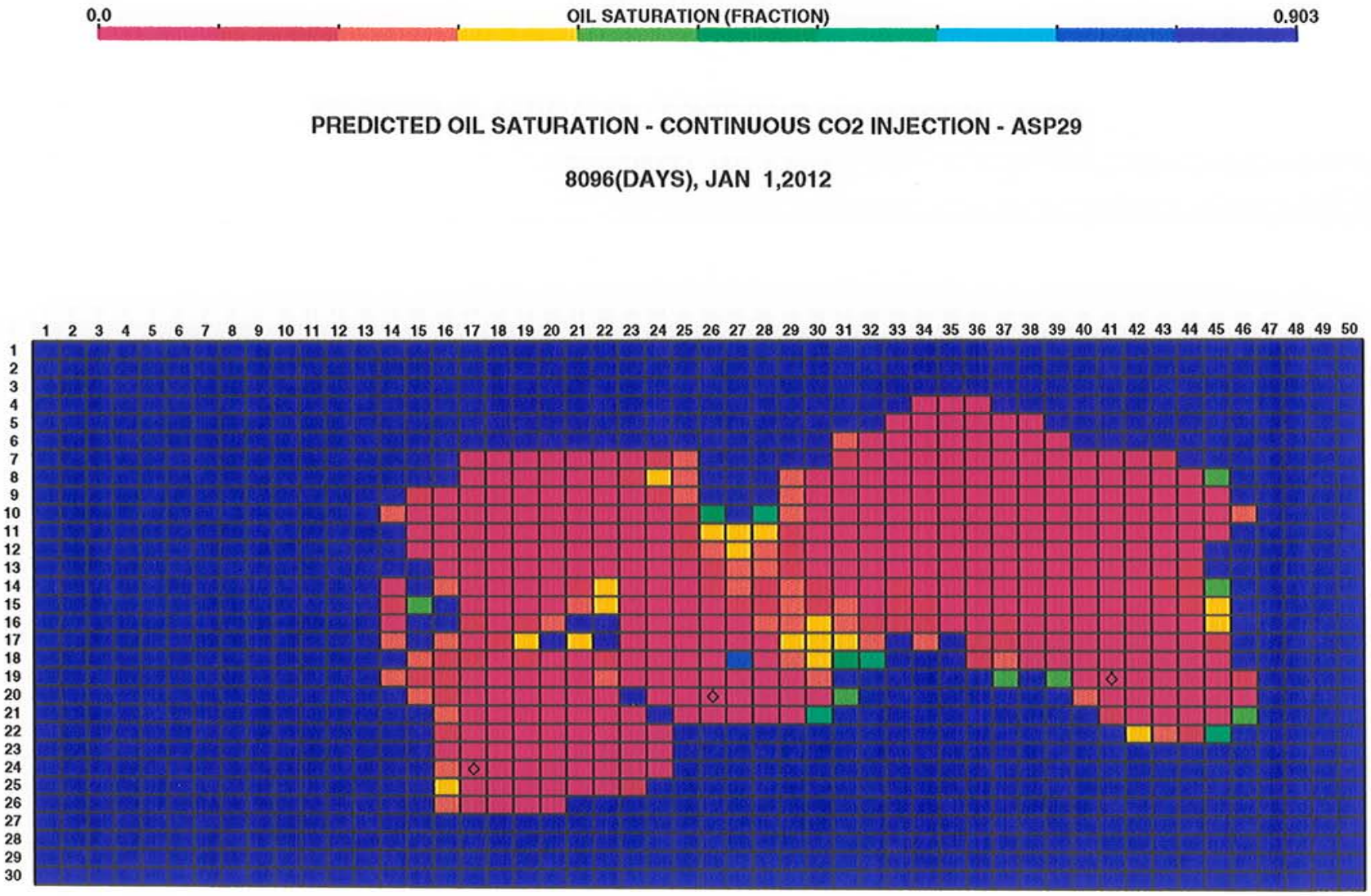

Figure 15-31 Oil Saturation Distribution
Z-Direction Map - Layer 12 in Phylloid Algal Limestone

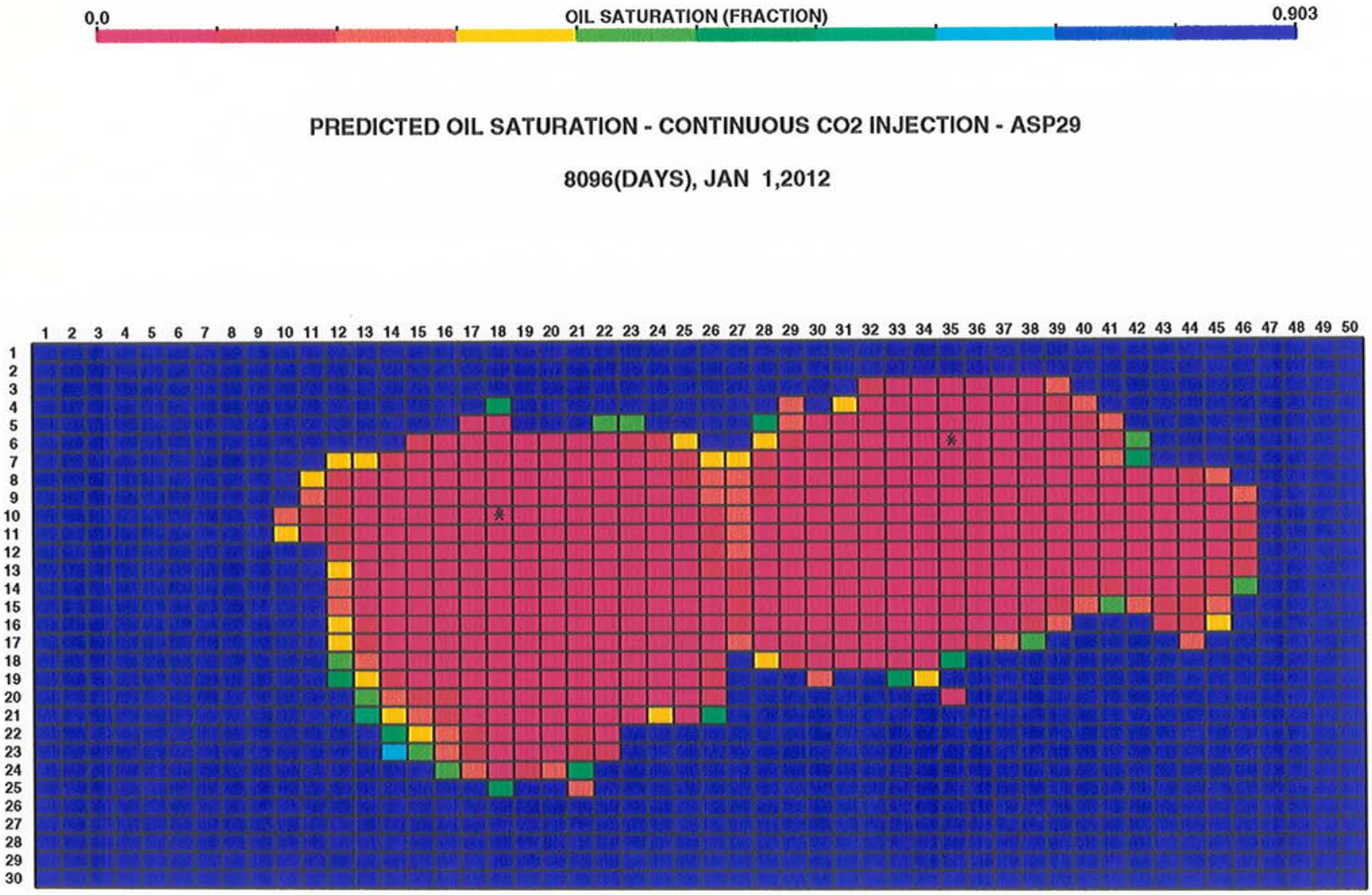

Figure 15-32 Oil Saturation Distribution
Z-Direction Map - Layer 5 in Supramound Interval

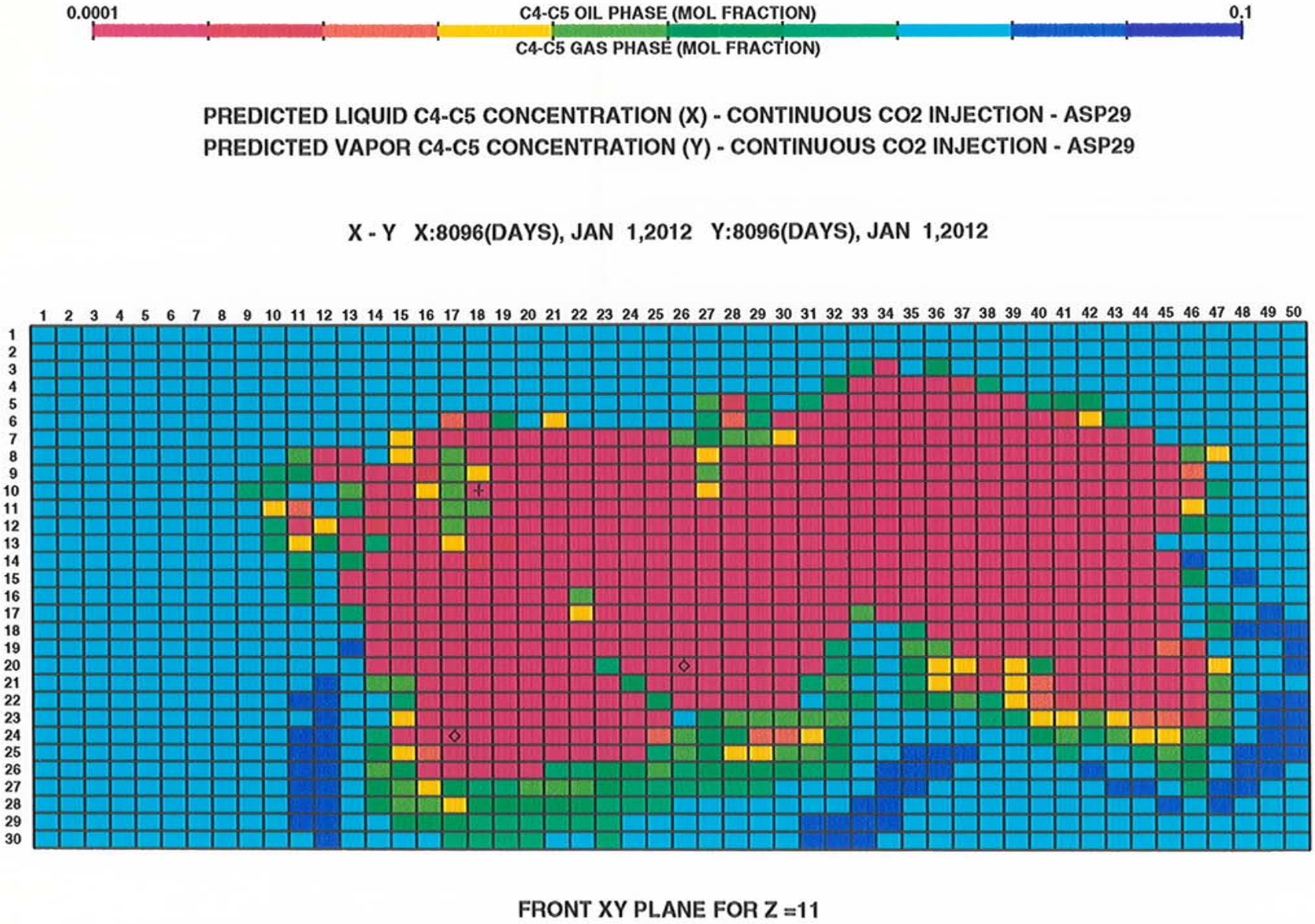

Figure 15-33 C4-C5 Liquid Mole Fraction Minus C4-C5 Vapor Mole Fraction Z-Direction Map - Layer 11 in Phylloid Algal Limestone

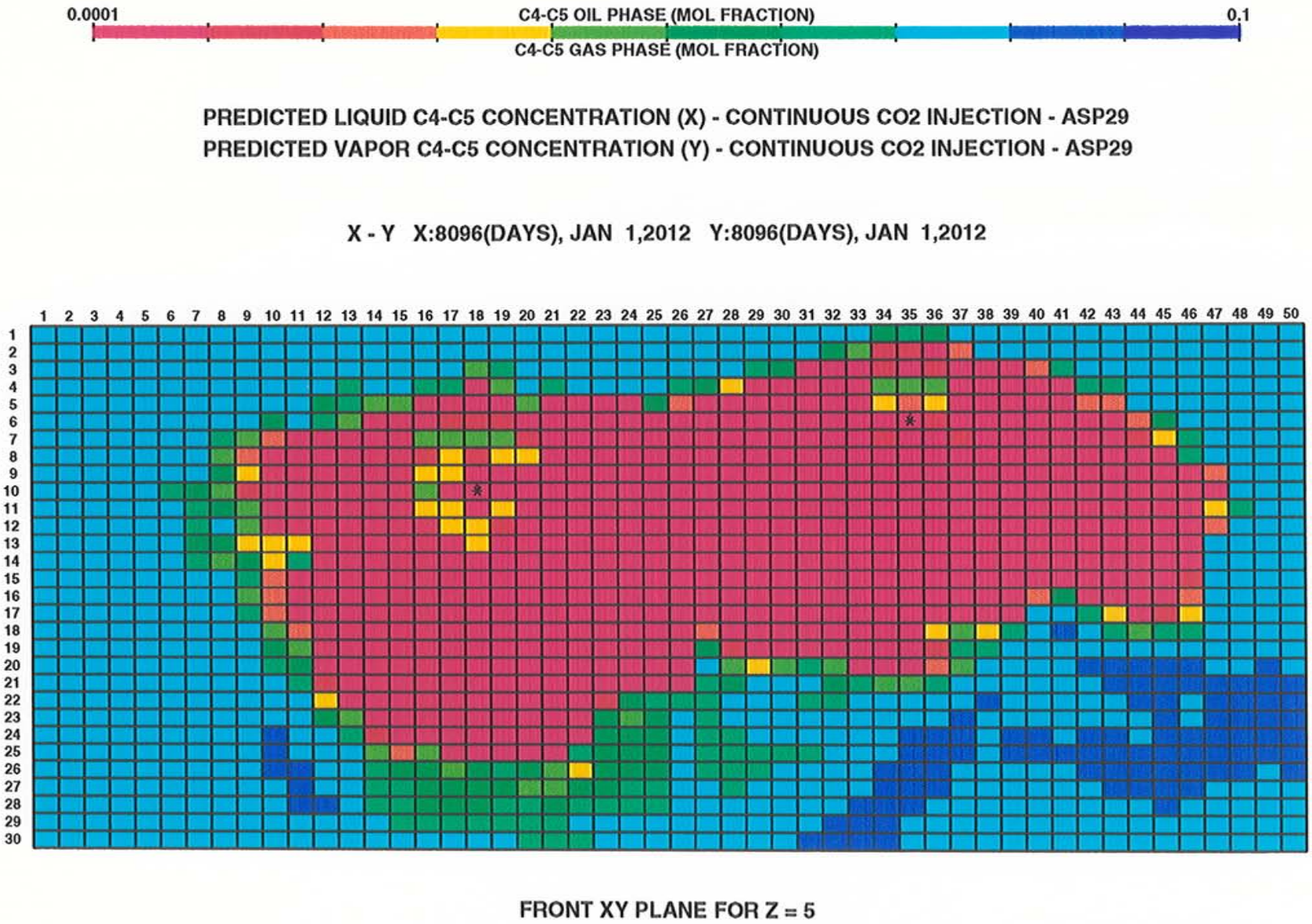

Figure 15-34 C4-C5 Liquid Mole Fraction Minus C4-C5 Vapor Mole Fraction Z-Direction Map - Layer 5 in Supramound Interval

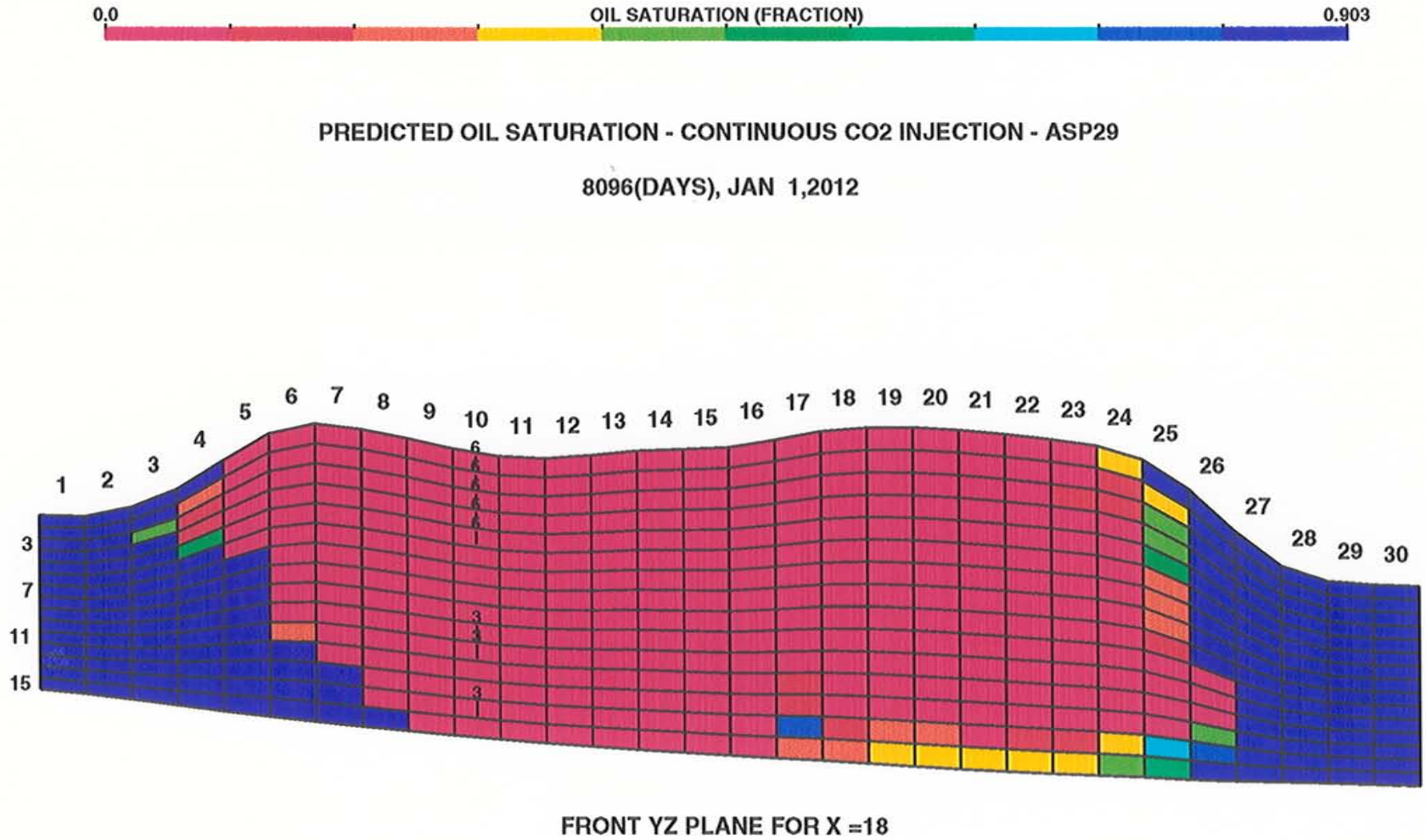

Figure 15-35 Oil Saturation Distribution

X-Direction Cross Section at Anasazi Mound Injector and Anasazi Well No 6H-1

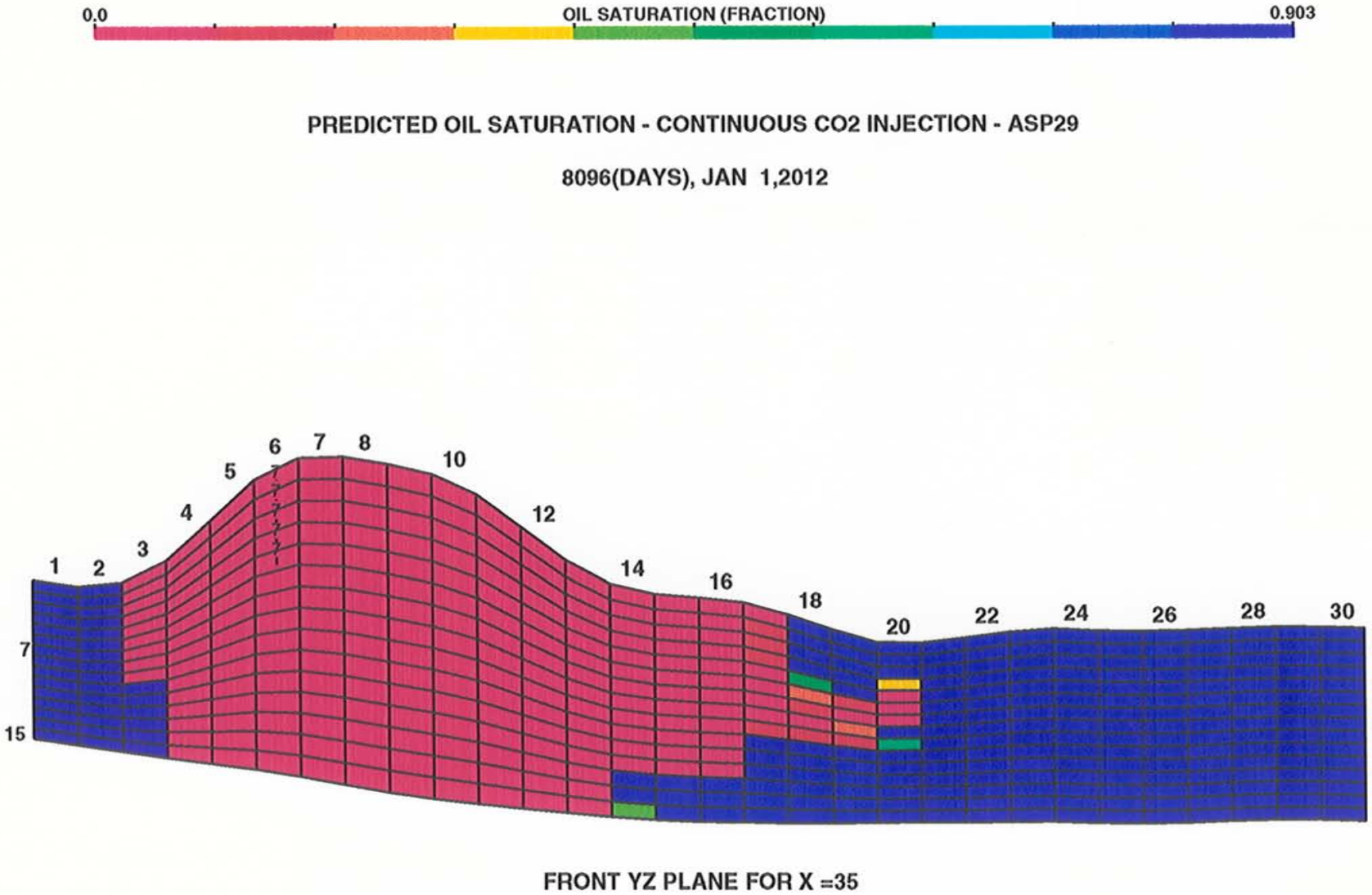

Figure 15-36 Oil Saturation Distribution

X-Direction Cross Section at Sahgzie Mound Injector

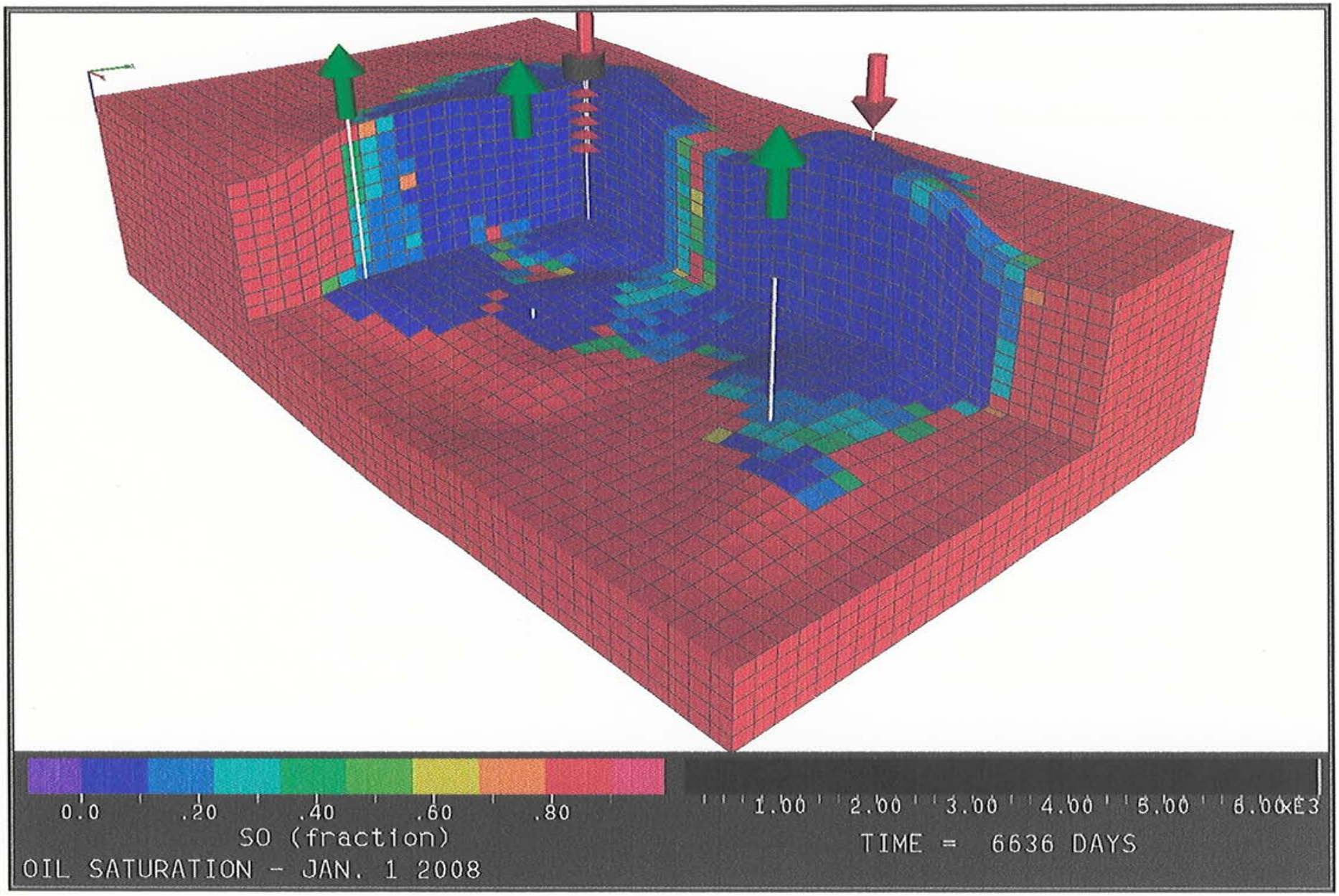

Figure 15-37 3-D Oil Saturation Distribution

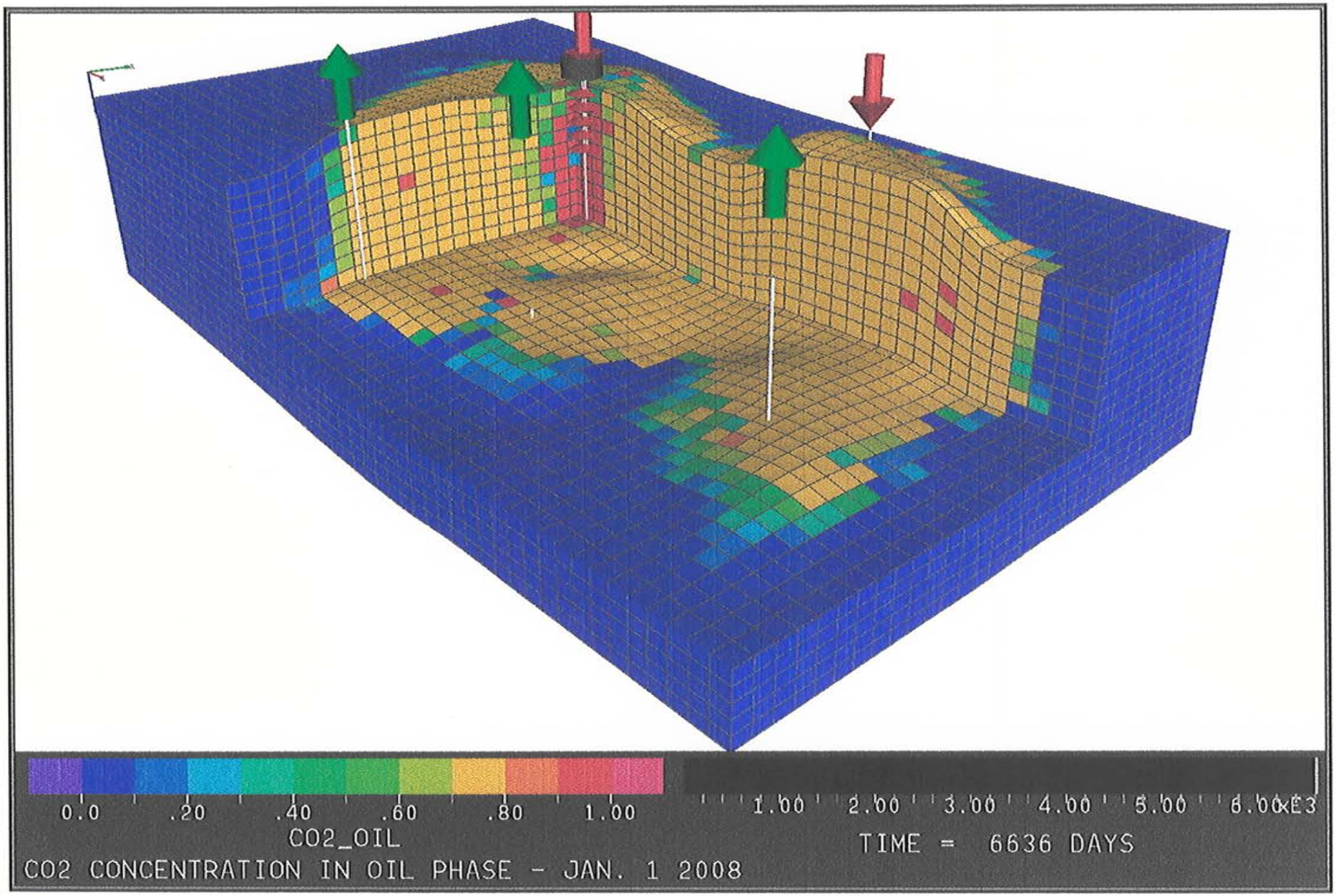

Figure 15-38 3-D Liquid Phase CO2 Mole Fraction Distribution

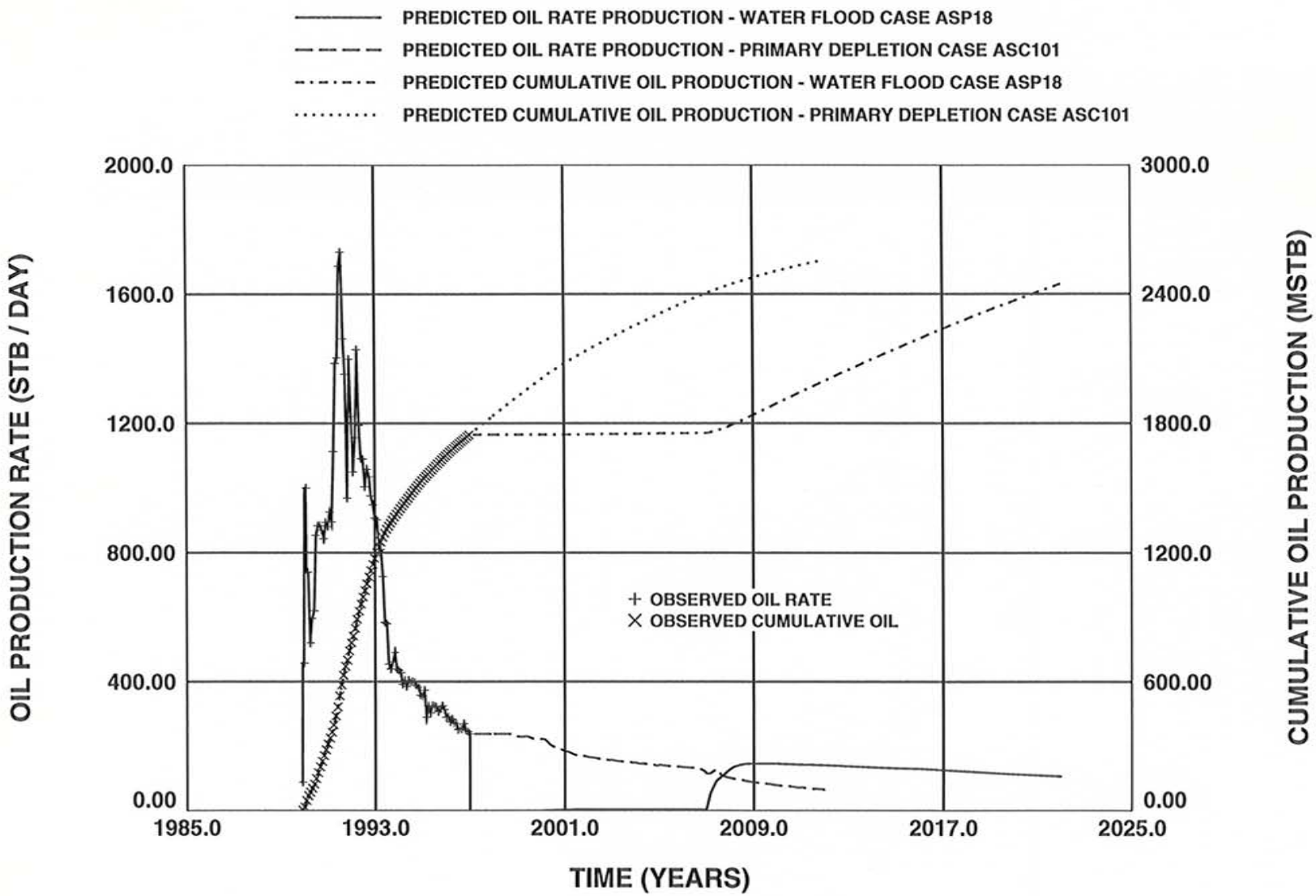

Figure 15-39 Field Level Oil Production - Water Flood versus Primary

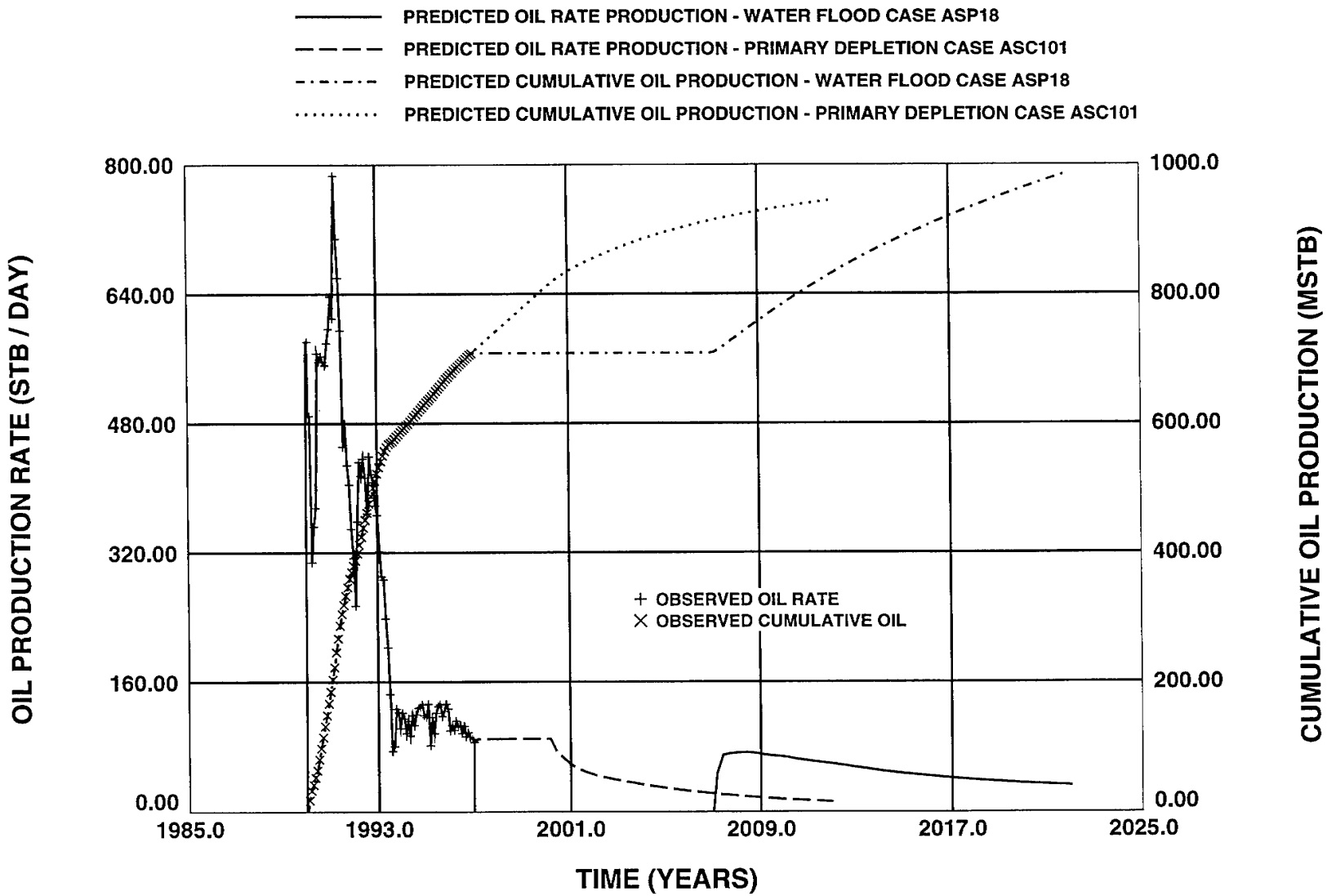

Figure 15-40 Anasazi Well No 1 Oil Production - Water Flood versus Primary

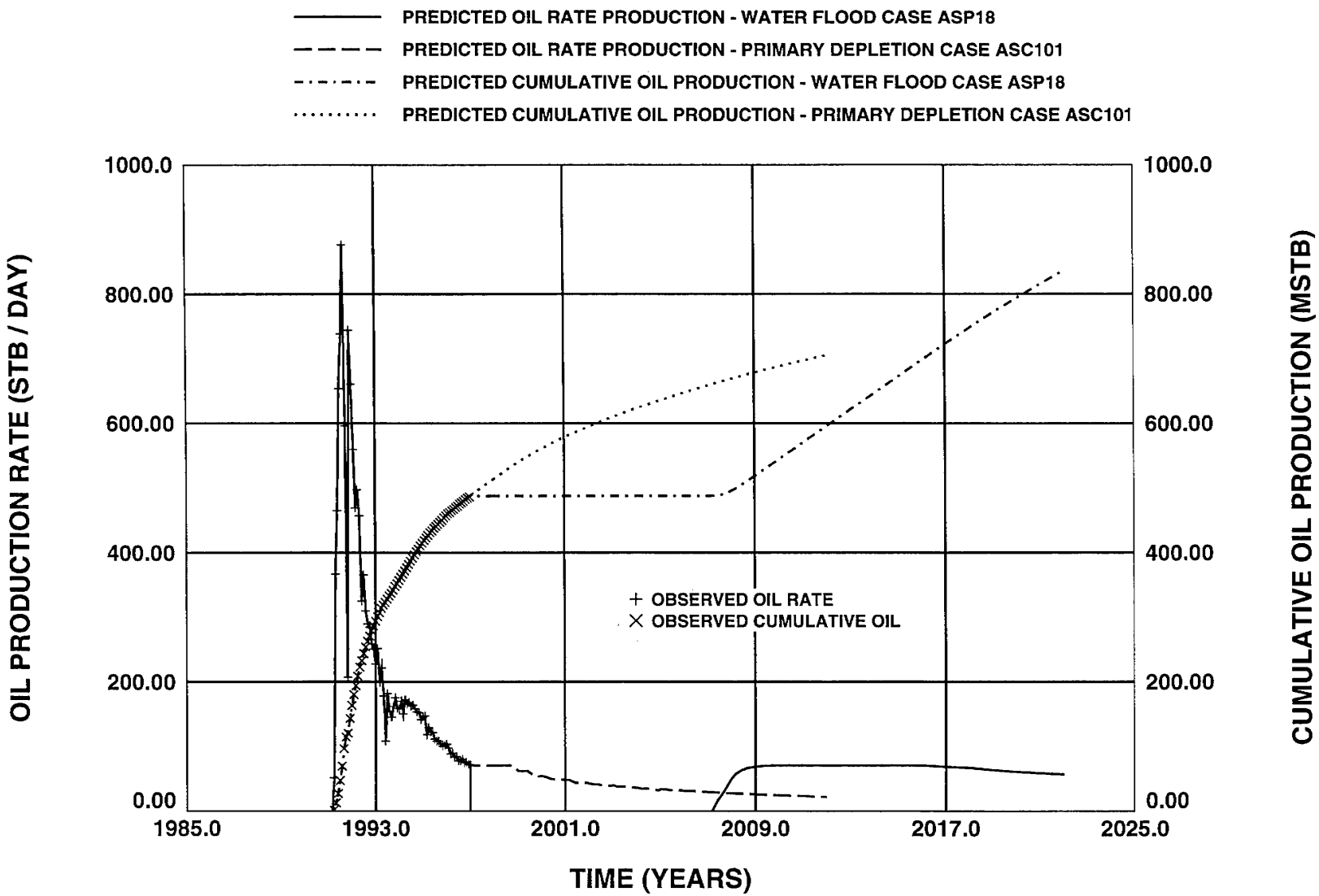

Figure 15-41 Anasazi Well No 5L-3 Oil Production - Water Flood versus Primary

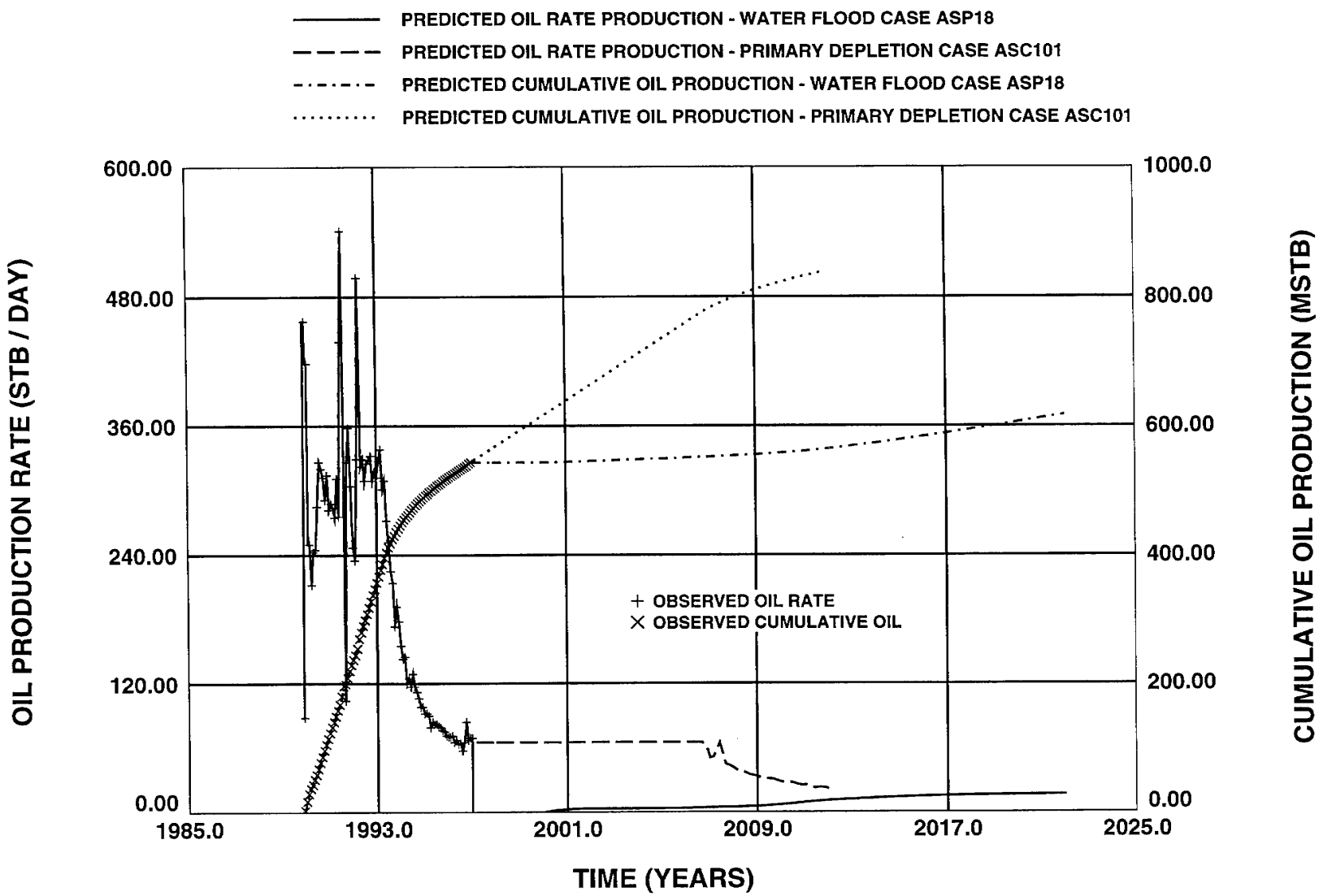

Figure 15-42 Sahgzie Well No 1 Oil Production - Water Flood versus Primary

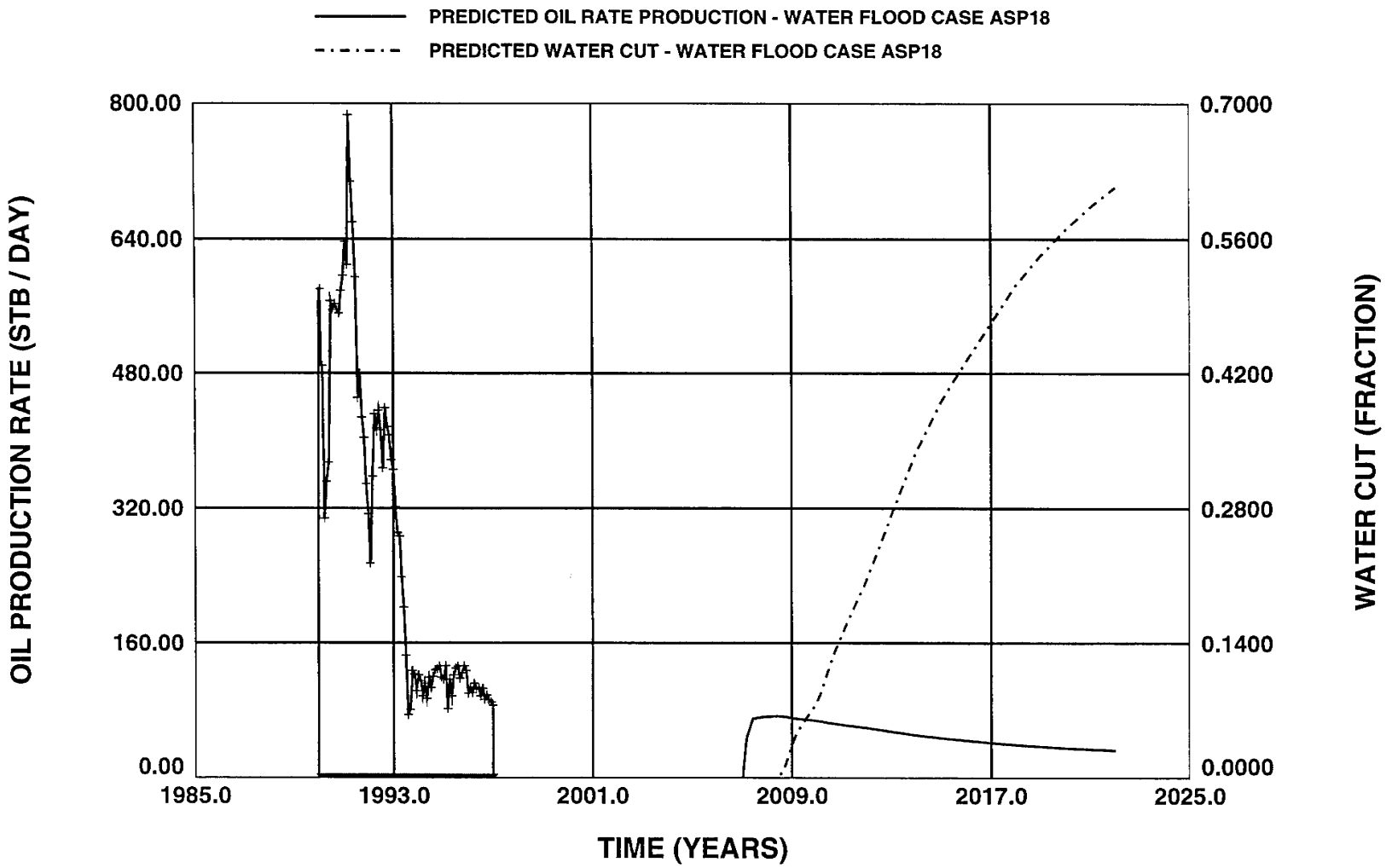

Figure 15-43 Anasazi Well No 1 Oil Rate and Water Cut - Water Flood

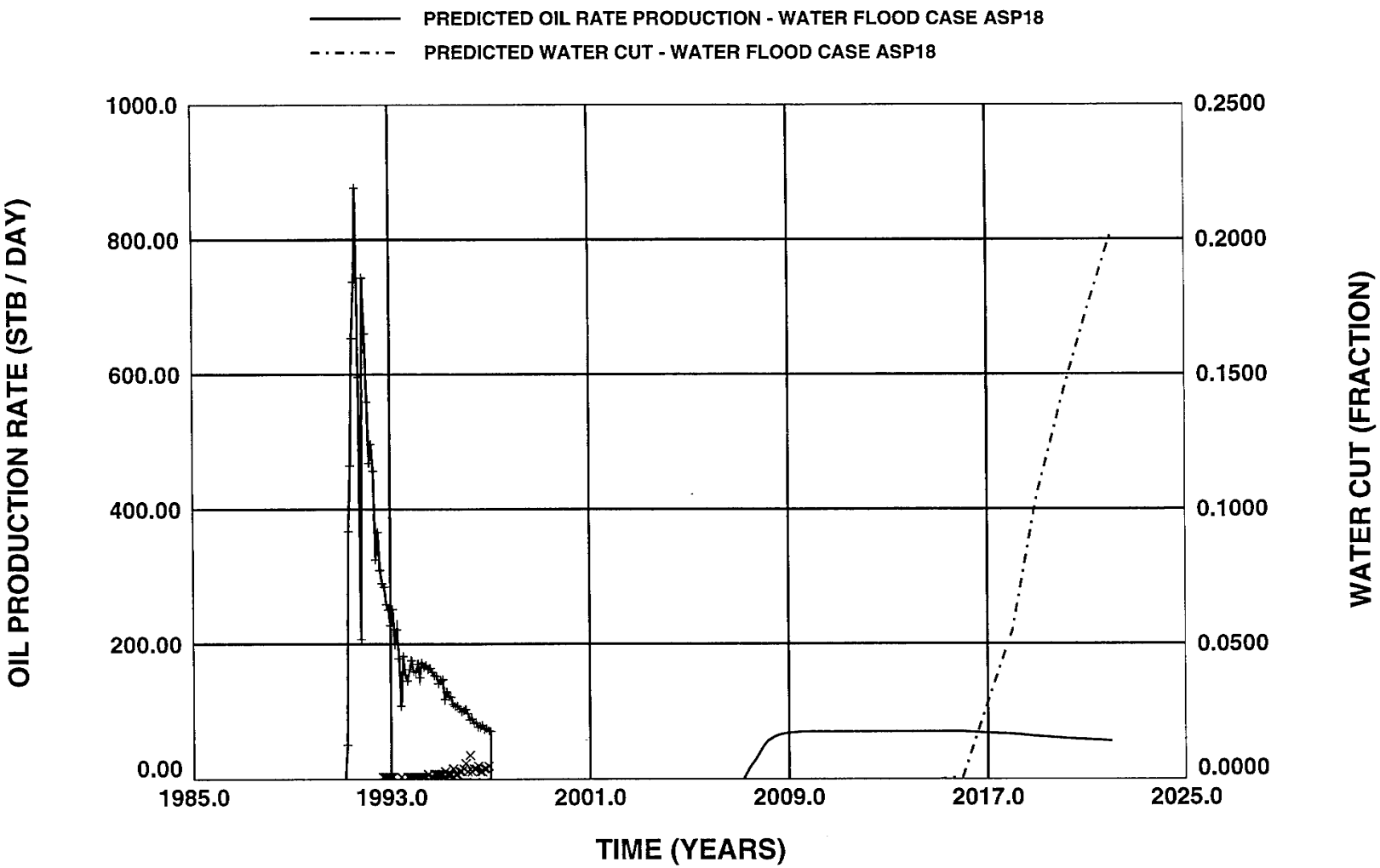

Figure 15-44 Anasazi Well No 5L-3 Oil Rate and Water Cut - Water Flood

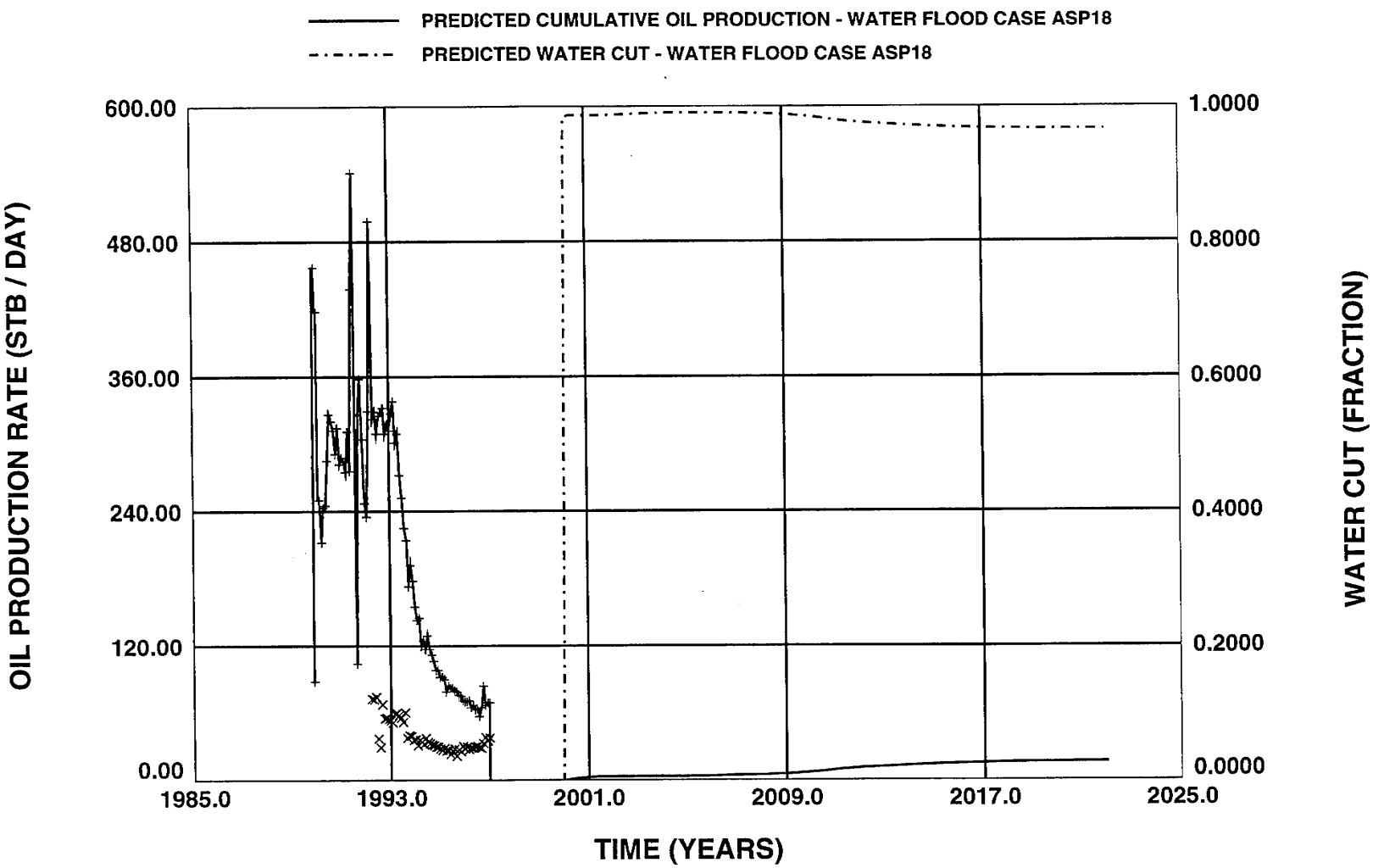

Figure 15-45 Sahgzie Well No 1 Oil Rate and Water Cut - Water Flood

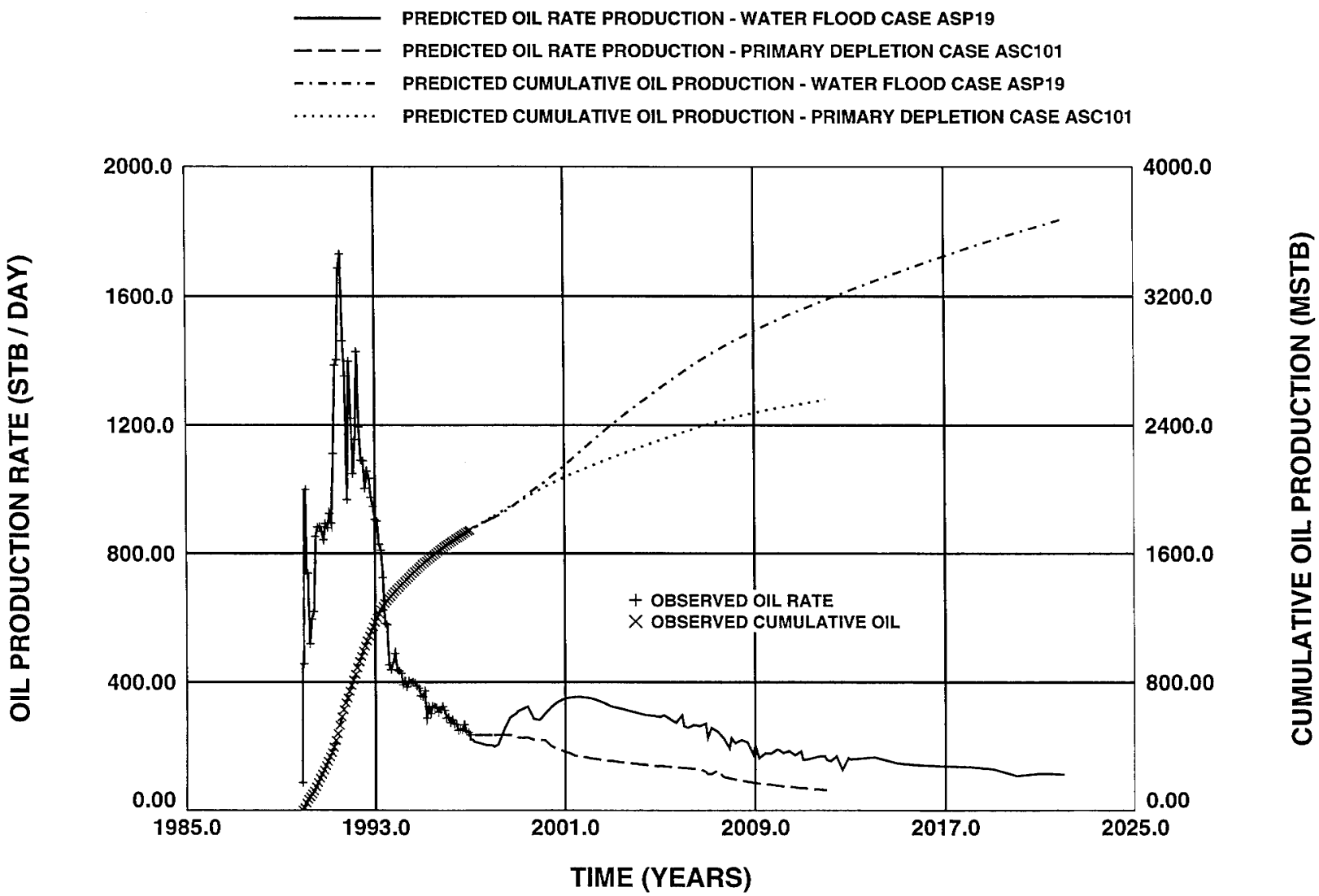

Figure 15-46 Field Level Oil Production - Water Flood versus Primary

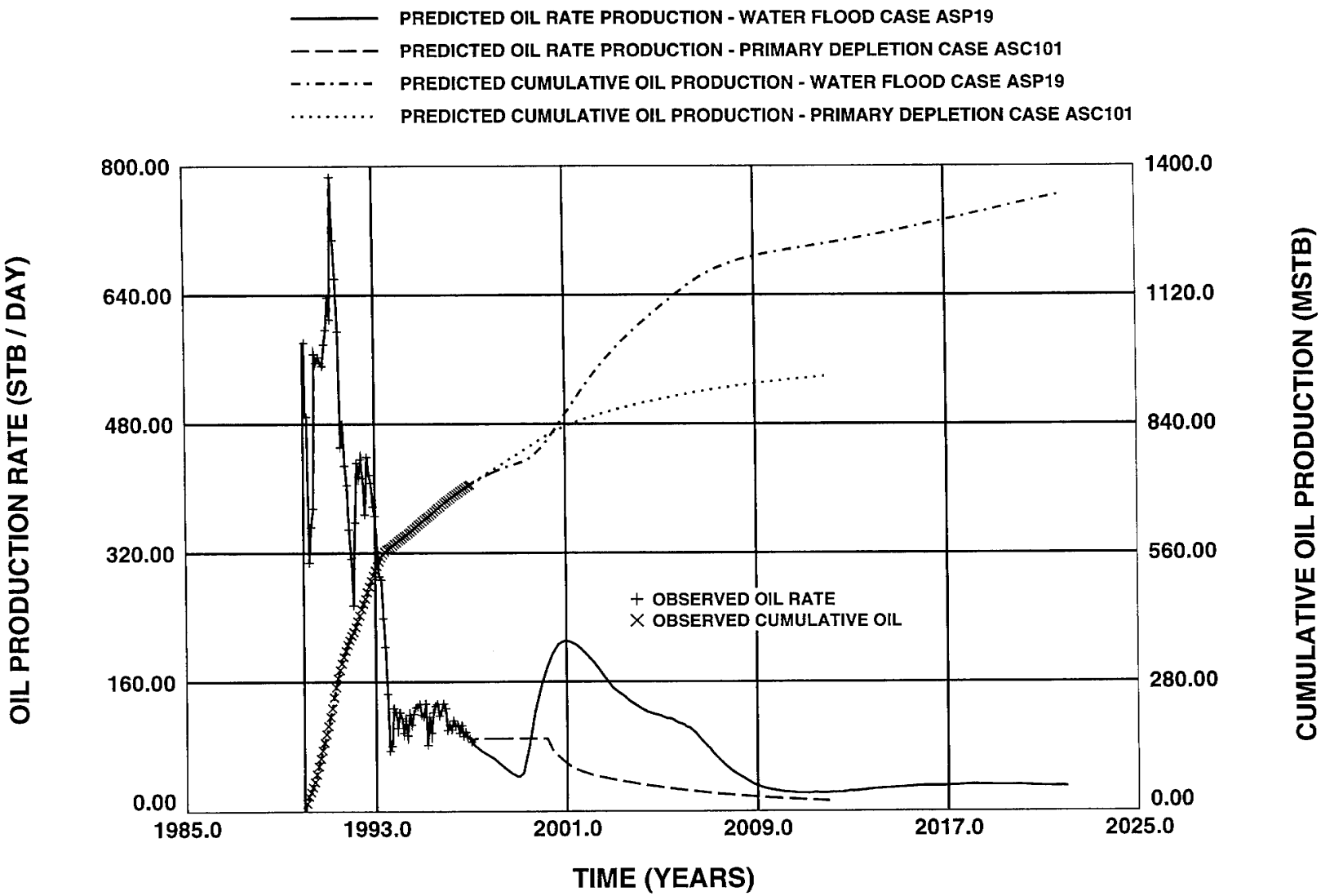

Figure 15-47 Anasazi Well No 1 Oil Production - Water Flood versus Primary

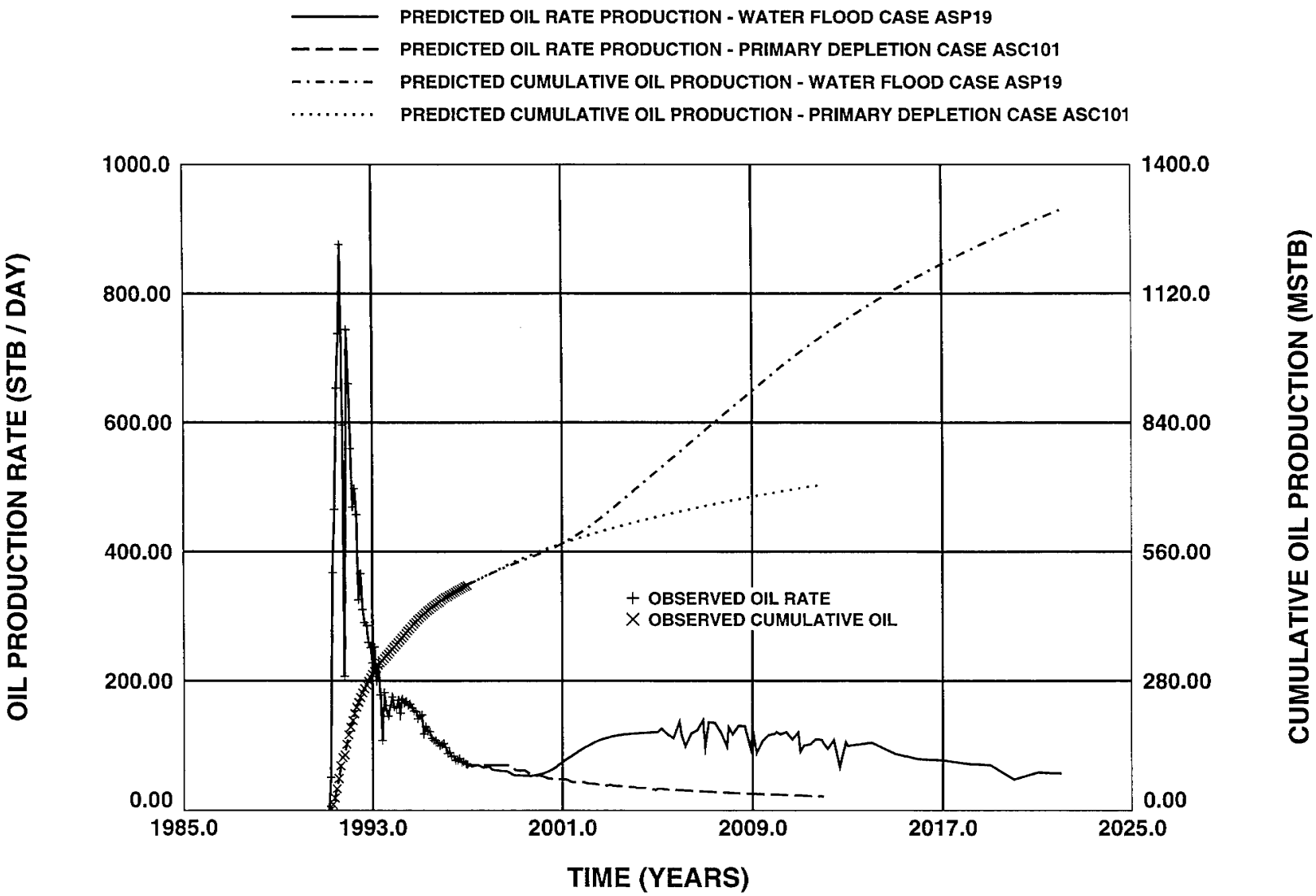

Figure 15-48 Anasazi Well No 5L-3 Oil Production - Water Flood versus Primary

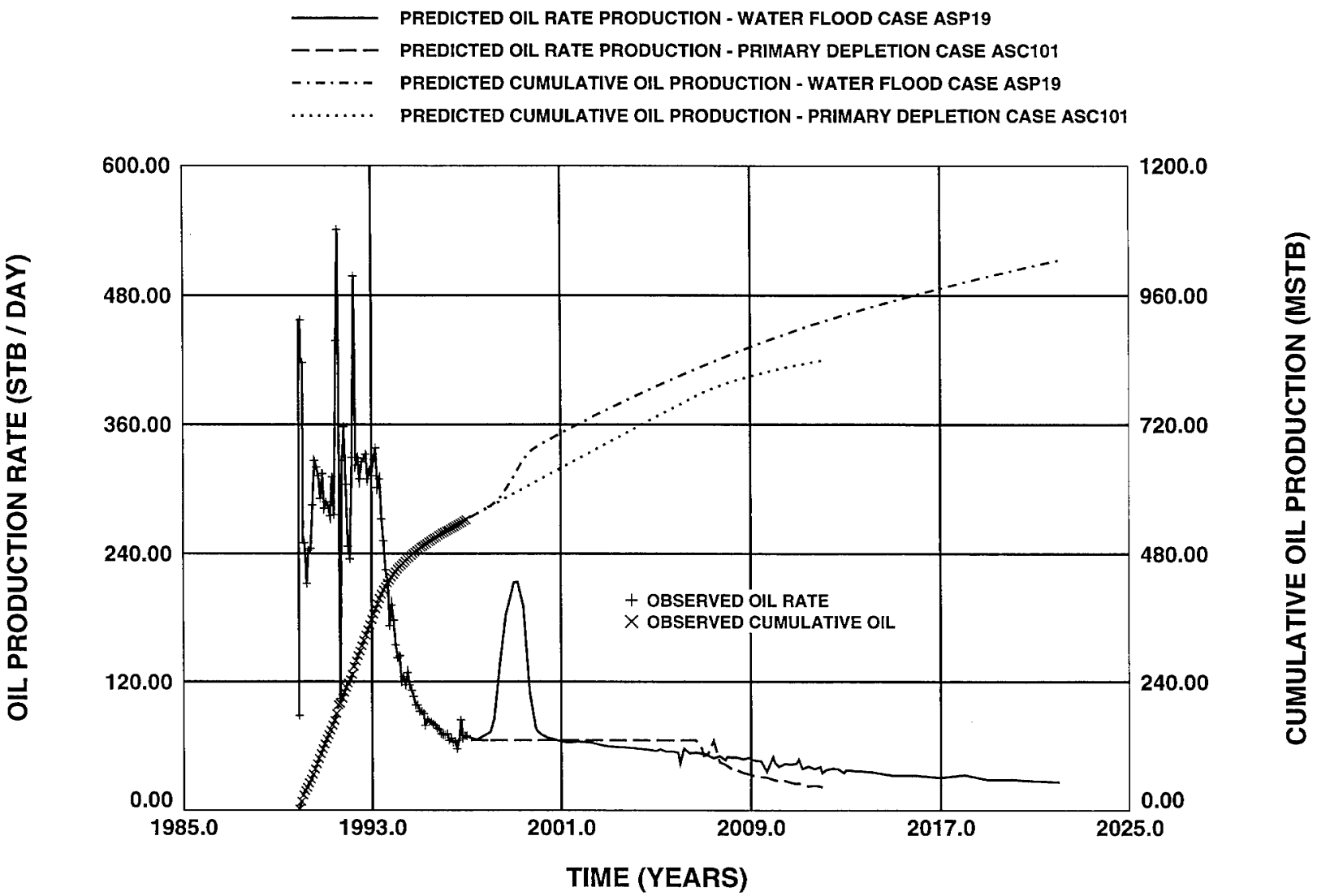

Figure 15-49 Sahgzie Well No 1 Oil Production - Water Flood versus Primary

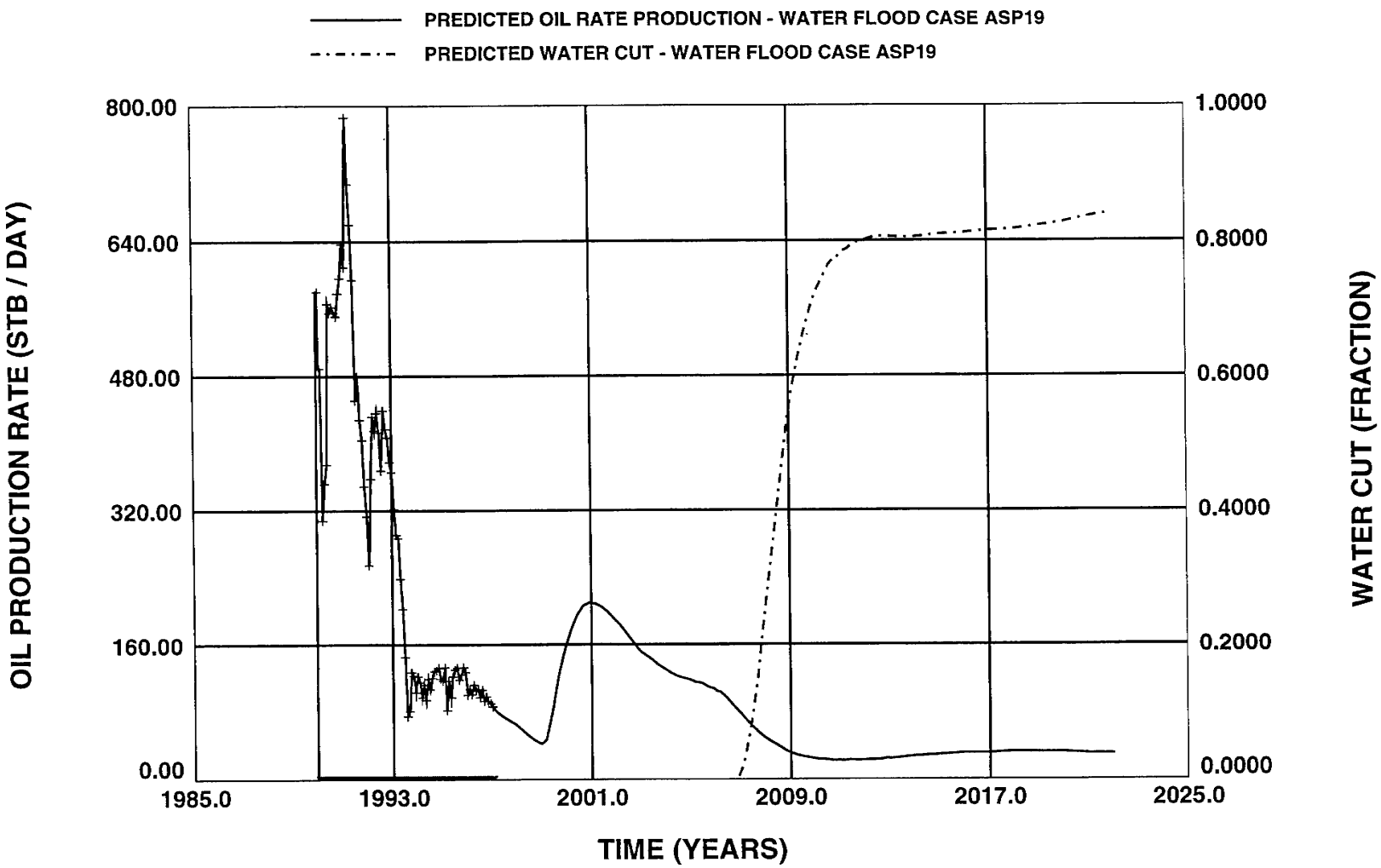

Figure 15-50 Anasazi Well No 1 Oil Rate and Water Cut - Water Flood

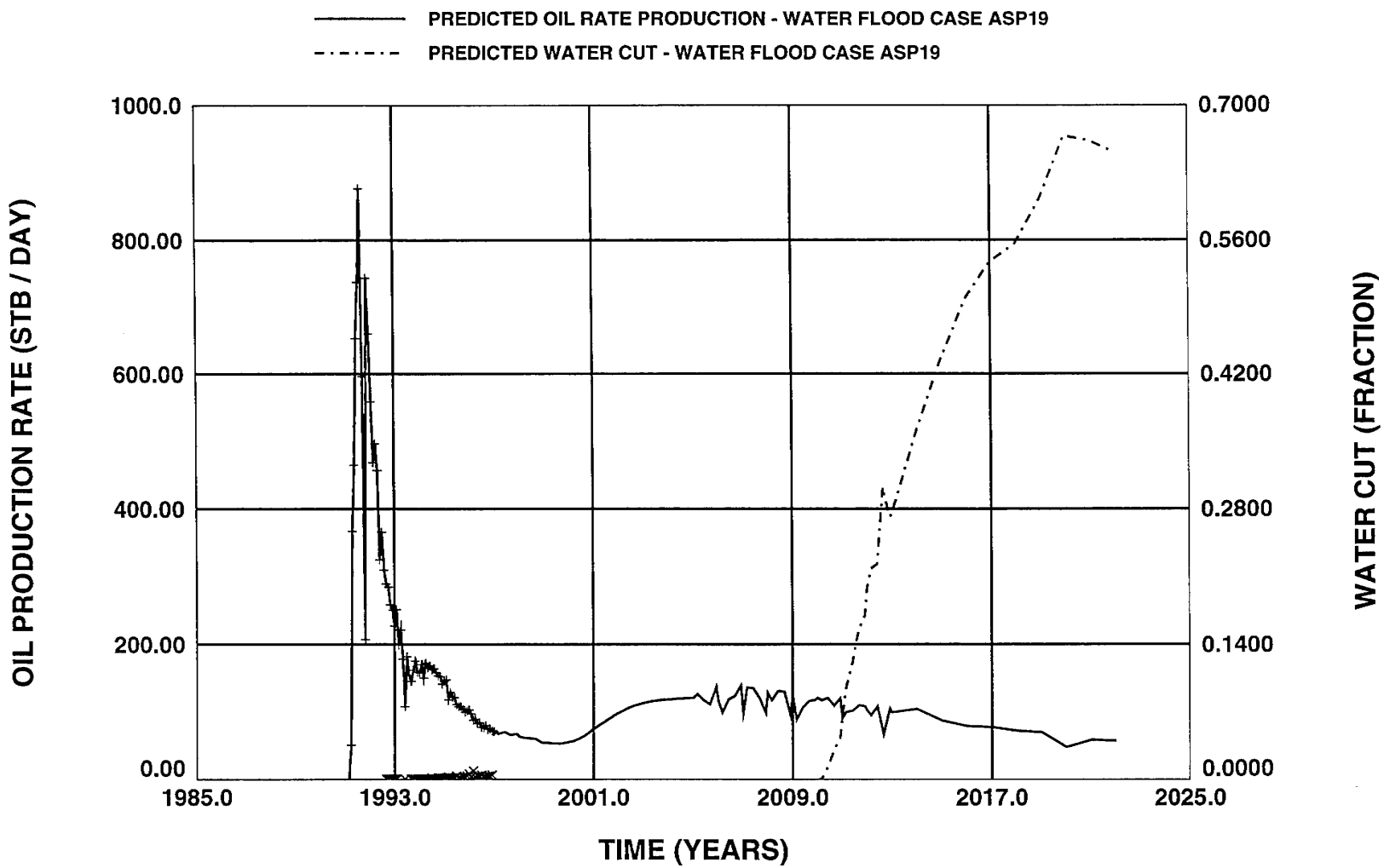

Figure 15-51 Anasazi Well No 5L-3 Oil Rate and Water Cut - Water Flood

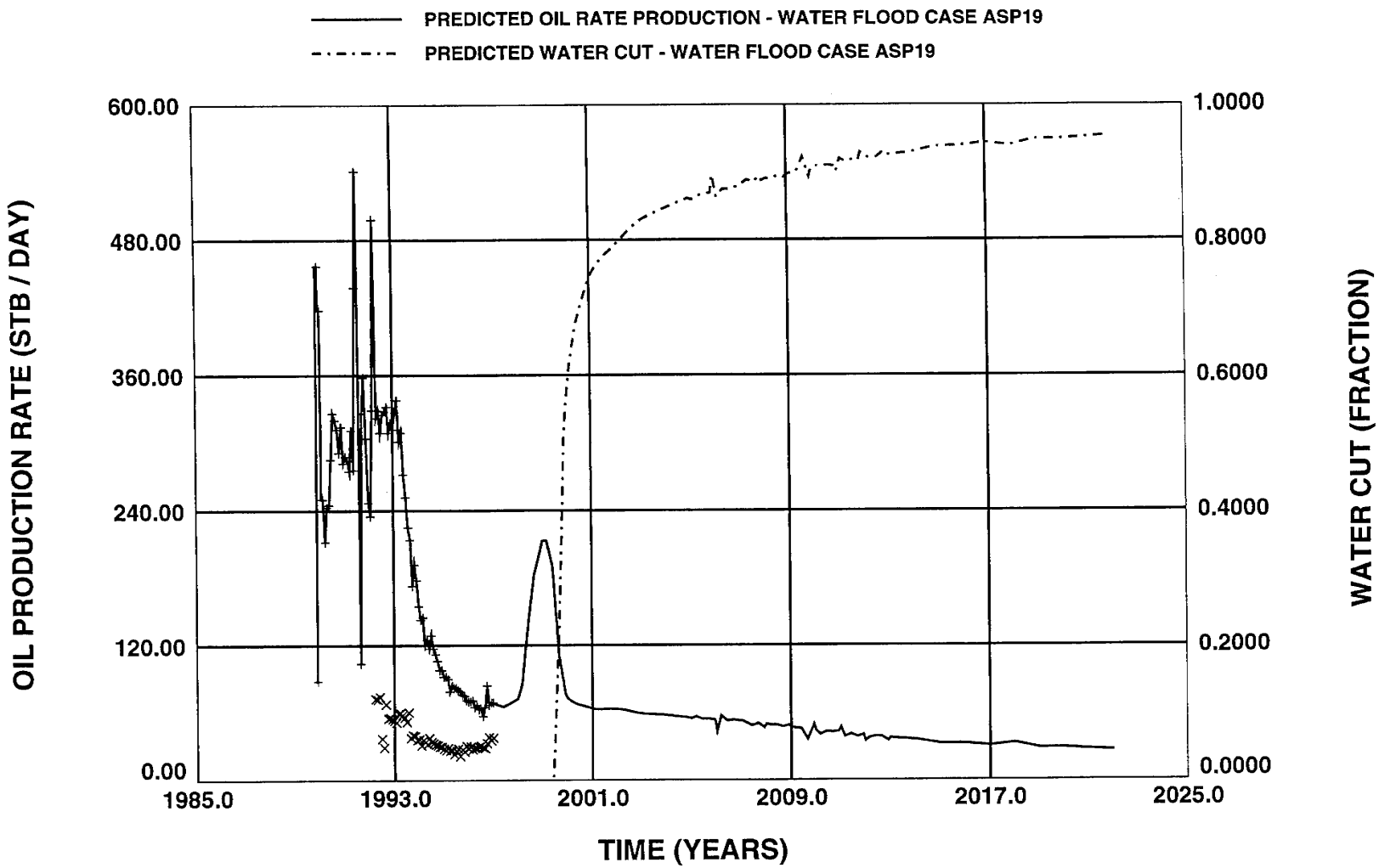

Figure 15-52 Sahgzie Well No 1 Oil Rate and Water Cut - Water Flood

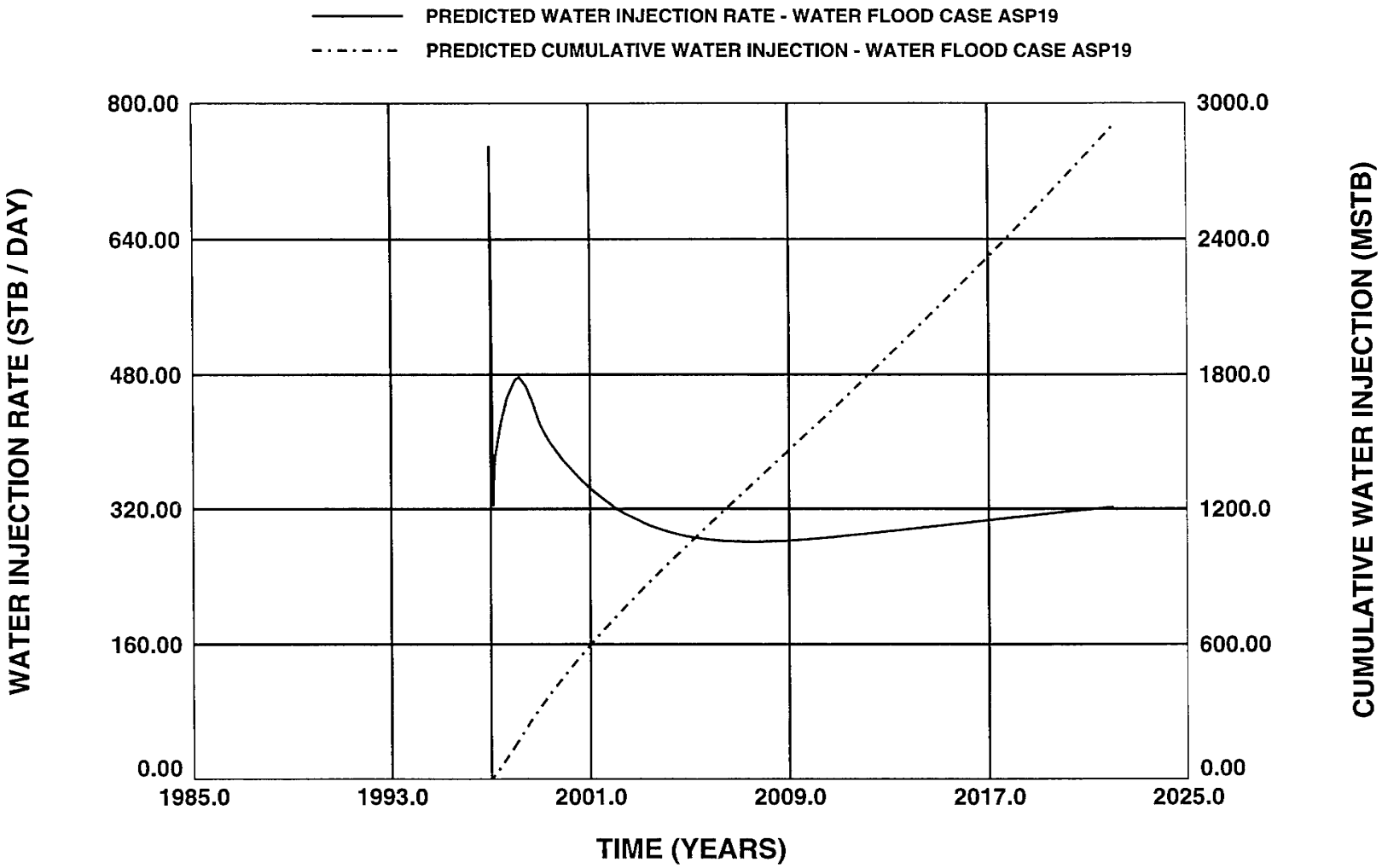

Figure 15-53 Water Injection Data - Anasazi Mound Injector

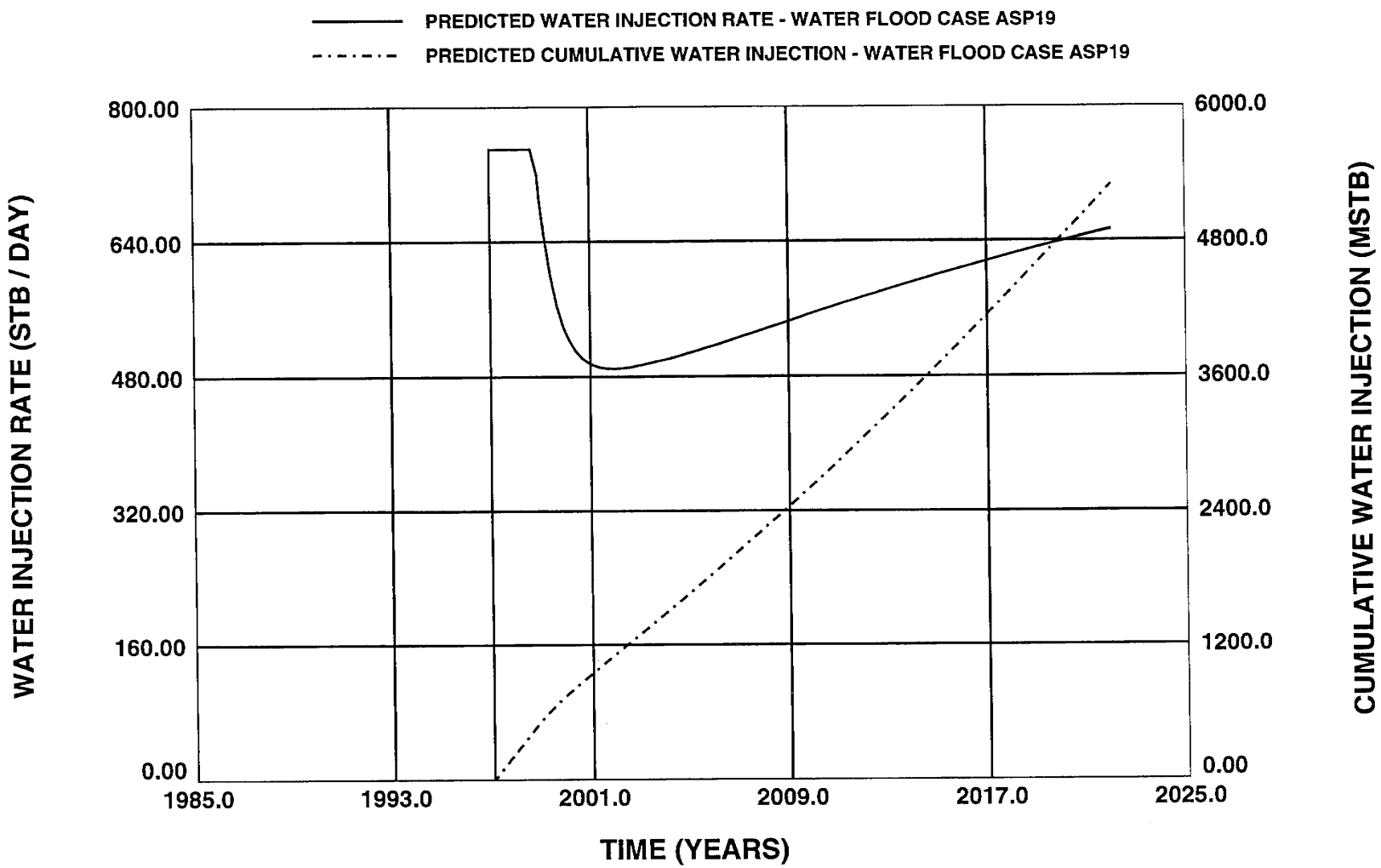

Figure 15-54 Water Injection Data - Sahgzie Mound Injector

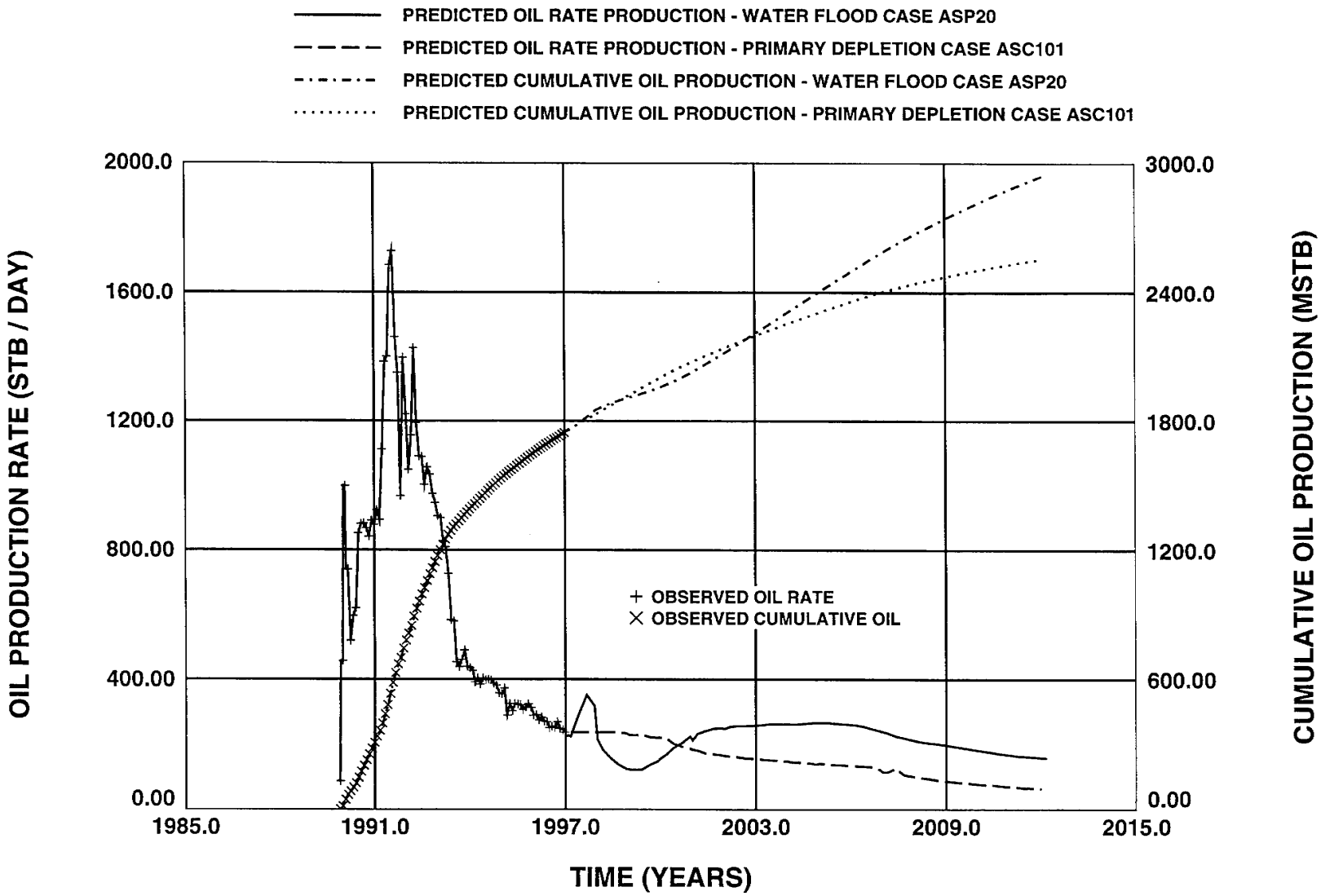

Figure 15-55 Field Level Oil Production - Water Flood Versus Primary

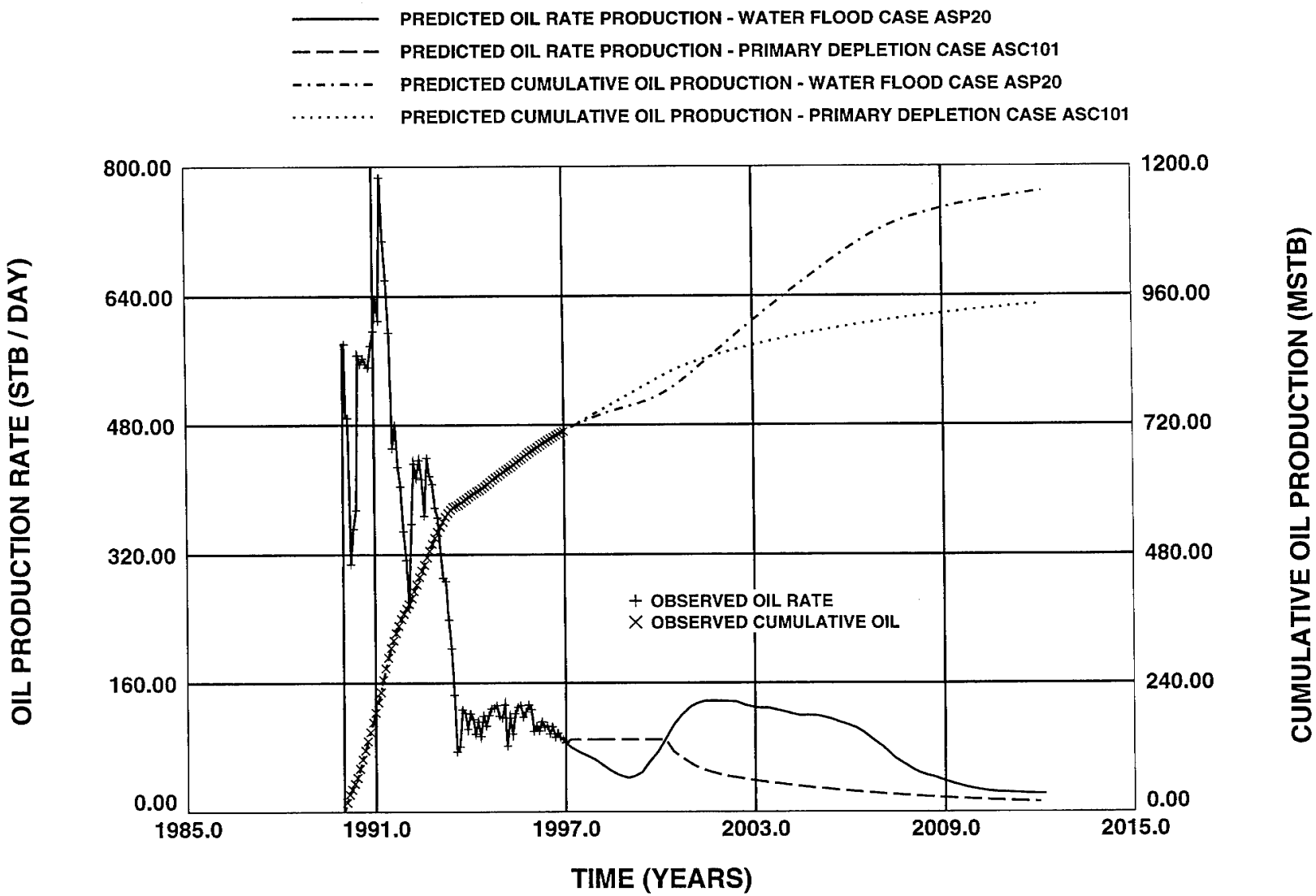

Figure 15-56 Anasazi Well No 1 Oil Production - Water Flood versus Primary

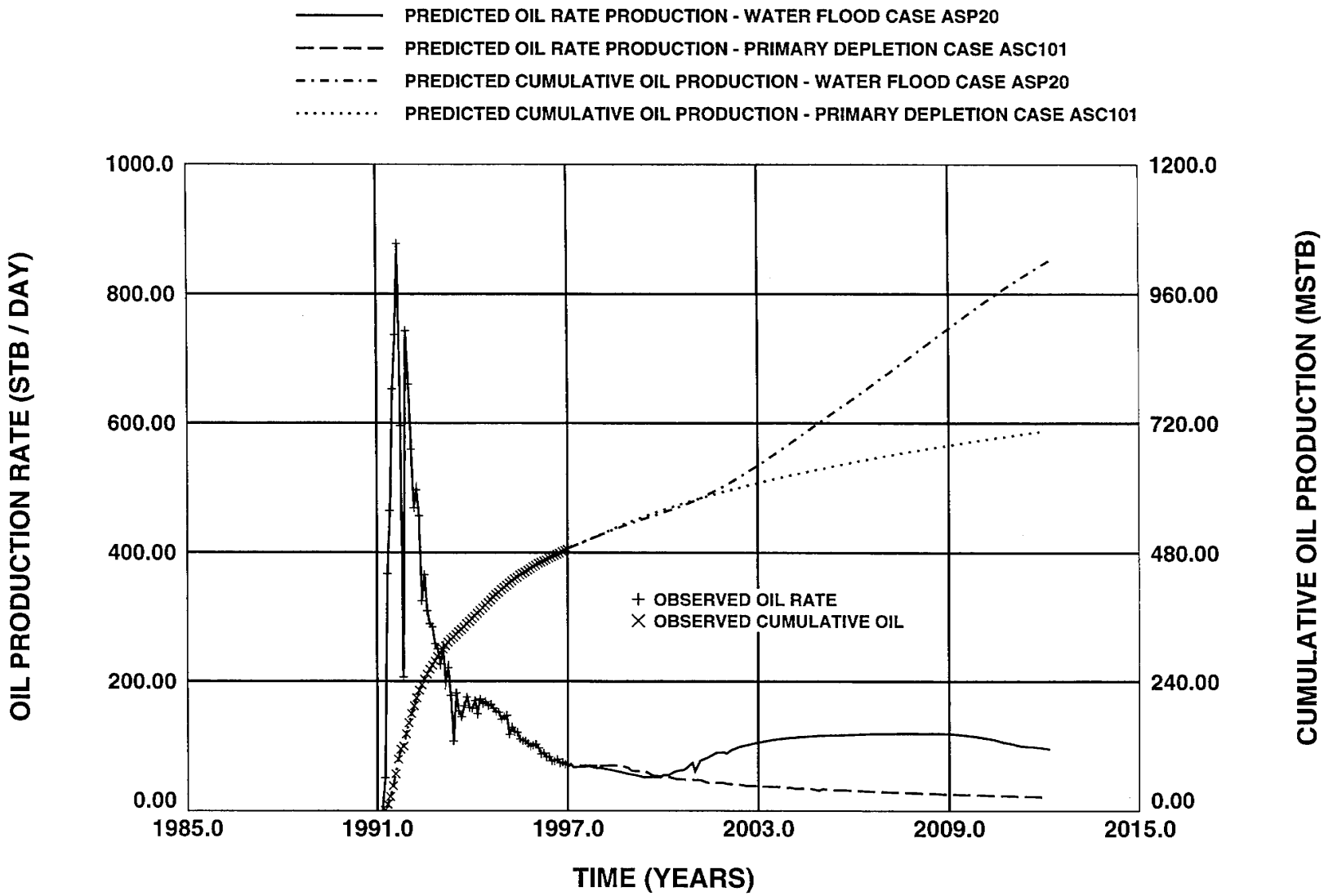

Figure 15-57 Anasazi Well No 5L-3 Oil Production - Water Flood versus Primary

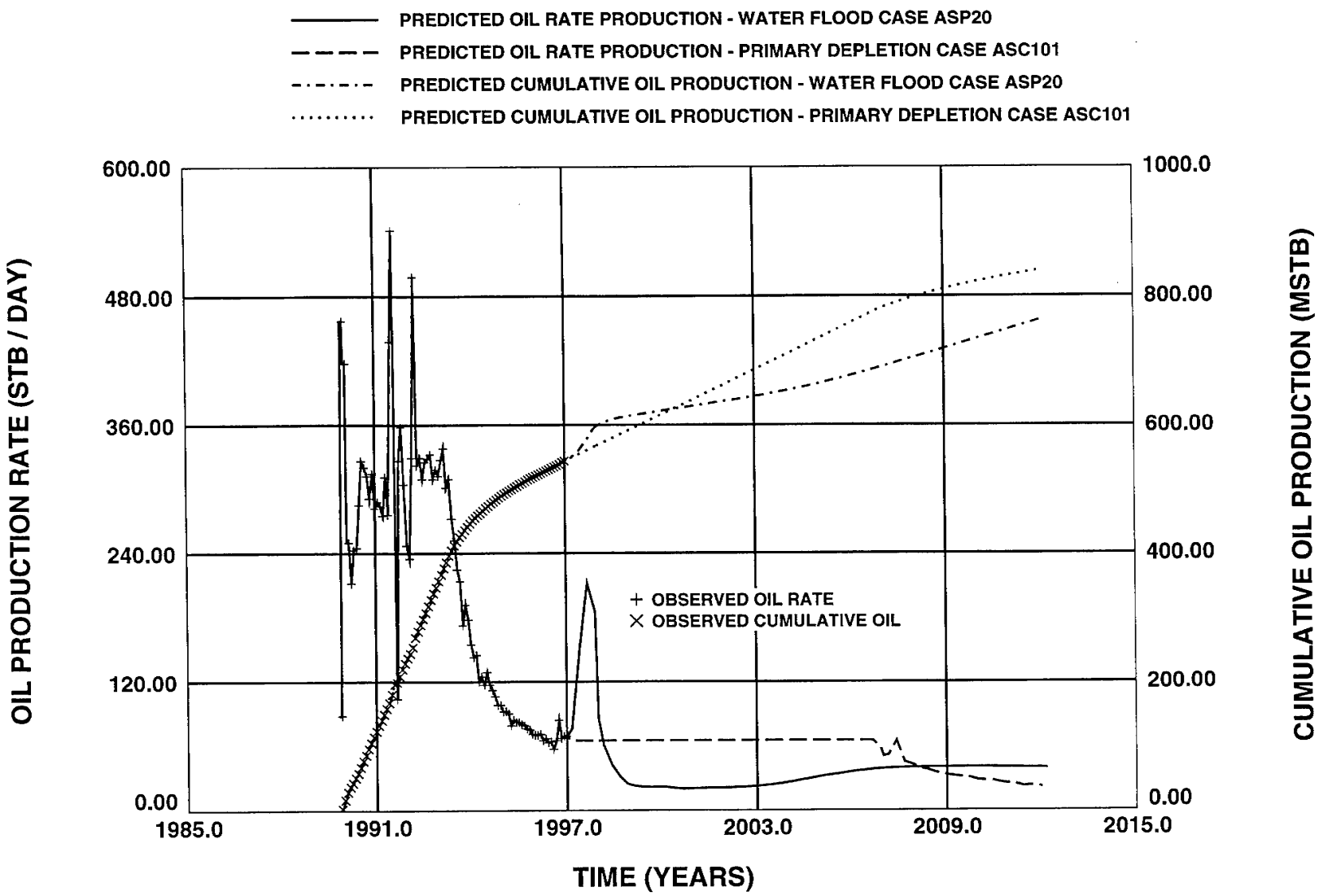

Figure 15-58 Sahgzie Well No 1 Oil Production - Water Flood versus Primary

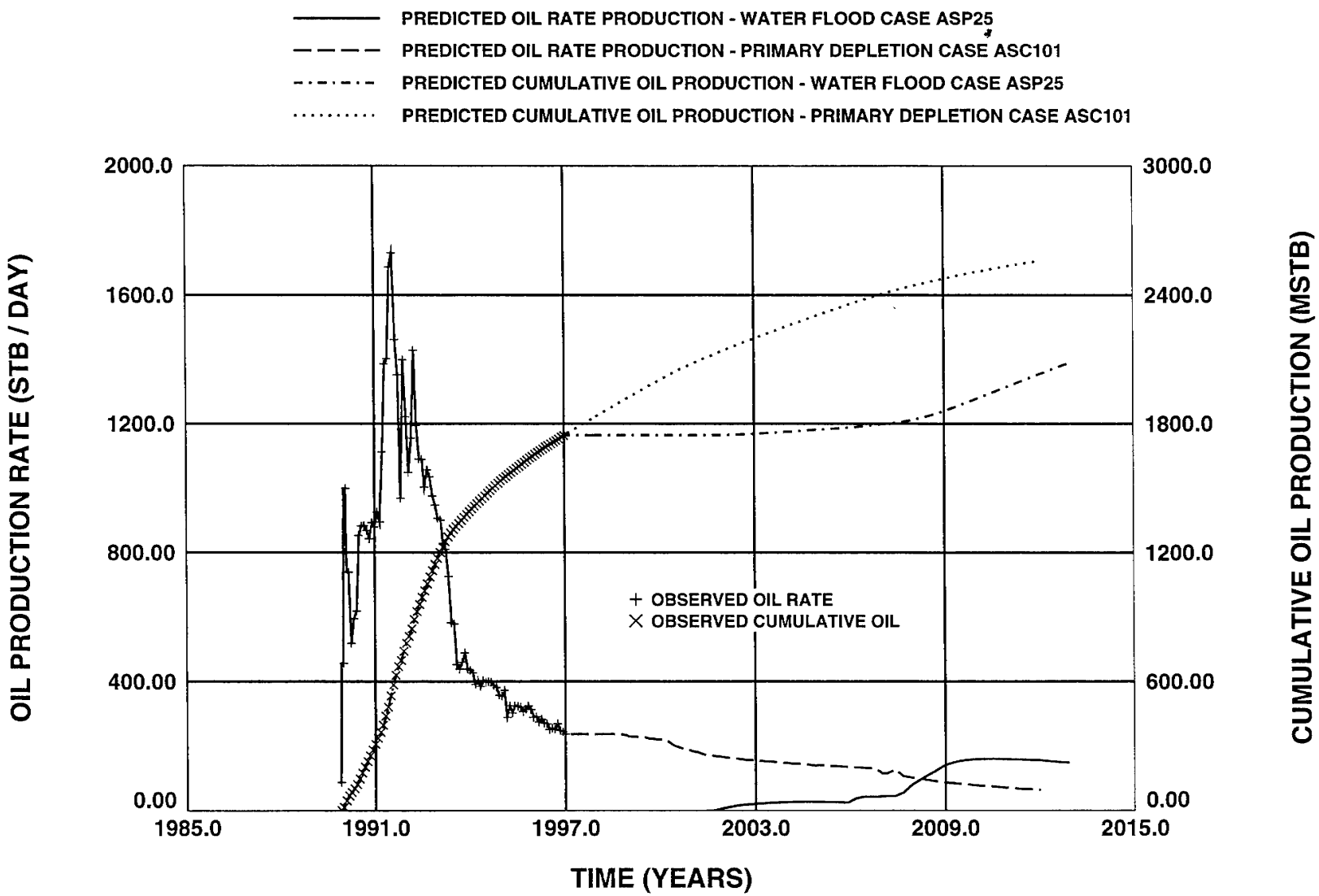

Figure 15-59 Field Level Oil Production - Water Flood versus Primary

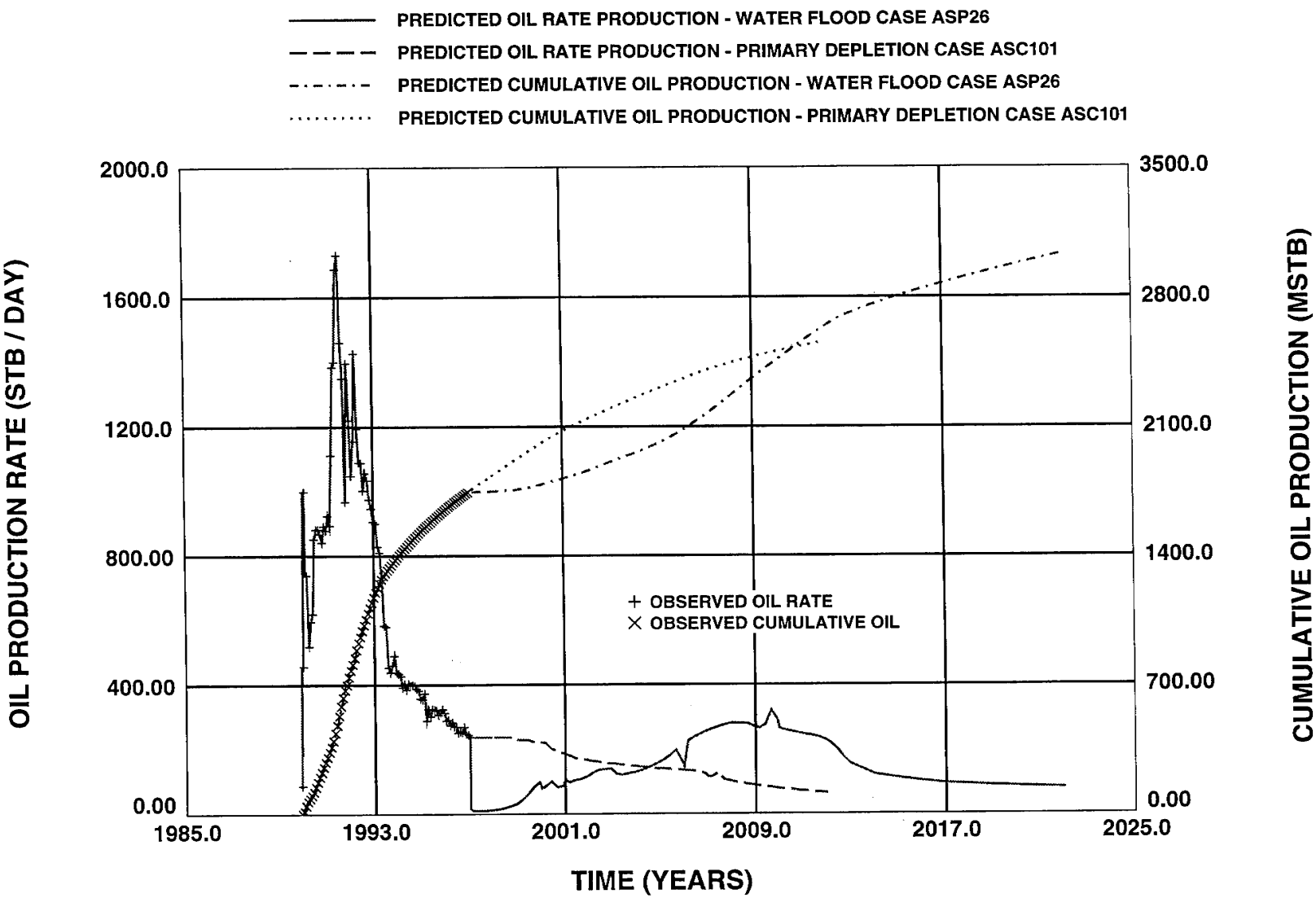

Figure 15-60 Field Level Oil Production - Water Flood versus Primary

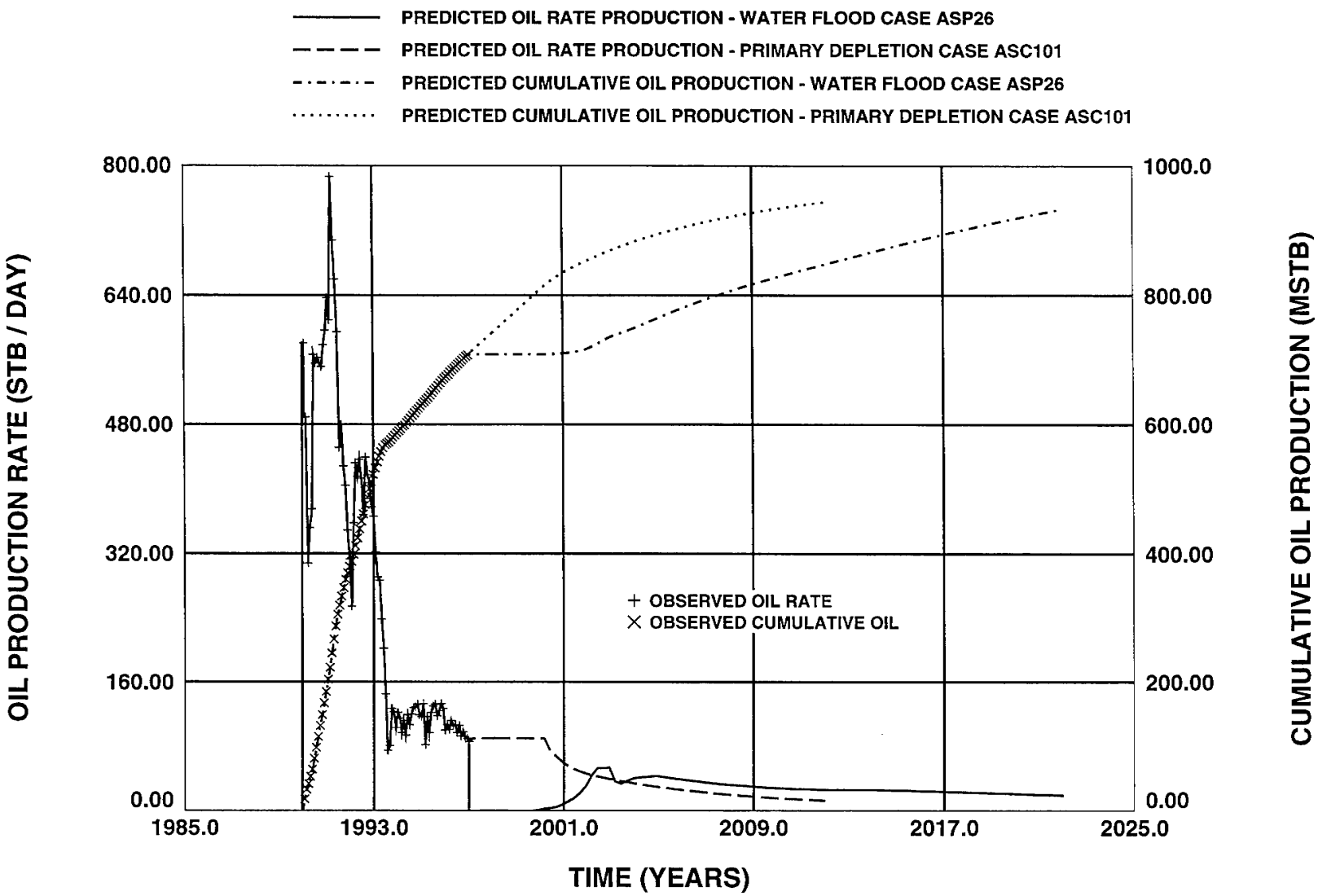

Figure 15-61 Anasazi Well No 1 Oil Production - Water Flood versus Primary

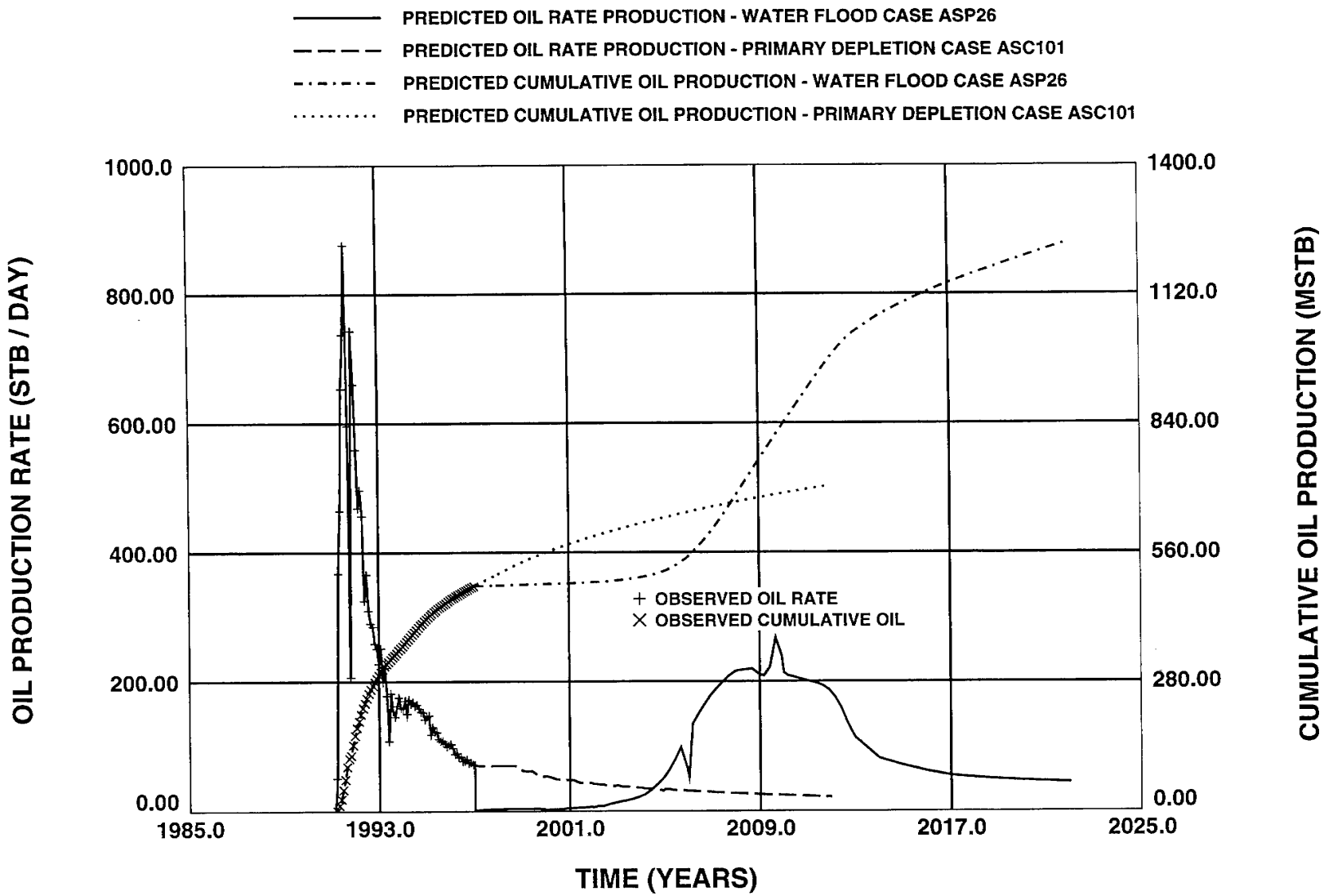

Figure 15-62 Anasazi Well No 5L-3 Oil Production - Water Flood versus Primary

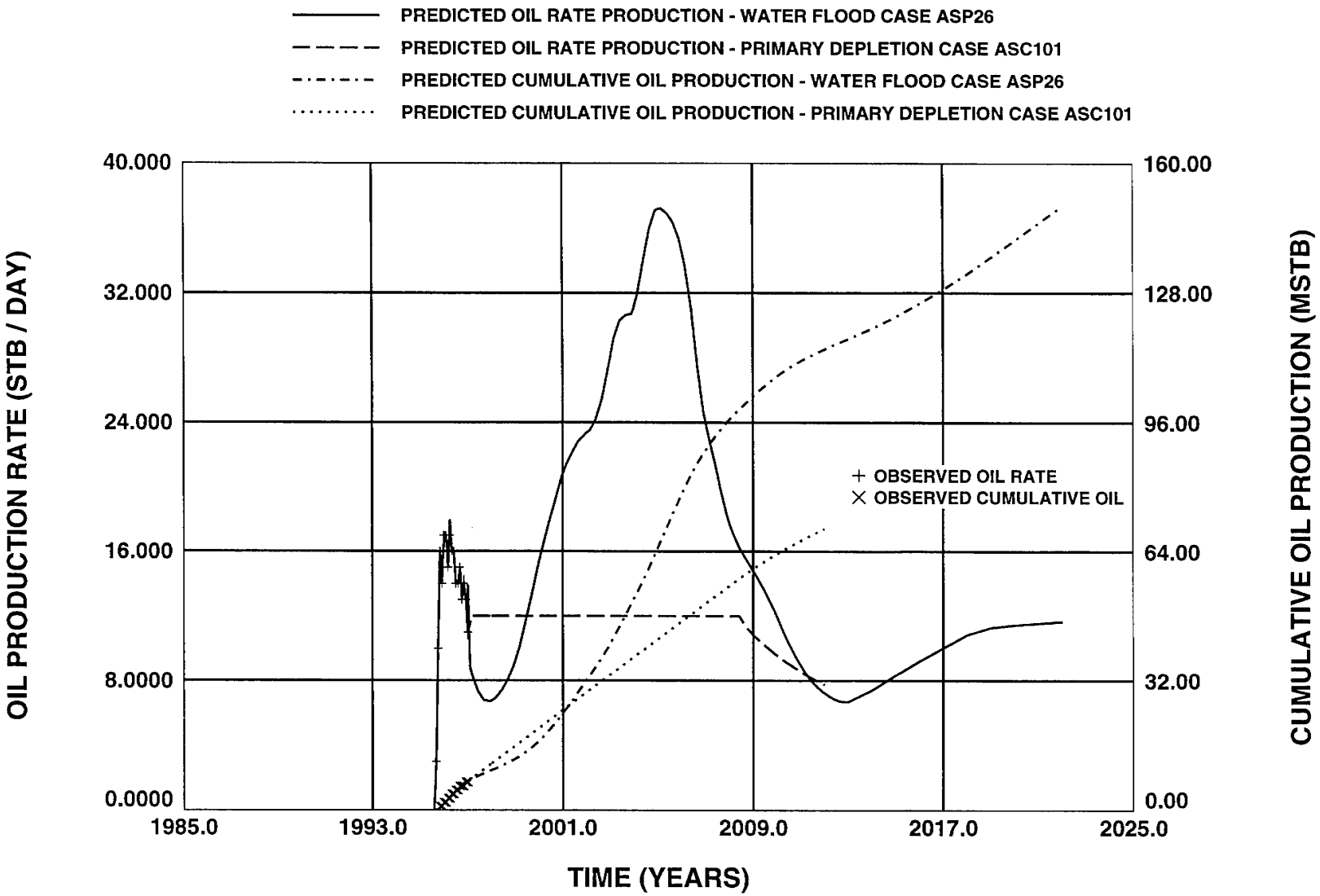

Figure 15-63 Anasazi Well No 6H-1 Oil Production - Water Flood versus Primary

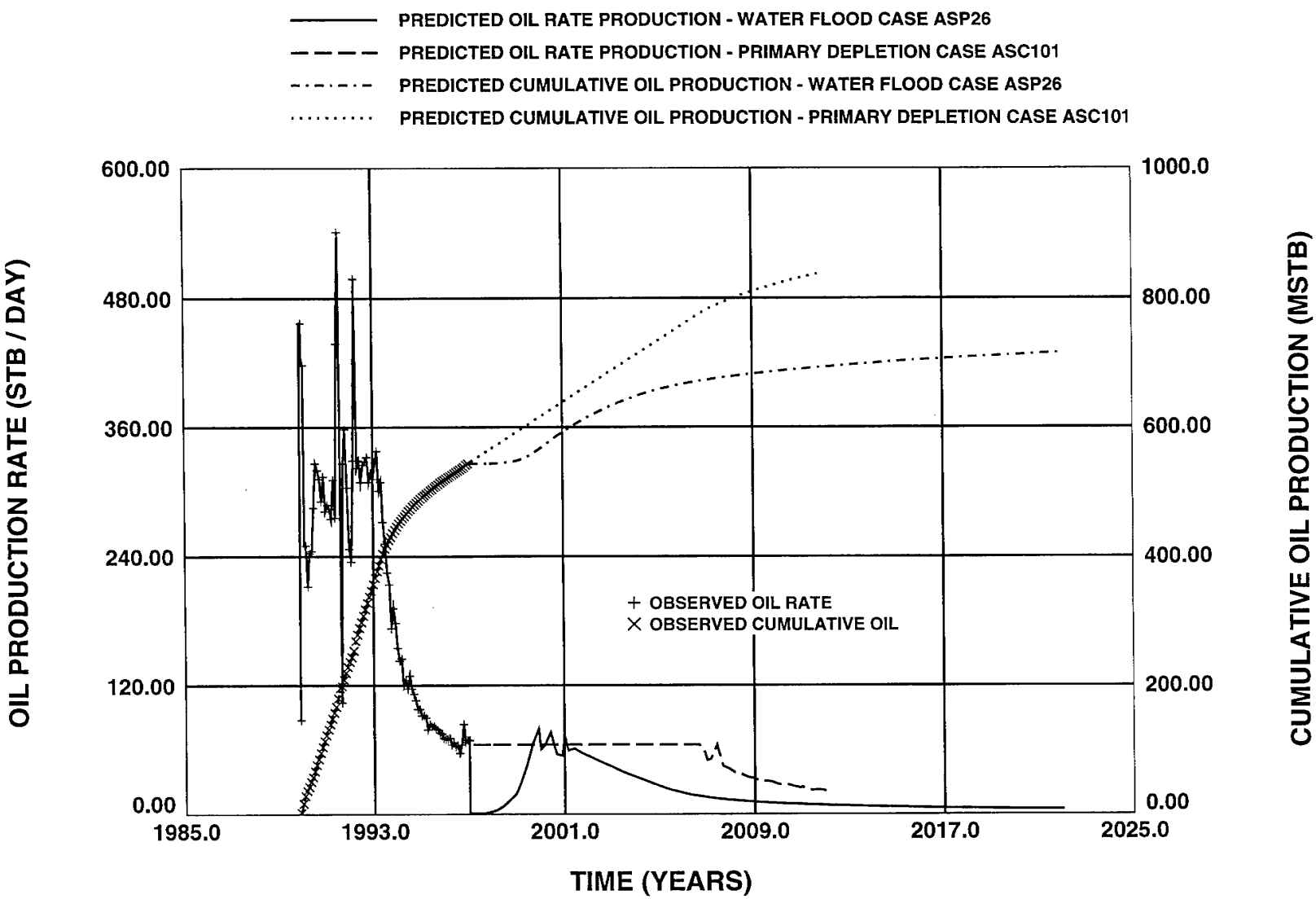

Figure 15-64 Sahgzie Well No 1 Oil Production - Water Flood versus Primary

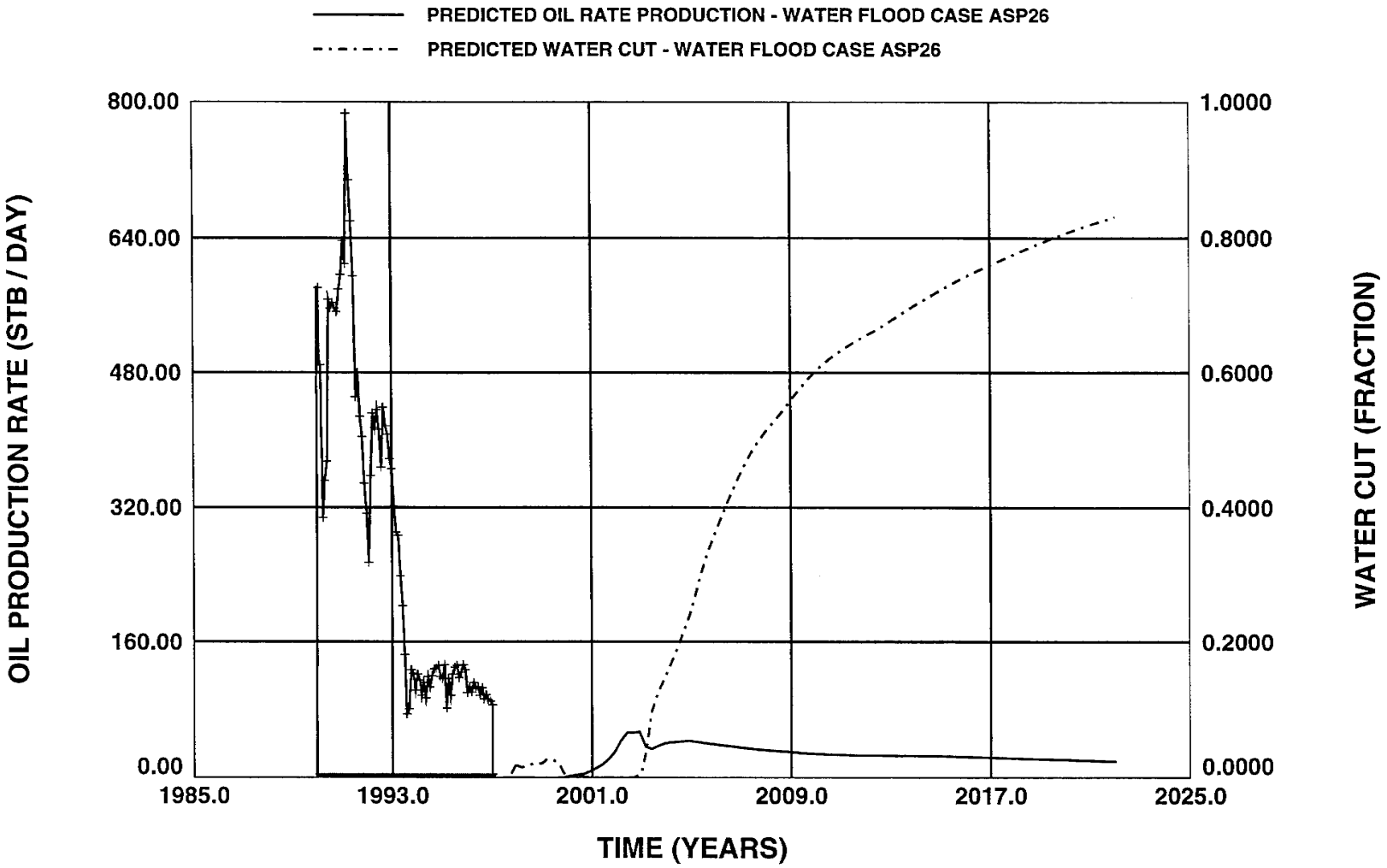

Figure 15-65 Anasazi Well No 1 Oil Rate and Water Cut - Water Flood

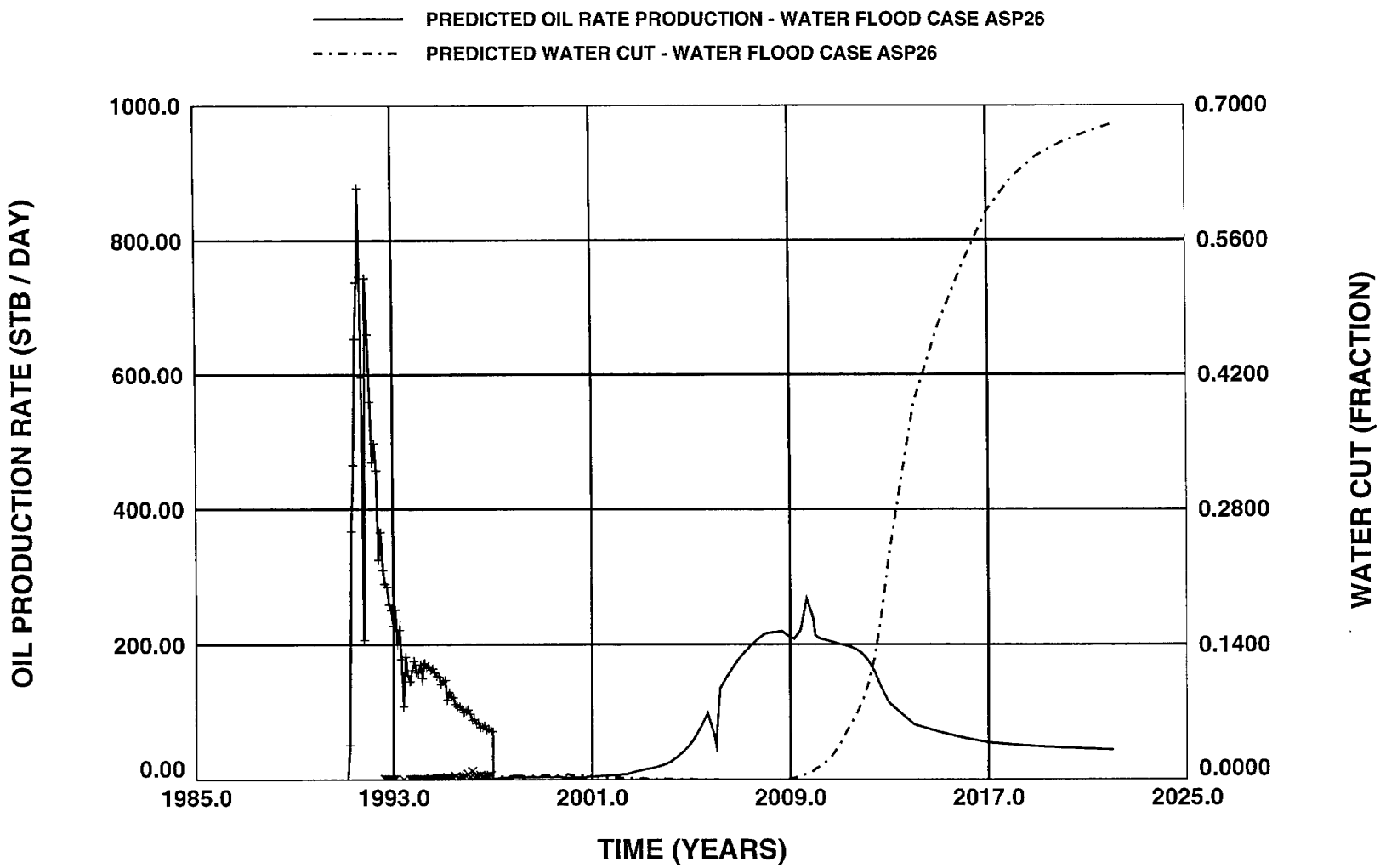

Figure 15-66 Anasazi Well No 5L-3 Oil Rate and Water Cut - Water Flood

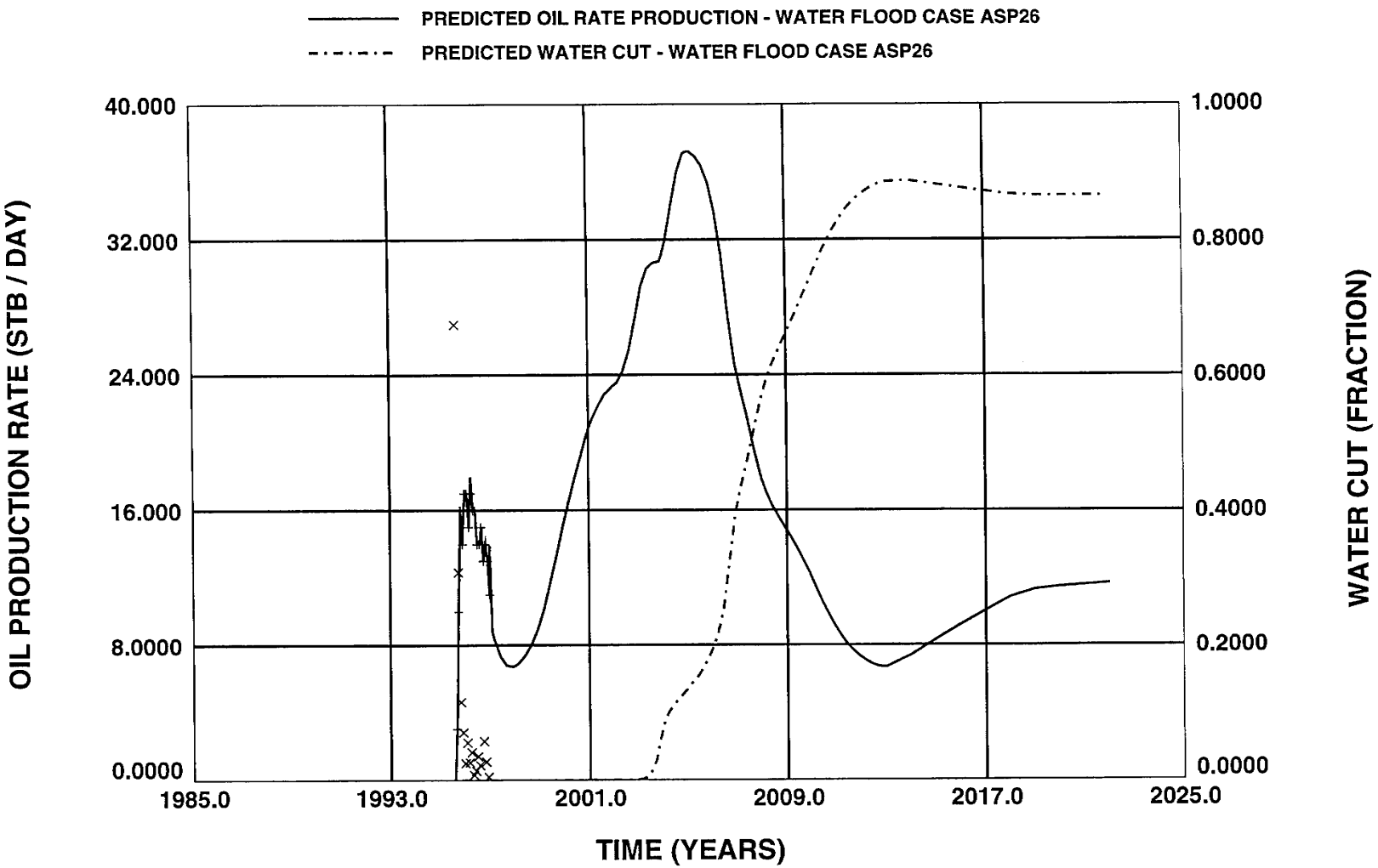

Figure 15-67 Anasazi Well No 6H-1 Oil Rate and Water Cut - Water Flood

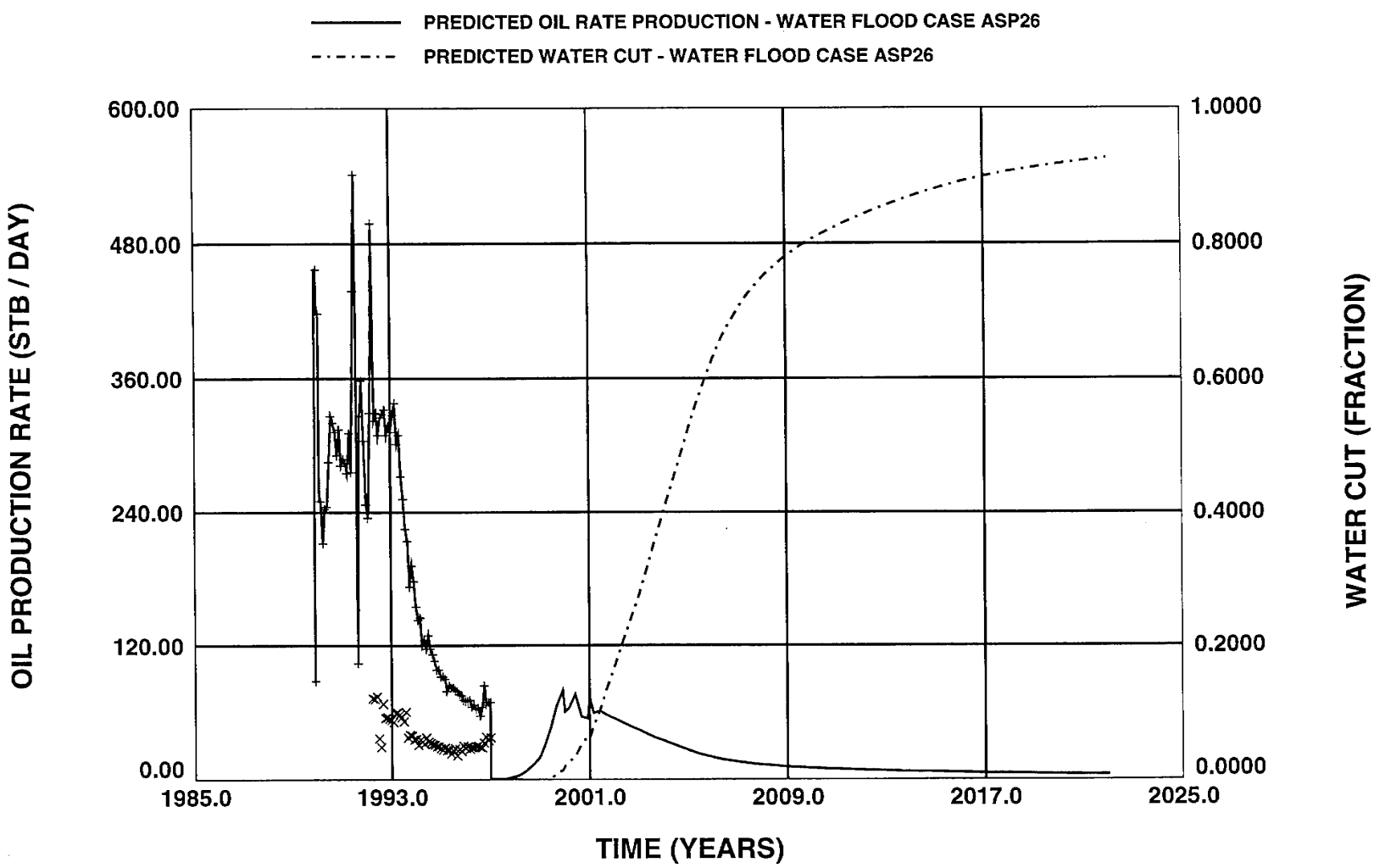

Figure 15-68 Sahgzie Well No 1 Oil Rate and Water Cut - Water Flood

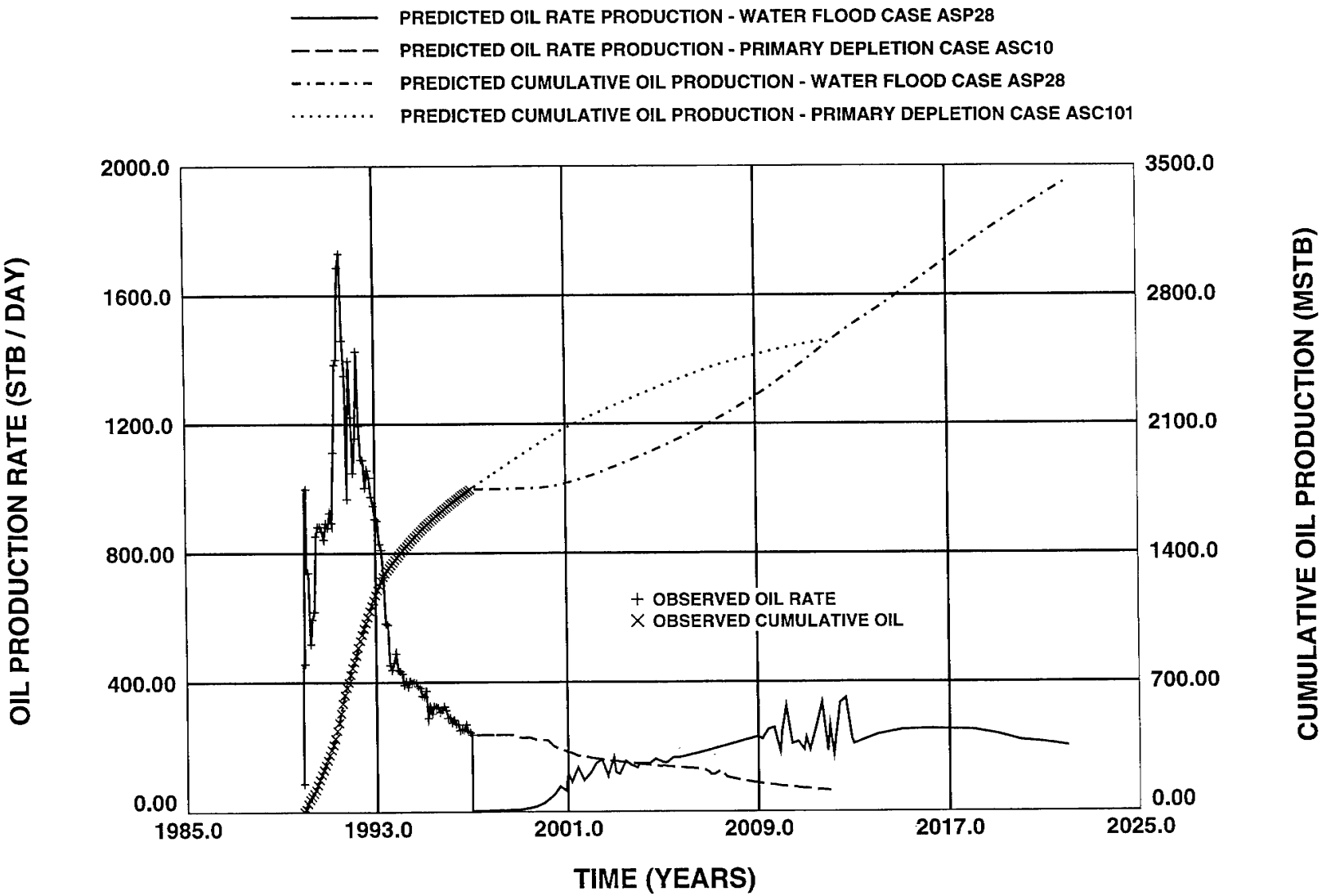

Figure 15-69 Field Level Oil Production - Water Flood versus Primary

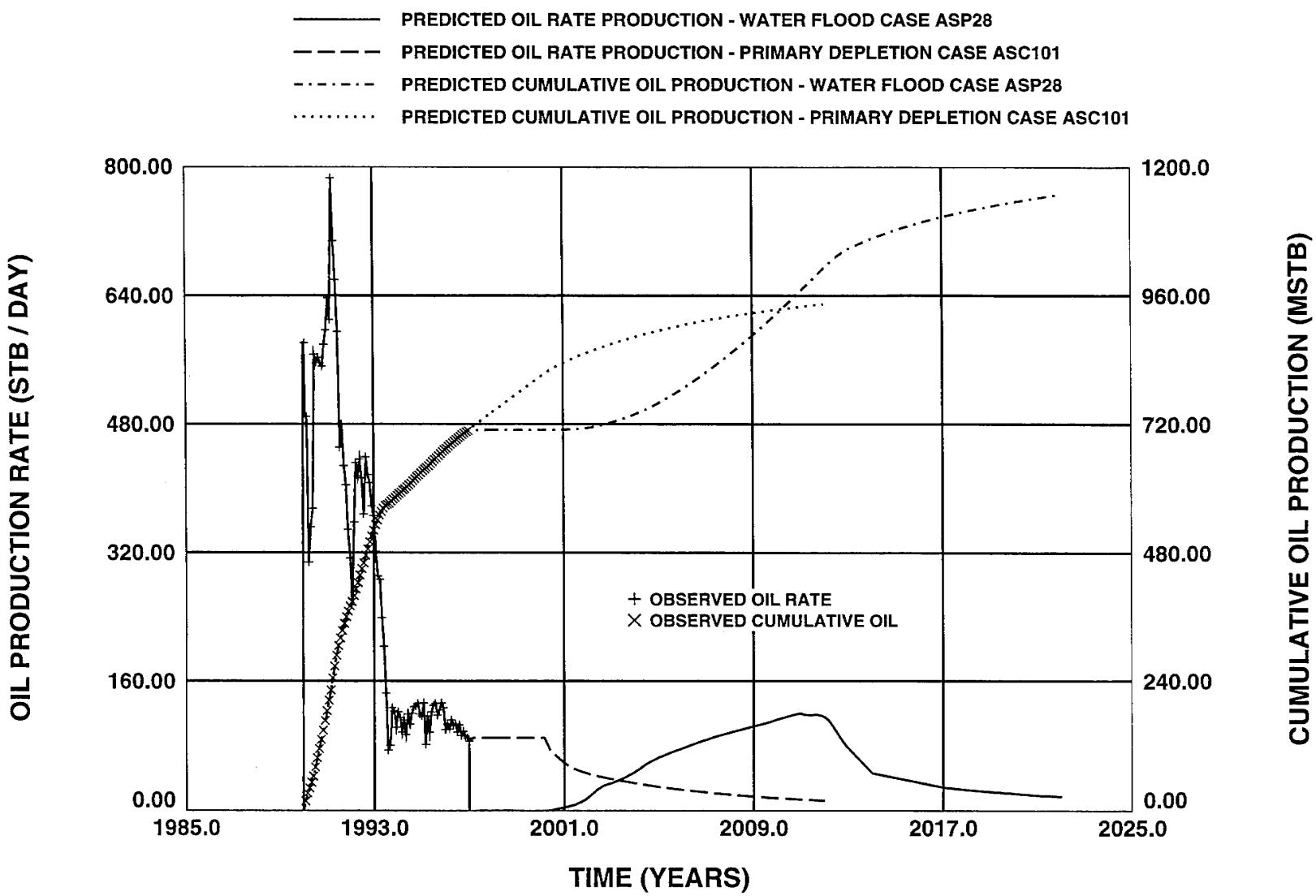

Figure 15-70 Anasazi Well No 1 Oil Production - Water Flood versus Primary

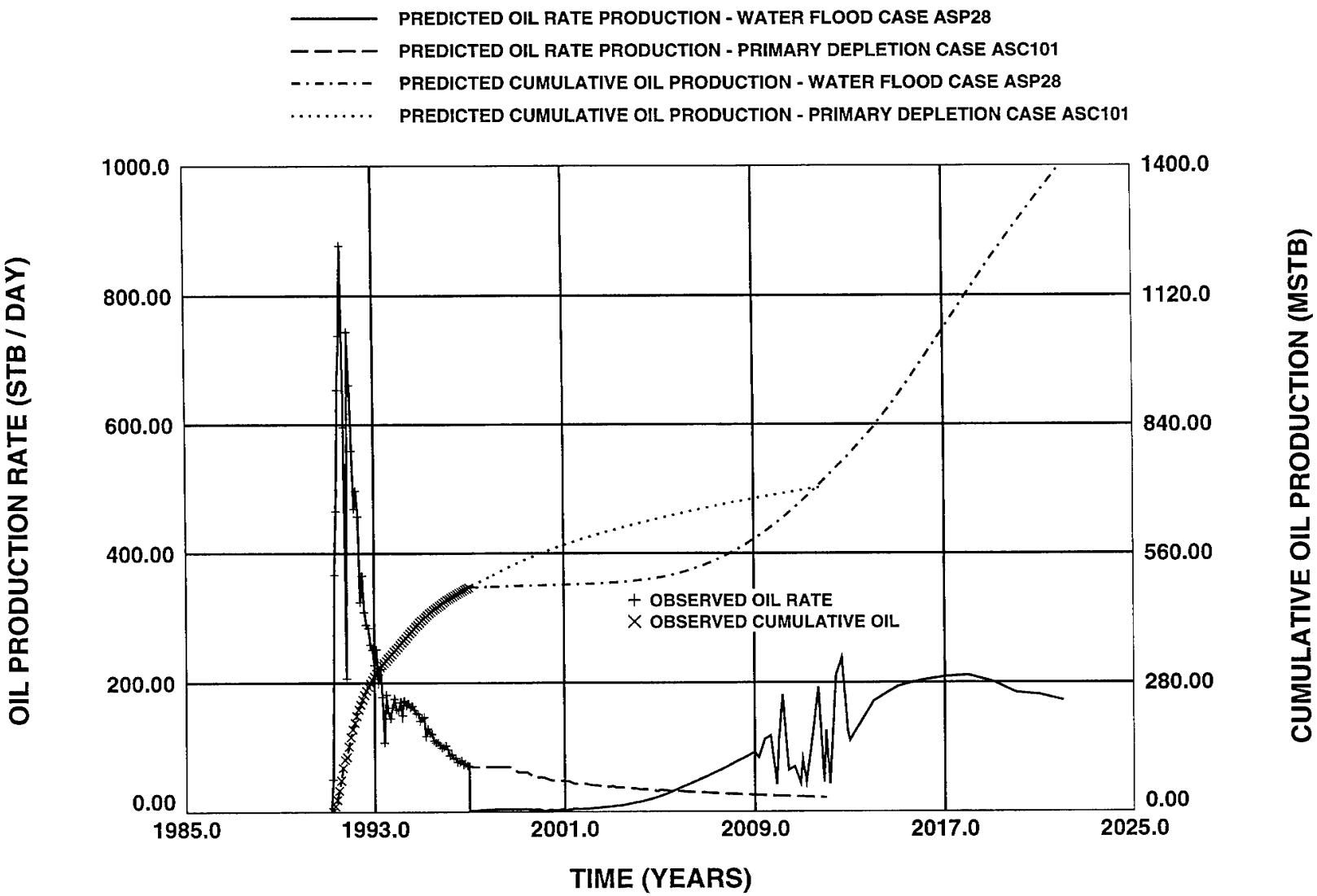

Figure 15-71 Anasazi Well No 5L-3 Oil Production - Water Flood versus Primary

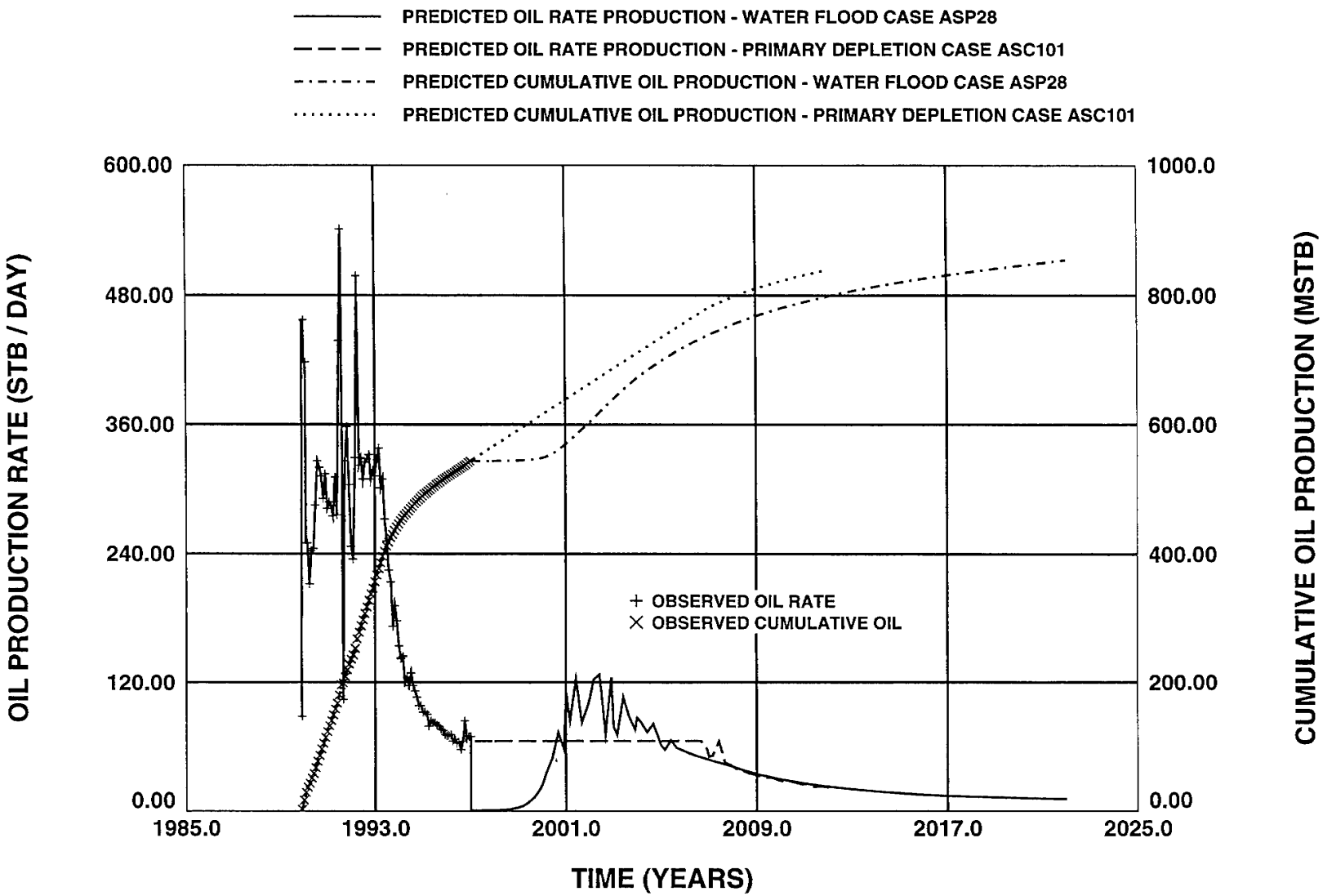

Figure 15-72 Sahgzie Well No 1 Oil Production - Water Flood versus Primary

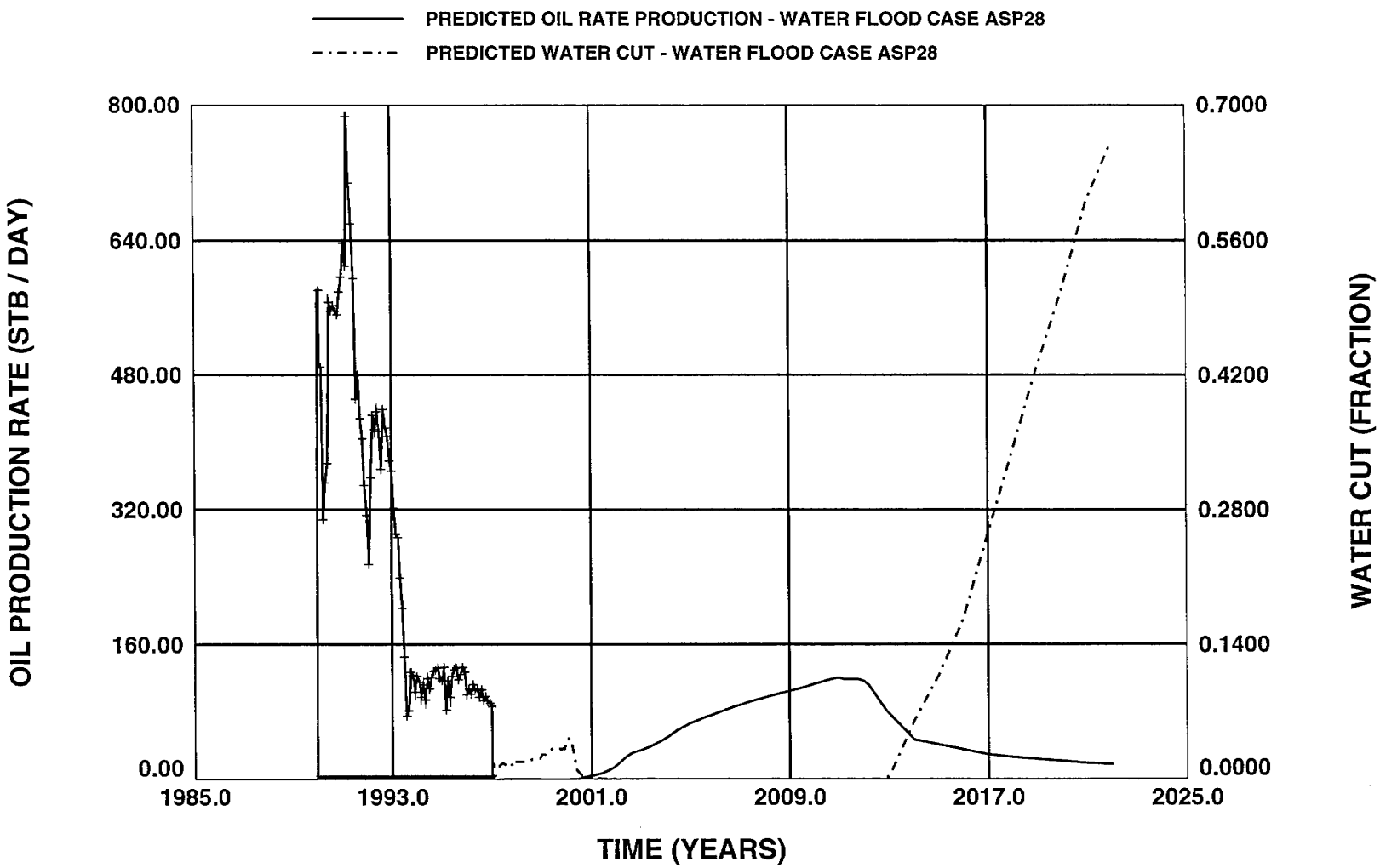

Figure 15-73 Anasazi Well No 1 Oil Rate and Water Cut - Water Flood

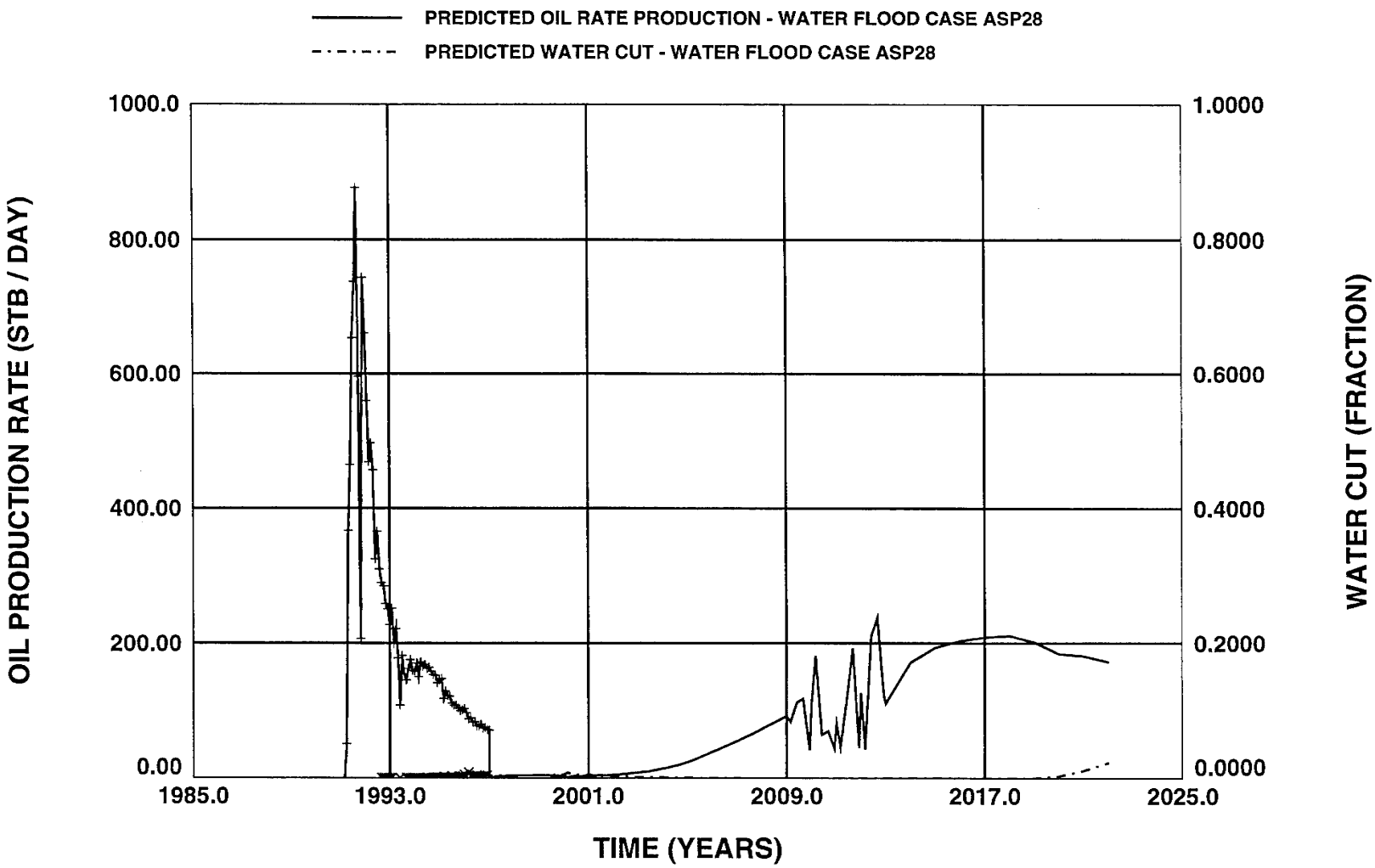

Figure 15-74 Anasazi Well No 5L-3 Oil Rate and Water Cut - Water Flood

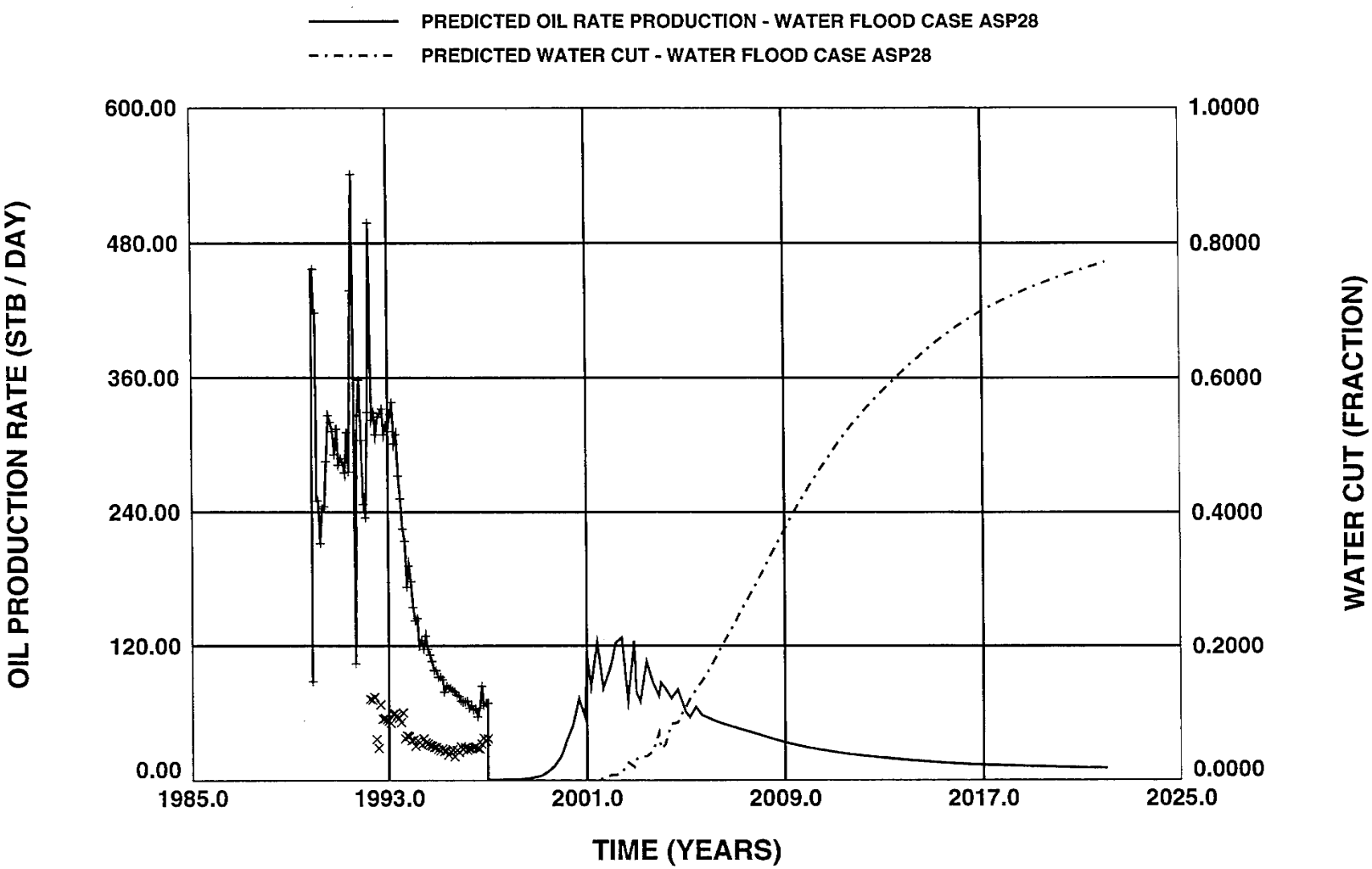

Figure 15-75 Sahgzie Well No 1 Oil Rate and Water Cut - Water Flood

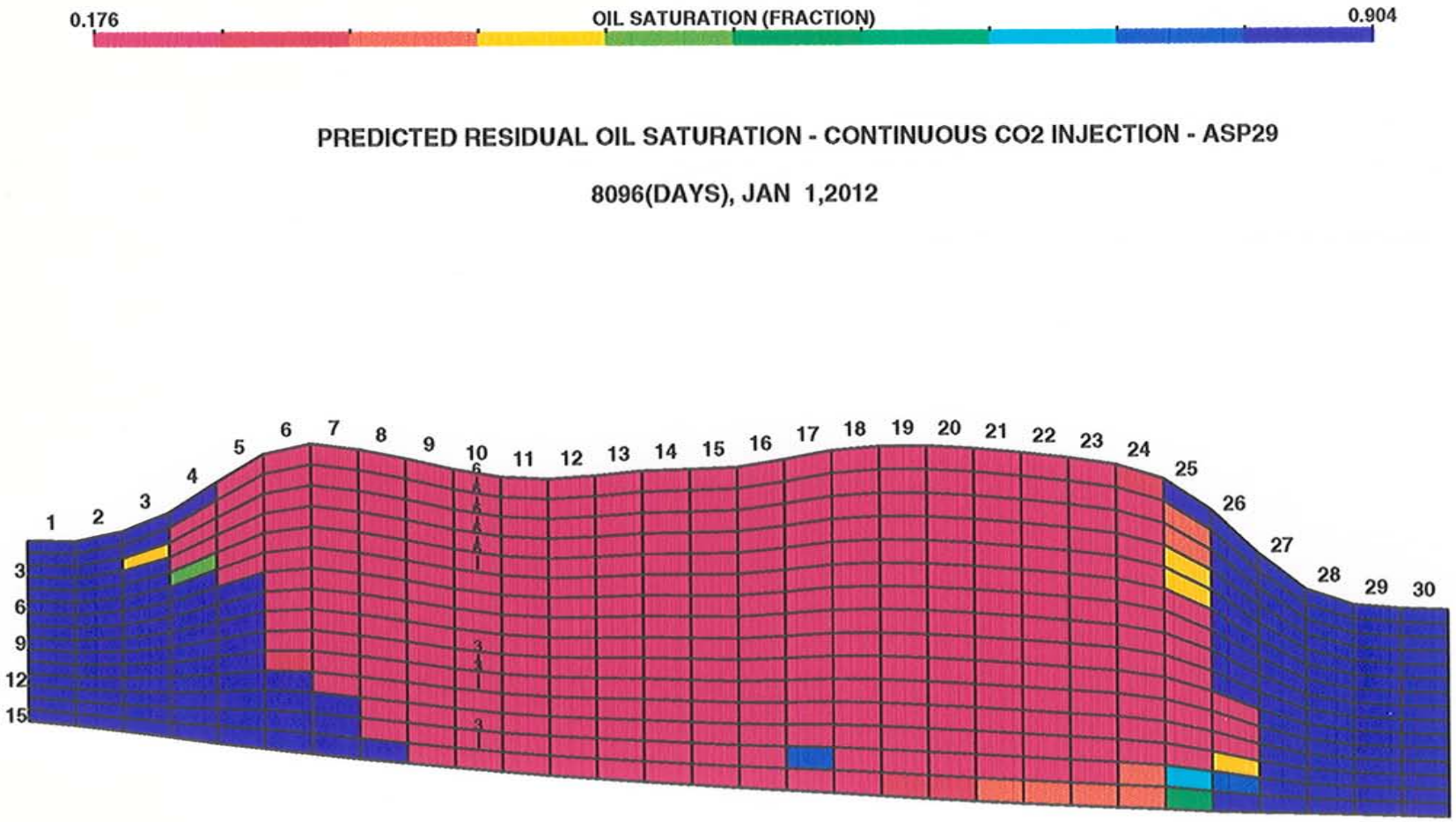

Figure 15-76 Residual Oil Saturation after CO2 Flooding

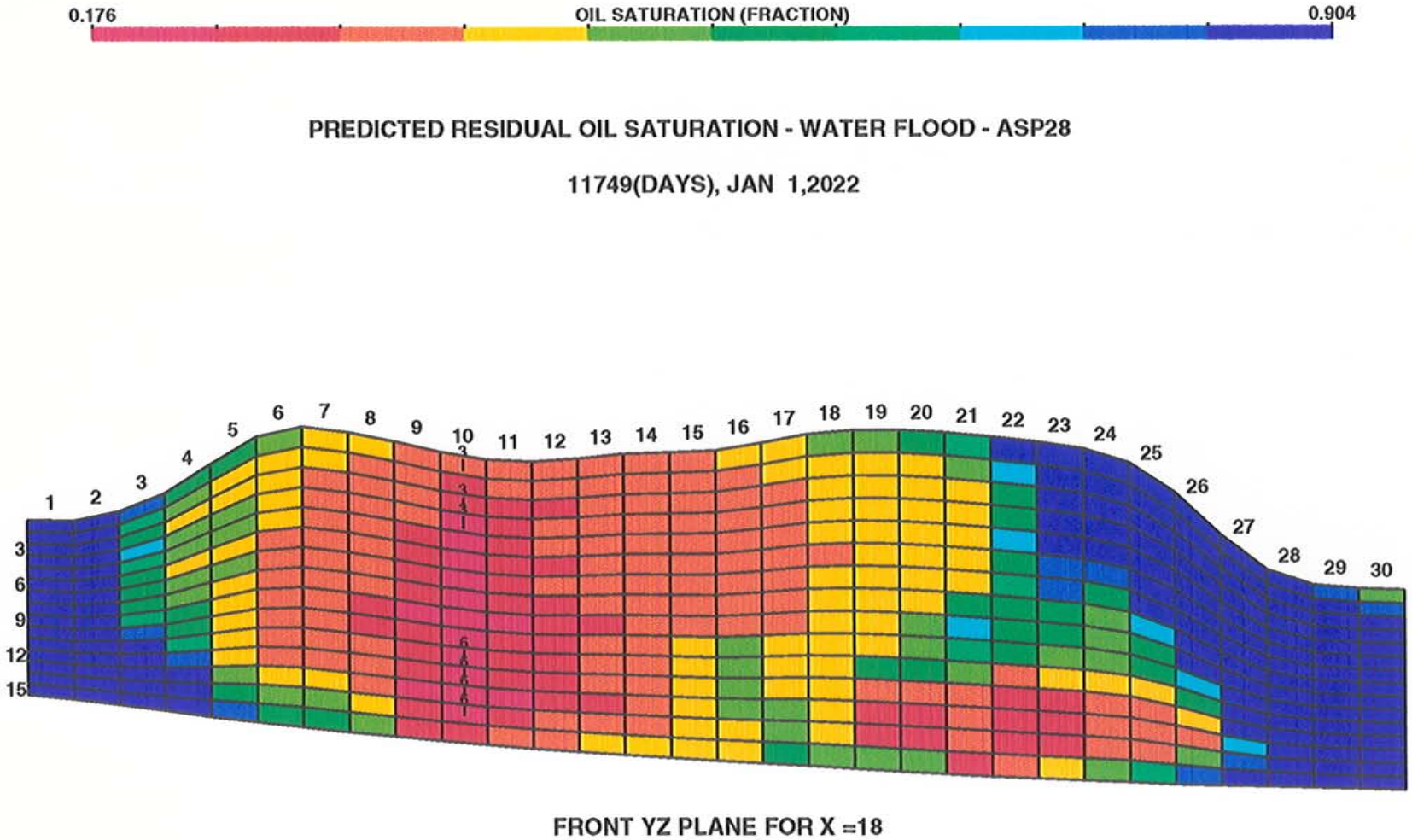

Figure 15-77 Residual Oil Saturation after Water Flooding